TKI - Innovative mooring in the Port of the Future

ShoreTension moored ship scale model tests

Deltares

TKI - Innovative mooring in the Port of the Future

ShoreTension moored ship scale model tests

S.P. Reijmerink
N. Bruinsma
A.J. van der Hout

Deltares

Title
TKI - Innovative mooring in the Port of the Future

Client	Project	Attribute	Pages
ShoreTension	11202696-000	11202696-000-HYE-0010	53

Keywords
ShoreTension, physical scale model, moored vessel, shallow water, jetty, validation database, innovative mooring techniques, Port of the Future

Summary
The overall aim of this project was to explore the limits and possibilities of innovative mooring of vessels in the Port of the Future and to provide a solid database for validation of numerical models simulating the performance of these innovative mooring solution. The mooring technique studied in this project was the ShoreTension (ST) system. This system is used in combination with conventional mooring lines and actively controls the line forces by giving out or hauling in the mooring lines, and therewith minimizing the motions of a moored vessel. With respect to the ST system, the main system-specific goals of this project were to verify the application limits of the ST system with respect to wave height (for the most critical response periods) and to optimise the system settings to maximise the applicability range of the system. In this way the applicability limits of the system may be enlarged compared to present understanding and expectations of the system.

To reach those goals, physical scale model tests of a moored vessel were performed within Deltares' Delta Basin with one vessel size/type and one draft-depth ratio for four different mooring configurations. The vessel has been tested in three series of different types of wave conditions with increasing complexity (monochromatic, bi-chromatic and irregular waves) and wave heights. The wave periods of these wave conditions were selected such that they corresponded to, or were almost equal to, the natural periods of the moored vessel. In this way the tested situations corresponded to the most challenging wave conditions for the ST system.

The tests showed that the ST system effectively reduces low-frequency horizontal wave motions (surge, sway and yaw). In traditional ports these are generally normative. When developing new port concepts in which innovative mooring techniques are applied it should be considered that other aspects will become normative (e.g. roll motions). To be able to assess these situations, well-validated numerical tools are necessary. The systematically generated measurement database together with this report provide a proper basis for the validation of numerical representations of the ST system.

The scale model results form a solid verification of the functionality and performance of the innovative mooring system. The results will help to increase acceptability of the ST system (and similar techniques) throughout the waterborne transport community and for use in the Port of the Future. In addition, the explored applicability limits of the ST system may diversify and extend the fields of application of the system.

References
TKI proposal, 'Innovatief afmeren van schepen in de haven van de toekomst', dated 3 February 2018
TKI award document, T-DEL/2018/05 – DEL083 – 'innovatief afmeren van schepen', dated 05 March 2018
Project plan - Innovatief afmeren van schepen in de haven van de toekomst, Reference: 11202696-000-HYE-0002, Dated 11-Jun-2018.

Version	Date	Author	Initials	Review	Initials	Approval	Initials
Draft	Jan. 2019	S.P. Reijmerink et al.		M.P.C. de Jong		J. Schouten	
Final	Mar. 2019	S.P. Reijmerink N. Bruinsma A.J. van der Hout		M.P.C. de Jong		J. Schouten	

Status
final

Please note that due to reasons of confidentiality, some parts of this document have been removed and are not publicly available.

Contents

1 Introduction **1**
1.1 Background 1
1.2 TKI project and partners 1
1.3 Objective 1
1.4 Project approach 2
1.5 Project team 3
1.6 Content of the report 3

2 Physical model setup **5**
2.1 Test facility 5
2.1.1 Facts and figures 5
2.1.2 Applied basin setup 6
2.2 Scaling 8
2.2.1 Froude scaling 8
2.2.2 Considerations on accuracy at the chosen model scale 8
2.3 Hydrodynamic conditions 9
2.3.1 Water depth 9
2.3.2 Wave condition types 9
2.4 Vessel 10
2.4.1 Vessel particulars 10
2.4.2 Decay tests 12
2.5 Mooring configuration 12
2.5.1 Mooring equipment 12
2.5.2 Cases A, B and C 16
2.5.3 Cases D 17
2.6 Measurement equipment 18
2.6.1 Hydrodynamic measurements 19
2.6.2 Motion measurements 20
2.6.3 Force measurements 21
2.7 General testing procedure 21
2.7.1 Calibration of instruments 21
2.7.2 Decay tests 21
2.7.3 Wave calibration 21
2.7.4 Application of line/fender pretension 22
2.7.5 Zero-measurements 22
2.7.6 Test duration and timing 23

3 Test programme **25**
3.1 Case A: Head-on waves 25
3.2 Case B: Beam-on waves 26
3.3 Case C: Bow-quartering waves 28
3.4 Case D 30

4 Test results cases A, B and C **31**
4.1 Decay tests 31
4.1.1 Decay tests without ShoreTension system active 31
4.1.2 Decay test with ShoreTension system active 33

4.1.3 Delivery of data 34
4.2 Wave calibration 34
4.3 Wave reflection analysis 36
4.4 Presentation of time series and interpretation 38
4.4.1 Description of the measured timeseries 38
4.4.2 Case A: Head-on waves 39
4.4.3 Case B: Beam-on waves 40
4.4.4 Case C: Bow-quartering waves 42

5 Test results Case D 45
5.1 Decay tests 45
5.2 Wave calibration 46
5.3 Wave reflection analysis 48
5.4 Presentation of time series and interpretation 49

6 Conclusions 51
6.1 Project context 51
6.2 Main conclusions 51
6.3 Summary of observations related to effectiveness of the ST system 52
6.4 Closing remarks 52

References 53

Appendices

A Photo report damping material A-1

B Folder AukePC B-1

C Technical note by RHDHV on mooring arrangement in the scale model C-1

D Calibration plots of mooring lines and fenders D-1

E Wave calibration and reflection E-1
E.1 Cases A, B and C E-1
E.2 Reflection analyses Cases A, B and C E-2
E.3 Case D E-3
E.4 Reflection analyses Case D E-4

F Test ID tables F-1

G Results G-1
G.1 Cases A, B and C G-1
G.1.1 Result plots G-1
G.1.2 Tables with standard deviations of ship motions G-2
G.1.3 Tables with absolute maxima of ship motions G-6
G.2 Case D G-10
G.2.1 Result plots G-10
G.2.2 Tables with standard deviations of ship motions G-11
G.2.3 Tables with absolute maxima of ship motions G-12

1 Introduction

1.1 Background

Within the Port of the Future ships will be moored in an innovative way that allows for an optimal loading and unloading strategy while the port layout has a minimal impact on the coastline. Such an innovative mooring technique is the ShoreTension (ST) system.

ShoreTension has indicated that the ability of the ST system to reduce wave-generated vessel motions is presently largely based on experience at sheltered locations (in port) with modest wave conditions. In case it can be proven that the ST system also has benefits in more exposed locations (i.e. in more open port layouts), the system may provide a mooring solution in situations where otherwise breakwaters would be required. This may lead to significant cost reductions. Deltares also sees these more open port layouts as a very promising development and has published and presented a number of reports and papers on this concept (e.g. De Jong et al., 2012).

Testing ST under relatively high wave conditions in the field implies practical problems, costs and risks. Furthermore, the test conditions cannot be (sufficiently) controlled or predicted in the field. Therefore, the principal participant (ShoreTension) presently considered physical scale model tests of the ST system. A ST system on model scale (model ST) had already been developed by ShoreTension, as a first preparation step towards physical model tests. This scale model version of the ST system has now been used in the Delta Basin at Deltares, a professional multidirectional physical scale model facility. The results of the physical scale model test could be used to validate a numerical implementation of the ST system. With this validated numerical implementation, it will be possible to already assess the application of the ST system in the design stage of to-be-developed terminals.

1.2 TKI project and partners

This project has been performed as a TKI subsidized project (reference number DEL083) together with the following external partners and their respective tasks:

- **ShoreTension:** preparation of ST scale model units and performing tests
- **Royal HaskoningDHV:** preparing the scaled “real life” mooring arrangement and numerical modelling of ST in aNySIM using the scale model results
- **Shell:** consulting on daily practice in terminals
- **Vopak:** consulting on daily practice in terminals and delivering a report on the analysis of the port of Fujairah, UAE (Witteveen+Bos, 2018).
- **Marin:** Second opinion and hydrodynamic input

Following the TKI terms and conditions, this report will be published on the Deltares virtual knowledge centre. Moreover, the results of this project will also be published to the public as a conference paper to be presented at an upcoming relevant conference by Deltares together with the partners.

1.3 Objective

The overall aim of the project is exploring (the limits of) the possibilities of innovative mooring of vessels in the Port of the Future. Physical scale modelling tests will be the main approach to reach that goal. Such tests will make it possible to consider an innovative mooring technique (the ST system is applied here as one of the new systems available) subjected to the complex wave conditions that can occur inside and around a port. In the future, such wave conditions may become even more critical if ports will be designed with a more open layout or even using floating port infrastructure to limit the effects of such large infrastructural developments on the coastal region. Climate change may also lead to more complex wave conditions in new and existing ports and can as such be seen as one of the drivers to apply new port concepts and innovative mooring techniques.

With respect to the ST system the project has the following system-specific aims:

- Verify the application limits of the ST system with respect to wave height (for the most critical response periods) and to optimise the system settings to maximise the applicability range of the system. In this way the applicability limits of the system may be enlarged compared to present understanding and expectations of the system.
- The scale model outcomes are intended to form a solid (conceptual) and undisputed verification of the functionality and performance of the system, which is expected to increase acceptability of the system throughout the waterborne transport community. In addition, the project outcomes may diversify and extend the fields of application of the system.
- Last, the measurement database can be used as a validation database of implementations of the ST system in numerical moored-ship simulations (dynamic mooring analyses, DMAs).

1.4 Project approach

The physical model test programme consists of four different mooring cases (i.e. combinations of mooring configurations and specific wave conditions) divided over two project phases. In the first phase a fundamental mooring layout has been tested and in the second phase a more realistic mooring layout has been tested. The line characteristics of the first situation were based on those of the latter realistic mooring layout.

The activities performed within the phases consisted of the following:

- Phase 1: In this phase three fundamental symmetrical mooring configurations are considered in which the waves (which are sent out perpendicular to the wave board) come from respectively head-on, beam-on and bow-quartering direction. The vessel is moored symmetrically with conventional lines, i.e. two lines in longitudinal direction at the bow and stern (spring lines) and four lines perpendicularly near the bow and stern of the ship (bow and stern lines). Depending on the orientation either two or four ST modules are included in the configuration. These mooring layouts were chosen to serve as fundamental validation data for numerical DMA models, by providing the possibility to identify specific characteristics of the mooring system. By using wave conditions with increasing complexity (from theoretical/schematic up to field conditions), the result is a well-defined mooring system in which the exact behaviour of the ship can be related to certain wave conditions. In this phase different settings of the ST modules have also been considered.
- Phase 2: For the “real-life” mooring configuration considered in this phase, the ship is moored along a jetty. The spring stiffness characteristics of the (symmetrical) mooring configuration of Phase 1 are translated into corresponding spring characteristics for both the conventional and ST (4 modules) breast and spring mooring lines. Different than for Phase 1, the waves are sent out in three different directions while the ship orientation within the basin remained constant. In this phase focus was given to more realistic spectral wave conditions.

All tests have included one vessel size/type and one draft-depth ratio. The ship has been ballasted according to a predeveloped (calculated/theoretically derived) weight distribution to ensure optimal representation of moments of inertia. The natural periods of the scaled vessel have been checked by performing free-floating and conventionally moored (i.e. without ST) decay tests at the start of each of the two phases. The natural periods found formed input for the wave periods of the conditions to be included in the test programme. This is because the largest motion responses of the vessel and the most challenging conditions for the ST system to mitigate will be at or around those conditions. In total three types of wave conditions have been considered: monochromatic, bi-chromatic and spectral wave conditions. Starting with more simple (fundamental/schematic) wave conditions allowed analysing the fundamental aspects of the system, prior to proceeding with more complex conditions. This allowed a progressive build-up of understanding and insights.

1.5 Project team

The following team members from Deltares contributed to this study:

Technical experts:

- Niek Bruinsma, scale model testing analysis and reporting
- Bas Reijmerink, scale model testing analysis and reporting
- Arne van der Hout, project management and senior nautical specialist
- Martijn de Jong, senior specialist ports and waterways (quality assurance)

Laboratory technicians:

- Jaap Schipper, mechanical engineer
- Frans de Vreede, instrument technician
- Jelle Molenaar, instrument technician
- Peter Alberts, model assistant
- Richard Tuin, model assistant
- Job Waaijerink, model carpentry
- Richard Boele, project technician

From ShoreTension Chris Clement, Karel Roozen and Patrick Boon contributed to the execution of the scale model tests.

The design work of the “real life” mooring layout of Royal HaskoningDHV was led by Alex van Deyzen.

1.6 Content of the report

In Chapter 2 the different aspects of the physical scale model are discussed, Here information can be found on the test facility, scaling, the hydrodynamic conditions, the vessel, the mooring configurations, the measurement equipment and the general testing procedures. The test program is discussed in detail in Chapter 3. The test results of the first and second phase of the project are presented and discussed in respectively Chapters 4 and 5. Chapter 6 finalizes the report with conclusions.

2 Physical model setup

2.1 Test facility

2.1.1 Facts and figures

The tests have been performed at the Deltares' Delta Basin (Figure 2.1 and Figure 2.2). The Delta Basin (outer dimensions: 50 x 50 m, effective model area: 40 x 40 m) is a multidirectional wave basin, equipped with a multidirectional wave generator with a length of 40 m (100 segments). The wave generator is capable of generating both regular (periodic) as irregular (random) long-crested or short-crested waves according to user-defined (e.g. from literature) frequency-directional distributions. The wave generator is equipped with state-of-the-art online Active Reflection Compensation, which effectively eliminates re-reflections of waves from the wave board. Also wave board control for random second-order waves is operational to minimise spurious waves while generating the target wave conditions. When generating waves, the Dalrymple method[1] (Dalrymple, 1989) can be applied to generate a wave train at a specified location, which effectively increases the model area that can be used. The maximum water depth that can be applied in the basin is 1.0 m (model scale). The basin does not allow for the generation of tidal flow or wind influences.

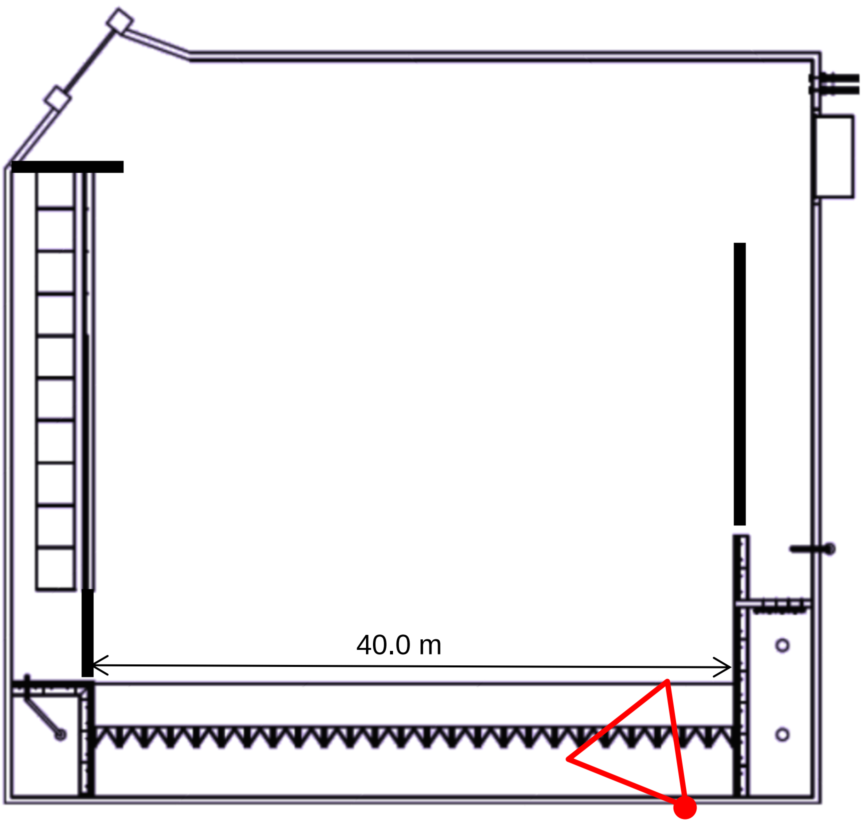

Figure 2.1 Left: Delta Basin floorplan. Viewpoint of Figure 2.2 indicated in red.

[1] *The Dalrymple method entails sending out waves directed towards the side wall where they reflect and line up with waves generated directly from the wave boards. This technique delivers a virtual extension of the wave board by mirroring in the side wall.*

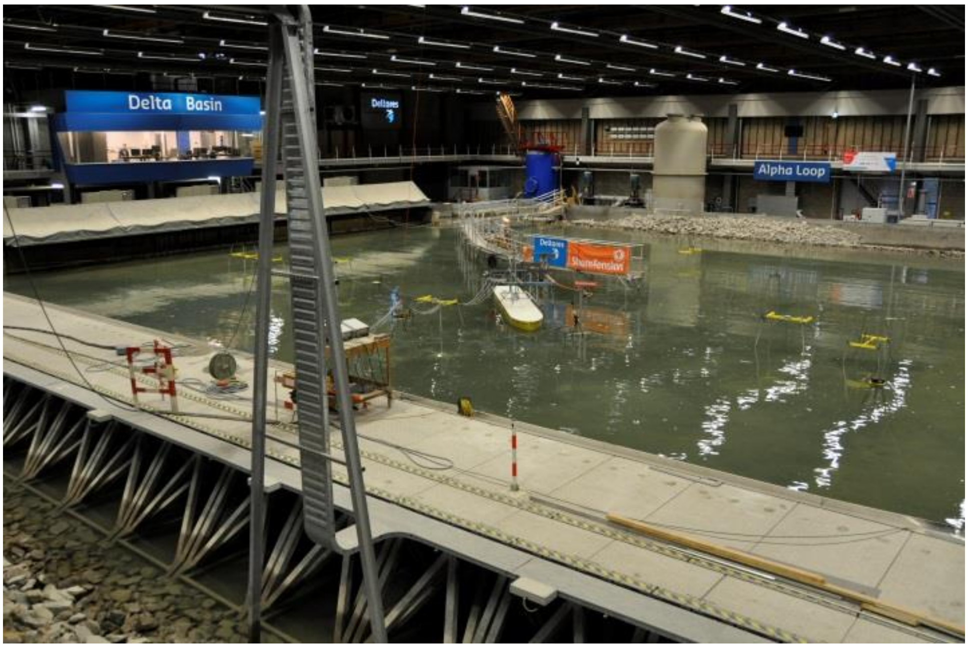

Figure 2.2 Overview photo of Delta Basin (Case D).

2.1.2 Applied basin setup

Wave generator

By applying the Dalrymple method (Dalrymple, 1989) it was possible to generate all envisaged wave conditions at the location of the centre of gravity (CoG) of the ship (see Section 2.3.2 for details on the wave condition types and Sections 4.2 and 0 for the wave calibration results of respectively phases one and two).

Wave damping

Since relatively long (low-frequency) waves have been considered within this project (up to 80 s wave periods on full scale), it was very important to install sufficient wave damping with gentle slopes along the vertical basin edges to absorb as much wave energy as possible. Particularly longer waves are difficult to damp out fully with the confinements of any wave basin and some reflection will be inevitable, still measures were taken to ensure maximum damping effects within the space available. Two means were used for this (see Figure 2.3):

- rubble mound slopes along the vertical edges (indicated in blue in Figure 2.3), and
- a metal parabolic beach shape (surface: 2.5x2.5 m, height 0.60 m, indicated in green in Figure 2.3), elevated on concrete blocks at the basin entrance.

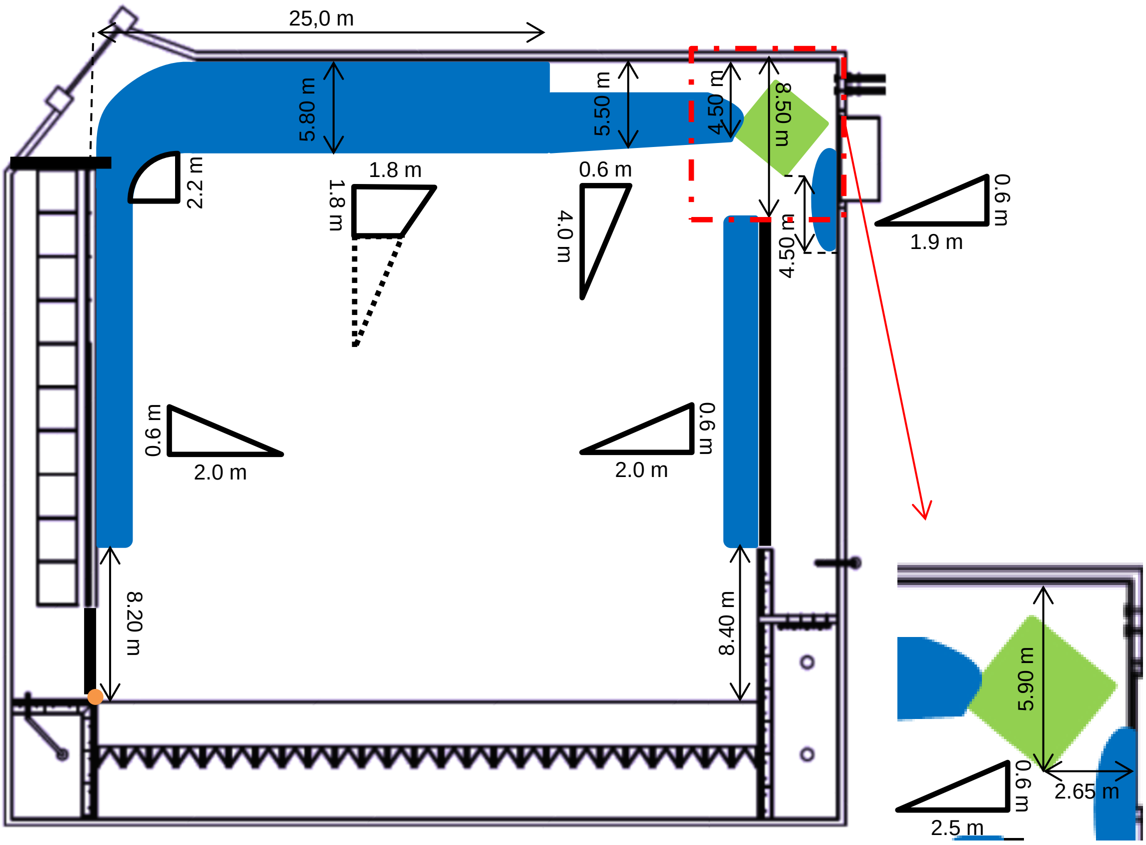

Figure 2.3 Schematic overview of locations and extents of damping material applied during tests. Blue surfaces represent riprap slopes. The green surface represents a metal parabolic beach shape. The orange dot in the lower left corner of the basin represents the (0,0) coordinate of the Delta Basin used throughout the tests and recording and reporting of results. Insert shows detail of location of metal parabolic beach shape.

The aim was to build a geometry configuration that was as symmetric as possible, to create a situation in which the total wave field (incoming + reflected waves) is well defined and therewith most easily analysed and understood. As can be seen from Figure 2.3, this was not possible everywhere (e.g. because of doors in the walls of the basin used to bring in and remove materials in between tests) and therefore some practical compromises had to be made. For recording purposes, detailed photos of the configuration of the installed wave damping are included in the photo report of Appendix A. The data in this section combined with the photos of Appendix A can for example be used if the scale model results need to be reproduced numerically at a later stage.

Although the wave damping was installed with care, not all wave energy could be absorbed by the installed wave damping during the tests. Depending on the wave condition approximately 20% to 35% of the wave height (4-13% of the wave energy) was reflected at each slope (see Sections 4.3 and 5.3). Waves (re-)reflecting at multiple damping slopes experience a cumulative damping effect. However, some (small levels of) remaining wave energy could still reach the wave maker. To prevent unwanted wave re-reflections of these waves the Active Reflection Compensation (ARC) system on the wave maker was activated during all tests. This system absorbs all (spurious) remaining wave energy that reaches the wave board by sending out anti-waves that cancel out the arriving wave signals, while at the same time generating the targeted incoming wave conditions. The damping materials along the edges of the basin and the use of ARC on the wave maker were combined with the aim to introduce sufficient energy sinks to avoid resonant spurious wave energy build-up. Results of the tests have been analysed and checked throughout performing the tests, and as part of subsequent detailed analyses, to verify that this approach was successful.

2.2 Scaling

2.2.1 Froude scaling

The scale used in this project to translate the conditions in the field to model scale is n_L = 1/40. All hydrodynamic parameters, the mooring system and structure dimensions are scaled using Froude scaling laws to preserve the ratio between the most relevant forces. For the free surface waves and the motion of the ship these are the gravitational and inertial forces. This ratio is preserved by maintaining a constant value for the Froude number:

$$Fr = \sqrt{u^2/_{gl}}$$

With *u* a velocity, *g* the gravitational acceleration and *l* a length. For waves the relevant *l* is the water depth. For floating bodies, the relevant *l* is usually the ship's length. As *g* is a constant, the Froude number relates lengths to velocities and thereby also to duration (time). With the selected geometrical scale factor of n_L = 1/40, retaining the Froude number leads to the following scaling factors for other parameters:

- Distances and dimensions, water depth, wave length, wave height, motions (translations etc. in [m]: n_L 1/40
- Durations, including wave period, expressed in [s]: $\sqrt{n_L}$ $1/\sqrt{40} \approx 1/6.3$
- Volumes [m^3], masses [kg] and forces [kN] (for the same density): $(n_L)^3$ $(1/40)^3 = 1/6.4*10^4$

Angles and rotations are not affected by scaling. Note that forces in reality are often related to salt water, whereas the scale model tests are performed using fresh water[2].

In this report all values are reported on full scale, unless stated otherwise. No corrections have been applied for the difference in specific density between fresh and salt water. Where relevant, this should to be taken into account when considering the relevant forces.

2.2.2 Considerations on accuracy at the chosen model scale

The choice of the scale factor is generally a consideration of practical manageability (magnitude of forces, sizes of vessel/basin and costs) and accuracy (measuring accuracy and scale effects). A scale factor of 1:40 is therefore a typical value for the type of tests performed in this project. Considering the above, the scale factor can have an influence on the achievable accuracy in various ways. This has been discussed in detail below.

The first relevant aspect is wave generation. The chosen scale factor leads to wave heights (H_s) as small as ~1 cm on model scale (0.4 m in full scale). The waves are still large enough to avoid any capillarity effects. Through the wave calibrations it is assured that the correct wave height is achieved at the centre of gravity of the ship (CoG); the accuracy is determined by the accuracy of the wave measurements. General experience, including calibration studies, shows that the wave height probes used have an accuracy of about 1 mm. At a scale of 1:40 this is

[2] This is because of practical reasons, with fresh water being much less corrosive and therefore impacting much less the equipment of the facility and the measurement probes.

an accuracy of 4 cm on full scale, which is 8% of the lowest wave height specified (0.5 m). Experiences from other projects, in which also low wave height conditions were generated, show that the accuracy of the wave probes is sufficient and that they have been successfully applied for scales up to 1:100.

The second attention point relates to the motion response of the moored ship. Waves and motions of vessels in waves are primarily potential flow related phenomena and these are insensitive to scale effects. The non-potential flow issues (i.e. viscous effects and damping) are very relevant for motions at the natural frequencies and are more sensitive to scale. For such aspects applying any model scale applied could significantly influence (and contaminate) results relative to the targeted situation as would occur in the field. This may not be fully avoidable, given a practical range of possible scale factors (say 1:40 – 1:100). The scale of 1:40 means that these effects have been limited as much as possible.

The third attention point is that the motion response is also dependent on the accurate reproduction of the line and fender characteristics. These are made to scale and the applied calibration curves (line forces and fender deflection forces) are included in this report. The fender friction forces are not always known accurately for a given type of fender. Moreover, particularly that aspect of the fender is difficult to represent on model scale, even with the same material used, because the friction in the model will often be too high. Therefore, in the scale model the fender friction was minimised by using plates of nylon, to ensure that a very low friction was present. A low friction was preferred, in consultation with the participants, over an arbitrary higher friction value with unknown reliability and accuracy (see Section 2.5.1 for further details on the modelled fenders). This low friction value can be taken into account in further numerical analyses.

Due care has been taken to avoid unwanted friction in the model equipment (e.g. hinges and pulleys). The motions of the ship are measured with an optical system, ensuring high precision in the measurements, and avoiding any contact (generating damping) with the moving ship (see Section 2.6.2 for a further description of this part of the scale model setup).

Based on the considerations above, it is concluded that a good accuracy can be reached at a scale of 1:40, provided that all related elements are given due attention.

2.3 Hydrodynamic conditions

2.3.1 Water depth

During all tests a constant water depth of 18 m was applied (0.45 m model scale). This fairly shallow water depth can be seen as a typical water depth at locations for which the open ports concept is considered (e.g. West Africa). This value was based on input from the participants.

2.3.2 Wave condition types

To fully understand the ship behaviour under different wave loads in the four mooring cases, three longcrested[3] wave condition types with increasing complexity and low and high frequencies have been considered. In this case low-frequency waves refer to waves with wave periods larger than 30 seconds and high frequency waves (‘wave-frequency’ / primary waves) refer to waves with periods ranging from 8 to 25 seconds.

---

[3] *All waves have the same direction, i.e. without directional spreading.*

- Monochromatic waves: by forcing the ship with regular long (low-frequency[4]) waves, the exact ship response to the specific frequency can be considered. By choosing the wave periods/frequencies such that they correspond to the natural periods of the ship, the clearest response (surge/sway/roll/yaw) can be considered as a worst-case scenario. This way the application boundaries of the ST system can also be considered best, since the large motions at the natural period of the vessel are the hardest to compensate for. Last, this analytical wave load allows for validating the numerical implementation of the ST system as accurate as possible (in a follow-up task/project).
- Bi-chromatic waves: by combining two high(er) frequency sine waves with similar wave frequencies, a third second-order low frequency wave with a small amplitude is generated[5]. By applying this type of wave load it was possible to excite the ship with two natural frequencies simultaneously, e.g. with both the roll and surge frequencies.
- Spectral waves: as most complete and realistic wave condition type, a long-crested (1D) wave spectrum was considered with a relatively high peak frequency equal to the natural roll period of the loaded ship. The wave signal based on this spectrum also includes the low-frequency wave energy as considered with the monochromatic and bi-chromatic wave signals, but less distinct because of the presence of several frequencies. The ship behaviour under this load type can be analysed in more detail using the results of the two other wave load types.

All wave steering files for the wave generator have been generated prior to the test series with the Deltares wave software package for experimental facilities: AukePC (see Appendix B for details). The maximum wave amplitude or height from a series of similar tests was used in the generation of the signal. When another wave amplitude or height from that timeseries was needed during the wave calibration or test execution phase, this could simply be achieved by changing the ‘gain’ setting of the wave generator, which can be seen as a scaling factor.

The wave steering files have all been written in a cyclic way, i.e. the wave signals would continue again smoothly from the start when the end of the signal is reached. For the monochromatic and bi-chromatic conditions the signals are repeated after 42 low-frequency waves while for the spectral conditions the signals are repeated after 1200 waves.

2.4 Vessel

2.4.1 Vessel particulars

The scale model of the ship used during this test series is *“The Flying Dutchman”,* which is a Capesize dry bulk carrier. This vessel was selected from the archive of Deltares and it has been made available for use during this project at no costs. In shape and size it quite closely resembles a big Aframax or a small Suezmax tanker which it is intended to represent in these tests. The ships line plan is displayed in Figure 2.4, the scale model is shown in Figure 2.5, and the ships main particulars are presented in Table 2.1. Please note that the draft of 16.3 m is applied for the scale model in combination with the fresh water density in the test basin, which corresponds to a slightly lower weight.

[4] *Note that long infra-gravity type waves were generated here as free waves in the cases without carrier waves present. This allowed those tests (and related analyses) to focus only on those long-period effects. In reality these waves would be bound to wave groups and therewith have shorter wave lengths related to the velocity of the wave group, c_g. For an 80 s wave at 18 m depth this difference is approximately 117 m (L_{bound} = 944 m and L_{free} = 1061 m).*

[5] *The low frequency wave frequency occurs at the difference frequency of the two higher frequency waves:*

$$1/T_{3,LF} = \left|1/T_{1,HF} - 1/T_{2,HF}\right|$$

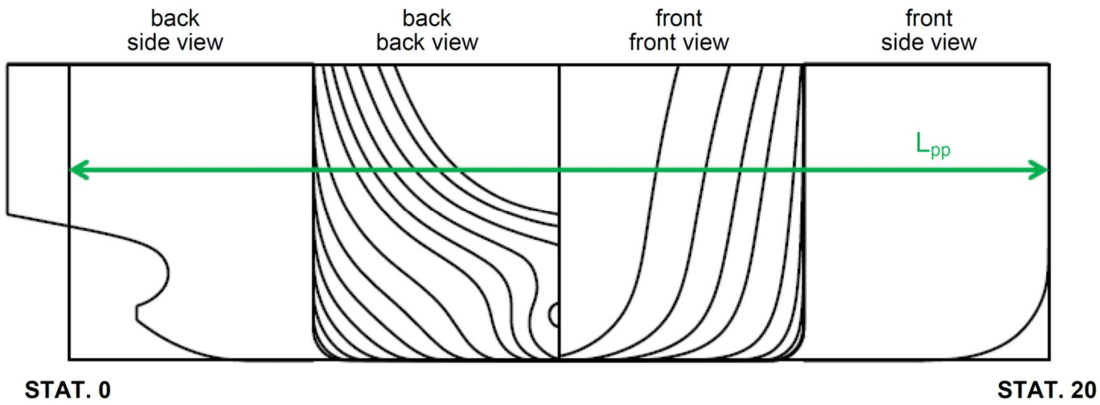

Figure 2.4 Line plan of the used bulk carrier.

Figure 2.5 Scale model of the bulk carrier.

Table 2.1 Ship particulars bulk carrier (Updated version: 14 June 2019).

Designation	Symbol	Unit	Value
Length between Perpendiculars	L_{pp}	m	252.00
Breadth	B	m	40.00
Draft fore	TF	m	16.30
Draft mid	TM	m	16.30
Draft aft	TA	m	16.30
Displacement volume	D	m^3	133169
Waterline area	AWL	m^2	9307.976
Centre of Gravity above base	KG	m	13.61
Centre of Gravity forward of st10	LCG	m	5.80
Transverse metacentric height	GMt	m	3.37
Roll radius of gyration	k_{xx}	m	11.45
Pitch radius of gyration	k_{yy}	m	73.72
Yaw radius of gyration	k_{zz}	m	73.75
Water depth	WD	m	18.00

2.4.2 Decay tests

The ship was carefully ballasted to match the particulars mentioned in the previous section. Subsequently a series of decay tests was performed to analyse the natural periods of the predominant ship motions. A decay test is a test in still water (i.e. no waves), where the vessel is displaced from its equilibrium with a certain translation or rotation (offset) and let go to oscillate back to its equilibrium.

The following set of decay tests was performed:

- Free floating roll decay tests;
- Moored surge, sway, roll and yaw decay tests.

The moored decay tests were performed for the different mooring cases, see Section 2.5. Note that the heave and pitch decay tests are not performed as the high damping characteristics of the vessel made it impractical (and unnecessary) to perform these tests.

2.5 Mooring configuration

The test program in this project is split in two phases, see Section 1.4. In the first phase three fundamental symmetrical mooring configurations are considered and in the second phase the “real-life” mooring configuration considered. The mooring configurations used in the test campaign are presented schematically in Figure 2.6. The ship is moored with conventional mooring lines (indicated in black) with the addition of the innovative ShoreTension (ST) mooring system (indicated in yellow) for all tests (Cases A to D). In the “real-life” mooring configuration, Case D, the ship is also moored against four fenders (see Figure 2.12 for a detail of the mooring configuration). Reference tests were also performed without the ST system to better understand the effect of this innovative mooring system.

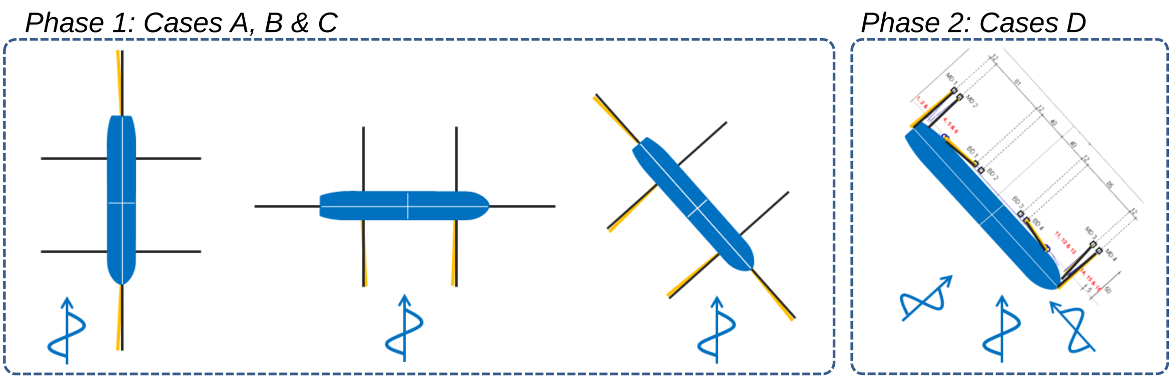

Figure 2.6 Schematical representation of the mooring configurations for the four different test cases. The black lines represent conventional mooring lines and the yellow lines represent ST mooring lines.

The mooring system for the two phases of the physical model tests are described in Section 2.5.2 and 2.5.3 respectively. Their characteristics, e.g. mooring stiffness, are based on the technical note provided to the participants by Royal HaskoningDHV as part of this project, see Appendix C.

2.5.1 Mooring equipment

Mooring lines

The Aframax and Suezmax tankers are moored with 16 combi-lines: steel wires with a 11 m synthetic tail. The tail is usually fabricated from polyester or polypropylene or a mixture and has a Minimum Breaking Load (MBL) of 100 tonnes. The steel wire has a MBL of 80 tonnes.

For this research project the relevant property of the mooring lines is the individual line stiffness. The individual line stiffness depends on the length of the steel wire, the length of the tail, the tail material and the wire and tail diameter (MBL). All these parameters have been taken into account to derive the stiffness of the different lines to be included in the scale model. The resulting line characteristics of the individual mooring lines for the various mooring setups are presented in Appendix D.

In Figure 2.7 the physical scale model of the mooring lines is shown. These mooring lines are anchored on a force transducer mounted on top of a vertical pile. The lines are constructed with a thin steel wire and a vertically mounted linear spring to simulate the desired line characteristics[6]. Note that the mooring lines are simulated with a single linear spring because of the linear nature of the applied load-elongation curves (presented in Appendix C). The calibration plots for the individual mooring lines, showing the target and measured load-elongation curve, are presented in Appendix D.

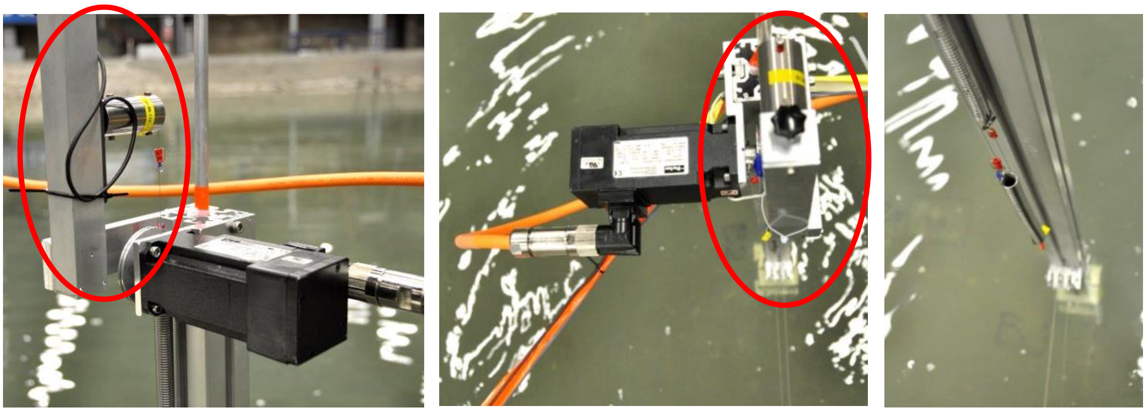

Figure 2.7 The mooring lines with force transducers and vertically mounted springs. Left: force transducer mounted on top of mooring pile (indicated by red oval). Note that the black box represents a scaled ShoreTension model (see next paragraph). Middle: top view of force transducer (indicated by red oval). Right: springs to represent the desired line characteristics. The lines are being led horizontally towards the ship via pulleys mounted on the pile at the same height of the ship fairleads.

ShoreTension system

The ShoreTension (ST) system can be used in addition to the conventional mooring lines, as can be seen in the left image in Figure 2.8, depicting a situation of the ST system applied in practice. The middle and right images in Figure 2.8 show the model scale ST system as used in the physical model experiments. This is an electric motor, programmed and controlled from a central control unit to function in the same way as one of their prototype hydraulic systems. [The following content has been removed for reasons of confidentiality

] The modelled ST system and its behaviour has been developed and validated by ShoreTension itself, prior to this project. ShoreTension provided Deltares with the modelled system (including four electric motors) to use within the physical scale model. Checking/validating the behaviour of the modelled ST system with a prototype ST system was done earlier as part of developing those scale model versions of the ST system and was therefore not part of this project.

---

[6] *Please note that the lines used in the scale model are far too stiff to represent elongation behavior of the actual mooring line. Additional springs are used to introduce the proper force-elongation characteristic, assuming (practically) no elongation of the scale model line itself.*

Please note that it is not required, and also impractical, to scale all the different (hydraulic) parts of the ST system, since that would correspond to very small elements that will most likely result in significant scaling effects. Using an electro motor to mimic the resulting behaviour of the ST system and its effect on the mooring line is an efficient and reliable way of introducing the ST system behaviour in the physical scale model.

Figure 2.8 Left: Hydraulic ST system on prototype scale on a quayside. Middle: (black) Electrical motor with wheel representing the behaviour of ST system on model scale. Right: force transducers mounted on the ship to measure the forces in the ST lines (Case B).

[The following content has been removed for reasons of confidentiality

]

Fenders

The fenders specified for this project are four cone fenders of capacity SCN1800-F1.0. These fenders have a height (thickness) of 1.8 m, can absorb 2327 kNm of energy and have a maximum reaction force of 2171.5 kN, see Appendix C for a detailed description of the fender characteristics. The force generated by the fenders is represented in the model by a fender mechanism, shown in Figure 2.9. For measuring the transverse force the system is mounted to a force gauge which is fixed to the jetty.

In the scale model, the front pad of the fender consists of a metal bolt, with a rounded head, which has been polished to reduce friction between the ship's hull and the fender. The round bolt shape ensures that the contact with the ship model is properly modelled, even if the ship shows roll motions. The friction between the model fender and the vessel is further reduced by attaching nylon (polyamide, PA) plates to the ships with a lightly waxed coating (see also Section 2.2.2).

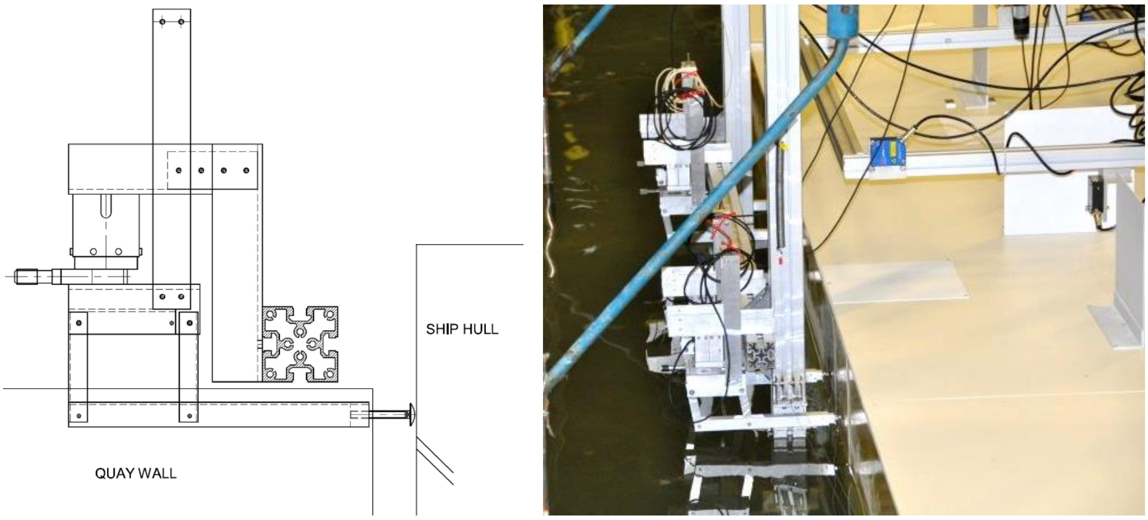

Figure 2.9 Left: Schematic representation of the fender model. Right: image of the model scale fender.

Figure 2.10 shows the targeted load-deflection curve of the fender with in blue the schematization applied in the fender model with a single linear spring[7]. The slope of the adopted linear approach is selected to correspond approximately to the same amount of energy absorption over the full compression of the fender length. This setting was selected in consultation with the participants. To represent the same amount of energy absorption, the reaction force of the scale model fender was chosen such that it is at its maximum when the compression of the actual cone fender is at 50% (red circle in Figure 2.10). This resulted in a linear spring stiffness of 2171.5 / (0.5 * 1.8) = 2413 kN/m of the scaled fender. Appendix D (Figure D.8) contains the calibration plots for the fender springs.

[7] A combination of two springs, of different stiffness, could be used to represent different parts of the force-elongation graph. However, such a combination will always first show the lower stiffness and, once that spring is fully elongated, only then the larger stiffness. Here the opposite is required (first stiff, then softer), which only leaves the option of using one spring as most fitting approximation.

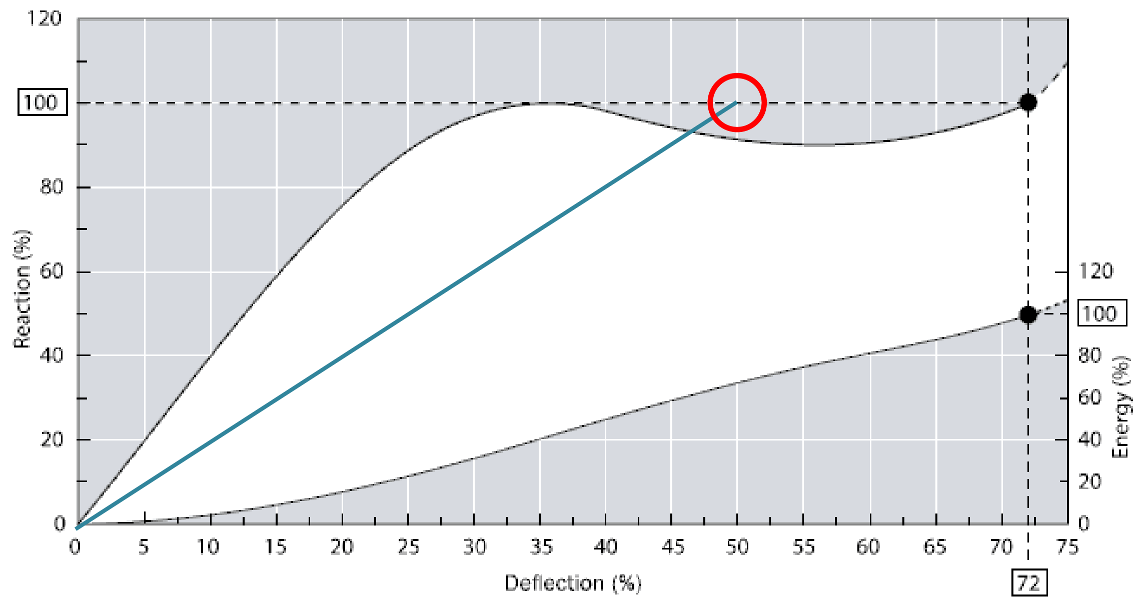

Figure 2.10 Load-deflection curve cone fenders. Blue line shows the linear load-deflection curve representing the cone fenders in the physical model setup. The red circle indicates the maximum force of the scaled fender when the deflection of the actual is at 50%.

2.5.2 Cases A, B and C

In the first phase of the tests, Cases A, B and C, the waves (which are sent out perpendicular to the wave board) come respectively from head-on, beam-on and bow-quartering direction. The vessel is moored symmetrically with conventional lines, i.e. two lines in longitudinal direction at the bow and stern and four lines perpendicularly near the bow and stern of the ship (see Figure 2.11 and Table 2.2). Note that the mooring configuration is the same for all three cases except for the vessel orientation with respect to the wave maker and the number of active ShoreTension (ST) modules, see Figure 2.6. In all three test series (A-C) the CoG of the ship is located at x = 20 m and y = 16 m (model scale) from the (0,0) coordinate of the Delta Basin (Figure 2.1). Both the conventional and the ST mooring lines are mounted horizontally with the fairlead and anchor points at 4 m above still water level.

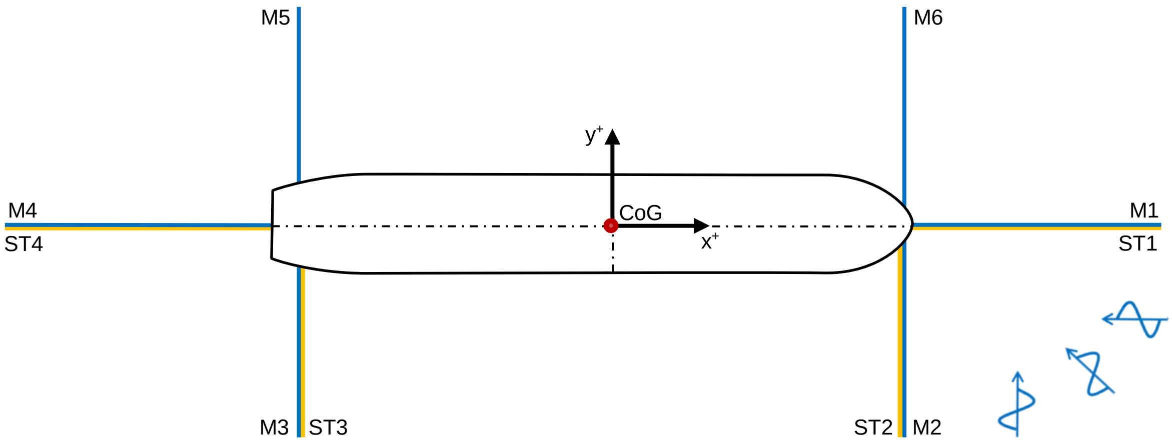

Figure 2.11 Schematic representation of the mooring configuration for phase one, test Cases A, B and C. The blue lines represent conventional mooring lines and the yellow lines represent ST mooring lines, denoted by M and ST respectively. The blue arrows indicate the incoming wave directions relative to the orientation of the vessel.

Table 2.2 The fairlead and bollard points of the mooring system with respect to the CoG for Cases A, B and C. The CoG of the ship is located at x = 20 m and y = 16 m (model scale) from the (0,0) coordinate of the Delta Basin. Both conventional and ST lines are installed horizontally at 4 m above still water level.

Designation	Symbol (Figure 2.11)	Spring nr. (see App. D)	Stiffness (target /achieved)	Fairlead location w.r.t. CoG		Bollard location w.r.t. CoG	
			[kN/m]	X [m]	Y [m]	X [m]	Y [m]
Conv. mooring 1	M1	11	816/827	121.0	0.0	208.2	0.0
Conv. mooring 2	M2	1	1152/1155	116.7	-8.2	116.7	-88.0
Conv. mooring 3	M3	2	1152/1159	-128.3	-16.5	-128.3	-88.0
Conv. mooring 4	M4	10	816/828	-137.6	0.0	-227.2	0.0
Conv. mooring 5	M5	3	1152/1149	-128.3	16.5	-128.3	88.0
Conv. mooring 6	M6	4	1152/1148	116.7	8.2	116.7	88.0
ShoreTension 1	ST1	5	1888/1897	121.8	0.0	208.2	-0.8
ShoreTension 2	ST2	9	1888/1902	116.7	-9.0	117.5	-88.0
ShoreTension 3	ST3	8	1888/1902	-128.3	-17.3	-129.1	-88.0
ShoreTension 4	ST4	7	1888/1894	-138.4	0.0	-227.2	-0.8

2.5.3 Cases D

In Phase 2 of the tests, Cases D, the ship is moored in a the “realistic” configuration along a jetty. The ship is moored under an angle of 45 degrees with respect to the wave maker like in Case C of Phase 1. Different than for Phase 1, the waves are now sent out by the wave maker in three different directions (in each test one main direction), while the ship orientation within the basin remained constant. The mooring configuration is presented in Figure 2.12 and Table 2.3. The vessel is moored using six conventional lines, four ST systems and four fenders. Note that the conventional mooring lines in the scale model represent multiple mooring lines in reality[8], see Appendix C for a detailed description of the mooring setup. The CoG of the ship in test series D is located at x = 22 m and y = 13 m (model scale) from the (0,0) coordinate of the Delta Basin, see Figure 2.1. Both the conventional and the ST mooring lines are mounted horizontally with the fairlead and anchor points 4 m above still water level. The fenders are mounted 2 m above still water level. The mooring configuration, including the heights of fenders and anchor points, was selected in consultation with, and based on input from, the participants.

[8] *For example: two lines of a given stiffness in practice can be approximated in the scale model by one line with double that stiffness.*

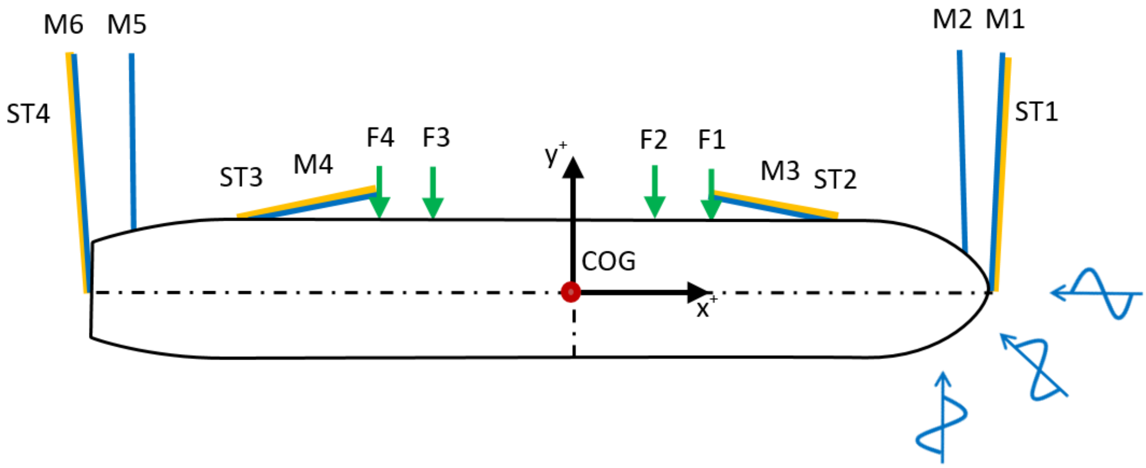

Figure 2.12 Schematic representation of the mooring configuration for phase two, test Cases D. The blue lines connected to the vessel represent conventional mooring lines and the yellow lines represent ST mooring lines, denoted M and ST respectively. The green arrows represent the four fenders. The blue arrows indicate the incoming wave direction relative to the orientation of the vessel.

Table 2.3 The fairlead and bollard points of the mooring system with respect to the CoG for Cases D. The CoG of the ship is located at x = 20 m and y = 16 m (model scale) from the (0,0) coordinate of the Delta Basin.

Designation	**Symbol (Figure 2.12)**	**Spring nr. (See App. D)**	**Stiffness (target/ achieved)**	**Fairlead location w.r.t. CoG**		**Bollard location w.r.t. CoG**	
			[kN/m]	X [m]	Y [m]	X [m]	Y [m]
Conv. mooring 1	M1	16	1120/1121	121.0	0.0	129.2	60.0
Conv. mooring 2	M2	18	1232/1227	116.7	8.2	104.2	60.0
Conv. mooring 3	M3	20	784/783	67.2	20.0	24.2	24.0
Conv. mooring 4	M4	22	784/785	-78.8	20.0	-35.8	24.0
Conv. mooring 5	M5	19	1232/1238	-128.3	16.5	-115.8	60.0
Conv. mooring 6	M6	17	1120/1124	-137.6	0.0	-140.8	60.0
ShoreTension 1	ST1	30	1600/1602	121.8	0.0	130.0	60.0
ShoreTension 2	ST2	9	1888/1902	67.2	20.8	24.2	24.8
ShoreTension 3	ST3	8	1888/1902	-78.8	20.8	-35.8	24.8
ShoreTension 4	ST4	31	1600/1597	-138.4	0.0	-141.6	60.0
Fender 1	F1	24	2416/2448	30.0	20.0	n.a.	n.a.
Fender 2	F2	26	2416/2449	20.0	20.0	n.a.	n.a.
Fender 3	F3	25	2416/2439	-20.0	20.0	n.a.	n.a.
Fender 4	F4	27	2416/2450	-30.0	20.0	n.a.	n.a.

2.6 Measurement equipment

In this section the measurement techniques as applied for the scale model tests are presented. Subsections are dedicated to hydrodynamic, motion and force measurements. All electronic measurement signals (except video recordings) are sampled at 20 Hz (model scale), with an analogue low-pass filter applied of 90 Hz[9] as part of the data collection equipment, so prior to recording of the raw data. This means that any noise present above the cut-off frequency is removed from the signals, leaving a cleaner measurement signal.

[9] No influence of any high-frequency interference source was observed during calibration tests of the measurement equipment. Therefore, the highest possible value for the cut-off frequency was chosen to influence the measurement signal as little as possible.

2.6.1 Hydrodynamic measurements

Figure 2.13 and Table 2.4 present the locations of the wave height meters (WHM) and directional wave height meters (combined wave height and electro-magnetic current velocity meters, WHM/EMS). Flow velocities are measured with electro-magnetic current velocity meters (type EMS-30, developed in-house by Deltares), these can also be used to determine wave directions. These instruments measure at 5 cm (model scale) above the seabed. A minimum distance above the seabed is applied to ensure that the proper velocity is measured but also because at too small distances from the bed level the magnetic field of the probe may be distorted, leading to errors in measured values.

The water level fluctuations are measured by means of resistance-type wave gauges (type WHM-50). Eight WHMs (WHM01-WHM08) were used for all tests and during wave calibration tests, in which the vessel was not yet present, an additional WHM (WHM09a) was positioned at the location of the CoG of the ship to carefully calibrate the undisturbed wave heights at the planned location of the vessel. Note that in Case D this additional measurement device was placed at a location WHM09b after the wave calibration tests. The wave height meters were placed at strategic intervals for reflection analysis of the wave field in the basin, for which a non-equidistant distribution is beneficial for accurate wave splitting.

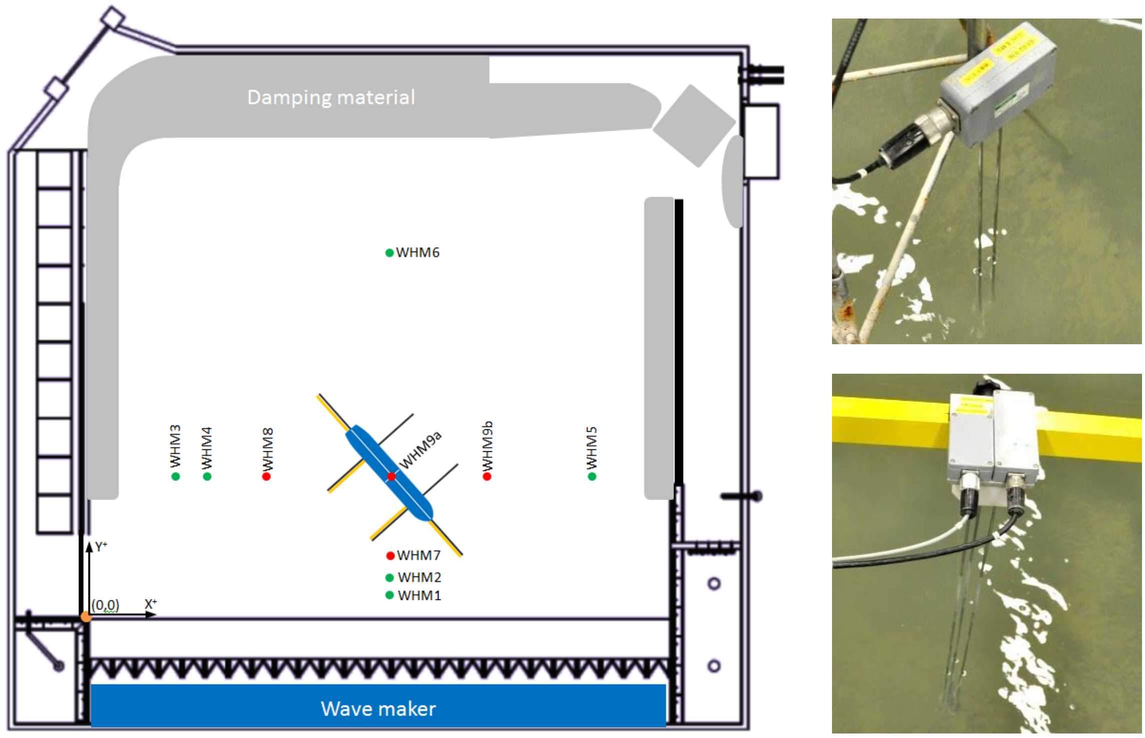

Figure 2.13 Left: Schematic representation of the locations of the wave height meters (WHM, indicated in green) and of the locations of the directional wave height meters (WHM and EMS, indicated in red) in the basin. Right: WHM (top) and directional wave height meter (combined WHM and EMS, bottom). Note that WHM09b was only present in the tests of Case D.

Table 2.4 Overview of the location of hydrodynamic instrumentation, presented in x and y distances from the zero point in the basin (model scale) for Cases A, B and C and Case D.

Designation	**Location Cases A, B and C**		**Location Case D**	
	X [m]	Y [m]	X [m]	Y [m]
WHM01	20.0	7.25	22.0	7.25
WHM02	20.0	7.95	22.0	7.95
WHM03	7.0	16.0	7.0	13.0
WHM04	8.75	16.0	8.75	13.0
WHM05	33.0	16.0	33.0	13.0
WHM06	20.0	26.5	22.0	26.5
WHM/EMS07	20.0	9.0	22.0	9.0
WHM/EMS08	13.0	16.0	13.0	13.0
WHM/EMS09a	20.0	16.0	22.0	13.0
WHM/EMS09b	-	-	31.0	13.0

2.6.2 Motion measurements

The six degrees of freedom (6-DOF) motions of the ship are measured during the physical model tests. Deltares' in-house developed laser positioning system is used to track the motions of the ship, see Figure 2.14.

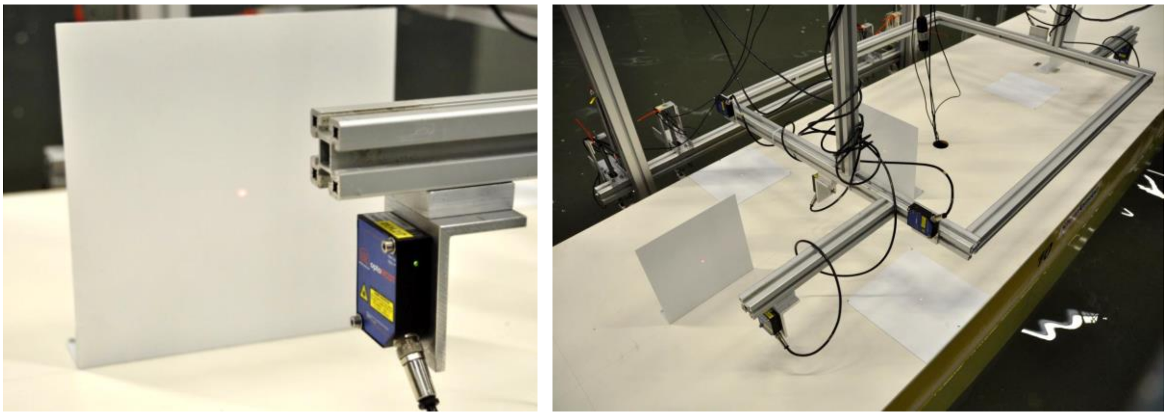

Figure 2.14 Left: Laser distance measurement sensor. Right: Overview motion detection system setup.

Six lasers sensors are strategically pointed at an orthogonal setup on the deck of the ship with the sensors mounted in an earth fixed frame. In this way the vessel motions are measured without any electrical cables or other elements connected to the vessel that would otherwise interfere with the motion behaviour of the vessel. The lasers each measure accurately the distance to the moving ship model. This system uses aluminium reflector plates which are mounted on deck and sprayed with a white paint to make them non-scattering and to ensure accurate distance measurements. The six measured distances are post-processed into the 6-DOF motions of the vessel around its the Centre of Gravity (CoG, see Figure 2.15).

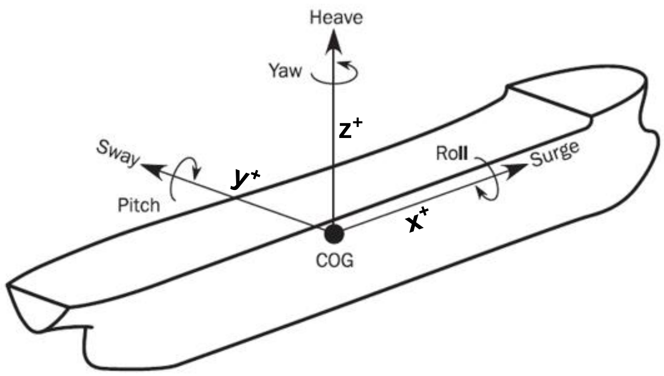

Figure 2.15 The 6-DOF motions of a ship at CoG.

2.6.3 Force measurements

The line forces in both the conventional and the ShoreTension (ST) lines were measured in all the performed tests. The force transducers in the conventional lines were placed at the anchor point of the mooring line, while the force in the ST lines was measured at the fairlead of the line, where it is connected to the ship. For test Cases D the fender forces were also measured. Additionally, the cylinder position of the ST modules were recorded.

2.7 General testing procedure

In this section the general testing procedure for Cases A to D is described. Sections 2.7.2 and 2.7.5 also describe the specific procedures for case D including fenders.

2.7.1 Calibration of instruments

All instruments were calibrated and checked for linearity in the scale model workshop prior to their installation in the scale model. The calibration takes into account the known effects on the measurement signal caused by the cables used to connect the instrument in the basin to the data acquisition system in the measurement data-acquisition system of the Delta Basin.

2.7.2 Decay tests

After ballasting the vessel such that it represents a real-life loaded condition and before each of the two phases the vessel has been brought under the motion measurement system and free (roll) and moored (surge/sway/roll/yaw) decay tests were performed. The values derived from the test setup corresponded very well to the theoretic target values. The derived values were used as input, for selecting the wave periods considered in the test program. This has been worked out in more detail in Sections 2.4.2 and 4.1 (cases A, B and C) and Section 5.1 (case D).

2.7.3 Wave calibration

With the results of the decay tests available and the test programme filled out, the wave maker steering files were generated for all considered wave conditions (see Section 2.3.2). Wave calibration tests were performed at the start of each of the two test phases to ensure that the specified wave conditions at the CoG of the ship were realised (see Section 2.5). During these tests the ship was moved towards a sheltered location in the basin where the wave load was minimal, and it was moored temporarily. At the location of the CoG of the ship in the moored situation a water level probe was installed which was used to calibrate the wave signals.

During calibration the aim was to achieve the specified total wave height (combined effect of incoming and reflected waves)[10] and wave period at the location of the probe. The first could be achieved by adjusting the gain level of the wave generator, while the latter was determined by the wave steering file and could only be adjusted by generating a new steering file. After each calibration test the measured signal was post-processed into a wave spectrum and the result checked with the aimed values. The final results of the calibration tests (i.e. achieved wave parameters and wave spectra for each wave condition) are presented in Sections 4.2 and 0 for test phases one (Cases A-C) and two (Case D) respectively.

2.7.4 Application of line/fender pretension

At the start of each test case (A to D), the zero levels of the force measuring instruments were checked and, if needed, corrected. After that, the zero position of the ship model was set by fixing the ship model to its equilibrium position using weight blocks at the bottom of the basin and distance blocks, assuring the correct distance between the ship and the positions of the boulders/dolphins and of the zero-load position of the fenders. Then the mooring lines were all attached, and the fenders were positioned such that they just touched the hull of the ship. Last, the pre-tension in the mooring lines and fenders was applied. This was done as follows.

The pretensions as described in Section 2.5 are valid for the ship in the equilibrium position, leaning into the fenders in reaction to the line loads. The introduction of such pretension can be cumbersome in scale model testing practice, since each adjustment causes a shift in the vessels position, causing changes in the other line loads. As an efficient solution to this, after applying these different pre-tensions, the weight blocks and distance blocks were taken away and the target pre-tension values were checked and adjusted if needed.

After each test, and after the waves in the basin have dissipated, the vessel should return to the same initial position (the position including the effect of the pre-tension) and the mooring lines and the fenders should show the same pre-tension values as the start of the test. This was checked after each test to ensure that all the relevant equipment had performed well during the test and to verify that the set-up was ready for the next test, without further adjustments being required.

2.7.5 Zero-measurements

In between tests, or from day to day, measurement probes can in principle start to show a slight deviation from the zero level. Because of this the probes need to be checked and readjusted where needed on a regular interval. Therefore, at the start of each testing day the definition/verification of the zero levels of the different measurement probes and the pre-tension were checked as follows:

- The water depth in the basin was checked and corrected if necessary.
- The wave gauges were cleaned, and the basin was allowed to come to a complete still water surface. The zero levels of the wave gauges were then checked and corrected if necessary.
- The zero-levels for the force gauges of lines and fenders were checked; the “zero levels” for the mooring lines and fenders corresponded to the targeted pretension values (i.e. if 50 N pretension was applied, a value of 50 N was considered as the zero/reference-value).

[10] For possible numerical modelling of the tests in later project phases, the incoming wave height should be isolated from the total wave signals or for given reflection values of edge materials the same targeted total wave height could be considered. These values can be derived from the results presented in Section 4.3.

- The position of the ship was checked by ensuring that the distance lasers all were positioned in/near the middle of their measuring range.
- A zero-measurement test was performed of 180 s, measuring the test setup without any (wave) forcing.

If necessary, e.g. when a mooring line got disconnected and had to be repositioned, the processes of Section 2.7.2 and 2.7.5 were repeated.

2.7.6 Test duration and timing

Typically, a minimum number of wave periods need to be included in a test duration to achieve reliable results. The duration of each test was dependent of the type of wave condition and the (second order low-frequency) wave period considered. Regular wave signals (because of their repetitive nature) can be analysed based on shorter tests, whereas a test for a complete wave spectrum (irregular waves) requires a longer duration. In case of:

- monochromatic wave tests, the duration of a test was equal to 42 times the wave period of the sine wave. In this way it was ensured that the correct wave period/frequency would be found when the water levels signals were processed into wave spectra (spike signal). This is because the resolution of the wave spectrum derived from a time series is dependent on the duration of the signal. Including a round number of wave periods in the measurement signal means that the spectrum derived includes a peak at the exact frequency of the targeted sine wave (spike), which would otherwise be ‘smeared out’ over multiple (misaligned) frequency bins resulting in an incorrect spectral representation[11].
- bi-chromatic wave tests, the duration of a test was equal to exactly 42 times the second order low-frequency wave period determined by the periods of the two high(er)-frequency sine waves[12]. This way, as with the monochromatic waves, it was ensured that the correct wave periods/frequencies would be found when the water levels signals were processed into wave spectra (spike signals).
- spectral wave tests, the duration of a test was equal to exactly 1200 times the peak wave period of the wave spectrum. This number of waves was chosen to ensure that a statistically well-defined spectrum could be determined from the measured water level signal during post-processing.

Before the actual measurements were started, the wave generator was started to let a stationary wave field develop. Since the wave steering files (as calibrated) are exactly as long as the measuring period and are used in a cyclic way, the specific moment of starting the measurement (also in case of a wave spectrum) had no impact on the test results.

The test procedure consisted of the following practical steps:

- send the steering file to the wave generator and turn up the gain on the steering board to the value as determined in the wave calibrations,
- fill in the correct duration and test ID of the measurement in the Deltares measurement software
- after the waves have filled the basin and a spatially stationary situation has established: start data acquisition,
- after the end of the measurement: stop the wave machine or adjust the gain of the wave generator in preparation of the next condition in the test series.

---

[11] Please note that in case of a full wave spectrum (irregular waves) this typically is less critical because of the several different wave frequencies included in such a wave signal.

[12] Please note that if the low-frequency wave is included a round number of times in the signal this automatically means that also the primary carrier waves are included a round number of times.

After this the energy density spectra of motions and forces and exceedance curves were generated and checked. If no errors were observed, the test was finished, and the data was stored for later use and analyses.

3 Test programme

The test programme consists of four test series (A to D) which can be subdivided into two phases. In the first phase, Cases A, B and C, an analytical (symmetrical) mooring layout is tested and in the second phase, Case D, a more realistic mooring layout is tested. In the following sections the summaries of the characteristics of these test series are presented in a set of tables. The type, periods, heights and direction of the wave conditions and the particulars of the ShoreTension (ST) system are presented. Next to the standard ST setting the following special settings where tested:
[The following content has been removed for reasons of confidentiality

] Next to the tests with special settings, also tests without the ST system in place (noST) were performed as well as transition tests (Transition) for a selected number of conditions in which the ST system was deactivated halfway the measurement. Please note that the transition tests are not mentioned in the tables below, but the results of those tests are presented along with the outcomes of the other tests in Chapters 4 and 5.

Please note that these tests were designed to test system to the limits of its capacity and therefore some tests could not be performed or were prematurely stopped, these are marked red and orange respectively. For test with beam-on and bow-quarterly waves this was mostly caused by the ship making contact with the bottom due to too large roll motions. In case of head-on wave tests, both the surge motions and the line forces became too large. Please note that this does not imply failing or errors of the ST system, it merely shows that in order to determine (and extend) the application limits of the ST system we first had to exceed them. In most cases this involved deliberately generating wave conditions most difficult for the system to deal with.

3.1 Case A: Head-on waves

Table 3.1 Test conditions of Case A. With the test IDs, primary/secondary/low wave periods, T_1/ T_2/ T_{low},, wave heights, H, vessel-oriented wave direction in degrees, ST settings, the amount of ST lines and the duration of the test. (Part 1)

TestID	Wave period [s]			γ [-]	Wave heigth [m]	Wave direction	ST-Setting	ST-lines	Duration [s]
	T_1	T_2	T_{low}		H/H_{m0}	[°]			
A1_M610a	61	-	-	-	0.20	180	Standard	2	2562
A1_M610b					0.40				2562
A1_M610c					0.60				2562
A1_M800a	80	-	-	-	0.20	180	Standard	2	3360
A1_M800b					0.40				3360
A1_M800c					0.60				3360

Table 3.2 Test conditions of Case A (Part 2).

TestID	Wave period [s]			γ [-]	Wave heigth [m]	Wave direction [°]	ST-Setting	ST-lines	Duration [s]
	T_1	T_2	T_{low}		H/H_{m0}				
A2_B610a_noST	15.6	20.96	61.0	-	1.00	180	Off	0	2562
A2_B610b_noST					1.25				2562
A2_B610c_noST					1.50				2562
A2_B610d_noST					1.75				2562
A2_B610e_noST					2.00				2562
A2_B800a_noST		19.38	80.0	-	1.00	180	Off	0	3360
A2_B800b_noST					1.25				3360
A2_B800c_noST					1.50				3360
A2_B800d_noST					1.75				3360
A2_B800e_noST					2.00				3360
A2_B610a	15.6	20.96	61.0	-	1.00	180	Standard	2	2562
A2_B610b					1.25				2562
A2_B610c					1.50				2562
A2_B610d					1.75				2562
A2_B610e					2.00				2562
A2_B610f					3.00				2562
A2_B800a		19.38	80.0	-	1.00	180	Standard	2	3360
A2_B800b					1.25				3360
A2_B800c					1.50				3360
A2_B800d					1.75				3360
A2_B800e					2.00				3360
A2_B800f					3.00				3360
A3_M610e_sga	61.0	-	-	-	0.40	180	sga	2	2562
A3_M610e_ssk					0.40		ssk		2562
A3_M610e_ssk_sga					0.40		ssk+sga		2562
A3_B610e_sga	15.6	19.38	61.0	-	2.00	180	sga	2	2562
A3_B610e_ssk					2.00		ssk		2562
A3_B610e_ssk_sga					2.00		ssk+sga		2562
A3_B610e_200t					2.00		200t		2562
A3_B610f_200t					3.00		200t		2562
A3_B800e_200t	15.6	20.96	80.0	-	2.00	180	200t	2	3360
A3_B800f_200t					3.00		200t		3360
A4_I156a	15.6	-	-	5.0	0.50	180	Standard	2	18720
A4_I156b					1.00				18720
A4_I156c					1.50				18720
A4_I156d					2.00				18720
A4_I156e					2.50				18720

3.2 Case B: Beam-on waves

Table 3.3 As Table 3.1, now for Case B (Part 1).

TestID	Wave period [s]			γ [-]	Wave heigth [m]	Wave direction [°]	ST-Setting	ST-lines	Duration [s]
	T_1	T_2	T_{low}		H/H_{m0}				
B1_M80a	8.0	-	-	-	0.75	90	Standard	2	336
B1_M80b					1.50				336
B1_M80a_noST	8.0	-	-	-	0.75	90	Off	0	336
B1_M80b_noST					1.50				336

Table 3.4 As Table 3.1, now for Case B (Part 2).

TestID	Wave period [s]			γ [-]	Wave heigth [m]	Wave direction [°]	ST-Setting	ST-lines	Duration [s]
	T_1	T_2	T_{low}		H/H_{m0}				
B1_M140f	14.0	-	-	-	0.25	90	Standard	2	588
B1_M140g					0.50				588
B1_M140h					0.75				588
B1_M140a					1.00				588
B1_M140b					1.25				588
B1_M140c					1.50				588
B1_M140d					1.75				588
B1_M140e					2.00				588
B1_M140a_lwv	14.0	-	-	-	1.00	90	lwv	2	588
B1_M140a_sk					1.00		sk		588
B1_M156f	15.6	-	-	-	0.25	90	Standard	2	655
B1_M156g					0.50				655
B1_M156h					0.75				655
B1_M156a					1.00				655
B1_M156b					1.25				655
B1_M156c					1.50				655
B1_M156d					1.75				655
B1_M156e					2.00				655
B1_M172f	17.2	-	-	-	0.25	90	Standard	2	722
B1_M172g					0.50				722
B1_M172h					0.75				722
B1_M172a					1.00				722
B1_M172b					1.25				722
B1_M172c					1.50				722
B1_M172d					1.75				722
B1_M172e					2.00				722
B1_M800e	80.0	-	-	-	0.05	90	Standard	2	3360
B1_M800d					0.10				3360
B1_M800e_noST	80.0	-	-	-	0.05	90	Off	0	3360
B2_B610f_noST	15.6	20.96	61.0	-	0.25	90	Off	0	2562
B2_B610g_noST					0.50				2562
B2_B610h_noST					0.75				2562
B2_B800f_noST		19.38	80.0	-	0.25	90	Off	0	3360
B2_B800g_noST					0.50				3360
B2_B800h_noST					0.75				3360
B2_B610f	15.6	20.96	61.0	-	0.25	90	Standard	2	2562
B2_B610g					0.50				2562
B2_B610h					0.75				2562
B2_B610a					1.00				2562
B2_B610b					1.25				2562
B2_B800f	15.6	19.38	80.0	-	0.25	90	Standard	2	3360
B2_B800g					0.50				3360
B2_B800h					0.75				3360
B2_B800a					1.00				3360
B2_B800b					1.25				3360

Table 3.5 As Table 3.1, now for Case B (Part 3).

TestID	Wave period [s]			γ [-]	Wave heigth [m]	Wave direction [°]	ST-Setting	ST-lines	Duration [s]
	T_1	T_2	T_{low}		H/H_{m0}				
B3_M156f_sga	15.6	-	-	-	0.25	90	sga	2	655
B3_M156f_sk					0.25		sk		655
B3_M156f_ssk					0.25		ssk		655
B3_M156f_ssk_sga					0.25		ssk+sga		655
B3_M156f_50t					0.25		50t		655
B3_M156f_200t					0.25		200t		655
B3_B800f_sga	80.0	-	-	-	0.05	90	sga	2	3360
B3_B800f_sk					0.05		sk		3360
B3_B800f_ssk					0.05		ssk		3360
B3_B800f_ssk_sga					0.05		ssk+sga		3360
B3_B800f_50t					0.05		50t		3360
B3_B800f_200t					0.05		200t		3360
B3_B156f_sga	15.6	19.38	80.0	-	0.50	90	sga	2	3360
B3_B156f_sk					0.50		sk		3360
B3_B156f_ssk					0.50		ssk		3360
B3_B156f_ssk_sga					0.50		ssk+sga		3360
B3_B156f_50t					0.50		50t		3360
B3_B156f_200t					0.50		200t		3360
B4_I156a	15.6	-	-	5.0	0.50	90	Standard	2	655
B4_I156b					1.00				655
B4_I156c					1.50				655
B4_I156d					2.00				655
B4_I156e					2.50				655

3.3 Case C: Bow-quartering waves

Table 3.6 As Table 3.1, now for Case C (Part 1).

TestID	Wave period [s]			γ [-]	Wave heigth [m]	Wave direction [°]	ST-Setting	ST-lines	Duration [s]
	T_1	T_2	T_{low}		H/H_{m0}				
C1_B610a	15.6	20.96	61.0	-	1.00	135	Standard	4	2562
C1_B610b					1.25				2562
C1_B610c					1.50				2562
C1_B610d					1.75				2562
C1_B610e					2.00				2562
C1_B800a	15.6	19.38	80.0	-	1.00	135	Standard	4	3360
C1_B800b					1.25				3360
C1_B800c					1.50				3360
C1_B800d					1.75				3360
C1_B800e					2.00				3360
C2_B610c_sga	15.6	20.96	61.0	-	1.50	135	sga	4	2562
C2_B610c_sk					1.50		sk		2562
C2_B610c_ssk					1.50		ssk		2562
C2_B610c_ssk_sga					1.50		ssk+sga		2562
C2_B610c_200t					1.50		200t		2562

Table 3.7 As Table 3.1, now for Case C (Part 2).

TestID	Wave period [s]			γ [-]	Wave heigth [m]	Wave direction [°]	ST-Setting	ST-lines	Duration [s]
	T_1	T_2	T_{low}		H/H_{m0}				
C3_I140a	14.0	-	-	3.3	0.50	135	Standard	4	16800
C3_I156a	15.6	-	-	5.0	0.50	135	Standard	4	18720
C3_I156b	15.6	-	-	5.0	1.00	135	Standard	4	18720
C3_I156c	15.6	-	-	5.0	1.50	135	Standard	4	18720
C3_I156d	15.6	-	-	5.0	2.00	135	Standard	4	18720
C3_I156e	15.6	-	-	5.0	2.50	135	Standard	4	18720
C4_M140a	14.0	-	-	-	1.00	135	Standard	4	588
C4_M140b	14.0	-	-	-	1.25	135	Standard	4	588
C4_M140c	14.0	-	-	-	1.50	135	Standard	4	588
C4_M140d	14.0	-	-	-	1.75	135	Standard	4	588
C4_M140e	14.0	-	-	-	2.00	135	Standard	4	588
C4_M156a	15.6	-	-	-	1.00	135	Standard	4	655
C4_M156b	15.6	-	-	-	1.25	135	Standard	4	655
C4_M156c	15.6	-	-	-	1.50	135	Standard	4	655
C4_M156d	15.6	-	-	-	1.75	135	Standard	4	655
C4_M156e	15.6	-	-	-	2.00	135	Standard	4	655
C4_M156a_noST	15.6	-	-	-	1.00	135	Off	0	655
C4_M156b_noST	15.6	-	-	-	1.25	135	Off	0	655
C4_M156c_noST	15.6	-	-	-	1.50	135	Off	0	655
C4_M156d_noST	15.6	-	-	-	1.75	135	Off	0	655
C4_M156e_noST	15.6	-	-	-	2.00	135	Off	0	655
C4_M172a	17.2	-	-	-	1.00	135	Standard	4	722
C4_M172b	17.2	-	-	-	1.25	135	Standard	4	722
C4_M172c	17.2	-	-	-	1.50	135	Standard	4	722
C4_M172d	17.2	-	-	-	1.75	135	Standard	4	722
C4_M172e	17.2	-	-	-	2.00	135	Standard	4	722
C4_M172a_noST	17.2	-	-	-	1.00	135	Off	0	722
C4_M172b_noST	17.2	-	-	-	1.25	135	Off	0	722
C4_M172c_noST	17.2	-	-	-	1.50	135	Off	0	722
C4_M172d_noST	17.2	-	-	-	1.75	135	Off	0	722
C4_M172e_noST	17.2	-	-	-	2.00	135	Off	0	722
C4_M330a	33.0	-	-	-	0.25	135	Standard	4	1386
C4_M330a_noST	33.0	-	-	-	0.25	135	Off	0	1386
C4_M360a	36.0	-	-	-	0.25	135	Standard	4	1512
C4_M360a_noST	36.0	-	-	-	0.25	135	Off	0	1512
C4_M360c_sga	36.0	-	-	-	0.25	135	sga	4	1512
C4_M360c_sk	36.0	-	-	-	0.25	135	sk	4	1512
C4_M360c_ssk	36.0	-	-	-	0.25	135	ssk	4	1512
C4_M360c_ssk_sga	36.0	-	-	-	0.25	135	ssk+sga	4	1512
C4_M360c_200t	36.0	-	-	-	0.25	135	200t	4	1512
C4_M380a	38.0	-	-	-	0.25	135	Standard	4	1596
C4_M380a_noST	38.0	-	-	-	0.25	135	Off	0	1596

Table 3.8 As Table 3.1, now for Case C (Part 3).

TestID	Wave period [s]			γ [-]	Wave heigth [m]	Wave direction [°]	ST-Setting	ST-lines	Duration [s]
	T_1	T_2	T_{low}		H/H_{m0}				
C4_M610a	61.0	-	-	-	0.20	135	Standard	4	2562
C4_M610b					0.40				2562
C4_M610c					0.60				2562
C4_M610a_noST					0.20		Off	0	2562
C4_M800a	80.0	-	-	-	0.05	135	Standard	4	3360
C4_M800b					0.10				3360
C4_M800c					0.20				3360
C4_M800a_noST					0.05		Off	0	3360

3.4 Case D

Table 3.9 As Table 3.1, now for Case D.

TestID	Wave period [s]			γ [-]	Wave heigth [m]	Wave direction [°]	ST-Setting	ST-lines	Duration [s]
	T_1	T_2	T_{low}		H/H_{m0}				
D1_I162e	16.2	-	-	3.3	1.00	180	Standard	4	19440
D1_I162d					2.00				19440
D1_I162e_noST					1.00		Off	0	19440
D1_I162f_noST					2.00				19440
D1_I80a	8.00	-	-	3.3	1.00	135	Standard	4	9600
D1_I80b					1.50				9600
D1_I120a	12.00	-	-	3.3	1.00				14400
D1_I120b					1.50				14400
D1_I162a	16.2	-	-	5.0	1.00				19440
D1_I162b					1.50				19440
D1_I80c	8.0	-	-	3.3	0.50	90	Standard	4	9600
D1_I80d					1.00				9600
D1_I120c	12.0	-	-	3.3	0.50				14400
D1_I120d					1.00				14400
D1_I162c	16.2	-	-	5.0	0.50				19440
D1_I162d					1.00				19440
D2_M156a	15.6	-	-	-	0.50	135	Standard	4	655
D2_M156b					1.00				655
D2_M156c					1.50				655
D2_M156a_noST					0.50		Off	0	655
D2_M162a	16.2	-	-	-	0.50	135	Standard	4	680
D2_M162b					1.00				680
D2_M162c					1.50				680
D2_M162a_noST					0.50		Off	0	680
D2_M330a	33.0	-	-	-	0.25	135	Standard	4	1386
D2_M330a_noST					0.25		Off	0	1386
D2_M7312a	73.12	-	-	-	0.20	135	Standard	4	3071
D2_M7312b					0.40				3071
D2_M7312c					0.60				3071
D2_M7312a_noST					0.20		Off	0	3071
D3_B7312a	16.2	20.81	73.12	-	0.50	135	Standard	4	3071
D3_B7312b					1.00				3071
D3_B7312c					1.50				3071
D3_B7312a_noST					0.50		Off	0	3071

4 Test results cases A, B and C

4.1 Decay tests

4.1.1 Decay tests without ShoreTension system active

This section discusses the decay tests performed in still water conditions. From these tests the natural period T_n can be determined. This partly serves as a validation of the test setup and partly to setup the hydrodynamic conditions as described in Section 2.7. The natural period, T_n, is derived from the period with which the vessel comes back to an equilibrium position from a forced and instantaneously released offset. The free natural roll period and subsequently the moored surge, sway, roll and yaw periods of the ship are evaluated in the mooring setup used for test Cases A, B and C. Each decay test is performed twice to check the reproducibility and the natural period is based on the average of the two measurements. Note that the value of the initial displacement (within a practical range) does not influence the period of the oscillations. For this reason, all signals presented in this Section have been normalised by the initial offset. The displacement signals of the relevant motions from the free roll and moored surge, sway, roll and yaw tests are presented in Figure 4.1, Figure 4.2, Figure 4.3, Figure 4.4 and Figure 4.5 respectively. The natural frequencies are summarised in Table 4.1.

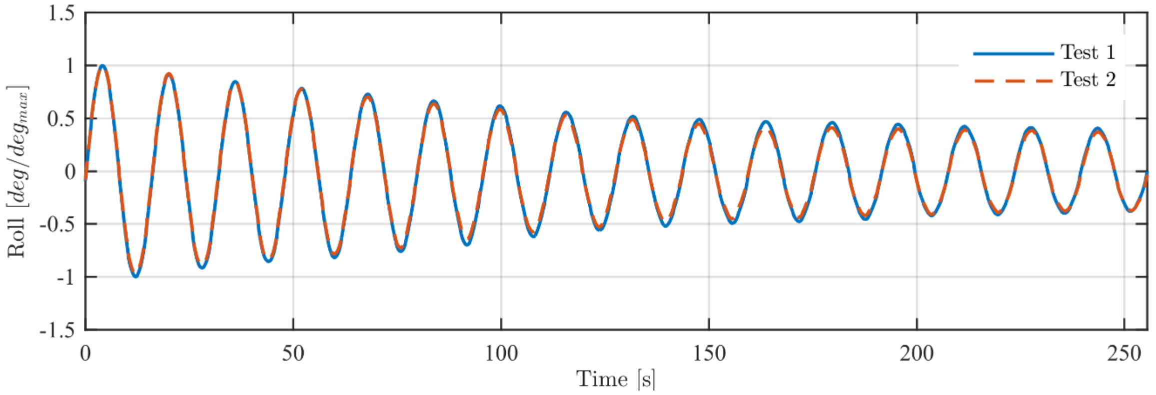

Figure 4.1 Normalised free roll decay tests without mooring system.

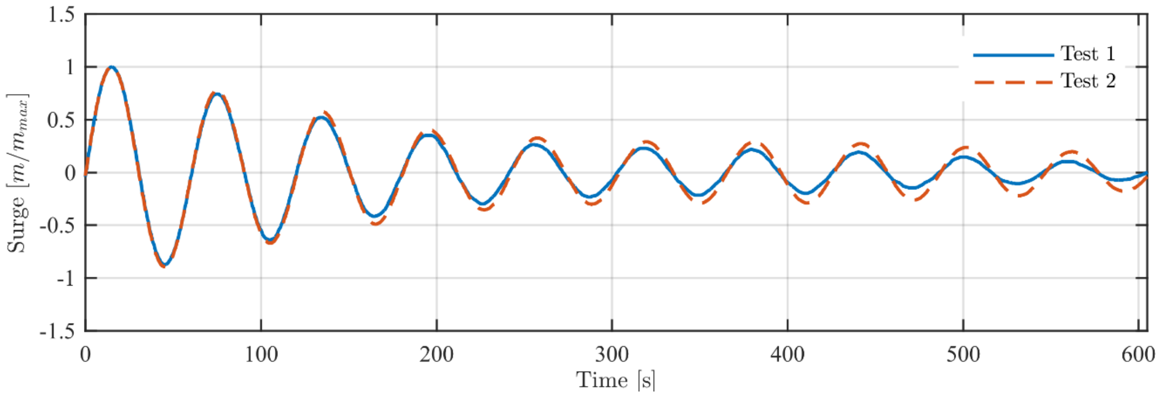

Figure 4.2 Normalised moored surge decay tests for mooring configuration Cases A, B and C.

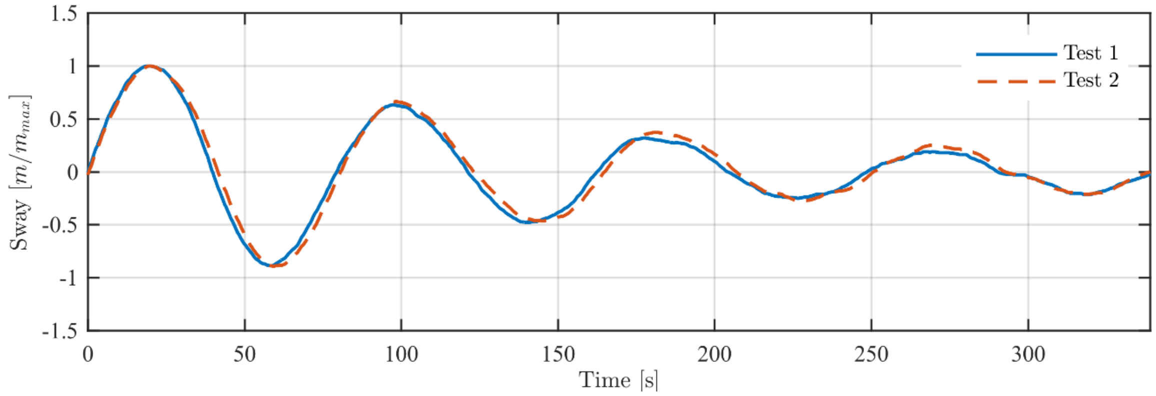

Figure 4.3 Normalised moored sway decay tests for mooring configuration Cases A, B and C.

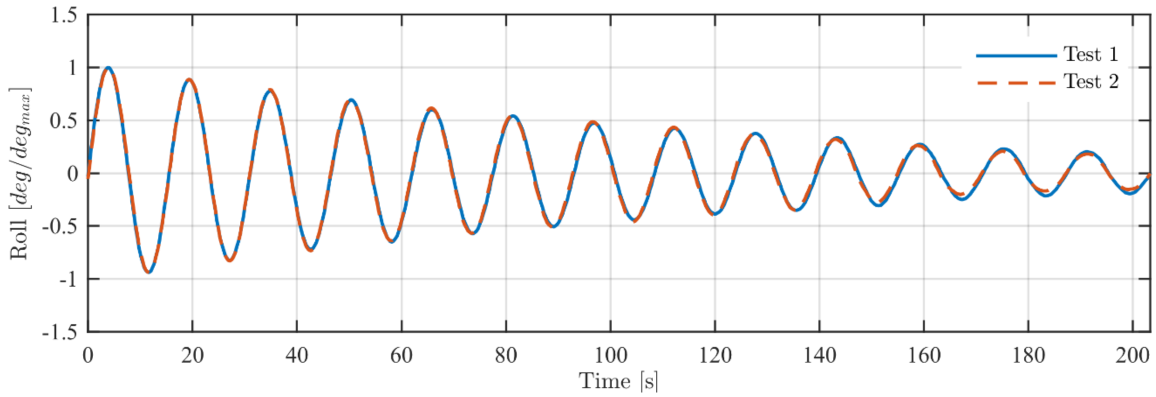

Figure 4.4 Normalised moored roll decay tests for mooring configuration Cases A, B and C.

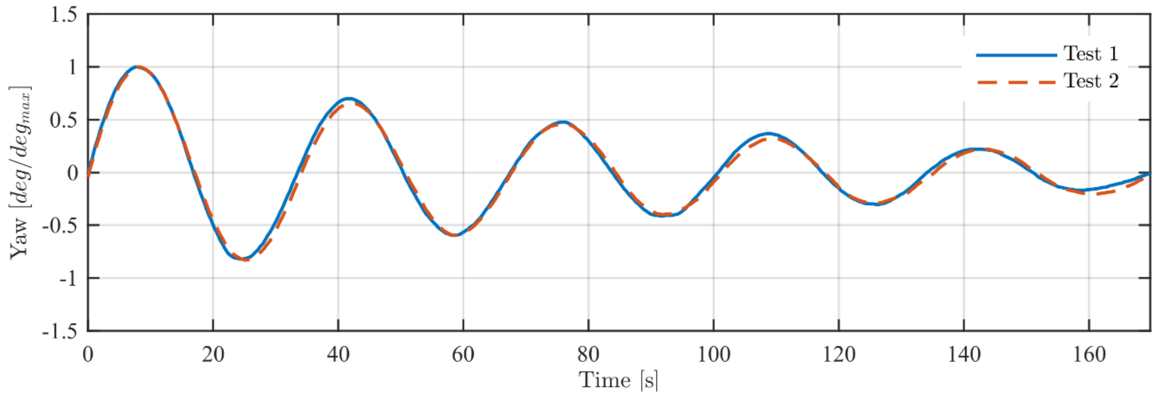

Figure 4.5 Normalised moored yaw decay tests for mooring configuration Cases A, B and C.

From the figures above and Table 4.1 it is observed that the natural periods of all degrees of freedom are very similar in the first and second tests, which confirms good reproducibility.

Table 4.1 Comparison of the free roll and moored surge, sway, roll and yaw natural periods for Cases A, B and C.

Designation	Natural period T_n [s]		Average natural period T_n [s]
	Test 1	Test 2	
Free Roll	15.95	15.96	15.96
Moored Surge	60.75	61.18	60.96
Moored Sway	78.12	81.91	80.01
Moored Roll	15.63	15.63	15.63
Moored Yaw	32.94	33.16	33.05

4.1.2 Decay test with ShoreTension system active

[The following content has been removed for reasons of confidentiality

]

4.1.3 Delivery of data

The motion data (including ST cylinder positions) of the decay tests have been saved to “comma separated value”-files (.csv) per degree of freedom. These csv-files have been delivered together with this report. Each file is named after the specific degree of freedom (free/moored/ST) and contains the following signals:

- Time in [s]
- Motions (6 DoF) at centre of gravity of the ship (CoG) in [m] or [°]: surge, sway, heave, roll, pitch and yaw)
- ST cylinder position in [m]: xST01 to xST04

4.2 Wave calibration

As described in Section 2.7.3, the main calibration parameters were the (total/spectral) wave height(s) and (peak) wave period(s) at WHM09 (see Section 2.6.1). The resulting wave parameters were determined based on the results of a 1D spectral analysis on the signal of the total water level signal (net result of incoming + reflected waves): H and T for the mono- and bi-chromatic wave conditions and H_{m0} and T_p for the spectral wave conditions. The most detailed calibration would have been based on the incoming wave only. However, this would require much more iterations of performing a test, applying wave splitting and redoing the test with new settings in a number of steps. Since numerical calculations primarily require that it should be known which conditions were present, and do not require a perfect calibration based on incoming wave heights only, calibration on total wave height was applied in order to leave more time for performing the main tests, which could then cover a wider range of wave conditions and ST system settings.

Since the bi-chromatic wave conditions consist of three separate waves (two higher frequency waves and a second-order low frequency wave), the spectral analysis was performed for three individual ranges of frequencies (also taking into account higher order wave components). This resulted in three individual wave heights (H_1, H_2 and H_{low}) and periods (T_1, T_2 and T_{low}). The total wave height of a wave test was considered as the sum of the two high-frequency carrier wave components ($H_{1,2} = H_1 + H_2$).

A calibration test was considered to be successful when the (total/spectral) wave height deviated less than 3 percent from the target wave heights and the (peak) periods deviated not more than 5 percent from the target periods. These are accuracies typically applied in physical scale model tests.

For the irregular wave conditions not only the spectral wave height, H_{m0}, and the peak period, T_p, were considered during the calibration, but also the spectral shape was checked. Since the specific value of the computed peak period was sensitive to the settings of the spectral analysis tool[13], the parameters were not considered alone, but in combination with the achieved spectral shape. If for example the wave height was correct, but a small deviation of the targeted peak period was found, the calibration was still considered to be successful if the spectral shape followed the targeted spectral shape adequately[14].

Table 4.2, Table 4.3 and Table 4.4 present the numerical calibration results for respectively the monochromatic, bi-chromatic and irregular wave conditions considered for Cases A, B and C. For the bi-chromatic wave conditions the wave height and period of the low frequency component, H_{low} and T_{low}, are also presented in Table 4.3, although these were not a calibration parameter, but a result of the calibrated high-frequency carries wave conditions.

In Appendix E.1 the calibration results are also presented by a plot of the variance density spectra[15] and, in case of irregular wave conditions, a plot of the exceedance curves of individual wave heights based on a Rayleigh distribution (not relevant for mono- or bi-chromatic wave conditions). In the second column of Table 4.2, Table 4.3 and Table 4.4 the appendix ID per test is denoted. In each of the plots in the appendix both the targeted (dashed black lines) and achieved (solid red lines) spectra and curves are presented. Please note that the presented target spectra and lines represent the deep-water situation (i.e. excluding influences of the shallow bottom) without reflections, while the measured signals are influenced by the (shallow) water depth in the basin and reflections coming from the damping material and basin wall. Therefore, no influences of second-order low/high frequency wave components or reflections are included in the targeted spectra and exceedance curves, while these do can be seen in the achieved spectra (e.g. higher harmonic wave components due to the shallow water situation and unequal peak values for the bi-chromatic wave conditions due to differences in reflection per carrier wave). This has not been considered critical in relation to the present application because similar effects are inevitable and will also be present in reality at locations close to the coast. Please note that when generating the wave signals, the second order effects were taken into account by the wave maker.

Note that for a number of intermediate bi-chromatic and irregular wave conditions, no dedicated calibration tests have been performed (see Table 4.3 and Table 4.4). This was because the results from earlier calibration tests showed a clear linear behaviour of the wave maker ‘gain’ setting, allowing for straightforward definition of these conditions.

The water level measurement data of the calibration tests have been saved to “comma separated value”-files (.csv) per wave condition. These csv-files have been delivered together with this report. Each file is named after the specific wave condition and contains the following signals:

---

[13] The resulting peak period can be influenced by the choice of the number of frequency bins over which is smoothed and by the number of data segments over which is averaged. For the overall irregular spectra (i.e. full frequency range) smoothing over 20 frequency bins has been applied in combination with averaging over 2 data segments (i.e. time series were cut in half). For the low frequency ranges of the irregular spectra, no smoothing was applied. This holds for all wave spectra of irregular wave conditions presented in this report.

[14] Note that for some spectra in Appendix E.1 large peaks can be observed that do not follow the target spectrum shape, even after smoothing of the spectrum. This indicates that a standing wave pattern might have been present in the basin with a node at the CoG of the ship. These peaks disappear when spectra are generated from the separated signals (incoming and reflection). The latter can be seen in the results of Section 4.3).

[15] In case of bi-chromatic and irregular wave conditions also a zoom plot is given of the low frequency wave components (no smoothing or averaging applied).

- Time in [s]
- Water level in [m]: WHM01 to WHM09
- Decomposed current velocities in [m/s]: EMS07x to EMS09x and EMS07y to EMS09y

4.3 Wave reflection analysis

Prior to the start of the physical scale model tests there were some concerns on the possible resonating behaviour of the Delta Basin (eigenmodes of the scale model basin, leading to spurious influences) when very long waves would be generated with the wave machine. It was also unclear how much reflection could be expected with both damping materials installed and the “Active Reflection Compensation” (ARC) of the wave machine activated. Therefore, extra attention was given to these processes before starting with the actual tests of the main test program (see Chapter 3).

To check whether basin resonance was present, the signals of each of the wave gauges in the basin were converted into wave spectra after each calibration test and checked for low frequency wave energy at the eigenfrequencies of the basin[16] ($f_{eigen,1}$ = 0.002 Hz, $f_{eigen,2}$ = 0.006 Hz, $f_{eigen,3}$ = 0.010 Hz). No apparent wave energy increases were observed at these specific frequencies other than the intended wave energy that was generated by the wave machine. Therefore, it was concluded that no basin resonance is expected for the scale model tests and that the wave signals do not have to be corrected. Apparently, the damping materials combined with the ARC of the wave maker ensures that reflection of waves is limited and that any remaining wave energy that does reflect back towards the wave maker is absorbed adequately, therewith ensuring that spurious basin resonance effects cannot arise.

Wave reflections were observed in the basin during the calibration tests. A reflection analysis was performed on the calibration tests. This was done by the separation of incident and reflected waves according to the Mansard-Funke procedure (Mansard & Funke, 1980). For the wave periods smaller than or equal to 33 s WHM01, WHM02 and WHM07 (see Figure 2.13) were used, while for the longer waves the selected wave gauges for the analysis were placed wider apart, namely WHM01, WHM07 and WHM09 (see Figure 2.13). The results of the reflection analyses are presented in Appendix E.2 and represent the conditions at the location of wave probe WHM01. The figures in the appendix show how the measured signals were decomposed into incoming and reflected wave signals. Surface elevation signals and variance density plots are presented. The general result of this analysis is that, depending on the wave height and length, the wave height, *H*, of the reflected wave, as a percentage relative to the incoming wave signal is in the order of 20 to 40 percent. General trends are that, as can be expected from theory, the reflection value lowers with increasing wave height (at a constant wave period) and increases with decreasing wave frequency (at a constant wave height). For the present application this is deemed acceptable. Practically speaking a reflection level of 0 is impossible to reach in laboratory practice, particularly for longer wave periods. This is not critical as long as the reflection levels that occur are known so that they can be used as input for possible numerical analyses.

*[16] Assuming that the wave machine acts as an open boundary with ARC activated and assuming that the installed damping material has no influence on the very low-frequency basin resonance waves, the first three eigenmode-waves have lengths of respectively 6400 m (L_{basin} = L/4), 2133 m (L_{basin} = 3*L/4) and 1280 m (L_{basin} = 5*L/4) at a water depth of 18 m.*

Table 4.2 Calibration parameter results monochromatic wave conditions for Cases A, B and C

Cond.	App. ID	Target H [m]	Achieved H [m]	Target T [s]	Achieved T [s]
M140a	F.1.01	1.00	1.00	14.00	14.00
M140b	F.1.02	1.25	1.25	14.00	14.00
M140c	F.1.03	1.50	1.50	14.00	14.00
M140d	F.1.04	1.75	1.77	14.00	14.00
M140e	F.1.05	2.00	2.01	15.60	14.00
M156a	F.1.06	1.00	1.01	15.60	15.66
M156b	F.1.07	1.25	1.26	15.60	15.66
M156c	F.1.08	1.50	1.50	15.60	15.66
M156d	F.1.09	1.75	1.76	15.60	15.66
M156e	F.1.10	2.00	2.01	15.60	15.66
M172a	F.1.11	1.00	0.99	17.20	17.17
M172b	F.1.12	1.25	1.25	17.20	17.17
M172c	F.1.13	1.50	1.51	17.20	17.17
M172d	F.1.14	1.75	1.76	17.20	17.17
M172e	F.1.15	2.00	2.02	17.20	17.17
M610a	F.1.16	0.20	0.21	61.00	60.99
M610b	F.1.17	0.40	0.41	61.00	60.99
M610c	F.1.18	0.60	0.59	61.00	60.99
M800a	F.1.19	0.20	0.20	80.00	79.96
M800b	F.1.20	0.40	0.40	80.00	79.96
M800c	F.1.21	0.60	0.59	80.00	79.96

Table 4.3 Calibration parameter results bi-chromatic wave conditions for Cases A, B and C

Cond.	App. ID	Target $H_{1,2}$ [m]	Achieved $H_{1,2}$ [m]	Target T_1 [s]	Achieved T_1 [s]	Target T_2 [s]	Achieved T_2 [s]	Target T_{low} [s]	Achieved T_{low} [s]	Achieved H_{low} [m]
B610a	F.1.22	1.00	1.01	15.60	15.62	21.00	20.96	61.00	60.99	0.04
B610b	-	1.25	-	15.60	-	-	20.96	61.00	-	-
B610c	-	1.50	-	15.60	-	-	20.96	61.00	-	-
B610d	-	1.75	-	15.60	-	-	20.96	61.00	-	-
B610e	F.1.23	2.00	2.03	15.60	15.62	21.00	20.96	61.00	60.99	0.19
B800a	F.1.24	1.00	1.02	15.60	15.62	19.40	19.38	80.00	80.05	0.02
B800b	-	1.25	-	15.60	-	-	19.38	80.00	-	-
B800c	F.1.25	1.50	1.53	15.60	15.62	19.41	19.38	80.00	81.91	0.03
B800d	-	1.75	-	15.60	-	-	19.38	80.00	-	-
B800e	F.1.26	2.00	2.00	15.60	15.62	19.40	19.38	80.00	80.05	0.05

Table 4.4 Calibration parameter results irregular wave conditions for Cases A, B and C

Cond.	App. ID	Target H_{m0} [m]	Achieved H_{m0} [m]	Target T_p [s]	Achieved T_p [s]
I156a	F.1.27	0.50	0.52	15.60	15.60
I156b	-	1.000	-	15.60	-
I156c	-	1.500	-	15.60	-
I156d	-	2.000	-	15.60	-
I156e	F.1.28	2.50	2.51	15.60	15.37

4.4 Presentation of time series and interpretation

4.4.1 Description of the measured timeseries

As mentioned in Section 2.6 time series of water levels, currents, line forces, fender forces and the position of the (analytical) modelled ShoreTension (ST) cylinders have been measured on model scale and stored for each performed model test. Subsequently, these time series have been converted into prototype signals by multiplying them with the correct scale factor (see Section 2.2) and have been saved to “comma separated value”-files (.csv) per test. These csv-files have been delivered together with this report. Each file is named after the specific test and contains the following (synchronised) signals:

- Time in [s]
- Water level in [m]: WHM01 to WHM09
- Decomposed current velocities in [m/s]: EMS07x to EMS09x and EMS07y to EMS09y
- Line forces of conventional mooring lines in [kN]: Fconv01 to Fconv06
- Fender forces in [kN]: Ffend01 to Ffend04
- Line forces of ST mooring lines in [kN]: FST01 to FST04
- ST cylinder position in [m]: xST01 to xST04
- Motions (6 DoF) at centre of gravity of the ship (CoG) in [m] or [°]: surge, sway, heave, roll, pitch and yaw)

If no data was available for a certain signal (e.g. the fender signals for cases A, B and C), all values of this signal have been filled with ‘NaN’(‘Not a Number’) within the csv-file.

The prototype signals of all tests have also been visualized in three figures for each test separately to give a overview of the measured signals. For this each performed test has been given a unique index, which can be found in the tables of Appendix G. With these tables the correct result plot figures can be found in Appendix G.1.1 for Cases A, B and C. These indices can be found in the second columns of the following tables in Appendix G per case:

- Case A (Head-on waves): Table F.1 and Table F.2
- Case B (Beam-on waves): Table F.3 and Table F.4
- Case C (Beam-quartering waves): Table F.5, Table F.6 and Table F.7

Next to the indices of the figures, the tables also give a quick overview of the specific test settings that have been applied.

The three figures per test of Appendix G.1.1 present the following information:

- Figure 1: Four panels with respectively the time series of 1) water levels w.r.t. still water level (SWL) for each of the eight wave gauges, 2) line forces of each of the six conventional mooring lines, 3) line forces of each of the two or four active ST modules and 4) cylinder positions of each of the active two or four active ST modules.
- Figure 2: Twelve panels divided over two columns. The six panels of the first column present the time series of the motions of the CoG of the ship in the six degrees of freedom. The panels of the second column present the unsmoothed motion spectra of the six degrees of freedom around the CoG of the ship. Last, below the twelve panels the standard deviations of the time series of each motion in the six degrees of freedom are presented as a measure of the amount of motion in a certain direction.
- Figure 3: Eight panels divided over two columns presenting the ST F-x characteristics (line force plotted against cylinder position) in the first column and the

F-x' characteristics (line force plotted against cylinder velocity) in the second column. For each test, only the signals of the active ST modules are presented.

Note that the limits of the y-axis of each panel in the three figures are kept constant for all tests to facilitate an easy comparison between tests. The only exceptions of this rule are the y-axis of the motion spectra; these were adjusted automatically to the value limits for visibility purposes.

To be able to quickly evaluate the influence of certain parameters on the movements of the moored ship, the standard deviation of the CoG motion timeseries, presented in Figure 2 and the absolute maxima of each test, have also been presented into tables in Appendix G.1.2 and G.1.3 respectively:

Standard deviations[17]
- Case A: Table G.1
- Case B: Table G.2 and Table G.3
- Case C: Table G.4 and Table G.5

Absolute maxima
- Case A: Table G.6
- Case B: Table G.7 and Table G.8
- Case C: Table G.9 and Table G.10

The results described above have not been interpreted thoroughly as part of this project, but some quick observations have been listed in the following sub-sections per test case per wave type. These observations can be used as starting point for further analyses.

4.4.2 Case A: Head-on waves

A1: Monochromatic waves
Considering long waves with a period near the natural period of the mooring configuration with conventional mooring lines, relatively large surge motions for both considered wave periods (61 and 80 s) can be observed (even with the ST system active). Different than expected on beforehand, a much stronger surge motion for the 80 s wave was observed than for the 61 s wave. The opposite was expected because the 61 s period is closer to the natural period of the moored ship. When looking in more detail to the water level signals of tests with comparable wave height, it could be concluded that for the 80 s wave condition the CoG of the ship was situated at a node, leading to a significantly higher incoming (and reflected) wave conditions than measured at the CoG (total signal: incoming + reflected wave signal). Therefore, a comparison of the ship motions for tests with equal wave height at the CoG of the ship is not fair in this case. A fairer comparison would be to compare tests with similar overall wave heights, e.g. A1_M610b (H.002) with A1_B800a (H.005). In that case the surge motion is indeed more prominent for the 61 s wave condition while the sway motion is more pronounced for the 80 s wave condition. Note that no monochromatic wave condition tests have been performed without the ST active, because very large surge motions were expected that could damage the scale model setup and measuring devices.

[17] *No standard deviations have been presented for the transition test because here the standard deviation has no statistical relevance.*

Another observation is that even though the ship experienced head-on waves, relatively large sway motions were observed for the 80 s wave conditions. Since the eigenperiod of the ship in sway direction is equal to 80 s and since there is no active damping in the mooring configuration in that direction, this is no strange behaviour: only a small amount of energy in combination with a small yaw angle can already lead to large sway-motions even when the ship is aimed to be moored head-on with respect to the incoming wave direction.

A2: Bi-chromatic waves
Other than for the monochromatic waves, the largest surge motions can be observed for the bi-chromatic wave conditions with 61 s low frequency wave component. This can be explained by the fact that the wave height of the low frequency wave component is higher for the B610-conditions than for the comparable B800-conditions (see Table 4.3).

From the transition tests (i.e. the ST system was deactivated halfway: transition from situation with the system active to a situation without) and the tests with the ST system deactivated, it can be clearly observed what the added value of ShoreTension is: the surge motions become much smaller when the system is active (factor 2 to 6). For test B610e without the ST system active (B610e_noST) the surge motions became even so large that the slack/inactive ST lines were tensed.

A3: Special ST settings
[The following content has been removed for reasons of confidentiality

]

A4: Irregular waves
In the considered cases the magnitude of the motions of the vessel at CoG shows a linear behaviour related to the applied wave height of the wave condition. The vessel motions under these wave conditions are relatively small compared to the motions observed for the monochromatic and bi-chromatic wave conditions. This is because the wave energy is now distributed over a larger range of wave frequencies, instead of being focussed at one of the natural periods of the moored ship. As expected for the head-on mooring configuration, the surge motions of the ship are the largest, followed by the sway motions.

4.4.3 Case B: Beam-on waves

B1: Monochromatic waves
The following observations could be made for the monochromatic beam-on wave tests:

- The ship shows little to no effect to the short but high 8 s waves. No difference in ship motions can be observed when the ST modules are activated or deactivated.
- A moored ship experiencing beam-on monochromatic waves that have a period equal or close to the roll-eigenperiod of the ship reacts strongly to these waves with (relatively) large sway, heave and roll motions.

- Although the roll eigenperiod of the moored ship (15.6 s) does not coincide with the sway (80 s) or heave eigenperiod (not determined but >15.6 s), the vessel also moves along with the primary wave excitation: all vessel motion spectra of the test show clear peaks at the considered wave periods.
- No specific tests with ShoreTension switched off have been performed for the relatively long high-frequency wave conditions (T>8 s) since the vessel motions in these tests were dominated by (too) large roll motions. It was expected that turning off ShoreTension in those cases would lead to even larger motions, which was not preferred.
- The vessel showed the strongest response for the longest considered "short" monochromatic wave (T =17.2 s). A clear surge motion at the surge eigenperiod was observed under these wave conditions although no forcing at that period was present in the basin. This surge motion was not observed in repeat tests with the same wave height or tests with lower wave heights and an equal period. It is therefore believed that this undamped motion was somehow introduced unintentionally. It should be filtered out when used in later project phases. In none of the other test conditions such a spurious wave effect was found.
- The tests with 80 s waves clearly show that ST has a damping effect for the low-frequency sway motion. The sway motion becomes three times smaller when the ST modules are active compared to the situation without ST applied.
- The damping effect of ST on roll is small. Because this motion is mostly a vertical motion at the fairleads of the ship (connection point of lines in scale model) and therewith strongly influenced by gravity, it is very hard to damp this motion with ST (or any other method), which is primarily intended for forces in the horizontal plane. This was known beforehand and this expectation was merely verified in these tests.

B2: Bi-chromatic waves

Tests with lower wave heights were performed once it became clear that the originally foreseen wave heights (1 m or higher) of the bi-chromatic tests (see Section 3.2) resulted in unacceptably large roll motions. As expected for the beam-on mooring configuration, it followed from the tests that both the sway and roll motions are significantly larger compared to the other motions. Other than for the monochromatic waves with a period of 80 s, the sway motion does not become significantly larger when ST is deactivated. The sway motion spectra from the bi-chromatic tests, indicate that this sway motion is a high-frequency motion (related to the high-frequency roll motion) and not a low-frequency motion as for the monochromatic test. [The following content has been removed for reasons of confidentiality] Deactivating ST therefore has no effect on the (high-frequency) sway motions[18] in these cases.

B3: Special ST settings

[The following content has been removed for reasons of confidentiality

]

B4: Irregular waves

When performing the tests with irregular wave conditions, it turned out quickly that it was not possible to perform all tests because the ship was making contact with the bottom due to too

[18] *Note that the low-frequency sway energy does become larger when ST is deactivated*

large roll (and heave) motions. Only one test, with the smallest considered wave height, could be performed without contact with the bottom. A full comparison between irregular wave tests is therefore not possible.

4.4.4 Case C: Bow-quartering waves

C1: Bi-chromatic waves
The bi-chromatic tests performed for Case C showed linear behaviour in the ship motions with increasing wave height. The results showed that the 61 s wave period tests resulted in larger sway motions than the 80 s wave period tests with equal wave heights. When comparing the motion spectra of the different tests for surge and sway, it turned out that the moored ship in the bow-quarterly orientation was much more sensitive to the second wave component (T_2 = 20.96 s) of the B610 wave conditions than for the second wave component (T_2 = 19.38 s) of the B800 wave conditions. This difference is linked to a different motion response of the ship at those carrier wave frequencies.

C2: Special ST settings
[The following content has been removed for reasons of confidentiality

]

C3: Irregular waves
The irregular wave tests performed for Case C also showed linear behaviour in the ship motions with increasing wave height. The ship motions showed not to be very sensitive for the short-wave spectra in this mooring configuration. No specific tests with ST deactivated were performed because it was not expected that this would lead to an increase of vessel motions, also considering experiences of previous tests.

C4: Monochromatic waves
During the execution of the test program, originally only containing test series C1, C2 and C3, it was decided, in consultation with the participants, to also include a large set of monochromatic wave tests to the program. This new test series, C4, included all monochromatic wave conditions which were calibrated during the calibration phase (see Table 4.2) and some uncalibrated wave conditions (see Section 4.1.2).

From the tests with the calibrated relatively “short” wave conditions it followed that the ship motions were not very sensitive to these conditions. No large structural differences in ship motions were observed between the situations in which the ST system was activated and deactivated: some motion became slightly smaller and some motion became slightly larger.

As expected from theory, the ship motions were much more sensitive for the calibrated “long” waves. For the transition test of the M610a (H = 0.200 m, T = 61.00 s) wave condition for example, the surge motion ramped up to almost 3 meters in amplitude. The added value of the ST system is very clear in that situation.

With the uncalibrated wave conditions used for principle tests it was tried to check how the moored system, including the ST system, would react when it was loaded with a wave condition of which the wave period coincided with the (pseudo-) surge eigenperiod (33-36 s) of the combined stiff system. To do so three wave conditions were tested with wave periods in the range of 33 to 36 seconds and a small wave height of around 0.25 m. The latter was chosen such that the line force would remain below the limit of the ST system, which would therefore not be triggered to actively respond. It should be noted that by selecting this range, the vessel would also be triggered at its natural period for yaw when ST would be deactivated (T = 33 s, see Table 4.1).

As expected, the test with the 33 s wave led to a strong amplification of the yaw-motion of the ship, when ST was deactivated compared to when it was activated[19]. The surge motion on the other hand became smaller when the ST system was deactivated. A similar response for the surge motion was observed for both the 36 s and 38 s wave condition with a decreasing influence of the yaw-motion with increasing wave period.

Also, some test with special ST settings were performed for the 36 s wave condition. From these tests no clear positive or negative effect of applying special ST settings on the motions could be observed.

[19] In case ST is activated, the mooring configuration becomes stiffer, leading to a shift of the yaw natural period to a higher frequency (shorter period) and therewith not triggered by a 33 s wave.

5 Test results Case D

5.1 Decay tests

This section discusses the decay tests performed in still water conditions with mooring setup for Case D. During these decay tests the ShoreTension (ST) system was not active. From these tests the natural period, T_n, can be determined. This partly serves as a validation of the test setup and partly to setup the hydrodynamic conditions as described in Section 2.7. The natural period, T_n, is derived from the period with which the vessel comes back to an equilibrium position from a forced and instantaneously released offset. The moored surge, roll and yaw periods of the ship are evaluated in the mooring setup used for test Case D. Each decay test is performed twice to check the reproducibility and the natural period is based on the average of the two measurements. Note that the value of the initial displacement does not influence the period of the oscillations. For this reason, all signals presented in this Section have been normalised. The displacement signals of the relevant motions from the moored surge, roll and yaw tests are presented in Figure 5.1, Figure 5.2 and Figure 5.3 respectively. The natural frequencies are summarised in Table 5.1.

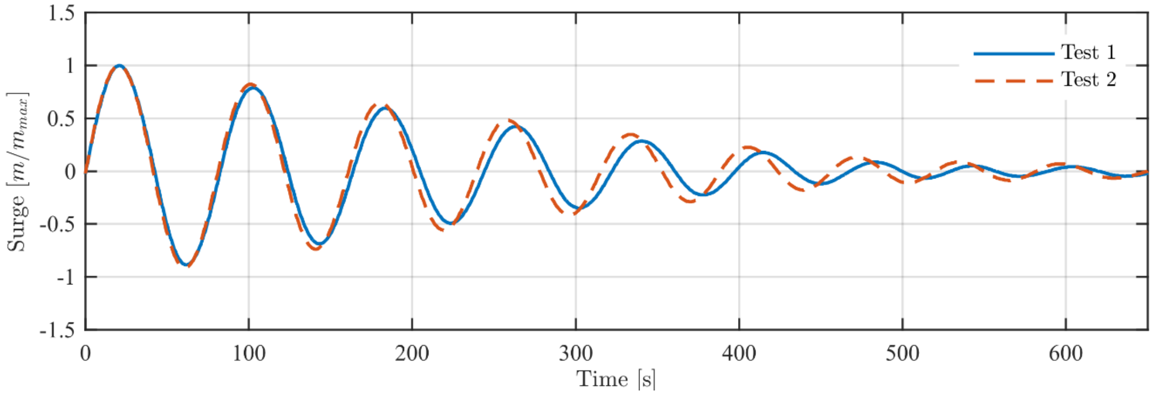

Figure 5.1 Normalised moored surge decay tests for mooring configuration Case D.

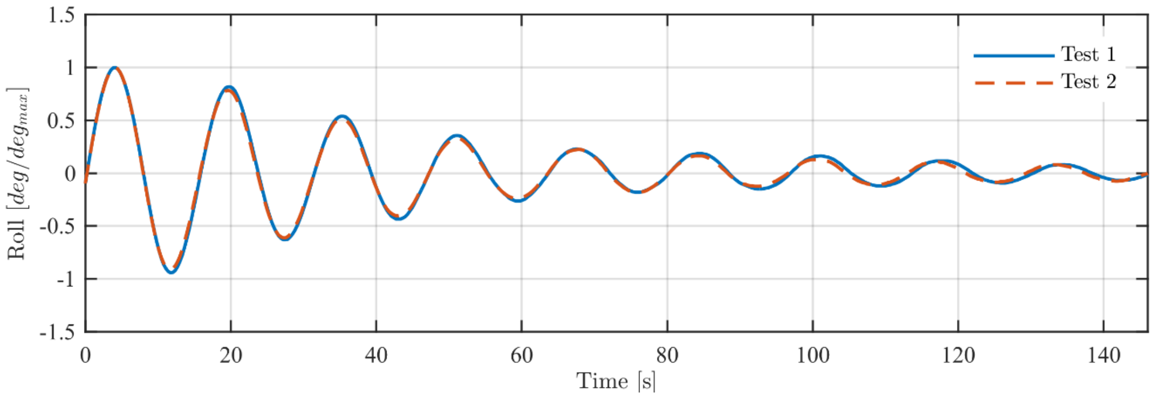

Figure 5.2 Normalised moored roll decay tests for mooring configuration Case D.

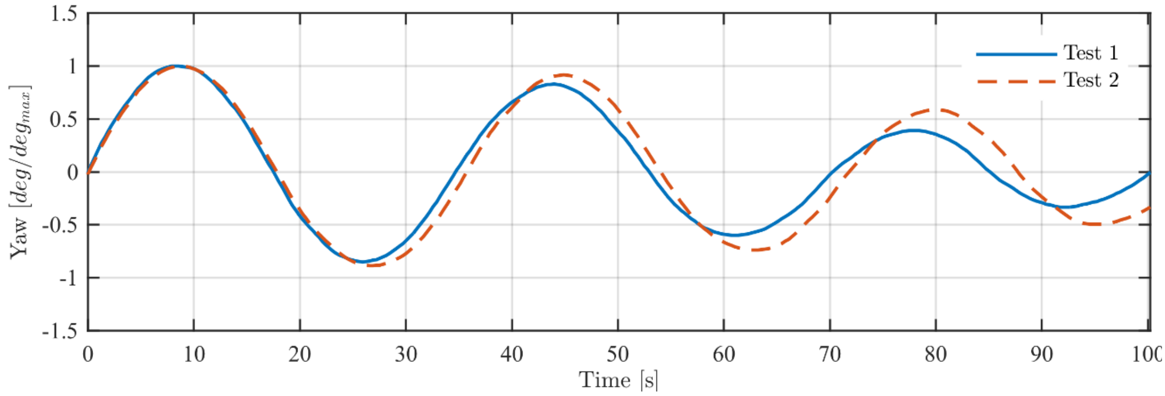

Figure 5.3 Normalised moored yaw decay tests for mooring configuration Case D.

From the figures and Table 5.1 it is observed that the roll period test is well replicated, while minor differences in amplitude and period are found in the two surge and yaw decay tests. The latter is expected to be caused by the influence of the fenders on the vessel surge and yaw motions. Although small, the friction of the fenders on the hull has a certain influence on the natural period of these motions. This influence becomes more pronounced when the amplitude decays (i.e. influence of friction increases). The latter leads to an elongation of the motion: the natural period increases. The latter was not expected to lead to problem during the measurements, since the ship was constantly kept in motion by the waves during the tests.

Table 5.1 Comparison of the moored surge, roll and yaw natural periods for Case D.

Designation	**Natural period T_n [s]**		**Average natural period T_n [s]**
	test 1	**test 2**	
Moored Surge	73.62	72.62	73.12
Moored Roll	16.29	16.17	16.23
Moored Yaw	34.00	32.06	33.03

The motion data of the decay tests have been saved to “comma separated value”-files (.csv) per degree of freedom. These csv-files have been delivered together with this report. Each file is named after the specific degree of freedom and contains the following signals:

- Time in [s]
- Motions (6 DoF) at centre of gravity of the ship (CoG) in [m] or [°]: surge, sway, heave, roll, pitch and yaw)

5.2 Wave calibration

For the calibration of the wave conditions for Case D the same procedure was followed as for the calibration tests of the wave conditions for Cases A, B and C. One is therefore referred to Sections 2.7.3 and 4.2 for more information on this procedure.

Table 5.2, Table 5.3 and Table 5.4 present the numerical calibration results for respectively the monochromatic, bi-chromatic and irregular wave conditions considered for Case D. For the bi-chromatic wave conditions the wave height and period of the low-frequency component, H_{low} and T_{low}, are also presented in Table 5.3, although these were not calibration parameters, but a result of the high-frequency wave components.

In Appendix E.3 the calibration results are also presented visually by two plots with variance density spectra[20] and exceedance curves of individual wave heights. In the second column of Table 5.2, Table 5.3 and Table 5.4 the appendix ID per test is denoted. In each of the plots both the targeted (dashed black lines) and achieved (solid red lines) spectra and curves are presented. Please note that the target spectra and lines represent the deep-water situation (i.e. excluding influences of the shallow water depth) without reflections, while the measured signals are influenced by the (shallow) water depths and reflections coming from the damping material and basin wall. Therefore, no influences of second-order low and/or high wave components are included in the target spectra and exceedance curves, while these are present in the achieved spectra (e.g. higher order wave components) and exceedance curves (higher individual waves due to shallower wave troughs and steeper wave peaks). This has not been considered critical in relation to the present application because similar effects are inevitable and will also be present in reality at locations close to the coast.

Table 5.2 Calibration parameter results monochromatic wave conditions for Case D.

Cond.	App. ID	Wave heading	Target	Achieved	Target	Achieved
			H [m]	H [m]	T [s]	T [s]
M156a	F.3.01	Bow-quartering	0.50	0.49	15.60	15.66
M156b	F.3.02	Bow-quartering	1.00	1.00	15.60	15.66
M156c	F.3.03	Bow-quartering	1.50	1.49	15.60	15.66
M162a	F.3.04	Bow-quartering	0.50	0.51	16.20	16.26
M162b	F.3.05	Bow-quartering	1.00	1.01	16.20	16.26
M162c	F.3.06	Bow-quartering	1.50	1.50	16.20	16.26
M330a	F.3.07	Bow-quartering	0.50	0.51	33.00	32.98
M330b	F.3.08	Bow-quartering	1.00	1.01	33.00	32.98
M330c	F.3.09	Bow-quartering	1.50	1.49	33.00	32.98
M330d	F.3.10	Bow-quartering	2.00	1.96	33.00	32.98
M7312a	F.3.11	Bow-quartering	0.20	0.20	73.12	73.18
M7312b	F.3.12	Bow-quartering	0.40	0.40	73.12	73.18
M7312c	F.3.13	Bow-quartering	0.60	0.60	73.12	73.18

Table 5.3 Calibration parameter results bi-chromatic wave conditions for Case D (Ach. =Achieved).

Cond.	App. ID	Wave heading	Target	Ach.	Target	Ach.	Target	Ach.	Target	Ach.	Ach.
			$H_{1,2}$ [m]	$H_{1,2}$ [m]	T_1 [s]	T_1 [s]	T_2 [s]	T_2 [s]	T_{low} [s]	T_{low} [s]	H_{low} [m]
B7312a	F.3.14	Bow-quart.	0.50	0.51	16.20	16.18	20.81	20.77	73.12	73.18	0.01
B7312b	F.3.15	Bow-quart.	1.00	1.00	16.20	16.18	20.81	20.77	73.12	73.18	0.05
B7312c	F.3.16	Bow-quart.	1.50	1.51	16.20	16.18	20.81	20.77	73.12	73.18	0.11
B7312d	F.3.17	Bow-quart.	2.00	1.99	16.20	16.18	20.81	20.77	73.12	73.18	0.20

[20] *In case of bi-chromatic and irregular wave conditions also a zoom plot is given of the low frequency wave components.*

Table 5.4 Calibration parameter results irregular wave conditions for Case D.

Cond.	App. ID	Wave heading		Achieved	Target	Achieved
			H_{m0} [m]	H_{m0} [m]	T_p [s]	T_p [s]
I180a	F.3.18	Bow-quartering	1.00	1.00	8.00	7.48
I180b	F.3.19	Bow-quartering	1.50	1.49	8.00	7.99
I80c	F.3.20	Beam-on	0.50	0.49	8.00	7.83
I80d	F.3.21	Beam-on	1.00	0.98	8.00	7.81
I120a	F.3.22	Bow-quartering	1.00	1.00	12.00	12.37
I120b	F.3.23	Bow-quartering	1.50	1.49	12.00	12.35
I120c	F.3.24	Beam-on	0.50	0.51	12.00	11.98
I120d	F.3.25	Beam-on	1.00	1.01	12.00	12.00
I162a	F.3.26	Bow-quartering	1.00	1.01	16.20	15.83
I162b	F.3.27	Bow-quartering	1.50	1.49	16.20	17.02
I162c	F.3.28	Beam-on	0.50	0.50	16.20	16.07
I162d	F.3.29	Beam-on	1.00	1.00	16.20	16.09
I162e	F.3.30	Head-on	1.00	0.99	16.20	15.99
I162f	F.3.31	Head-on	2.00	2.00	16.20	16.09

5.3 Wave reflection analysis

A significant change from Cases A, B and C to Case D is the fact that waves are also generated under an angle of 45 or 135 degrees with respect to the wave board instead of only perpendicular to the wave board. From visual observations and by checking the 2D wave spectra at the location of the ship (WHM09, see Table 2.4) during the calibration phase, it was concluded that due to the fact that waves, generated under an angle, have to reflect three times to return to the vessel location and to the wave board, no significant influence of reflected waves could be observed at the location of the ship. An example of such a 2D spectrum is shown in Figure 5.4 for test I162e (waves sent out under an angle of 135° with respect to the wave board). Here, no wave energy is observed coming back from the wave damping material (i.e. only one peak of incoming wave energy is visible and no other peaks of significant/detectable height).

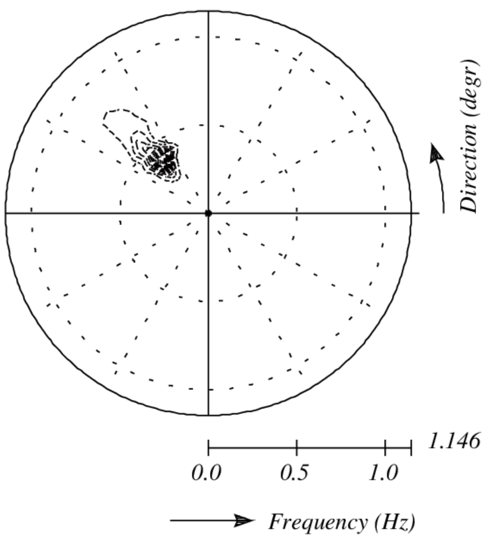

Figure 5.4 2D wave spectrum of location WHM09 for calibration test I162e

For the waves generated perpendicular to the wave board, wave reflection analyses have been performed for the configuration of Case D. The same approach as for the wave conditions of the first project phase (Cases A-C) has been applied. The results of the reflection analyses are presented in Appendix E.4 and represent the conditions at the location of wave probe WHM01. The general result of the analyses is that, depending on the wave height and length, the wave height, *H*, of the reflected wave, as a percentage relative to the incoming wave signal is in the order of 20 to 60 percent. General trends are that, as can be expected from theory, the reflection value lowers with increasing wave height (at a constant wave period) and increases with decreasing wave frequency (at a constant wave height). For the present application this is deemed acceptable. Practically speaking a reflection level of 0 is impossible to reach in laboratory practice, particularly for longer wave periods. This is not critical as long as the reflection levels that occur are known so that they can be used as input for possible numerical analyses.

5.4 Presentation of time series and interpretation

Similar as for the tests performed for Cases A, B and C, all time series measured during the tests of Case D have been saved to “comma separated value”-files (.csv) per test as prototype values and have been visualized in three figures for each test separately (using the same formatting as presented in Section 4.4) to give an overview of the measured signals. For this, each performed test has been given a unique index, which can be found in the tables of Appendix G. With these tables the correct result plot figures can be found in Appendix G.2.1 for Case D. These indices can be found in the second column of Table F.8 in Appendix F.

A description of the layout of these figures can be found in Section 4.4. Please note that other than for Cases A, B and C the first figure of each test from Case D contains five panels instead of four. These panels present respectively the time series of 1) water levels with respect to still water level (SWL) for each of the eight wave gauges, 2) line forces of each of the six conventional mooring lines, 3) fenders forces of each of the four fenders, 4) line forces of each of the two or four active ST modules and 5) cylinder positions of each of the active two or four active ST modules. The layout of the other two figures have not changed compared to the plots used to present results of Cases A to C in Chapter 4.

Note that the limits of the y-axis of each panel in the three figures are kept constant for all tests to facilitate an easy comparison between tests. The only exceptions of this rule are the y-axis of the motion spectra; these were adjusted automatically to the value limits.

To be able to quickly evaluate the influence of certain parameters on the motions of the moored ship, the standard deviation of the CoG motion timeseries, presented in Figure 2 of each test, have also been presented into Table G.11 in Appendix G.2.2 (see footnote 17). The absolute maxima of the CoG motion timeseries have been presented into Table G.12 in Appendix G.2.3.

As was mentioned in Section 4.4, the results of the tests have not been interpreted thoroughly as part of this project, but some quick observations have been listed in the following sub-sections per wave type. These observations can be used as starting point for further analyses.

D1: Irregular waves

In the irregular wave test results with a small peak wave period value (T_p = 8 or 12 s) it is observed that the moored ship does not react strongly to the waves, because these periods do not coincide with the natural periods of the ship and therefore do not trigger large motions. The strongest reaction for these waves can be seen in sway and roll for the highest and longest wave condition of that set: I120d.

For the irregular wave tests with a peak period of 16.2 s it followed that the beam-on condition with a significant wave height of 1.00 m could not be performed due to too large roll motions (ship making contact with the bottom). Also, the head-on wave conditions showed more significant motions, but then for the surge direction. For the latter test, also test with ST deactivated were performed. In those cases, the surge motions became twice as large, while the other motions remained more or less the same as in the situation with ST activated.

D2: Monochromatic waves
For the monochromatic wave conditions only bow-quartering tests were performed.

A remarkable result was that for wave condition M156a (H = 0.5 m), for which the wave period coincides with the free roll period of the ship, a decrease in the sway and roll motions was observed when ST was deactivated, while the opposite was expected. For wave condition M162a (H = 0.5 m), for which the wave period coincides with the moored roll period of the ship in case D, this increase was observed.

The added value of ST can clearly be seen in the tests performed for the monochromatic wave conditions with a wave period equal to the natural surge period of case D without ST activated (T = 73.12 s). For the tests with wave condition M7312a (H = 0.20 m) the surge motion decreases from 0.86 m to 0.02 m when ST is active (4200% decrease). It should be noted here that the mooring configuration becomes significantly stiffer when ST is activated, leading to a shift of the natural surge period to higher frequencies. Mostly this influences the response of the vessel.

D3: Bi-chromatic waves
The bi-chromatic tests (only bow-quartering waves) show a linear increase in motions with increasing wave height. Remarkably, the sway and roll motions decrease somewhat when the ST system is deactivated for wave condition M7312a. This shows that the ST system can sometimes increase the ship motions instead of decreasing them. It should be noted that these are only minor differences (<0.05 m and <0.05° for the considered condition) and is not expected to influence or limit the applicability of the ST system in practice.

6 Conclusions

6.1 Project context

The overall aim of this project was to explore the limits and possibilities of innovative mooring of vessels in the Port of the Future and to provide a solid database for validation of numerical models simulating the performance of these innovative mooring solution. The innovative mooring technique studied in this project was the ShoreTension (ST) system. With respect to the ST system, the main system-specific goals of this project were to verify the application limits of the ST system with respect to wave height (for the most critical response periods) and to optimise the system settings to maximise the applicability range of the system. In this way the applicability limits of the system may be enlarged compared to present understanding and expectations of the system.

To reach those goals, physical scale model tests of a moored vessel were performed within Deltares' Delta Basin with one vessel size/type and one draft-depth ratio for four different mooring configurations: three analytical configurations and one realistic configuration. The vessel has been tested in three series of different types of wave loads with increasing wave heights: monochromatic, bi-chromatic and irregular wave conditions. The wave periods of these wave conditions were selected such that they corresponded to, or were almost equal to, the eigenfrequencies of the moored vessel. In this way the tested situations corresponded to the most challenging wave conditions for the ST system.

6.2 Main conclusions

The following main conclusions have been drawn from the project:

- The ST system performs well under heavy wave loads and can significantly lower ship motions in the horizontal degrees of freedom of the ship (surge, sway and yaw). It is especially effective in minimizing the low-frequency motions of which the periods are equal or close to the moored vessel's natural periods (conventionally moored).
- [The following content has been removed for reasons of confidentiality

  ]
- The motions in the vertical degrees of freedom (heave, roll and pitch) were almost not, or much less, damped by the ST system. This system characteristic was known beforehand and confirmed by the scale model. The system has not been designed to cope with those forces, which, in general, are too high to control. Furthermore, in many cases the vertical motions are not the main factor influencing workability limits for (off-)loading a moored ship in a port.
- Especially for beam-on waves, the ship experienced large roll motions for relatively low wave heights. The test results showed that changing the vessel heading relative to the incoming wave direction has much more effect on the roll motions in those cases than applying the ST system.
- The wave basin and wave maker used for the physical scale model tests allowed for a wide range of wave conditions to be generated (up to 80 s period). Reflection material along the outer edges of the basin and the state-of-the-art "Active Reflection Compensation" (ARC) of the wave maker ensured that no significant spurious basin resonance modes arose, even for the longest wave periods generated.
- Wave splitting has been used to determine accurately the height of the incoming and reflected waves in the basin. This analysis resulted in reflection values of 20-60% for the total range of wave periods considered.

- The model version of the ST system performed well and has reproduced the characteristics of the system accurately and reliably based on information provided by ShoreTension to Deltares.

6.3 Summary of observations related to effectiveness of the ST system

The tests showed that the ST system effectively reduces low-frequency horizontal wave motions (surge, sway and yaw). In traditional ports these are generally normative. For higher frequency horizontal motions, the ST system also has a positive effect, though somewhat smaller due to the relatively long response times of the system compared to the wave motions (i.e. the system cannot fully keep up with the high-frequency motions).

The results of the tests with the considered vessel have been qualitatively summarized in Table 6.1. It should be noted that this table only holds for large vessels with similar dimensions and free/moored natural periods as the vessel considered in this study. The results presented should be considered general observations based on the scale model tests as performed; the suitability and effectiveness of the ST system for a specific location will require dedicated analyses and validations.

Table 6.1 Effectiveness of the ST system in damping vessel motions for different ranges of wave periods.

Degree of Freedom	Wind sea waves (T < 12 s)	Swell waves (T = 15-25 s)	Low-frequency waves (T > 30 s)
Surge (horizontal)	o	+	++
Sway (horizontal)	o	+	++
Heave (vertical)	x	x	x
Roll (vertical)	x	x	x
Pitch (vertical)	x	x	x
Yaw (horizontal)	o	+	++

Meaning of symbols:
++ = Most effective
\+ = Effective
o = No or little vessel response due to unsensitivity of vessel to wind sea waves
x = Almost not, or much less effective because the system is not designed for damping vertical motions

6.4 Closing remarks

When developing new port concepts in which innovative mooring techniques are applied, it should be considered that other aspects will become normative (e.g. roll motions). To be able to assess these situations, well-validated numerical tools are necessary. The systematically generated measurement database together with this report provide a proper basis for the validation of numerical representations of the ST system.

The scale model results form a solid verification of the functionality and performance of the innovative mooring system. The results will help to increase acceptability of the ST system (and similar techniques) throughout the waterborne transport community and for use in the Port of the Future. In addition, the explored applicability limits of the ST system may diversify and extend the fields of application of the system.

Last, it is concluded that applying innovative mooring techniques in existing ports or future open port concepts may significantly alleviate possible hindrance of swell or low-frequency waves on moored vessels. By doing so, this may open up possibilities for both existing or future ports to shorten, replace or even leave out mitigating measures like breakwaters, which, by itself, can have a positive effect on the coastal impact and may save large investments.

References

Dalrymple, R.A., 1989, Directional wavemaker theory with sidewall reflection, J. of Hydraulic Research, vol. 27, no. 1, pp. 23-34, 1989.

De Jong, M.P.C., O.M. Weiler, J. Schouten, 2012, Open water ports – a sustainable design approach, Third International Engineering Systems Symposium CESUN 2012, Delft University of Technology, 18-20 June 2012.

Mansard, E. P., & Funke, E. R. (1980). The measurement of incident and reflected spectra using a least squares method. In Coastal Engineering 1980 (pp. 154-172).

Witteveen+Bos, 2018, Dynamic Mooring Analysis, Phase 4 – ShoreTension, Vopak Horizon Fujairah Limited, 104481-RPT-002-RevA, 27-03-2018.

A Photo report damping material

In this Appendix detailed photos are presented of the damping material in the Delta Basin. The configuration of the damping material did not change throughout the project and is the same for each of the four considered mooring cases.

Next to each photo it is shown in a map plot from which location the photo was taken together with the orientation of the photo. A number of photos were taken from within the Delta Basin itself; in this case the location and orientation are represented by a red dot (location) and triangle (orientation). Other photos were taken from the overhead balustrades of the Hydro Hall; in that case the location and orientation are represented by a red dot (location) and oval/circle (orientation).


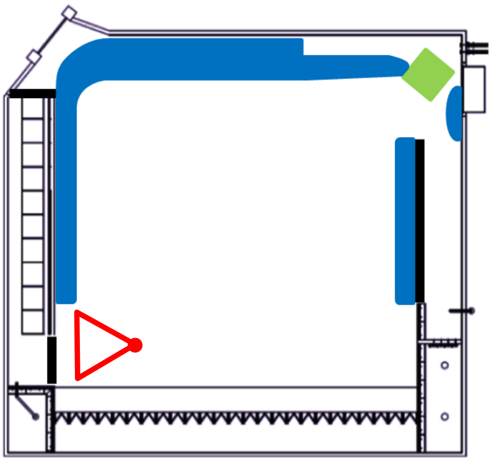

Figure A.1 Left vertical reflection wall near the wave board (X = 0 m)


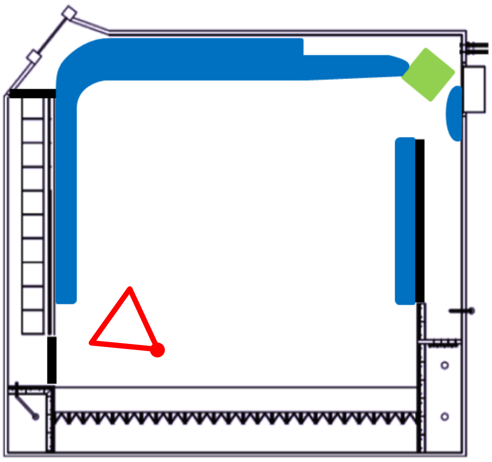

Figure A.2 Lower view of damping material along left boundary of the Delta Basin (X =0 m). Wooden plates are placed along the not used second wave machine.

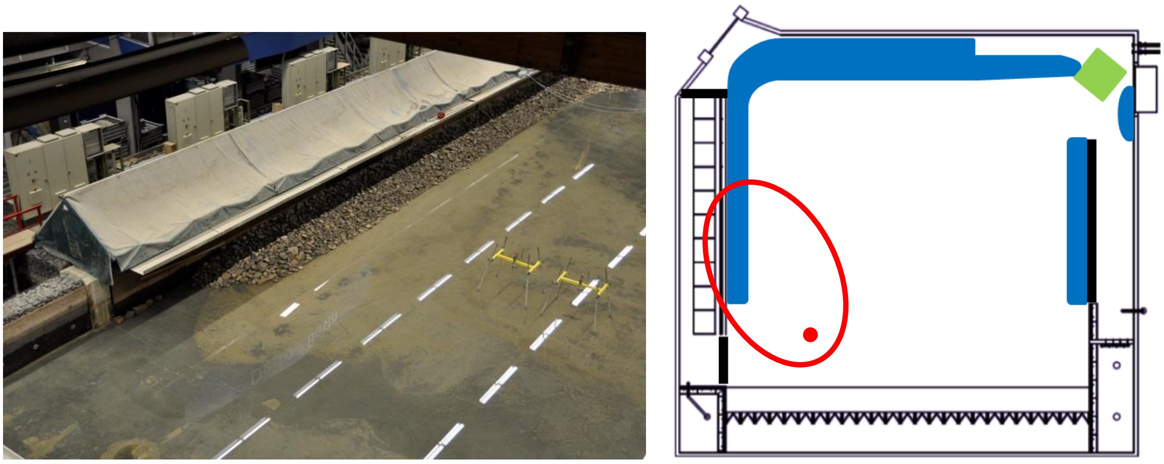

Figure A.3 Top view of damping material along left boundary of the Delta Basin (X =0 m).

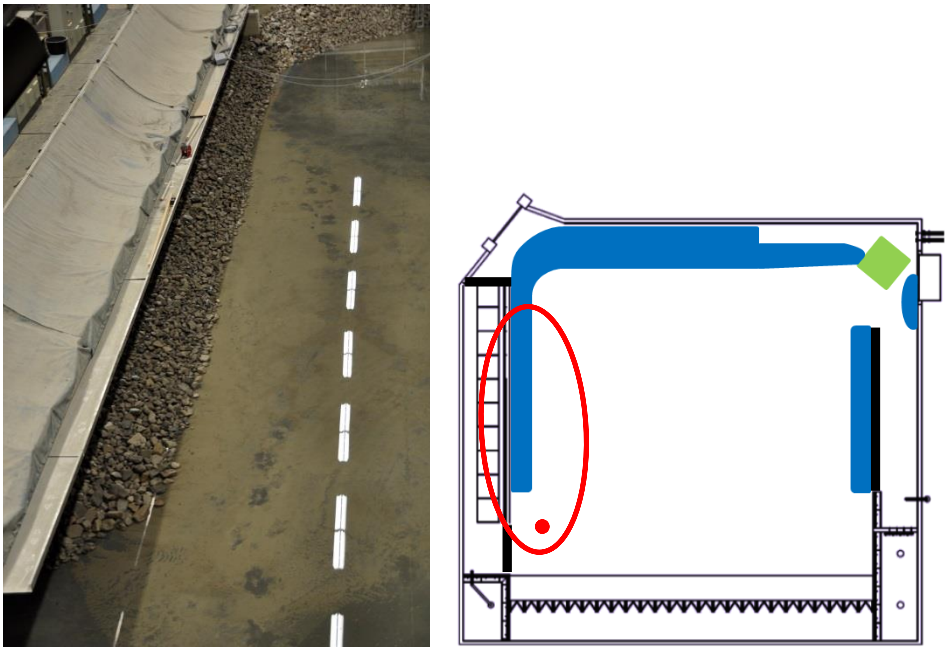

Figure A.4 Top view of damping material along left boundary of the Delta Basin (X =0 m).

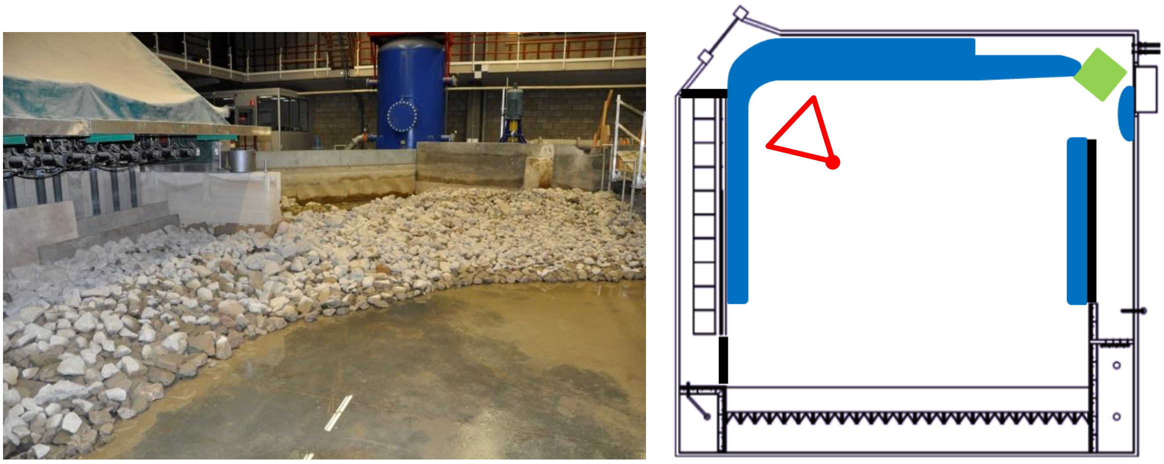

Figure A.5 Lower view of damping material in the upper left corner of the Delta Basin (X = 0 m, Y = 40 m).

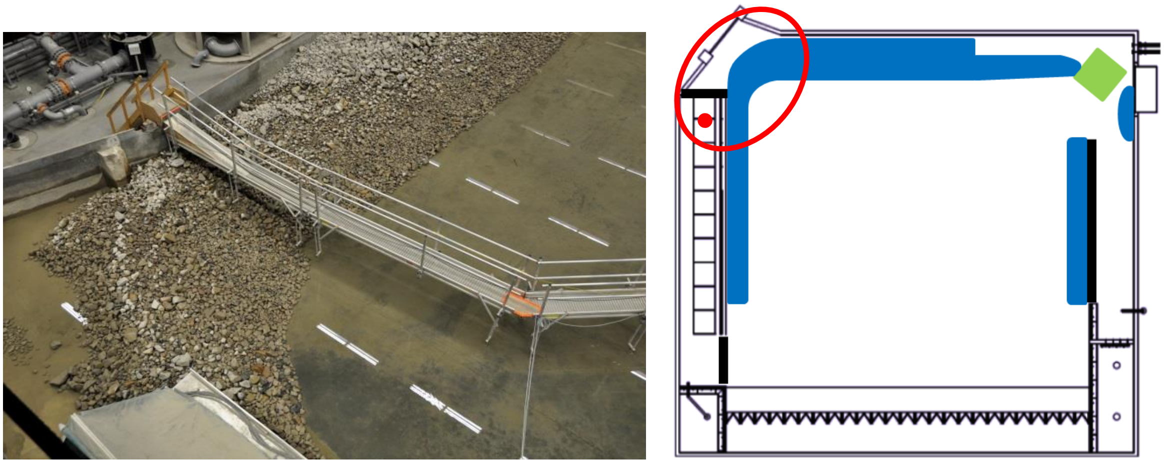

Figure A.6 Top view of damping material in the upper left corner of the Delta Basin (X = 0 m, Y = 40 m).

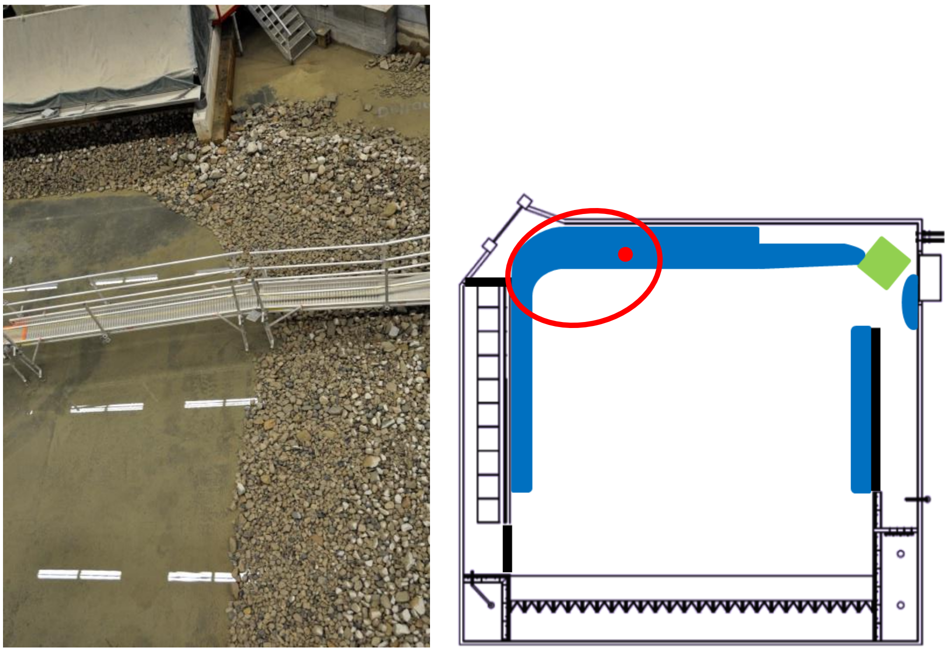

Figure A.7 Top view of damping material in the upper left corner of the Delta Basin (X = 0 m, Y = 40 m).

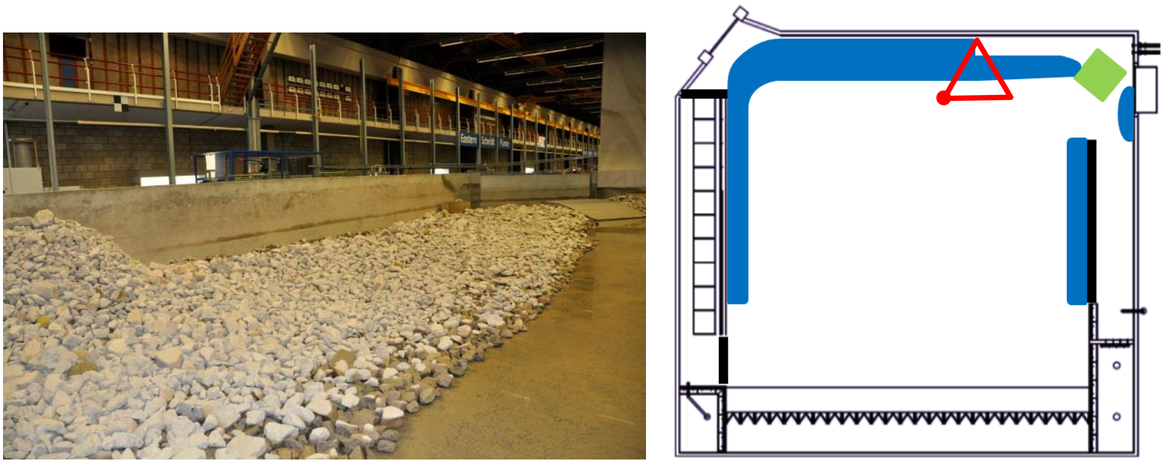

Figure A.8 Lower view of damping material along the upper wall of the Delta Basin (Y = 40 m)

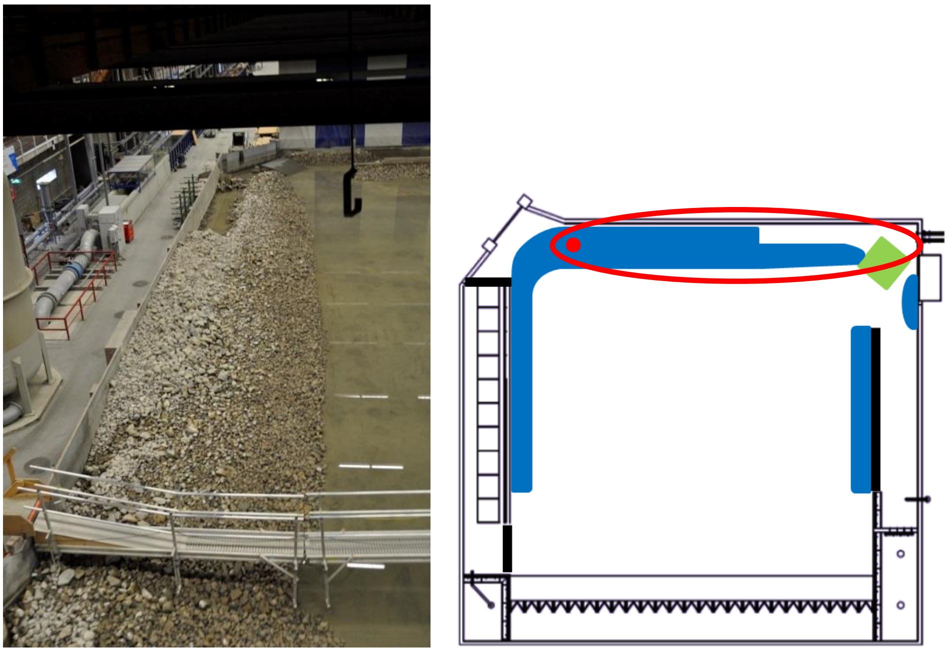

Figure A.9 Top view of damping material along the upper wall of the Delta Basin (Y = 40 m).

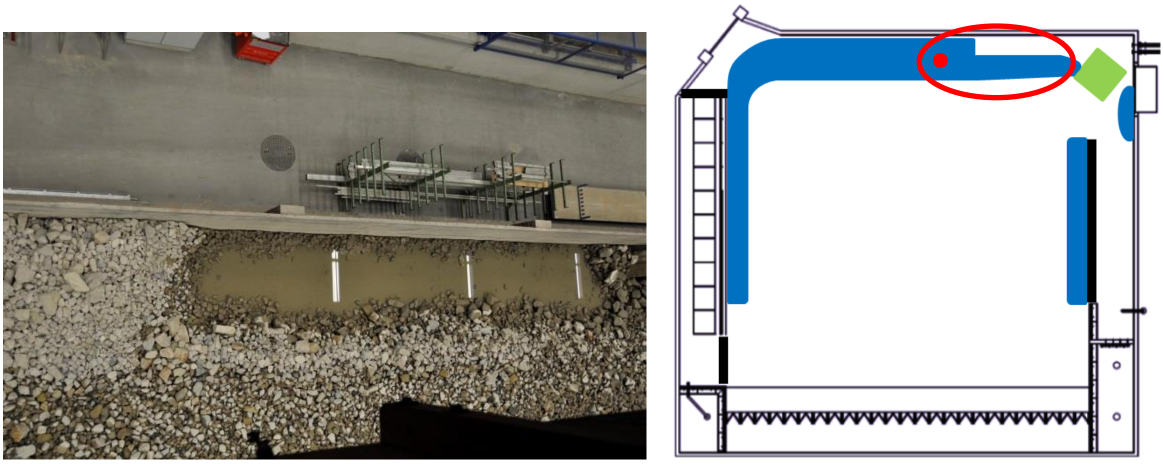

Figure A.10 Top view of damping material along the upper wall of the Delta Basin (Y = 40 m).

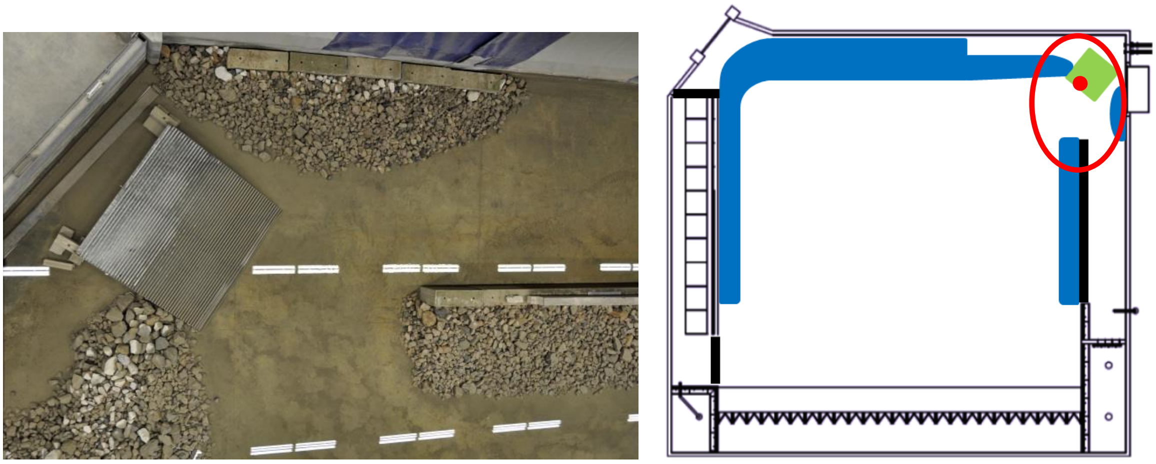

Figure A.11 Top view of damping material in the upper right corner of the Delta Basin (X = 40 m, Y = 40 m).

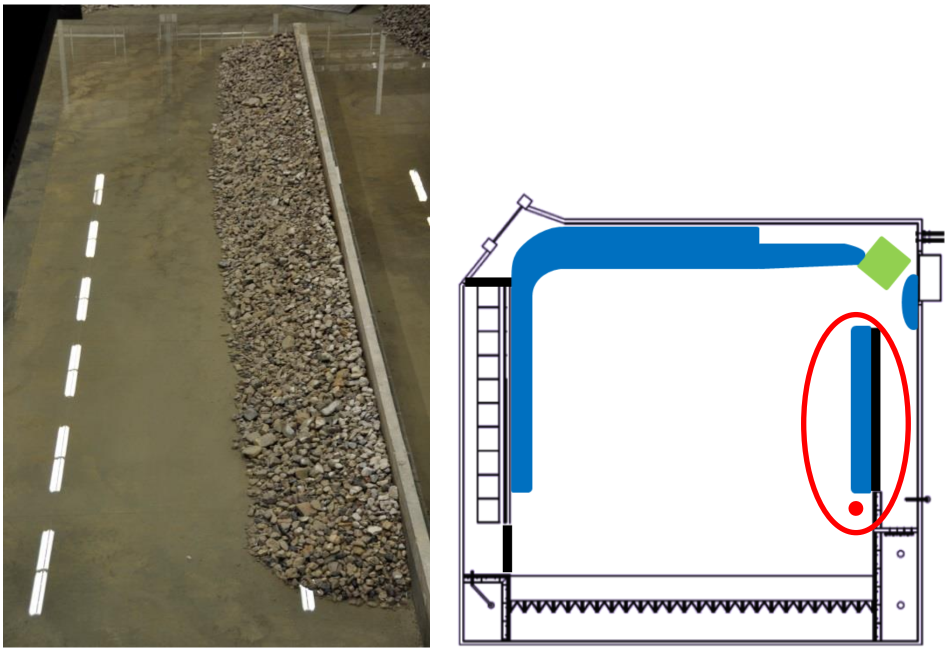

Figure A.12 Top view of damping material along the right wall of the Delta Basin (X = 40 m).

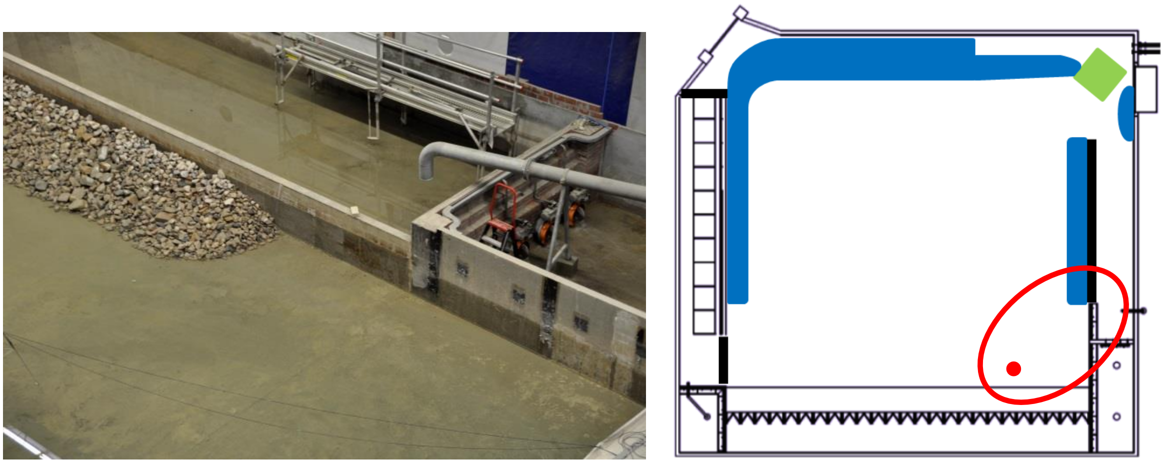

Figure A.13 Top view of damping material in the lower right corner of the Delta Basin (X = 40 m, Y = 0 m).

B Folder AukePC

Wave software for experimental facilities

AukePC

Deltares systems

Deltares

Enabling Delta Life

Wave software for experimental facilities

AukePC

Deltares systems

Deltares conducts experiments in its own facilities for among others water research. The results of these experiments allow us to validate our models and to test, for example, the optimal design of harbours, breakwaters and dikes, or the response of dune to wave load.
A lot of these experiments involve waves. These waves must be generated by a wave generator and at strategically chosen points in the experimental facility they must be measured. The measured waves must be processed and analysed. For these purposes the software package AukePC has been developed to generate, measure and process waves.

General

AukePC is a software package for use in hydraulic laboratory facilities. It has been developed at Deltares.

The software package AukePC consists of the following modules:

- **AukePC/Generate**
  This module computes the motion of the wave board segment(s) that is required to obtain the desired wave conditions.

- **AukePC/Process**
  This module handles the processing of wave data by a set of programs

- **AukePC/ARC**
  The aim of the ARC functionality is to reduce unwanted re-reflections of waves against the wave board by absorbing the waves coming from the flume or basin at the moment they reach the wave board.

- **AukePC/Measure**
  This module is a data acquisition system, comprising both hardware and software.

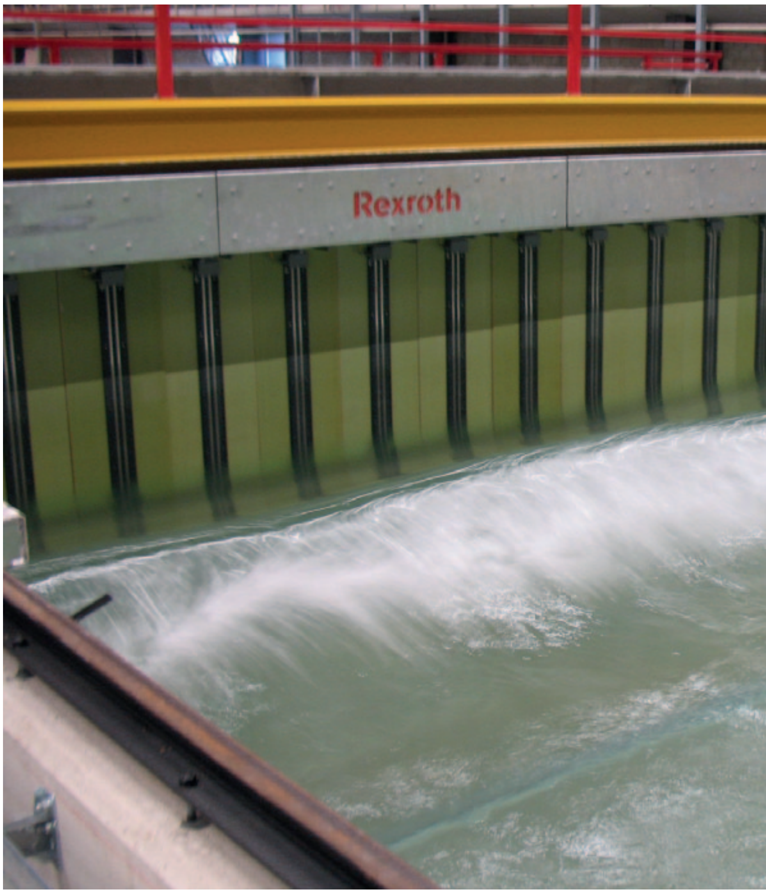

Wave generator in Atlantic Basin

AukePC/Generate

AukePC/Generate is wave generation software developed by Deltares. This software computes the motion of the wave board segment(s) that is required to obtain the desired wave conditions. The software can be used for both single-segmented wave generators (e.g., for uni-directional wave generation in a flume) and multi-segmented wave generators (e.g., for multi-directional wave generation in a basin). Depending on the type of wave generator, the following modules are available:

- **Single-segmented wave generator:**
  - AukePC/Generate: first-order module.
  - AukePC/Generate: second-order module (optional).
  - AukePC/Generate: ARC preconditioning module (optional).

- **Multi-segmented wave generator:**
  - AukePC/Generate: first-order module.
  - AukePC/Generate: second-order module (optional).
  - AukePC/Generate: ARC preconditioning module (optional).
  - AukePC/Generate: Dalrymple side-wall reflection module (optional).

Wave generator creating a small wave

The first-order module is mandatory. The optional modules are add-ons, and can be purchased independently of each other.

All AukePC/Generate modules can be used for the following most-commonly used types of wave boards:

- Translatory (piston motion) wave boards.
- Rotating (flap motion) wave boards with a variable hinge position. The hinge position may be between the floor and the still water level, or below the floor (a so-called virtual hinge postion).

- **First-order module**
  The first-order module of AukePC/Generate is capable of computing wave board signals for a number of wave types based on first-order (linear) theory:
  - Regular waves.
  - Multi-chromatic waves.
  - Irregular (random) waves, satisfying a user-defined energy density spectrum with a pre-defined shape (e.g., JONSWAP, Pierson-Moskowitz) or user-defined shape (in the form of a table)

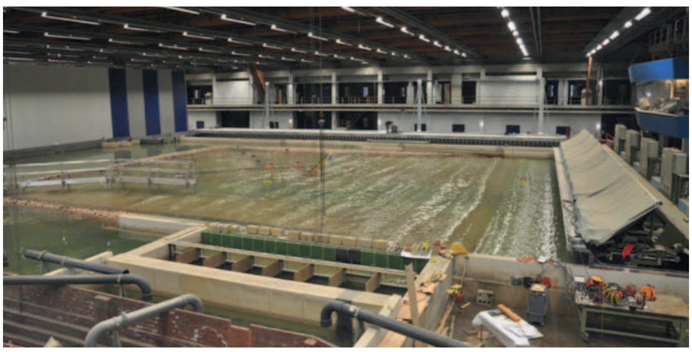

Delta Basin wave generator in action

For multi-segmented machines, the software include the generation of:

- Long-crested waves in perpendicular (=flume mode) or oblique direction.
- Short-crested (multi-directional) waves, satisfying a user-defined directional spreading with a pre-defined shape (e.g., cos2s and normal distribution) or user-defined shape (in the form of a table). The latter includes the generation of 2D frequency-directional spectra from a table (so-called 'bimodal seas' or 'wind sea – swell systems').

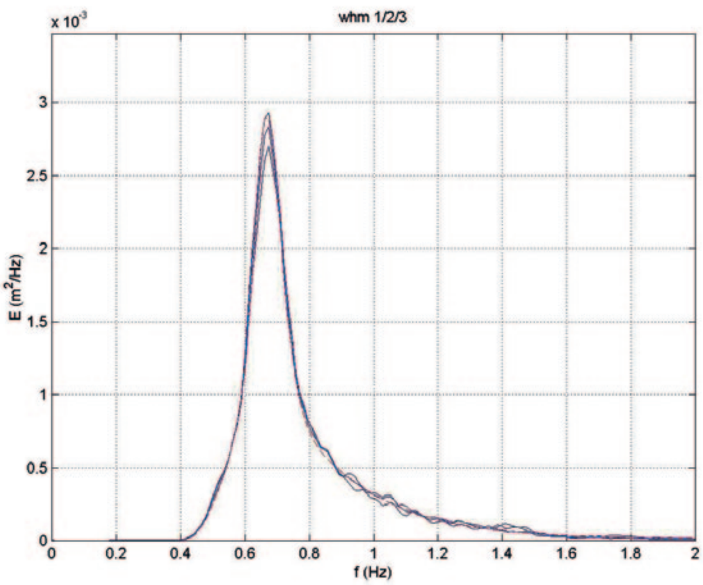

Spectrum of irregular waves in a flume. Red line: imposed spectrum; blue lines: measured spectrum at three distinct locations

Special features in the software are:

- Reproduction of a wave elevation time trace at a specific location in the flume or basin (long-crested waves only).
- Generation of wave groups with pre-selected group steepness and group length characteristics.
- Correction of the imposed wave board signal through a frequency-dependent correction factor file, for improved matching to the target spectrum.

- **Second-order module**
  While the first-order module of AukePC/Generate is capable of generating highly accurate waves, there are some physical phenomena which will disturb the wave field. One aspect is that the wave board motion should account for the second-order sub-harmonic and super-harmonic bound frequencies to the specified wave field. If this is not the case, spurious free waves are generated at the wave board. The second-order module of AukePC/Generate includes corrections to the wave generation signal up to second-order (according to Stokes' theory). This enhances the wave field as produced by the wave generator. An example of a measured wave train and a comparison to fully nonlinear theory (Rienecker & Fenton (1981), 'A Fourier approximation method for steady water waves.' J. Fluid Mech., vol. 104, pp. 119-137) is shown in the figure.

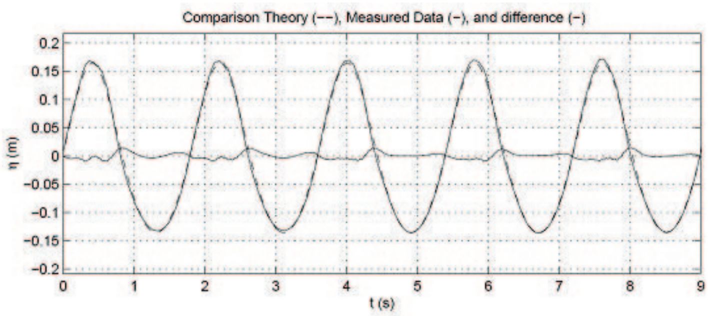

Comparison of measured wave train, generated with the second-order module, against the theoretical wave train

The second-order module is available for the generation of long-crested waves (regular, multi-chromatic and irregular) in perpendicular and oblique directions.

- **ARC preconditioning module**
  In case the Active Reflection Compensation (ARC) functionality is purchased (see further on), improved performance is obtained by a suitable preconditioning (offline adaptation) of the wave signal. This is done by the AukePC/Generate ARC preconditioning module. Time delay in the ARC feedback loop and a reduced mechanical transfer at high frequencies lead to inconsistencies in the treatment of the wave signals as measured by the ARC wave gauges: part of the imposed incident wave signal becomes interpreted incorrectly as a reflecting wave that needs to be absorbed. It is possible to anticipate for these inaccuracies. This is done in the ARC preconditioning module.

- **Dalrymple side-wall reflection module**
  The finite length of a wave generator and the presence of reflective side-walls create, in case of waves in oblique directions, so-called shadow areas in the laboratory basin. This limits the effective basin area. For the situation as shown in the figure, the red line shows the effective area at a distance *D* from the wave board. Note that, for ease of discussion, diffraction effects are omitted in the figure.

  The Side-Wall Reflection method (Dalrymple, R.A. (1989). 'Directional wavemaker theory with sidewall reflection.' J. of

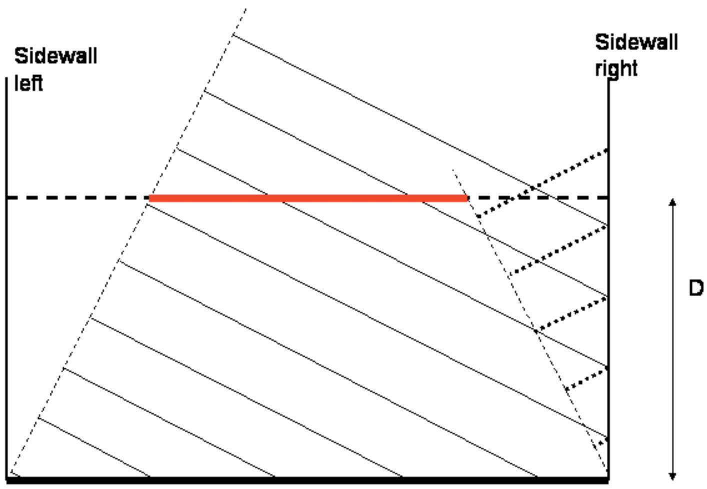

Reduction of effective area in a basin in case of oblique wave directions

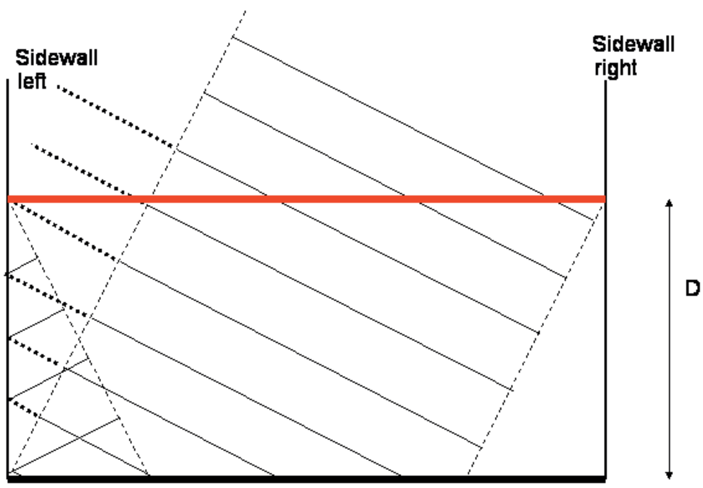

Application of the Dalrymple's Side-Wall Reflection method to increase effective basin area

Hydraulic Research, vol. 27, no. 1, pp. 23-34) accounts for the linear diffraction effects and uses side-wall reflection to generate a user-specified wave train at a specified distance from wave generator over the entire width between the side-walls. Putting it simply and referring to the situation sketched in the figure: the most right part of the wave generator is not generating waves (to avoid reflections against the right side-wall which will then propagate in the wrong direction); the central part of the wave generator is generating the user-specified waves; the most left part of the wave generator is generating a combined wave field consisting of the user-specified waves and waves to be reflected (on purpose!) at the left side-wall. This effectively increases the model area which can be used, as illustrated in the figure.

AukePC/Process

AukePC/Process handles the processing of wave data by a set of programs. Wave data can come from laboratory instruments such as:

- **Wave gauges:** time series of surface elevation
- **Pressure sensors:** time series of pressures
- **GRSM gauges:** time series of surface elevation and horizontal orbital velocities in the same location.

The input data of an AukePC/Process program may be a wave data signal obtained in an experimental facility (as above) or the result of a previous processing program. The results are shown in tabular and graphical form and are written to file. AukePC/Process has a special plotting program (Aukeplot) that is used to make the graphs, and provides the user with optimal control.

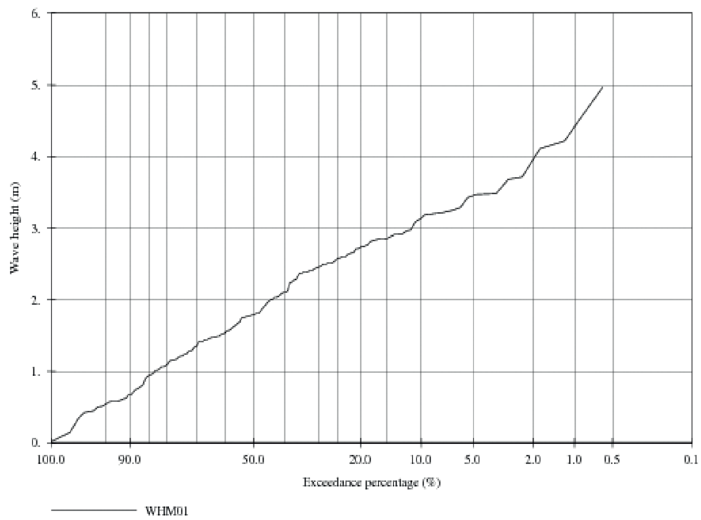

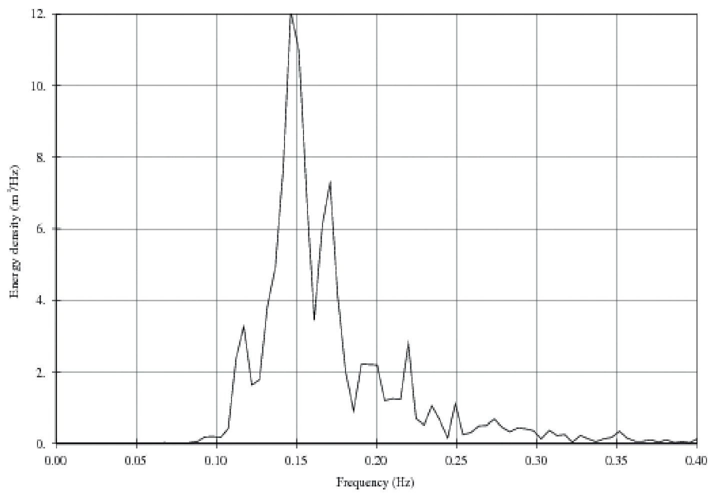

Example of time domain (wave height exceedance curve) and frequency domain (wave spectrum) processing

In AukePC/Process there are three types of programs:

- Non directional processing programs
- Directional processing programs
- Auxiliary programs

They are discussed below.

- **Non directional processing programs**
  These programs are used to process non-directional data.
  - **DistanceMF**: Advises the user about the position of wave gauges for reflection measurements.
  - **Filter:** Filtering of series with an equidistant time step: derivative, Hilbert Transform, integration.
  - **Harmo:** Harmonic analysis of regular waves.
  - **ReflecMF:** Incident and reflected spectrum computation based on the method developed by Mansard and Funke (1980), incl. spectral parameters of incoming waves
  - **Spectrum:** Computation of variance density spectra and spectral parameters in the frequency domain. Various windows and tapers (Hanning, overlap, rectangle, cosine, sine) can be used. The parameters are the significant height Hm0, the spectral moments mi, the peak frequency fp, peak period Tp, weighted peak period TpD, spectral periods such as Tm0,1 and Tm0,2 as well as spectral narrowness parameter $\varepsilon2$ and the broadness parameter $\varepsilon4$.
  - **Waves:** Wave parameter computation in the time domain. Output includes root-mean-square wave height Hrms, maximum wave height Hmax, significant wave height H1/3, T1/3, H1/10, T1/10 (both up-crossing and down-crossing methods), the exceedance probability of wave height, the groupiness κ and the coefficient of linear correlation r.

- **Directional processing programs**
  These programs are for use for data with directional information. The data is processed to obtain 2D frequency-directional spectra on the basis of simultaneous recordings of surface elevation and velocities.
  - **Maxent:** Computation of directional information with the Maximum Entropy Method.
  - **Polar:** Polar presentation of directional spreading.
  - **Thr3D:** Three dimensional presentation of directional spreading.

Waves in the Atlantic Basin

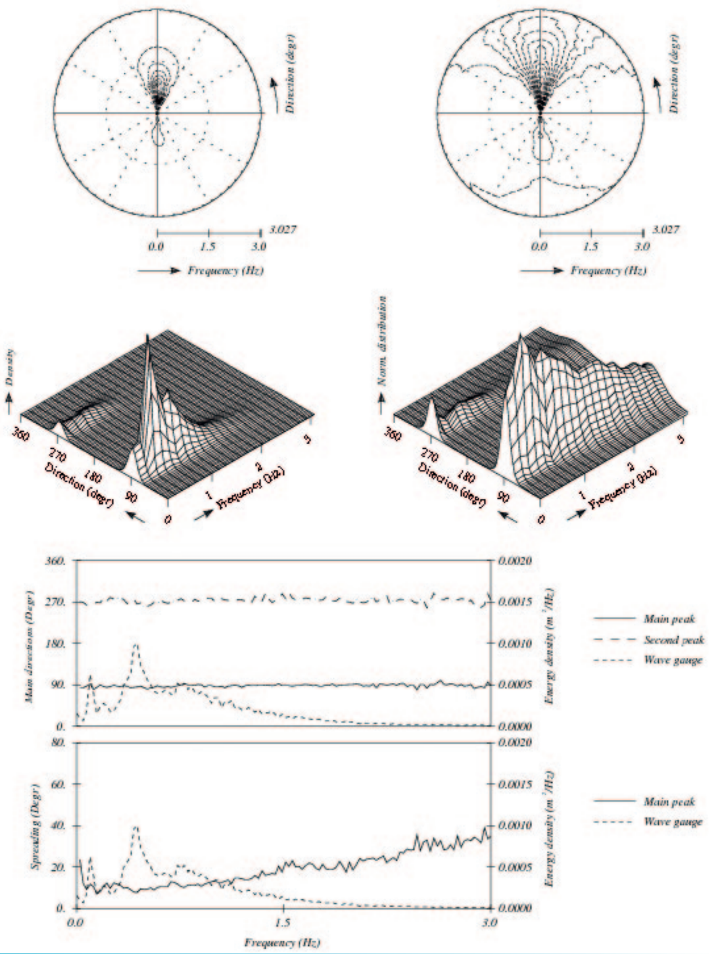

Example of directional processing

- **Auxiliary programs**
  These programs support the processing.
  - **Ascii:** Conversion of binary data to Ascii.
  - **Aukeplot:** General AukePC/Process plotting program.
  - **Conasc:** Conversion of Ascii-files to binary data files.
  - **Extract:** Extraction of series from various series files which are combined to a new series file.
  - **Extreme:** Determination of extreme values
  - **Parplot:** Combining parameter values to series for plotting.
  - **Partable:** Write parameter values in a table.
  - **Statist:** Computation of statistical parameters such as mean, standard deviation, skewness, kurtosis.

AukePC/Active Reflection Compensation

A Significant improvement in the wave field in flumes and wave basins can be made by equipping the wave generator with the Active Reflection Compensation (ARC) functionality. The aim of the ARC functionality is to reduce unwanted re-reflections of waves against the wave board by absorbing the waves coming from the flume or basin at the moment they reach the wave board. ARC is running simultaneously with generation of the target incident waves, so the wave board generates the target incident waves and absorbs the unwanted waves at the same time. Equipping a wave generator with the ARC functionality requires additional hardware and software, and a real-time connection to the wave generator control system. The additional hardware concerns ARC wave gauges mounted to the wave boards and the related wave signal data acquisition. The AukePC/ARC software computes real-time the additional motion that the wave generator must make in order to absorb the undesired waves. This information must real-time be transferred to the wave generator control system.

The ARC functionality can be incorporated in existing wave generators, provided they satisfy certain hardware and software characteristics. Please use the contact information in this document for more on this.

In case of buying a new wave generator, we recommend to purchase a Bosch Rexroth wave generator and equip it with the ARCH functionality. Here, ARCH stands for Active Reflection Compensation HyPCoS. In the ARCH software, the Active Reflection Compensation software by Deltares cooperates with the HyPCoS wave generator control software by Bosch Rexroth. From experience (Marin, Coppetec, Deltares (two machines), Hannover), we know that the Bosch Rexroth hardware (wave generators) and software (HyPCoS) operate very well with the AukePC/ARC software.

Installation of the ARC functionality in your wave maker system leads to a tremendous reduction of the re-reflections in a facility (flume or basin). As a consequence, the resulting wave field is much more similar to the desired wave field than in case no ARC is employed.

- **Motivation for using Active Reflection Compensation**
  Active reflection compensation (ARC) in the present context refers to the use of the wave maker not only as a wave generating device, but also as a wave absorbing device. Wave generation and active wave absorption can be executed simultaneously. In fact, this is the default way of working. There are various reasons for employing ARC:
  - To avoid spurious re-reflections from the wave maker, thereby spoiling the target incident waves.
  - To prevent resonant oscillations in the flume or basin, which reduce the maximum test operation.
  - To reduce the flume or basin stilling time between tests substantially (say, from an hour to a couple of minutes) by quickly removing the otherwise slowly damped low-frequency oscillations.
  - To make the experimental results less sensitive to the placing of artificial boundaries constituted by wave makers, and thus to make them easier to interpret.

In order to explain the necessity of having ARC in a facility, consider first the prototype situation, see Figure 1. This is the real-life situation somewhere out there in the field. The wave field near the structure (a harbour, a breakwater, a dike, a coastline, etc) always consists of an incident part (the incoming waves) propagating towards the structure, and the reflected waves propagating seawards (away) from the structure.

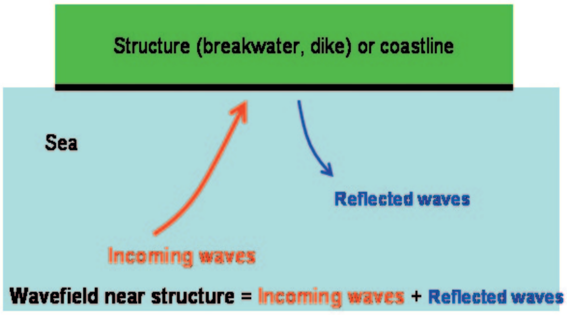

Figure 1. Prototype situation, to be modeled in the lab

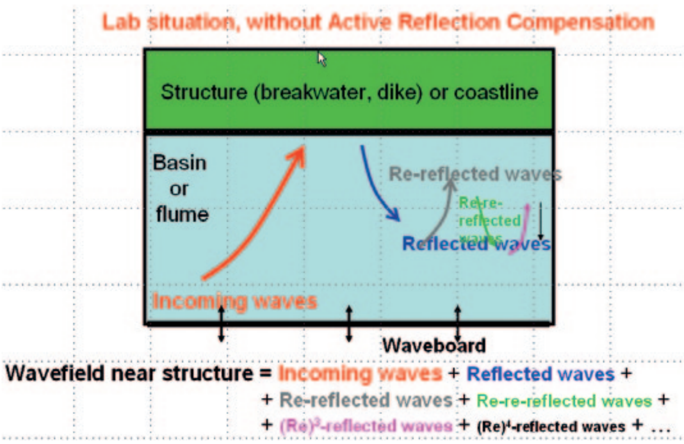

Figure 2. Laboratory model situation, without ARC

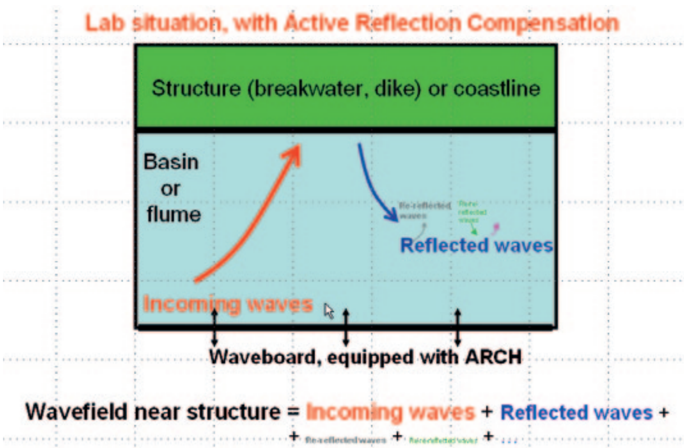

Figure 3. Laboratory model situation, with ARC

The next step is to make a laboratory model of the prototype situation. It is inevitable that additional model boundaries are introduced. These boundaries are formed by the side-walls of the facility and by the wave maker. The model boundaries lead to unwanted (because not present in the prototype situation) reflections. Therefore, at the side-walls of basins often gravel beaches are employed to provide additional damping (passive). Also the wave board itself gives – without arc – significant reflections. In other words, in a facility the wave field consists of two parts:

- The wanted part. This consists of the target incoming waves (provided by the wave maker) and the reflected waves (the target waves that have reflected at the structure, and may interact with the target incoming waves).
- The unwanted part. This part consists of the re-reflected waves (reflection of the reflected waves at the wave board), the re-re-reflected waves (reflection of the re-reflected waves at the structure), the re-re-re-reflected waves (reflection of the re-re-reflected waves at the wave board), and so on.

This leads to a polluted wave field, as graphically depicted in Figure 2.

In case ARC is employed, the re-reflection at the wave board is significantly reduced. Of course, also the subsequent re-re-reflections are reduced significantly, to a point of non-existence. This leads to a much less spoiled wave field, as depicted in Figure 3.

To estimate the amount of wave field pollution due to the absence of ARC, and the effect that inclusion of ARC has, a crude model is devised. Let the wave height of the wanted wave field be indicated by H_{wanted}, and the wave height of the unwanted wave field by $H_{unwanted}$. Furthermore, let the reflection coefficient (defined in terms of wave height) at the structure be denoted by r_s, and the reflection coefficient at the wave board by r_w. It is precisely this coefficient r_w that ARC aims to reduce. It is not hard to prove that the ratio R between the wanted wave height and the unwanted wave height is given by:

$$R = \frac{H_{unwanted}}{H_{wanted}} = \frac{r_w r_s}{\sqrt{1 - r_w^2 r_s^2}}$$

The value for R should be as small as possible, with R=0 being the ideal situation. Let's now insert some representative values. Assume a value for the reflection coefficient of the structure: r_s= 0.4. As mentioned, the influence of ARC lies in the coefficient r_w.

- No ARC included. With a typical value of r_w= 0.9, we get: R= 0.39. This means that the wave field is significantly spoiled. This situation must be considered as unacceptable.
- With ARC included. With a typical value of r_w= 0.1, we get: R= 0.04. This means that the wave field is hardly spoiled with undesired re-reflections. This is considered as acceptable.

- **ARC software and hardware**

  Getting ARC operational in a facility, requires installation of the ARC software and hardware. The ARC software uses the surface elevation measured by an ARC wave gauge mounted at each wave board segment, and computes a real-time correction to the wave board motion, see the figure.

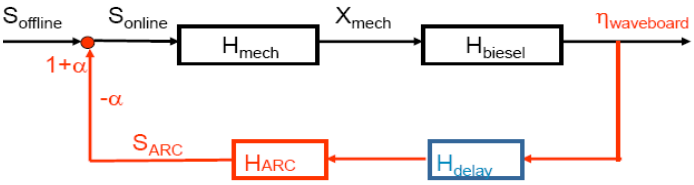

Diagram of the wave generator, with the ARCH feed-back loop in red

Here, $S_{offline}$ is the offline wave board signal as computed by AukePC/Generate. The ARC correction S_{corr} is added to the offline signal, leading to the online signal S_{online}=(1+α)$S_{offline}$-αS_{corr} The factor α, which is unity by default, controls the relative influence of the ARC motion on the total signal. The wave board signal S_{online} leads to a mechanical motion X_{mech} of the wave board, with H_{mech} representing the mechanical transfer function. The motion of the wave board leads, through the Biésel transfer function, to a target incident wave η_{target}. The measured total wave signal at the wave board, η_{meas}, contains not only the target incident wave (η_{target}), but also the reflected wave $\eta_{ref\ 1}$. The latter needs to be absorbed. This is done by suitable adjustment of the total wave board signal. The ARC routine computes the required correction $S_{corr}$to the wave board signal.

- **Expected performance**

  The performance of ARC, i.e. the amount in which re-reflections at the wave board are suppressed (i.e. the value of r_w), depends on various aspects, such as the type of wave generator (piston or flap), the quality of the hardware and software, the stiffness of the machine, the power of the machine engines, the machine electronics etc.. Also, the ARCH performance of a given system varies somewhat with the water depth and the wave conditions. Based on results in the past, typical values of r_w range between 5% and 15% for the most relevant wave conditions. Some results obtained in a flume which is perfectly equiped for ARC (the Scheldt flume at Deltares) are shown in the figure.

  As mentioned above, the un-wanted re-reflections can cause a significant amount of undesired wave field ‘pollution’. The figure shows a target spectrum (in black) and two measured spectra. The green line is obtained with ARC on, while the red line is obtained with ARC switched off. The strong spurious peaks occur at the resonance frequencies of the basin. These peaks constitute significant deviations from the target wave field.

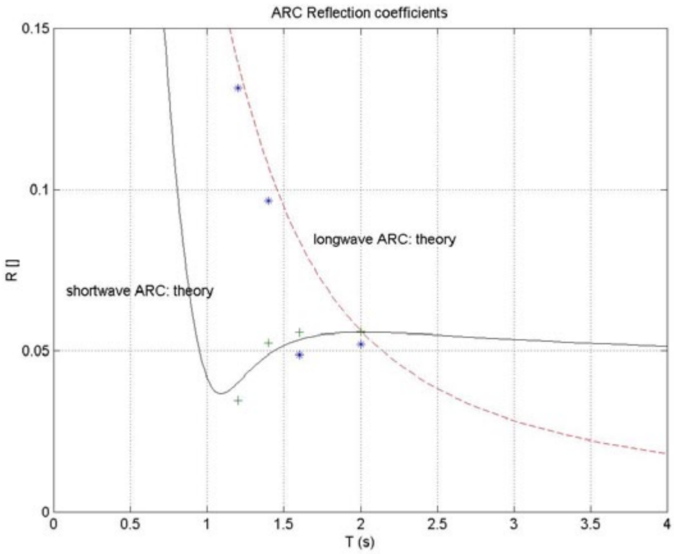

Reflection coefficients in Scheldt flume. Theoretical curves and observations

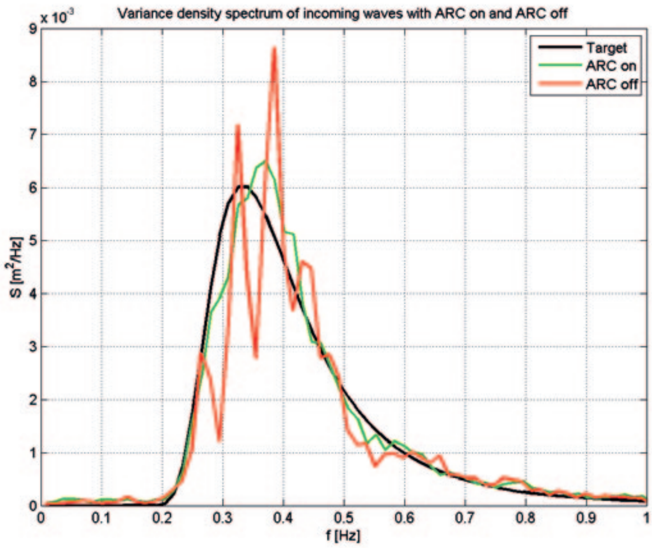

Target spectrum (in black) and two measured spectra

AukePC/Measure

The module AukePC/Measure is a data acquisition system, comprising both hardware and software. It is configured for operation in a PC environment under MS Windows. The standard version is primarily intended to acquire data of analogue instruments. On request digital instruments, e.g. counters and serial devices, can also be supported. The operator controls AukePC/Measure via a graphical user interface. Essential functions like set-up, data acquisition and performance monitoring are supported. While data acquisition is in progress, acquired data are graphically visualised in strip chart fashion and also displayed numerically. Most importantly, the data values are recorded in file (ASCII or binary).

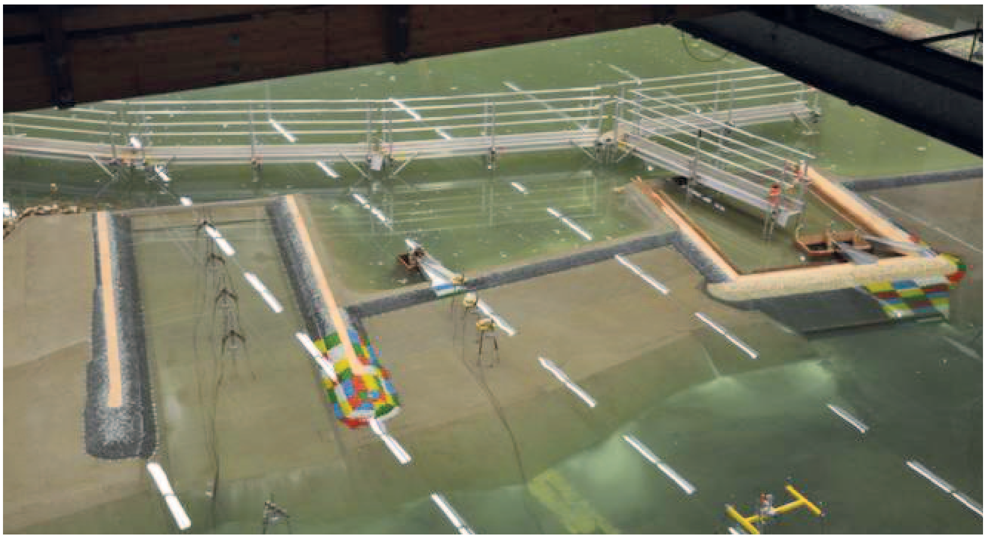

Scale model of part of harbour lay-out

ARC wave gauge

- **Hardware**

  AUKE/Measure supports a large variety of data acquisition hardware, e.g. internal cards, external cards, USB based, Ethernet based and others. The performance depends upon the capabilities of the data acquisition hardware, the type of PC interface and the performance of the PC. Typical data acquisition hardware supports 4 to 64 analogue input channels at a digital resolution of 14 or 16 bits. Input channels can be single ended or differential (hardware dependant). On most data acquisition hardware, the input gain can be adjusted under software control.

  Essential for the data acquisition hardware is that it supports the range of the signal voltages to be acquired. Some standard industrial output signal ranges are 0 to 5, 1 to 5, 0 to 10, -10 to +10, 2 to 10 Volt. The 1 to 5 (and 2 to 10) voltage ranges typically pertain to current loop signals (4 to 20 mA) with the loop closed by a resistor. The output signals of the Deltares' standard laboratory instruments like PEMS, UHCM, OSLIM, OPCON, ASTM, WAVO, GHM and PV-09/11, have output ranges from -10 to +10 volts or 0 to 10 volts. However, AUKE/Measure supports any instrument of any manufacturer provided the instrument output analogue signal is compatible with the input range of the data acquisition hardware. Most data acquisition hardware can accommodate instruments producing smaller output signals by stepping-up the input gain, support of mixed input gain settings is rather common. The input impedance is high, which limits signal loss over longer cables. The standard hardware supports BNC input connectors, bulkhead version. To accommodate easy access, the input connectors have been installed in one or more rows on a terminal box, the latter is connected to the data acquisition hardware. Other connection techniques, e.g. by screw terminals, can be delivered upon request. The figure shows a 'Channel Settings' window with a typical variety of supported instruments.

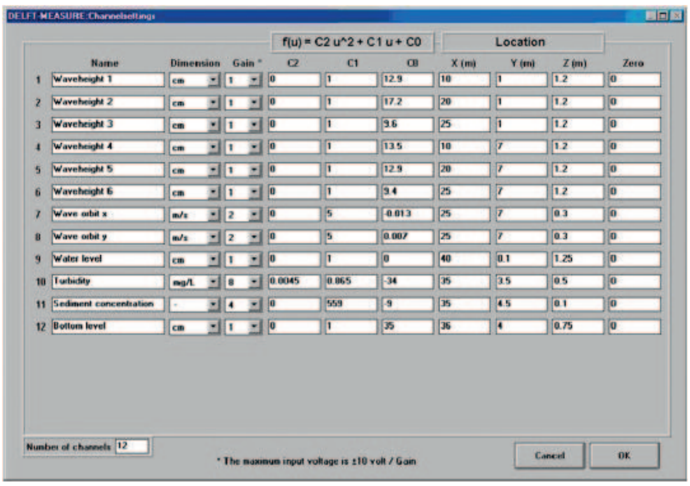

DELFT-MEASURE:Channelsettings

				f(u) = C2 u^2 + C1 u + C0			Location			
	Name	Dimension	Gain *	C2	C1	C0	X (m)	Y (m)	Z (m)	Zero
1	Waveheight 1	cm	1	0	1	12.9	10	1	1.2	0
2	Waveheight 2	cm	1	0	1	17.2	20	1	1.2	0
3	Waveheight 3	cm	1	0	1	9.6	25	1	1.2	0
4	Waveheight 4	cm	1	0	1	13.5	10	7	1.2	0
5	Waveheight 5	cm	1	0	1	12.9	20	7	1.2	0
6	Waveheight 6	cm	1	0	1	9.4	25	7	1.2	0
7	Wave orbit x	m/s	2	0	5	-0.013	25	7	0.3	0
8	Wave orbit y	m/s	2	0	5	0.007	25	7	0.3	0
9	Water level	cm	1	0	1	0	40	0.1	1.25	0
10	Turbidity	mg/L	8	0.0045	0.865	-34	35	3.5	0.5	0
11	Sediment concentration	-	4	0	559	-9	35	4.5	0.1	0
12	Bottom level	cm	1	0	1	35	36	4	0.75	0

Number of channels 12

* The maximum input voltage is ±10 volt / Gain

Cancel OK

A 'Channel Settings' window with a typical variety of supported instruments.

- **Software**

  The AUKE/Measure software assists the operator in setting up a measurement, provides supervision of the data acquisition process and stores acquired data in various file types. File naming can be automatic or manual; the automatic file naming system also supports recording in consecutive files of equal length. This feature is in particular advantageous to limit file size when acquiring data from a large number of channels at a high sampling rate. The pass-over from the one file to the next is loss free, i.e. no samples will be skipped when closing the one file and opening the next. Several file formats are supported,e.g. numbered comma separated columns, tabbed columns and binary AUKE compatible. In setup files also naming, scaling, offset, dimensions and other parameters of individual data acquisition channels are recorded.

The graphic output supports visualisation of any combination of four out of n channels versus time. Both time and parameter axes can be adjusted to the specific needs of the project. The scale of the time axis is operator adjustable over a wide range, e.g. 1 second for fast signals to 3600 seconds for very slow signals; the maximum scale is 10000 seconds.

- **Specifications**

  The standard version of AUKE/Measure does not support RS232 interfaces; however, specific instruments can be supported upon request provided that the communication protocol is well defined. It should be noted that the specifications are typical for the supported hardware; the actual specification of a specific product may be different. Please contact Deltares for technical details about specific products. AUKE/Measure software and hardware are delivered as a fully working combination together with the required drivers and installation software. Installation is straight forward and simple to execute.

- **Some typical properties**
  - interfaces USB, PCI, Ethernet, RS232
  - input channels 4, 8, 16 or 64
  - mixed gain e.g. 1, 2, 4, 8 or 1, 10, 100
  - resolution 12, 14 (standard), 16 bits
  - data rate several ks/s
  - connection type SE / Differential
  - input impedance 1 MOhm

Waves on a grass dike

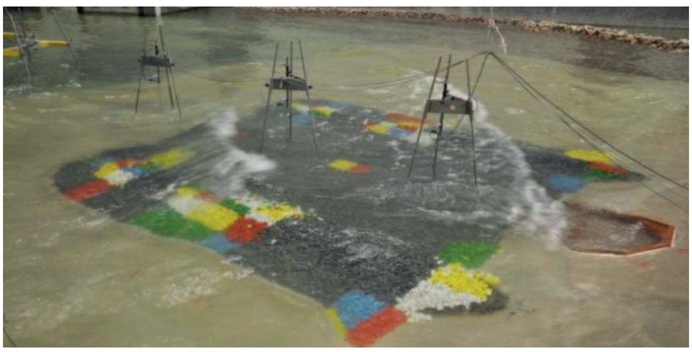

Waves over a submerged structure

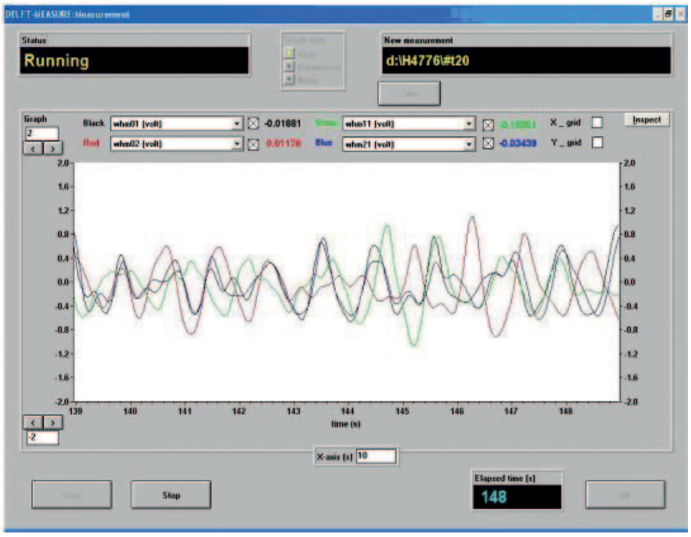

Visualisation of AUKEPC/Measure during an experiment

Manual

AUKEPC comes with a digital User & Technical manual, which contains all necessary information to use the program and understand the underlying formulae. This manual is available in pdf-format.

System requirements

AUKEPC is supported on Microsoft Windows XP or higher. The advised minimum requirements are a configuration consisting of:

	Minimal
Processor	1 GHz
Memory	1 GB
Disk free	1 GB

For AukePC/ARC and AukePC/Measure, dedicated hardware is required.

License

For this software package, node locked and floating licences can be issued. For more information on how to purchase this package please contact: delftchess.info@deltares.nl or visit our web site: www.deltaressystems.nl

Support

Deltares systems tools are supported by Deltares. A group of 70 people in software development ensures continuous research and development. Support is provided by the developers and if necessary by the appropriate Deltares experts. These experts can provide consultancy backup as well.

Deltares systems

PO Box 177
2600 MH Delft
Rotterdamseweg 185
2629 HD Delft
The Netherlands

+31 (0)88 335 83 00
delftchess.info@deltares.nl
www.deltaressystems.nl

C Technical note by RHDHV on mooring arrangement in the scale model

Note / Memo

HaskoningDHV Nederland B.V.
Maritime & Aviation

To: Arne van der Hout, Bas Reijmerink, Chris Clement, Gert van der Burg, Peter Bos, Willem van der Zon, Karel Roozen, Anastasia Karamperidou, Willemijn Pauw
From: Alex van Deyzen
Date: 11 December 2018
Copy: Cock van der Lem

Our reference: M&ANT1810161516
Classification: Restricted

Subject: **Mooring arrangement for ShoreTension model experiments**

1 Introduction

ShoreTension, Deltares, Royal HaskoningDHV, Vopak, Shell and Marin want to carry out physical model tests to explore the limits of the innovative ShoreTension mooring system for mooring locations exposed to waves [REF1].

The project plan [REF1] defines four cases for one moored ship:

A. In this case two ShoreTension units work strictly in longitudinal direction of the ship, as do the waves;
B. In this case two ShoreTension units work strictly in lateral direction of the ship, as do the waves;
C. In this case the ShoreTension units work in both longitudinal and lateral direction of the ship, but the relative wave directions are head on, beam on and bow-quarterly (basically a combination of Case A & B);
D. This case resembles a “real life” mooring arrangement, with mooring and breasting dolphins, spring and breast lines and fenders and ShoreTension units;

Figure 1-1 depicts sketches of mooring case A, B and C. The HMPE lines of ShoreTension are depicted in (——). A number of conventional mooring (— —) lines run parallel with the ShoreTension lines (similar to current practice) and some conventional lines (——) are used to keep the vessel at its place.

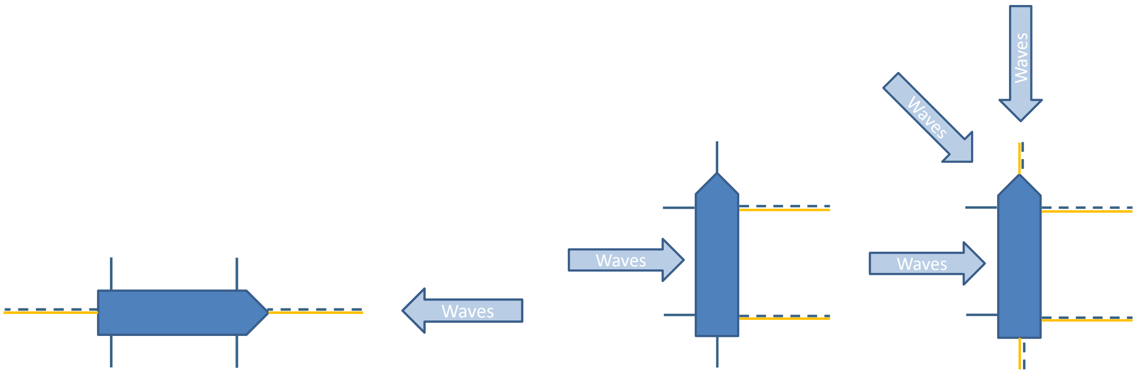

Figure 1-1: Sketch Case A, B & C

Currently, it is not known what spring stiffness to choose for the number of conventional mooring lines (— — & ——) for mooring case A, B and C nor what the stiffness of the HMPE lines of ShoreTension should be (——).

In this note, a reasonable stiffness for the conventional mooring lines for Case A, B & C and the stiffness of the HMPE lines attached to ShoreTension cylinders based on a more realistic mooring arrangement (Case D) is determined. For this a mooring arrangement for Case D needs to be designed based on OCIMF Mooring Equipment Guidelines [REF2]. The individual stiffness of each lines (dependent on the line properties and total length) and the horizontal and vertical angles determine the restoring force in surge, sway and yaw direction. The restoring force in surge, sway and yaw for Case D determine the spring stiffness to choose for the number of conventional mooring lines (— — & ——) for mooring case A, B and C. Four ShoreTension units are deployed for Case D: two as added to the spring lines and two added as breast lines.

Chapter 2 describes the mooring setup, i.e. ship main dimensions, line and fender specifications and the mooring arrangement for Case D according to OCIMF [REF2].

Chapter 3 presents the natural periods for surge, sway and yaw for the conventional mooring arrangement without ShoreTension® and stiffness of the individual lines for Case A & B & C based on Case D.

All presented values are on full scale.

2 Mooring setup

2.1 Ship

The ship that will be used for the experiments is the bulk carrier “The Flying Dutchmen”. Table 2-1 depicts its main dimensions. Originally, “The Flying Dutchmen” is a Capesize dry bulk carrier but for these model tests it has been assumed that it represents a big Aframax or a small Suezmax tanker.

Table 2-1: Main dimensions bulk carrier “The Flying Dutchmen”

Description	Symbol	Unit	Value
Length overall	L_{oa}	m	257
Length between perpendiculars	L_{pp}	m	252
Breadth	B	m	40
Depth	D	m	~20
Draft (loaded)	T	m	16.3
Displacement	Δ	t	135303.85
Block coefficient	c_b	-	0.84
Deadweight	DWT	t	~115,000

2.2 Lines

Aframax and Suezmax tankers carry 16 combi-lines (www.q88.com), i.e. steel wire and a 11 m synthetic tail. The tail is mostly fabricated from polyester or polypropylene or a mixture, but sometimes out of nylon. The Minimum Breaking Load (MBL) lies between 70-100 t. OCIMF Mooring Equipment Guidelines prescribes that the tails should have a 1.25 times higher MBL than the steel wire in case of a polyester or polypropylene tail [REF2].

For this research project the relevant property of the mooring lines is the individual line stiffness The exact MBL or tail material is not relevant. The individual line stiffness depends on the length of the steel wire, the length of the tail, the tail material and the wire and tail diameter (MBL). Figure 2-1 depicts the load-extension characteristics for different line materials.

For this project the following has been chosen:

- 16 mooring lines;
- Steel wire, MBL=80 t;
- 11 m Polyester tail, MBL=100 t;

Pre-tension is normally in the order of 5-10% of the MBL.

The HMPE lines have an MBL of 200 t.

2.3 Fenders

Based on a berthing energy calculation according to PIANC guidelines [REF6] a cone fender of capacity SCN1800-F1.0 has been selected. Table 2-2 presents the fender characteristics. Figure 2-2 depicts the load-deflection curve. The required berthing energy is 1962 kNm based on the following assumptions:

- Berthing speed: 120mm/s
- Berthing angle: 5°
- Construction: Jetty berthing, open structure
- Impact point: 33% from bow
- Underkeel Clearance: 1.7 m
- Safety factor abnormal berthing: 1.5
- Min / max. temperature: 0°C - 30°C

The minimum energy absorption capacity is 2250 kNm taking into account performance tolerance, angle factor, temperature factor and velocity factor. Trelleborg's cone fender SCN1800-F1.0 is suitable to absorb this berthing energy[1].

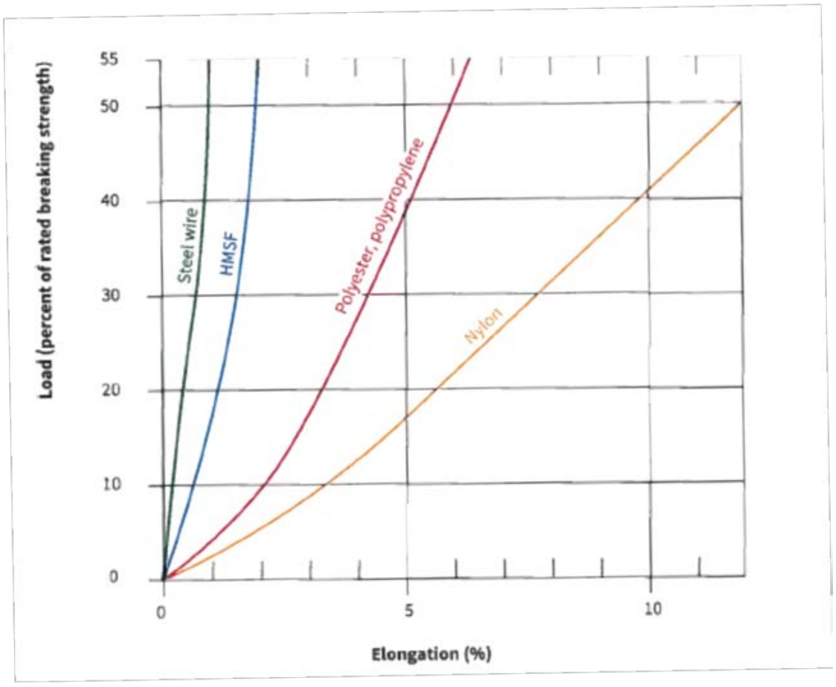

Figure 2-1: Load-extension characteristics mooring lines [REF2]

Table 2-2: Fender characteristics (source: Trelleborg)

Description	Unit	Cone fender SCN1800-F1.0
Height	m	1.8
Number	-	4
Energy	kNm	2327
Reaction force	kN	2171.5
Fender friction	-	to be discussed

[1] *Another fender type, e.g. floating foam fender, could also suffice. The load-deflection curve fir such a fender, however, is different. A floating foam fender has softer response characteristics than a cone fender.*

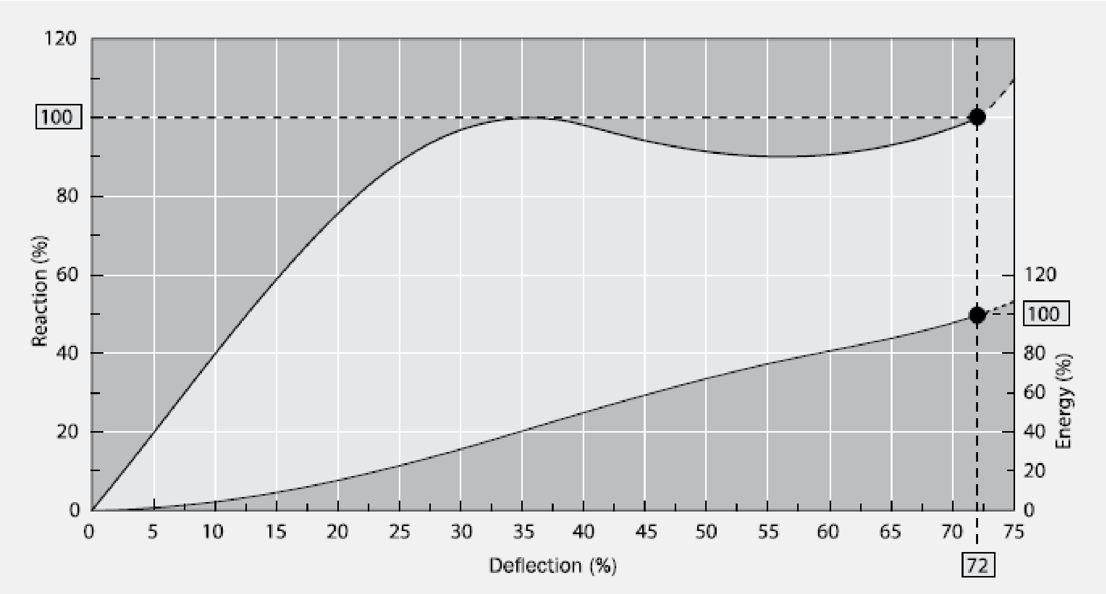

Figure 2-2: Load-deflection characteristic cone fenders (source: Trelleborg)

2.4 Mooring arrangement Case D

A conventional mooring arrangement according to the guidelines of OCIMF Mooring Equipment Guidelines has been designed [REF2]. The fairlead positions have been based on three Suezmax oil tankers: Meltemi, Eton and Brasil Voyager (respectively IMO 9298741, 9311610 & 9637777) [REF4, REF5]. Appendix 1 presents the fairlead coordinates. A port mooring has been assumed, based on the provided sketch of the mooring layout in the basin (Presentation Kick off_10-09-2018_Technical Part). The jetty will not be positioned in between ship and wave maker. Figure 2-2 depicts the top view of this mooring arrangement (without ShoreTension). The line lengths and horizontal line angles are according to the guidelines. For this project the spring lines are deployed to the outer breasting dolphins so that lines and fender equipment on model scale do not touch or cross[2].

For the vertical line angles the following parameters are relevant: water depth, tide, ballasted and loaded draft, depth and height of fairleads above main deck and height dolphins. The following values for these parameters have been assumed:

- Water depth and tidal range: Respectively 18 m and -0.7 - +1.5 m relative to Mean Sea Level (yielding a minimum underkeel clearance of 1 m in loaded condition);
- Ballasted draft: 12 m;
- All fairleads are 50 cm above main deck, the depth is assumed to be 20 m;
- Height dolphins and mooring points on dolphins: 4 m above 0 m tidal range[3];

Figure 2-4 depicts the front view of the mooring layout; loaded condition at low tide (-0.7 m + CD) and ballasted condition at high tide (+1.5 m +CD). The vertical line angles are for both loading conditions and water levels according to the guidelines.

[2] *In reality, there is also an option to deploy the spring lines to the inner breasting dolphins and to move the outer breasting dolphins further apart. This would restrict the yaw motion more. The effect of the fenders on the yaw motion, however, are not of interest for this study (i.e. in Case A, B and C there are no fenders).*

[3] *The height of the dolphins for jetties fully exposed to swell is probably more than 10 m. For this study, however, the exact height of the dolphins is not relevant. It would change the vertical angles of the mooring lines. This (slightly) diminished the contribution of each line to the restoring force in surge, sway or yaw direction. This influence, however, is not relevant for outcome of this study.*

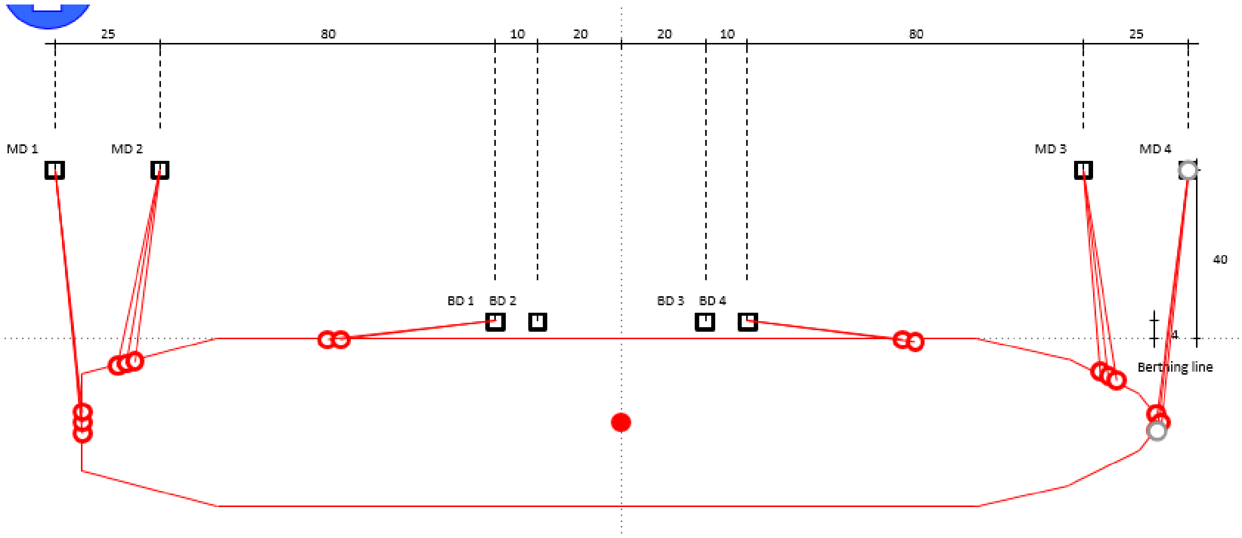

Figure 2-3: Top view mooring layout without ShoreTension units

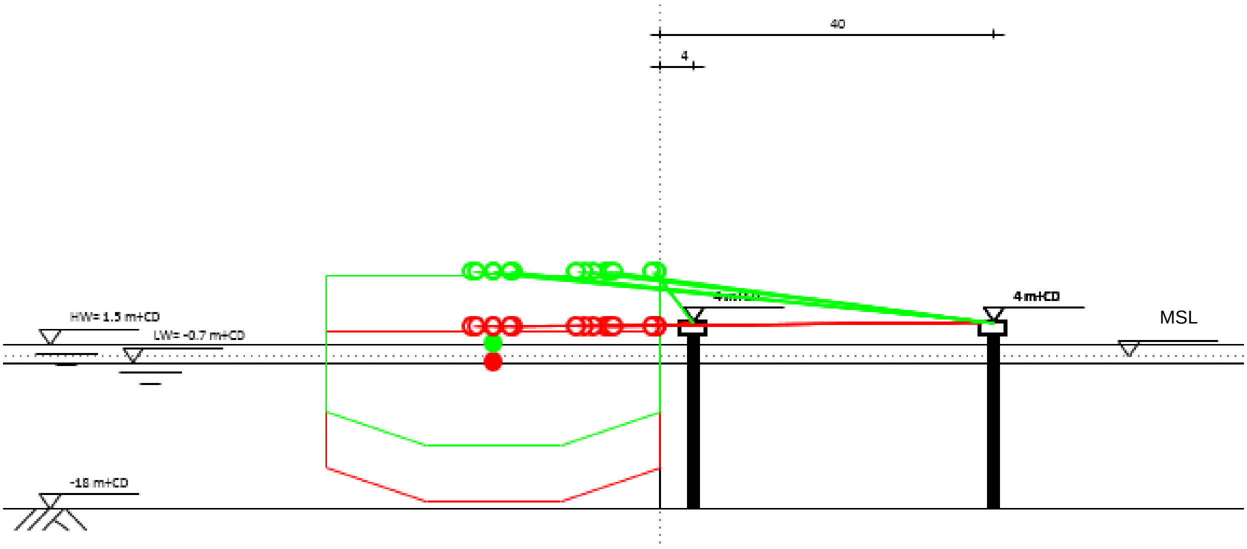

Figure 2-4: Front view mooring layout

For this research project the relevant aspects of the mooring arrangement are the total line lengths and angles. Table 2-3 depicts the suspended line lengths and the line angles for "The Flying Dutchmen" in loaded condition at Chart Datum. The lines are numbered from stern to bow. The horizontal angles for the breast lines are defined as the angle between the line and the perpendicular to the ship and for the spring lines as the angle between the line and the berthing line. For the line length on deck 5 m has been assumed for the breast lines and 20 m for the spring lines. The winches on the fore and aft deck are located in the vicinity of the fairleads. The winches for the spring lines are often located near the centre line of a Aframax or Suezmax tanker (B/2 = 20 m). The vertical angle is negligibly small. It has no effect on the restoring force in surge, sway and yaw direction.

For this research project it is also relevant to determine where the ShoreTension units are deployed. The black lines in Figure 2-5 show the deployment of two units on the bow/stern lines and two on the spring lines. The HMPE lines need to be deployed from the bow and stern because there are not enough fairleads available next to lines deployed to mooring dolphin 2 and 3. The line lengths and angles of the four HMPE lines is very similar to line 3, 7, 10 and 14 in Table 2-3. The suspended line lengths and angle for each HMPE line (numbered from stern to bow) are:

1. 56 m, 7° and 1°;
2. 43 m, 5° and 1°;
3. 43 m, 5° and 1°;
4. 58 m, 8° and 1°;

It has been assumed that a bollard in the vicinity of the fairlead is available to attach the HMPE line to. The line length on deck is therefore assumed to be 5 m for all HMPE lines.

The fenders are located on the four breasting dolphins; the centre of the fender panel is located 2 m above MSL.

Table 2-3: Suspended line lengths and line angles at Chart Datum in loaded condition

Vessel 1			**The Flying Dutchmen**						
ML #	Type line	Length [m]	Hor.angle [degrees]	Vert.angle [degrees]	ML #	Type line	Length [m]	Hor.angle [degrees]	Vert.angle [degrees]
1	Bow/ stern line	63	6	1	16	Bow/ stern line	63	7	1
2	Bow/ stern line	60	6	1	15	Bow/ stern line	60	6	1
3	Bow/ stern line	58	6	1	14	Bow/ stern line	59	7	1
4	Breast line	48	12	1	13	Breast line	51	9	1
5	Breast line	47	10	1	12	Breast line	49	7	1
6	Breast line	46	8	1	11	Breast line	48	5	1
7	Spring line	40	6	1	10	Spring line	40	6	1
8	Spring line	37	7	1	9	Spring line	37	7	1

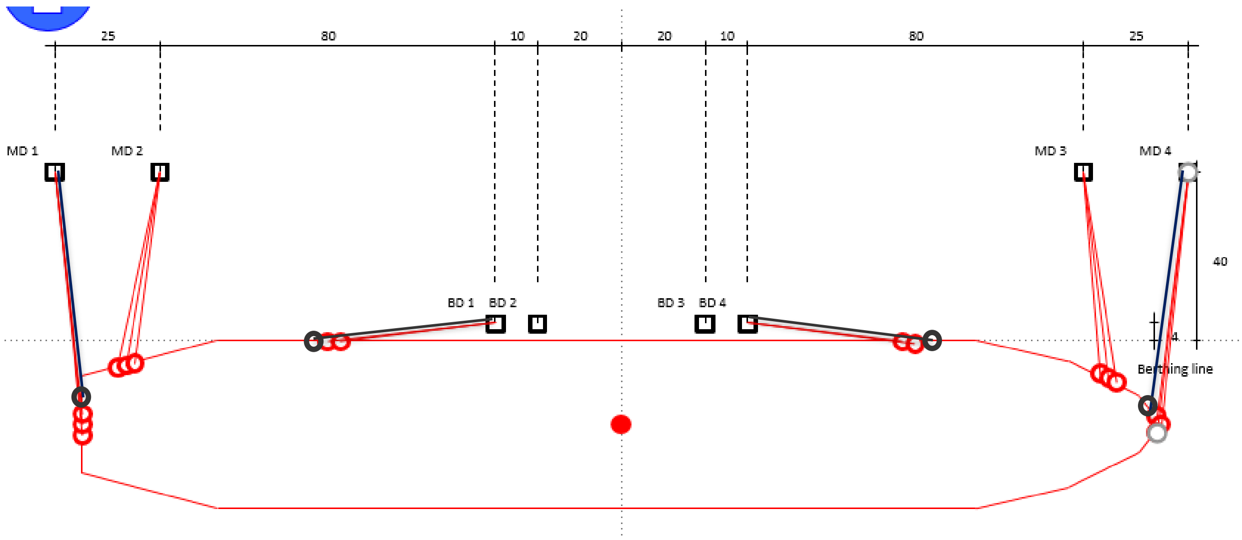

Figure 2-5: Top view mooring layout with four ShoreTension units

3 Dynamic properties mooring

3.1 Natural periods surge, sway and yaw

The natural periods for the surge, sway and yaw motion depend on the total spring constant in surge, sway and yaw direction and the mass for surge and sway and the mass moment of inertia for yaw. The mass of the ship is 135303.85 t (refer to Table 2-1) and the radius of gyration around the vertical axis is assumed to be 75.6 m (30% of L_{pp}). The added mass has been taken from the hydrodynamic file generated by Marin.

The steps to determine the total spring constant in surge, sway and yaw direction are:

1. Determine stiffness individual lines;
2. Decompose stiffness each line in surge, sway and yaw direction;
3. Add contribution of each line in each direction;

To determine the individual stiffness of each mooring line the load-elongation curve will be linearised around the origin. The load-elongation curves for steel wire-polyester tail combination lines are determined for the unique length of the steel wire (refer to Table 2-3). The tail length is constant (11 m). Figure 3-1, Figure 3-2 and Figure 3-3 (all below) depict the load-elongation curves for respectively line 2, 4 and 7. The load elongation curves for respectively line 15, 11 and 10 are exactly the same. The curves for other respectively bow/stern, breast or spring lines are very similar because the lengths do not differ much. The load-elongation curves are fairly linear. Table 3-1 shows the individual line stiffnesses.

Table 3-1: Individual line stiffness mooring arrangement Case D [kN/m]

1	2	3	4	5	6	7	8	9	10	11	12	13	14	15	16
367	373	380	408	411	413	386	395	395	386	406	403	399	378	373	368

The total spring constants and natural periods without added mass are:

- Surge: 1625 kN/m and 57 s;
- Sway: 4616 kN/m and 34 s;
- Yaw: 69036334 kNm/rad and 21 s;

The added mass at these periods and the natural periods including added mass are:

- Surge: 2.25×10^4 t and 62 s;
- Sway: 5.37×10^5 t and 76 s;
- Yaw: 1.16×10^9 tm^2 and 33 s;

The added mass in sway and yaw direction on shallow water is large. Hence, the steep increase of the natural period.

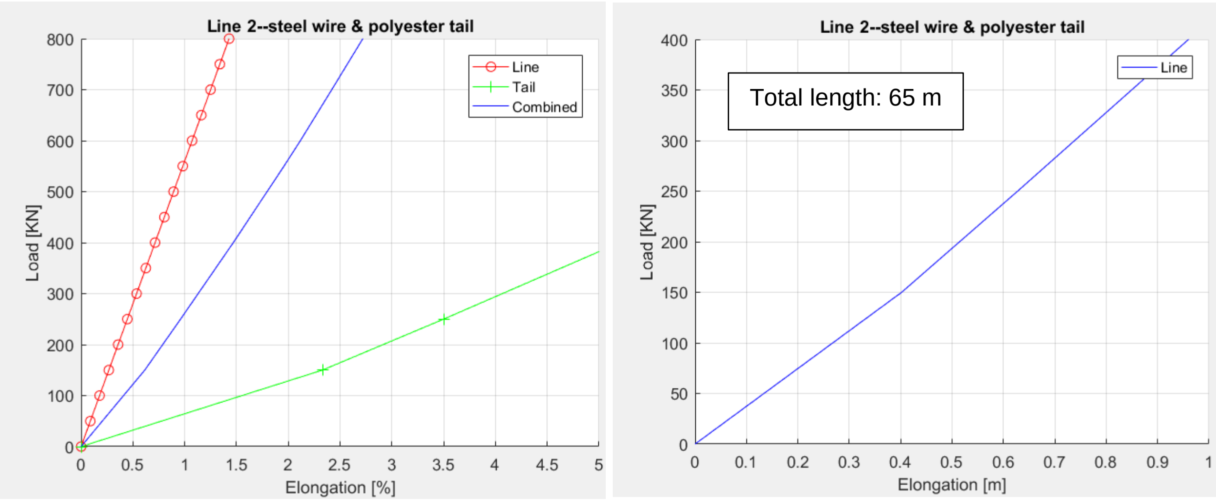

Figure 3-1: Load-elongation curve line 2 (stern line)

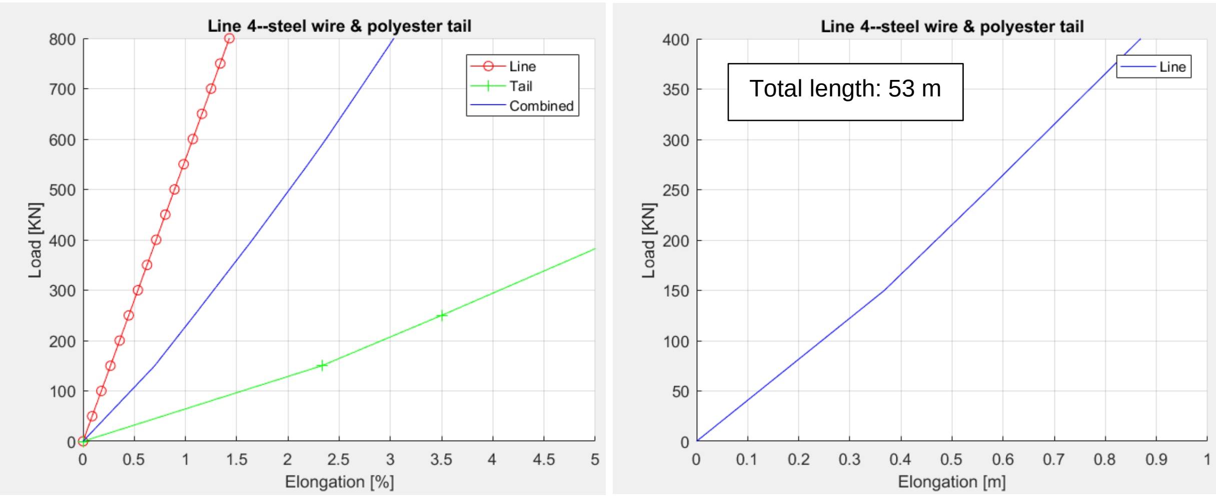

Figure 3-2: Load-elongation curve line 4 (breast line)

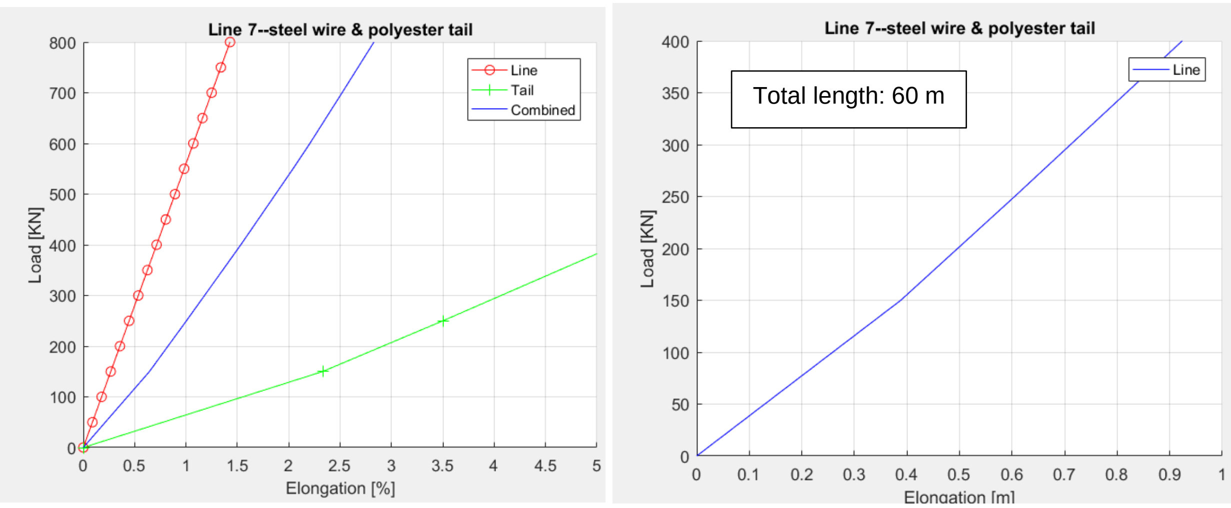

Figure 3-3: Load-elongation curve line 7 (spring line)

3.2 Stiffness individual lines for Case A, B & C

The line stiffness for the conventional lines for mooring arrangement A, B and C (refer to Figure 1-1) based on a real-life mooring arrangement Case D (refer to Figure 2-3) becomes:

- 2 Spring lines: Spring constant in surge direction /2 = 1625/2 = 812.5 kN/m;
- 4 Breast lines: Spring constant in sway direction /4 = 4620[4]/4 = 1155 kN/m;

The spring constant in yaw direction determines where the springs should be mounted in lengthwise direction relative to midship (L is defined as the distance between breast lines fore and aft):

- The elongation of the breast lines in Case A, B and C for 1 rad yaw angle is: dy= L/2 x dψ [m];
- The force in 1 breast line at 1 rad yaw is equal to c22' x dy = c22' x L/2 x dψ [kN];
  - Where c22' the individual line stiffness of the breast lines in Case A, B and C (1155 kN/m);
- The total force fore (or aft) at 1 rad yaw becomes c22' x L x dψ [kN] (two breast lines);
- The total couple becomes c22' x L^2 x dψ [kNm];
- The total couple is also equal to the spring constant in yaw direction times the yaw angle;
- Combining the last two expressions determines that L is the square root of the ratio between the total spring constant in yaw direction over the individual line stiffness of the breast lines;

The distance L is therefore equal to sqrt(69036334/1155) = 245.5 m.

The line stiffness for the HMPE for mooring arrangement A, B and C (refer to Figure 1-1) based on a real-life mooring arrangement Case D (refer to Figure 2-5) becomes (refer to Figure 2-1):

- Spring lines: Spring constant HMPE line for 48 m = 1275 kN/m;
- Breast lines: Spring constant HMPE line for 62 m: = 980 kN/m;

Both the horizontal and vertical angle have been neglected. The spring constant is solely based on the line lengths. Furthermore, the contribution of the HMPE breast lines in Case D to the line stiffness of the spring lines in Case C and the contribution of the HMPE spring lines in Case D to the line stiffness of the breast lines in Case C is nearly equal.

[4] *Spring stiffnes mentioned in Section 3.1 ceiled to 4620 kN.*

References

REF1. Deltares. Bijlage A – Project plan – Innovatief afmeren van schepen in de haven van de toekomst. 11202696-000HYE-0002. 13 April 2018

REF2. OCIMF. Mooring equipment guidelines. 4th Edition, 2018

REF3. Deltares. Minutes of Meeting, Kick-off meeting 11 Sept 2018. 11202696-000-0001. 12 Sept 2018

REF4. Significant Ships (2006). The Royal Institute of Naval Architects

REF5. Significant Ships (2013). The Royal Institute of Naval Architects

REF6. PIANC. Guidelines for the design of fender systems. 2002

Appendix 1: Fairlead positions

Fairleads coordinates relative to midship, centre line and main deck (depth) for conventional mooring lines.

Fairlead	X to midship [m]	Y to midship [m]	Z to main deck [m]
1	-128.5	-2.5	0.5
2	-128.5	0.0	0.5
3	-128.5	2.5	0.5
4	-120.0	13.5	0.5
5	-118.0	14.0	0.5
6	-116.0	14.5	0.5
7	-70.0	19.6	0.5
8	-67.0	19.6	0.5
9	67.0	19.6	0.5
10	70.0	19.6	0.5
11	114.0	12.0	0.5
12	116.0	11.0	0.5
13	118.0	10.0	0.5
14	127.5	2.0	0.5
15	128.5	0.0	0.5
16	127.5	-2.0	0.5

Fairleads coordinates relative to midship, centre line and main deck (depth) for HMPE lines (attached to ShoreTension units).

Fairlead	X to midship [m]	Y to midship [m]	Z to main deck [m]
1	-128.5	5.0	0.5
2	-73.0	19.6	0.5
3	73.0	19.6	0.5
4	127.5	3.0	0.5

D Calibration plots of mooring lines and fenders

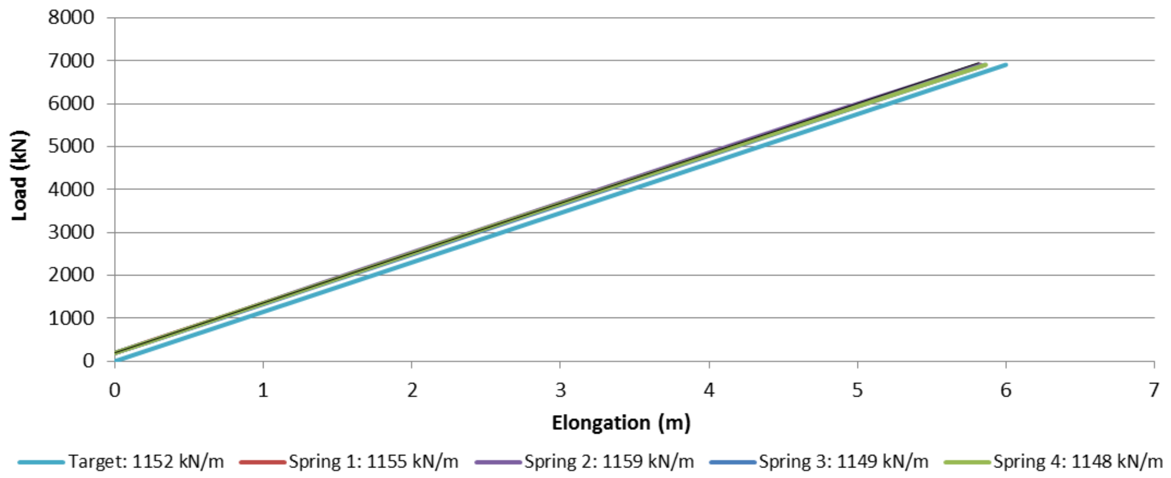

Figure D.1 Calibration plot of springs 1 to 4.

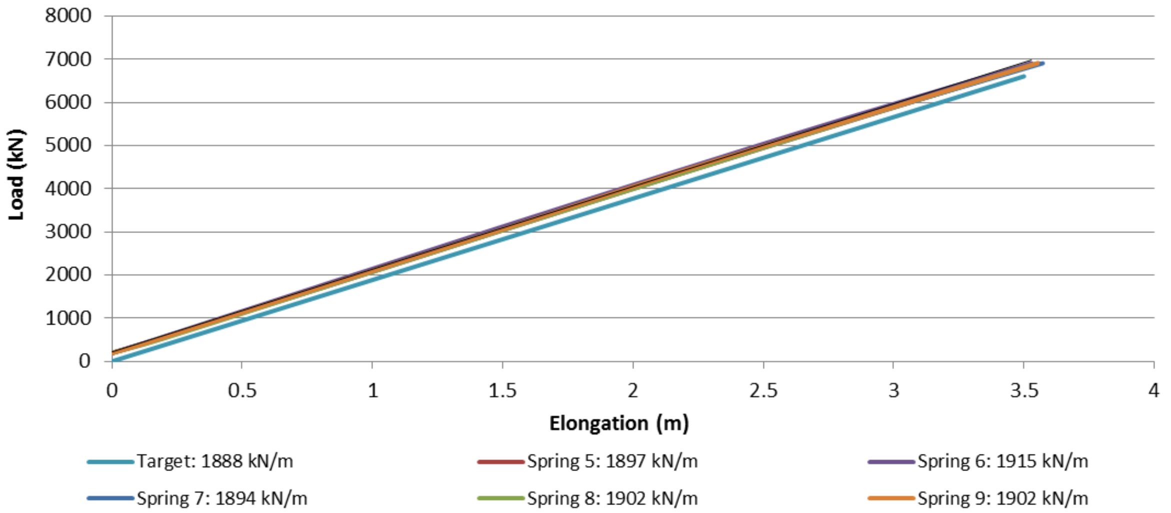

Figure D.2 Calibration plot of springs 5 to 9.

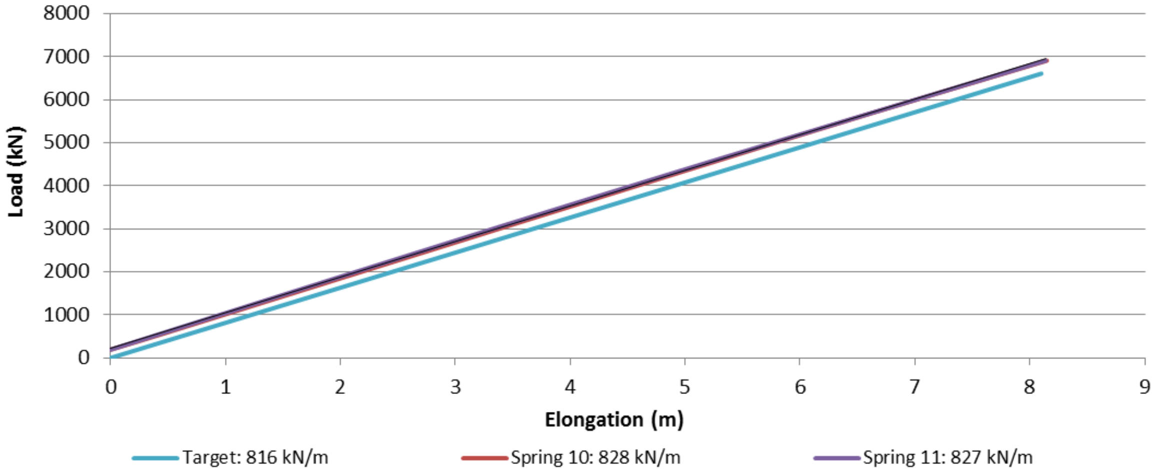

Figure D.3 Calibration plot of springs 10 and 11.

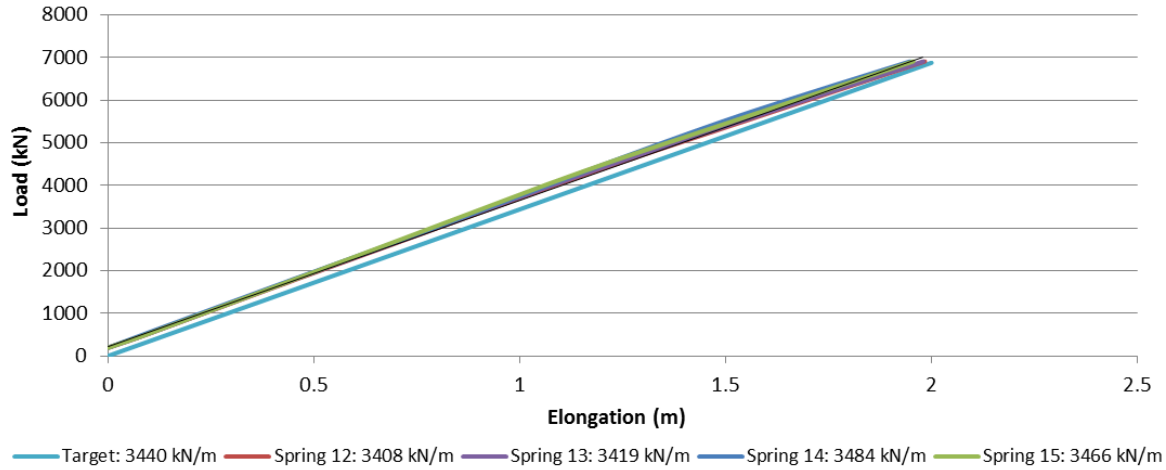

Figure D.4 Calibration plot of springs 12 to 15.

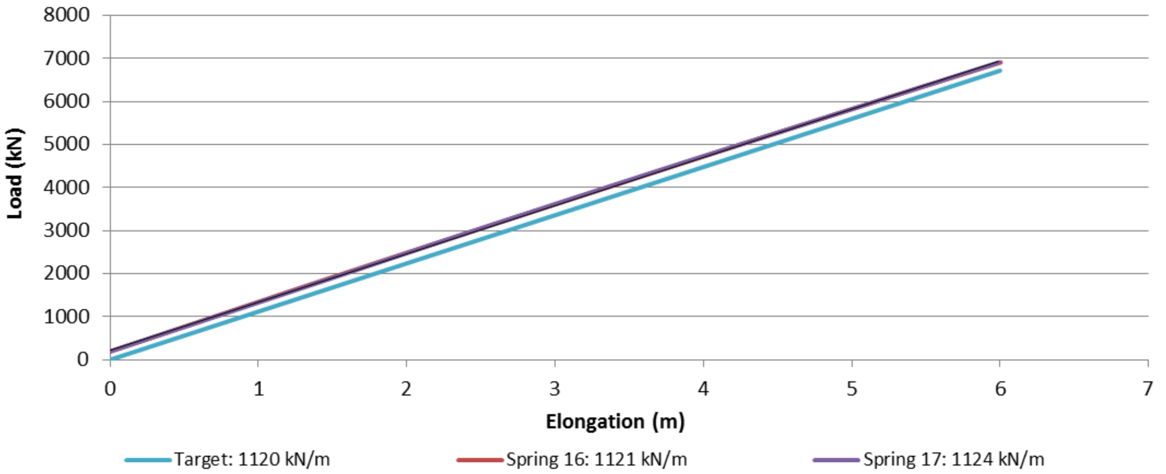

Figure D.5 Calibration plot of springs 16 and 17.

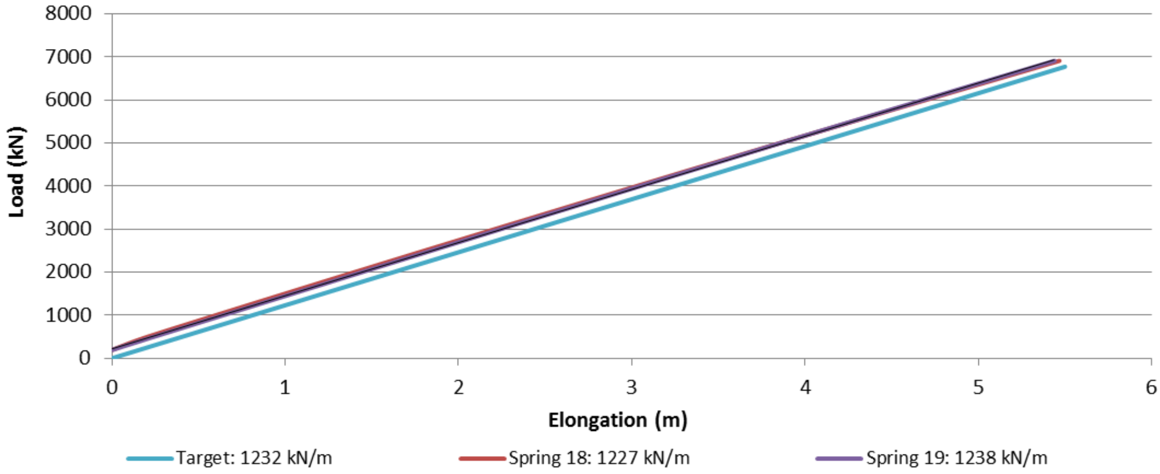

Figure D.6 Calibration plot of springs 18 and 19.

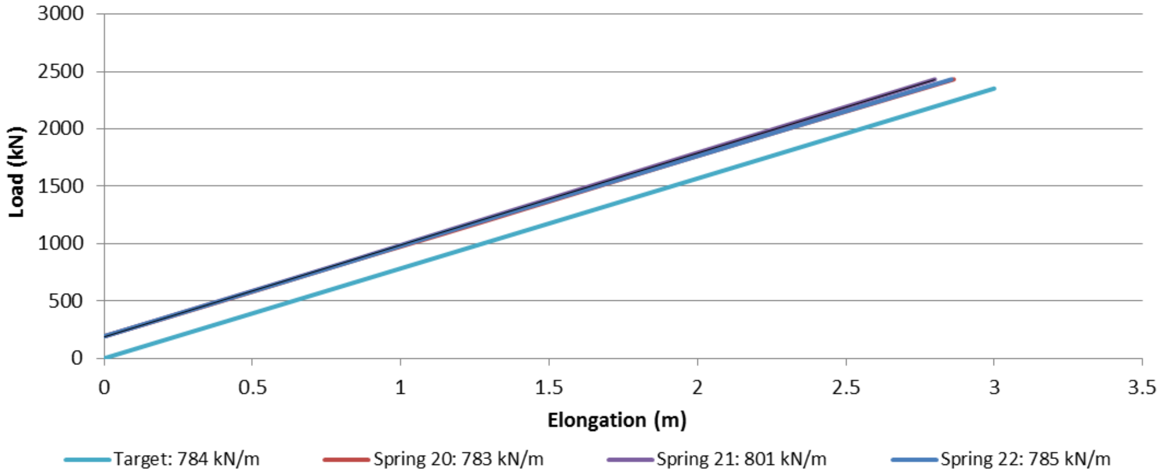

Figure D.7 Calibration plot of springs 20, 21 and 22.

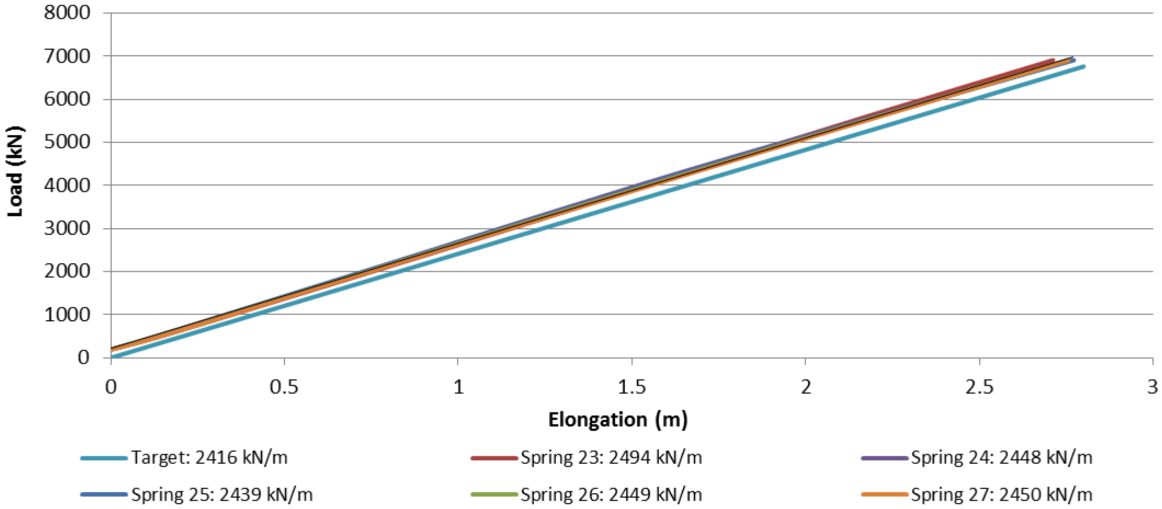

Figure D.8 Calibration plot of springs 23 to 27.

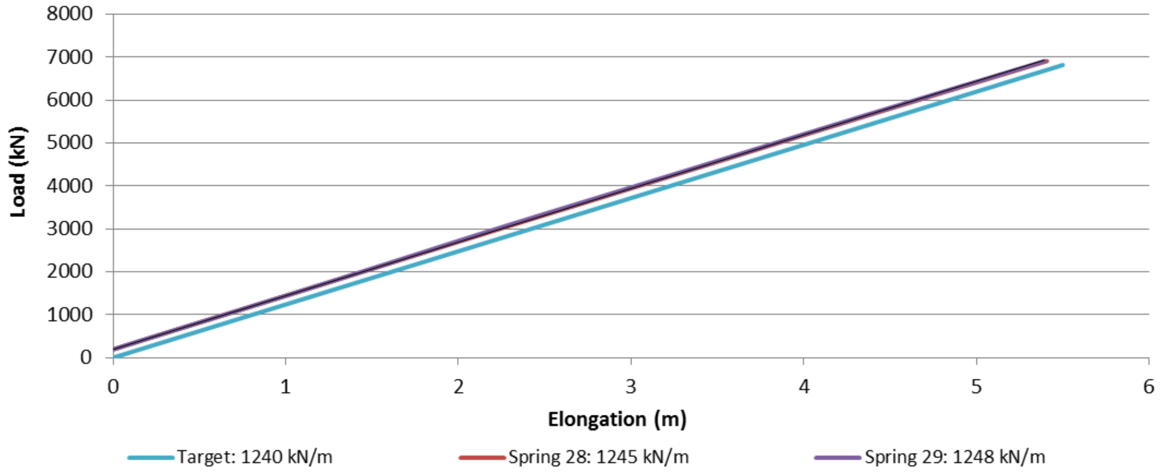

Figure D.9 Calibration plot of springs 28 and 29.

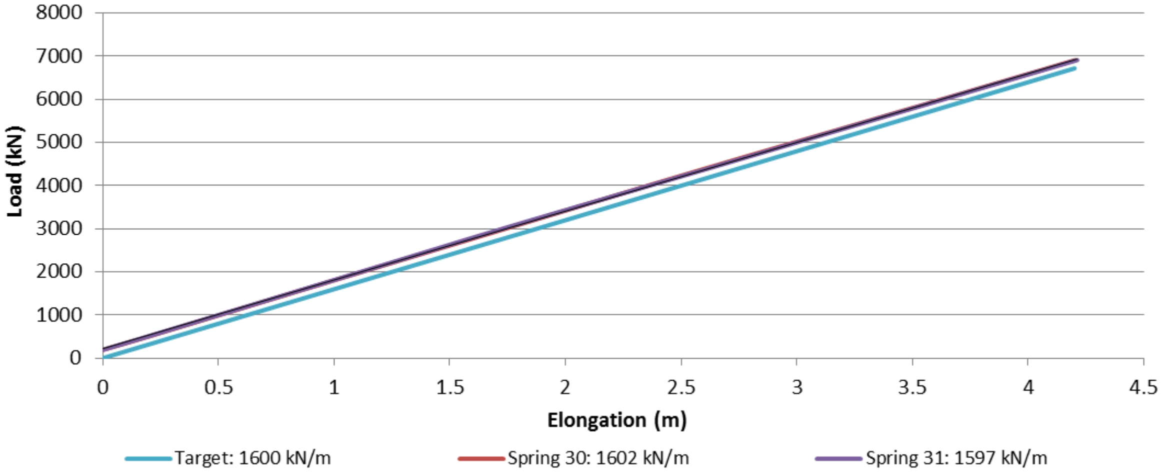

Figure D.10 Calibration plot of springs 30 and 31.

E Wave calibration and reflection

E.1 Cases A, B and C

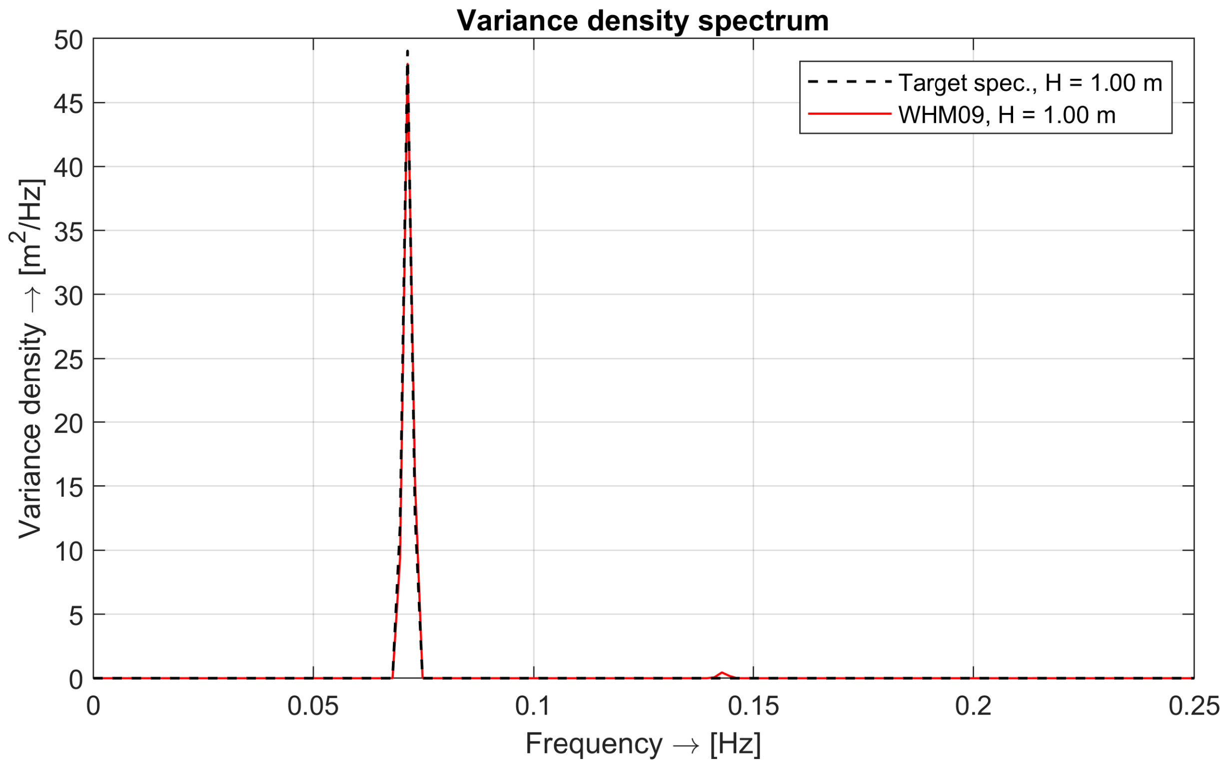

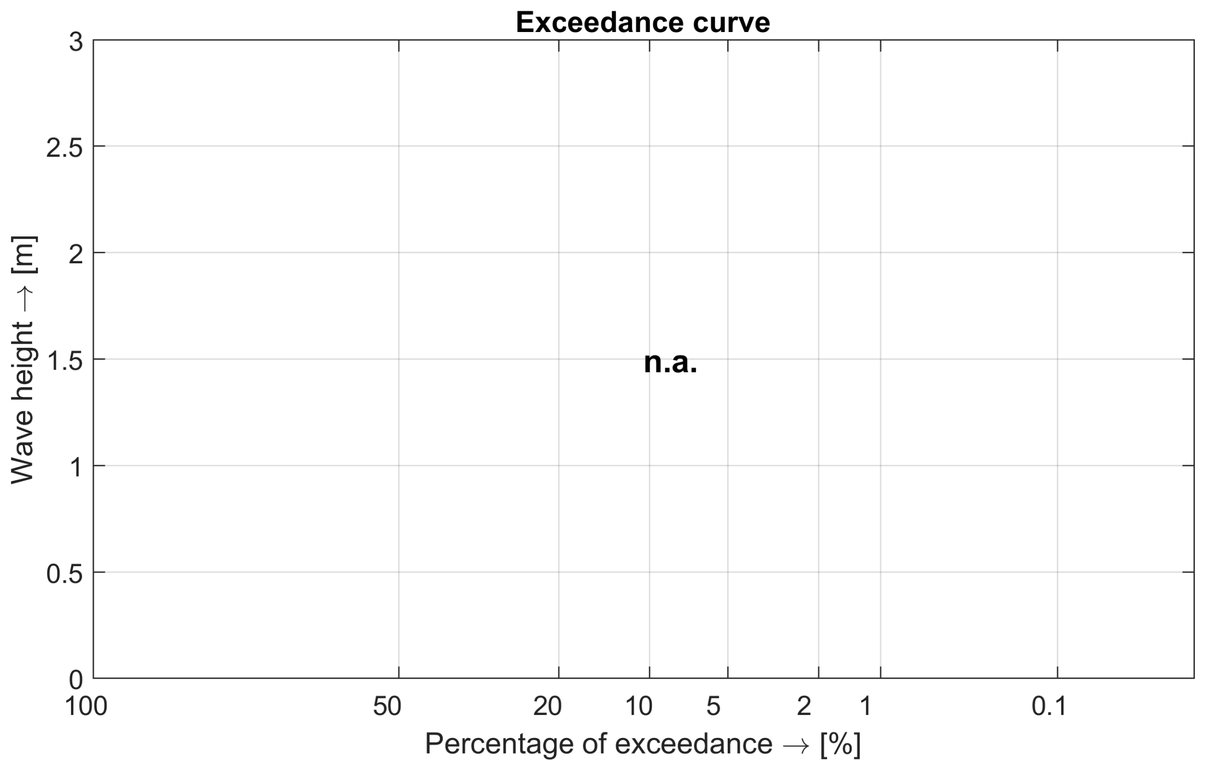

Results of wave generation calibration Depth = 18.0 m, H = 1.00 m, T = 14.00 s	Monochromatic	M140a
Deltares	11202696	App. E.1.01

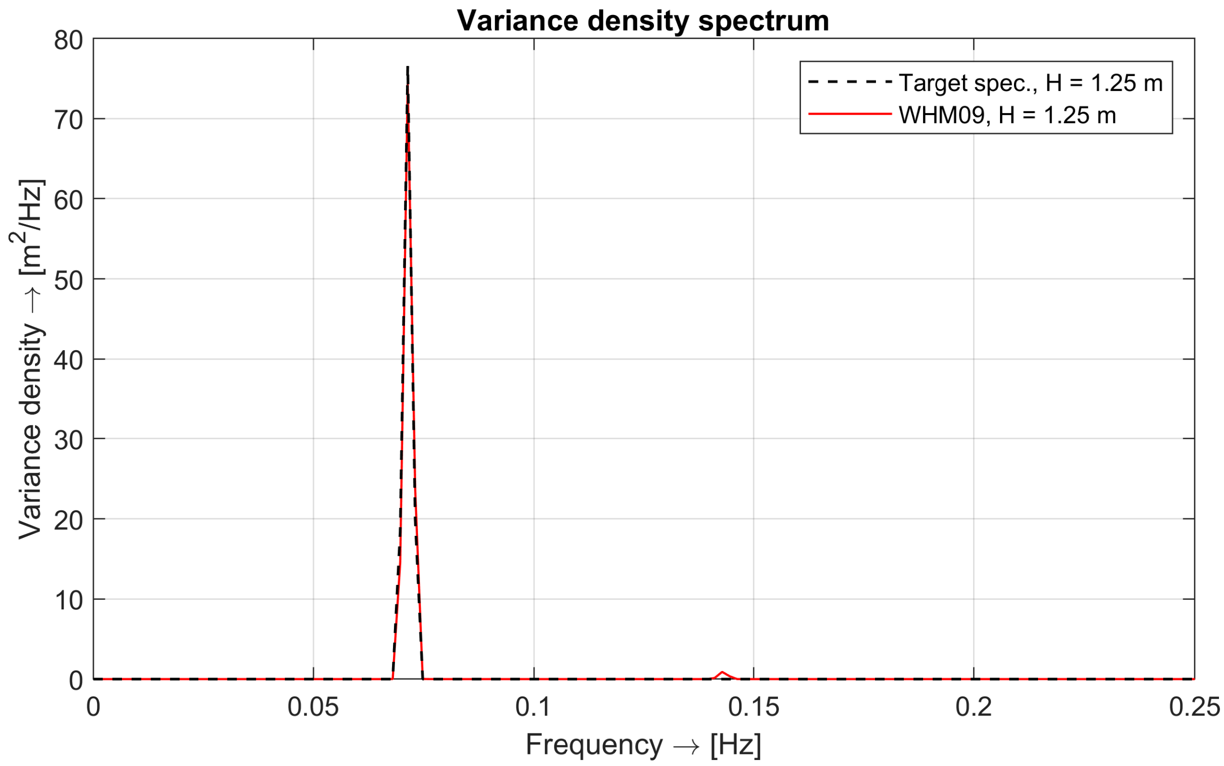

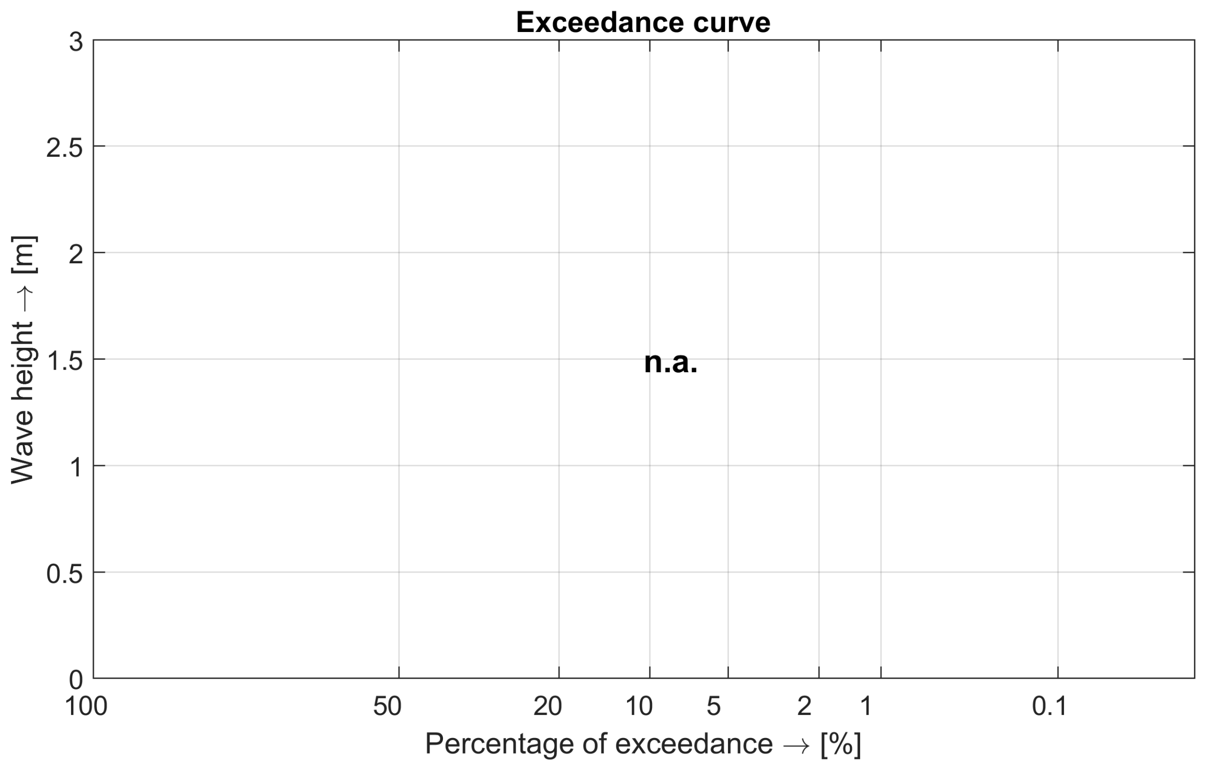

Results of wave generation calibration Depth = 18.0 m, H = 1.25 m, T = 14.00 s	Monochromatic	M140b
Deltares	11202696	App. E.1.02

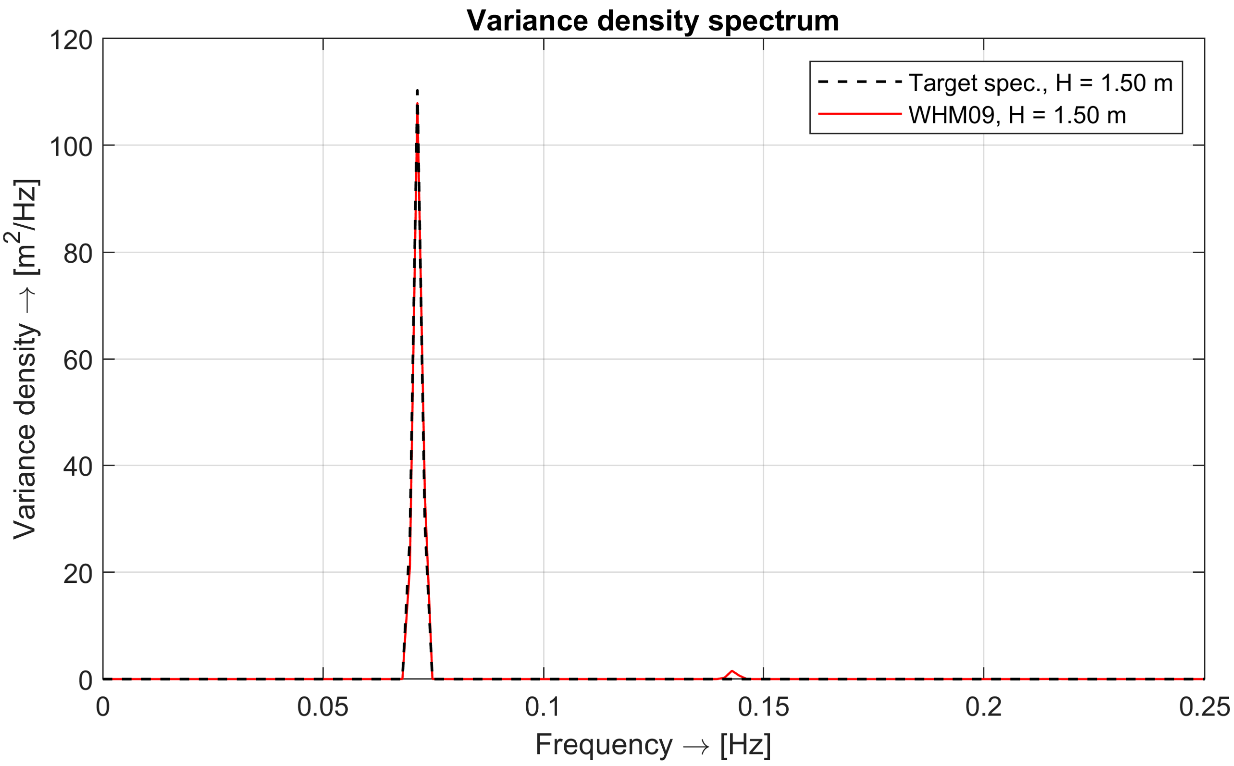

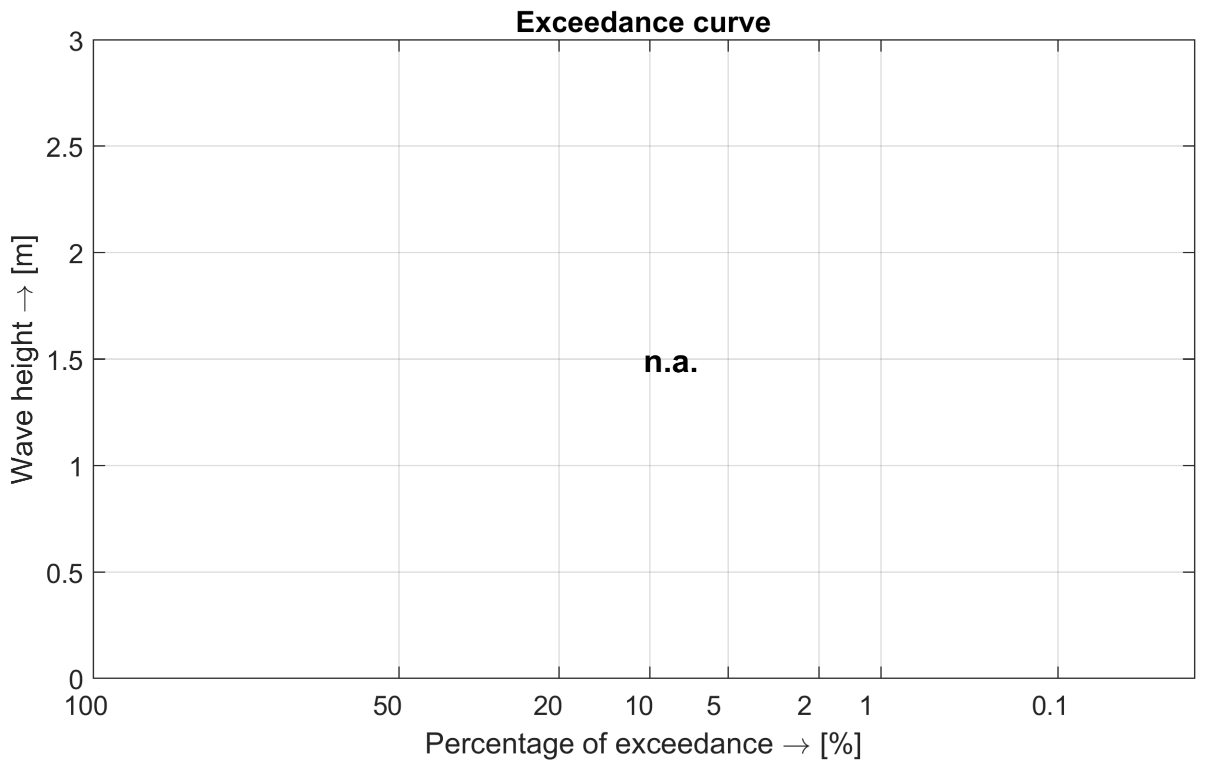

Results of wave generation calibration Depth = 18.0 m, H = 1.50 m, T = 14.00 s	Monochromatic	M140c
Deltares	11202696	App. E.1.03

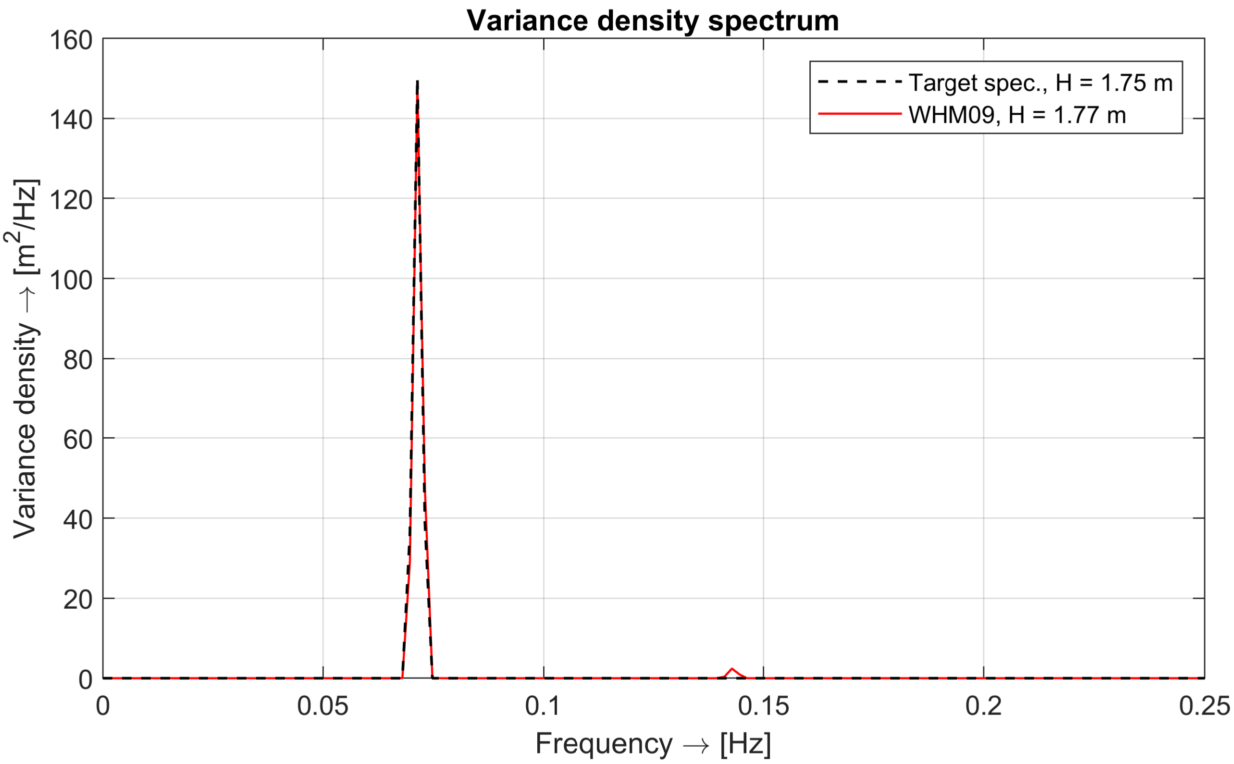

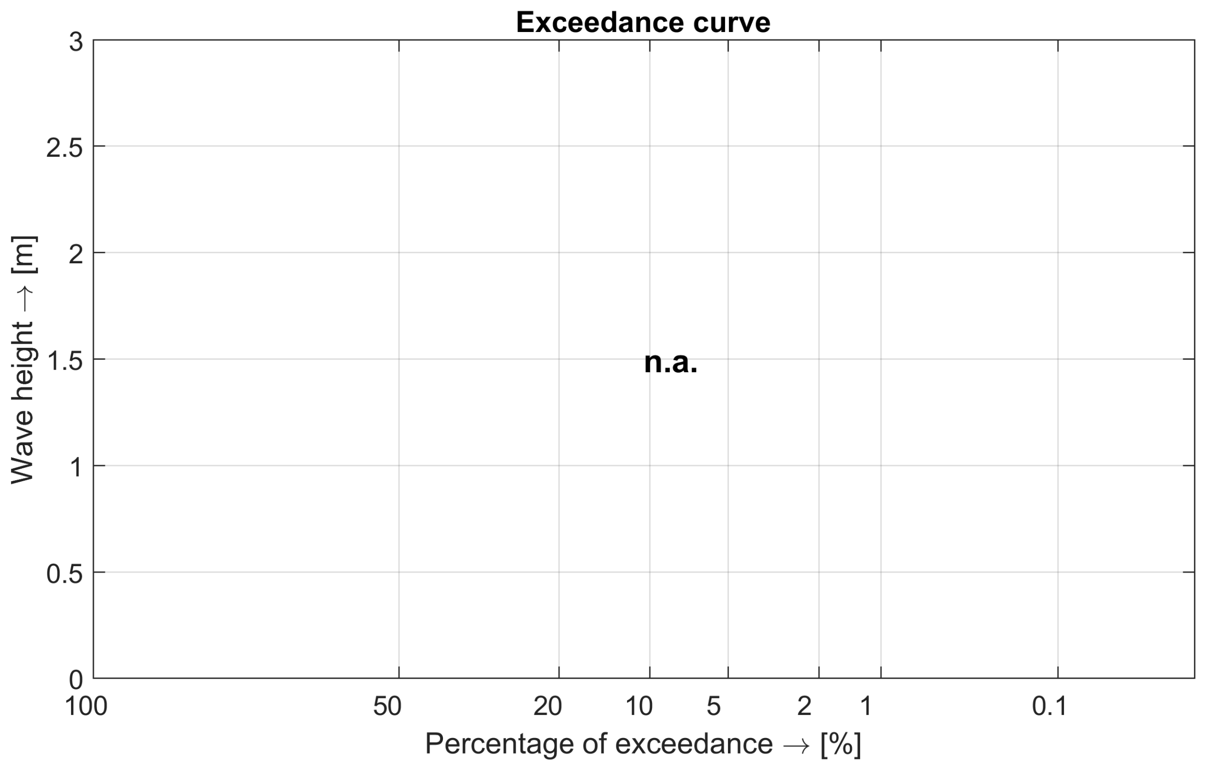

Results of wave generation calibration Depth = 18.0 m, H = 1.75 m, T = 14.00 s	Monochromatic	M140d
Deltares	11202696	App. E.1.04

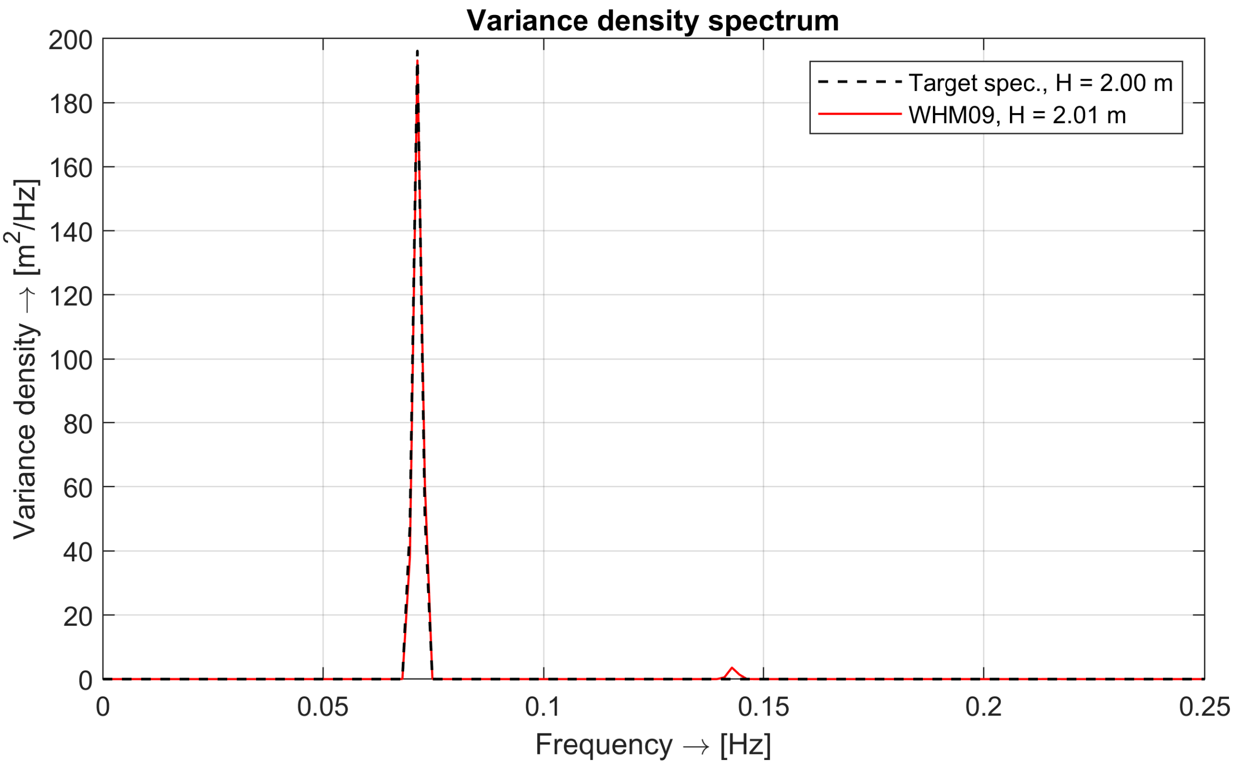

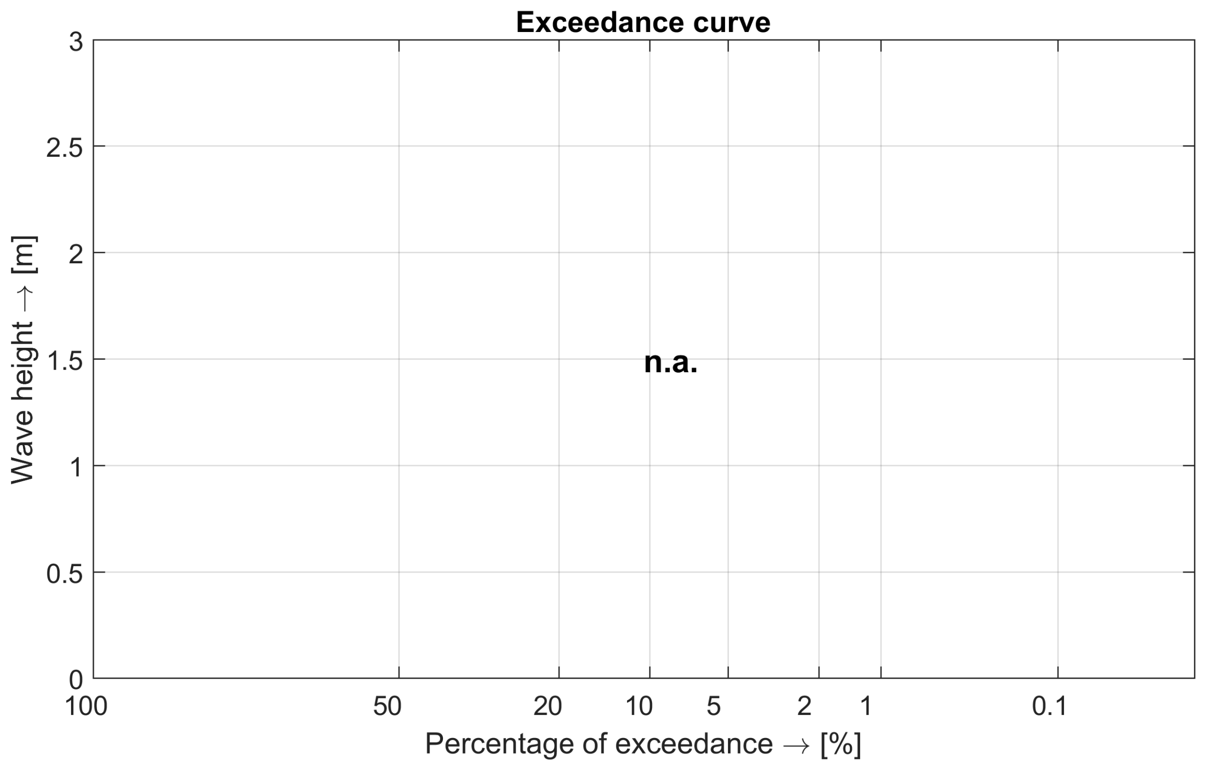

Results of wave generation calibration Depth = 18.0 m, H = 2.00 m, T = 14.00 s	Monochromatic	M140e
Deltares	11202696	App. E.1.05

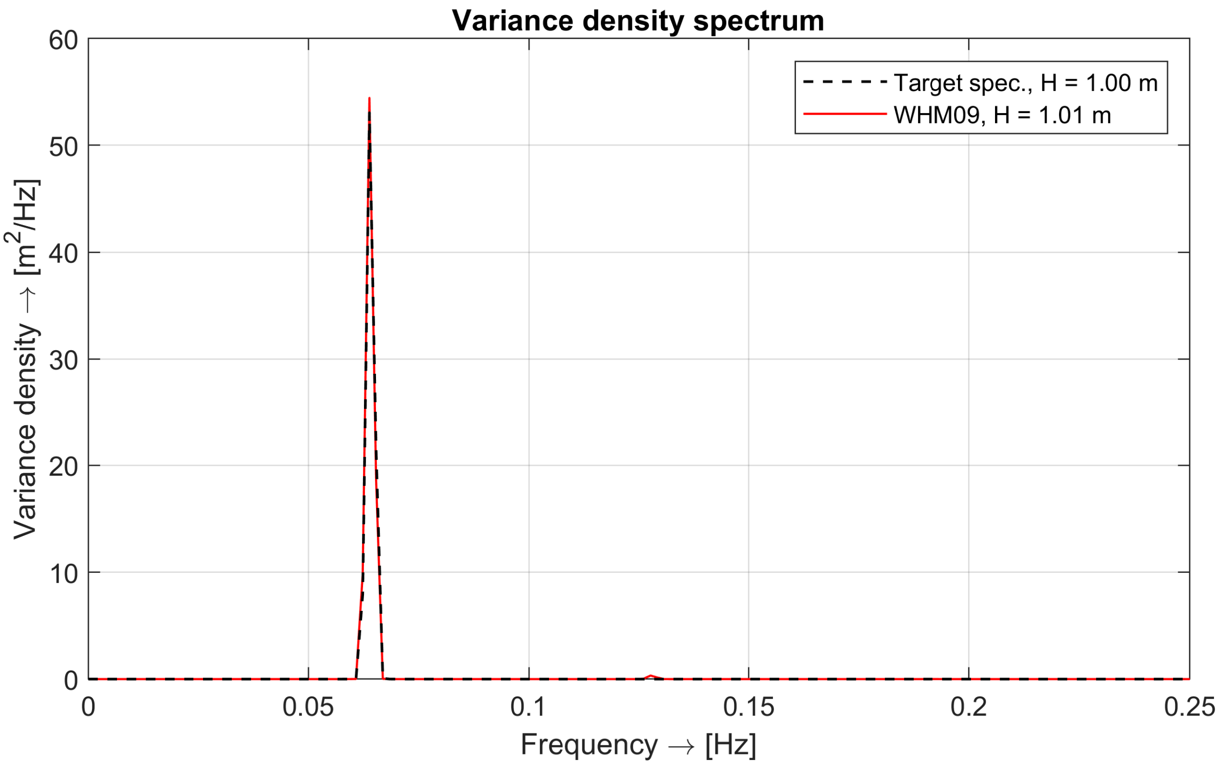

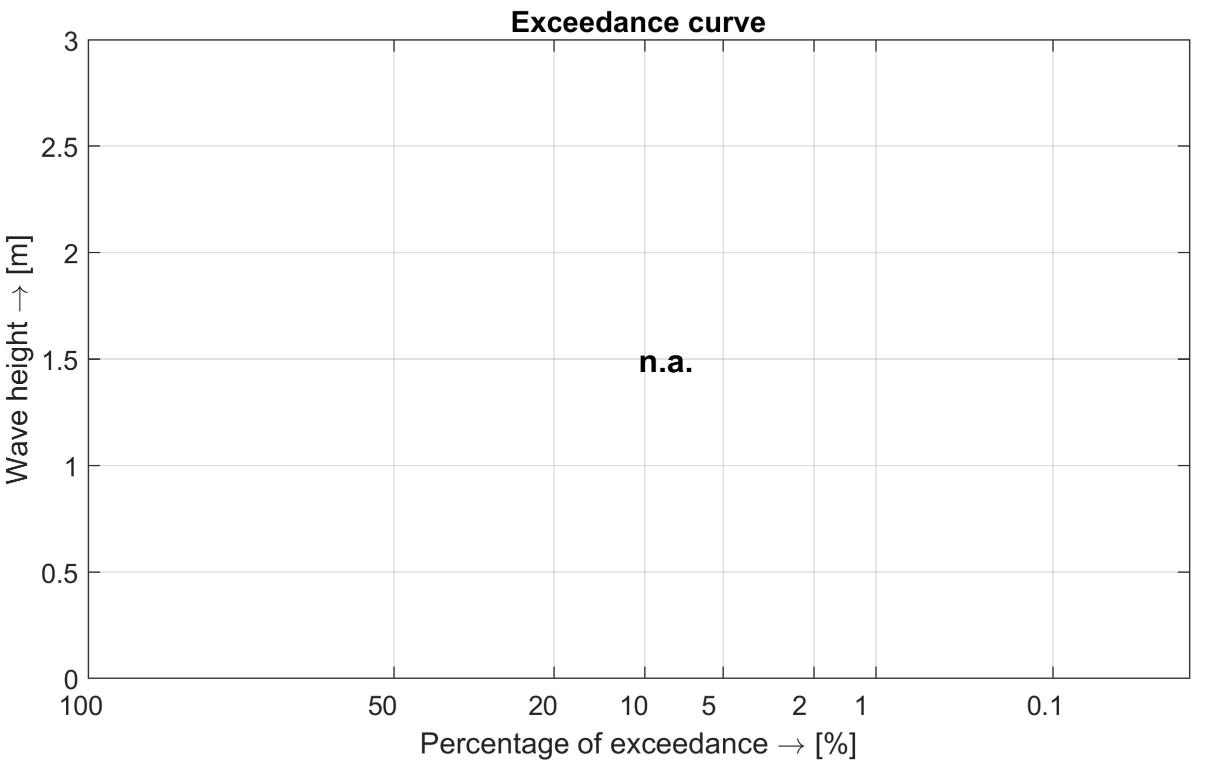

Results of wave generation calibration Depth = 18.0 m, H = 1.00 m, T = 15.60 s	Monochromatic	M156a
Deltares	11202696	App. E.1.06

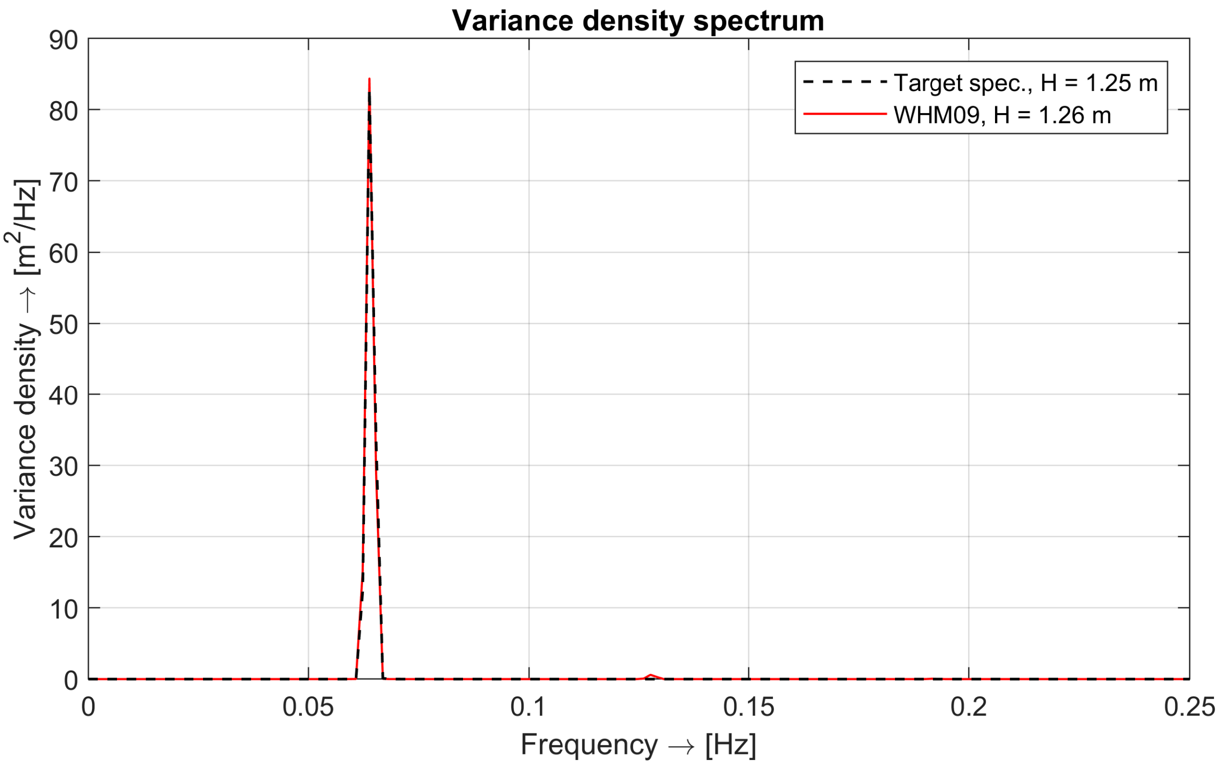

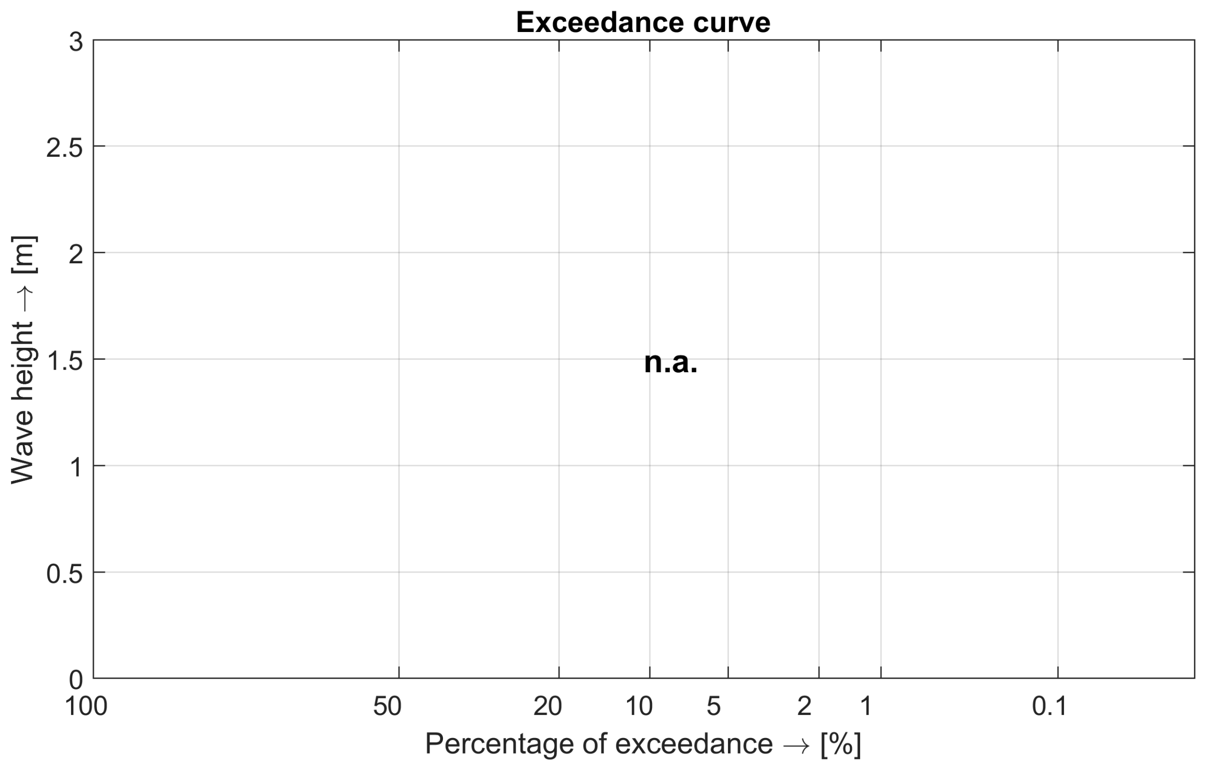

Results of wave generation calibration Depth = 18.0 m, H = 1.25 m, T = 15.60 s	Monochromatic	M156b
Deltares	11202696	App. E.1.07

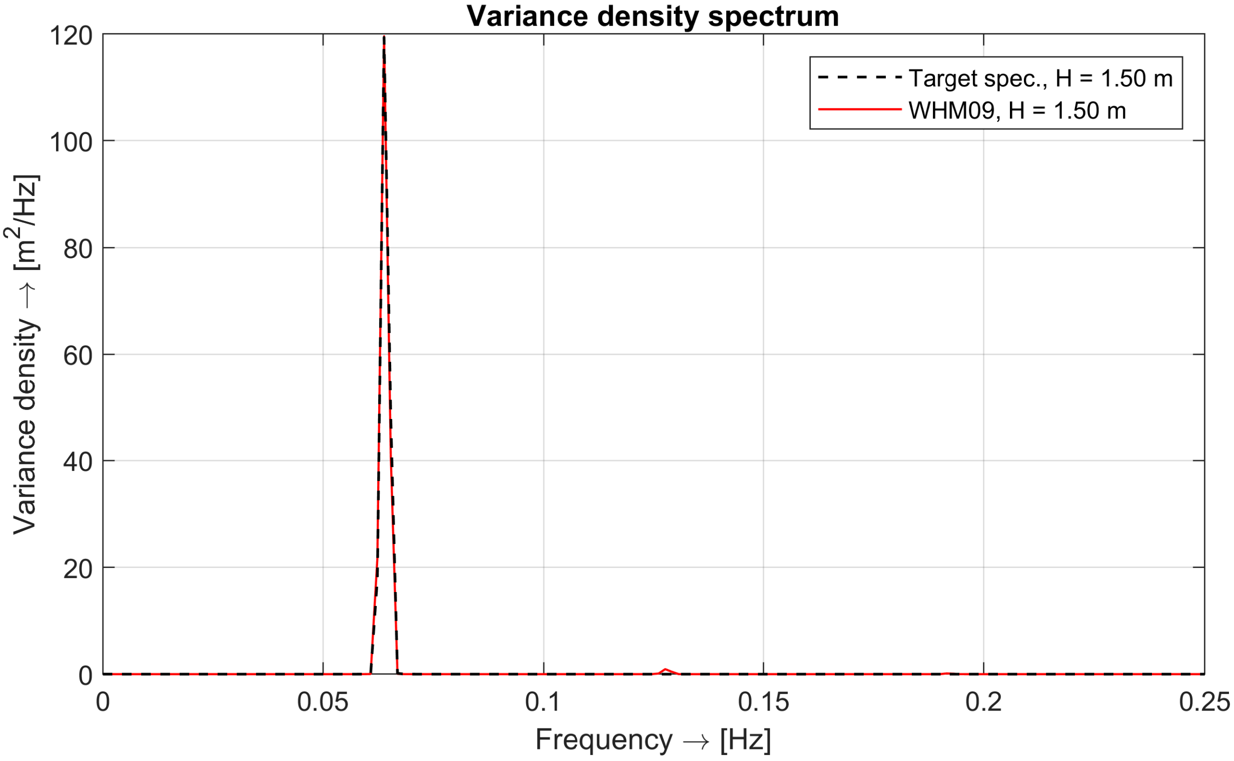

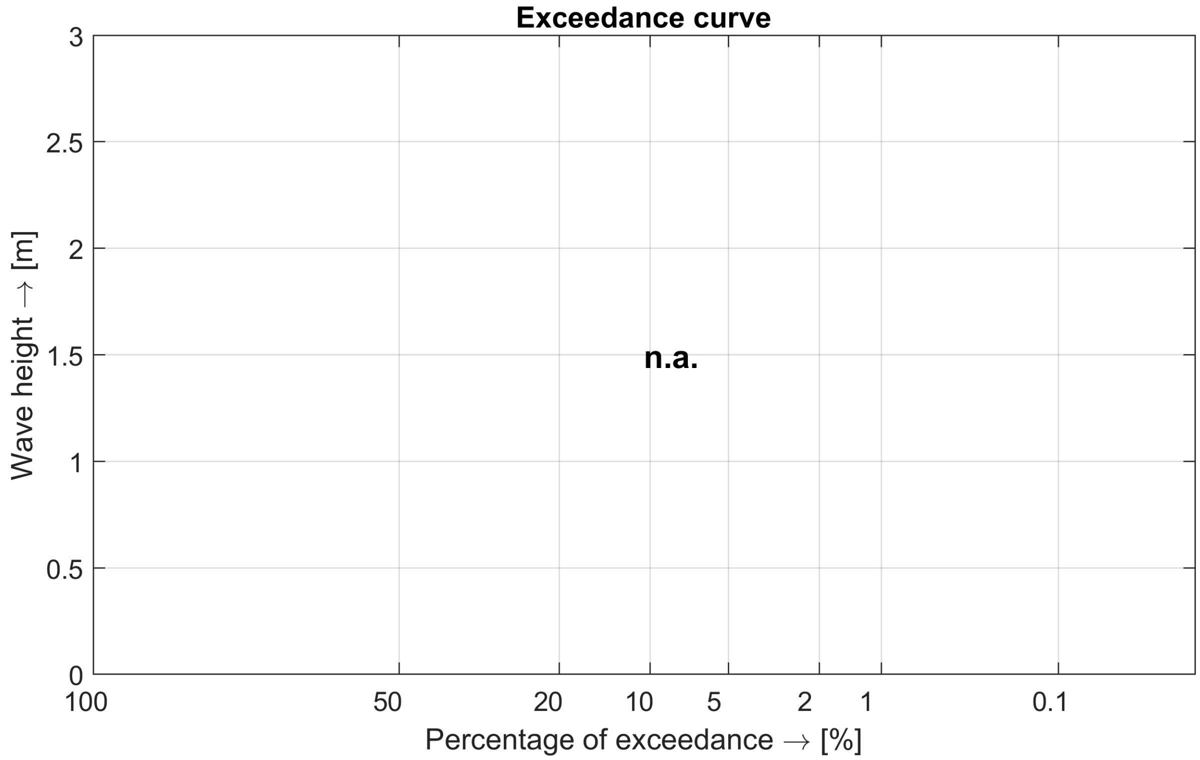

Results of wave generation calibration Depth = 18.0 m, H = 1.50 m, T = 15.60 s	Monochromatic	M156c
Deltares	11202696	App. E.1.08

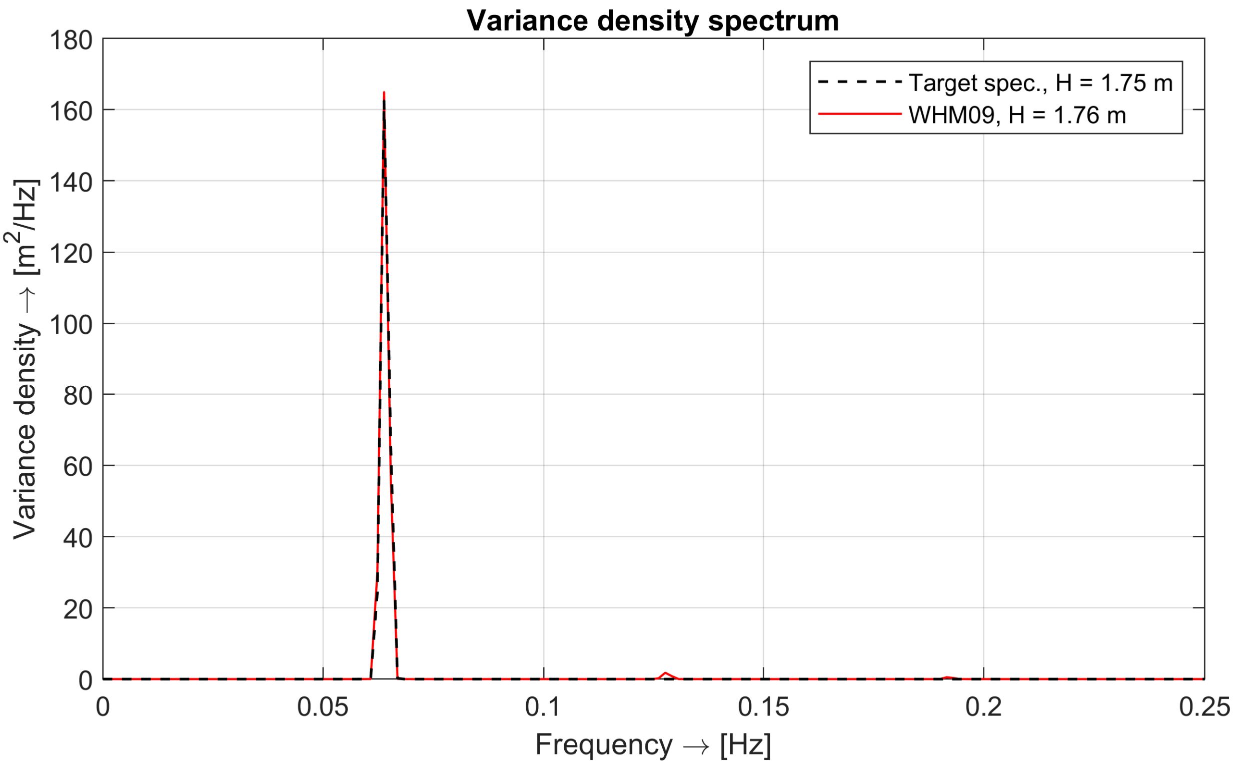

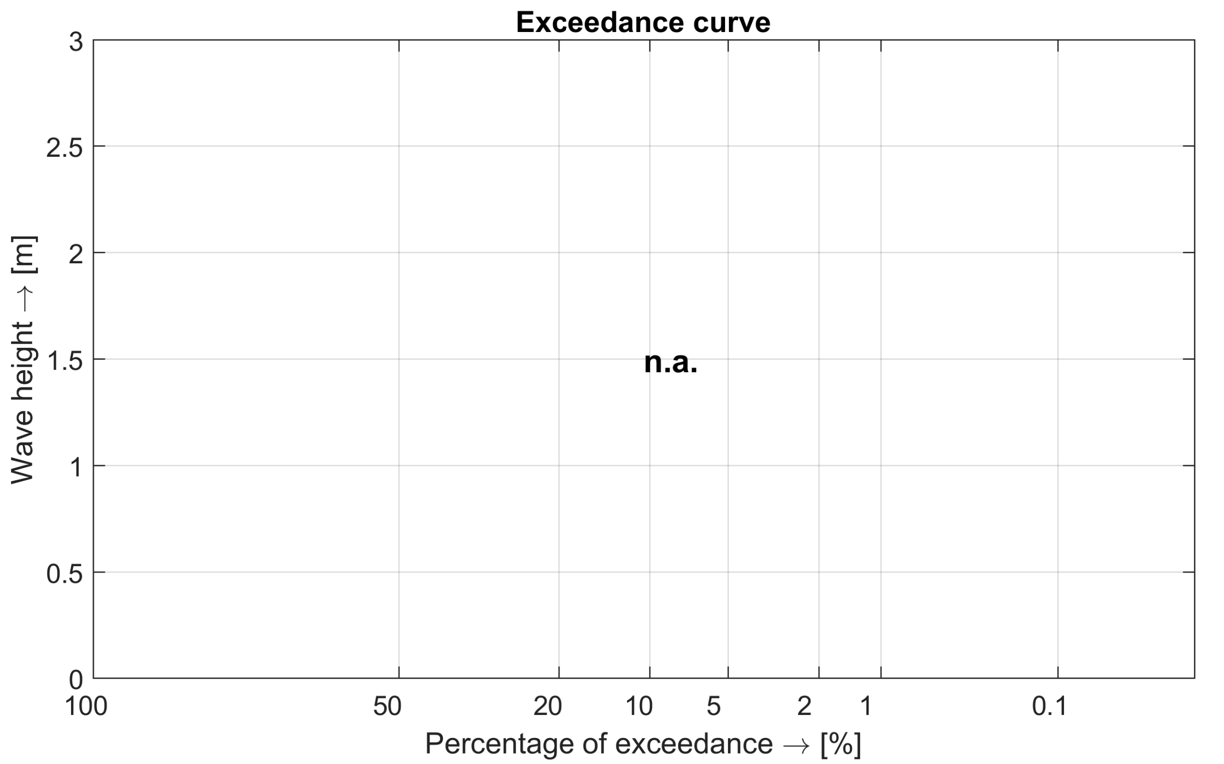

Results of wave generation calibration Depth = 18.0 m, H = 1.75 m, T = 15.60 s	Monochromatic	M156d
Deltares	11202696	App. E.1.09

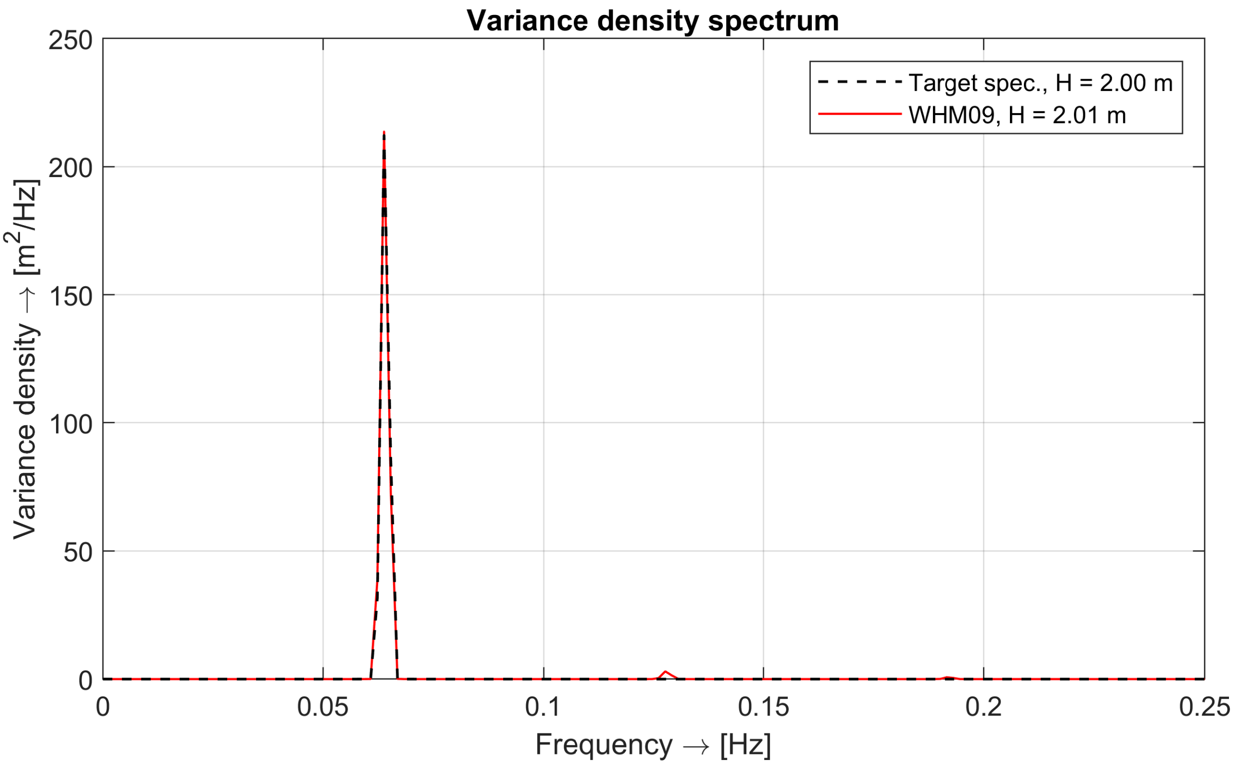

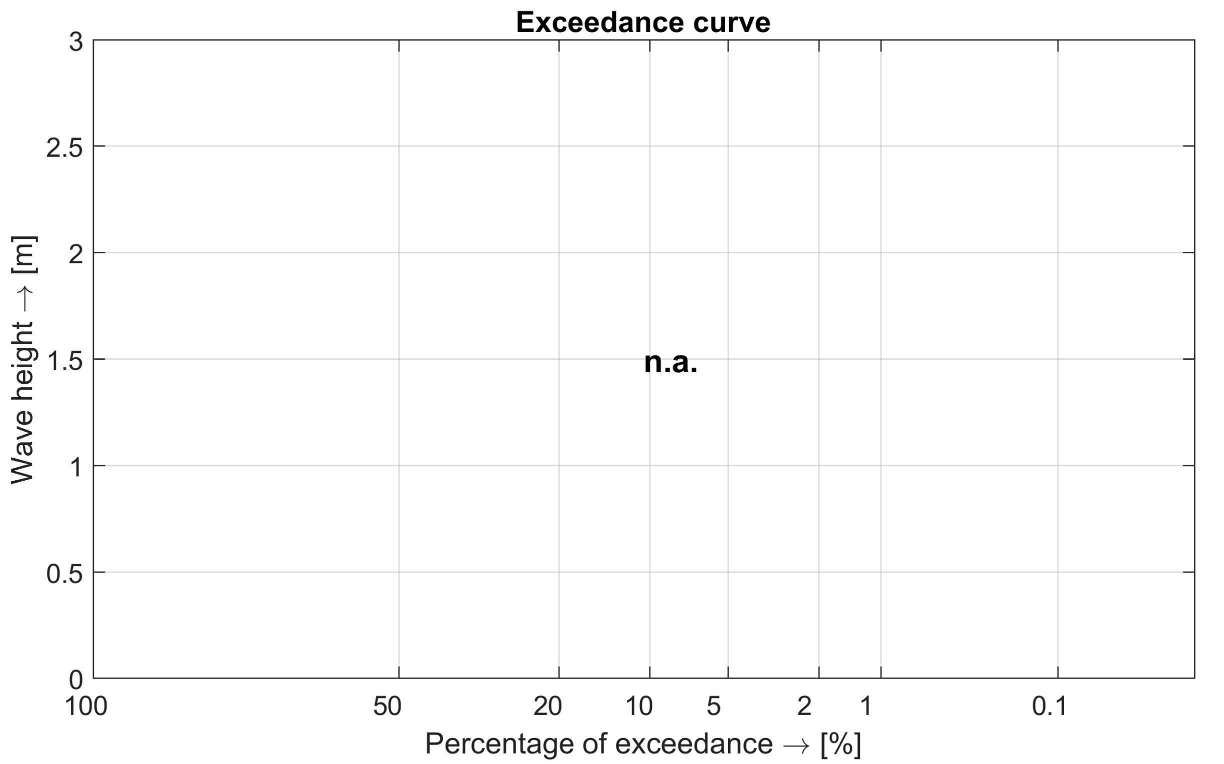

Results of wave generation calibration Depth = 18.0 m, H = 2.00 m, T = 15.60 s	Monochromatic	M156e
Deltares	11202696	App. E.1.10

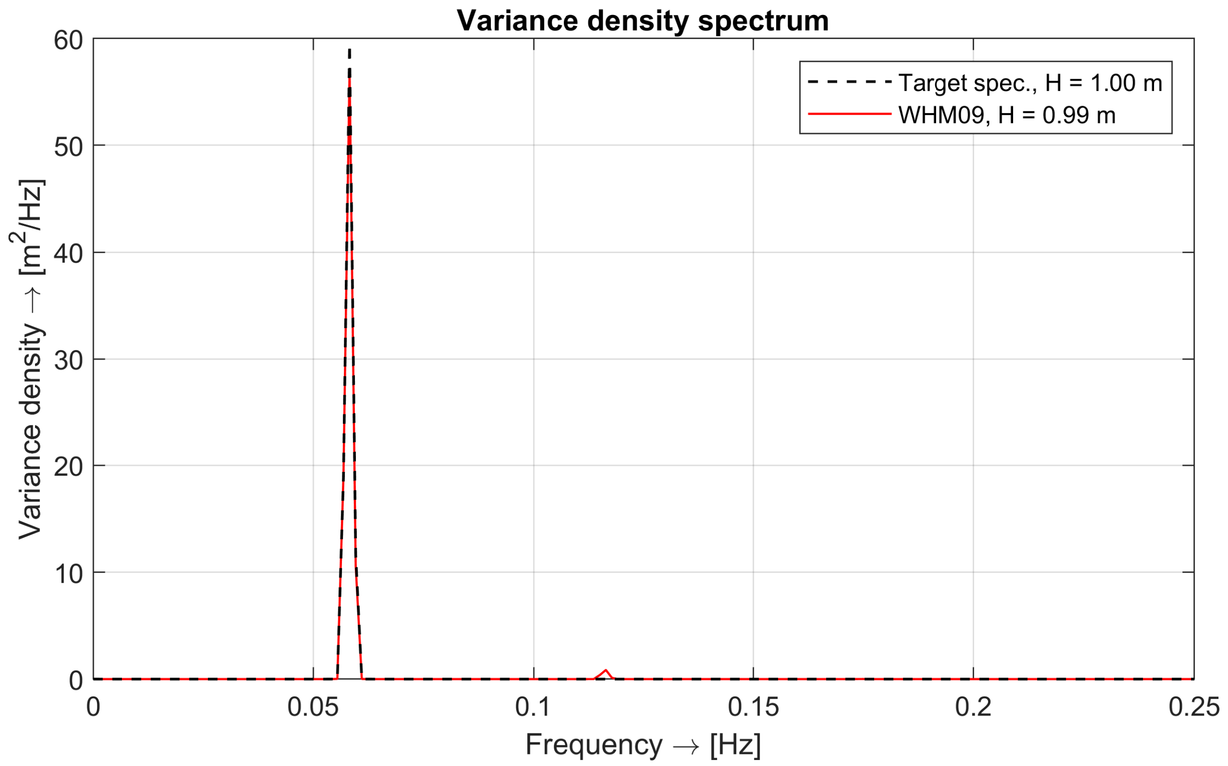

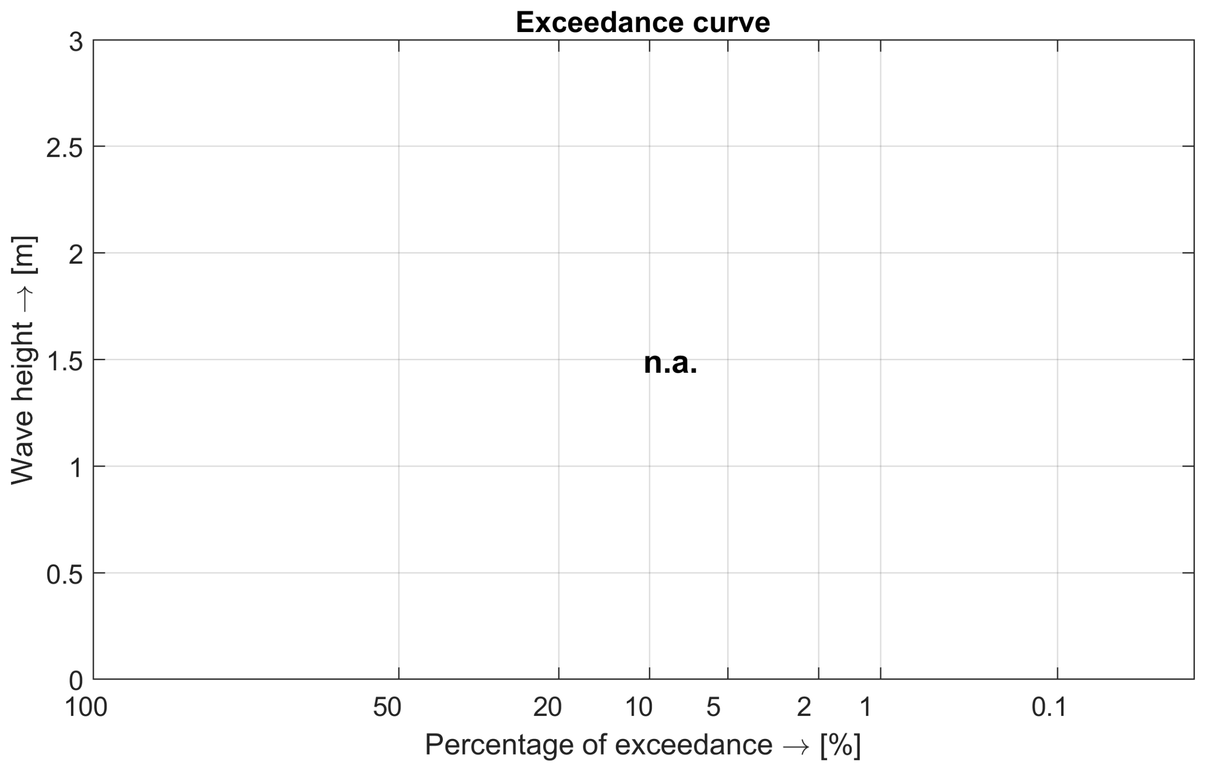

Results of wave generation calibration Depth = 18.0 m, H = 1.00 m, T = 17.20 s	Monochromatic	M172a
Deltares	11202696	App. E.1.11

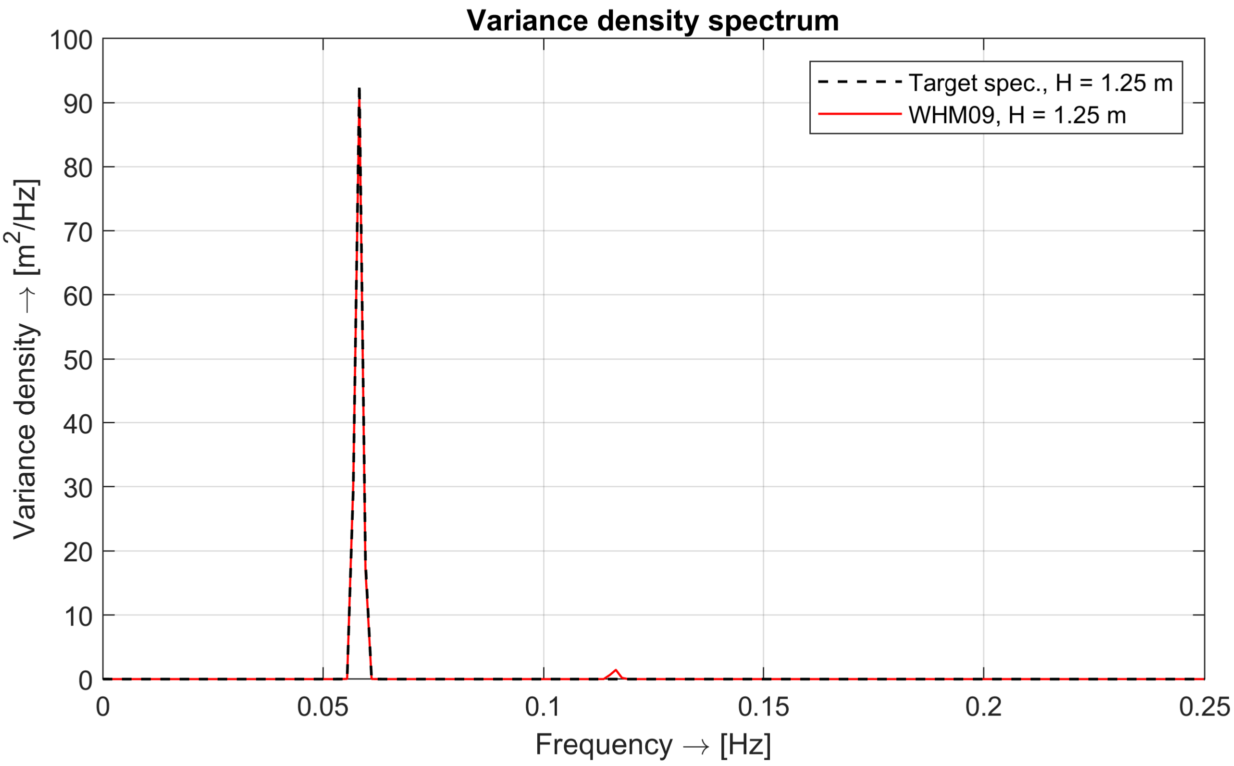

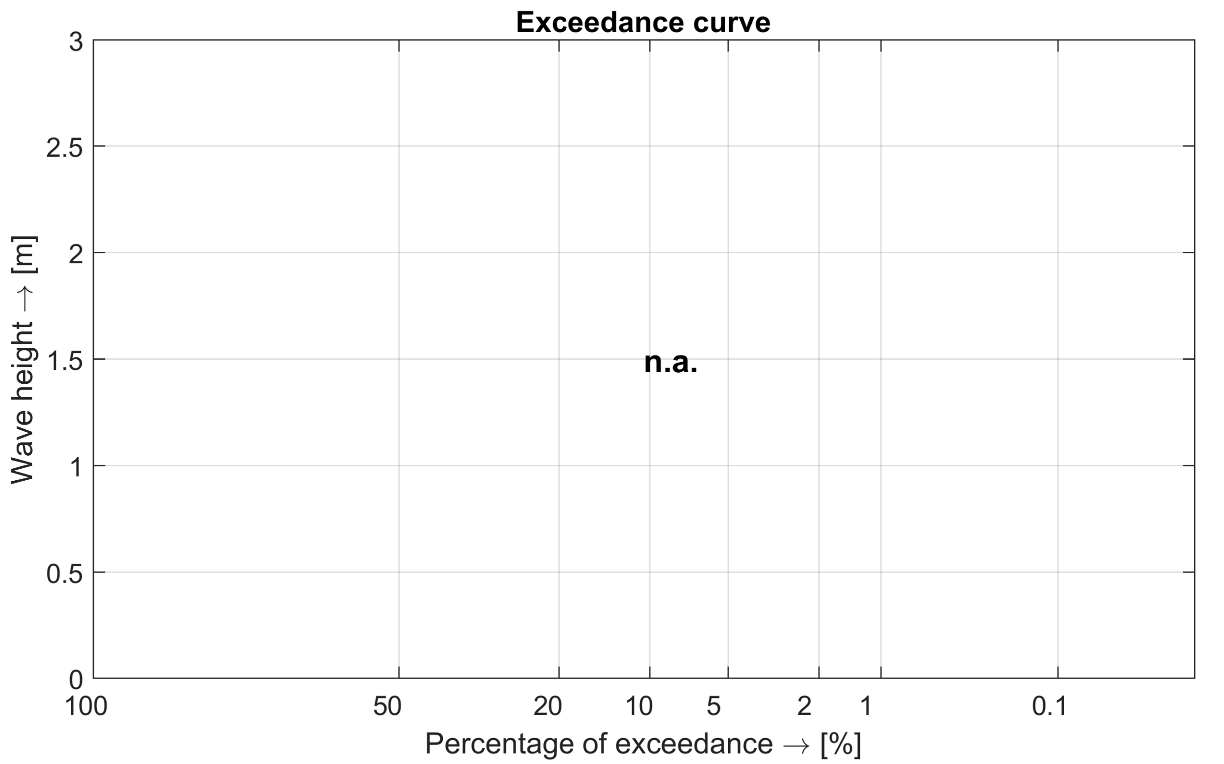

Results of wave generation calibration Depth = 18.0 m, H = 1.25 m, T = 17.20 s	Monochromatic	M172b
Deltares	11202696	App. E.1.12

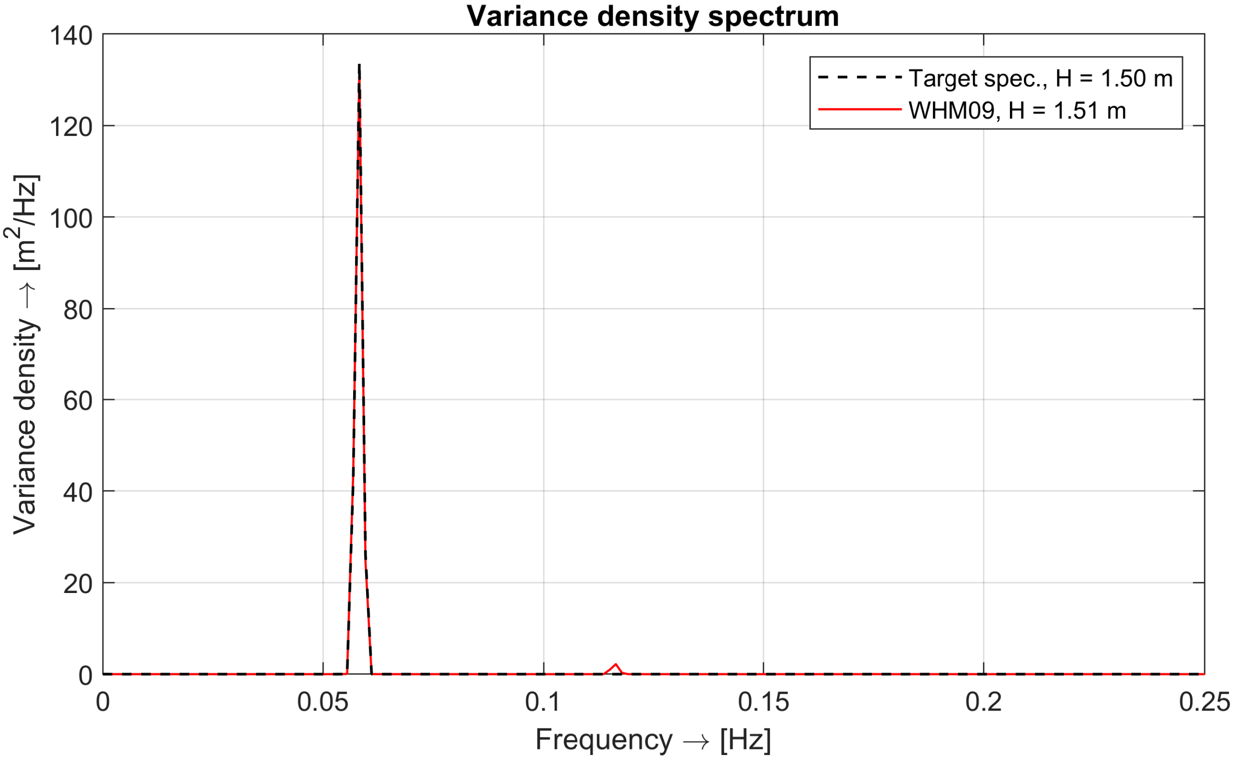

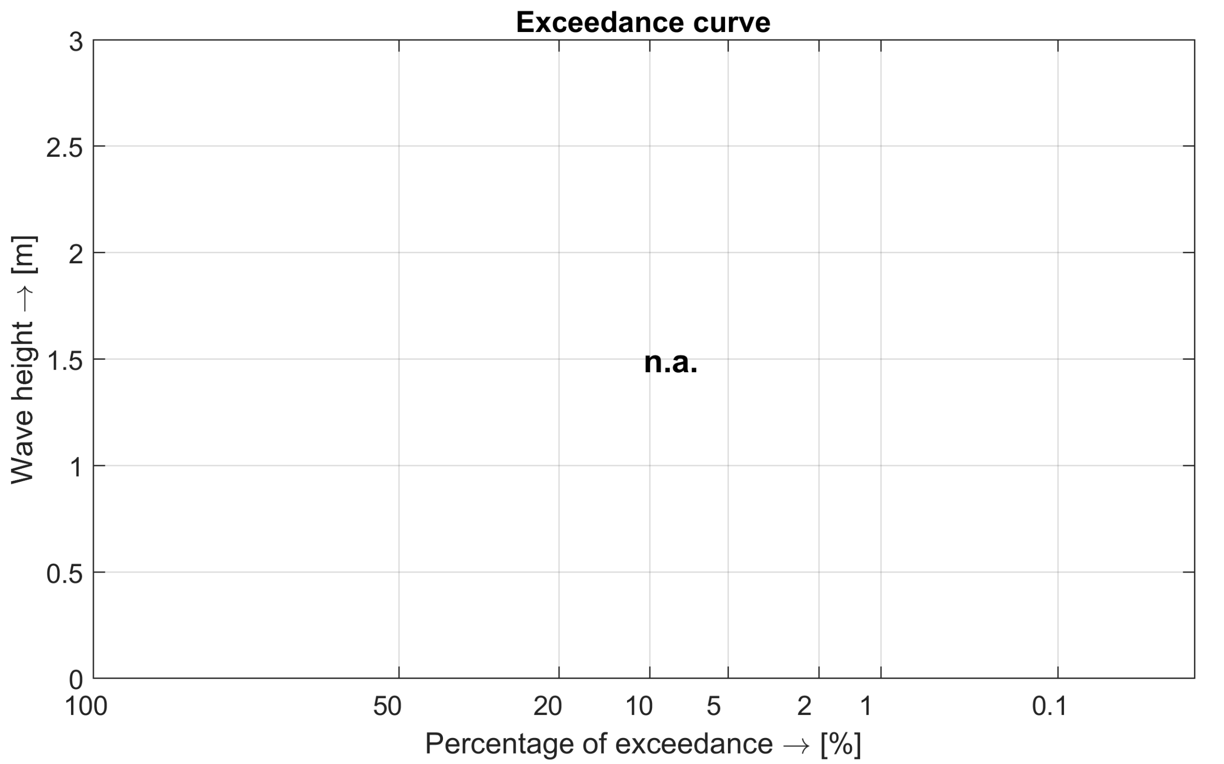

Results of wave generation calibration Depth = 18.0 m, H = 1.50 m, T = 17.20 s	Monochromatic	M172c
Deltares	11202696	App. E.1.13

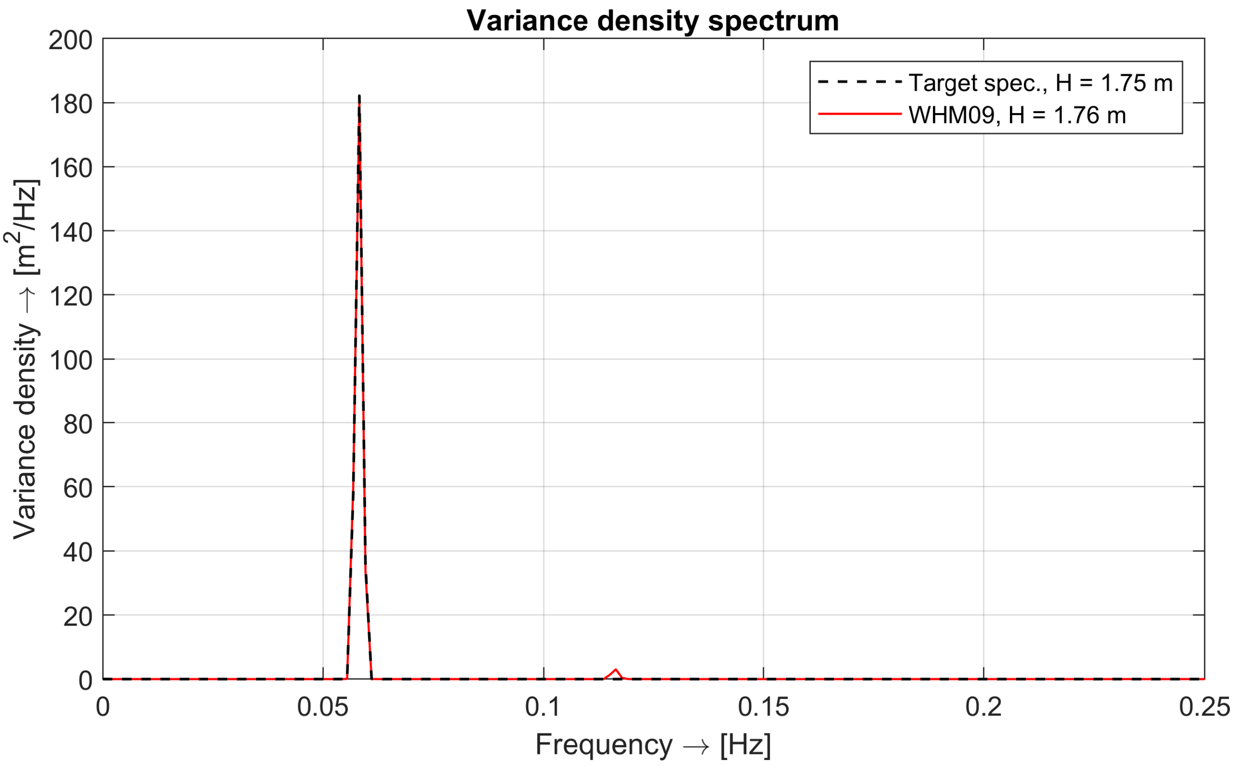

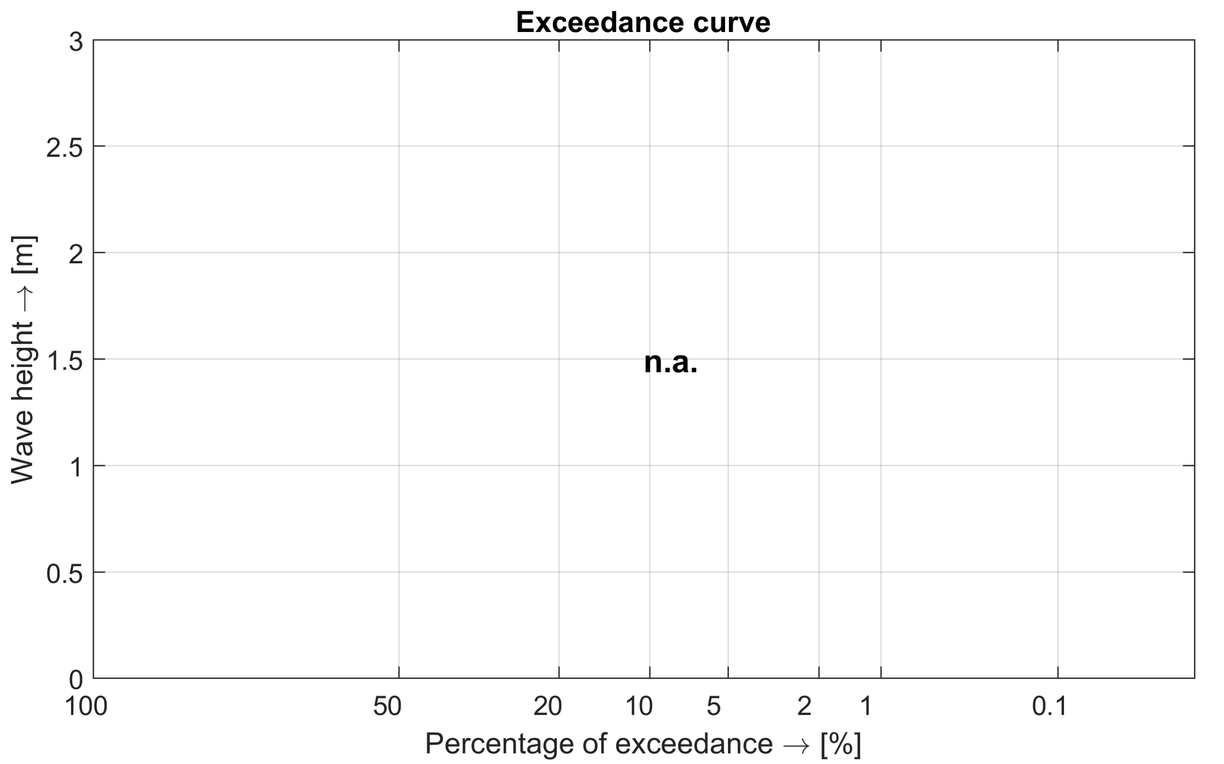

Results of wave generation calibration Depth = 18.0 m, H = 1.75 m, T = 17.20 s	Monochromatic	M172d
Deltares	11202696	App. E.1.14

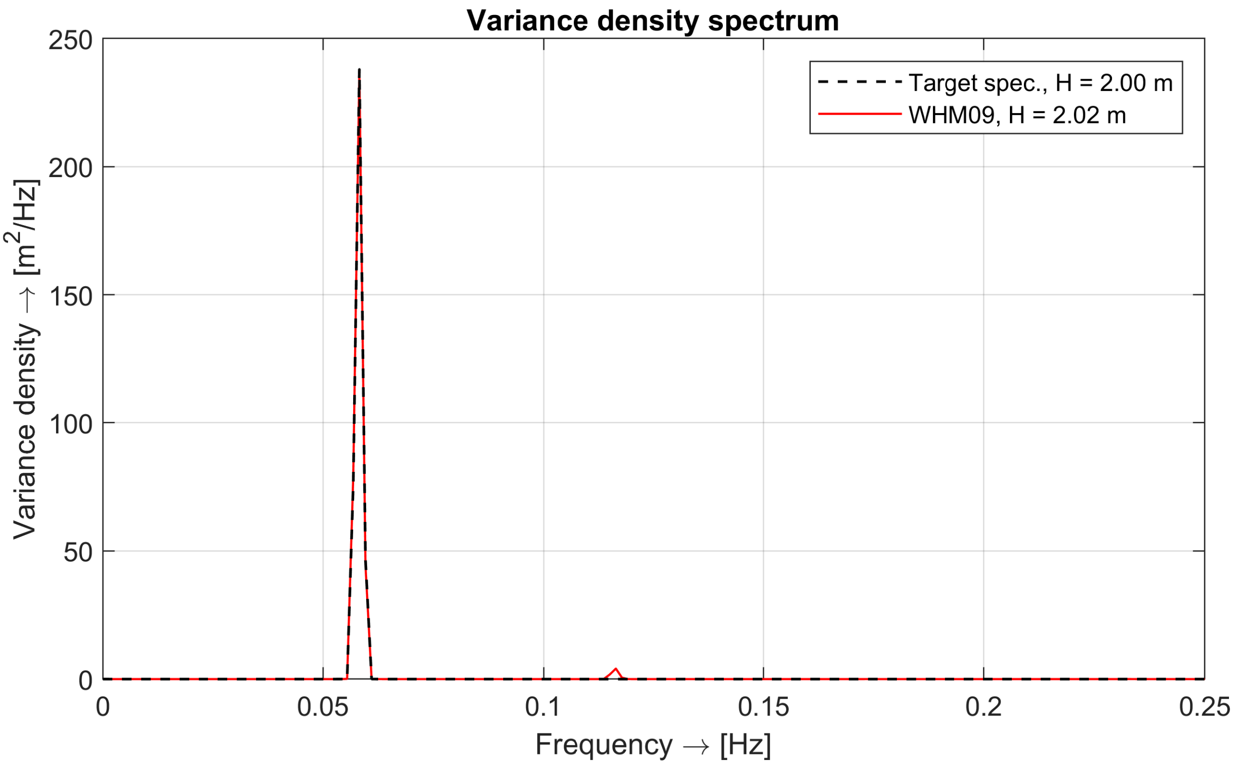

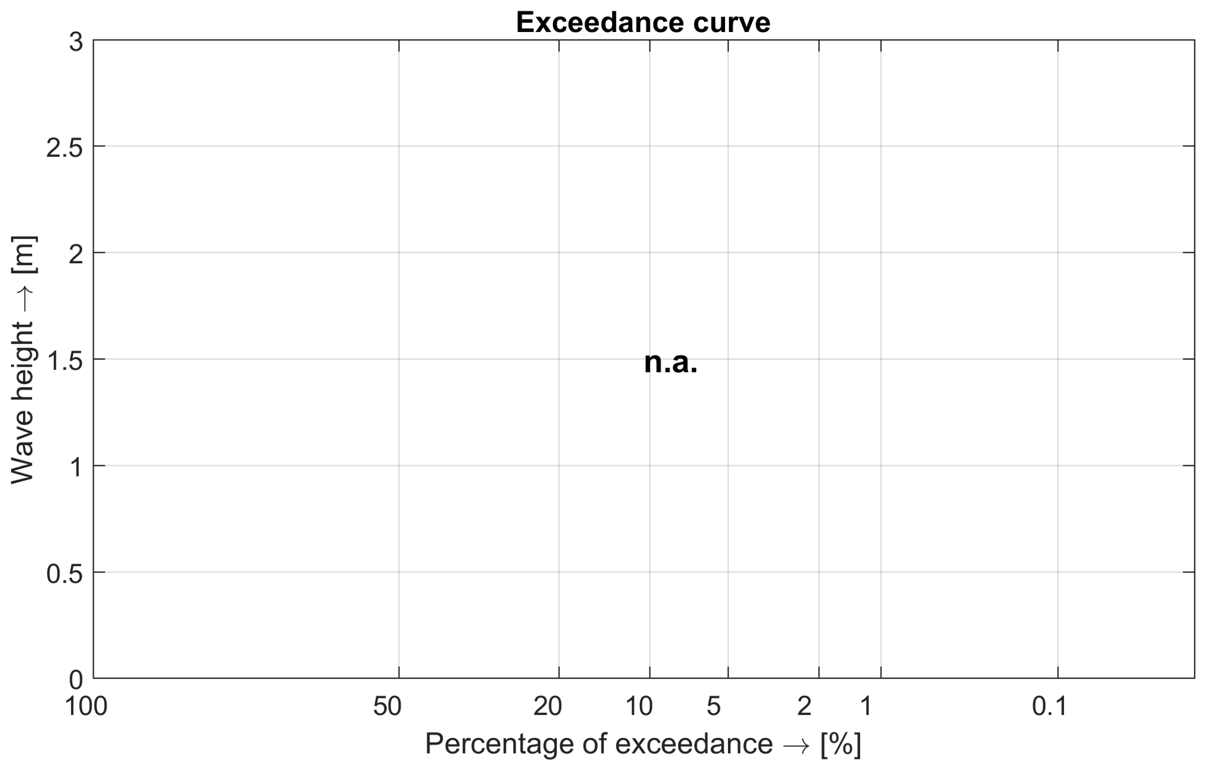

Results of wave generation calibration Depth = 18.0 m, H = 2.00 m, T = 17.20 s	Monochromatic	M172e
Deltares	11202696	App. E.1.15

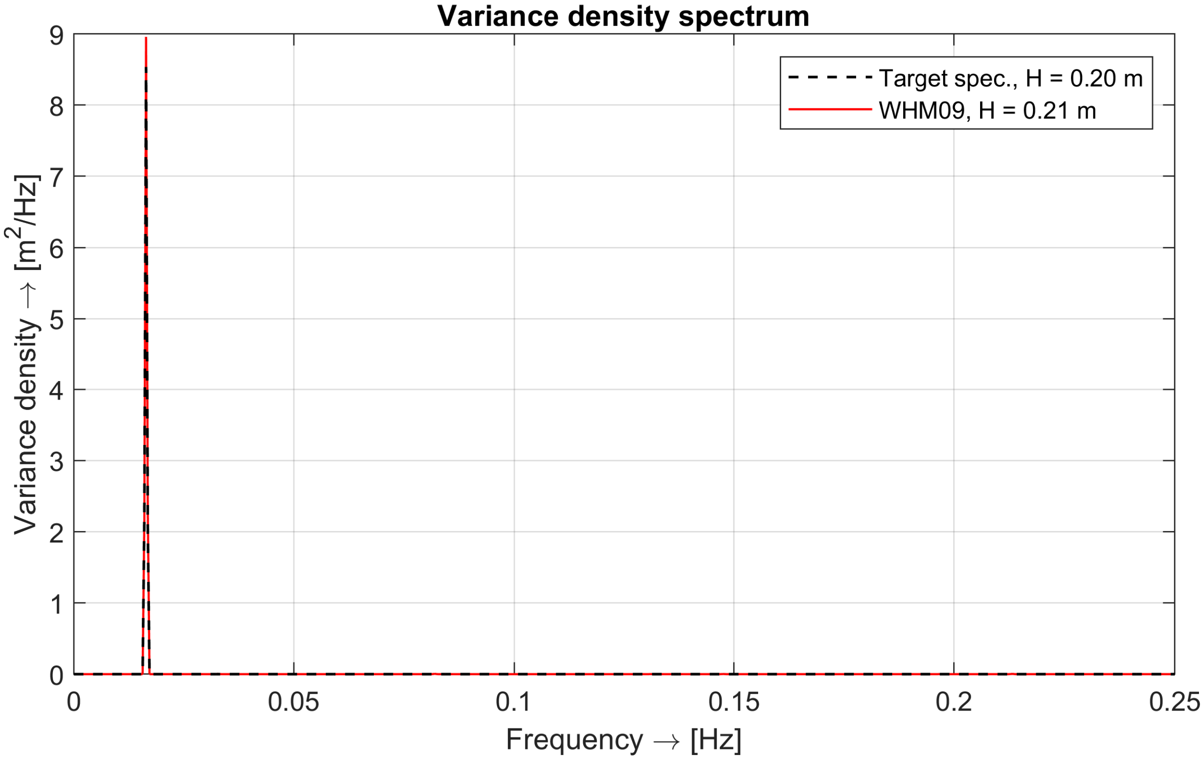

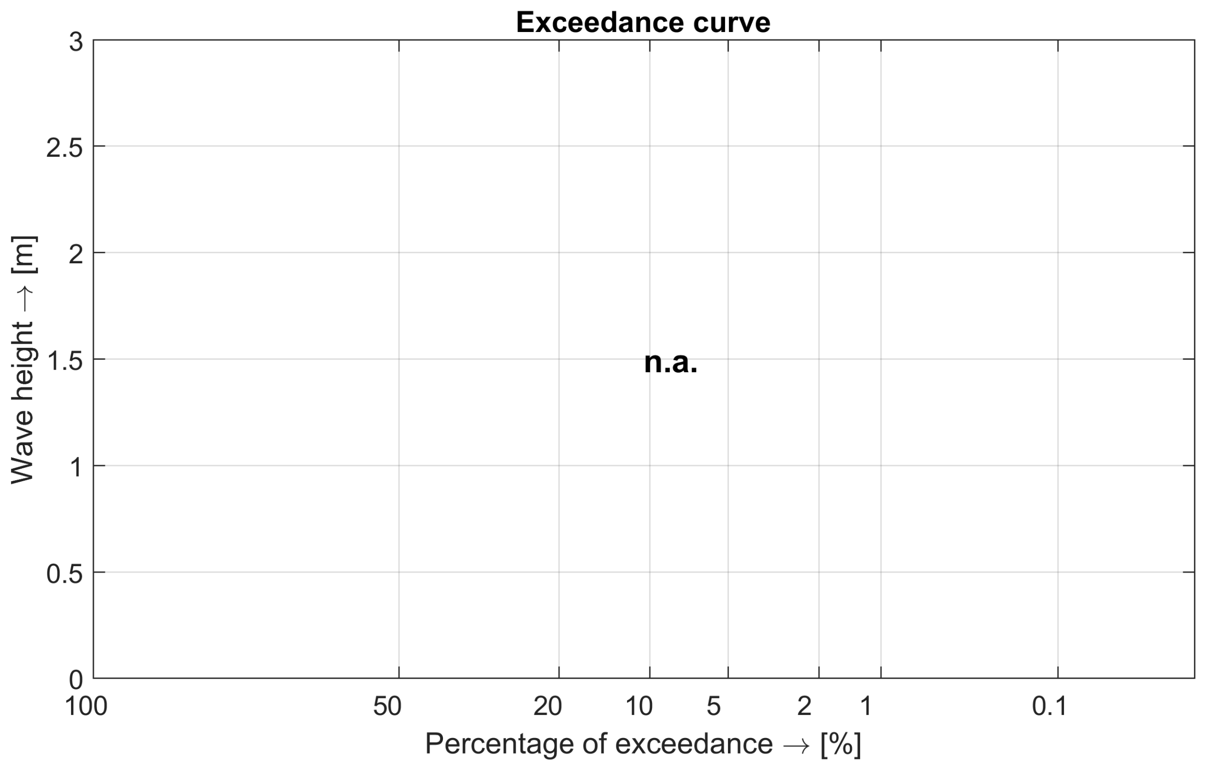

Results of wave generation calibration Depth = 18.0 m, H = 0.20 m, T = 61.00 s	Monochromatic	M610a
Deltares	11202696	App. E.1.16

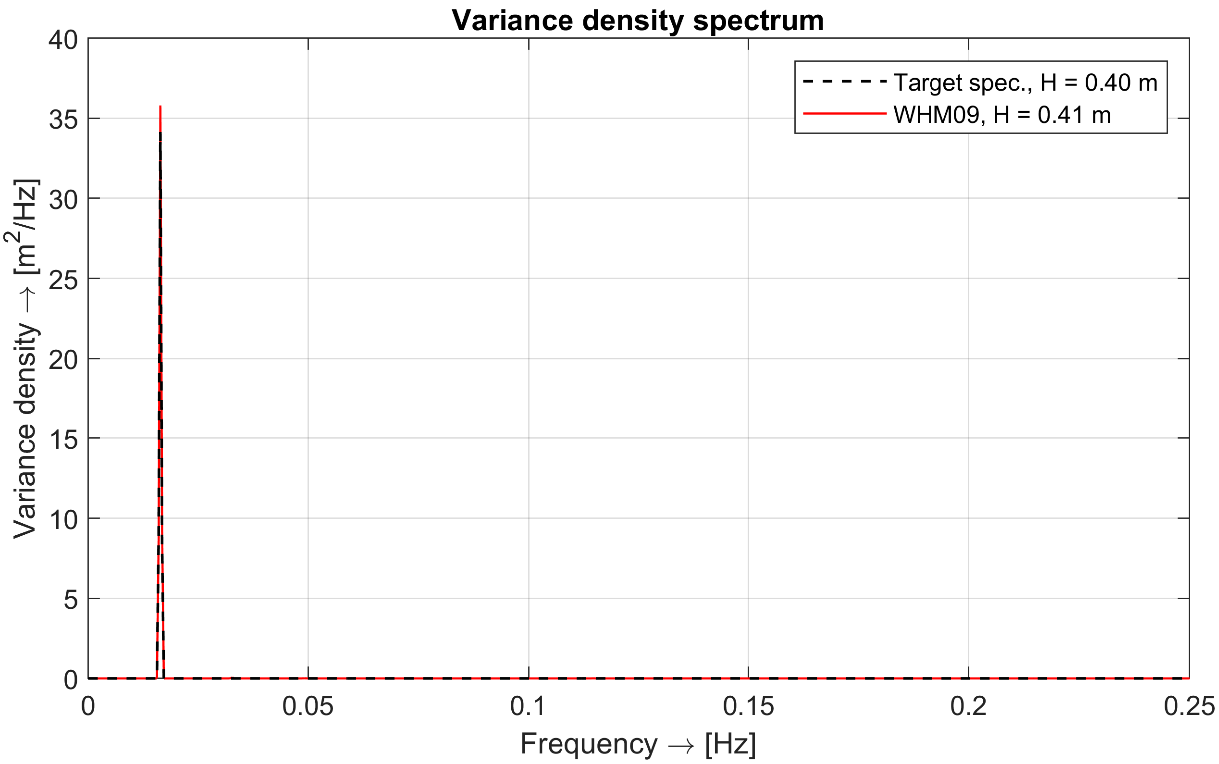

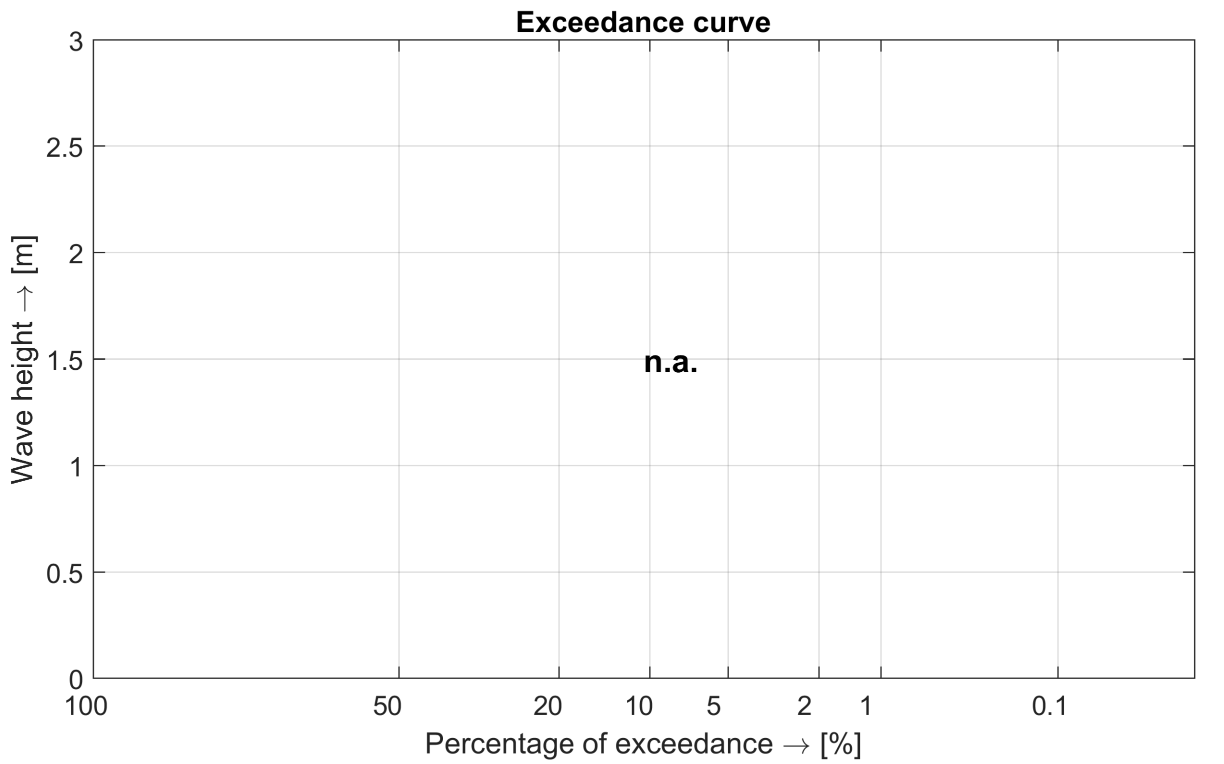

Results of wave generation calibration Depth = 18.0 m, H = 0.40 m, T = 61.00 s	Monochromatic	M610b
Deltares	11202696	App. E.1.17

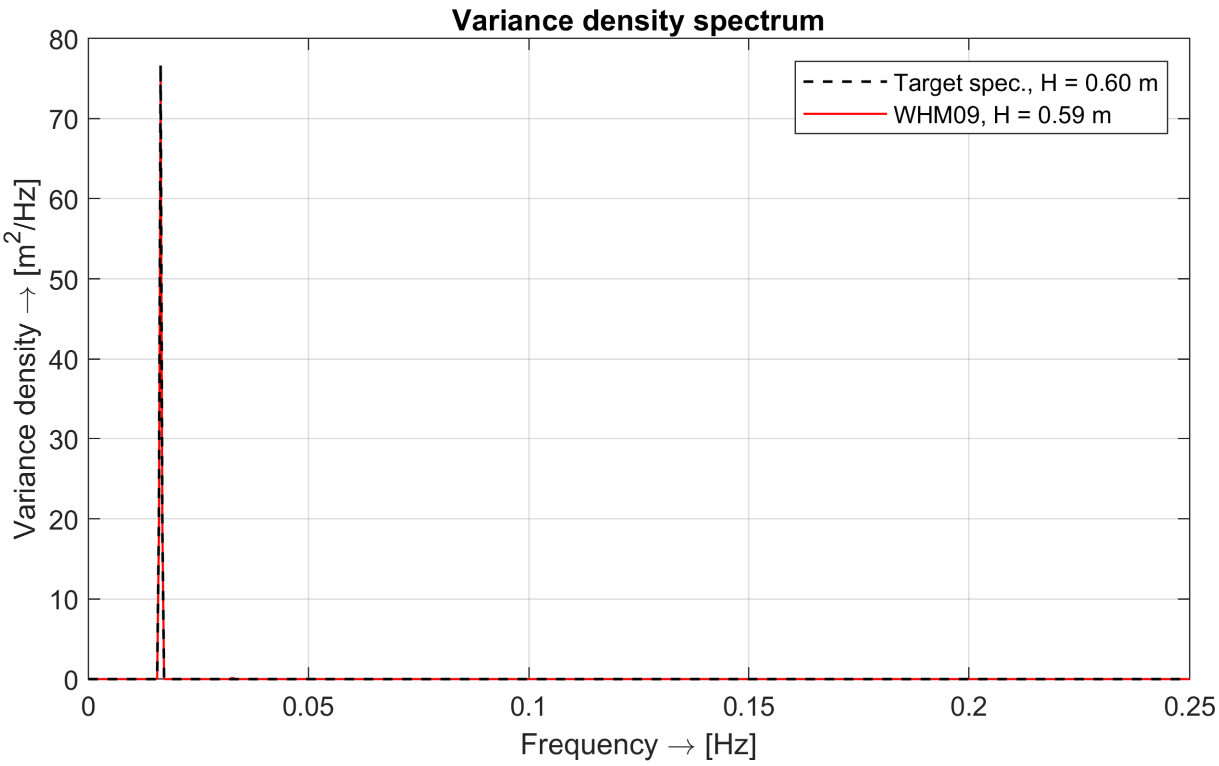

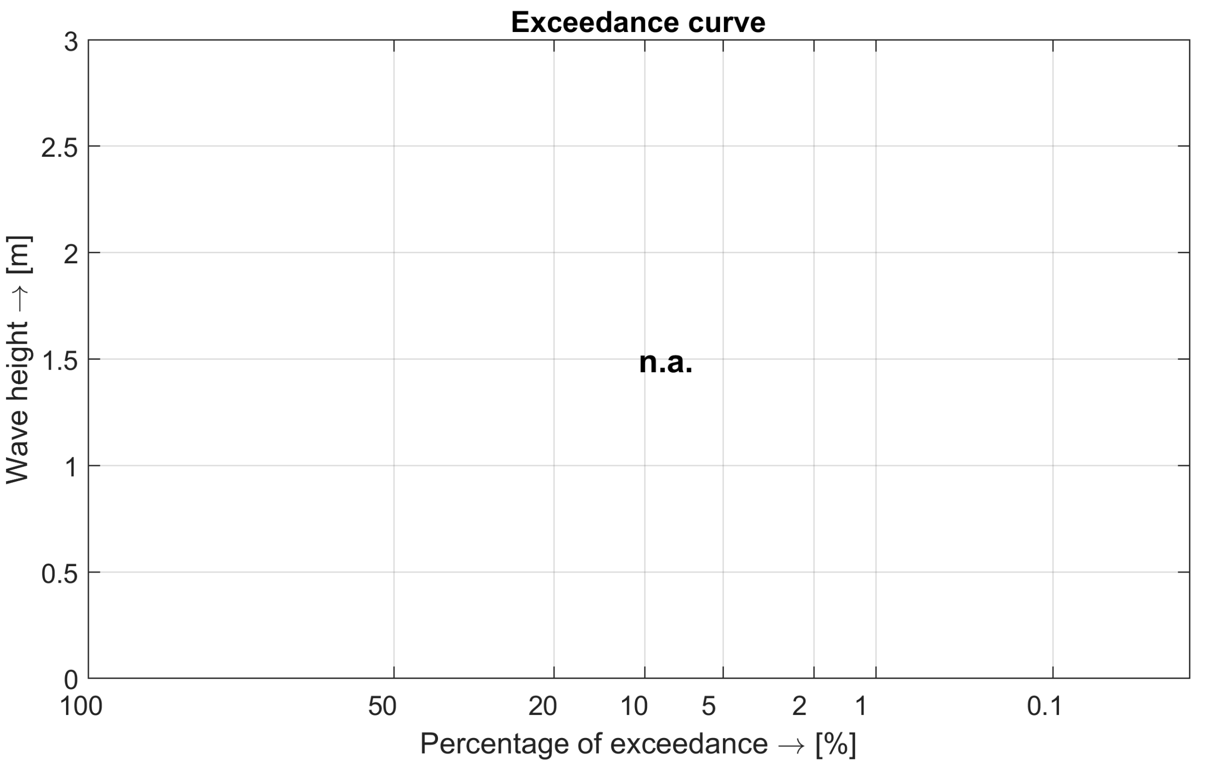

Results of wave generation calibration Depth = 18.0 m, H = 0.60 m, T = 61.00 s	Monochromatic	M610c
Deltares	11202696	App. E.1.18

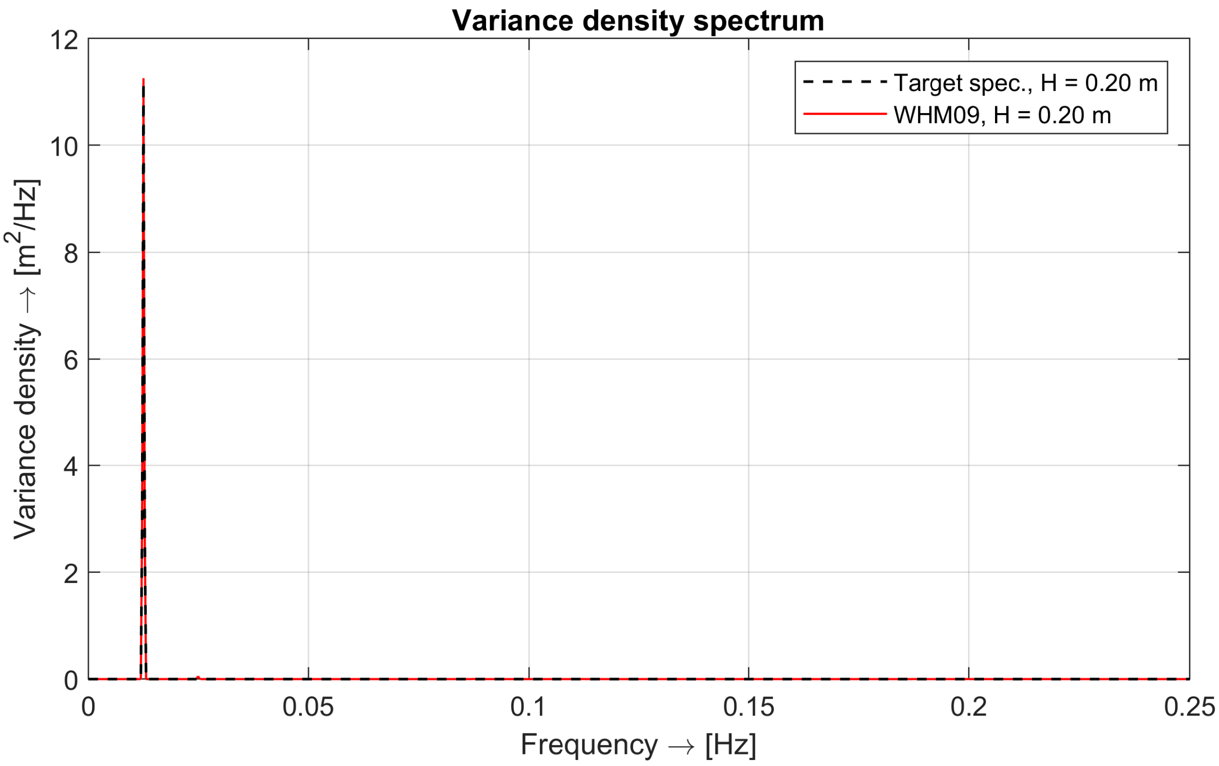

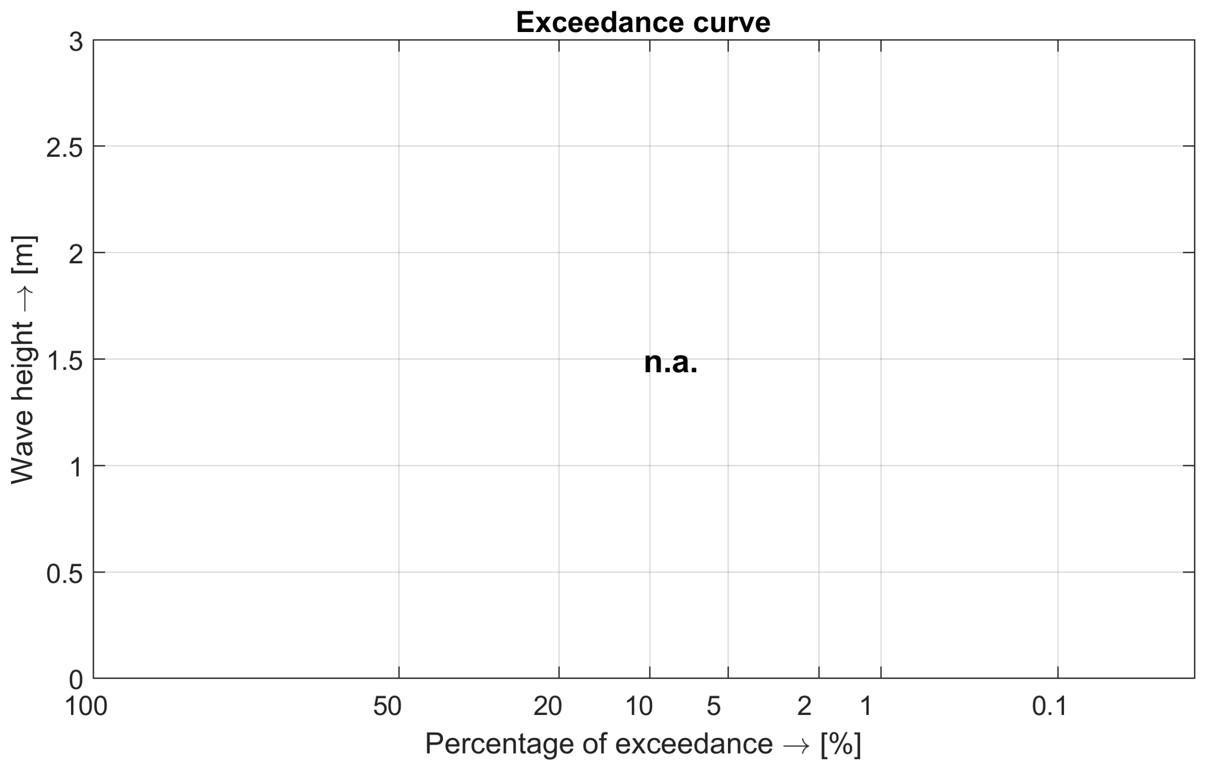

Results of wave generation calibration Depth = 18.0 m, H = 0.20 m, T = 80.00 s	Monochromatic	M800a
Deltares	11202696	App. E.1.19

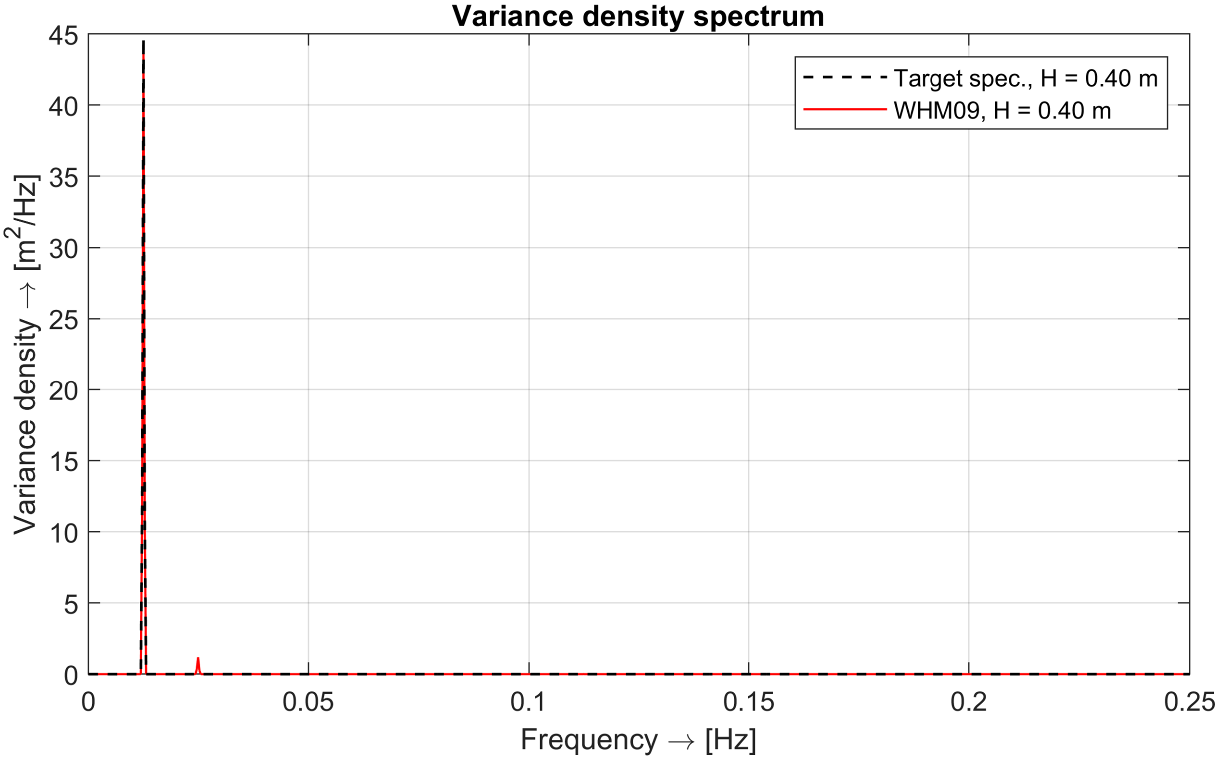

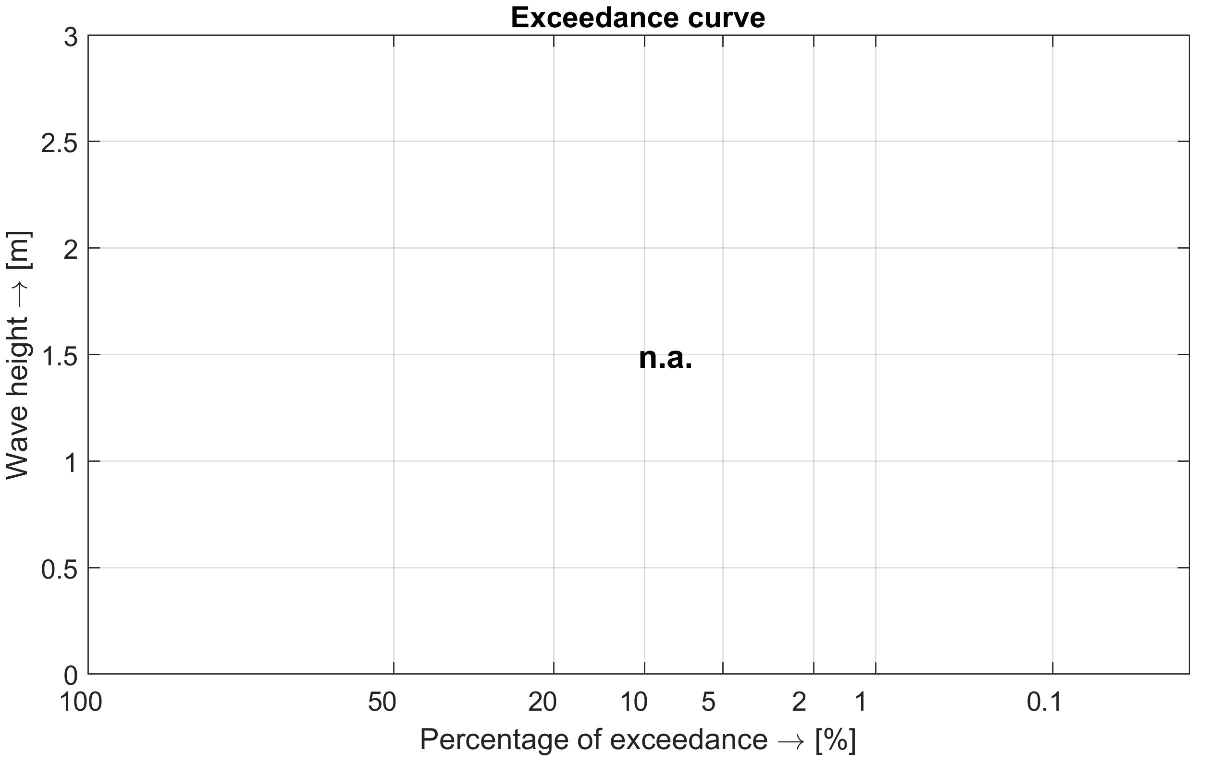

Results of wave generation calibration Depth = 18.0 m, H = 0.40 m, T = 80.00 s	Monochromatic	M800b
Deltares	11202696	App. E.1.20

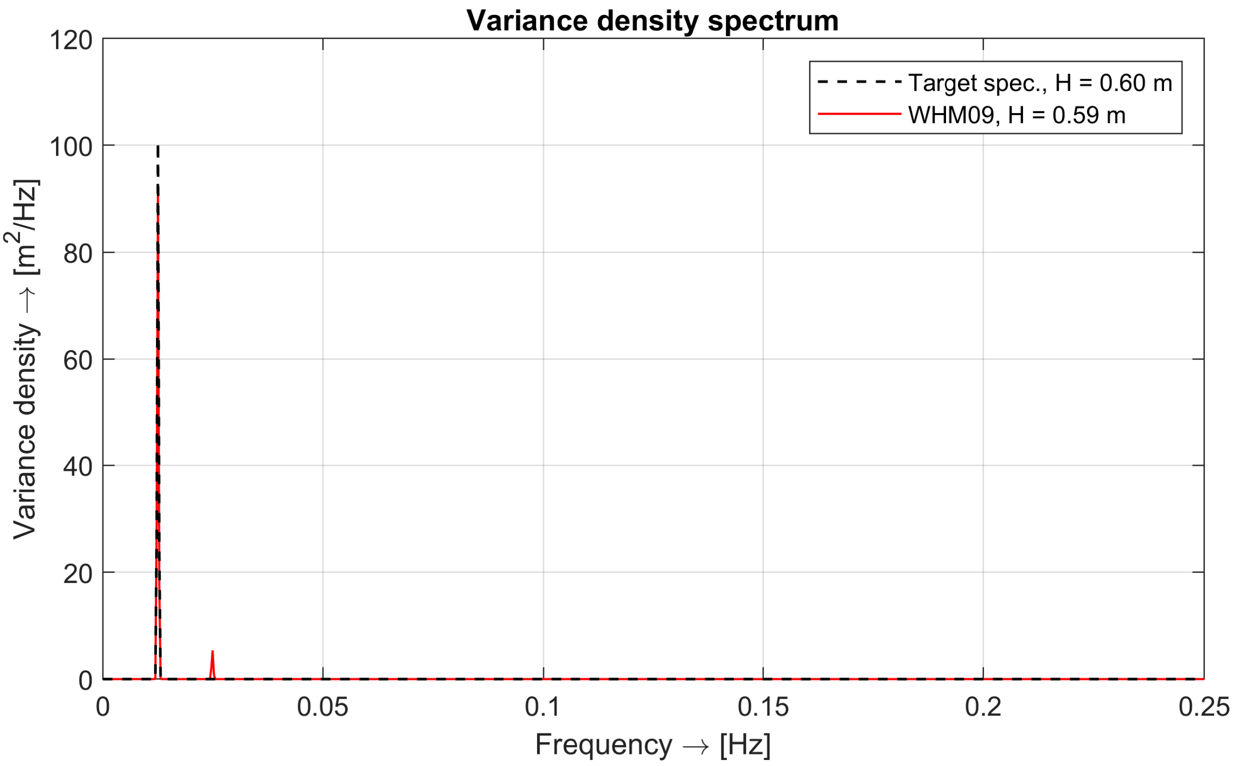

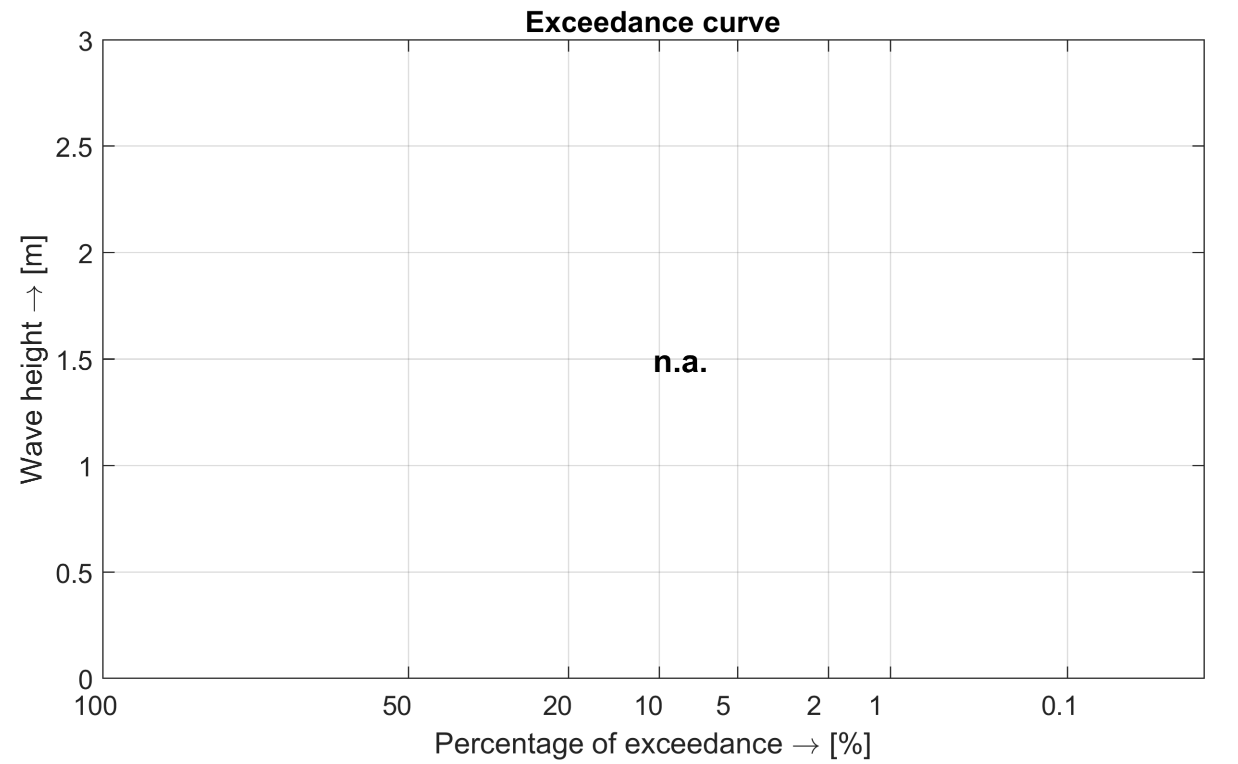

Results of wave generation calibration Depth = 18.0 m, H = 0.60 m, T = 80.00 s	Monochromatic	M800c
Deltares	11202696	App. E.1.21

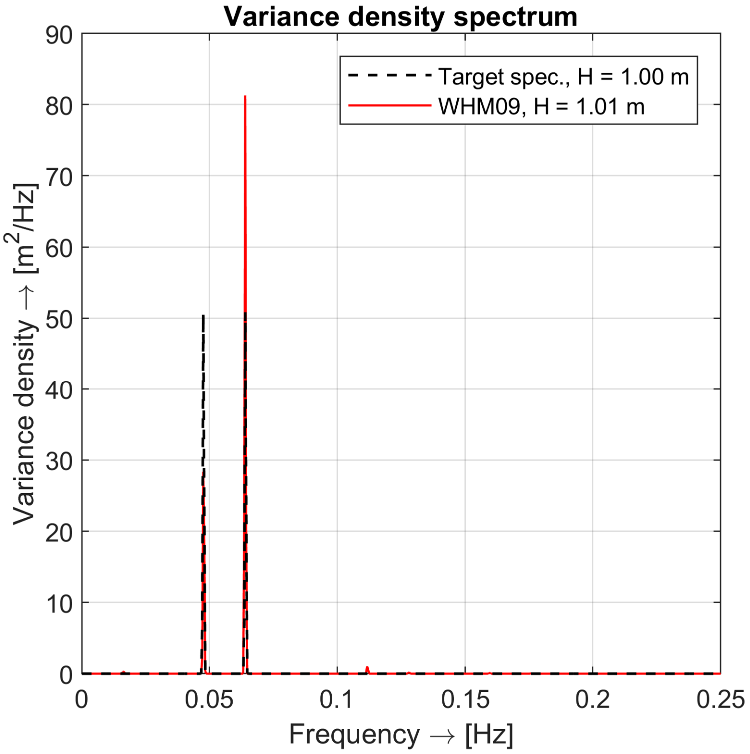

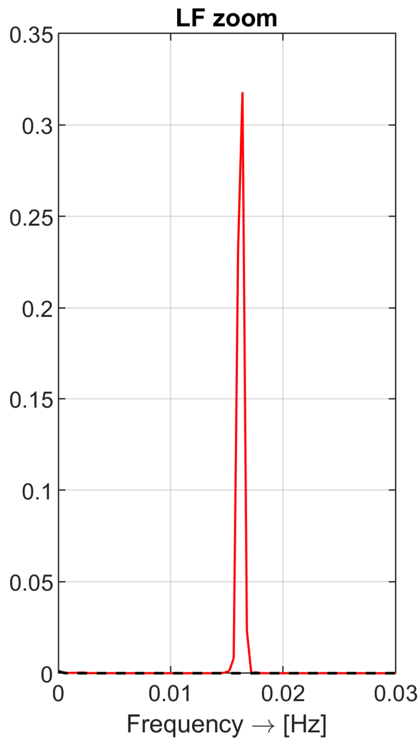

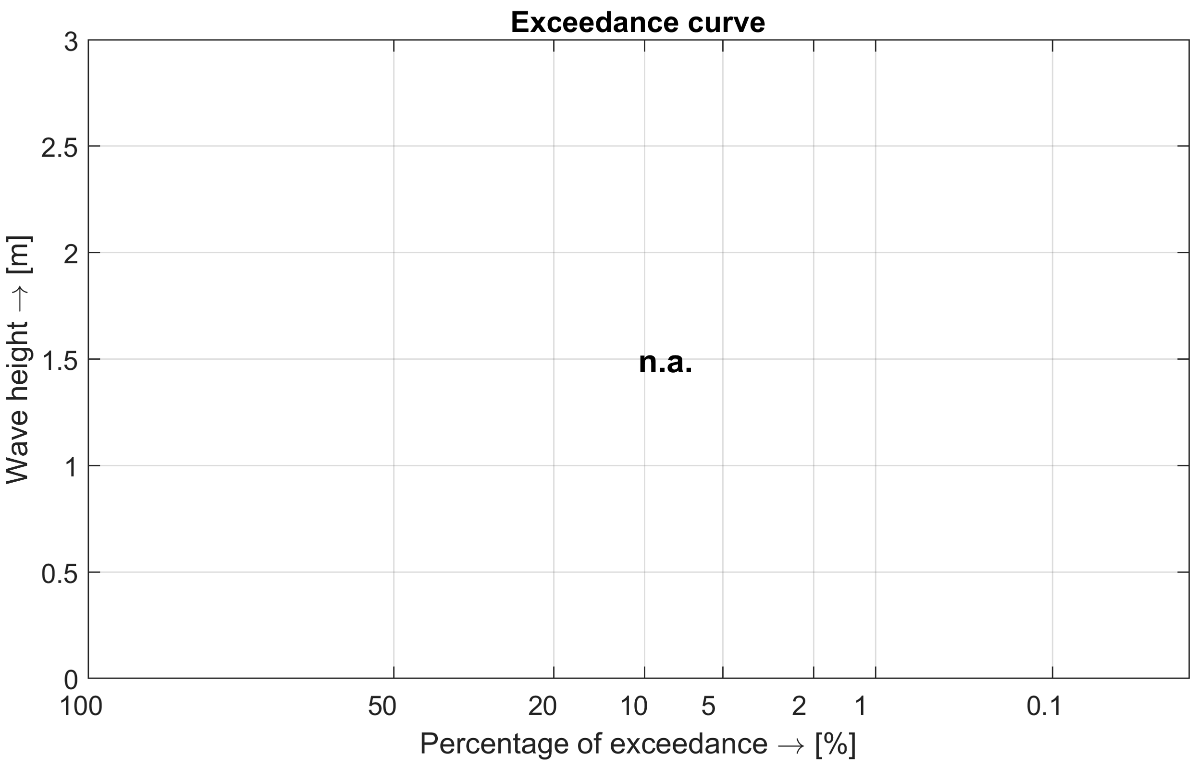

Results of wave generation calibration Depth = 18.0 m, H = 1.00 m, T_1 = 15.60 s, T_2 = 20.96 s	Bichromatic	B610a
Deltares	11202696	App. E.1.22

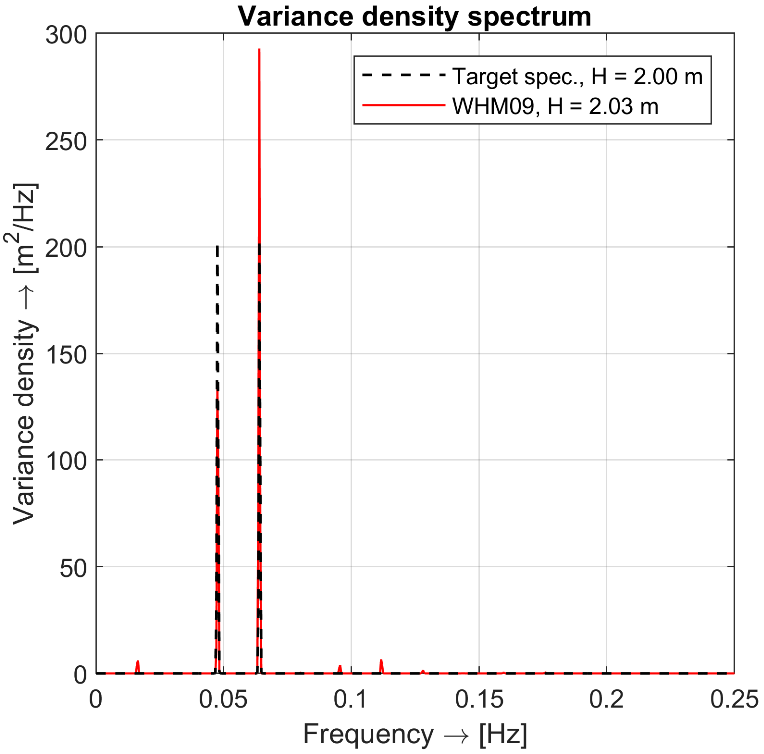

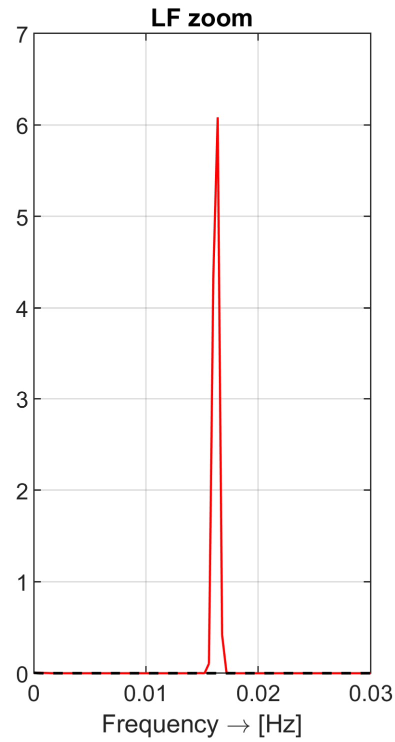

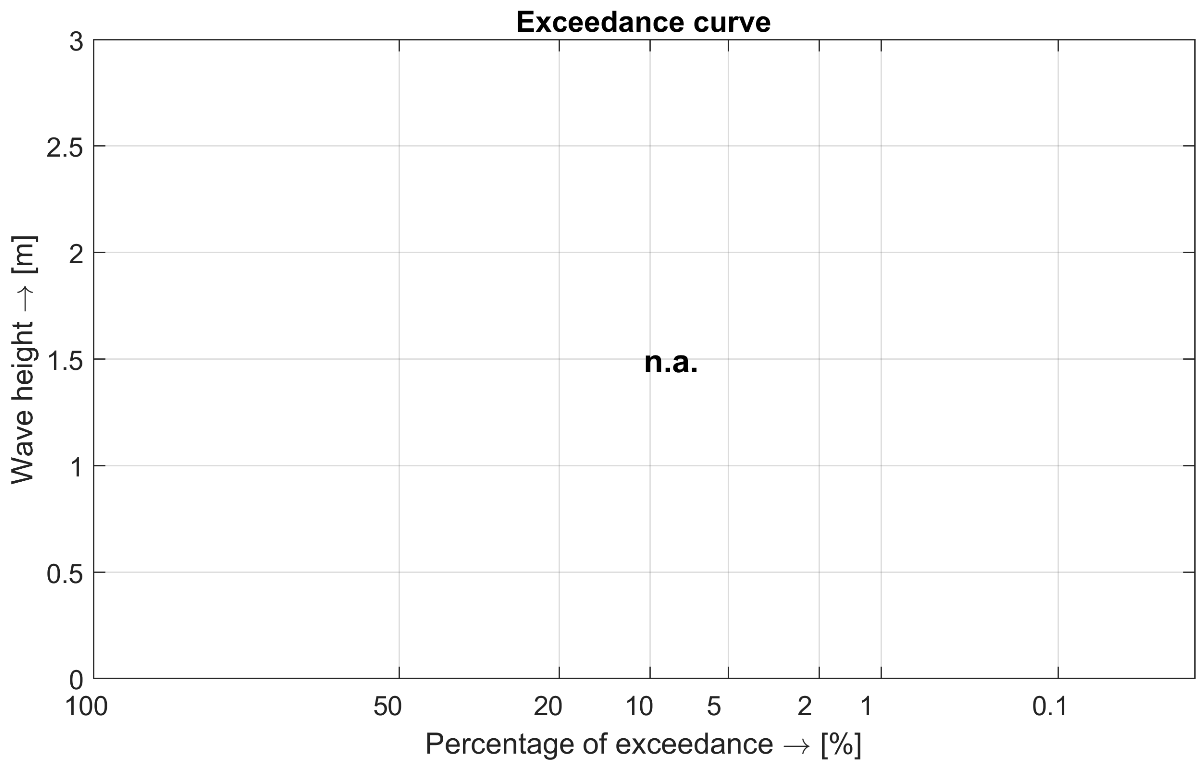

Results of wave generation calibration Depth = 18.0 m, H = 2.00 m, T_1 = 15.60 s, T_2 = 20.96 s	Bichromatic	B610e
Deltares	11202696	App. E.1.23

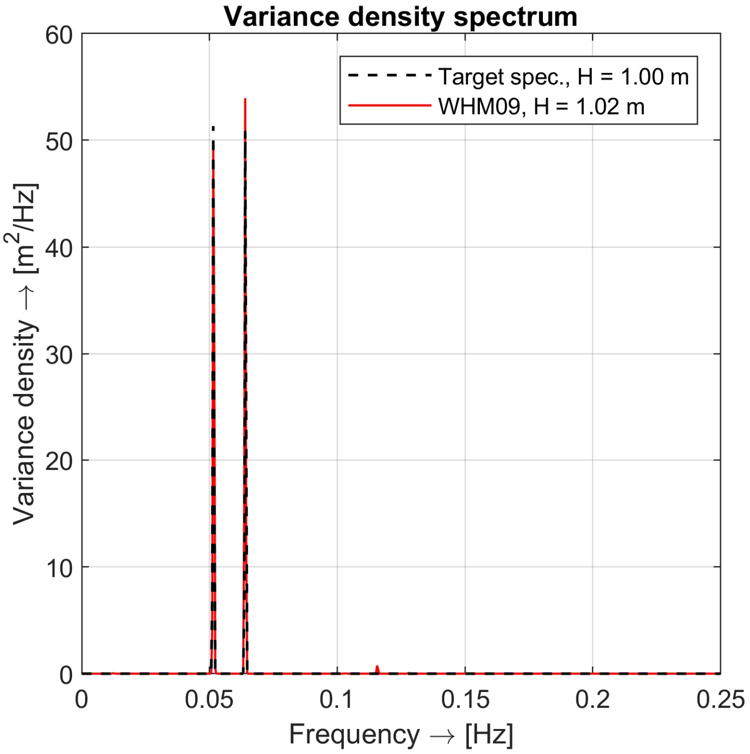

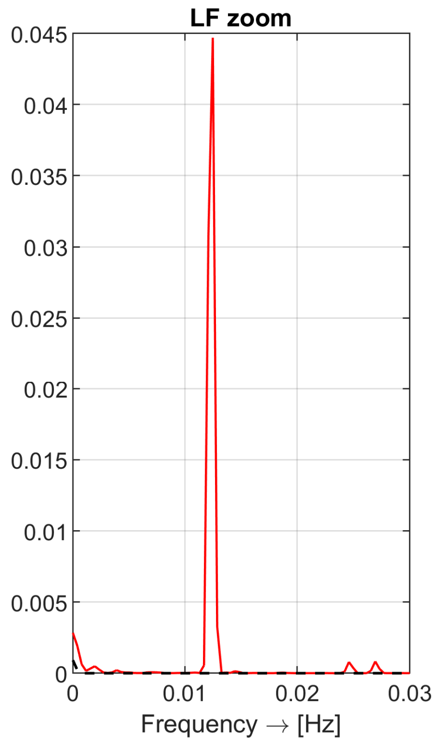

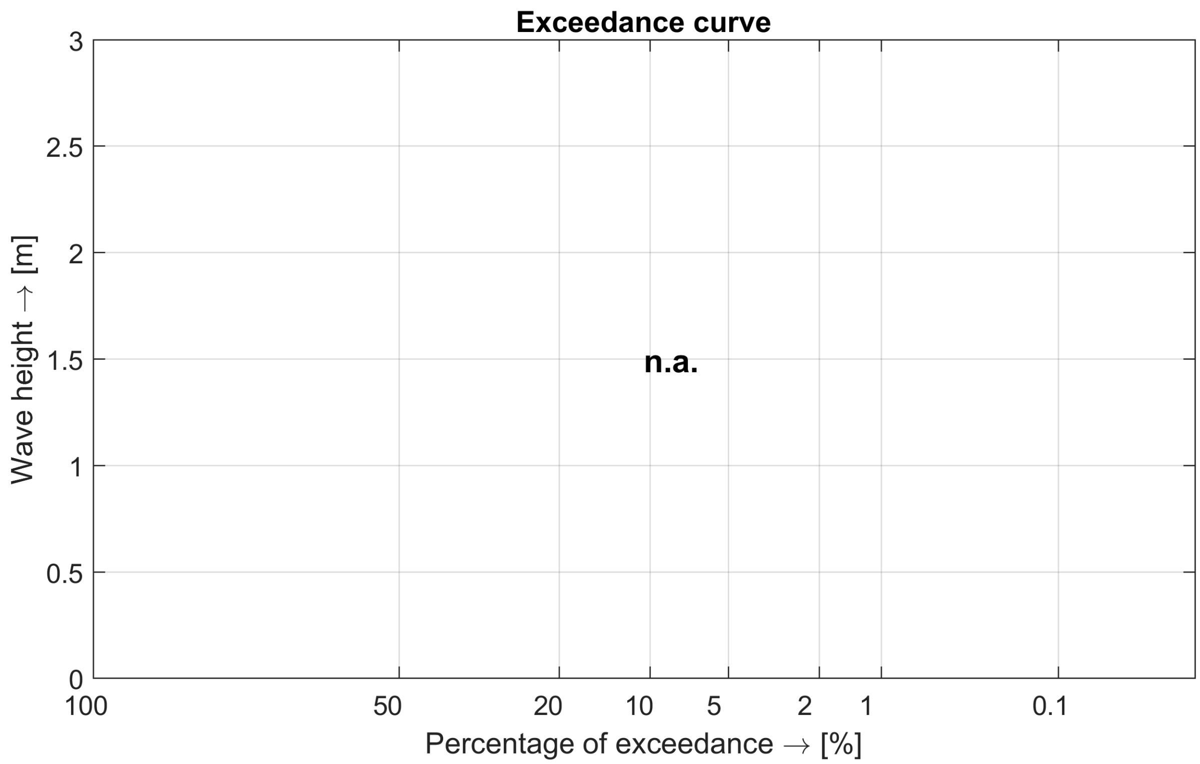

Results of wave generation calibration Depth = 18.0 m, H = 1.00 m, T_1 = 15.60 s, T_2 = 19.38 s	Bichromatic	B800a
Deltares	11202696	App. E.1.24

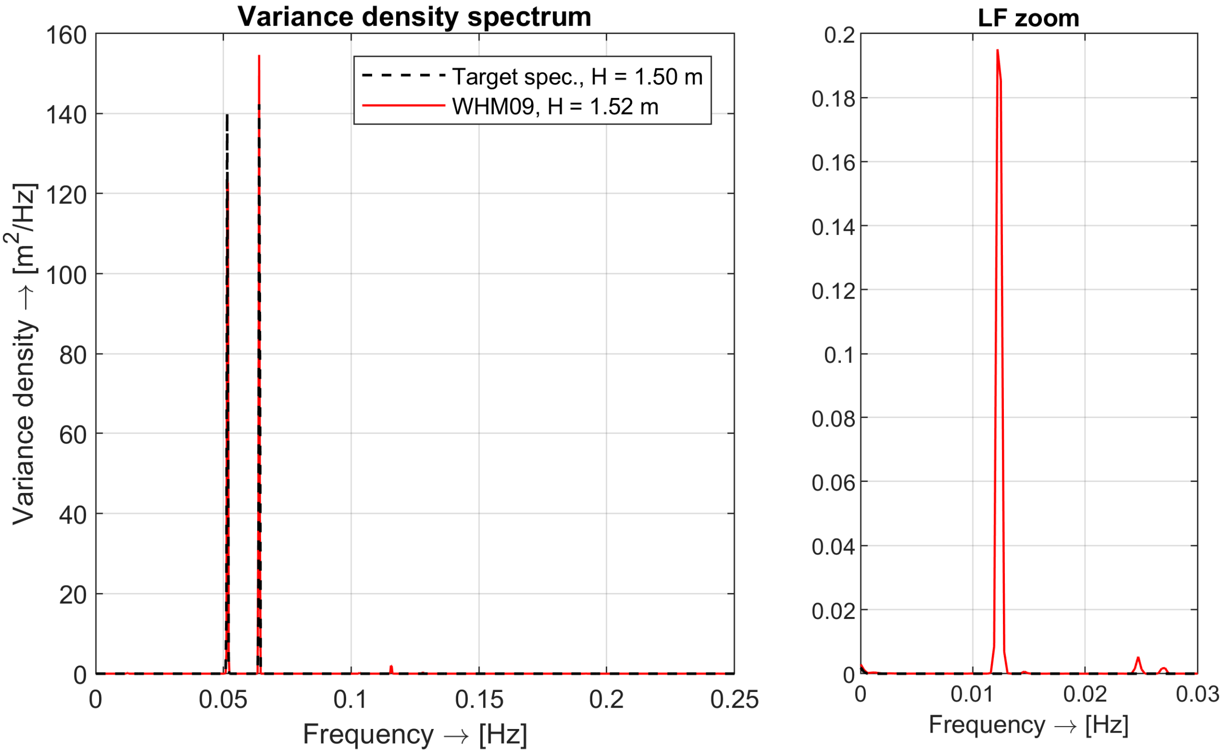

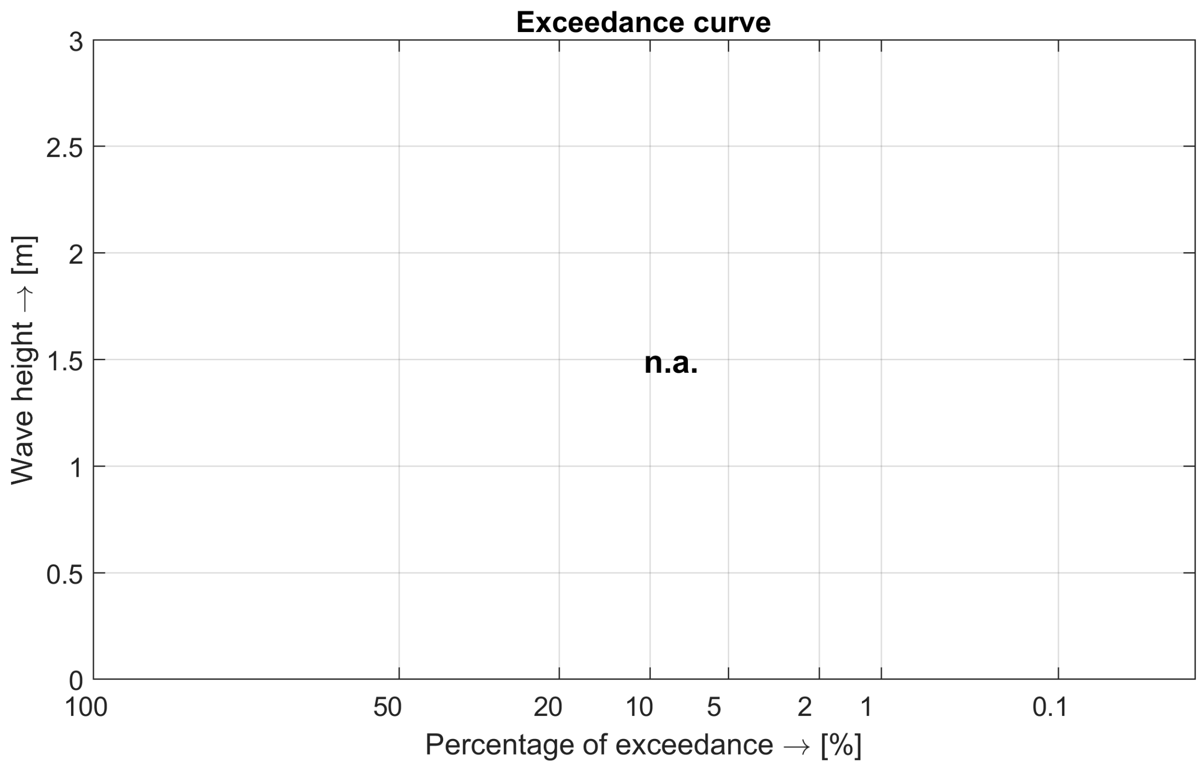

Results of wave generation calibration Depth = 18.0 m, H = 1.50 m, T_1 = 15.60 s, T_2 = 19.38 s	Bichromatic	B800c
Deltares	11202696	App. E.1.25

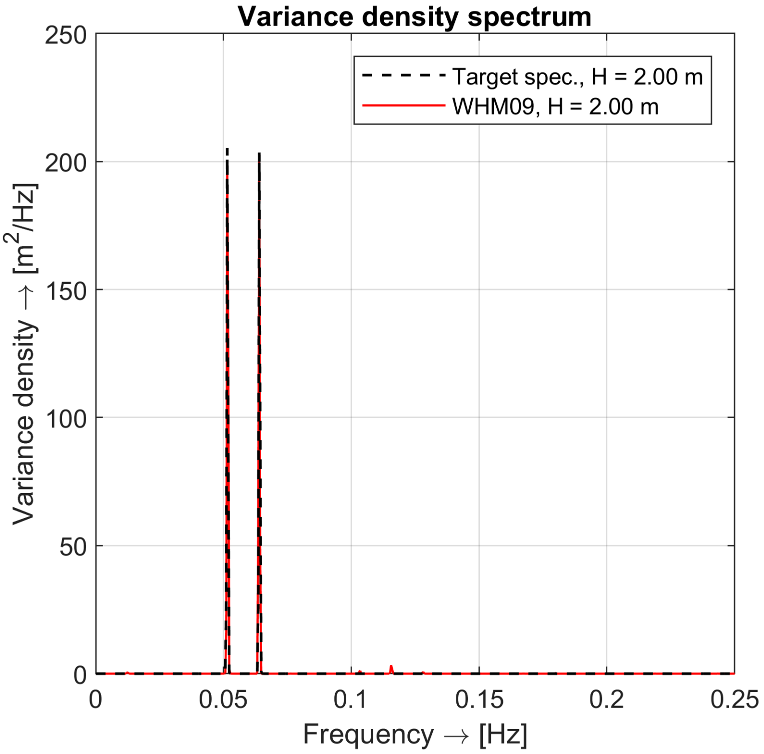

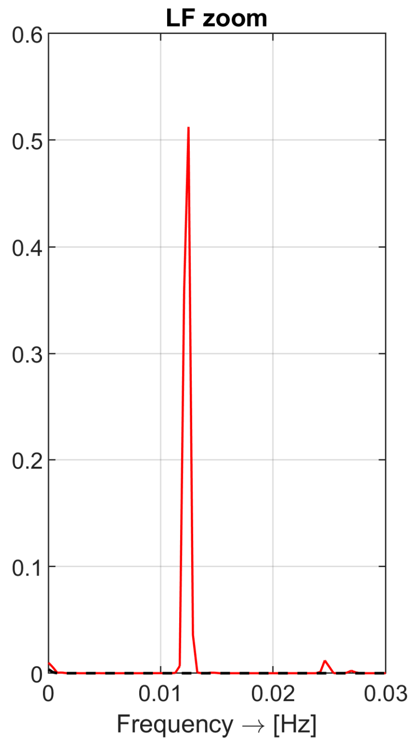

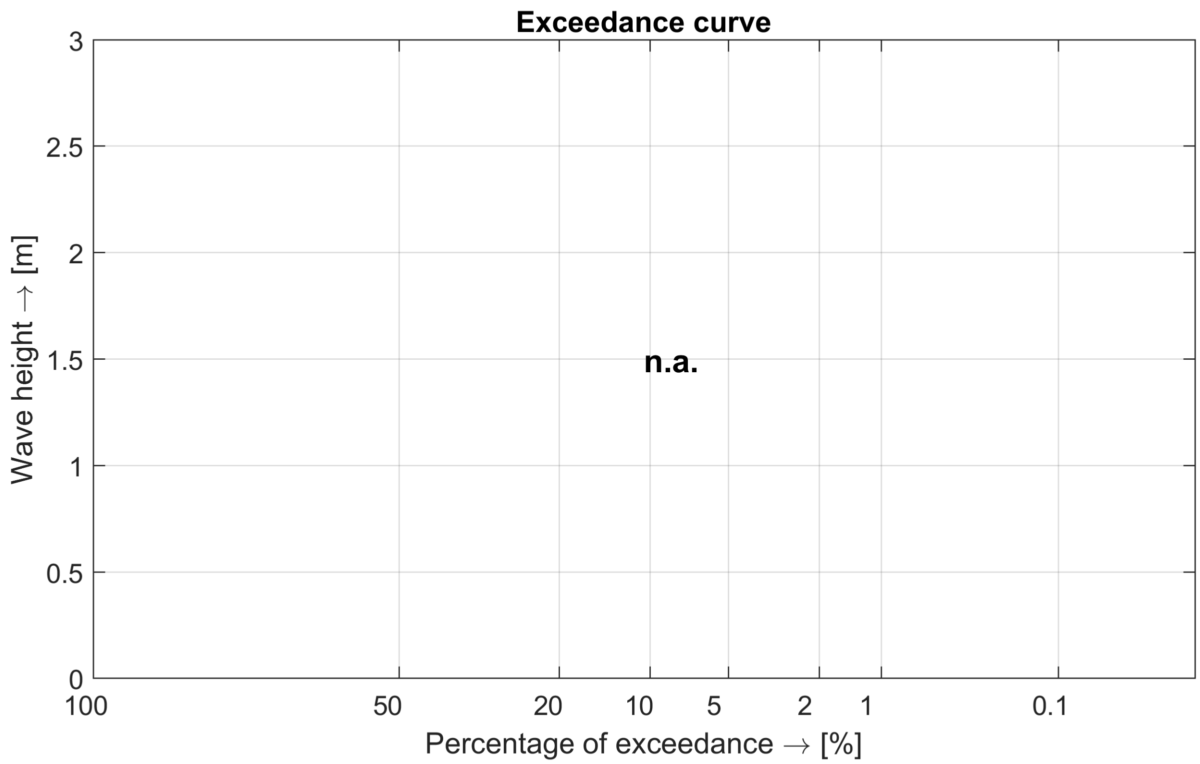

Results of wave generation calibration Depth = 18.0 m, H = 2.00 m, T_1 = 15.60 s, T_2 = 19.38 s	Bichromatic	B800e
Deltares	11202696	App. E.1.26

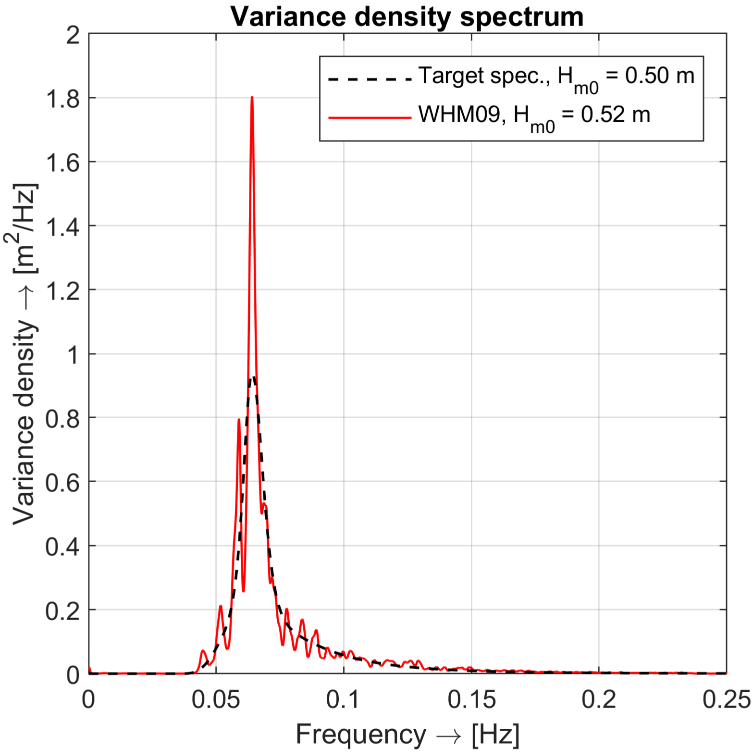

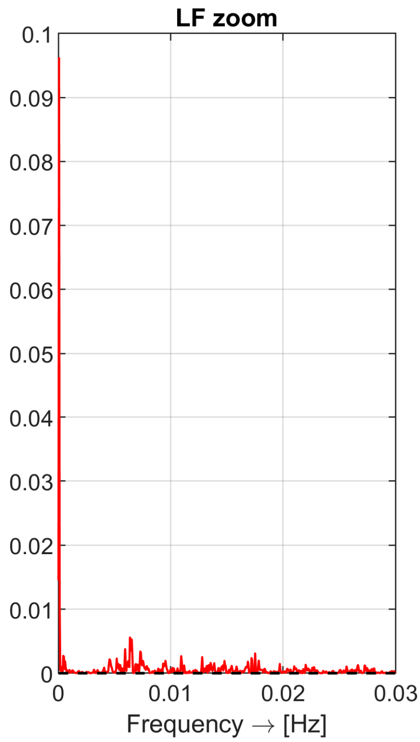

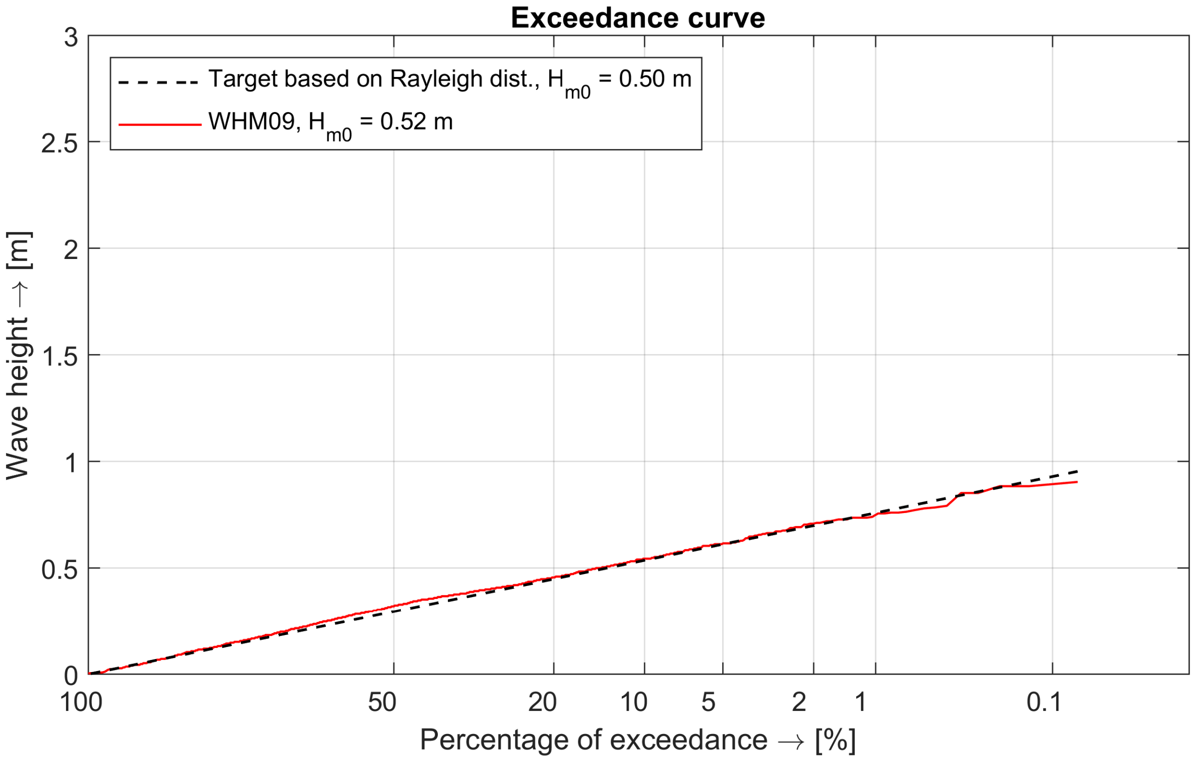

Results of wave generation calibration Depth = 18.0 m, H_{m0} = 0.50 m, T_p = 15.60 s, γ = 5.0	Irregular	I156a
Deltares	11202696	App. E.1.27

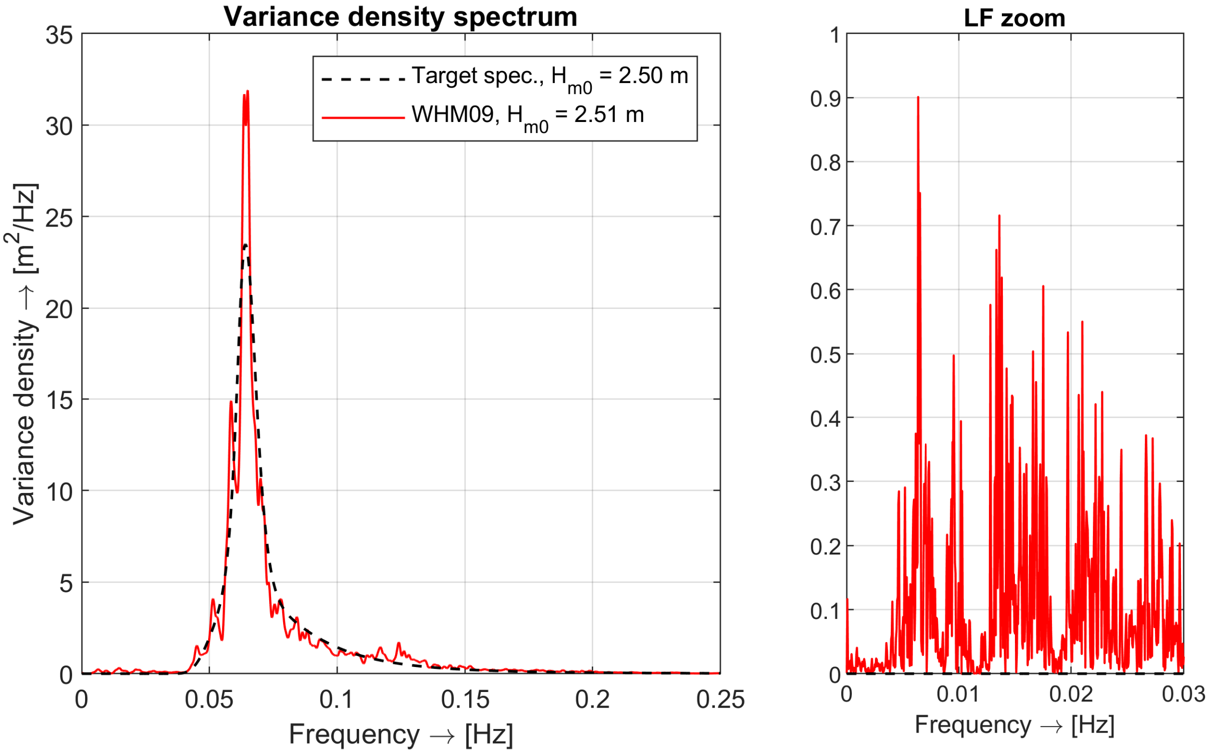

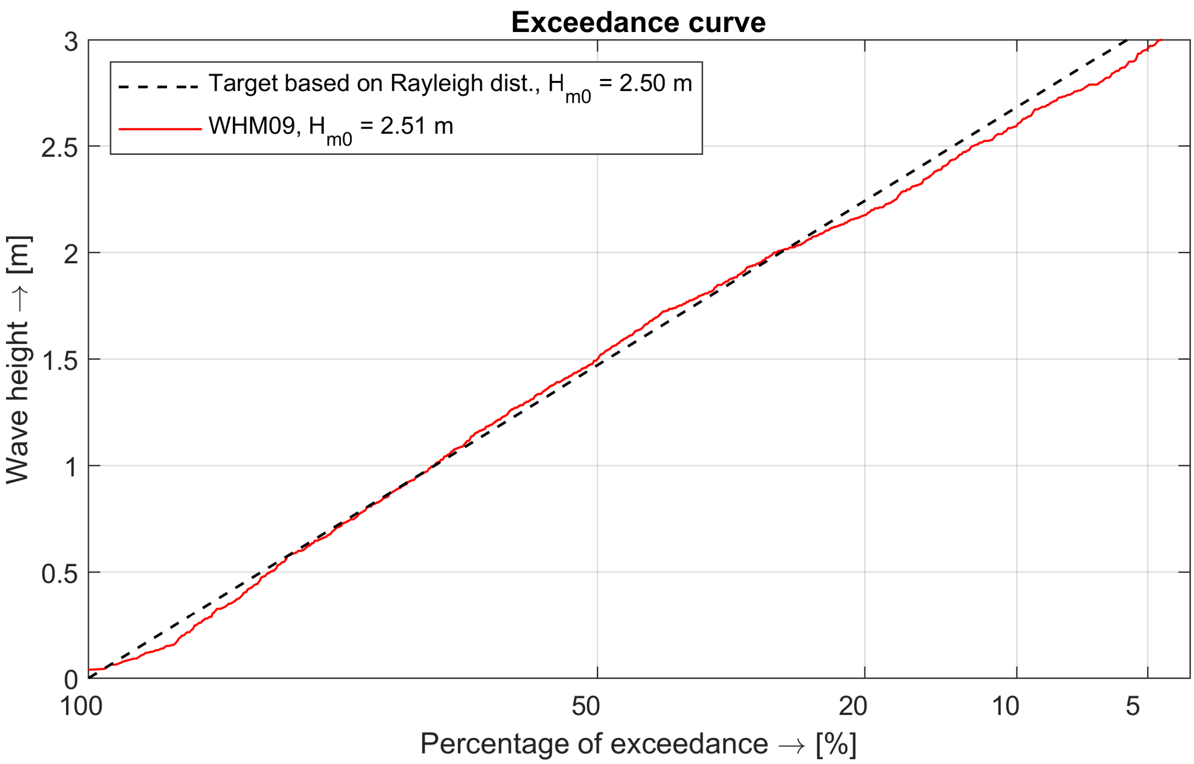

Results of wave generation calibration Depth = 18.0 m, H_{m0} = 2.50 m, T_p = 15.60 s, γ = 5.0	Irregular	I156e
Deltares	11202696	App. E.1.28

E.2 Reflection analyses Cases A, B and C

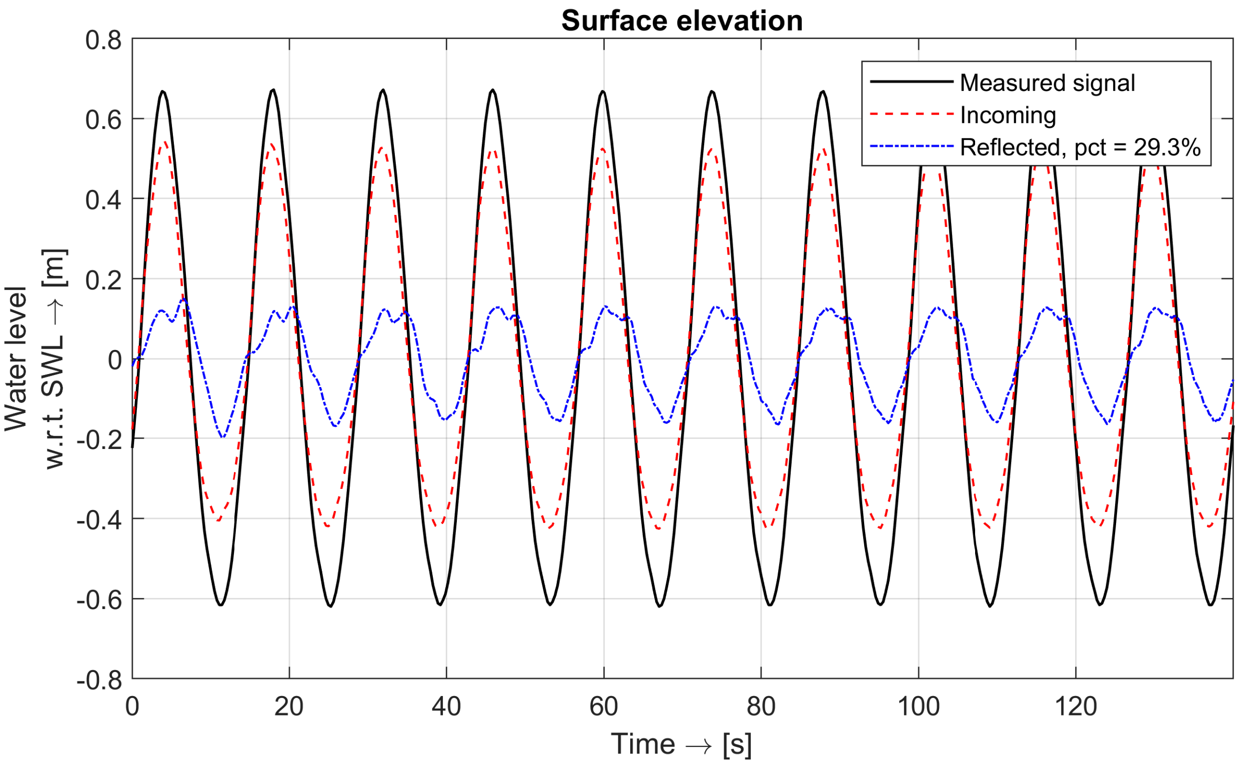

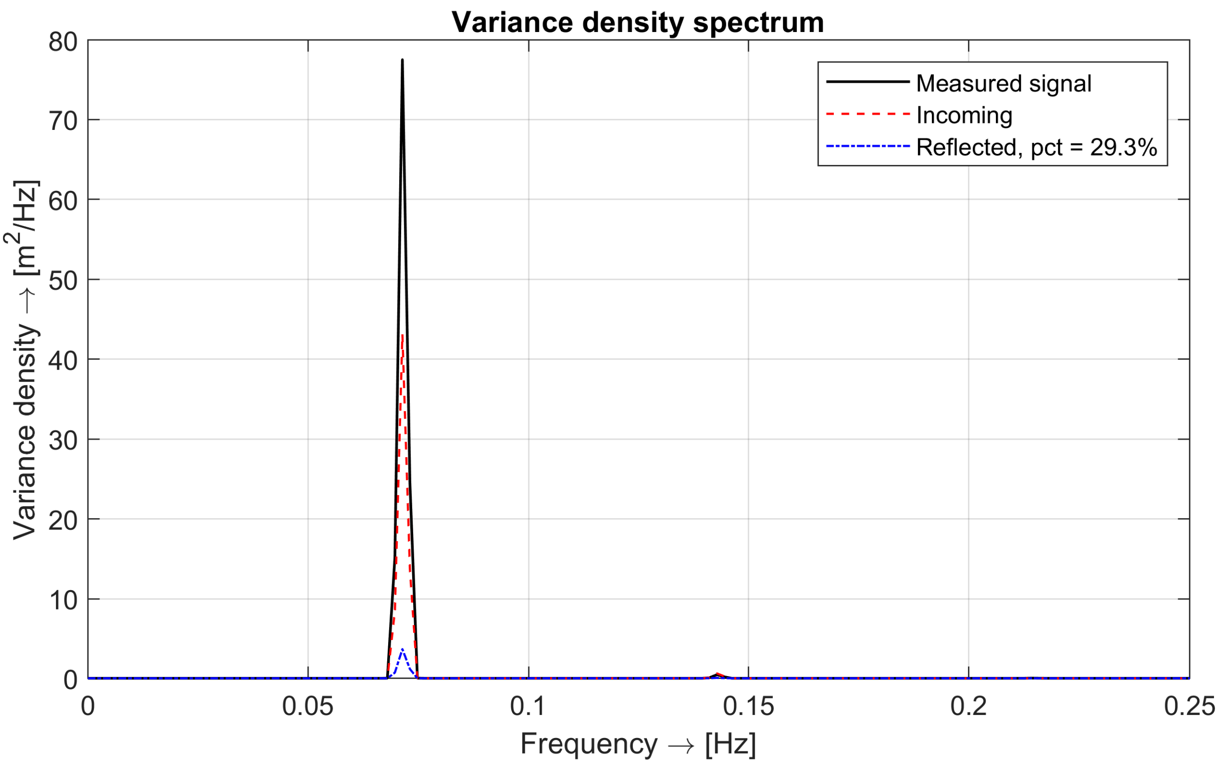

Reflection analysis using WHMs:01, 02 & 07	Monochromatic	M140a
Deltares	11202696	App. E.2.01

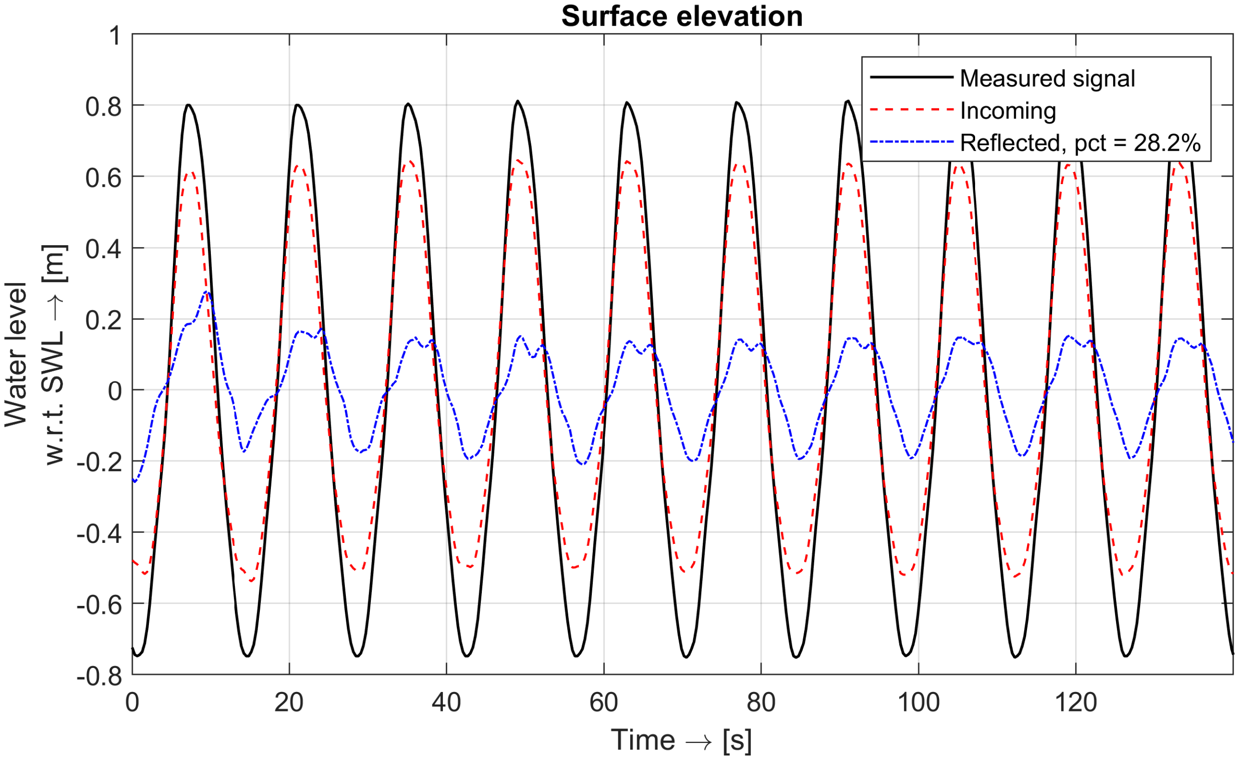

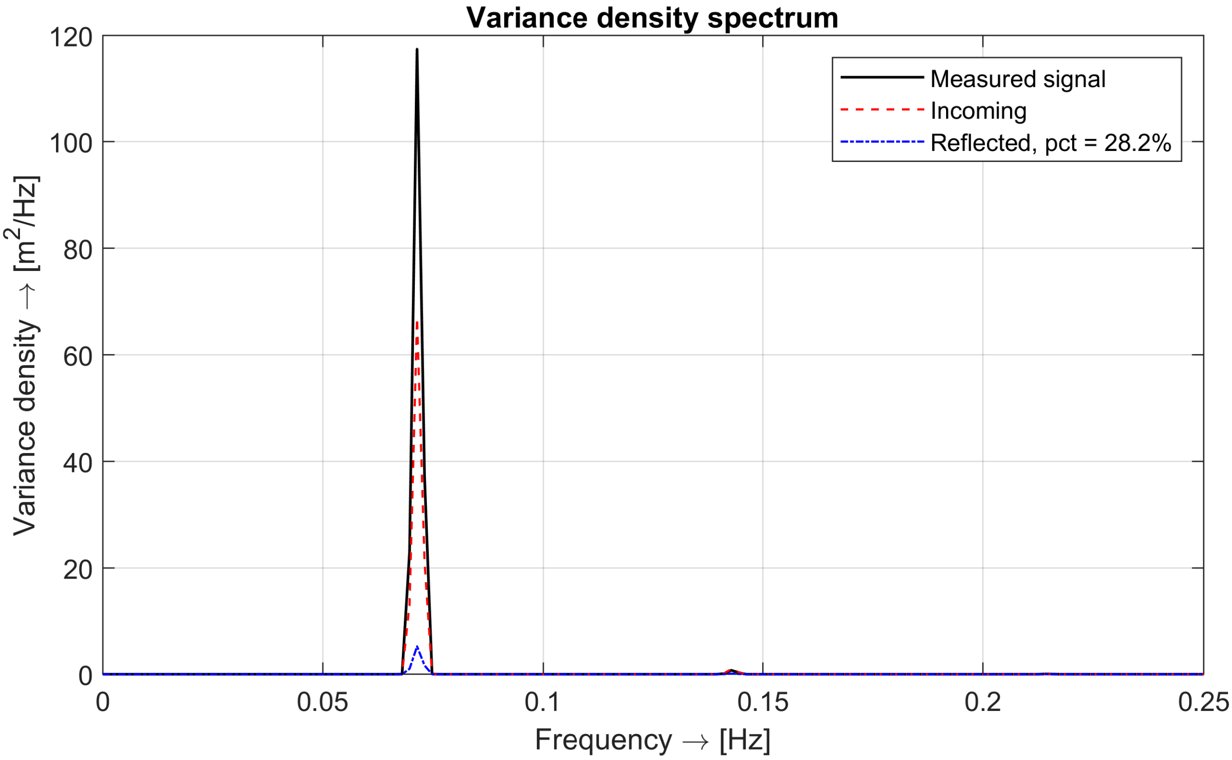

Reflection analysis using WHMs:01, 02 & 07	Monochromatic	M140b
Deltares	11202696	App. E.2.02

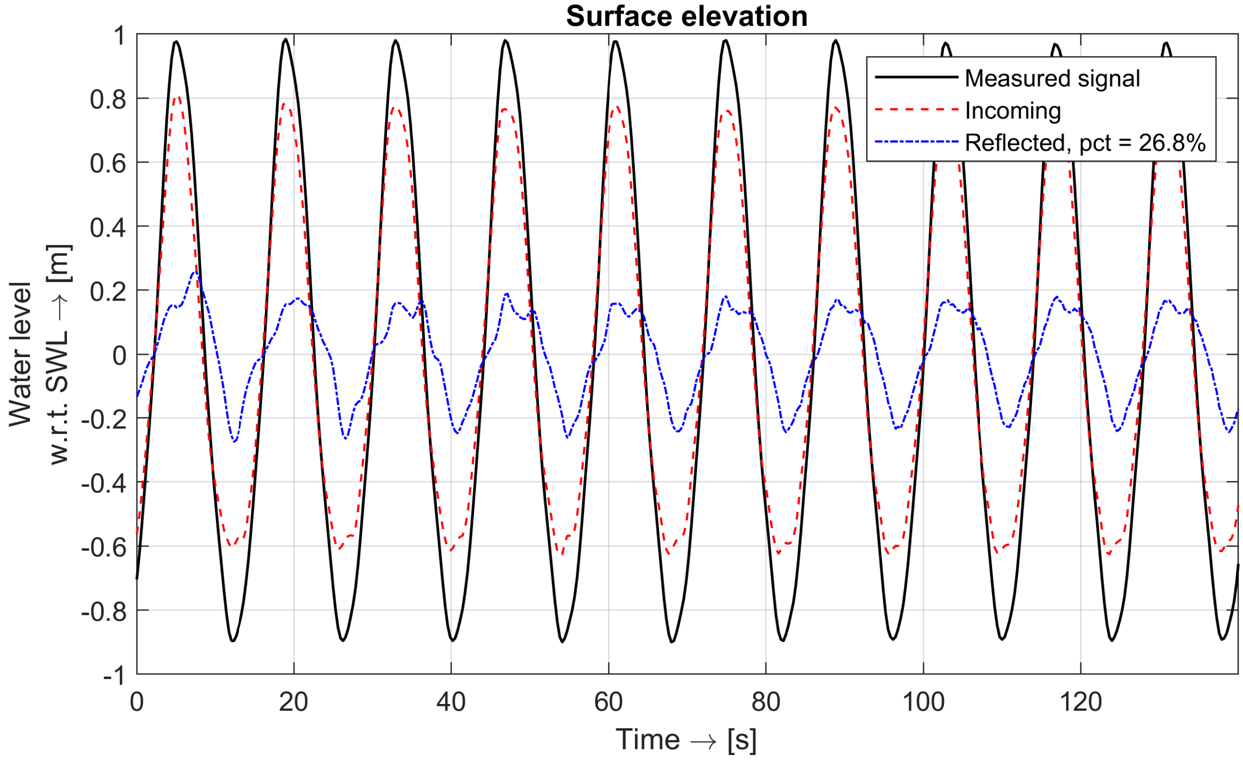

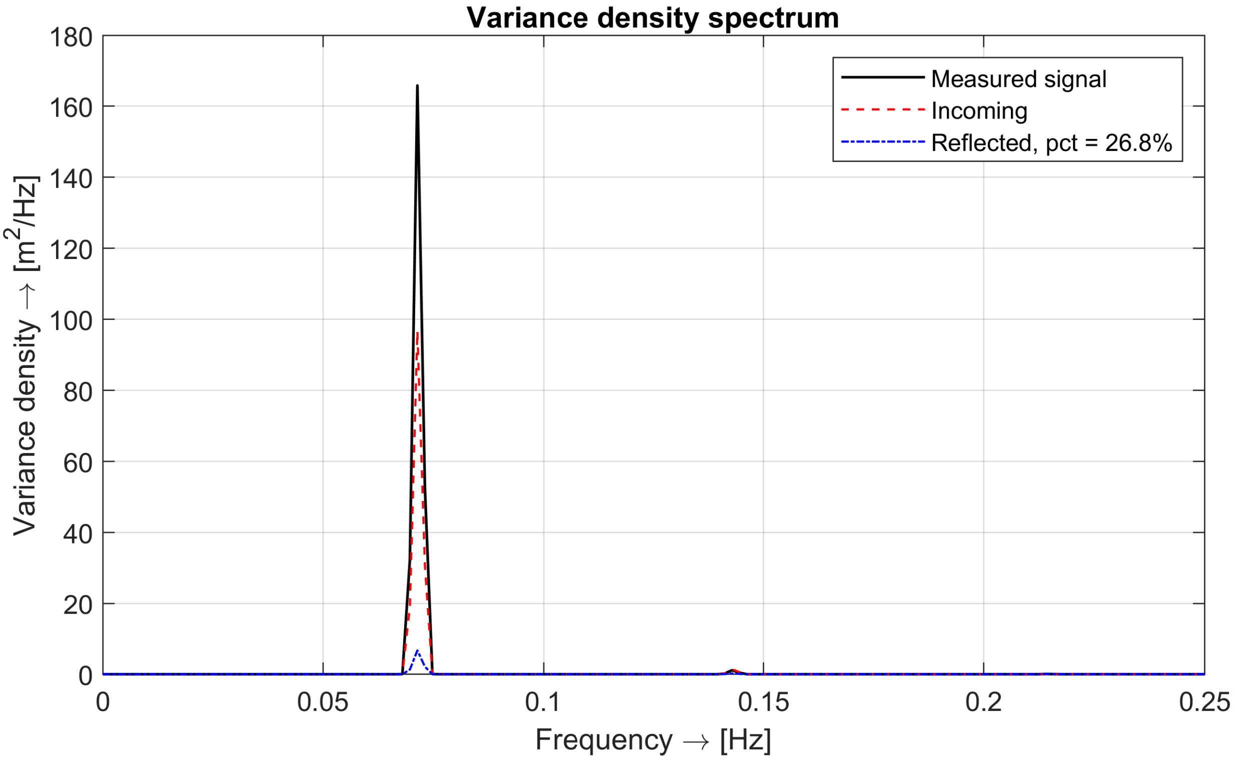

Reflection analysis using WHMs:01, 02 & 07	Monochromatic	M140c
Deltares	11202696	App. E.2.03

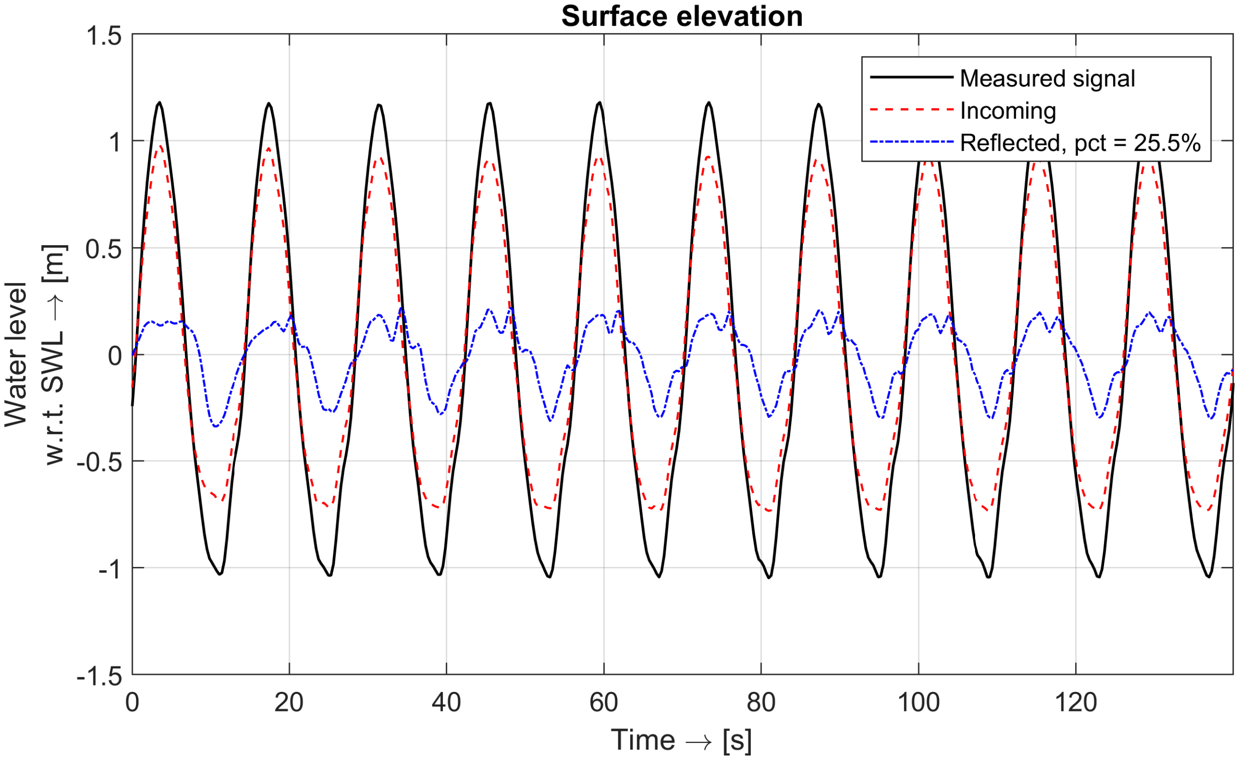

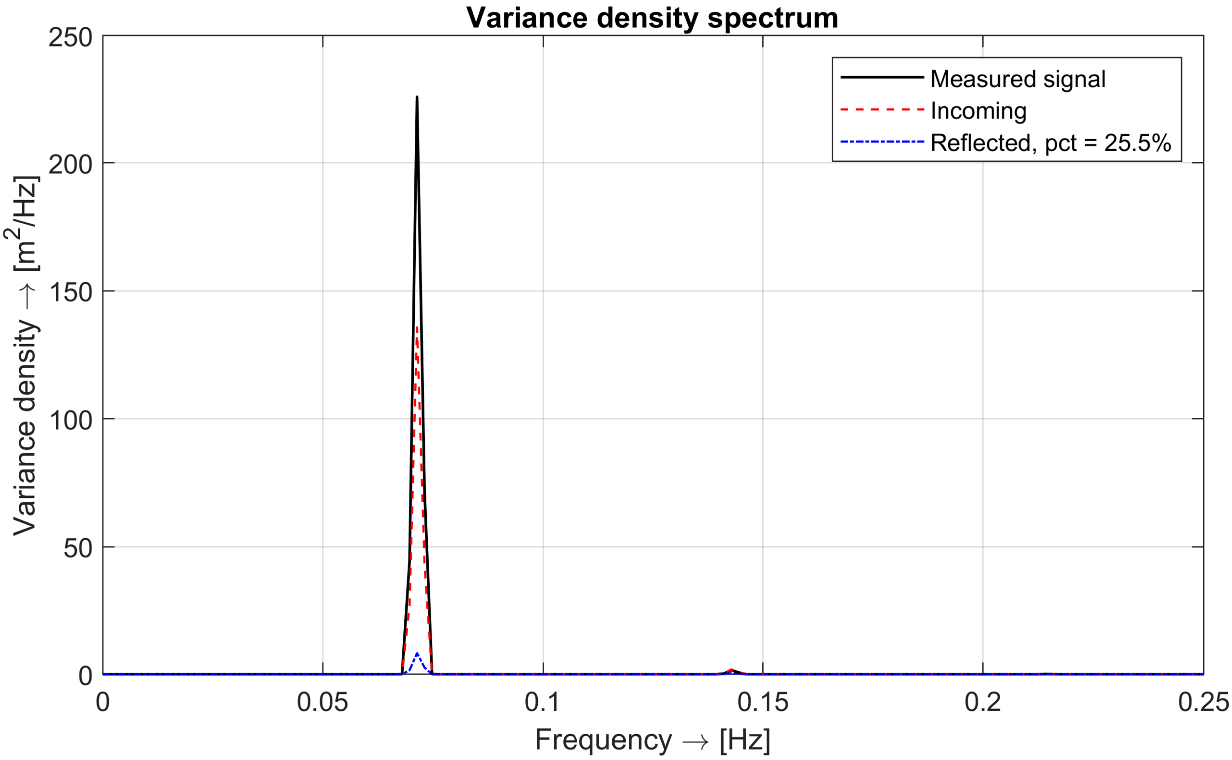

Reflection analysis using WHMs:01, 02 & 07	Monochromatic	M140d
Deltares	11202696	App. E.2.04

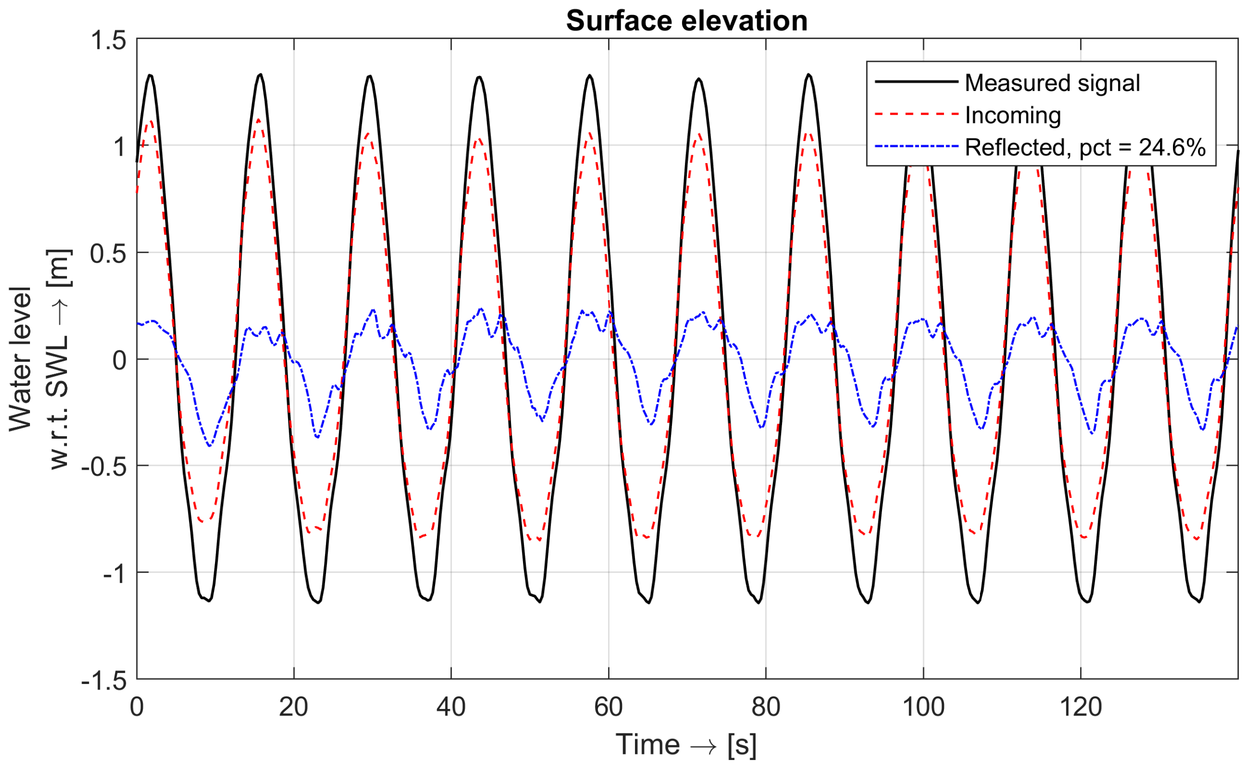

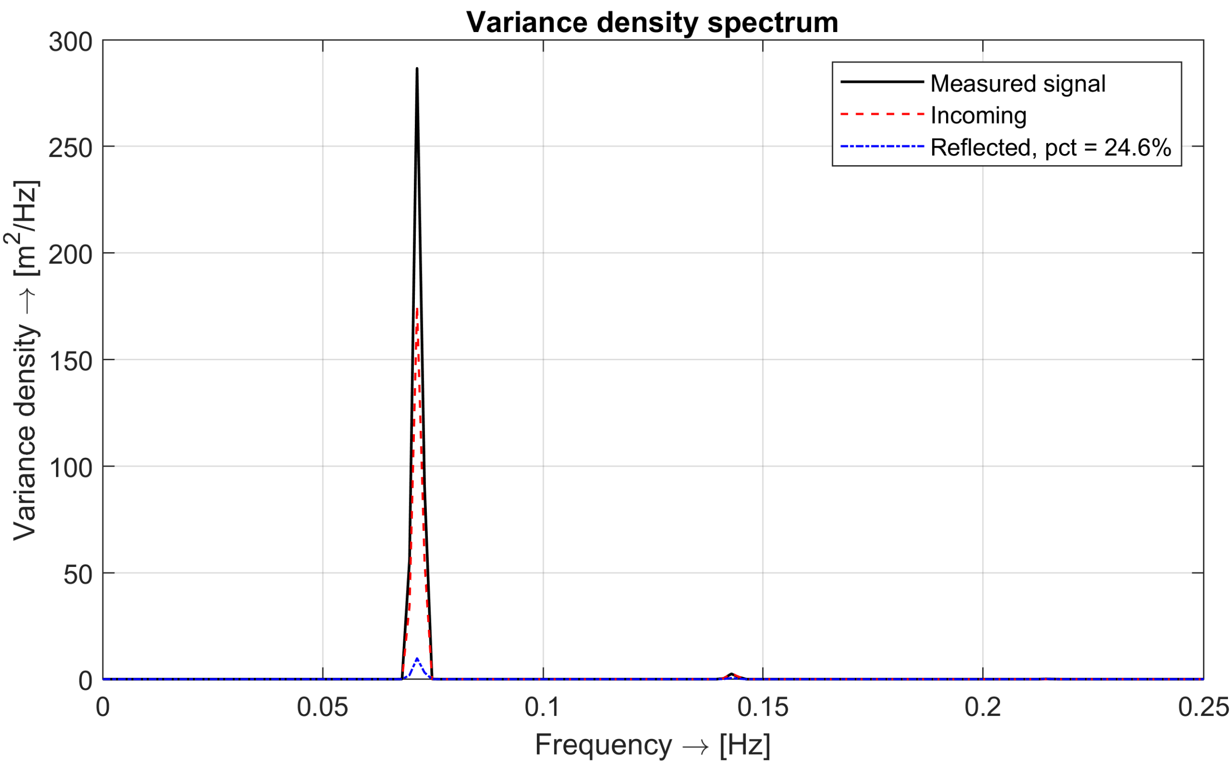

Reflection analysis using WHMs:01, 02 & 07	Monochromatic	M140e
Deltares	11202696	App. E.2.05

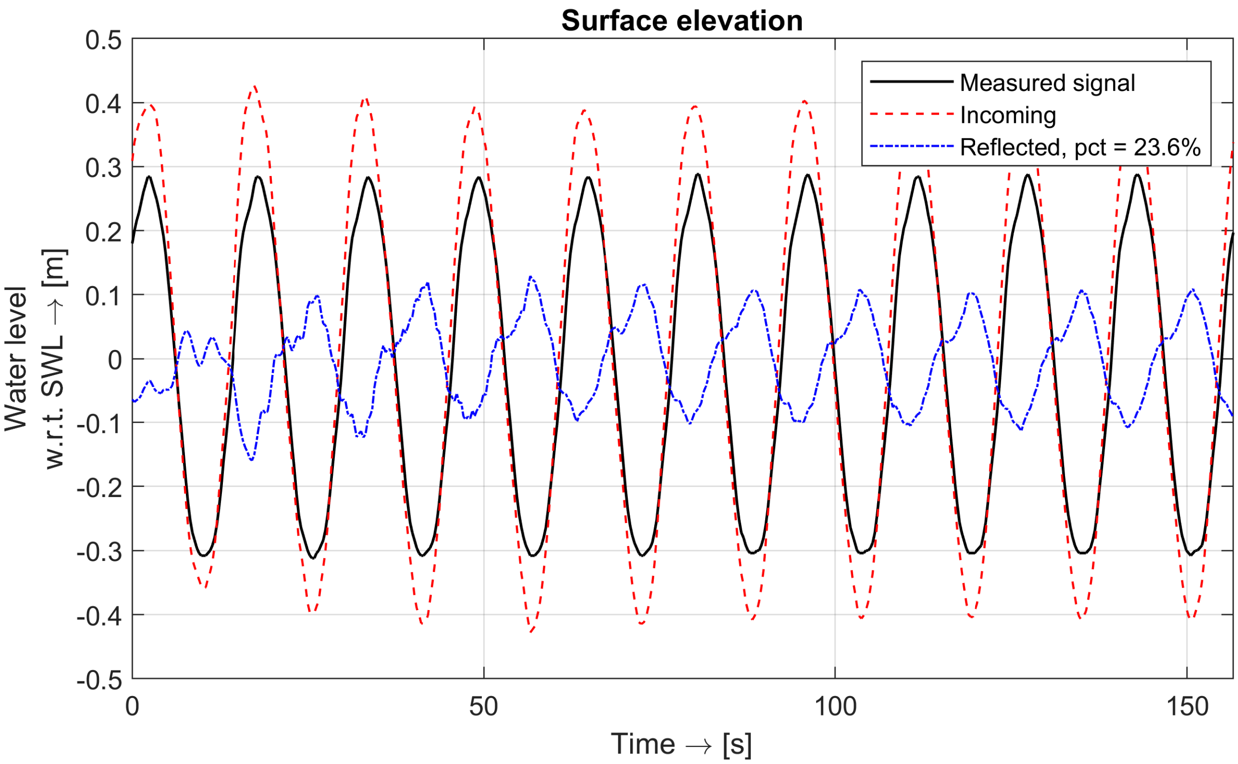

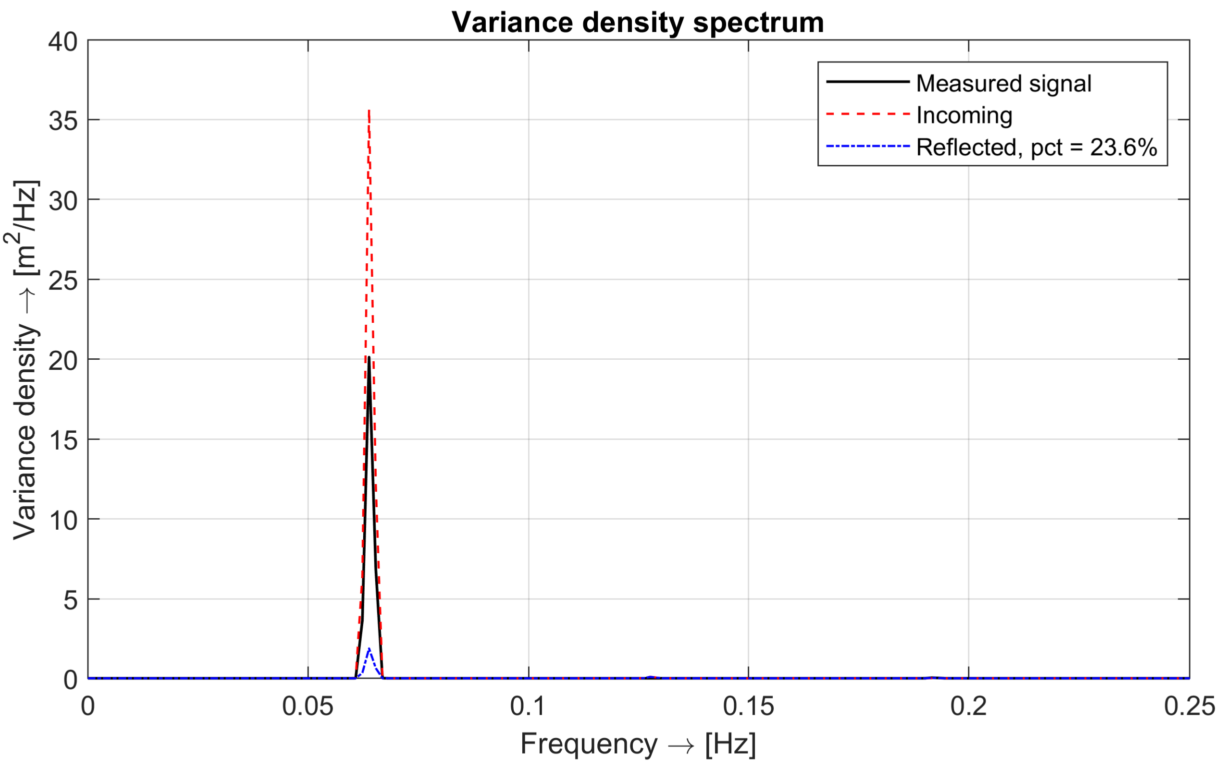

Reflection analysis using WHMs:01, 02 & 07	Monochromatic	M156a
Deltares	11202696	App. E.2.06

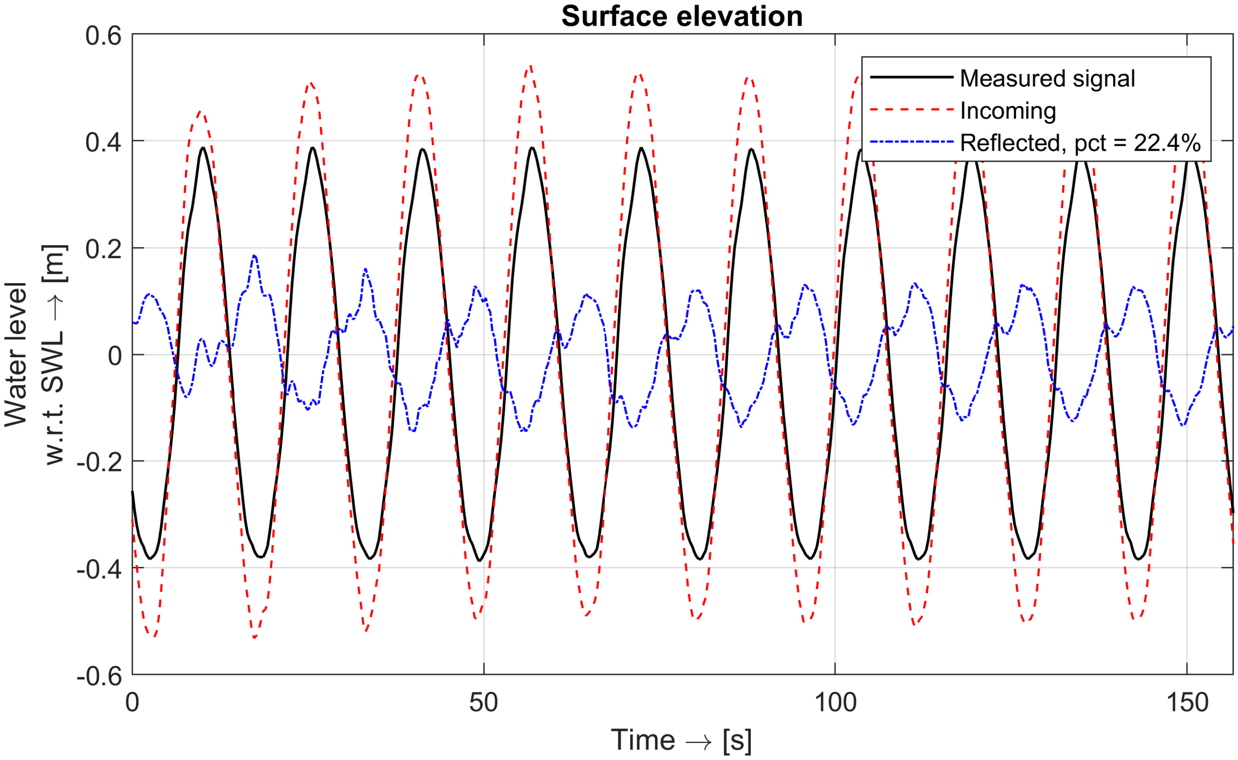

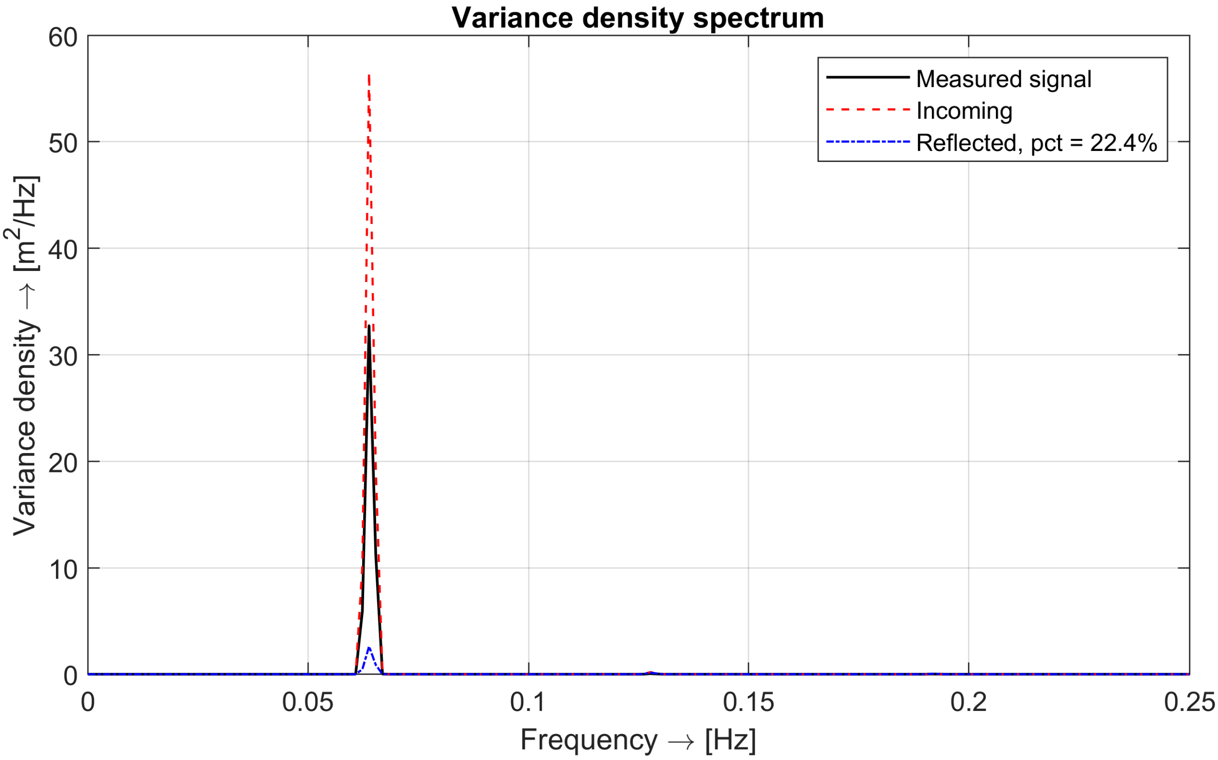

Reflection analysis using WHMs:01, 02 & 07	Monochromatic	M156b
Deltares	11202696	App. E.2.07

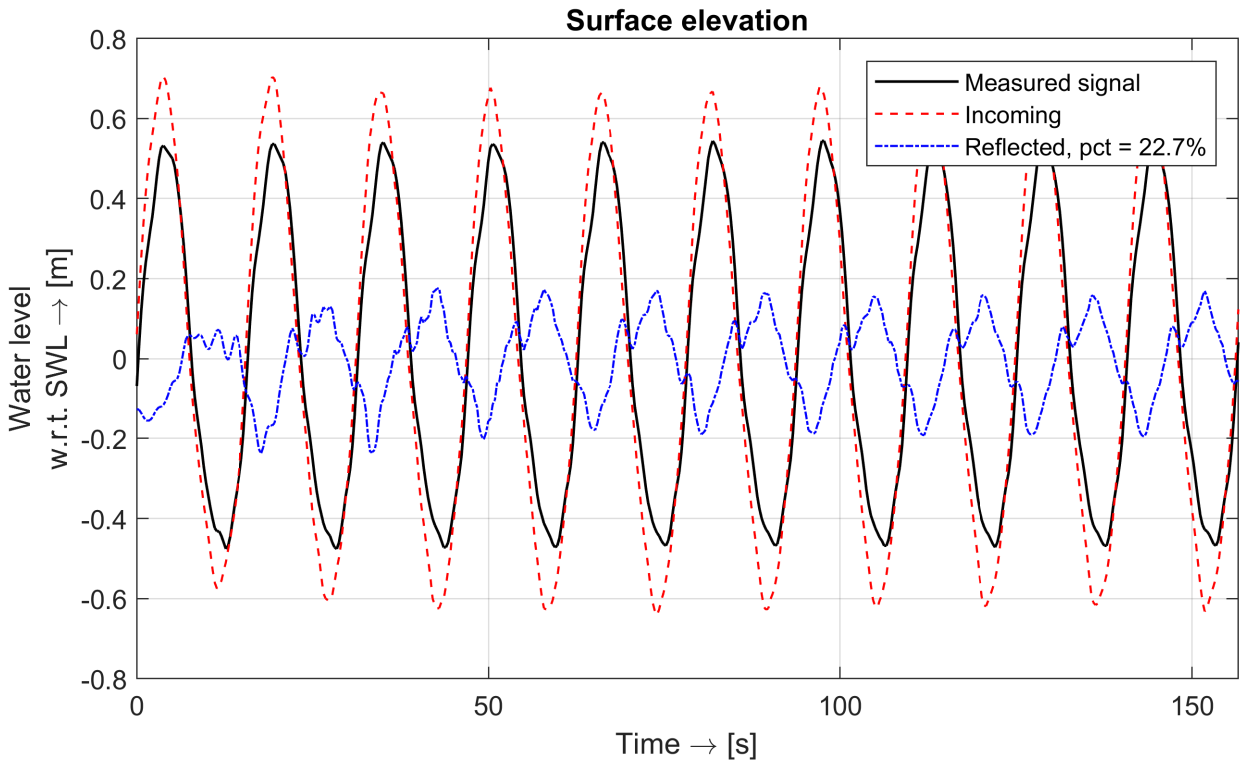

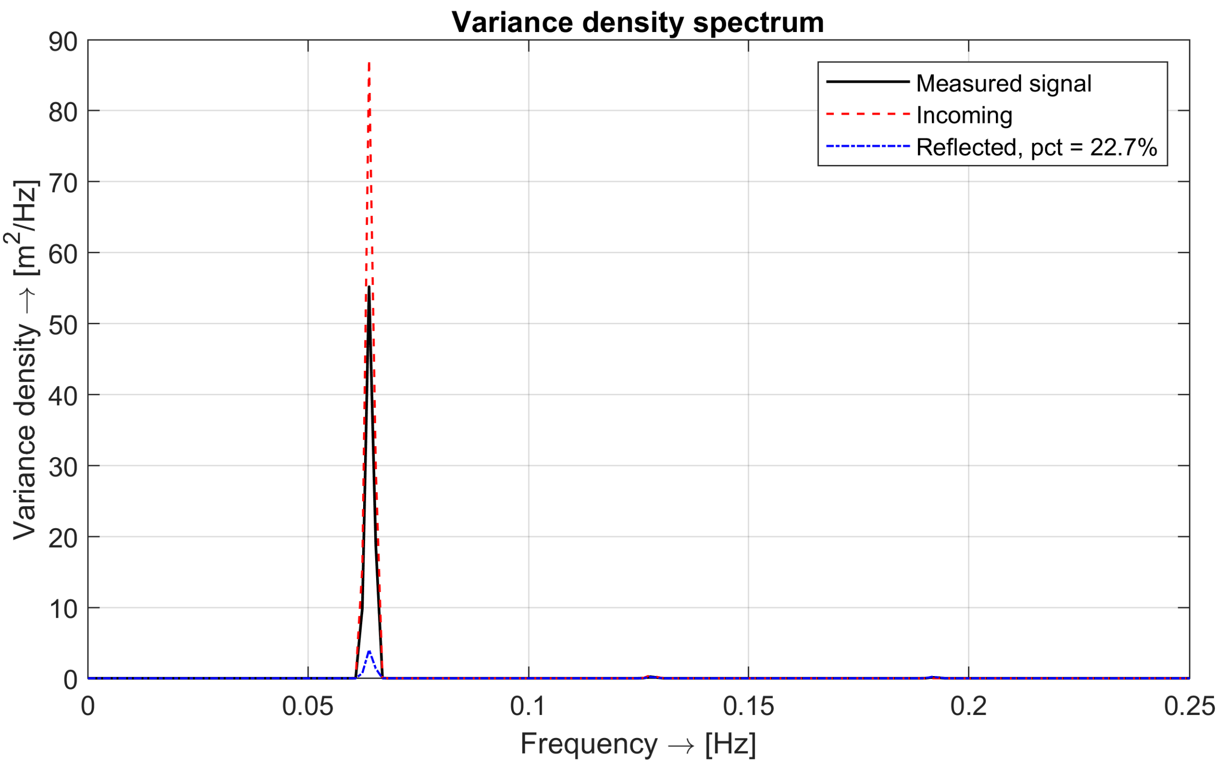

Reflection analysis using WHMs:01, 02 & 07	Monochromatic	M156c
Deltares	11202696	App. E.2.08

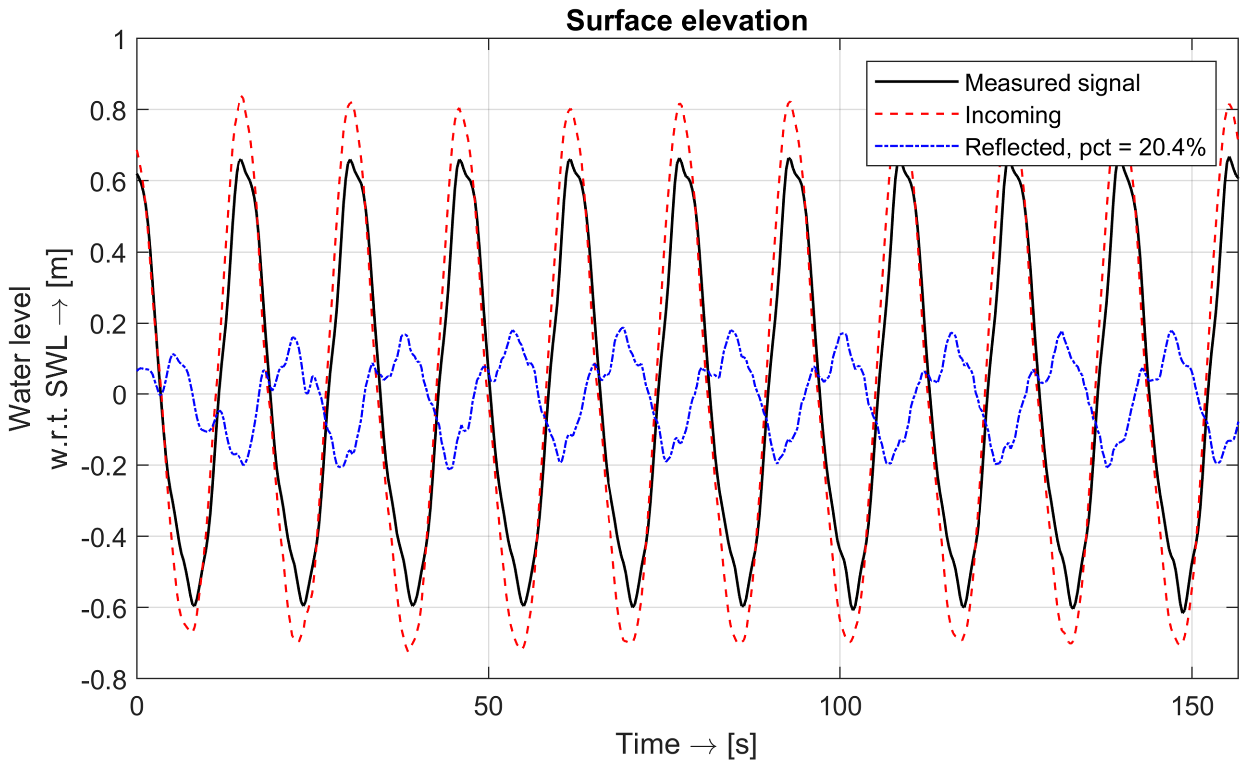

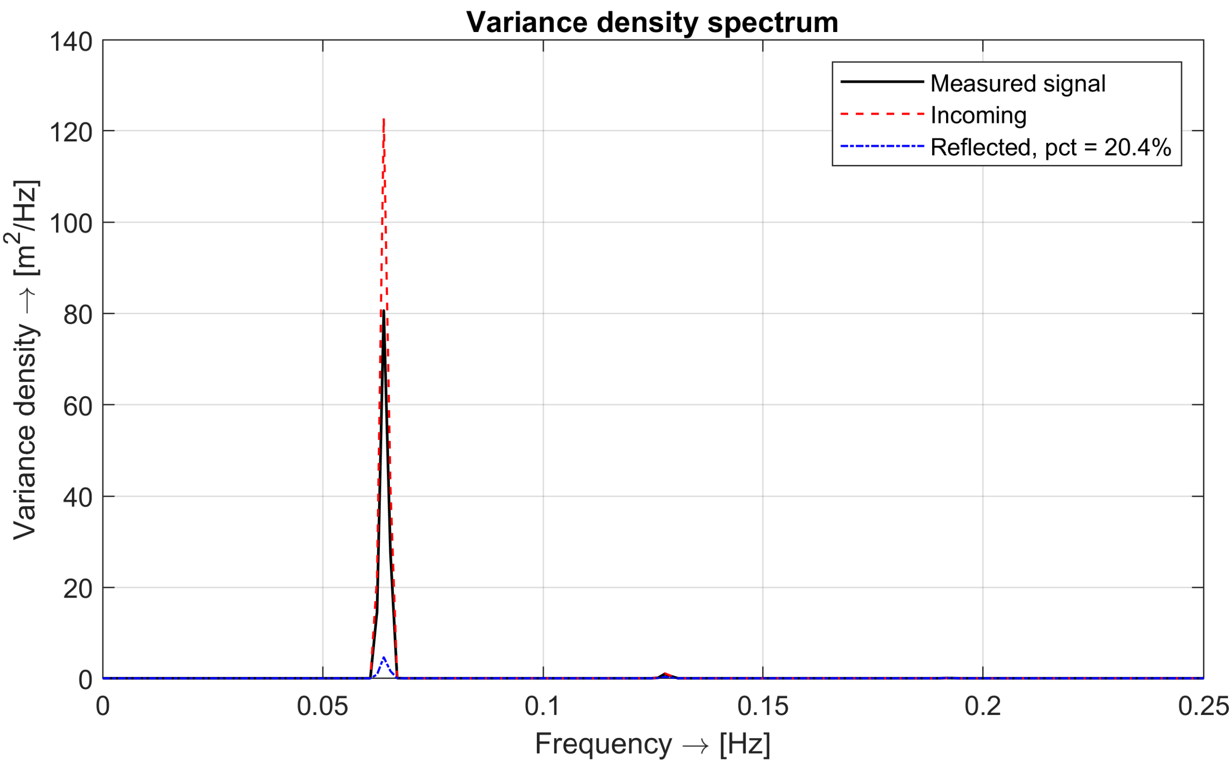

Reflection analysis using WHMs:01, 02 & 07	Monochromatic	M156d
Deltares	11202696	App. E.2.09

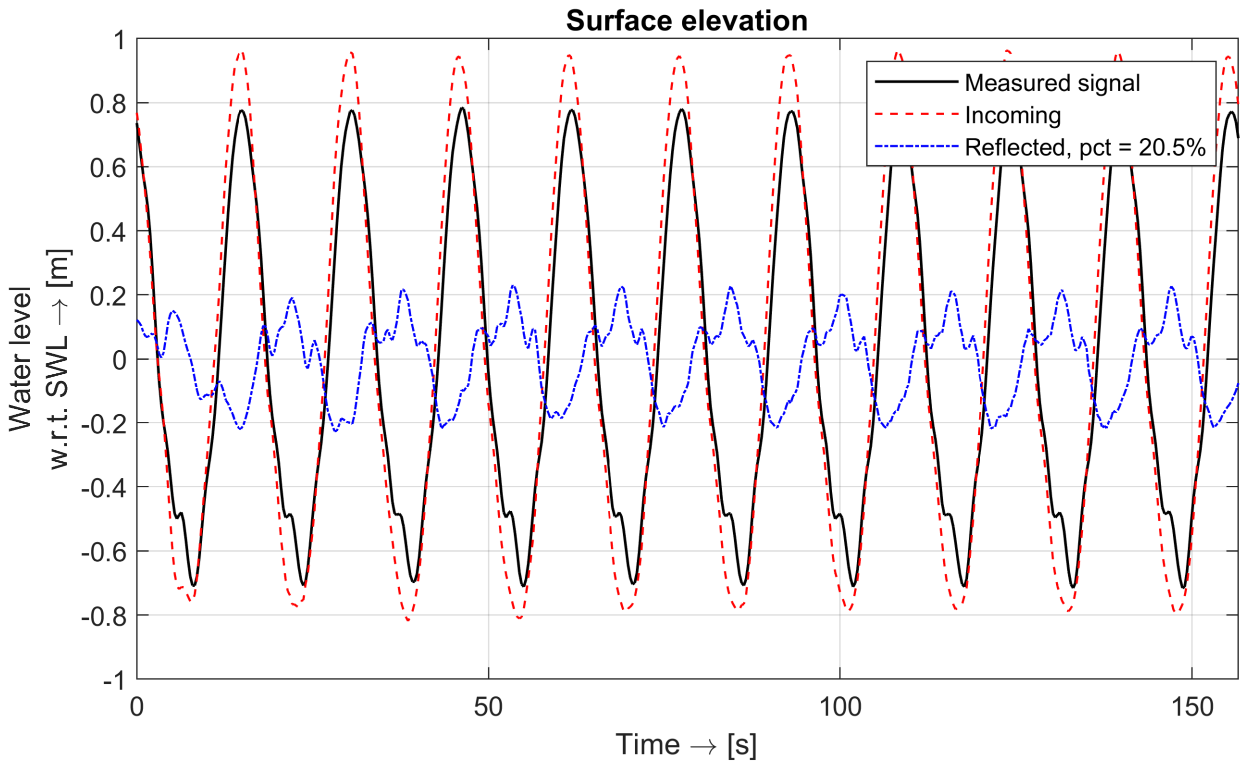

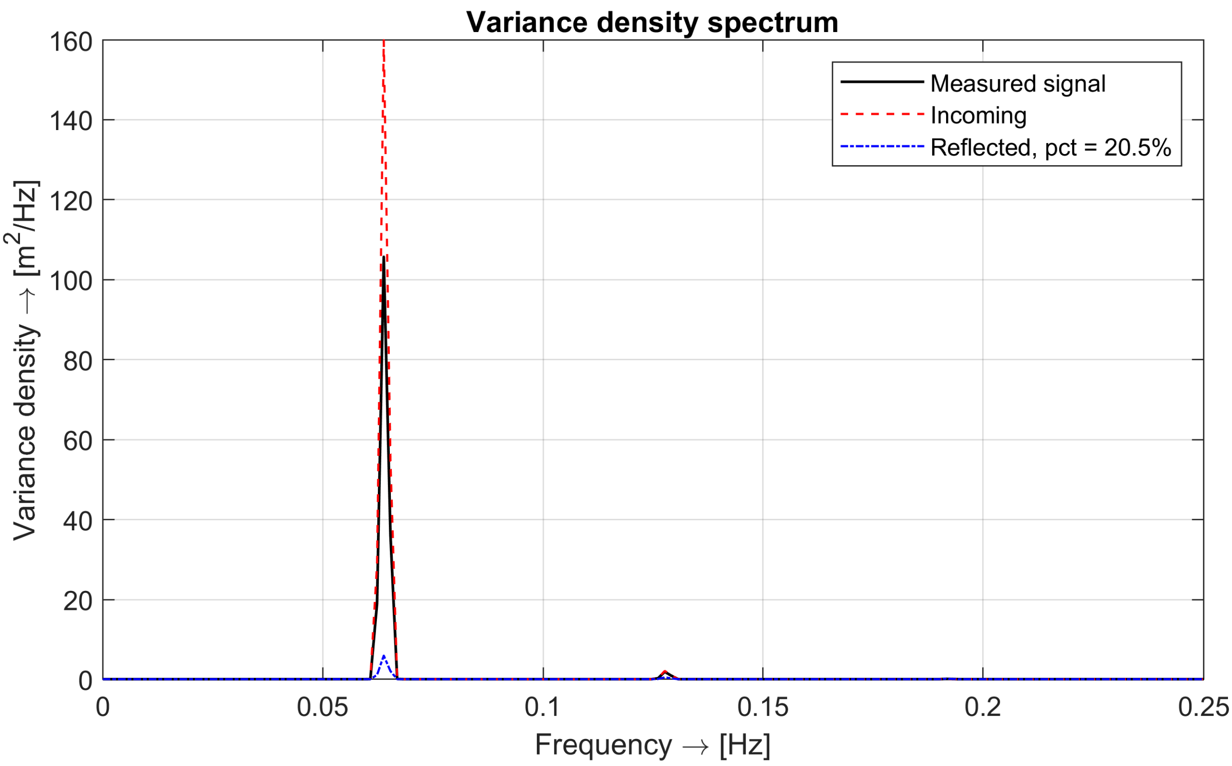

Reflection analysis using WHMs:01, 02 & 07	Monochromatic	M156e
Deltares	11202696	App. E.2.10

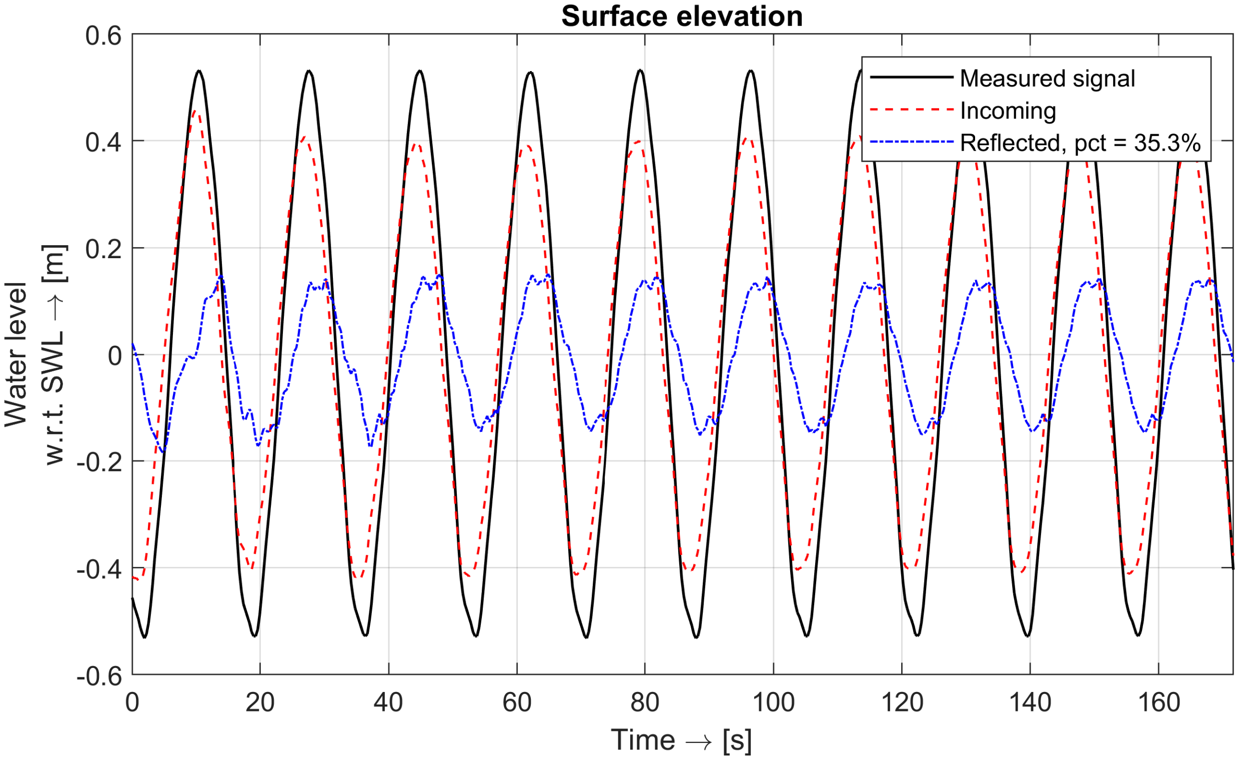

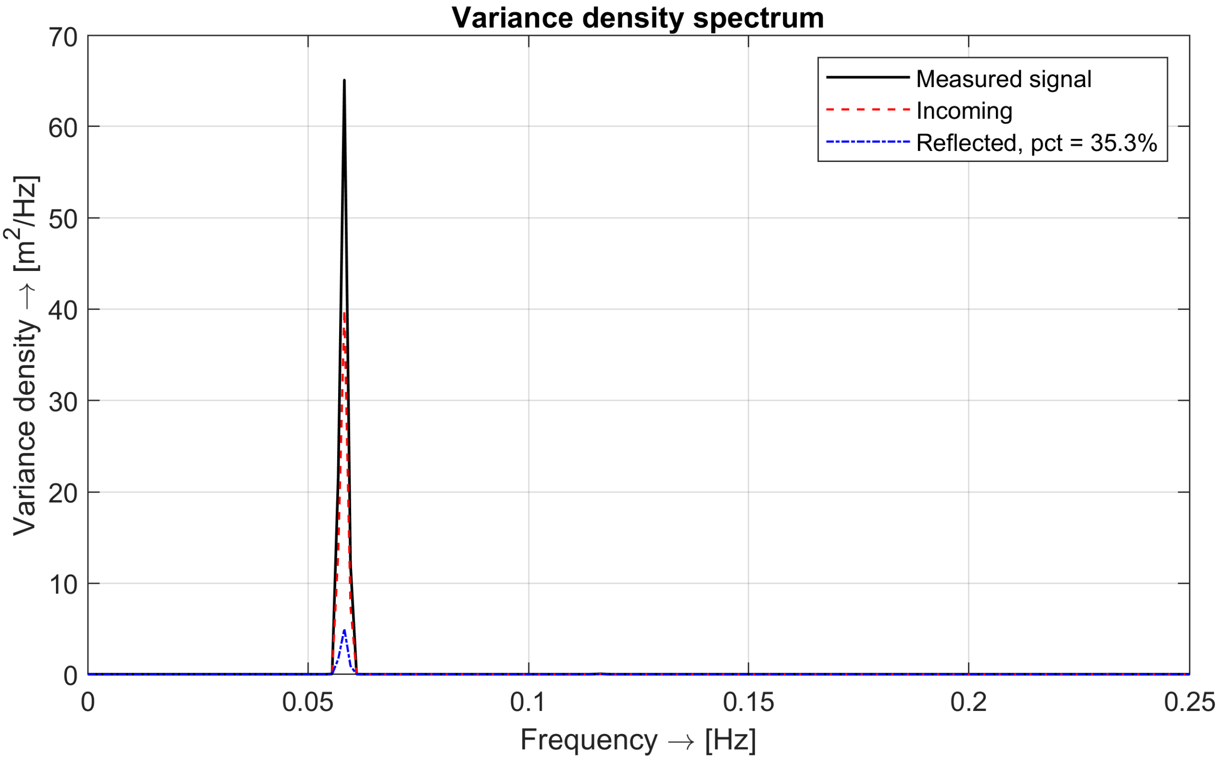

Reflection analysis using WHMs:01, 02 & 07	Monochromatic	M172a
Deltares	11202696	App. E.2.11

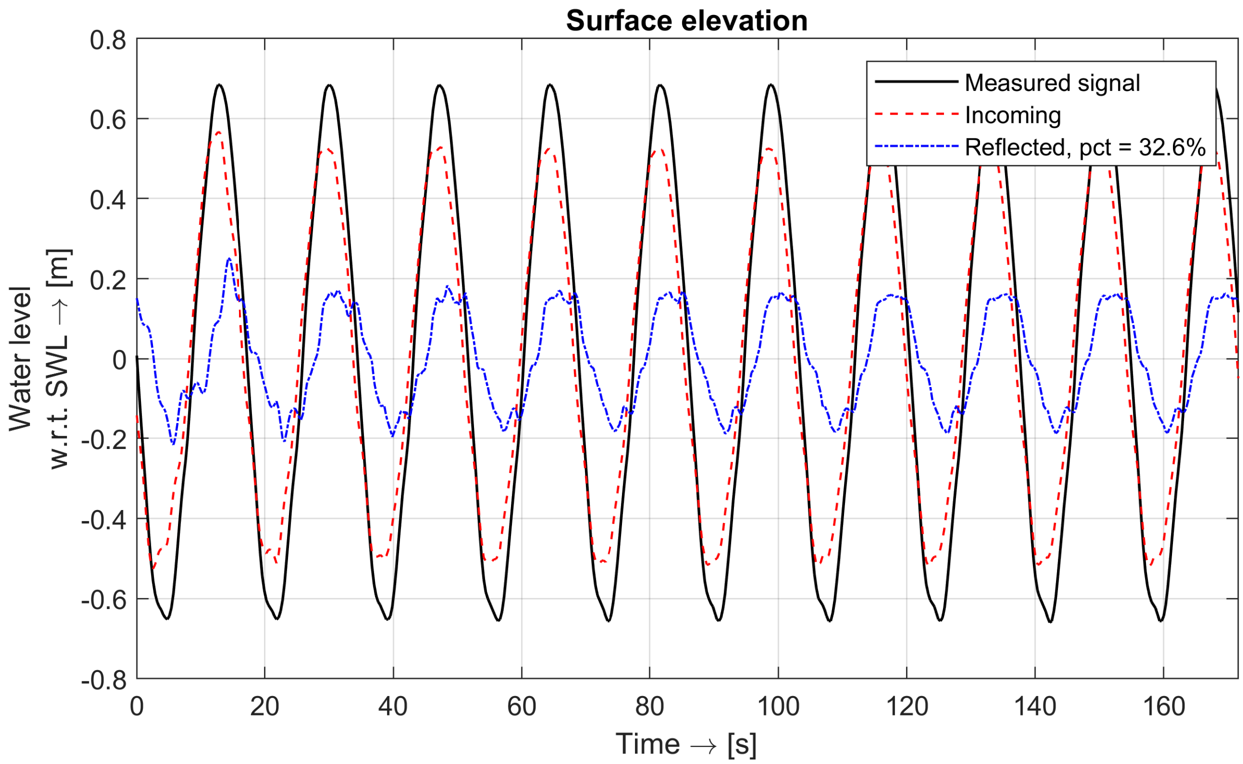

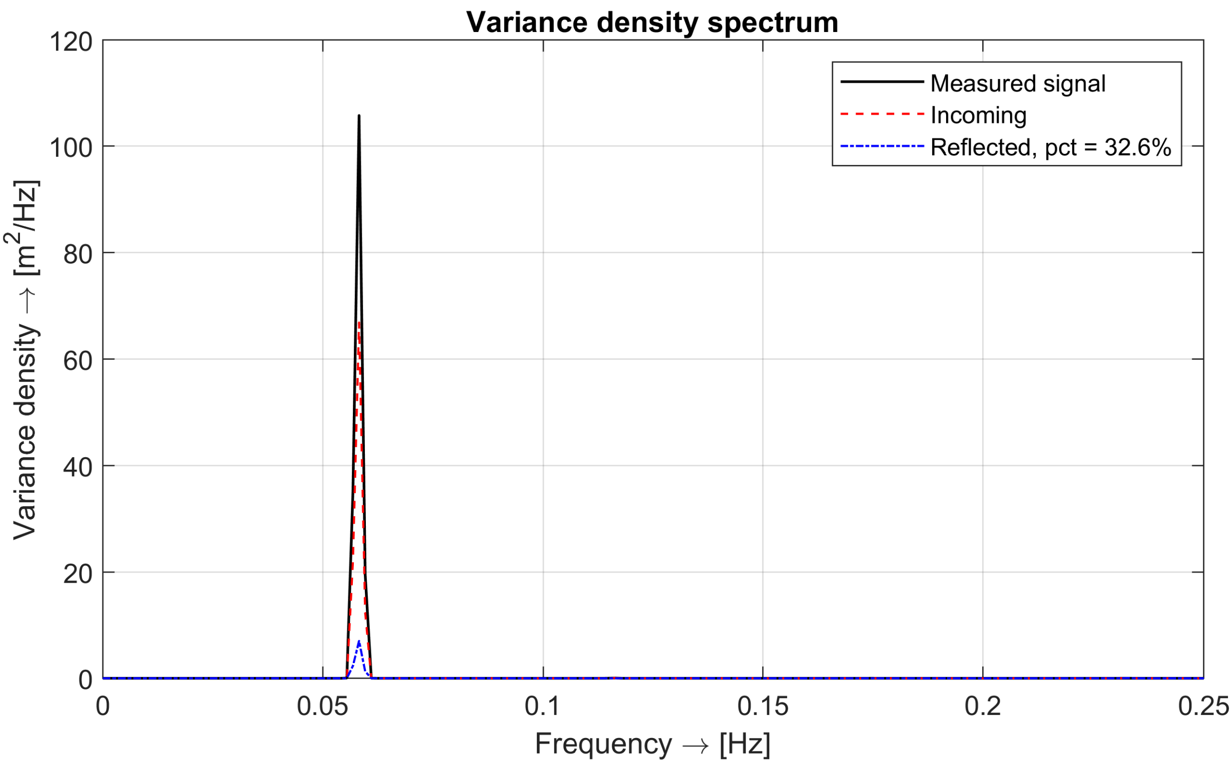

Reflection analysis using WHMs:01, 02 & 07	Monochromatic	M172b
Deltares	11202696	App. E.2.12

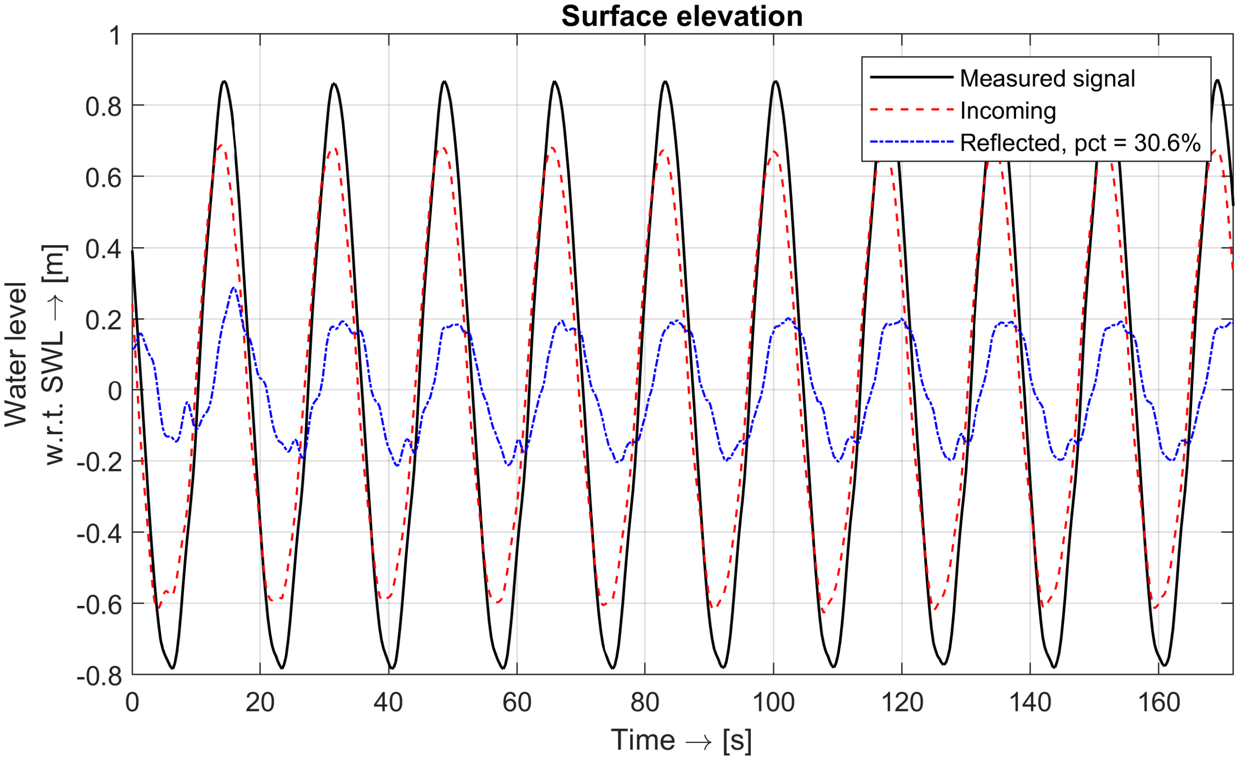

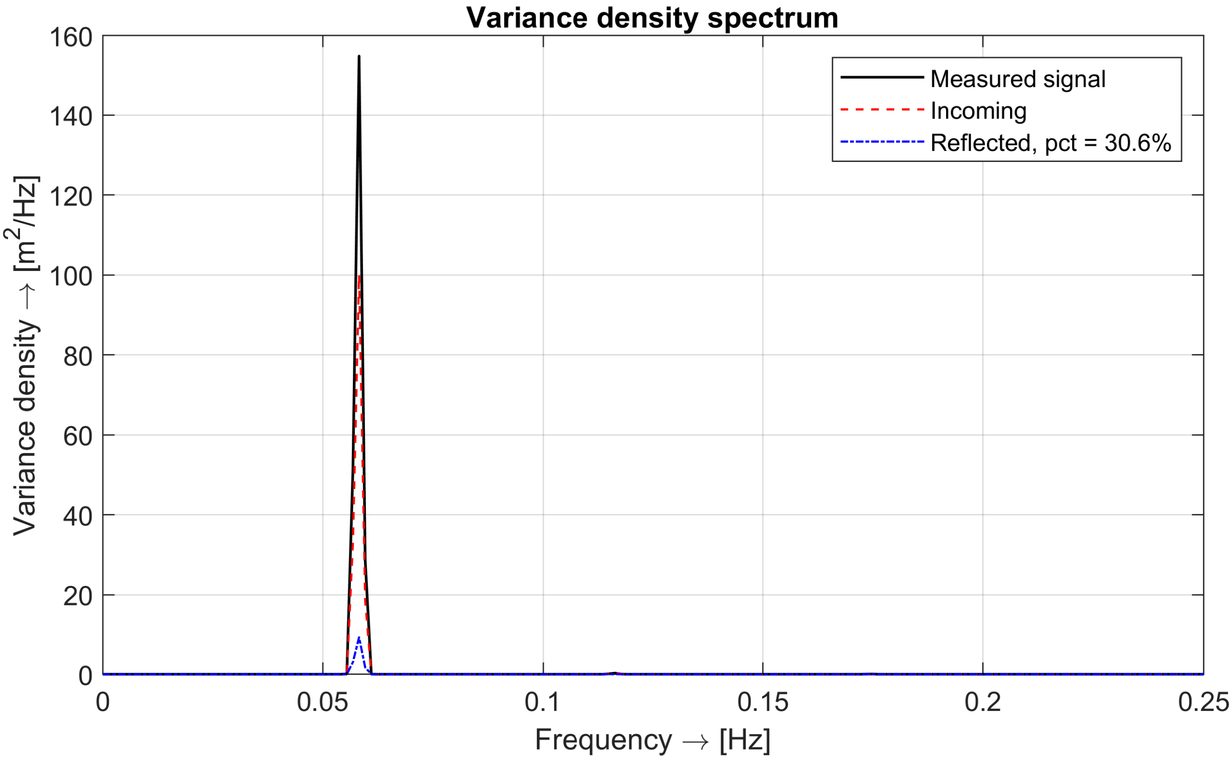

Reflection analysis using WHMs:01, 02 & 07	Monochromatic	M172c
Deltares	11202696	App. E.2.13

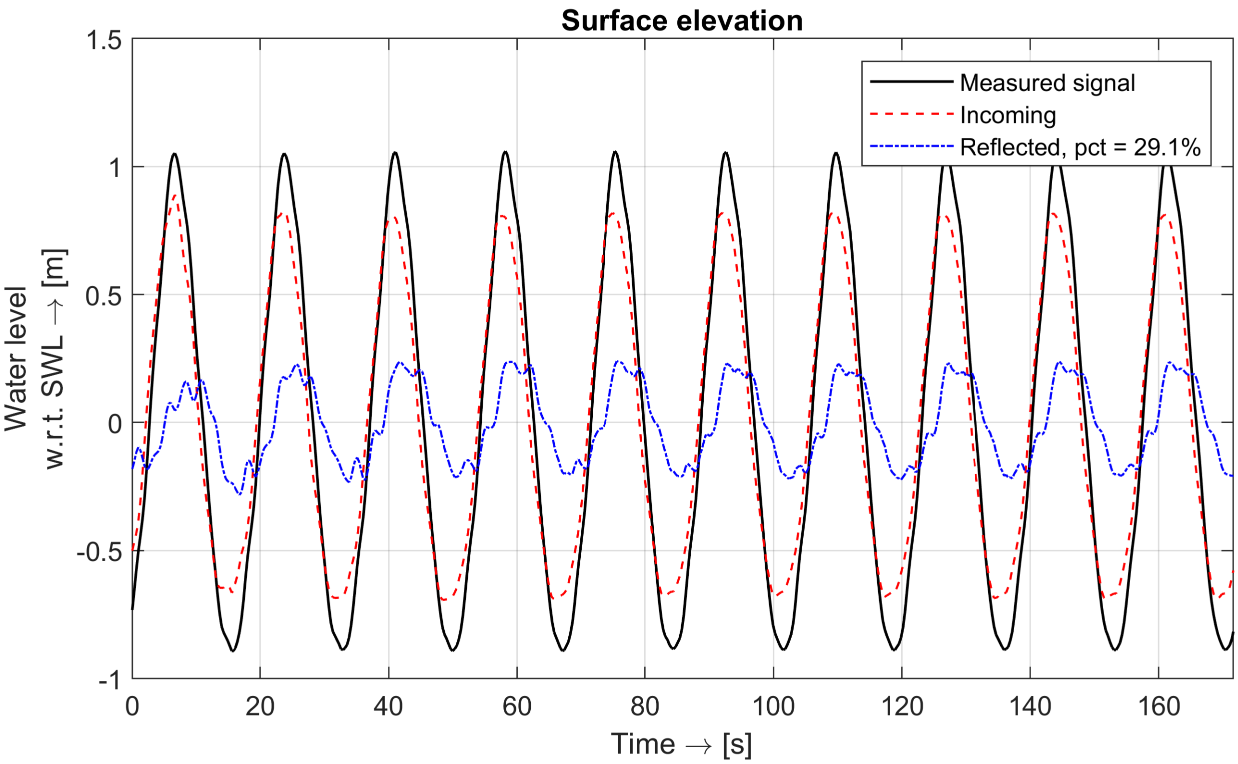

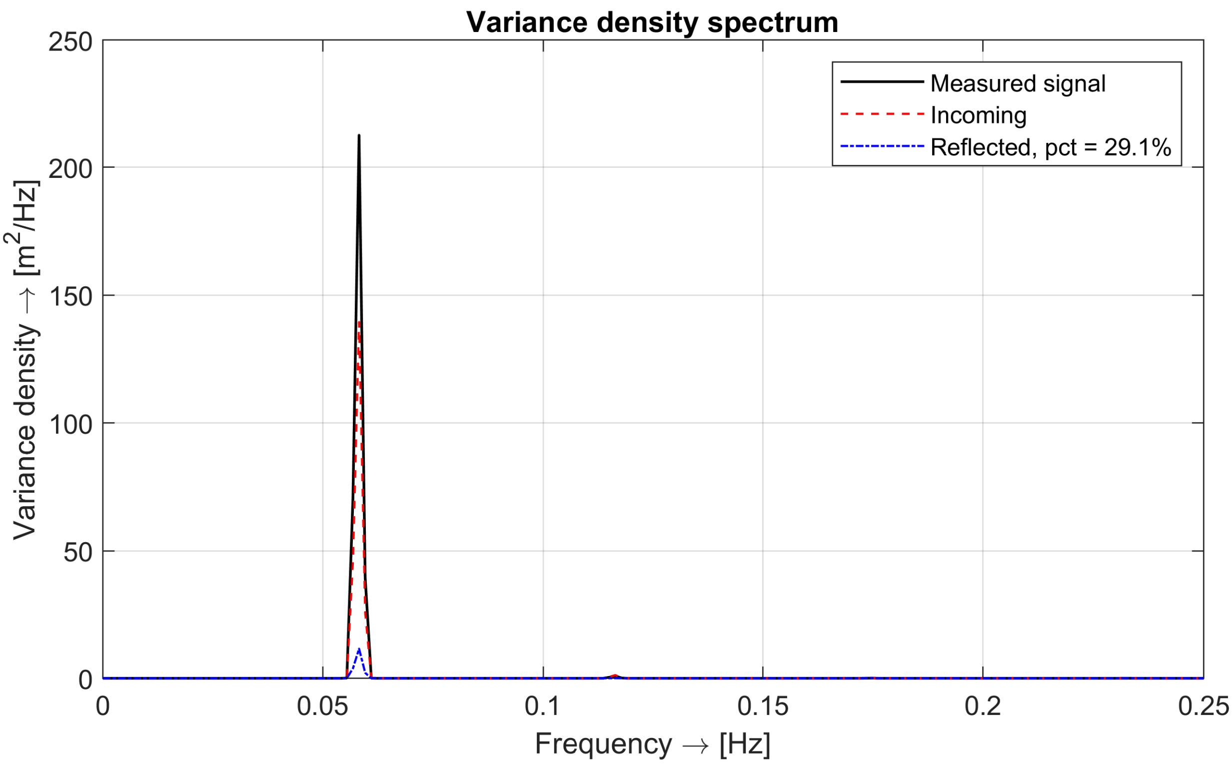

Reflection analysis using WHMs:01, 02 & 07	Monochromatic	M172d
Deltares	11202696	App. E.2.14

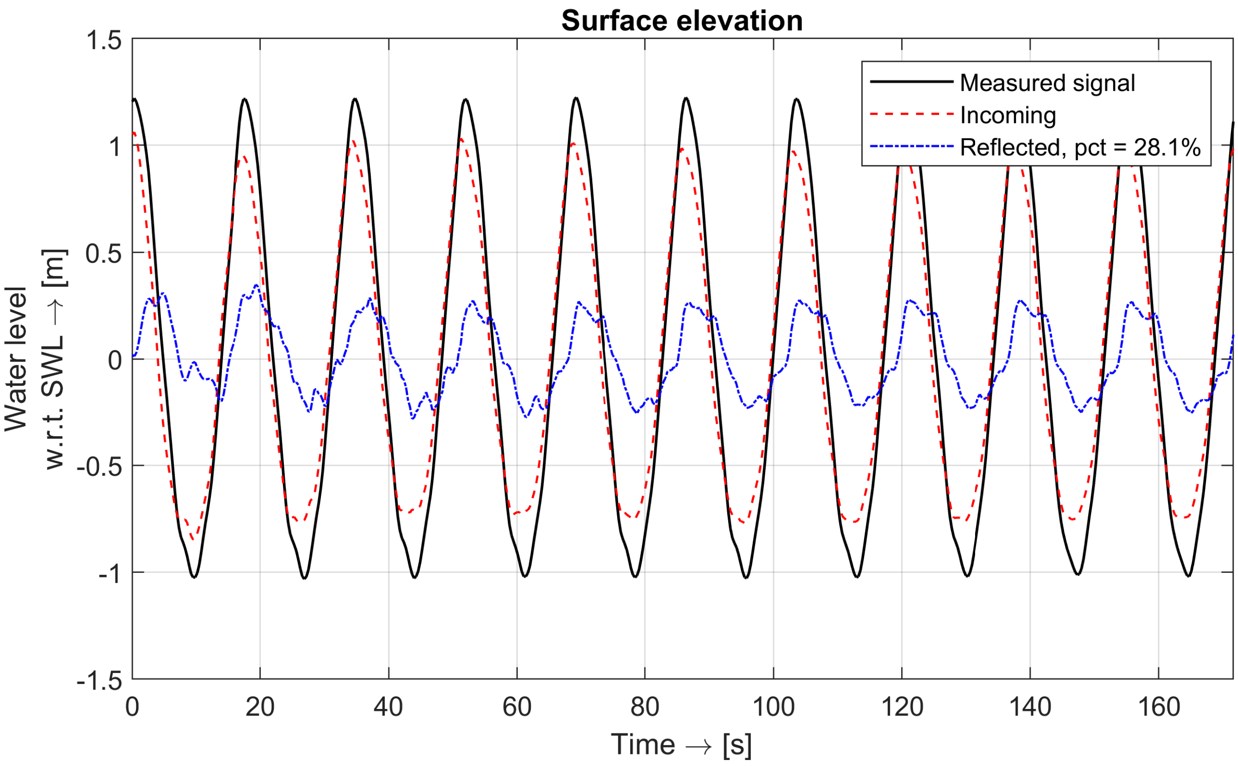

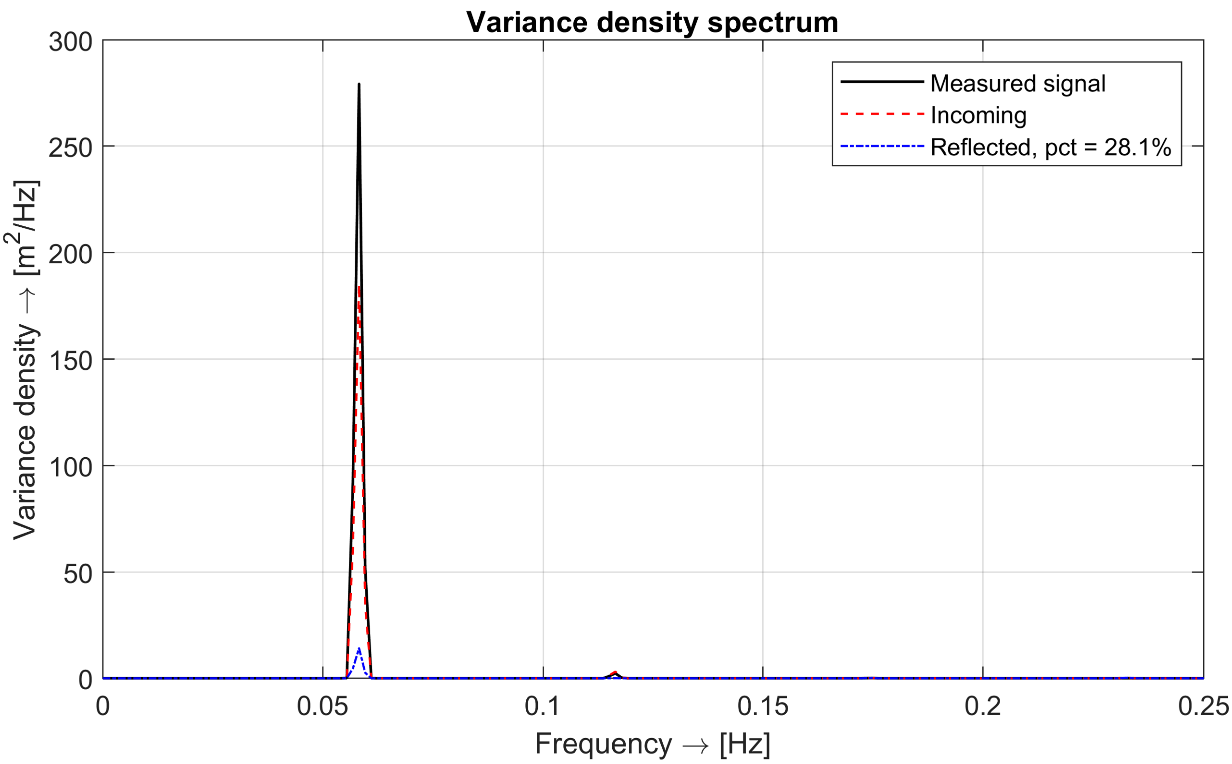

Reflection analysis using WHMs:01, 02 & 07	Monochromatic	M172e
Deltares	11202696	App. E.2.15

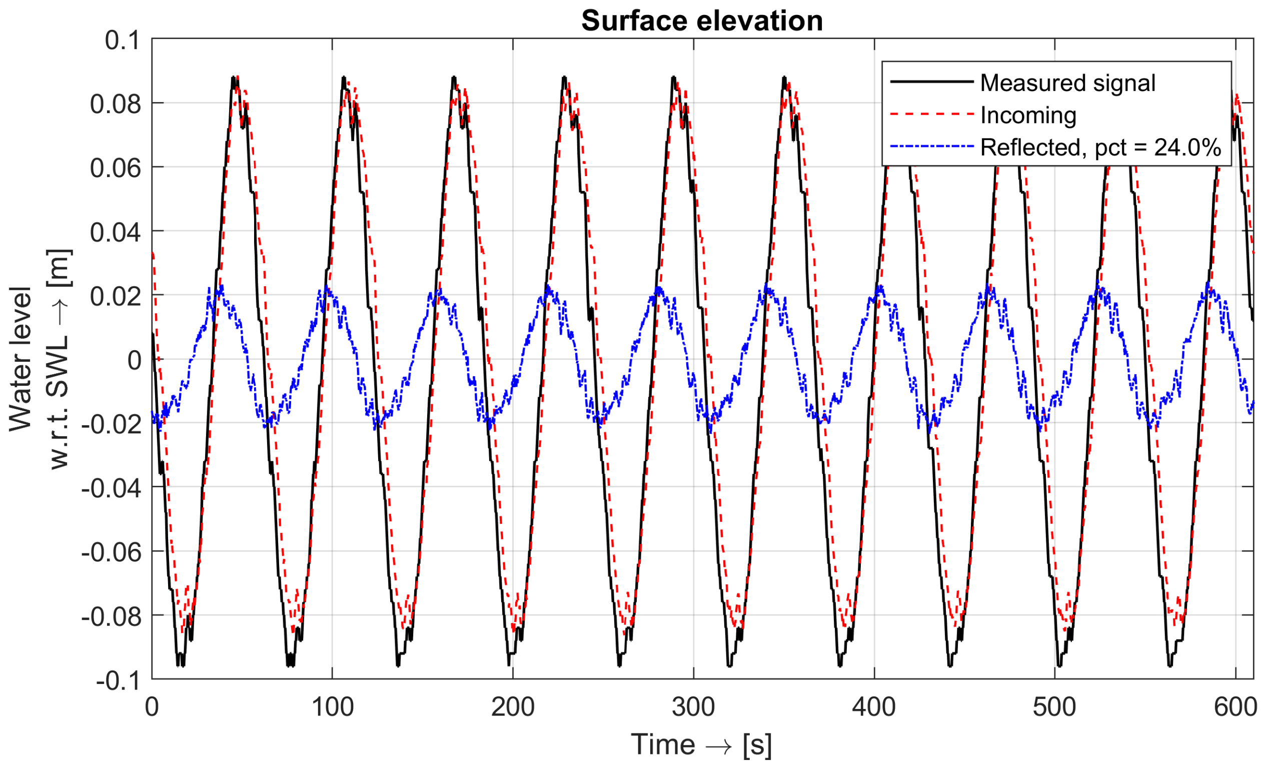

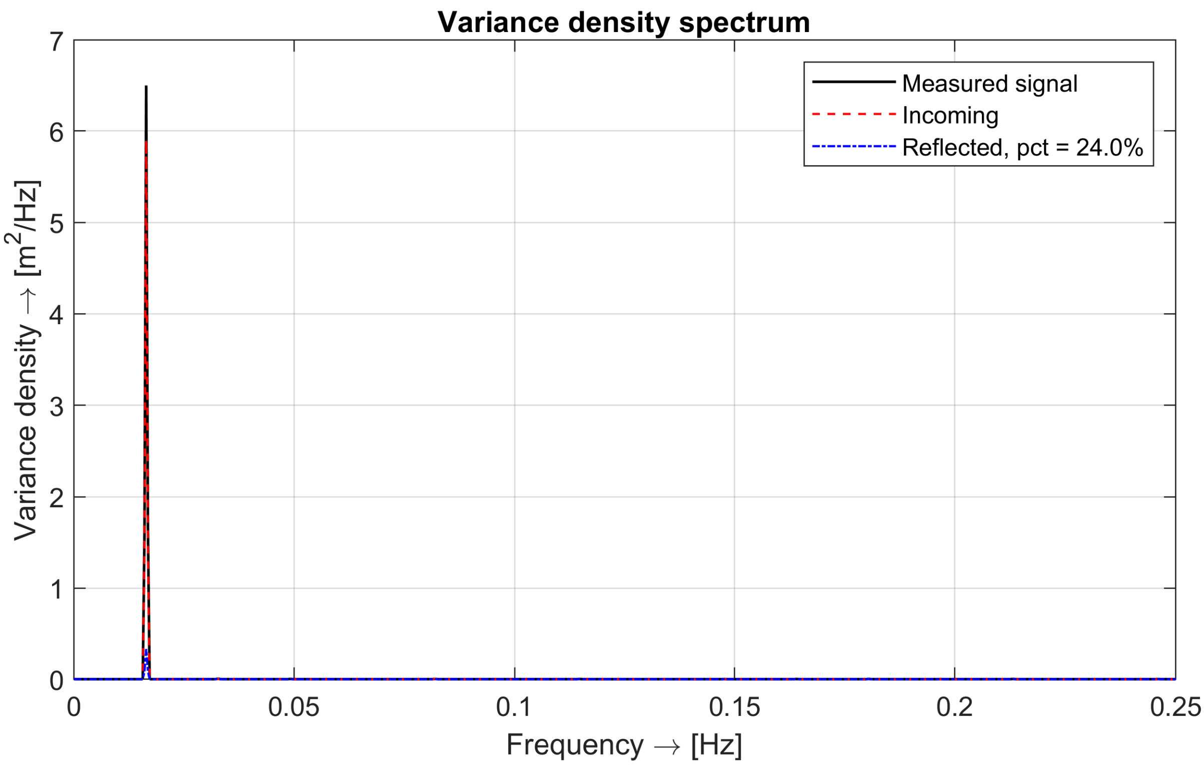

Reflection analysis using WHMs:01, 07 & 09	Monochromatic	M610a
Deltares	11202696	App. E.2.16

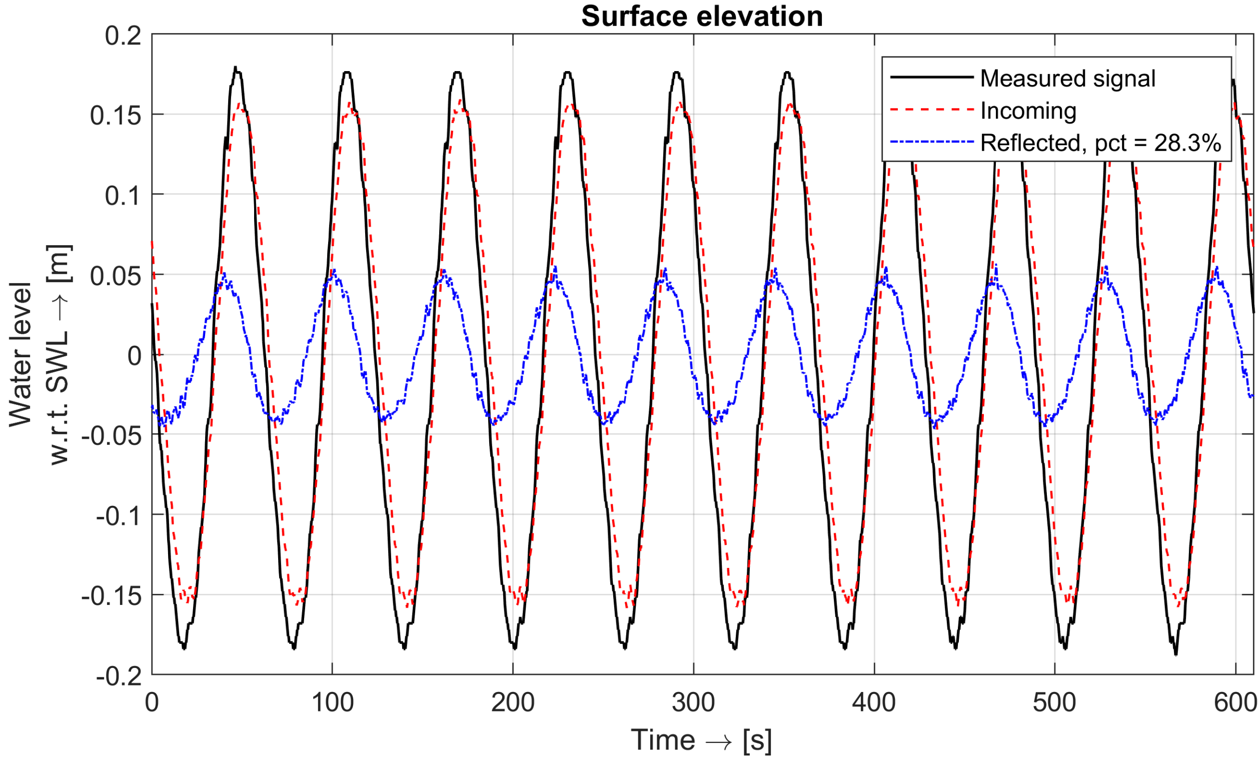

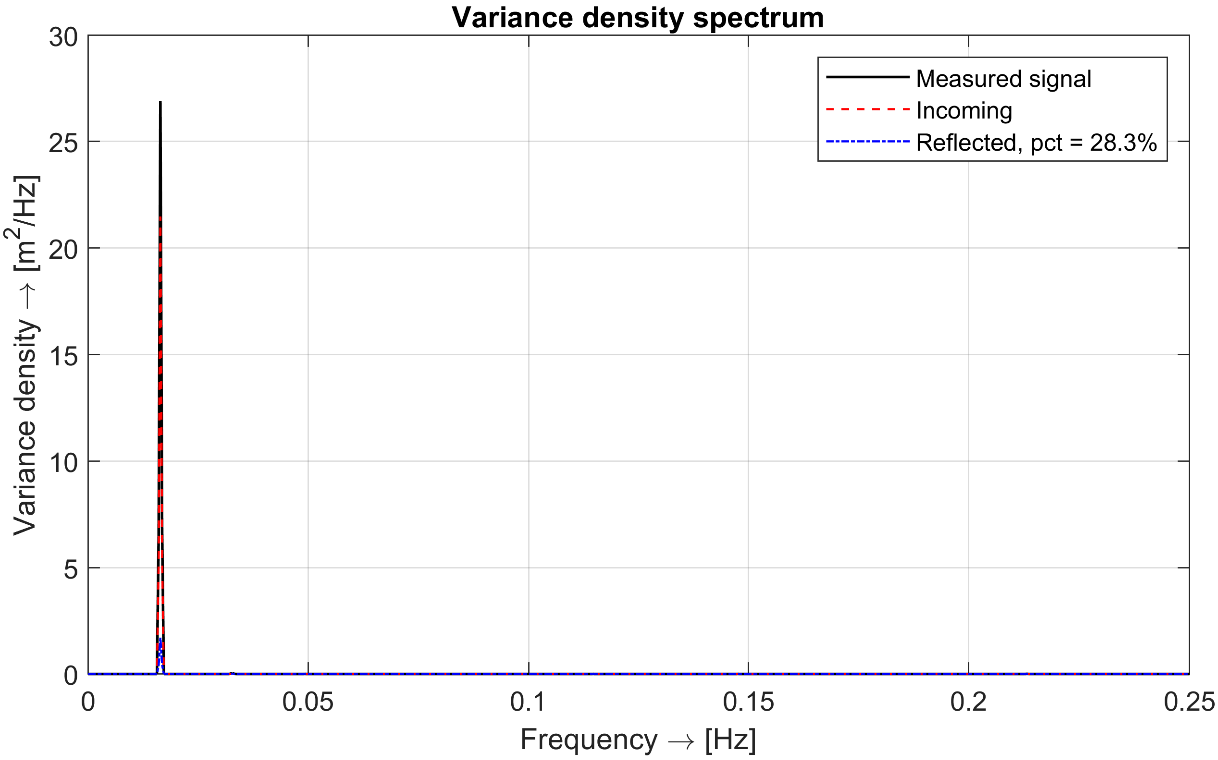

Reflection analysis using WHMs:01, 07 & 09	Monochromatic	M610b
Deltares	11202696	App. E.2.17

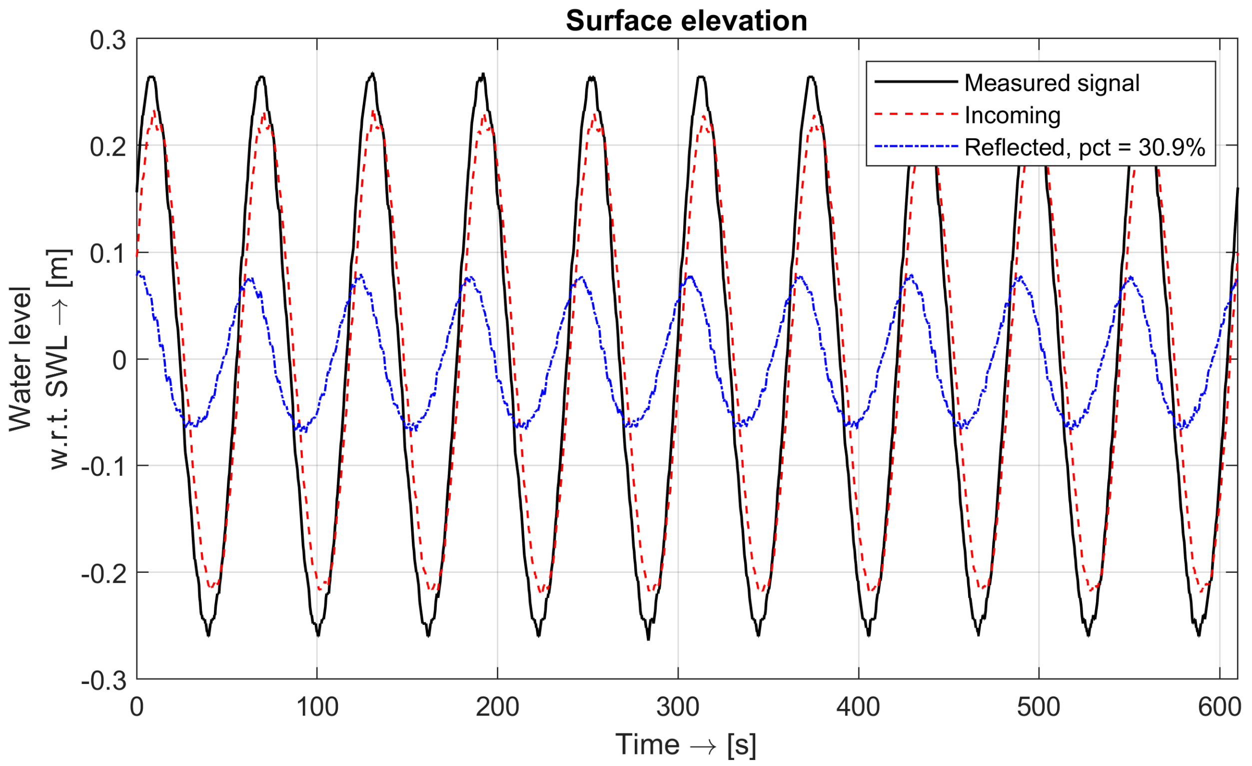

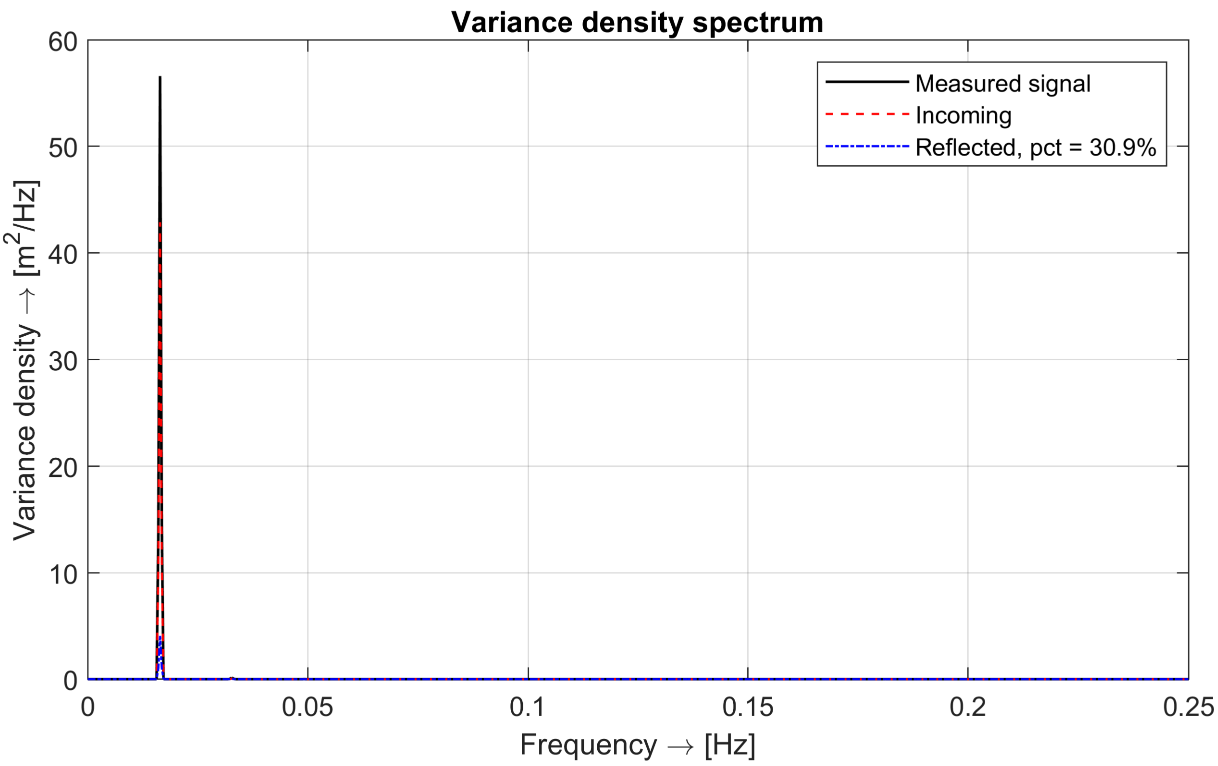

Reflection analysis using WHMs:01, 07 & 09	Monochromatic	M610c
Deltares	11202696	App. E.2.18

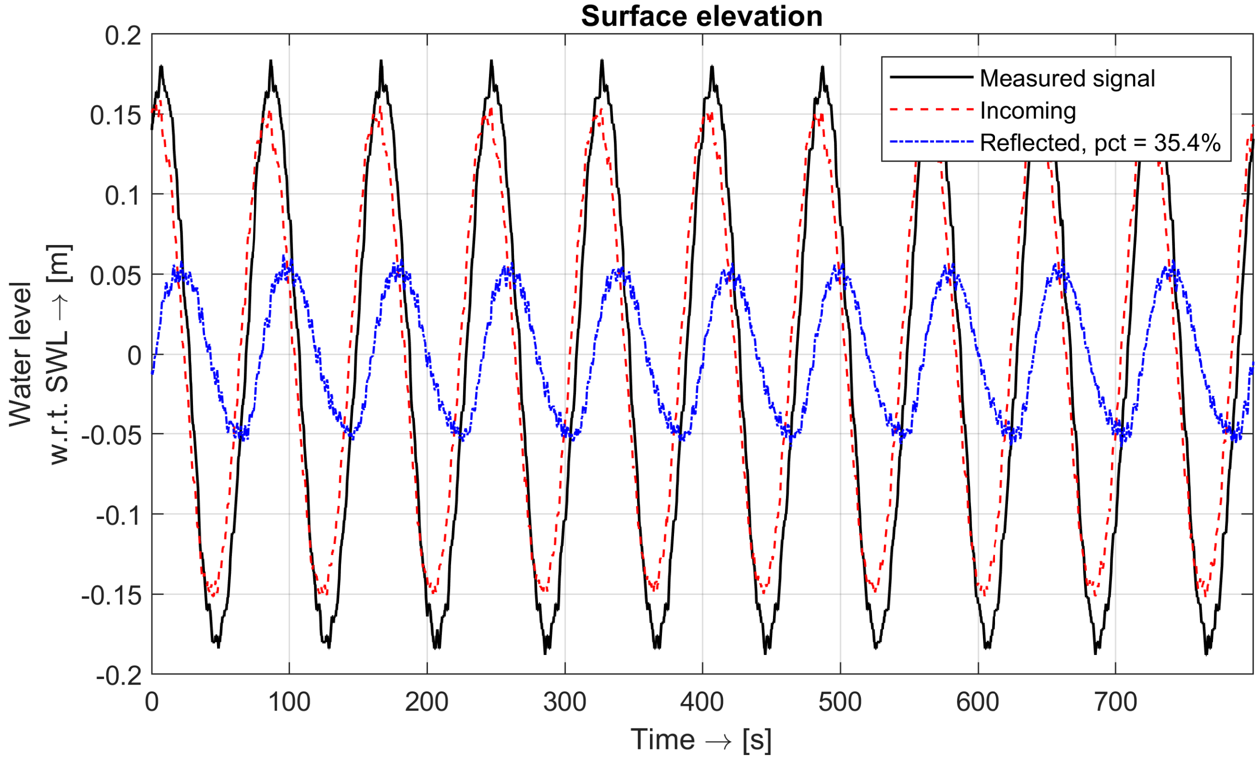

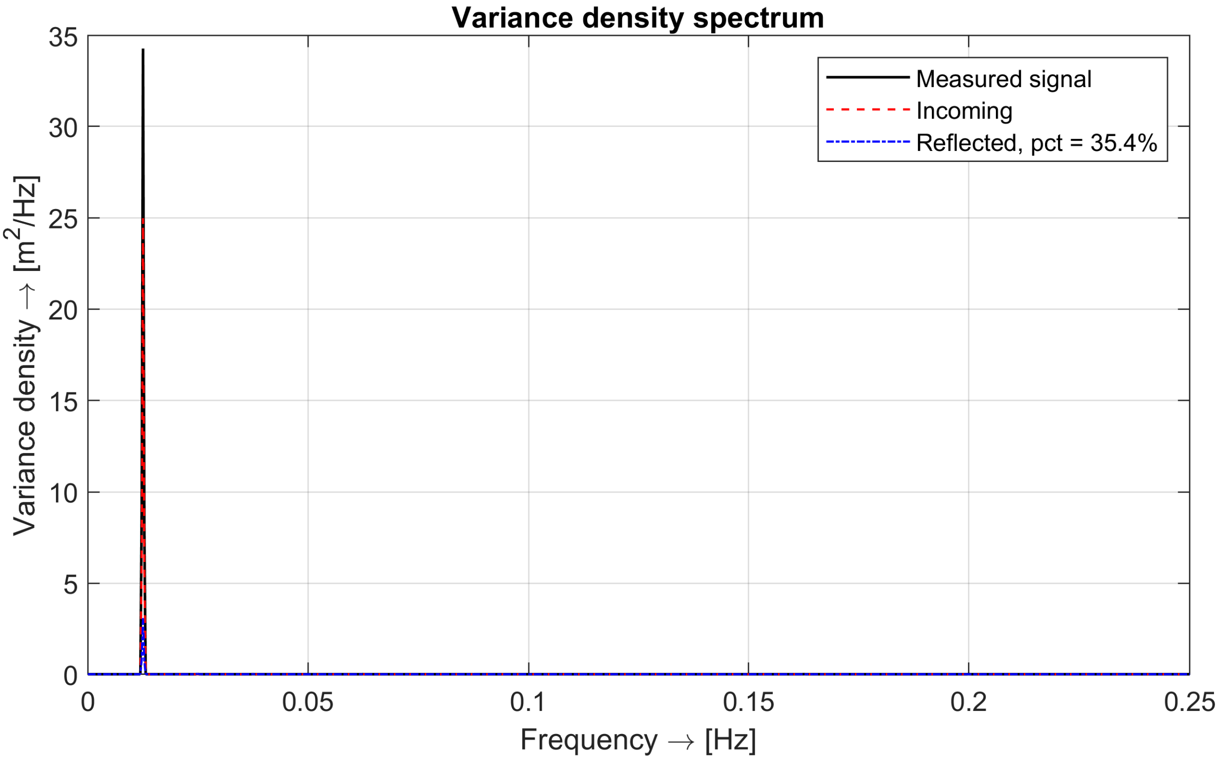

Reflection analysis using WHMs:01, 07 & 09	Monochromatic	M800a
Deltares	11202696	App. E.2.19

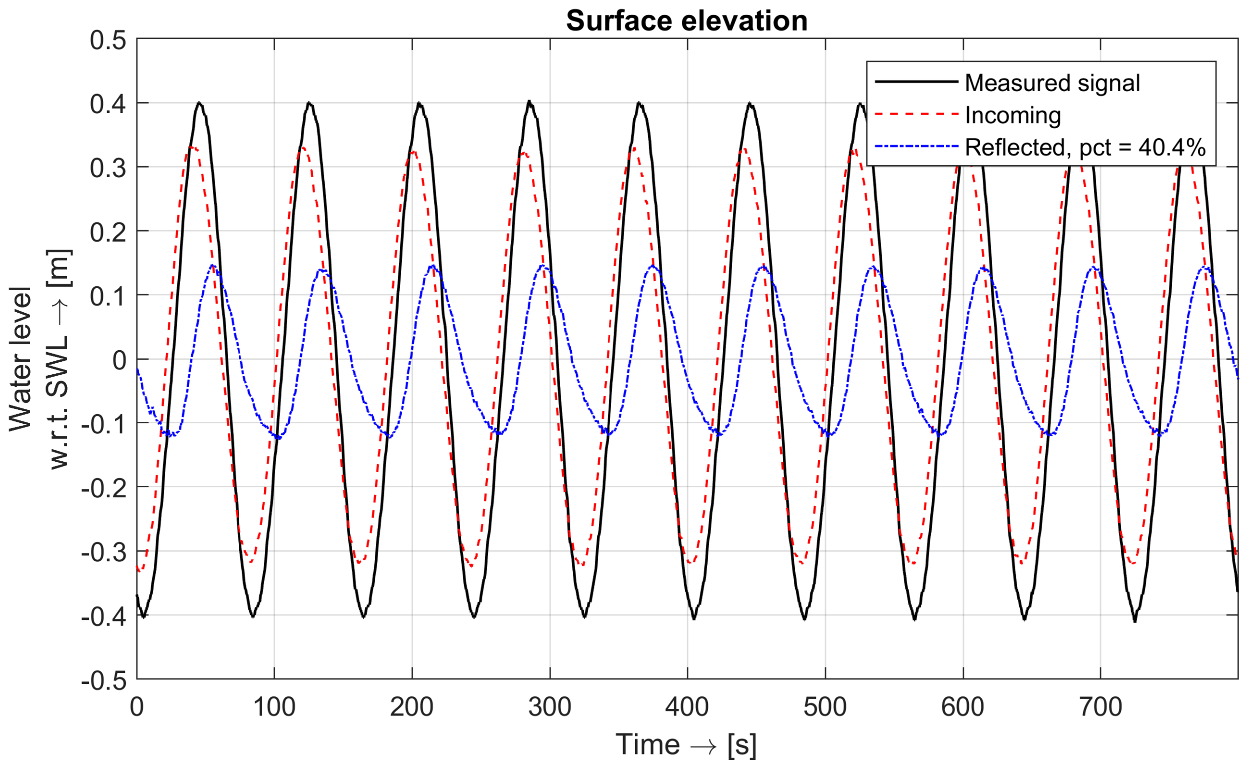

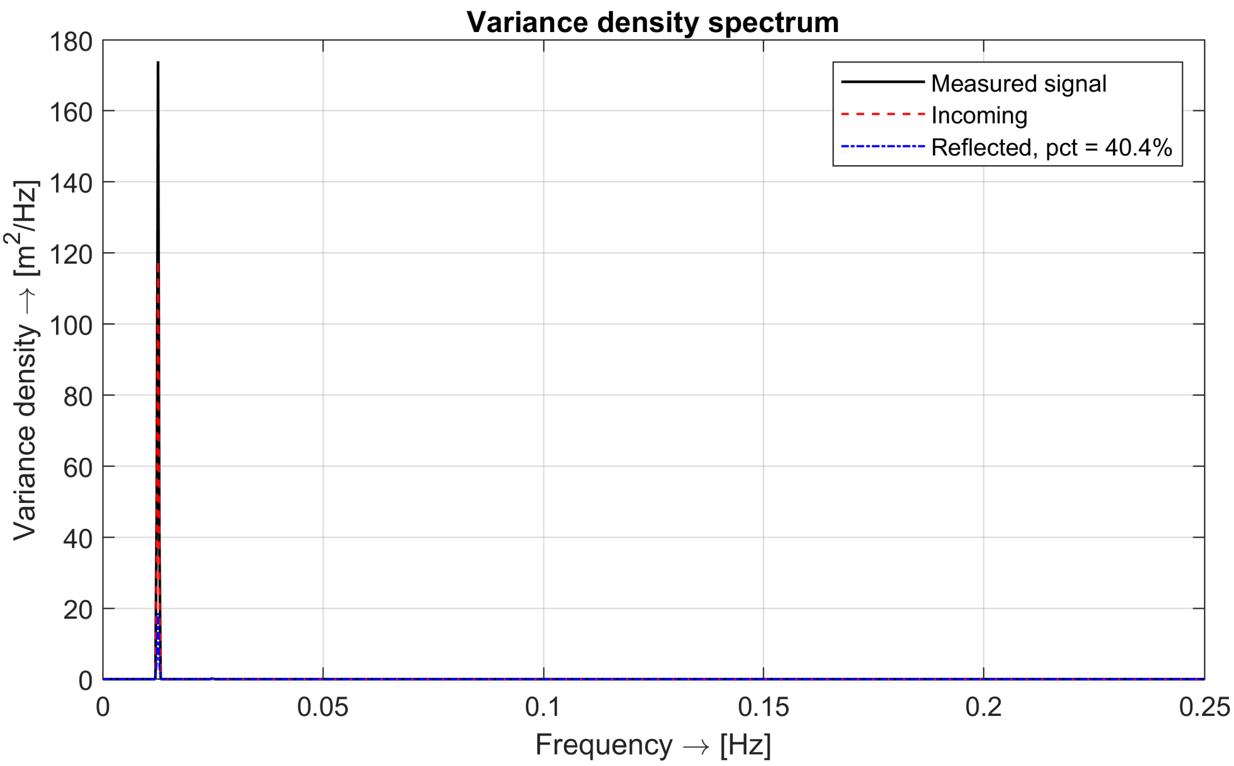

Reflection analysis using WHMs:01, 07 & 09	Monochromatic	M800b
Deltares	11202696	App. E.2.20

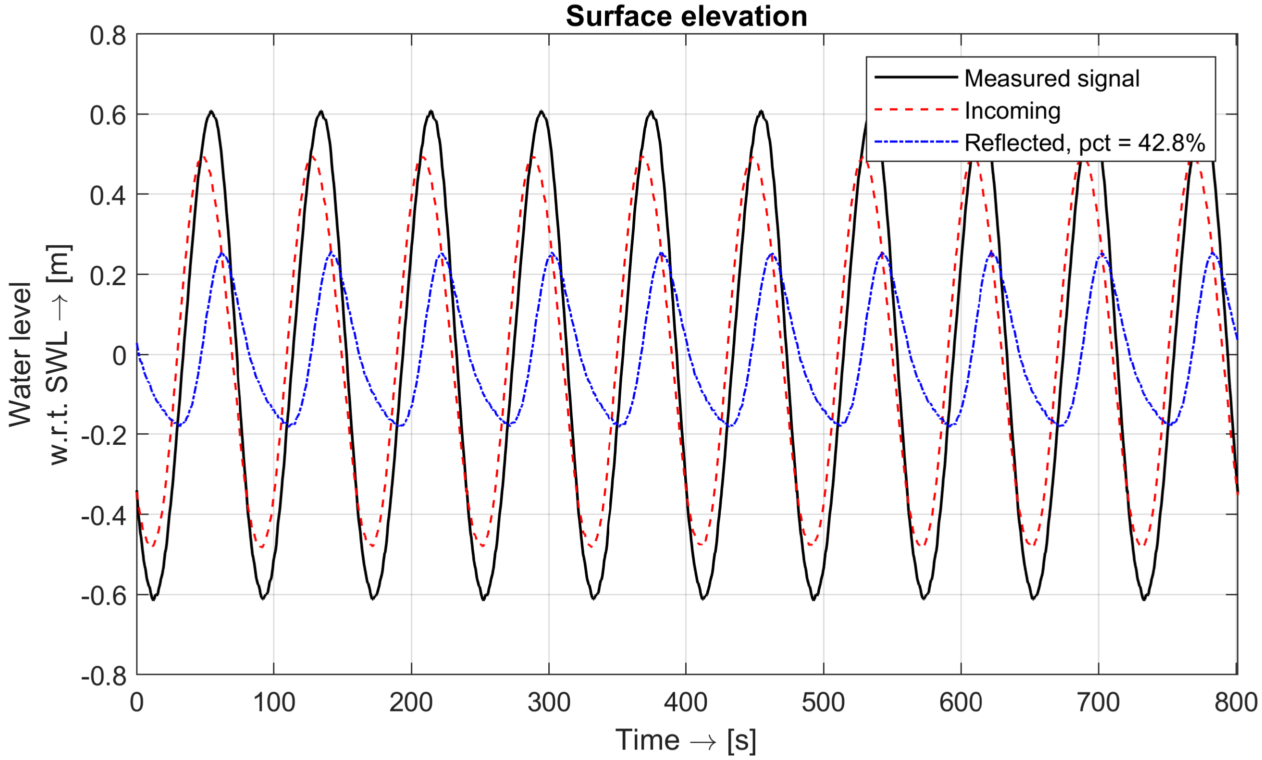

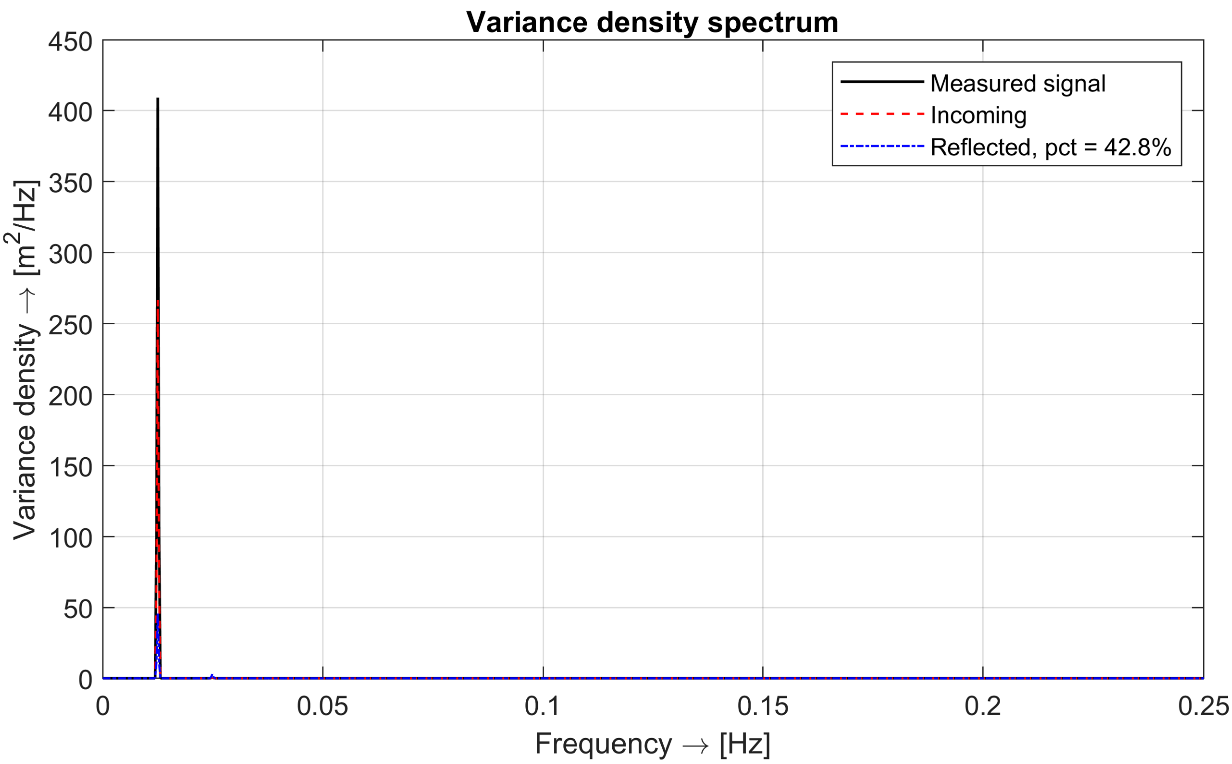

Reflection analysis using WHMs:01, 07 & 09	Monochromatic	M800c
Deltares	11202696	App. E.2.21

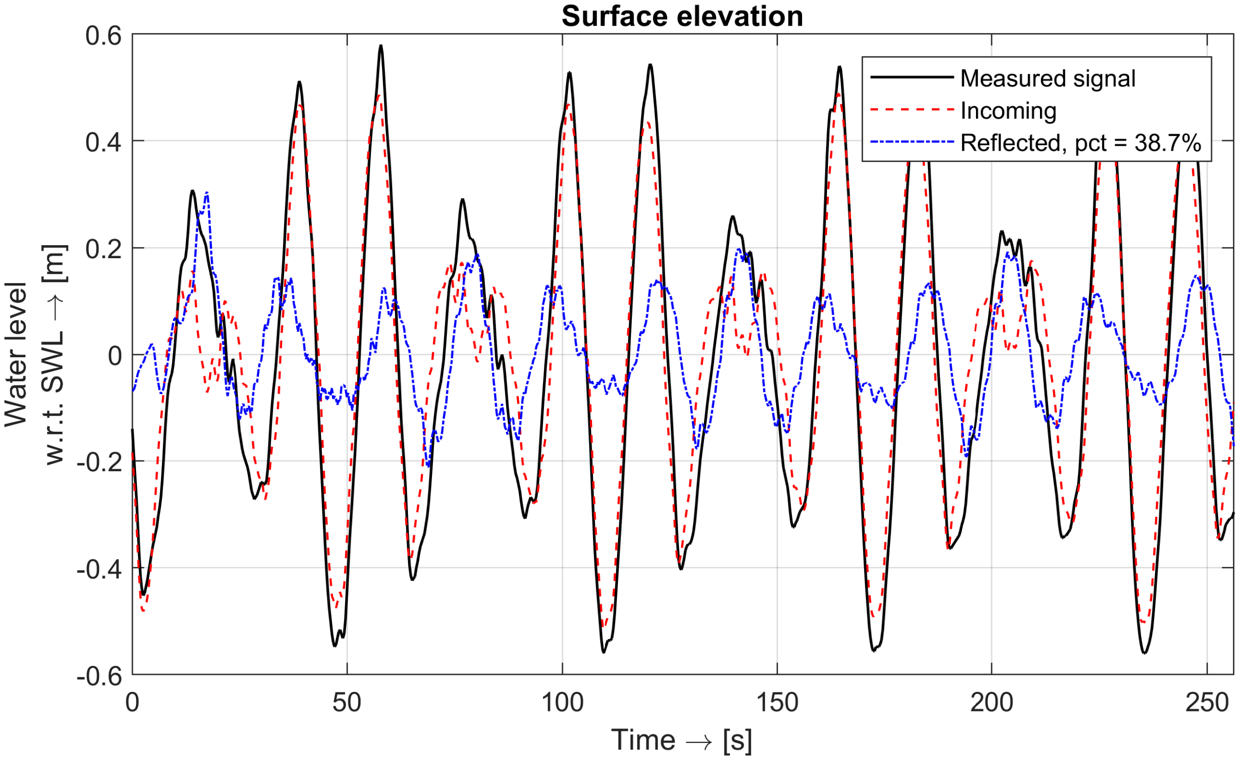

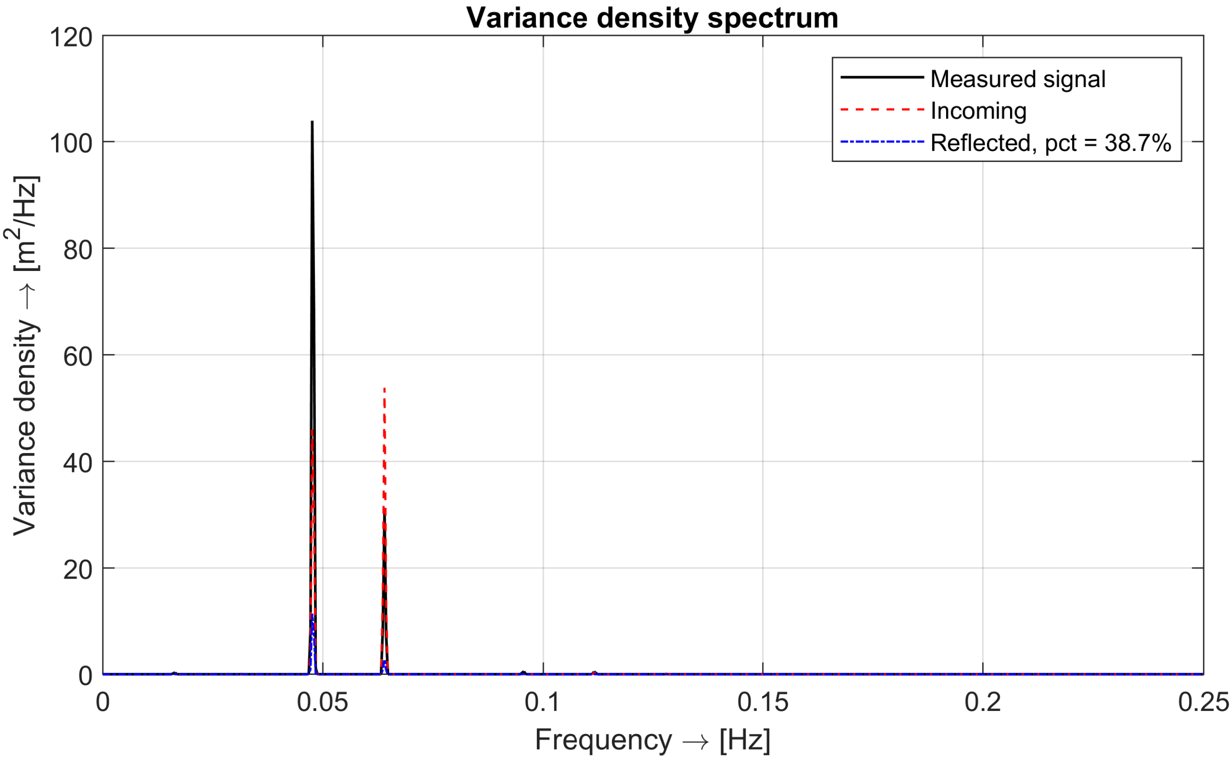

Reflection analysis using WHMs:01, 02 & 07	Bichromatic	B610a
Deltares	11202696	App. E.2.22

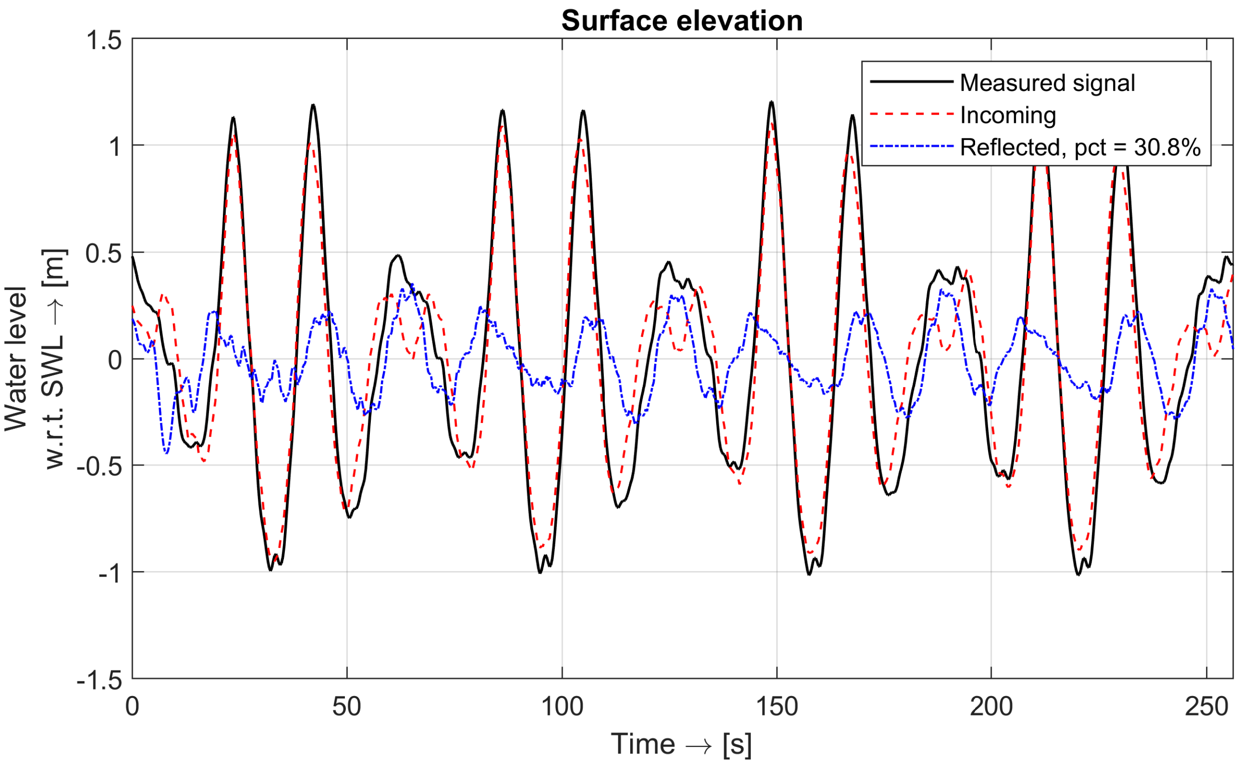

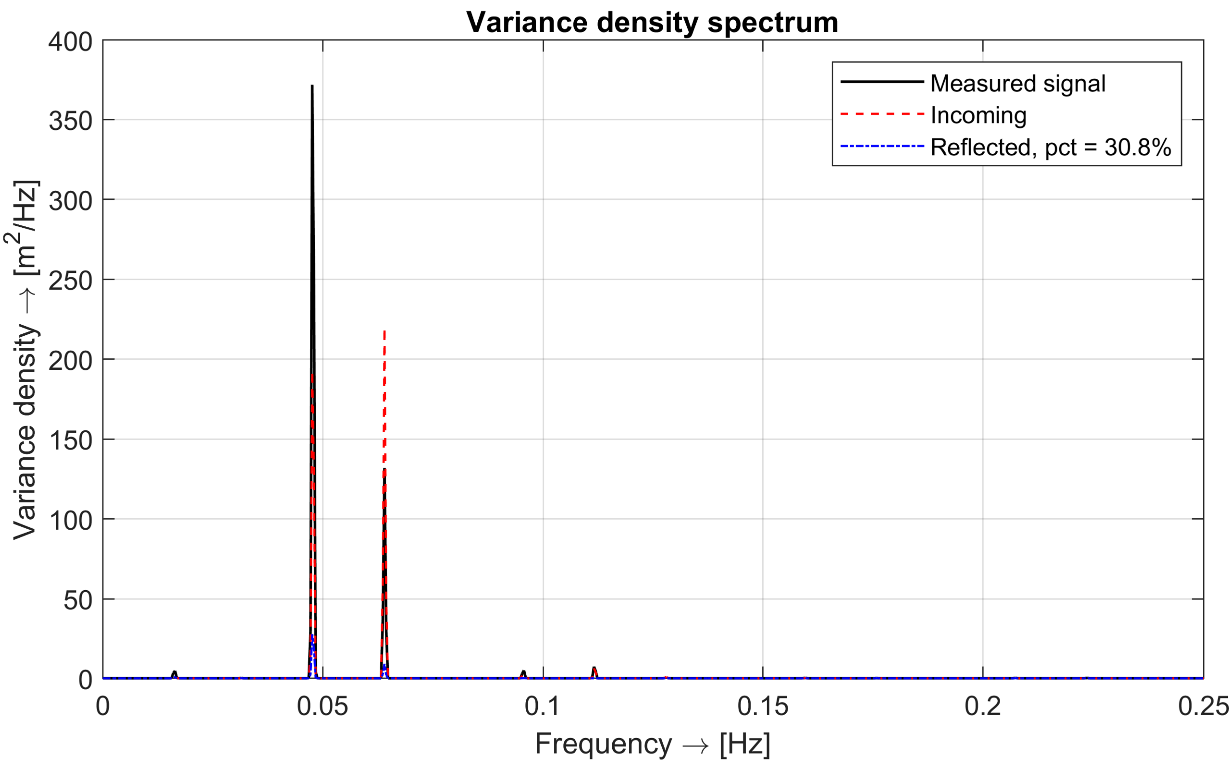

Reflection analysis using WHMs:01, 02 & 07	Bichromatic	B610e
Deltares	11202696	App. E.2.23

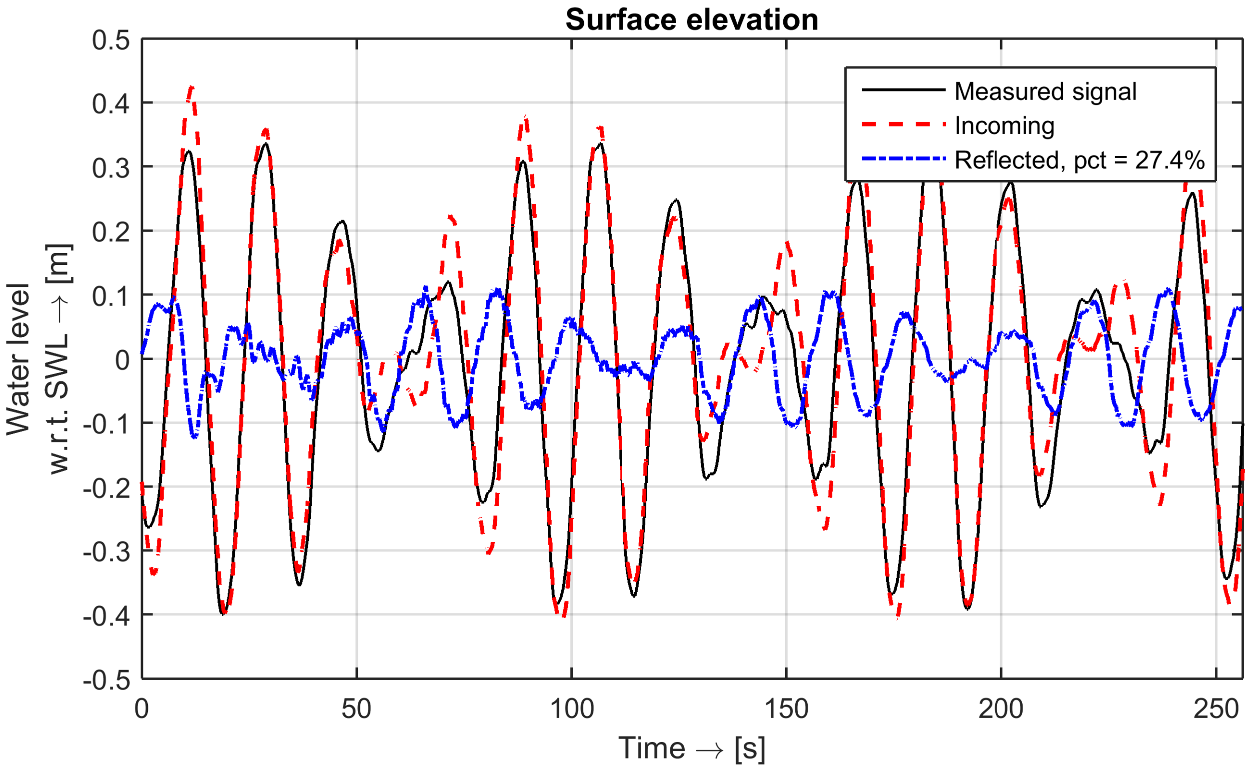

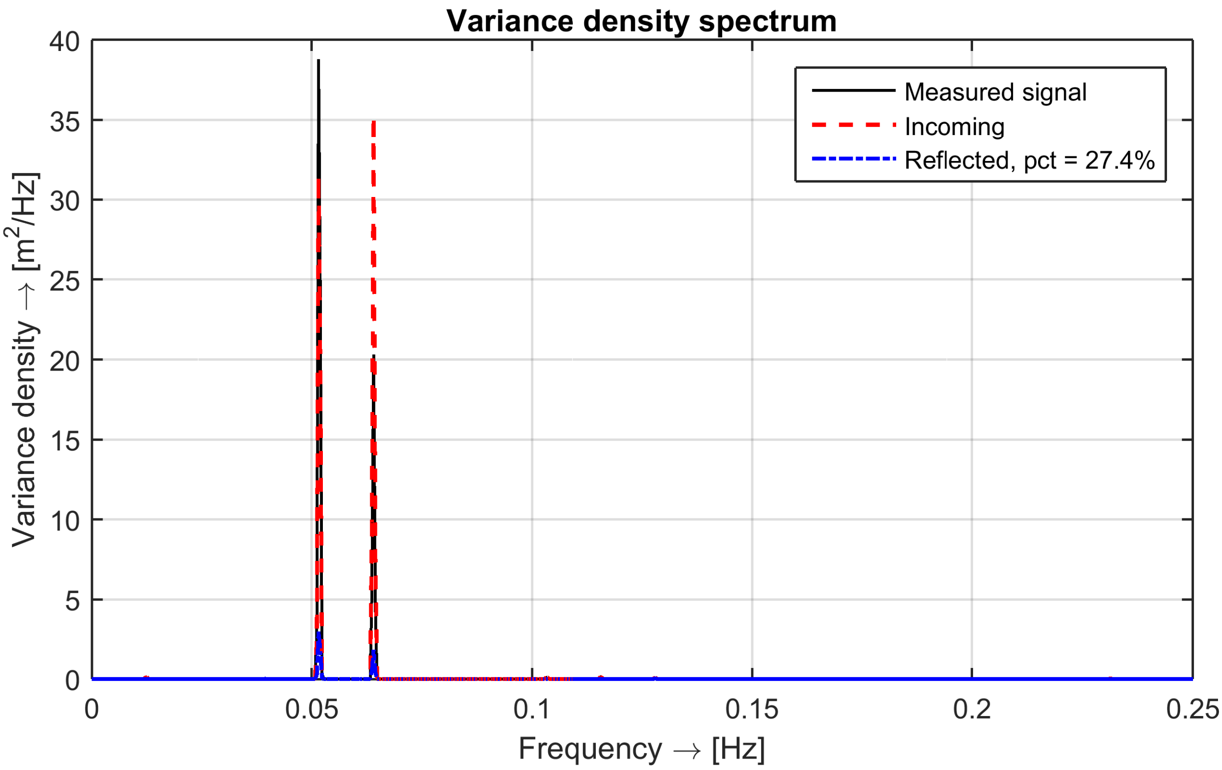

Reflection analysis with WHMs:01, 02 & 07	Bichromatic	B800a
Deltares	11202696	App. E.2.24

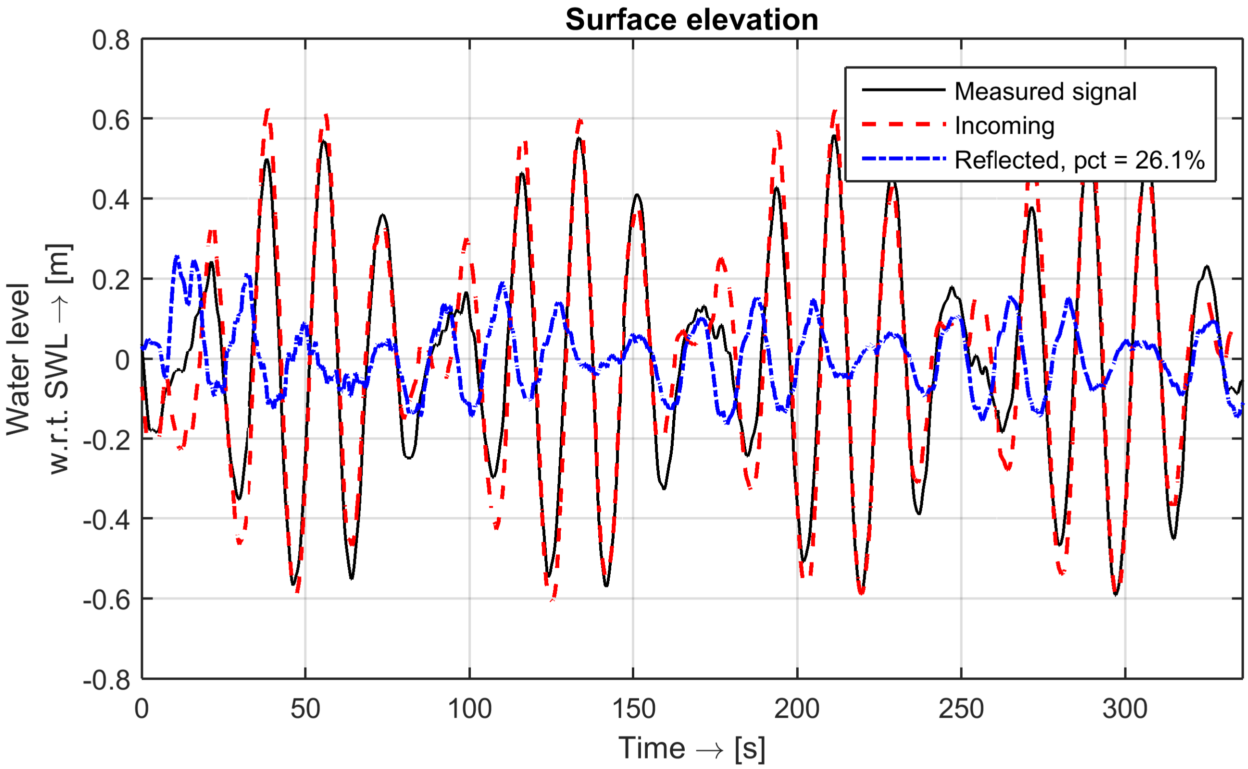

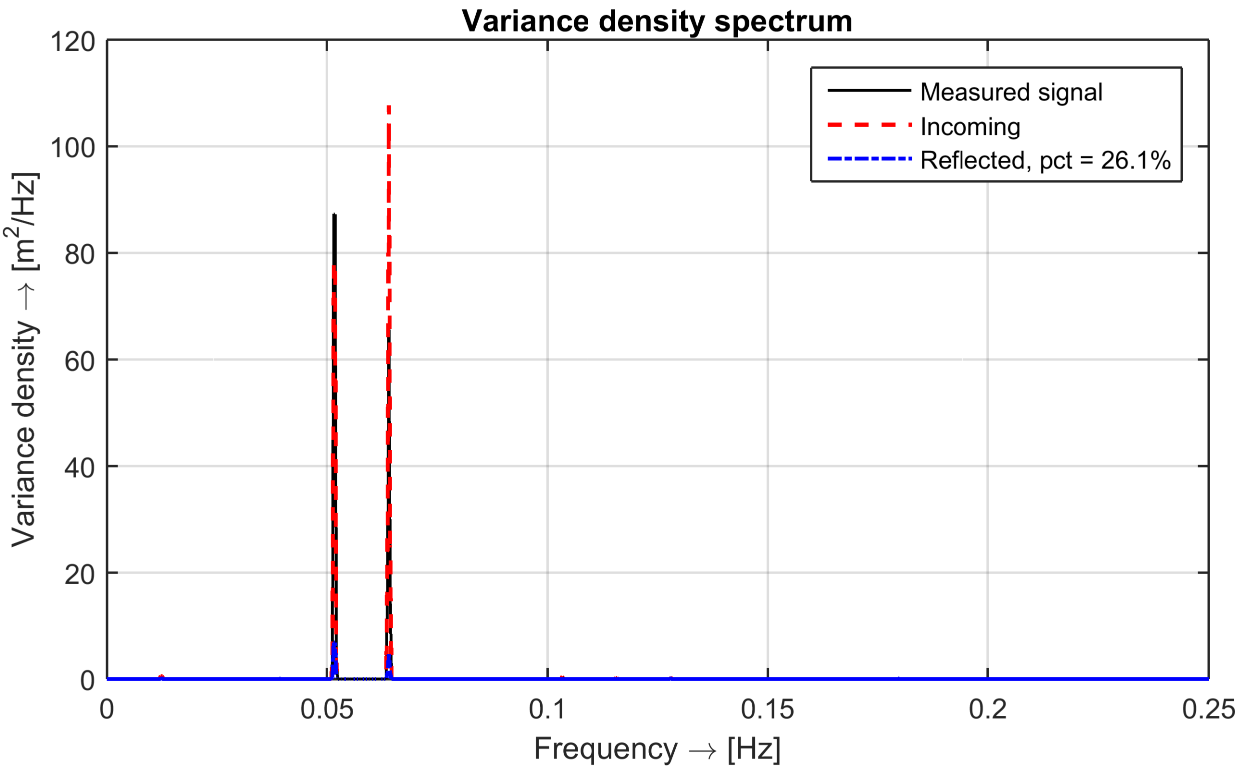

Reflection analysis with WHMs:01, 02 & 07	Bichromatic	B800c
Deltares	11202696	App. E.2.25

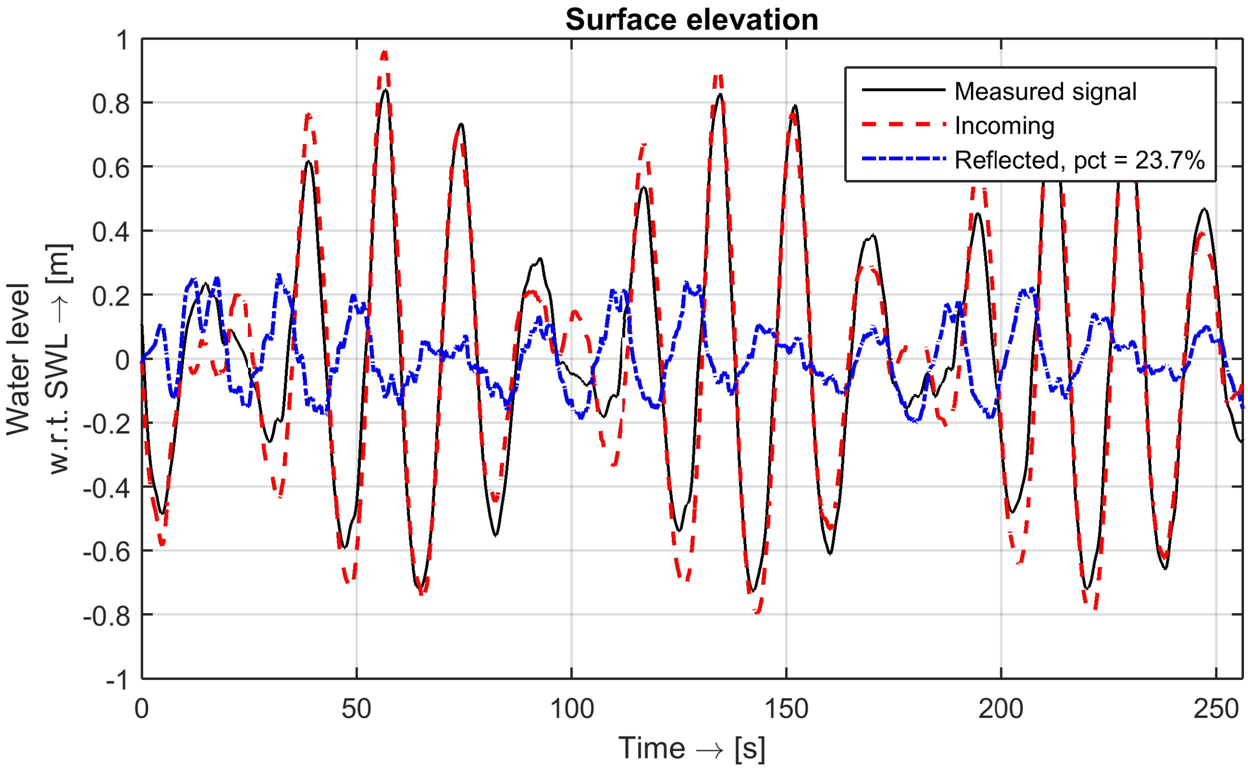

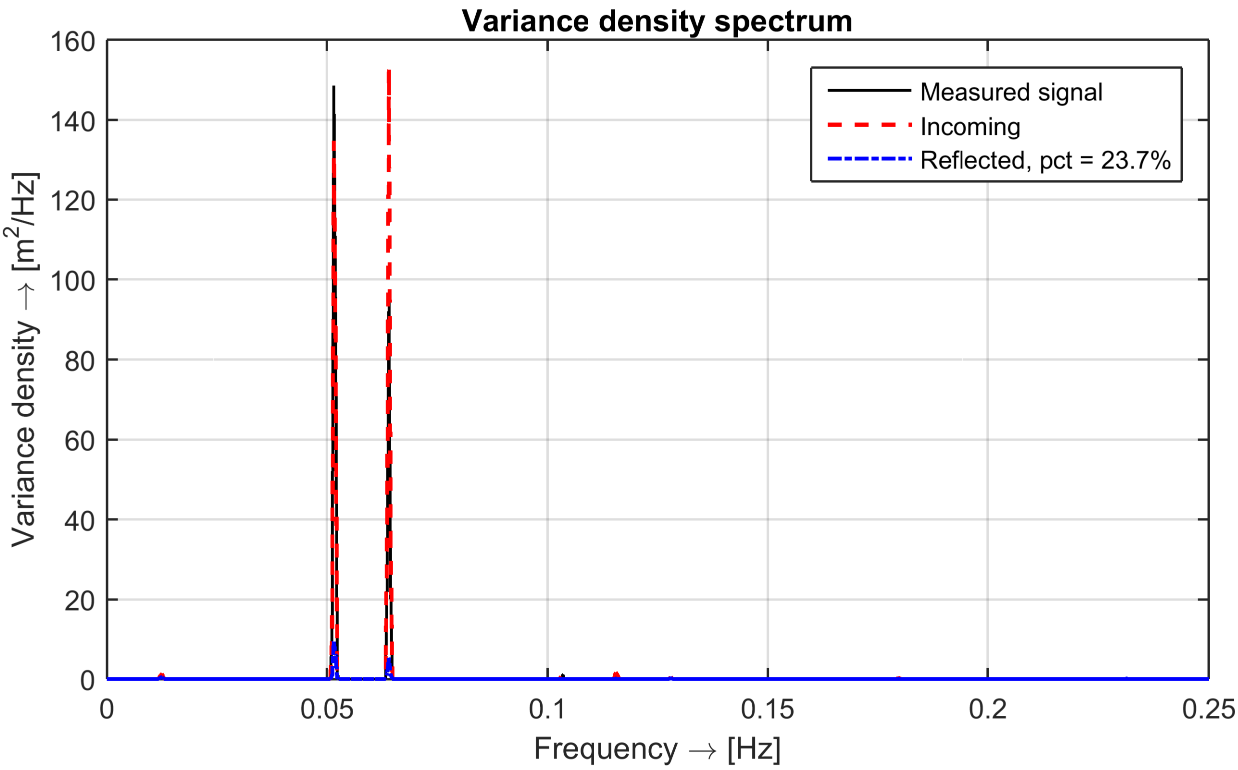

Reflection analysis with WHMs:01, 02 & 07	Bichromatic	B800e
Deltares	11202696	App. E.2.26

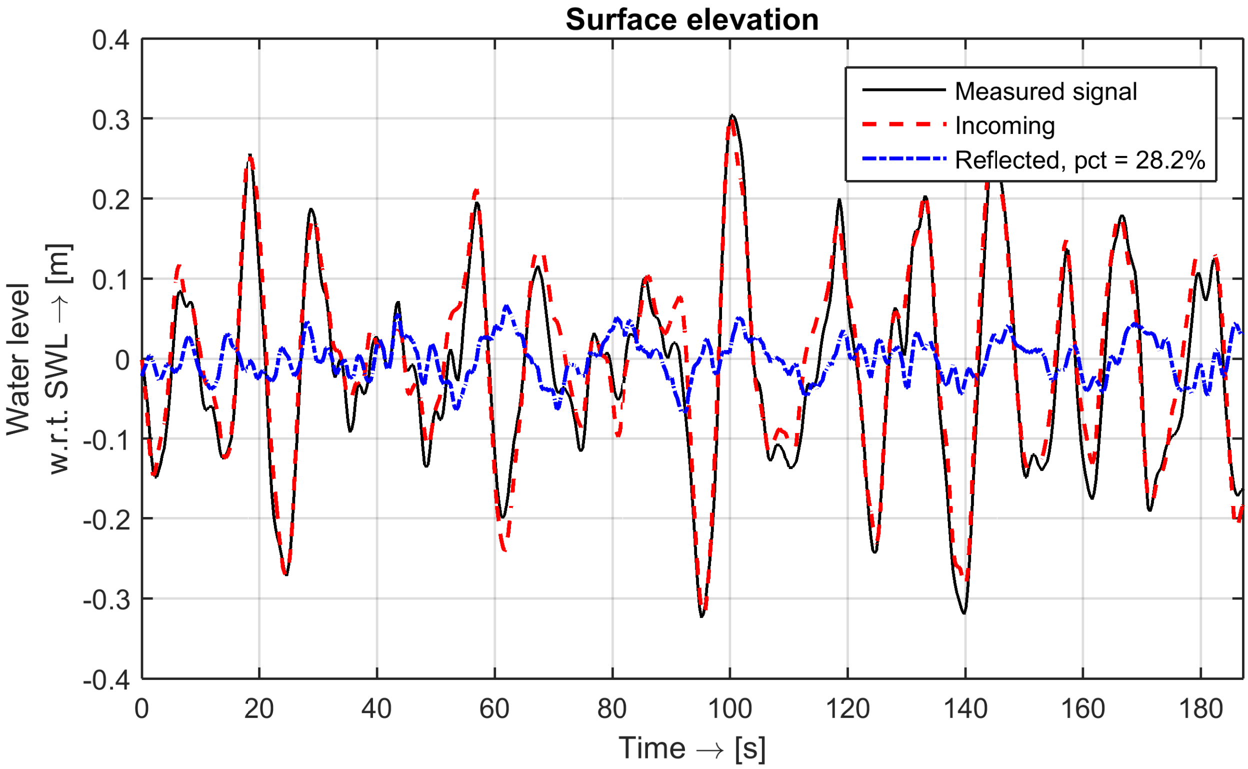

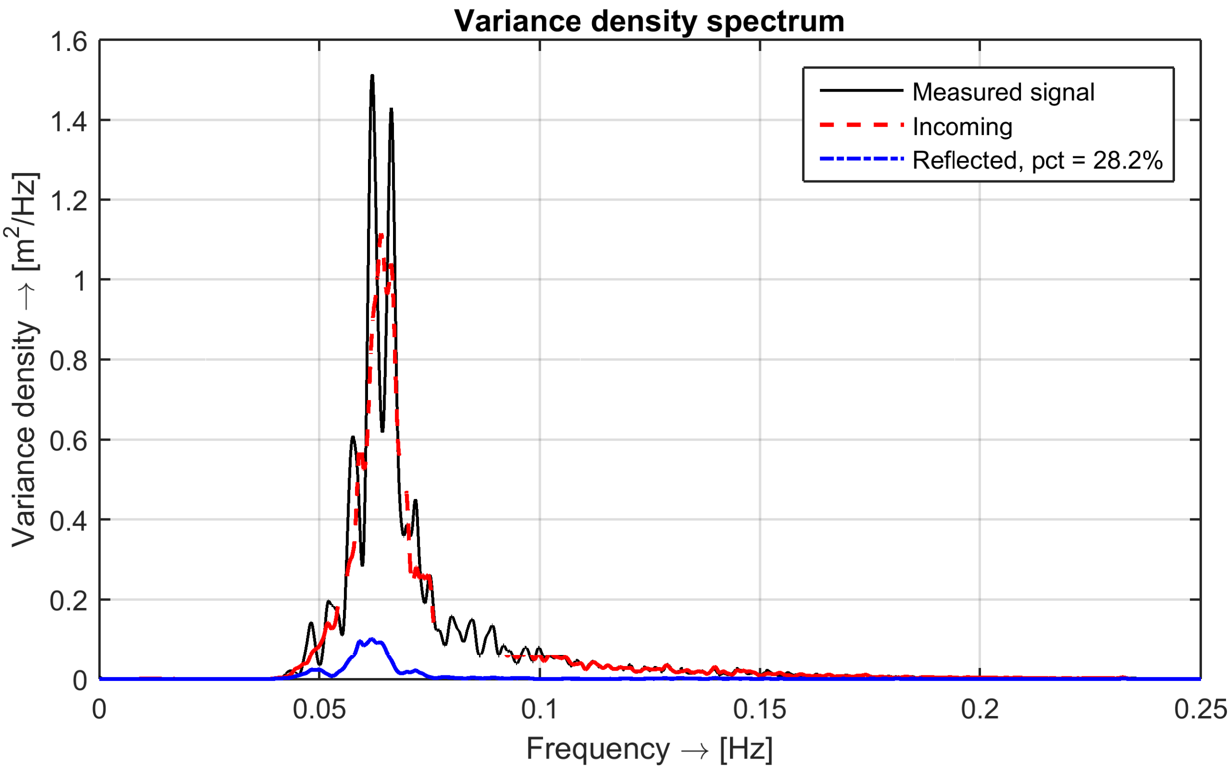

Reflection analysis with WHMs:01, 02 & 07	Irregular	I156a
Deltares	11202696	App. E.2.27

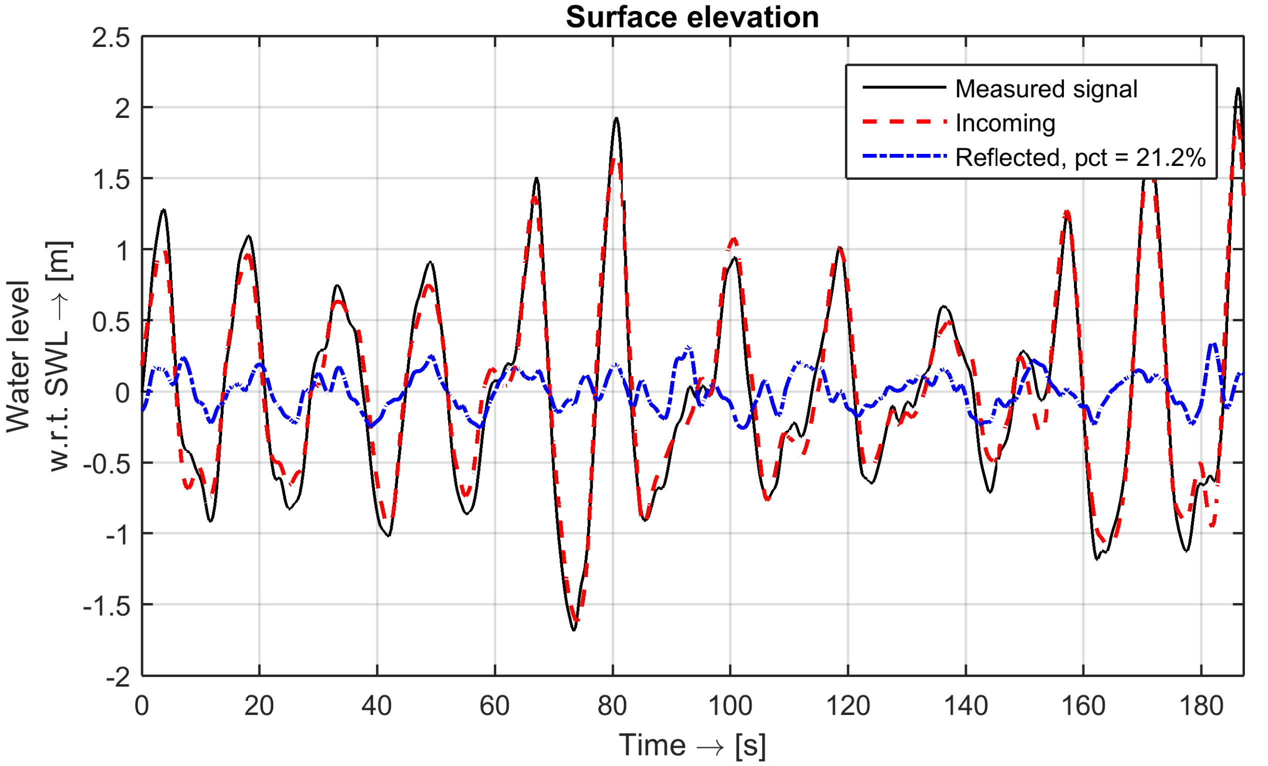

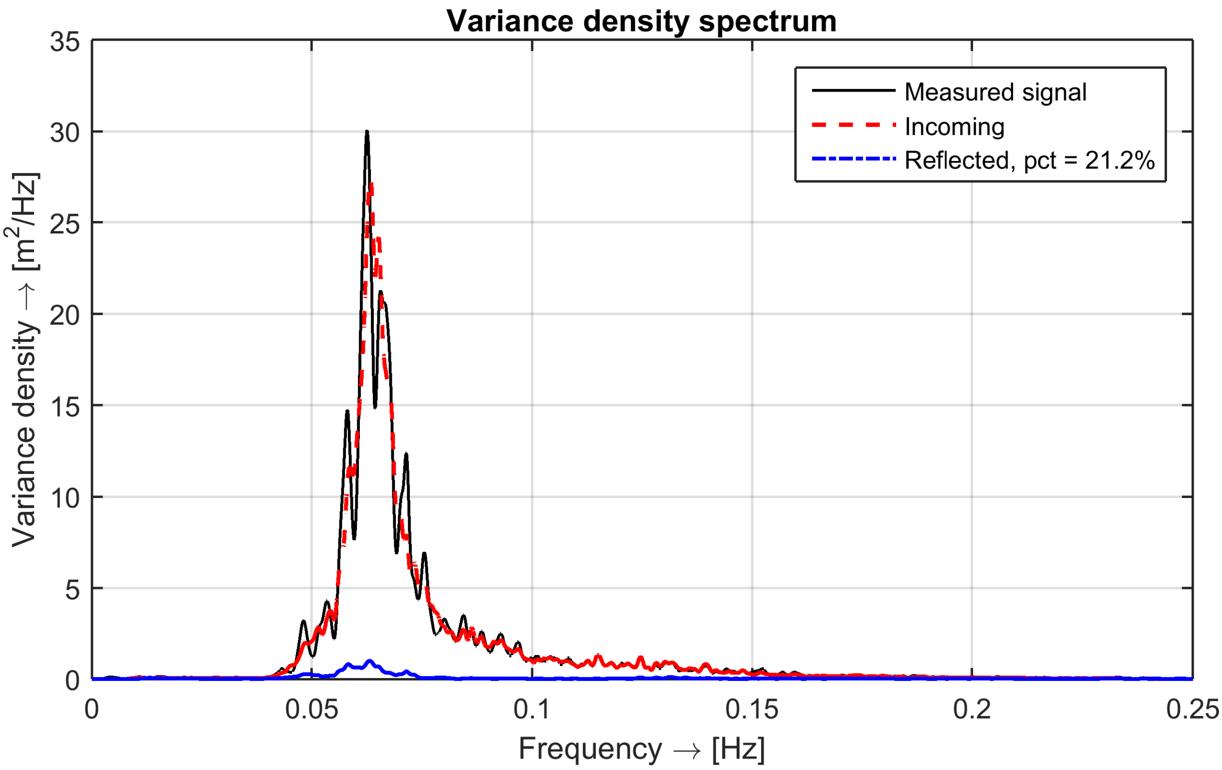

Reflection analysis with WHMs:01, 02 & 07	Irregular	I156e
Deltares	11202696	App. E.2.28

E.3 Case D

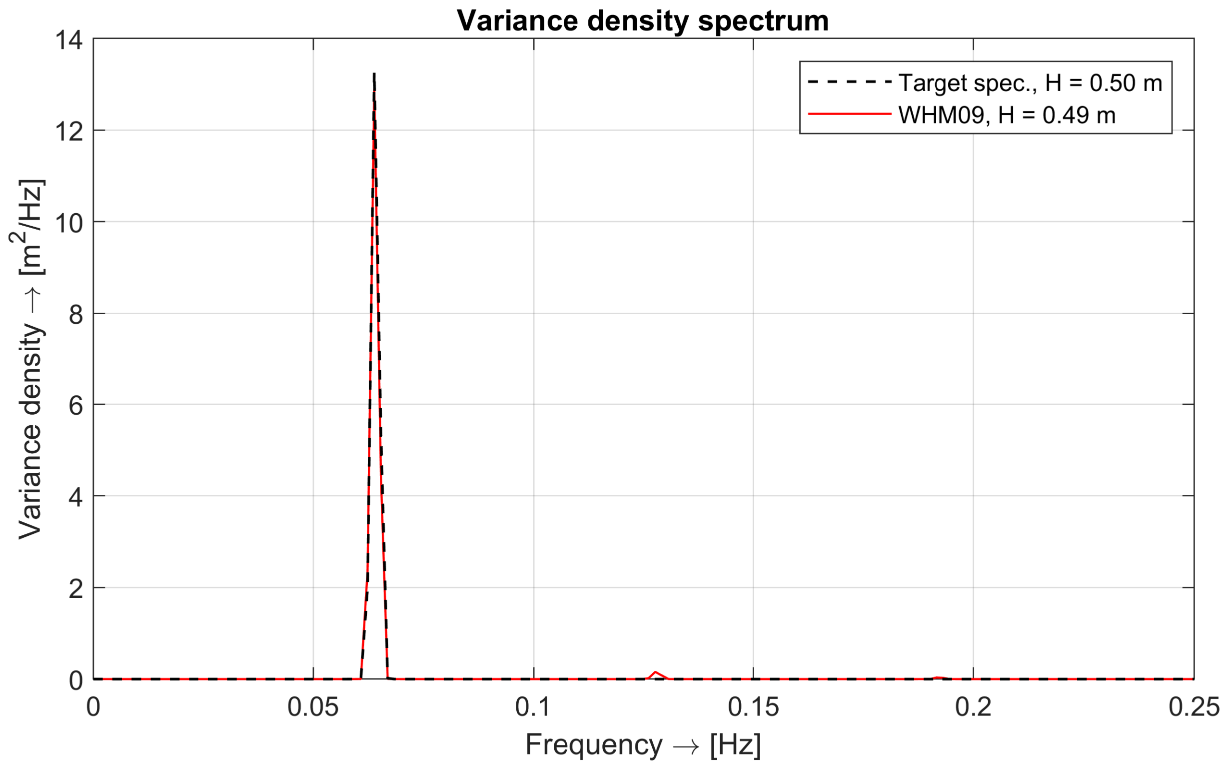

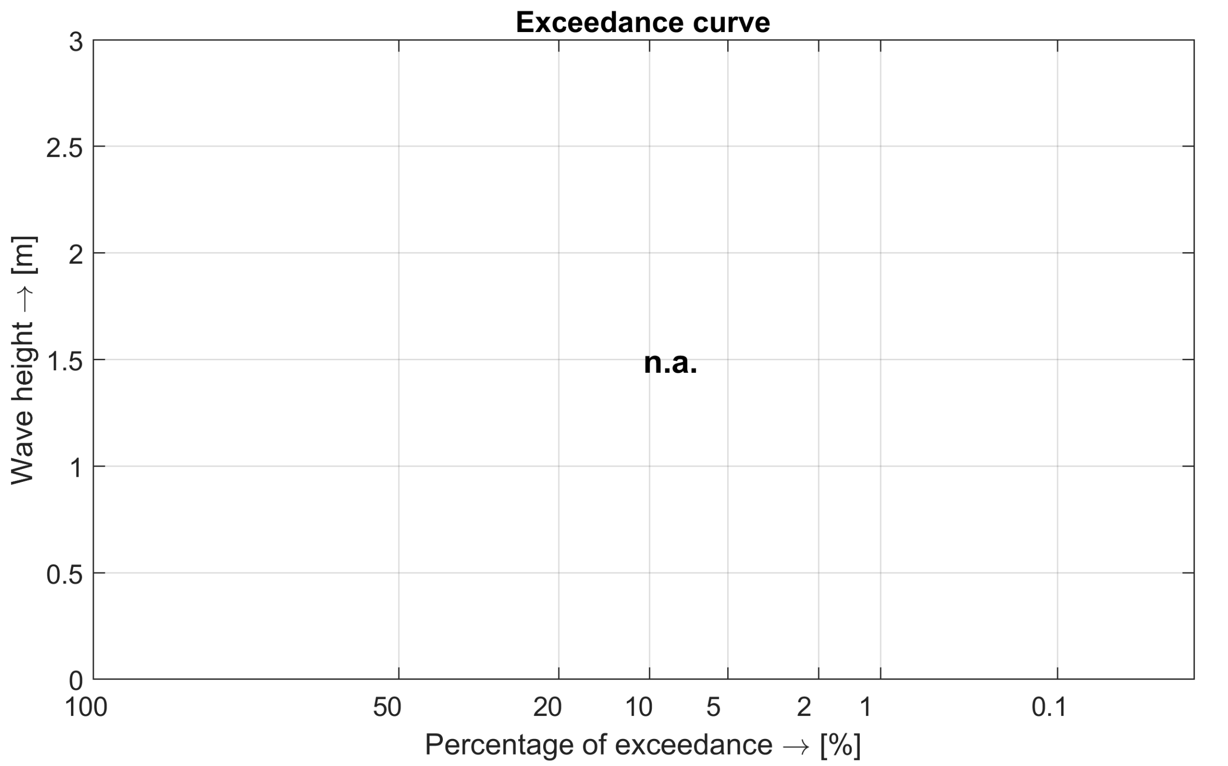

Results of wave generation calibration Depth = 18.0 m, H = 0.50 m, T = 15.60 s	Monochromatic	M156a
Deltares	11202696	App. E.3.01

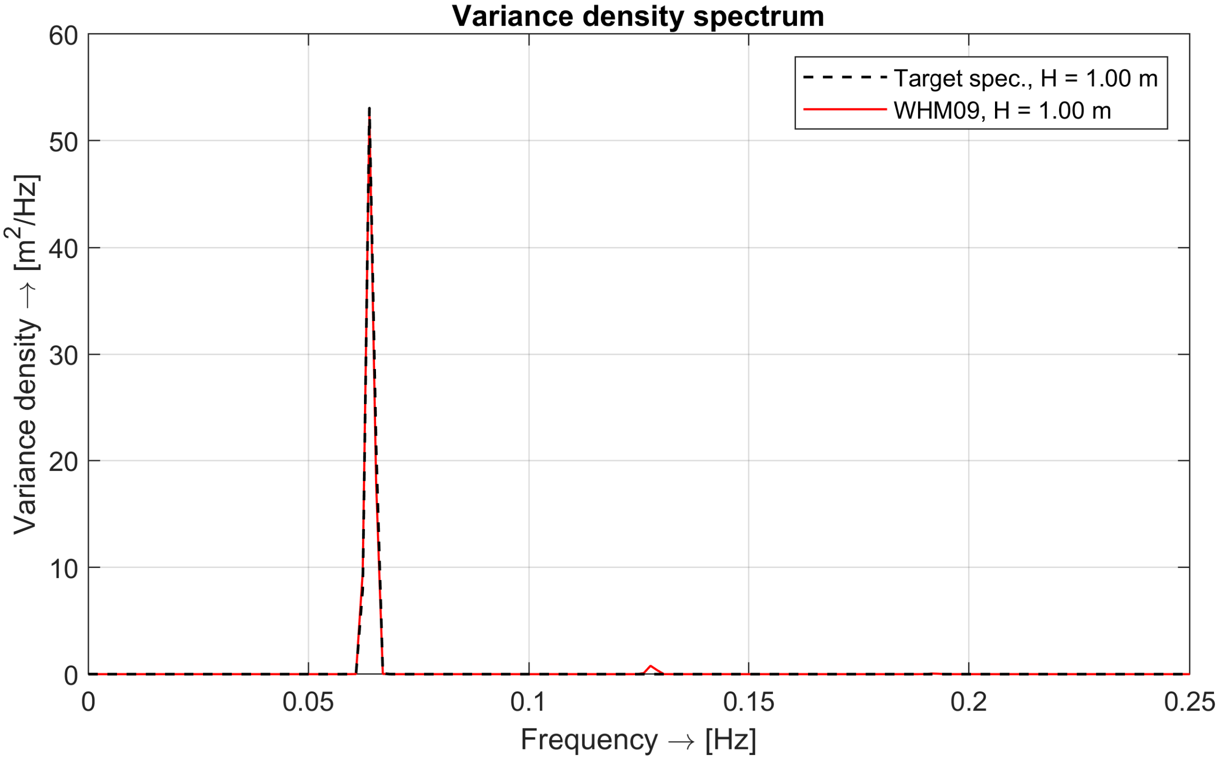

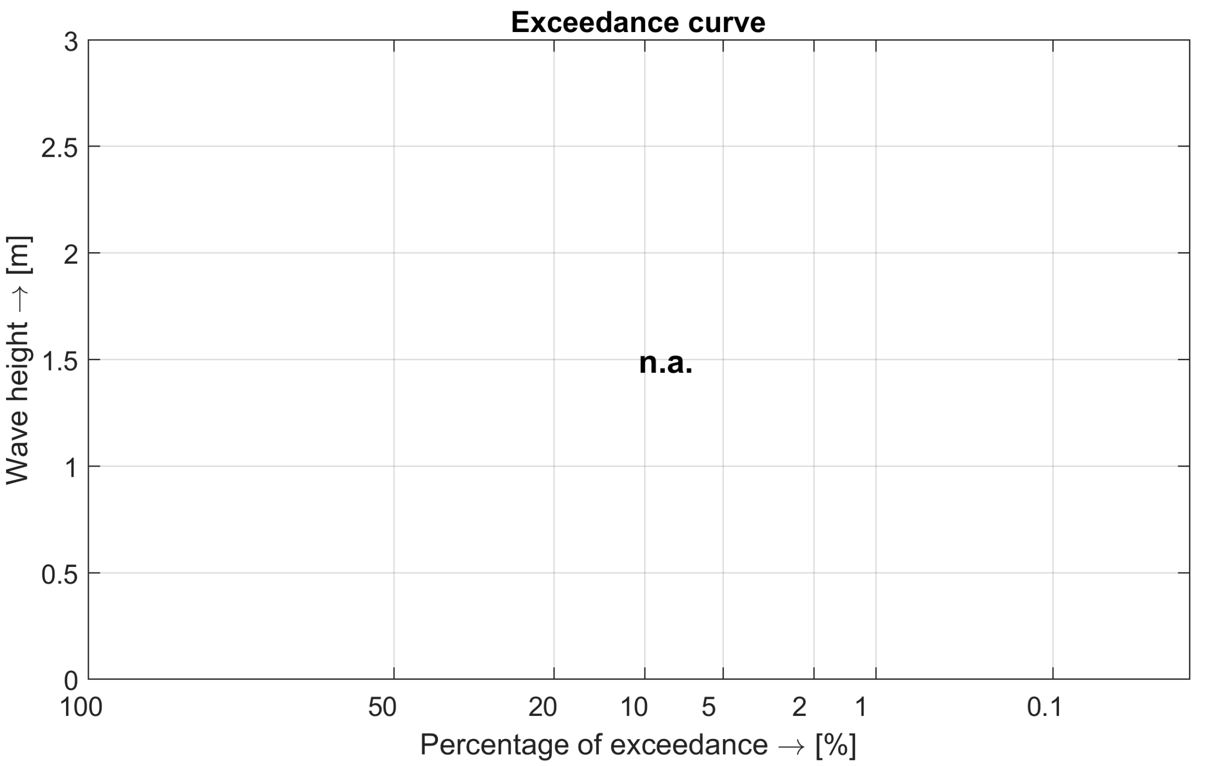

Results of wave generation calibration Depth = 18.0 m, H = 1.00 m, T = 15.60 s	Monochromatic	M156b
Deltares	11202696	App. E.3.02

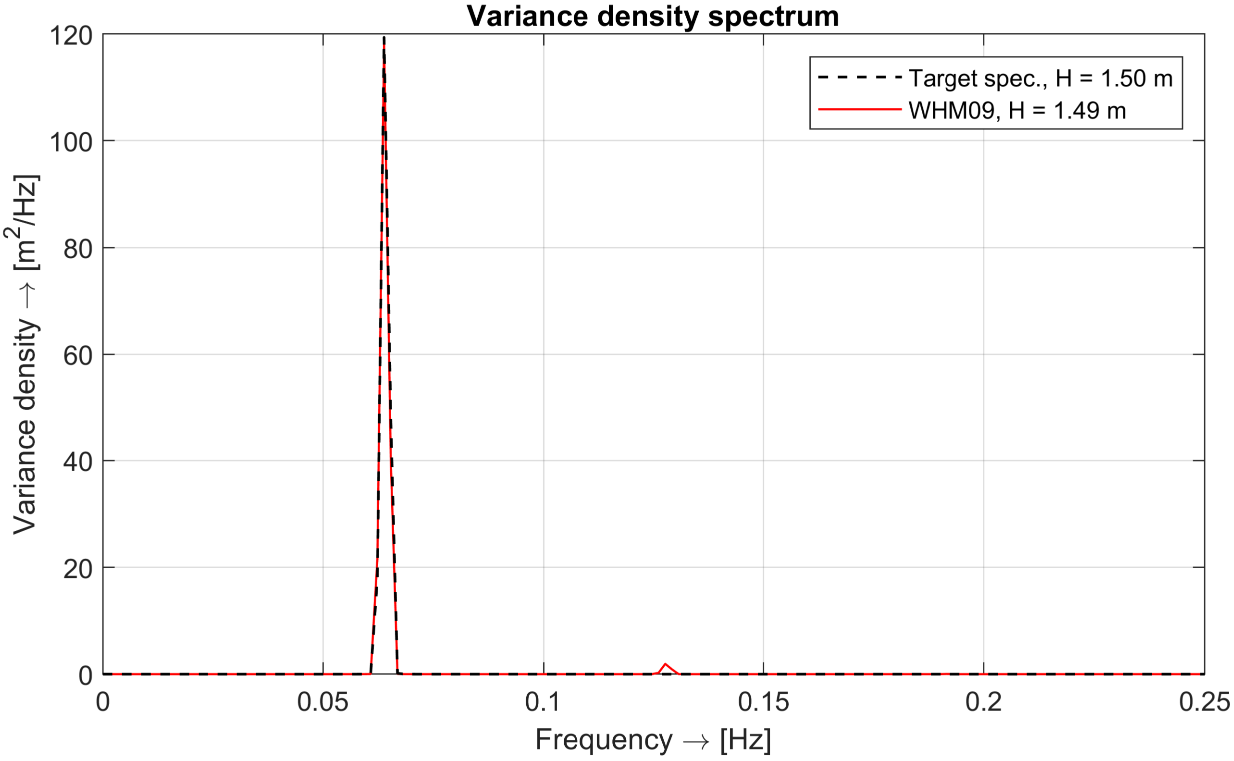

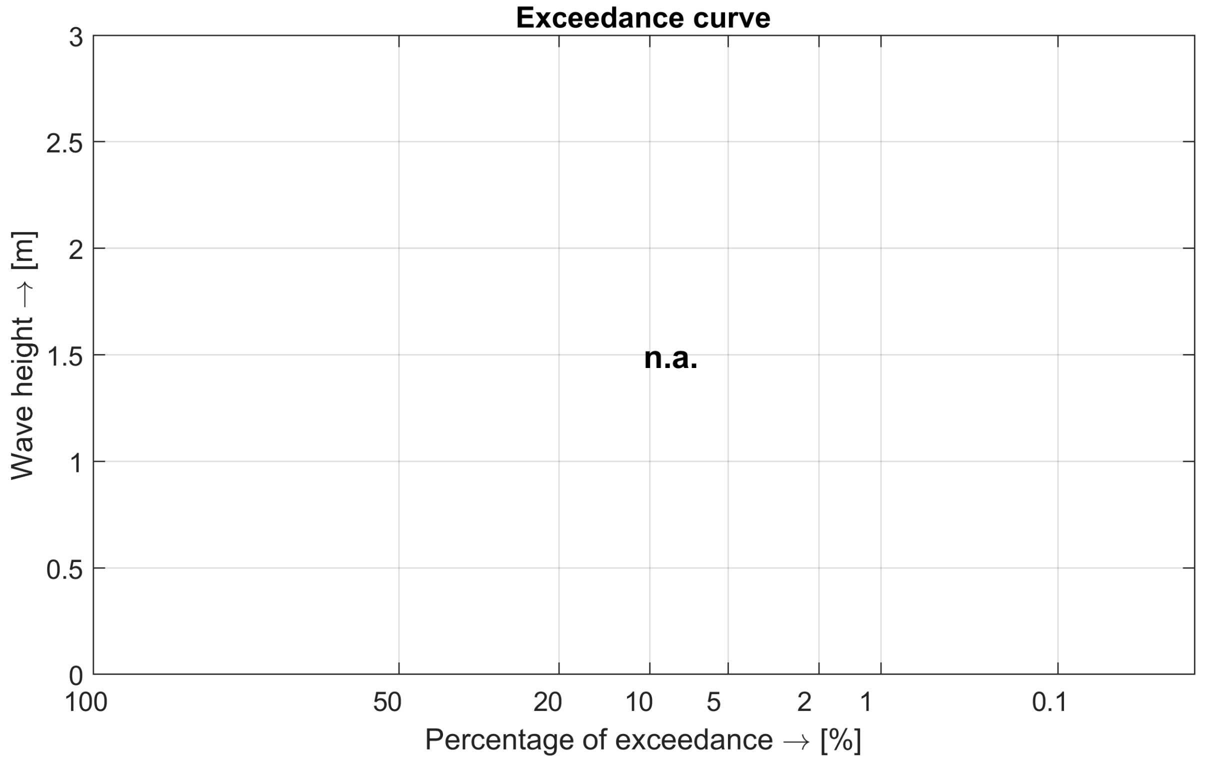

Results of wave generation calibration Depth = 18.0 m, H = 1.50 m, T = 15.60 s	Monochromatic	M156c
Deltares	11202696	App. E.3.03

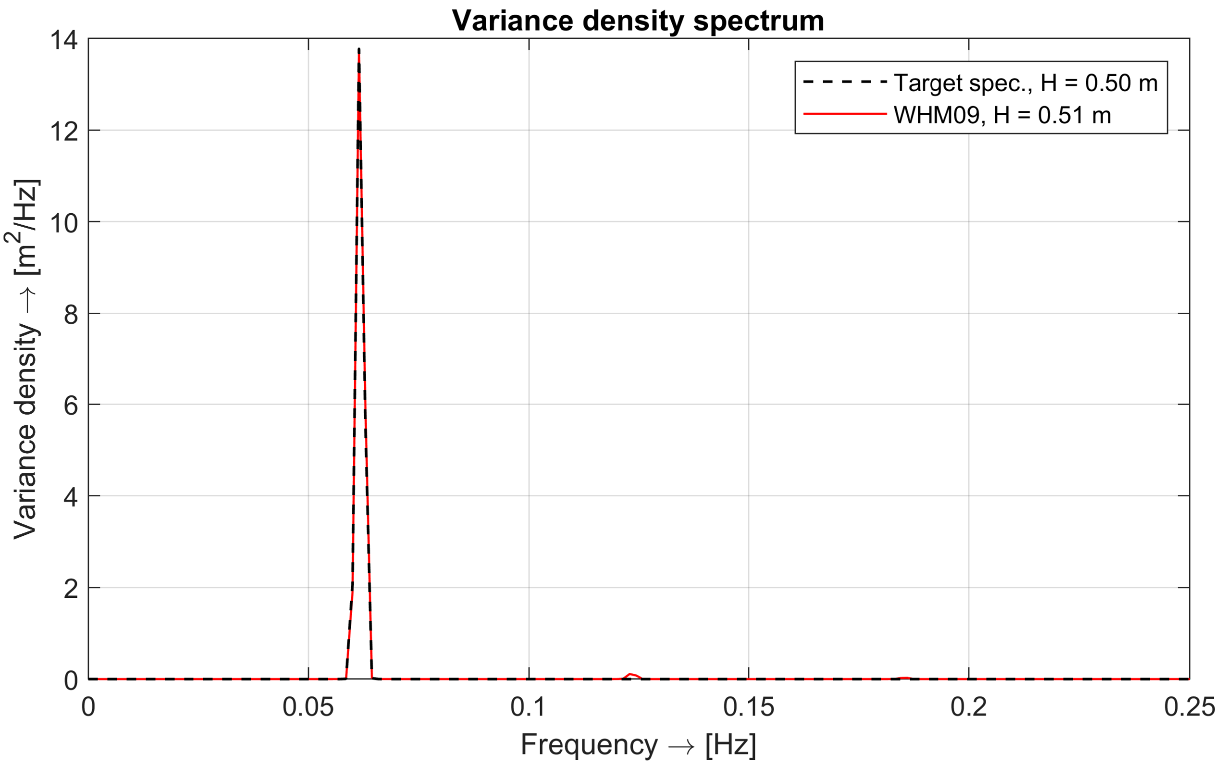

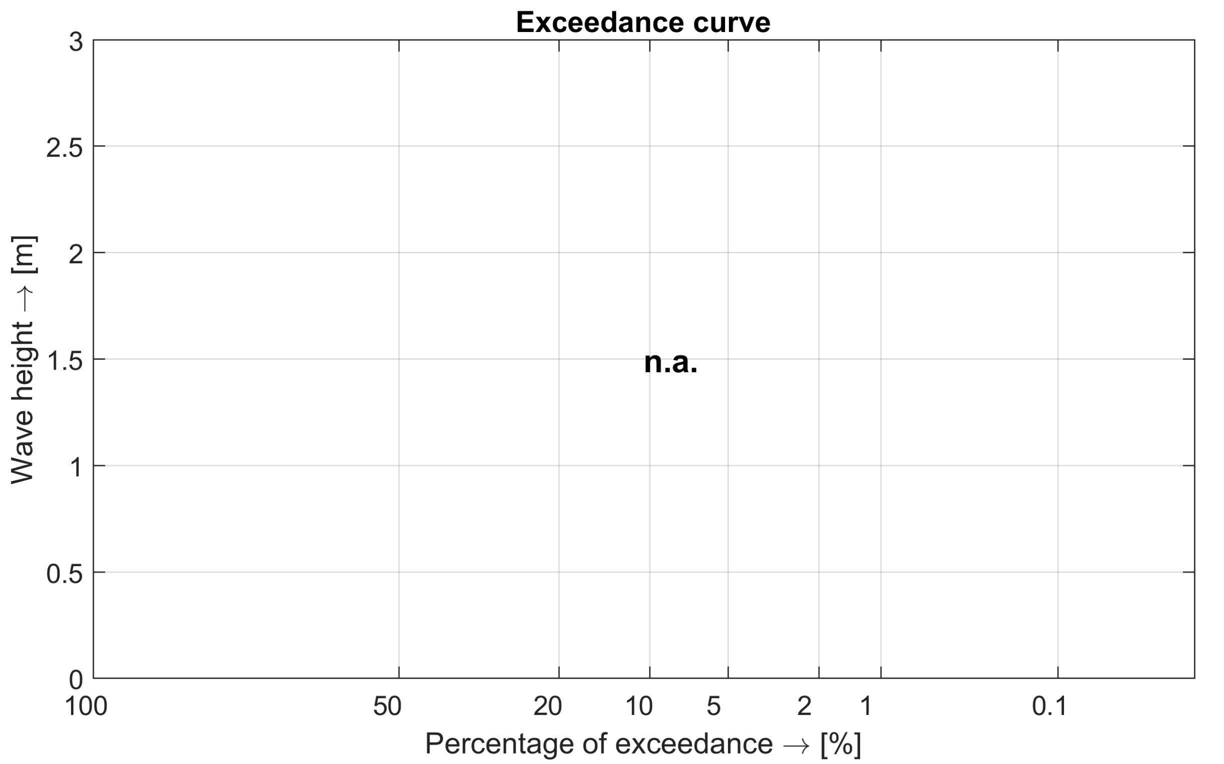

Results of wave generation calibration Depth = 18.0 m, H = 0.50 m, T = 16.20 s	Monochromatic	M162a
Deltares	11202696	App. E.3.04

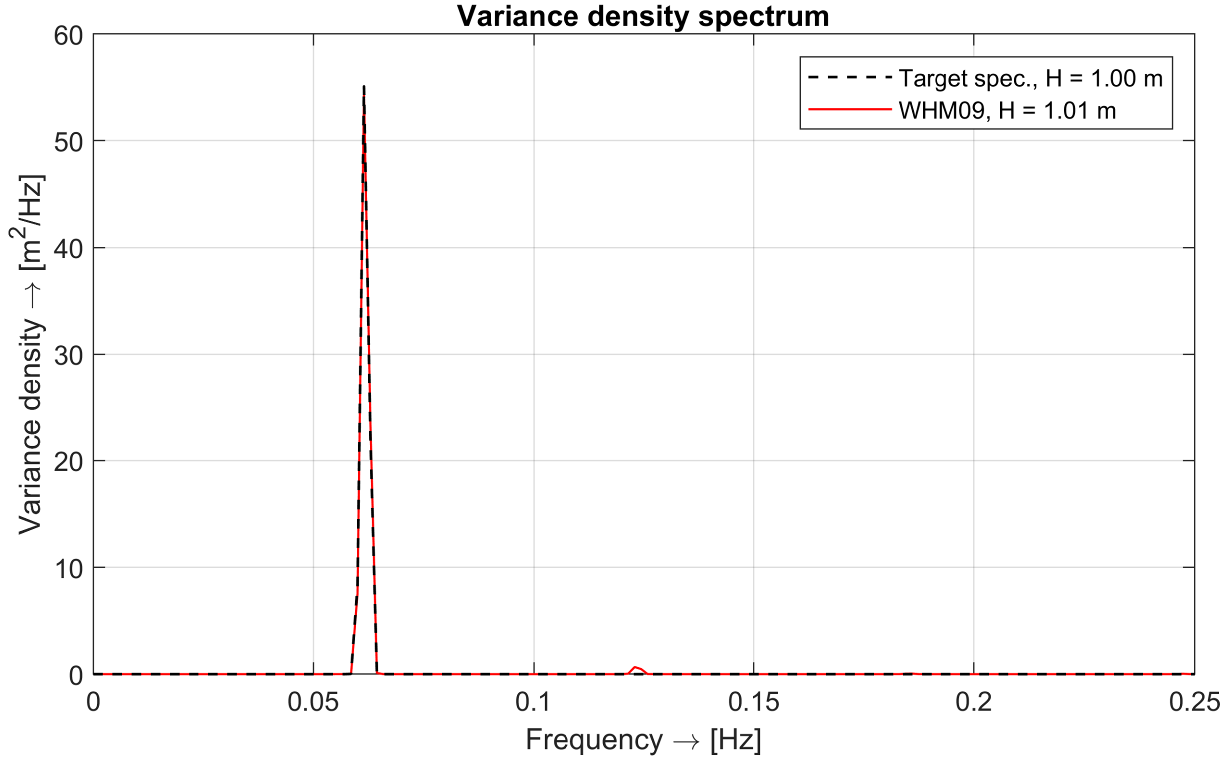

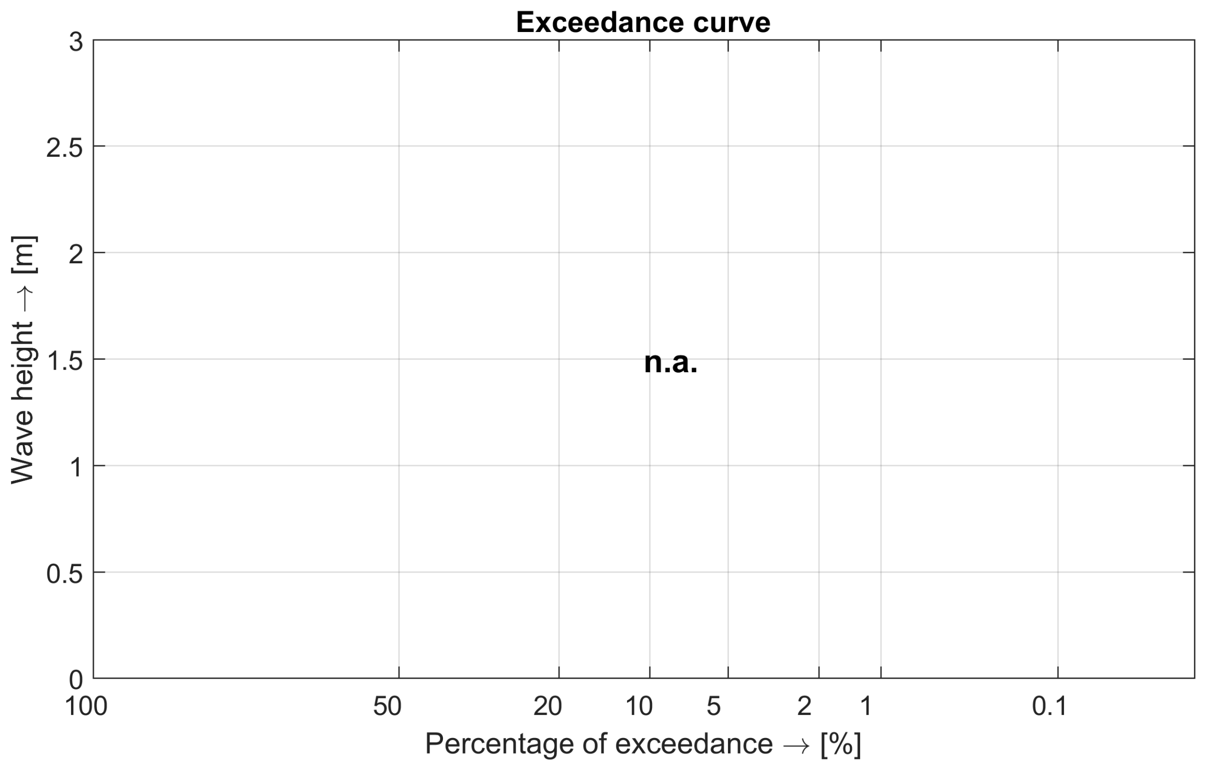

Results of wave generation calibration Depth = 18.0 m, H = 1.00 m, T = 16.20 s	Monochromatic	M162b
Deltares	11202696	App. E.3.05

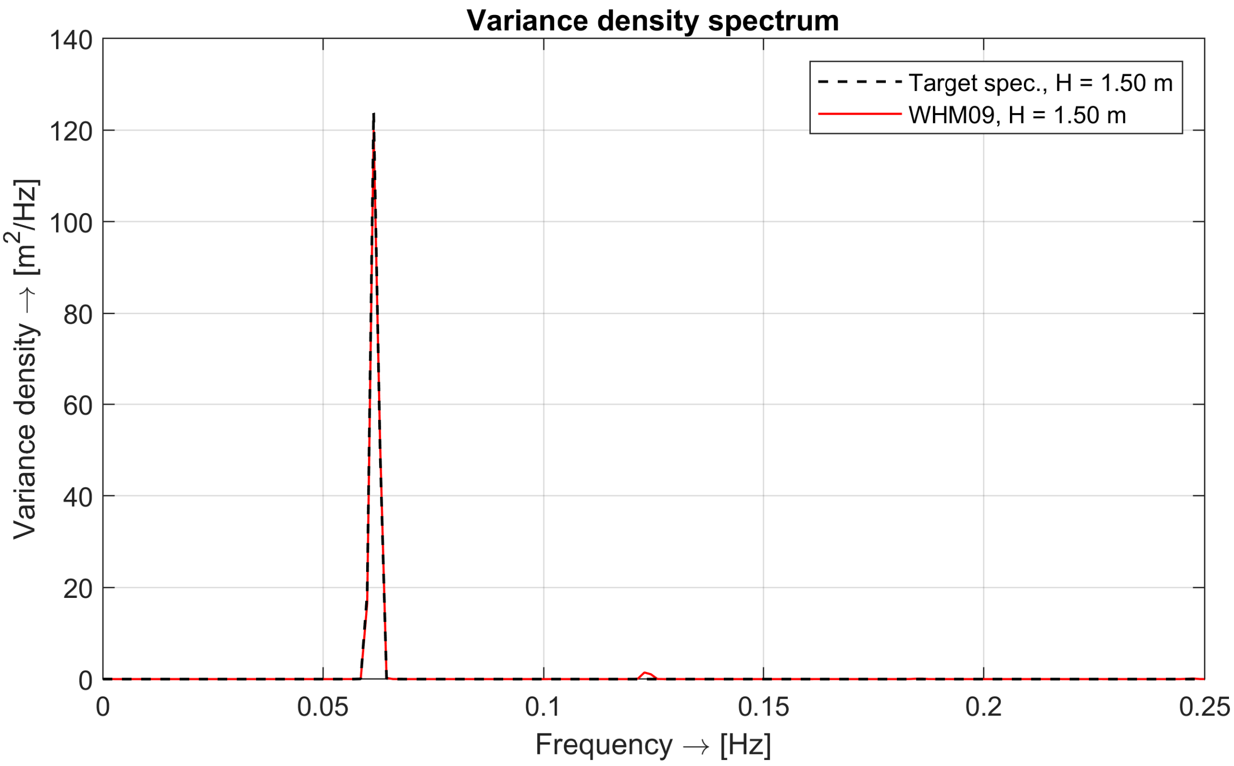

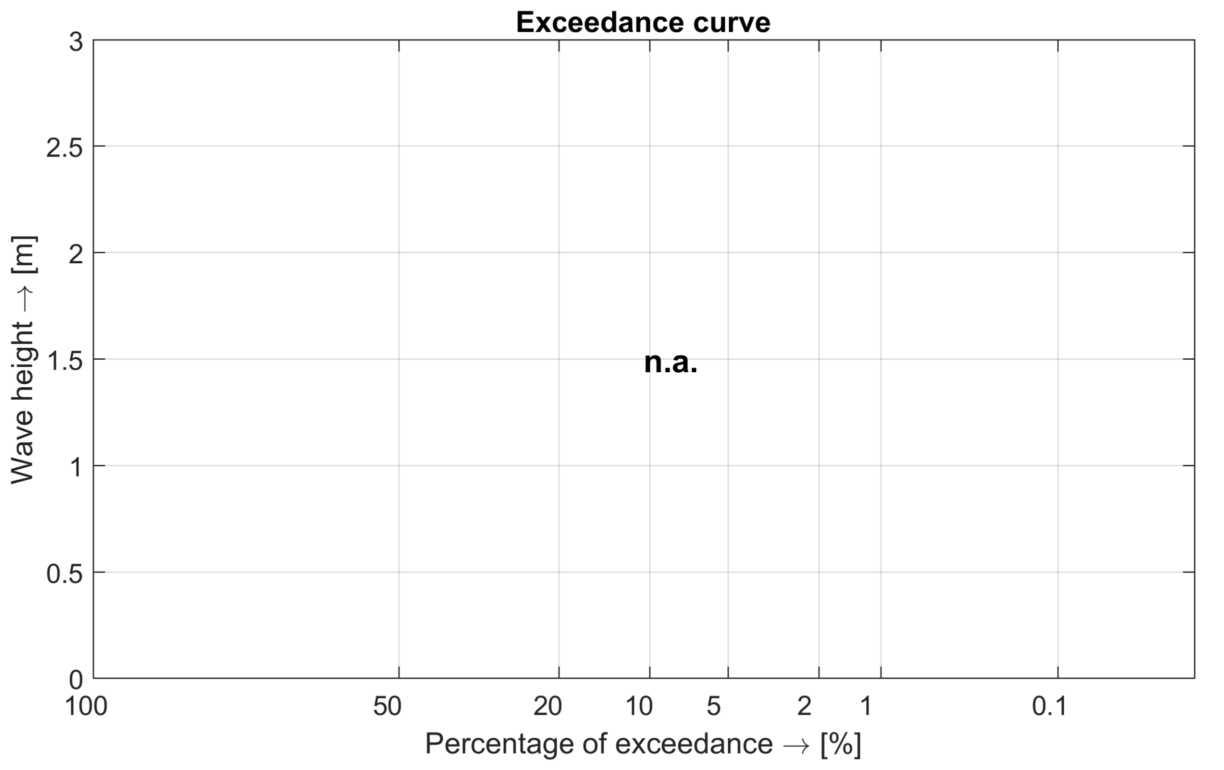

Results of wave generation calibration Depth = 18.0 m, H = 1.50 m, T = 16.20 s	Monochromatic	M162c
Deltares	11202696	App. E.3.06

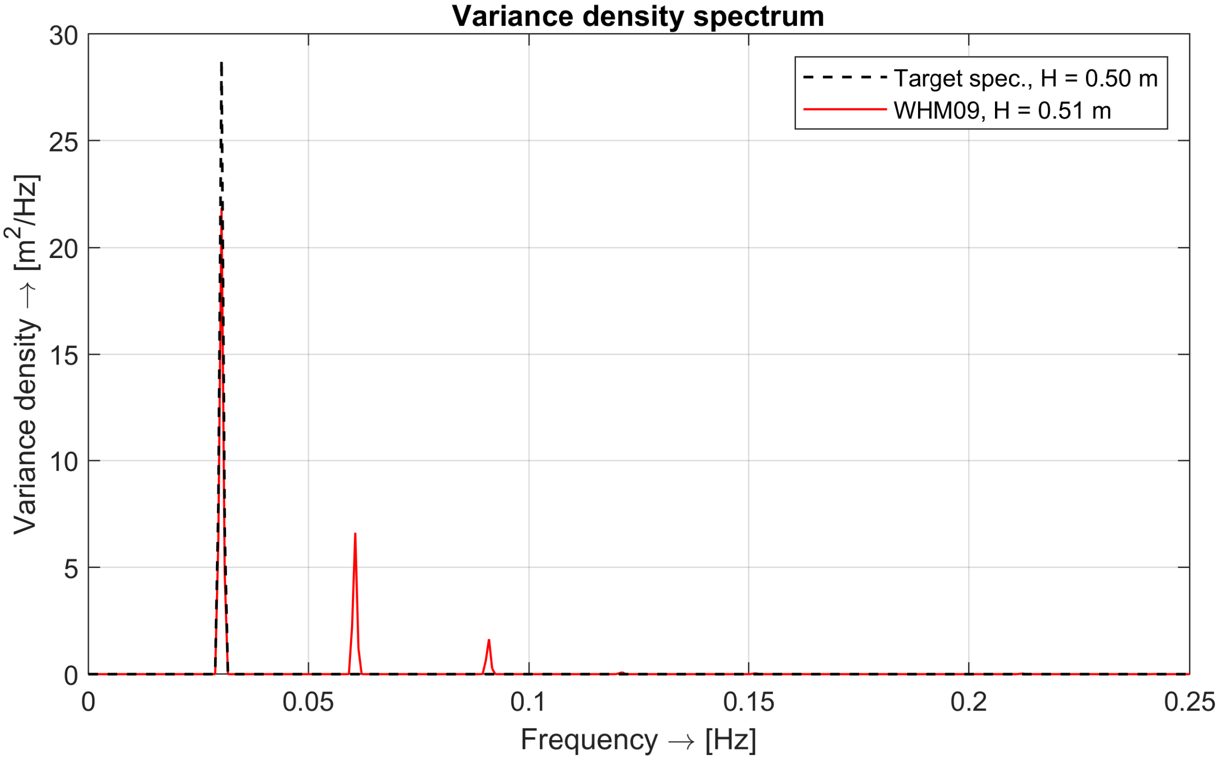

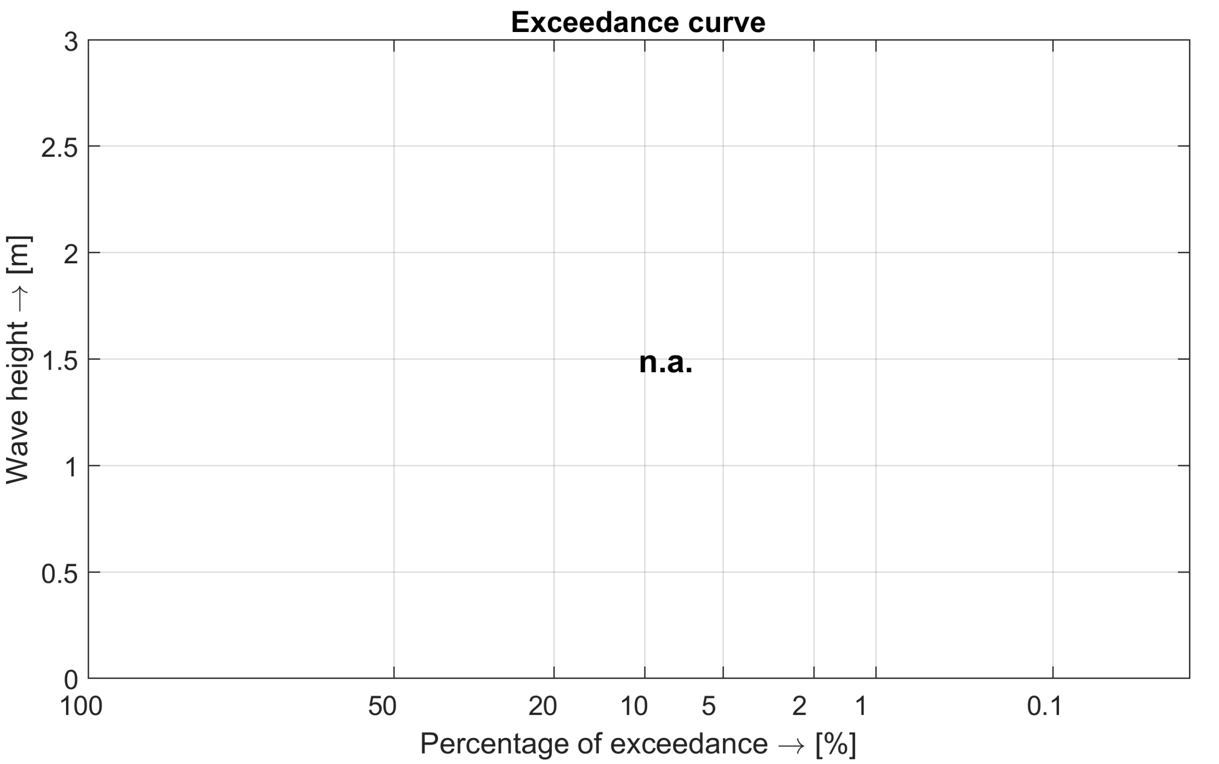

Results of wave generation calibration Depth = 18.0 m, H = 0.50 m, T = 33.00 s	Monochromatic	M330a
Deltares	11202696	App. E.3.07

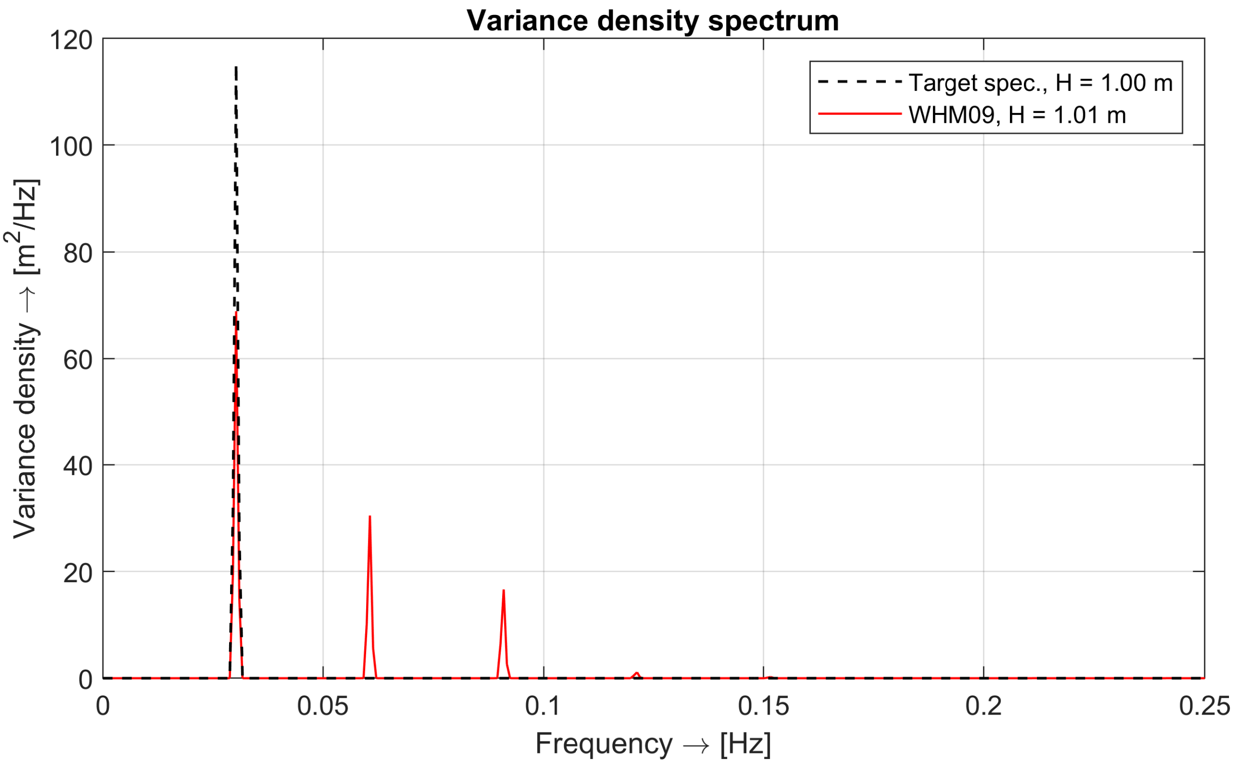

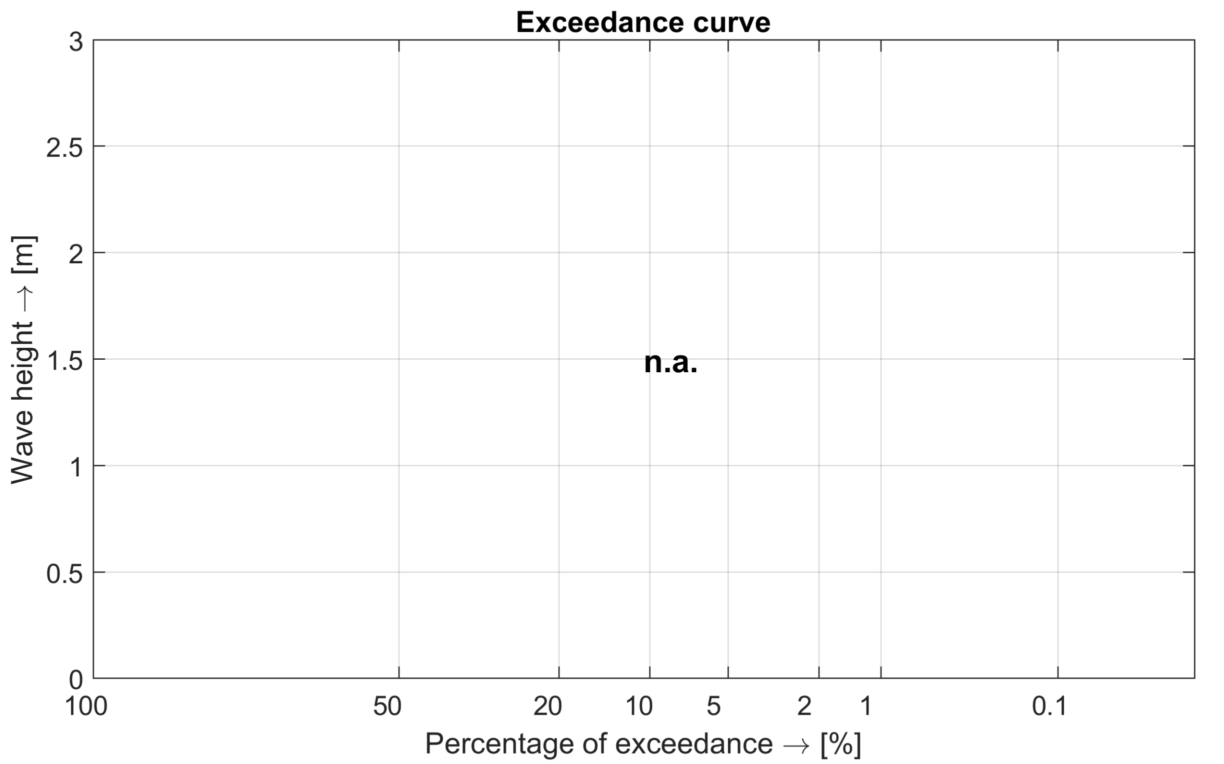

Results of wave generation calibration Depth = 18.0 m, H = 1.00 m, T = 33.00 s	Monochromatic	M330b
Deltares	11202696	App. E.3.08

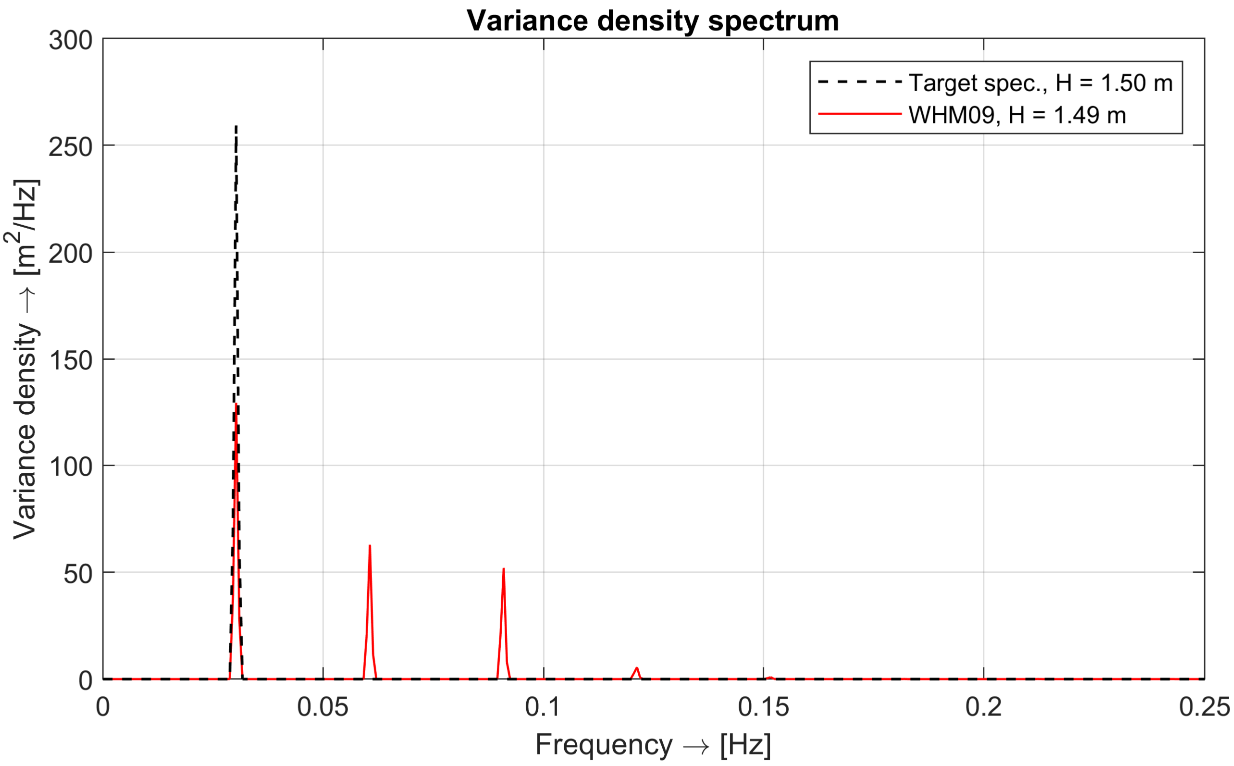

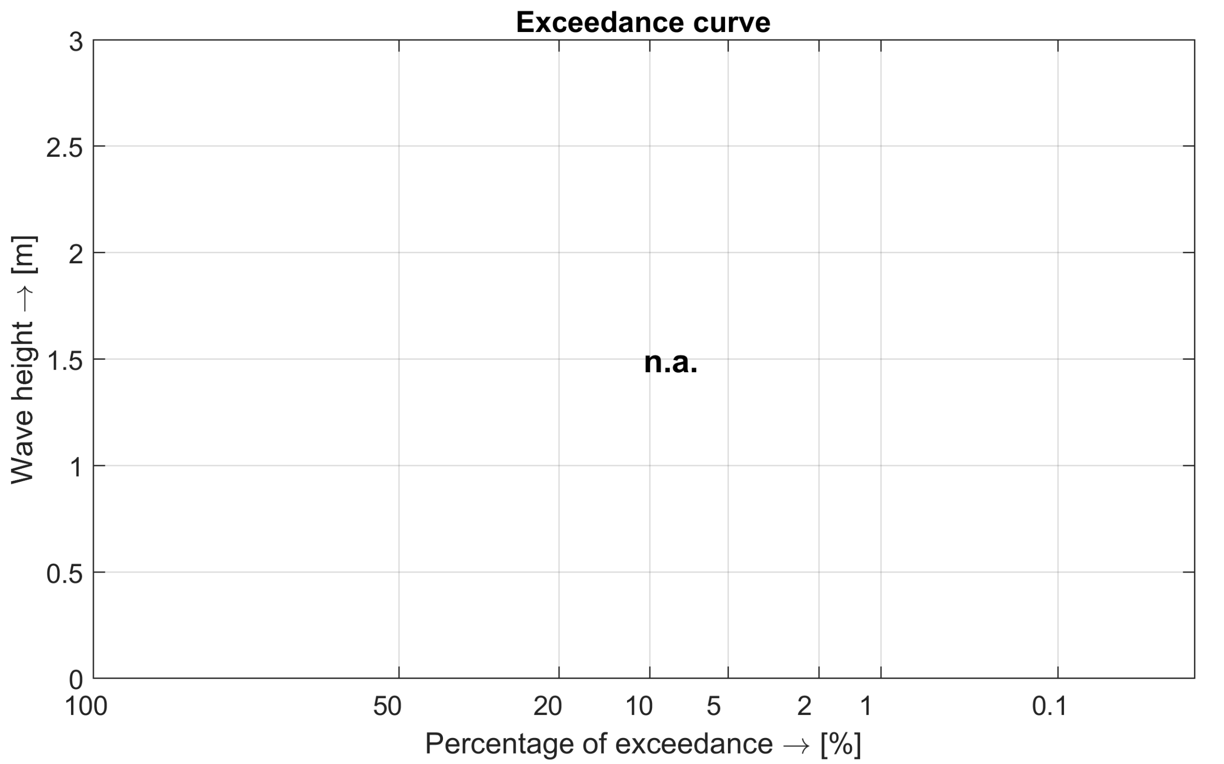

Results of wave generation calibration Depth = 18.0 m, H = 1.50 m, T = 33.00 s	Monochromatic	M330c
Deltares	11202696	App. E.3.09

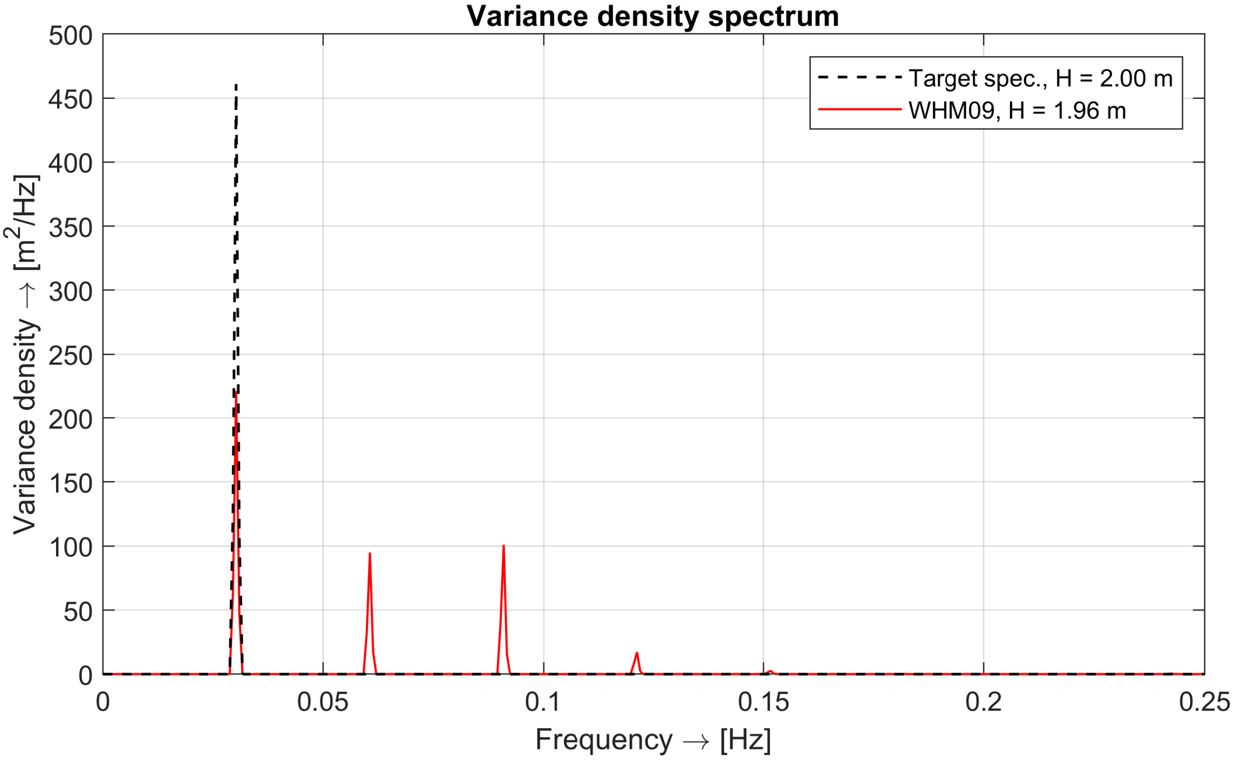

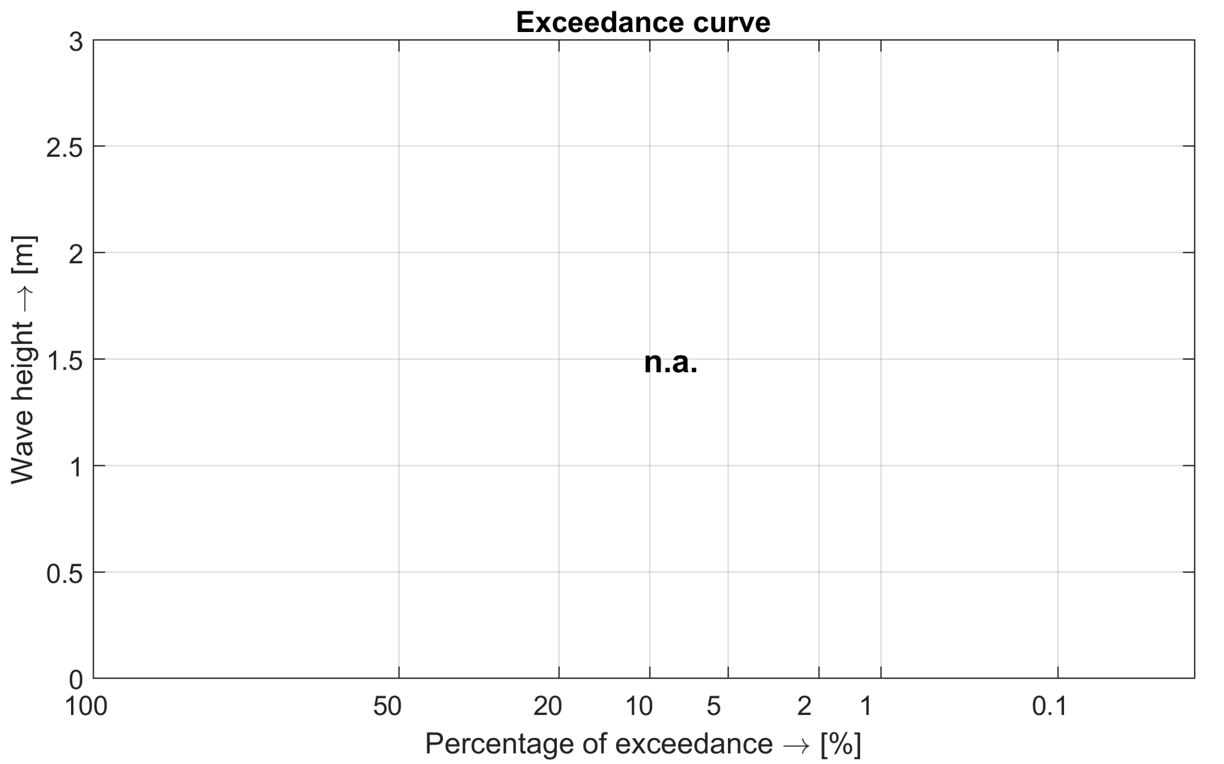

Results of wave generation calibration Depth = 18.0 m, H = 2.00 m, T = 33.00 s	Monochromatic	M330d
Deltares	11202696	App. E.3.10

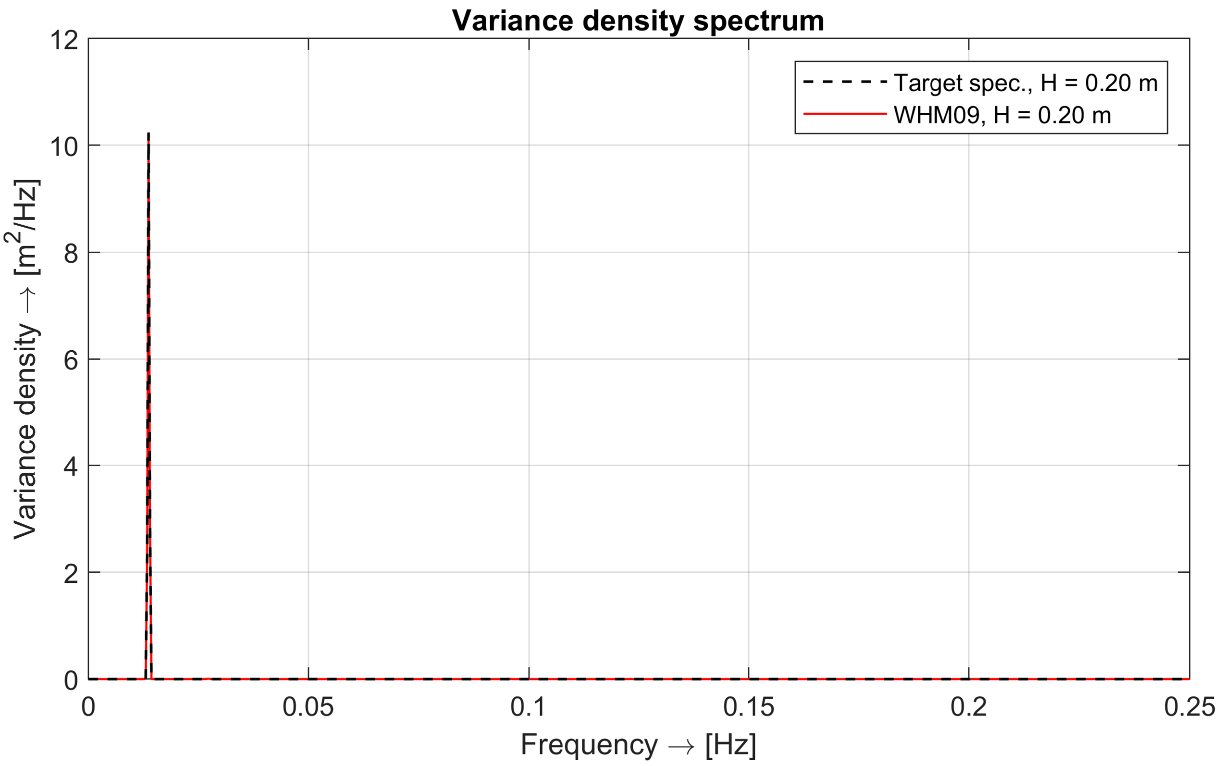

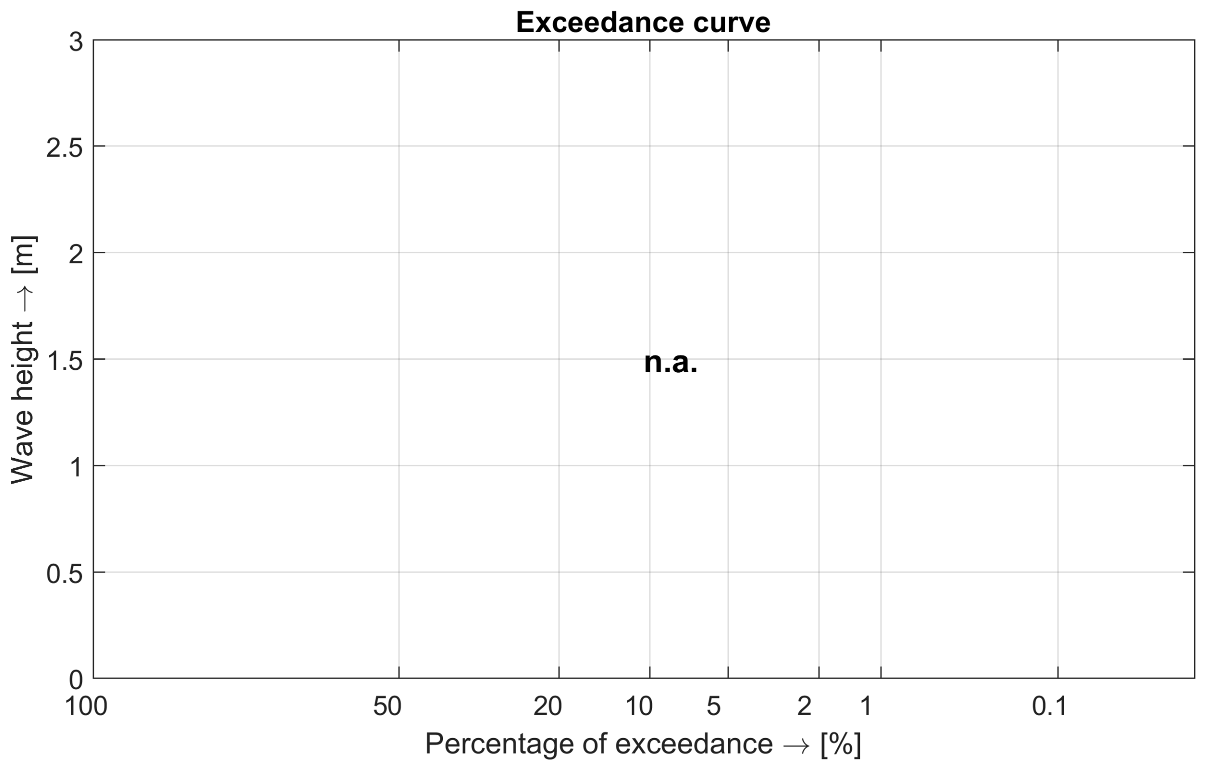

Results of wave generation calibration Depth = 18.0 m, H = 0.20 m, T = 73.12 s	Monochromatic	M7312a
Deltares	11202696	App. E.3.11

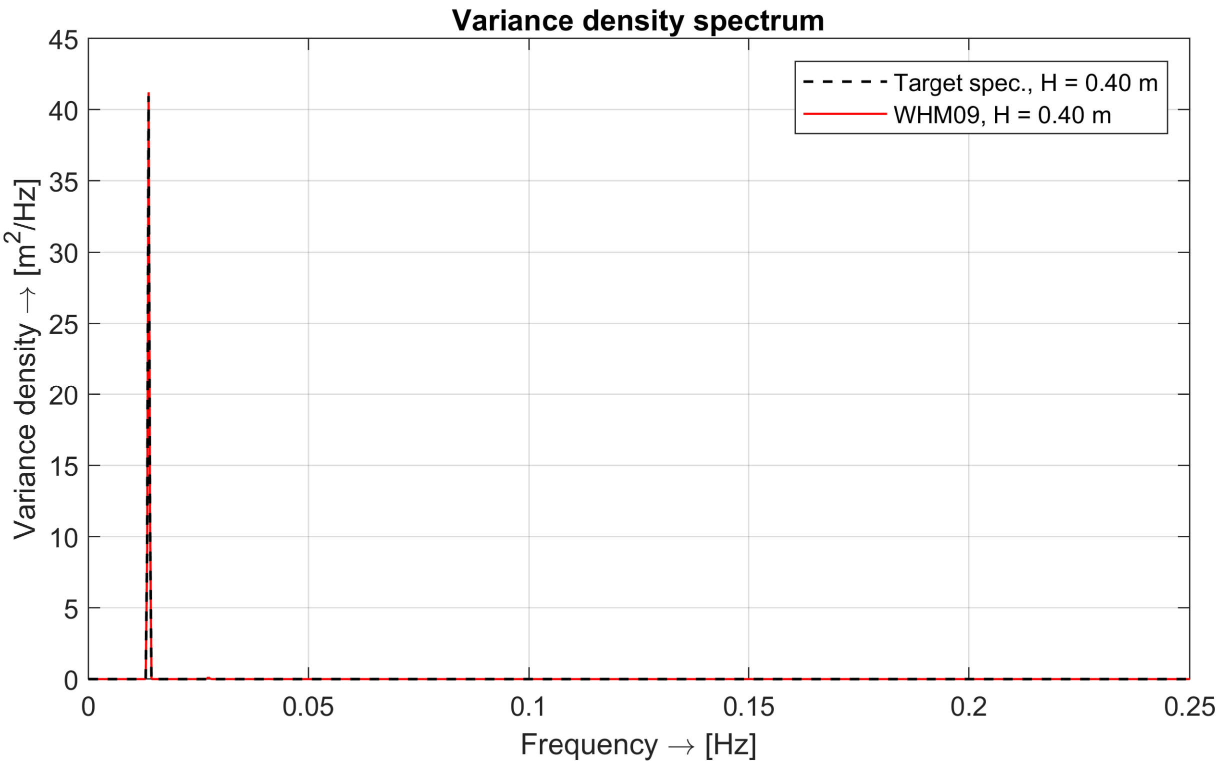

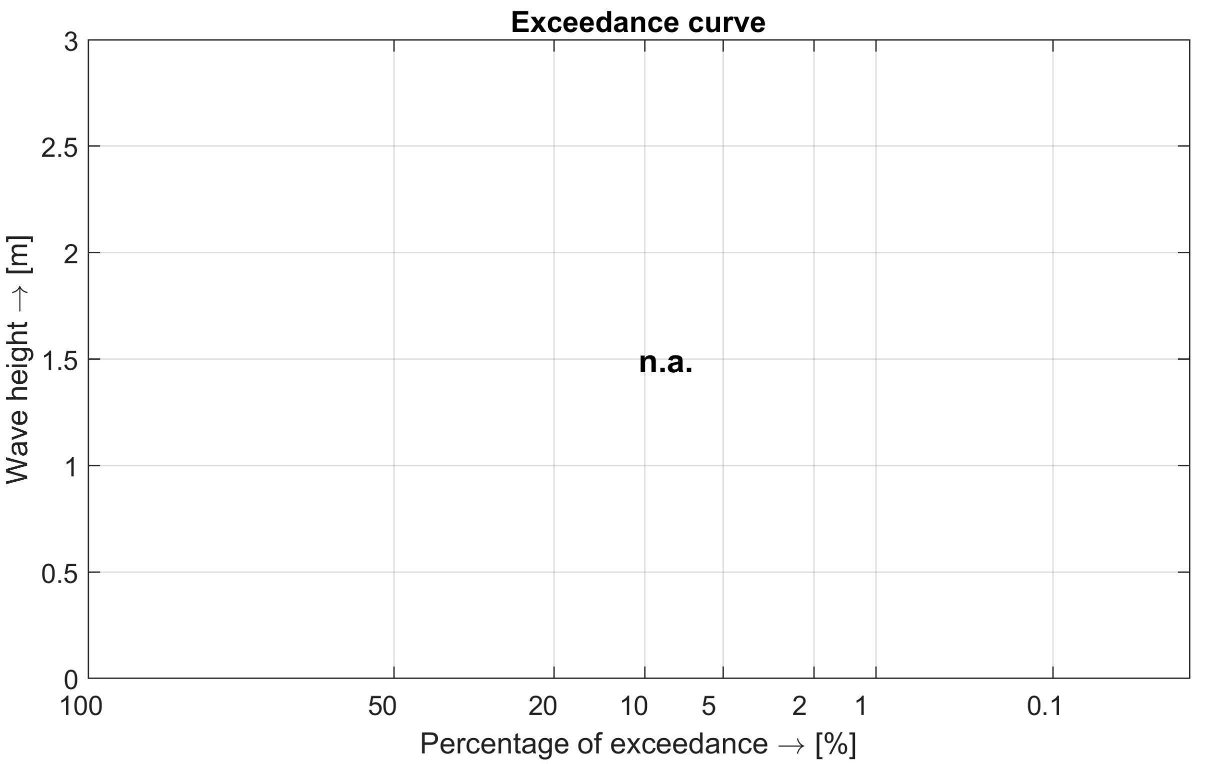

Results of wave generation calibration Depth = 18.0 m, H = 0.40 m, T = 73.12 s	Monochromatic	M7312b
Deltares	11202696	App. E.3.12

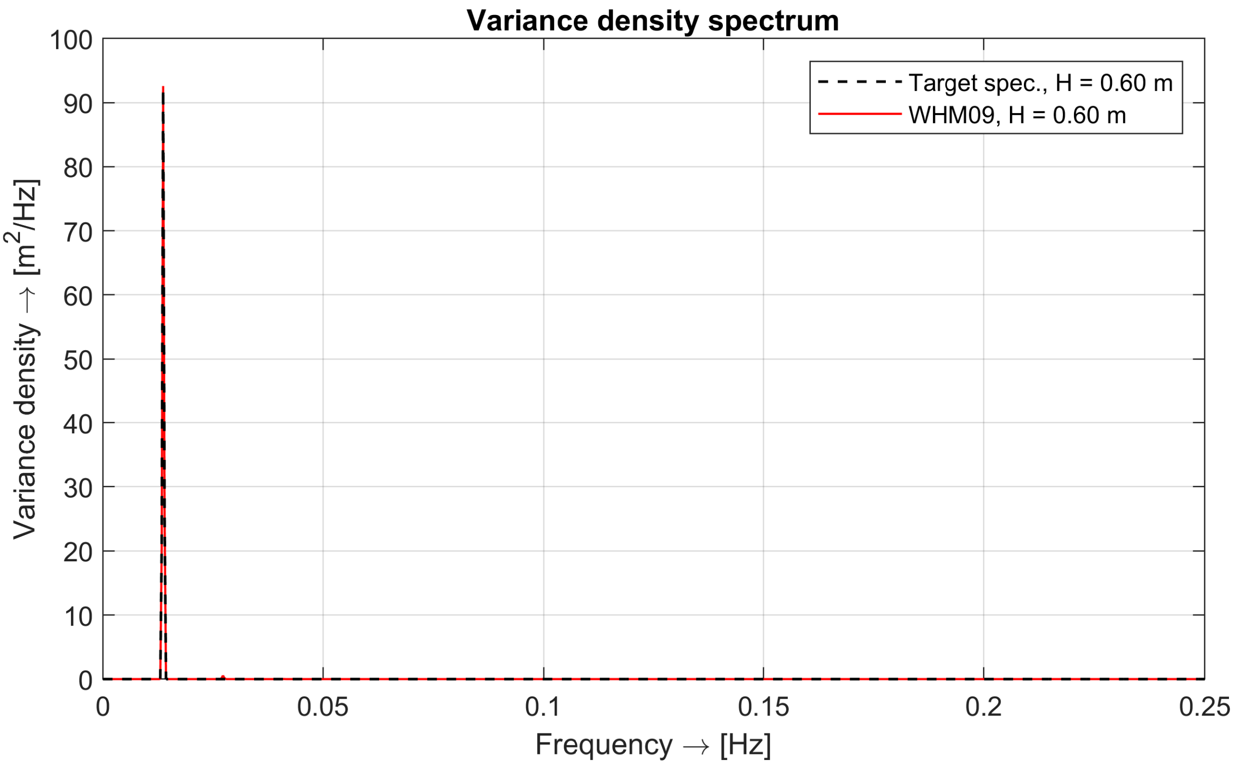

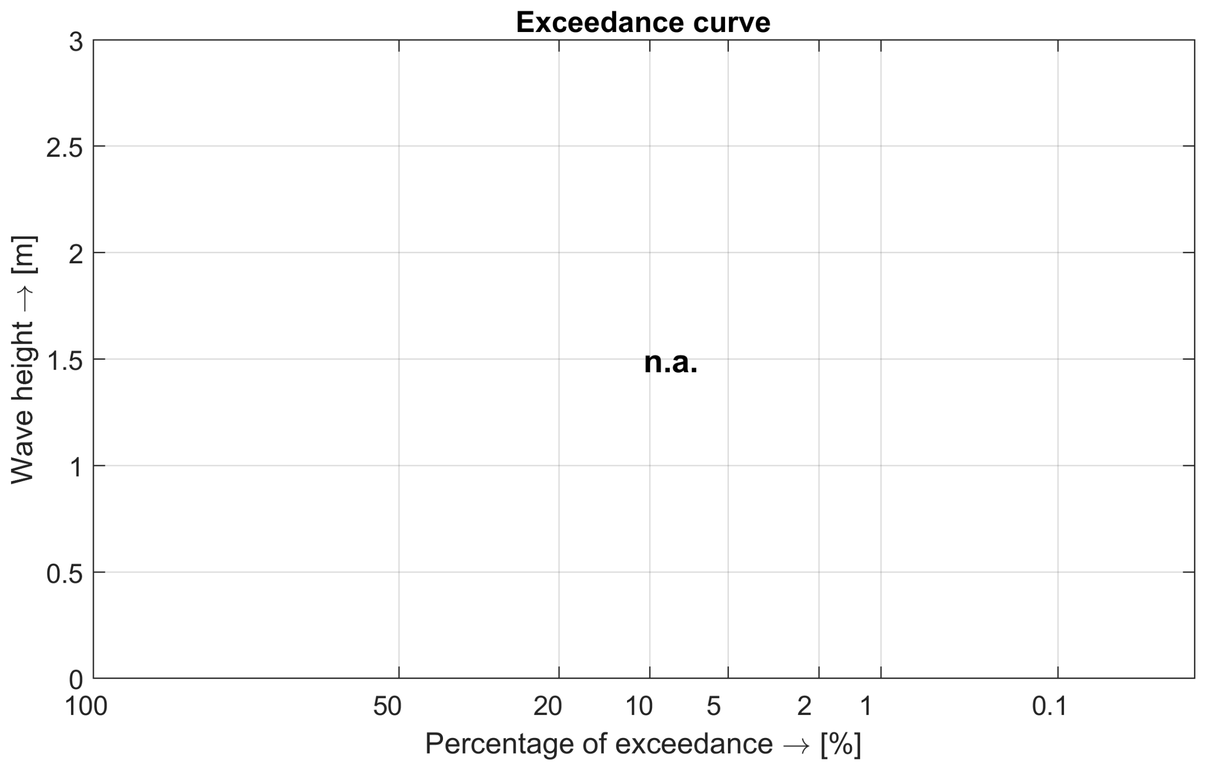

Results of wave generation calibration Depth = 18.0 m, H = 0.60 m, T = 73.12 s	Monochromatic	M7312c
Deltares	11202696	App. E.3.13

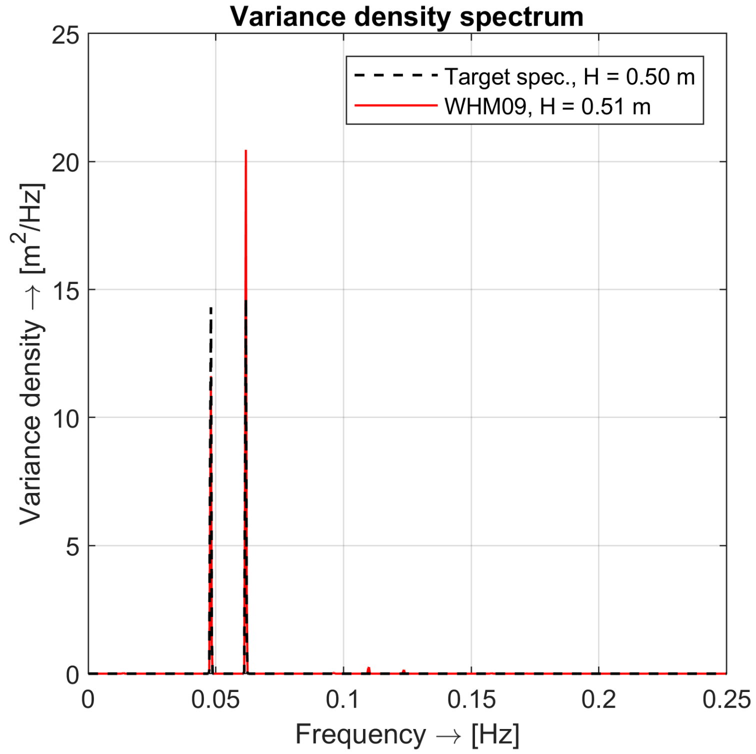

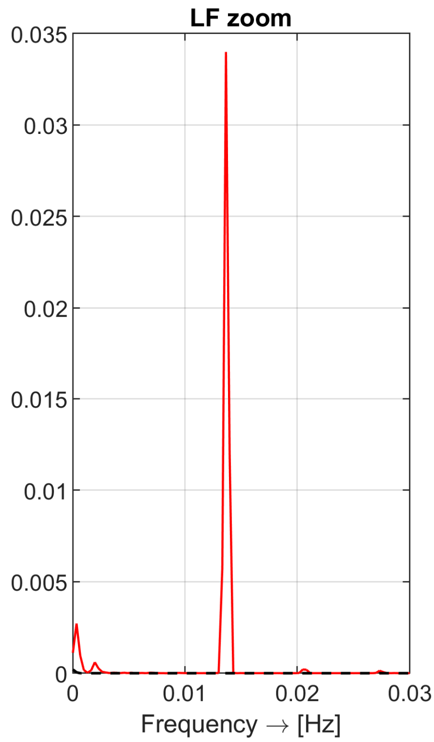

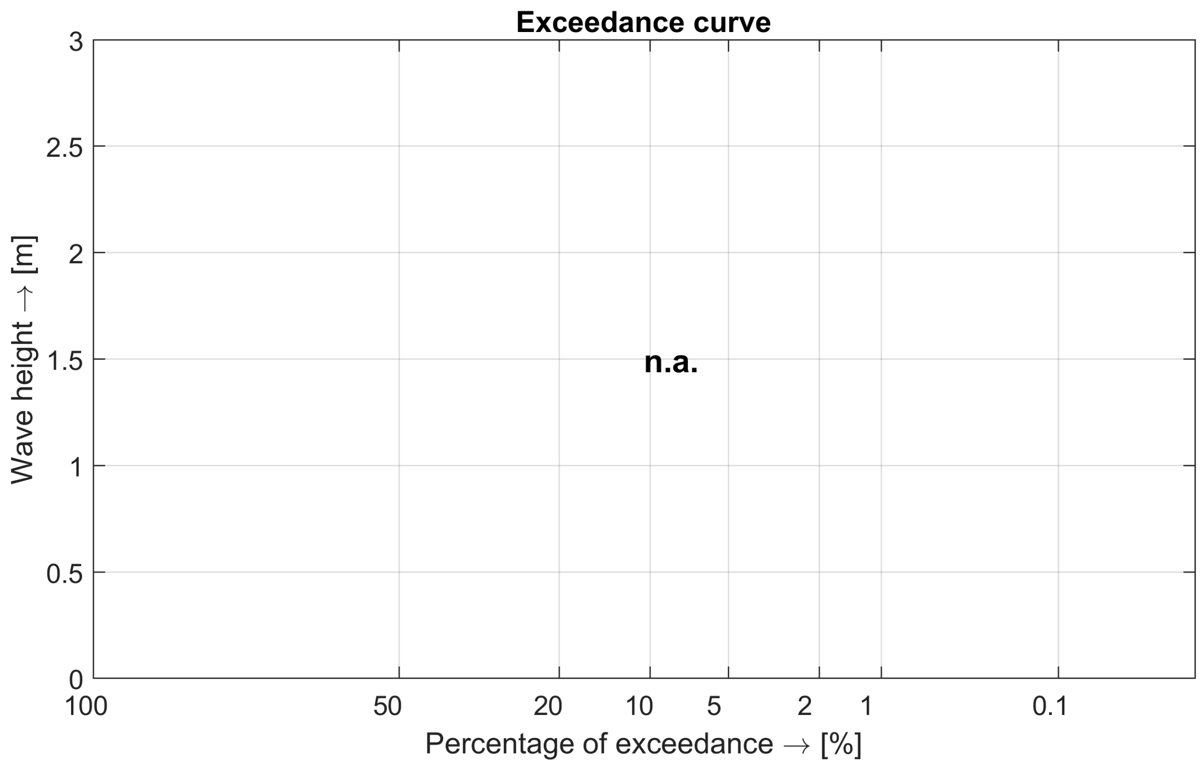

Results of wave generation calibration Depth = 18.0 m, H = 0.50 m, T_1 = 16.20 s, T_2 = 20.81 s	Bichromatic	B7312a
Deltares	11202696	App. E.3.14

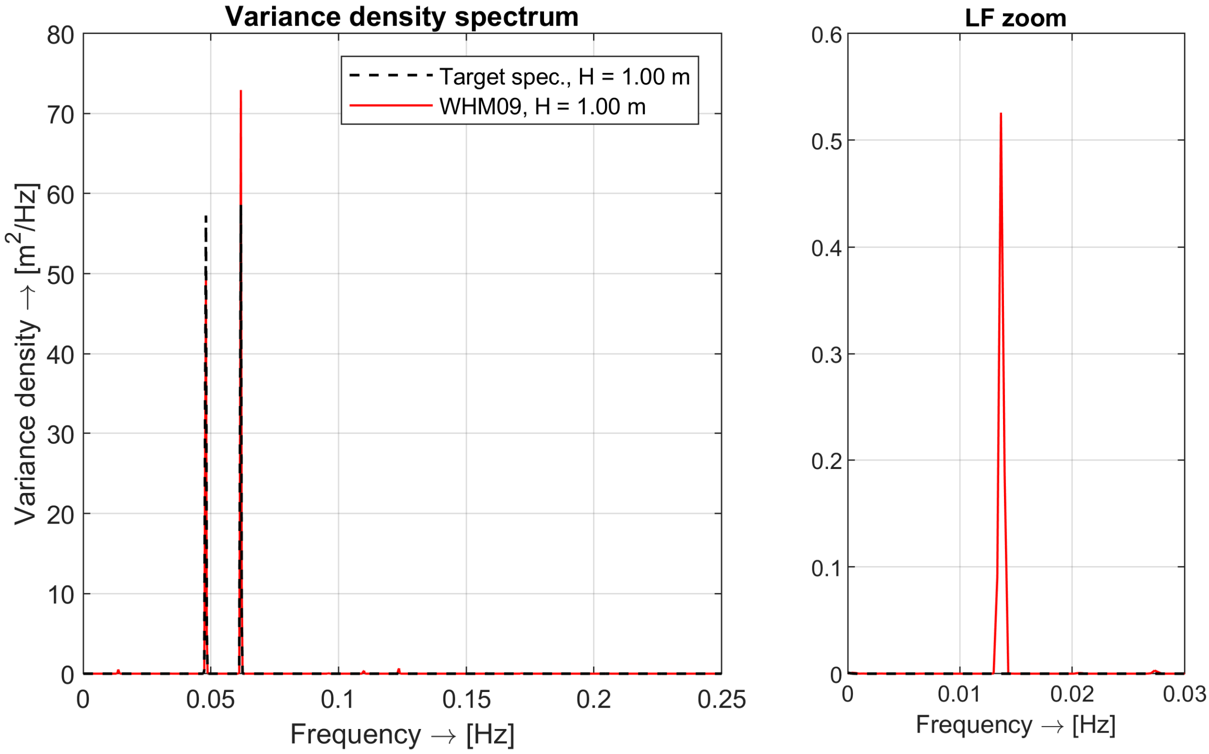

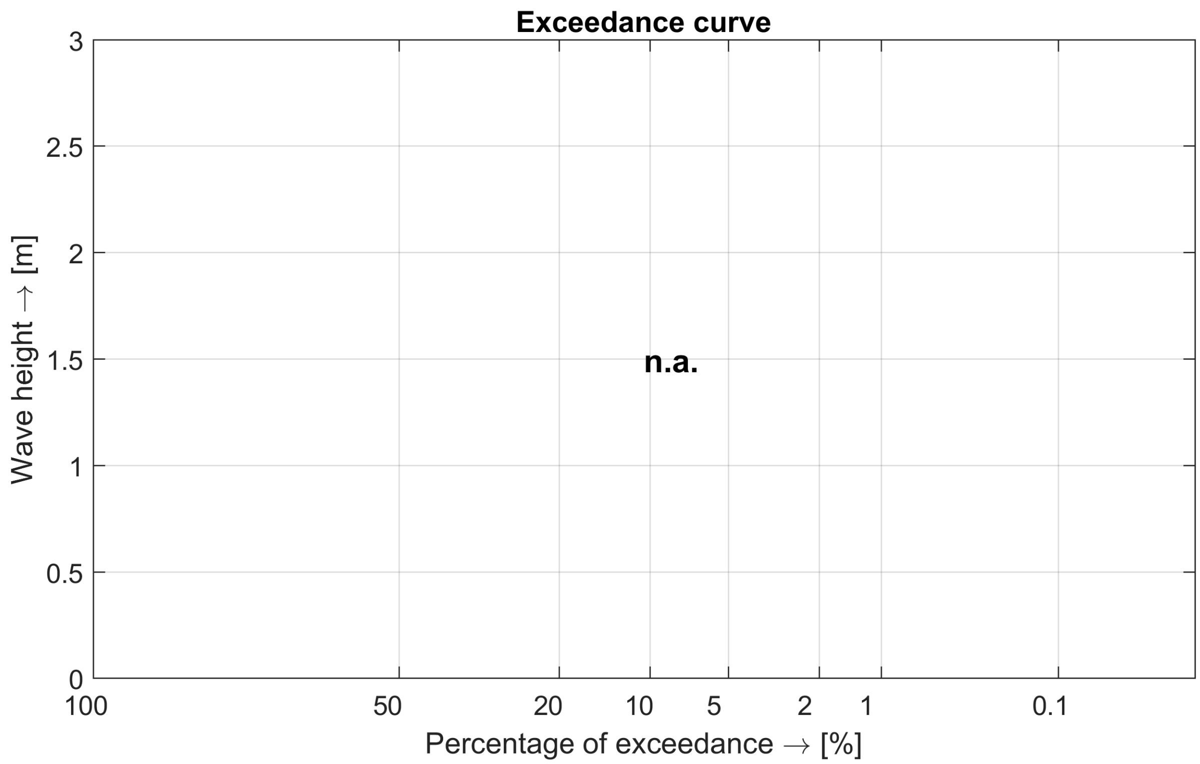

Results of wave generation calibration Depth = 18.0 m, H = 1.00 m, T_1 = 16.20 s, T_2 = 20.81 s	Bichromatic	B7312b
Deltares	11202696	App. E.3.15

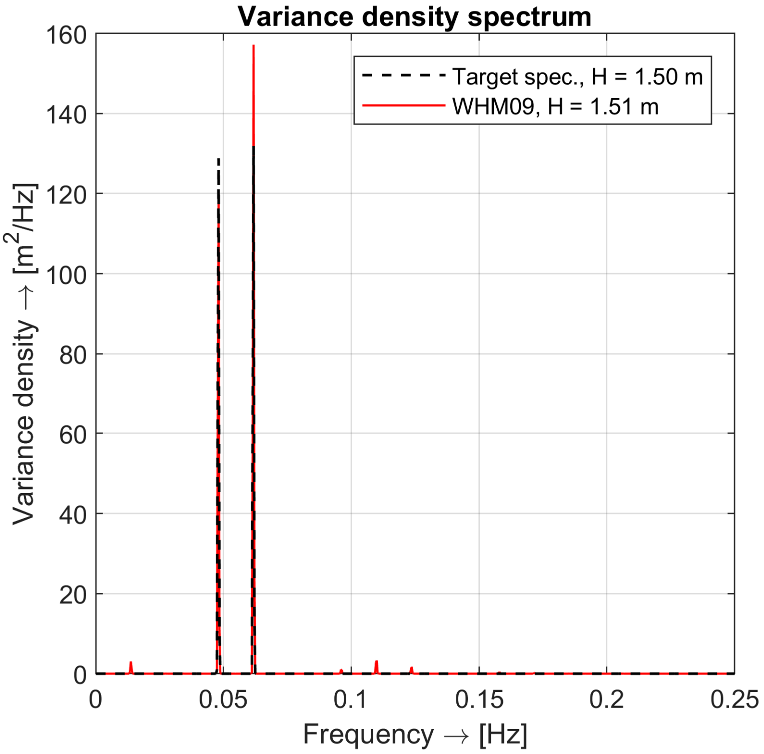

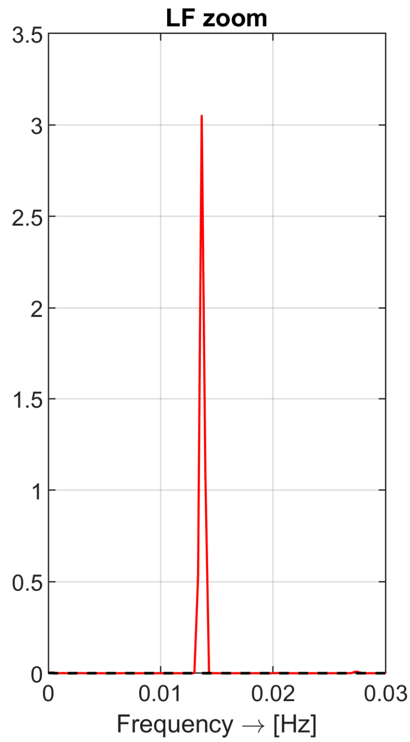

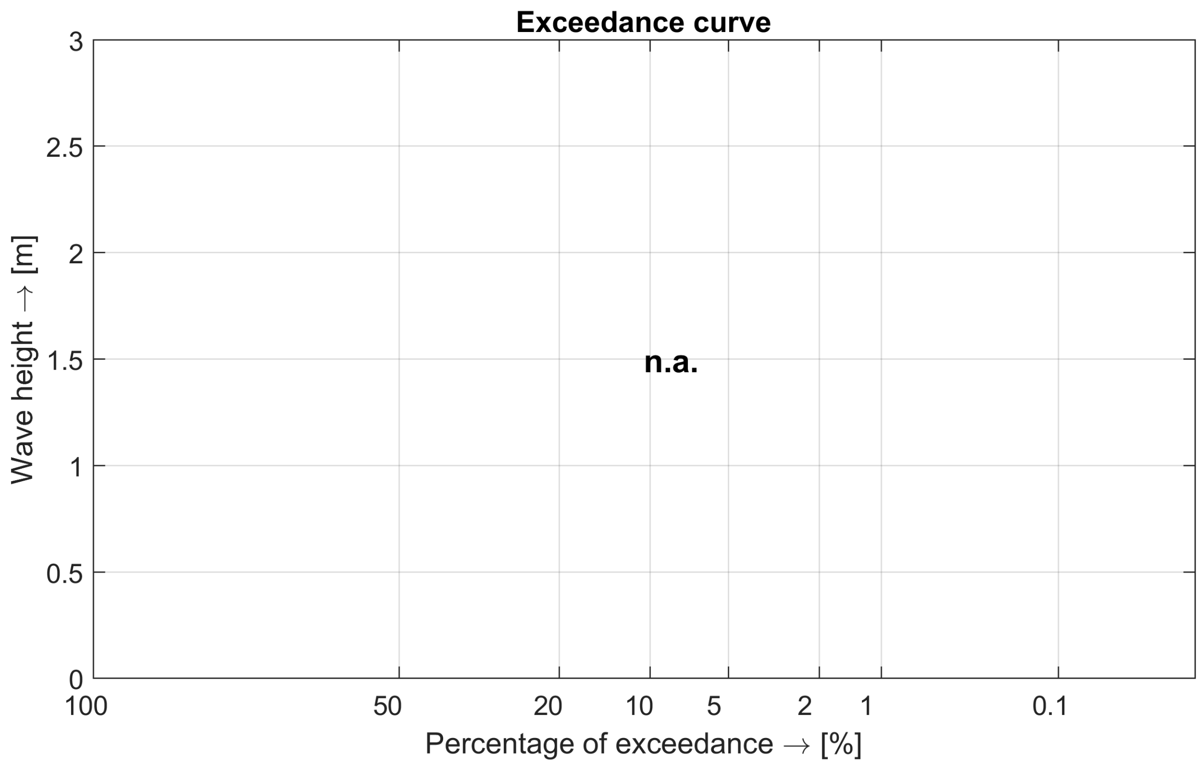

Results of wave generation calibration Depth = 18.0 m, H = 1.50 m, T_1 = 16.20 s, T_2 = 20.81 s	Bichromatic	B7312c
Deltares	11202696	App. E.3.16

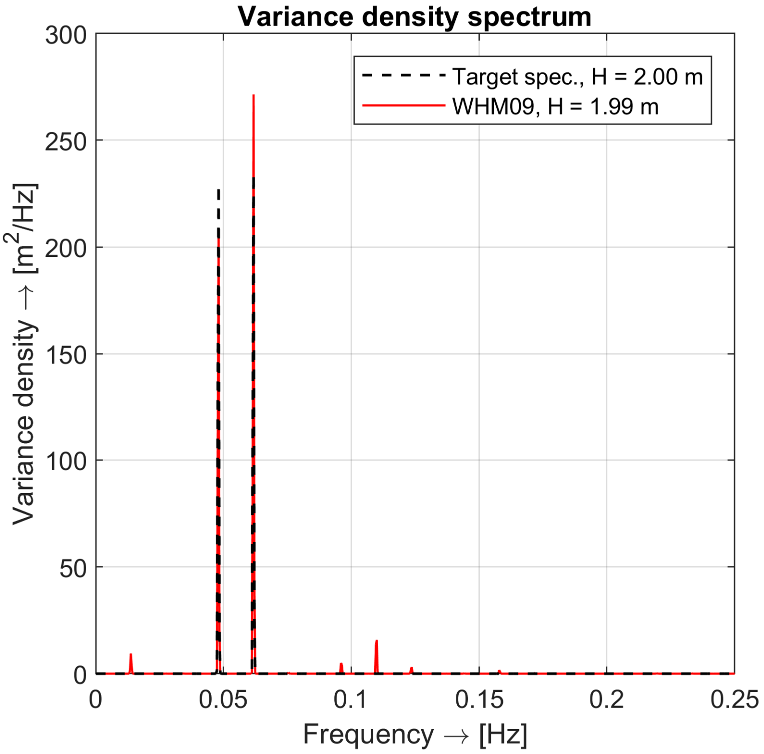

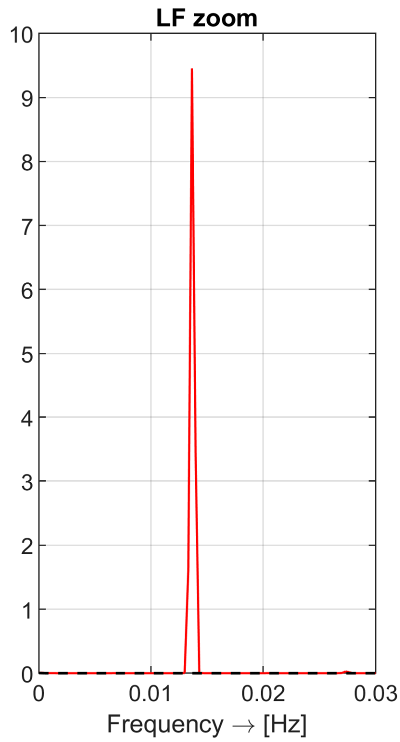

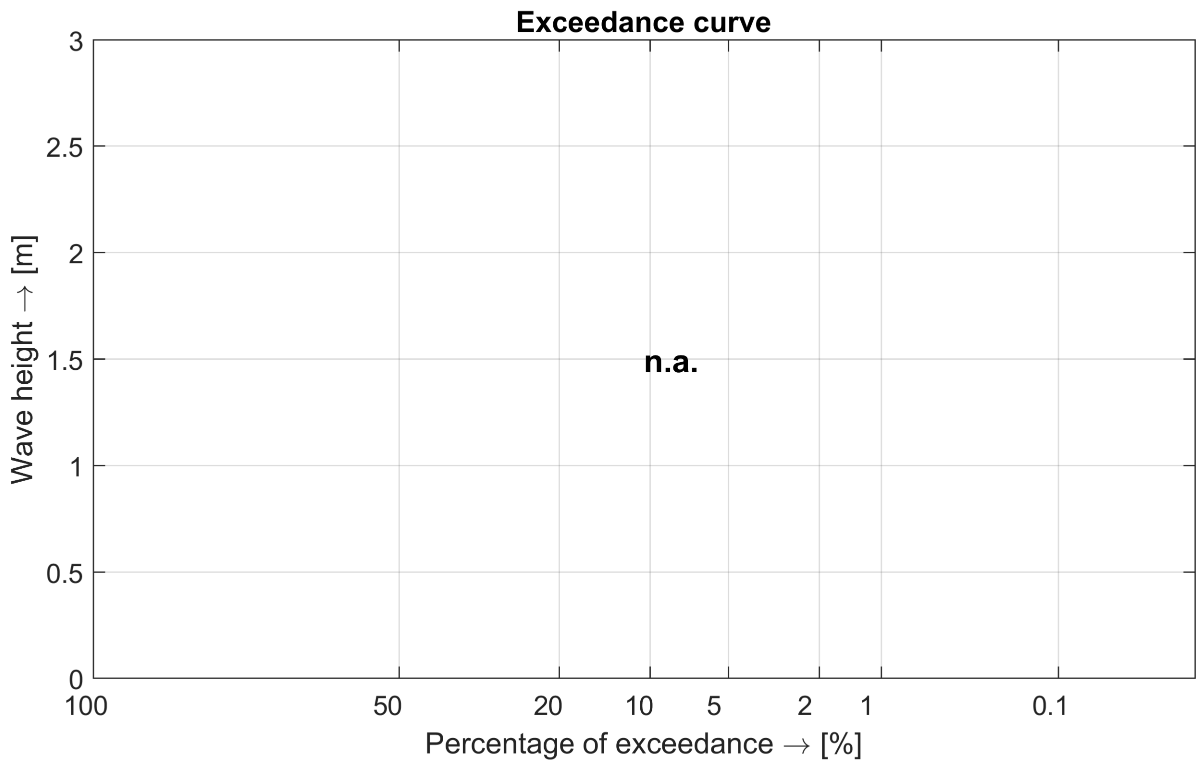

Results of wave generation calibration Depth = 18.0 m, H = 2.00 m, T_1 = 16.20 s, T_2 = 20.81 s	Bichromatic	B7312d
Deltares	11202696	App. E.3.17

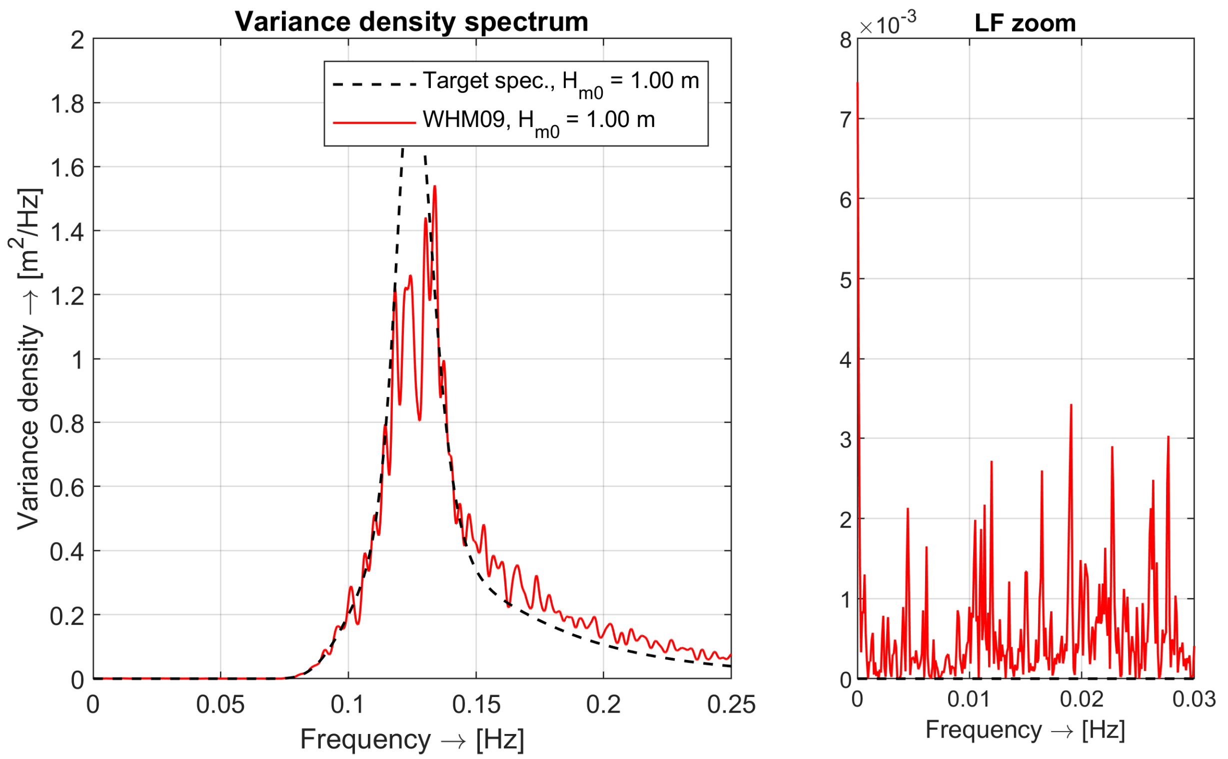

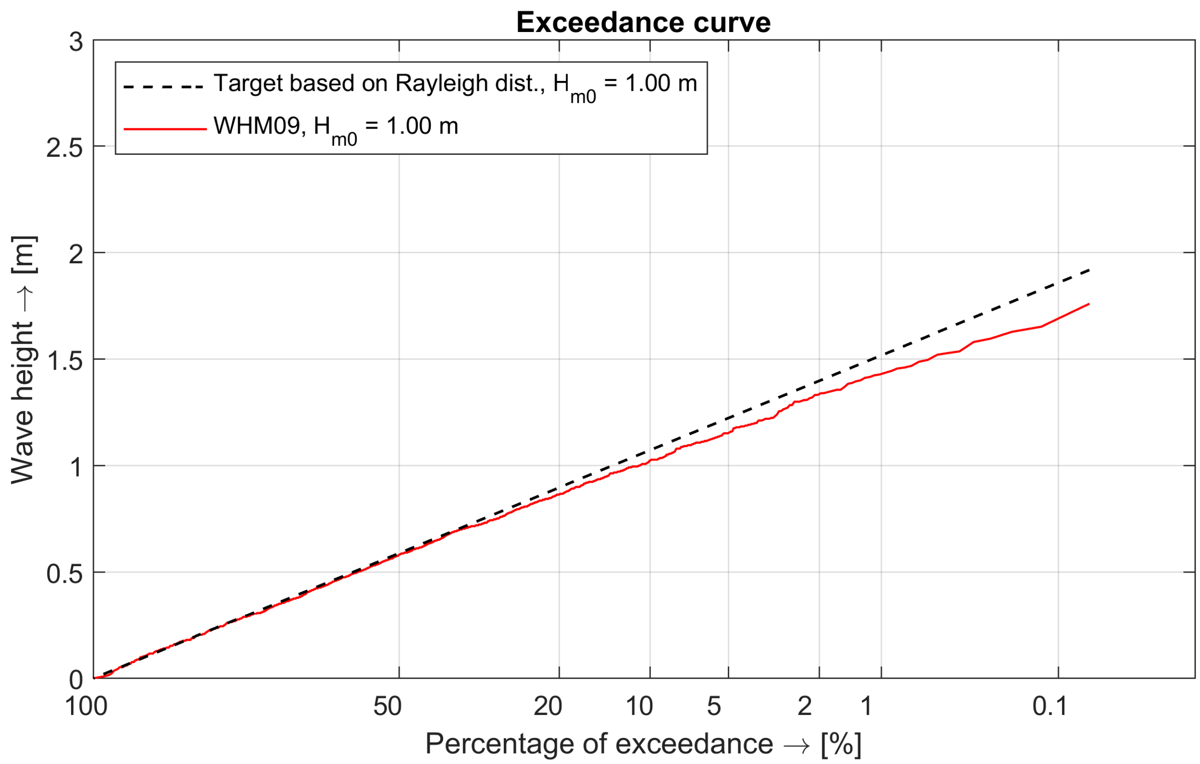

Results of wave generation calibration Depth = 18.0 m, H_{m0} = 1.00 m, T_p = 8.00 s, γ = 5.0	Irregular	I80a
Deltares	11202696	App. E.3.18

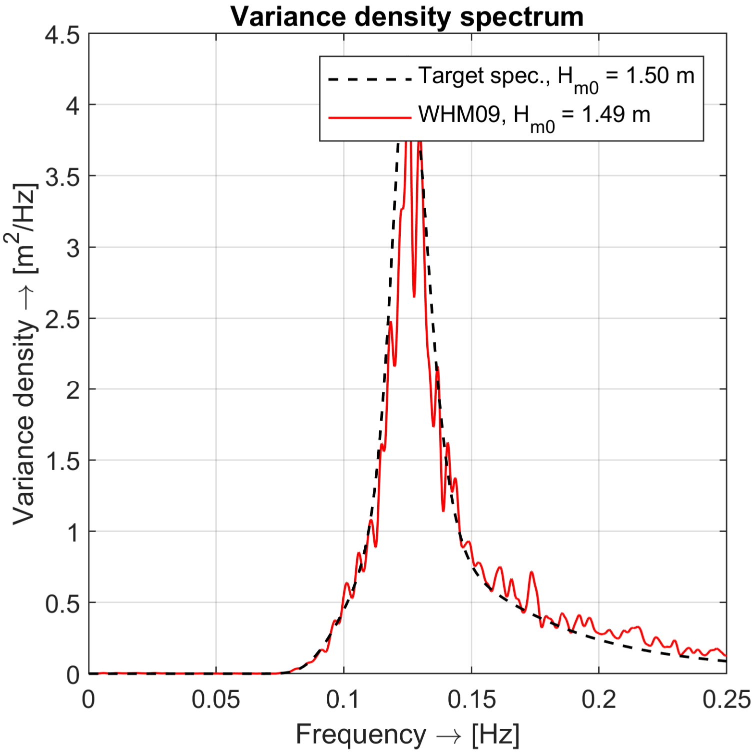

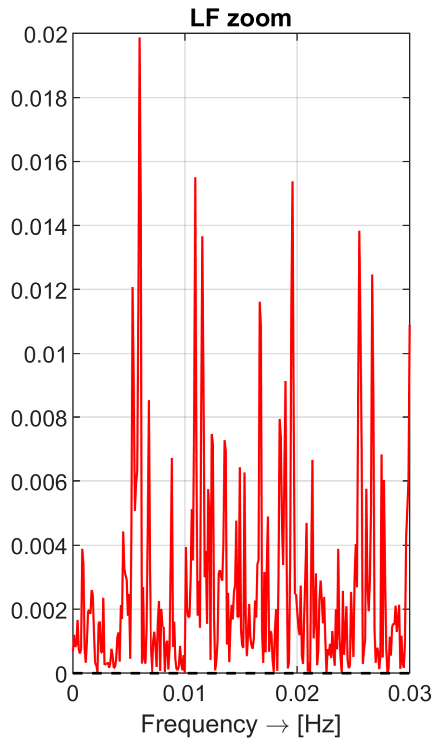

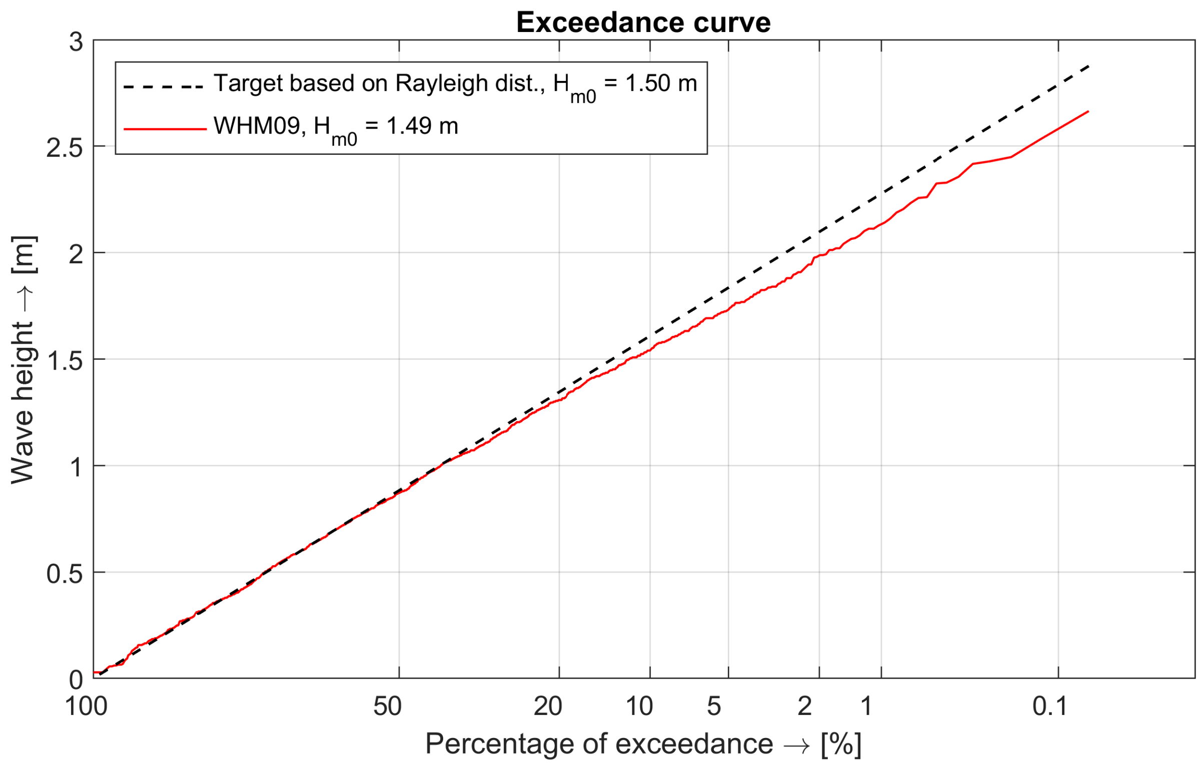

Results of wave generation calibration Depth = 18.0 m, H_{m0} = 1.50 m, T_p = 8.00 s, γ = 5.0	Irregular	I80b
Deltares	11202696	App. E.3.19

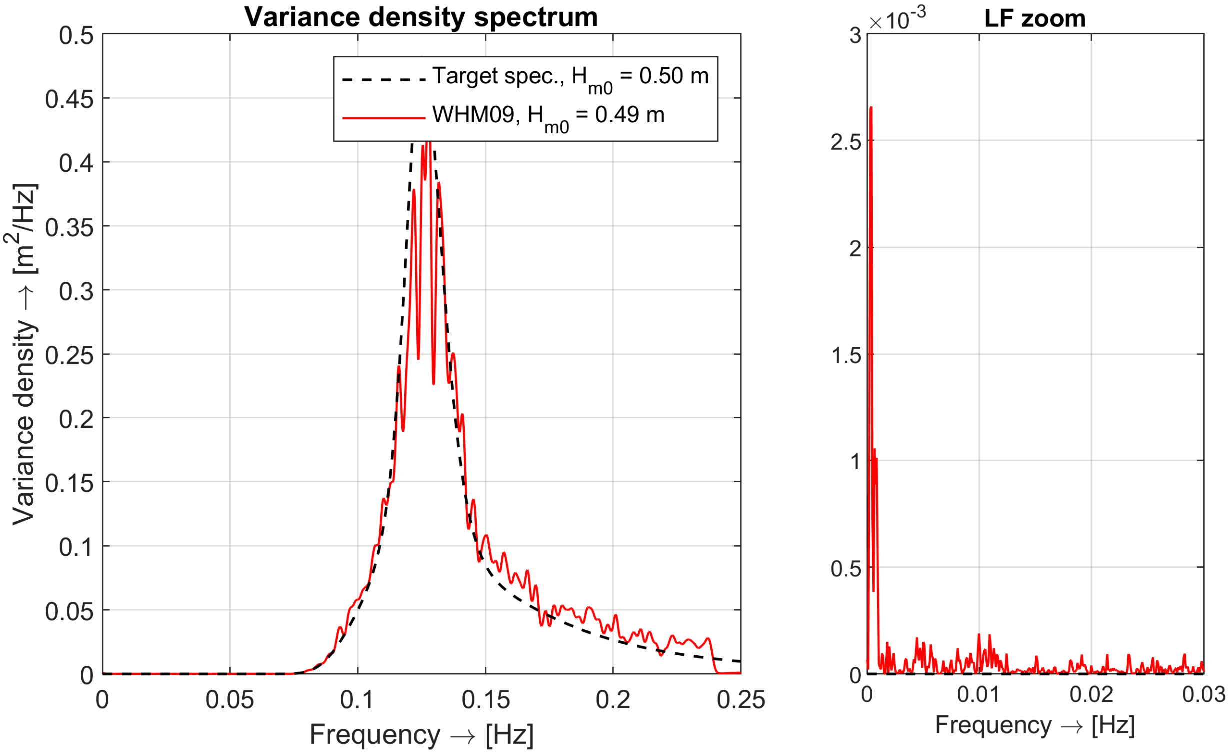

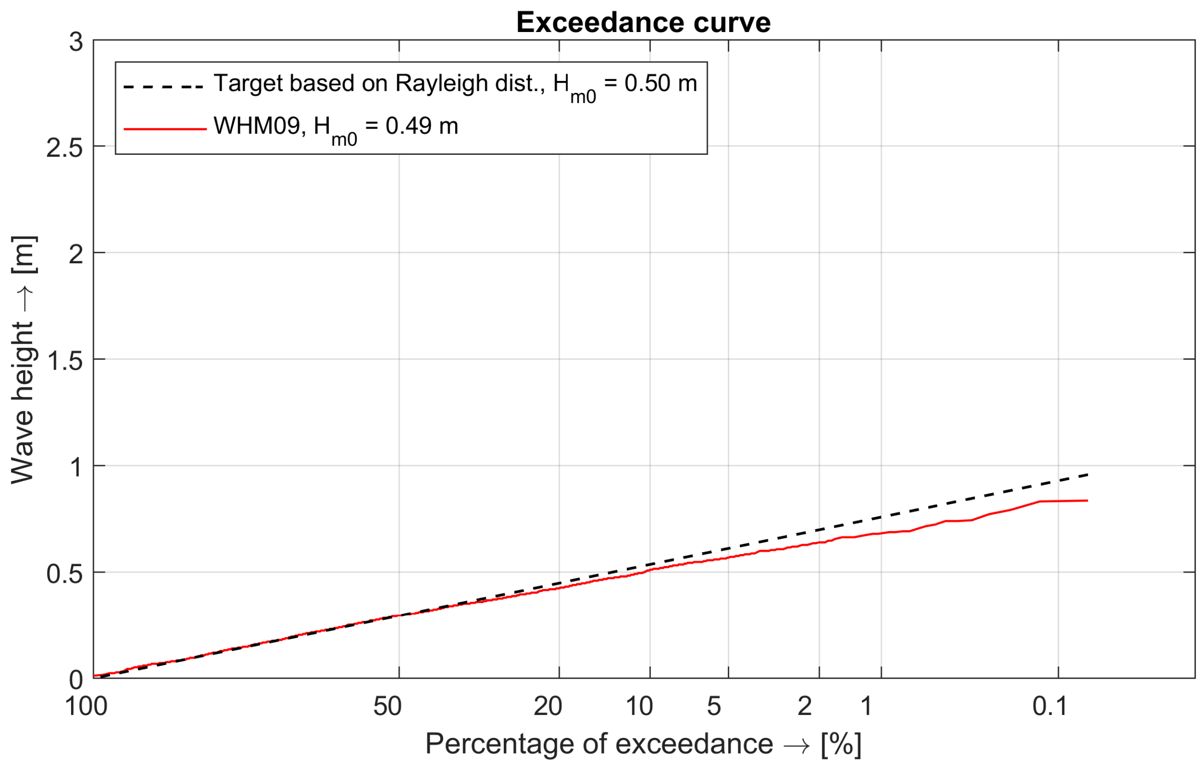

Results of wave generation calibration Depth = 18.0 m, H_{m0} = 0.50 m, T_p = 8.00 s, γ = 5.0	Irregular	I80c
Deltares	11202696	App. E.3.20

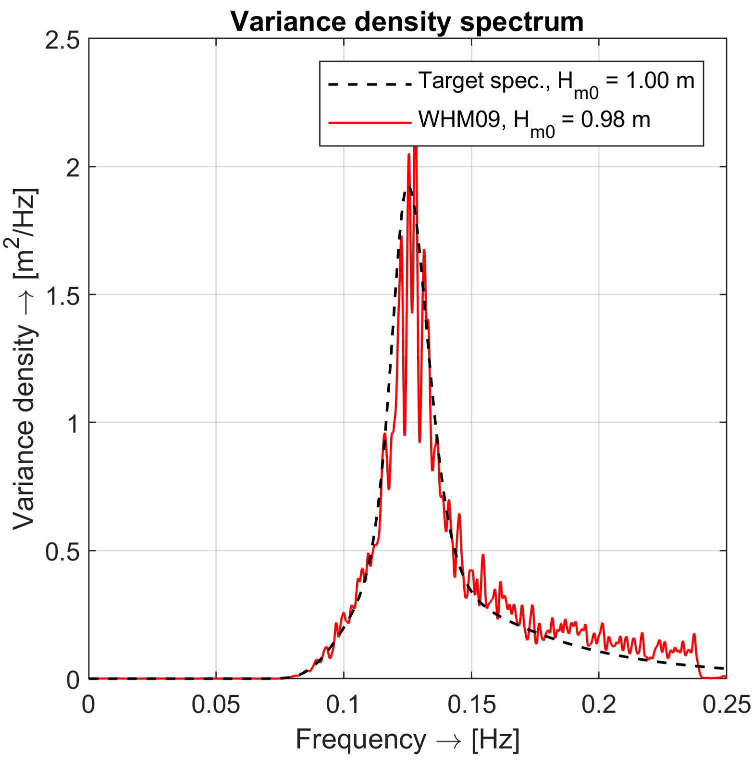

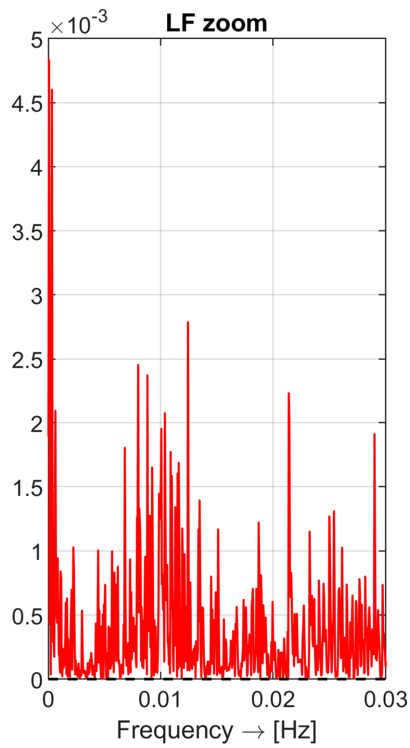

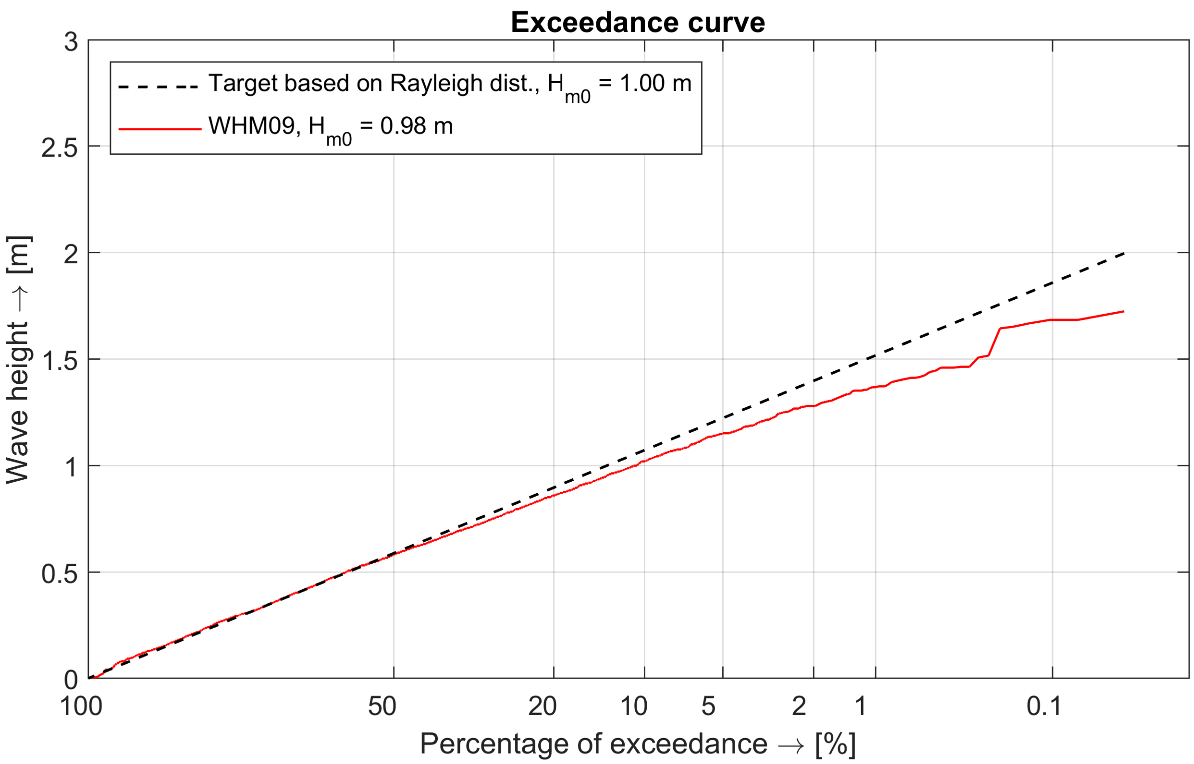

Results of wave generation calibration Depth = 18.0 m, H_{m0} = 1.00 m, T_p = 8.00 s, γ = 5.0	Irregular	I80d
Deltares	11202696	App. E.3.21

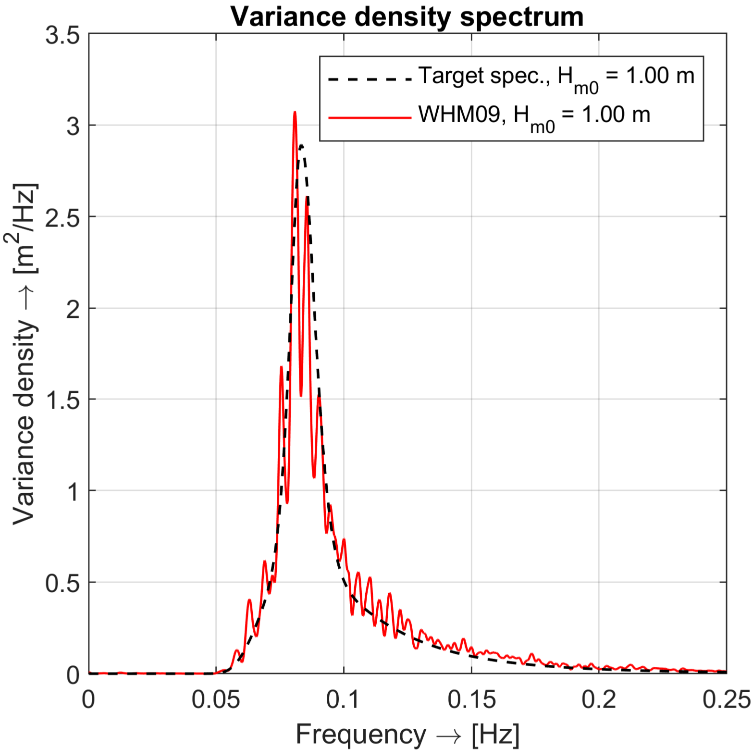

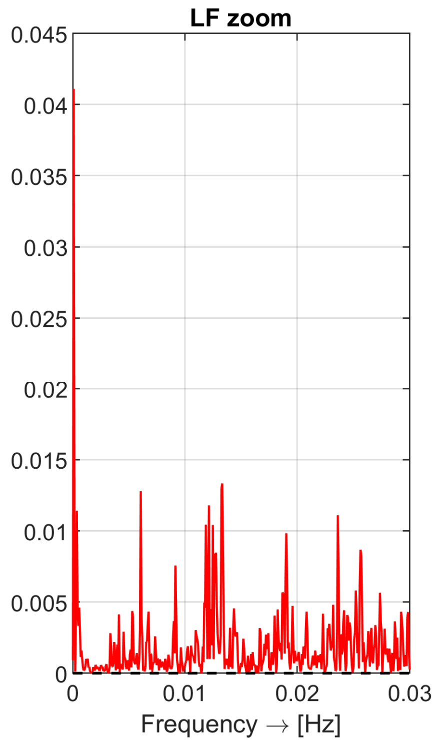

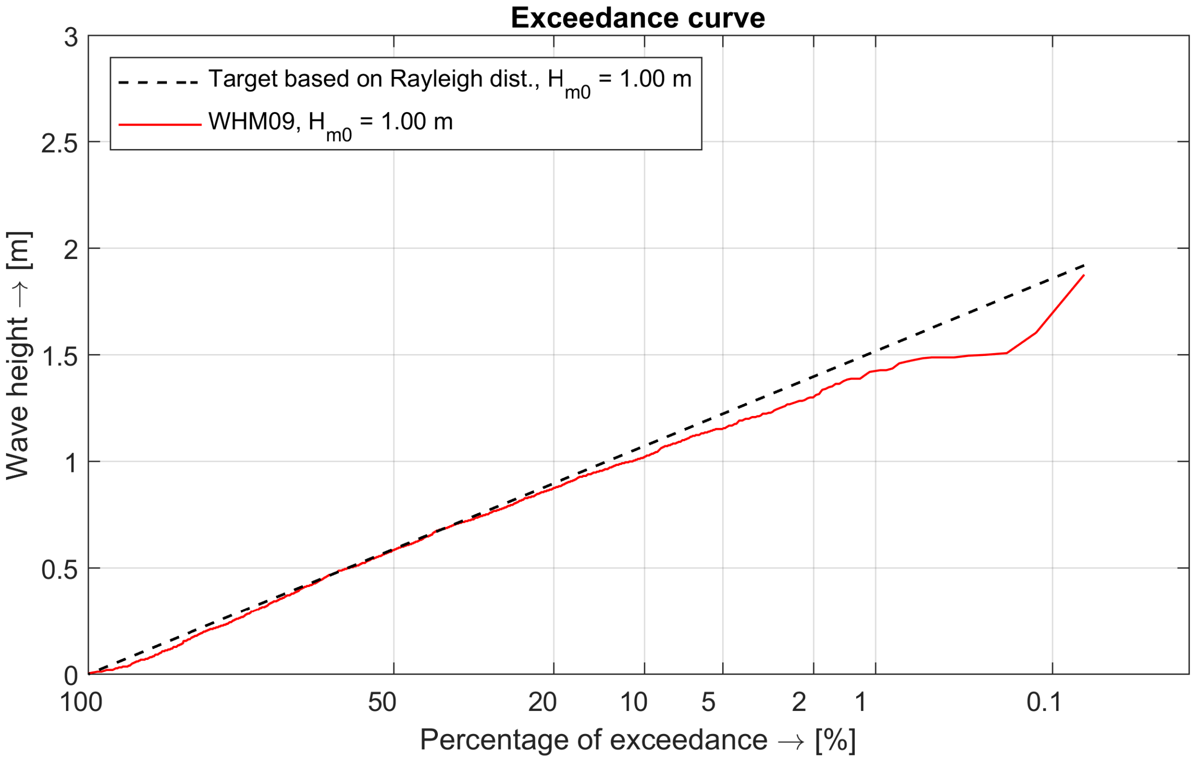

Results of wave generation calibration Depth = 18.0 m, H_{m0} = 1.00 m, T_p = 12.00 s, γ = 5.0	Irregular	I120a
Deltares	11202696	App. E.3.22

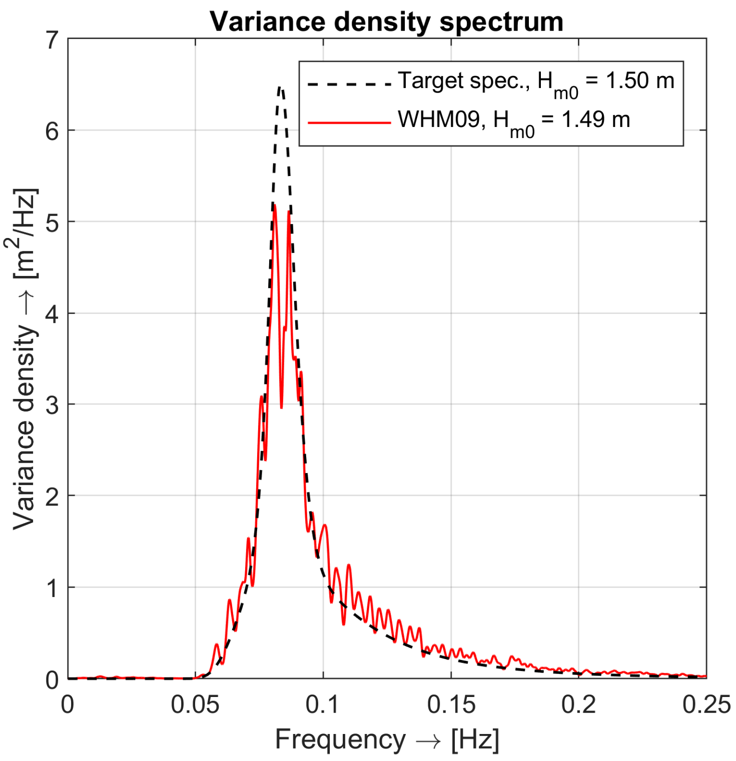

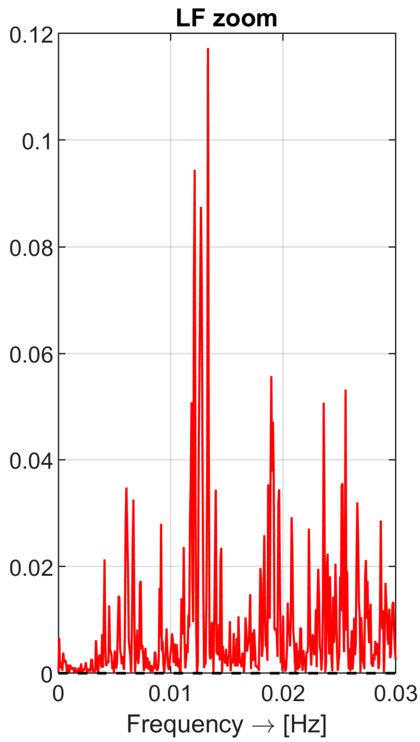

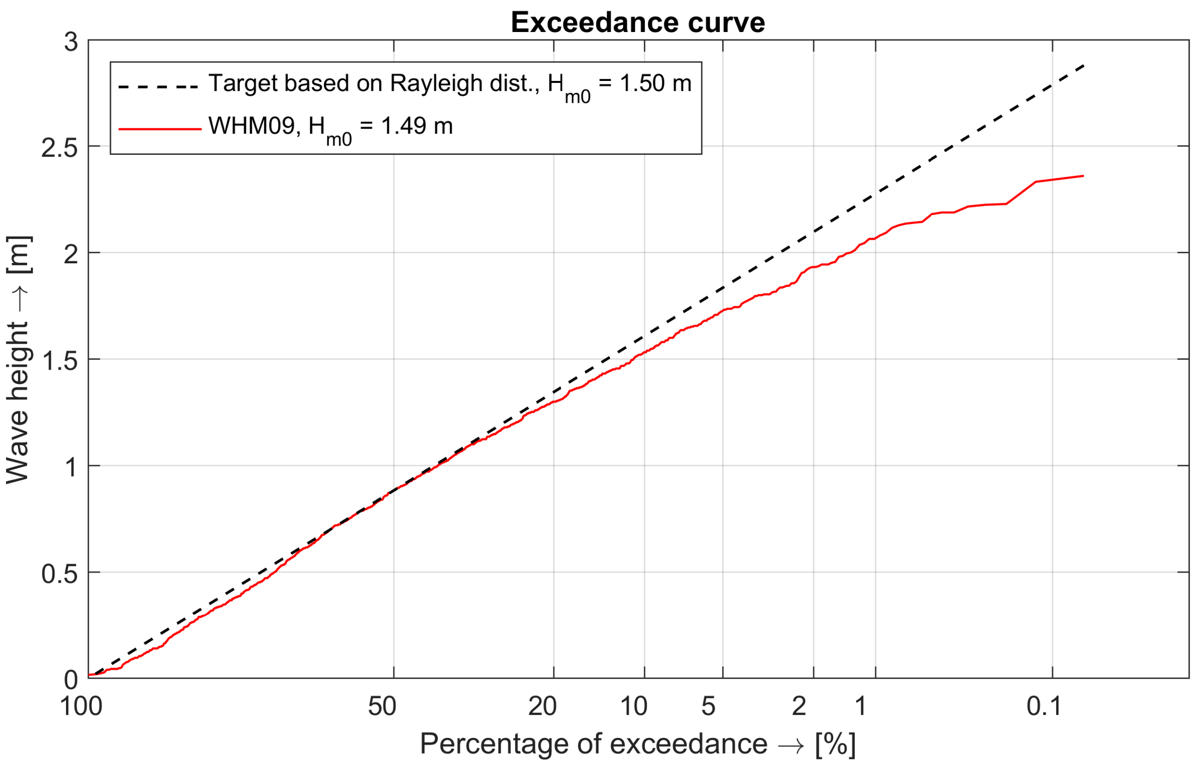

Results of wave generation calibration Depth = 18.0 m, H_{m0} = 1.50 m, T_p = 12.00 s, γ = 5.0	Irregular	I120b
Deltares	11202696	App. E.3.23

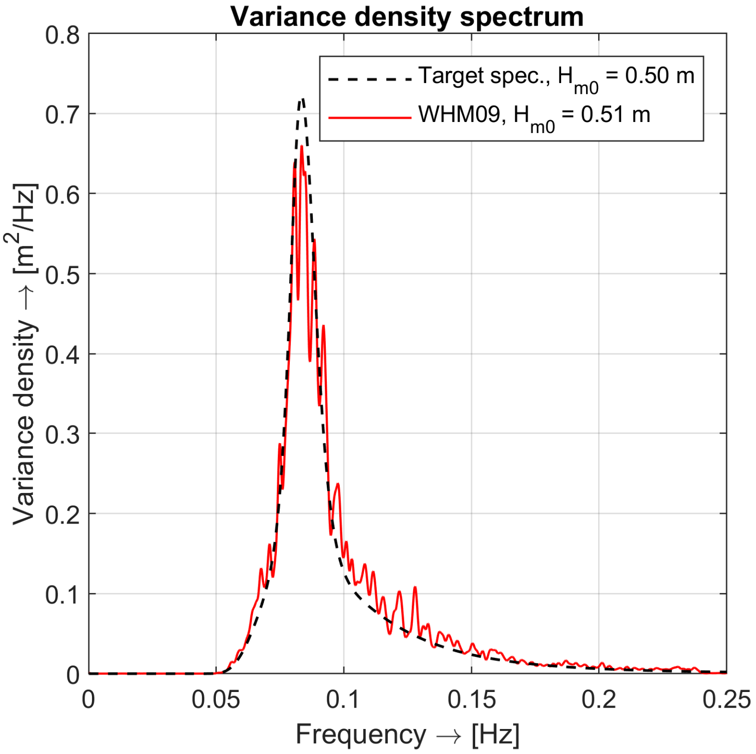

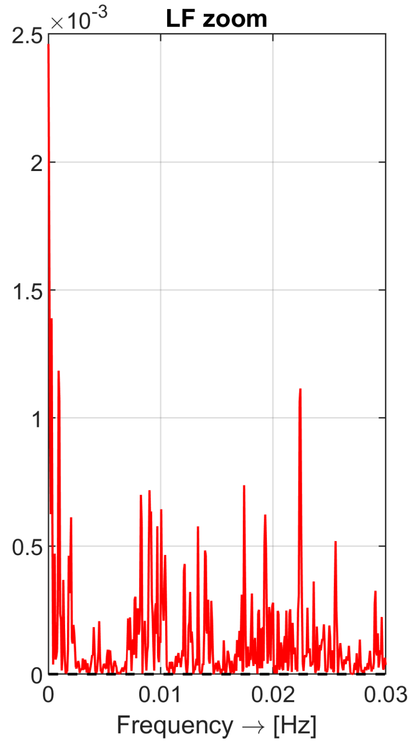

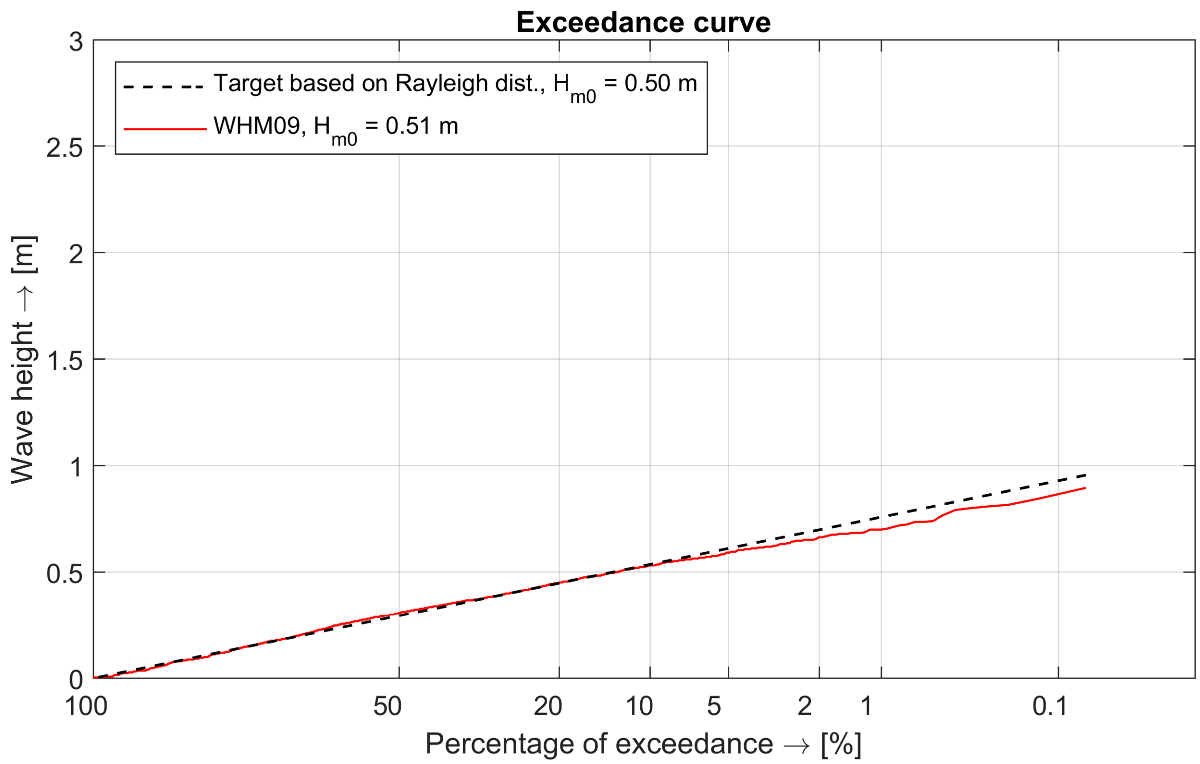

Results of wave generation calibration Depth = 18.0 m, H_{m0} = 0.50 m, T_p = 12.00 s, γ = 5.0	Irregular	I120c
Deltares	11202696	App. E.3.24

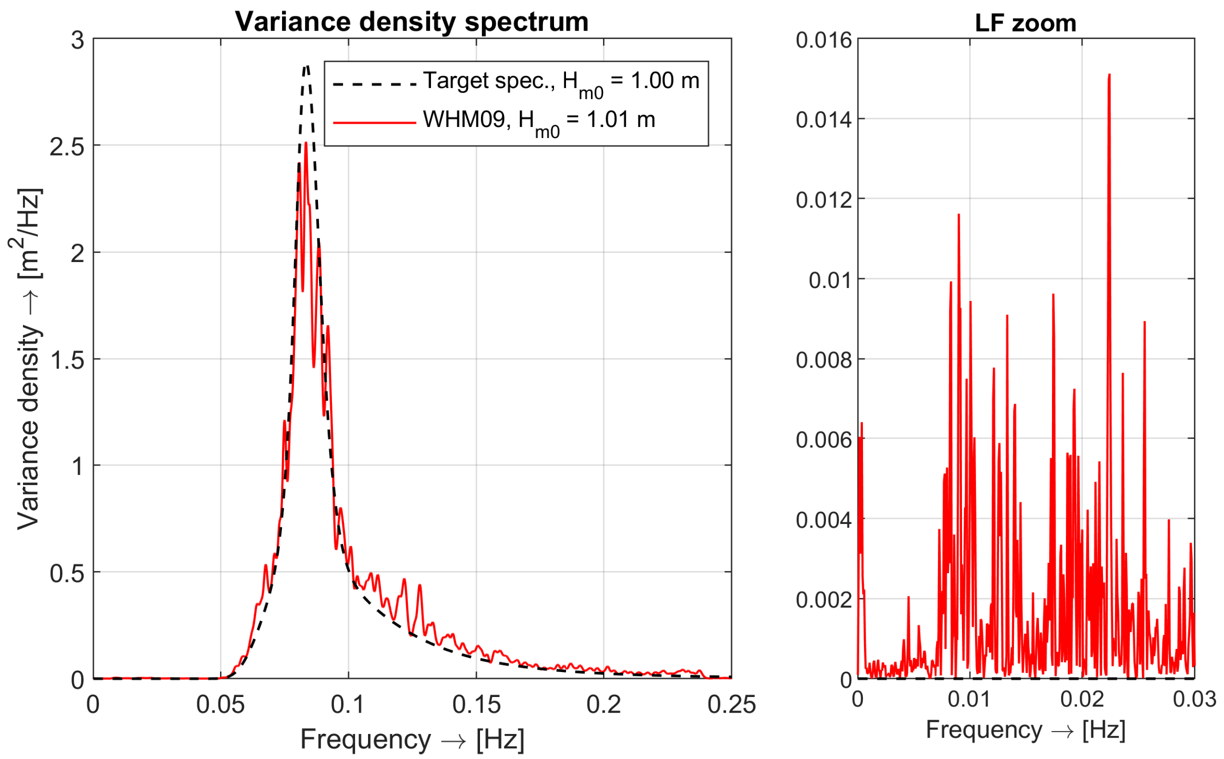

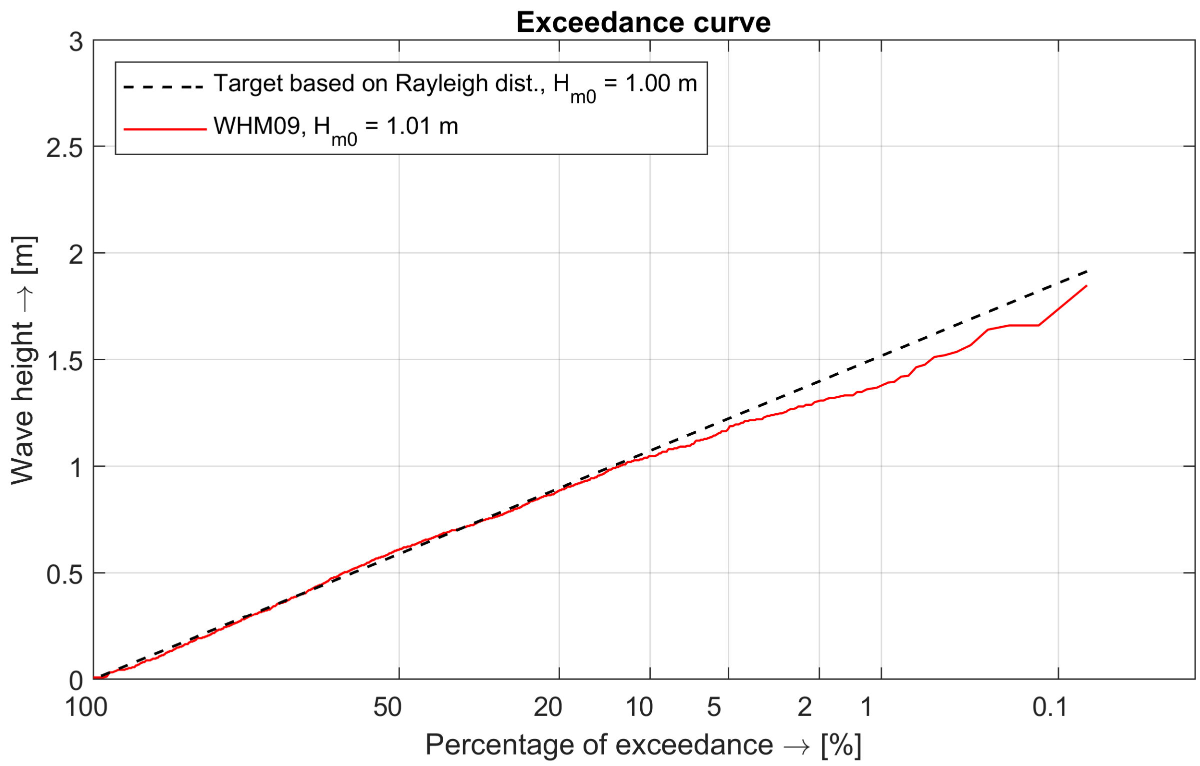

Results of wave generation calibration Depth = 18.0 m, H_{m0} = 1.00 m, T_p = 12.00 s, γ = 5.0	Irregular	I120d
Deltares	11202696	App. E.3.25

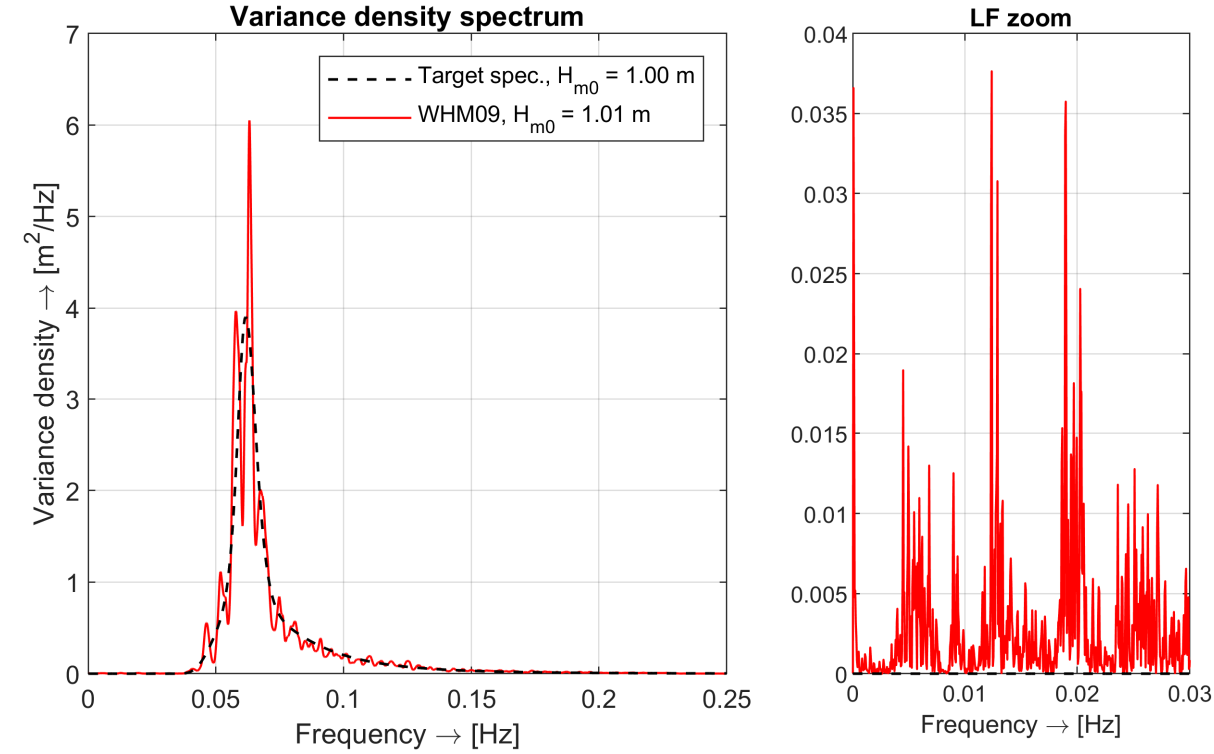

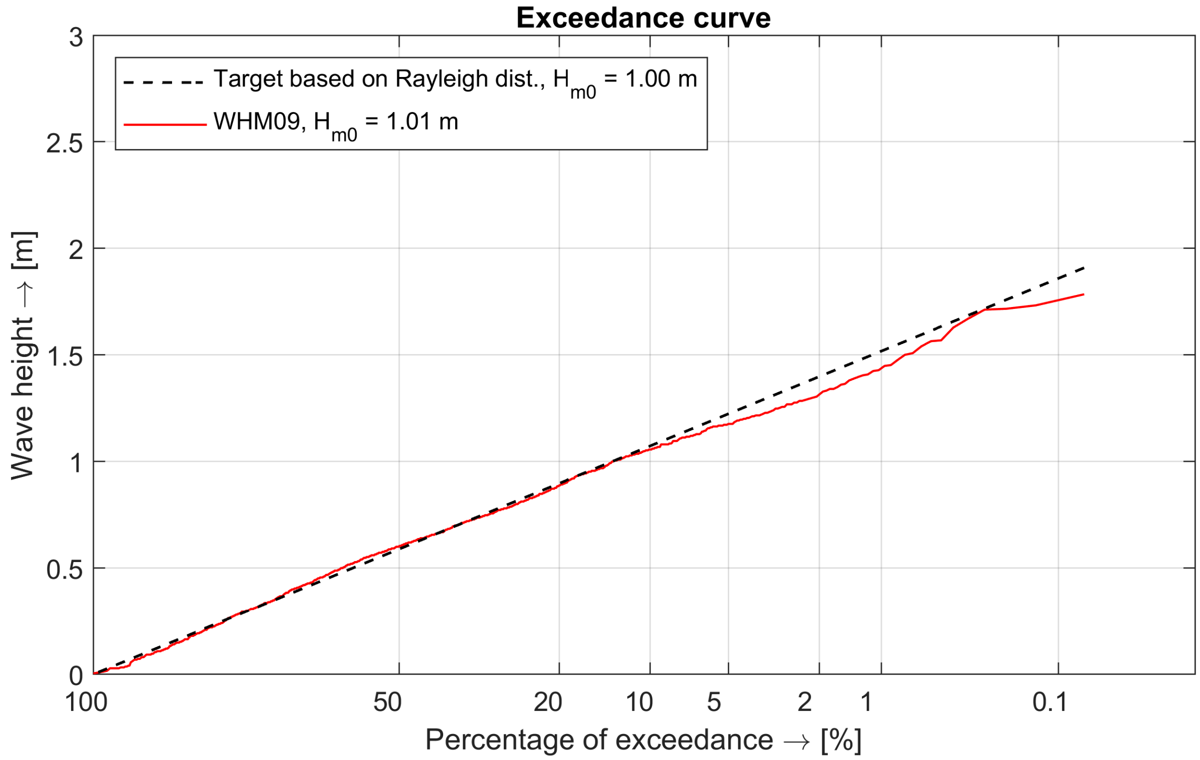

Results of wave generation calibration Depth = 18.0 m, H_{m0} = 1.00 m, T_p = 16.20 s, γ = 5.0	Irregular	I162a
Deltares	11202696	App. E.3.26

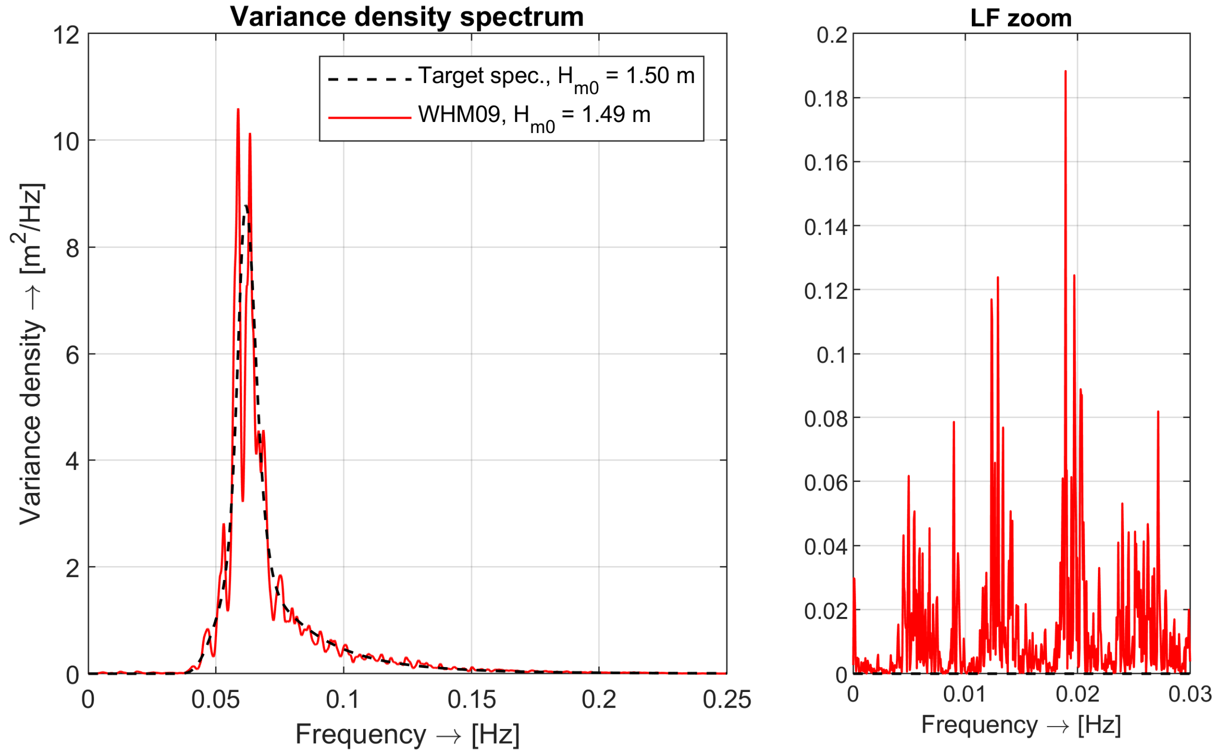

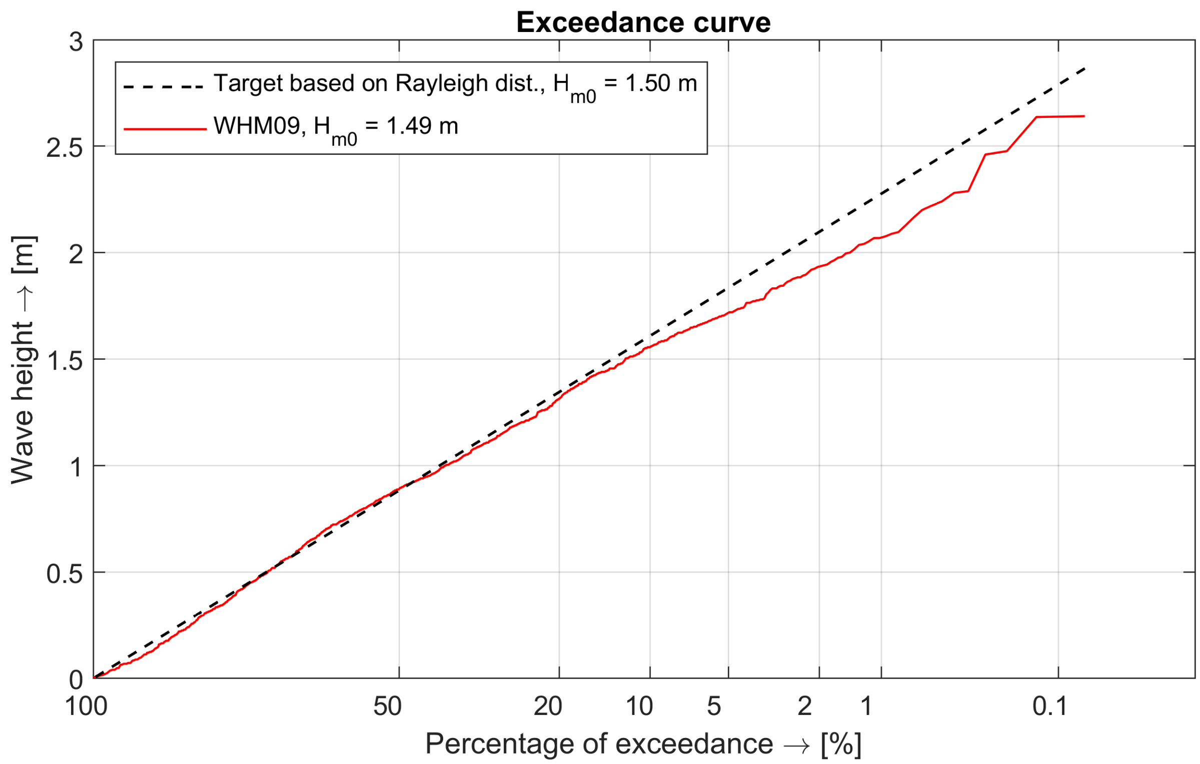

Results of wave generation calibration Depth = 18.0 m, H_{m0} = 1.50 m, T_p = 16.20 s, γ = 5.0	Irregular	I162b
Deltares	11202696	App. E.3.27

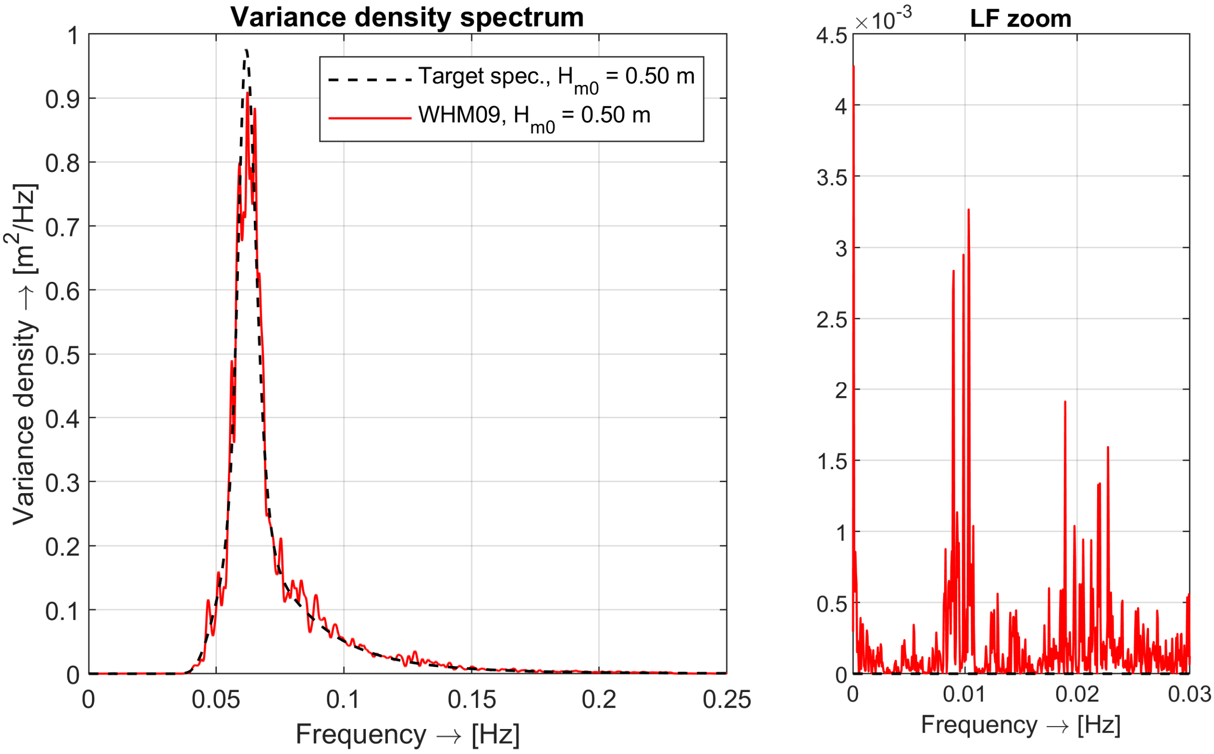

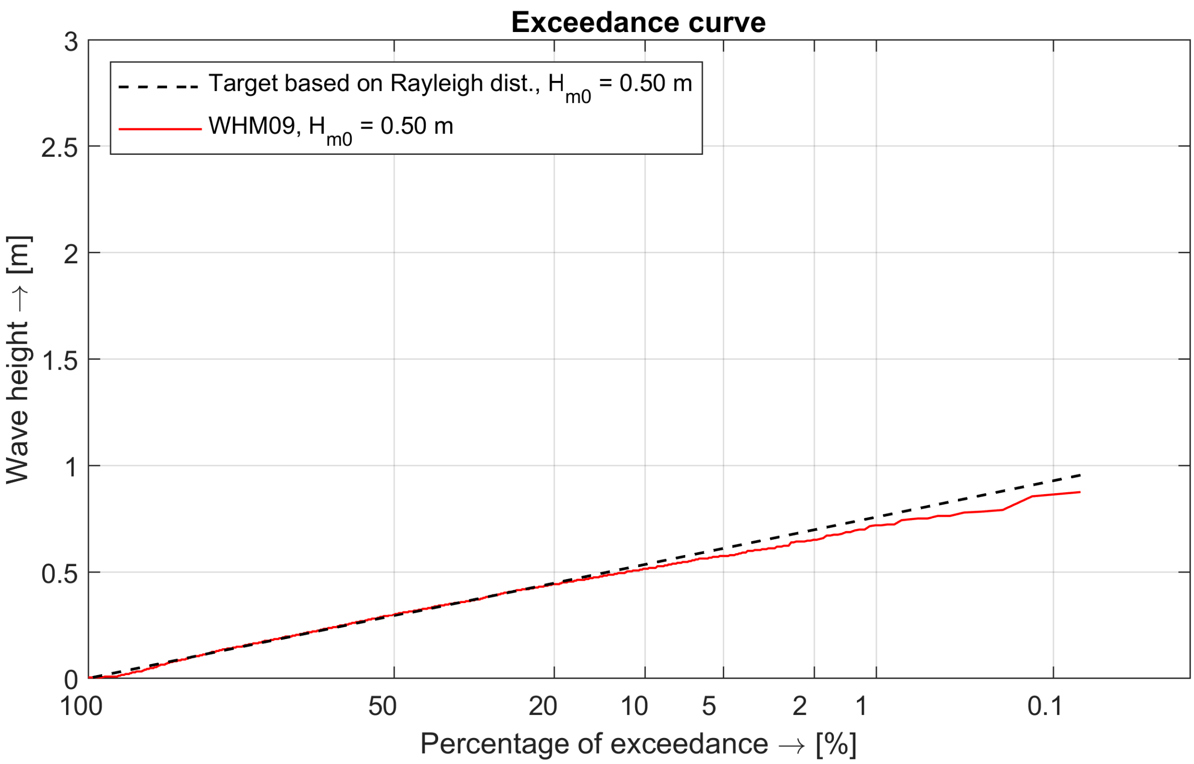

Results of wave generation calibration Depth = 18.0 m, H_{m0} = 0.50 m, T_p = 16.20 s, γ = 5.0	Irregular	I162c
Deltares	11202696	App. E.3.28

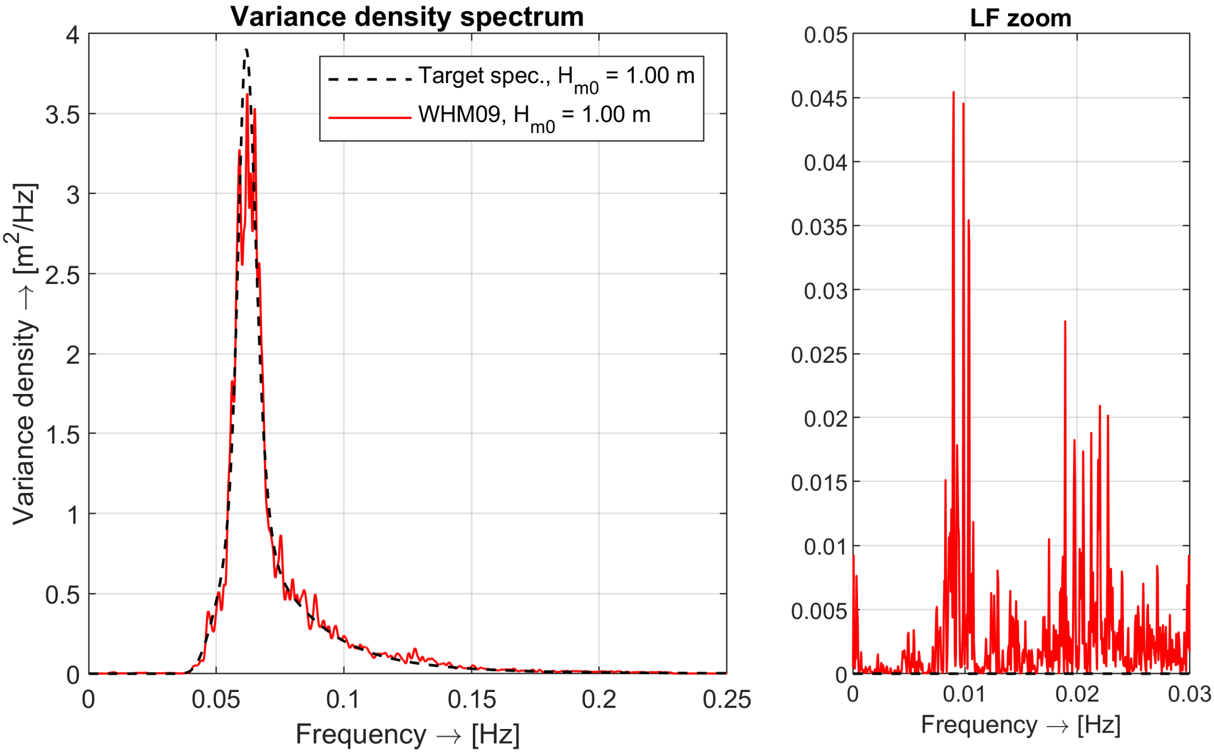

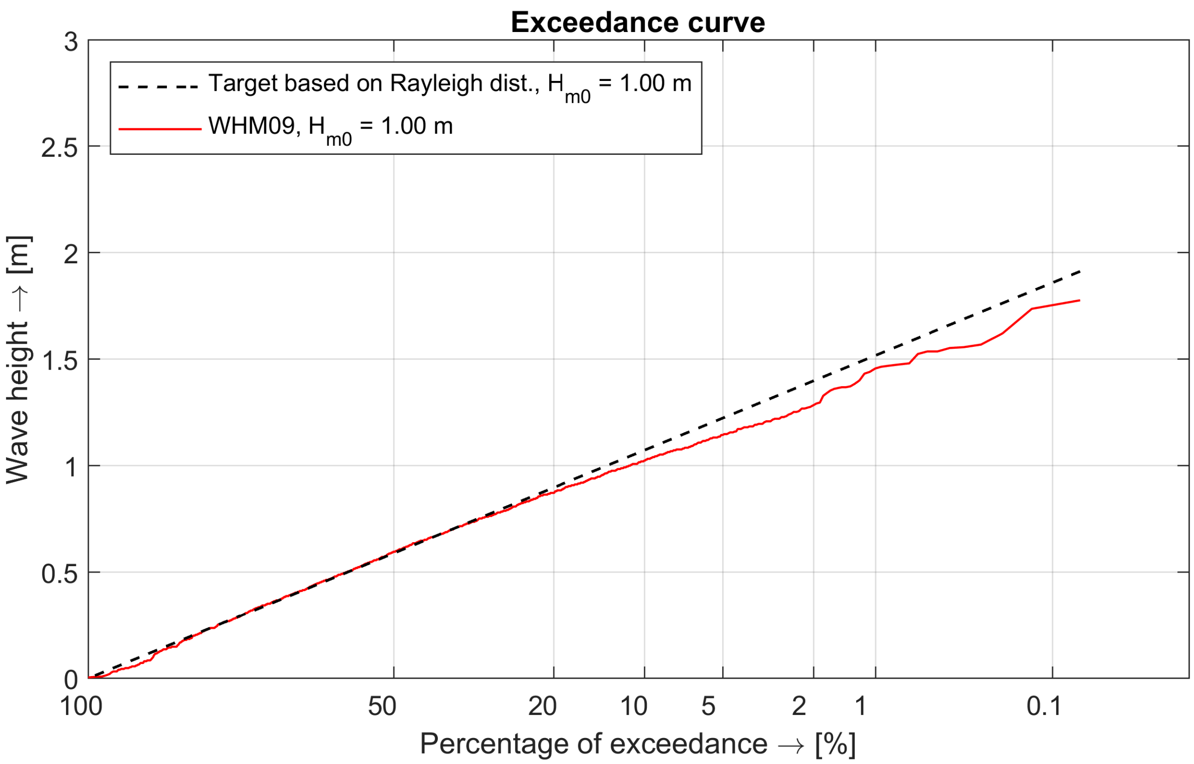

Results of wave generation calibration Depth = 18.0 m, H_{m0} = 1.00 m, T_p = 16.20 s, γ = 5.0	Irregular	I162d
Deltares	11202696	App. E.3.29

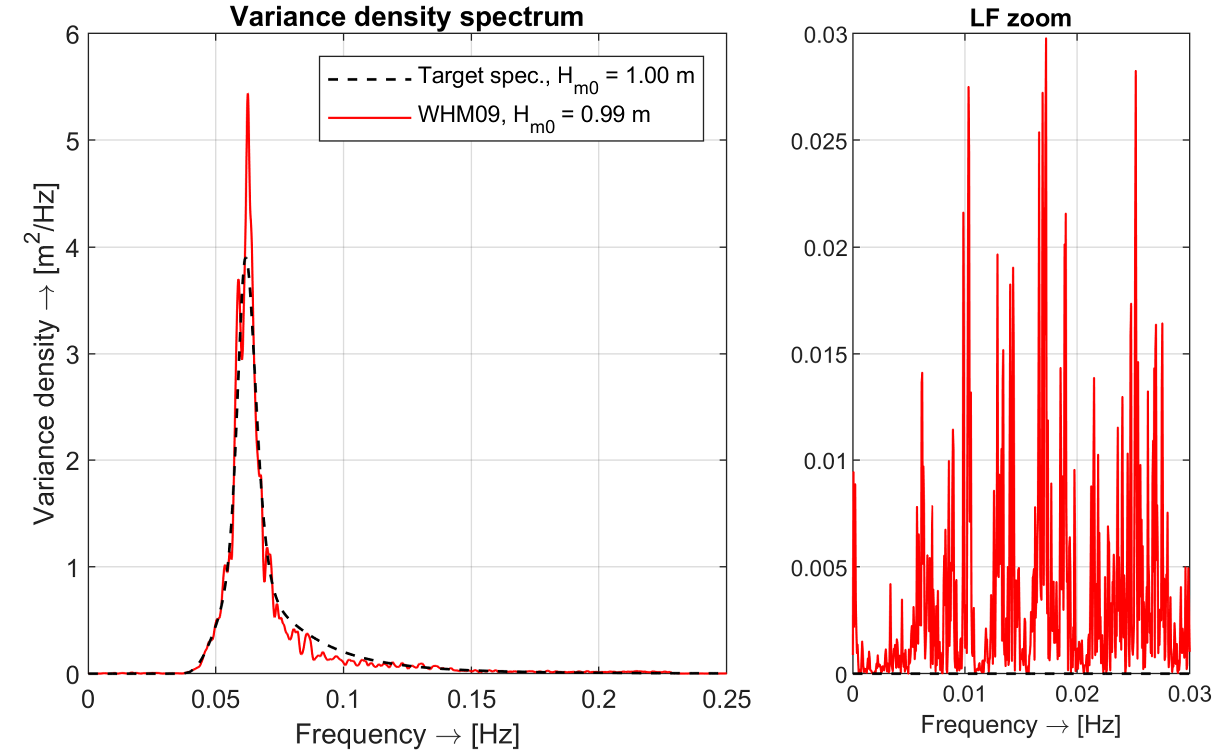

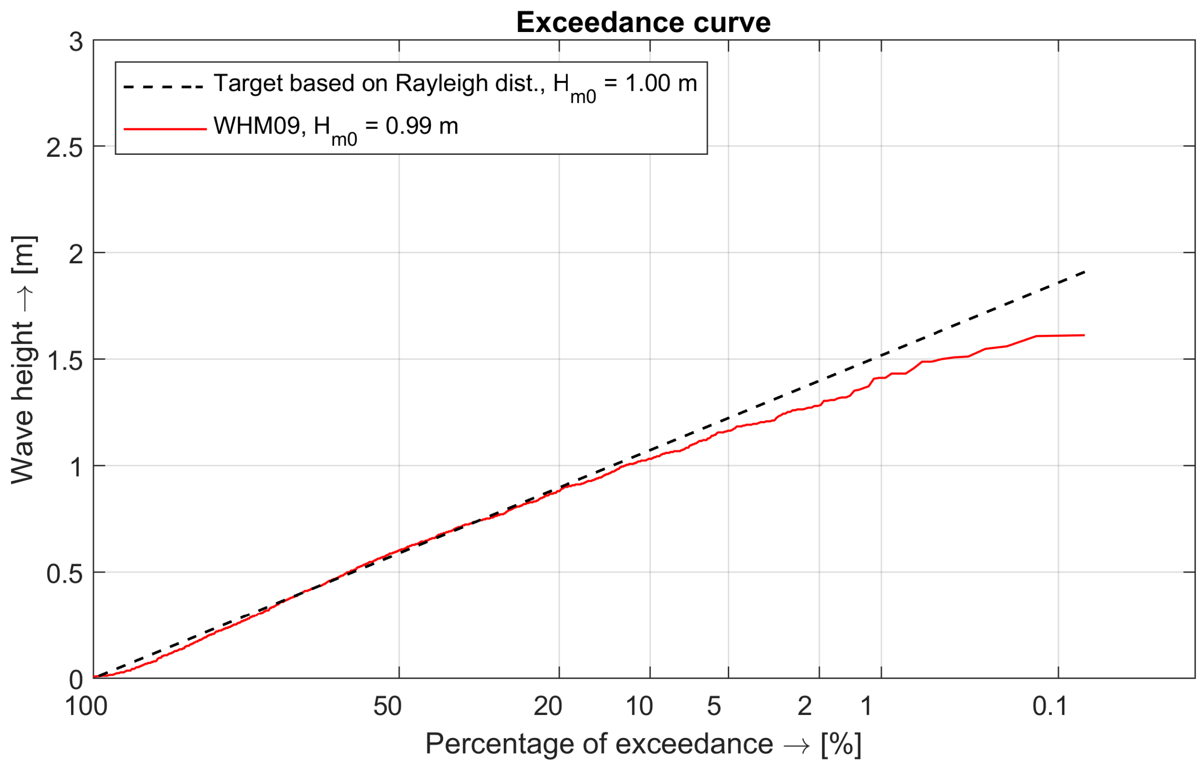

Results of wave generation calibration Depth = 18.0 m, H_{m0} = 1.00 m, T_p = 16.20 s, γ = 5.0	Irregular	I162e
Deltares	11202696	App. E.3.30

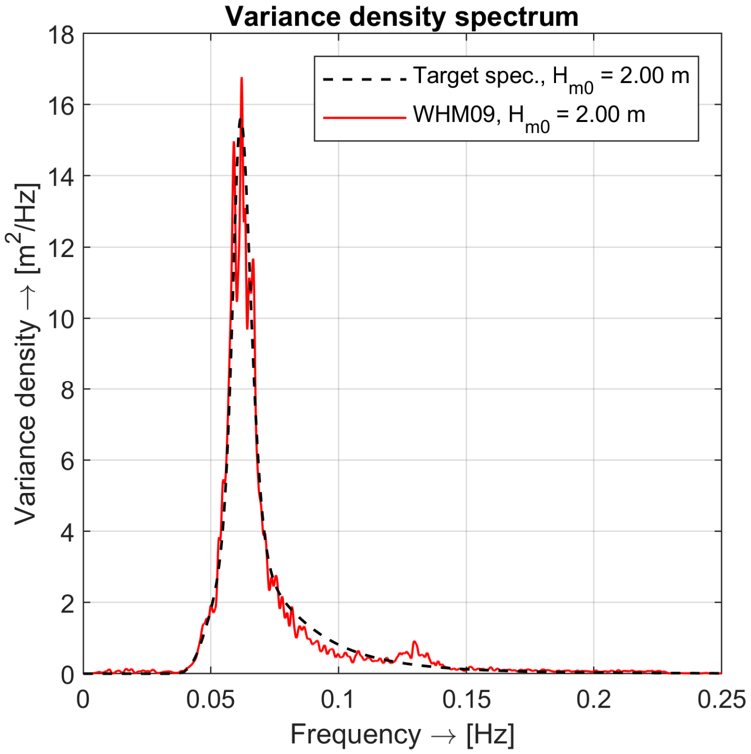

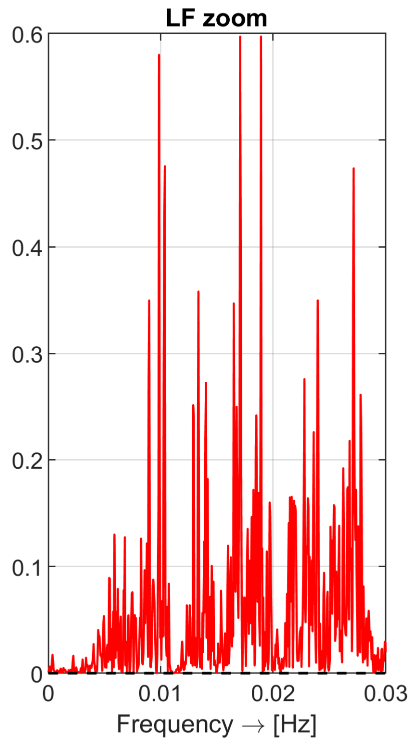

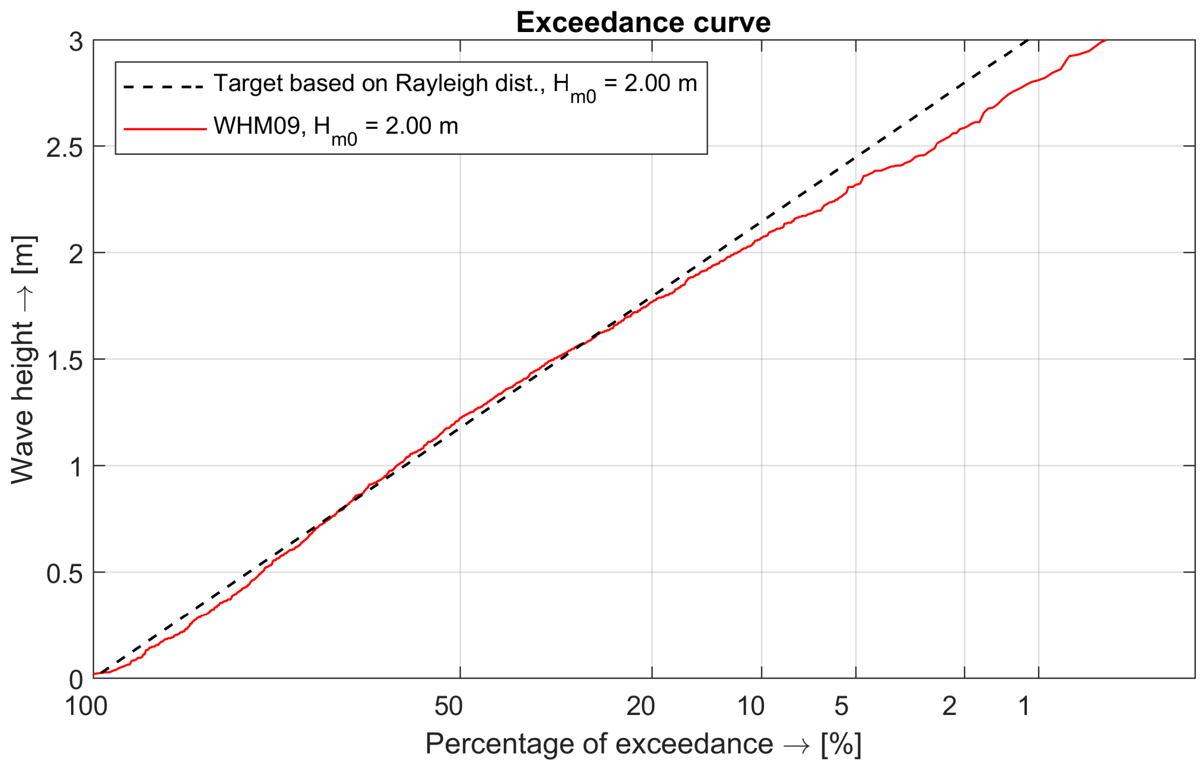

Results of wave generation calibration Depth = 18.0 m, H_{m0} = 2.00 m, T_p = 16.20 s, γ = 5.0	Irregular	I162f
Deltares	11202696	App. E.3.31

E.4 Reflection analyses Case D

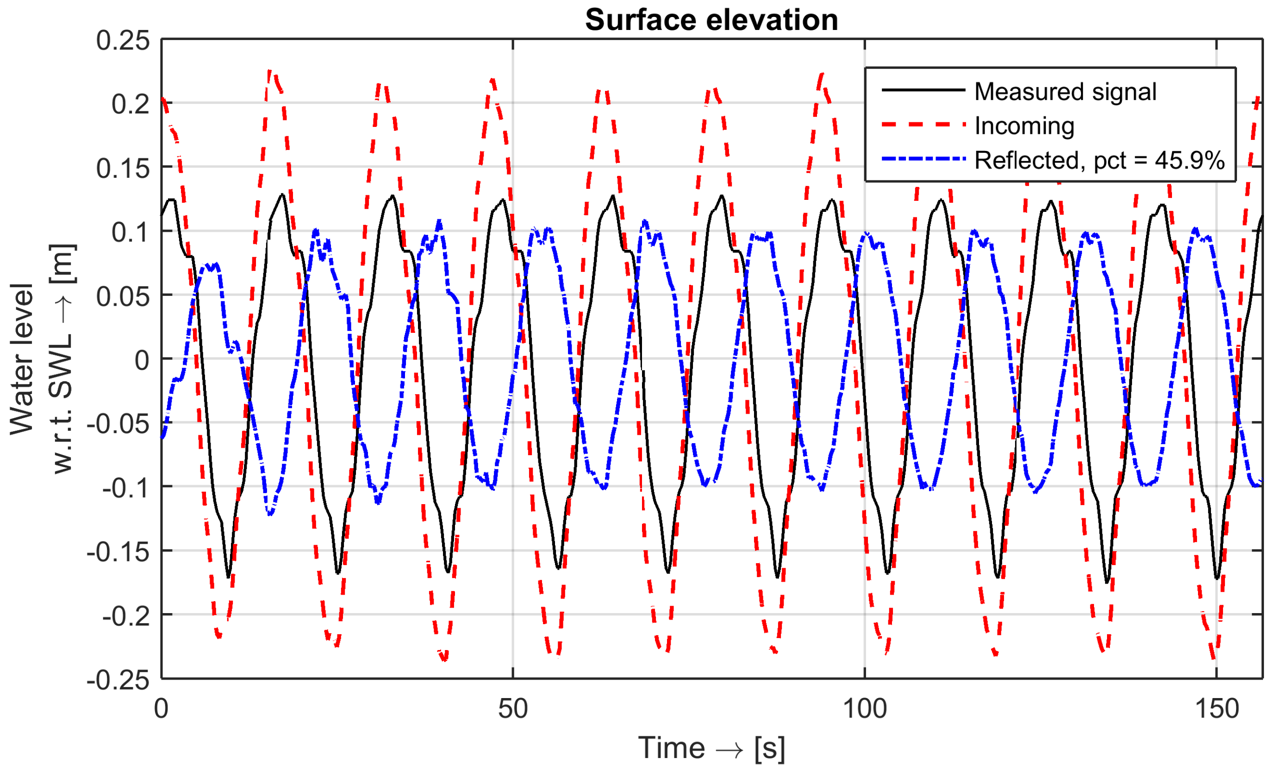

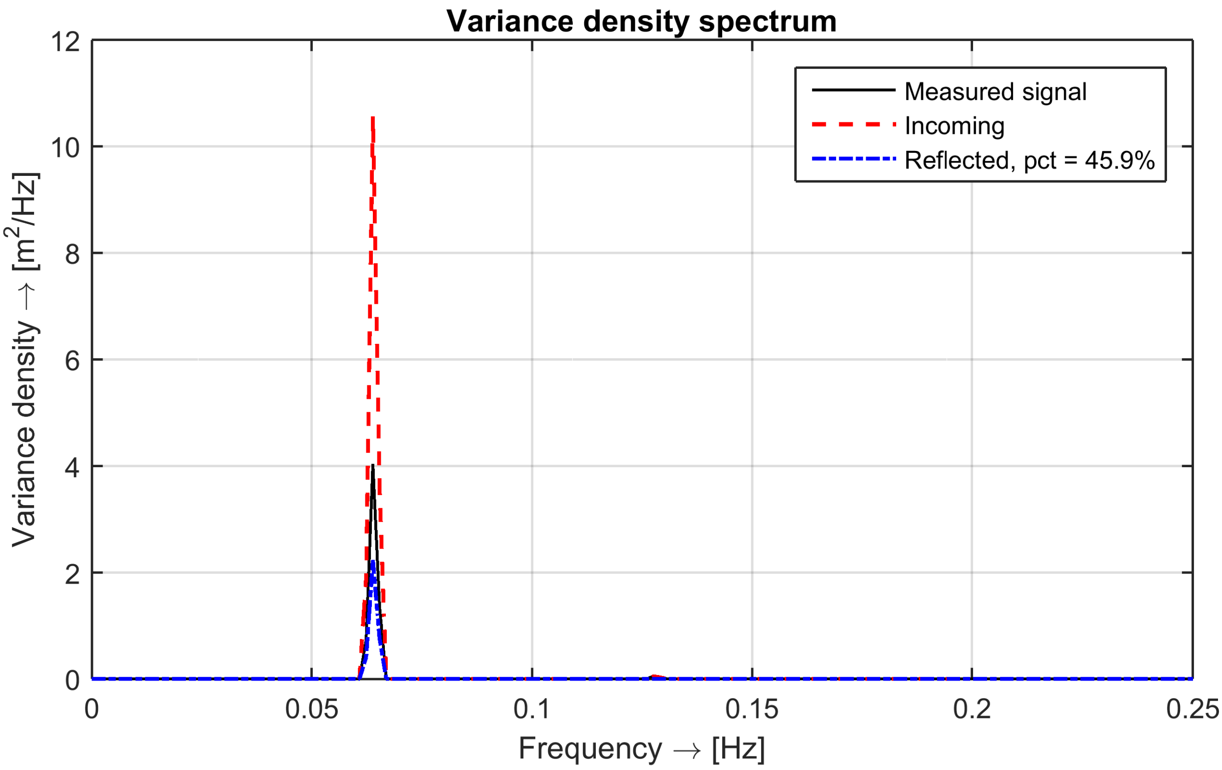

Reflection analysis using WHMs:01, 02 & 07	Monochromatic	M156a
Deltares	11202696	App. E.4.01

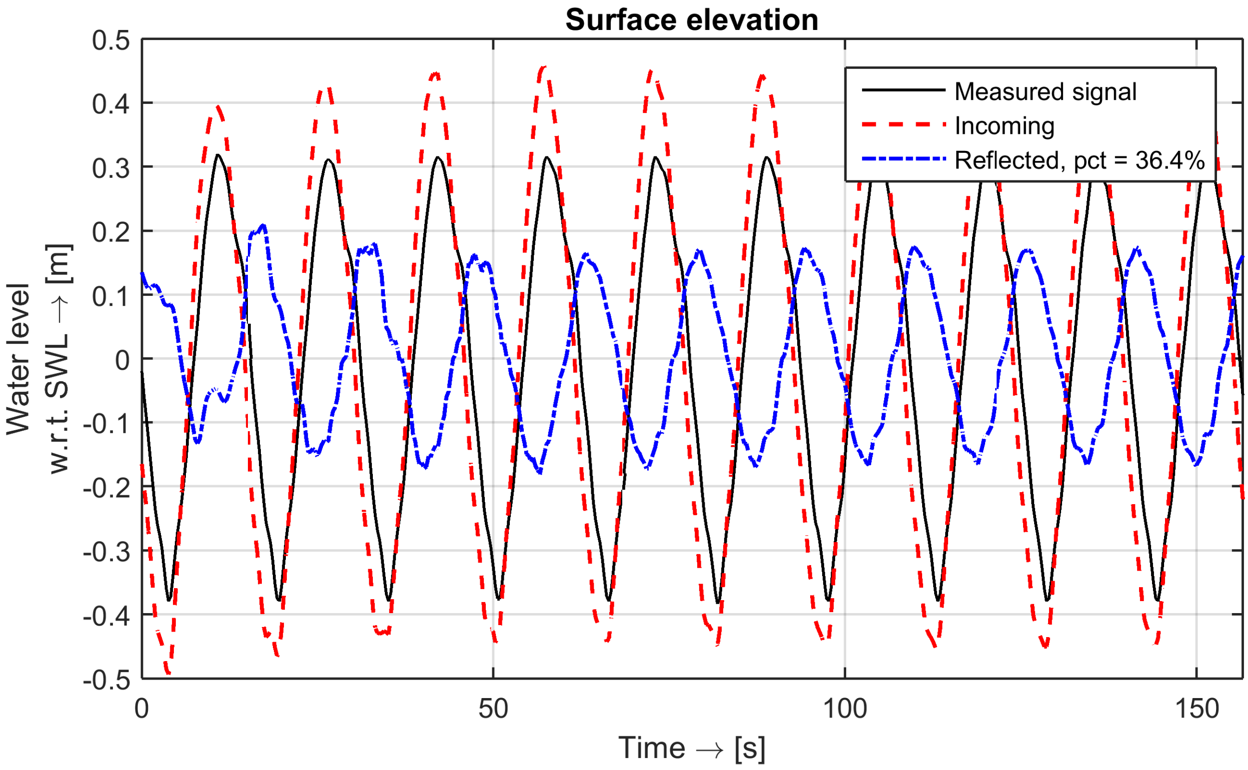

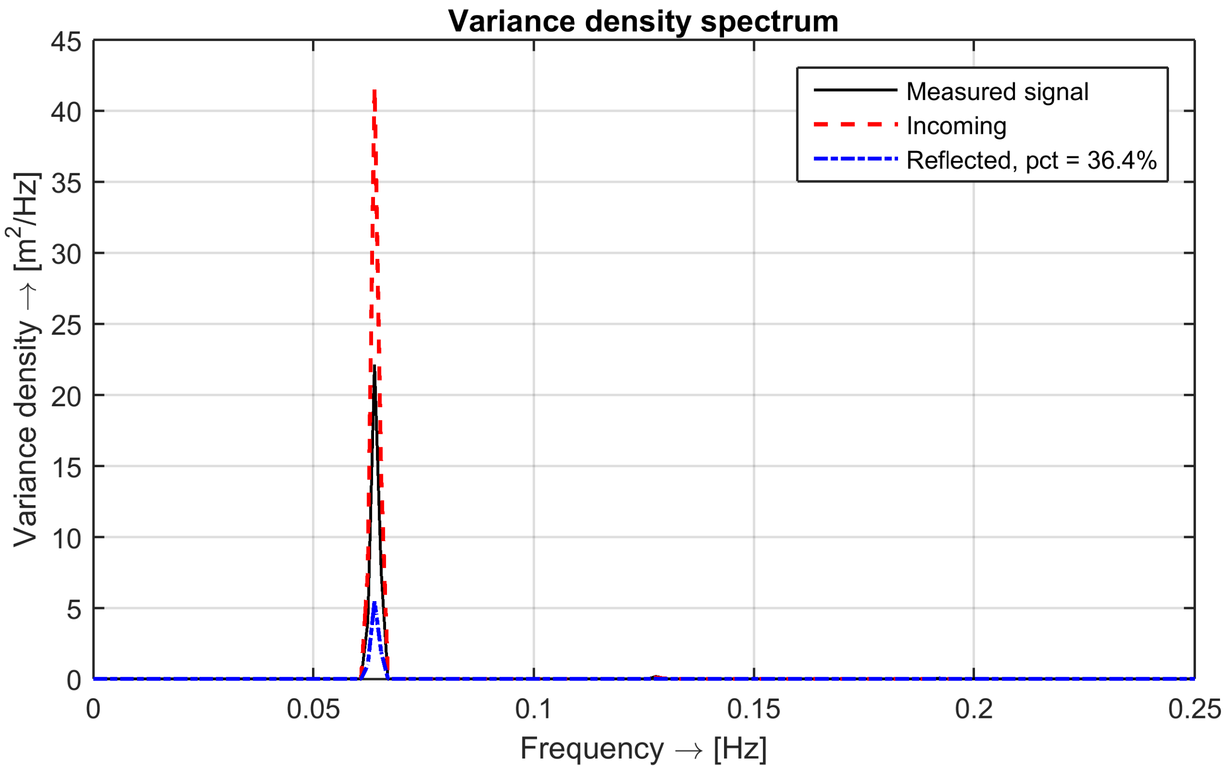

Reflection analysis using WHMs:01, 02 & 07	Monochromatic	M156b
Deltares	11202696	App. E.4.02

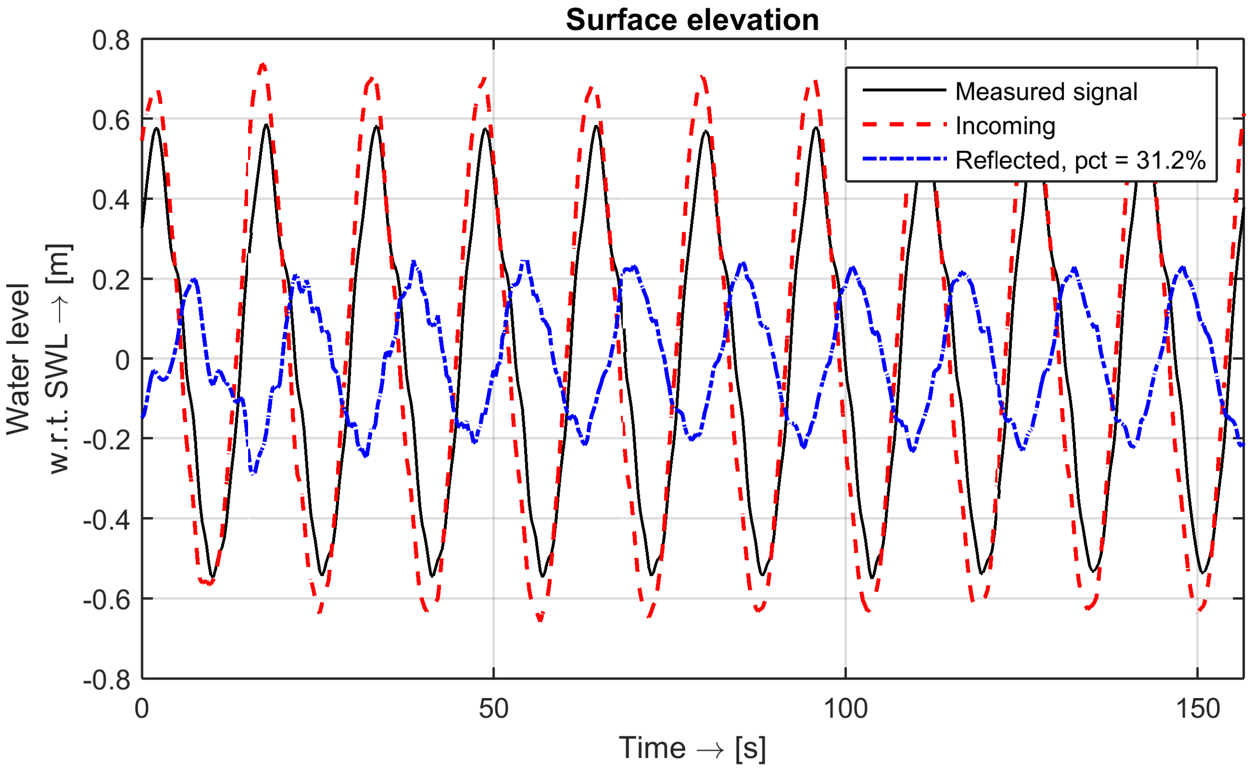

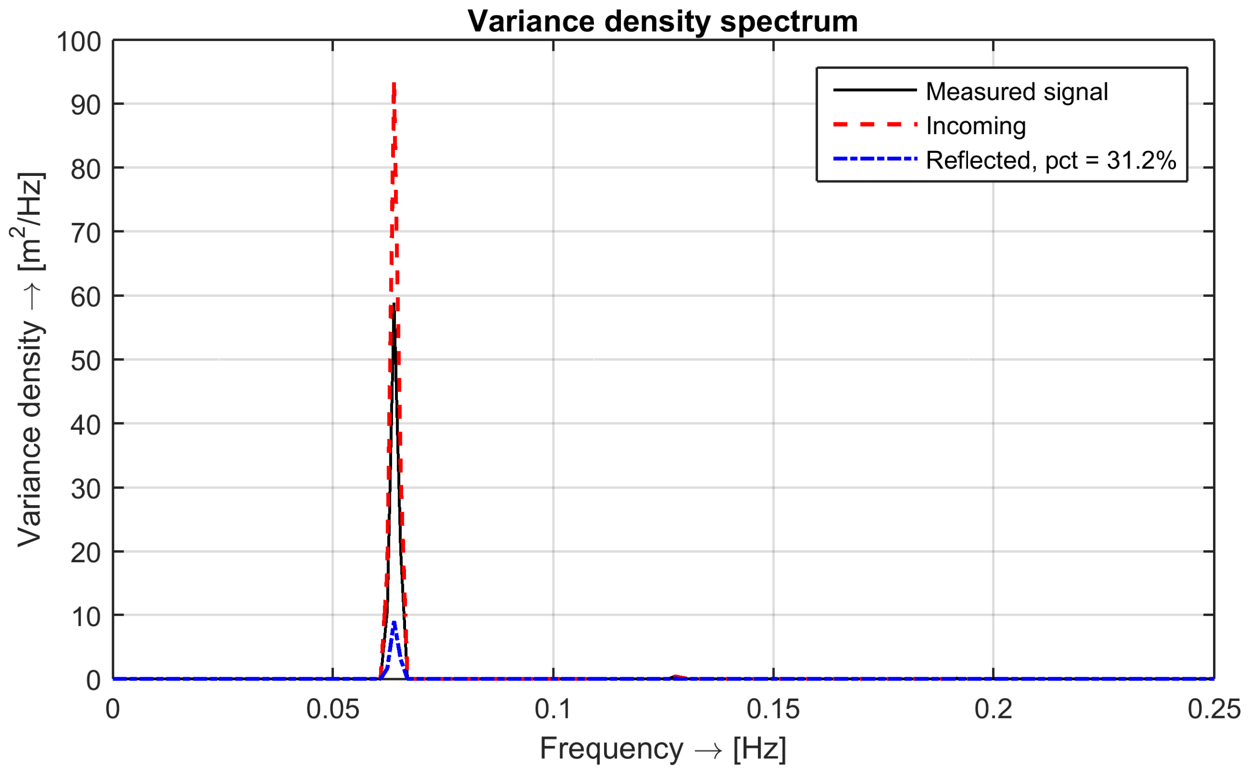

Reflection analysis using WHMs:01, 02 & 07	Monochromatic	M156c
Deltares	11202696	App. E.4.03

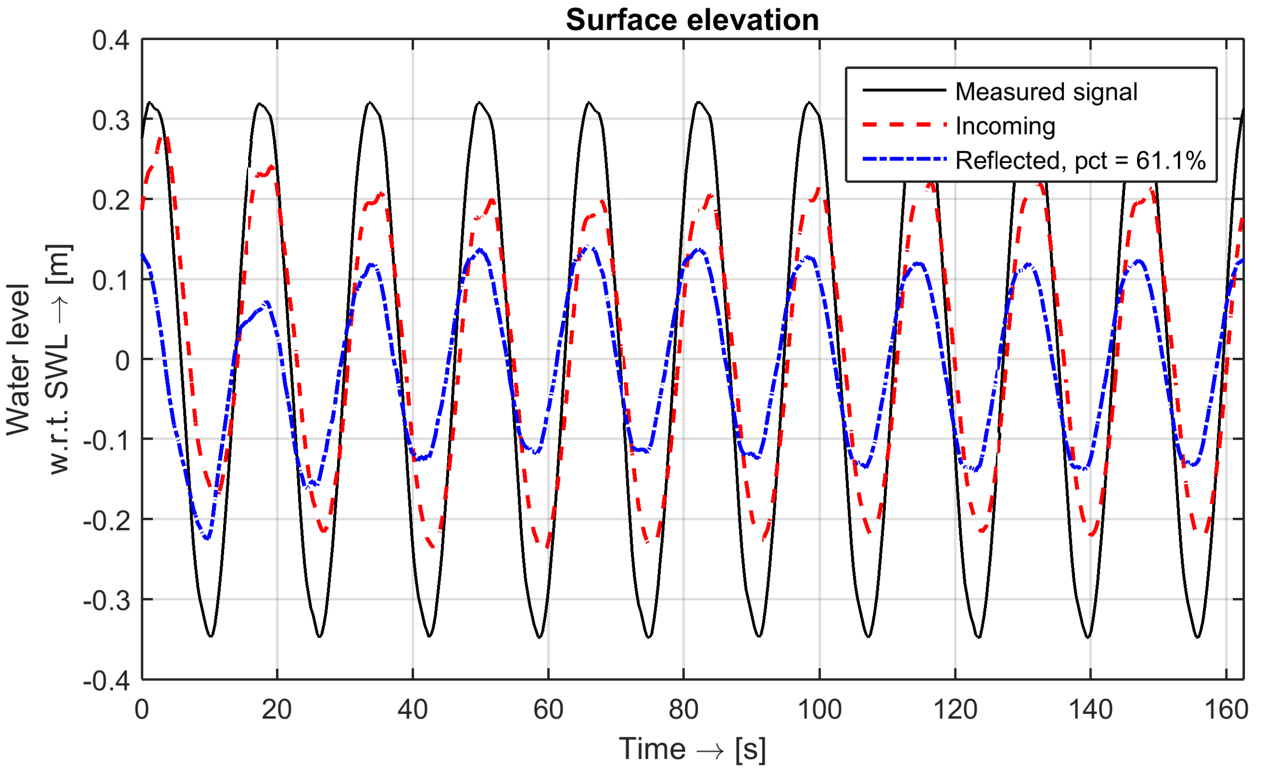

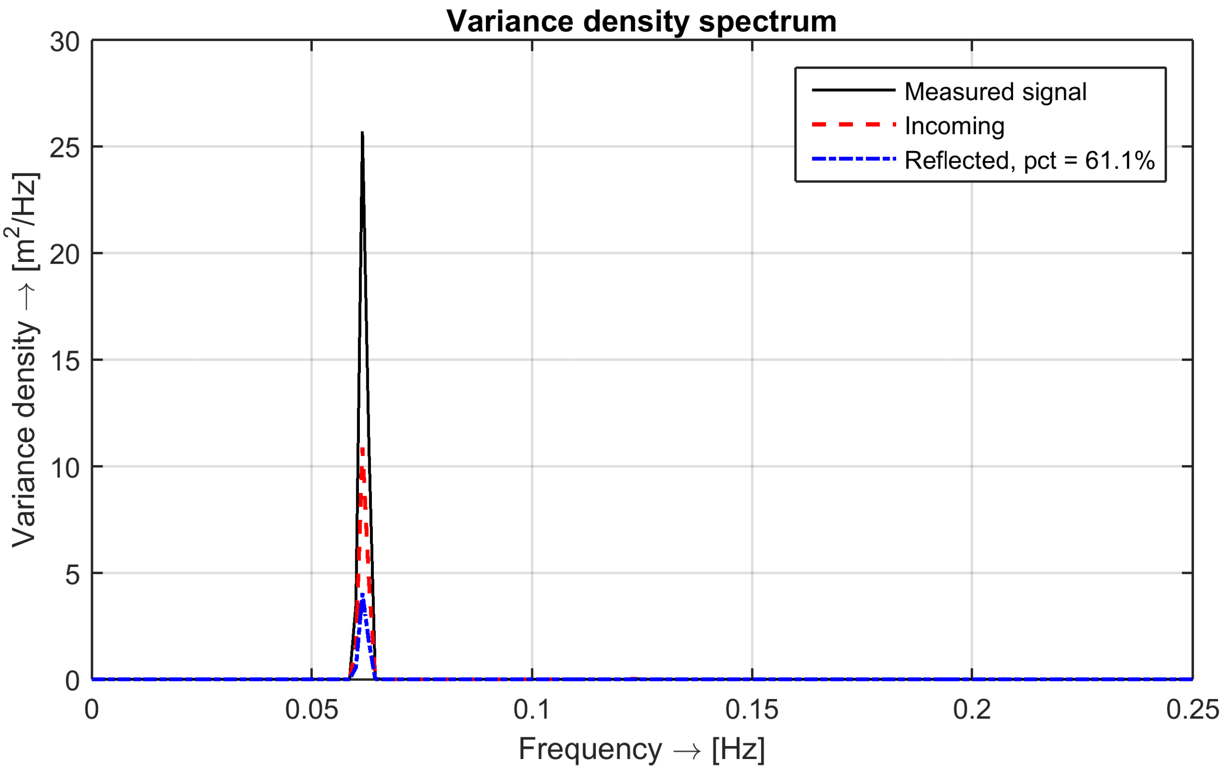

Reflection analysis using WHMs:01, 02 & 07	Monochromatic	M162a
Deltares	11202696	App. E.4.04

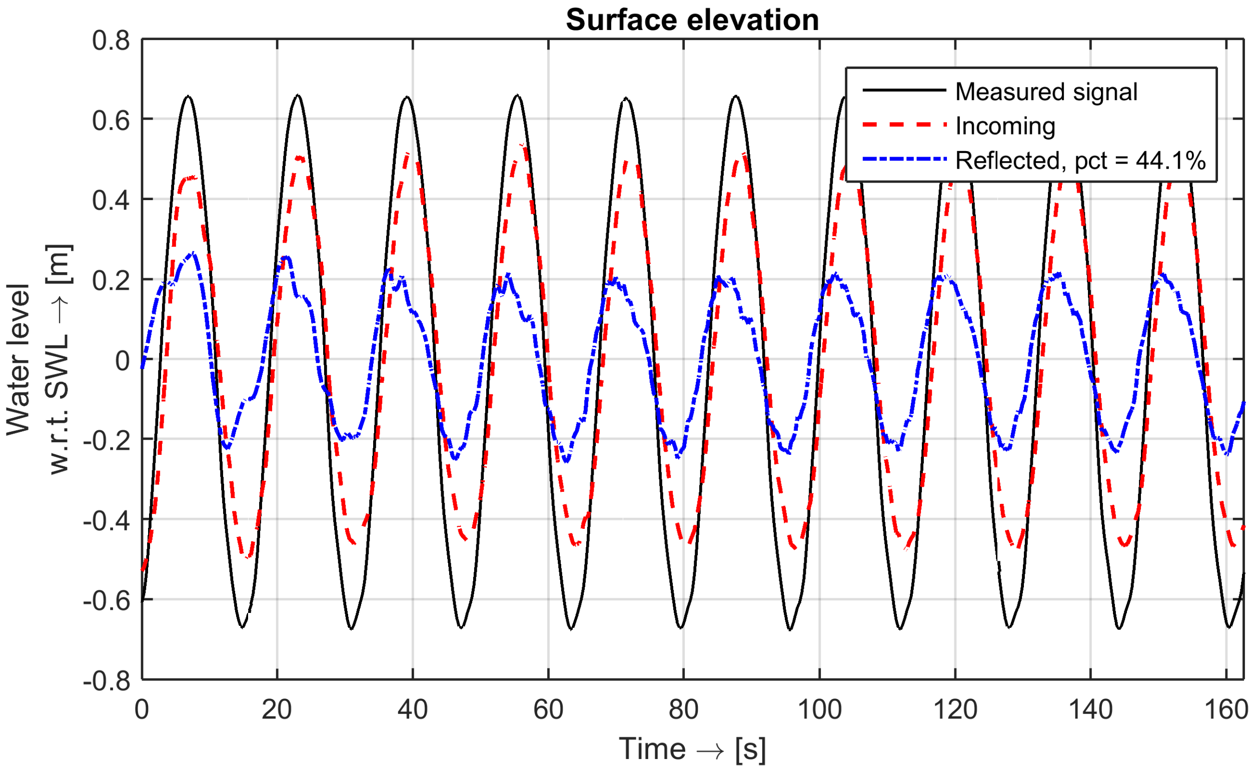

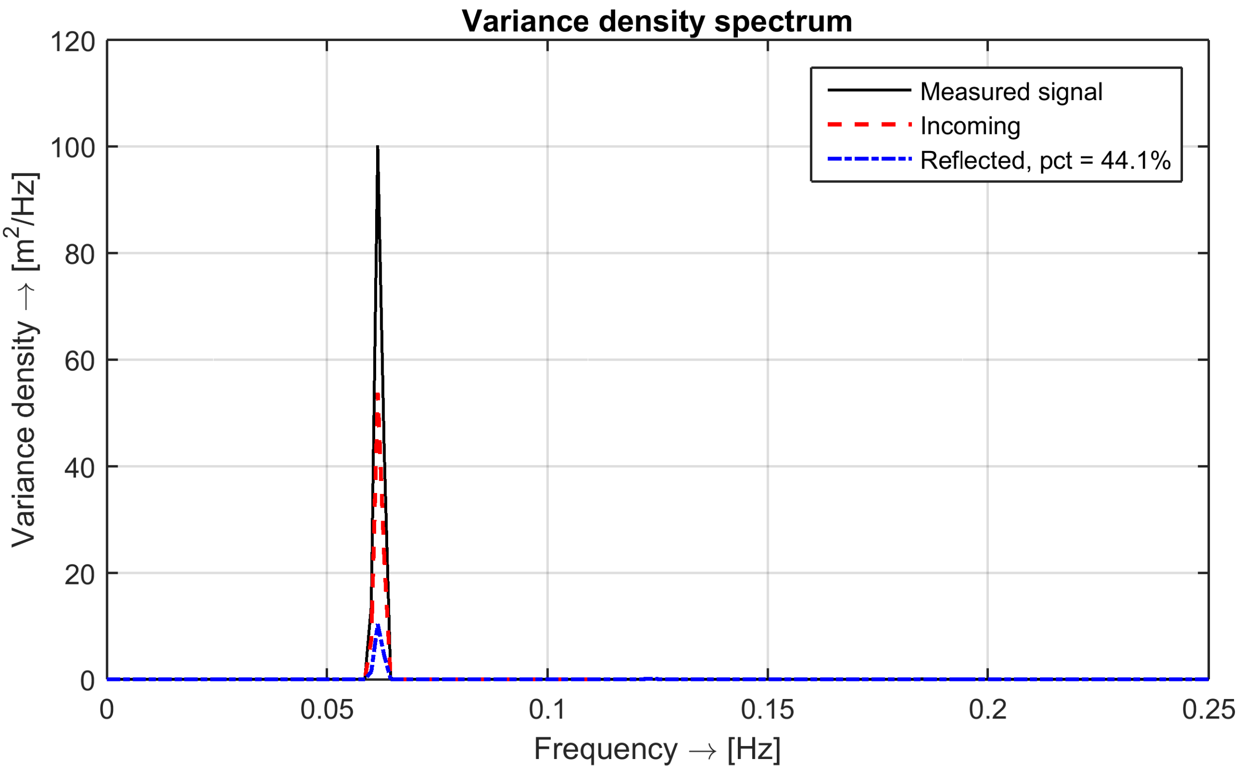

Reflection analysis using WHMs:01, 02 & 07	Monochromatic	M162b
Deltares	11202696	App. E.4.05

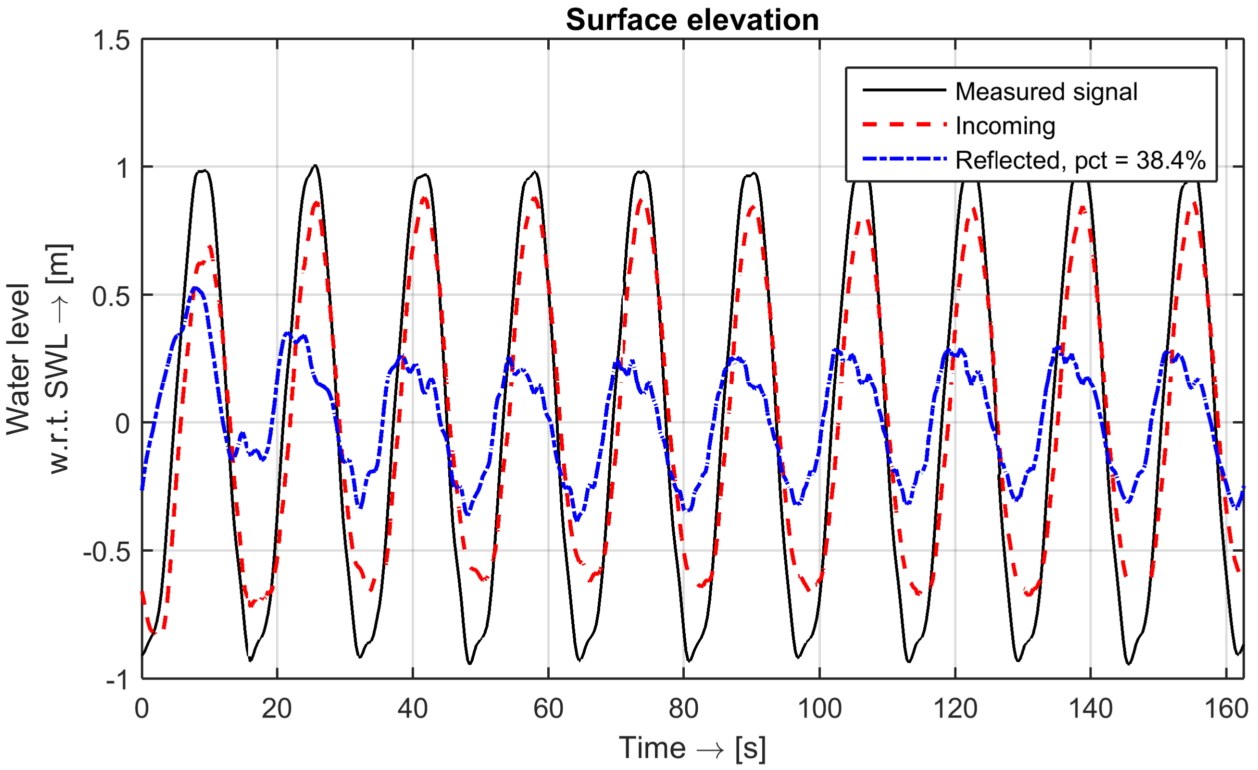

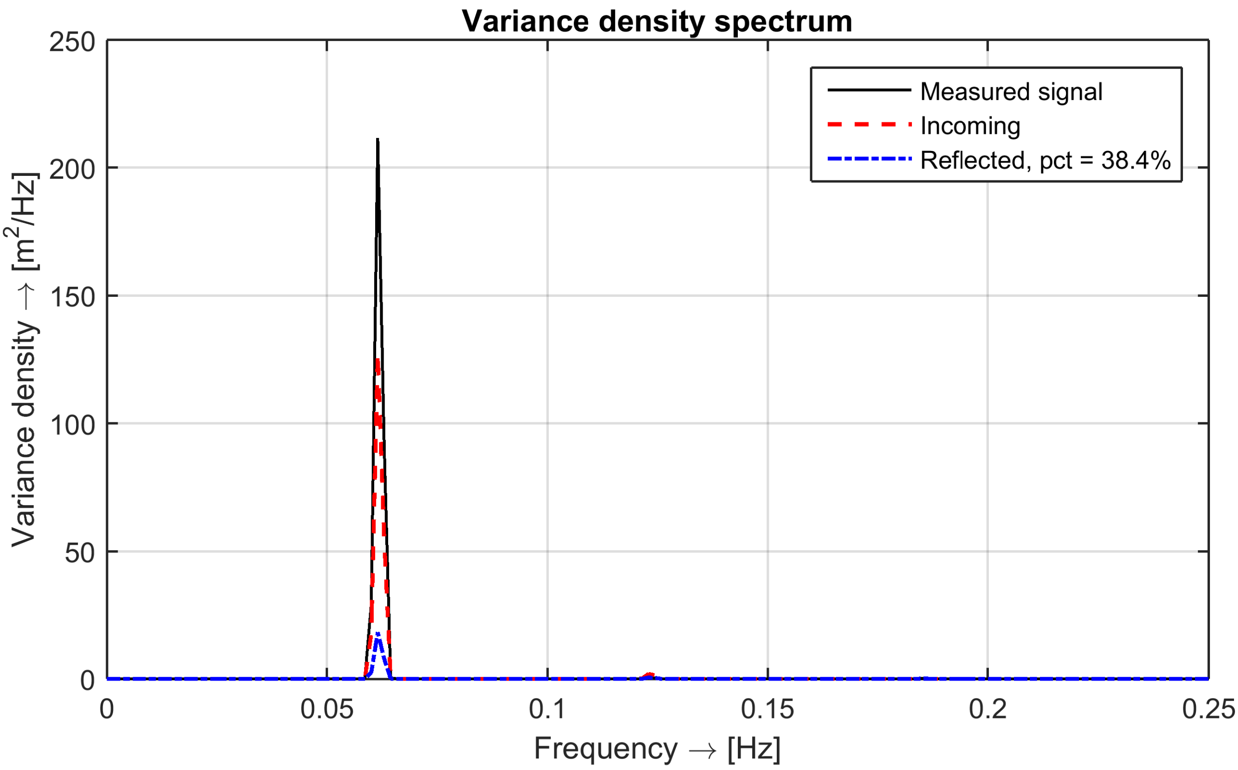

Reflection analysis using WHMs:01, 02 & 07	Monochromatic	M162c
Deltares	11202696	App. E.4.06

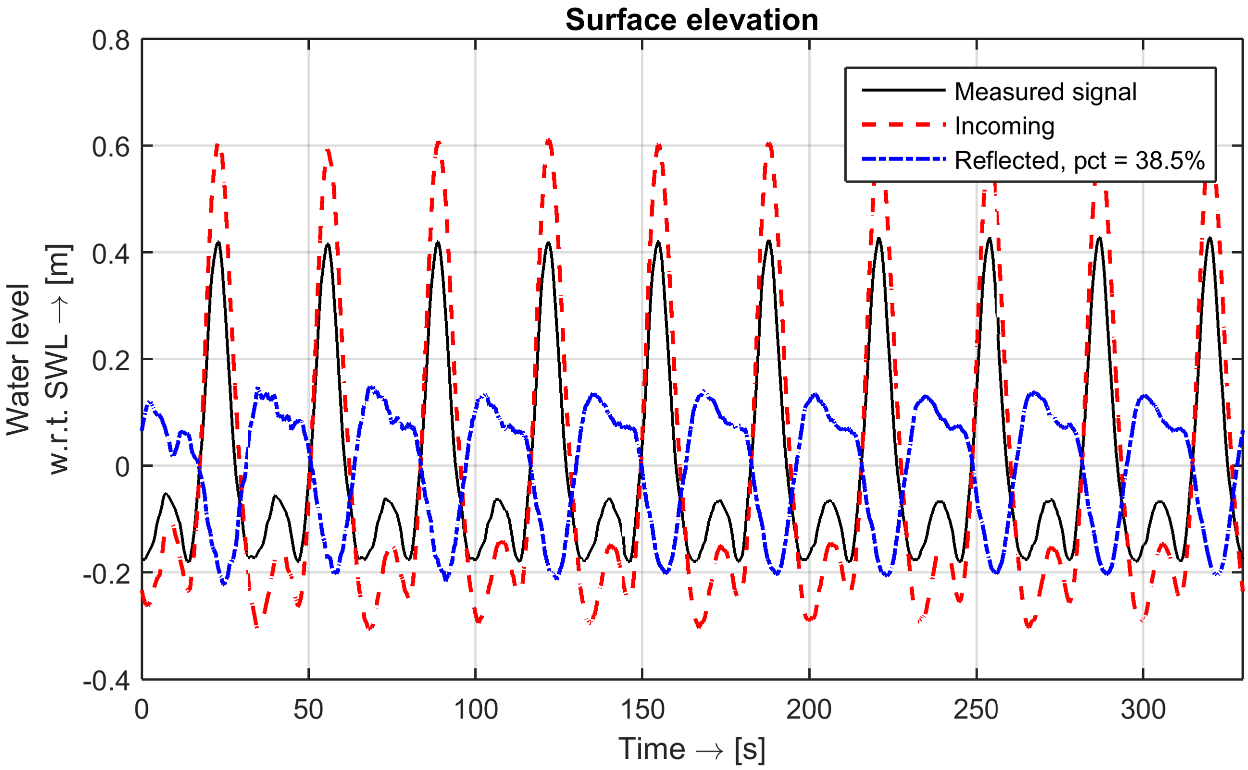

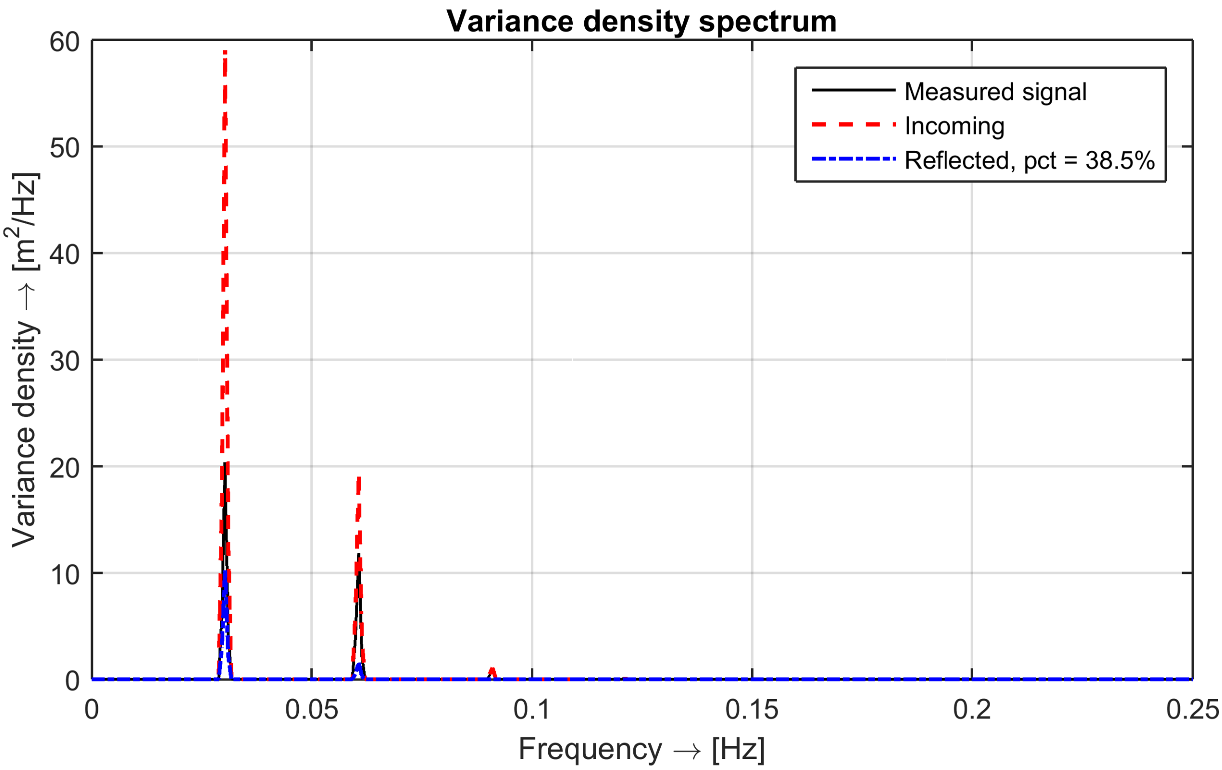

Reflection analysis using WHMs:01, 02 & 07	Monochromatic	M330a
Deltares	11202696	App. E.4.07

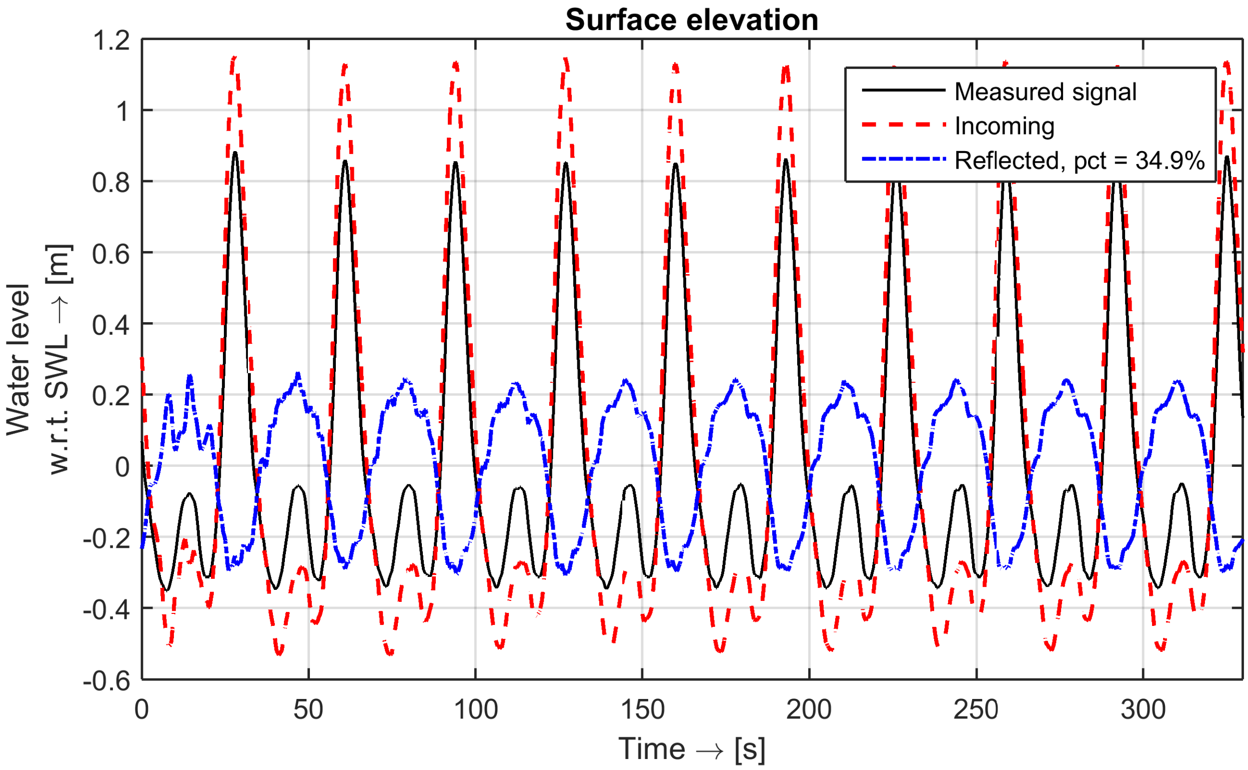

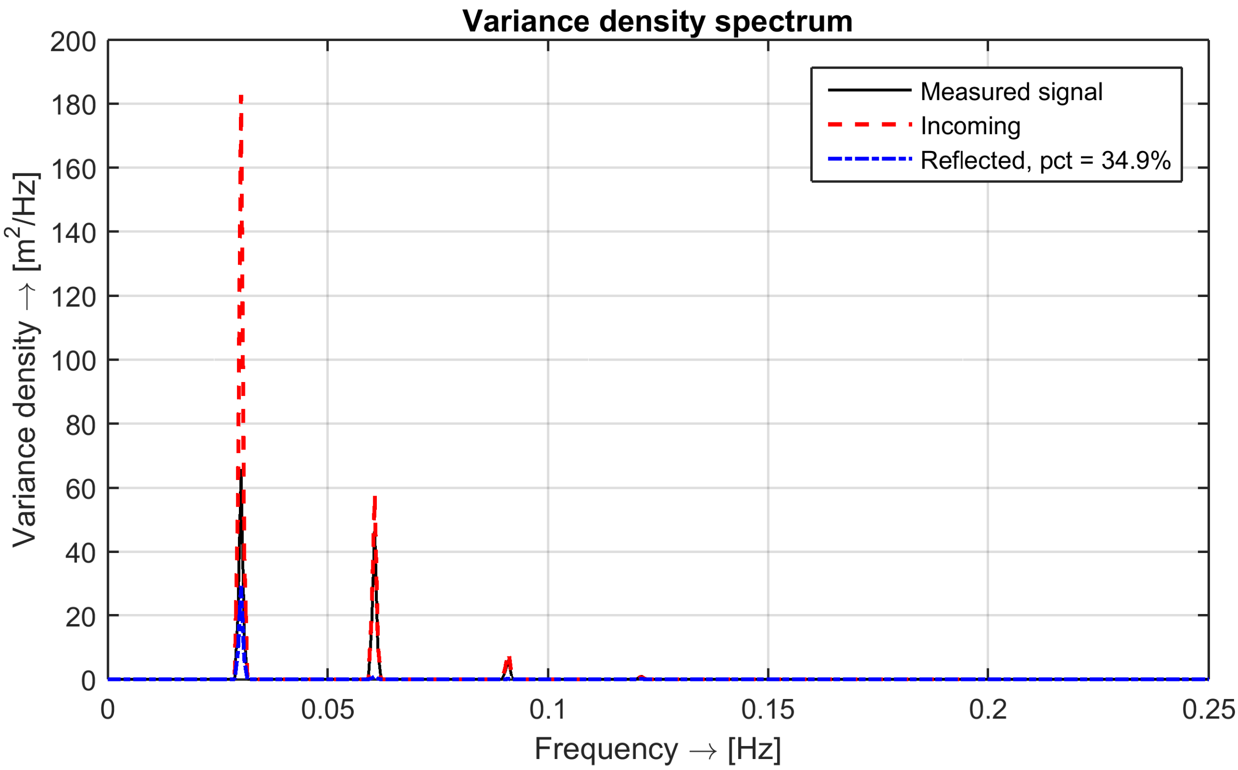

Reflection analysis using WHMs:01, 02 & 07	Monochromatic	M330b
Deltares	11202696	App. E.4.08

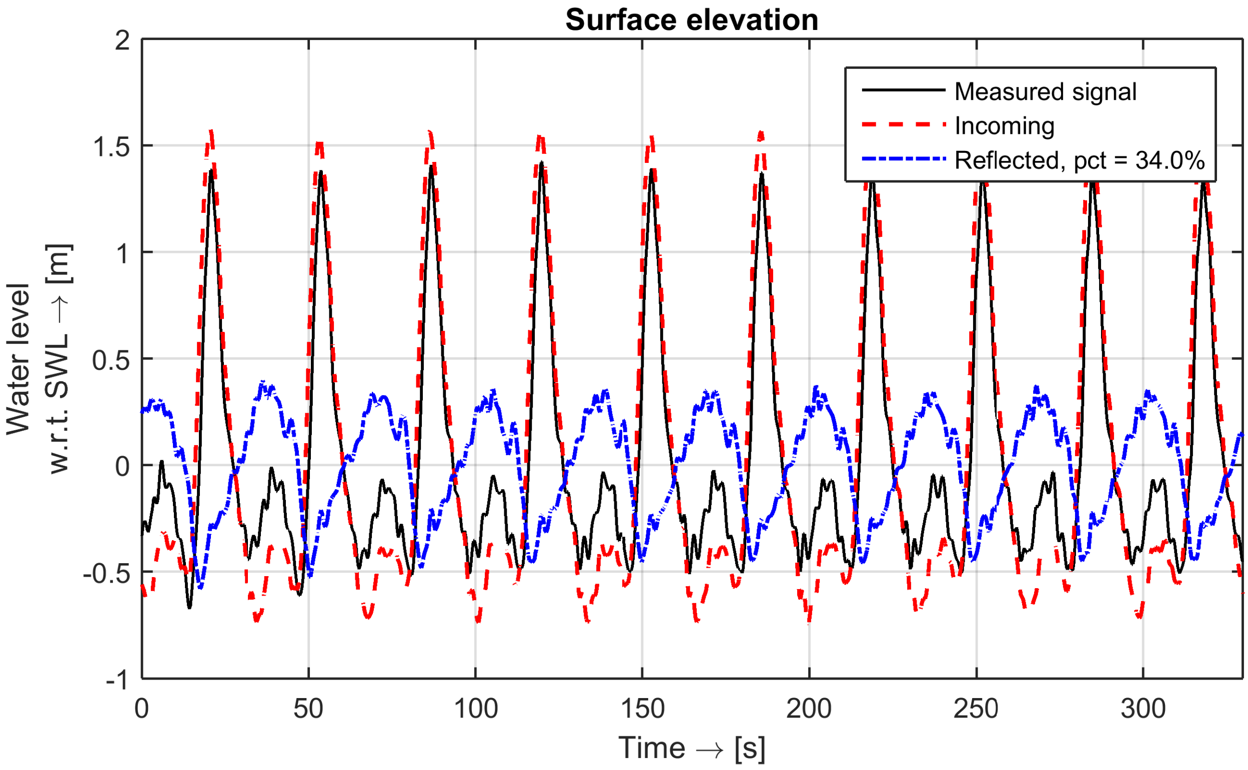

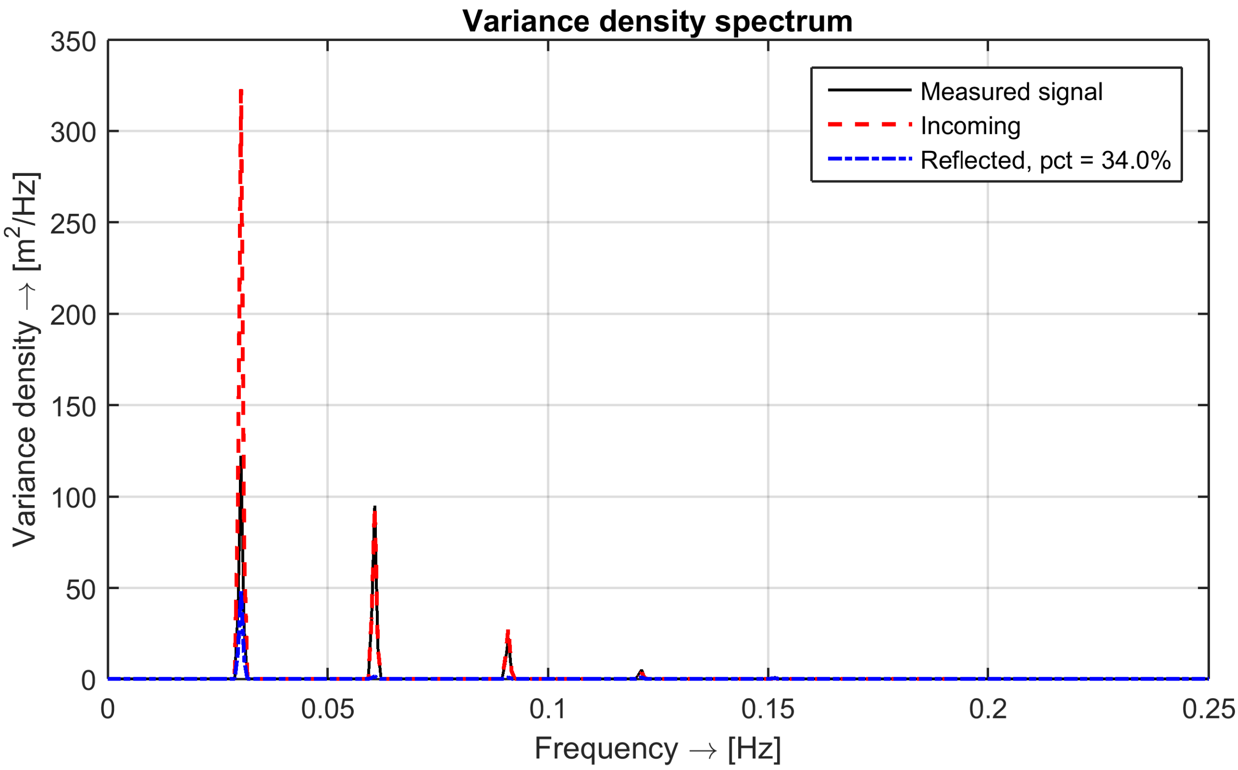

Reflection analysis using WHMs:01, 02 & 07	Monochromatic	M330c
Deltares	11202696	App. E.4.09

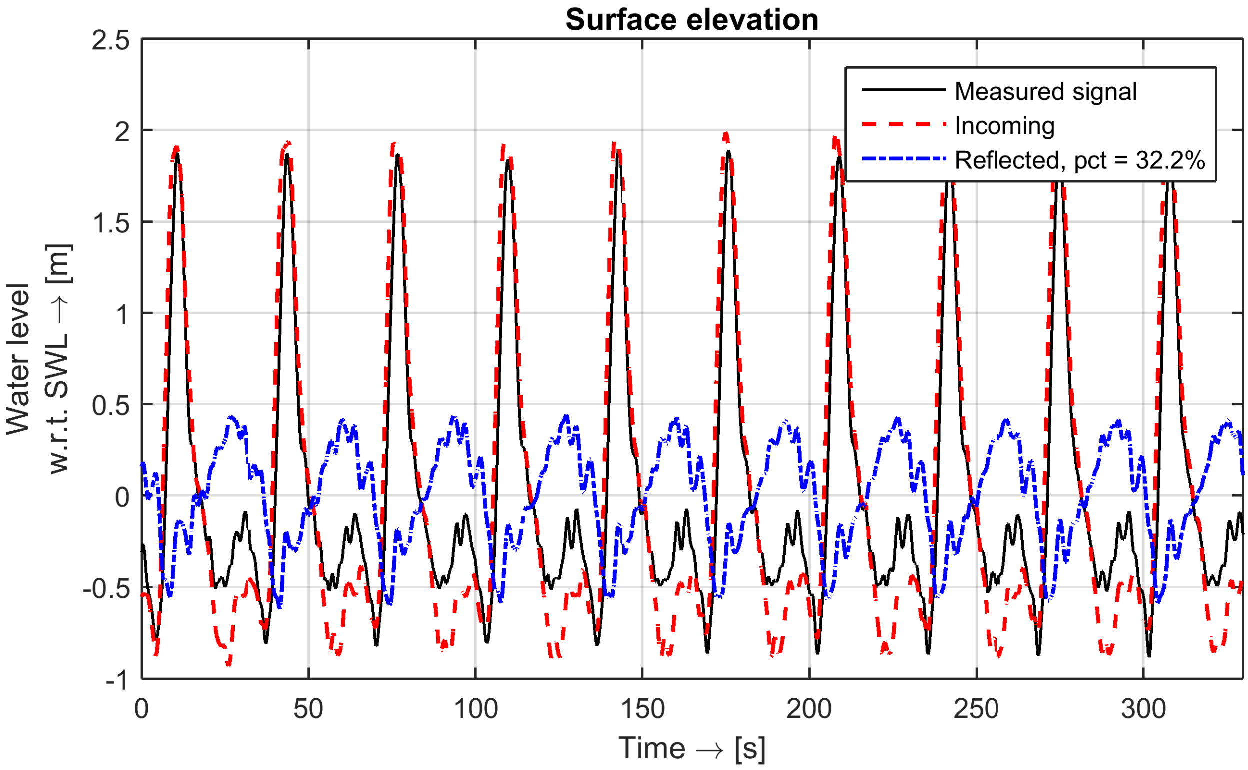

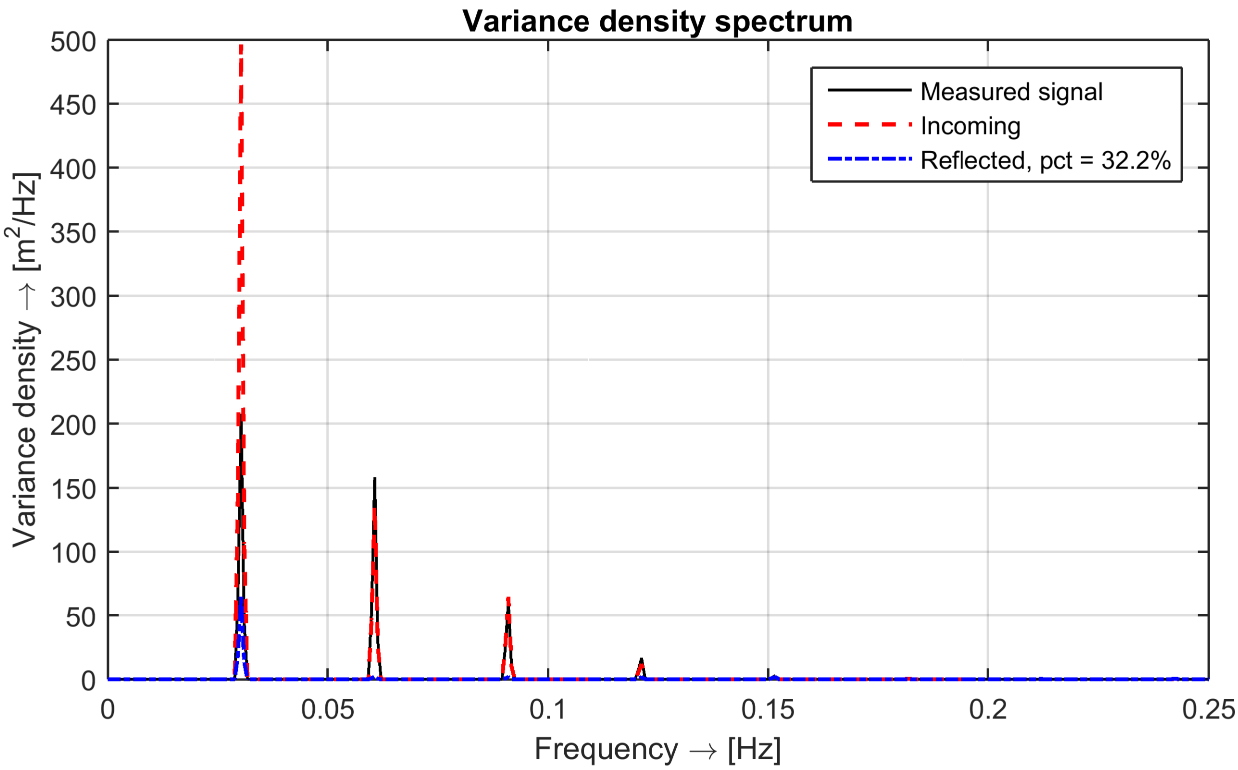

Reflection analysis using WHMs:01, 02 & 07	Monochromatic	M330d
Deltares	11202696	App. E.4.10

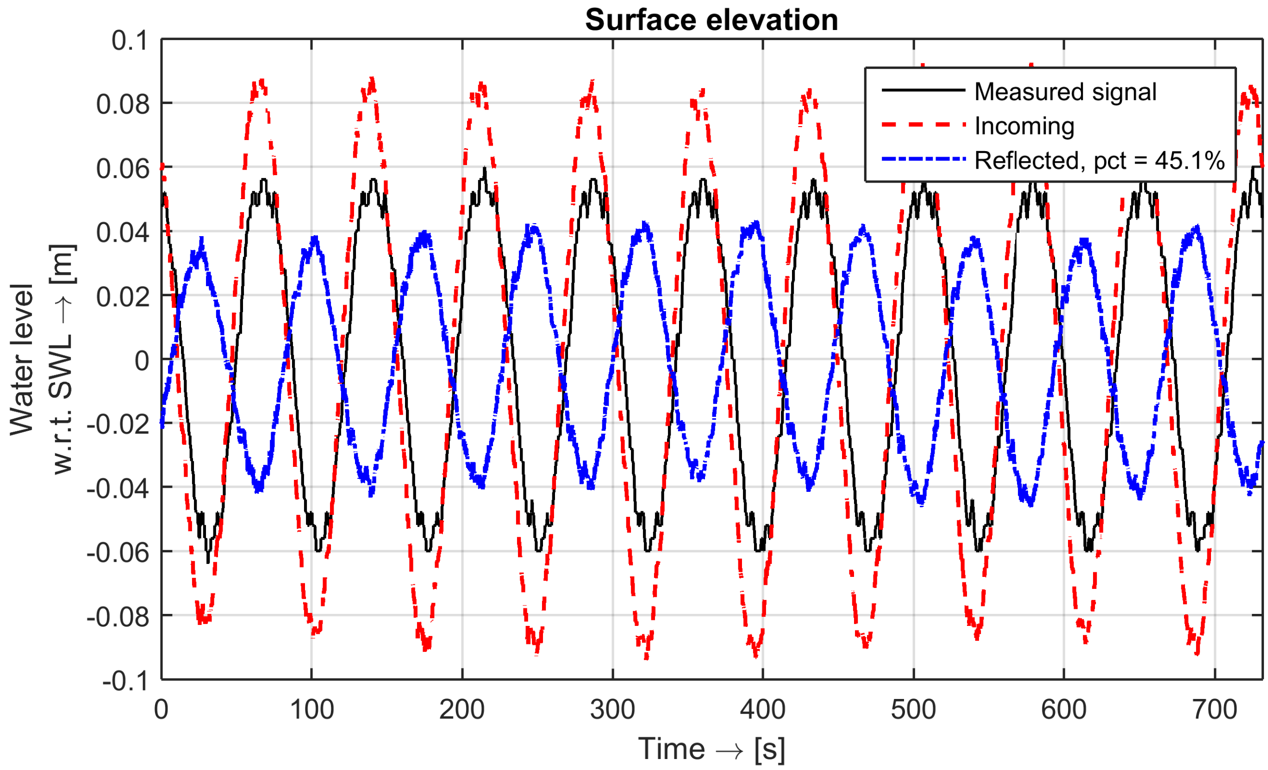

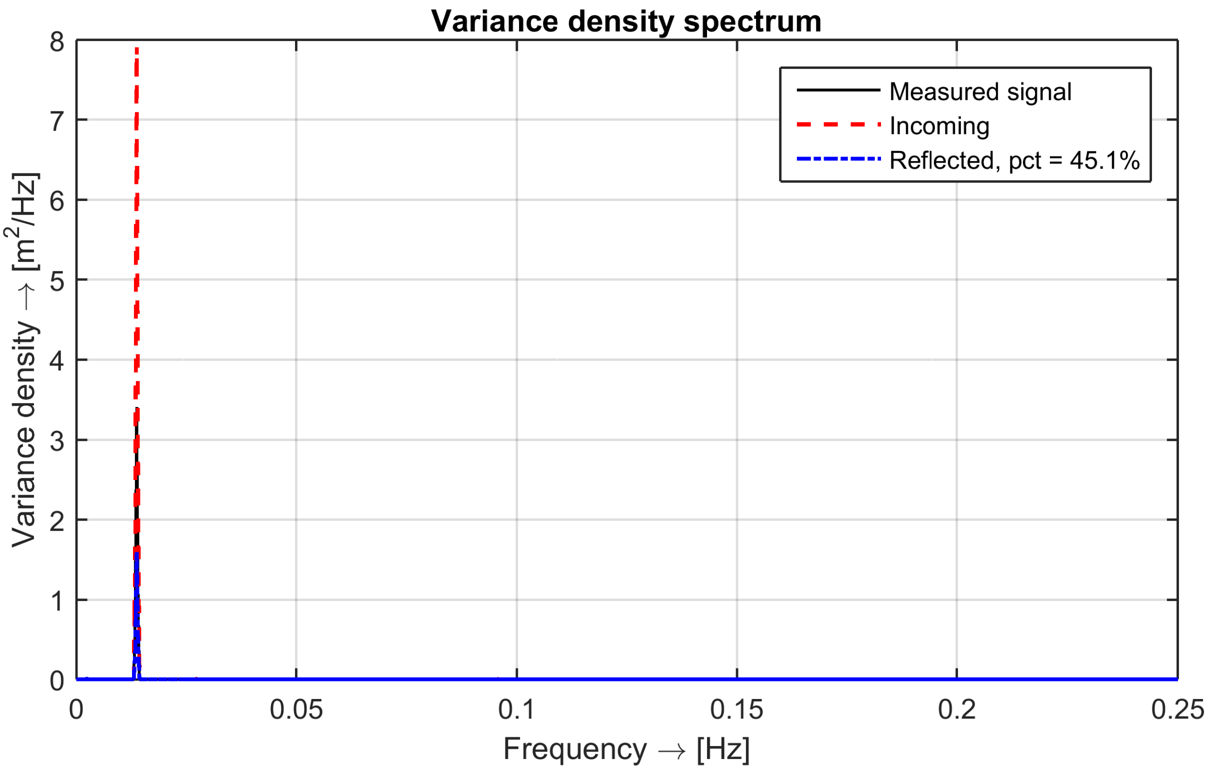

Reflection analysis using WHMs:01, 07 & 09	Monochromatic	M7312a
Deltares	11202696	App. E.4.11

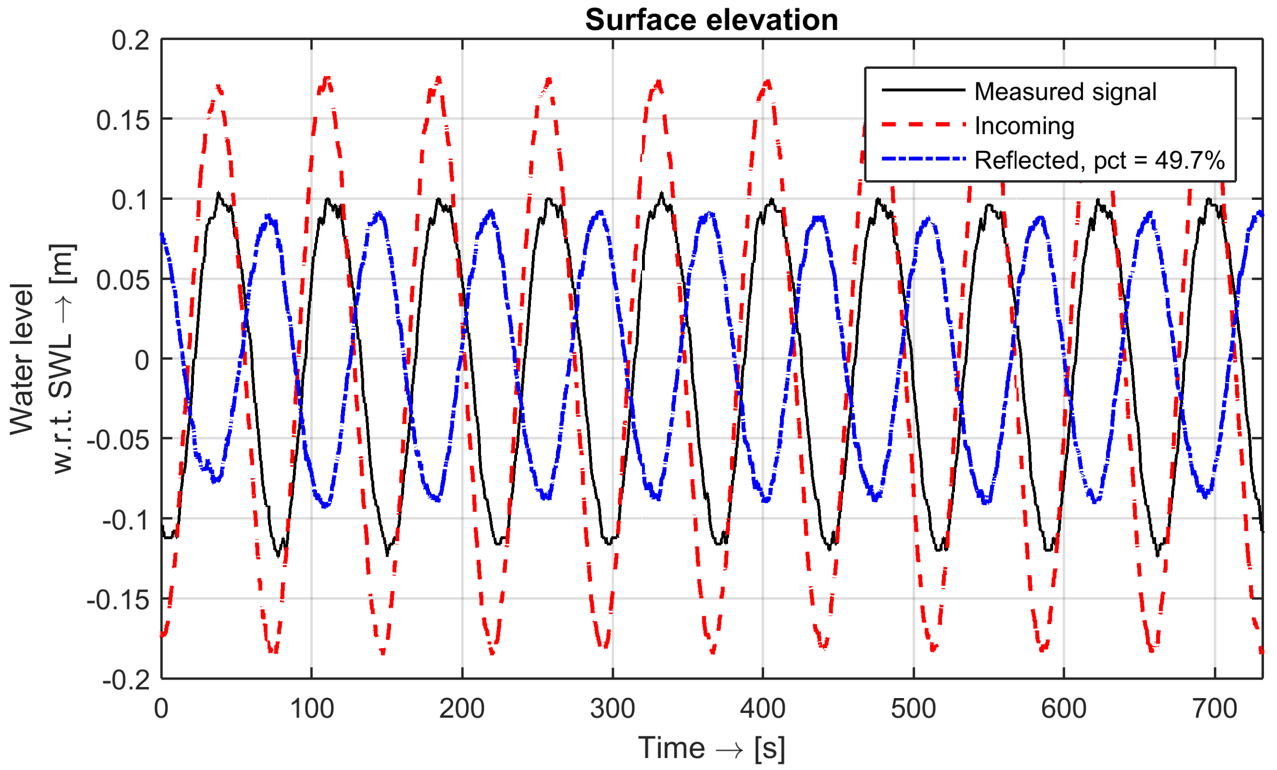

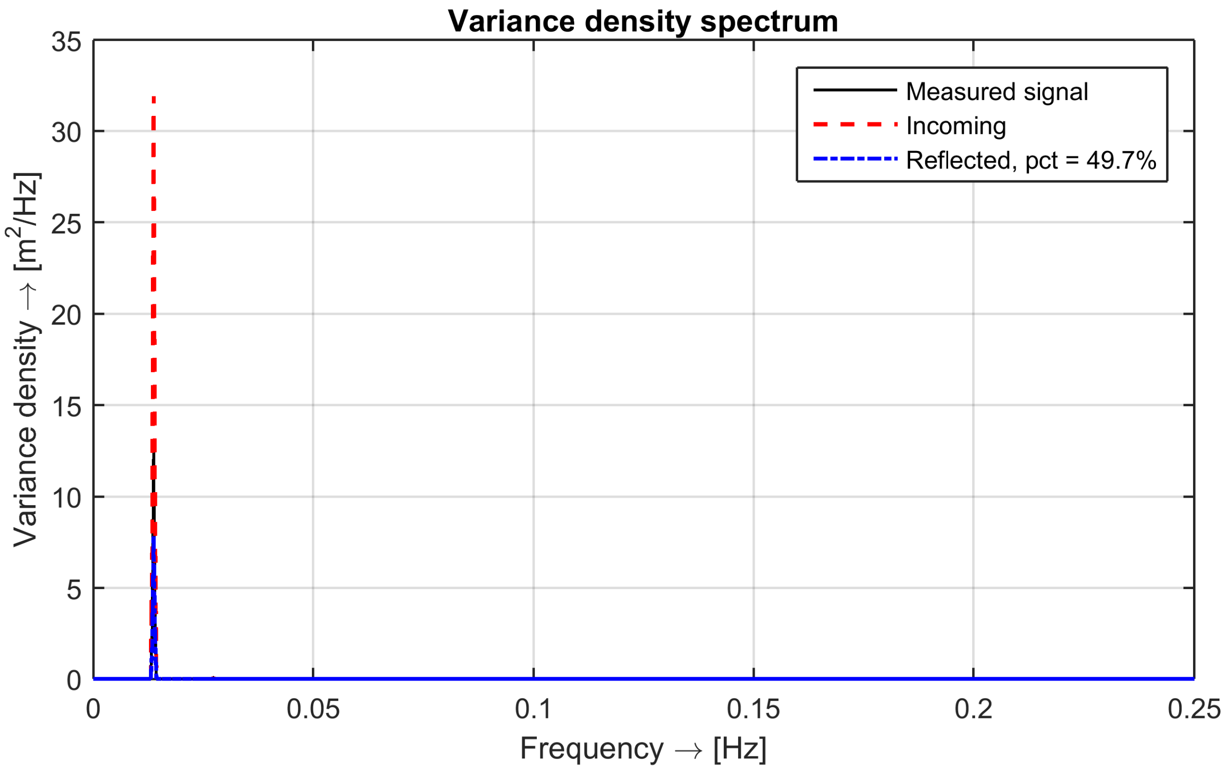

Reflection analysis using WHMs:01, 07 & 09	Monochromatic	M7312b
Deltares	11202696	App. E.4.12

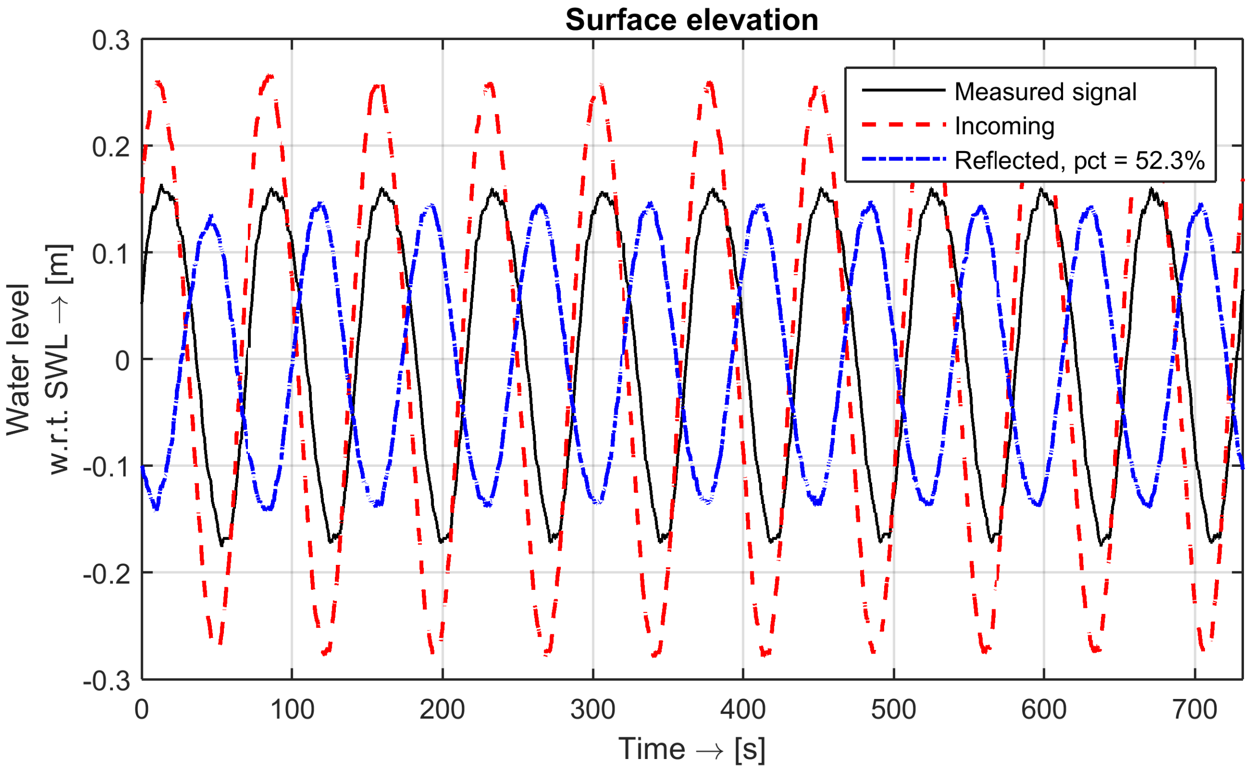

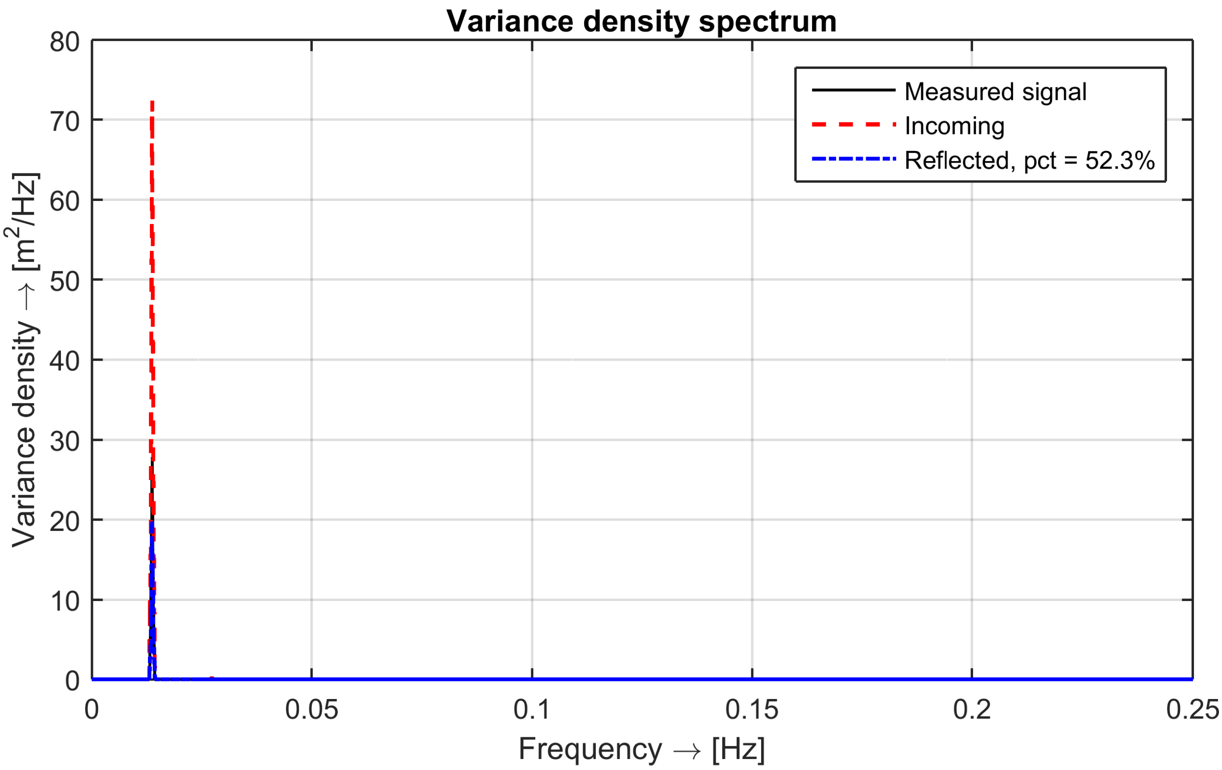

Reflection analysis using WHMs:01, 07 & 09	Monochromatic	M7312c
Deltares	11202696	App. E.4.13

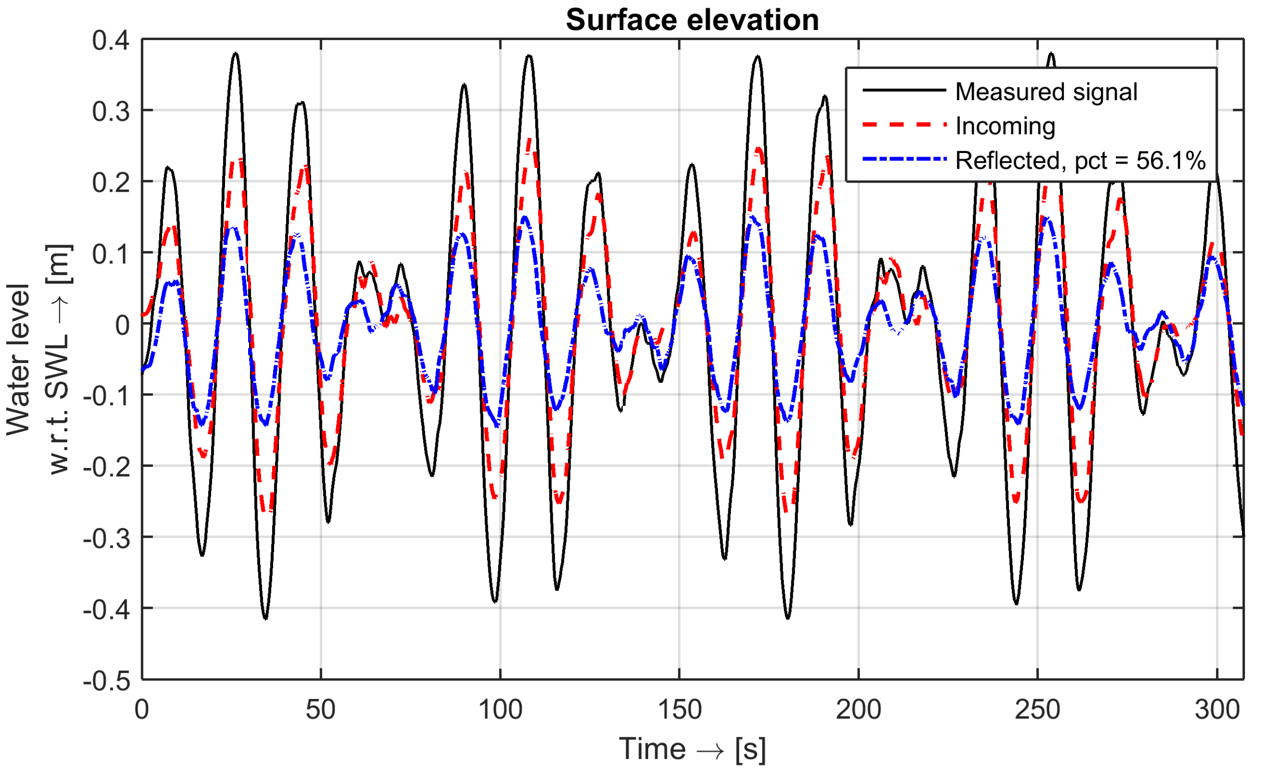

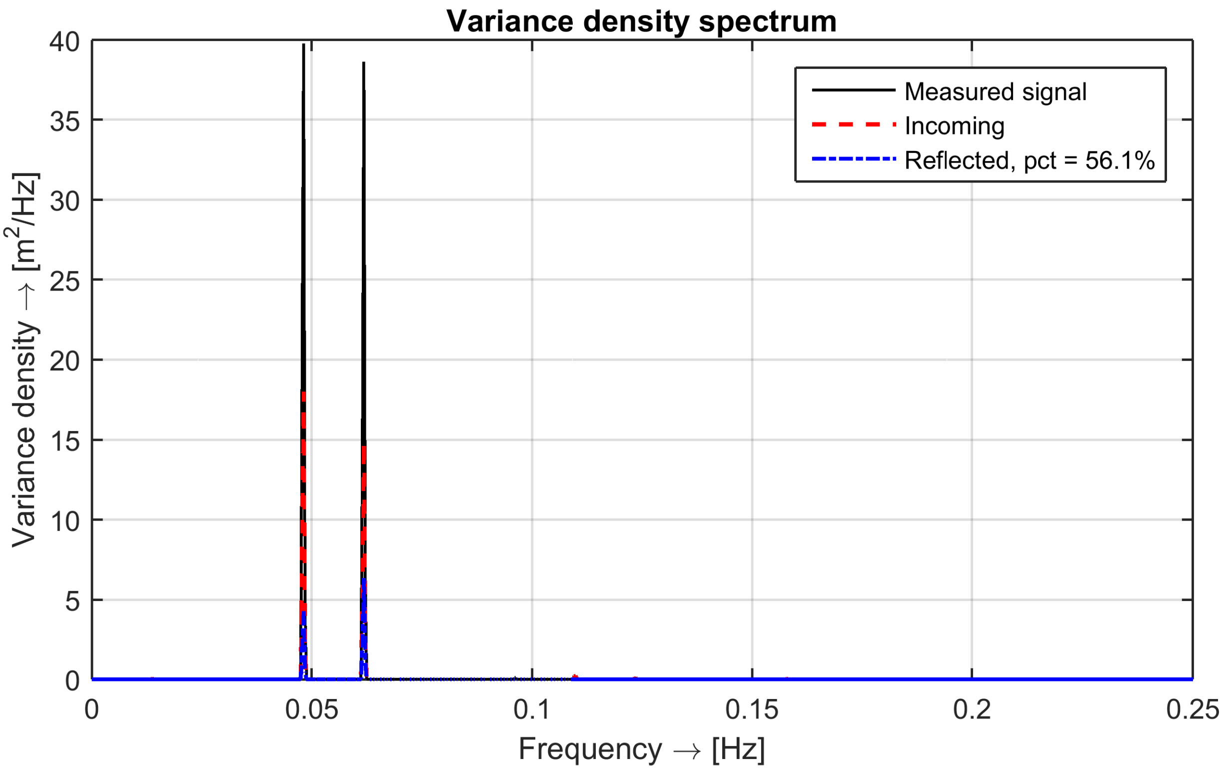

Reflection analysis using WHMs:01, 02 & 07	Bichromatic	B7312a
Deltares	11202696	App. E.4.14

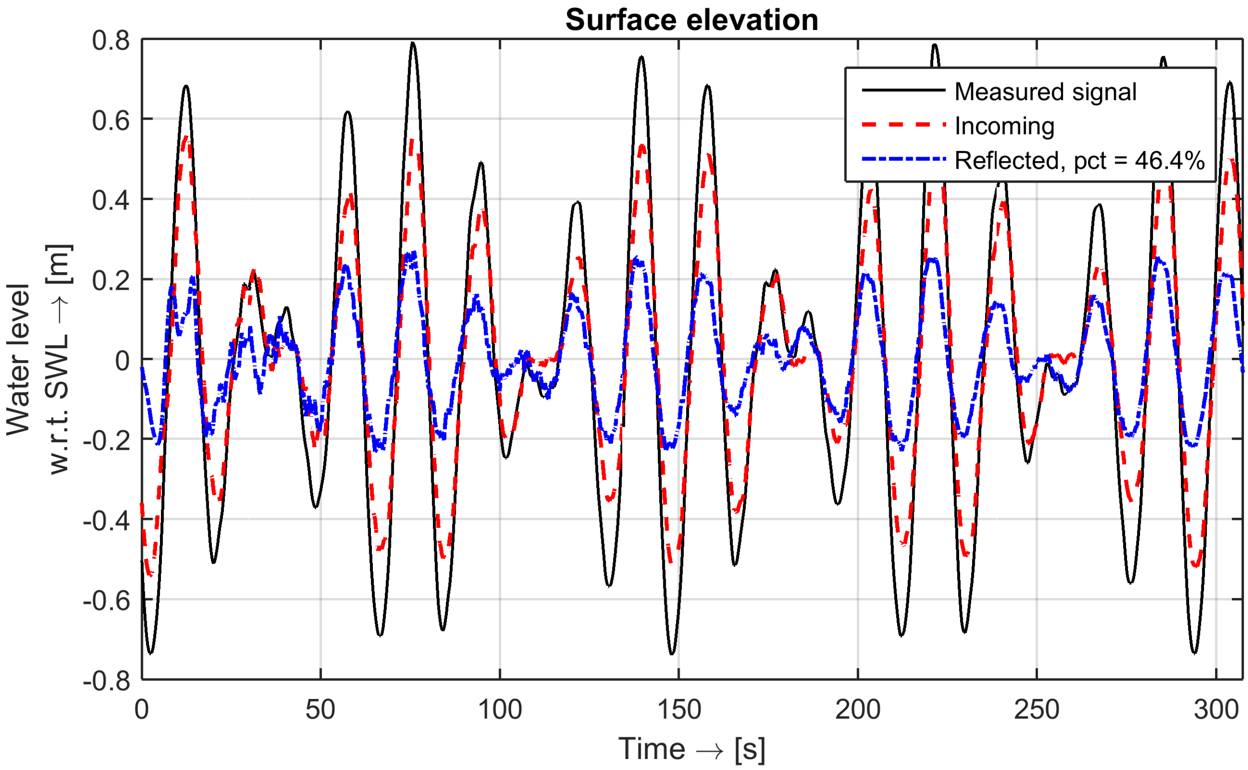

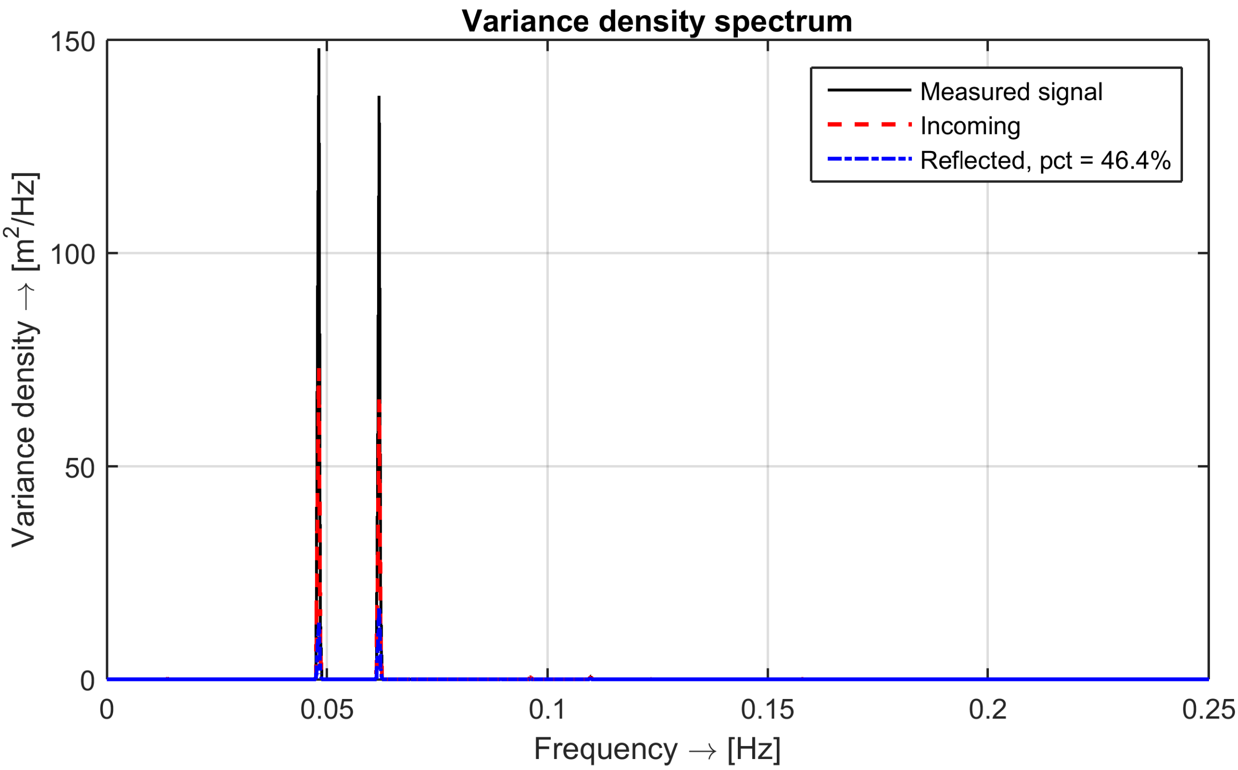

Reflection analysis using WHMs:01, 02 & 07	Bichromatic	B7312b
Deltares	11202696	App. E.4.15

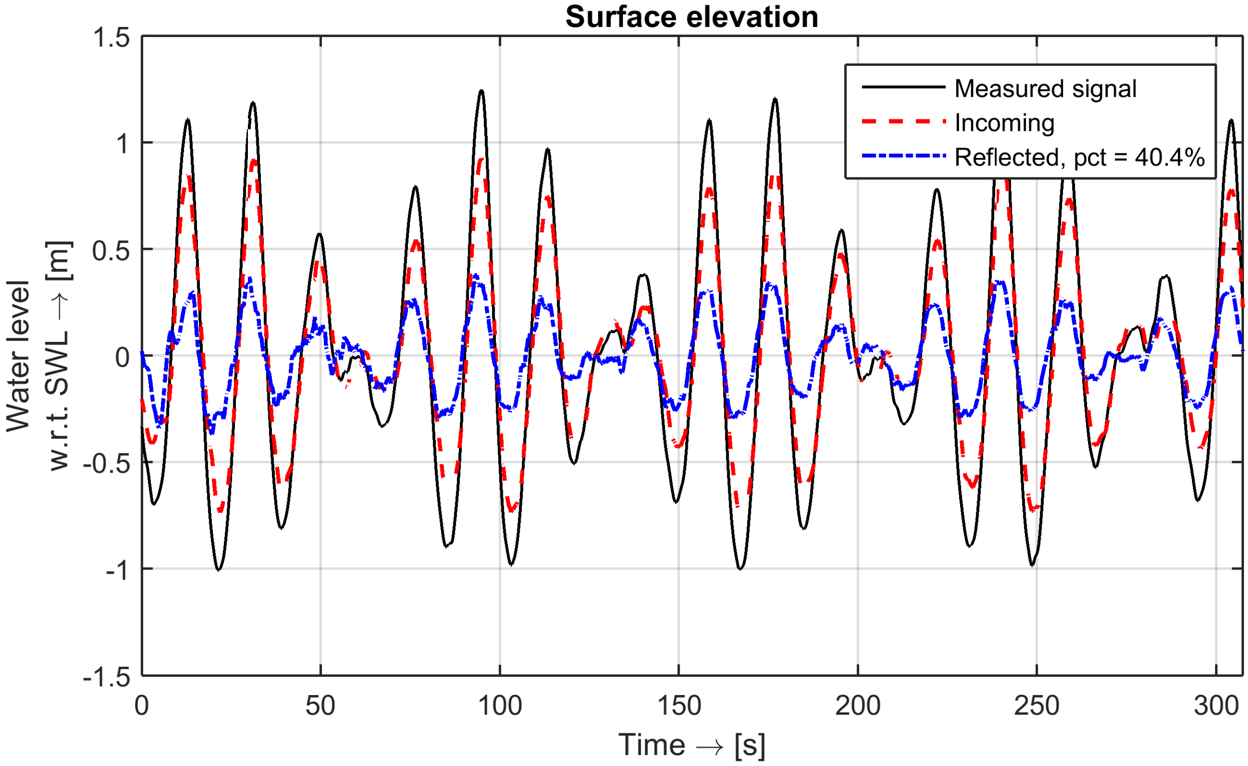

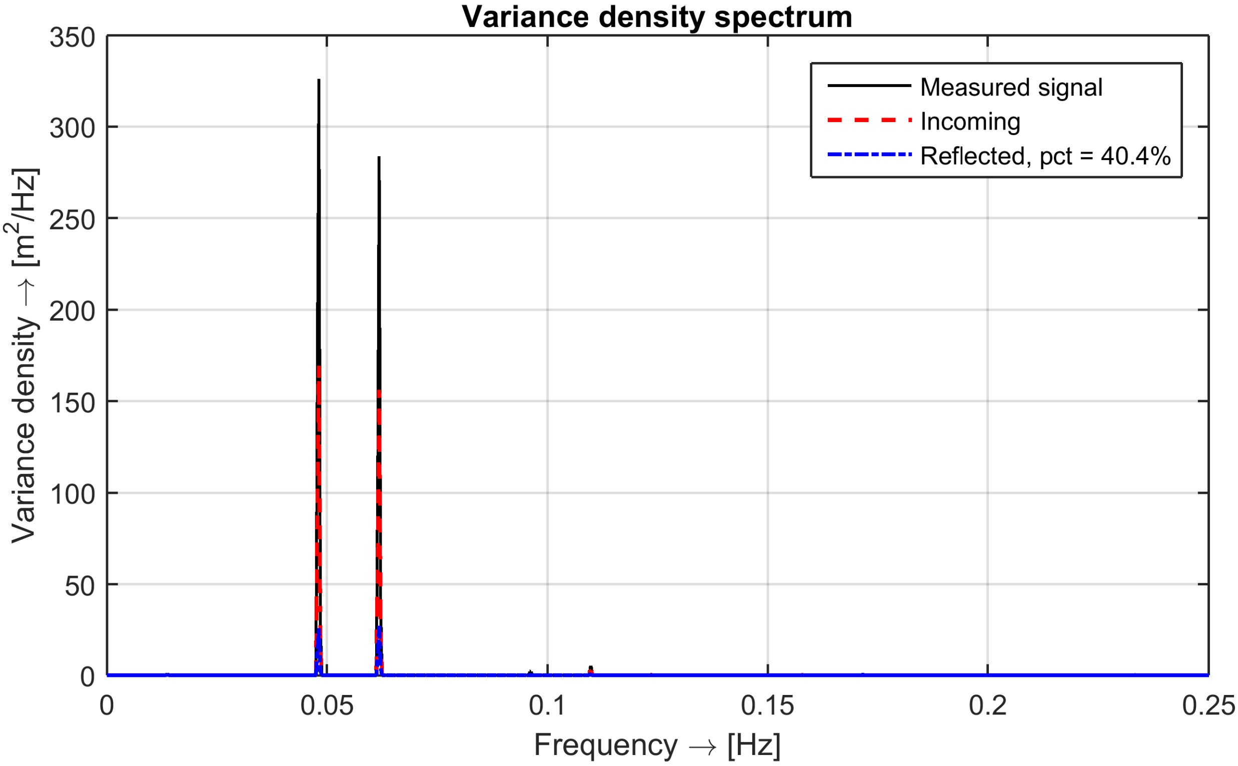

Reflection analysis using WHMs:01, 02 & 07	Bichromatic	B7312c
Deltares	11202696	App. E.4.16

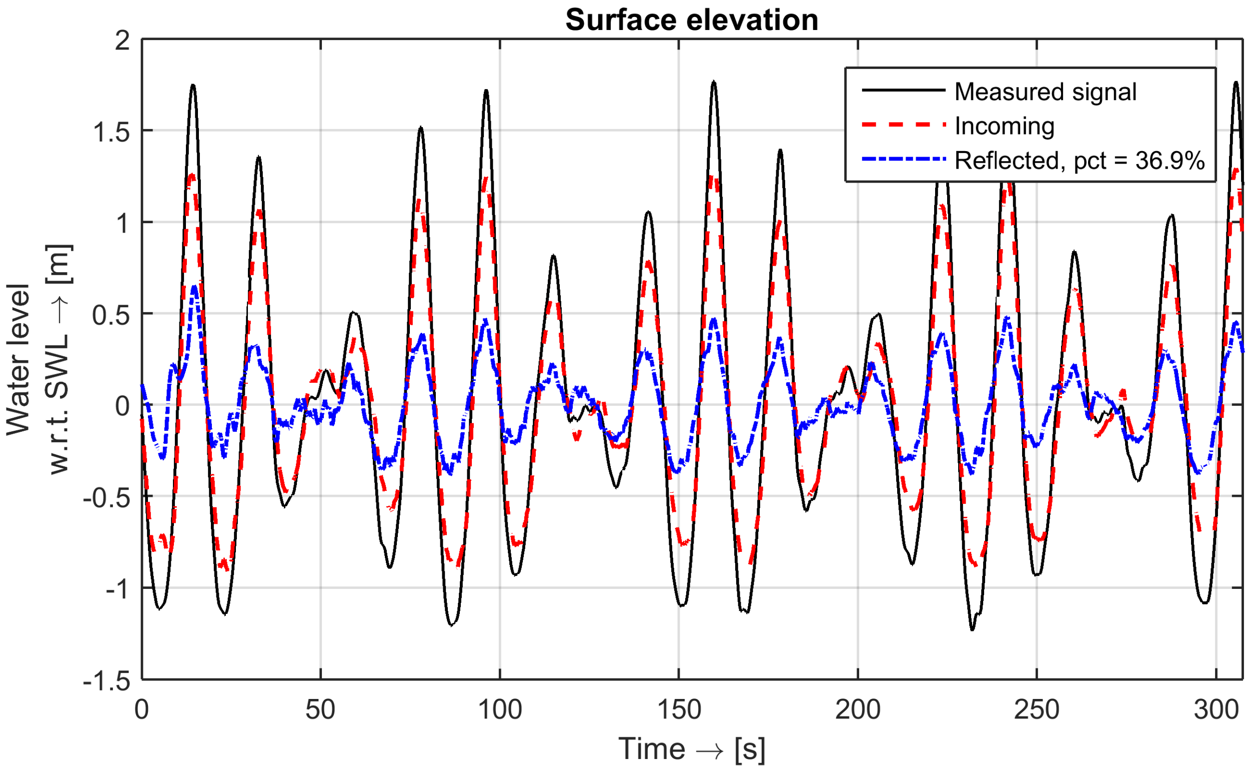

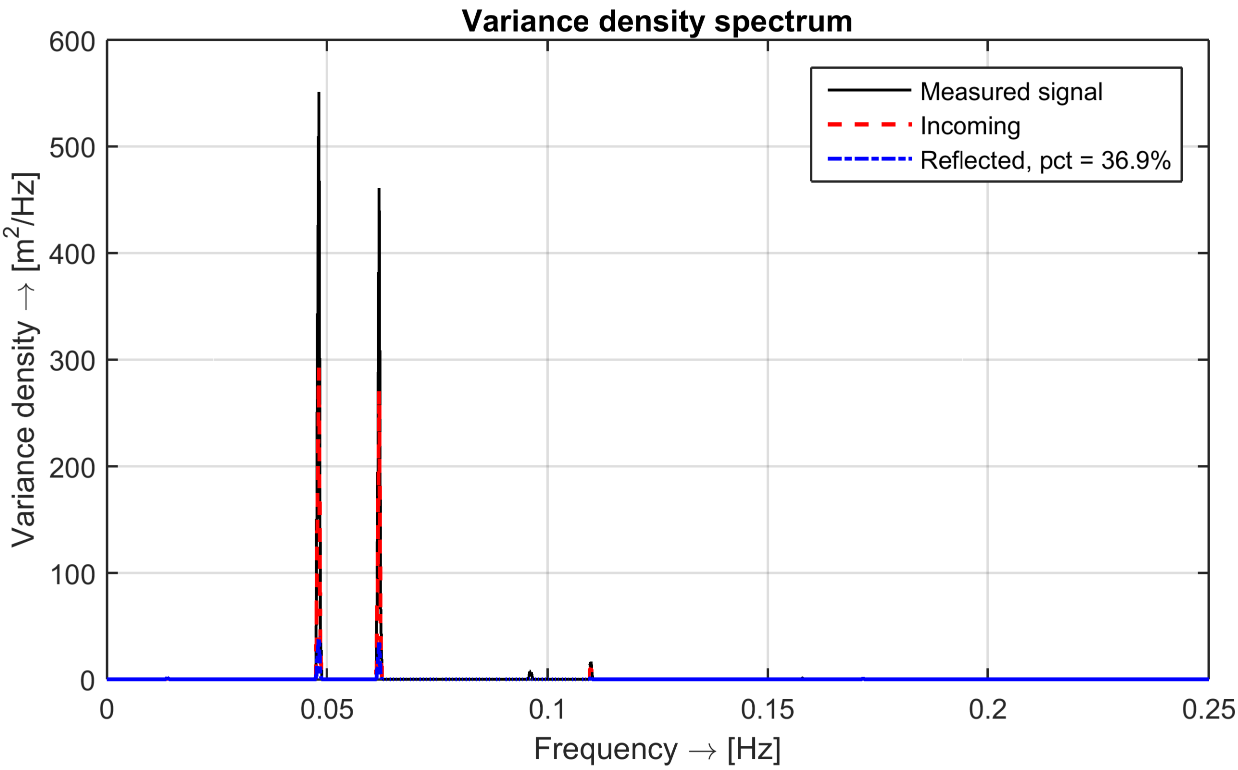

Reflection analysis using WHMs:01, 02 & 07	Bichromatic	B7312d
Deltares	11202696	App. E.4.17

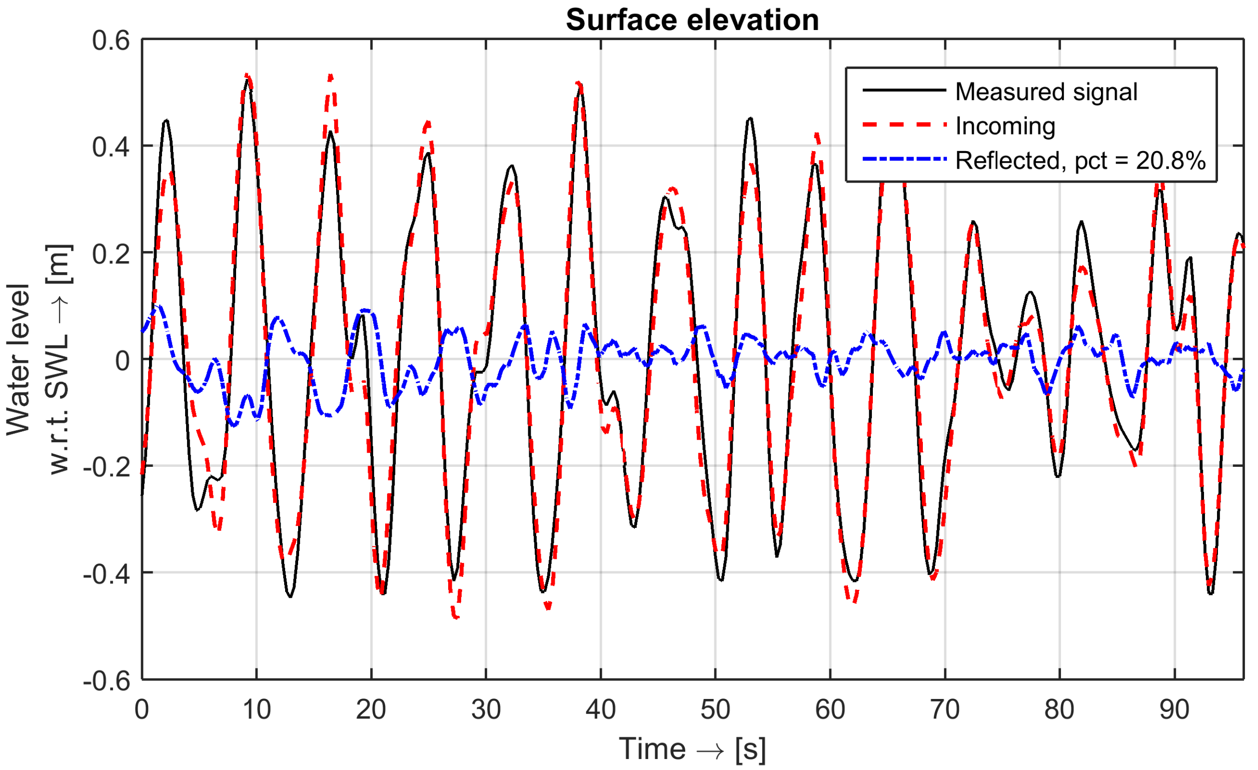

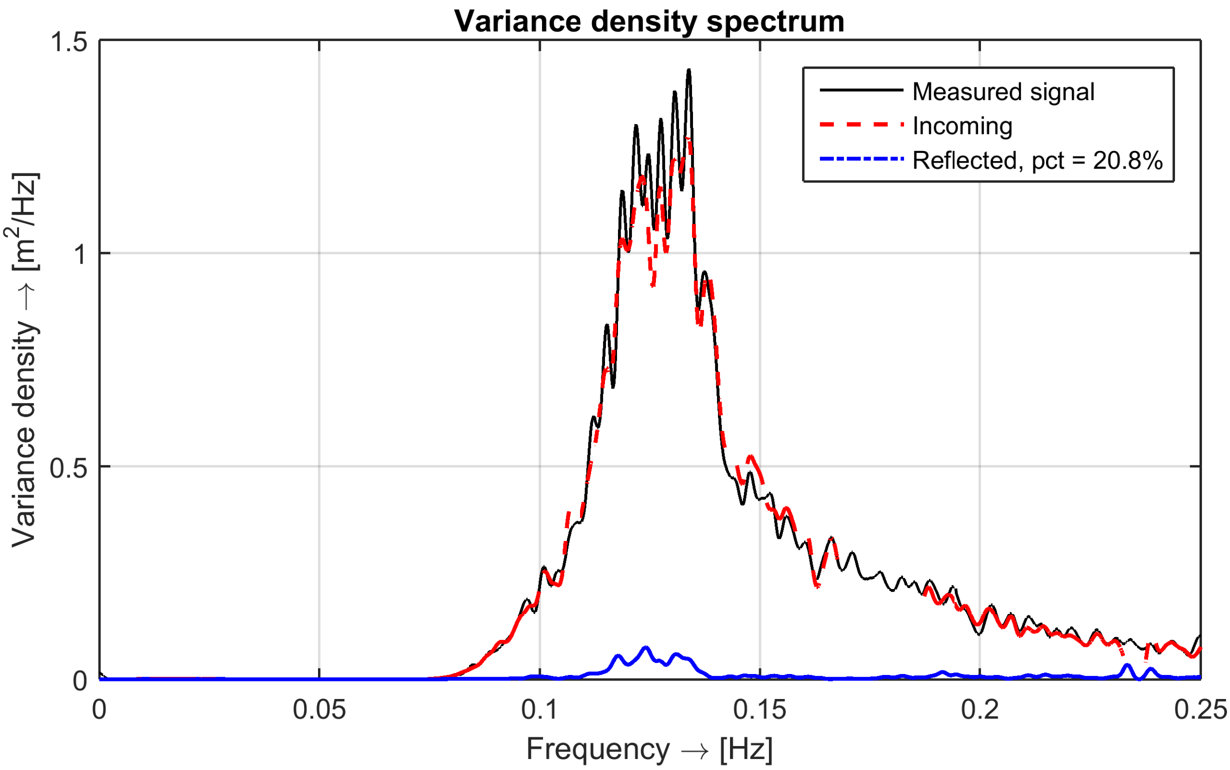

Reflection analysis using WHMs:01, 02 & 07	Irregular	I80a
Deltares	11202696	App. E.4.18

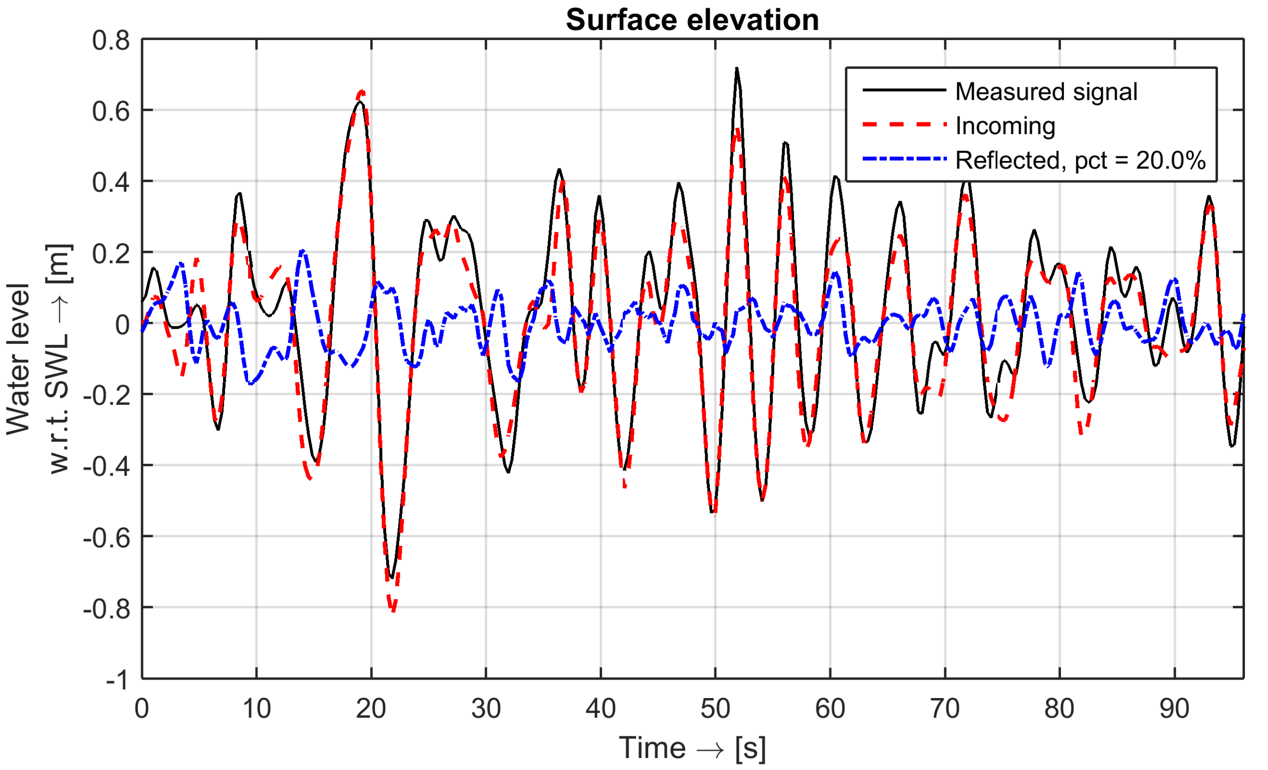

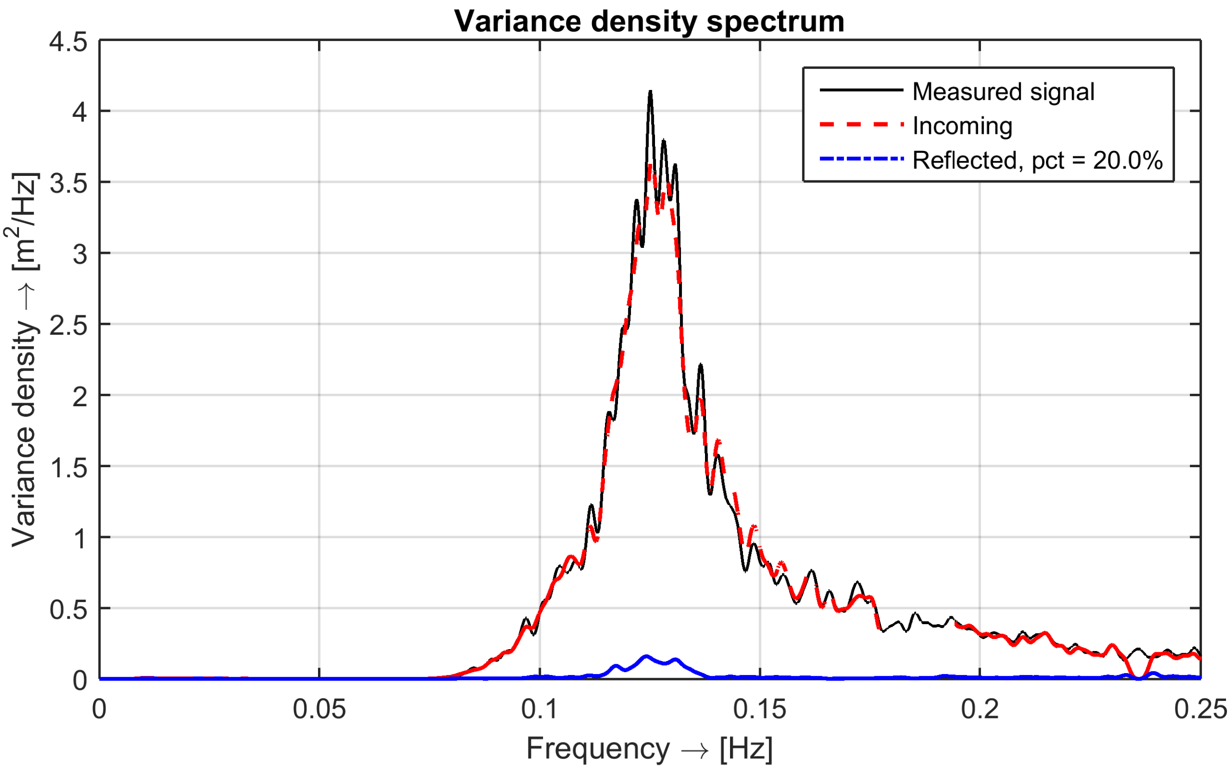

Reflection analysis using WHMs:01, 02 & 07	Irregular	I80b
Deltares	11202696	App. E.4.19

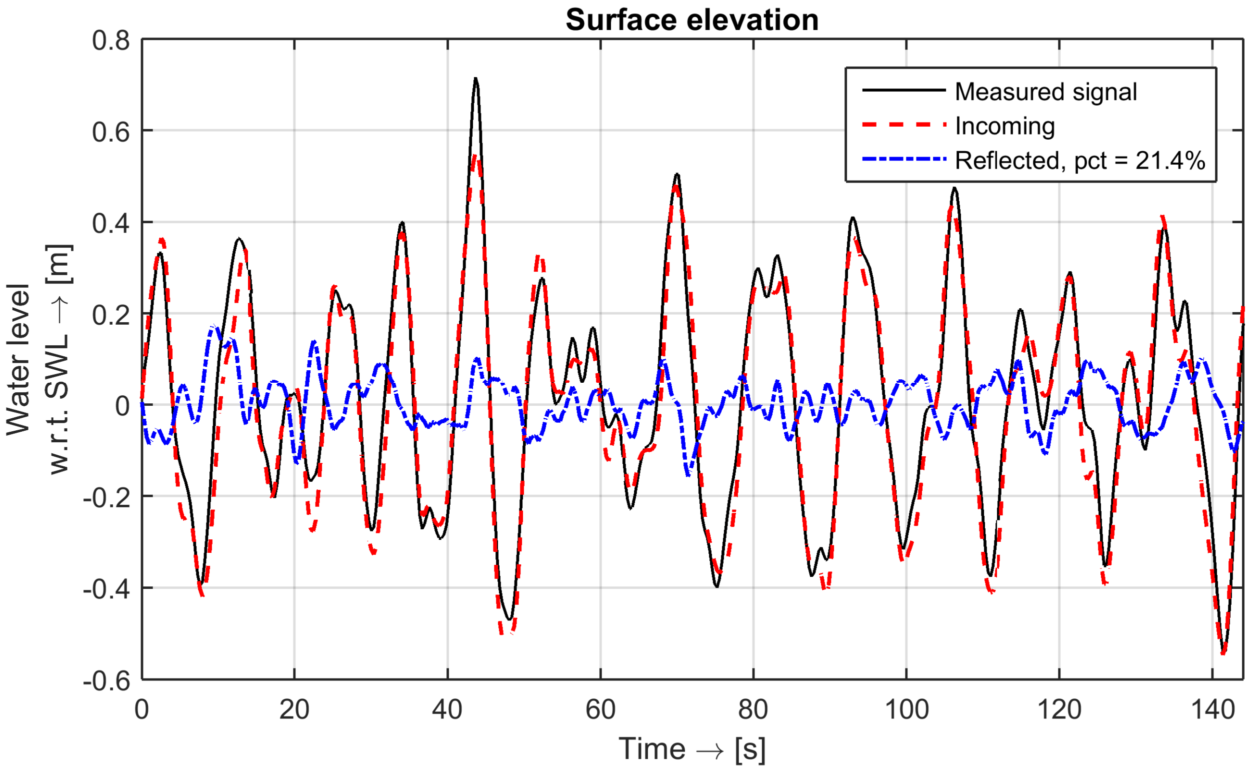

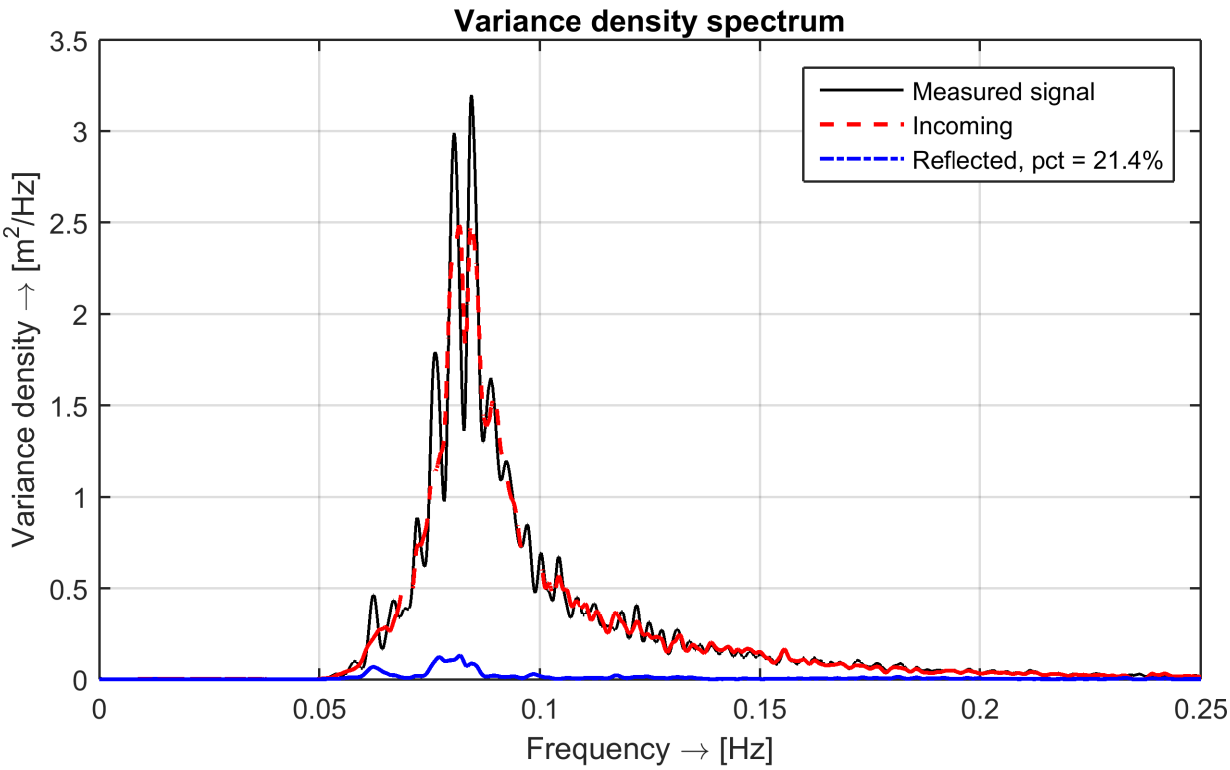

Reflection analysis using WHMs:01, 02 & 07	Irregular	I120a
Deltares	11202696	App. E.4.20

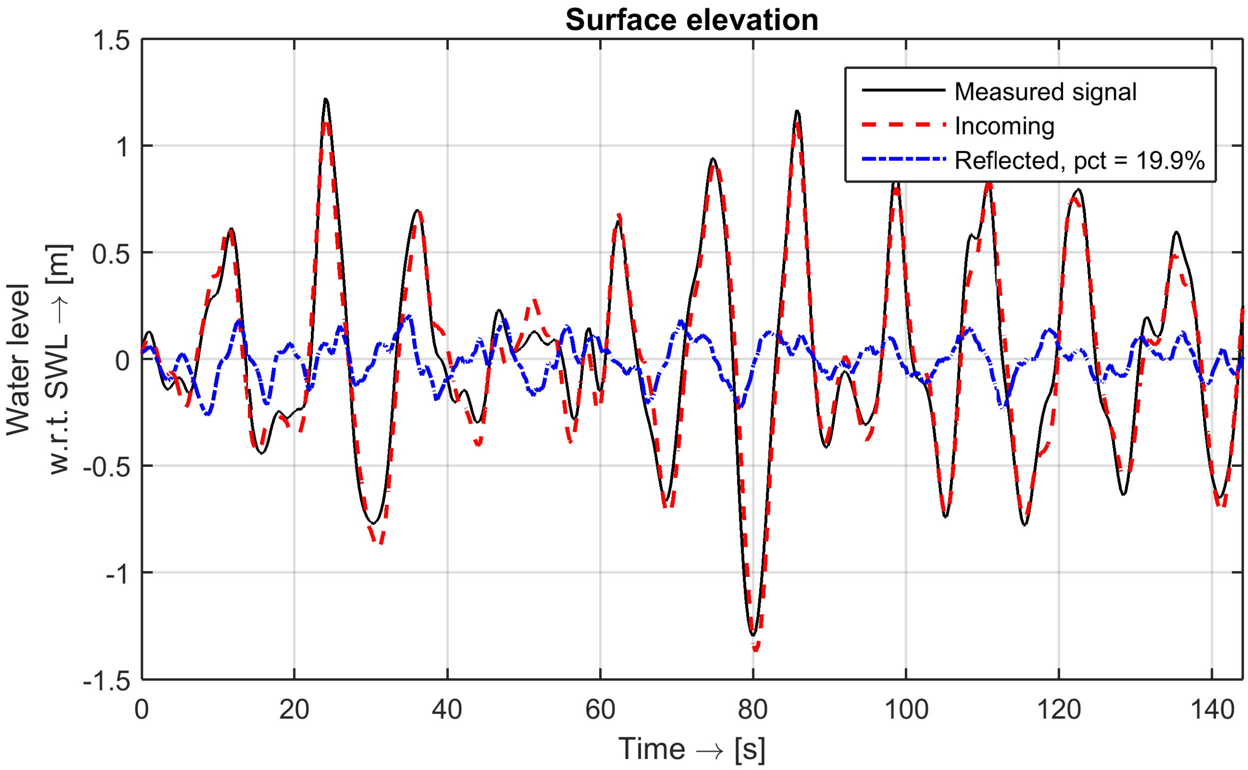

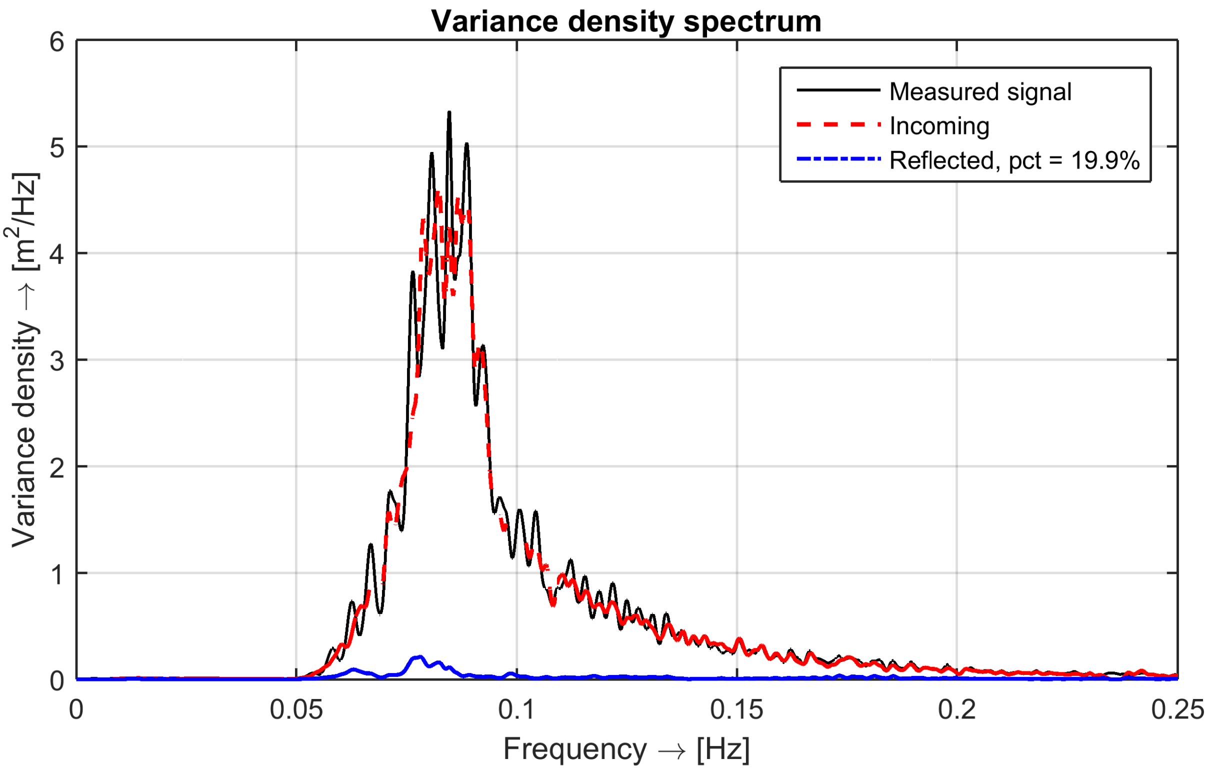

Reflection analysis using WHMs:01, 02 & 07	Irregular	I120b
Deltares	11202696	App. E.4.21

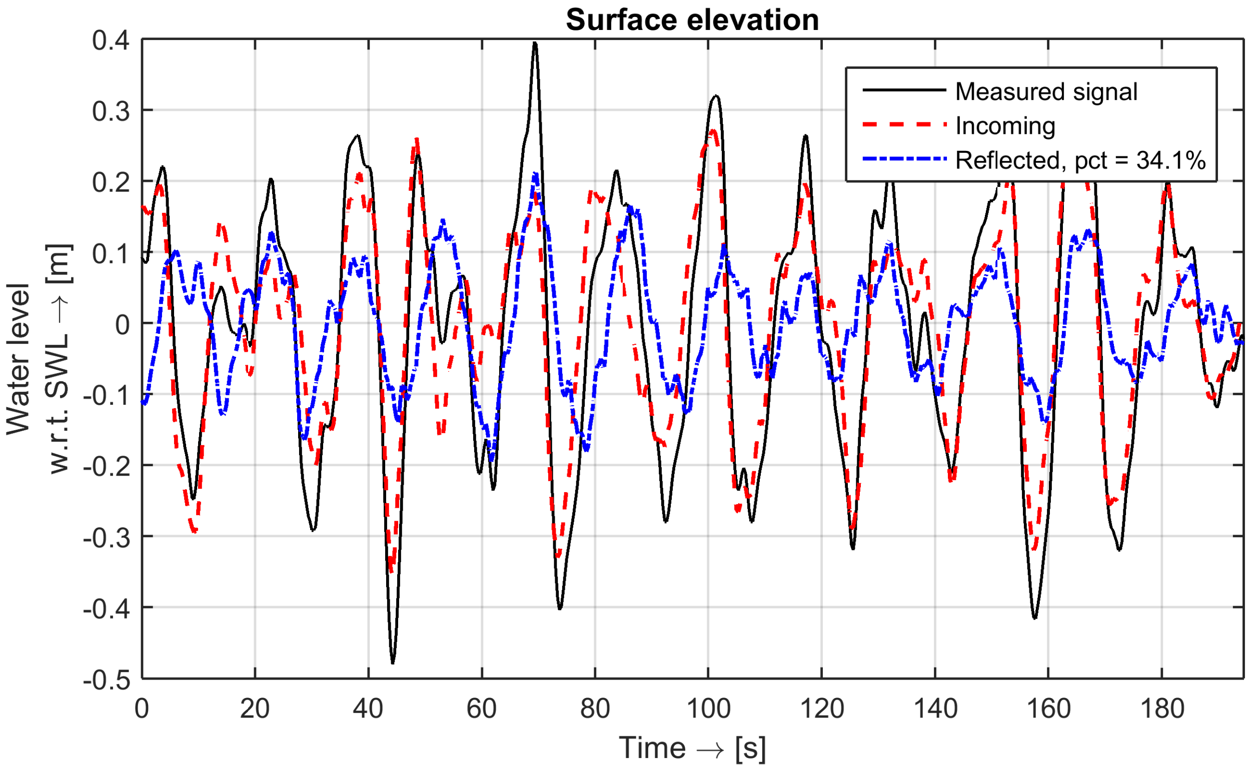

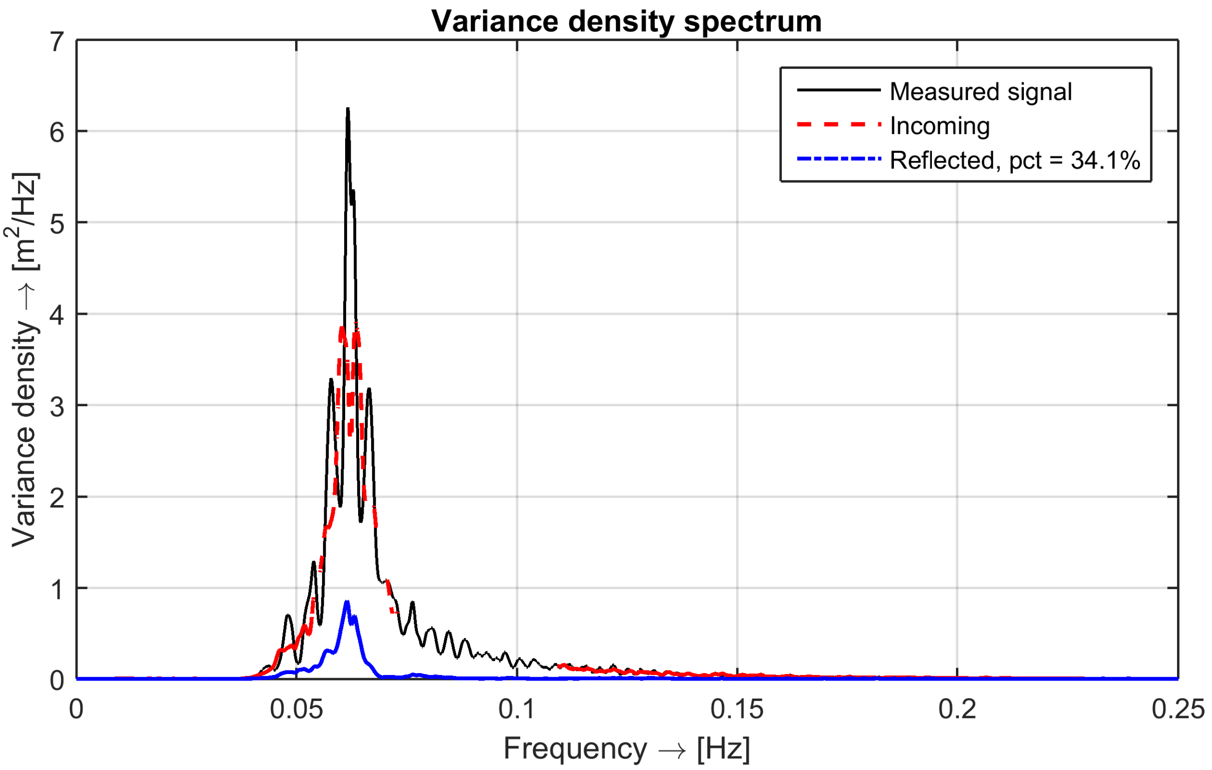

Reflection analysis using WHMs:01, 02 & 07	Irregular	I162a
Deltares	11202696	App. E.4.22

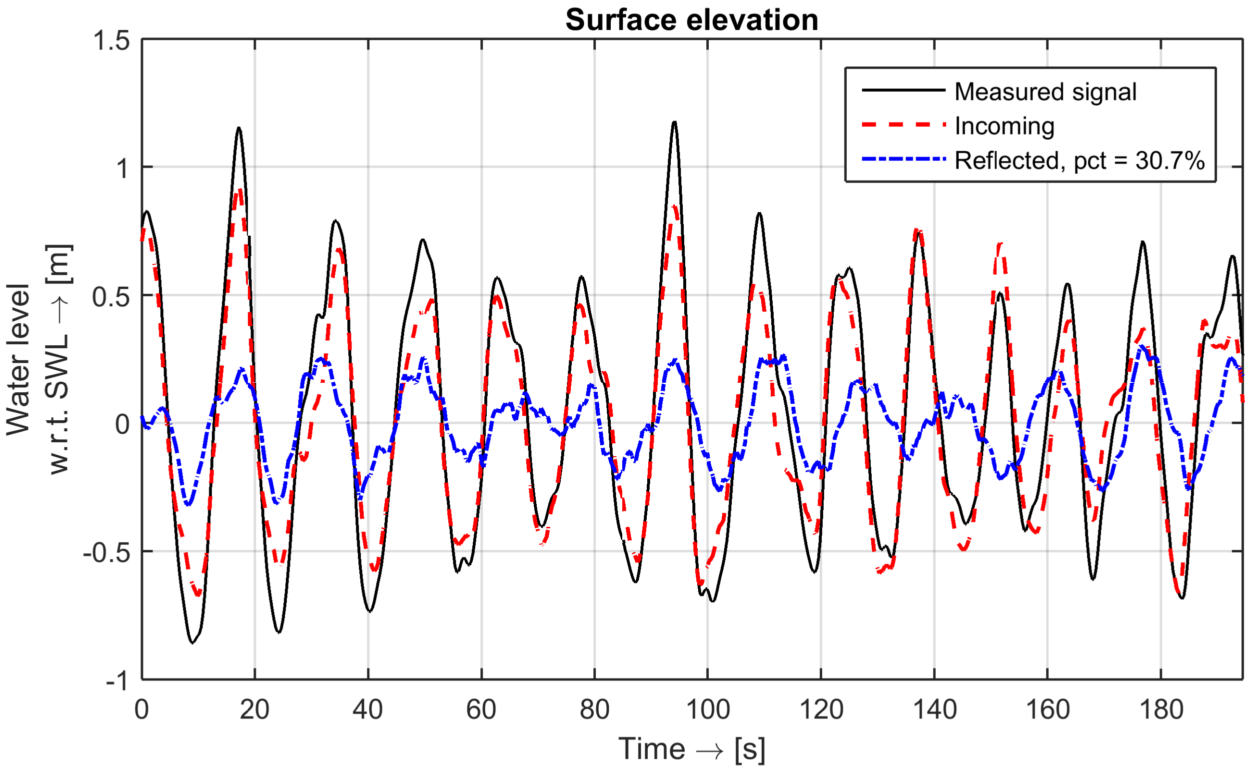

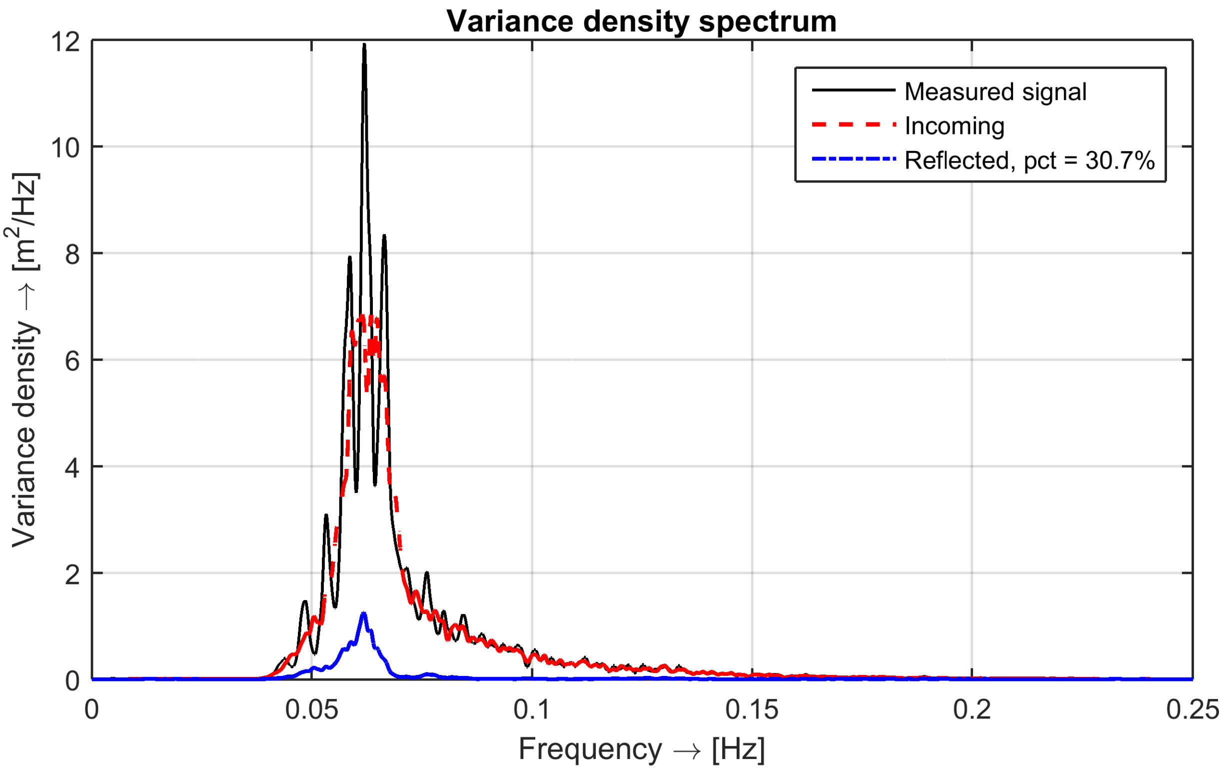

Reflection analysis using WHMs:01, 02 & 07	Irregular	I162b
Deltares	11202696	App. E.4.23

F Test ID tables

Special setting abbreviations:

- noST = ShoreTension (ST) system deactivated during the whole test
- Transition = ST system is deactivated halfway the measurement
- 50t = 50 tonnes ST module limit
- 200t = 200 tonnes ST module limit
- lwv = lowered friction of ducts (leidingweerstand verlaagd)
- sga = smart large battery (slimme grote accu)
- sk = swell chamber (swellkamer
- ssk = smart swell chamber (slimme swellkamer)

Table F.1 Overview of successfully executed tests Case A (Part 1)

Test ID	Index App. G.	ST activated	Special setting	Orientation	Wave type
A1_M610a	001	Yes	-	Head-on	Monochromatic
A1_M610b	002	Yes	-		Monochromatic
A1_M610c	003	Yes	-		Monochromatic
A1_M800a	004	Yes	-		Monochromatic
A1_M800b	005	Yes	-		Monochromatic
A2_B610a	006	Yes	-		Bi-chromatic
A2_B610a_Transition	007	Transition	-		Bi-chromatic
A2_B610a_noST	008	No	-		Bi-chromatic
A2_B610b	009	Yes	-		Bi-chromatic
A2_B610b_noST	010	No	-		Bi-chromatic
A2_B610c	011	Yes	-		Bi-chromatic
A2_B610c_noST	012	No	-		Bi-chromatic
A2_B610d	013	Yes	-		Bi-chromatic
A2_B610d_Transition	014	Transition	-		Bi-chromatic
A2_B610d_noST	015	No	-		Bi-chromatic
A2_B610e	016	Yes	-		Bi-chromatic
A2_B610e_noST	017	No	-		Bi-chromatic
A2_B610f	018	Yes	-		Bi-chromatic
A2_B800a	019	Yes	-		Bi-chromatic
A2_B800a_Transition	020	Transition	-		Bi-chromatic
A2_B800a_noST	021	No	-		Bi-chromatic
A2_B800b	022	Yes	-		Bi-chromatic
A2_B800b_noST	023	No	-		Bi-chromatic
A2_B800c	024	Yes	-		Bi-chromatic
A2_B800c_noST	025	No	-		Bi-chromatic
A2_B800d	026	Yes	-		Bi-chromatic
A2_B800d_noST	027	No	-		Bi-chromatic
A2_B800e	028	Yes	-		Bi-chromatic
A2_B800e_noST	029	No	-		Bi-chromatic
A2_B800f	030	Yes	-		Bi-chromatic

Table F.2 Overview of successfully executed tests Case A (Part 2)

Test ID	Index App. G.	ST activated	Special setting	Orientation	Wave type
A3_B610e_200t	031	Yes	200t	Head-on	Bi-chromatic
A3_B610e_sga	032	Yes	sga		Bi-chromatic
A3_B610e_ssk	033	Yes	ssk		Bi-chromatic
A3_B610e_ssk_sga	034	Yes	ssk+sga		Bi-chromatic
A3_B610f_200t	035	Yes	200t		Bi-chromatic
A3_B800e_200t	036	Yes	200t		Bi-chromatic
A3_B800f_200t	037	Yes	200t		Bi-chromatic
A3_M610b_sga	038	Yes	sga		Monochromatic
A3_M610b_ssk	039	Yes	ssk		Monochromatic
A3_M610b_ssk_sga	040	Yes	ssk+sga		Monochromatic
A4_I156a	041	Yes	-		Irregular
A4_I156b	042	Yes	-		Irregular
A4_I156c	043	Yes	-		Irregular
A4_I156d	044	Yes	-		Irregular
A4_I156e	045	Yes	-		Irregular

Table F.3 Overview of successfully executed tests Case B (Part 1).

Test ID	Index App. G.	ST activated	Special setting	Orientation	Wave type
B1_M80a	046	Yes	-	Beam-on	Monochromatic
B1_M80a_Transition	047	Transition	-		Monochromatic
B1_M80a_noST	048	No	-		Monochromatic
B1_M80b	049	Yes	-		Monochromatic
B1_M80b_Transition	050	Transition	-		Monochromatic
B1_M80b_noST	051	No	-		Monochromatic
B1_M140a	052	Yes	-		Monochromatic
B1_M140a_lwv	053	Yes	lwv		Monochromatic
B1_M140a_sk	054	Yes	sk		Monochromatic
B1_M140b	055	Yes	-		Monochromatic
B1_M140c	056	Yes	-		Monochromatic
B1_M140d	057	Yes	-		Monochromatic
B1_M140e	058	Yes	-		Monochromatic
B1_M140f	059	Yes	-		Monochromatic
B1_M140g	060	Yes	-		Monochromatic
B1_M140h	061	Yes	-		Monochromatic
B1_M156a	062	Yes	-		Monochromatic
B1_M156b	063	Yes	-		Monochromatic
B1_M156c	064	Yes	-		Monochromatic
B1_M156f	065	Yes	-		Monochromatic
B1_M156g	066	Yes	-		Monochromatic
B1_M156h	067	Yes	-		Monochromatic
B1_M172a	068	Yes	-		Monochromatic
B1_M172f	069	Yes	-		Monochromatic
B1_M172g	070	Yes	-		Monochromatic
B1_M172h	071	Yes	-		Monochromatic
B1_M800d	072	Yes	-		Monochromatic
B1_M800e	073	Yes	-		Monochromatic
B1_M800e_Transition	074	Transition	-		Monochromatic
B1_M800e_noS	075	No	-		Monochromatic

Table F.4 Overview of successfully executed tests Case B (Part 2).

Test ID	Index App. G.	ST activated	Special setting	Orientation	Wave type
B2_B610f	076	Yes	-	Beam-on	Bi-chromatic
B2_B610f_noST	077	No	-		Bi-chromatic
B2_B610g	078	Yes	-		Bi-chromatic
B2_B610g_noST	079	No	-		Bi-chromatic
B2_B610h	080	Yes	-		Bi-chromatic
B2_B610h_noST	081	No	-		Bi-chromatic
B2_B800f	082	Yes	-		Bi-chromatic
B2_B800f_noST	083	No	-		Bi-chromatic
B2_B800g	084	Yes	-		Bi-chromatic
B2_B800g_noST	085	No	-		Bi-chromatic
B2_B800h	086	Yes	-		Bi-chromatic
B2_B800h_noST	087	No	-		Bi-chromatic
B3_B800g_50t	088	Yes	50t		Bi-chromatic
B3_B800g_200t	089	Yes	200t		Bi-chromatic
B3_B800g_sga	090	Yes	sga		Bi-chromatic
B3_B800g_sk	091	Yes	sk		Bi-chromatic
B3_B800g_ssk	092	Yes	ssk		Bi-chromatic
B3_B800g_ssk_sga	093	Yes	ssk+sga		Bi-chromatic
B3_M156f_50t	094	Yes	50t		Monochromatic
B3_M156f_200t	095	Yes	200t		Monochromatic
B3_M156f_sga	096	Yes	sga		Monochromatic
B3_M156f_sk	097	Yes	sk		Monochromatic
B3_M156f_ssk	098	Yes	ssk		Monochromatic
B3_M156f_ssk_sga	099	Yes	ssk+sga		Monochromatic
B3_M800d_sk	100	Yes	sk		Monochromatic
B3_M800e_50t	101	Yes	50t		Monochromatic
B3_M800e_200t	102	Yes	200t		Monochromatic
B3_M800e_sga	103	Yes	sga		Monochromatic
B3_M800e_ssk	104	Yes	ssk		Monochromatic
B3_M800e_ssk_sga	105	Yes	ssk+sga		Monochromatic
B4_I156a	106	Yes	-		Irregular

Table F.5 Overview of successfully executed tests Case C (Part 1).

Test ID	Index App. G.	ST activated	Special setting	Orientation	Wave type
C1_B610a	107	Yes	-	Bow-quartering	Bi-chromatic
C1_B610b	108	Yes	-		Bi-chromatic
C1_B610c	109	Yes	-		Bi-chromatic
C1_B610d	110	Yes	-		Bi-chromatic
C1_B610e	111	Yes	-		Bi-chromatic
C1_B800a	112	Yes	-		Bi-chromatic
C1_B800b	113	Yes	-		Bi-chromatic
C1_B800c	114	Yes	-		Bi-chromatic
C1_B800d	115	Yes	-		Bi-chromatic
C1_B800e	116	Yes	-		Bi-chromatic
C2_B610c_200t	117	Yes	200t		Bi-chromatic
C2_B610c_sga	118	Yes	sga		Bi-chromatic
C2_B610c_sk	119	Yes	sk		Bi-chromatic
C2_B610c_ssk	120	Yes	ssk		Bi-chromatic
C2_B610c_ssk_sga	121	Yes	ssk+sga		Bi-chromatic

Table F.6 Overview of successfully executed tests Case C (Part 2).

Test ID	Index App. G.	ST activated	Special setting	Orientation	Wave type
C3_I120a	122	Yes	-	Bow-quartering	Irregular
C3_I140a	123	Yes	-		Irregular
C3_I156a	124	Yes	-		Irregular
C3_I156b	125	Yes	-		Irregular
C3_I156c	126	Yes	-		Irregular
C4_M140a	127	Yes	-		Monochromatic
C4_M140b	128	Yes	-		Monochromatic
C4_M140c	129	Yes	-		Monochromatic
C4_M140d	130	Yes	-		Monochromatic
C4_M140e	131	Yes	-		Monochromatic
C4_M156a	132	Yes	-		Monochromatic
C4_M156a_noST	133	No	-		Monochromatic
C4_M156b	134	Yes	-		Monochromatic
C4_M156b_noST	135	No	-		Monochromatic
C4_M156c	136	Yes	-		Monochromatic
C4_M156c_noST	137	No	-		Monochromatic
C4_M156d	138	Yes	-		Monochromatic
C4_M156d_noST	139	No	-		Monochromatic
C4_M156e	140	Yes	-		Monochromatic
C4_M156e_Transition	141	Transition	-		Monochromatic
C4_M156e_noST	142	No	-		Monochromatic
C4_M172a	143	Yes	-		Monochromatic
C4_M172a_Transition	144	Transition	-		Monochromatic
C4_M172a_noST	145	No	-		Monochromatic
C4_M172b	146	Yes	-		Monochromatic
C4_M172b_noST	147	No	-		Monochromatic
C4_M172c	148	Yes	-		Monochromatic
C4_M172c_noST	149	No	-		Monochromatic
C4_M172d	150	Yes	-		Monochromatic
C4_M172d_noST	151	No	-		Monochromatic
C4_M172e	152	Yes	-		Monochromatic
C4_M172e_noST	153	No	-		Monochromatic
C4_M330a	154	Yes	-		Monochromatic
C4_M330a_Transition	155	Transition	-		Monochromatic
C4_M330a_noST	156	No	-		Monochromatic
C4_M360a	157	Yes	-		Monochromatic
C4_M360a_Transition	158	Transition	-		Monochromatic
C4_M360a_noST	159	No	-		Monochromatic
C4_M360a_200t	160	Yes	200t		Monochromatic
C4_M360a_sga	161	Yes	sga		Monochromatic
C4_M360a_sk	162	Yes	sk		Monochromatic
C4_M360a_ssk	163	Yes	ssk		Monochromatic
C4_M360a_ssk_sga	164	Yes	ssk+sga		Monochromatic
C4_M380a	165	Yes	-		Monochromatic
C4_M380a_Transition	166	Transition	-		Monochromatic
C4_M380a_noST	167	No	-		Monochromatic

Table F.7 Overview of successfully executed tests Case C (Part 3).

Test ID	Index App. G.	ST activated	Special setting	Orientation	Wave type
C4_M610a	168	Yes	-	Bow-quartering	Monochromatic
C4_M610a_Transition	169	Transition	-		Monochromatic
C4_M610b	170	Yes	-		Monochromatic
C4_M610c	171	Yes	-		Monochromatic
C4_M800a	172	Yes	-		Monochromatic
C4_M800d	173	Yes	-		Monochromatic
C4_M800e	174	Yes	-		Monochromatic
C4_M800e_Transition	175	Transition	-		Monochromatic
C4_M800e_noST	176	No	-		Monochromatic

Table F.8 Overview of successfully executed tests Case D

Test ID	Index App. G.	ST activated	Special setting	Orientation	Wave type
D1_I80a	177	Yes	-	Bow-quartering	Irregular
D1_I80b	178	Yes	-	Bow-quartering	Irregular
D1_I80c	179	Yes	-	Beam-on	Irregular
D1_I80d	180	Yes	-	Beam-on	Irregular
D1_I120a	181	Yes	-	Bow-quartering	Irregular
D1_I120b	182	Yes	-	Bow-quartering	Irregular
D1_I120c	183	Yes	-	Beam-on	Irregular
D1_I120d	184	Yes	-	Beam-on	Irregular
D1_I162a	185	Yes	-	Bow-quartering	Irregular
D1_I162b	186	Yes	-	Bow-quartering	Irregular
D1_I162c	187	Yes	-	Beam-on	Irregular
D1_I162e	188	Yes	-	Head-on	Irregular
D1_I162e_noST	189	No	-	Head-on	Irregular
D1_I162f	190	Yes	-	Head-on	Irregular
D1_I162f_Transition	191	Transition	-	Head-on	Irregular
D1_I162f_noST	192	No	-	Head-on	Irregular
D2_M156a	193	Yes	-	Bow-quartering	Monochromatic
D2_M156a_noST	194	No	-	Bow-quartering	Monochromatic
D2_M156b	195	Yes	-	Bow-quartering	Monochromatic
D2_M156c	196	Yes	-	Bow-quartering	Monochromatic
D2_M162a	197	Yes	-	Bow-quartering	Monochromatic
D2_M162a_noST	198	No	-	Bow-quartering	Monochromatic
D2_M162b	199	Yes	-	Bow-quartering	Monochromatic
D2_M330e	200	Yes	-	Bow-quartering	Monochromatic
D2_M330e_noST	201	No	-	Bow-quartering	Monochromatic
D2_M7312a	202	Yes	-	Bow-quartering	Monochromatic
D2_M7312a_Transition	203	Transition	-	Bow-quartering	Monochromatic
D2_M7312a_noST	204	No	-	Bow-quartering	Monochromatic
D2_M7312b	205	Yes	-	Bow-quartering	Monochromatic
D2_M7312d_Transition	206	Transition	-	Bow-quartering	Monochromatic
D3_B7312a	207	Yes	-	Bow-quartering	Bi-chromatic
D3_B7312a_noST	208	No	-	Bow-quartering	Bi-chromatic
D3_B7312b	209	Yes	-	Bow-quartering	Bi-chromatic

G Results

G.1 Cases A, B and C

G.1.1 Result plots

Due to confidentiality, the figures including ST-results (i.e. forces, cylinder positions, characteristics) are not publicly available. Only the figures including the vessel motions have been published in this document.

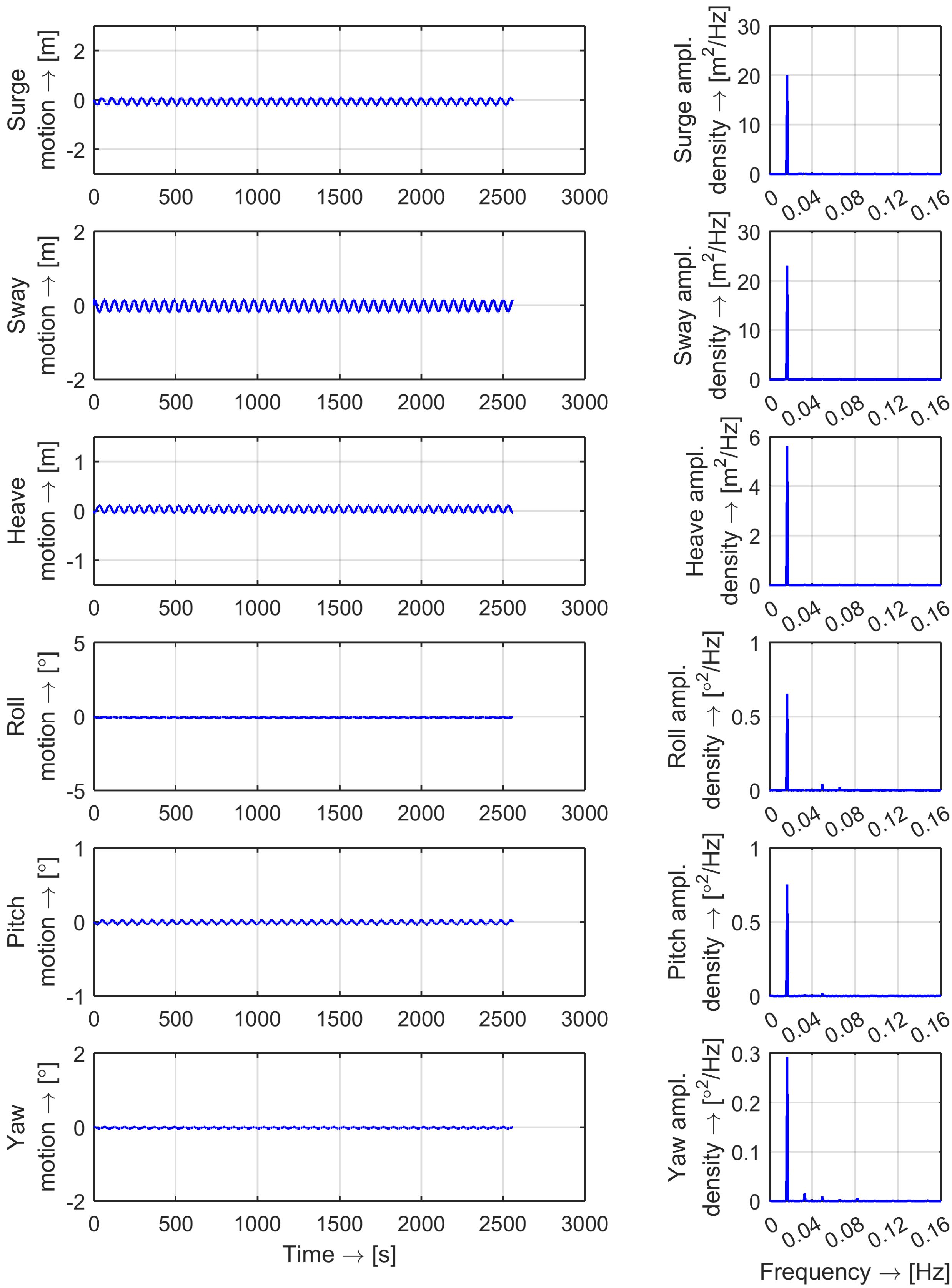

σ_{Surge} = 0.11 m, σ_{Sway} = 0.12 m, σ_{Heave} = 0.06 m, σ_{Roll} = 0.02°, σ_{Pitch} = 0.02°, σ_{Yaw} = 0.01°

Ship motions at centre of gravity (CoG) Depth = 18.0 m, H = 0.20 m, T = 61.00 s Head-on waves	Monochromatic	M610a
	A1_M610a	
Deltares	11202696	App. G.001-2

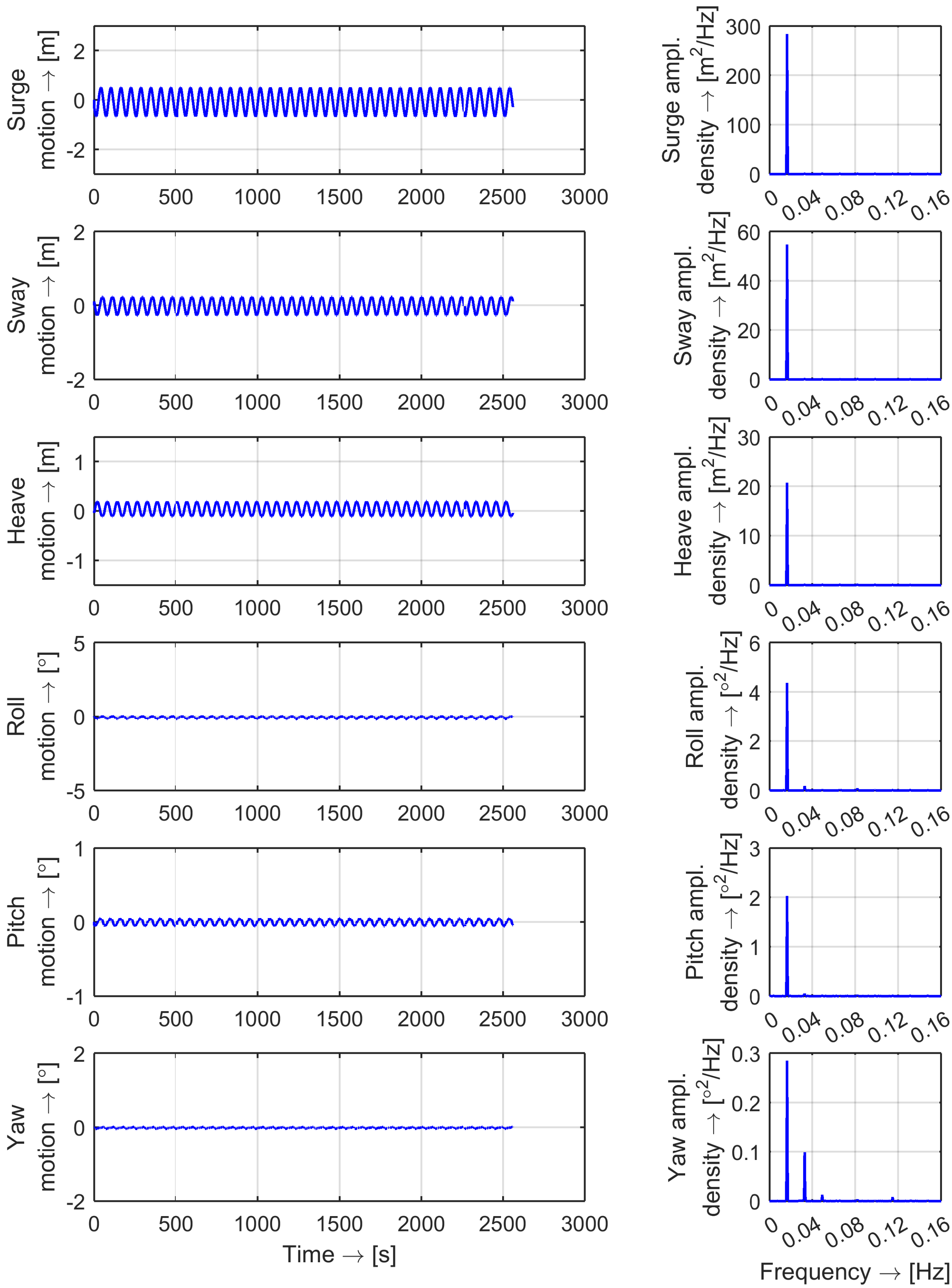

σ_{Surge} = 0.41 m, σ_{Sway} = 0.18 m, σ_{Heave} = 0.11 m, σ_{Roll} = 0.05°, σ_{Pitch} = 0.04°, σ_{Yaw} = 0.02°

Ship motions at centre of gravity (CoG) Depth = 18.0 m, H = 0.40 m, T = 61.00 s Head-on waves	Monochromatic	M610b
	A1_M610b	
Deltares	11202696	App. G.002-2

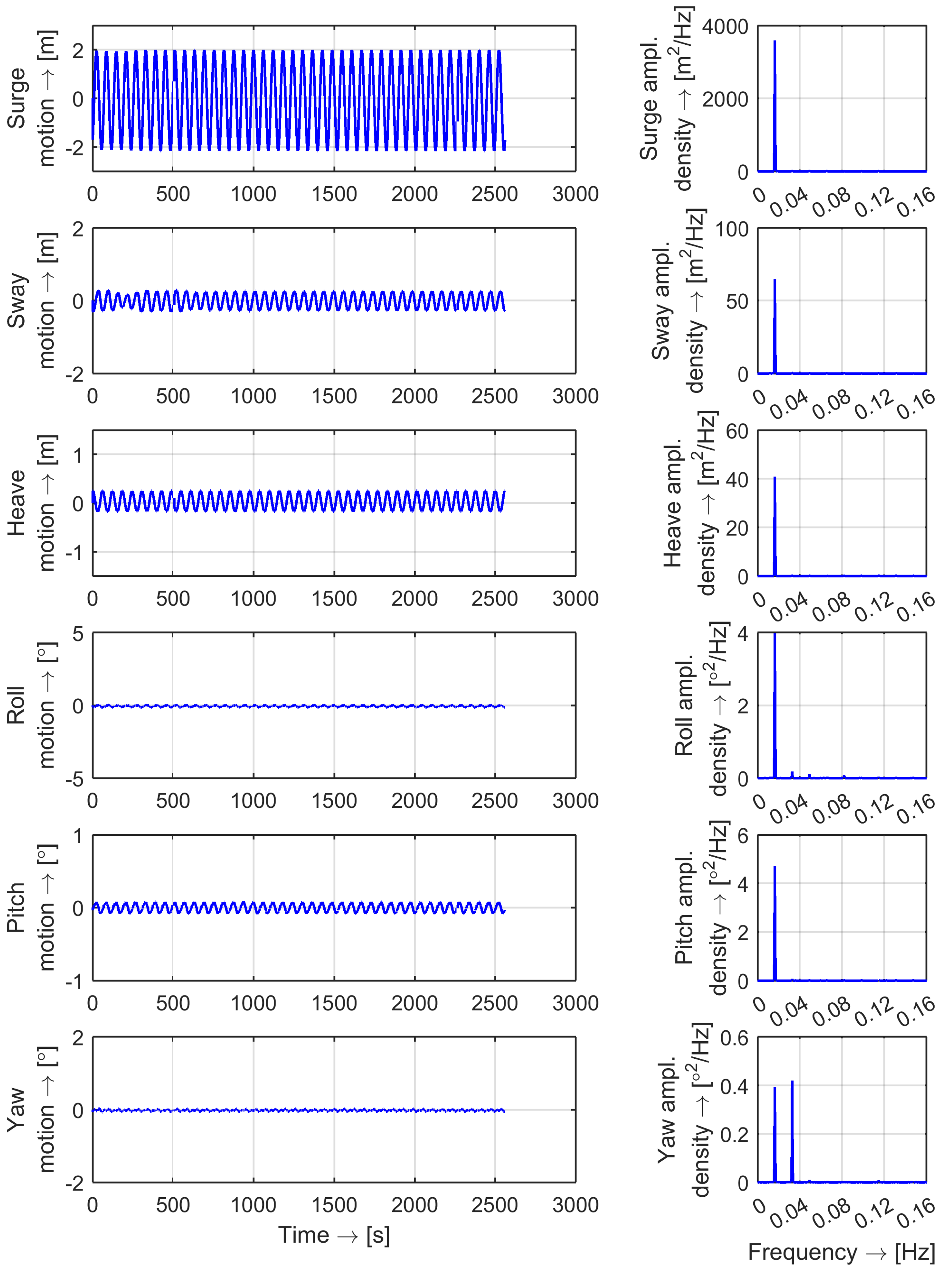

σ_{Surge} = 1.45 m, σ_{Sway} = 0.20 m, σ_{Heave} = 0.15 m, σ_{Roll} = 0.05°, σ_{Pitch} = 0.05°, σ_{Yaw} = 0.02°

Ship motions at centre of gravity (CoG) Depth = 18.0 m, H = 0.60 m, T = 61.00 s Head-on waves	Monochromatic	M610c
	A1_M610c	
Deltares	11202696	App. G.003-2

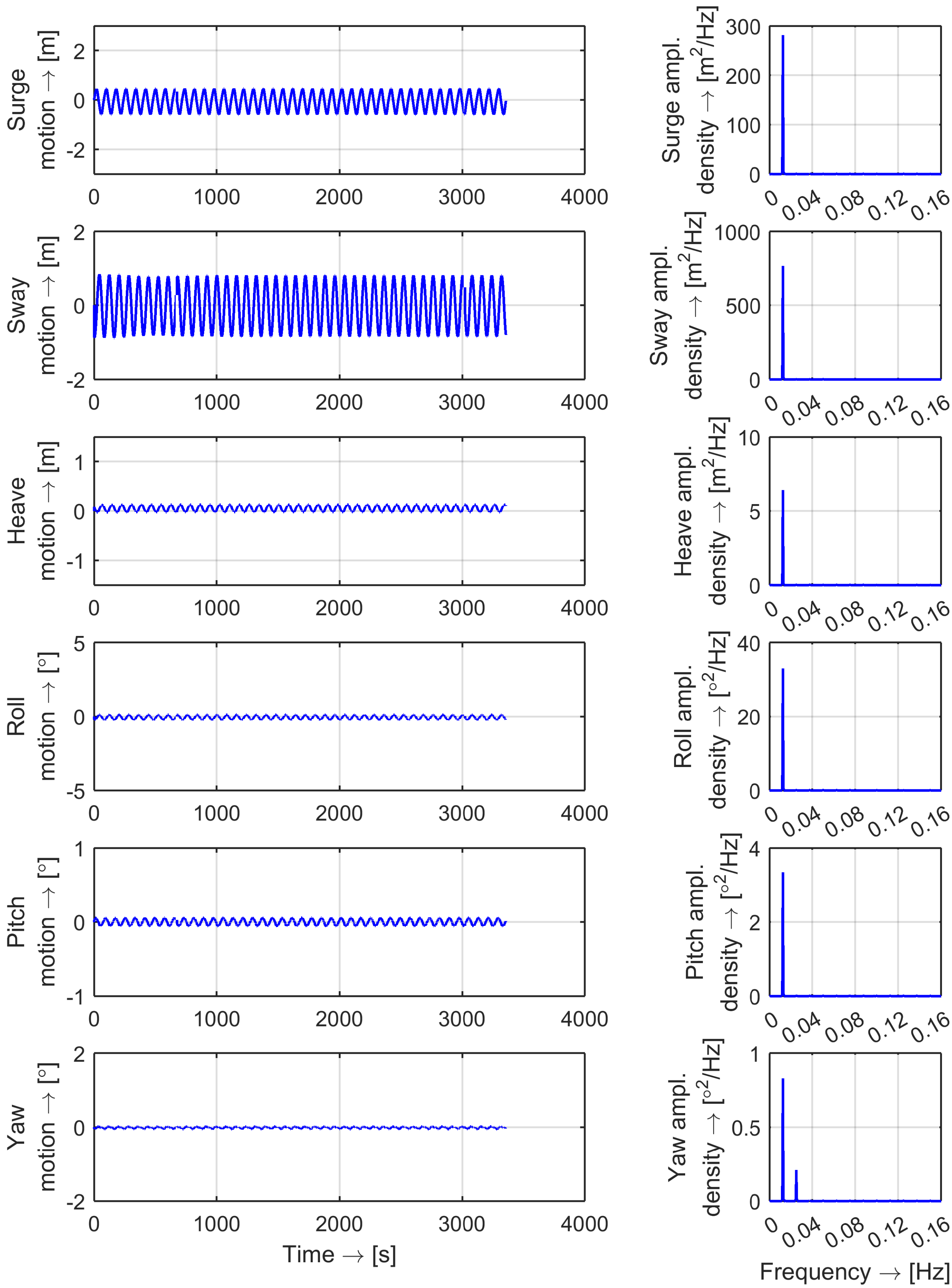

σ_{Surge} = 0.36 m, σ_{Sway} = 0.59 m, σ_{Heave} = 0.05 m, σ_{Roll} = 0.12°, σ_{Pitch} = 0.04°, σ_{Yaw} = 0.02°

Ship motions at centre of gravity (CoG) Depth = 18.0 m, H = 0.20 m, T = 80.00 s Head-on waves	Monochromatic	M800a
	A1_M800a	
Deltares	11202696	App. G.004-2

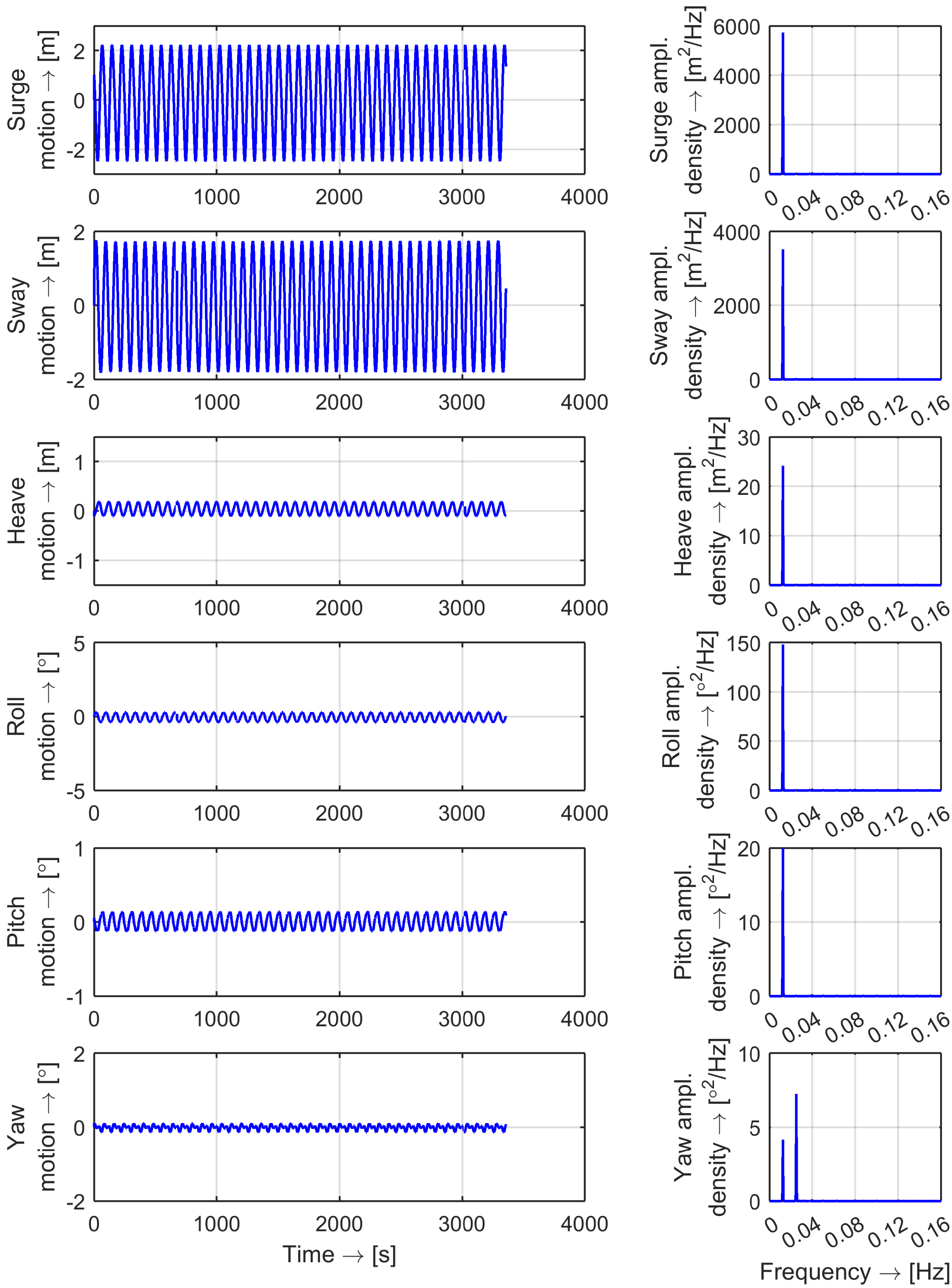

σ_{Surge} = 1.61 m, σ_{Sway} = 1.26 m, σ_{Heave} = 0.10 m, σ_{Roll} = 0.26°, σ_{Pitch} = 0.09°, σ_{Yaw} = 0.07°

Ship motions at centre of gravity (CoG) Depth = 18.0 m, H = 0.40 m, T = 80.00 s Head-on waves	Monochromatic	M800b
	A1_M800b	
Deltares	11202696	App. G.005-2

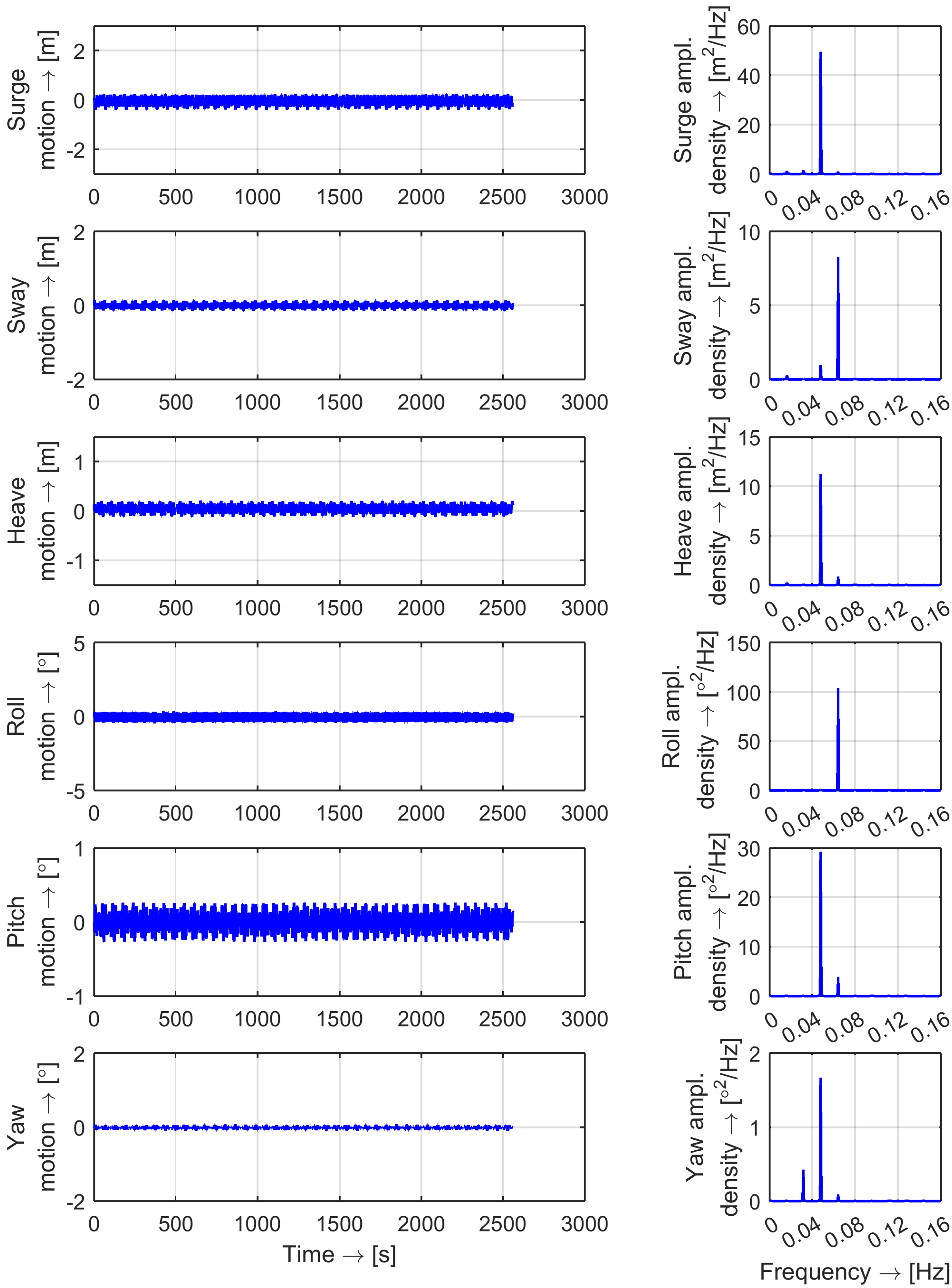

σ_{Surge} = 0.19 m, σ_{Sway} = 0.08 m, σ_{Heave} = 0.09 m, σ_{Roll} = 0.25°, σ_{Pitch} = 0.15°, σ_{Yaw} = 0.04°

Ship motions at centre of gravity (CoG) Depth = 18.0 m, H = 1.00 m, T_1 = 15.60 s, T_2 = 20.96 s Head-on waves	Bichromatic	B610a
	A2_B610a	
Deltares	11202696	App. G.006-2

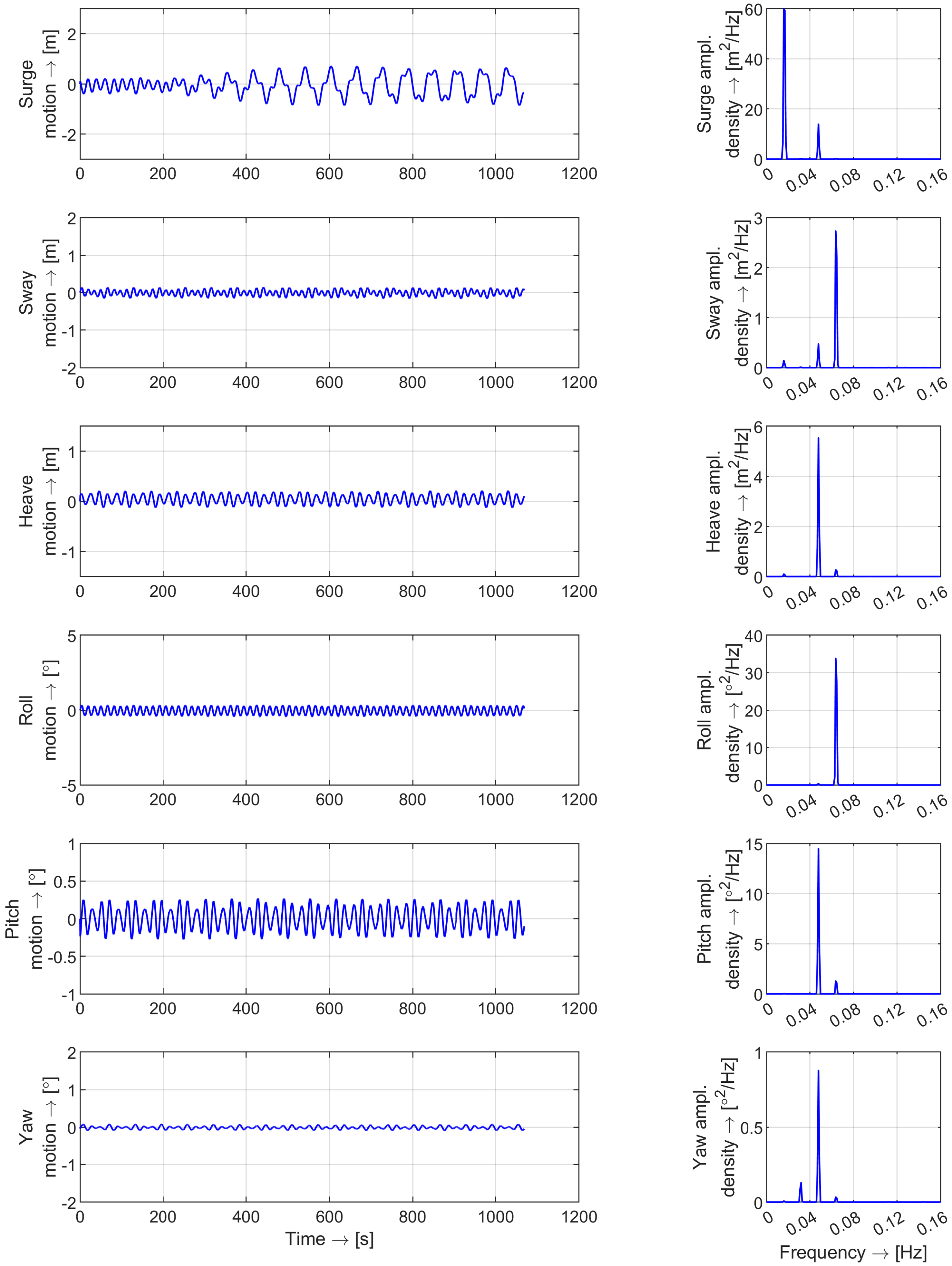

σ_{Surge} = n.a., σ_{Sway} = n.a., σ_{Heave} = n.a., σ_{Roll} = n.a., σ_{Pitch} = n.a., σ_{Yaw} = n.a.

Ship motions at centre of gravity (CoG) Depth = 18.0 m, H = 1.00 m, T_1 = 15.60 s, T_2 = 20.96 s Head-on waves	Bichromatic	B610a
	A2_B610a_Transition	
Deltares	11202696	App. G.007-2

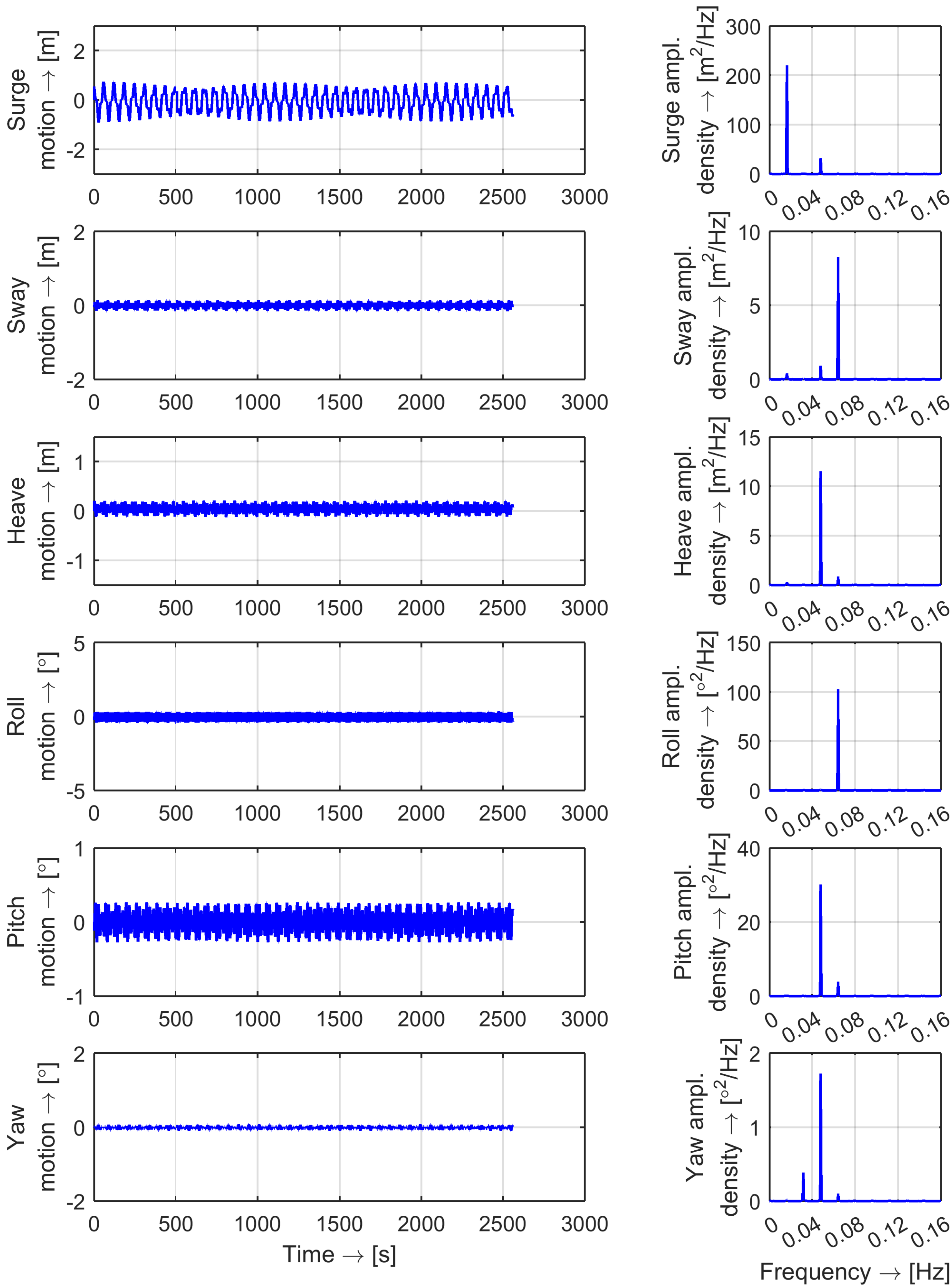

σ_{Surge} = 0.42 m, σ_{Sway} = 0.08 m, σ_{Heave} = 0.09 m, σ_{Roll} = 0.25°, σ_{Pitch} = 0.15°, σ_{Yaw} = 0.04°

Ship motions at centre of gravity (CoG) Depth = 18.0 m, H = 1.00 m, T_1 = 15.60 s, T_2 = 20.96 s Head-on waves	Bichromatic	B610a
	A2_B610a_noST	
Deltares	11202696	App. G.008-2

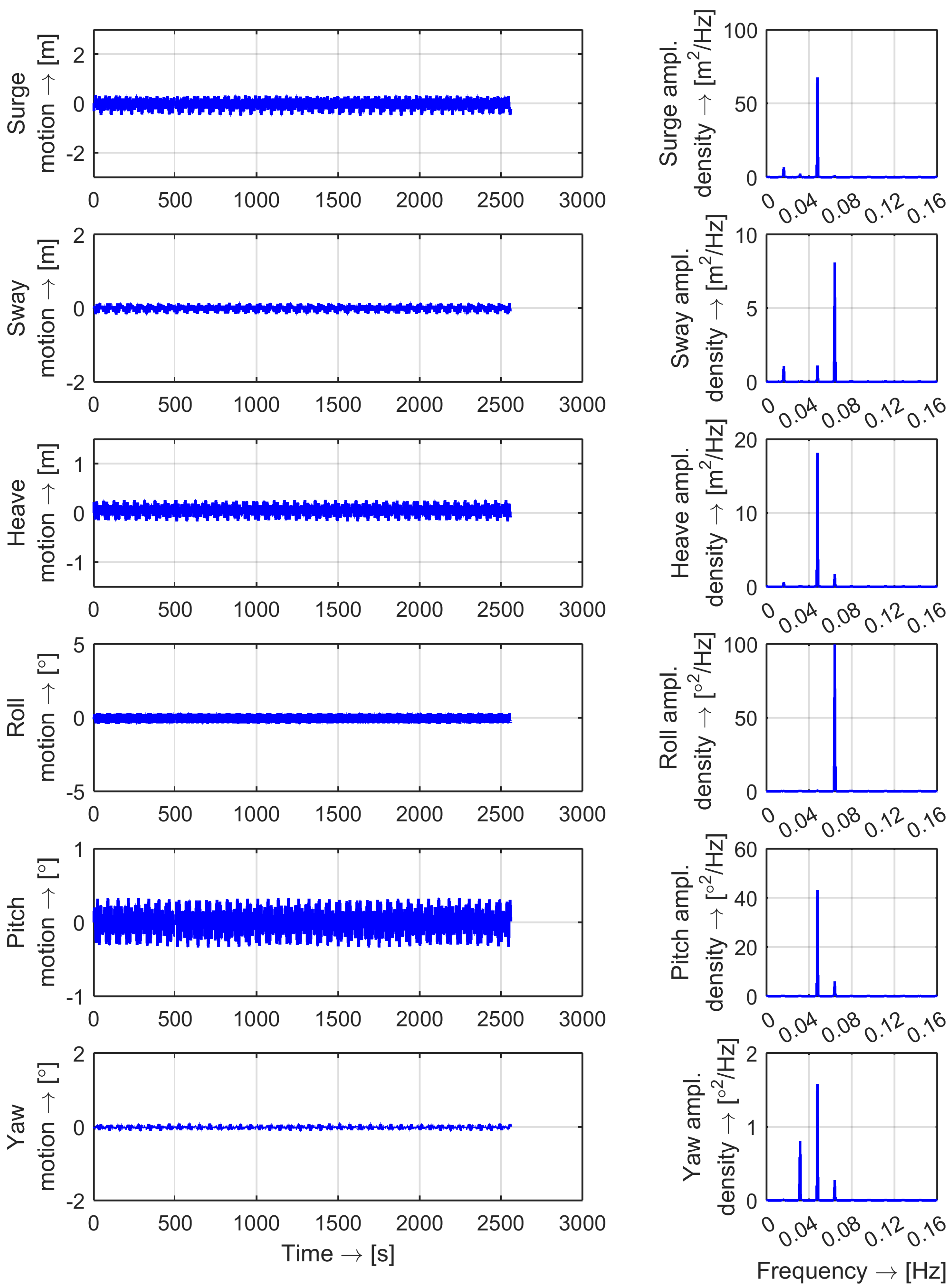

σ_{Surge} = 0.23 m, σ_{Sway} = 0.08 m, σ_{Heave} = 0.12 m, σ_{Roll} = 0.24°, σ_{Pitch} = 0.18°, σ_{Yaw} = 0.04°

Ship motions at centre of gravity (CoG) Depth = 18.0 m, H = 1.25 m, T_1 = 15.60 s, T_2 = 20.96 s Head-on waves	Bichromatic	B610b
	A2_B610b	
Deltares	11202696	App. G.009-2

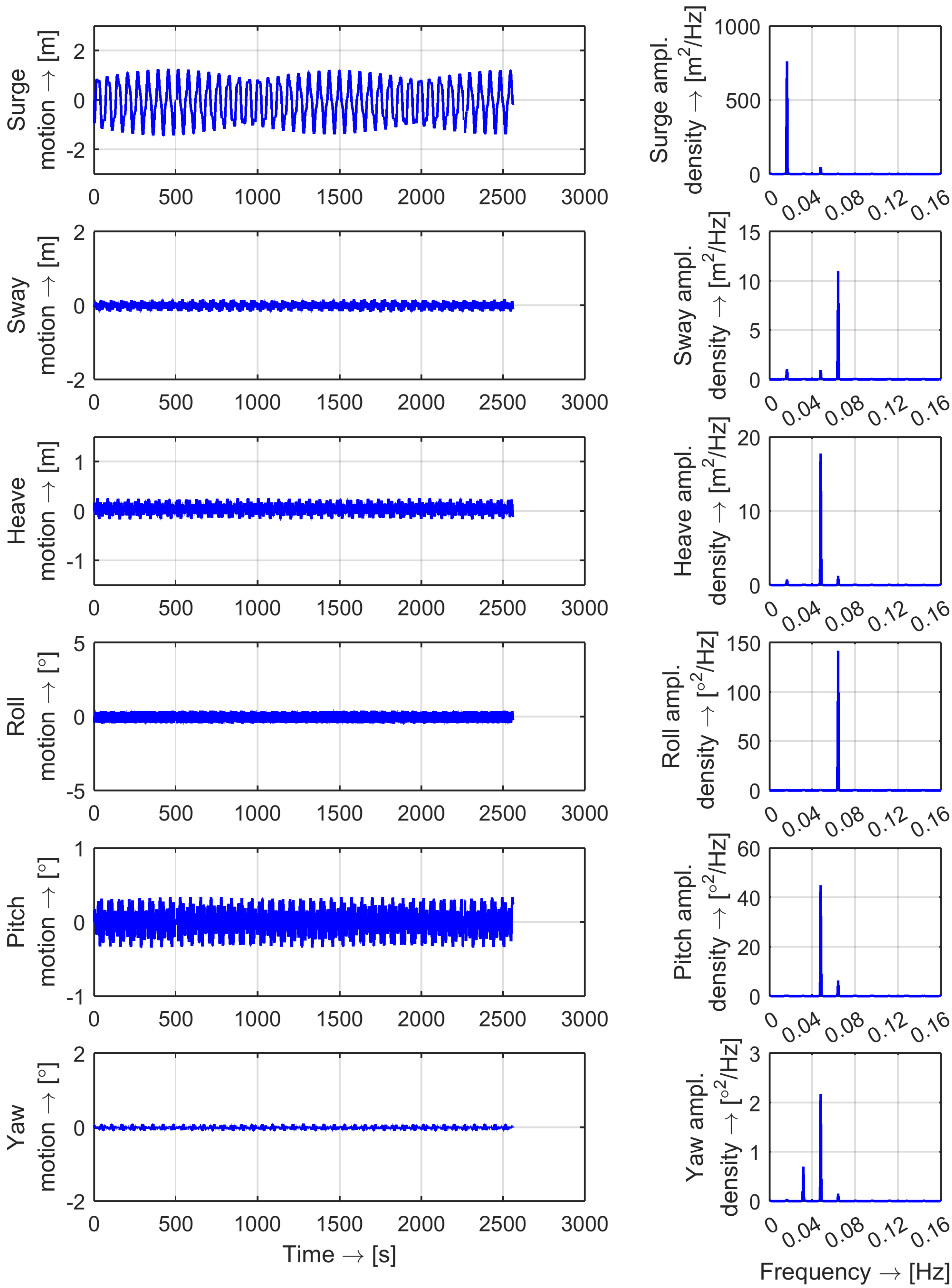

σ_{Surge} = 0.75 m, σ_{Sway} = 0.09 m, σ_{Heave} = 0.12 m, σ_{Roll} = 0.29°, σ_{Pitch} = 0.19°, σ_{Yaw} = 0.05°

Ship motions at centre of gravity (CoG) Depth = 18.0 m, H = 1.25 m, T_1 = 15.60 s, T_2 = 20.96 s Head-on waves	Bichromatic	B610b
	A2_B610b_noST	
Deltares	11202696	App. G.010-2

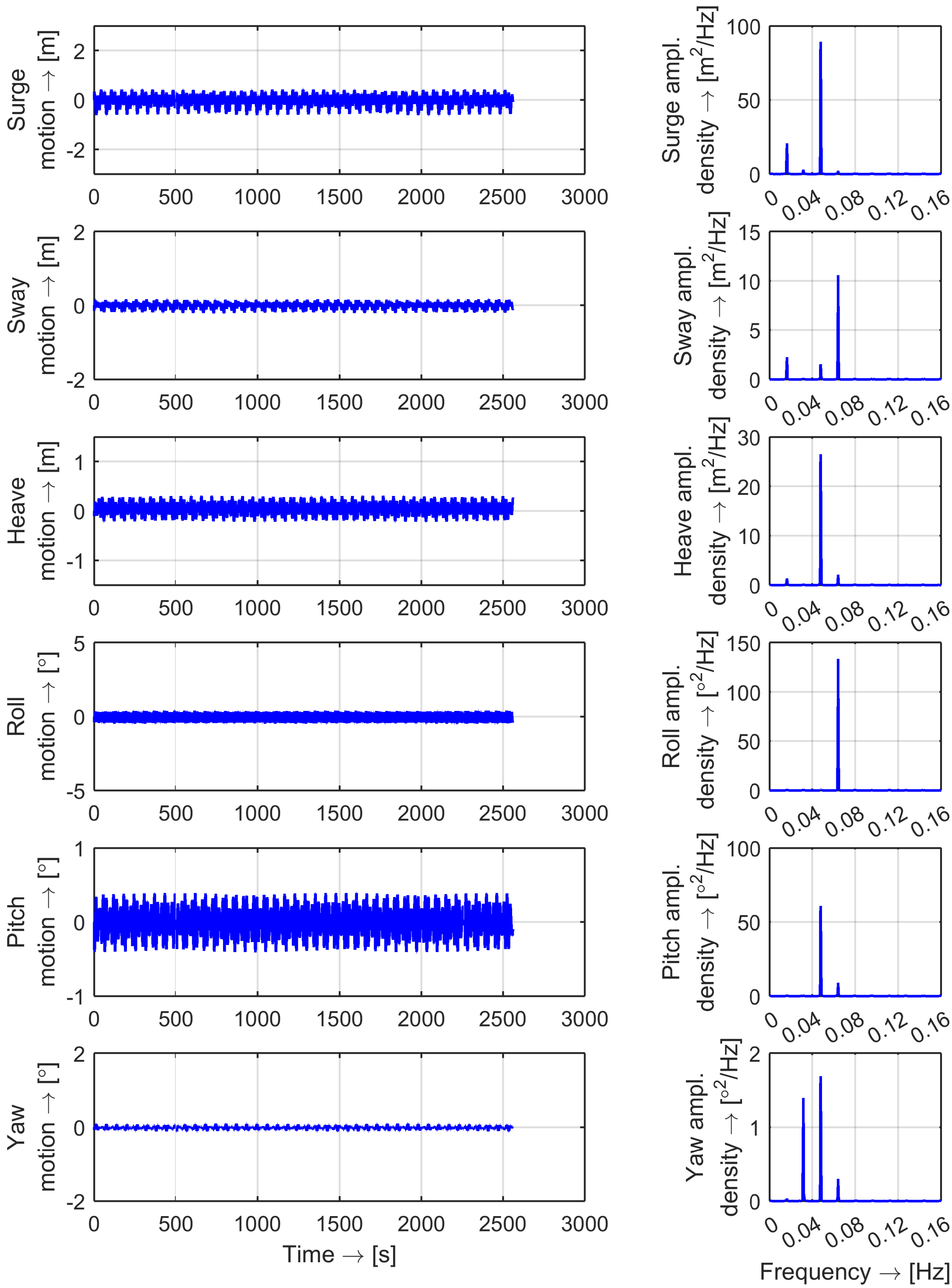

σ_{Surge} = 0.28 m, σ_{Sway} = 0.09 m, σ_{Heave} = 0.14 m, σ_{Roll} = 0.28°, σ_{Pitch} = 0.22°, σ_{Yaw} = 0.05°

Ship motions at centre of gravity (CoG) Depth = 18.0 m, H = 1.50 m, T_1 = 15.60 s, T_2 = 20.96 s Head-on waves	Bichromatic	B610c
	A2_B610c	
Deltares	11202696	App. G.011-2

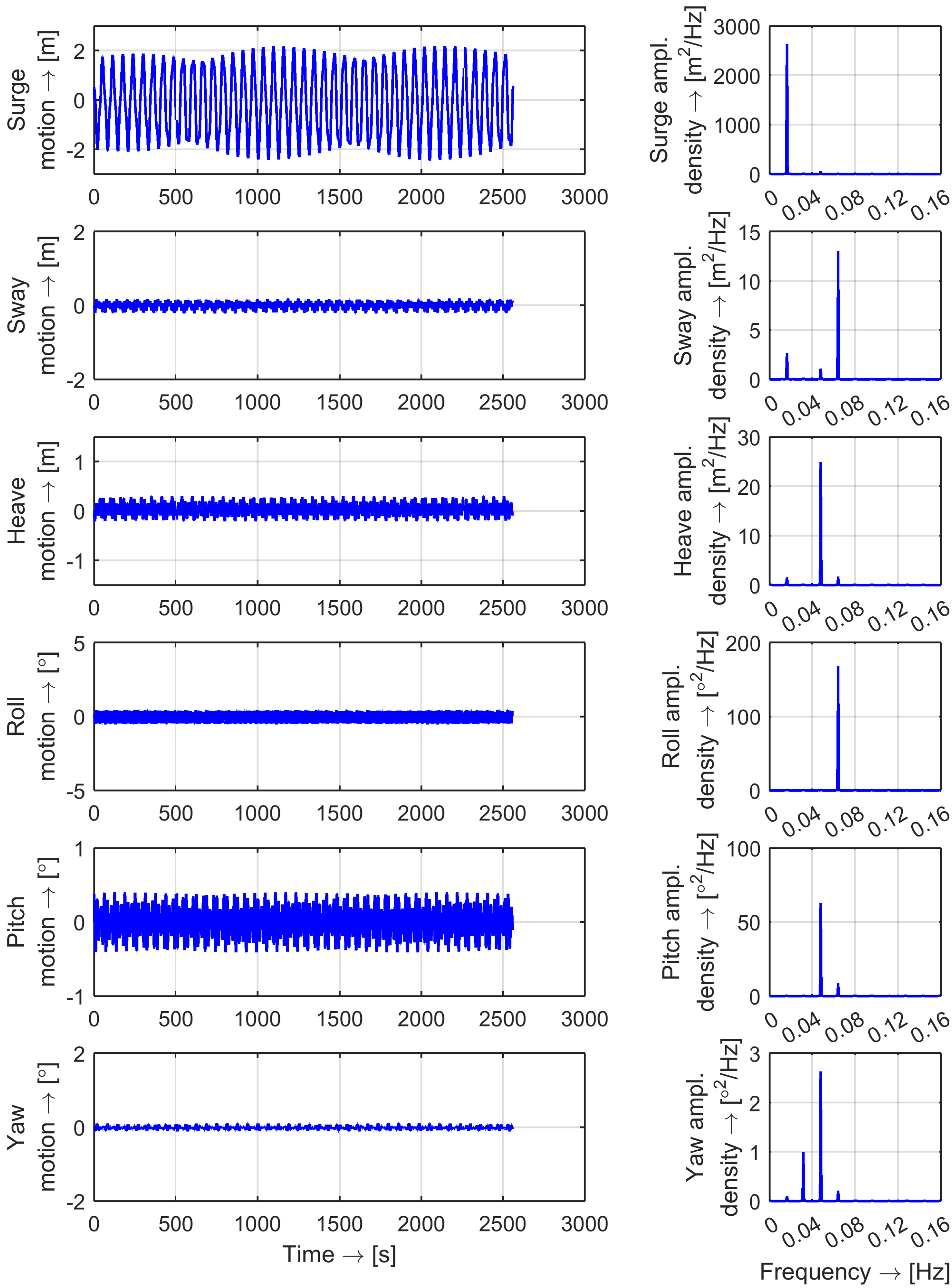

σ_{Surge} = 1.37 m, σ_{Sway} = 0.10 m, σ_{Heave} = 0.14 m, σ_{Roll} = 0.32°, σ_{Pitch} = 0.22°, σ_{Yaw} = 0.05°

Ship motions at centre of gravity (CoG) Depth = 18.0 m, H = 1.50 m, T_1 = 15.60 s, T_2 = 20.96 s Head-on waves	Bichromatic	B610c
	A2_B610c_noST	
Deltares	11202696	App. G.012-2

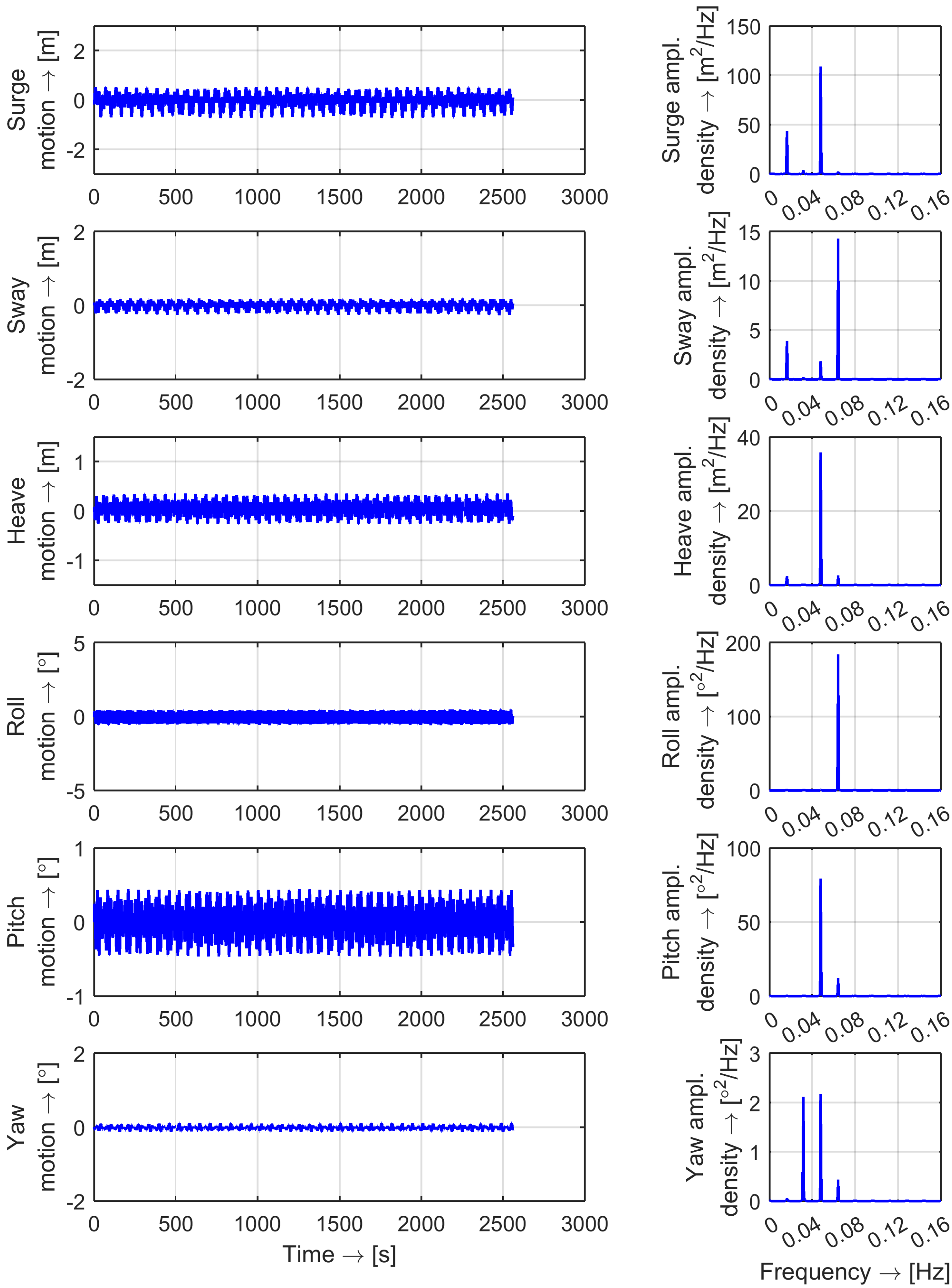

σ_{Surge} = 0.33 m, σ_{Sway} = 0.11 m, σ_{Heave} = 0.17 m, σ_{Roll} = 0.33°, σ_{Pitch} = 0.25°, σ_{Yaw} = 0.06°

Ship motions at centre of gravity (CoG) Depth = 18.0 m, H = 1.75 m, T_1 = 15.60 s, T_2 = 20.96 s Head-on waves	Bichromatic	B610d
	A2_B610d	
Deltares	11202696	App. G.013-2

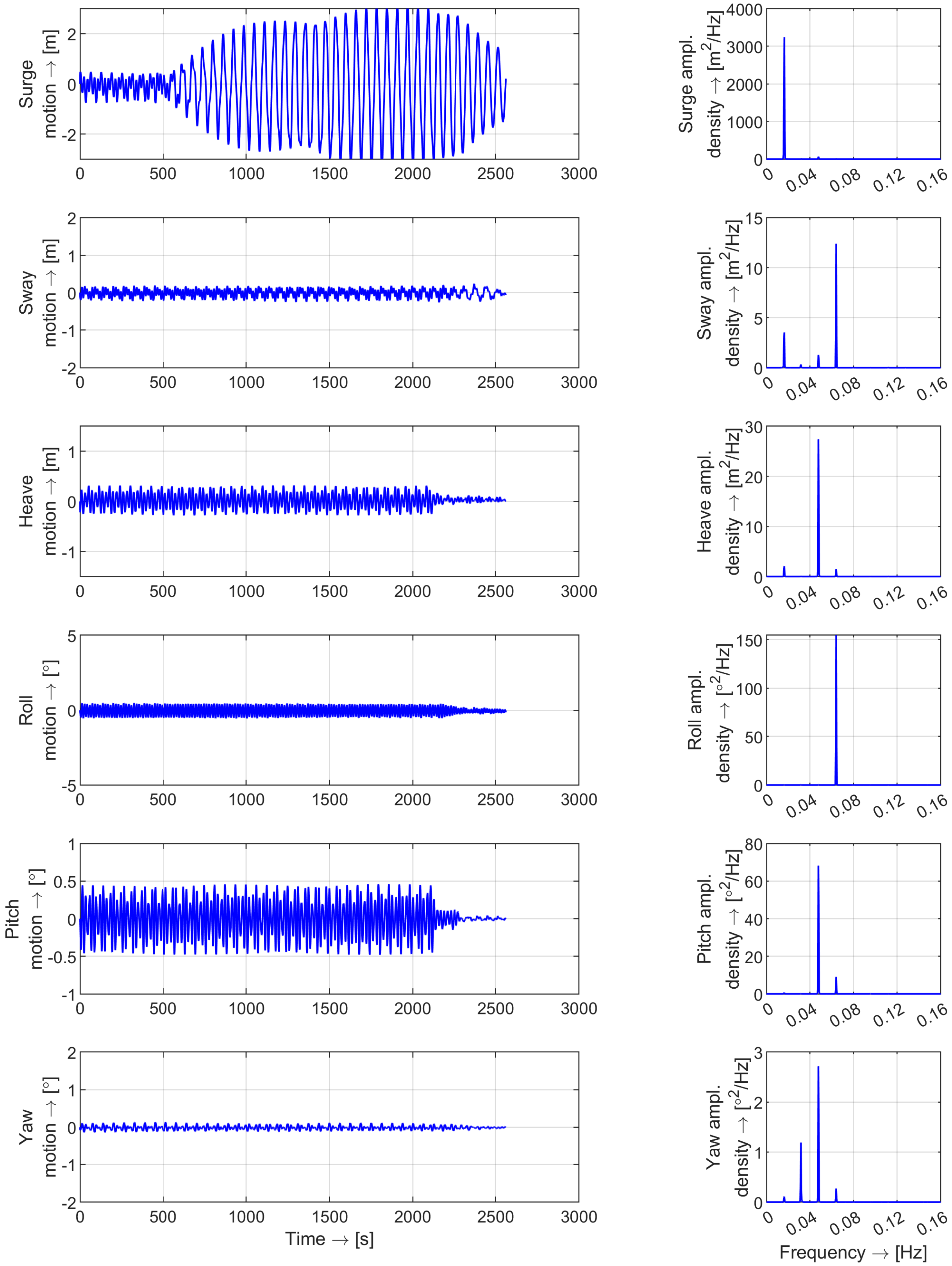

σ_{Surge} = n.a., σ_{Sway} = n.a., σ_{Heave} = n.a., σ_{Roll} = n.a., σ_{Pitch} = n.a., σ_{Yaw} = n.a.

Ship motions at centre of gravity (CoG) Depth = 18.0 m, H = 1.75 m, T_1 = 15.60 s, T_2 = 20.96 s Head-on waves	Bichromatic	B610d
	A2_B610d_Transition	
Deltares	11202696	App. G.014-2

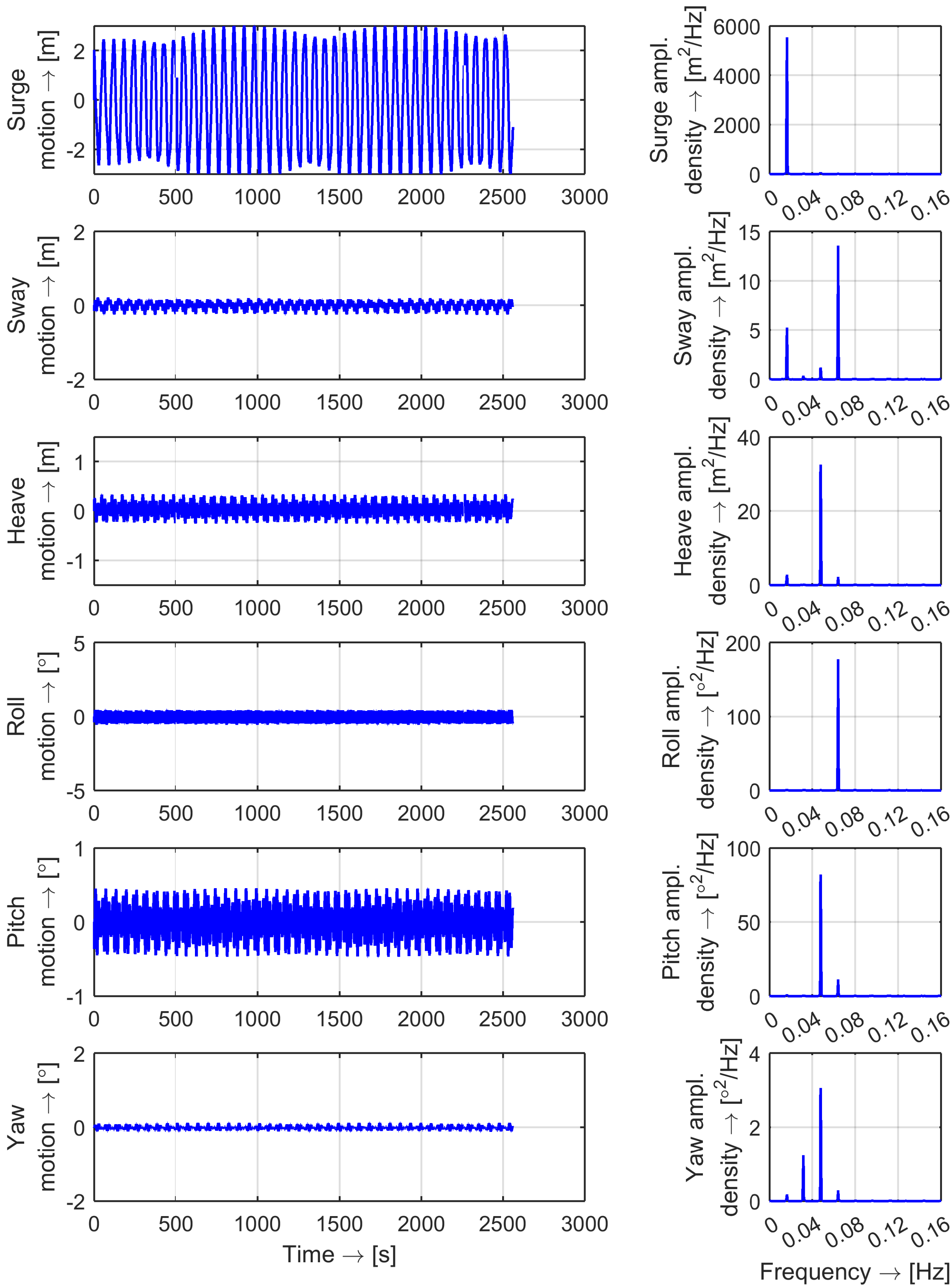

σ_{Surge} = 1.98 m, σ_{Sway} = 0.11 m, σ_{Heave} = 0.16 m, σ_{Roll} = 0.32°, σ_{Pitch} = 0.25°, σ_{Yaw} = 0.06°

Ship motions at centre of gravity (CoG) Depth = 18.0 m, H = 1.75 m, T_1 = 15.60 s, T_2 = 20.96 s Head-on waves	Bichromatic	B610d
	A2_B610d_noST	
Deltares	11202696	App. G.015-2

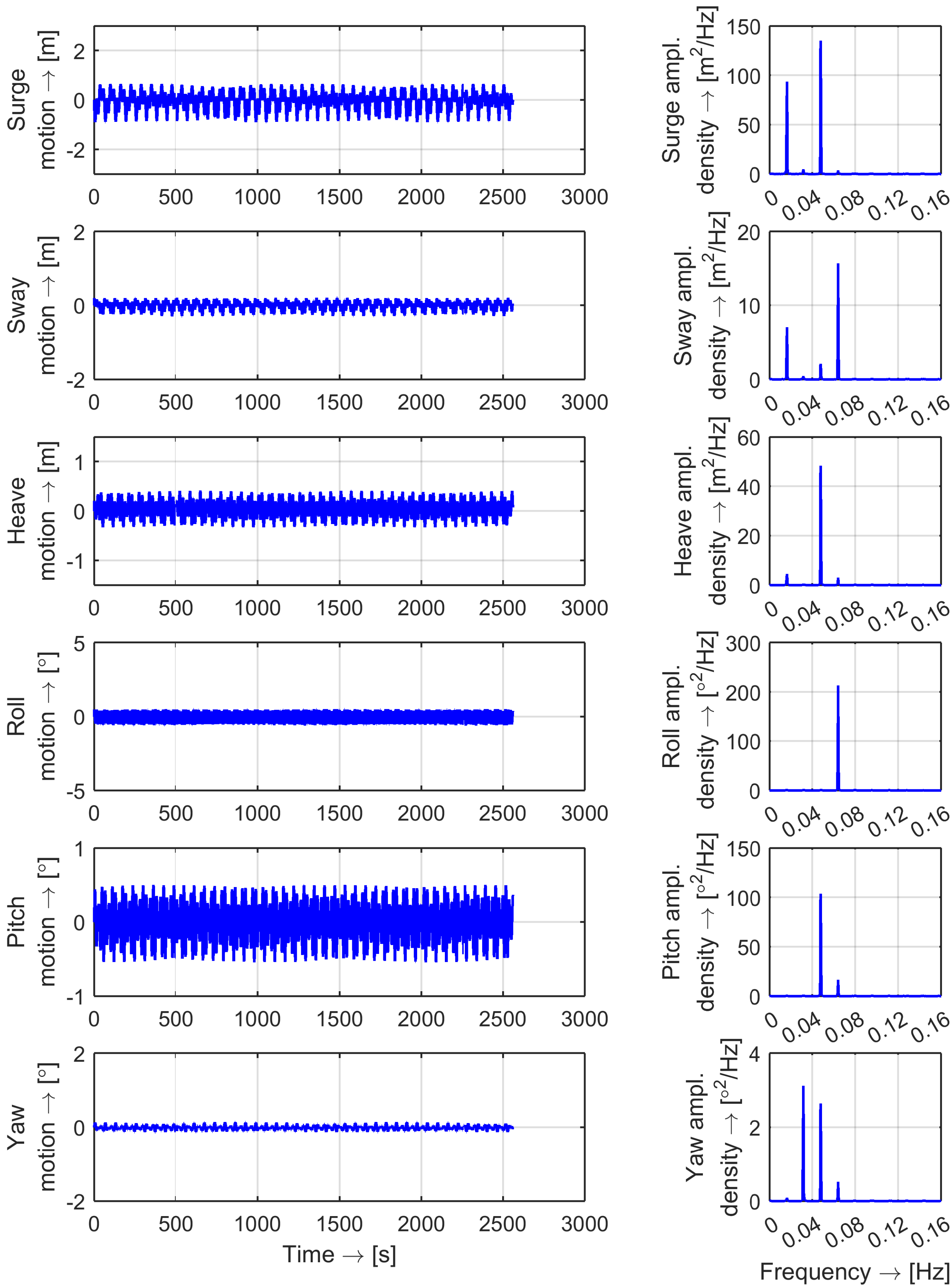

σ_{Surge} = 0.41 m, σ_{Sway} = 0.13 m, σ_{Heave} = 0.19 m, σ_{Roll} = 0.36°, σ_{Pitch} = 0.28°, σ_{Yaw} = 0.06°

Ship motions at centre of gravity (CoG) Depth = 18.0 m, H = 2.00 m, T_1 = 15.60 s, T_2 = 20.96 s Head-on waves	Bichromatic	B610e
	A2_B610e	
Deltares	11202696	App. G.016-2

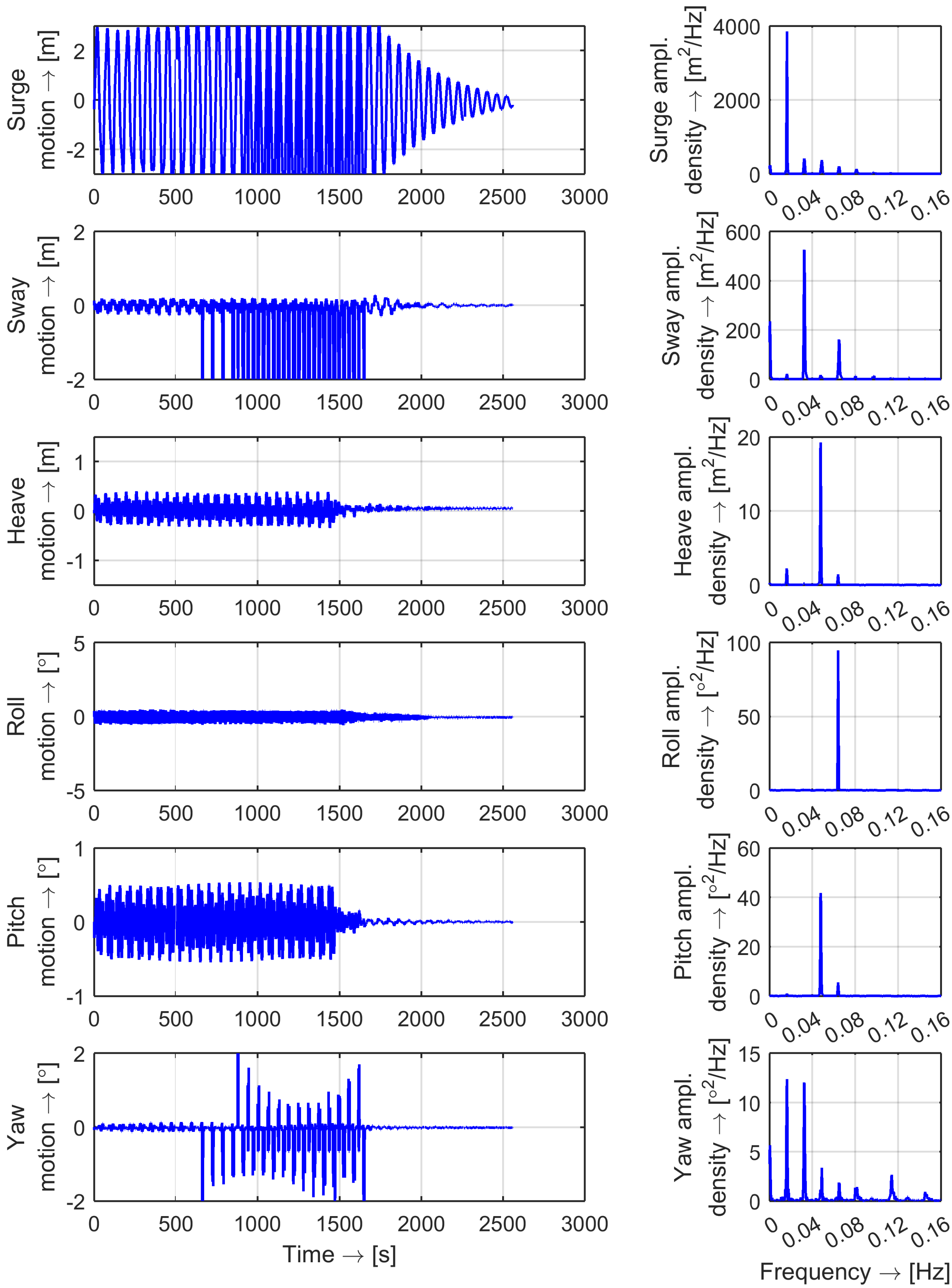

σ_{Surge} = 2.25 m, σ_{Sway} = 1.13 m, σ_{Heave} = 0.15 m, σ_{Roll} = 0.26°, σ_{Pitch} = 0.22°, σ_{Yaw} = 0.29°

Ship motions at centre of gravity (CoG) Depth = 18.0 m, H = 2.00 m, T_1 = 15.60 s, T_2 = 20.96 s Head-on waves	Bichromatic	B610e
	A2_B610e_noST	
Deltares	11202696	App. G.017-2

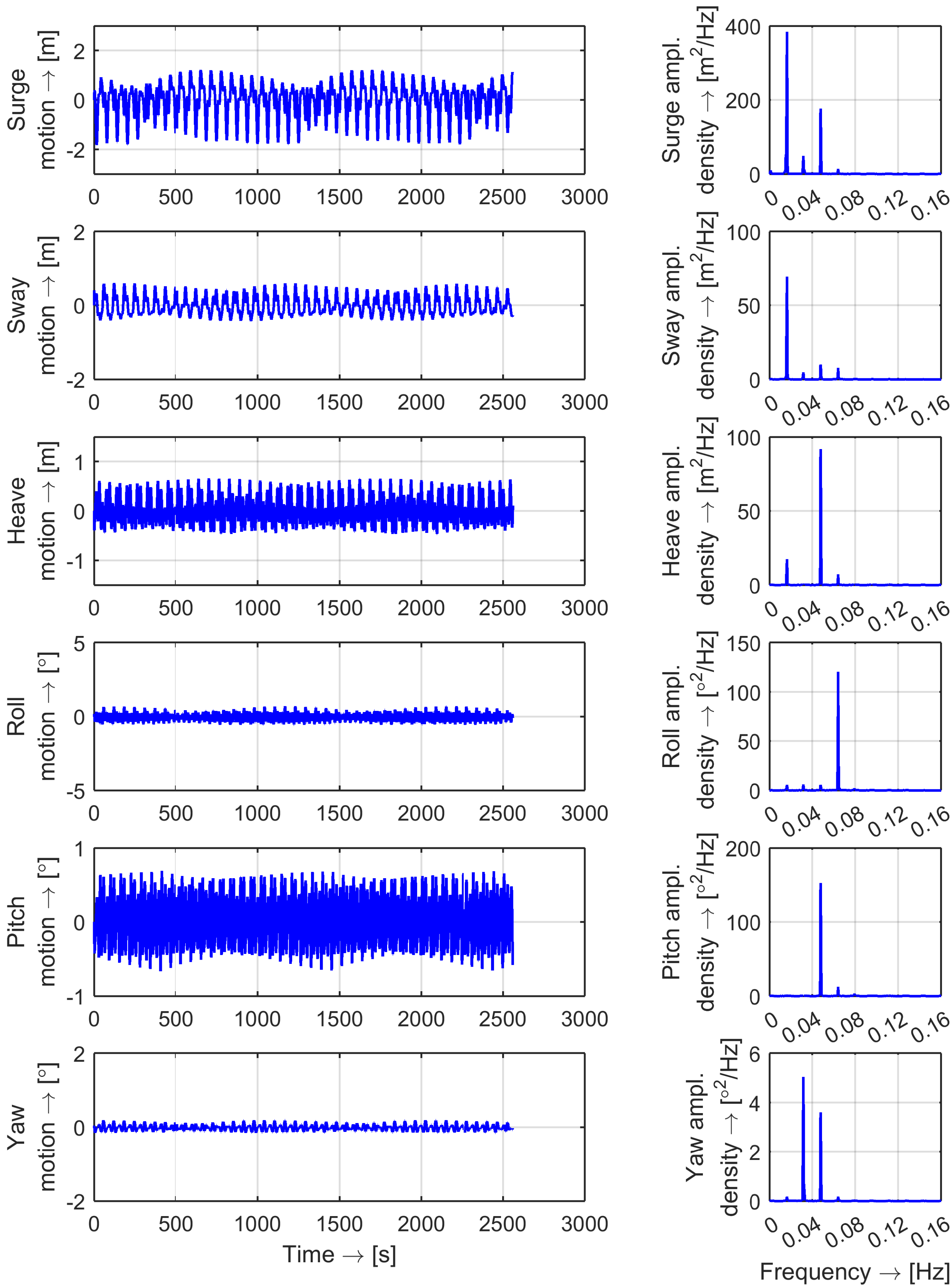

σ_{Surge} = 0.70 m, σ_{Sway} = 0.25 m, σ_{Heave} = 0.29 m, σ_{Roll} = 0.30°, σ_{Pitch} = 0.34°, σ_{Yaw} = 0.08°

Ship motions at centre of gravity (CoG) Depth = 18.0 m, H = 2.00 m, T_1 = 15.60 s, T_2 = 20.96 s Head-on waves	Bichromatic	B610e
	A2_B610f	
Deltares	11202696	App. G.018-2

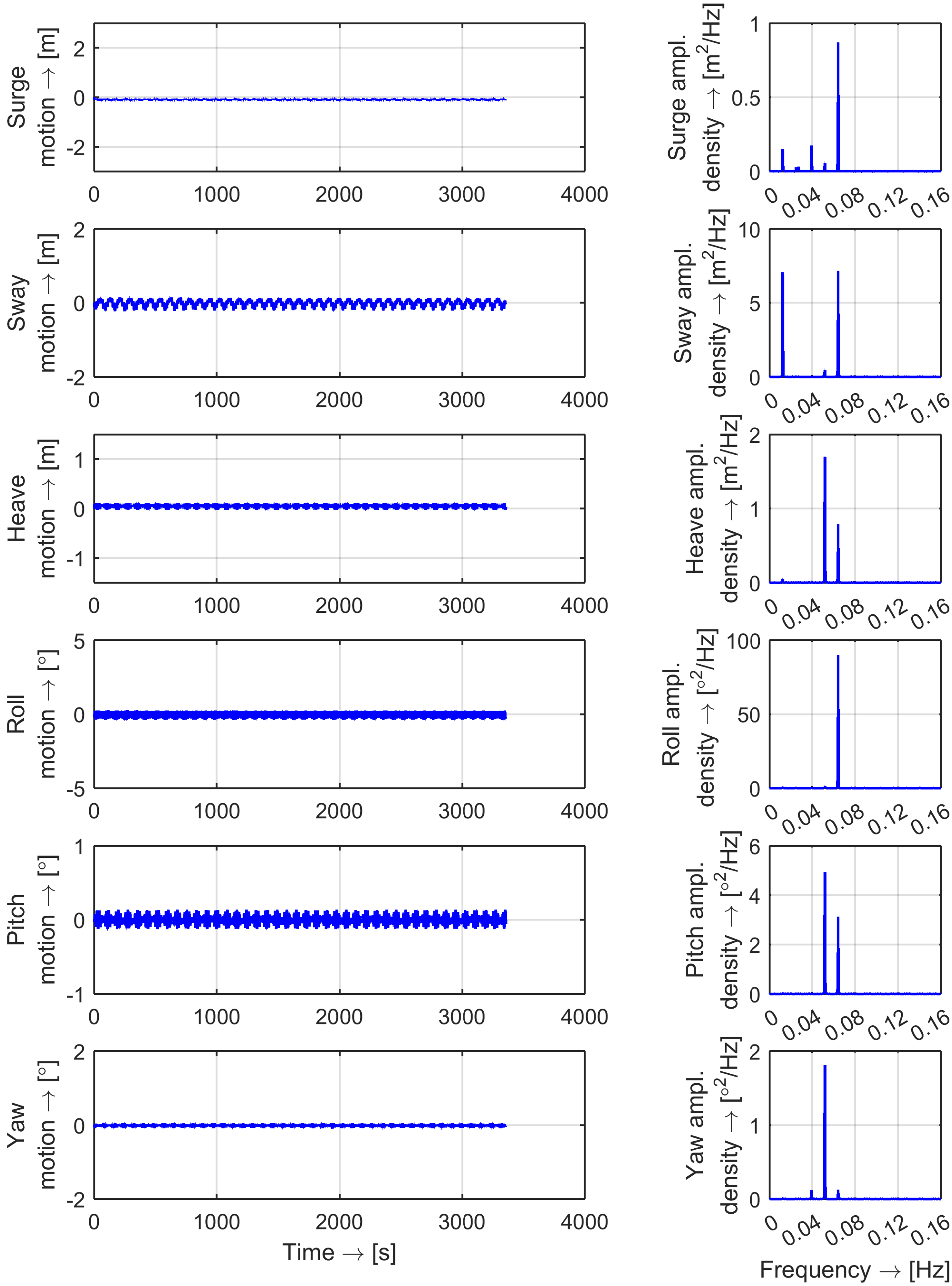

σ_{Surge} = 0.03 m, σ_{Sway} = 0.09 m, σ_{Heave} = 0.04 m, σ_{Roll} = 0.20°, σ_{Pitch} = 0.07°, σ_{Yaw} = 0.04°

Ship motions at centre of gravity (CoG) Depth = 18.0 m, H = 1.00 m, T_1 = 15.60 s, T_2 = 19.38 s Head-on waves	Bichromatic	B800a
	A2_B800a	
Deltares	11202696	App. G.019-2

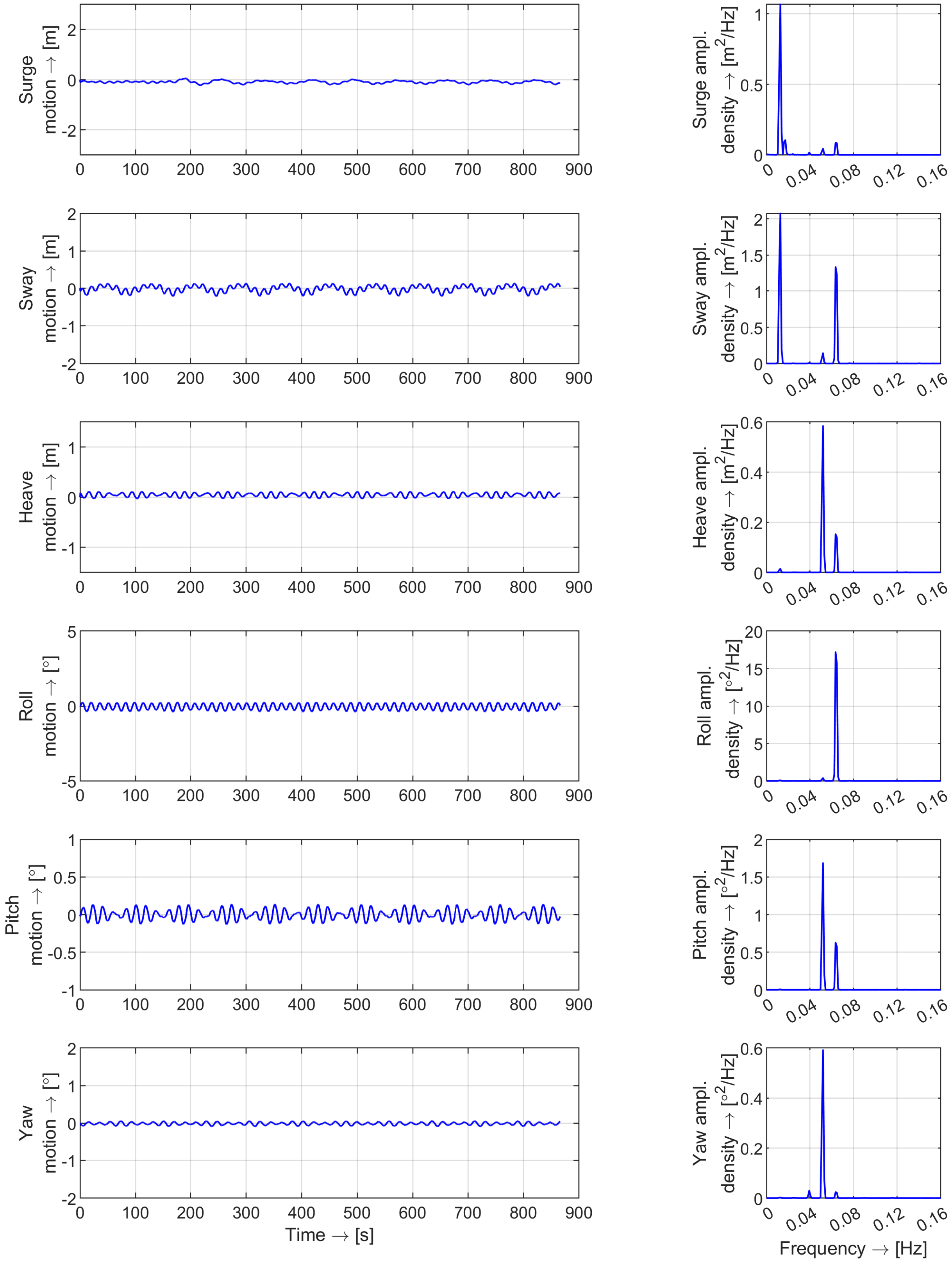

σ_{Surge} = n.a., σ_{Sway} = n.a., σ_{Heave} = n.a., σ_{Roll} = n.a., σ_{Pitch} = n.a., σ_{Yaw} = n.a.

Ship motions at centre of gravity (CoG) Depth = 18.0 m, H = 1.00 m, T_1 = 15.60 s, T_2 = 19.38 s Head-on waves	Bichromatic	B800a
	A2_B800a_Transition	
Deltares	11202696	App. G.020-2

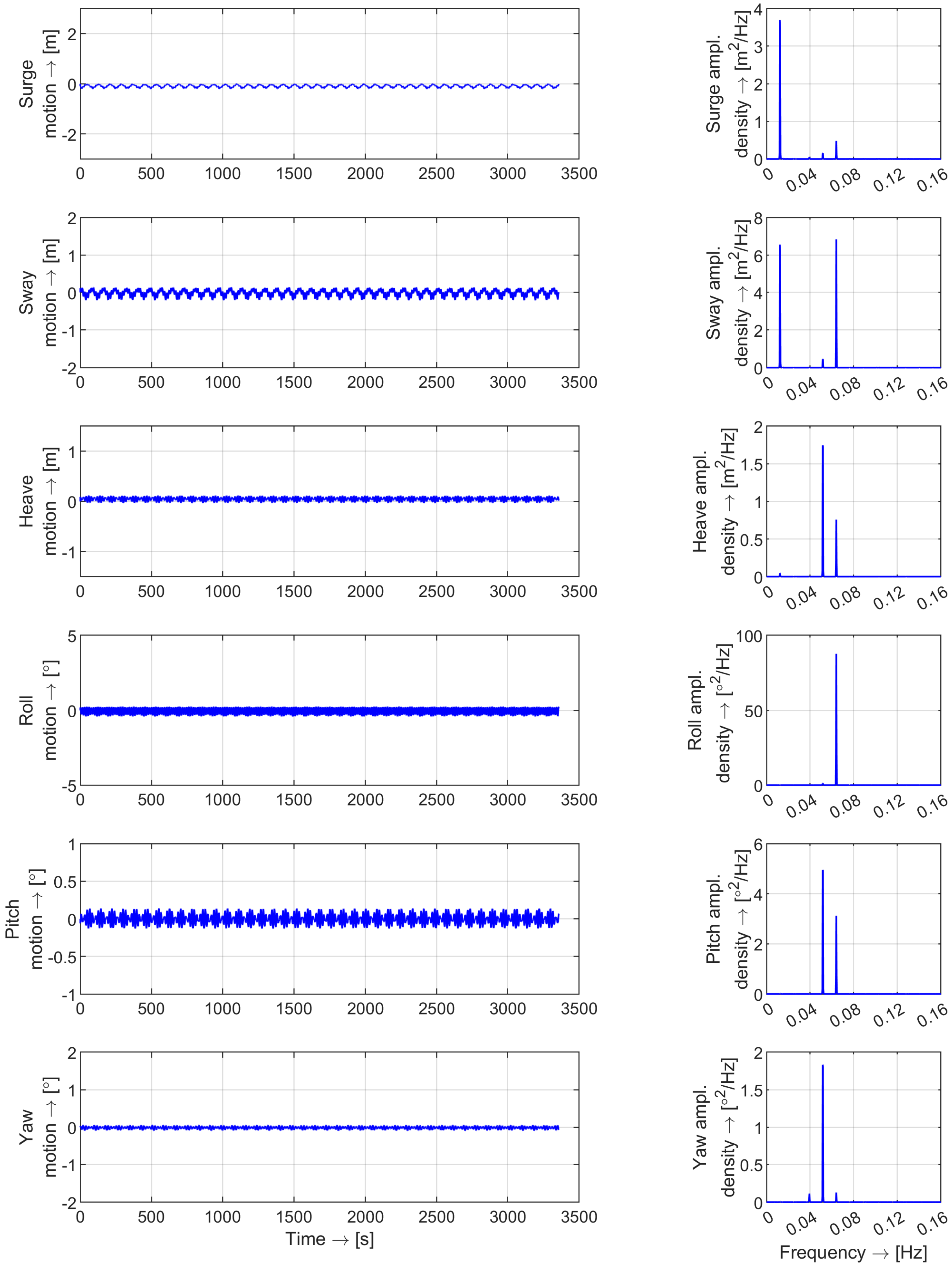

σ_{Surge} = 0.05 m, σ_{Sway} = 0.09 m, σ_{Heave} = 0.04 m, σ_{Roll} = 0.20°, σ_{Pitch} = 0.07°, σ_{Yaw} = 0.04°

Ship motions at centre of gravity (CoG) Depth = 18.0 m, H = 1.00 m, T_1 = 15.60 s, T_2 = 19.38 s Head-on waves	Bichromatic	B800a
	A2_B800a_noST	
Deltares	11202696	App. G.021-2

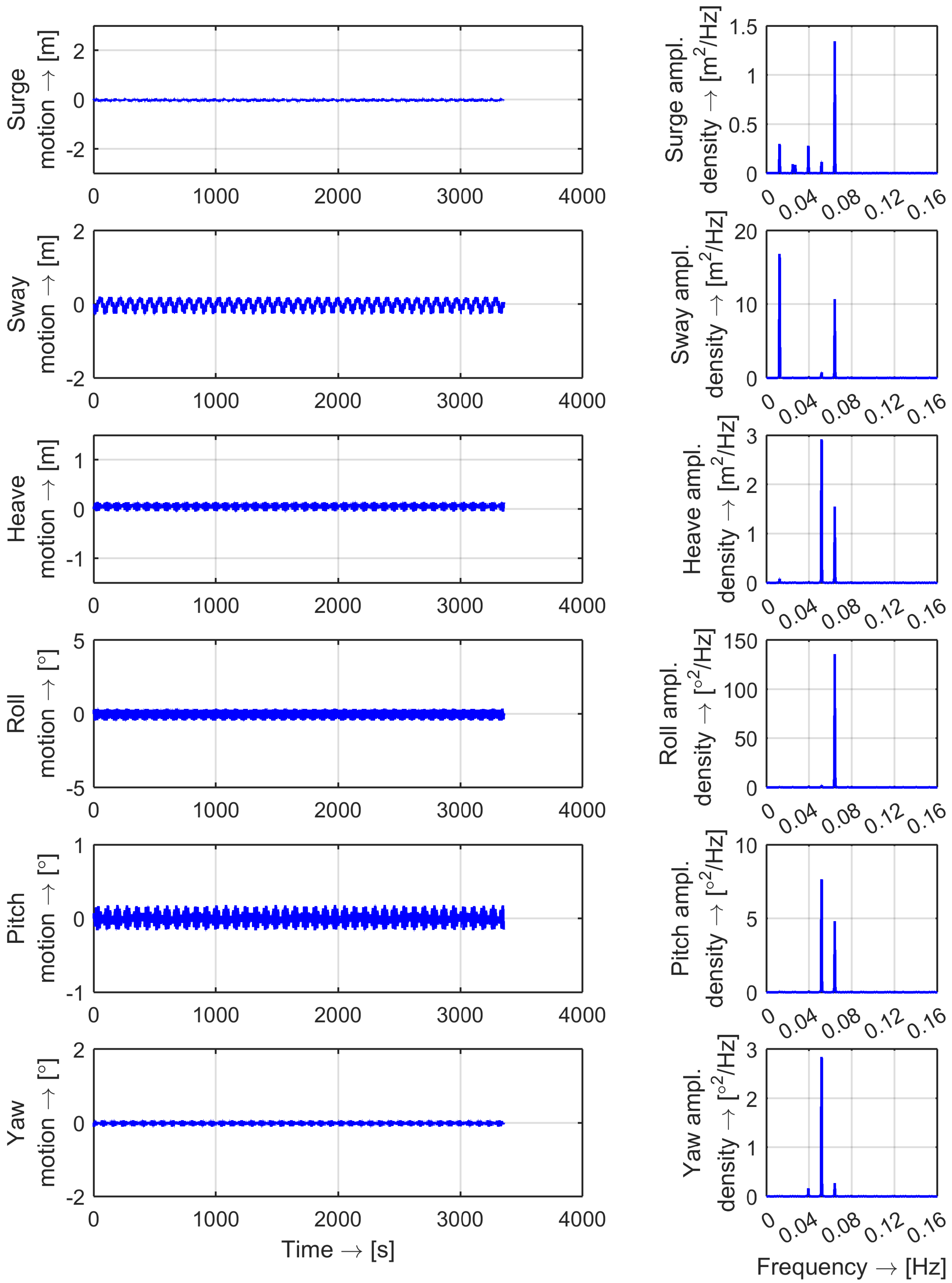

σ_{Surge} = 0.03 m, σ_{Sway} = 0.12 m, σ_{Heave} = 0.05 m, σ_{Roll} = 0.25°, σ_{Pitch} = 0.08°, σ_{Yaw} = 0.04°

Ship motions at centre of gravity (CoG) Depth = 18.0 m, H = 1.25 m, T_1 = 15.60 s, T_2 = 19.38 s Head-on waves	Bichromatic	B800b
	A2_B800b	
Deltares	11202696	App. G.022-2

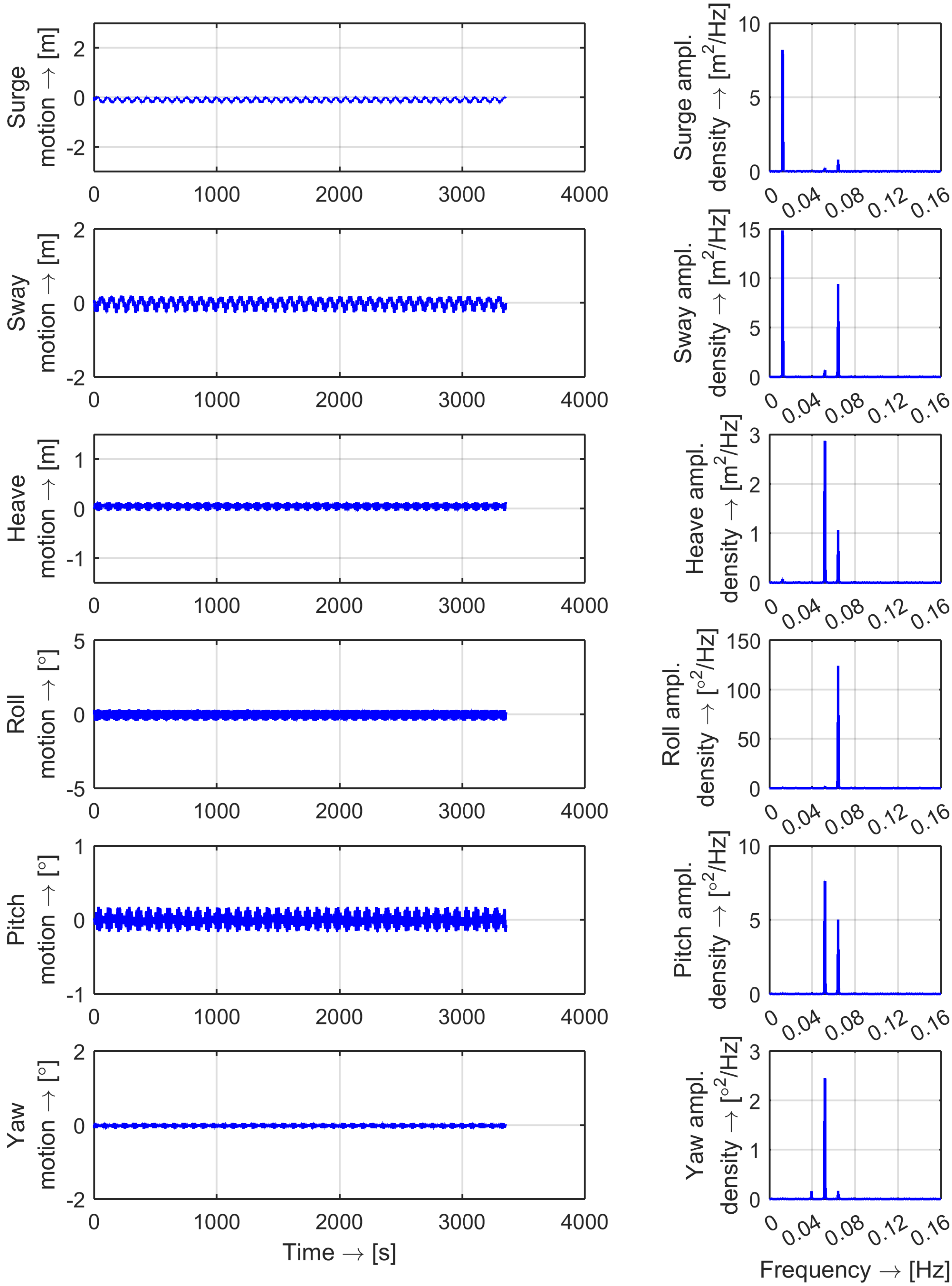

σ_{Surge} = 0.07 m, σ_{Sway} = 0.12 m, σ_{Heave} = 0.05 m, σ_{Roll} = 0.24°, σ_{Pitch} = 0.08°, σ_{Yaw} = 0.04°

Ship motions at centre of gravity (CoG) Depth = 18.0 m, H = 1.25 m, T_1 = 15.60 s, T_2 = 19.38 s Head-on waves	Bichromatic	B800b
	A2_B800b_noST	
Deltares	11202696	App. G.023-2

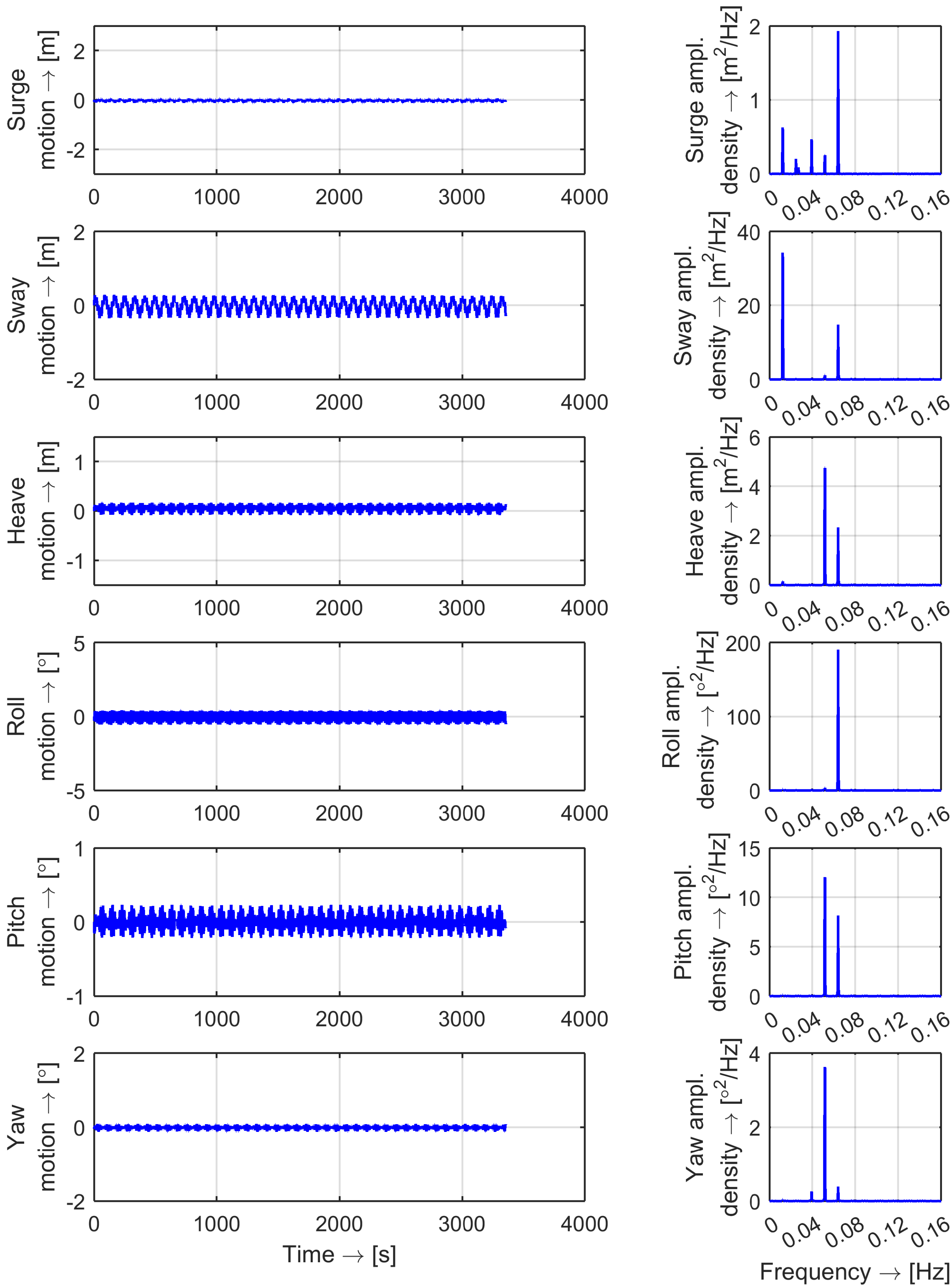

σ_{Surge} = 0.04 m, σ_{Sway} = 0.17 m, σ_{Heave} = 0.06 m, σ_{Roll} = 0.30°, σ_{Pitch} = 0.11°, σ_{Yaw} = 0.05°

Ship motions at centre of gravity (CoG) Depth = 18.0 m, H = 1.50 m, T_1 = 15.60 s, T_2 = 19.38 s Head-on waves	Bichromatic	B800c
	A2_B800c	
Deltares	11202696	App. G.024-2

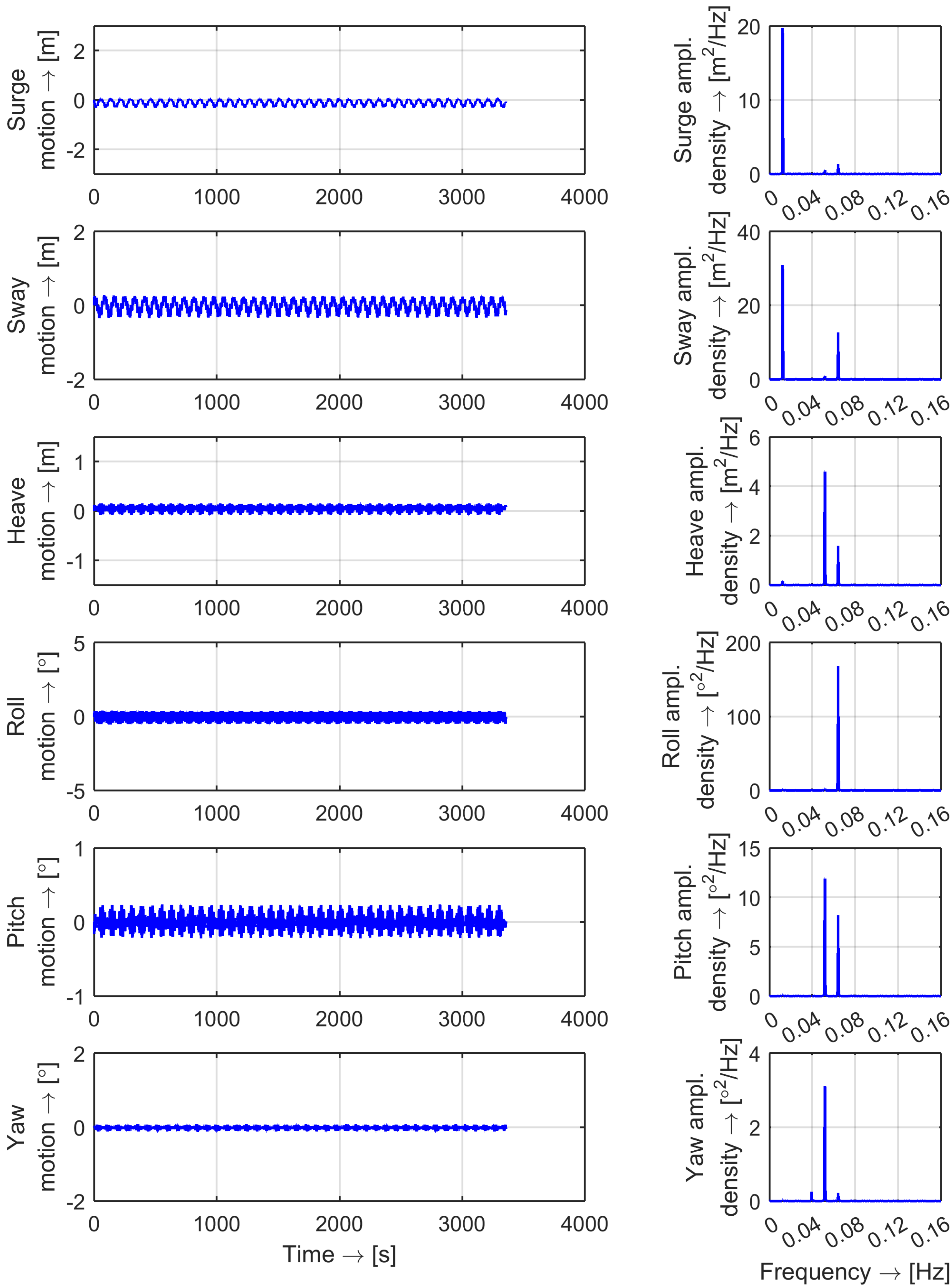

σ_{Surge} = 0.11 m, σ_{Sway} = 0.16 m, σ_{Heave} = 0.06 m, σ_{Roll} = 0.28°, σ_{Pitch} = 0.11°, σ_{Yaw} = 0.05°

Ship motions at centre of gravity (CoG) Depth = 18.0 m, H = 1.50 m, T_1 = 15.60 s, T_2 = 19.38 s Head-on waves	Bichromatic	B800c
	A2_B800c_noST	
Deltares	11202696	App. G.025-2

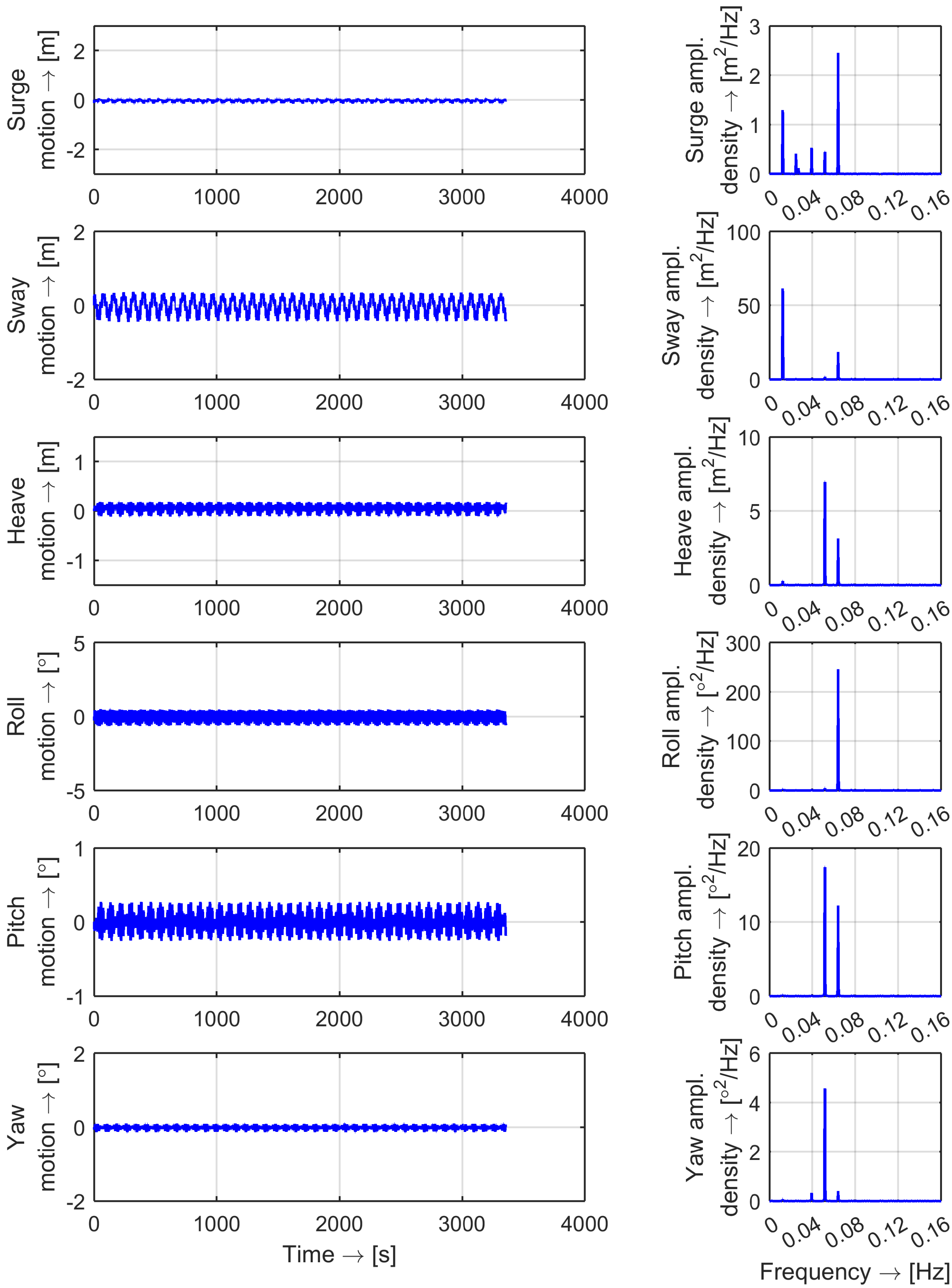

σ_{Surge} = 0.05 m, σ_{Sway} = 0.22 m, σ_{Heave} = 0.08 m, σ_{Roll} = 0.34°, σ_{Pitch} = 0.13°, σ_{Yaw} = 0.06°

Ship motions at centre of gravity (CoG) Depth = 18.0 m, H = 1.75 m, T_1 = 15.60 s, T_2 = 19.38 s Head-on waves	Bichromatic	B800d
	A2_B800d	
Deltares	11202696	App. G.026-2

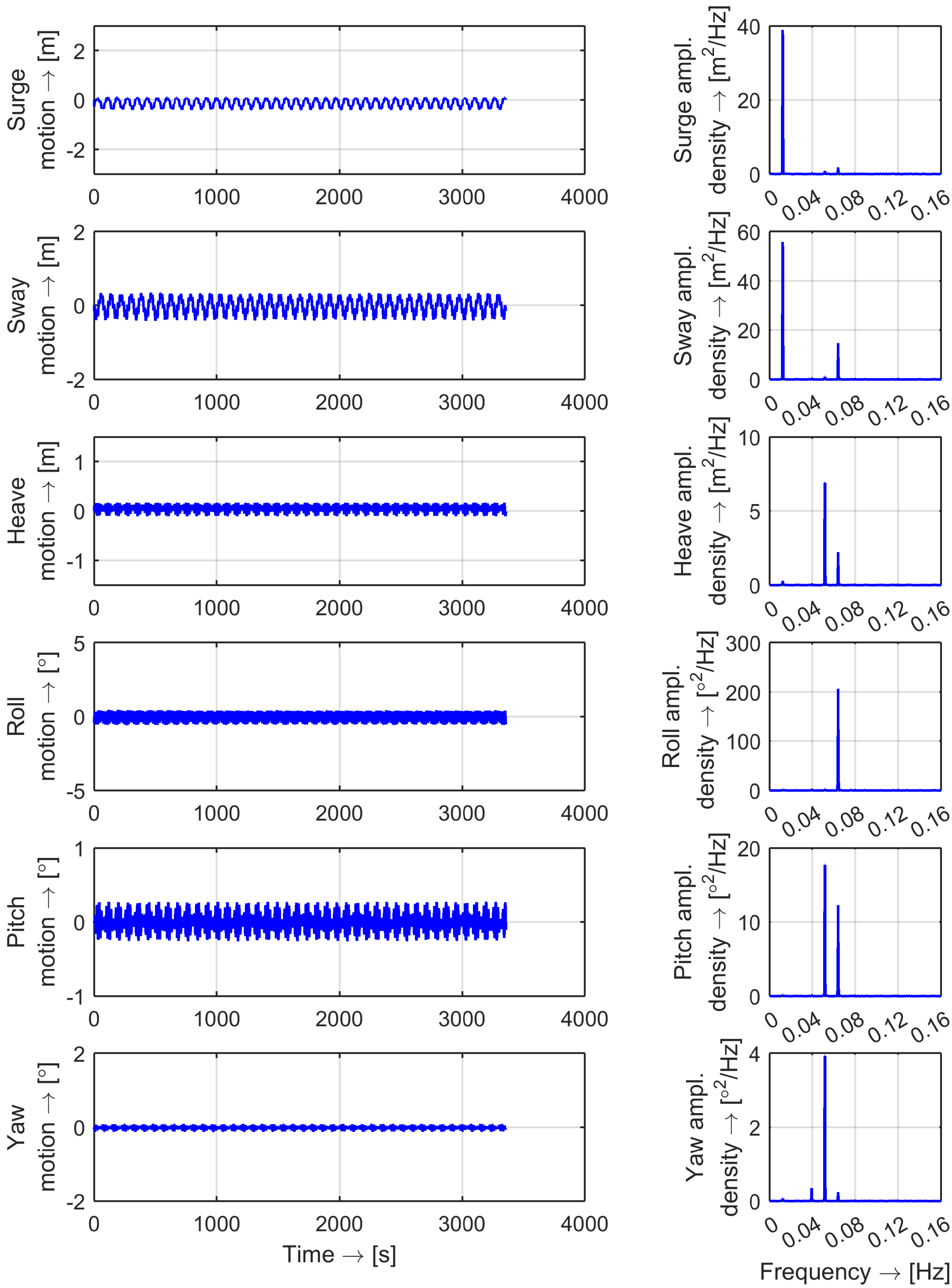

σ_{Surge} = 0.16 m, σ_{Sway} = 0.20 m, σ_{Heave} = 0.07 m, σ_{Roll} = 0.31°, σ_{Pitch} = 0.13°, σ_{Yaw} = 0.05°

Ship motions at centre of gravity (CoG) Depth = 18.0 m, H = 1.75 m, T_1 = 15.60 s, T_2 = 19.38 s Head-on waves	Bichromatic	B800d
	A2_B800d_noST	
Deltares	11202696	App. G.027-2

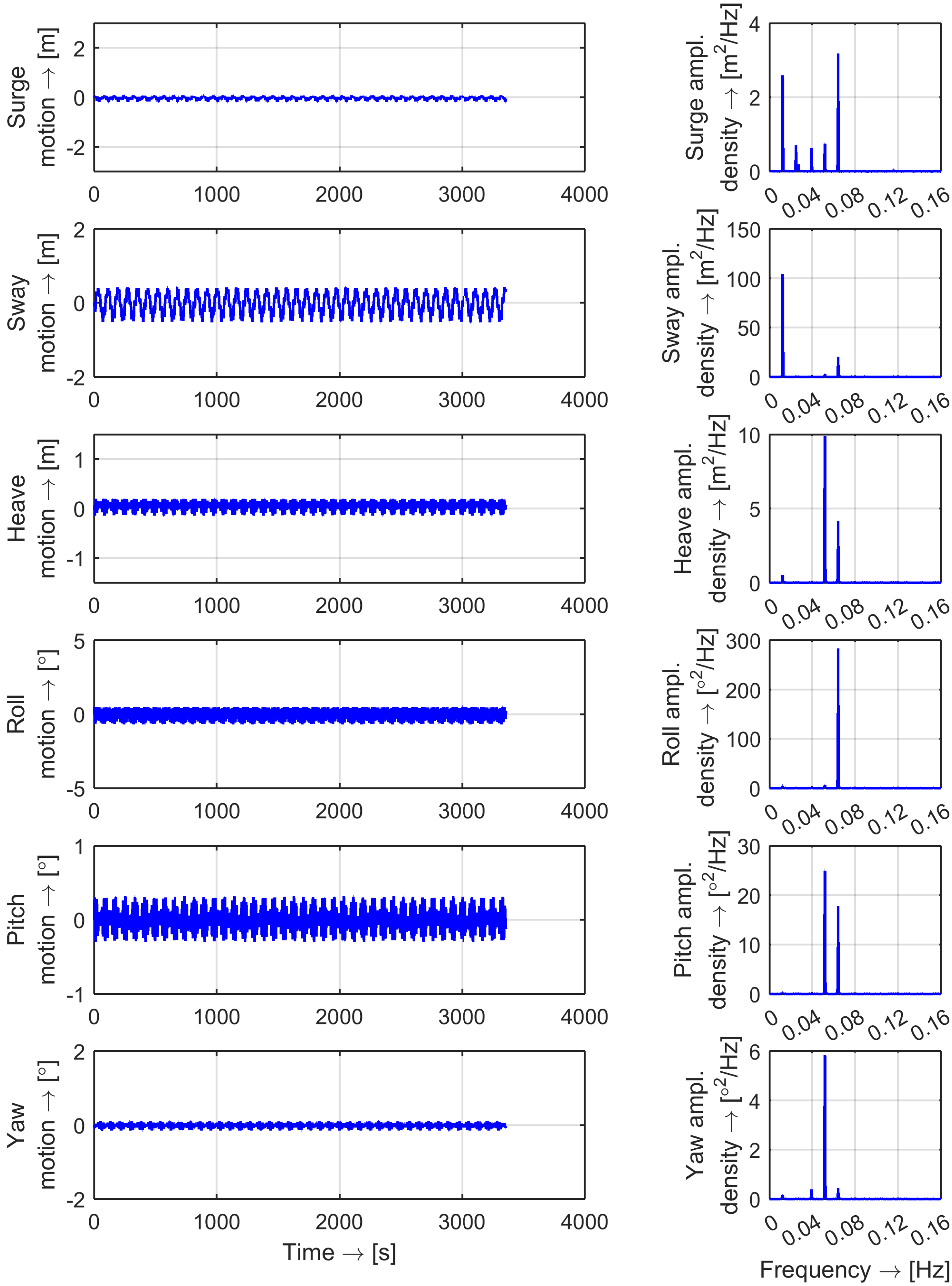

σ_{Surge} = 0.06 m, σ_{Sway} = 0.27 m, σ_{Heave} = 0.09 m, σ_{Roll} = 0.37°, σ_{Pitch} = 0.15°, σ_{Yaw} = 0.06°

Ship motions at centre of gravity (CoG) Depth = 18.0 m, H = 2.00 m, T_1 = 15.60 s, T_2 = 19.38 s Head-on waves	Bichromatic	B800e
	A2_B800e	
Deltares	11202696	App. G.028-2

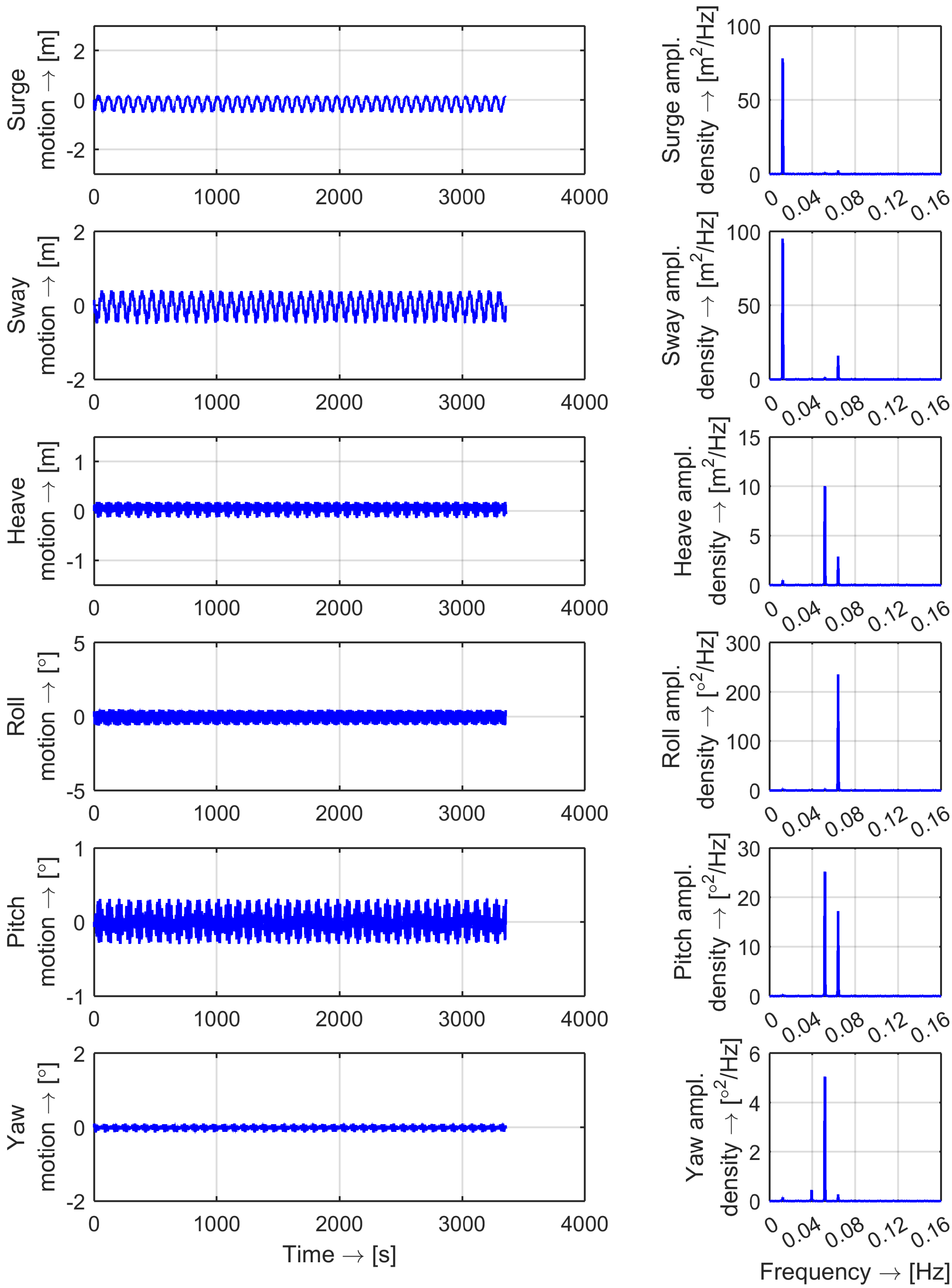

σ_{Surge} = 0.22 m, σ_{Sway} = 0.26 m, σ_{Heave} = 0.09 m, σ_{Roll} = 0.33°, σ_{Pitch} = 0.15°, σ_{Yaw} = 0.06°

Ship motions at centre of gravity (CoG) Depth = 18.0 m, H = 2.00 m, T_1 = 15.60 s, T_2 = 19.38 s Head-on waves	Bichromatic	B800e
	A2_B800e_noST	
Deltares	11202696	App. G.029-2

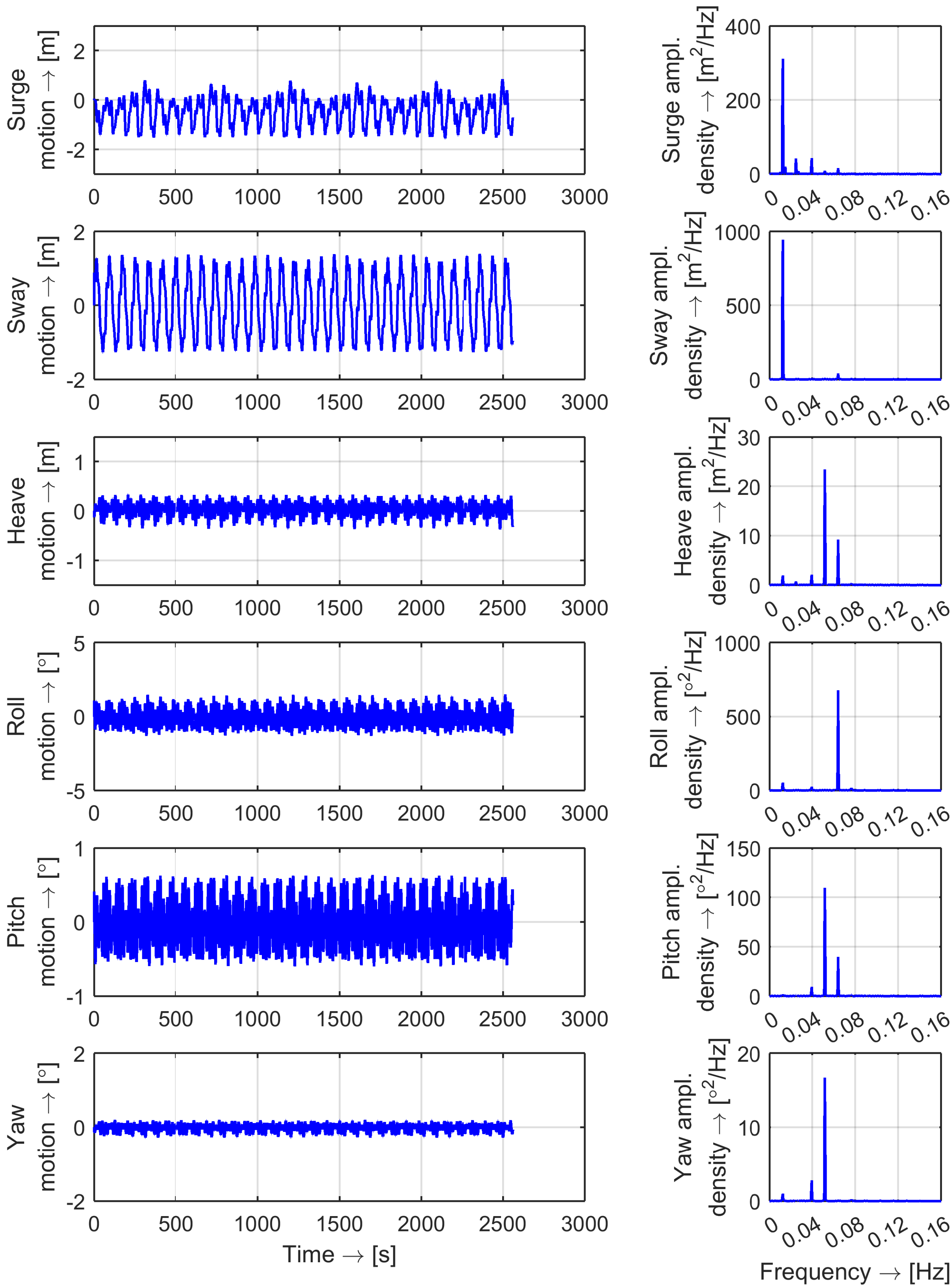

σ_{Surge} = 0.56 m, σ_{Sway} = 0.83 m, σ_{Heave} = 0.16 m, σ_{Roll} = 0.69°, σ_{Pitch} = 0.33°, σ_{Yaw} = 0.12°

Ship motions at centre of gravity (CoG) Depth = 18.0 m, H = 2.00 m, T_1 = 15.60 s, T_2 = 19.38 s Head-on waves	Bichromatic	B800e
	A2_B800f	
Deltares	11202696	App. G.030-2

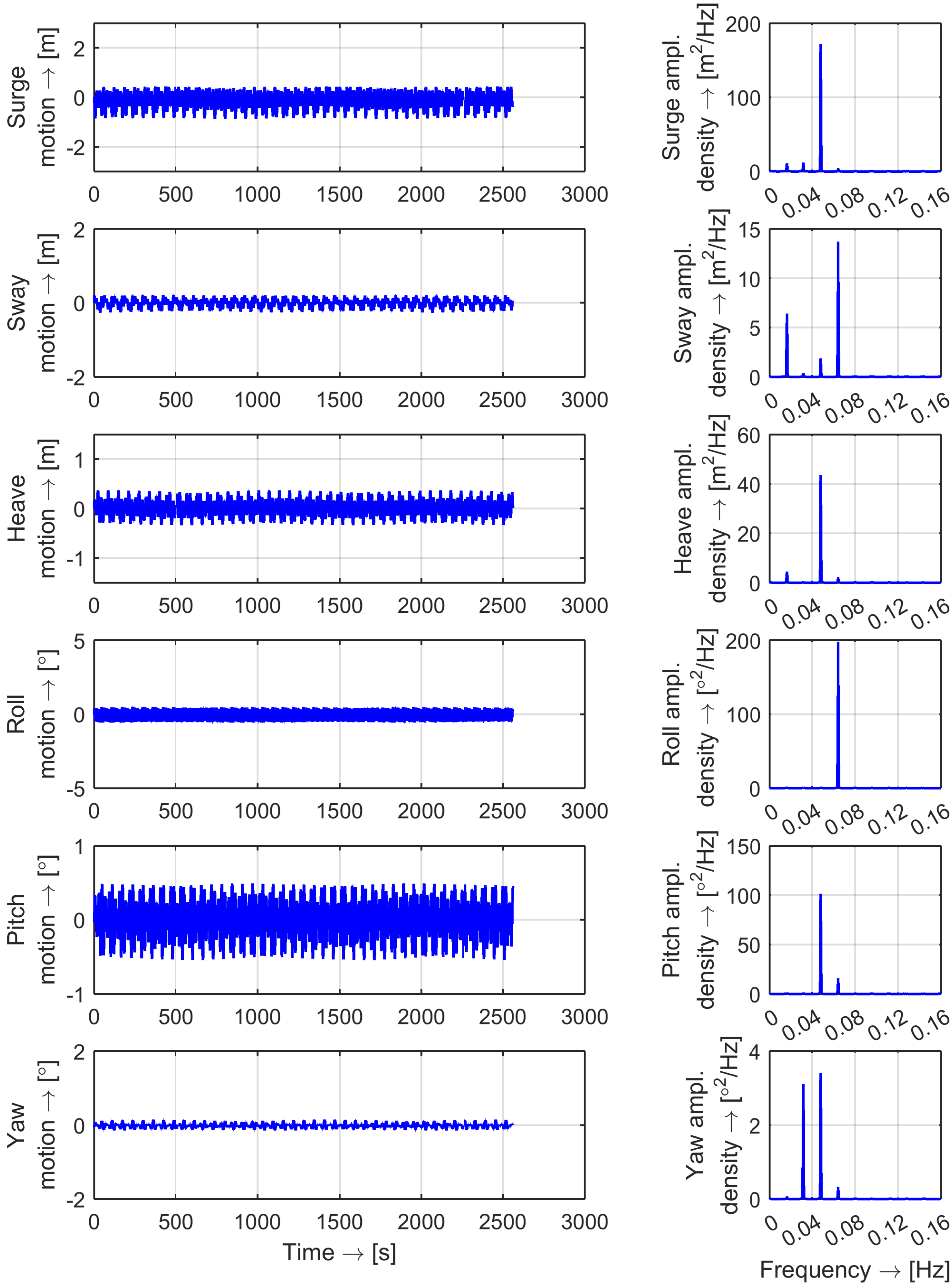

σ_{Surge} = 0.37 m, σ_{Sway} = 0.12 m, σ_{Heave} = 0.19 m, σ_{Roll} = 0.34°, σ_{Pitch} = 0.28°, σ_{Yaw} = 0.07°

Ship motions at centre of gravity (CoG) Depth = 18.0 m, H = 2.00 m, T_1 = 15.60 s, T_2 = 20.96 s Head-on waves	Bichromatic	B610e
	A3_B610e_200t	
Deltares	11202696	App. G.031-2

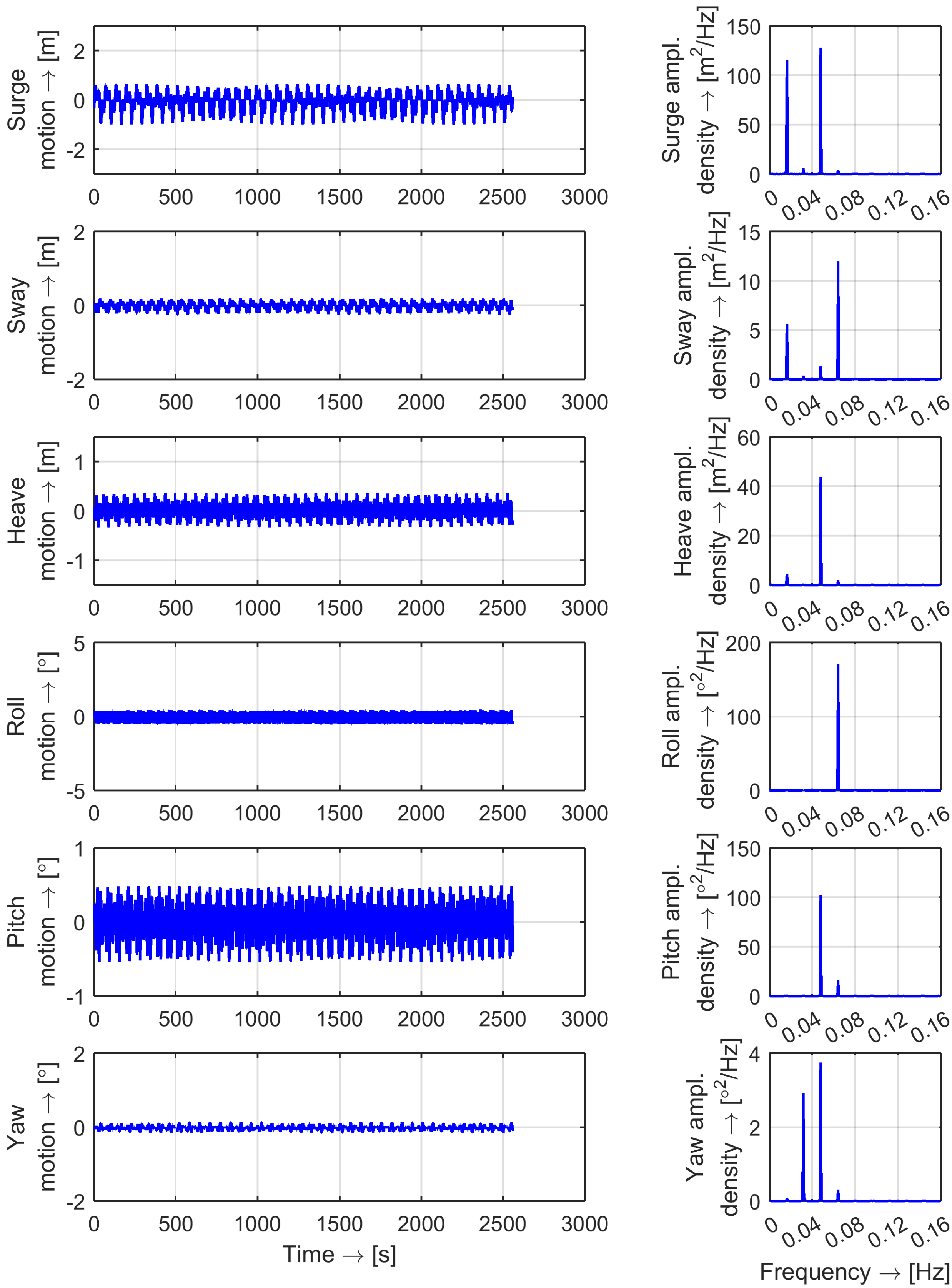

σ_{Surge} = 0.42 m, σ_{Sway} = 0.11 m, σ_{Heave} = 0.18 m, σ_{Roll} = 0.32°, σ_{Pitch} = 0.28°, σ_{Yaw} = 0.07°

Ship motions at centre of gravity (CoG) Depth = 18.0 m, H = 2.00 m, T_1 = 15.60 s, T_2 = 20.96 s Head-on waves	Bichromatic	B610e
	A3_B610e_sga	
Deltares	11202696	App. G.032-2

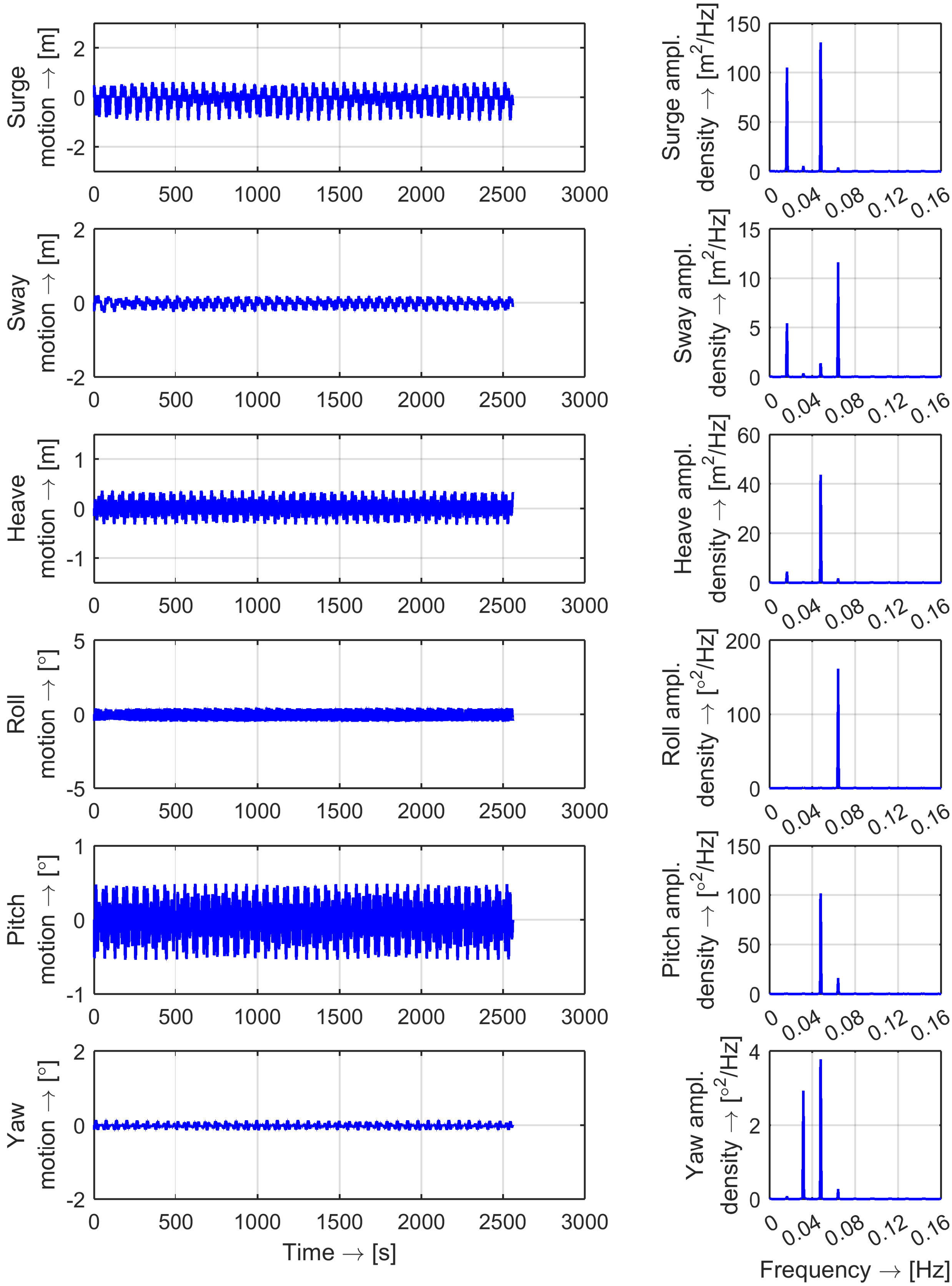

σ_{Surge} = 0.41 m, σ_{Sway} = 0.11 m, σ_{Heave} = 0.18 m, σ_{Roll} = 0.31°, σ_{Pitch} = 0.28°, σ_{Yaw} = 0.07°

Ship motions at centre of gravity (CoG) Depth = 18.0 m, H = 2.00 m, T_1 = 15.60 s, T_2 = 20.96 s Head-on waves	Bichromatic	B610e
	A3_B610e_ssk	
Deltares	11202696	App. G.033-2

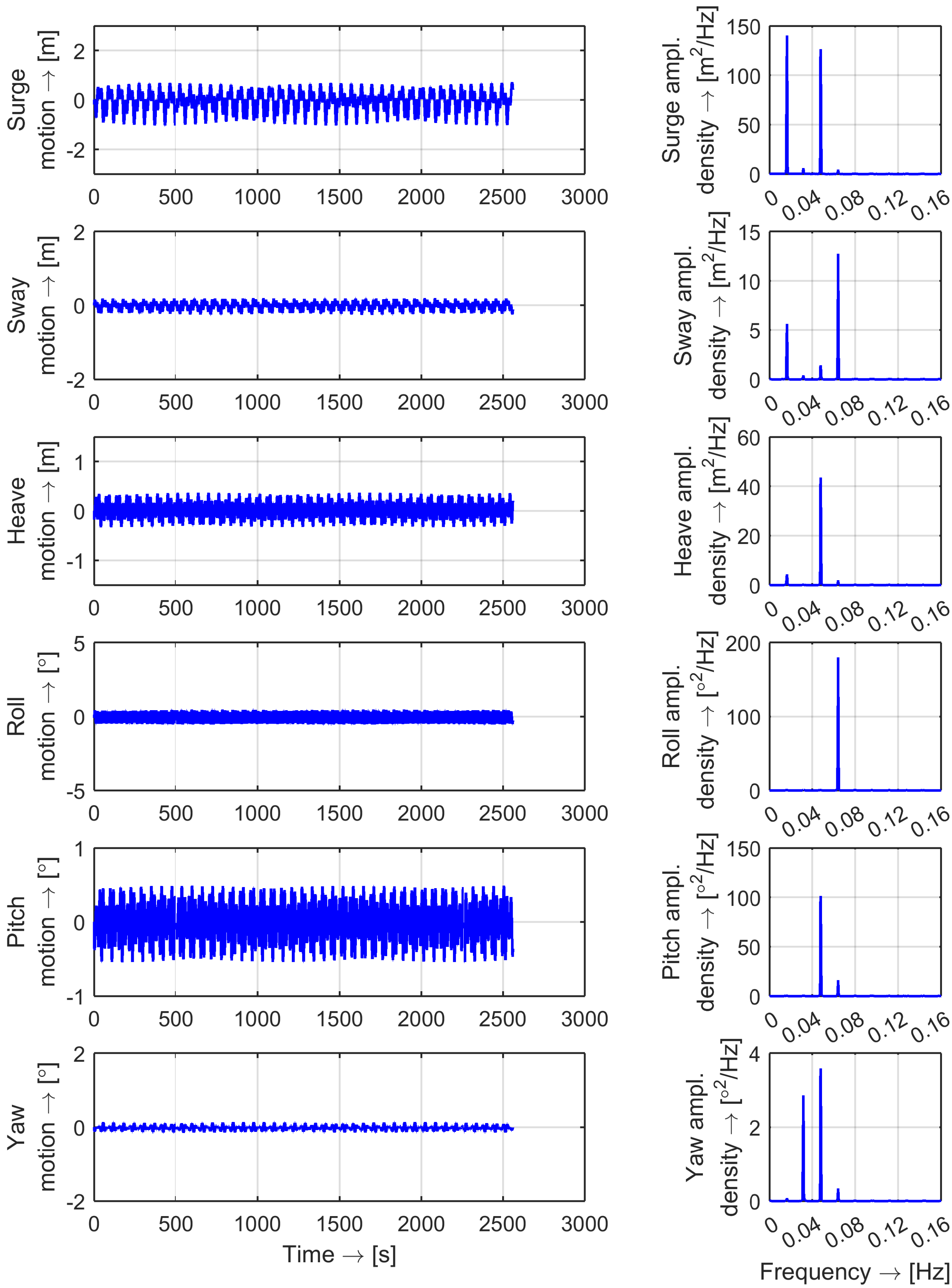

σ_{Surge} = 0.44 m, σ_{Sway} = 0.11 m, σ_{Heave} = 0.18 m, σ_{Roll} = 0.33°, σ_{Pitch} = 0.28°, σ_{Yaw} = 0.07°

Ship motions at centre of gravity (CoG) Depth = 18.0 m, H = 2.00 m, T_1 = 15.60 s, T_2 = 20.96 s Head-on waves	Bichromatic	B610e
	A3_B610e_ssk_sga	
Deltares	11202696	App. G.034-2

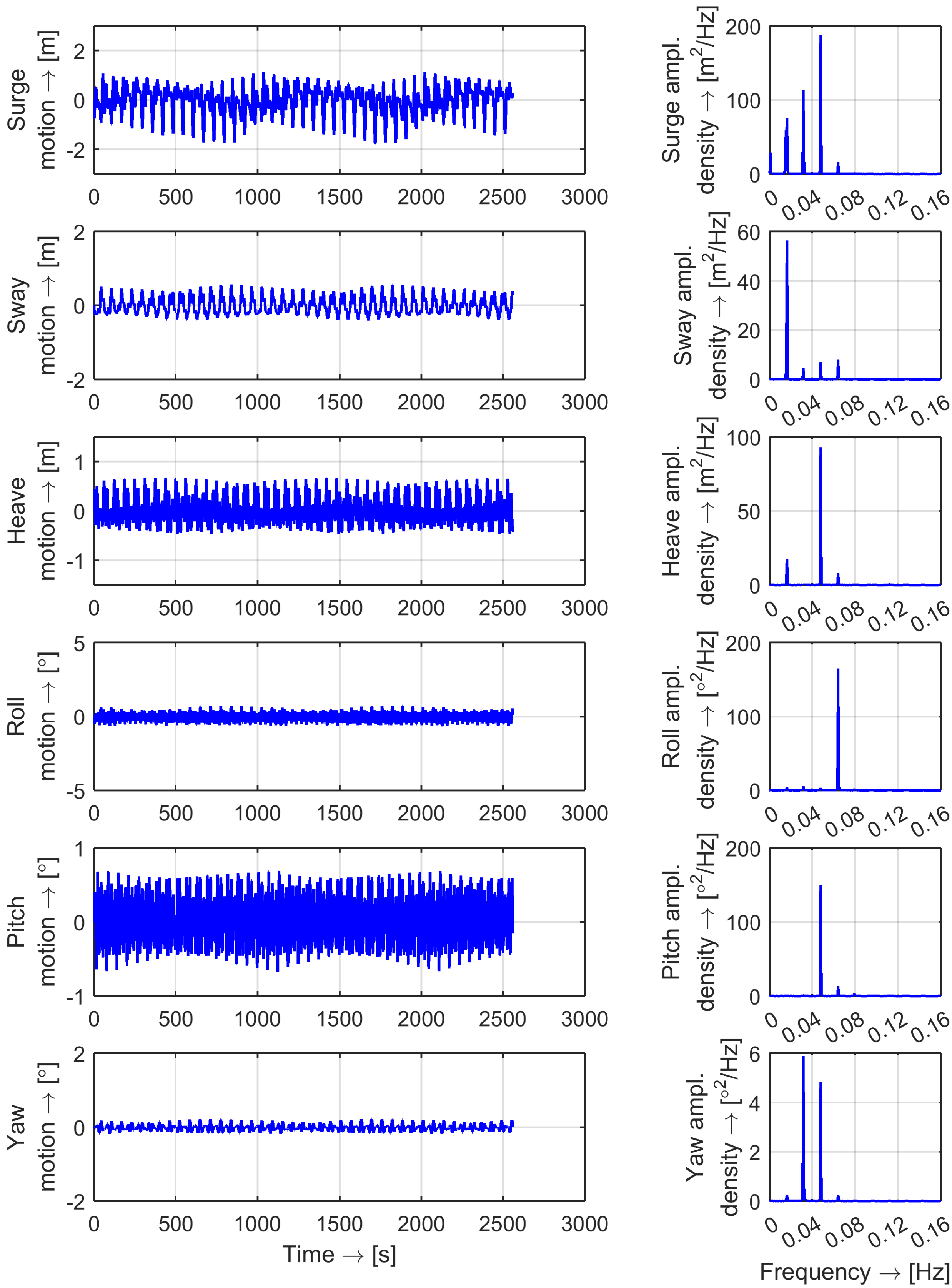

σ_{Surge} = 0.58 m, σ_{Sway} = 0.23 m, σ_{Heave} = 0.29 m, σ_{Roll} = 0.34°, σ_{Pitch} = 0.34°, σ_{Yaw} = 0.09°

Ship motions at centre of gravity (CoG) Depth = 18.0 m, H = 2.00 m, T_1 = 15.60 s, T_2 = 20.96 s Head-on waves	Bichromatic	B610e
	A3_B610f_200t	
Deltares	11202696	App. G.035-2

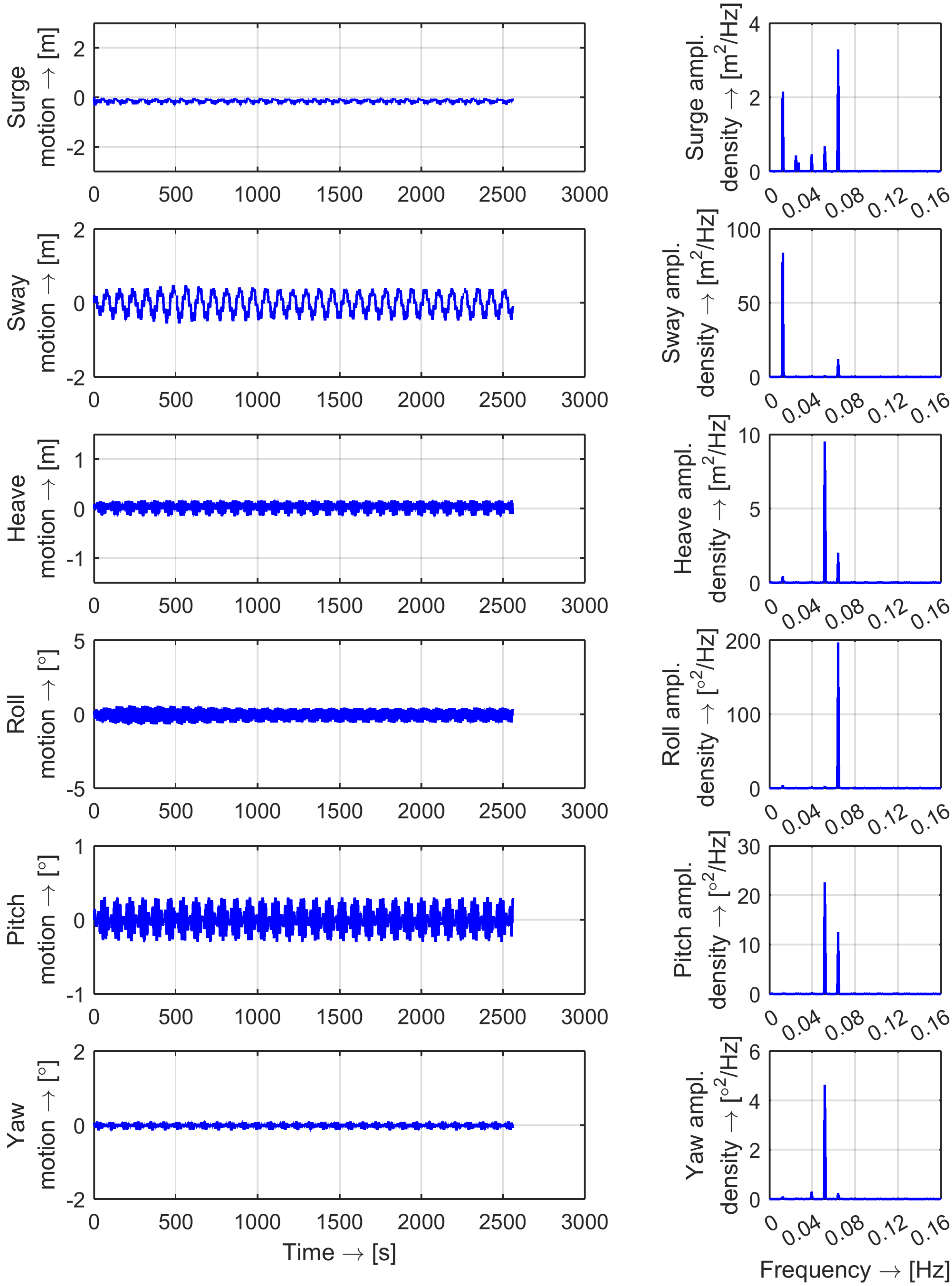

σ_{Surge} = 0.07 m, σ_{Sway} = 0.26 m, σ_{Heave} = 0.09 m, σ_{Roll} = 0.34°, σ_{Pitch} = 0.15°, σ_{Yaw} = 0.06°

Ship motions at centre of gravity (CoG) Depth = 18.0 m, H = 2.00 m, T_1 = 15.60 s, T_2 = 19.38 s Head-on waves	Bichromatic	B800e
	A3_B800e_200t	
Deltares	11202696	App. G.036-2

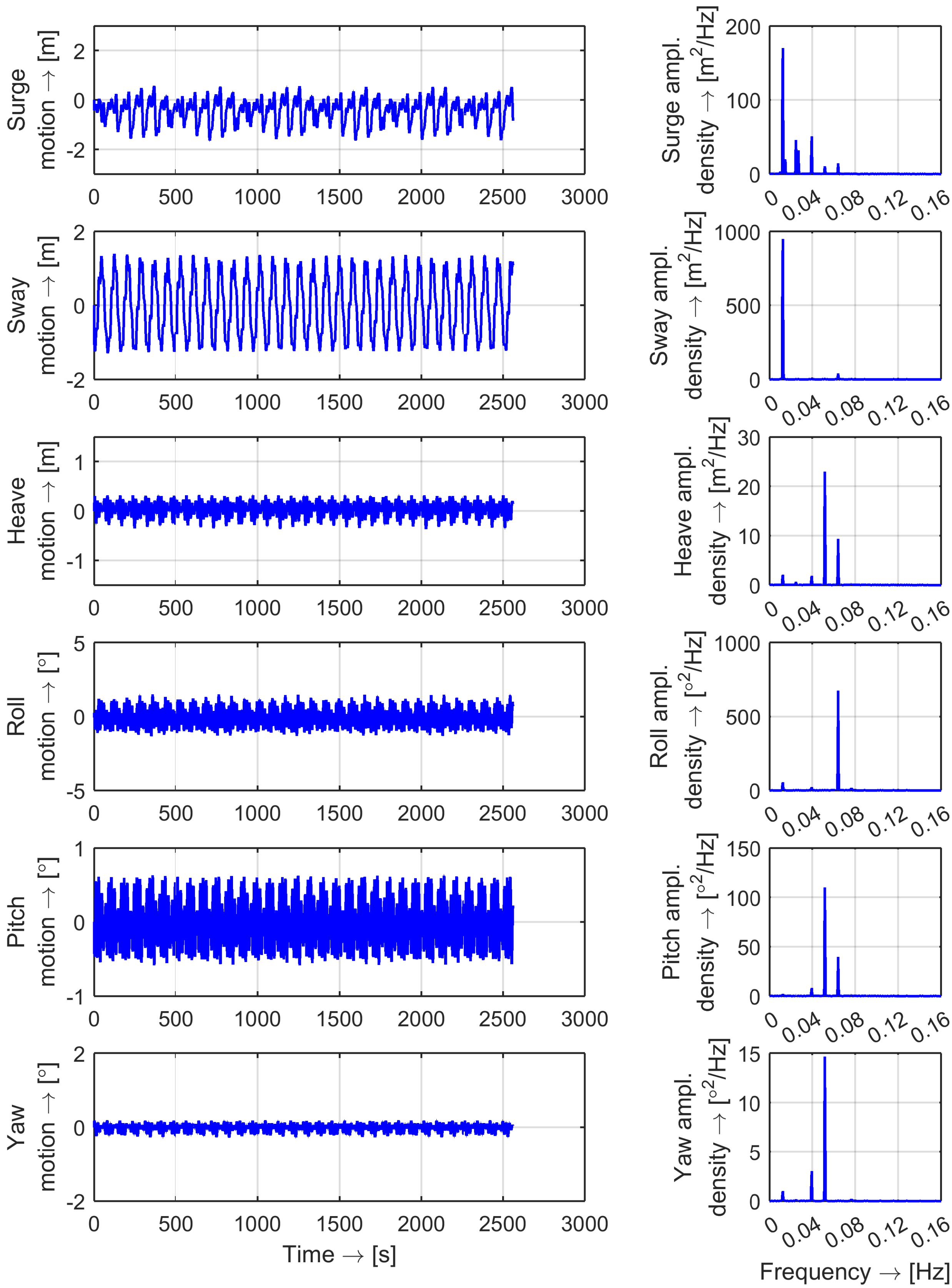

σ_{Surge} = 0.49 m, σ_{Sway} = 0.83 m, σ_{Heave} = 0.16 m, σ_{Roll} = 0.68°, σ_{Pitch} = 0.33°, σ_{Yaw} = 0.11°

Ship motions at centre of gravity (CoG) Depth = 18.0 m, H = 2.00 m, T_1 = 15.60 s, T_2 = 19.38 s Head-on waves	Bichromatic	B800e
	A3_B800f_200t	
Deltares	11202696	App. G.037-2

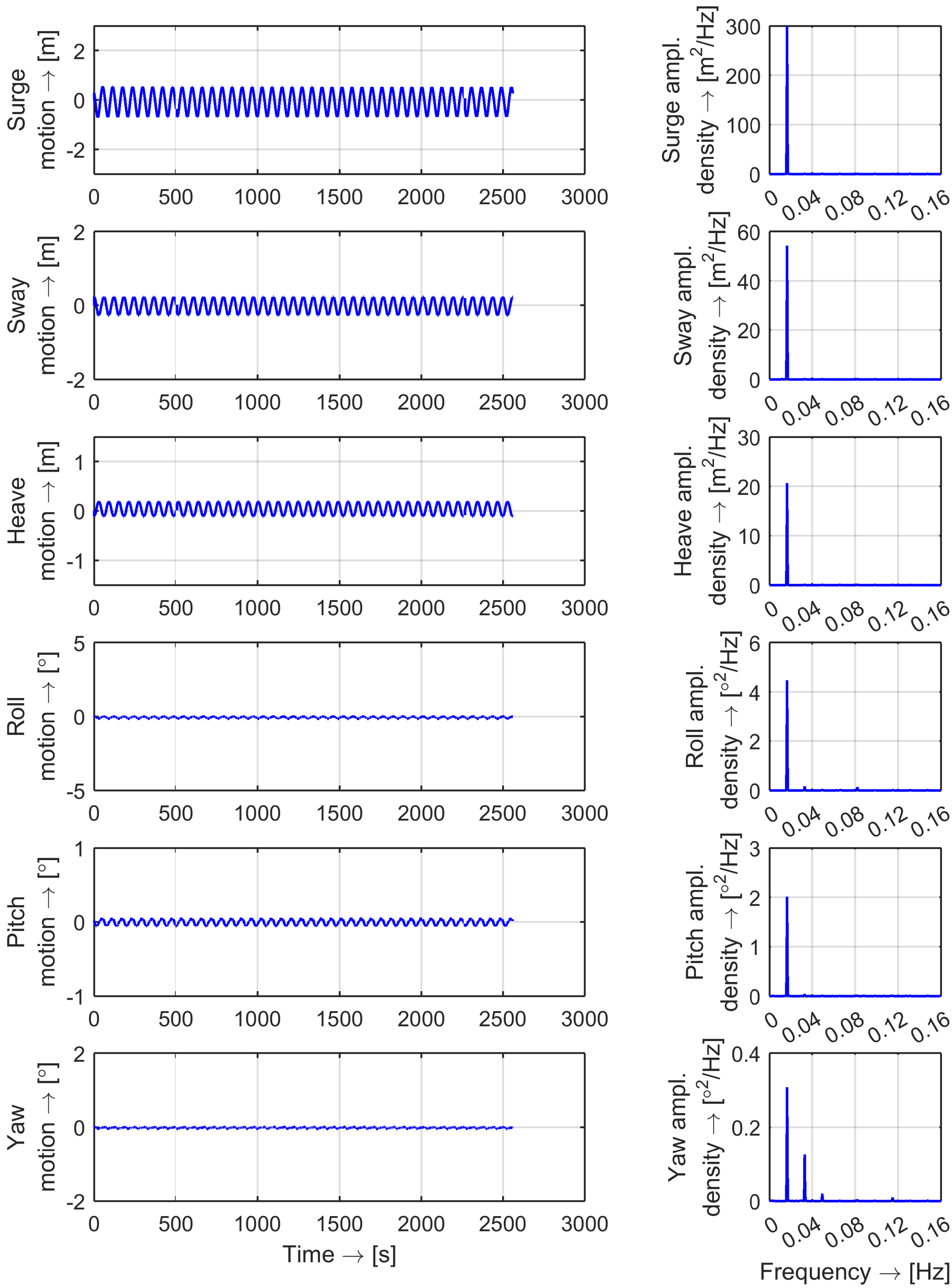

σ_{Surge} = 0.42 m, σ_{Sway} = 0.18 m, σ_{Heave} = 0.11 m, σ_{Roll} = 0.05°, σ_{Pitch} = 0.04°, σ_{Yaw} = 0.02°

Ship motions at centre of gravity (CoG) Depth = 18.0 m, H = 0.40 m, T = 61.00 s Head-on waves	Monochromatic	M610b
	A3_M610b_sga	
Deltares	11202696	App. G.038-2

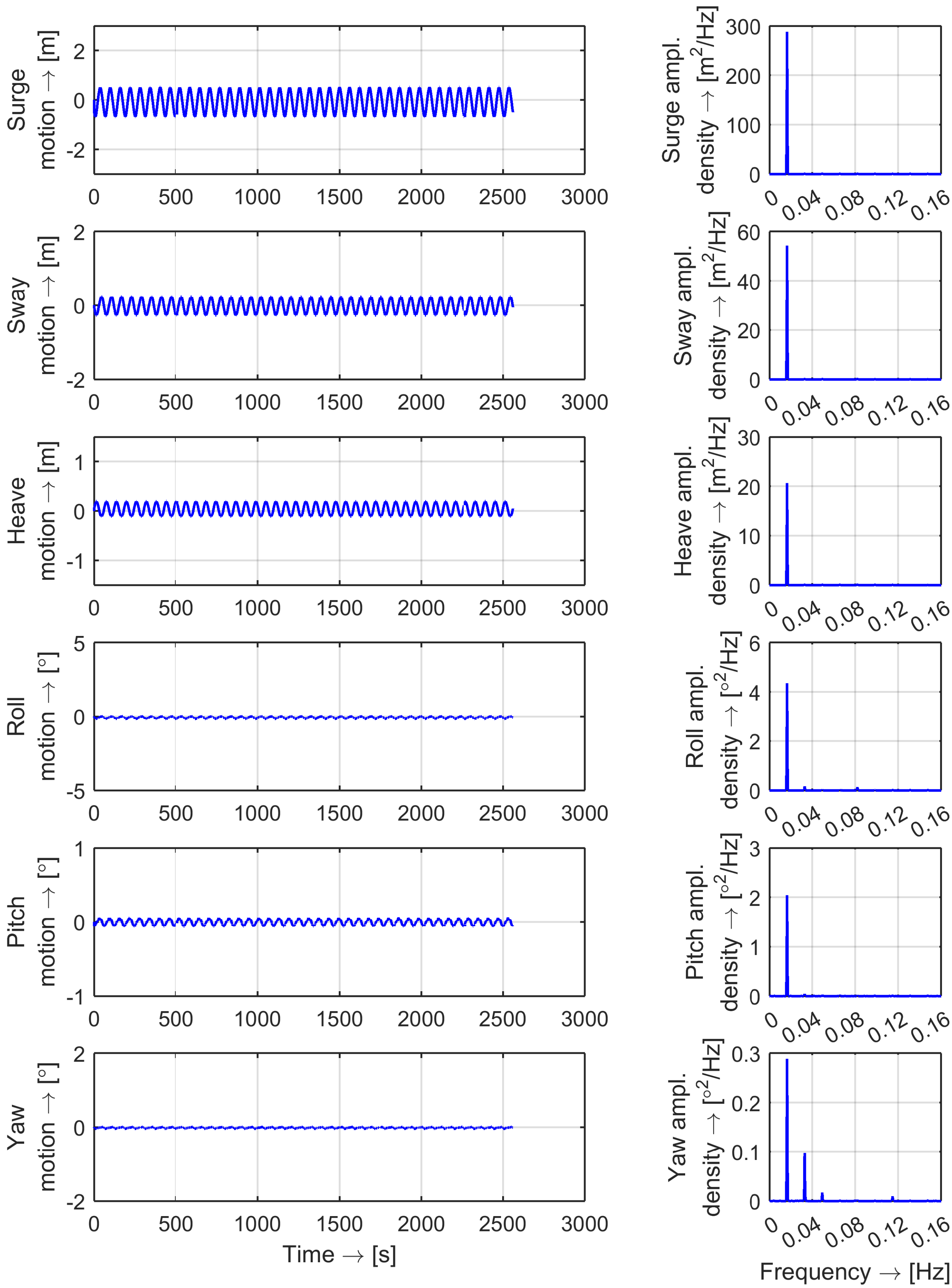

σ_{Surge} = 0.41 m, σ_{Sway} = 0.18 m, σ_{Heave} = 0.11 m, σ_{Roll} = 0.05°, σ_{Pitch} = 0.04°, σ_{Yaw} = 0.02°

Ship motions at centre of gravity (CoG) Depth = 18.0 m, H = 0.40 m, T = 61.00 s Head-on waves	Monochromatic	M610b
	A3_M610b_ssk	
Deltares	11202696	App. G.039-2

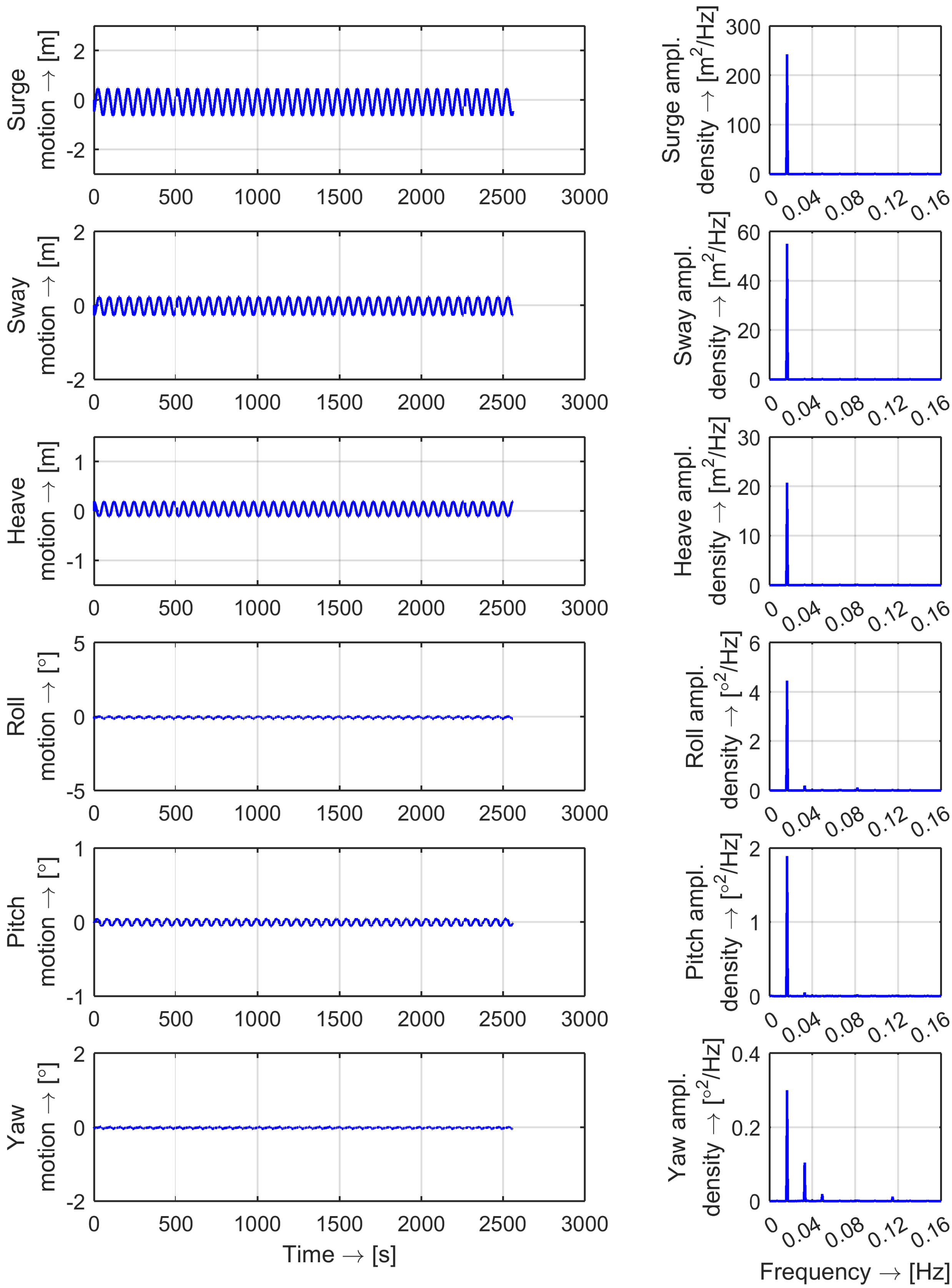

σ_{Surge} = 0.38 m, σ_{Sway} = 0.18 m, σ_{Heave} = 0.11 m, σ_{Roll} = 0.05°, σ_{Pitch} = 0.03°, σ_{Yaw} = 0.02°

Ship motions at centre of gravity (CoG) Depth = 18.0 m, H = 0.40 m, T = 61.00 s Head-on waves	Monochromatic	M610b
	A3_M610b_ssk_sga	
Deltares	11202696	App. G.040-2

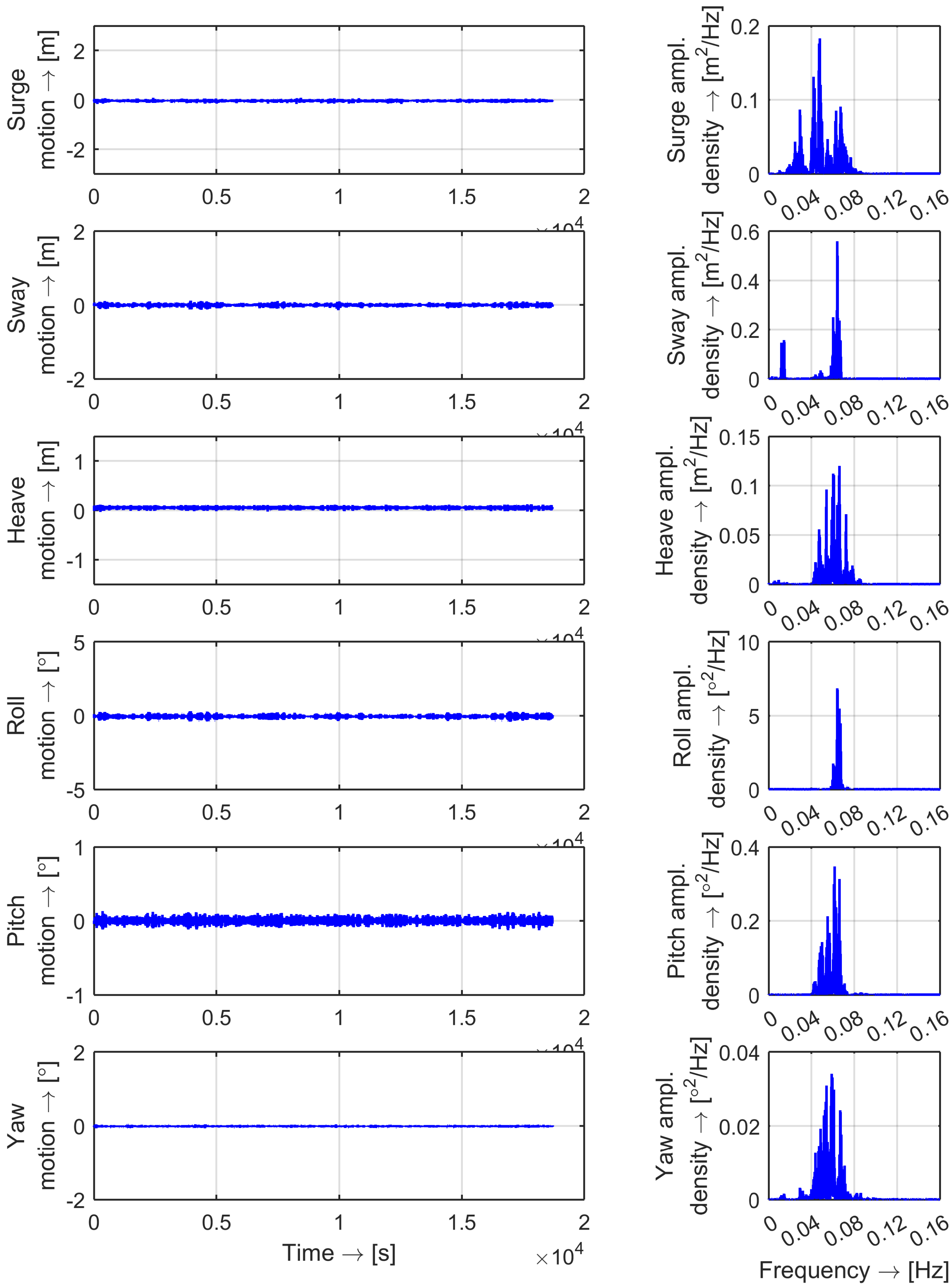

σ_{Surge} = 0.03 m, σ_{Sway} = 0.03 m, σ_{Heave} = 0.02 m, σ_{Roll} = 0.10°, σ_{Pitch} = 0.04°, σ_{Yaw} = 0.01°

Ship motions at centre of gravity (CoG) Depth = 18.0 m, H_{m0} = 0.50 m, T_p = 15.60 s, γ = 5.0 Head-on waves	Irregular	I156a
	A4_I156a	
Deltares	11202696	App. G.041-2

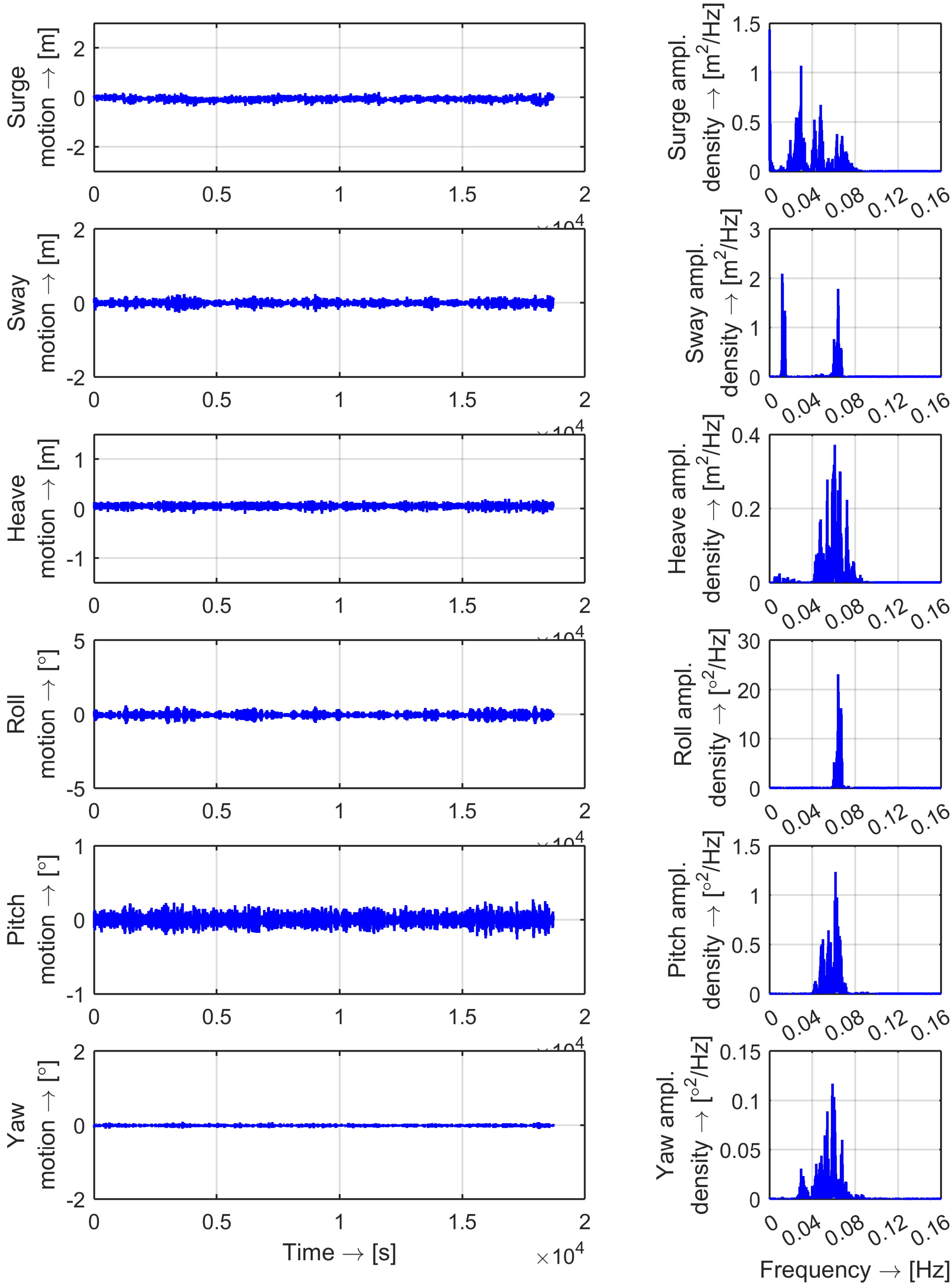

σ_{Surge} = 0.08 m, σ_{Sway} = 0.06 m, σ_{Heave} = 0.04 m, σ_{Roll} = 0.18°, σ_{Pitch} = 0.07°, σ_{Yaw} = 0.02°

Ship motions at centre of gravity (CoG) Depth = 18.0 m, H_{m0} = 1.00 m, T_p = 15.60 s, γ = 5.0 Head-on waves	Irregular	I156b
	A4_I156b	
Deltares	11202696	App. G.042-2

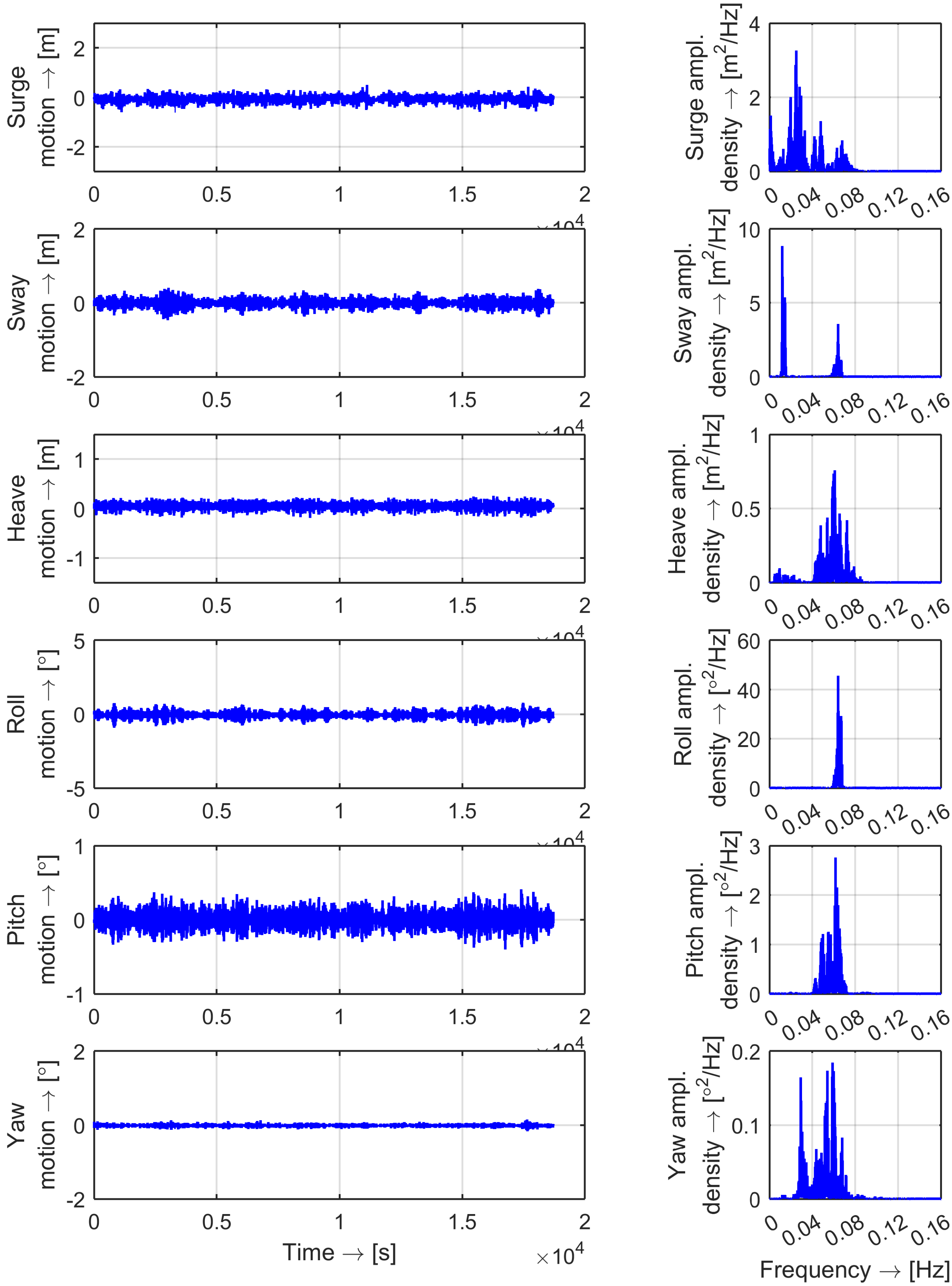

σ_{Surge} = 0.13 m, σ_{Sway} = 0.11 m, σ_{Heave} = 0.06 m, σ_{Roll} = 0.23°, σ_{Pitch} = 0.10°, σ_{Yaw} = 0.03°

Ship motions at centre of gravity (CoG) Depth = 18.0 m, H_{m0} = 1.50 m, T_p = 15.60 s, γ = 5.0 Head-on waves	Irregular	I156c
	A4_I156c	
Deltares	11202696	App. G.043-2

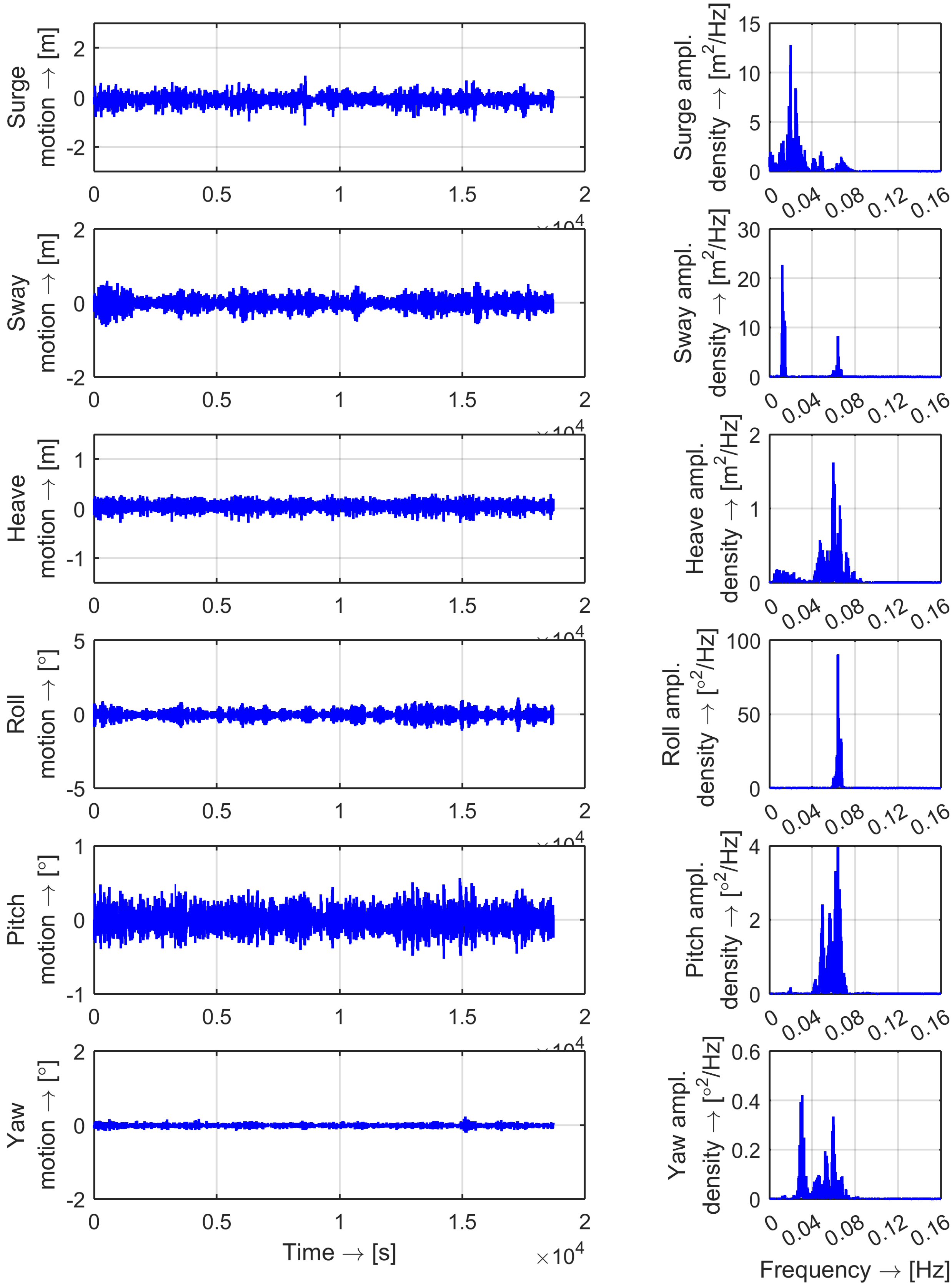

σ_{Surge} = 0.20 m, σ_{Sway} = 0.16 m, σ_{Heave} = 0.08 m, σ_{Roll} = 0.30°, σ_{Pitch} = 0.14°, σ_{Yaw} = 0.04°

Ship motions at centre of gravity (CoG) Depth = 18.0 m, H_{m0} = 2.00 m, T_p = 15.60 s, γ = 5.0 Head-on waves	Irregular	I156d
	A4_I156d	
Deltares	11202696	App. G.044-2

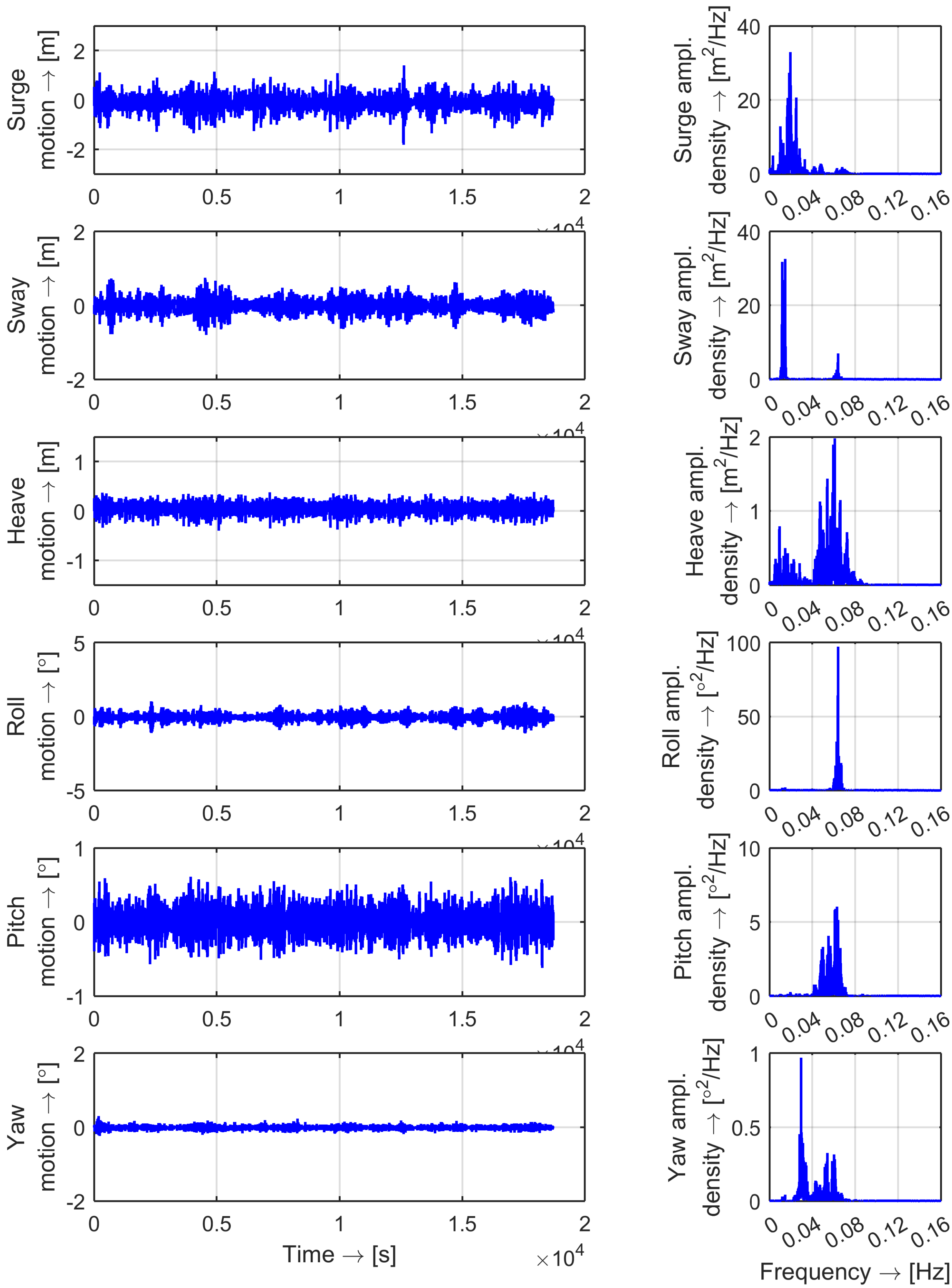

σ_{Surge} = 0.31 m, σ_{Sway} = 0.19 m, σ_{Heave} = 0.11 m, σ_{Roll} = 0.28°, σ_{Pitch} = 0.17°, σ_{Yaw} = 0.05°

Ship motions at centre of gravity (CoG) Depth = 18.0 m, H_{m0} = 2.50 m, T_p = 15.60 s, γ = 5.0 Head-on waves	Irregular	I156e
	A4_I156e	
Deltares	11202696	App. G.045-2

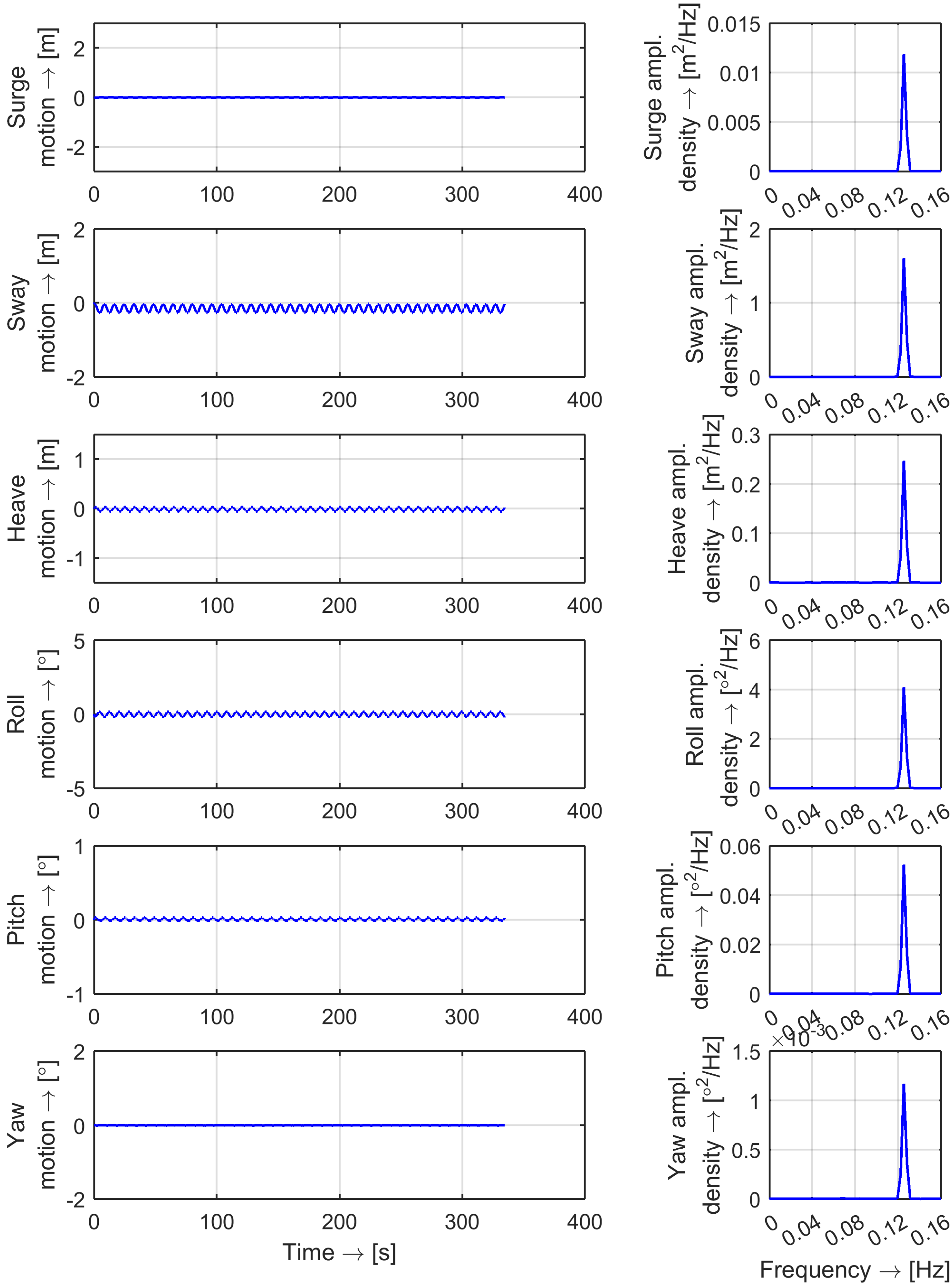

σ_{Surge} = 0.01 m, σ_{Sway} = 0.09 m, σ_{Heave} = 0.03 m, σ_{Roll} = 0.14°, σ_{Pitch} = 0.02°, σ_{Yaw} = 0.00°

Ship motions at centre of gravity (CoG) Depth = 18.0 m, H = 0.75 m, T = 8.00 s Beam-on waves	Monochromatic	M80a
	B1_M80a	
Deltares	11202696	App. G.046-2

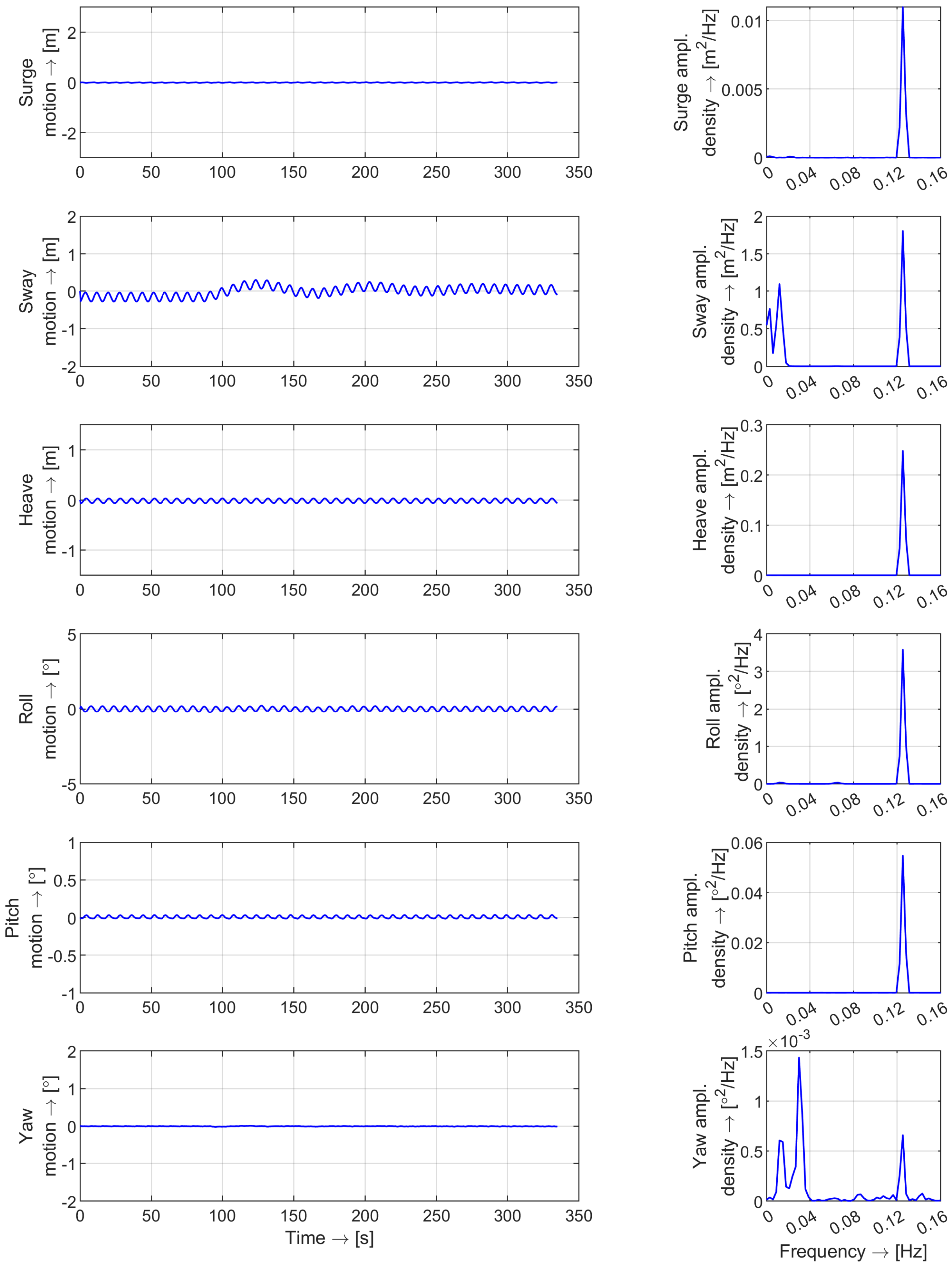

σ_{Surge} = n.a., σ_{Sway} = n.a., σ_{Heave} = n.a., σ_{Roll} = n.a., σ_{Pitch} = n.a., σ_{Yaw} = n.a.

Ship motions at centre of gravity (CoG) Depth = 18.0 m, H = 0.75 m, T = 8.00 s Beam-on waves	Monochromatic	M80a
	B1_M80a_Transition	
Deltares	11202696	App. G.047-2

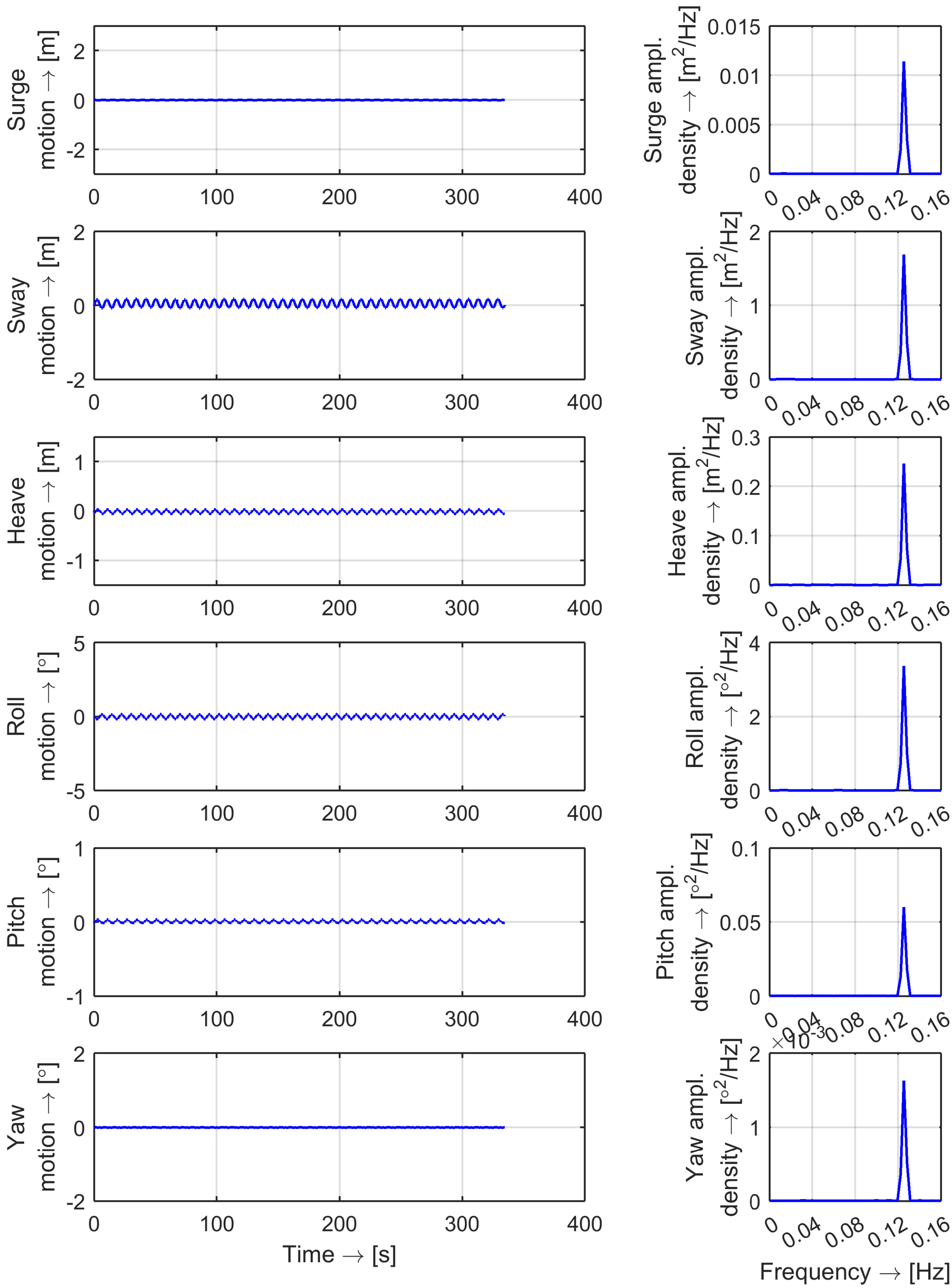

σ_{Surge} = 0.01 m, σ_{Sway} = 0.09 m, σ_{Heave} = 0.03 m, σ_{Roll} = 0.12°, σ_{Pitch} = 0.02°, σ_{Yaw} = 0.00°

Ship motions at centre of gravity (CoG) Depth = 18.0 m, H = 0.75 m, T = 8.00 s Beam-on waves	Monochromatic	M80a
	B1_M80a_noST	
Deltares	11202696	App. G.048-2

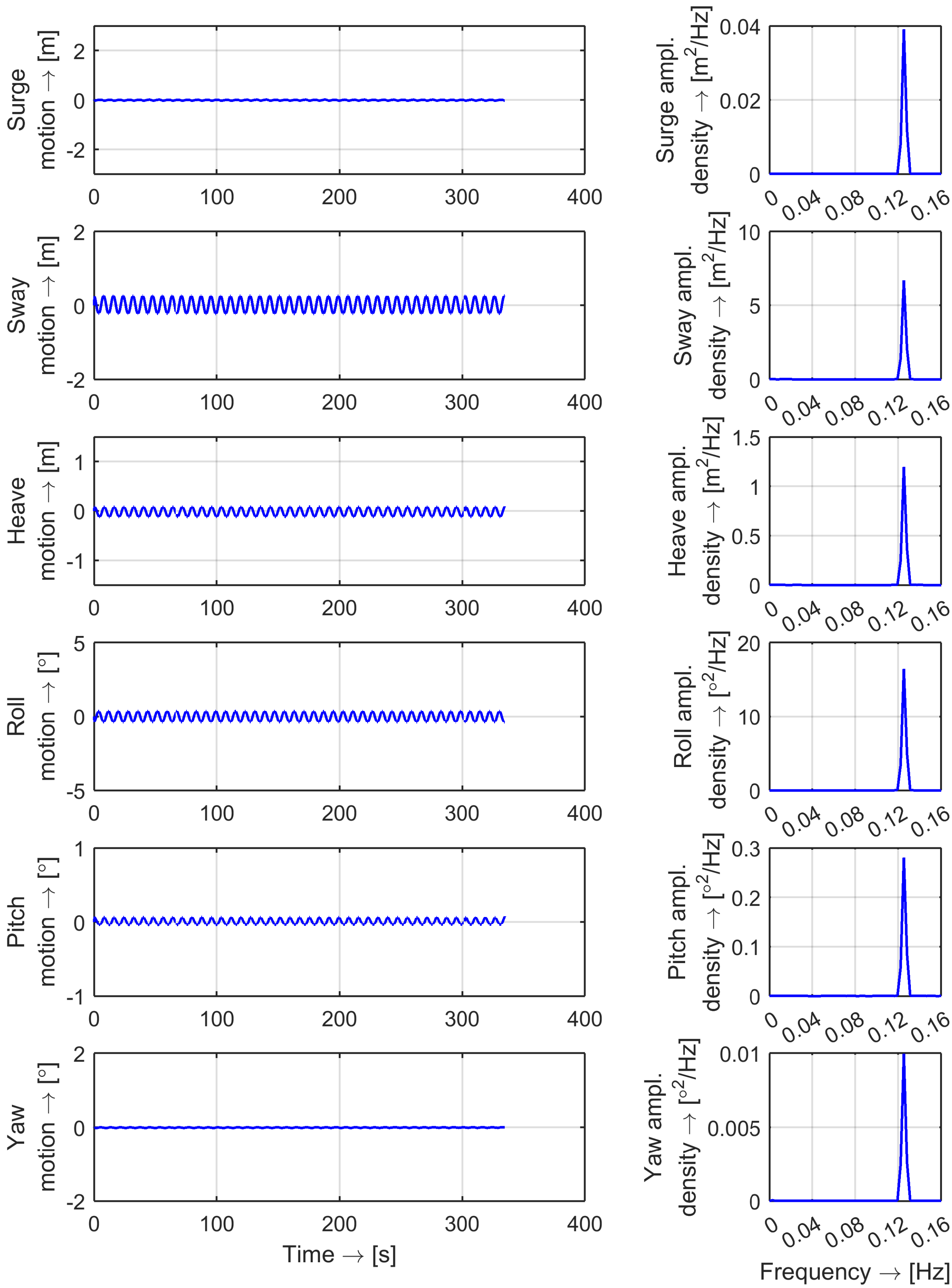

σ_{Surge} = 0.01 m, σ_{Sway} = 0.17 m, σ_{Heave} = 0.07 m, σ_{Roll} = 0.27°, σ_{Pitch} = 0.04°, σ_{Yaw} = 0.01°

Ship motions at centre of gravity (CoG) Depth = 18.0 m, H = 1.50 m, T = 8.00 s Beam-on waves	Monochromatic	M80b
	B1_M80b	
Deltares	11202696	App. G.049-2

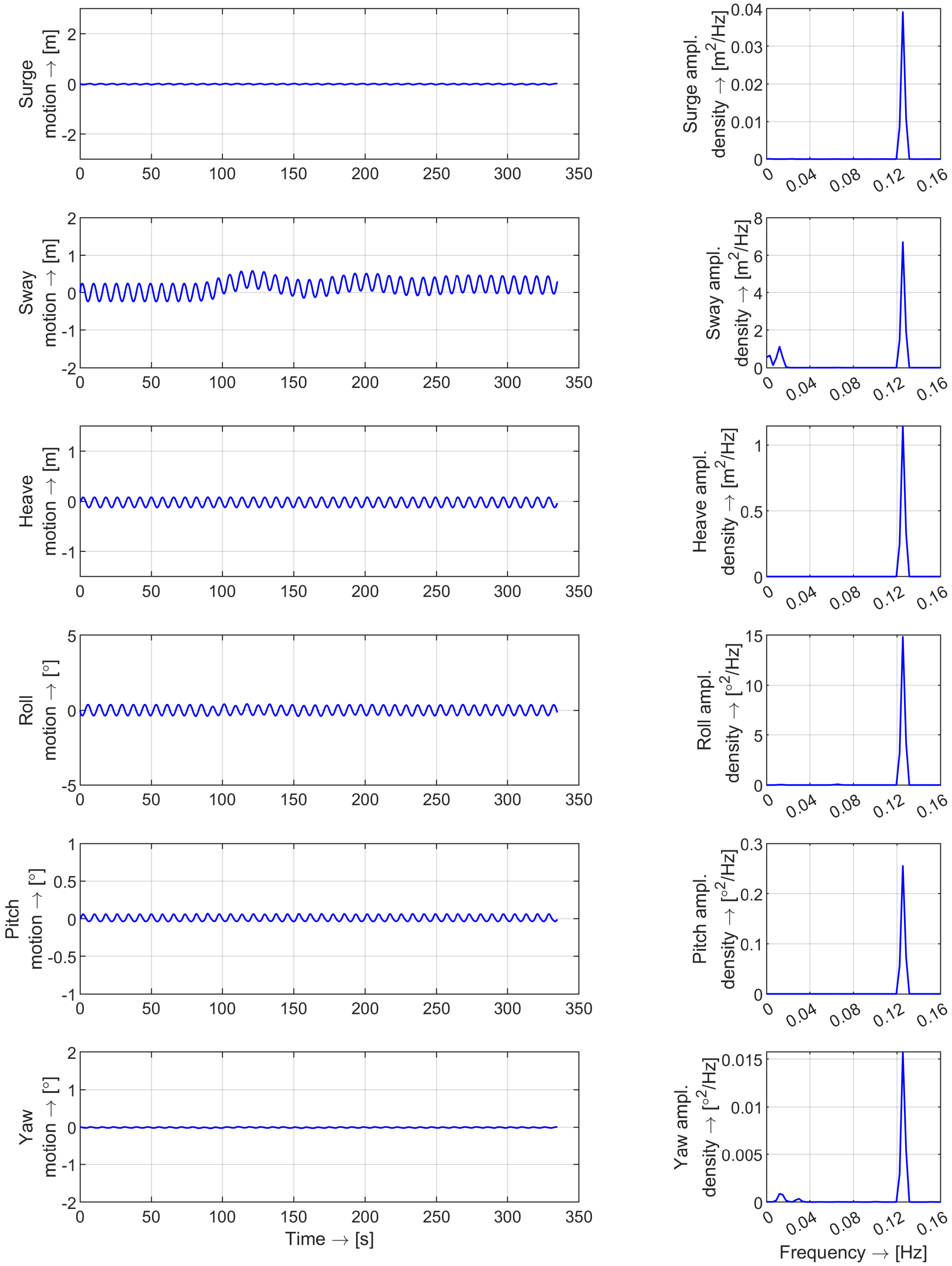

σ_{Surge} = n.a., σ_{Sway} = n.a., σ_{Heave} = n.a., σ_{Roll} = n.a., σ_{Pitch} = n.a., σ_{Yaw} = n.a.

Ship motions at centre of gravity (CoG) Depth = 18.0 m, H = 1.50 m, T = 8.00 s Beam-on waves	Monochromatic	M80b
	B1_M80b_Transition	
Deltares	11202696	App. G.050-2

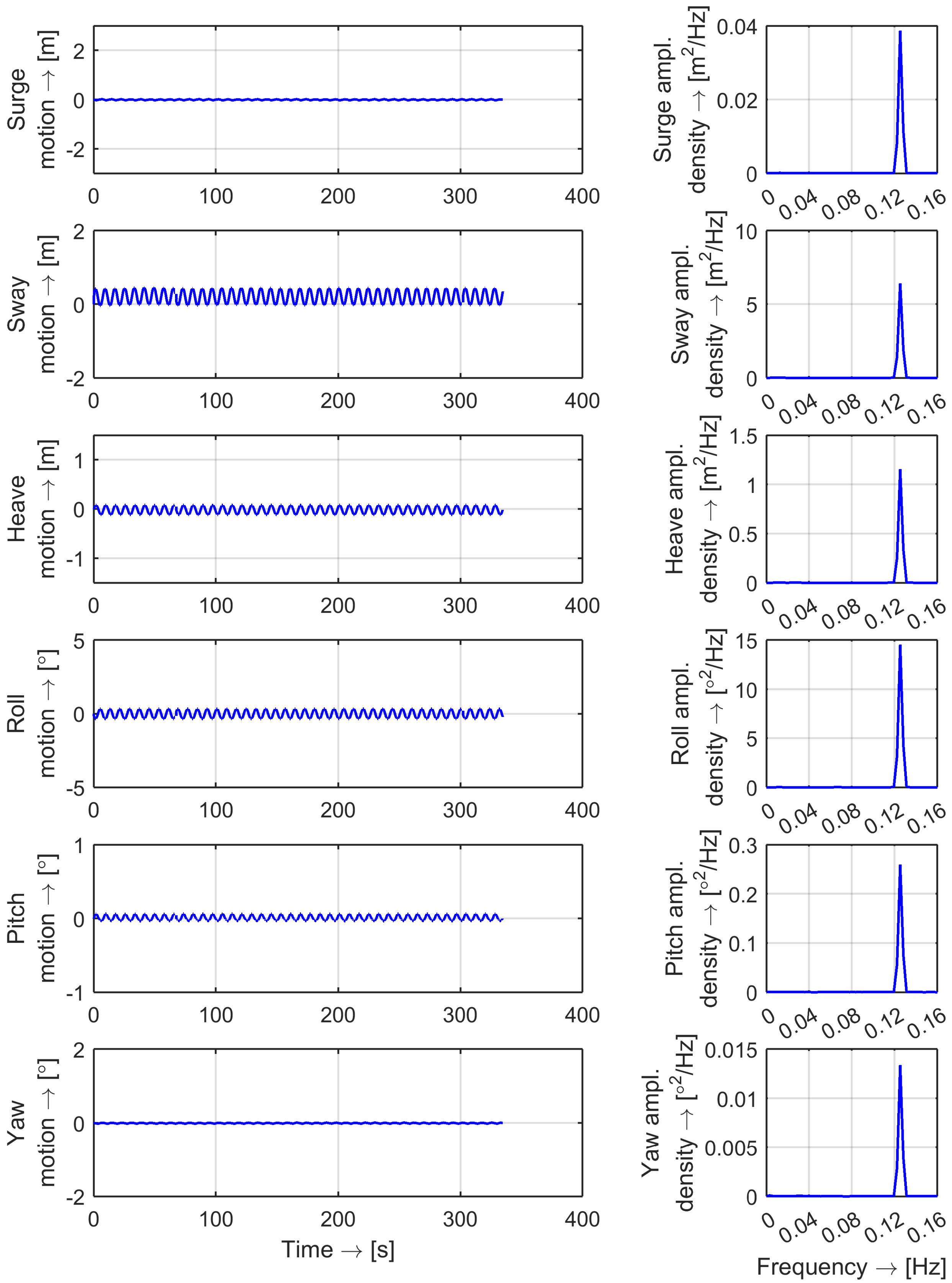

σ_{Surge} = 0.01 m, σ_{Sway} = 0.17 m, σ_{Heave} = 0.07 m, σ_{Roll} = 0.26°, σ_{Pitch} = 0.03°, σ_{Yaw} = 0.01°

Ship motions at centre of gravity (CoG) Depth = 18.0 m, H = 1.50 m, T = 8.00 s Beam-on waves	Monochromatic	M80b
	B1_M80b_noST	
Deltares	11202696	App. G.051-2

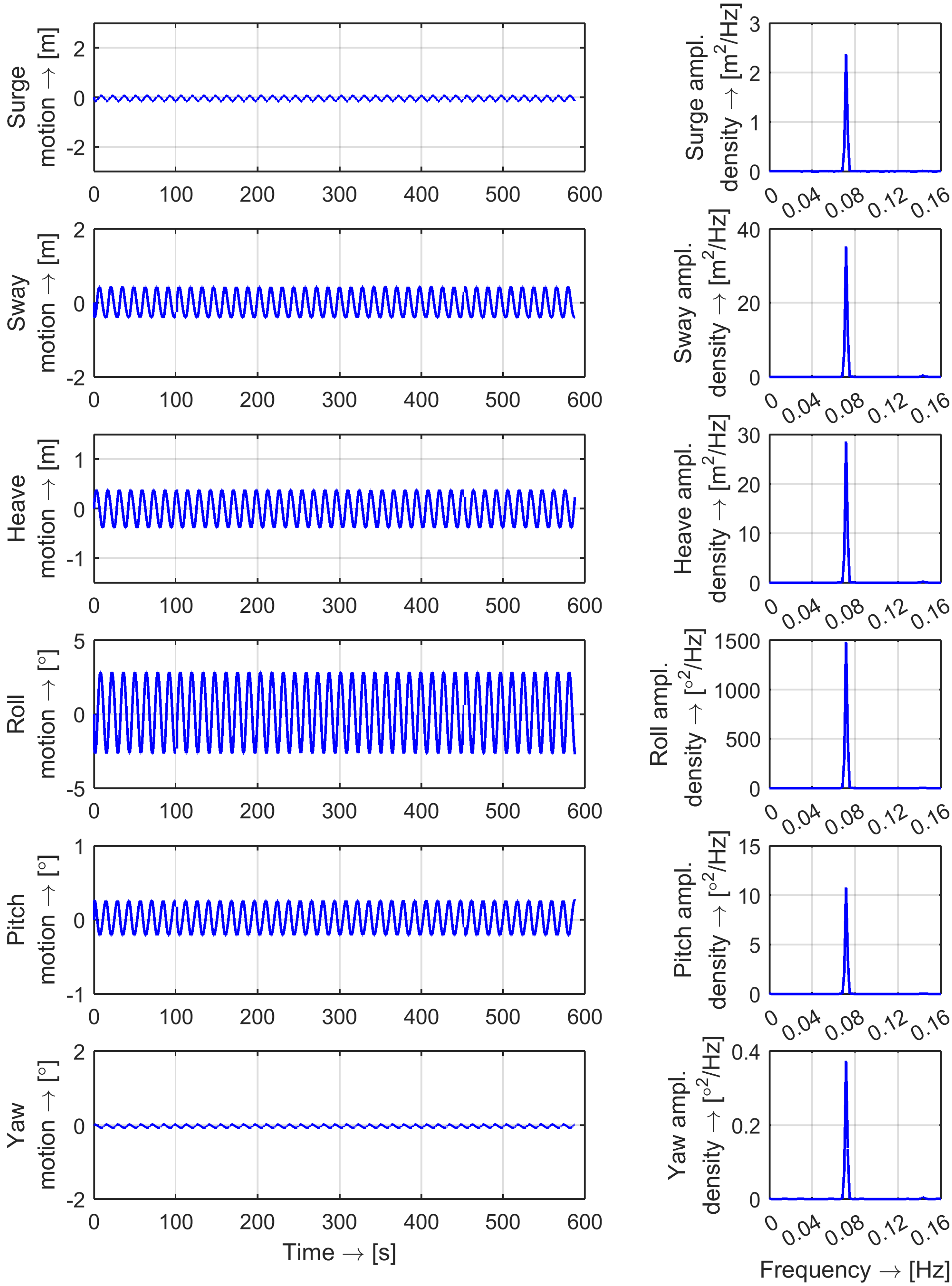

σ_{Surge} = 0.08 m, σ_{Sway} = 0.30 m, σ_{Heave} = 0.27 m, σ_{Roll} = 1.96°, σ_{Pitch} = 0.17°, σ_{Yaw} = 0.03°

Ship motions at centre of gravity (CoG) Depth = 18.0 m, H = 1.00 m, T = 14.00 s Beam-on waves	Monochromatic	M140a
	B1_M140a	
Deltares	11202696	App. G.052-2

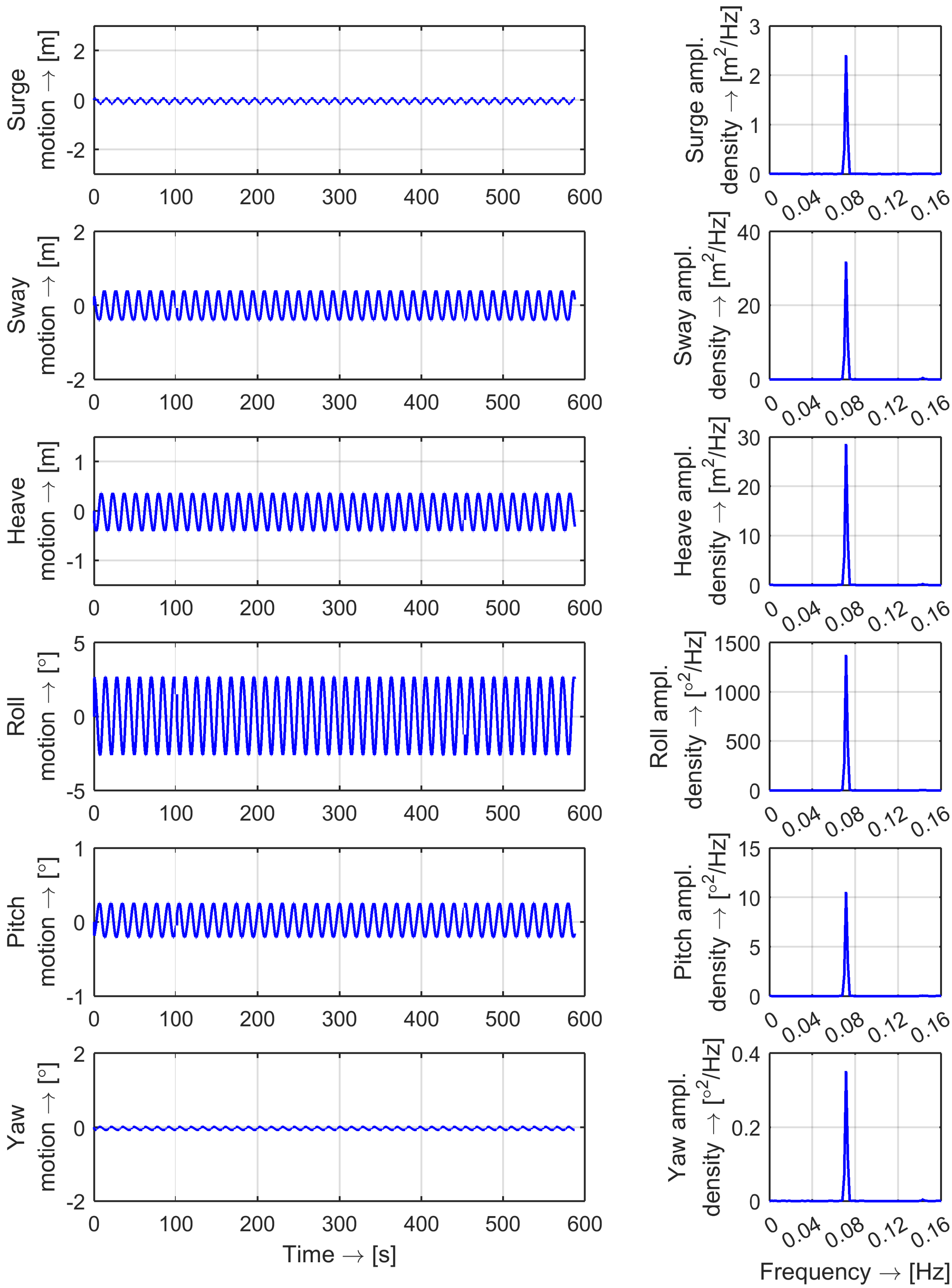

σ_{Surge} = 0.08 m, σ_{Sway} = 0.29 m, σ_{Heave} = 0.27 m, σ_{Roll} = 1.88°, σ_{Pitch} = 0.16°, σ_{Yaw} = 0.03°

Ship motions at centre of gravity (CoG) Depth = 18.0 m, H = 1.00 m, T = 14.00 s Beam-on waves	Monochromatic	M140a
	B1_M140a_lwv	
Deltares	11202696	App. G.053-2

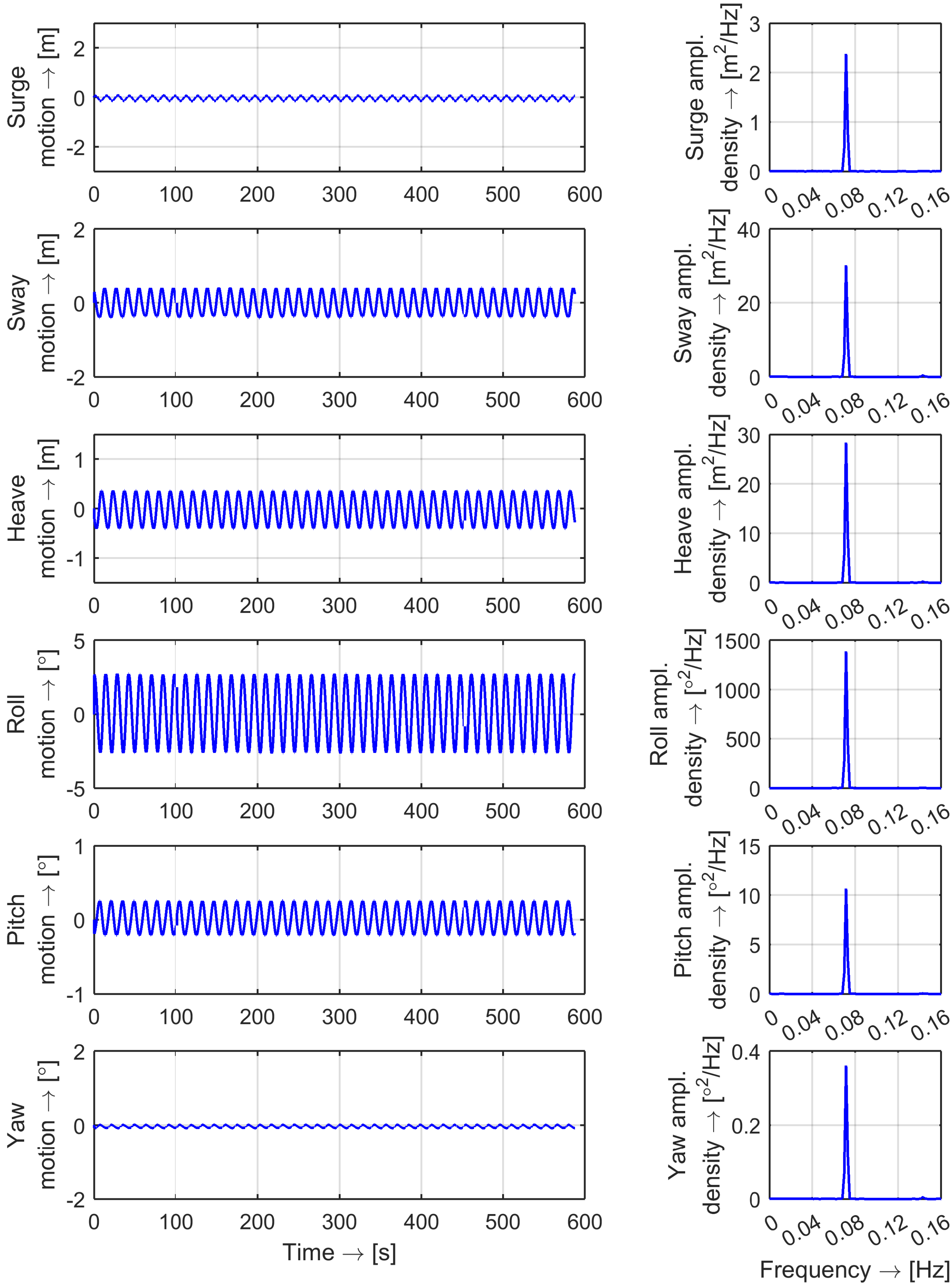

σ_{Surge} = 0.08 m, σ_{Sway} = 0.28 m, σ_{Heave} = 0.27 m, σ_{Roll} = 1.89°, σ_{Pitch} = 0.17°, σ_{Yaw} = 0.03°

Ship motions at centre of gravity (CoG) Depth = 18.0 m, H = 1.00 m, T = 14.00 s Beam-on waves	Monochromatic	M140a
	B1_M140a_sk	
Deltares	11202696	App. G.054-2

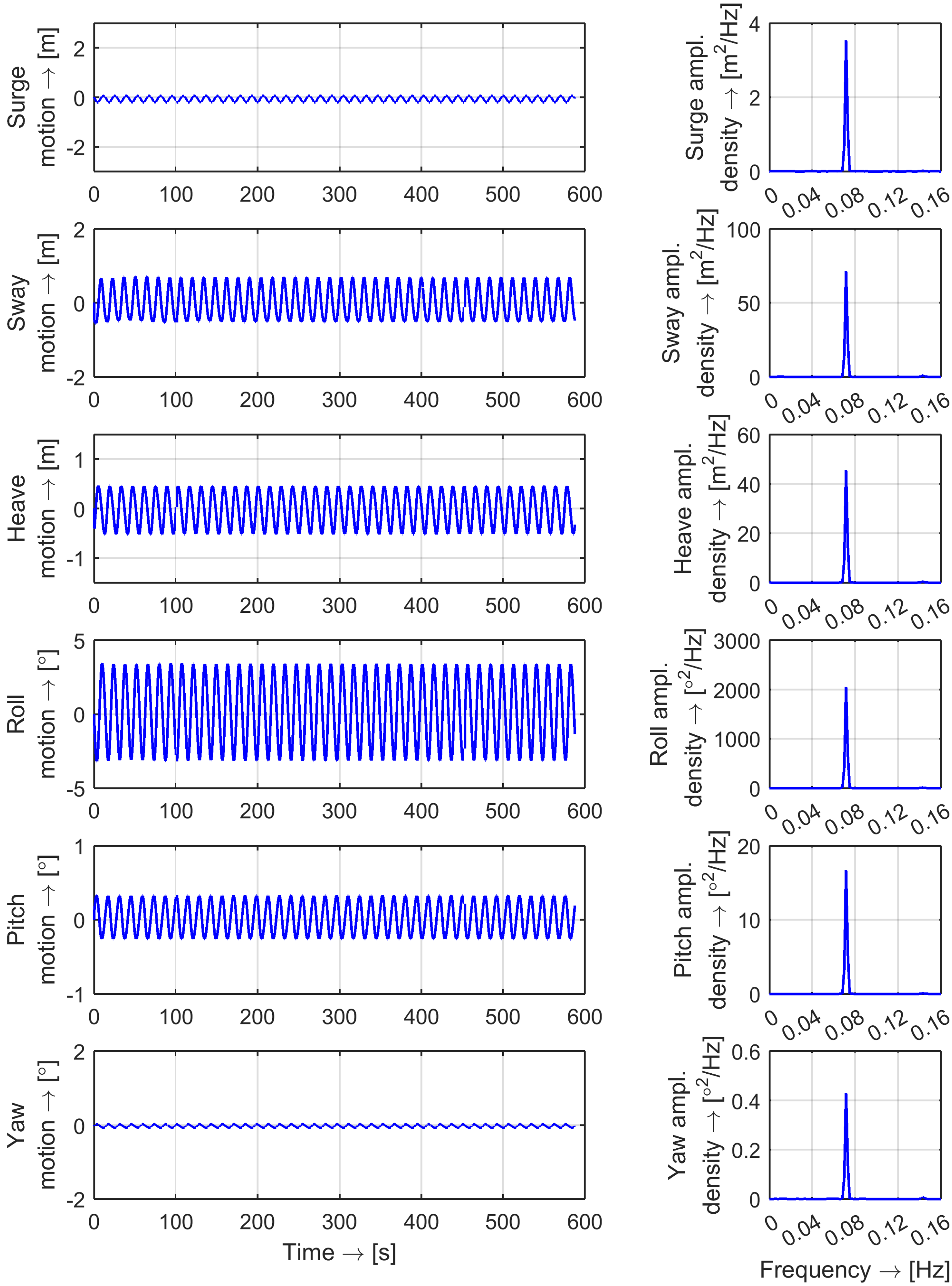

σ_{Surge} = 0.10 m, σ_{Sway} = 0.43 m, σ_{Heave} = 0.34 m, σ_{Roll} = 2.31°, σ_{Pitch} = 0.21°, σ_{Yaw} = 0.03°

Ship motions at centre of gravity (CoG) Depth = 18.0 m, H = 1.25 m, T = 14.00 s Beam-on waves	Monochromatic	M140b
	B1_M140b	
Deltares	11202696	App. G.055-2

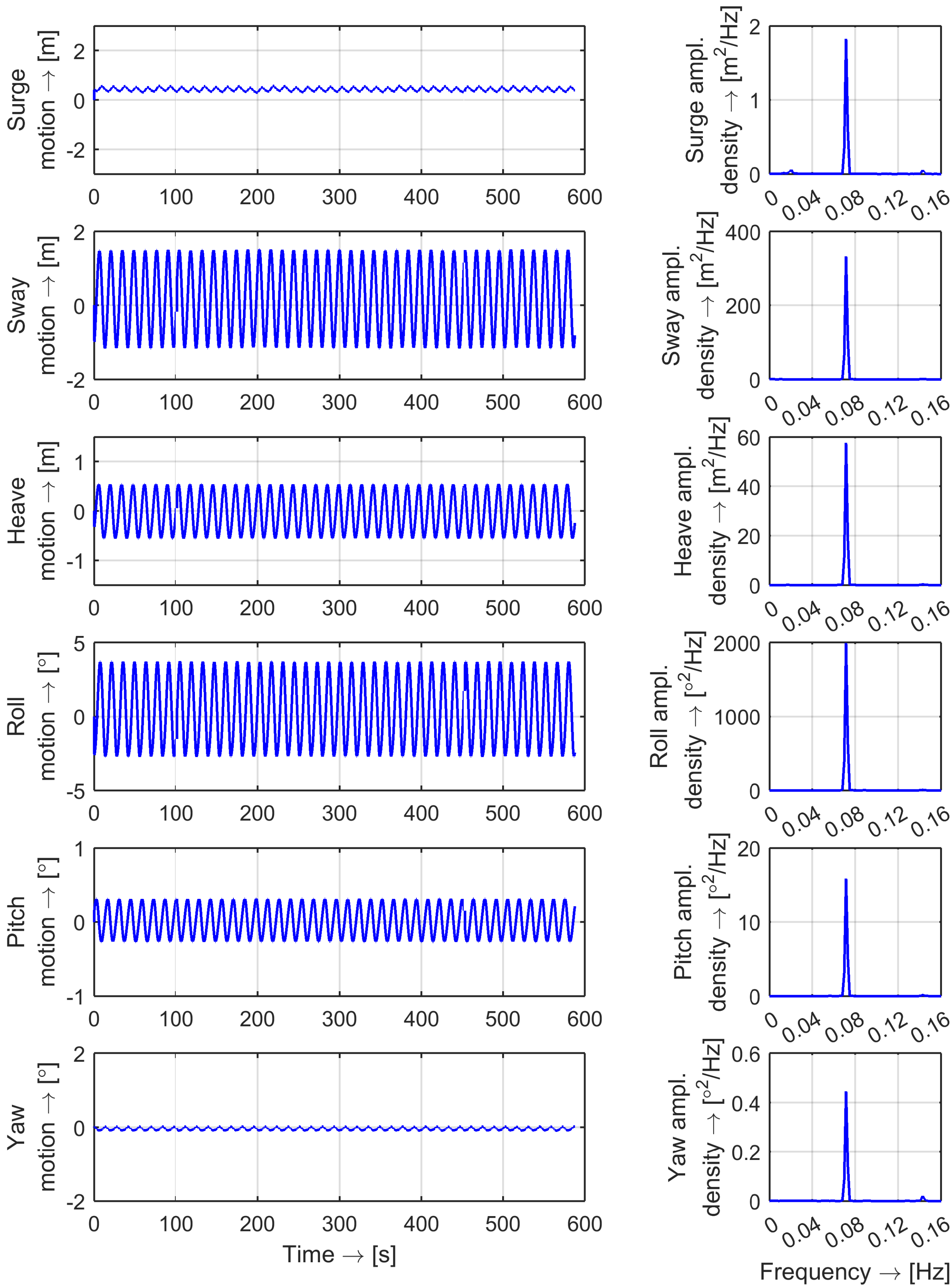

σ_{Surge} = 0.07 m, σ_{Sway} = 0.93 m, σ_{Heave} = 0.39 m, σ_{Roll} = 2.27°, σ_{Pitch} = 0.20°, σ_{Yaw} = 0.03°

Ship motions at centre of gravity (CoG) Depth = 18.0 m, H = 1.50 m, T = 14.00 s Beam-on waves	Monochromatic	M140c
	B1_M140c	
Deltares	11202696	App. G.056-2

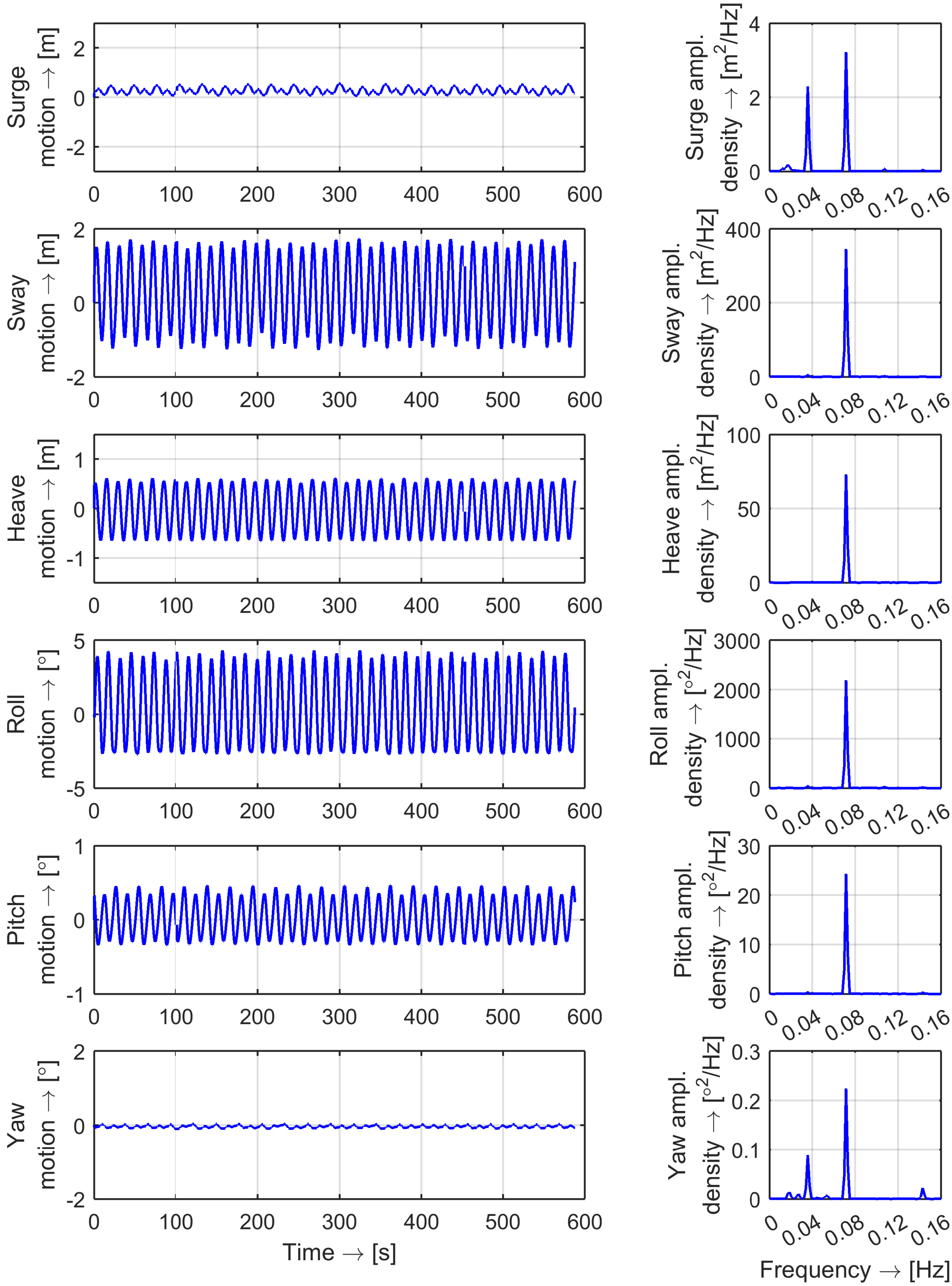

σ_{Surge} = 0.13 m, σ_{Sway} = 0.96 m, σ_{Heave} = 0.43 m, σ_{Roll} = 2.42°, σ_{Pitch} = 0.25°, σ_{Yaw} = 0.03°

Ship motions at centre of gravity (CoG) Depth = 18.0 m, H = 1.75 m, T = 14.00 s Beam-on waves	Monochromatic	M140d
	B1_M140d	
Deltares	11202696	App. G.057-2

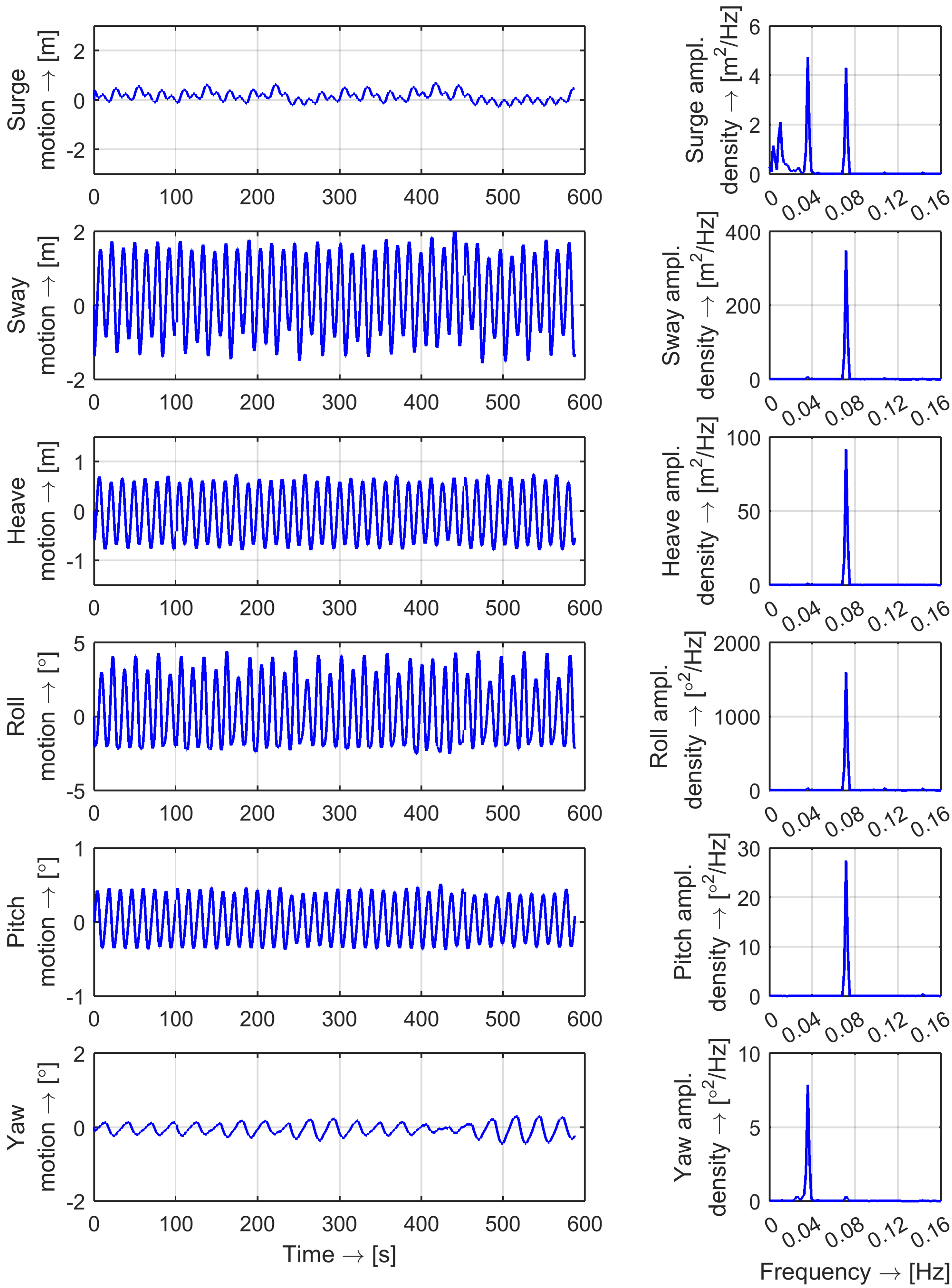

σ_{Surge} = 0.20 m, σ_{Sway} = 0.97 m, σ_{Heave} = 0.49 m, σ_{Roll} = 2.10°, σ_{Pitch} = 0.27°, σ_{Yaw} = 0.16°

Ship motions at centre of gravity (CoG) Depth = 18.0 m, H = 2.00 m, T = 14.00 s Beam-on waves	Monochromatic	M140e
	B1_M140e	
Deltares	11202696	App. G.058-2

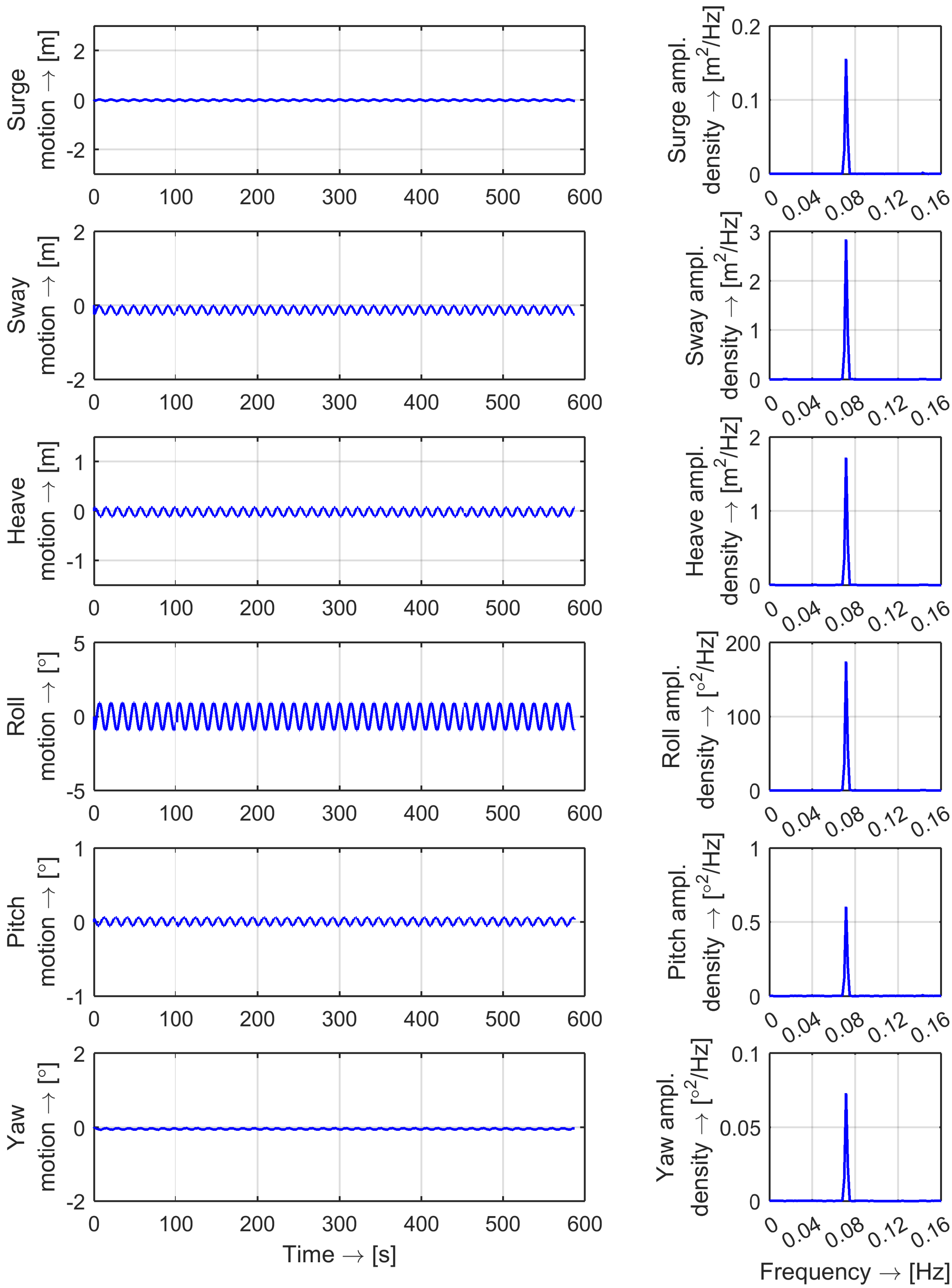

σ_{Surge} = 0.02 m, σ_{Sway} = 0.09 m, σ_{Heave} = 0.07 m, σ_{Roll} = 0.67°, σ_{Pitch} = 0.04°, σ_{Yaw} = 0.01°

Ship motions at centre of gravity (CoG) Depth = 18.0 m, H = 0.25 m, T = 14.00 s Beam-on waves	Monochromatic	M140f
	B1_M140f	
Deltares	11202696	App. G.059-2

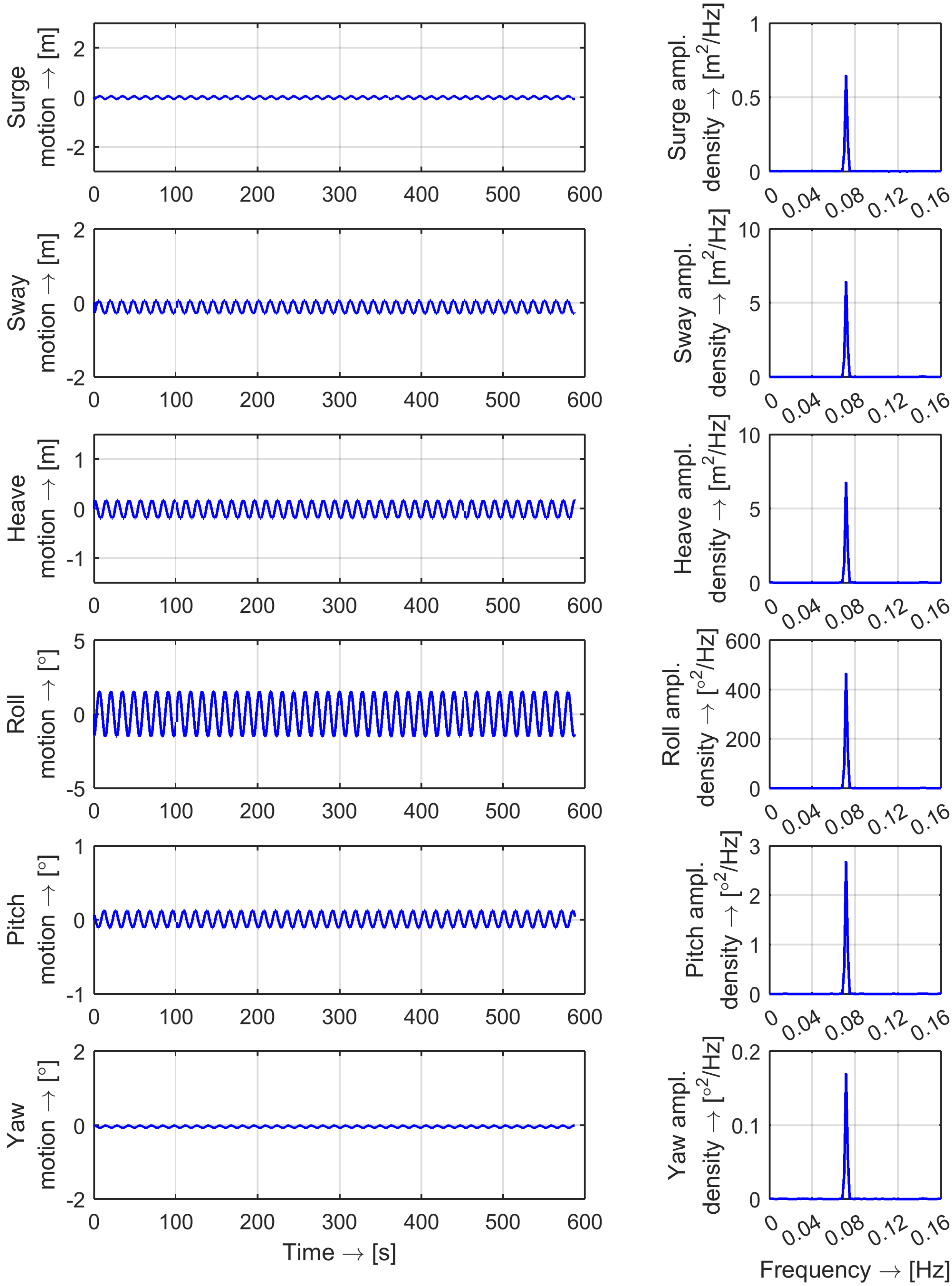

σ_{Surge} = 0.04 m, σ_{Sway} = 0.13 m, σ_{Heave} = 0.13 m, σ_{Roll} = 1.10°, σ_{Pitch} = 0.08°, σ_{Yaw} = 0.02°

Ship motions at centre of gravity (CoG) Depth = 18.0 m, H = 0.50 m, T = 14.00 s Beam-on waves	Monochromatic	M140g
	B1_M140g	
Deltares	11202696	App. G.060-2

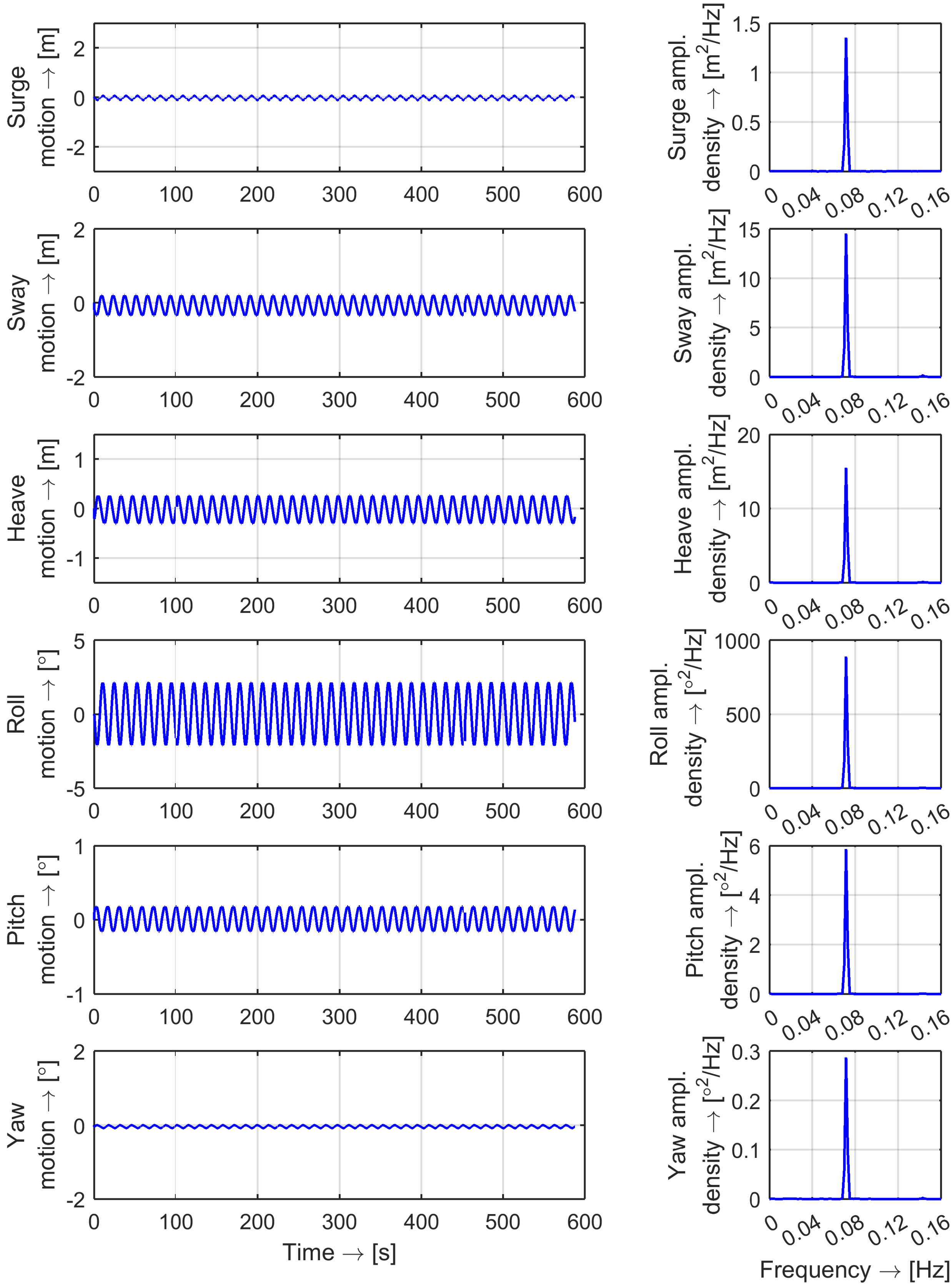

σ_{Surge} = 0.06 m, σ_{Sway} = 0.19 m, σ_{Heave} = 0.20 m, σ_{Roll} = 1.51°, σ_{Pitch} = 0.12°, σ_{Yaw} = 0.03°

Ship motions at centre of gravity (CoG) Depth = 18.0 m, H = 0.75 m, T = 14.00 s Beam-on waves	Monochromatic	M140h
	B1_M140h	
Deltares	11202696	App. G.061-2

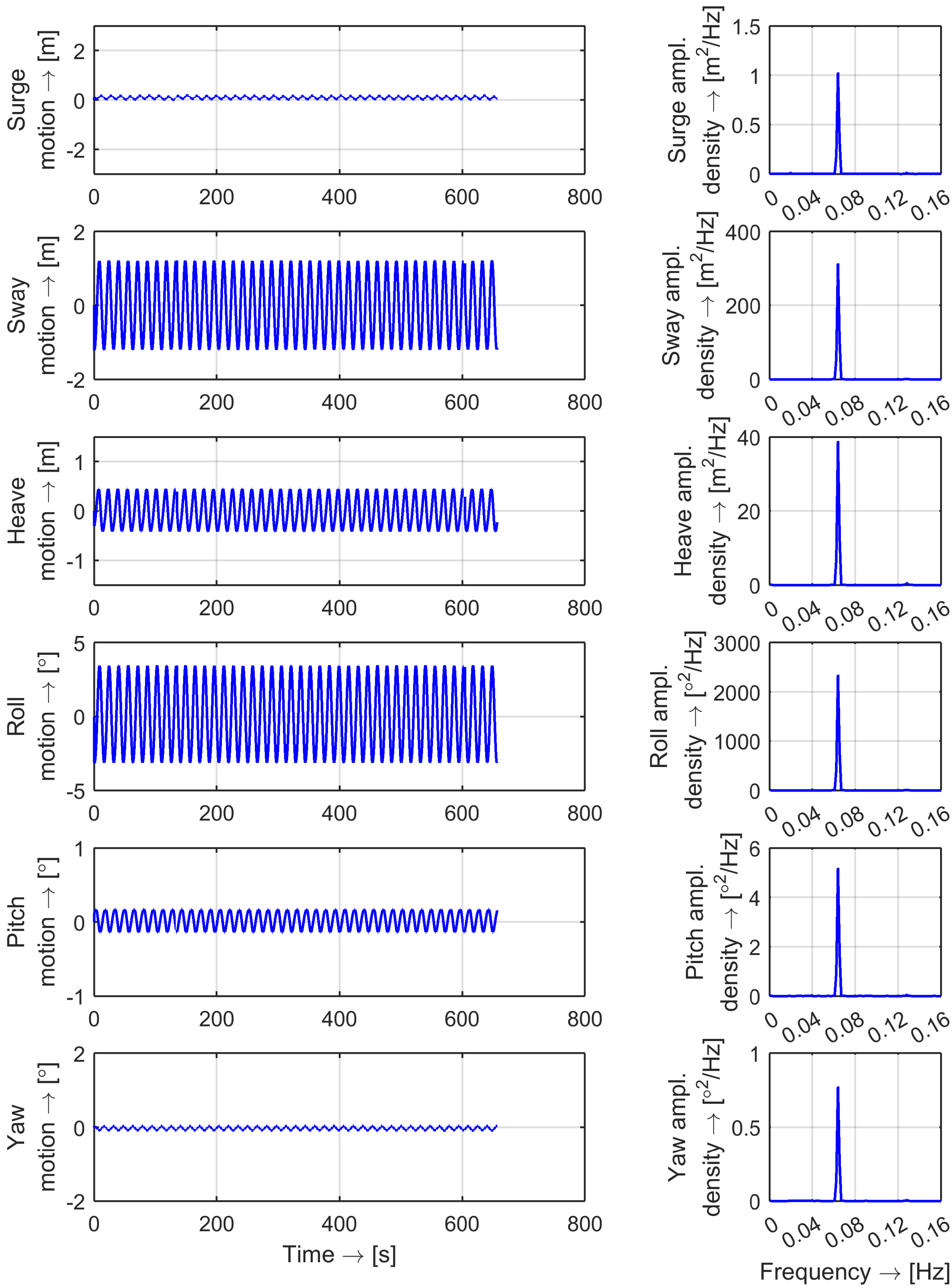

σ_{Surge} = 0.05 m, σ_{Sway} = 0.85 m, σ_{Heave} = 0.30 m, σ_{Roll} = 2.33°, σ_{Pitch} = 0.11°, σ_{Yaw} = 0.04°

Ship motions at centre of gravity (CoG) Depth = 18.0 m, H = 1.00 m, T = 15.60 s Beam-on waves	Monochromatic	M156a
	B1_M156a	
Deltares	11202696	App. G.062-2

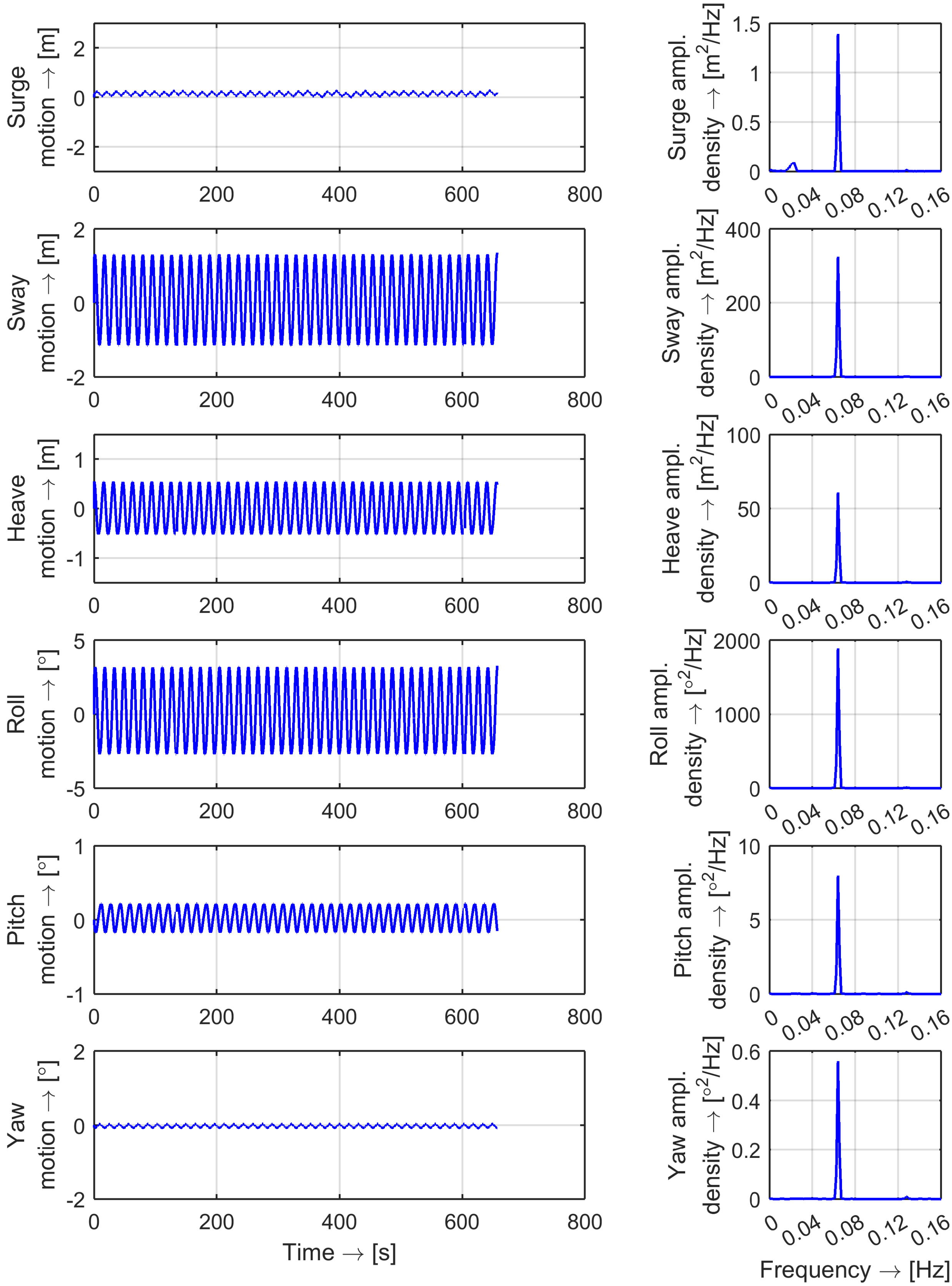

σ_{Surge} = 0.06 m, σ_{Sway} = 0.87 m, σ_{Heave} = 0.38 m, σ_{Roll} = 2.10°, σ_{Pitch} = 0.14°, σ_{Yaw} = 0.04°

Ship motions at centre of gravity (CoG) Depth = 18.0 m, H = 1.25 m, T = 15.60 s Beam-on waves	Monochromatic	M156b
	B1_M156b	
Deltares	11202696	App. G.063-2

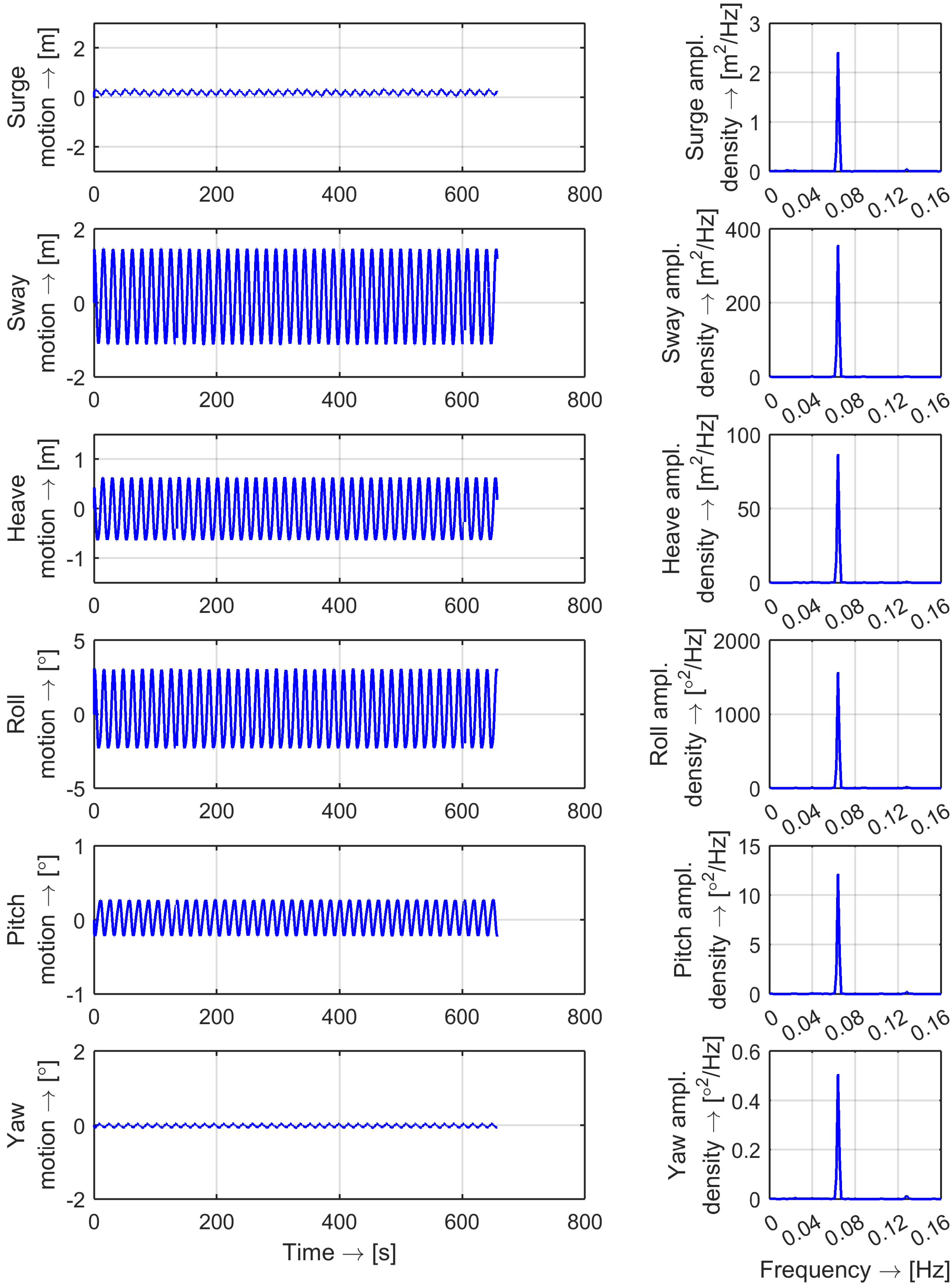

σ_{Surge} = 0.08 m, σ_{Sway} = 0.91 m, σ_{Heave} = 0.45 m, σ_{Roll} = 1.92°, σ_{Pitch} = 0.17°, σ_{Yaw} = 0.04°

Ship motions at centre of gravity (CoG) Depth = 18.0 m, H = 1.50 m, T = 15.60 s Beam-on waves	Monochromatic	M156c
	B1_M156c	
Deltares	11202696	App. G.064-2

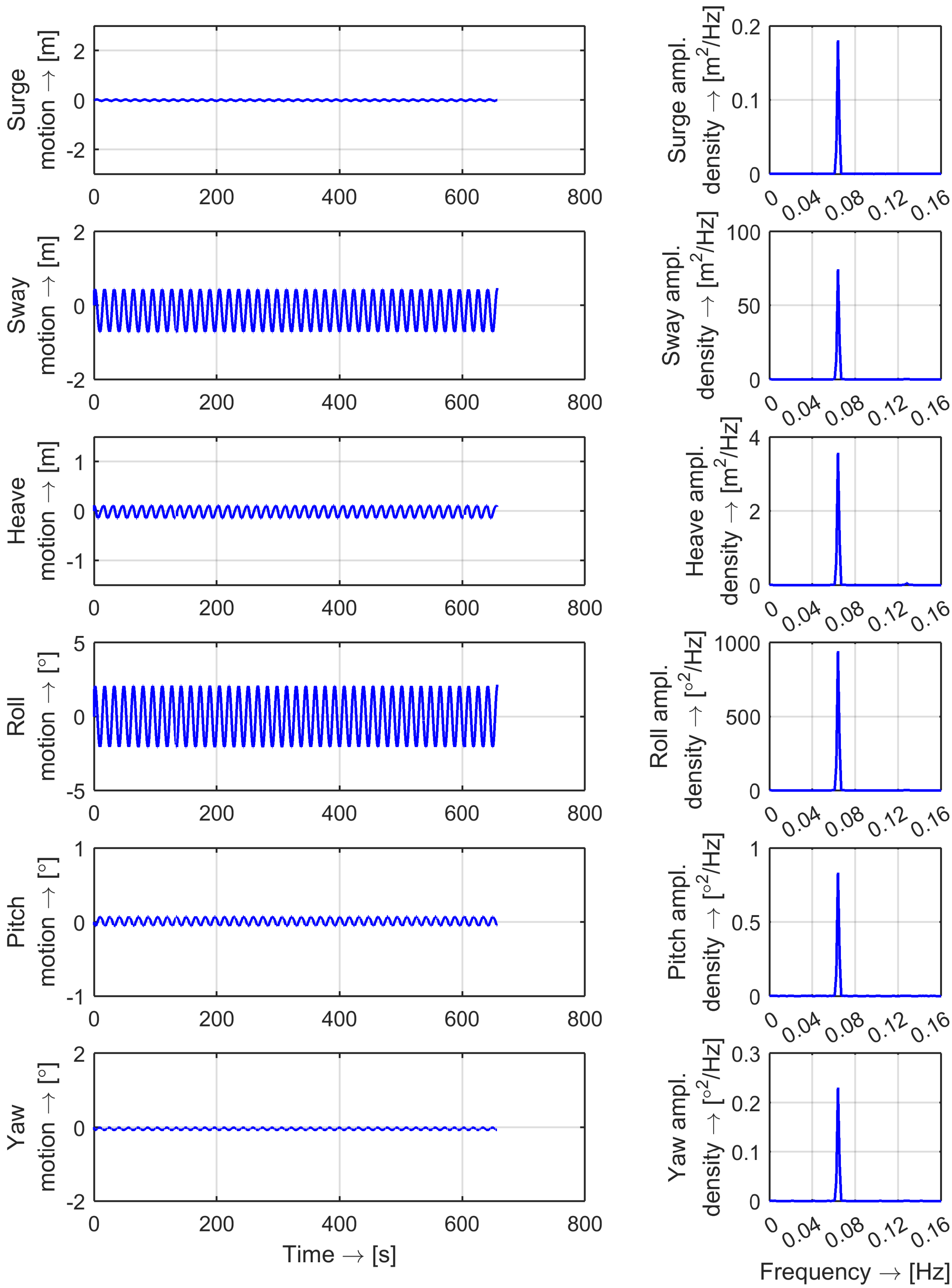

σ_{Surge} = 0.02 m, σ_{Sway} = 0.42 m, σ_{Heave} = 0.09 m, σ_{Roll} = 1.48°, σ_{Pitch} = 0.04°, σ_{Yaw} = 0.02°

Ship motions at centre of gravity (CoG) Depth = 18.0 m, H = 0.25 m, T = 15.60 s Beam-on waves	Monochromatic	M156f
	B1_M156f	
Deltares	11202696	App. G.065-2

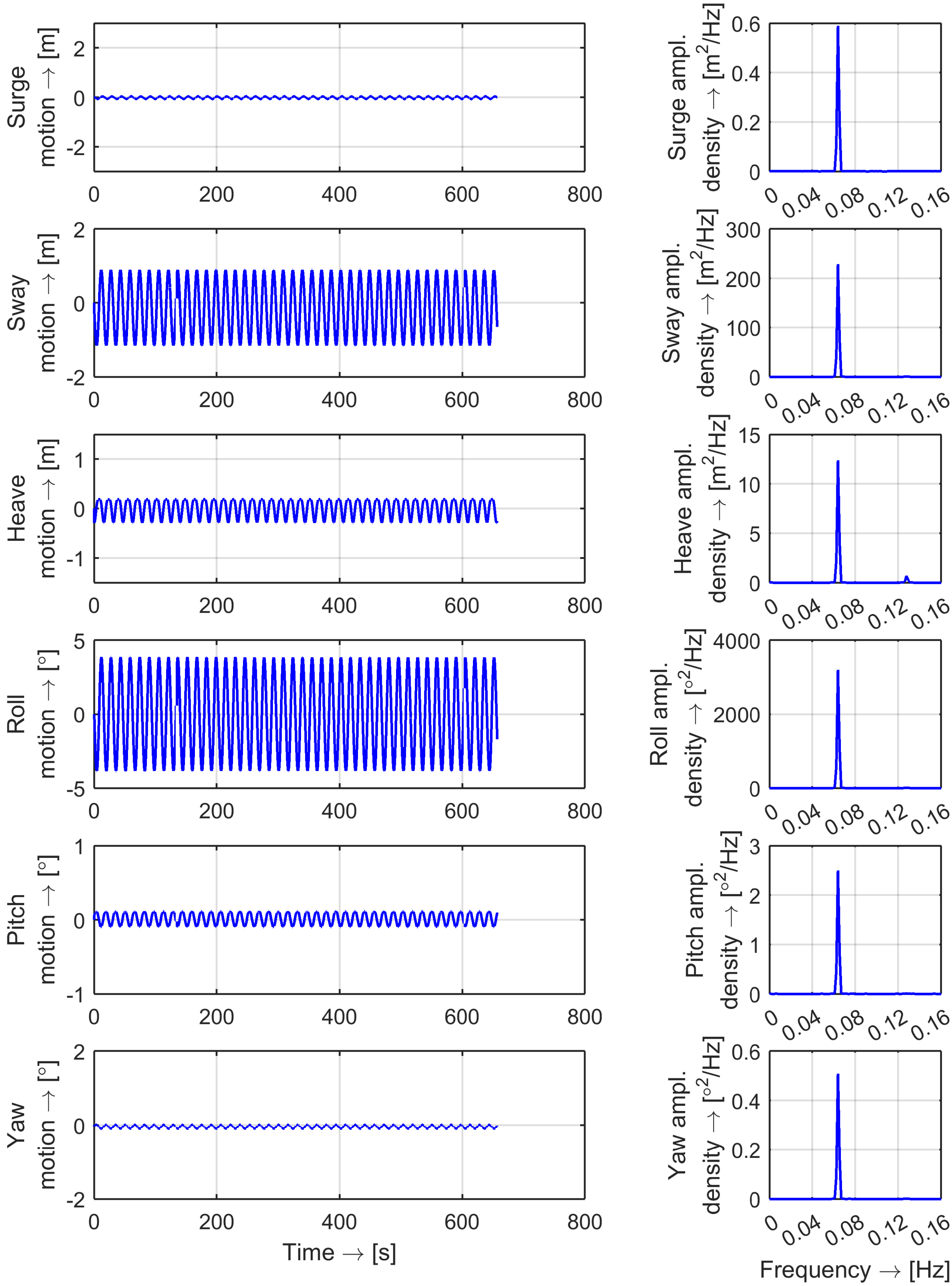

σ_{Surge} = 0.04 m, σ_{Sway} = 0.73 m, σ_{Heave} = 0.17 m, σ_{Roll} = 2.73°, σ_{Pitch} = 0.08°, σ_{Yaw} = 0.03°

Ship motions at centre of gravity (CoG) Depth = 18.0 m, H = 0.50 m, T = 15.60 s Beam-on waves	Monochromatic	M156g
	B1_M156g	
Deltares	11202696	App. G.066-2

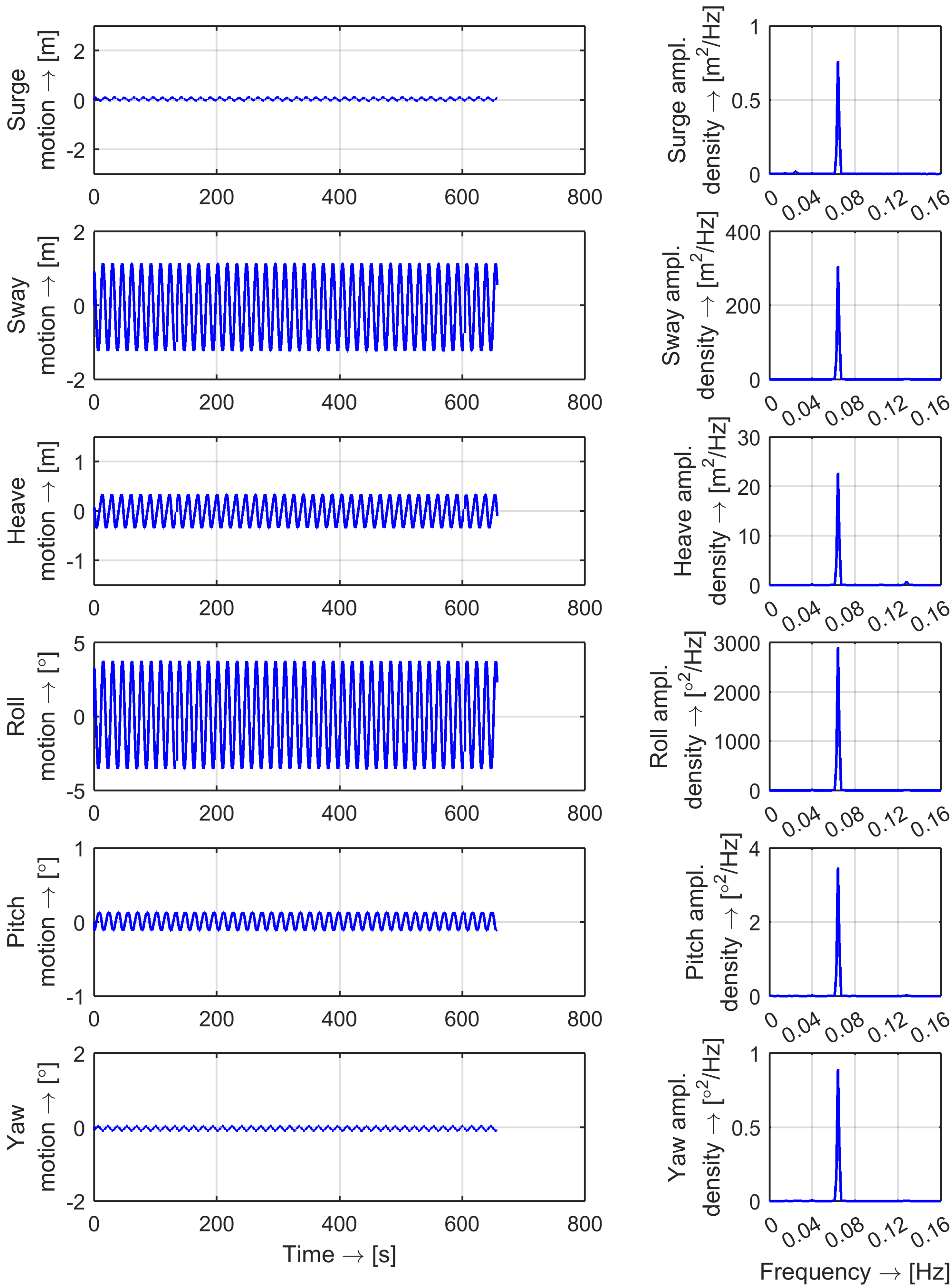

σ_{Surge} = 0.04 m, σ_{Sway} = 0.84 m, σ_{Heave} = 0.23 m, σ_{Roll} = 2.60°, σ_{Pitch} = 0.09°, σ_{Yaw} = 0.05°

Ship motions at centre of gravity (CoG) Depth = 18.0 m, H = 0.75 m, T = 15.60 s Beam-on waves	Monochromatic	M156h
	B1_M156h	
Deltares	11202696	App. G.067-2

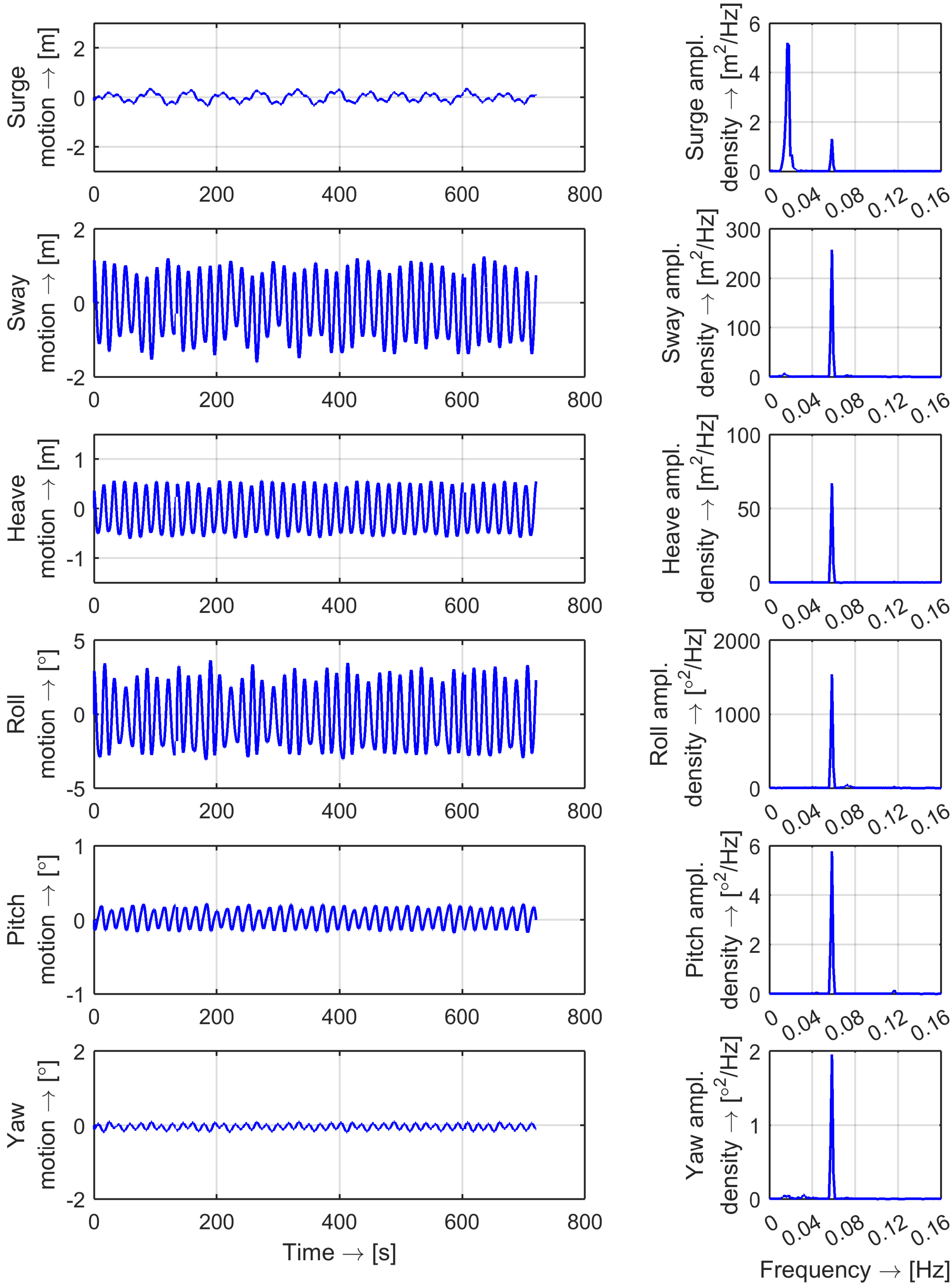

σ_{Surge} = 0.16 m, σ_{Sway} = 0.77 m, σ_{Heave} = 0.38 m, σ_{Roll} = 1.91°, σ_{Pitch} = 0.11°, σ_{Yaw} = 0.07°

Ship motions at centre of gravity (CoG) Depth = 18.0 m, H = 1.00 m, T = 17.20 s Beam-on waves	Monochromatic	M172a
	B1_M172a	
Deltares	11202696	App. G.068-2

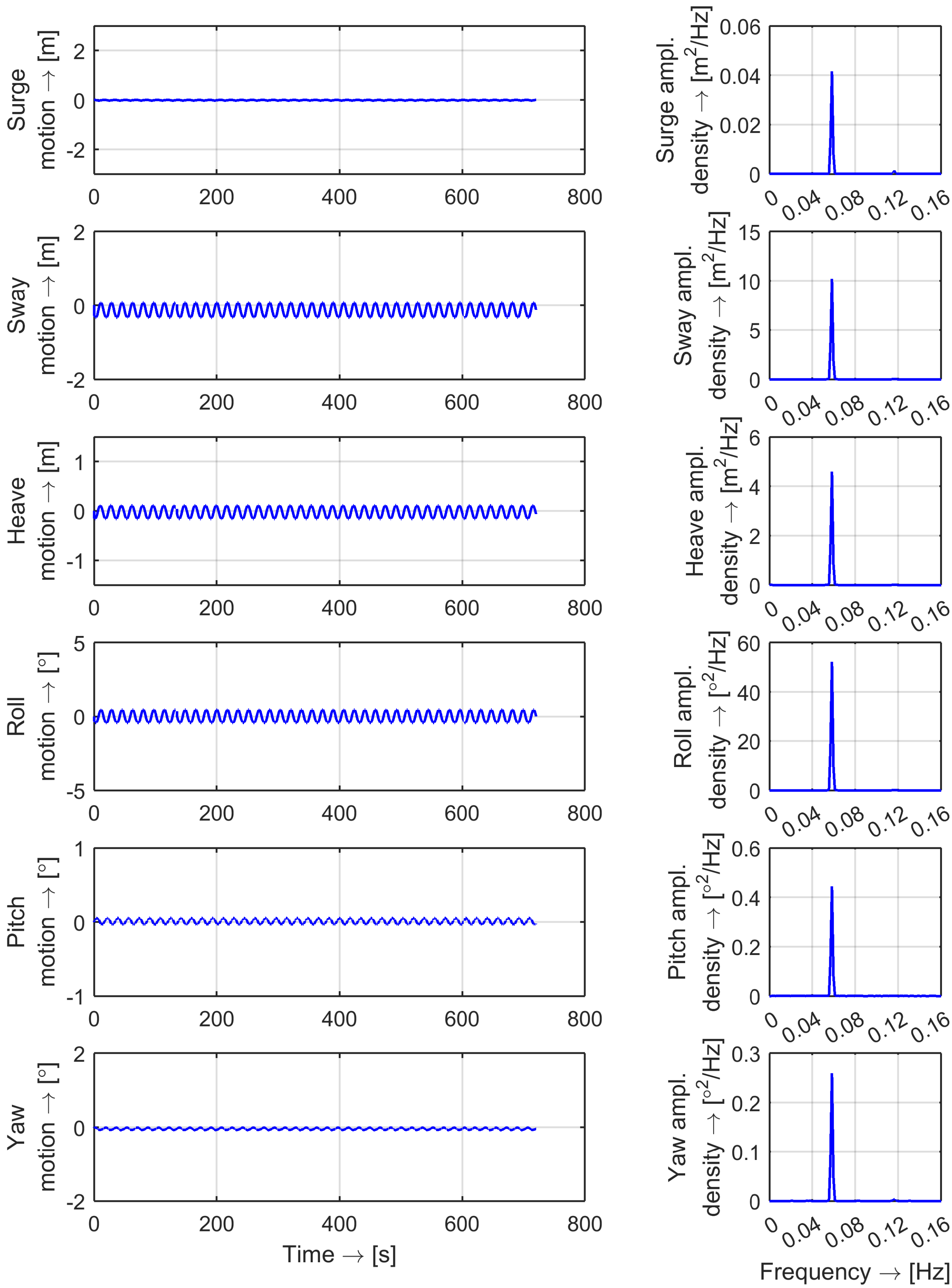

σ_{Surge} = 0.01 m, σ_{Sway} = 0.15 m, σ_{Heave} = 0.10 m, σ_{Roll} = 0.33°, σ_{Pitch} = 0.03°, σ_{Yaw} = 0.02°

Ship motions at centre of gravity (CoG) Depth = 18.0 m, H = 0.25 m, T = 17.20 s Beam-on waves	Monochromatic	M172f
	B1_M172f	
Deltares	11202696	App. G.069-2

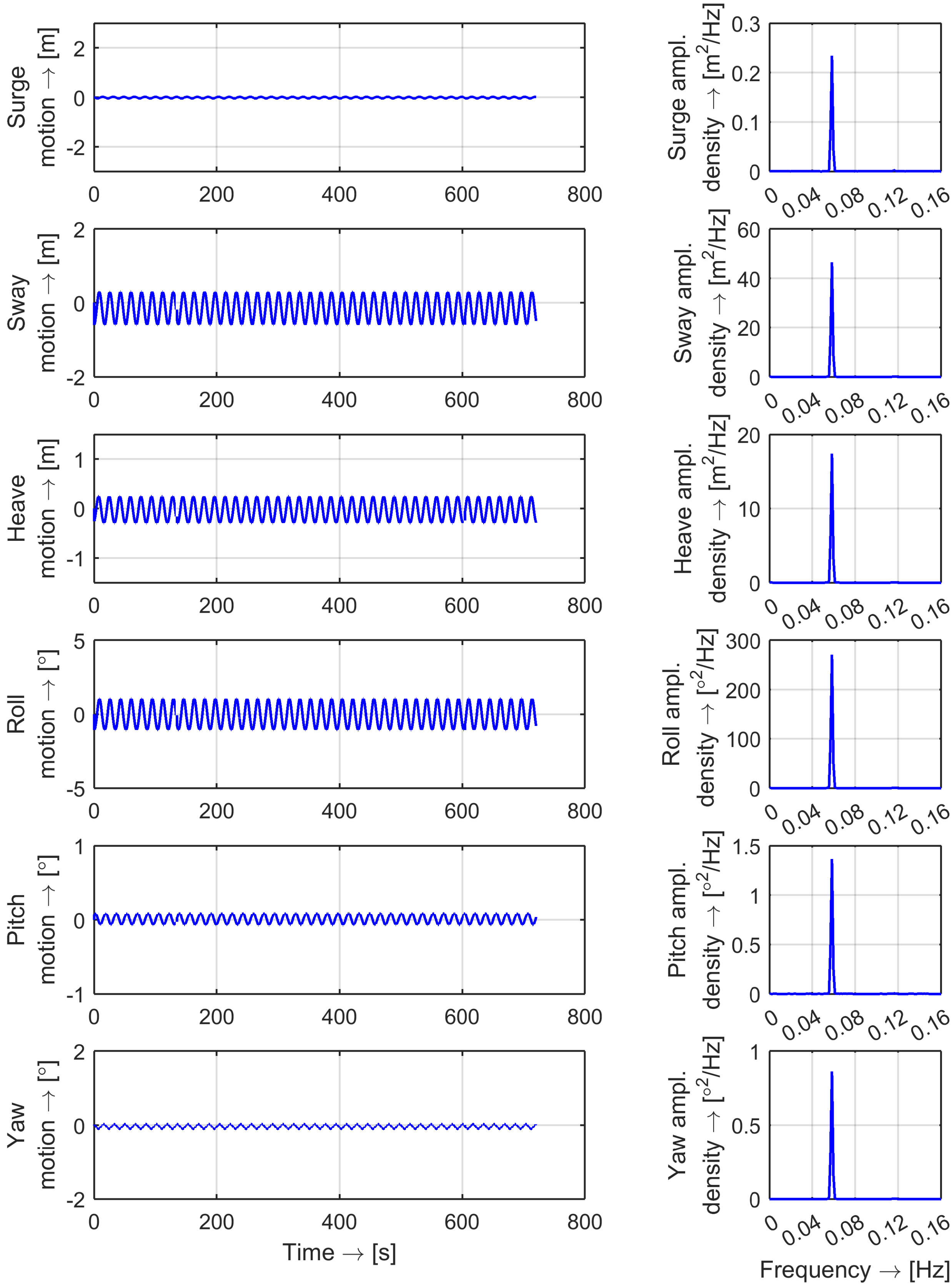

σ_{Surge} = 0.02 m, σ_{Sway} = 0.31 m, σ_{Heave} = 0.19 m, σ_{Roll} = 0.76°, σ_{Pitch} = 0.05°, σ_{Yaw} = 0.04°

Ship motions at centre of gravity (CoG) Depth = 18.0 m, H = 0.50 m, T = 17.20 s Beam-on waves	Monochromatic	M172g
	B1_M172g	
Deltares	11202696	App. G.070-2

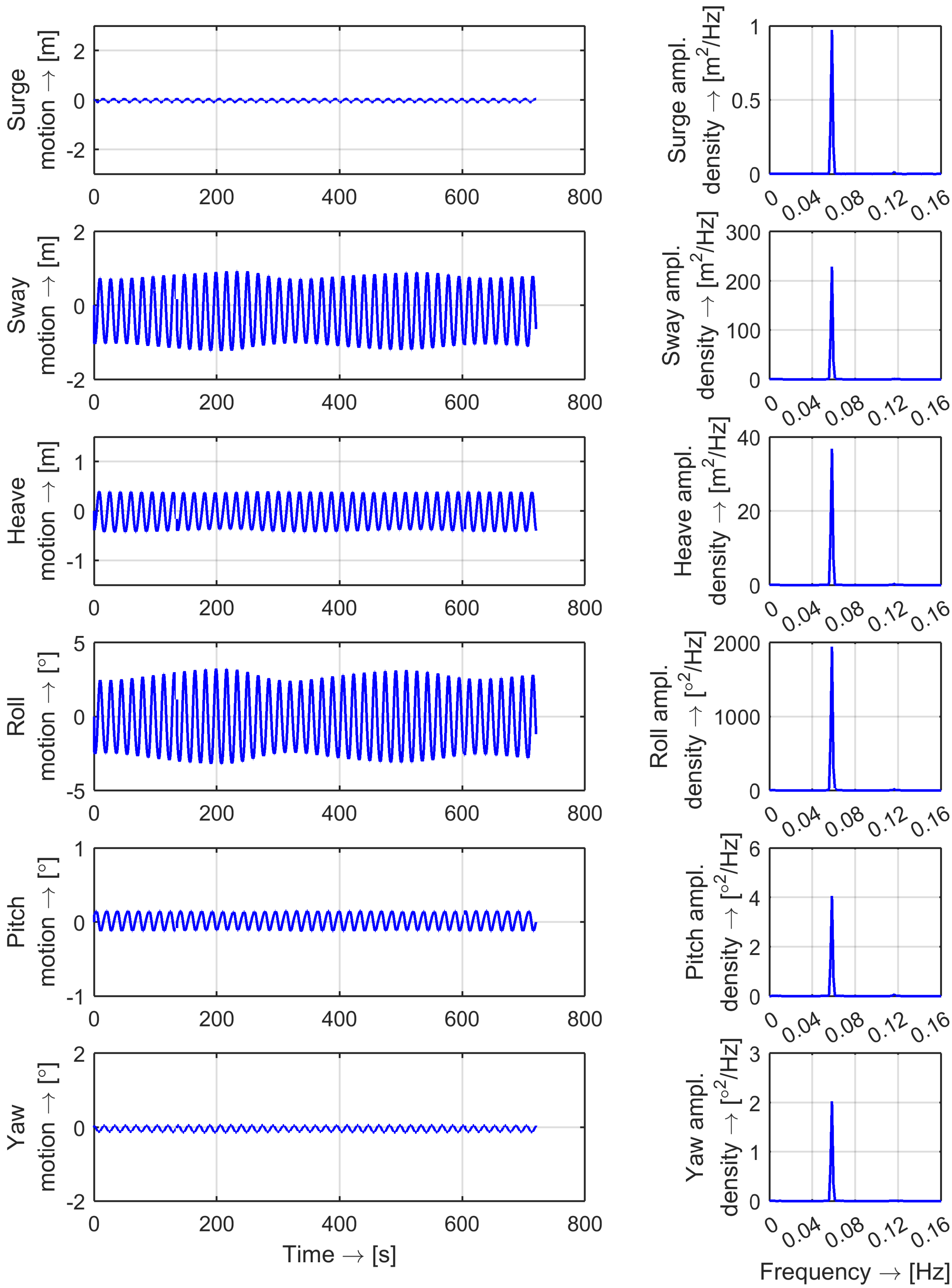

σ_{Surge} = 0.05 m, σ_{Sway} = 0.69 m, σ_{Heave} = 0.28 m, σ_{Roll} = 2.02°, σ_{Pitch} = 0.09°, σ_{Yaw} = 0.07°

Ship motions at centre of gravity (CoG) Depth = 18.0 m, H = 0.75 m, T = 17.20 s Beam-on waves	Monochromatic	M172h
	B1_M172h	
Deltares	11202696	App. G.071-2

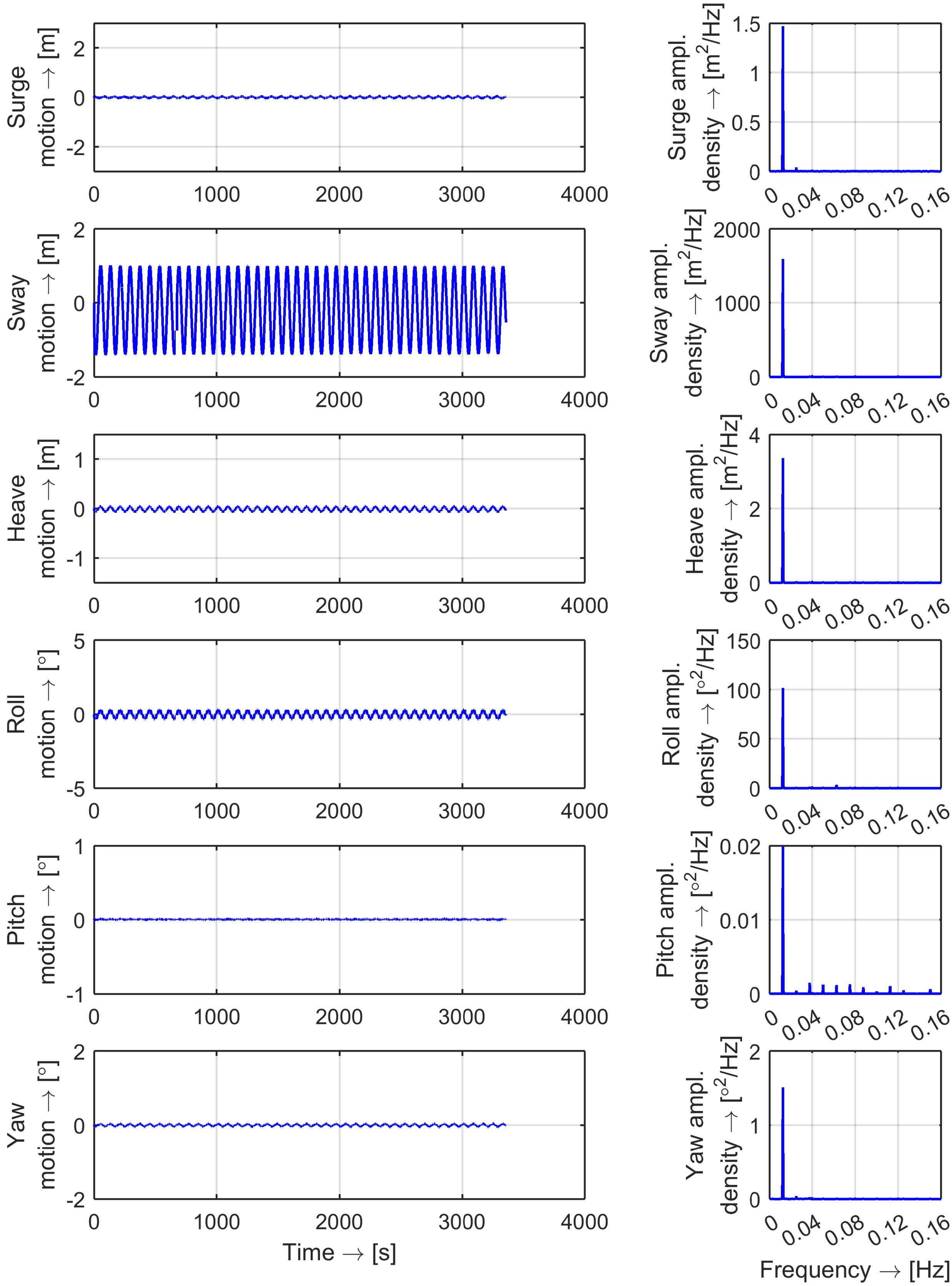

σ_{Surge} = 0.03 m, σ_{Sway} = 0.84 m, σ_{Heave} = 0.04 m, σ_{Roll} = 0.22°, σ_{Pitch} = 0.00°, σ_{Yaw} = 0.03°

Ship motions at centre of gravity (CoG) Depth = 18.0 m, H = 0.09 m, T = 80.00 s Beam-on waves	Monochromatic	M800d
	B1_M800d	
Deltares	11202696	App. G.072-2

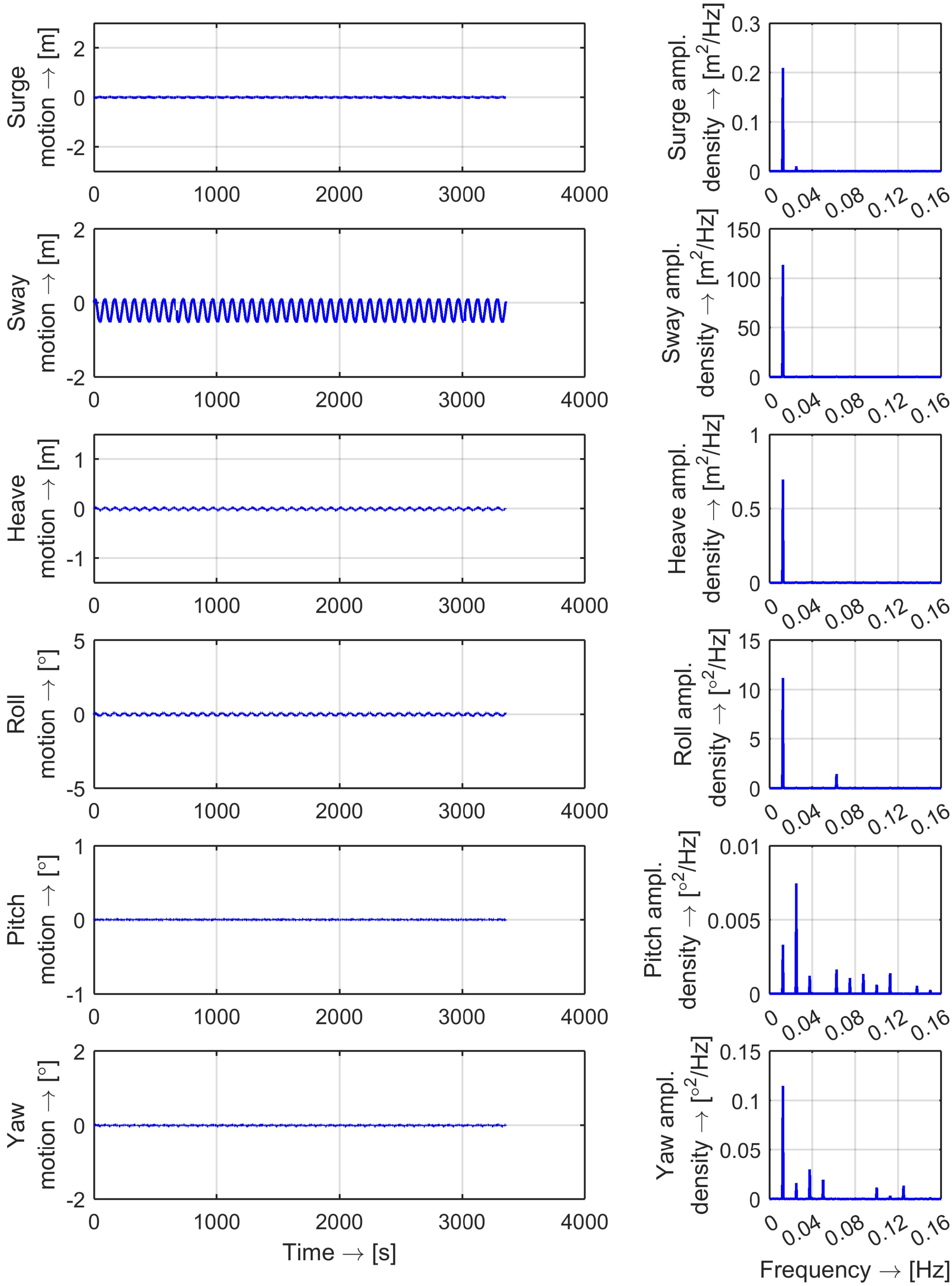

σ_{Surge} = 0.01 m, σ_{Sway} = 0.23 m, σ_{Heave} = 0.02 m, σ_{Roll} = 0.08°, σ_{Pitch} = 0.00°, σ_{Yaw} = 0.01°

Ship motions at centre of gravity (CoG) Depth = 18.0 m, H = 0.05 m, T = 80.00 s Beam-on waves	Monochromatic	M800e
	B1_M800e	
Deltares	11202696	App. G.073-2

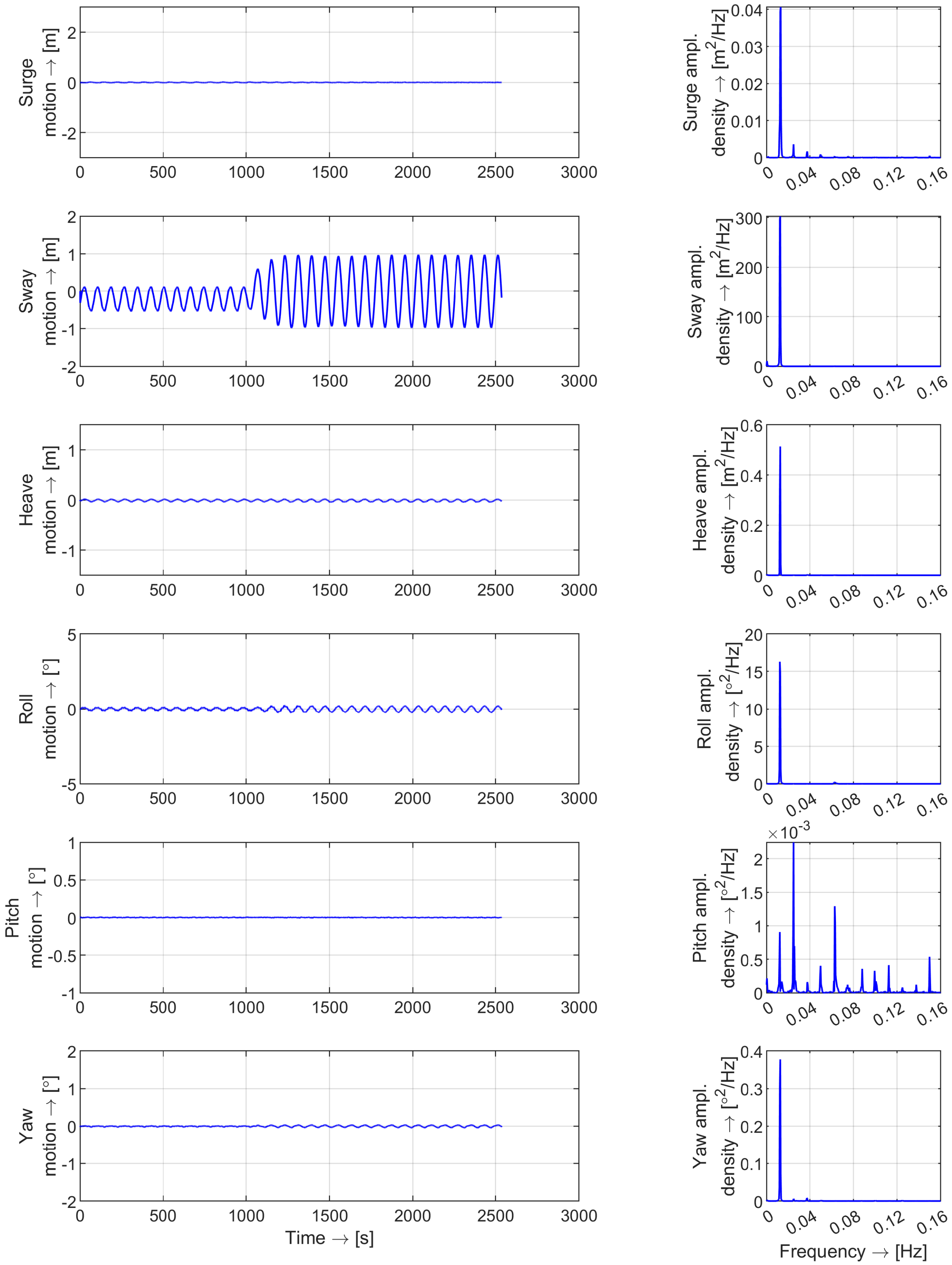

σ_{Surge} = n.a., σ_{Sway} = n.a., σ_{Heave} = n.a., σ_{Roll} = n.a., σ_{Pitch} = n.a., σ_{Yaw} = n.a.

Ship motions at centre of gravity (CoG) Depth = 18.0 m, H = 0.05 m, T = 80.00 s Beam-on waves	Monochromatic	M800e
	B1_M800e_Transition	
Deltares	11202696	App. G.074-2

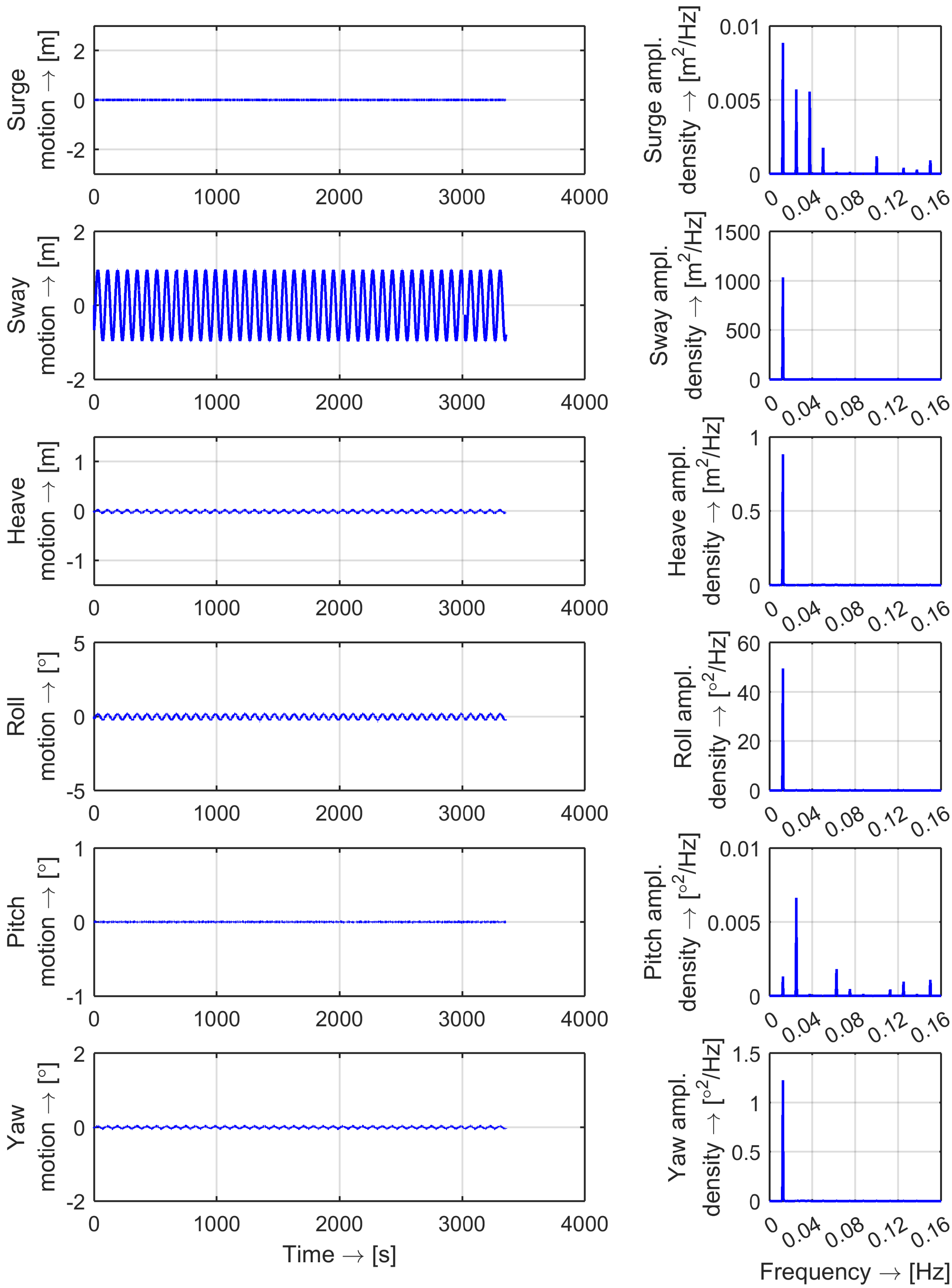

σ_{Surge} = 0.00 m, σ_{Sway} = 0.68 m, σ_{Heave} = 0.02 m, σ_{Roll} = 0.15°, σ_{Pitch} = 0.00°, σ_{Yaw} = 0.02°

Ship motions at centre of gravity (CoG) Depth = 18.0 m, H = 0.05 m, T = 80.00 s Beam-on waves	Monochromatic	M800e
	B1_M800e_noST	
Deltares	11202696	App. G.075-2

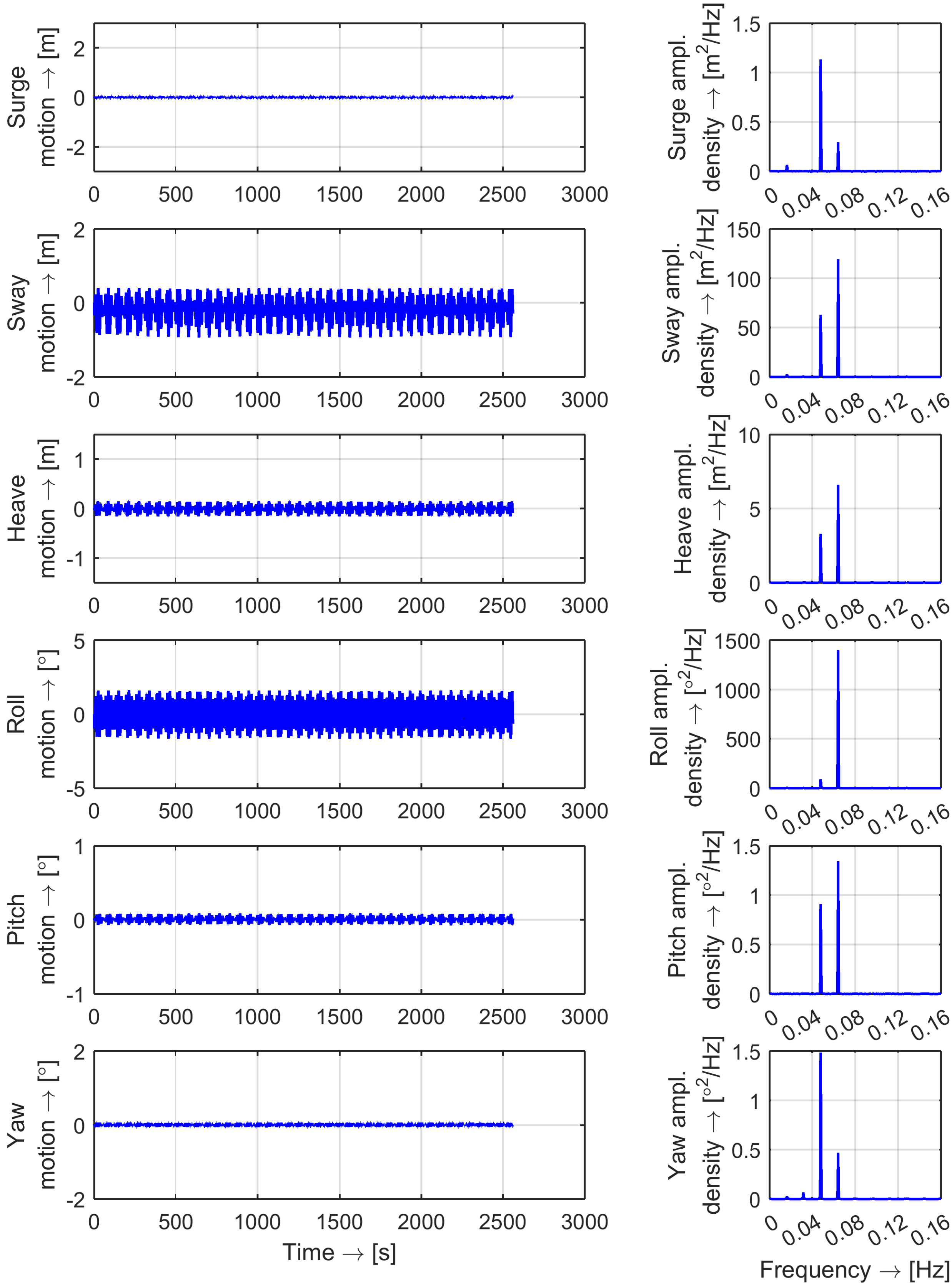

σ_{Surge} = 0.03 m, σ_{Sway} = 0.34 m, σ_{Heave} = 0.08 m, σ_{Roll} = 0.94°, σ_{Pitch} = 0.04°, σ_{Yaw} = 0.04°

Ship motions at centre of gravity (CoG) Depth = 18.0 m, H = 0.25 m, T_1 = 15.60 s, T_2 = 20.96 s Beam-on waves	Bichromatic	B610f
	B2_B610f	
Deltares	11202696	App. G.076-2

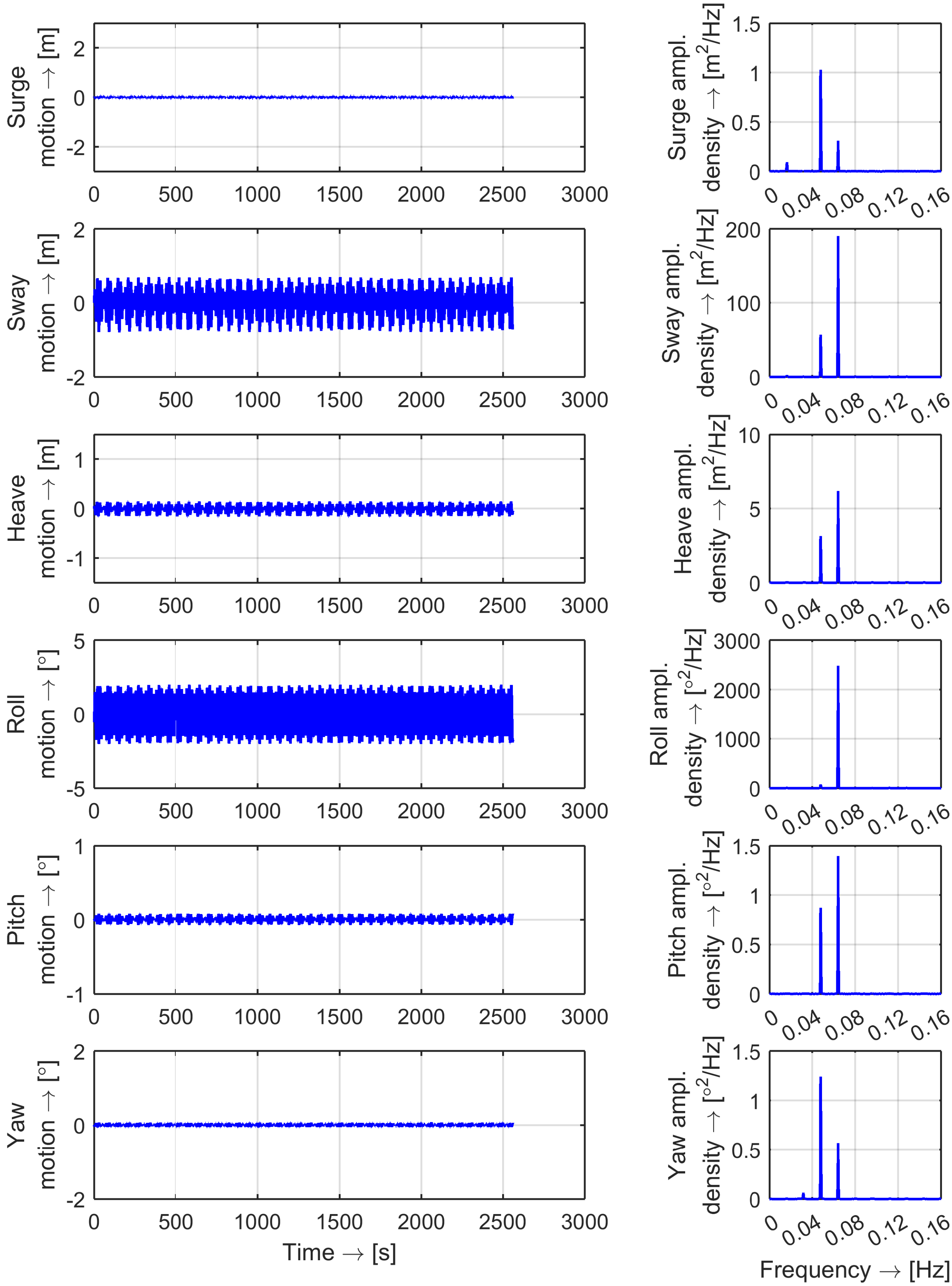

σ_{Surge} = 0.03 m, σ_{Sway} = 0.39 m, σ_{Heave} = 0.08 m, σ_{Roll} = 1.23°, σ_{Pitch} = 0.04°, σ_{Yaw} = 0.04°

Ship motions at centre of gravity (CoG) Depth = 18.0 m, H = 0.25 m, T_1 = 15.60 s, T_2 = 20.96 s Beam-on waves	Bichromatic	B610f
	B2_B610f_noST	
Deltares	11202696	App. G.077-2

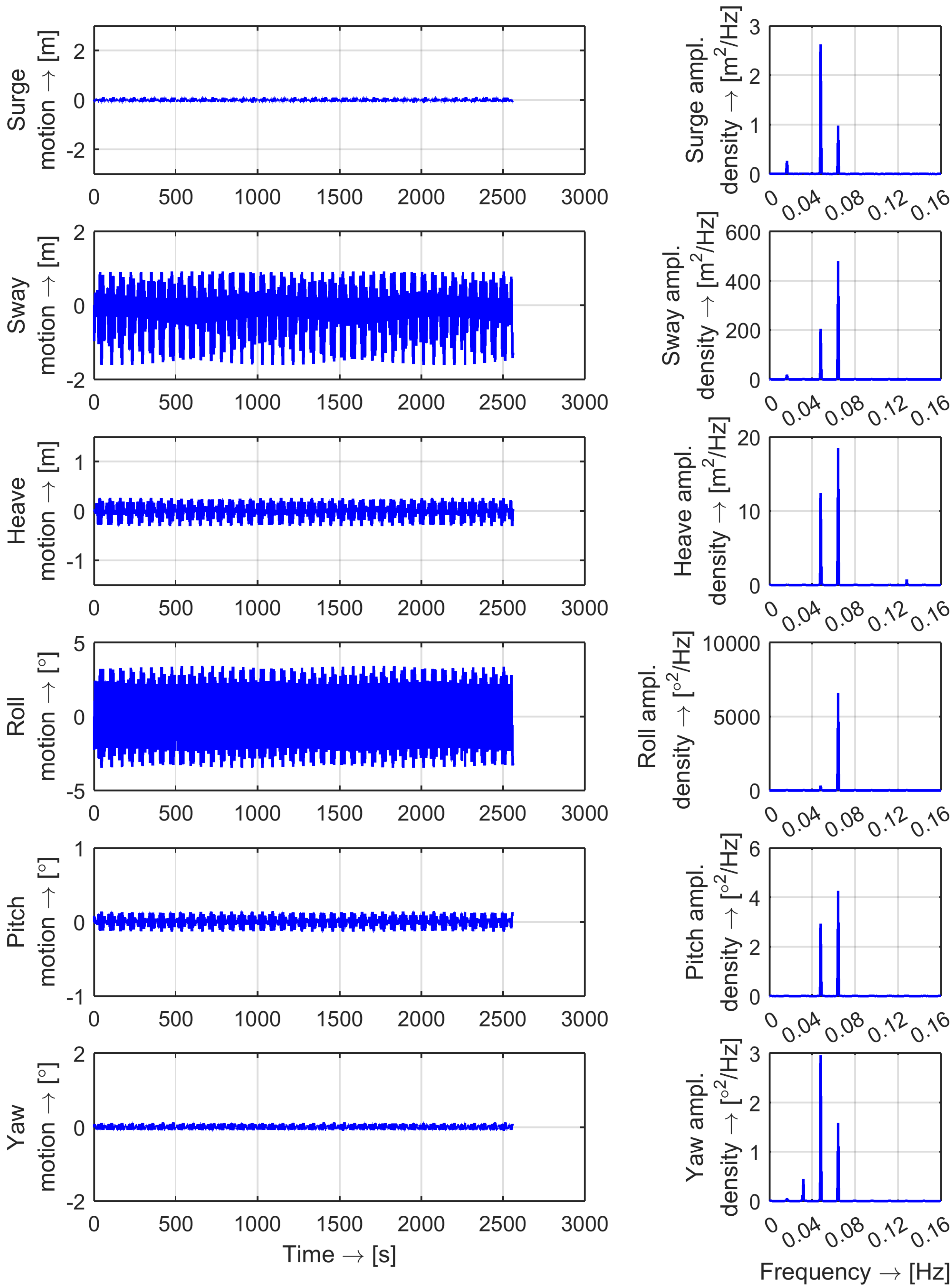

σ_{Surge} = 0.05 m, σ_{Sway} = 0.66 m, σ_{Heave} = 0.14 m, σ_{Roll} = 2.02°, σ_{Pitch} = 0.07°, σ_{Yaw} = 0.06°

Ship motions at centre of gravity (CoG) Depth = 18.0 m, H = 0.50 m, T_1 = 15.60 s, T_2 = 20.96 s Beam-on waves	Bichromatic	B610g
	B2_B610g	
Deltares	11202696	App. G.078-2

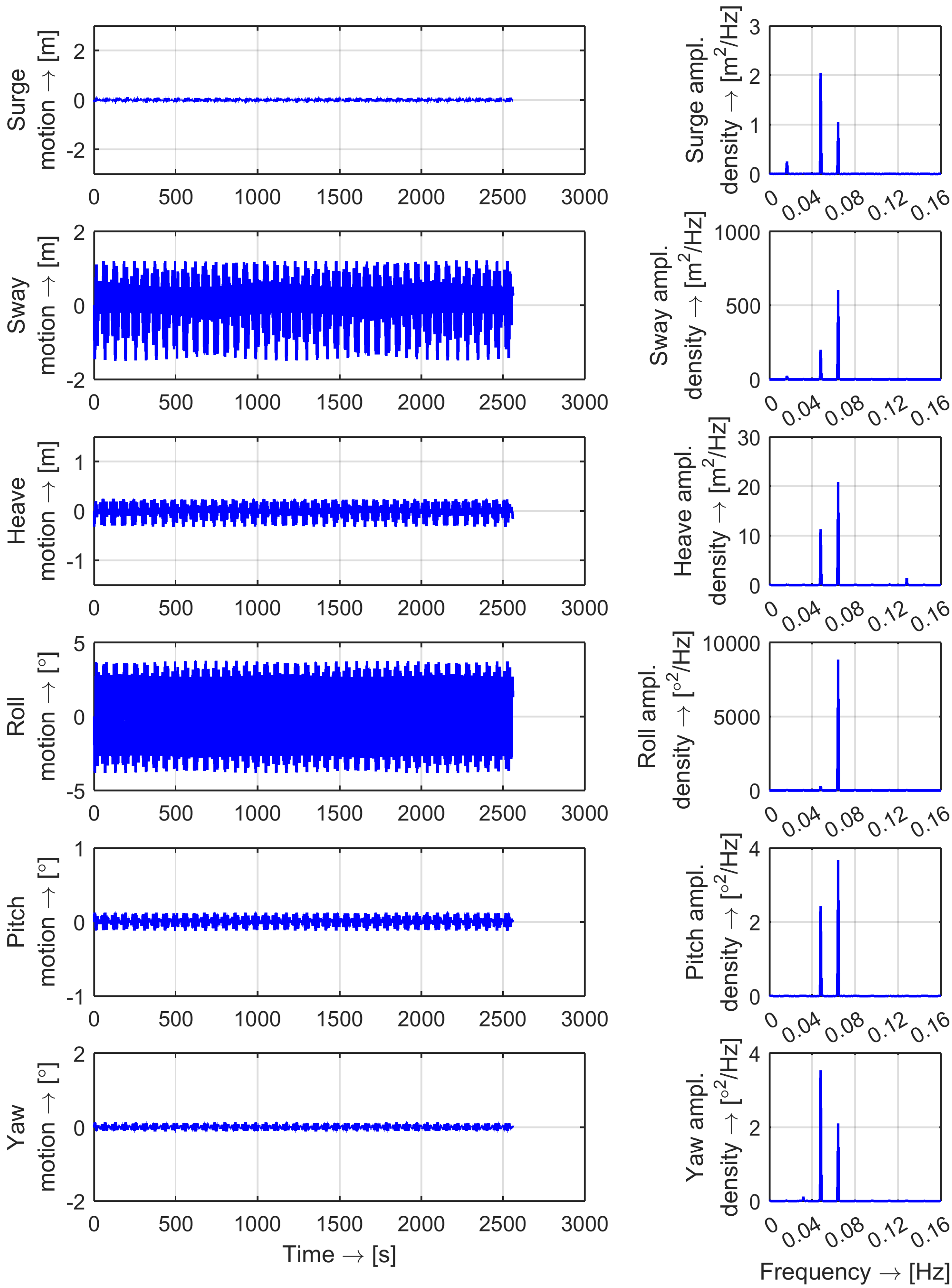

σ_{Surge} = 0.05 m, σ_{Sway} = 0.71 m, σ_{Heave} = 0.14 m, σ_{Roll} = 2.32°, σ_{Pitch} = 0.06°, σ_{Yaw} = 0.06°

Ship motions at centre of gravity (CoG) Depth = 18.0 m, H = 0.50 m, T_1 = 15.60 s, T_2 = 20.96 s Beam-on waves	Bichromatic	B610g
	B2_B610g_noST	
Deltares	11202696	App. G.079-2

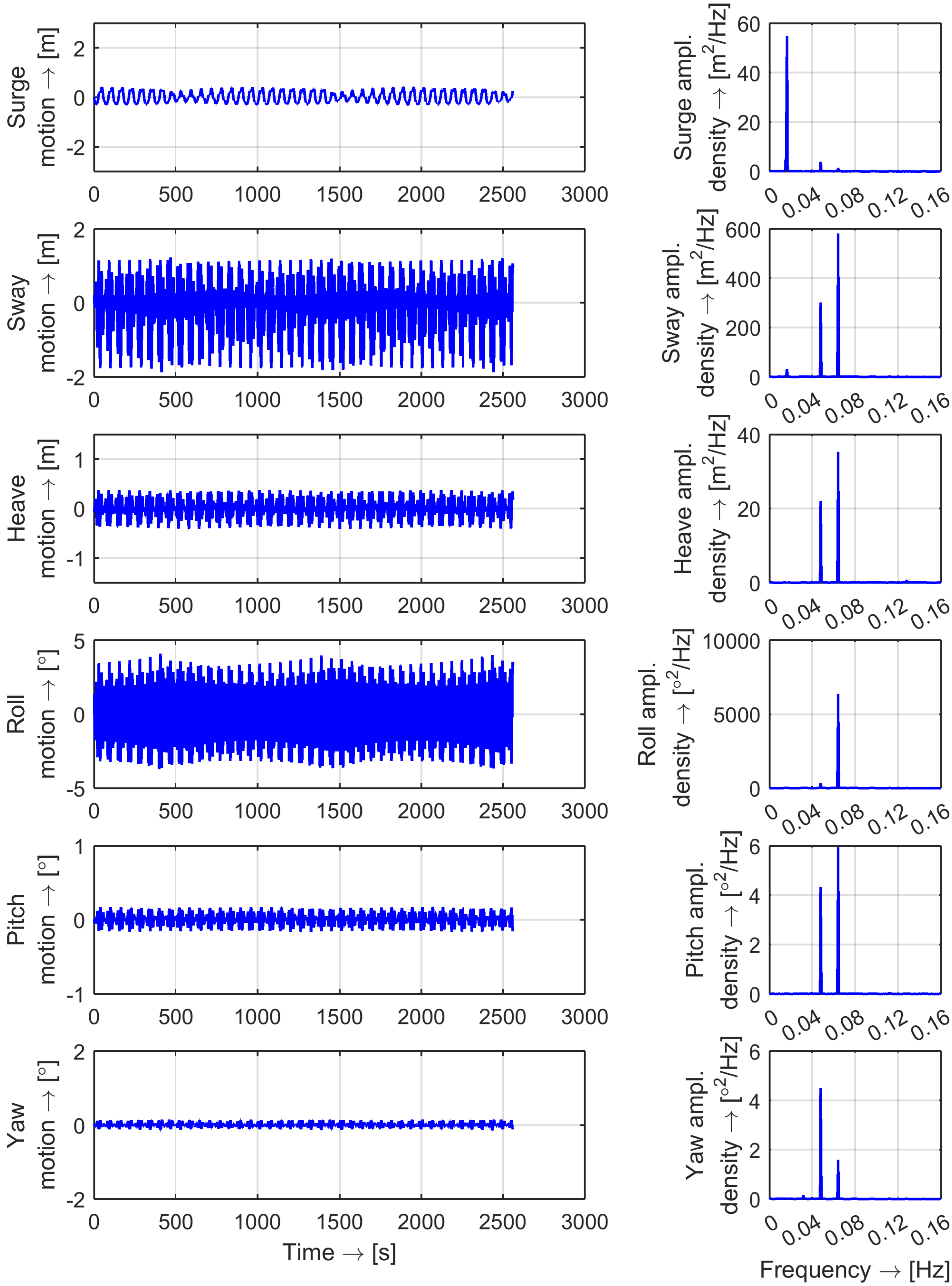

σ_{Surge} = 0.22 m, σ_{Sway} = 0.76 m, σ_{Heave} = 0.19 m, σ_{Roll} = 2.01°, σ_{Pitch} = 0.08°, σ_{Yaw} = 0.07°

Ship motions at centre of gravity (CoG) Depth = 18.0 m, H = 0.75 m, T_1 = 15.60 s, T_2 = 20.96 s Beam-on waves	Bichromatic	B610h
	B2_B610h	
Deltares	11202696	App. G.080-2

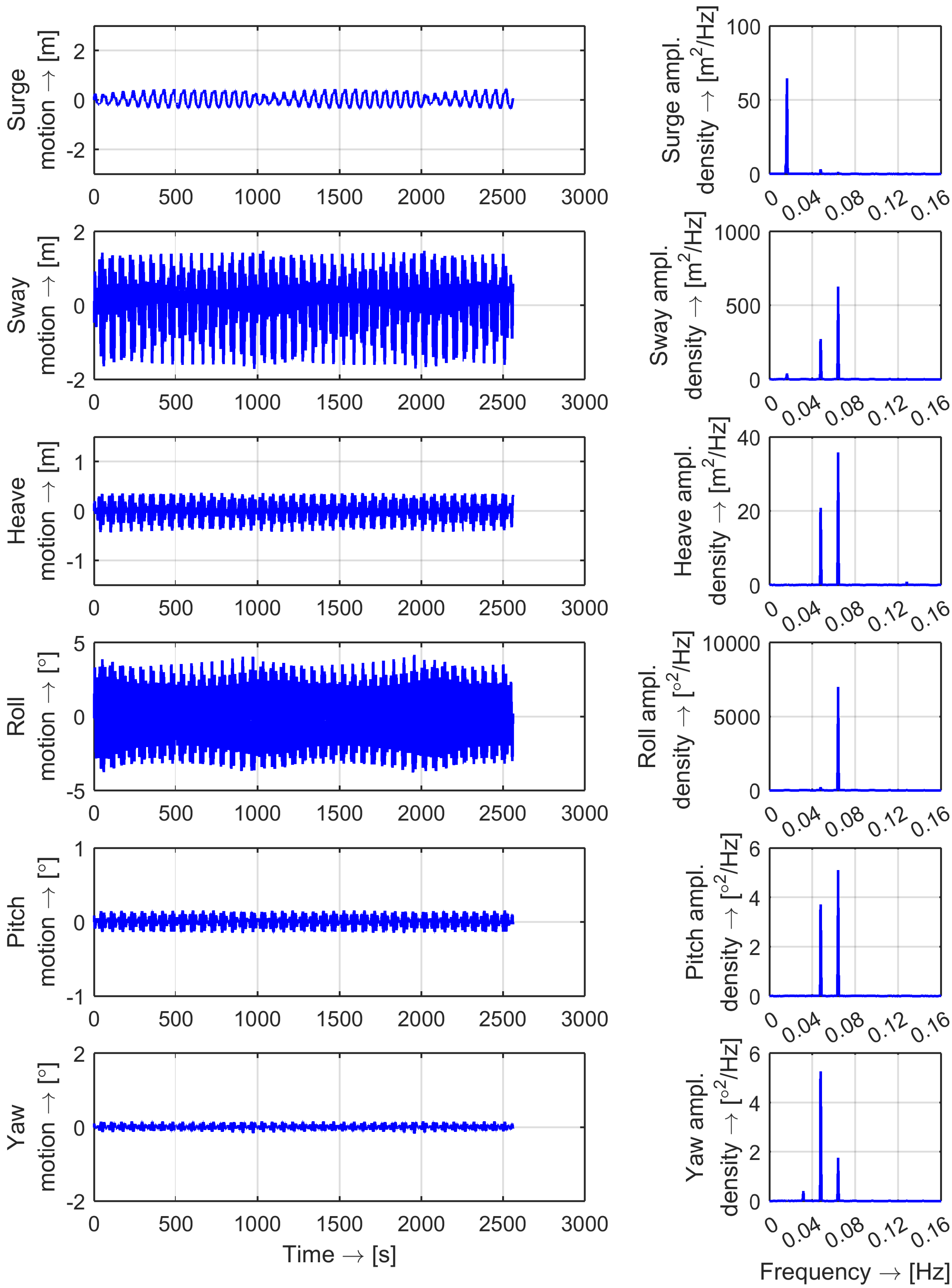

σ_{Surge} = 0.23 m, σ_{Sway} = 0.77 m, σ_{Heave} = 0.19 m, σ_{Roll} = 2.09°, σ_{Pitch} = 0.07°, σ_{Yaw} = 0.07°

Ship motions at centre of gravity (CoG) Depth = 18.0 m, H = 0.75 m, T_1 = 15.60 s, T_2 = 20.96 s Beam-on waves	Bichromatic	B610h
	B2_B610h_noST	
Deltares	11202696	App. G.081-2

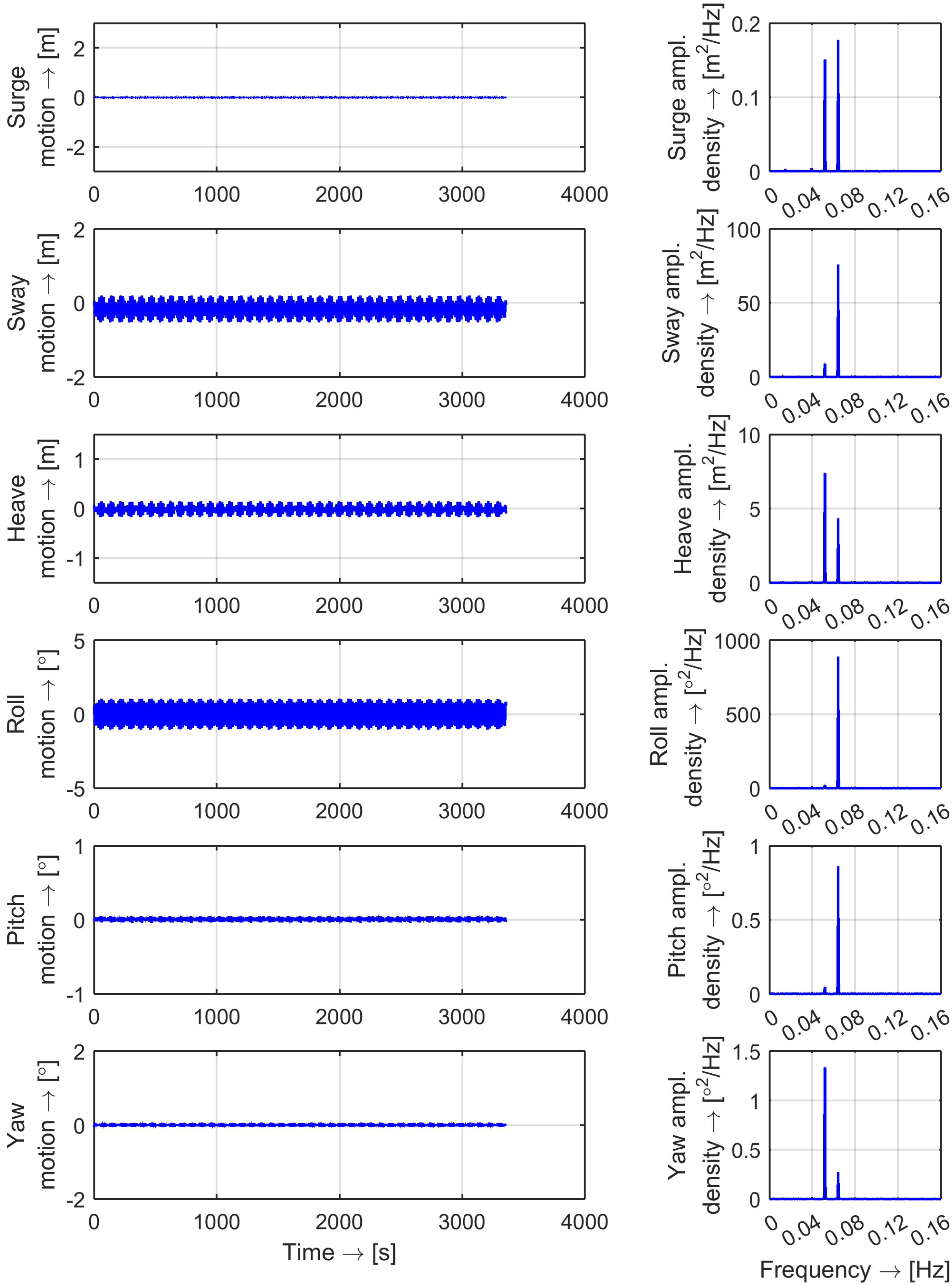

σ_{Surge} = 0.01 m, σ_{Sway} = 0.20 m, σ_{Heave} = 0.08 m, σ_{Roll} = 0.64°, σ_{Pitch} = 0.02°, σ_{Yaw} = 0.03°

Ship motions at centre of gravity (CoG) Depth = 18.0 m, H = 0.25 m, T_1 = 15.60 s, T_2 = 19.38 s Beam-on waves	Bichromatic	B800f
	B2_B800f	
Deltares	11202696	App. G.082-2

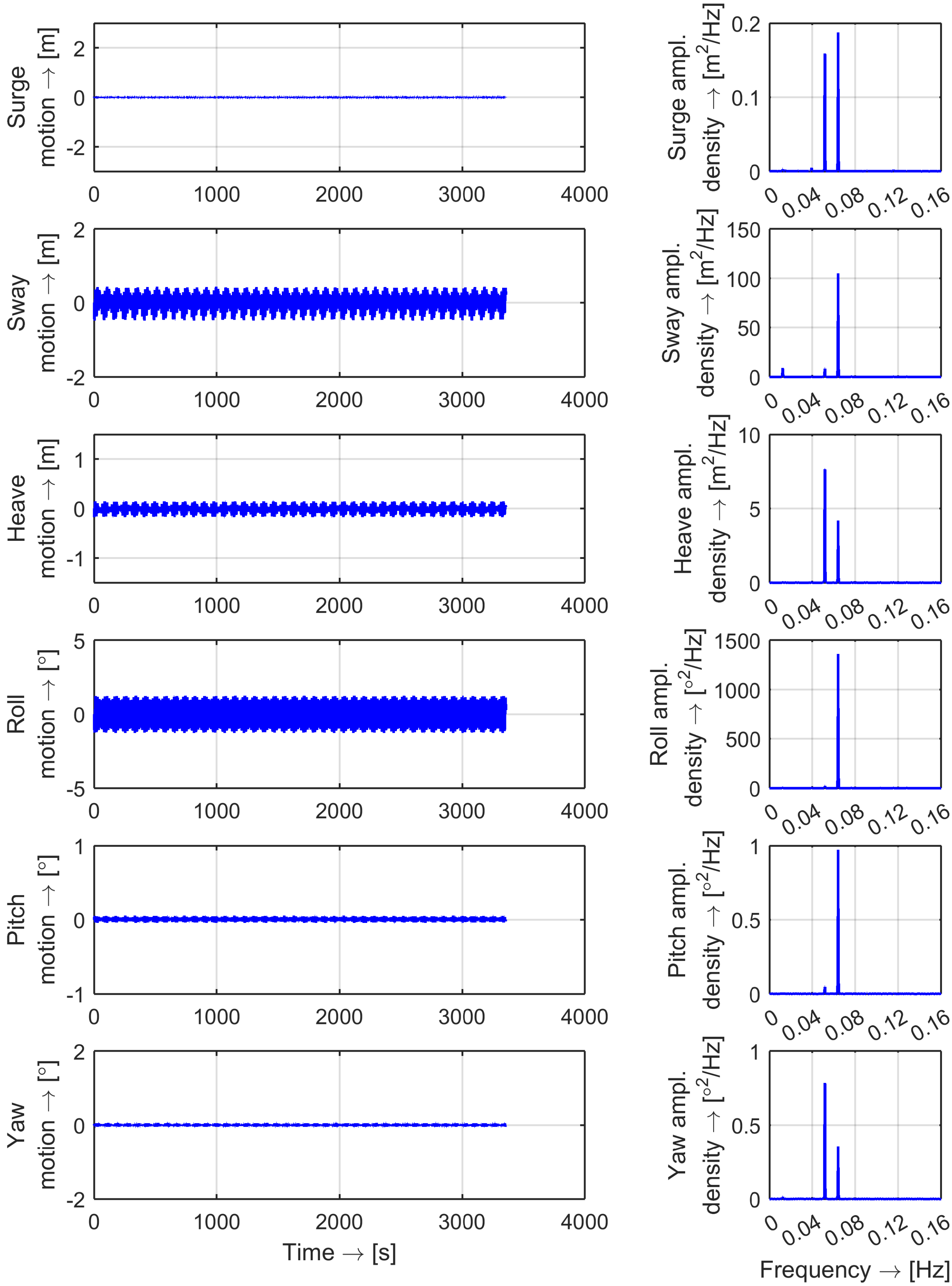

σ_{Surge} = 0.01 m, σ_{Sway} = 0.24 m, σ_{Heave} = 0.08 m, σ_{Roll} = 0.79°, σ_{Pitch} = 0.02°, σ_{Yaw} = 0.03°

Ship motions at centre of gravity (CoG) Depth = 18.0 m, H = 0.25 m, T_1 = 15.60 s, T_2 = 19.38 s Beam-on waves	Bichromatic	B800f
	B2_B800f_noST	
Deltares	11202696	App. G.083-2

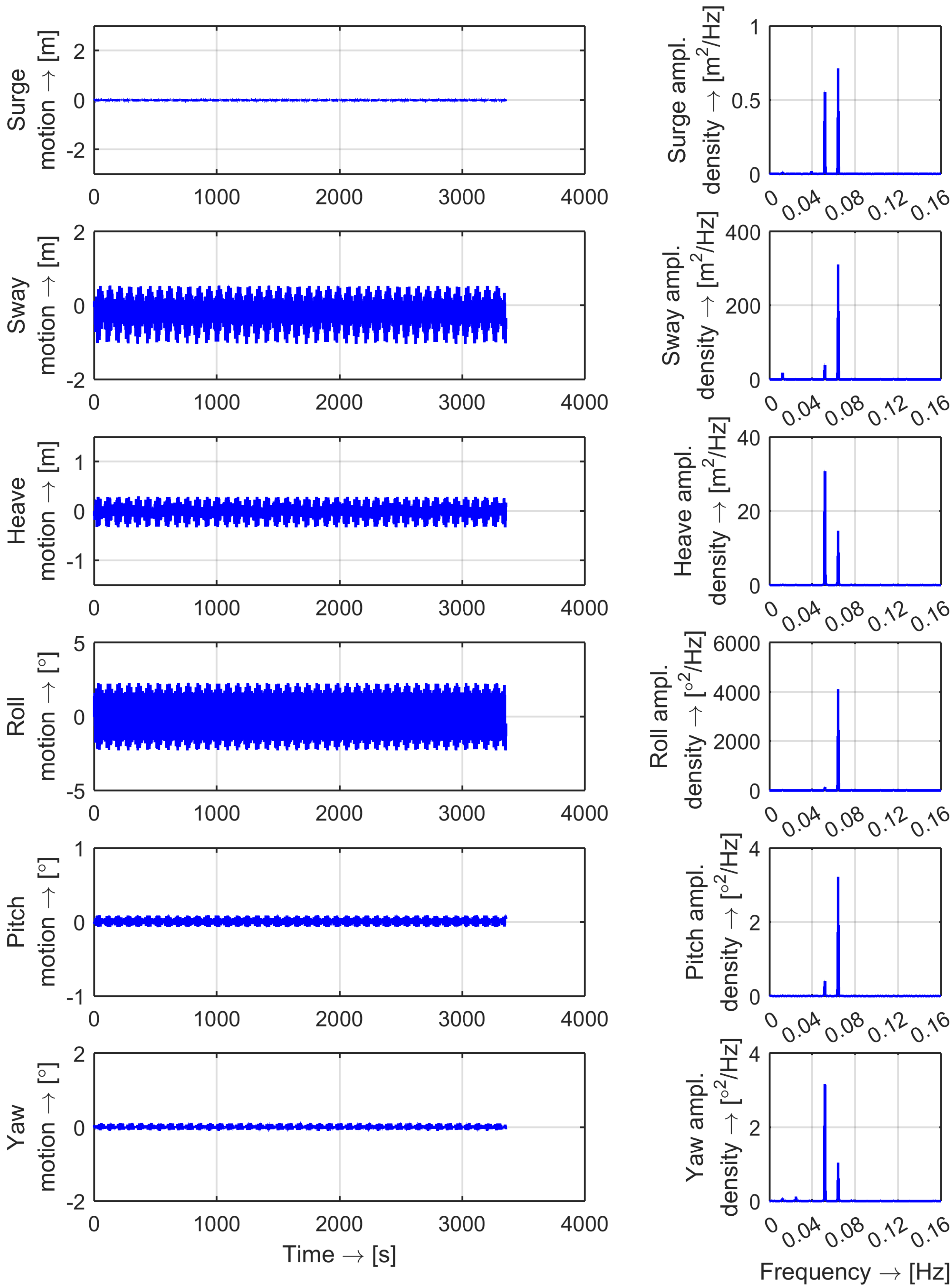

σ_{Surge} = 0.03 m, σ_{Sway} = 0.42 m, σ_{Heave} = 0.16 m, σ_{Roll} = 1.39°, σ_{Pitch} = 0.04°, σ_{Yaw} = 0.05°

Ship motions at centre of gravity (CoG) Depth = 18.0 m, H = 0.50 m, T_1 = 15.60 s, T_2 = 19.38 s Beam-on waves	Bichromatic	B800g
	B2_B800g	
Deltares	11202696	App. G.084-2

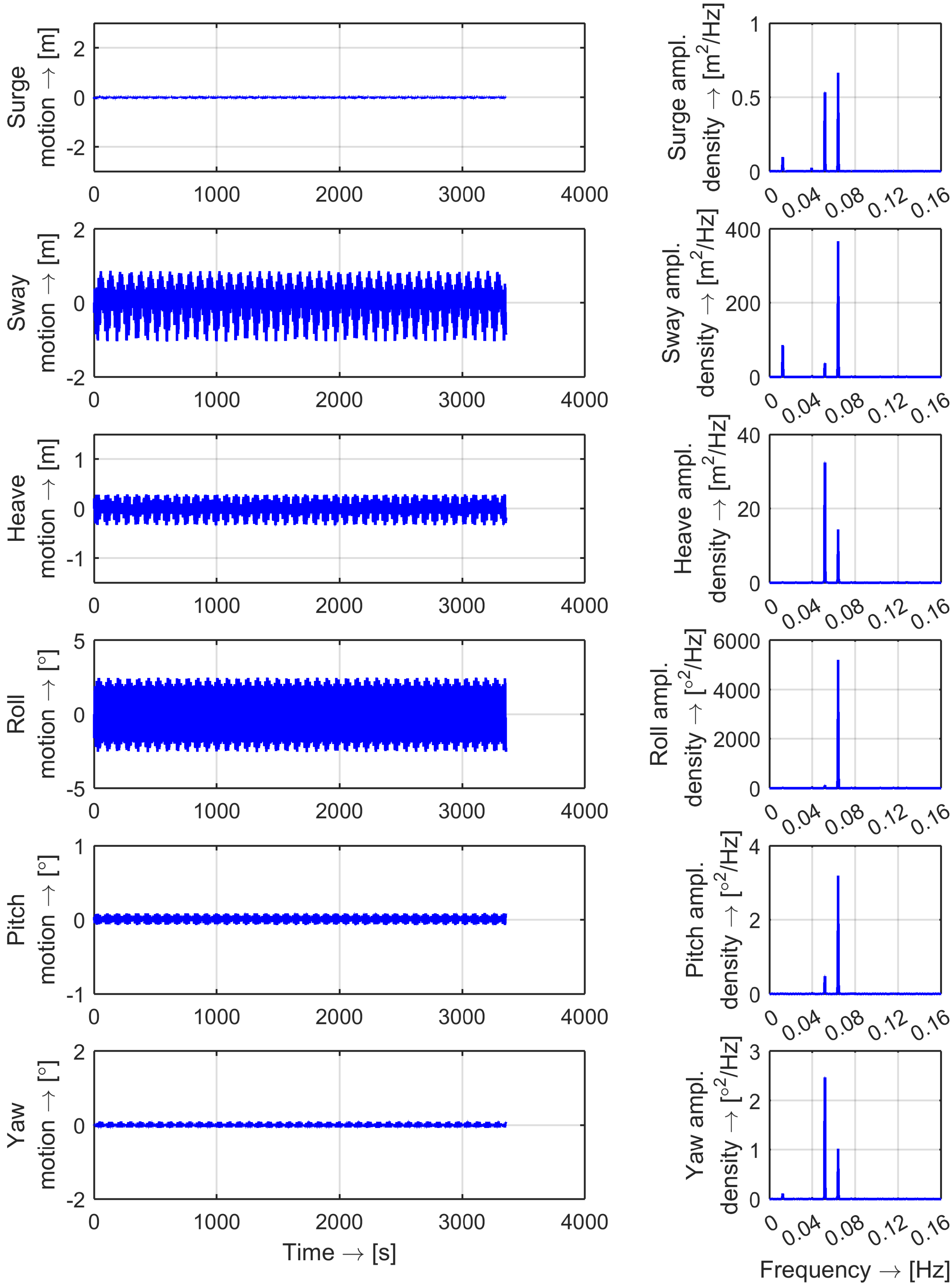

σ_{Surge} = 0.03 m, σ_{Sway} = 0.49 m, σ_{Heave} = 0.16 m, σ_{Roll} = 1.55°, σ_{Pitch} = 0.04°, σ_{Yaw} = 0.05°

Ship motions at centre of gravity (CoG) Depth = 18.0 m, H = 0.50 m, T_1 = 15.60 s, T_2 = 19.38 s Beam-on waves	Bichromatic	B800g
	B2_B800g_noST	
Deltares	11202696	App. G.085-2

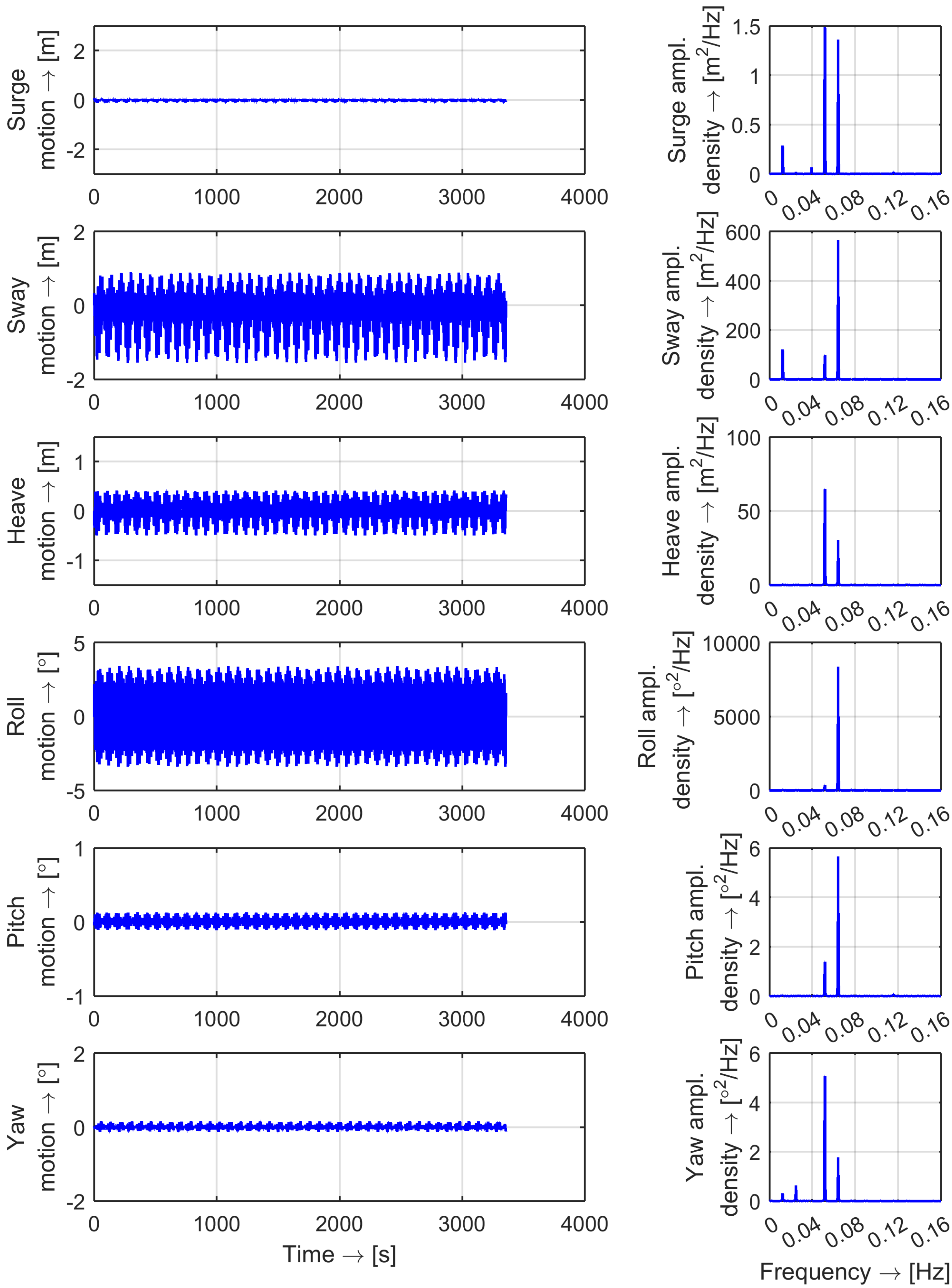

σ_{Surge} = 0.04 m, σ_{Sway} = 0.62 m, σ_{Heave} = 0.23 m, σ_{Roll} = 2.01°, σ_{Pitch} = 0.06°, σ_{Yaw} = 0.07°

Ship motions at centre of gravity (CoG) Depth = 18.0 m, H = 0.75 m, T_1 = 15.60 s, T_2 = 19.38 s Beam-on waves	Bichromatic	B800h
	B2_B800h	
Deltares	11202696	App. G.086-2

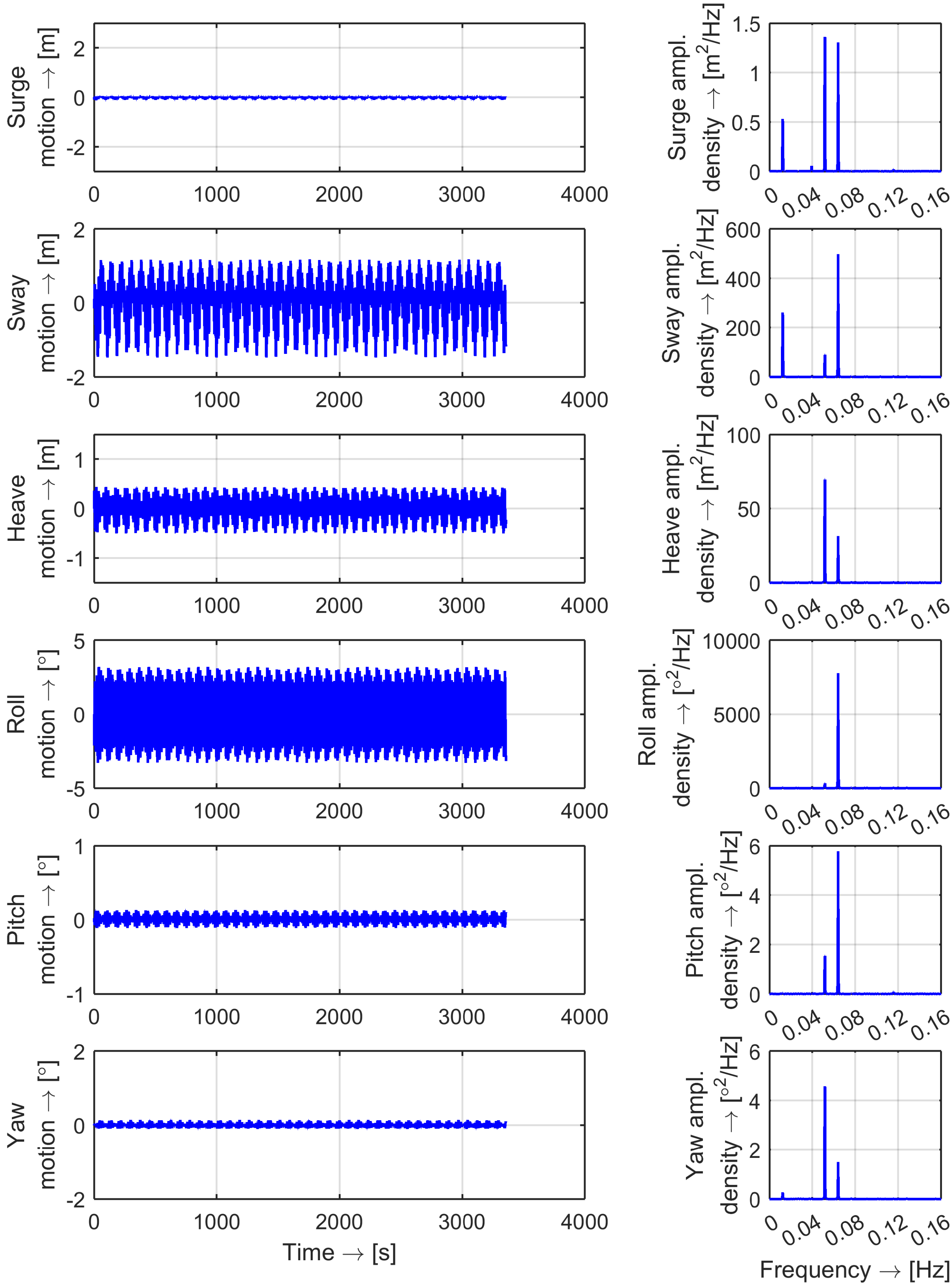

σ_{Surge} = 0.04 m, σ_{Sway} = 0.66 m, σ_{Heave} = 0.24 m, σ_{Roll} = 1.93°, σ_{Pitch} = 0.06°, σ_{Yaw} = 0.06°

Ship motions at centre of gravity (CoG) Depth = 18.0 m, H = 0.75 m, T_1 = 15.60 s, T_2 = 19.38 s Beam-on waves	Bichromatic	B800h
	B2_B800h_noST	
Deltares	11202696	App. G.087-2

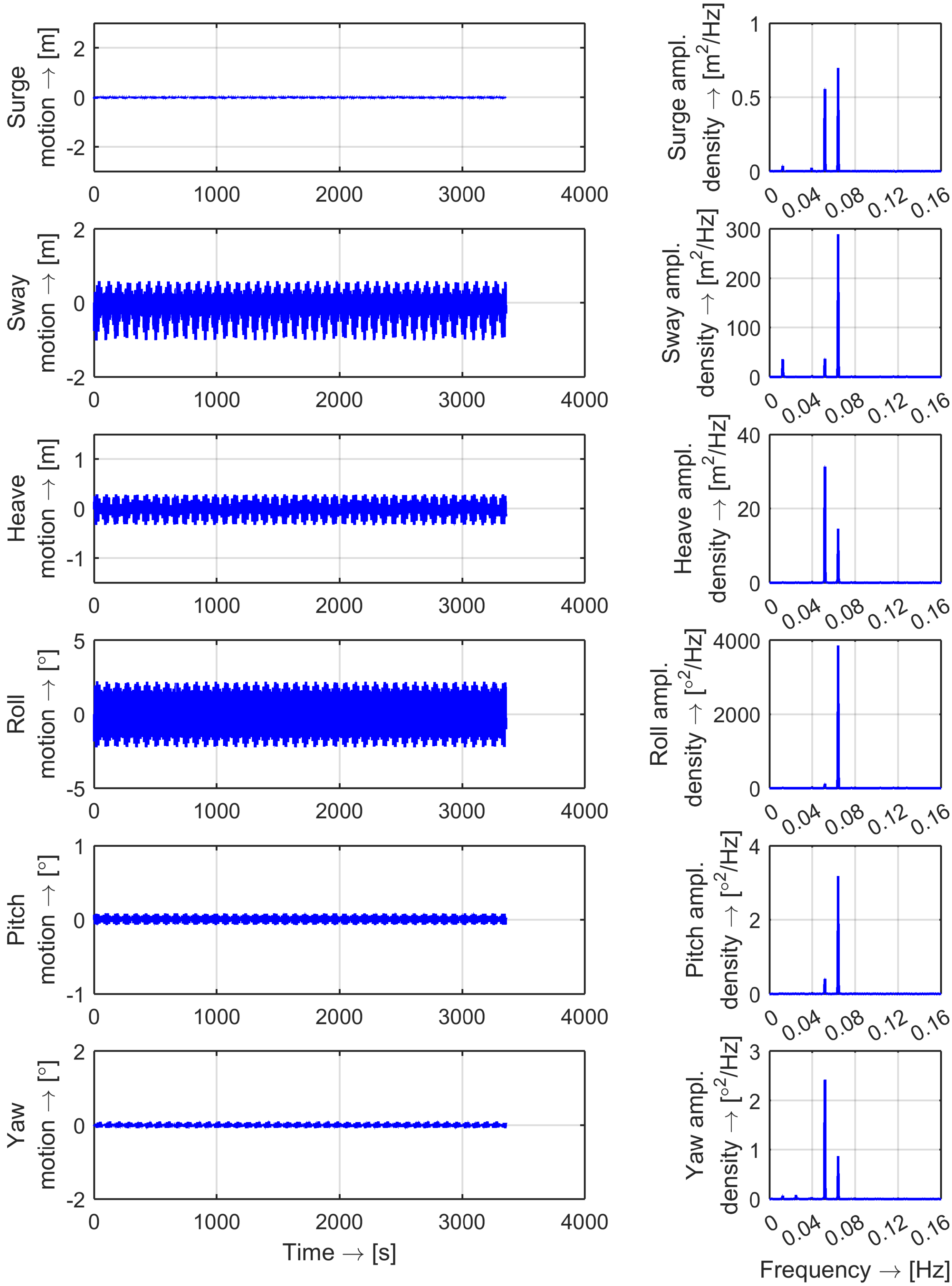

σ_{Surge} = 0.03 m, σ_{Sway} = 0.42 m, σ_{Heave} = 0.16 m, σ_{Roll} = 1.34°, σ_{Pitch} = 0.04°, σ_{Yaw} = 0.04°

Ship motions at centre of gravity (CoG) Depth = 18.0 m, H = 0.50 m, T_1 = 15.60 s, T_2 = 19.38 s Beam-on waves	Bichromatic	B800g
	B3_B800g_50t	
Deltares	11202696	App. G.088-2

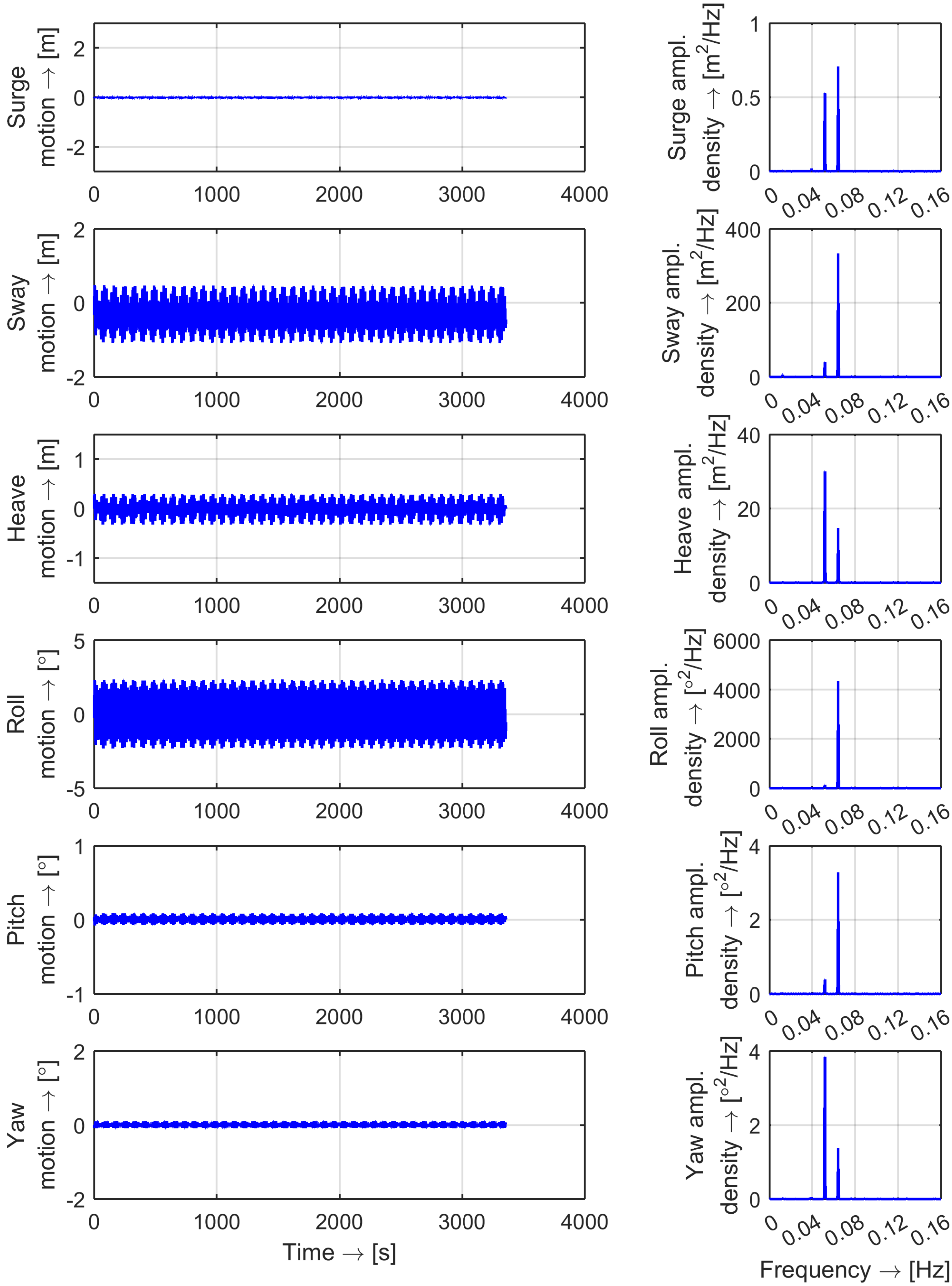

σ_{Surge} = 0.03 m, σ_{Sway} = 0.42 m, σ_{Heave} = 0.16 m, σ_{Roll} = 1.42°, σ_{Pitch} = 0.04°, σ_{Yaw} = 0.06°

Ship motions at centre of gravity (CoG) Depth = 18.0 m, H = 0.50 m, T_1 = 15.60 s, T_2 = 19.38 s Beam-on waves	Bichromatic	B800g
	B3_B800g_200t	
Deltares	11202696	App. G.089-2

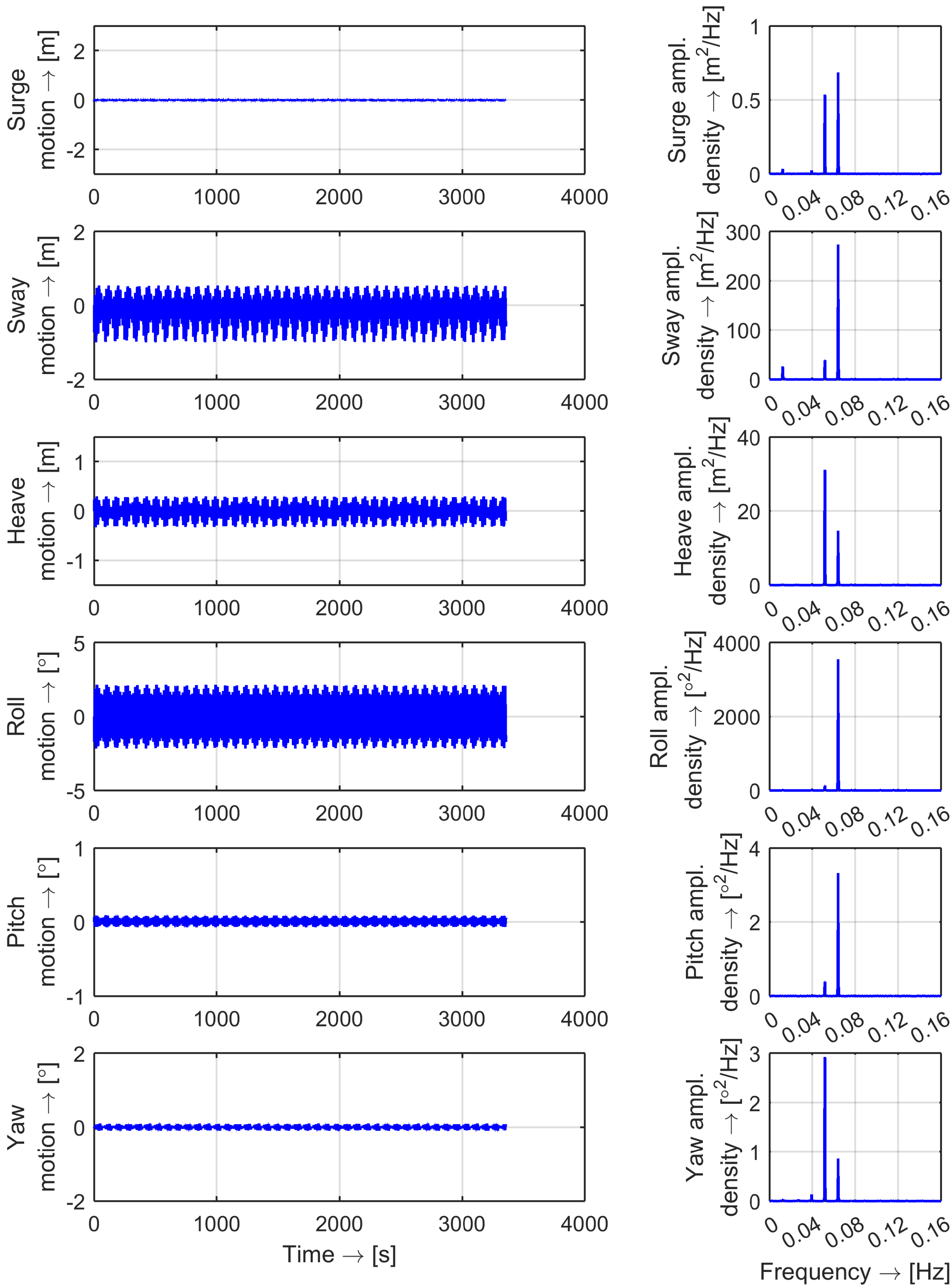

σ_{Surge} = 0.03 m, σ_{Sway} = 0.40 m, σ_{Heave} = 0.16 m, σ_{Roll} = 1.29°, σ_{Pitch} = 0.04°, σ_{Yaw} = 0.05°

Ship motions at centre of gravity (CoG) Depth = 18.0 m, H = 0.50 m, T_1 = 15.60 s, T_2 = 19.38 s Beam-on waves	Bichromatic	B800g
	B3_B800g_sga	
Deltares	11202696	App. G.090-2

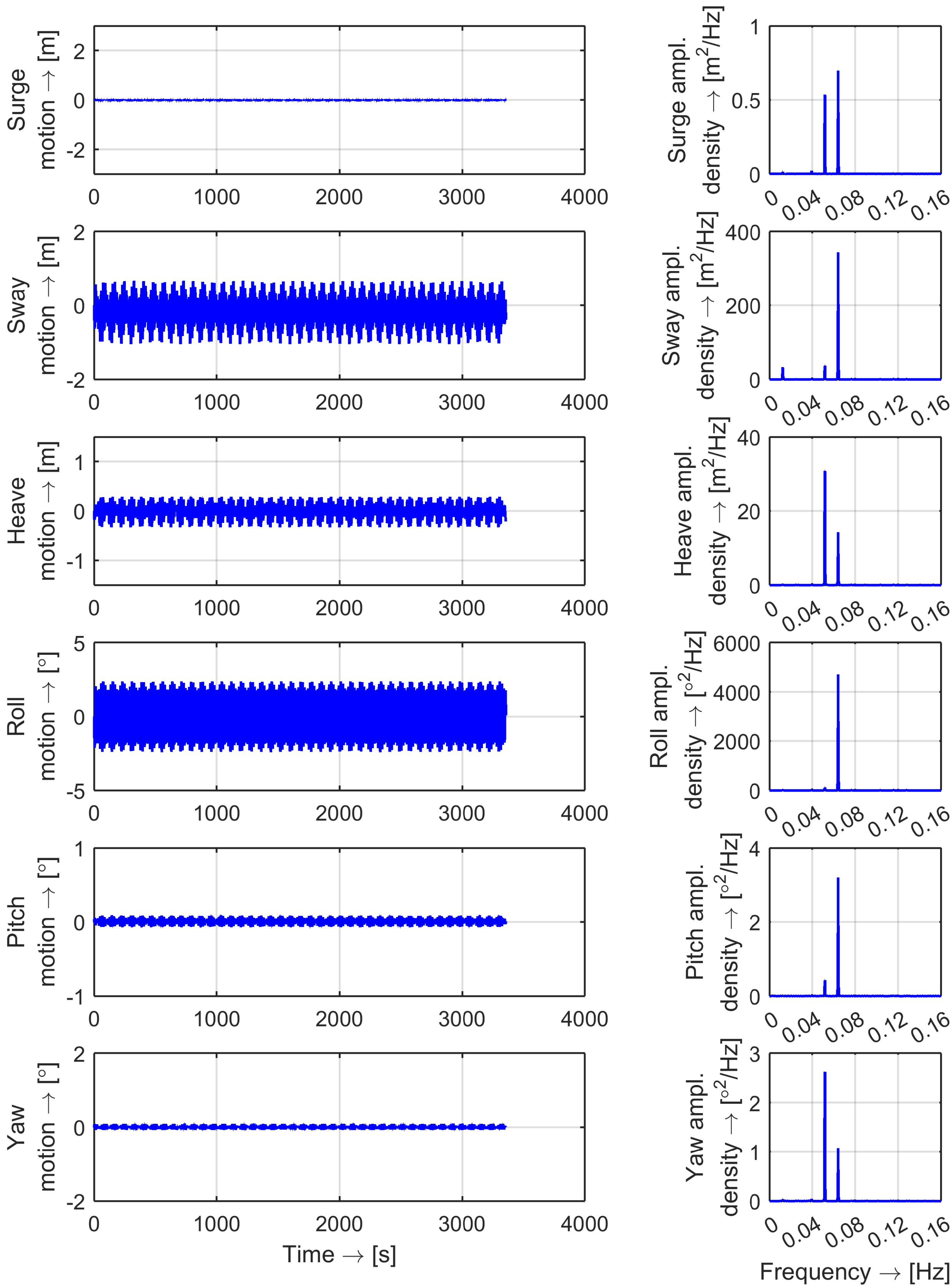

σ_{Surge} = 0.03 m, σ_{Sway} = 0.44 m, σ_{Heave} = 0.16 m, σ_{Roll} = 1.48°, σ_{Pitch} = 0.04°, σ_{Yaw} = 0.05°

Ship motions at centre of gravity (CoG) Depth = 18.0 m, H = 0.50 m, T_1 = 15.60 s, T_2 = 19.38 s Beam-on waves	Bichromatic	B800g
	B3_B800g_sk	
Deltares	11202696	App. G.091-2

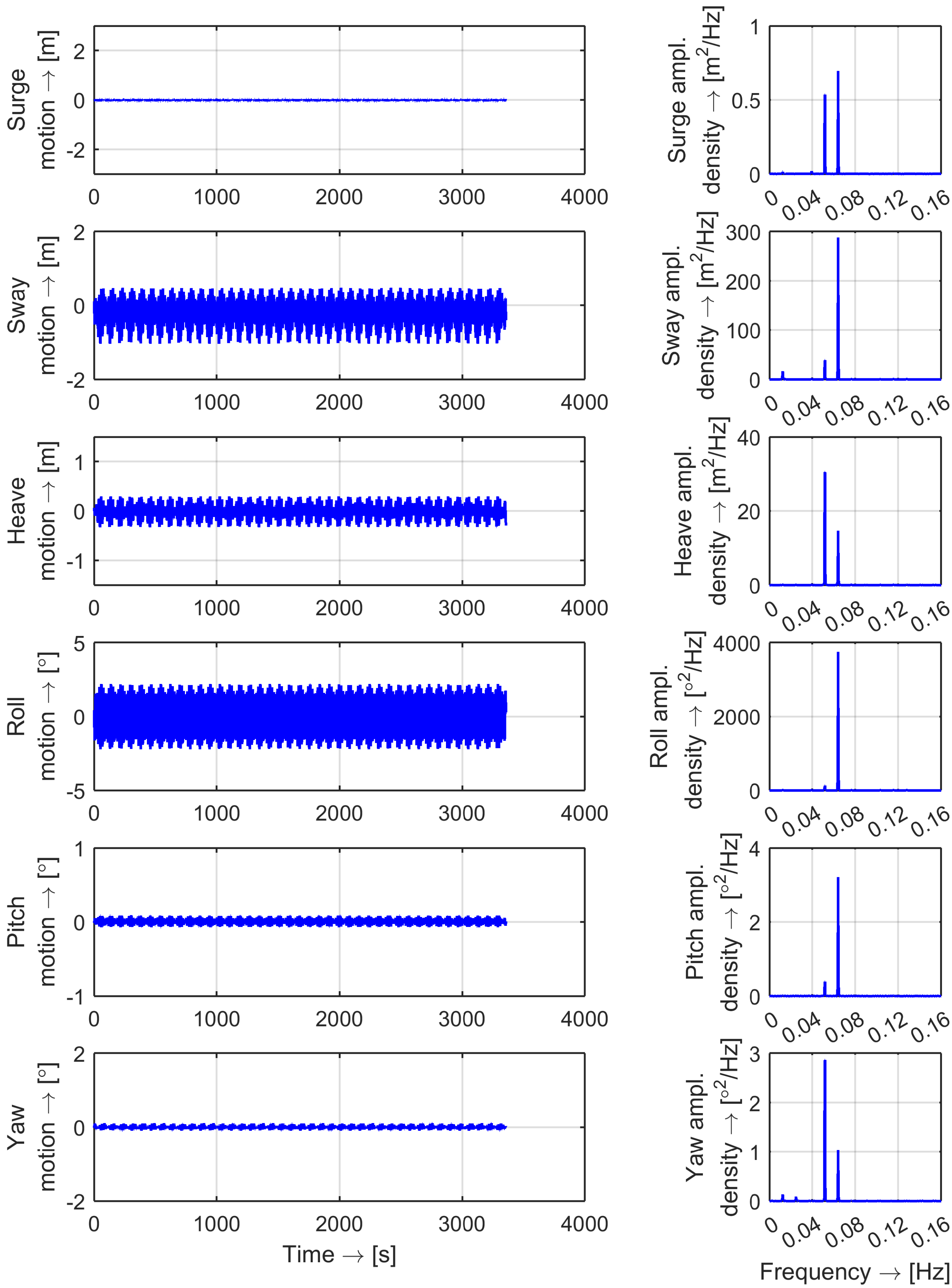

σ_{Surge} = 0.03 m, σ_{Sway} = 0.40 m, σ_{Heave} = 0.16 m, σ_{Roll} = 1.33°, σ_{Pitch} = 0.04°, σ_{Yaw} = 0.05°

Ship motions at centre of gravity (CoG) Depth = 18.0 m, H = 0.50 m, T_1 = 15.60 s, T_2 = 19.38 s Beam-on waves	Bichromatic	B800g
	B3_B800g_ssk	
Deltares	11202696	App. G.092-2

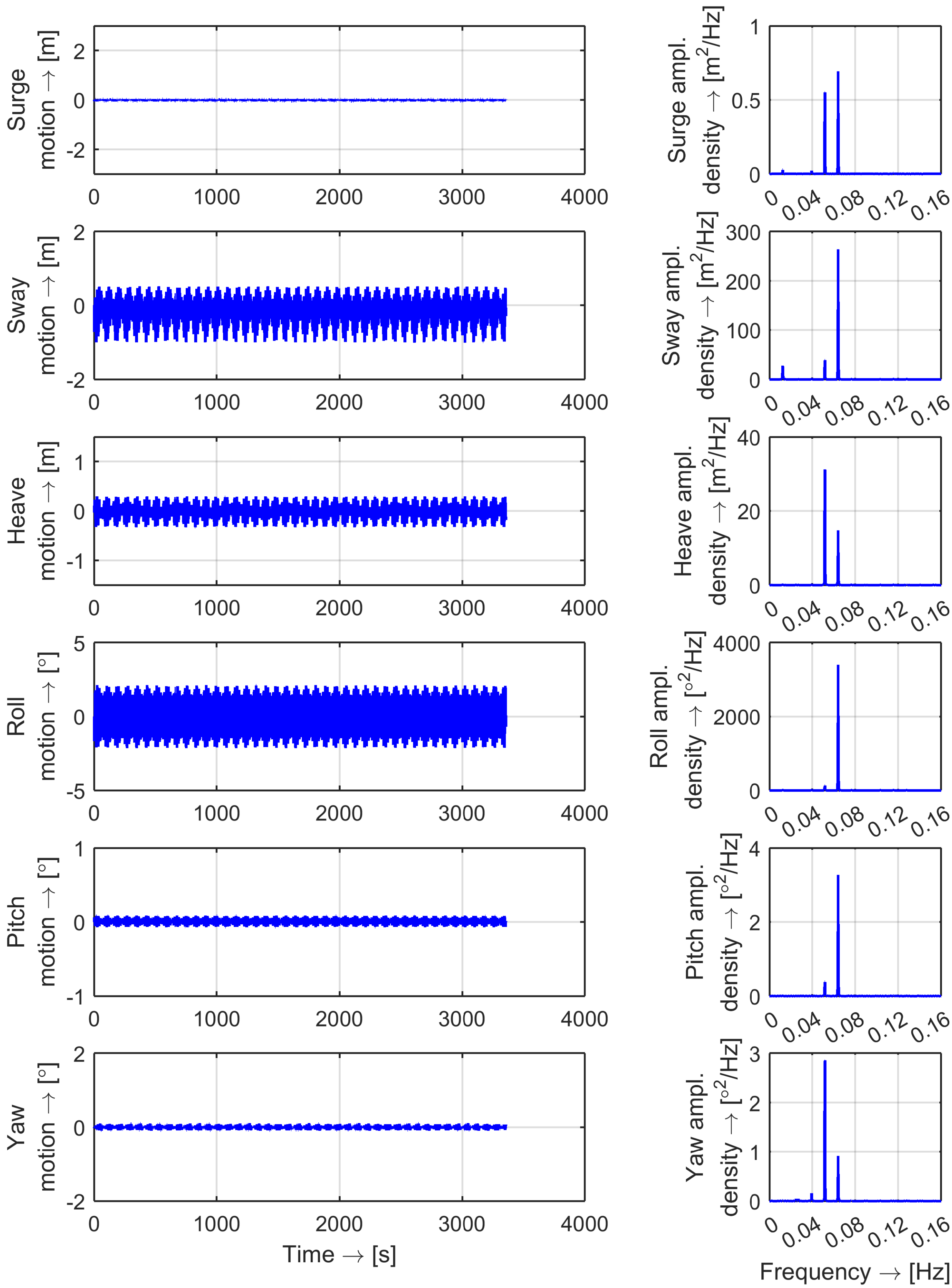

σ_{Surge} = 0.03 m, σ_{Sway} = 0.40 m, σ_{Heave} = 0.16 m, σ_{Roll} = 1.27°, σ_{Pitch} = 0.04°, σ_{Yaw} = 0.05°

Ship motions at centre of gravity (CoG) Depth = 18.0 m, H = 0.50 m, T_1 = 15.60 s, T_2 = 19.38 s Beam-on waves	Bichromatic	B800g
	B3_B800g_ssk_sga	
Deltares	11202696	App. G.093-2

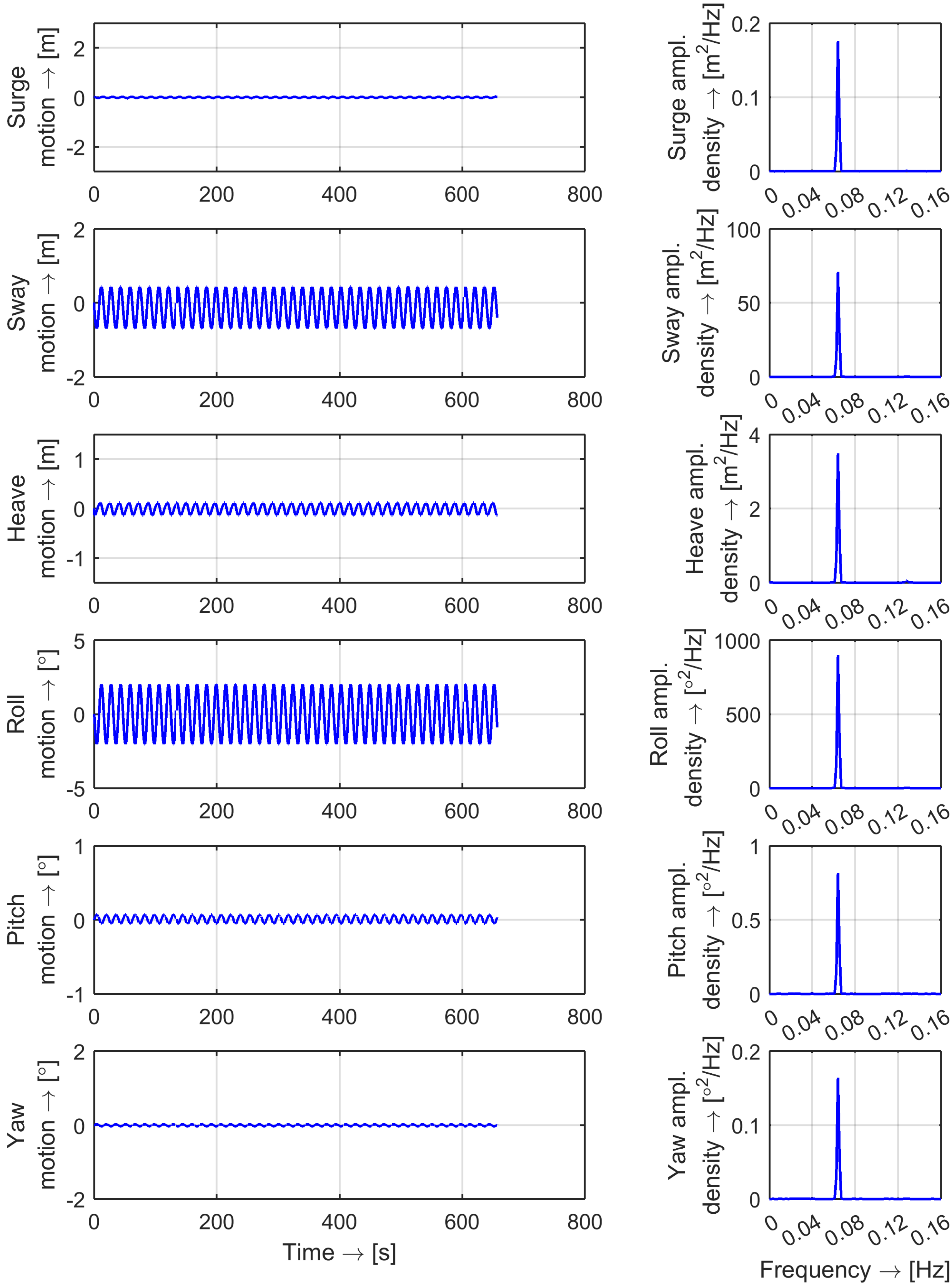

σ_{Surge} = 0.02 m, σ_{Sway} = 0.41 m, σ_{Heave} = 0.09 m, σ_{Roll} = 1.44°, σ_{Pitch} = 0.04°, σ_{Yaw} = 0.02°

Ship motions at centre of gravity (CoG) Depth = 18.0 m, H = 0.25 m, T = 15.60 s Beam-on waves	Monochromatic	M156f
	B3_M156f_50t	
Deltares	11202696	App. G.094-2

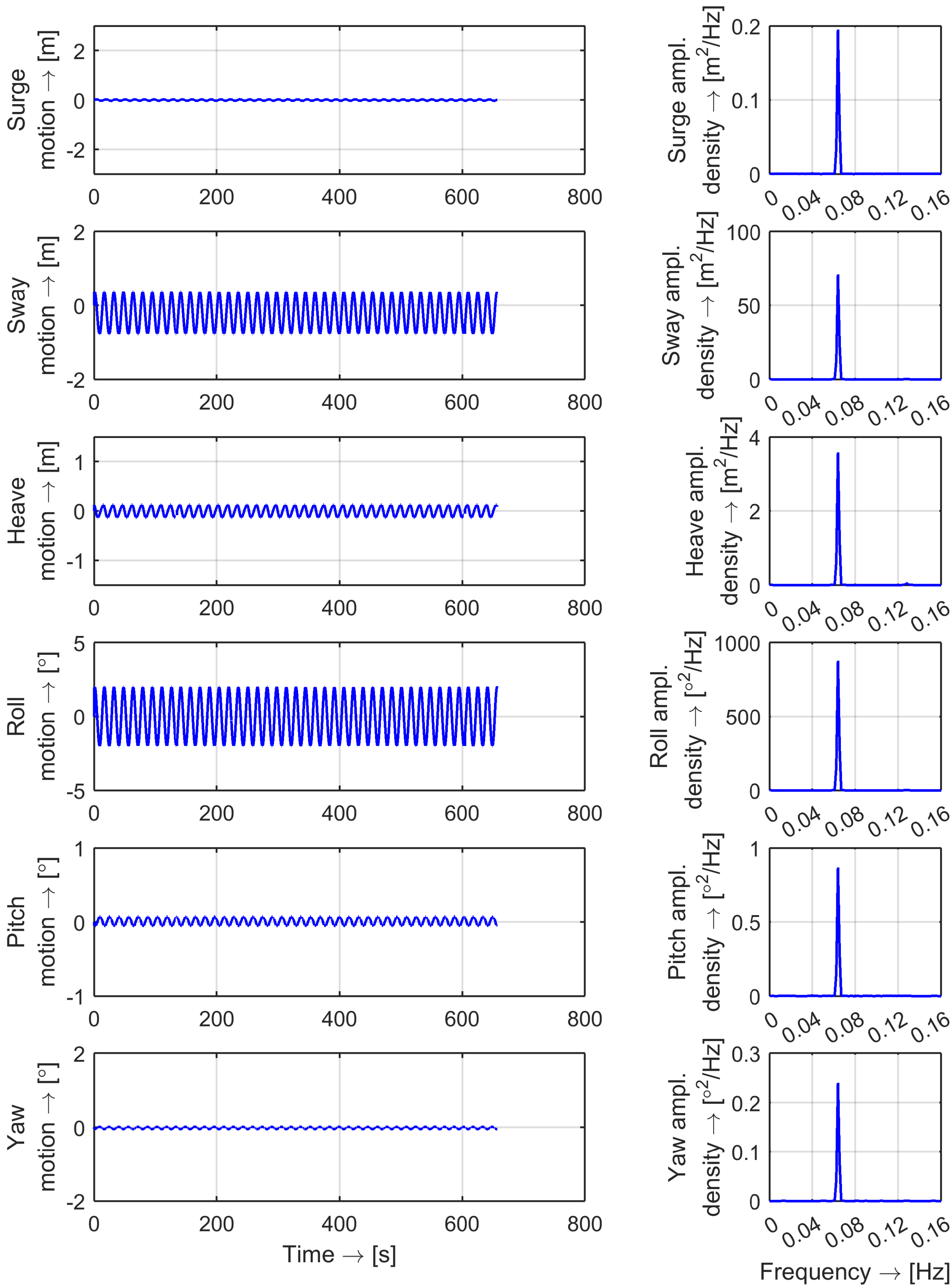

σ_{Surge} = 0.02 m, σ_{Sway} = 0.41 m, σ_{Heave} = 0.09 m, σ_{Roll} = 1.43°, σ_{Pitch} = 0.04°, σ_{Yaw} = 0.02°

Ship motions at centre of gravity (CoG) Depth = 18.0 m, H = 0.25 m, T = 15.60 s Beam-on waves	Monochromatic	M156f
	B3_M156f_200t	
Deltares	11202696	App. G.095-2

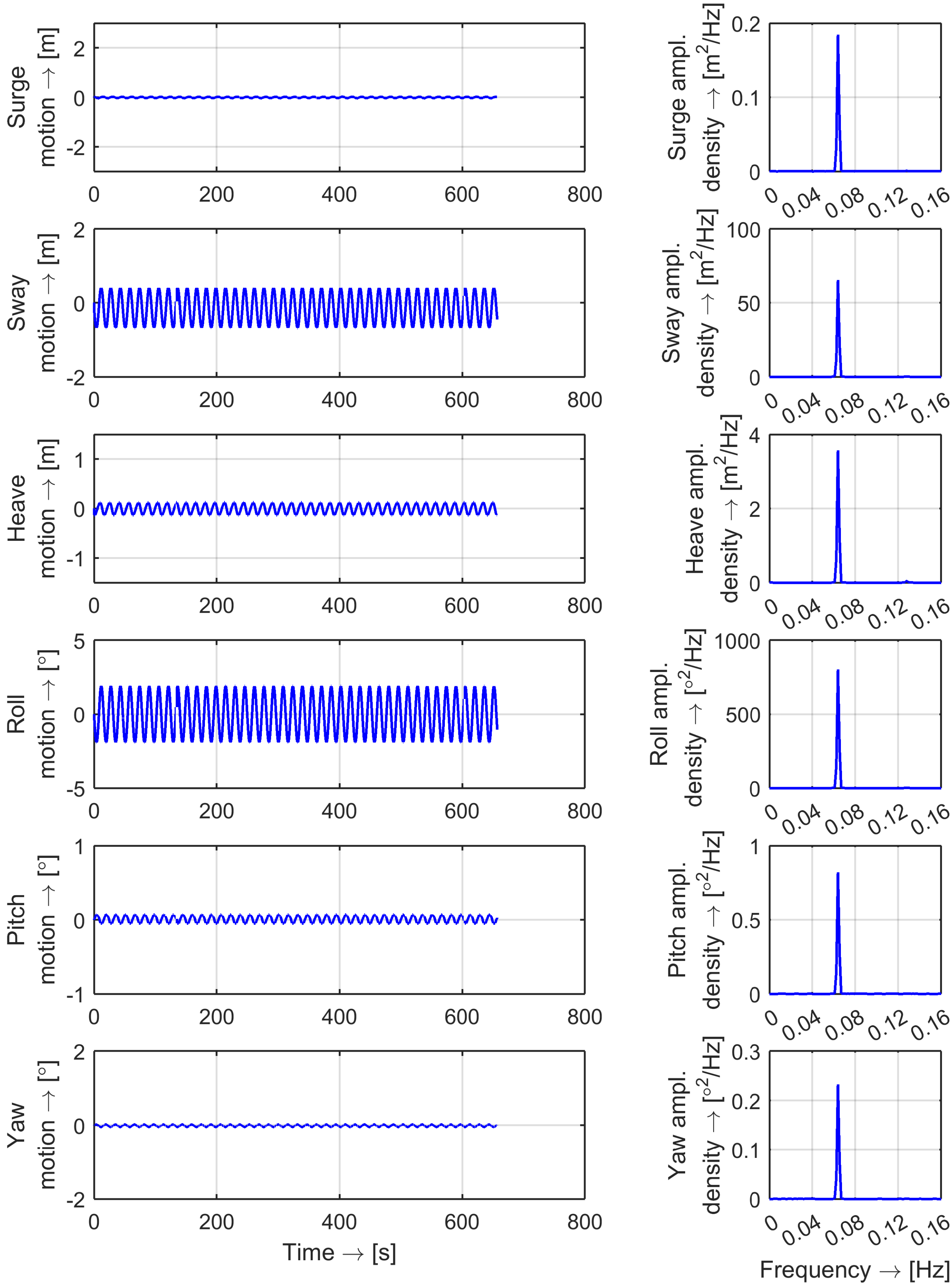

σ_{Surge} = 0.02 m, σ_{Sway} = 0.39 m, σ_{Heave} = 0.09 m, σ_{Roll} = 1.36°, σ_{Pitch} = 0.04°, σ_{Yaw} = 0.02°

Ship motions at centre of gravity (CoG) Depth = 18.0 m, H = 0.25 m, T = 15.60 s Beam-on waves	Monochromatic	M156f
	B3_M156f_sga	
Deltares	11202696	App. G.096-2

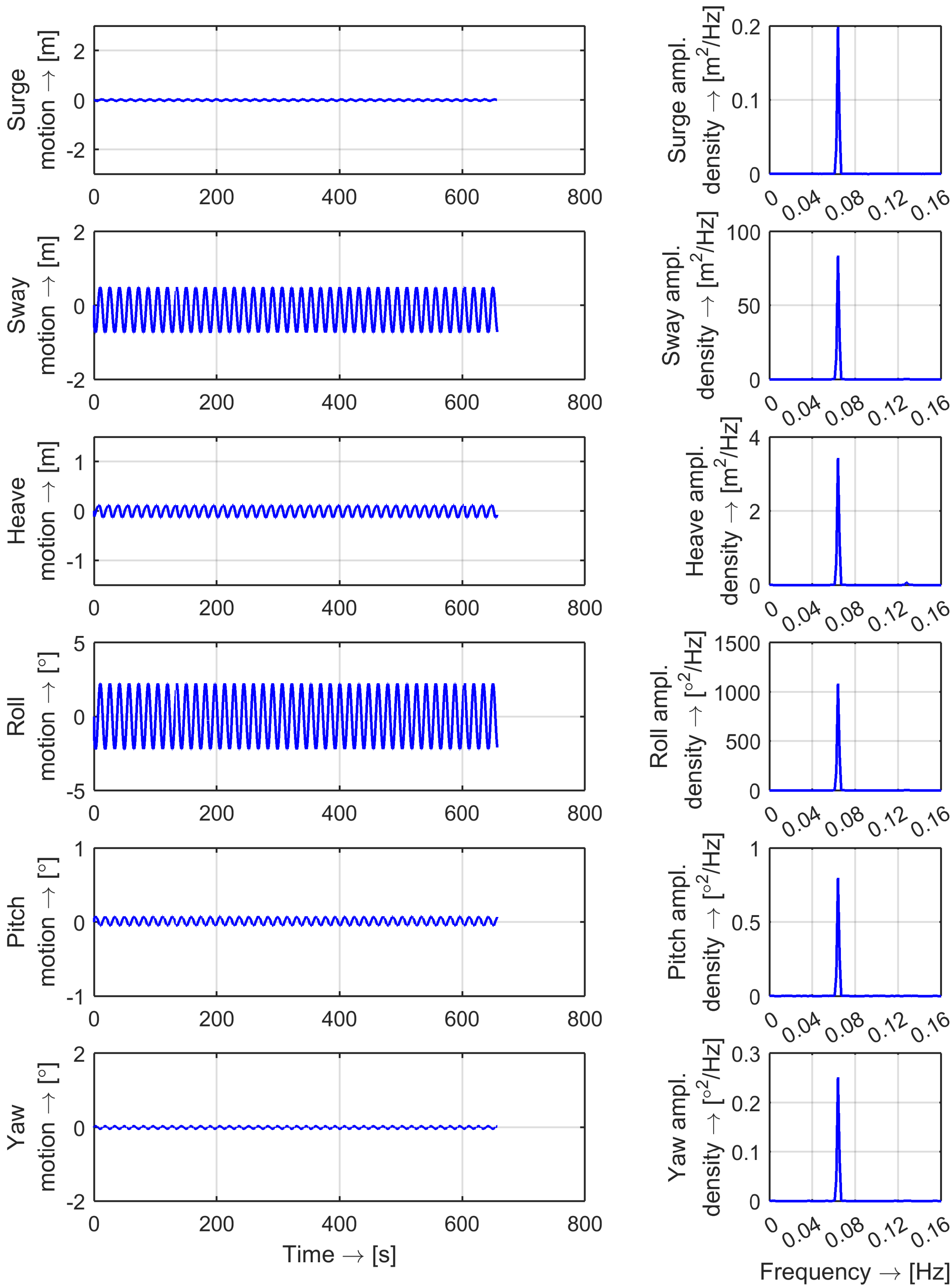

σ_{Surge} = 0.02 m, σ_{Sway} = 0.44 m, σ_{Heave} = 0.09 m, σ_{Roll} = 1.59°, σ_{Pitch} = 0.04°, σ_{Yaw} = 0.02°

Ship motions at centre of gravity (CoG) Depth = 18.0 m, H = 0.25 m, T = 15.60 s Beam-on waves	Monochromatic	M156f
	B3_M156f_sk	
Deltares	11202696	App. G.097-2

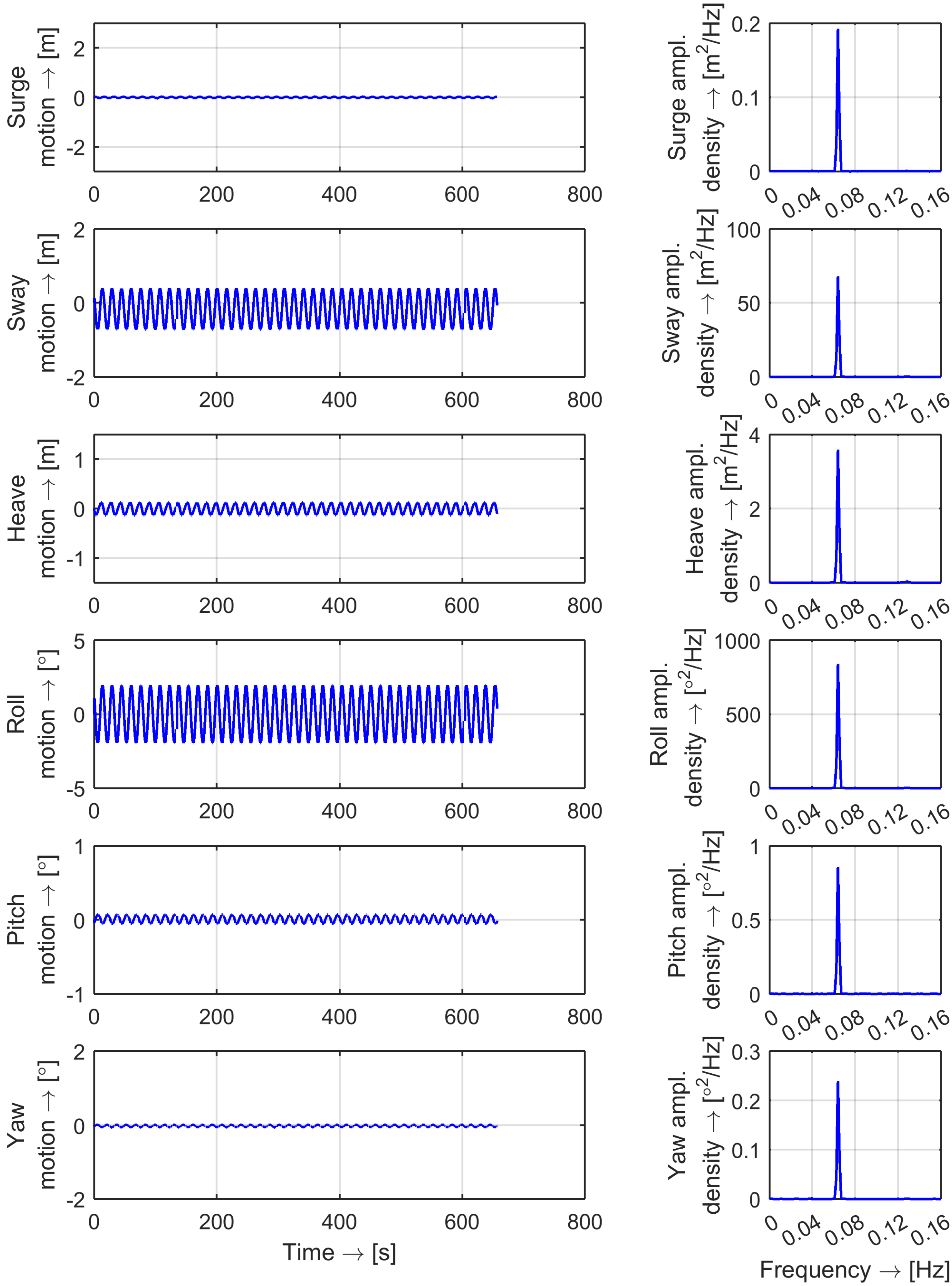

σ_{Surge} = 0.02 m, σ_{Sway} = 0.40 m, σ_{Heave} = 0.09 m, σ_{Roll} = 1.39°, σ_{Pitch} = 0.04°, σ_{Yaw} = 0.02°

Ship motions at centre of gravity (CoG) Depth = 18.0 m, H = 0.25 m, T = 15.60 s Beam-on waves	Monochromatic	M156f
	B3_M156f_ssk	
Deltares	11202696	App. G.098-2

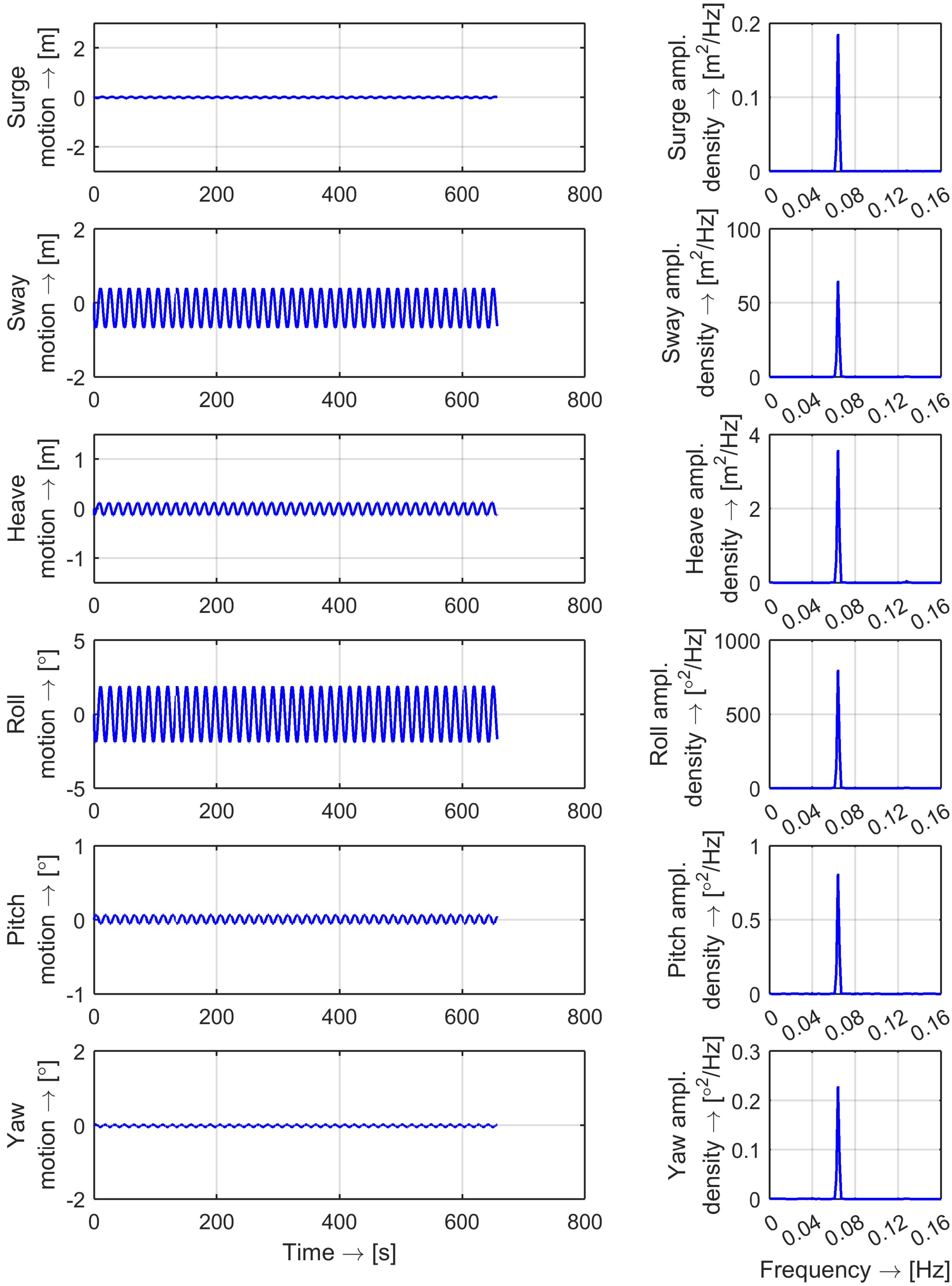

σ_{Surge} = 0.02 m, σ_{Sway} = 0.39 m, σ_{Heave} = 0.09 m, σ_{Roll} = 1.36°, σ_{Pitch} = 0.04°, σ_{Yaw} = 0.02°

Ship motions at centre of gravity (CoG) Depth = 18.0 m, H = 0.25 m, T = 15.60 s Beam-on waves	Monochromatic	M156f
	B3_M156f_ssk_sga	
Deltares	11202696	App. G.099-2

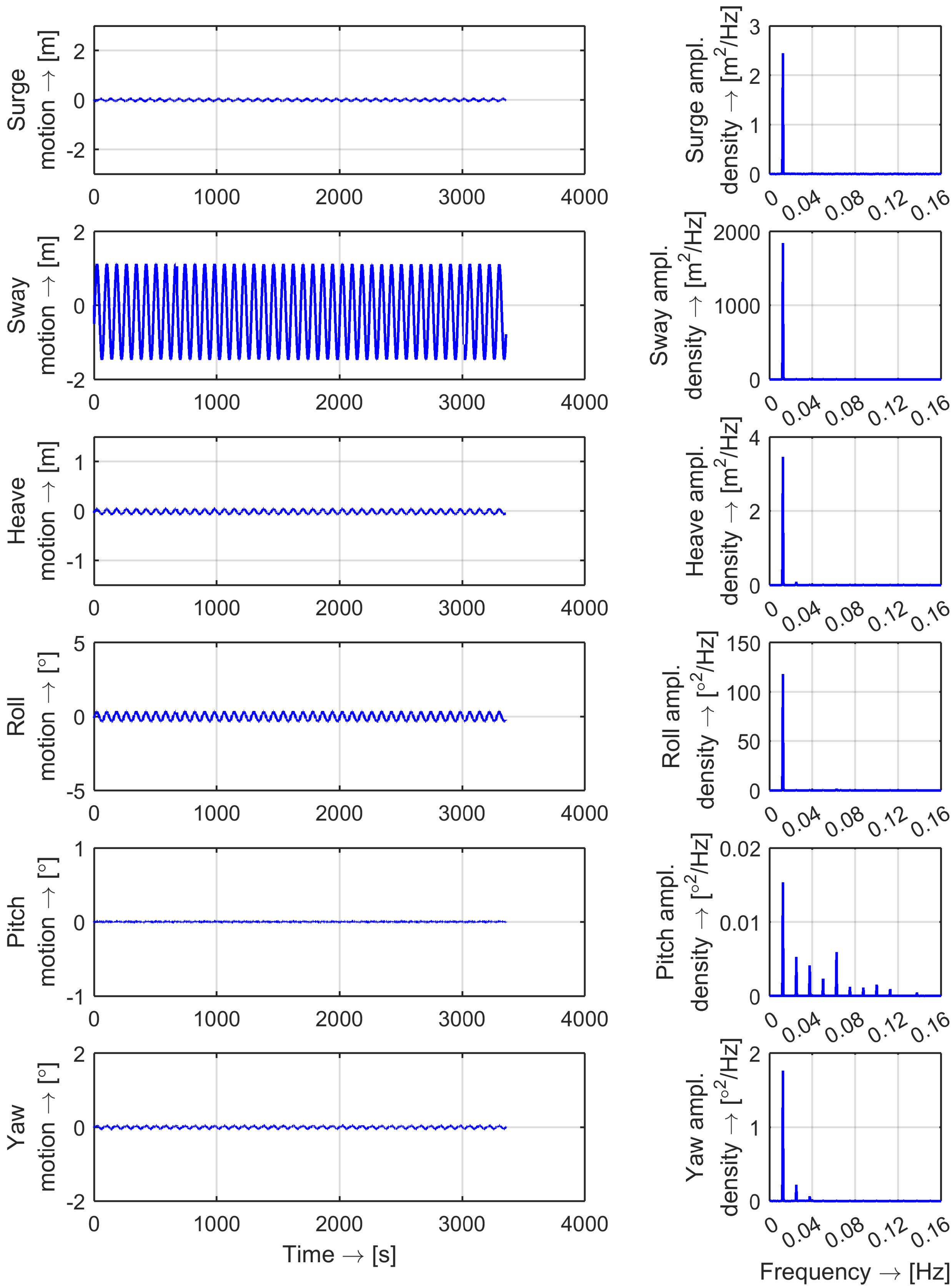

σ_{Surge} = 0.03 m, σ_{Sway} = 0.91 m, σ_{Heave} = 0.04 m, σ_{Roll} = 0.23°, σ_{Pitch} = 0.00°, σ_{Yaw} = 0.03°

Ship motions at centre of gravity (CoG) Depth = 18.0 m, H = 0.09 m, T = 80.00 s Beam-on waves	Monochromatic	M800d
	B3_M800d_sk	
Deltares	11202696	App. G.100-2

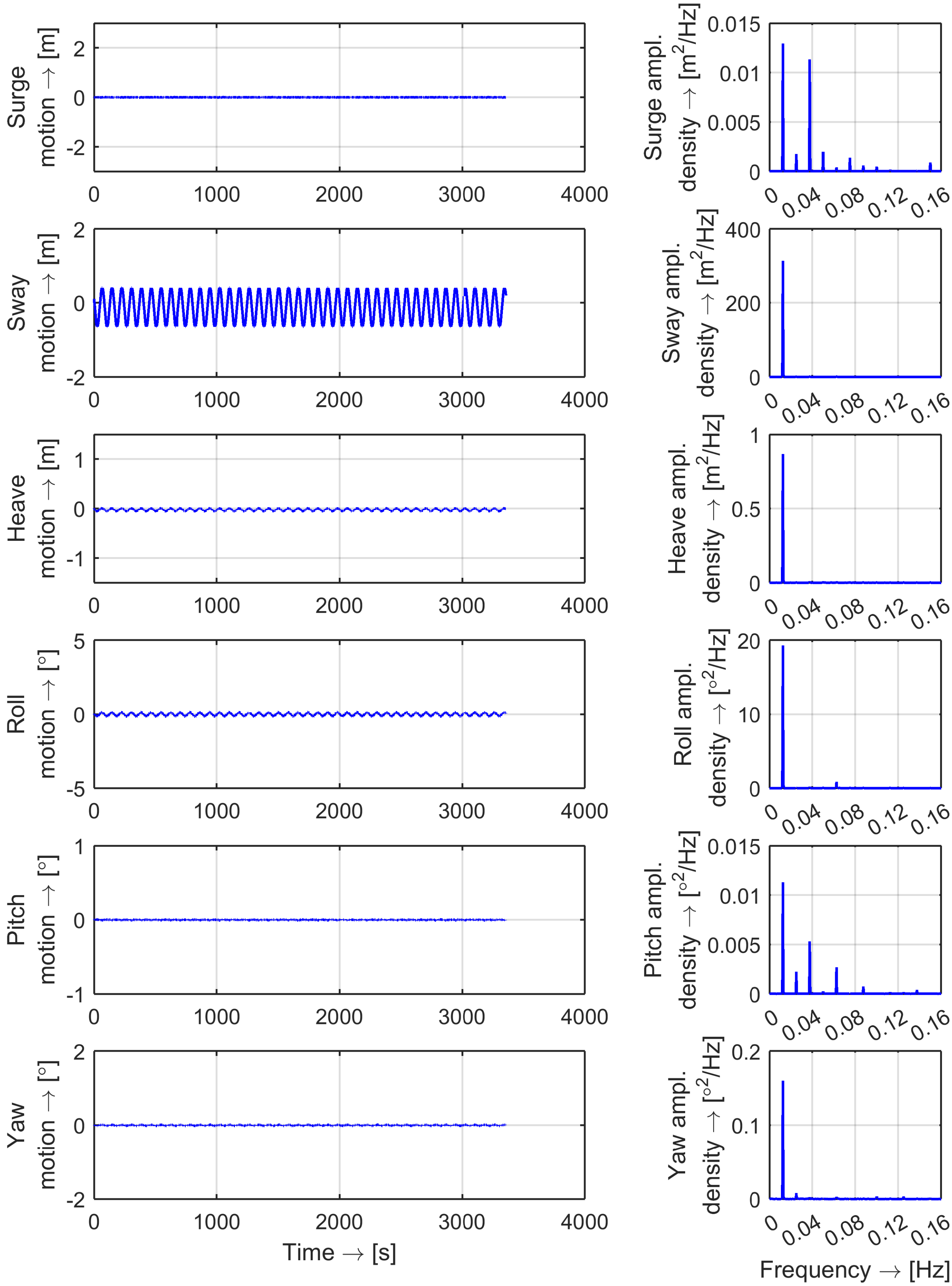

σ_{Surge} = 0.00 m, σ_{Sway} = 0.37 m, σ_{Heave} = 0.02 m, σ_{Roll} = 0.10°, σ_{Pitch} = 0.00°, σ_{Yaw} = 0.01°

Ship motions at centre of gravity (CoG) Depth = 18.0 m, H = 0.05 m, T = 80.00 s Beam-on waves	Monochromatic	M800e
	B3_M800e_50t	
Deltares	11202696	App. G.101-2

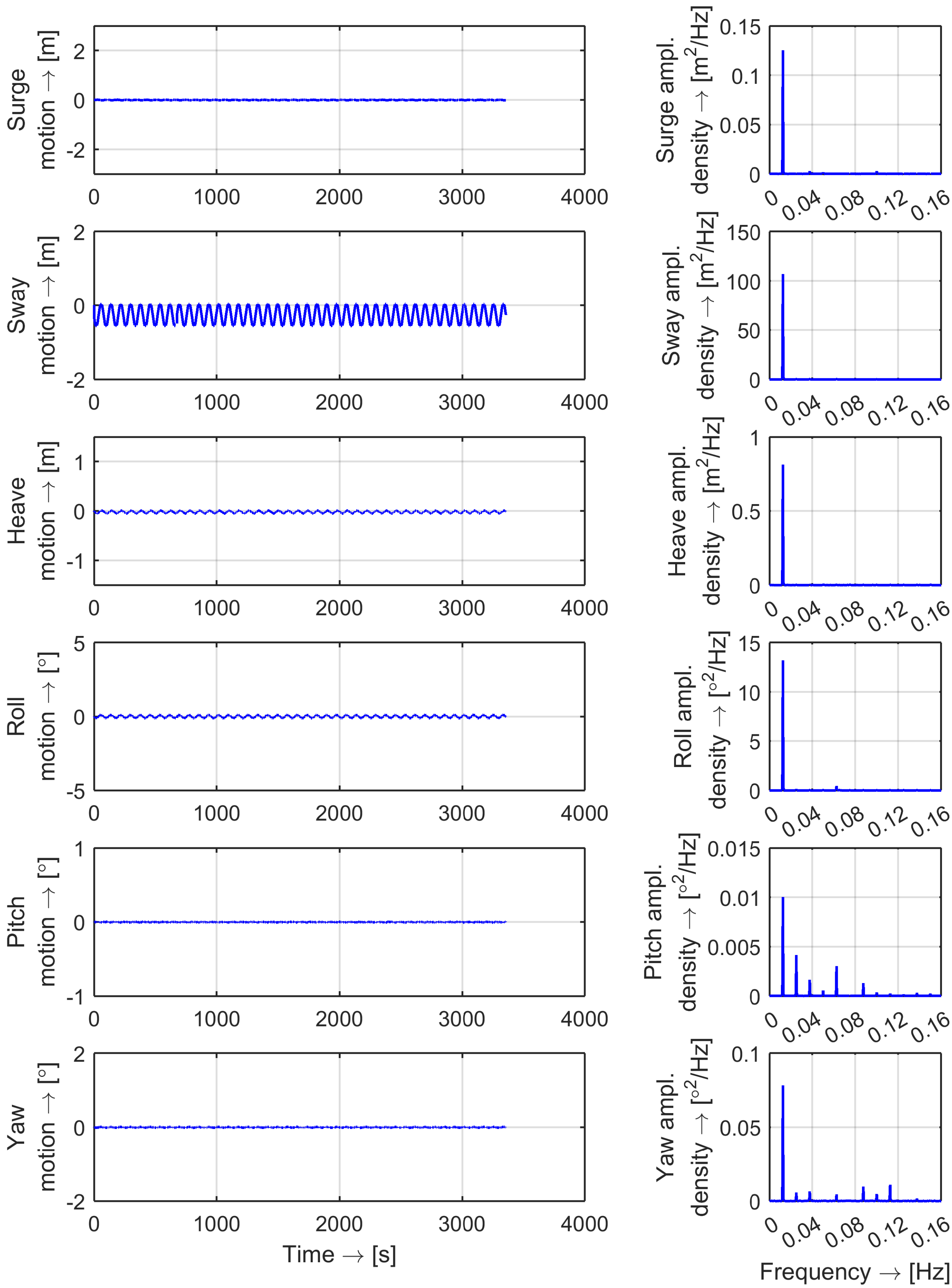

σ_{Surge} = 0.01 m, σ_{Sway} = 0.22 m, σ_{Heave} = 0.02 m, σ_{Roll} = 0.08°, σ_{Pitch} = 0.00°, σ_{Yaw} = 0.01°

Ship motions at centre of gravity (CoG) Depth = 18.0 m, H = 0.05 m, T = 80.00 s Beam-on waves	Monochromatic	M800e
	B3_M800e_200t	
Deltares	11202696	App. G.102-2

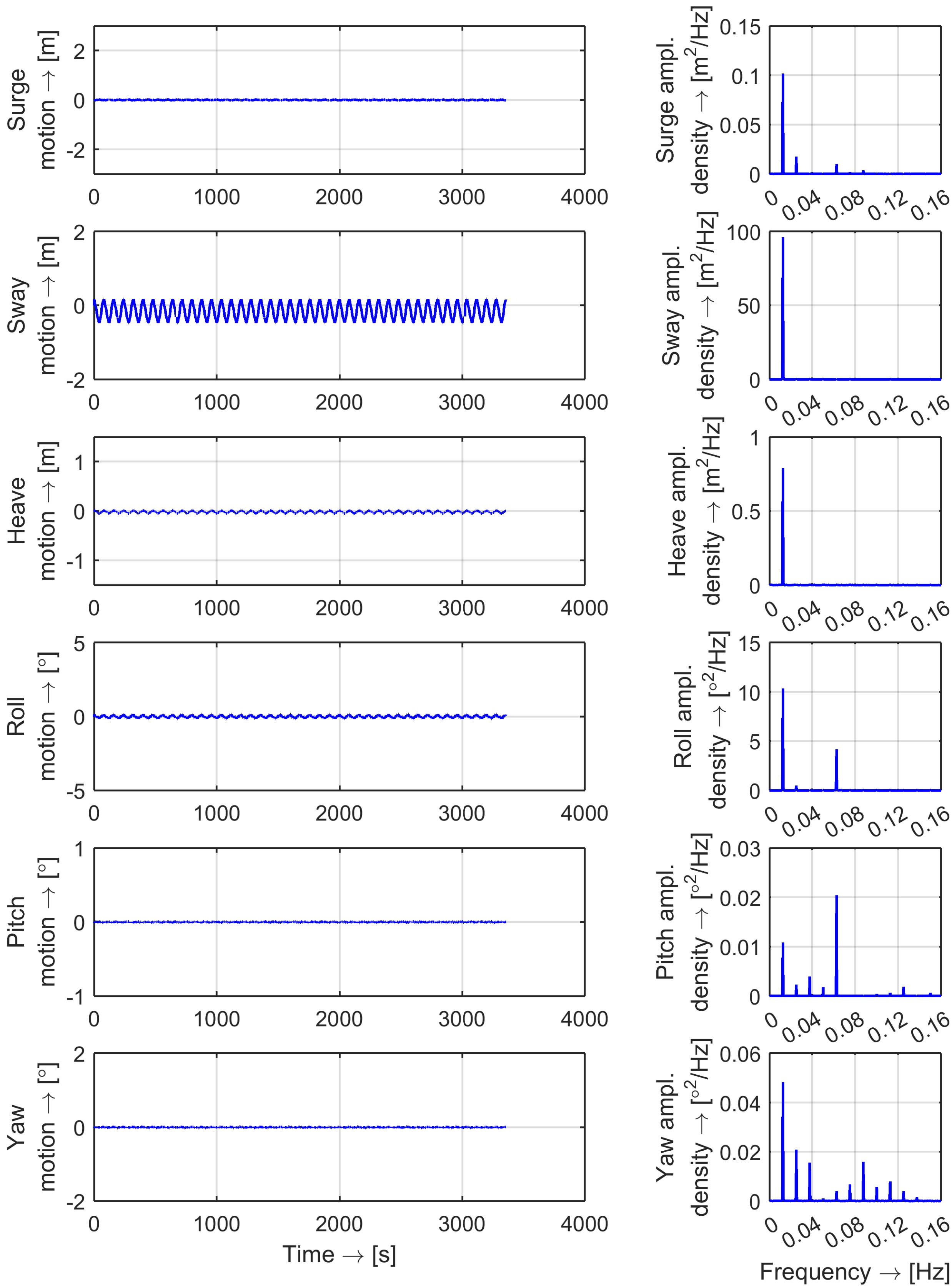

σ_{Surge} = 0.01 m, σ_{Sway} = 0.21 m, σ_{Heave} = 0.02 m, σ_{Roll} = 0.08°, σ_{Pitch} = 0.00°, σ_{Yaw} = 0.01°

Ship motions at centre of gravity (CoG) Depth = 18.0 m, H = 0.05 m, T = 80.00 s Beam-on waves	Monochromatic	M800e
	B3_M800e_sga	
Deltares	11202696	App. G.103-2

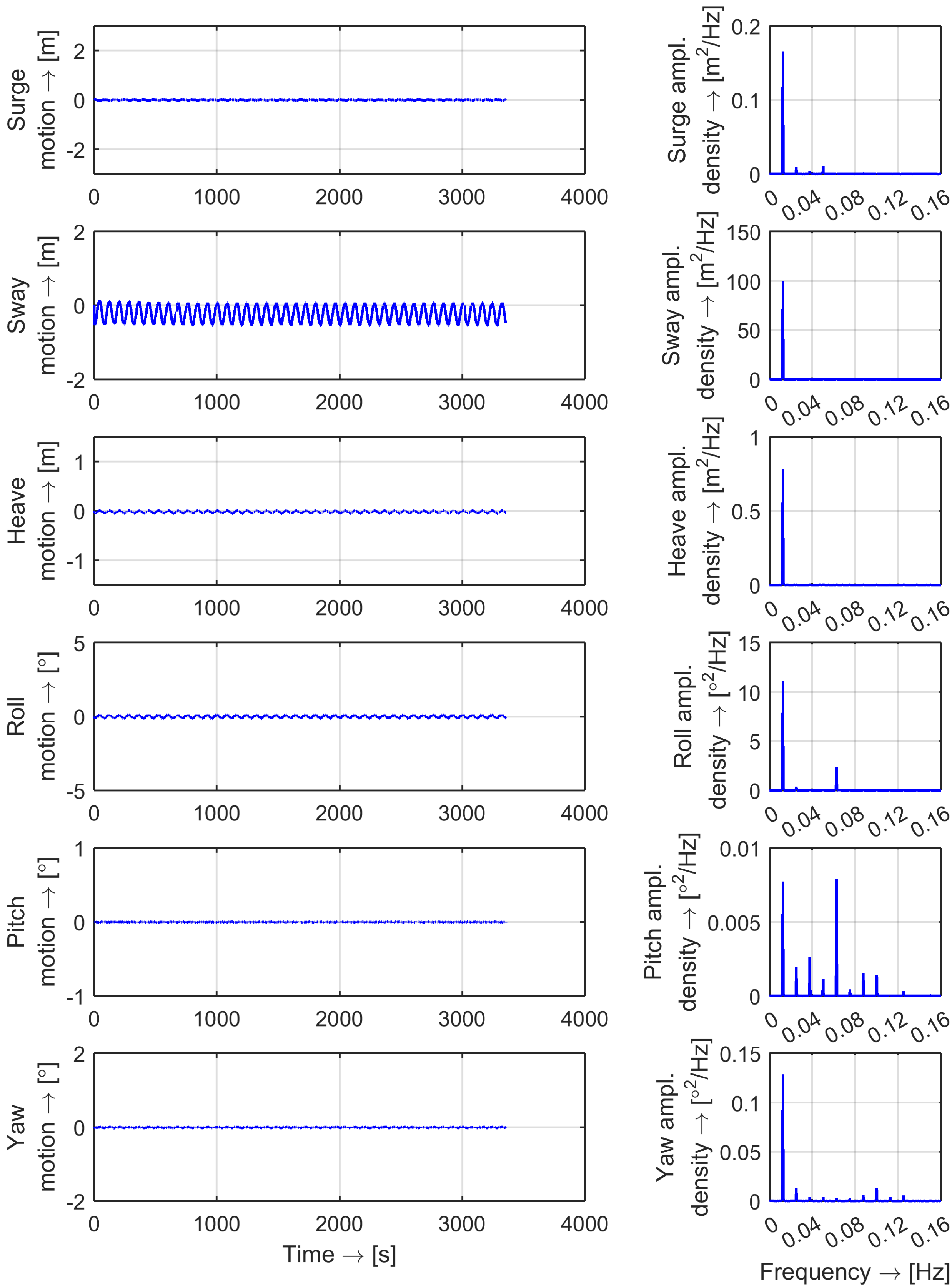

σ_{Surge} = 0.01 m, σ_{Sway} = 0.21 m, σ_{Heave} = 0.02 m, σ_{Roll} = 0.08°, σ_{Pitch} = 0.00°, σ_{Yaw} = 0.01°

Ship motions at centre of gravity (CoG) Depth = 18.0 m, H = 0.05 m, T = 80.00 s Beam-on waves	Monochromatic	M800e
	B3_M800e_ssk	
Deltares	11202696	App. G.104-2

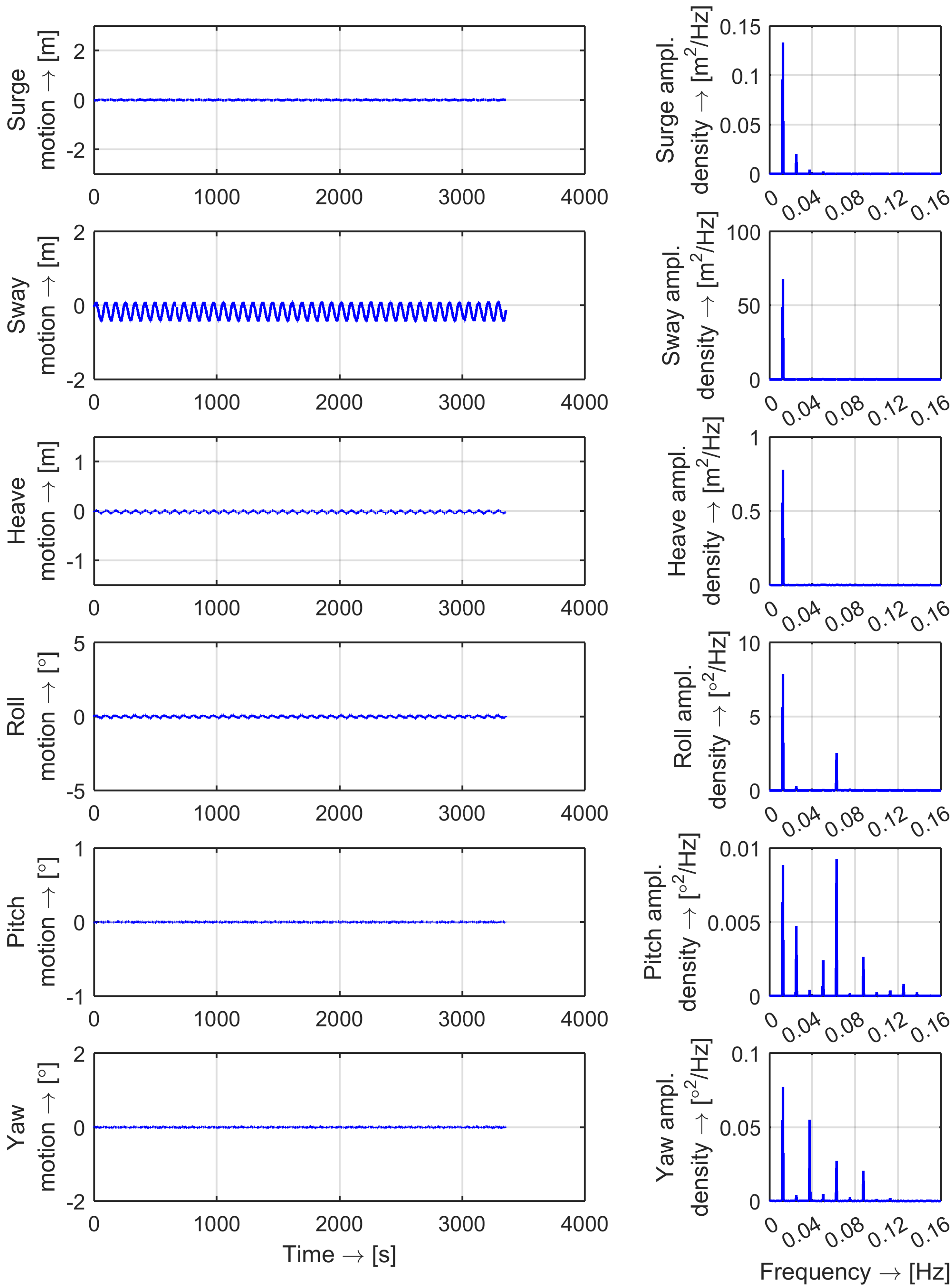

σ_{Surge} = 0.01 m, σ_{Sway} = 0.18 m, σ_{Heave} = 0.02 m, σ_{Roll} = 0.07°, σ_{Pitch} = 0.00°, σ_{Yaw} = 0.01°

Ship motions at centre of gravity (CoG) Depth = 18.0 m, H = 0.05 m, T = 80.00 s Beam-on waves	Monochromatic	M800e
	B3_M800e_ssk_sga	
Deltares	11202696	App. G.105-2

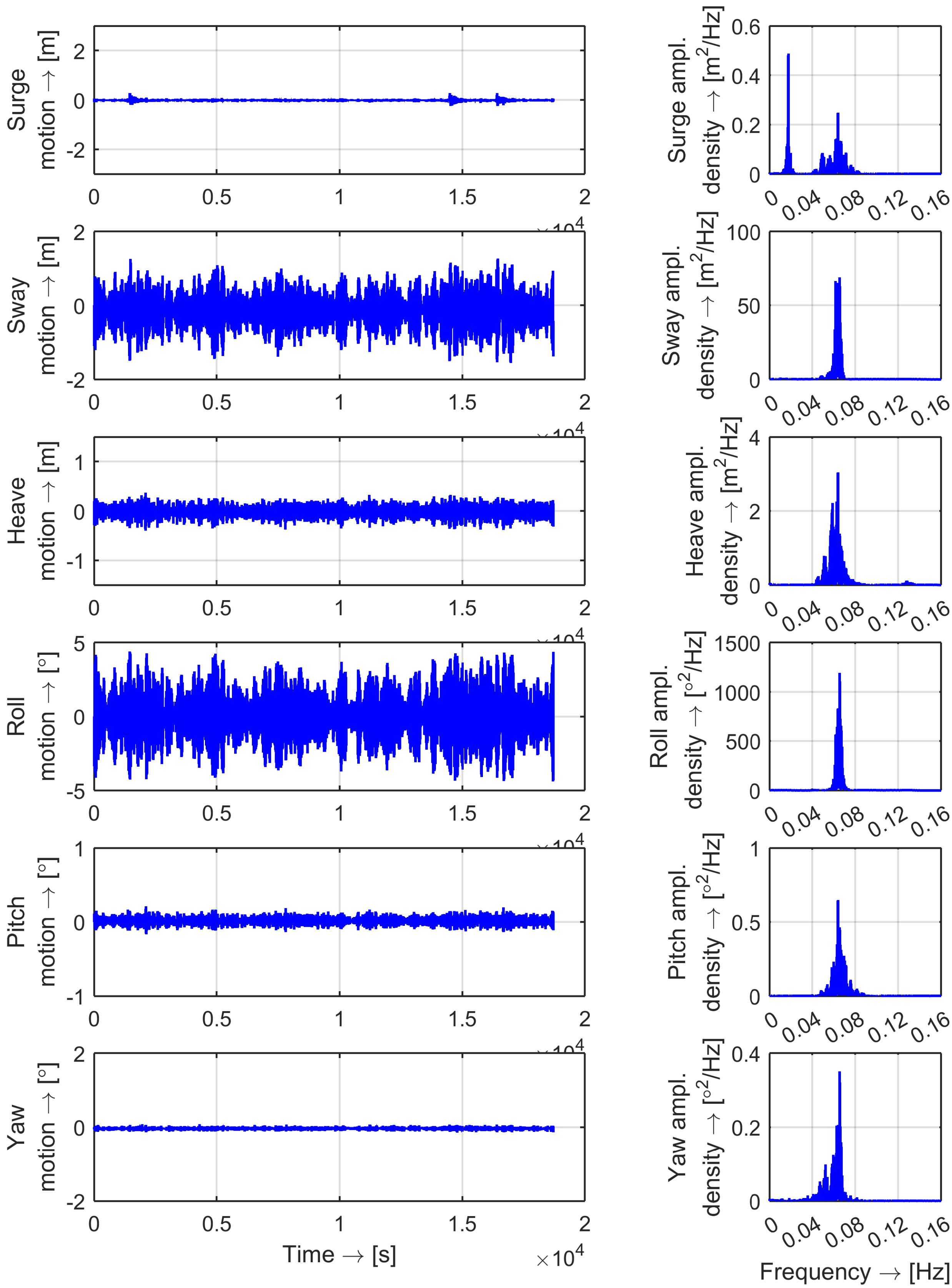

σ_{Surge} = 0.04 m, σ_{Sway} = 0.43 m, σ_{Heave} = 0.11 m, σ_{Roll} = 1.51°, σ_{Pitch} = 0.05°, σ_{Yaw} = 0.03°

Ship motions at centre of gravity (CoG) Depth = 18.0 m, H_{m0} = 0.50 m, T_p = 15.60 s, γ = 5.0 Beam-on waves	Irregular	I156a
	B4_I156a	
Deltares	11202696	App. G.106-2

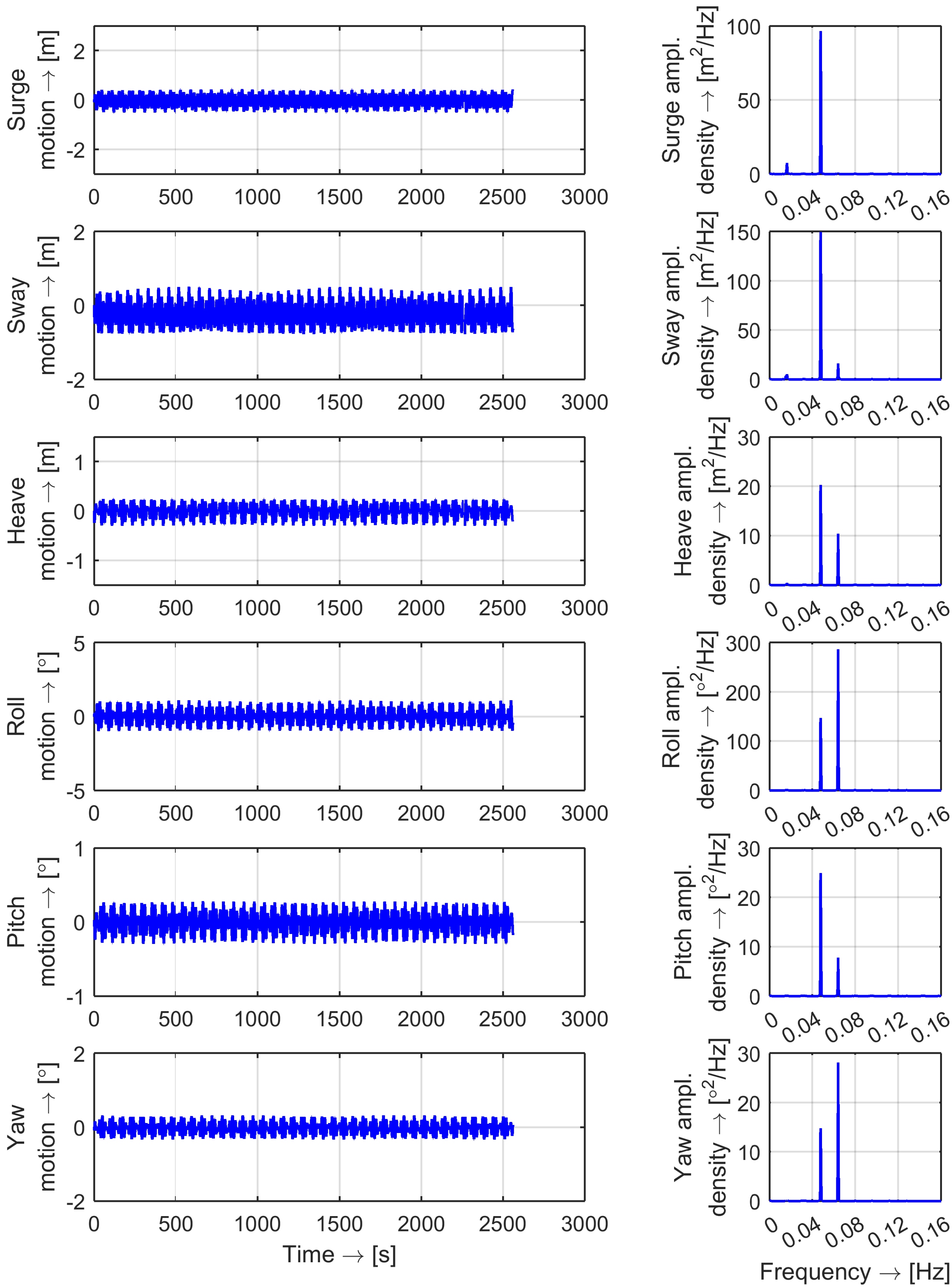

σ_{Surge} = 0.27 m, σ_{Sway} = 0.34 m, σ_{Heave} = 0.14 m, σ_{Roll} = 0.52°, σ_{Pitch} = 0.15°, σ_{Yaw} = 0.16°

Ship motions at centre of gravity (CoG) Depth = 18.0 m, H = 1.00 m, T_1 = 15.60 s, T_2 = 20.96 s Bow-quartering waves	Bichromatic	B610a
	C1_B610a	
Deltares	11202696	App. G.107-2

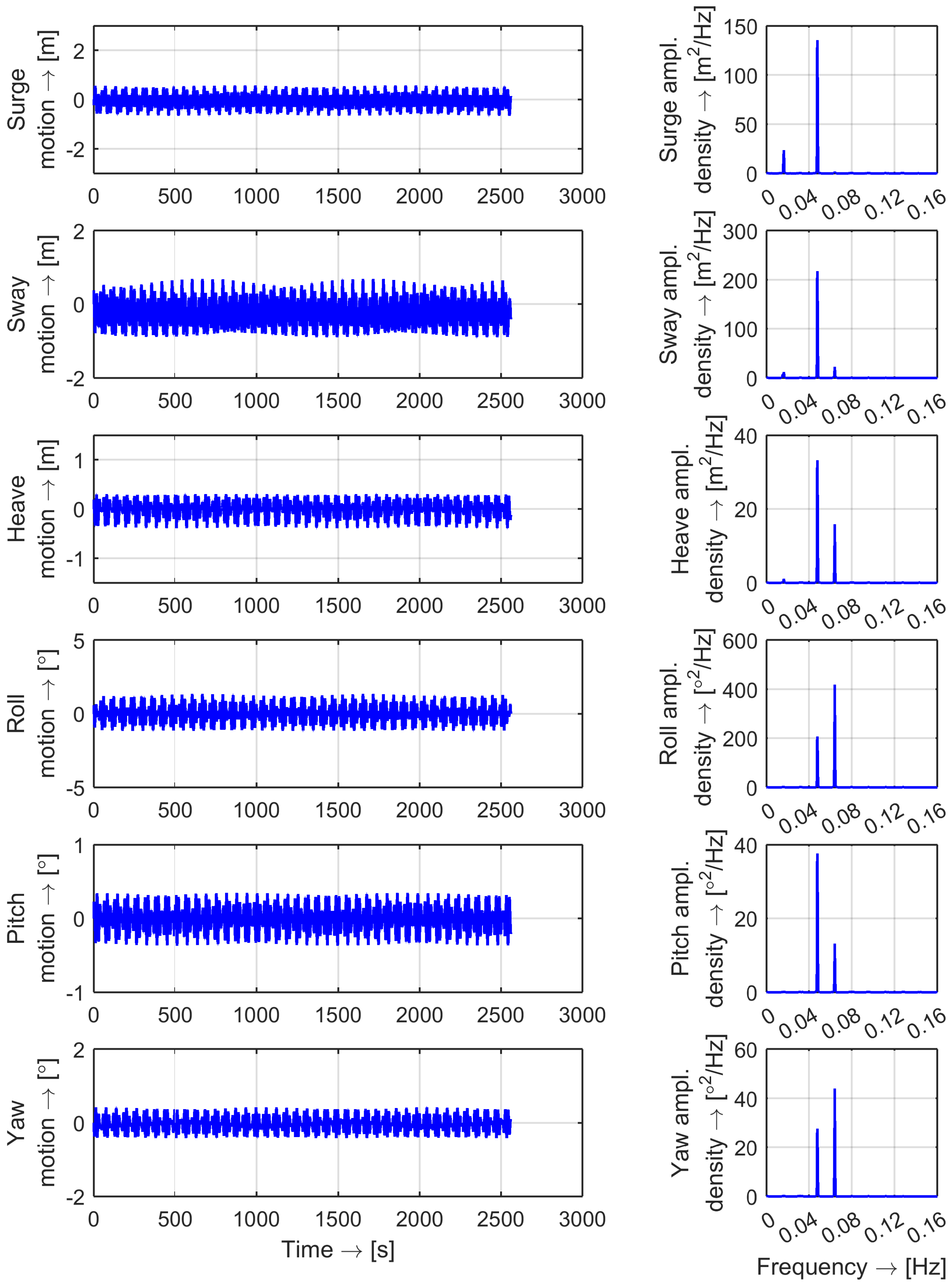

σ_{Surge} = 0.33 m, σ_{Sway} = 0.42 m, σ_{Heave} = 0.18 m, σ_{Roll} = 0.62°, σ_{Pitch} = 0.18°, σ_{Yaw} = 0.21°

Ship motions at centre of gravity (CoG) Depth = 18.0 m, H = 1.25 m, T_1 = 15.60 s, T_2 = 20.96 s Bow-quartering waves	Bichromatic	B610b
	C1_B610b	
Deltares	11202696	App. G.108-2

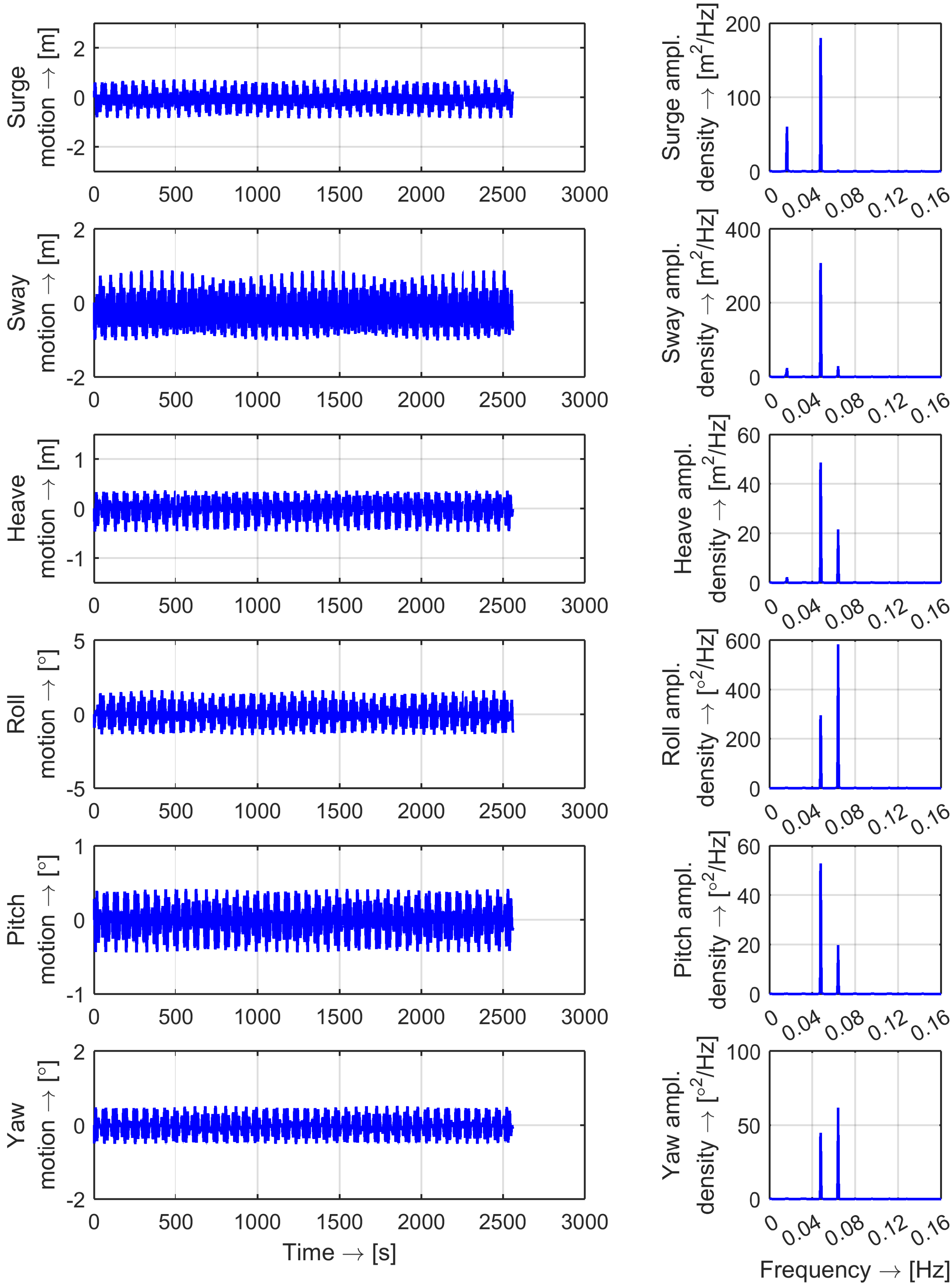

σ_{Surge} = 0.41 m, σ_{Sway} = 0.50 m, σ_{Heave} = 0.22 m, σ_{Roll} = 0.74°, σ_{Pitch} = 0.22°, σ_{Yaw} = 0.26°

Ship motions at centre of gravity (CoG) Depth = 18.0 m, H = 1.50 m, T_1 = 15.60 s, T_2 = 20.96 s Bow-quartering waves	Bichromatic	B610c
	C1_B610c	
Deltares	11202696	App. G.109-2

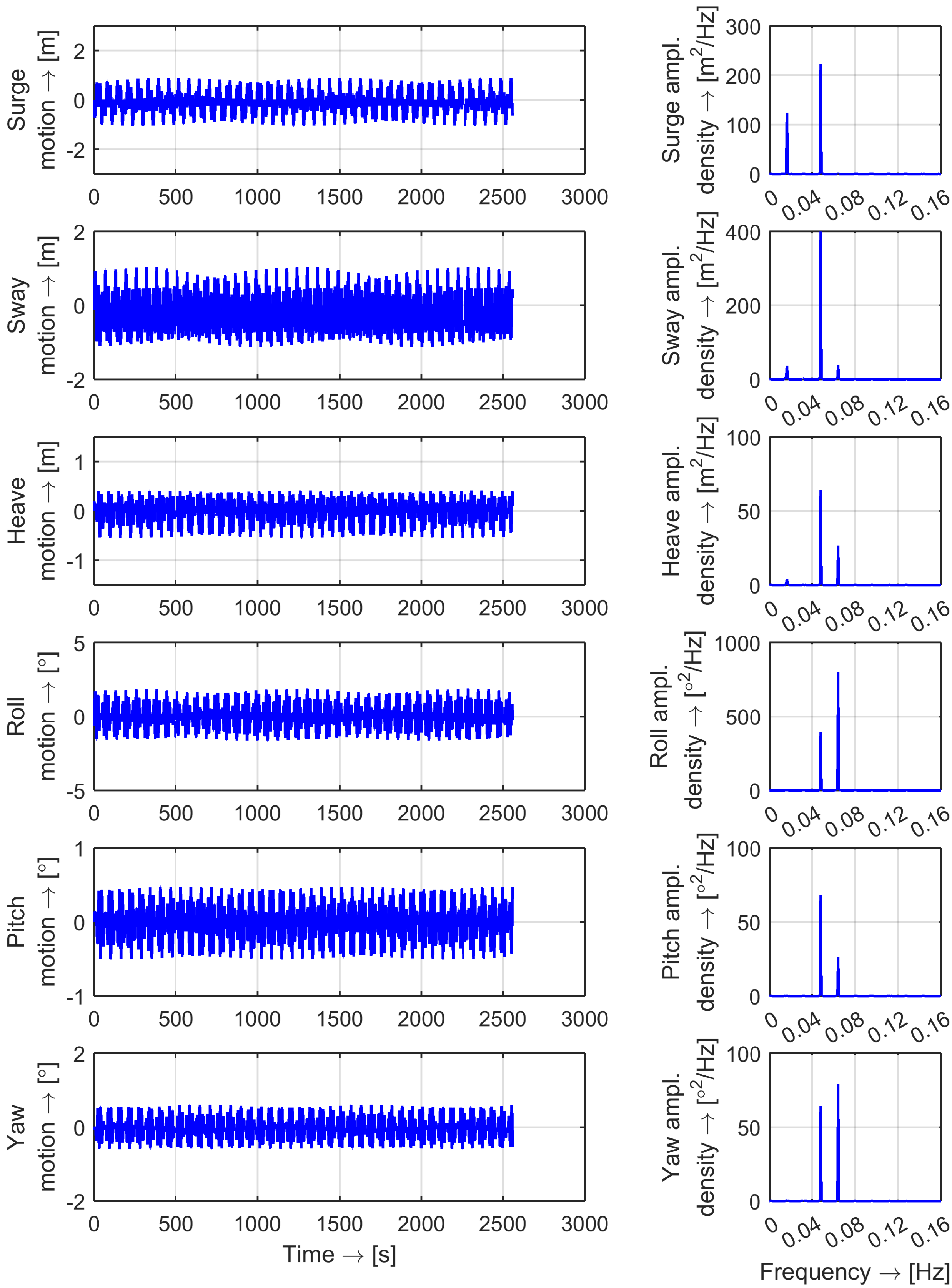

σ_{Surge} = 0.49 m, σ_{Sway} = 0.57 m, σ_{Heave} = 0.25 m, σ_{Roll} = 0.87°, σ_{Pitch} = 0.25°, σ_{Yaw} = 0.30°

Ship motions at centre of gravity (CoG) Depth = 18.0 m, H = 1.75 m, T_1 = 15.60 s, T_2 = 20.96 s Bow-quartering waves	Bichromatic	B610d
	C1_B610d	
Deltares	11202696	App. G.110-2

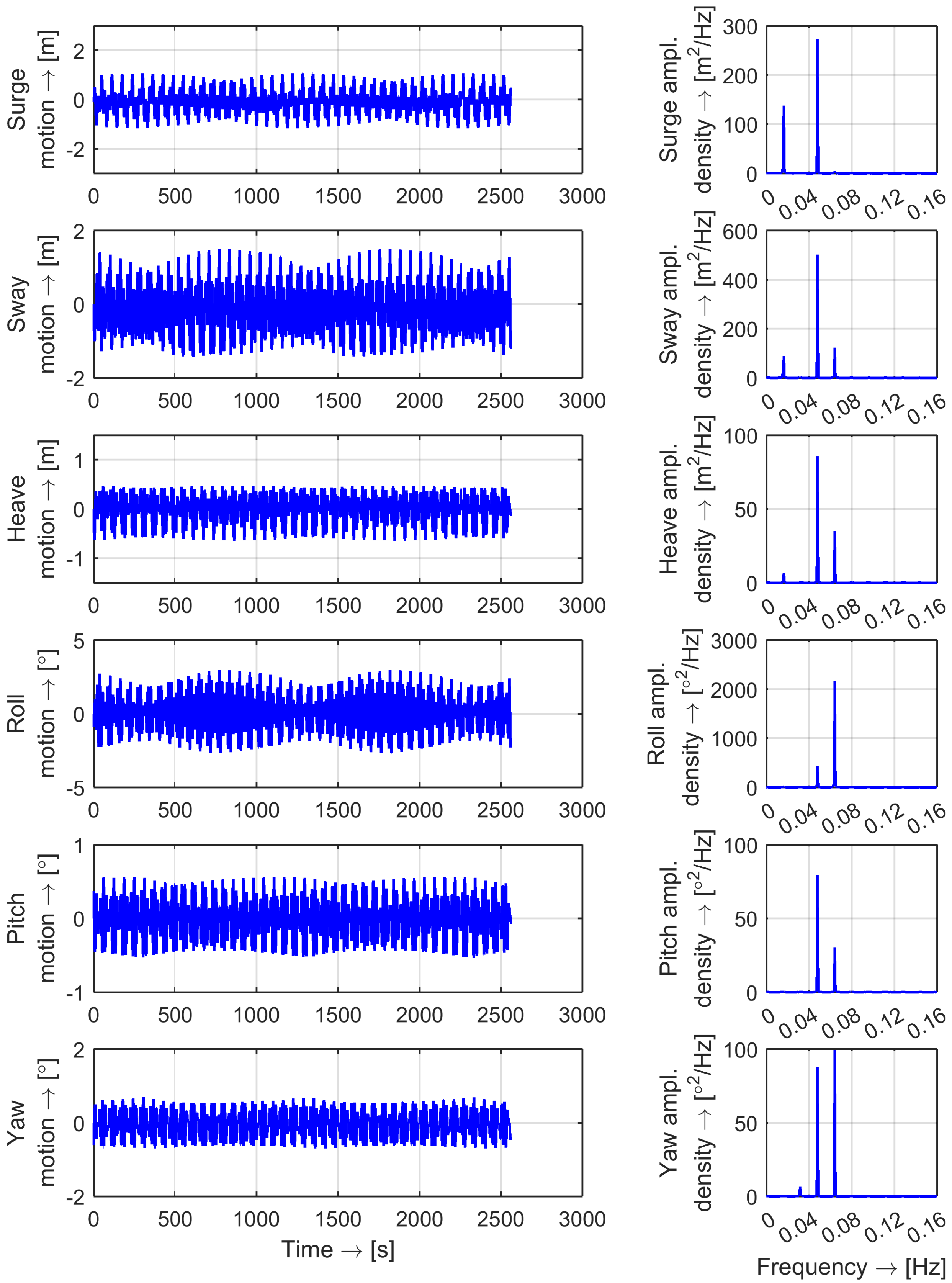

σ_{Surge} = 0.55 m, σ_{Sway} = 0.70 m, σ_{Heave} = 0.29 m, σ_{Roll} = 1.27°, σ_{Pitch} = 0.27°, σ_{Yaw} = 0.35°

Ship motions at centre of gravity (CoG) Depth = 18.0 m, H = 2.00 m, T_1 = 15.60 s, T_2 = 20.96 s Bow-quartering waves	Bichromatic	B610e
	C1_B610e	
Deltares	11202696	App. G.111-2

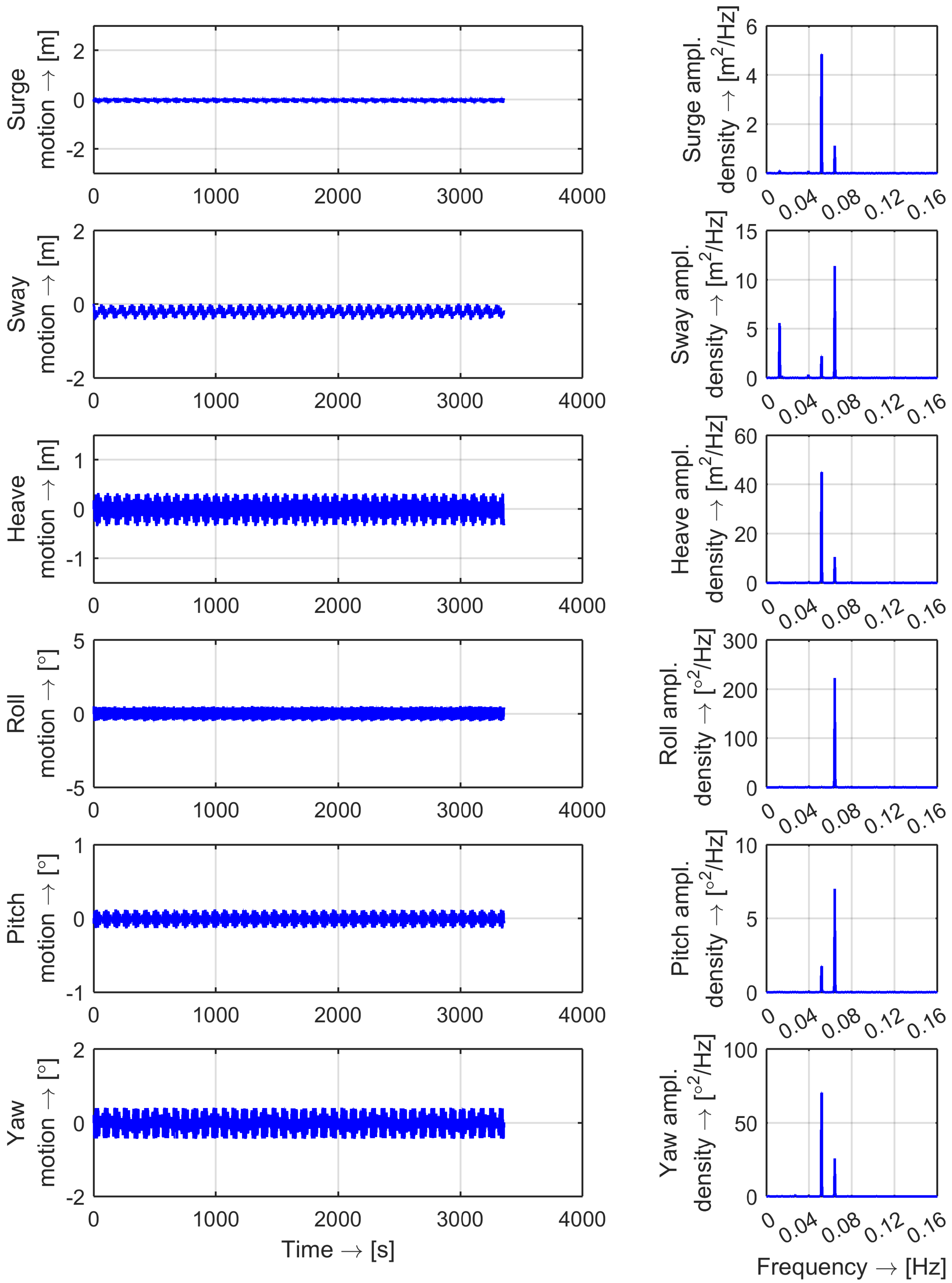

σ_{Surge} = 0.06 m, σ_{Sway} = 0.10 m, σ_{Heave} = 0.18 m, σ_{Roll} = 0.32°, σ_{Pitch} = 0.07°, σ_{Yaw} = 0.24°

Ship motions at centre of gravity (CoG) Depth = 18.0 m, H = 1.00 m, T_1 = 15.60 s, T_2 = 19.38 s Bow-quartering waves	Bichromatic	B800a
	C1_B800a	
Deltares	11202696	App. G.112-2

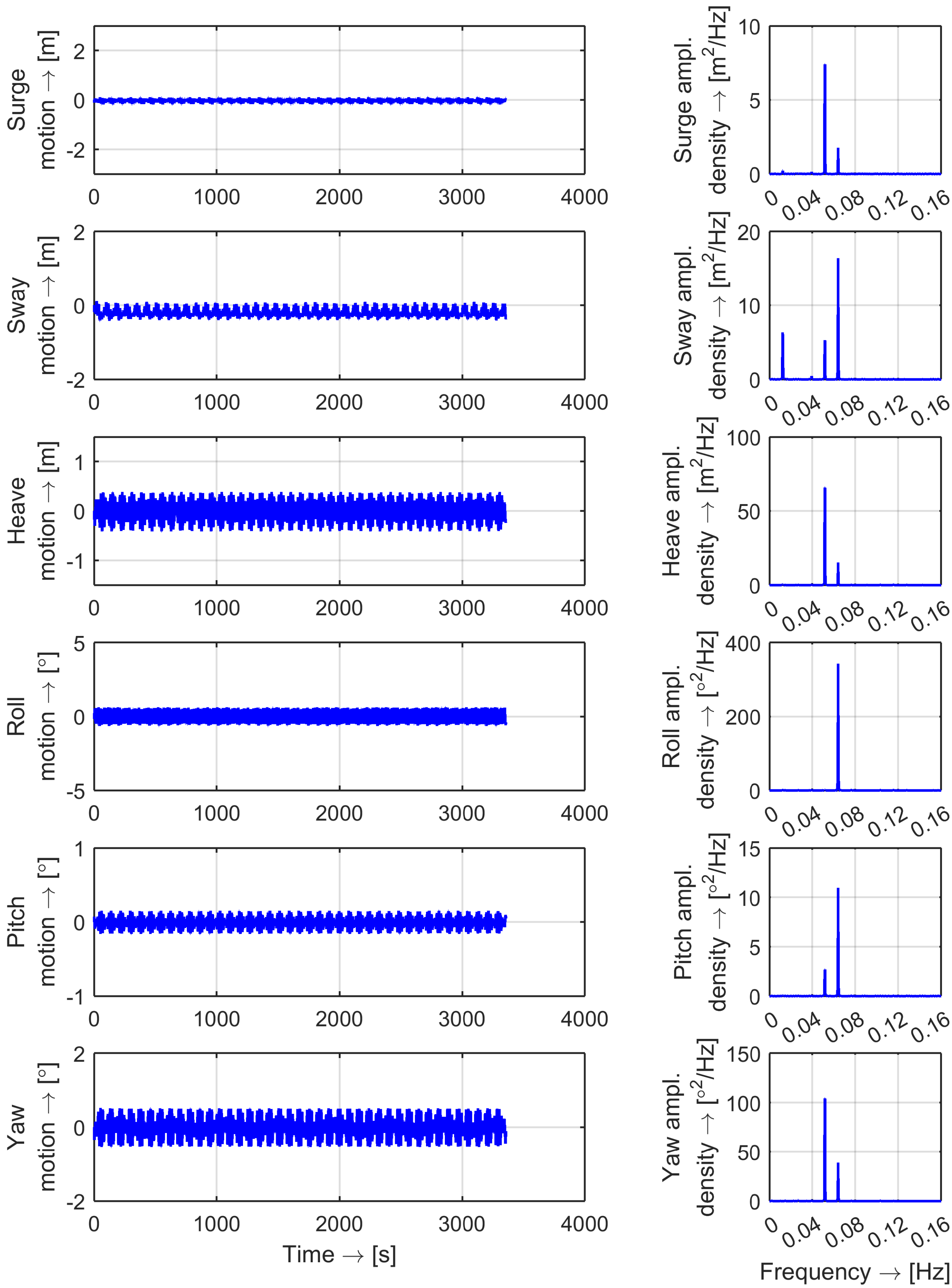

σ_{Surge} = 0.08 m, σ_{Sway} = 0.12 m, σ_{Heave} = 0.22 m, σ_{Roll} = 0.39°, σ_{Pitch} = 0.08°, σ_{Yaw} = 0.29°

Ship motions at centre of gravity (CoG) Depth = 18.0 m, H = 1.25 m, T_1 = 15.60 s, T_2 = 19.38 s Bow-quartering waves	Bichromatic	B800b
	C1_B800b	
Deltares	11202696	App. G.113-2

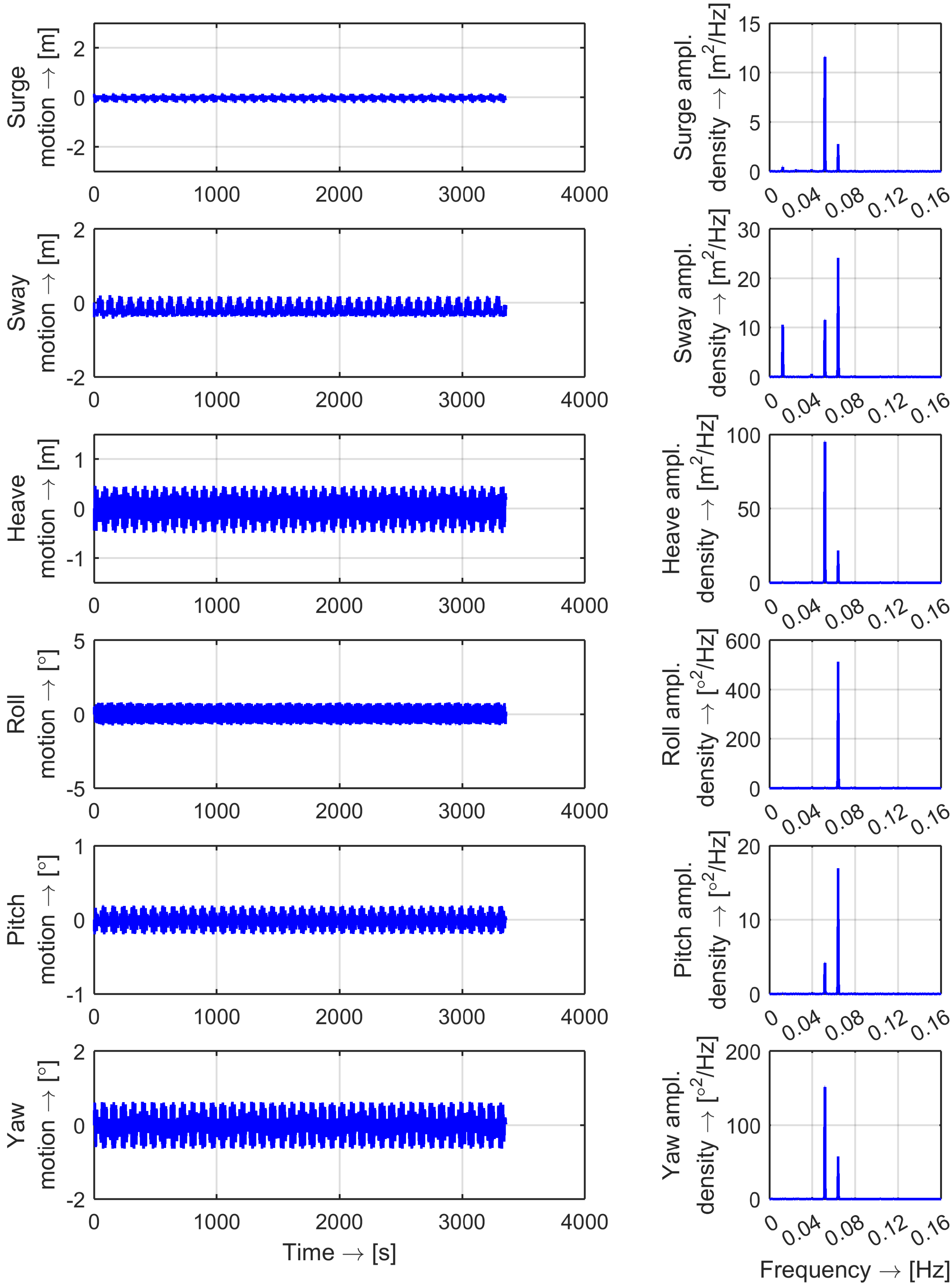

σ_{Surge} = 0.09 m, σ_{Sway} = 0.16 m, σ_{Heave} = 0.26 m, σ_{Roll} = 0.48°, σ_{Pitch} = 0.10°, σ_{Yaw} = 0.35°

Ship motions at centre of gravity (CoG) Depth = 18.0 m, H = 1.50 m, T_1 = 15.60 s, T_2 = 19.38 s Bow-quartering waves	Bichromatic	B800c
	C1_B800c	
Deltares	11202696	App. G.114-2

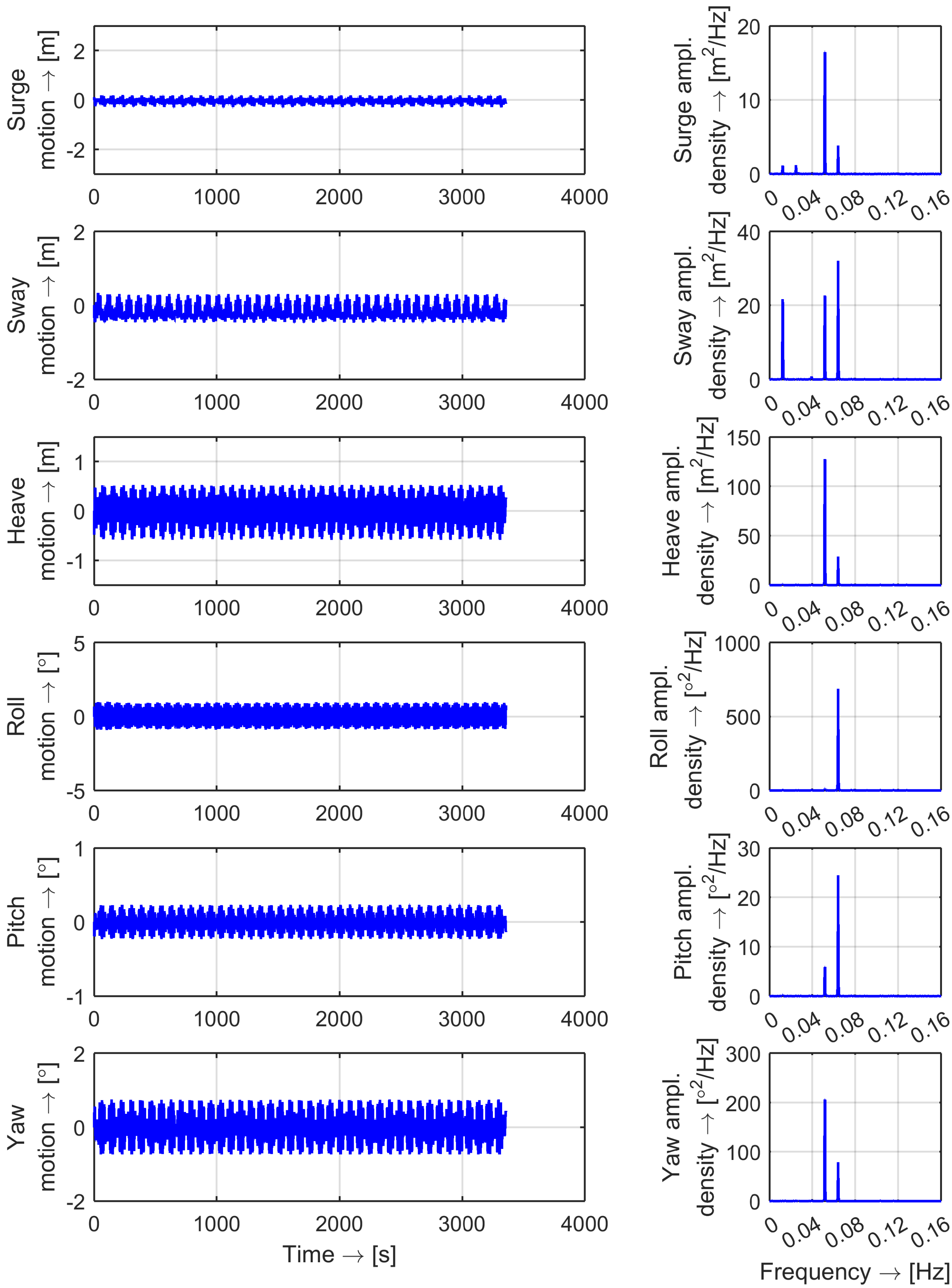

σ_{Surge} = 0.12 m, σ_{Sway} = 0.20 m, σ_{Heave} = 0.30 m, σ_{Roll} = 0.56°, σ_{Pitch} = 0.12°, σ_{Yaw} = 0.40°

Ship motions at centre of gravity (CoG) Depth = 18.0 m, H = 1.75 m, T_1 = 15.60 s, T_2 = 19.38 s Bow-quartering waves	Bichromatic	B800d
	C1_B800d	
Deltares	11202696	App. G.115-2

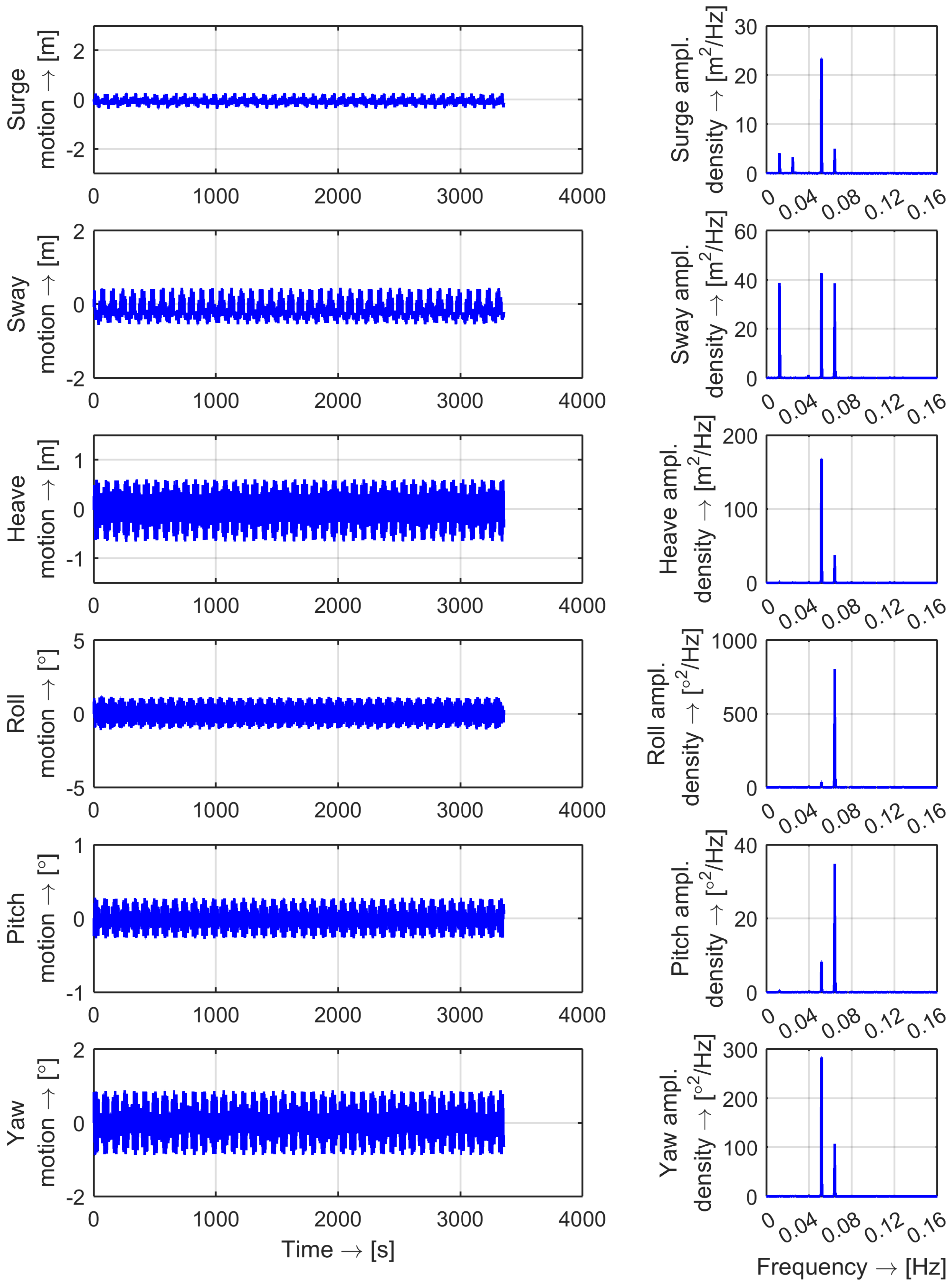

σ_{Surge} = 0.15 m, σ_{Sway} = 0.26 m, σ_{Heave} = 0.35 m, σ_{Roll} = 0.62°, σ_{Pitch} = 0.15°, σ_{Yaw} = 0.47°

Ship motions at centre of gravity (CoG) Depth = 18.0 m, H = 2.00 m, T_1 = 15.60 s, T_2 = 19.38 s Bow-quartering waves	Bichromatic	B800e
	C1_B800e	
Deltares	11202696	App. G.116-2

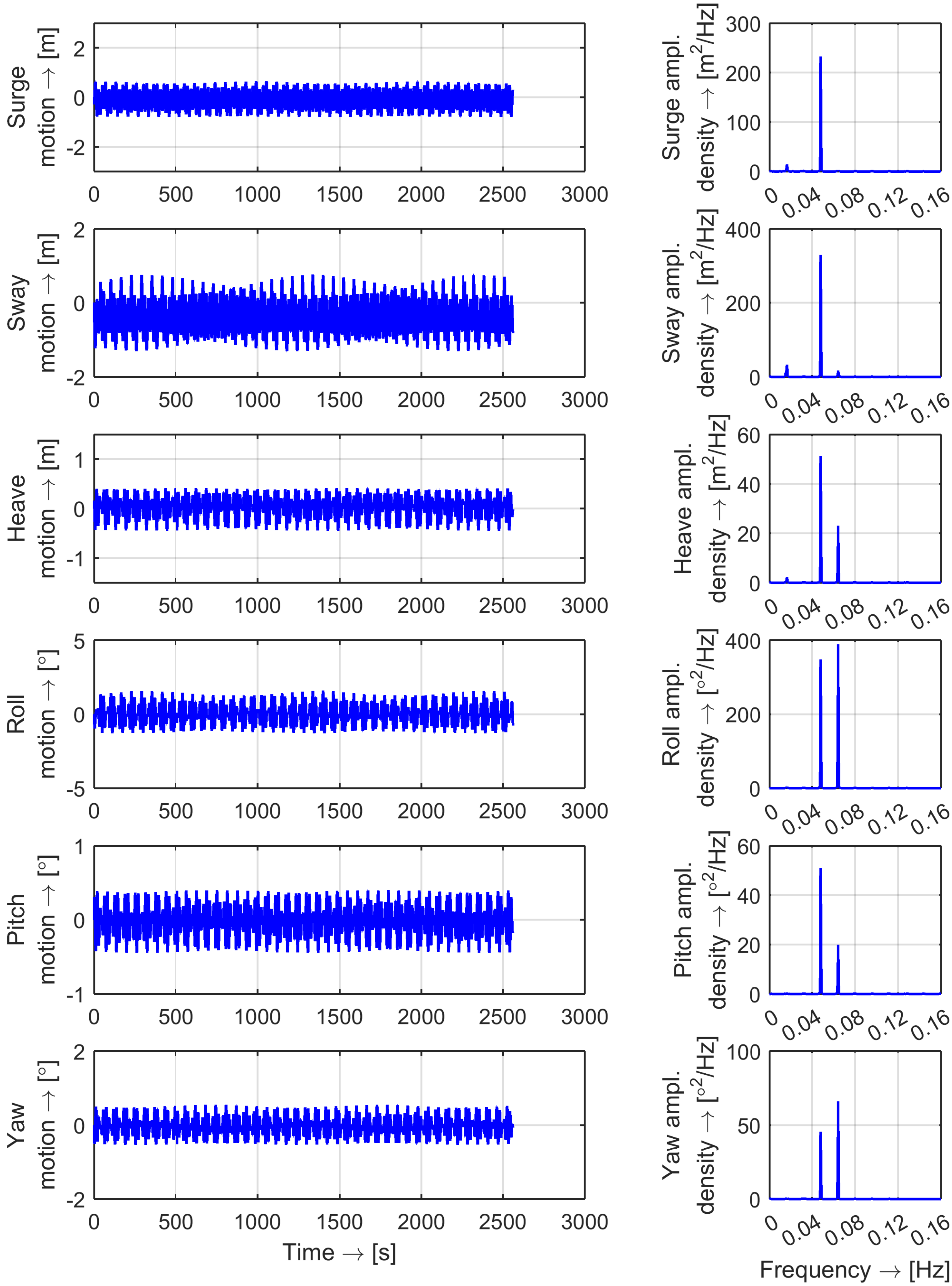

σ_{Surge} = 0.41 m, σ_{Sway} = 0.52 m, σ_{Heave} = 0.22 m, σ_{Roll} = 0.69°, σ_{Pitch} = 0.22°, σ_{Yaw} = 0.27°

Ship motions at centre of gravity (CoG) Depth = 18.0 m, H = 1.50 m, T_1 = 15.60 s, T_2 = 20.96 s Bow-quartering waves	Bichromatic	B610c
	C2_B610c_200t	
Deltares	11202696	App. G.117-2

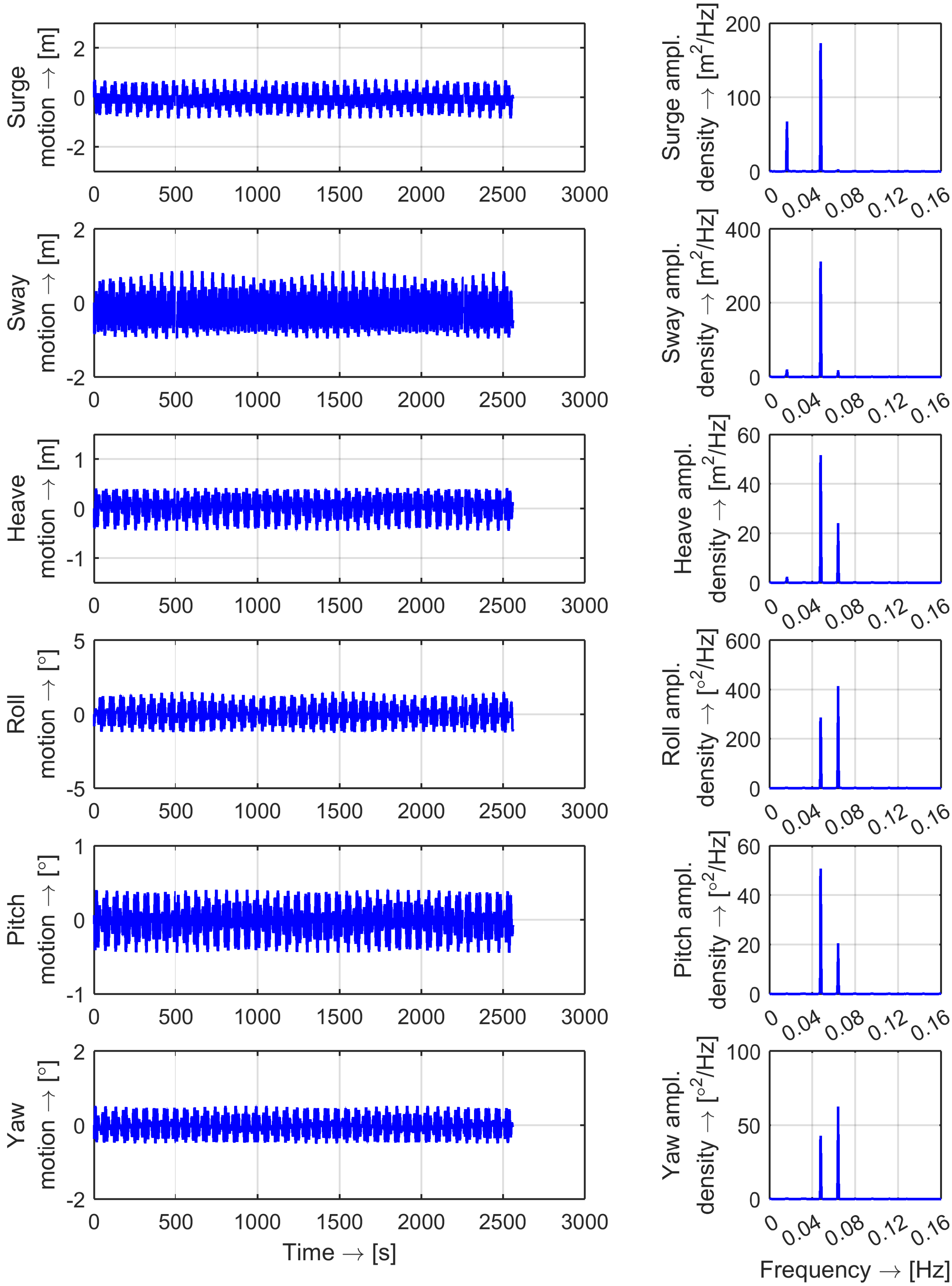

σ_{Surge} = 0.41 m, σ_{Sway} = 0.49 m, σ_{Heave} = 0.23 m, σ_{Roll} = 0.67°, σ_{Pitch} = 0.22°, σ_{Yaw} = 0.26°

Ship motions at centre of gravity (CoG) Depth = 18.0 m, H = 1.50 m, T_1 = 15.60 s, T_2 = 20.96 s Bow-quartering waves	Bichromatic	B610c
	C2_B610c_sga	
Deltares	11202696	App. G.118-2

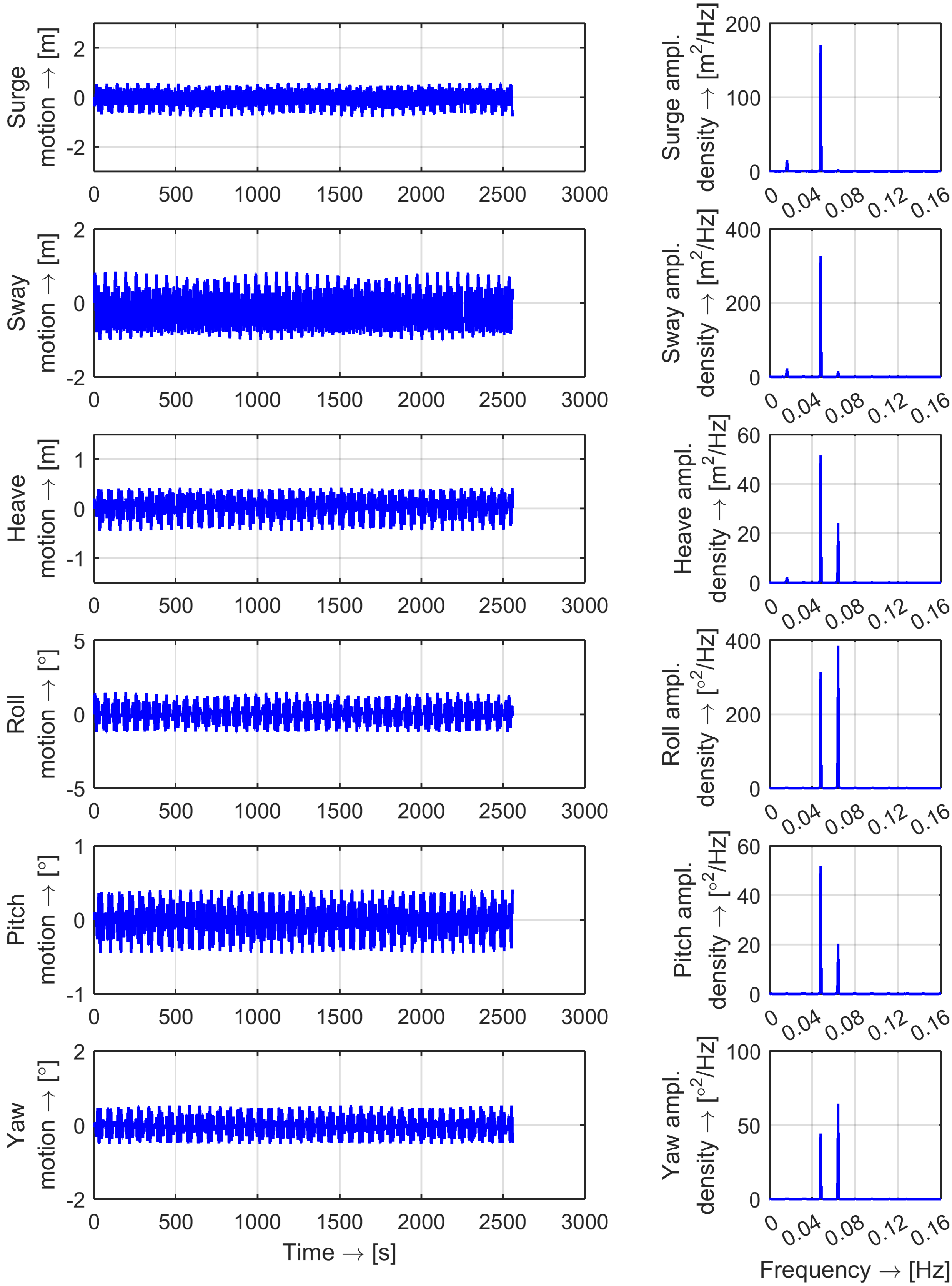

σ_{Surge} = 0.36 m, σ_{Sway} = 0.50 m, σ_{Heave} = 0.23 m, σ_{Roll} = 0.67°, σ_{Pitch} = 0.22°, σ_{Yaw} = 0.26°

Ship motions at centre of gravity (CoG) Depth = 18.0 m, H = 1.50 m, T_1 = 15.60 s, T_2 = 20.96 s Bow-quartering waves	Bichromatic	B610c
	C2_B610c_sk	
Deltares	11202696	App. G.119-2

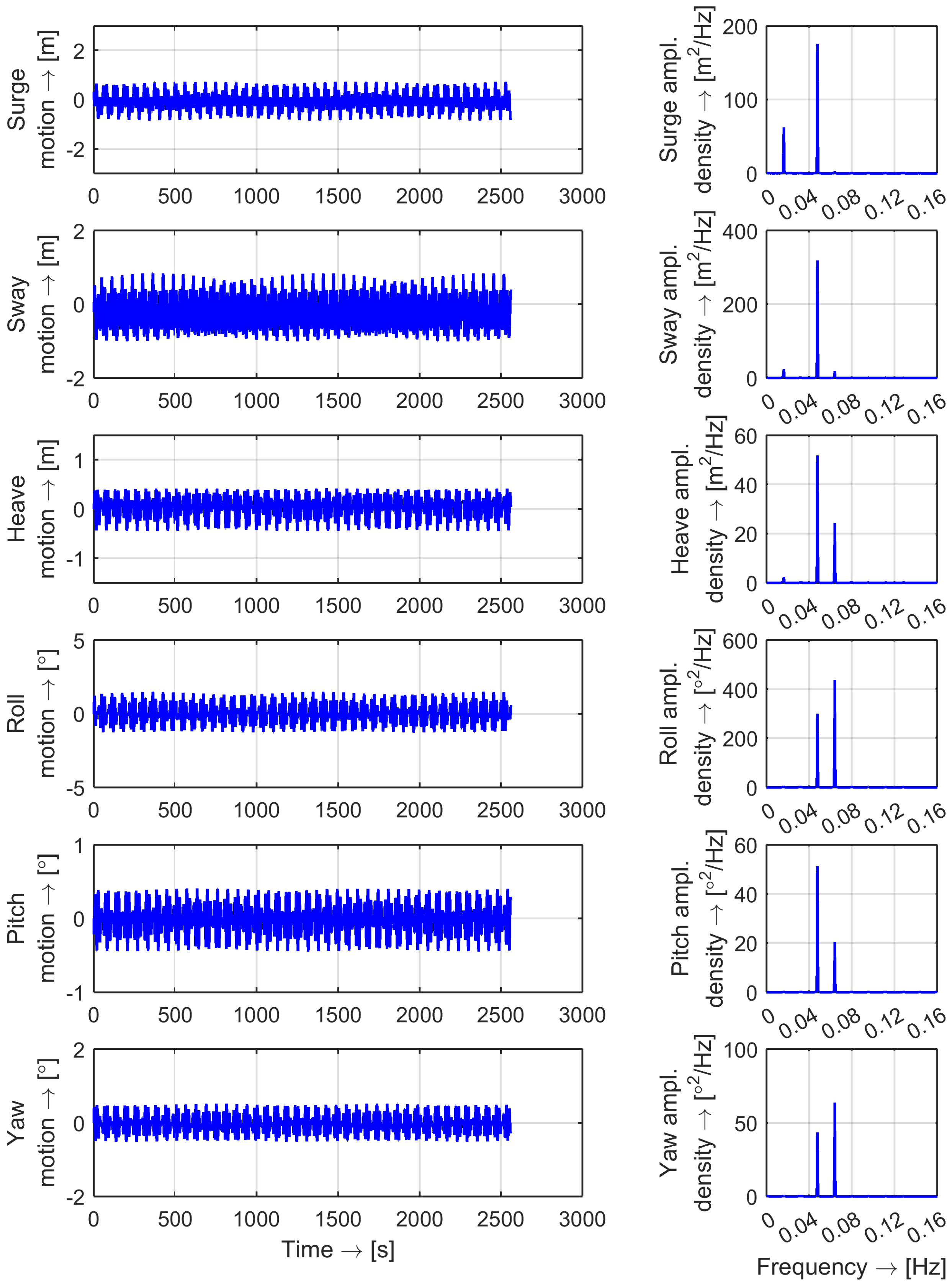

σ_{Surge} = 0.41 m, σ_{Sway} = 0.50 m, σ_{Heave} = 0.23 m, σ_{Roll} = 0.69°, σ_{Pitch} = 0.22°, σ_{Yaw} = 0.26°

Ship motions at centre of gravity (CoG) Depth = 18.0 m, H = 1.50 m, T_1 = 15.60 s, T_2 = 20.96 s Bow-quartering waves	Bichromatic	B610c
	C2_B610c_ssk	
Deltares	11202696	App. G.120-2

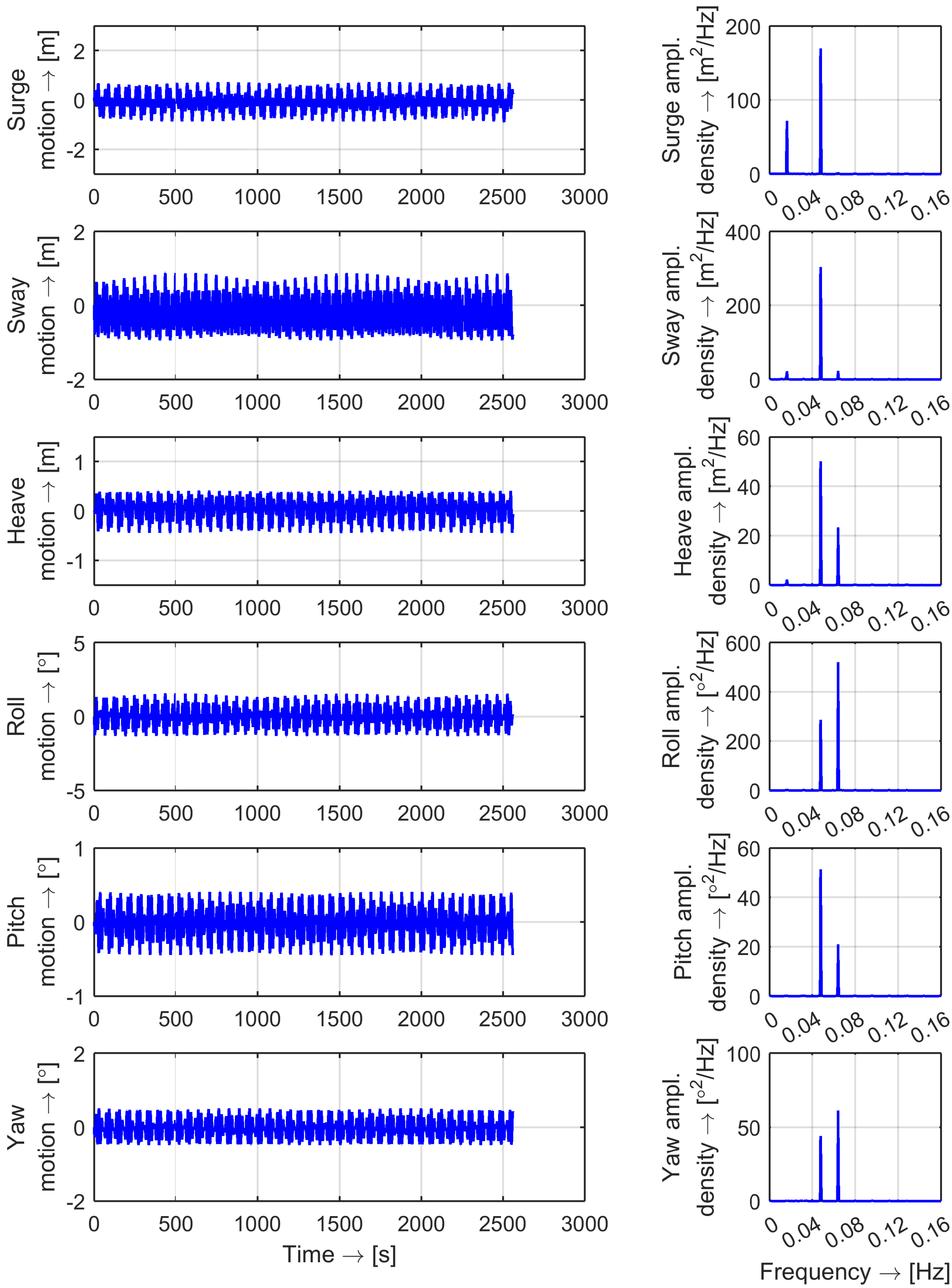

σ_{Surge} = 0.41 m, σ_{Sway} = 0.49 m, σ_{Heave} = 0.22 m, σ_{Roll} = 0.71°, σ_{Pitch} = 0.22°, σ_{Yaw} = 0.26°

Ship motions at centre of gravity (CoG) Depth = 18.0 m, H = 1.50 m, T_1 = 15.60 s, T_2 = 20.96 s Bow-quartering waves	Bichromatic	B610c
	C2_B610c_ssk_sga	
Deltares	11202696	App. G.121-2

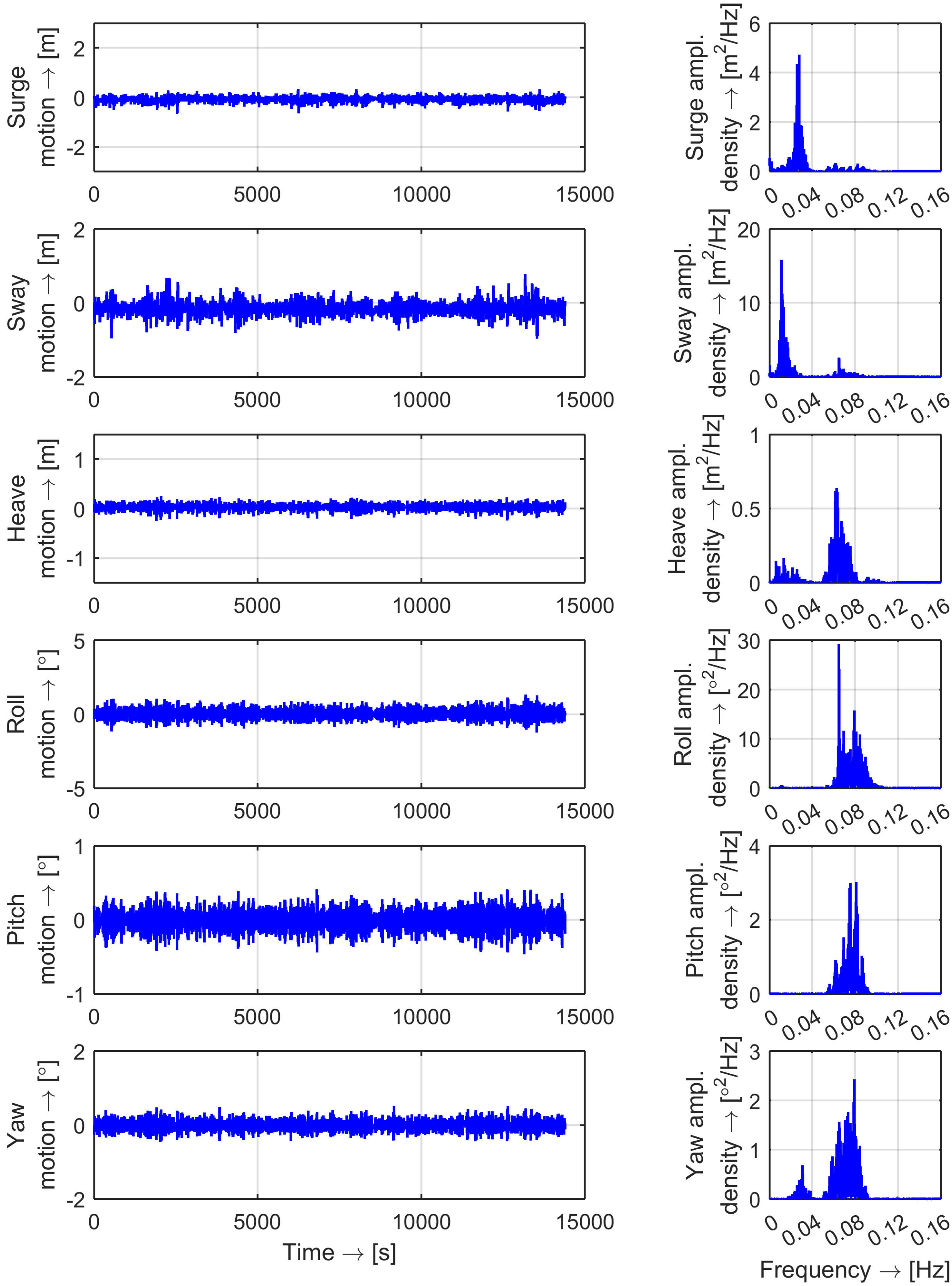

σ_{Surge} = 0.11 m, σ_{Sway} = 0.18 m, σ_{Heave} = 0.06 m, σ_{Roll} = 0.33°, σ_{Pitch} = 0.12°, σ_{Yaw} = 0.13°

Ship motions at centre of gravity (CoG) Depth = 18.0 m, H_{m0} = 1.00 m, T_p = 12.00 s, γ = 3.3 Bow-quartering waves	Irregular	I120a
	C3_I120a	
Deltares	11202696	App. G.122-2

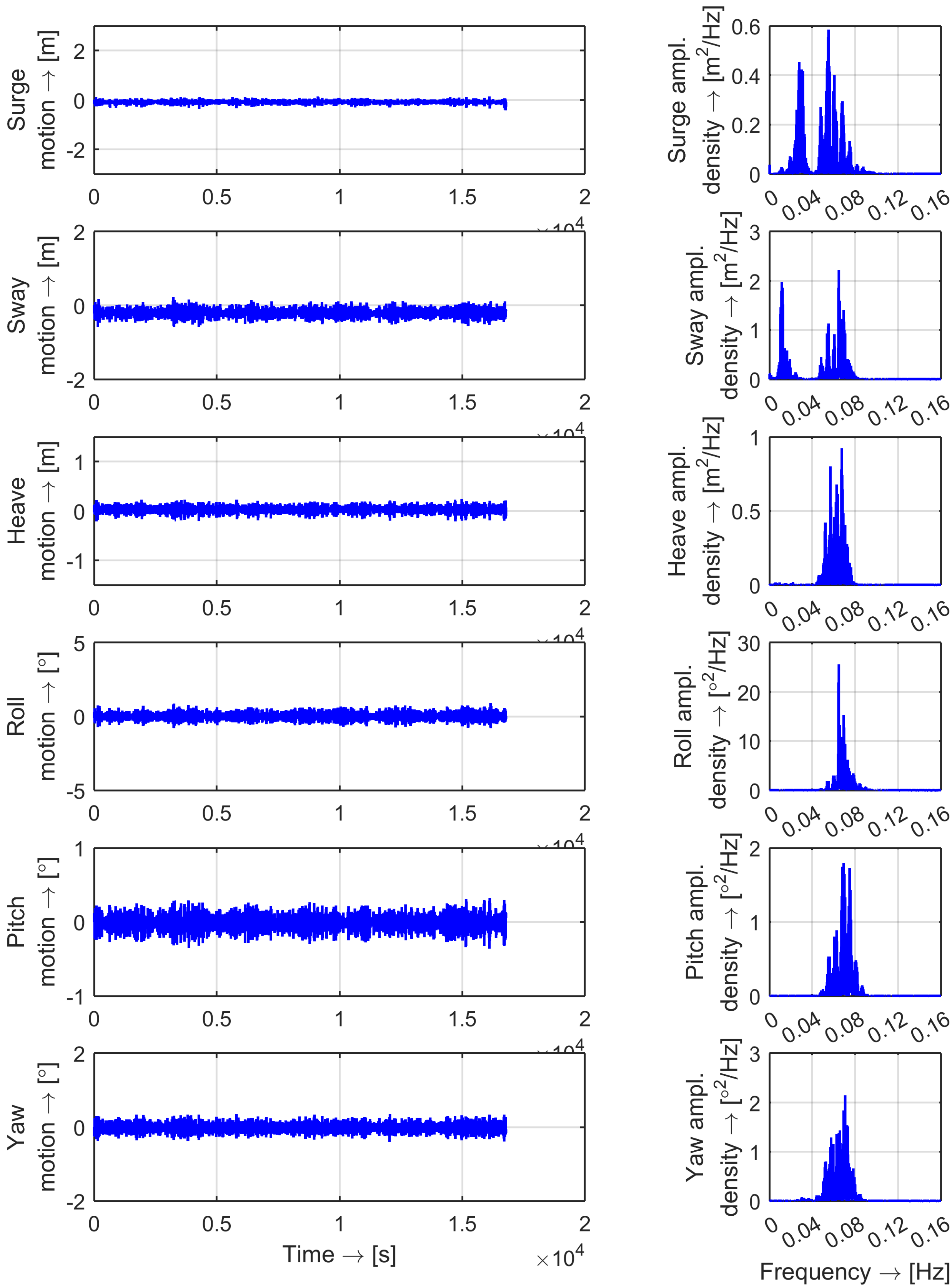

σ_{Surge} = 0.06 m, σ_{Sway} = 0.10 m, σ_{Heave} = 0.07 m, σ_{Roll} = 0.25°, σ_{Pitch} = 0.10°, σ_{Yaw} = 0.11°

Ship motions at centre of gravity (CoG) Depth = 18.0 m, H_{m0} = 0.50 m, T_p = 14.00 s, γ = 3.3 Bow-quartering waves	Irregular	I140a
	C3_I140a	
Deltares	11202696	App. G.123-2

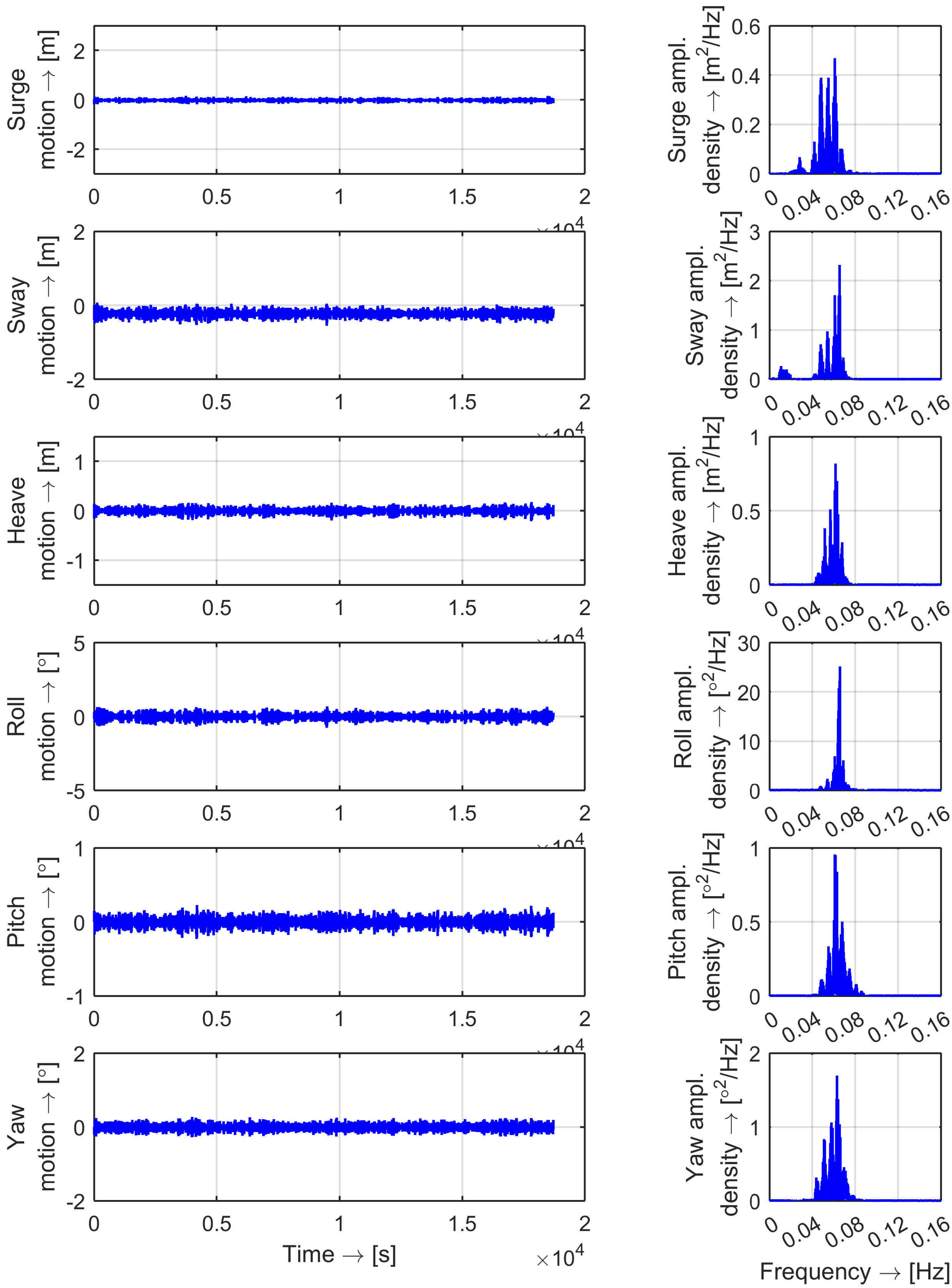

σ_{Surge} = 0.05 m, σ_{Sway} = 0.08 m, σ_{Heave} = 0.05 m, σ_{Roll} = 0.21°, σ_{Pitch} = 0.06°, σ_{Yaw} = 0.08°

Ship motions at centre of gravity (CoG) Depth = 18.0 m, H_{m0} = 0.50 m, T_p = 15.60 s, γ = 5.0 Bow-quartering waves	Irregular	I156a
	C3_I156a	
Deltares	11202696	App. G.124-2

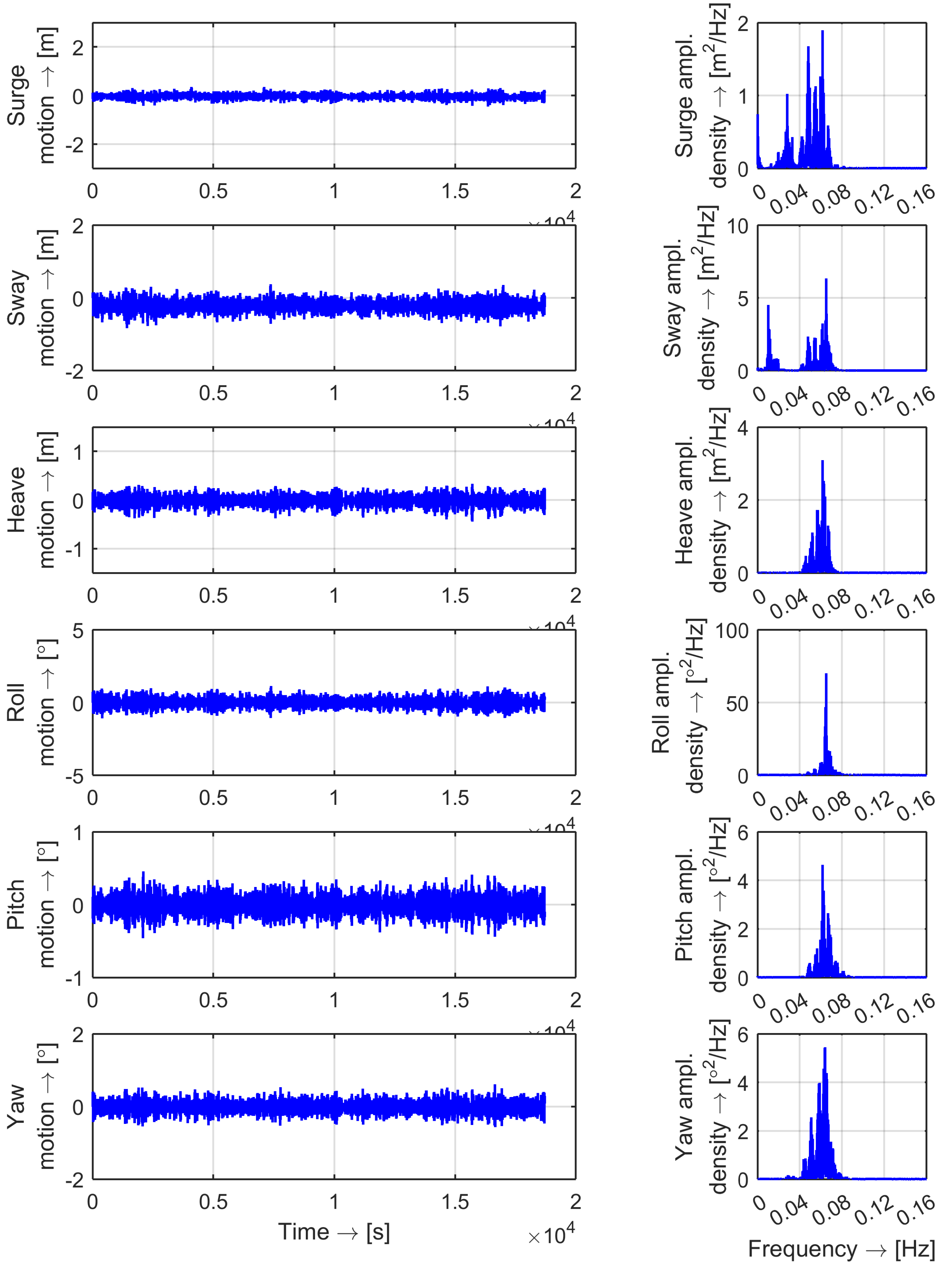

σ_{Surge} = 0.10 m, σ_{Sway} = 0.15 m, σ_{Heave} = 0.10 m, σ_{Roll} = 0.32°, σ_{Pitch} = 0.12°, σ_{Yaw} = 0.16°

Ship motions at centre of gravity (CoG) Depth = 18.0 m, H_{m0} = 1.00 m, T_p = 15.60 s, γ = 5.0 Bow-quartering waves	Irregular	I156b
	C3_I156b	
Deltares	11202696	App. G.125-2

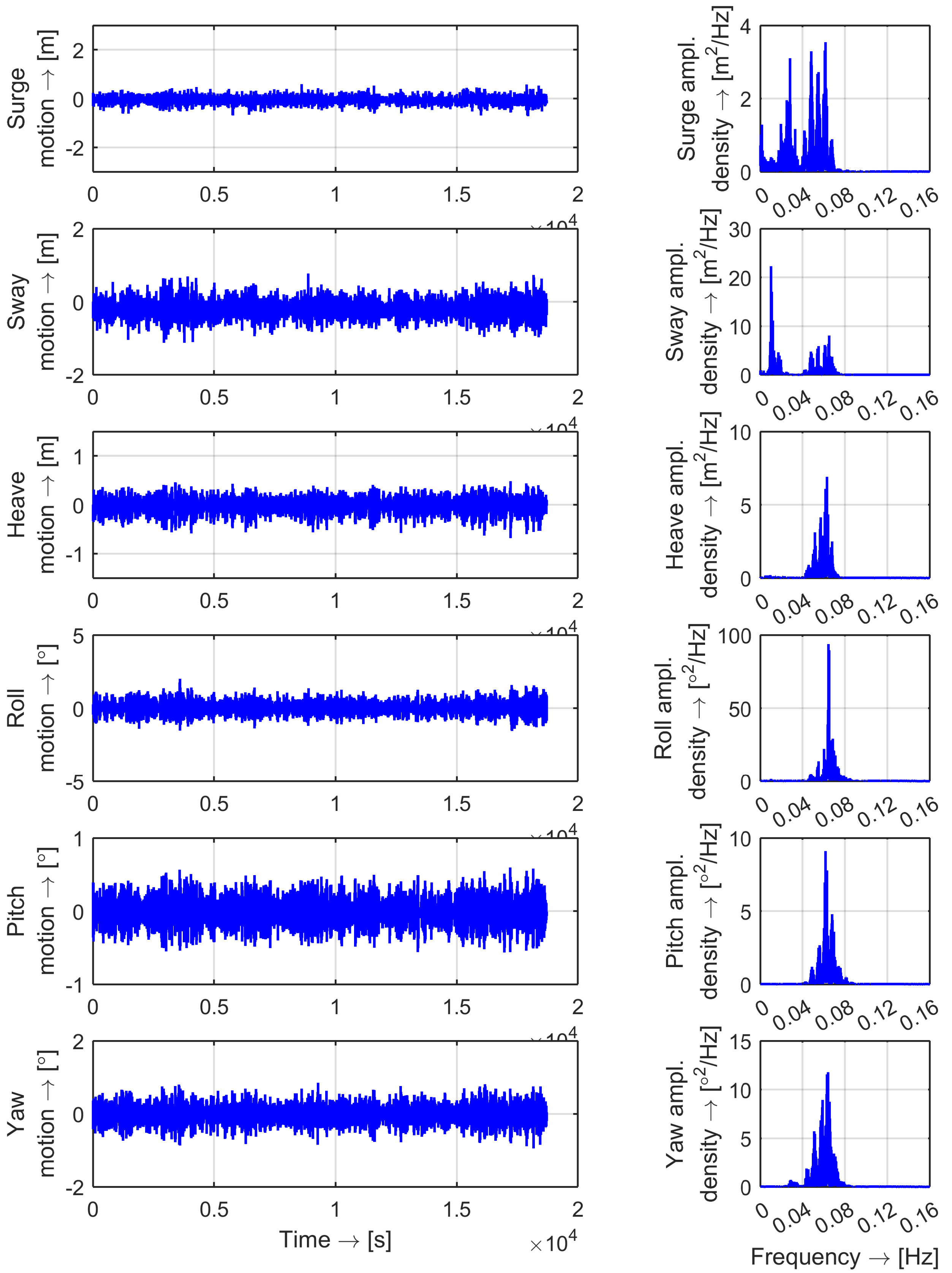

σ_{Surge} = 0.16 m, σ_{Sway} = 0.24 m, σ_{Heave} = 0.16 m, σ_{Roll} = 0.43°, σ_{Pitch} = 0.18°, σ_{Yaw} = 0.24°

Ship motions at centre of gravity (CoG) Depth = 18.0 m, H_{m0} = 1.50 m, T_p = 15.60 s, γ = 5.0 Bow-quartering waves	Irregular	I156c
	C3_I156c	
Deltares	11202696	App. G.126-2

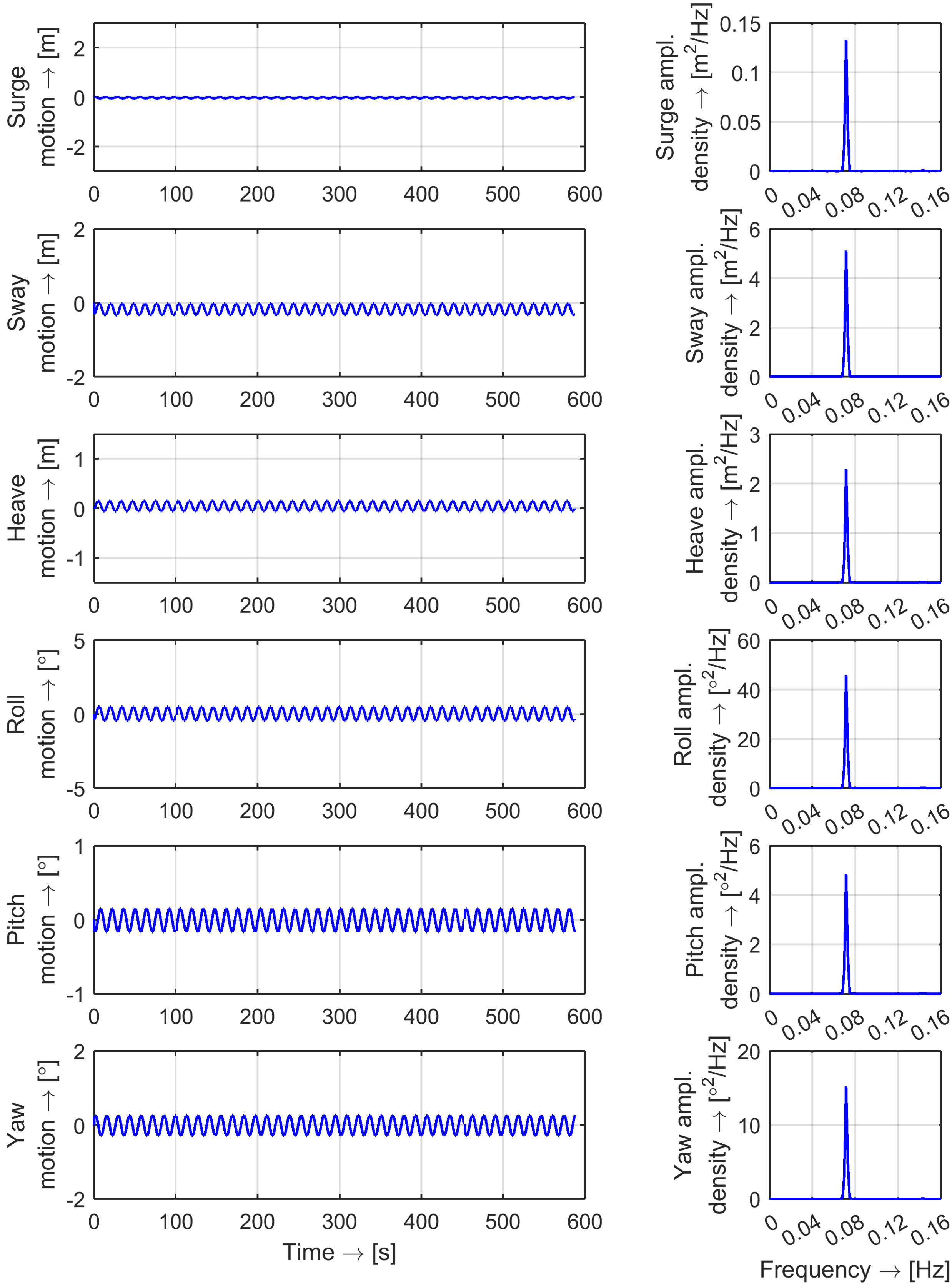

σ_{Surge} = 0.02 m, σ_{Sway} = 0.11 m, σ_{Heave} = 0.08 m, σ_{Roll} = 0.34°, σ_{Pitch} = 0.11°, σ_{Yaw} = 0.20°

Ship motions at centre of gravity (CoG) Depth = 18.0 m, H = 1.00 m, T = 14.00 s Bow-quartering waves	Monochromatic	M140a
	C4_M140a	
Deltares	11202696	App. G.127-2

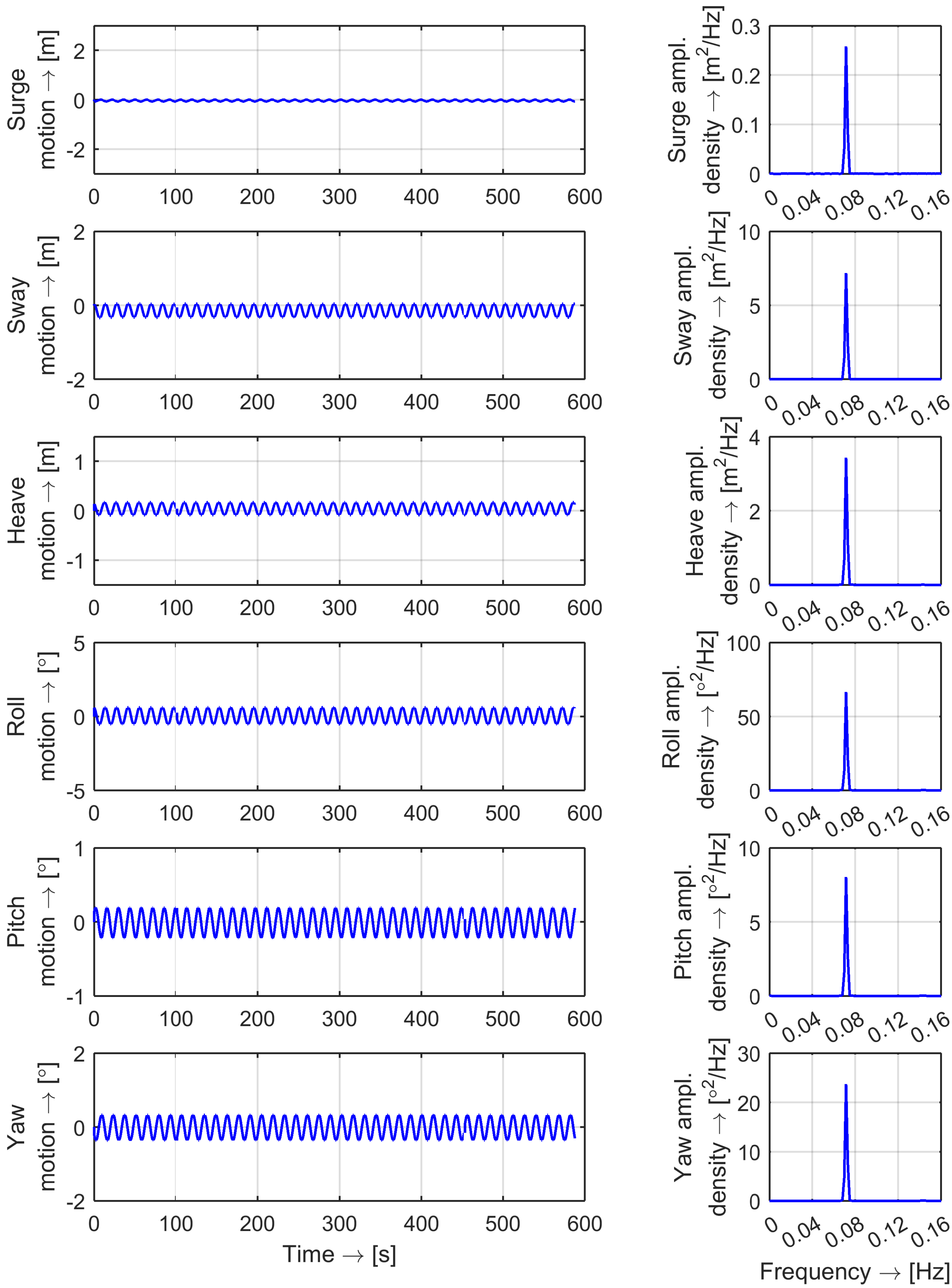

σ_{Surge} = 0.03 m, σ_{Sway} = 0.14 m, σ_{Heave} = 0.09 m, σ_{Roll} = 0.41°, σ_{Pitch} = 0.14°, σ_{Yaw} = 0.25°

Ship motions at centre of gravity (CoG) Depth = 18.0 m, H = 1.25 m, T = 14.00 s Bow-quartering waves	Monochromatic	M140b
	C4_M140b	
Deltares	11202696	App. G.128-2

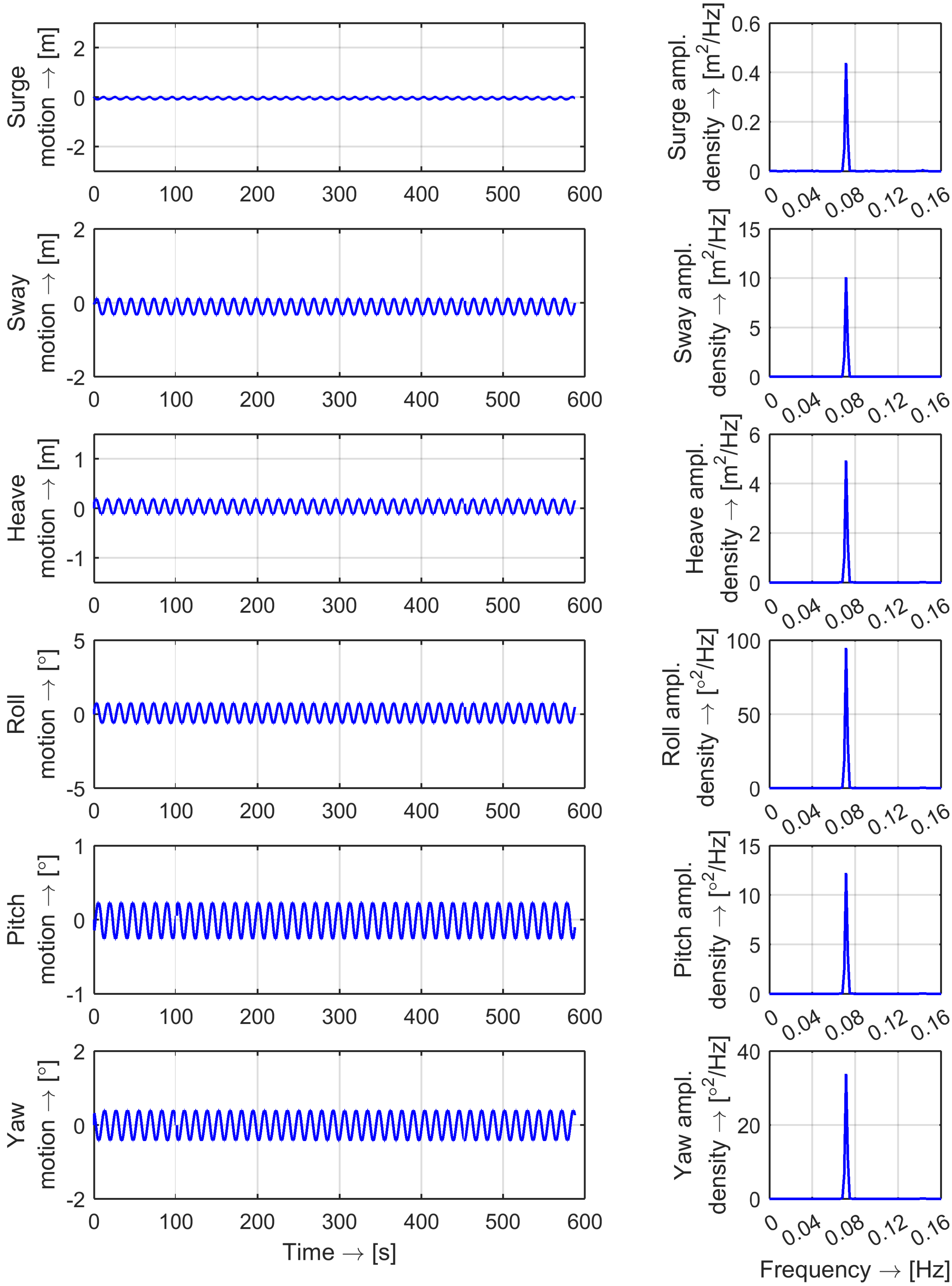

σ_{Surge} = 0.03 m, σ_{Sway} = 0.16 m, σ_{Heave} = 0.11 m, σ_{Roll} = 0.49°, σ_{Pitch} = 0.18°, σ_{Yaw} = 0.30°

Ship motions at centre of gravity (CoG) Depth = 18.0 m, H = 1.50 m, T = 14.00 s Bow-quartering waves	Monochromatic	M140c
	C4_M140c	
Deltares	11202696	App. G.129-2

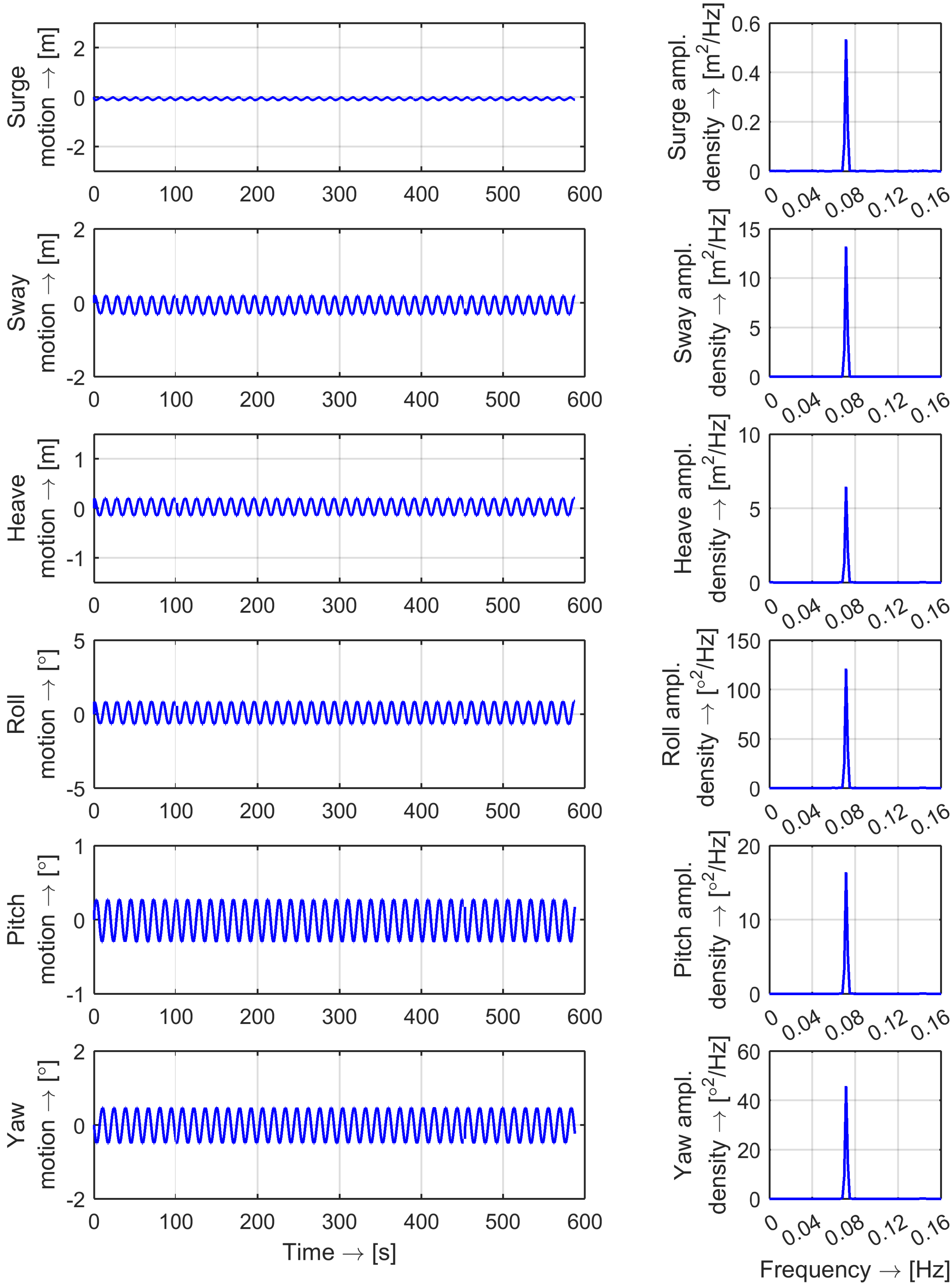

σ_{Surge} = 0.04 m, σ_{Sway} = 0.18 m, σ_{Heave} = 0.13 m, σ_{Roll} = 0.56°, σ_{Pitch} = 0.21°, σ_{Yaw} = 0.34°

Ship motions at centre of gravity (CoG) Depth = 18.0 m, H = 1.75 m, T = 14.00 s Bow-quartering waves	Monochromatic	M140d
	C4_M140d	
Deltares	11202696	App. G.130-2

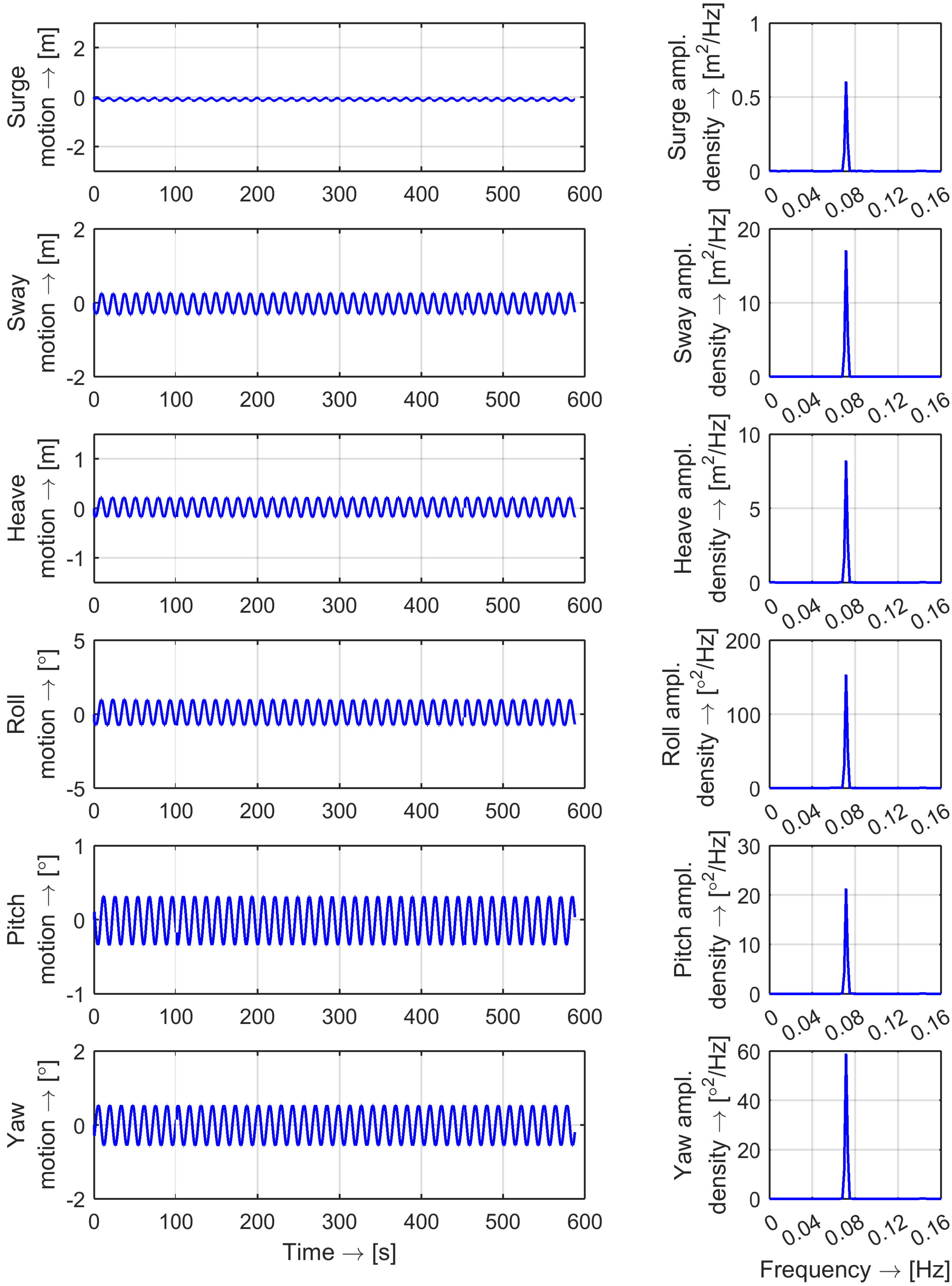

σ_{Surge} = 0.04 m, σ_{Sway} = 0.21 m, σ_{Heave} = 0.15 m, σ_{Roll} = 0.63°, σ_{Pitch} = 0.23°, σ_{Yaw} = 0.39°

Ship motions at centre of gravity (CoG) Depth = 18.0 m, H = 2.00 m, T = 14.00 s Bow-quartering waves	Monochromatic	M140e
	C4_M140e	
Deltares	11202696	App. G.131-2

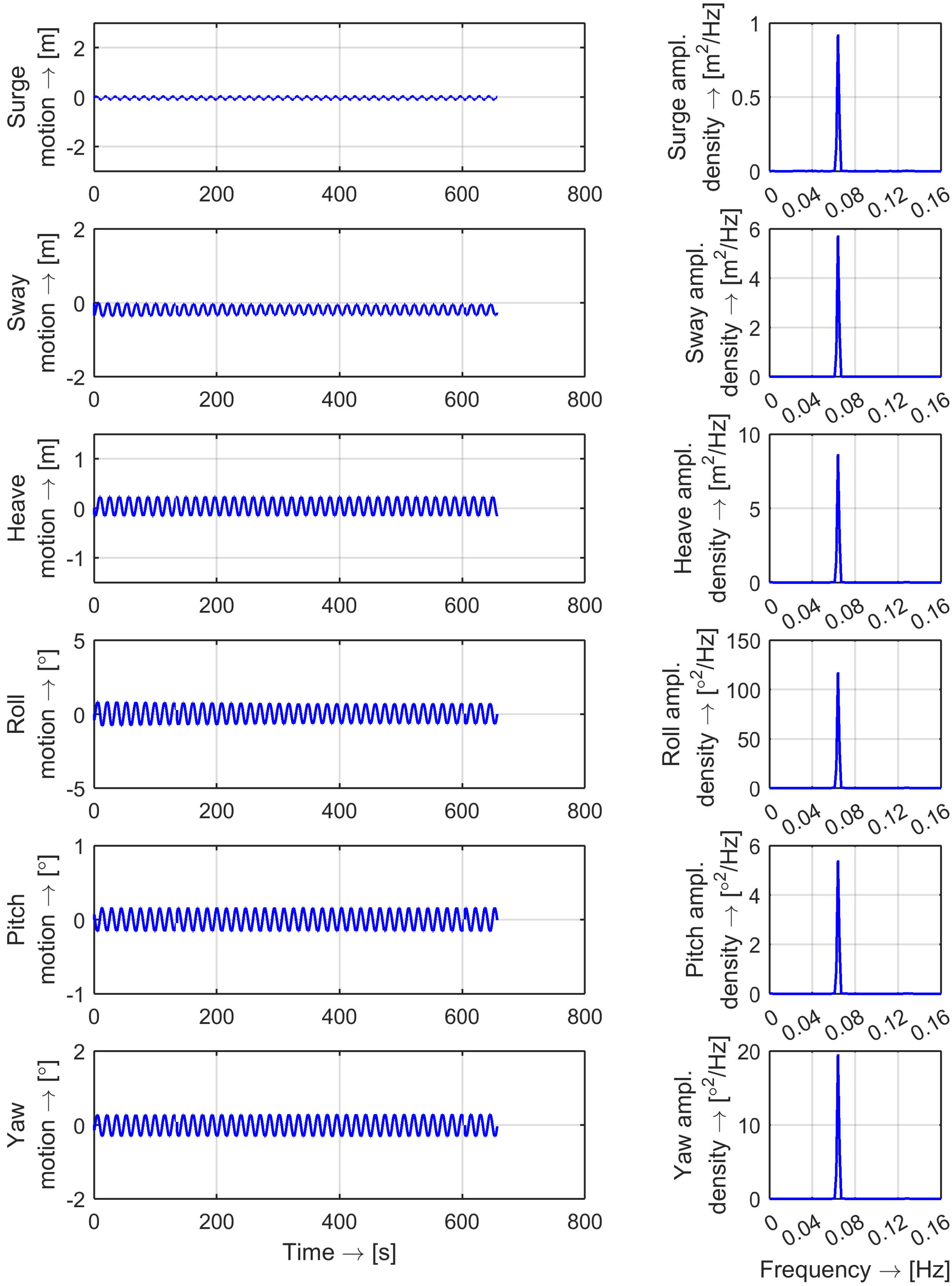

σ_{Surge} = 0.05 m, σ_{Sway} = 0.11 m, σ_{Heave} = 0.14 m, σ_{Roll} = 0.52°, σ_{Pitch} = 0.11°, σ_{Yaw} = 0.21°

Ship motions at centre of gravity (CoG) Depth = 18.0 m, H = 1.00 m, T = 15.60 s Bow-quartering waves	Monochromatic	M156a
	C4_M156a	
Deltares	11202696	App. G.132-2

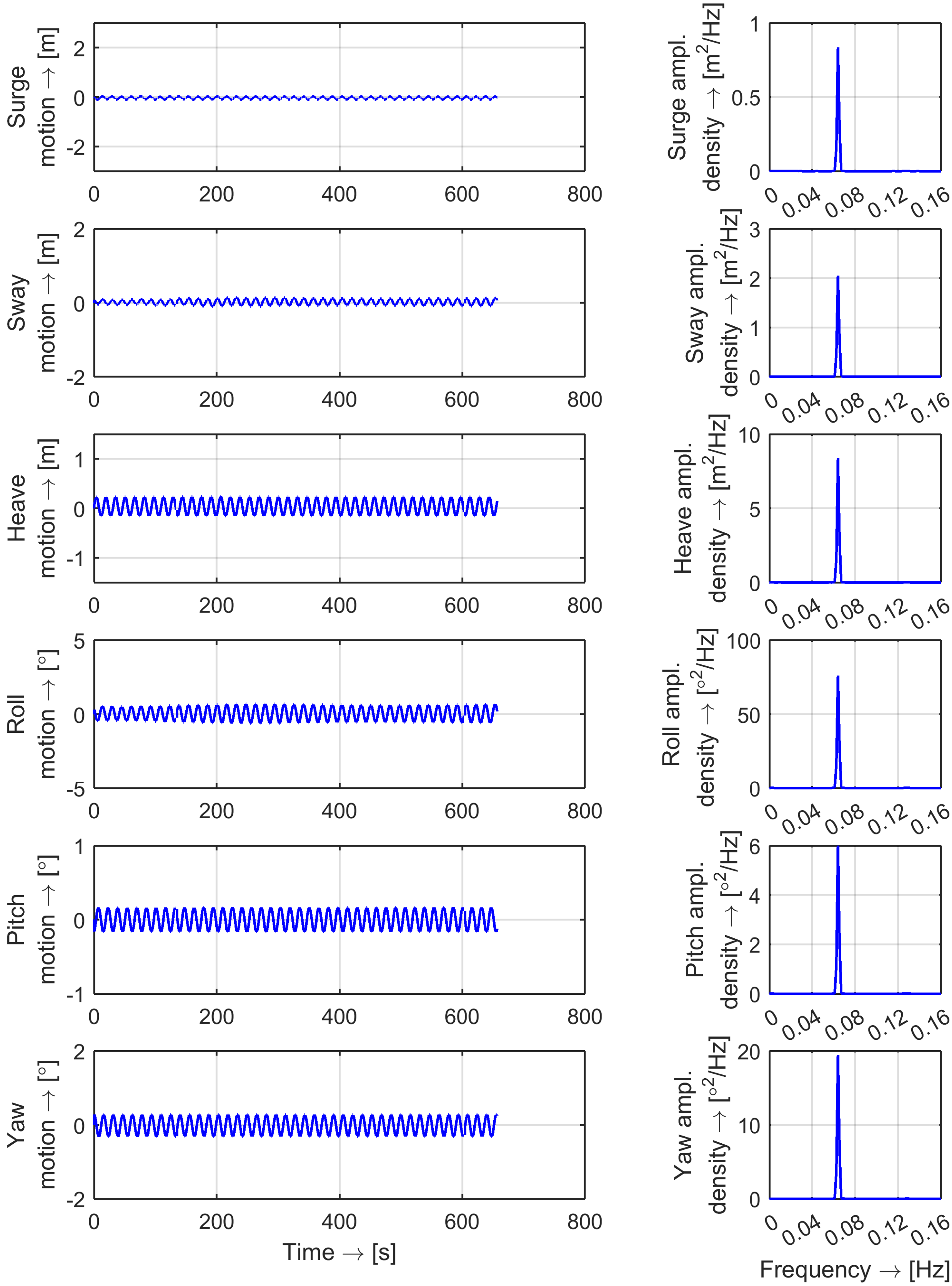

σ_{Surge} = 0.04 m, σ_{Sway} = 0.07 m, σ_{Heave} = 0.14 m, σ_{Roll} = 0.43°, σ_{Pitch} = 0.12°, σ_{Yaw} = 0.21°

Ship motions at centre of gravity (CoG) Depth = 18.0 m, H = 1.00 m, T = 15.60 s Bow-quartering waves	Monochromatic	M156a
	C4_M156a_noST	
Deltares	11202696	App. G.133-2

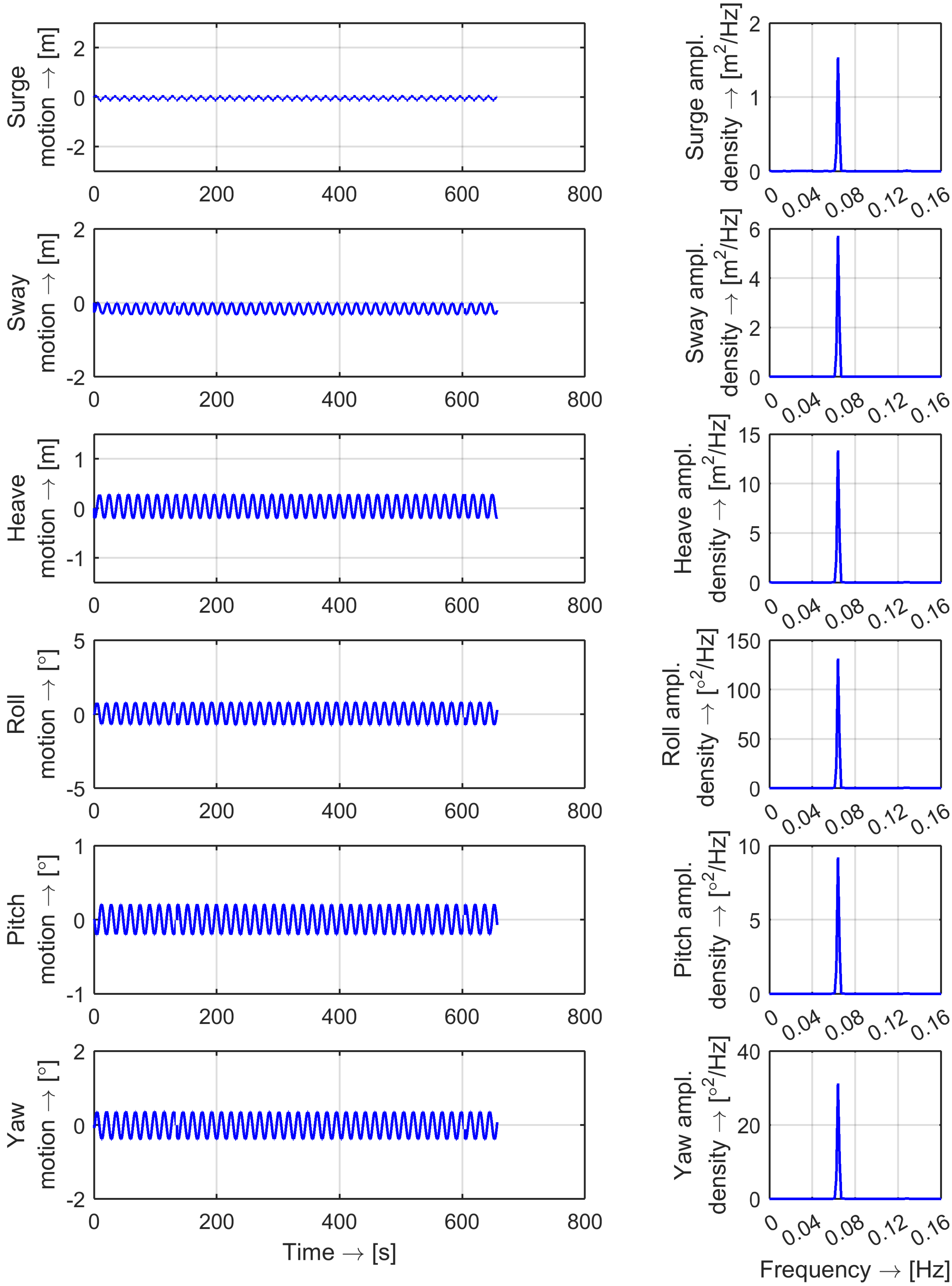

σ_{Surge} = 0.06 m, σ_{Sway} = 0.12 m, σ_{Heave} = 0.18 m, σ_{Roll} = 0.55°, σ_{Pitch} = 0.15°, σ_{Yaw} = 0.27°

Ship motions at centre of gravity (CoG) Depth = 18.0 m, H = 1.25 m, T = 15.60 s Bow-quartering waves	Monochromatic	M156b
	C4_M156b	
Deltares	11202696	App. G.134-2

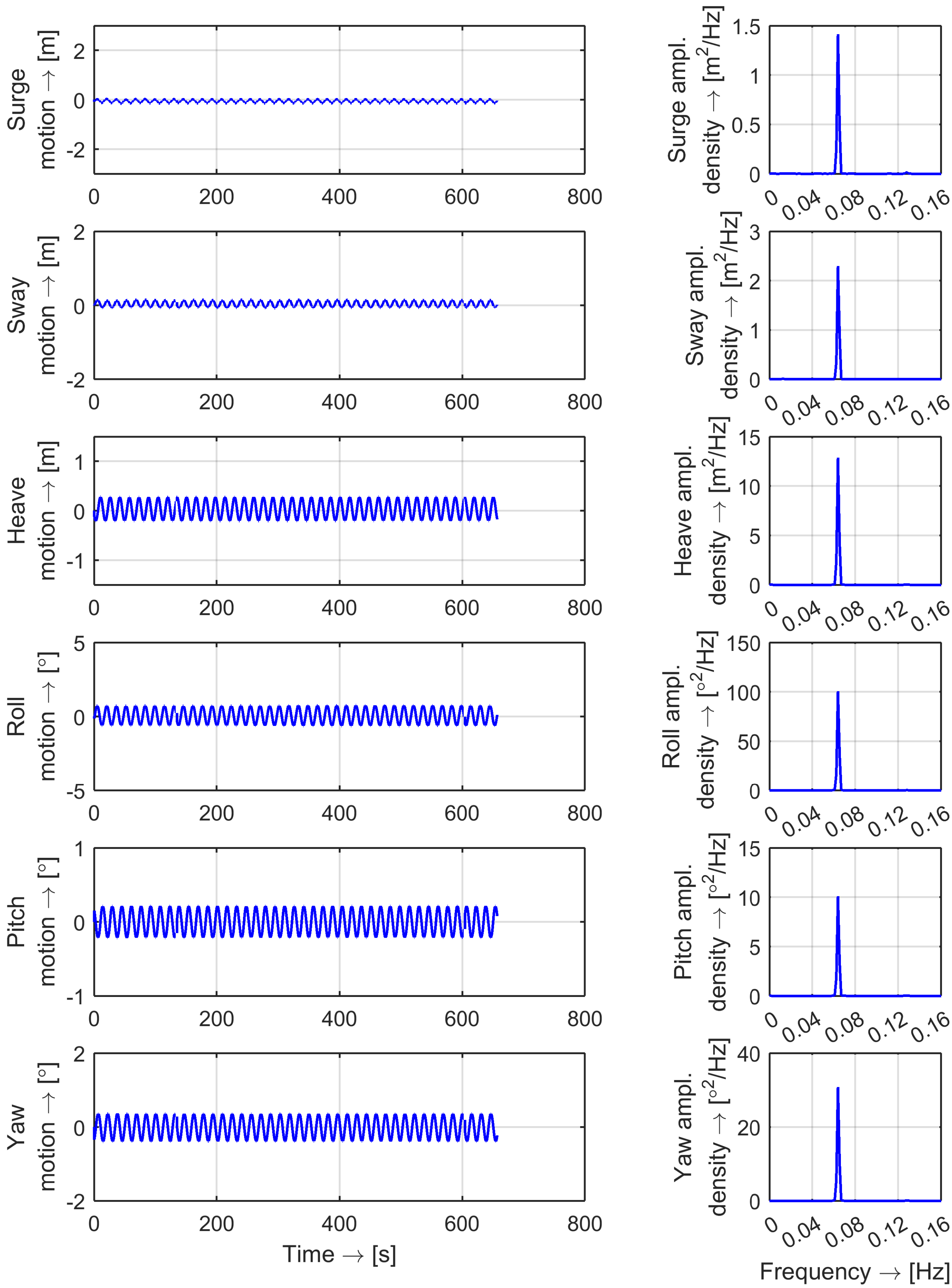

σ_{Surge} = 0.06 m, σ_{Sway} = 0.07 m, σ_{Heave} = 0.17 m, σ_{Roll} = 0.49°, σ_{Pitch} = 0.15°, σ_{Yaw} = 0.27°

Ship motions at centre of gravity (CoG) Depth = 18.0 m, H = 1.25 m, T = 15.60 s Bow-quartering waves	Monochromatic	M156b
	C4_M156b_noST	
Deltares	11202696	App. G.135-2

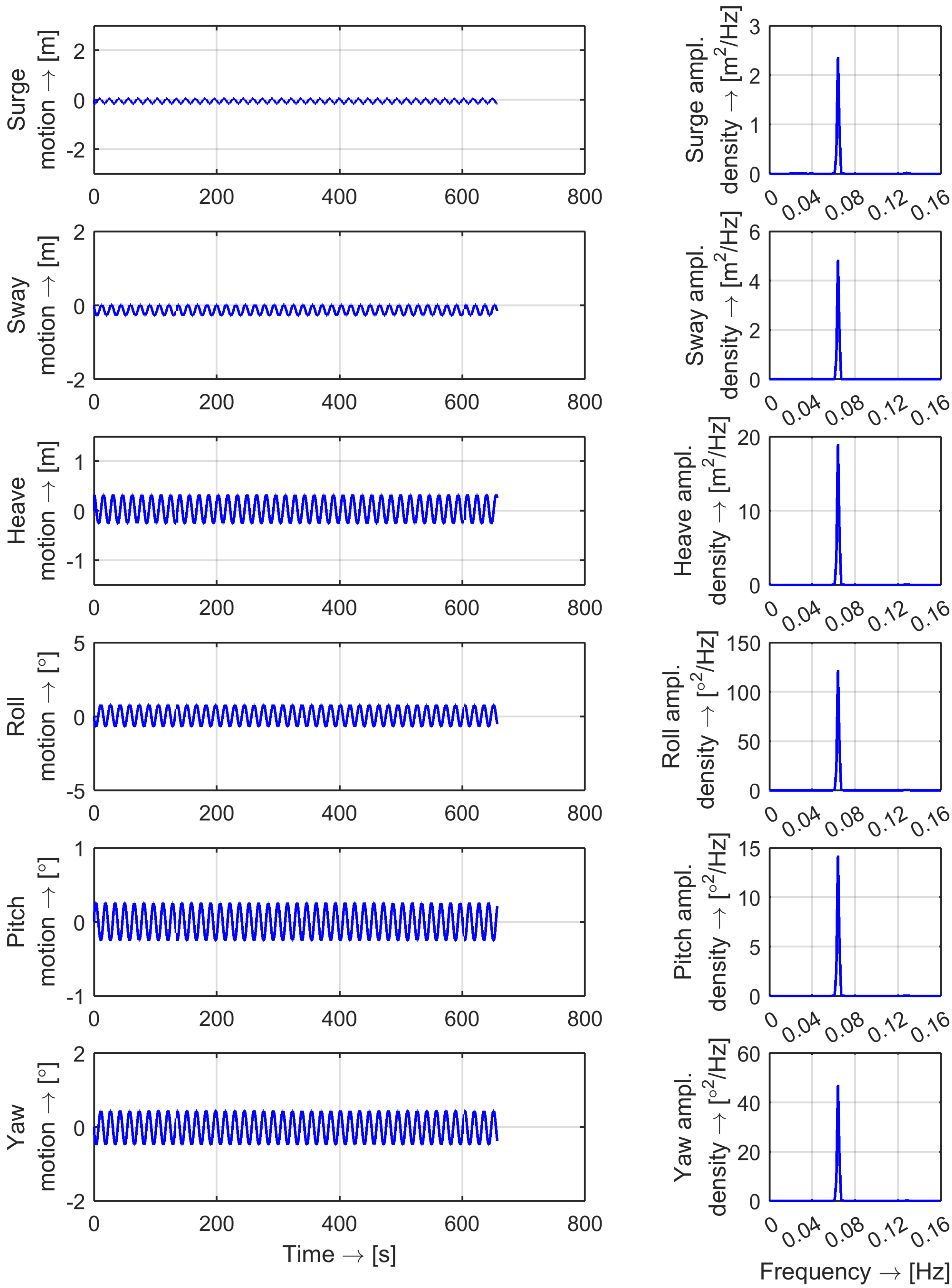

σ_{Surge} = 0.07 m, σ_{Sway} = 0.11 m, σ_{Heave} = 0.21 m, σ_{Roll} = 0.53°, σ_{Pitch} = 0.18°, σ_{Yaw} = 0.33°

Ship motions at centre of gravity (CoG) Depth = 18.0 m, H = 1.50 m, T = 15.60 s Bow-quartering waves	Monochromatic	M156c
	C4_M156c	
Deltares	11202696	App. G.136-2

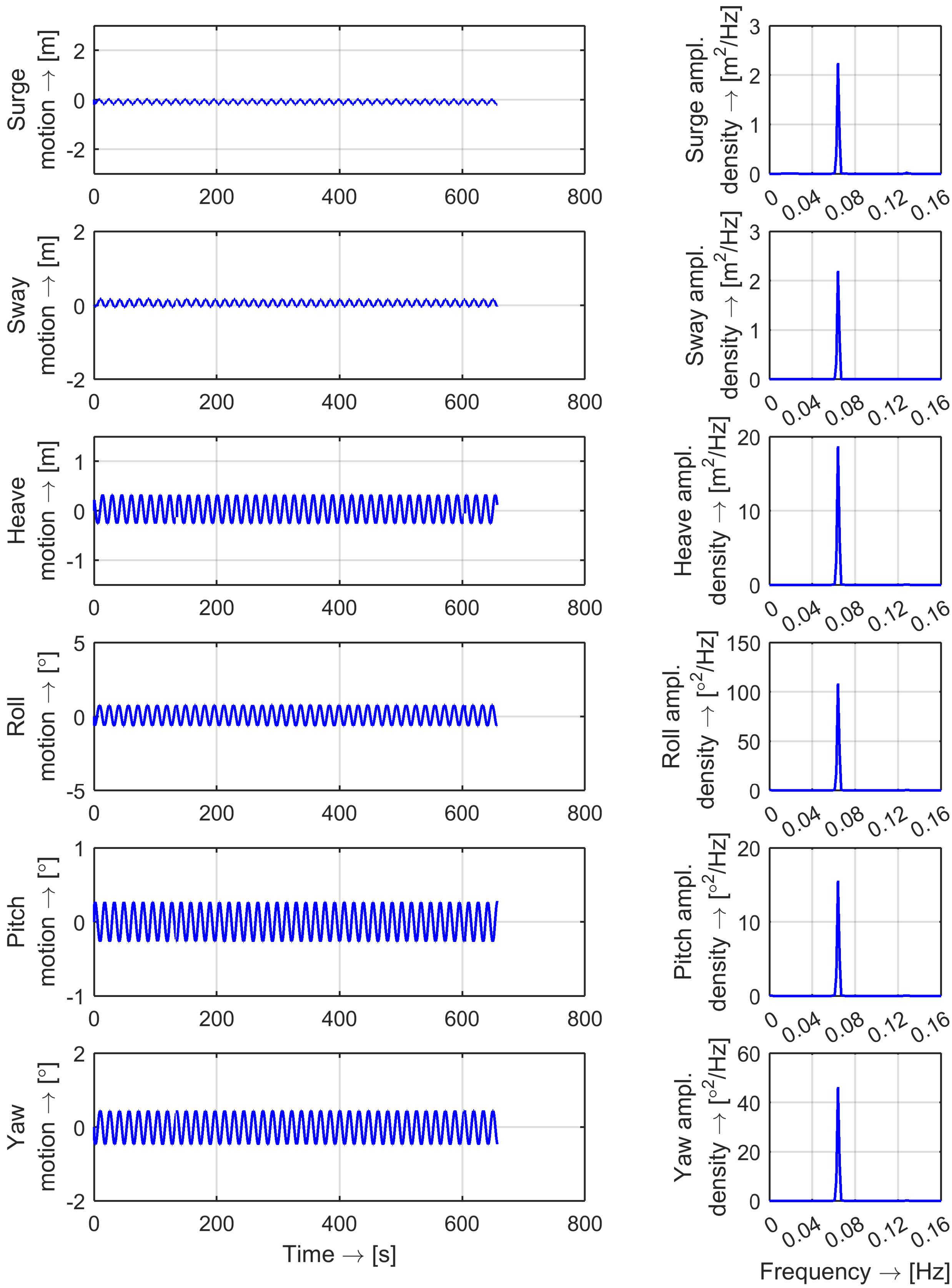

σ_{Surge} = 0.07 m, σ_{Sway} = 0.07 m, σ_{Heave} = 0.21 m, σ_{Roll} = 0.50°, σ_{Pitch} = 0.19°, σ_{Yaw} = 0.33°

Ship motions at centre of gravity (CoG) Depth = 18.0 m, H = 1.50 m, T = 15.60 s Bow-quartering waves	Monochromatic	M156c
	C4_M156c_noST	
Deltares	11202696	App. G.137-2

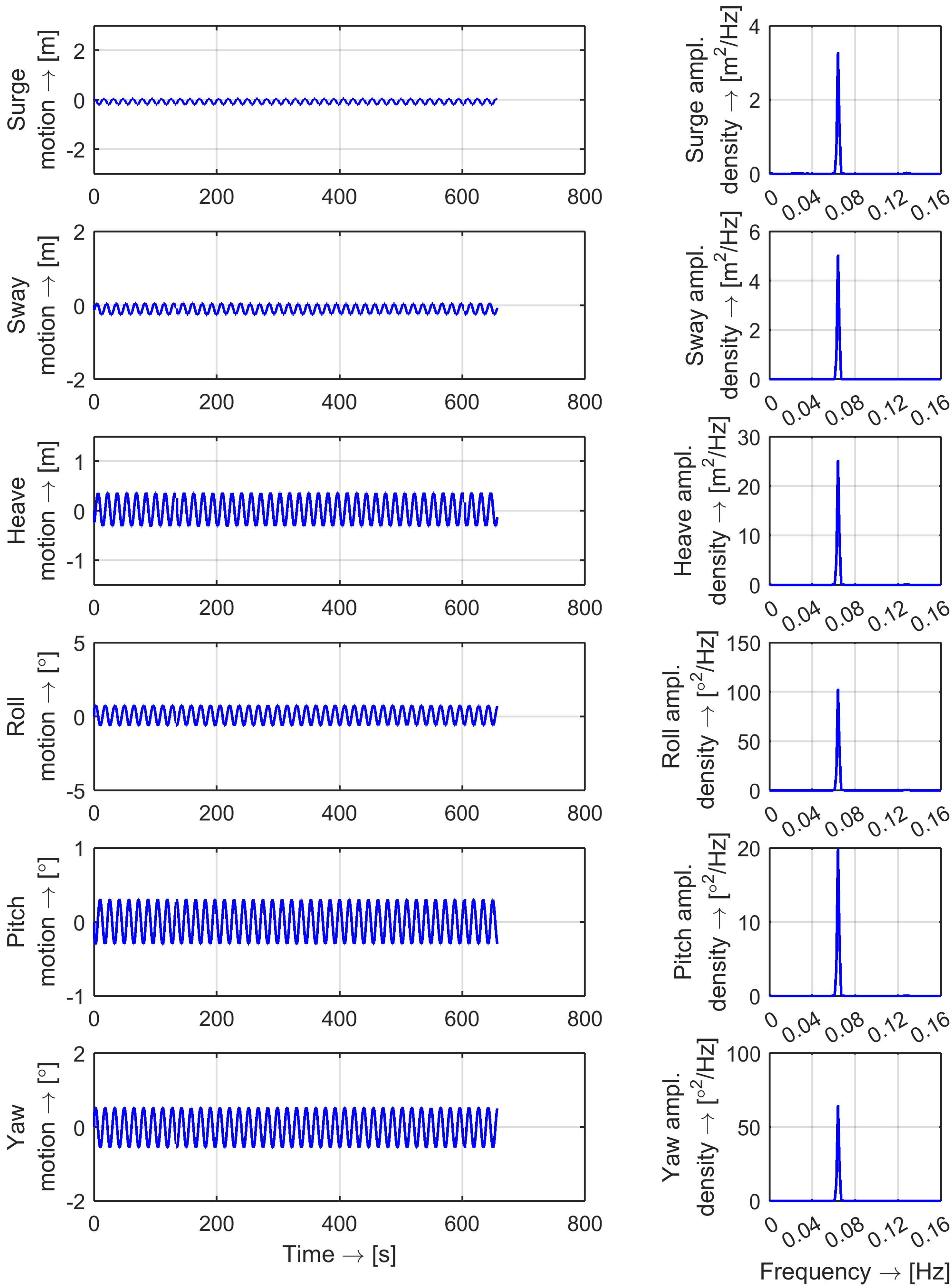

σ_{Surge} = 0.09 m, σ_{Sway} = 0.11 m, σ_{Heave} = 0.24 m, σ_{Roll} = 0.49°, σ_{Pitch} = 0.21°, σ_{Yaw} = 0.39°

Ship motions at centre of gravity (CoG) Depth = 18.0 m, H = 1.75 m, T = 15.60 s Bow-quartering waves	Monochromatic	M156d
	C4_M156d	
Deltares	11202696	App. G.138-2

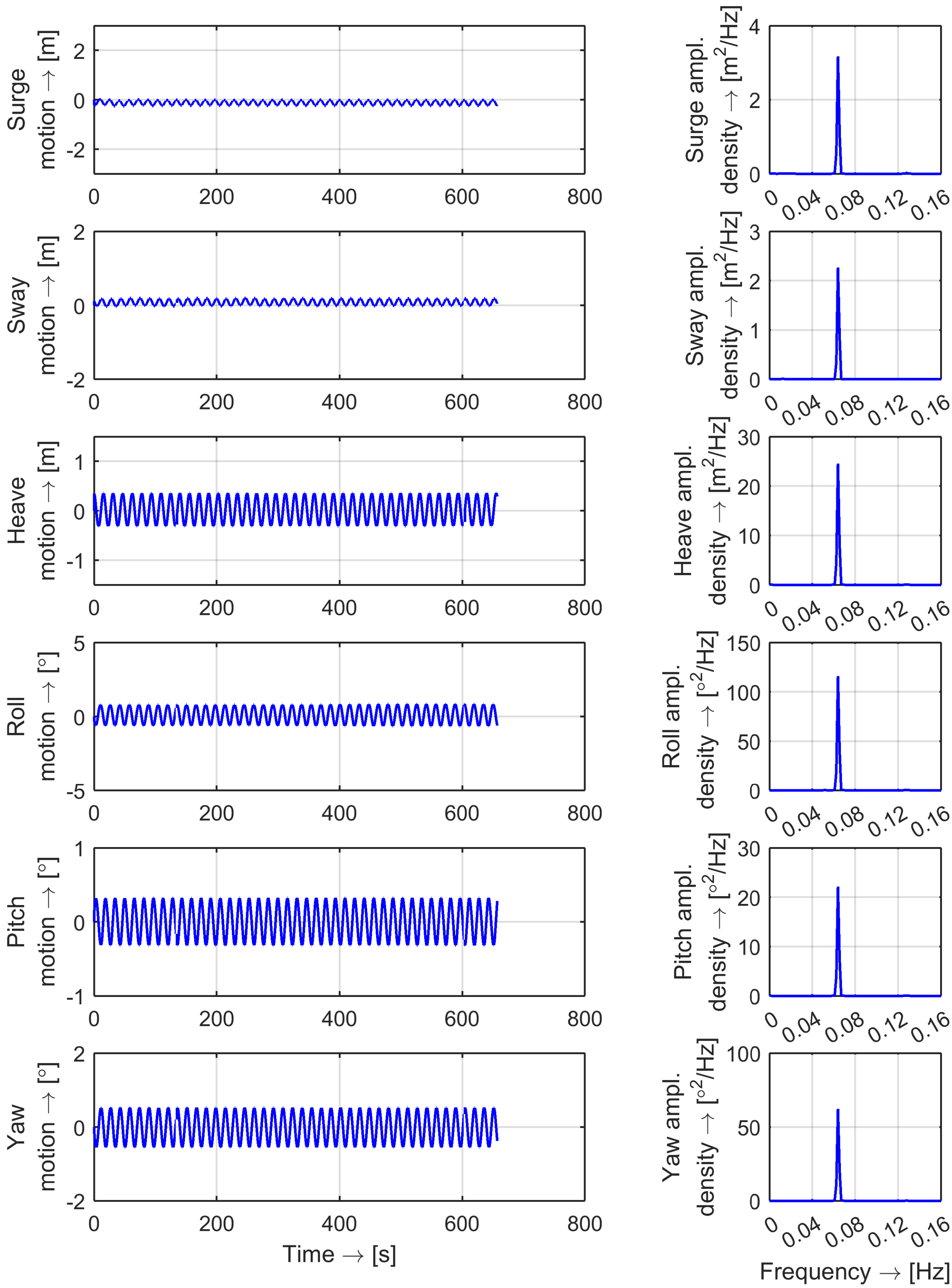

σ_{Surge} = 0.09 m, σ_{Sway} = 0.07 m, σ_{Heave} = 0.24 m, σ_{Roll} = 0.52°, σ_{Pitch} = 0.23°, σ_{Yaw} = 0.38°

Ship motions at centre of gravity (CoG) Depth = 18.0 m, H = 1.75 m, T = 15.60 s Bow-quartering waves	Monochromatic	M156d
	C4_M156d_noST	
Deltares	11202696	App. G.139-2

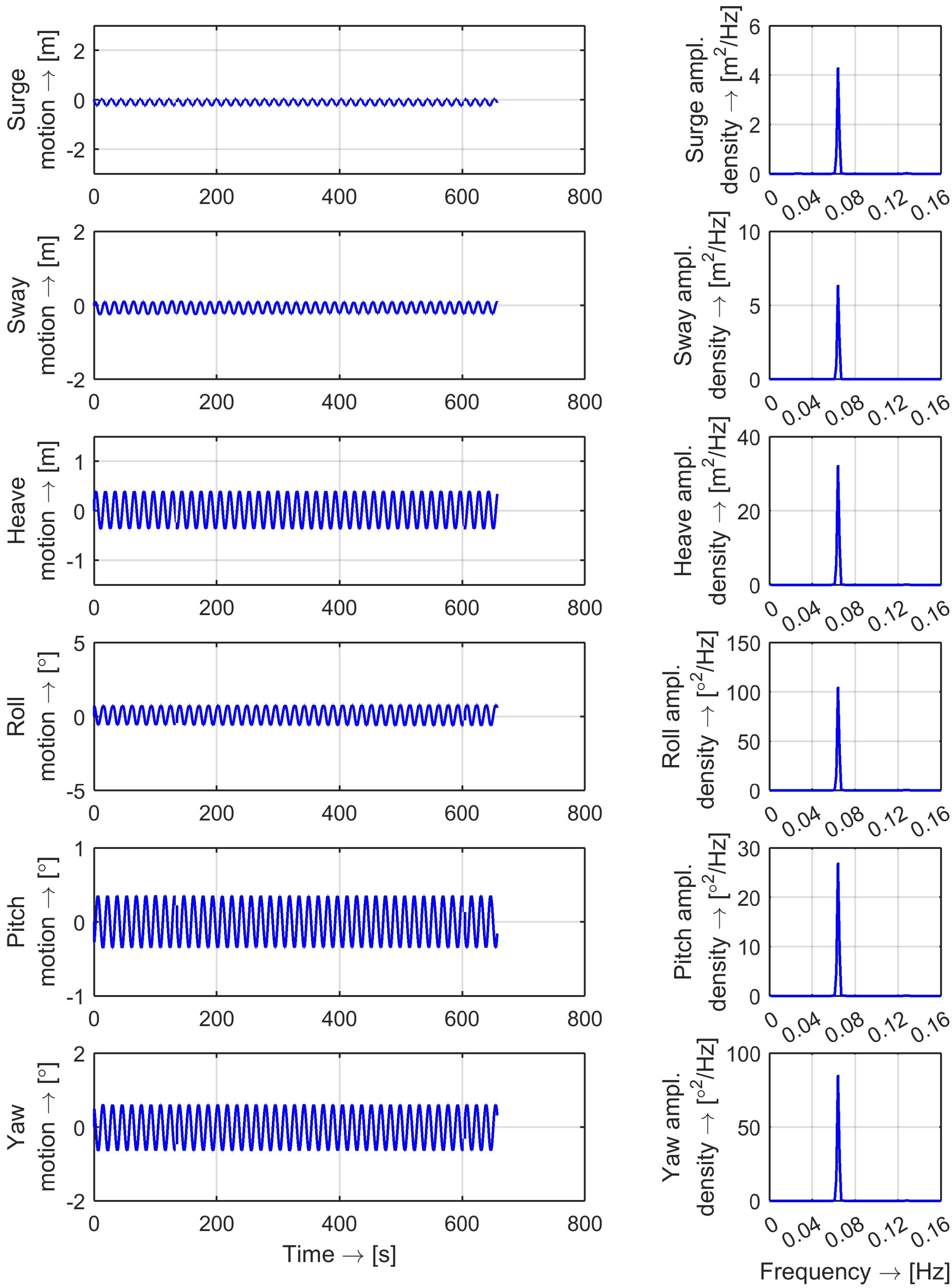

σ_{Surge} = 0.10 m, σ_{Sway} = 0.12 m, σ_{Heave} = 0.27 m, σ_{Roll} = 0.50°, σ_{Pitch} = 0.25°, σ_{Yaw} = 0.44°

Ship motions at centre of gravity (CoG) Depth = 18.0 m, H = 2.00 m, T = 15.60 s Bow-quartering waves	Monochromatic	M156e
	C4_M156e	
Deltares	11202696	App. G.140-2

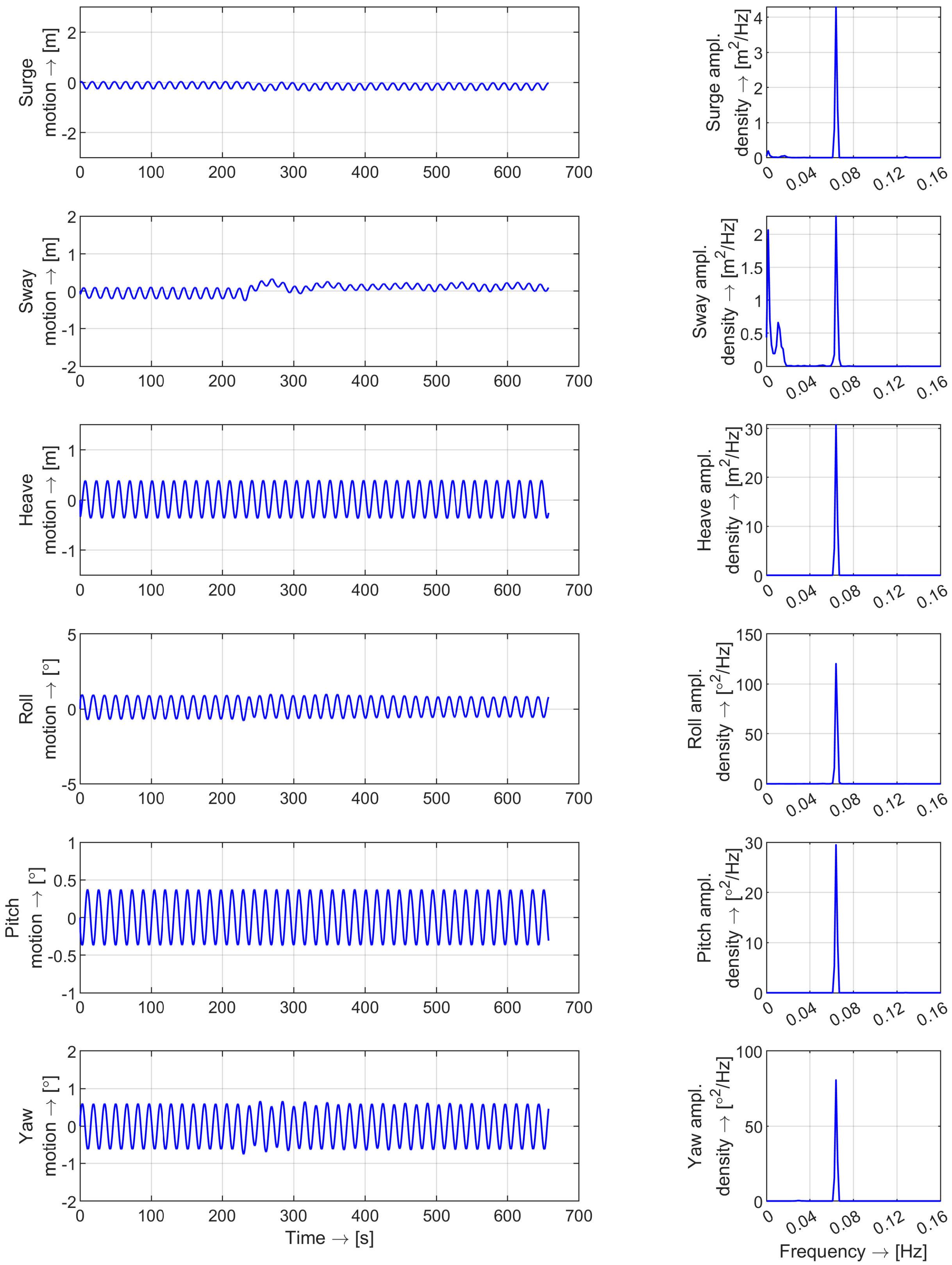

σ_{Surge} = n.a., σ_{Sway} = n.a., σ_{Heave} = n.a., σ_{Roll} = n.a., σ_{Pitch} = n.a., σ_{Yaw} = n.a.

Ship motions at centre of gravity (CoG) Depth = 18.0 m, H = 2.00 m, T = 15.60 s Bow-quartering waves	Monochromatic	M156e
	C4_M156e_Transition	
Deltares	11202696	App. G.141-2

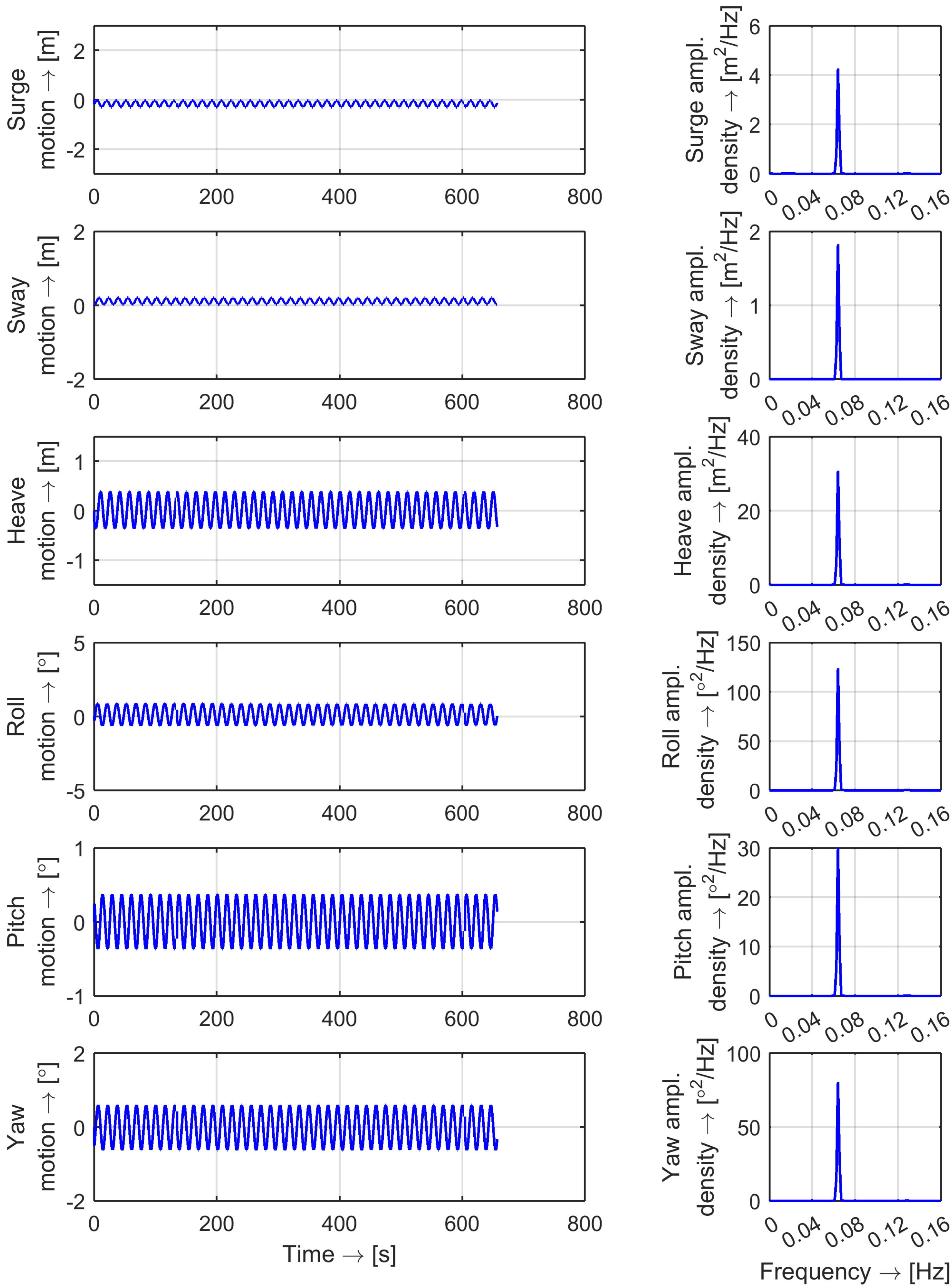

σ_{Surge} = 0.10 m, σ_{Sway} = 0.06 m, σ_{Heave} = 0.27 m, σ_{Roll} = 0.53°, σ_{Pitch} = 0.26°, σ_{Yaw} = 0.43°

Ship motions at centre of gravity (CoG) Depth = 18.0 m, H = 2.00 m, T = 15.60 s Bow-quartering waves	Monochromatic	M156e
	C4_M156e_noST	
Deltares	11202696	App. G.142-2

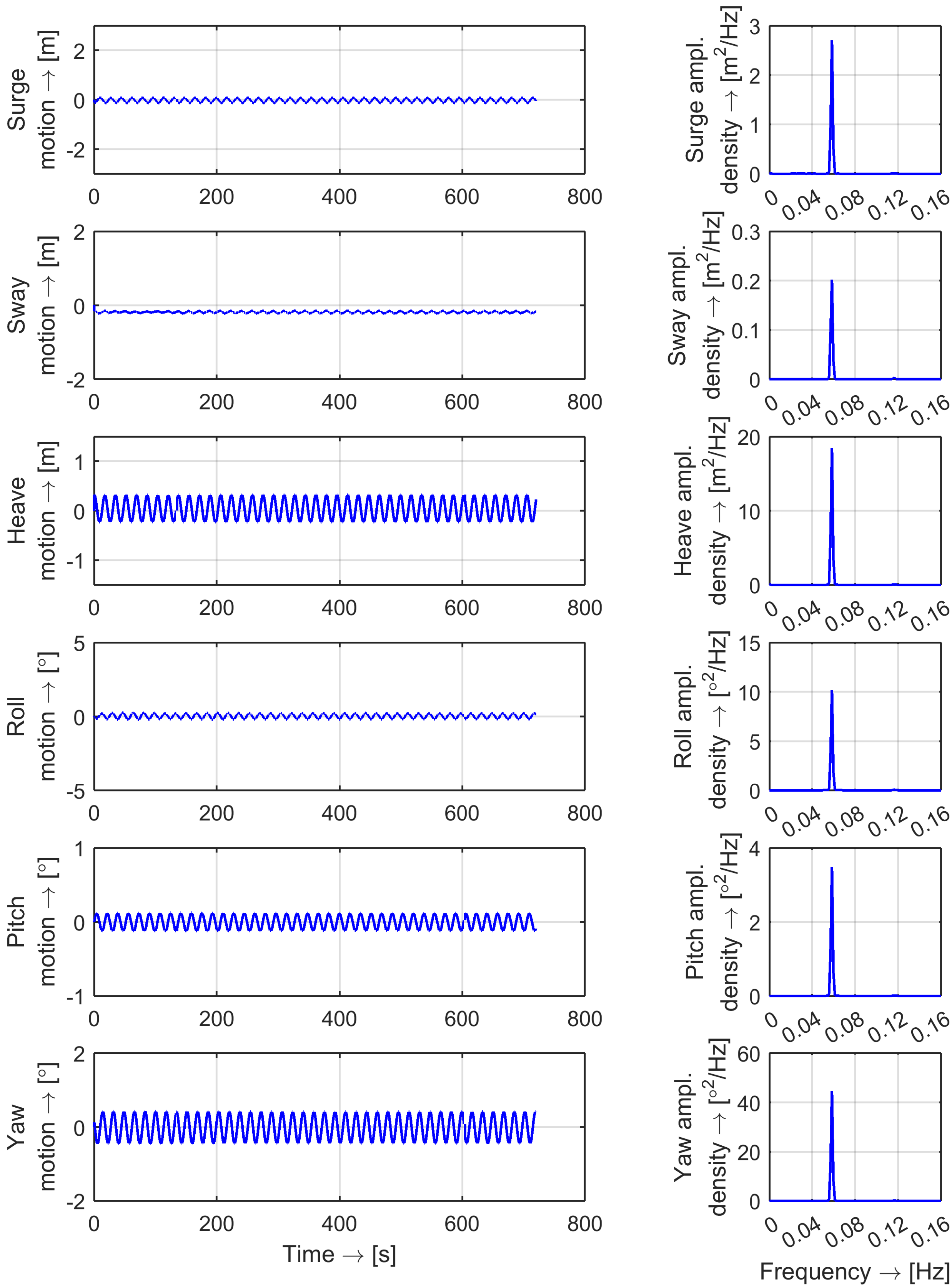

σ_{Surge} = 0.08 m, σ_{Sway} = 0.02 m, σ_{Heave} = 0.20 m, σ_{Roll} = 0.15°, σ_{Pitch} = 0.09°, σ_{Yaw} = 0.31°

Ship motions at centre of gravity (CoG) Depth = 18.0 m, H = 1.00 m, T = 17.20 s Bow-quartering waves	Monochromatic	M172a
	C4_M172a	
Deltares	11202696	App. G.143-2

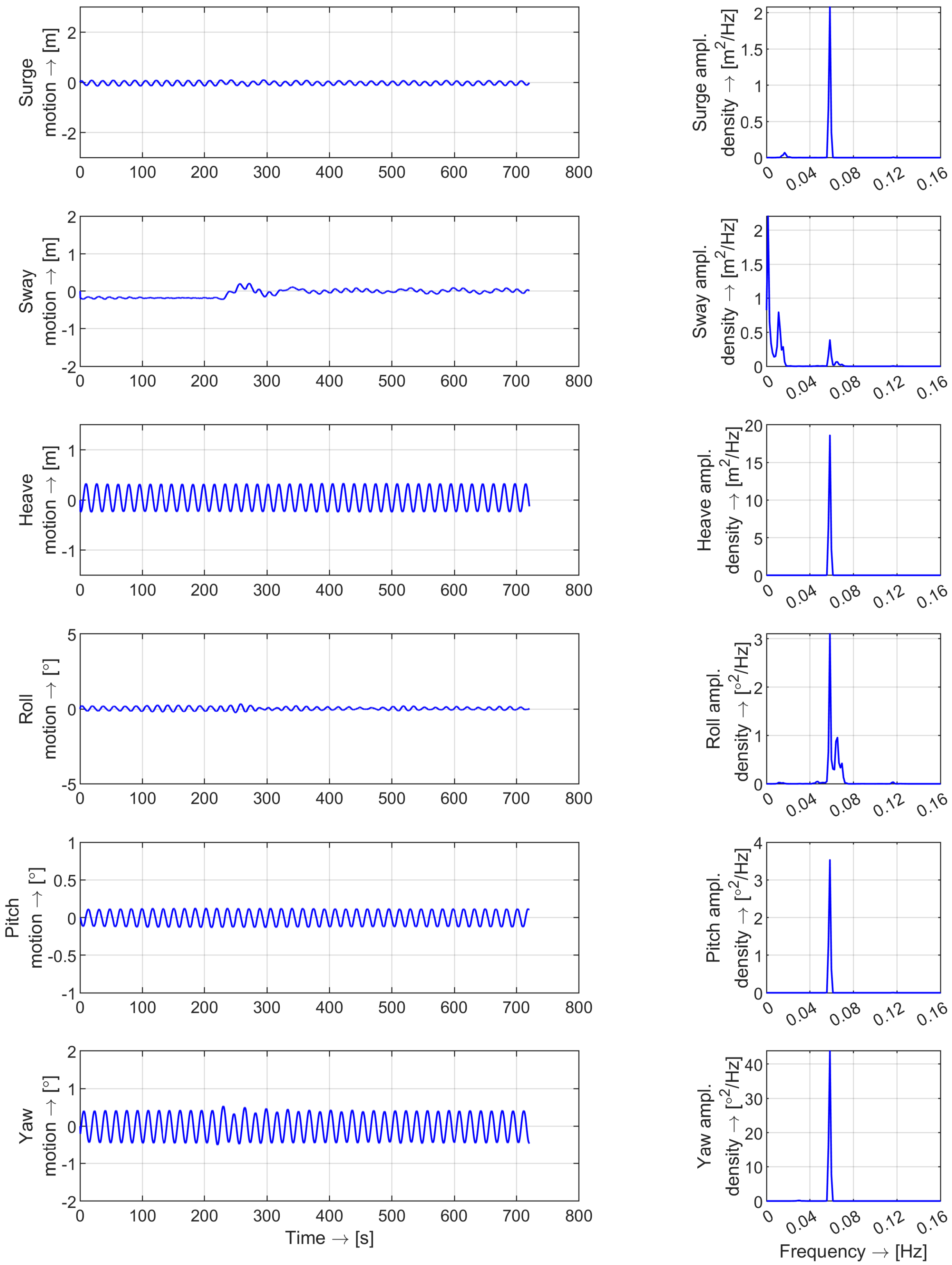

σ_{Surge} = n.a., σ_{Sway} = n.a., σ_{Heave} = n.a., σ_{Roll} = n.a., σ_{Pitch} = n.a., σ_{Yaw} = n.a.

Ship motions at centre of gravity (CoG) Depth = 18.0 m, H = 1.00 m, T = 17.20 s Bow-quartering waves	Monochromatic	M172a
	C4_M172a_Transition	
Deltares	11202696	App. G.144-2

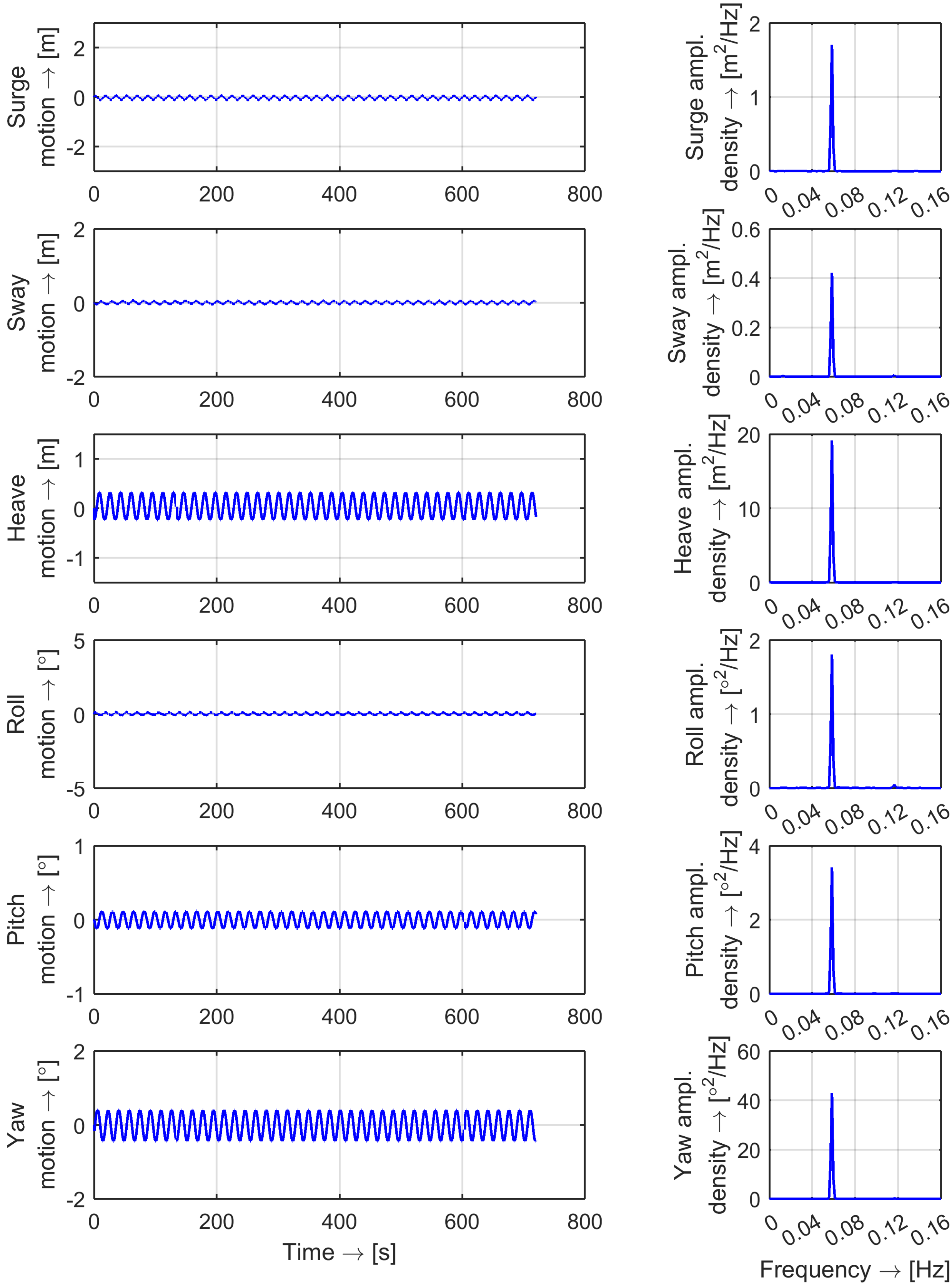

σ_{Surge} = 0.06 m, σ_{Sway} = 0.03 m, σ_{Heave} = 0.20 m, σ_{Roll} = 0.06°, σ_{Pitch} = 0.08°, σ_{Yaw} = 0.30°

Ship motions at centre of gravity (CoG) Depth = 18.0 m, H = 1.00 m, T = 17.20 s Bow-quartering waves	Monochromatic	M172a
	C4_M172a_noST	
Deltares	11202696	App. G.145-2

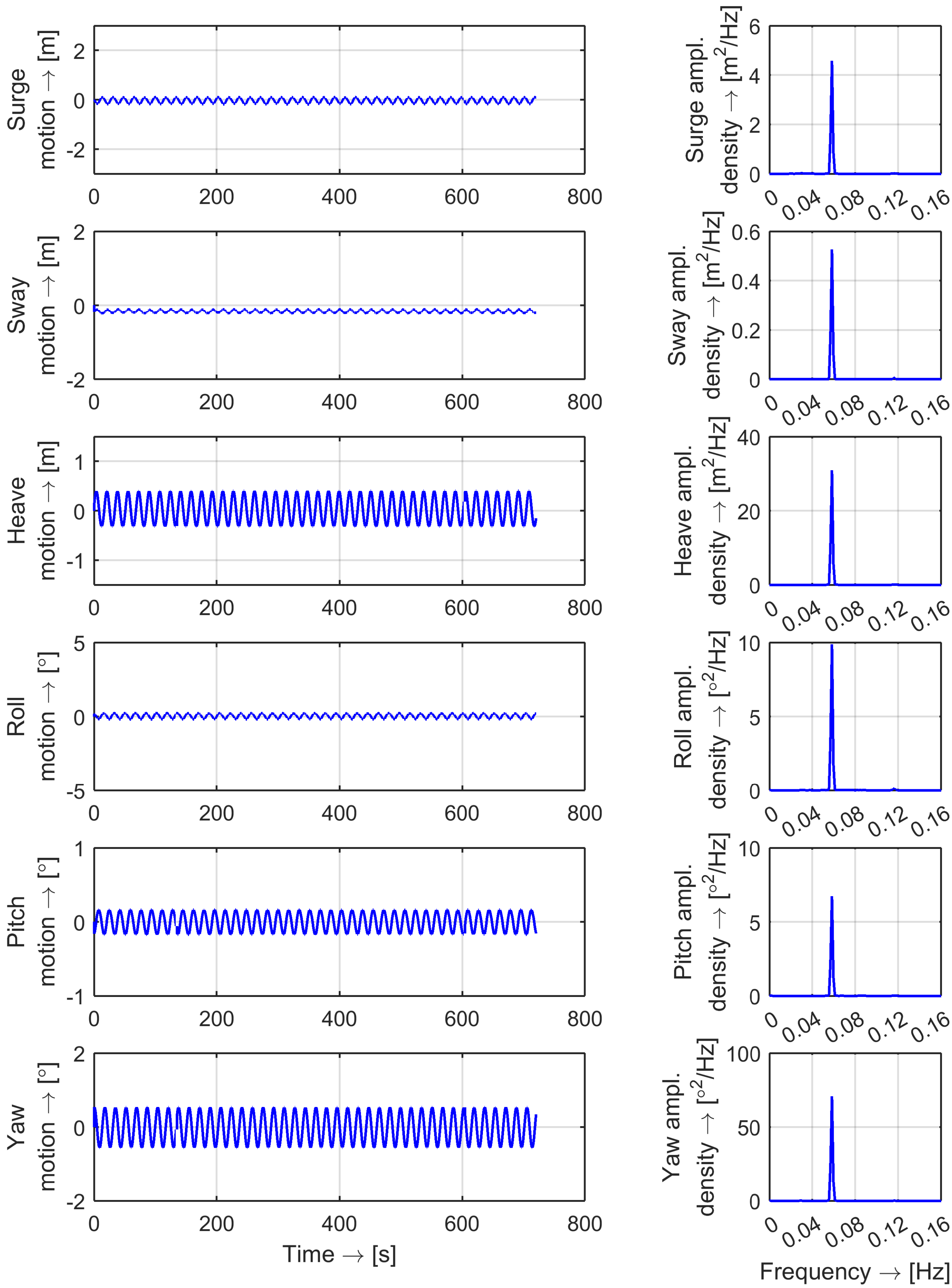

σ_{Surge} = 0.10 m, σ_{Sway} = 0.03 m, σ_{Heave} = 0.26 m, σ_{Roll} = 0.15°, σ_{Pitch} = 0.12°, σ_{Yaw} = 0.39°

Ship motions at centre of gravity (CoG) Depth = 18.0 m, H = 1.25 m, T = 17.20 s Bow-quartering waves	Monochromatic	M172b
	C4_M172b	
Deltares	11202696	App. G.146-2

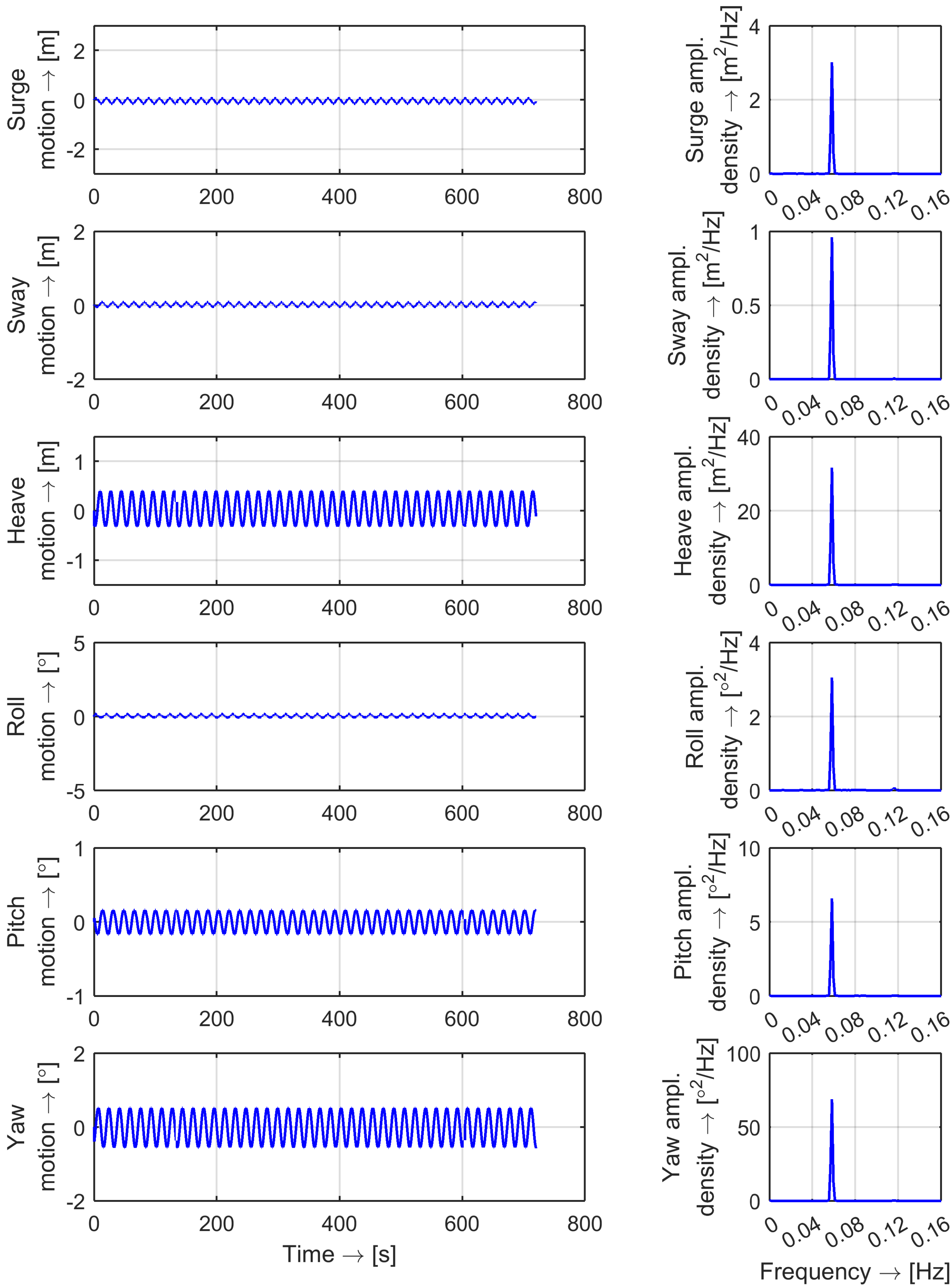

σ_{Surge} = 0.08 m, σ_{Sway} = 0.05 m, σ_{Heave} = 0.26 m, σ_{Roll} = 0.08°, σ_{Pitch} = 0.12°, σ_{Yaw} = 0.38°

Ship motions at centre of gravity (CoG) Depth = 18.0 m, H = 1.25 m, T = 17.20 s Bow-quartering waves	Monochromatic	M172b
	C4_M172b_noST	
Deltares	11202696	App. G.147-2

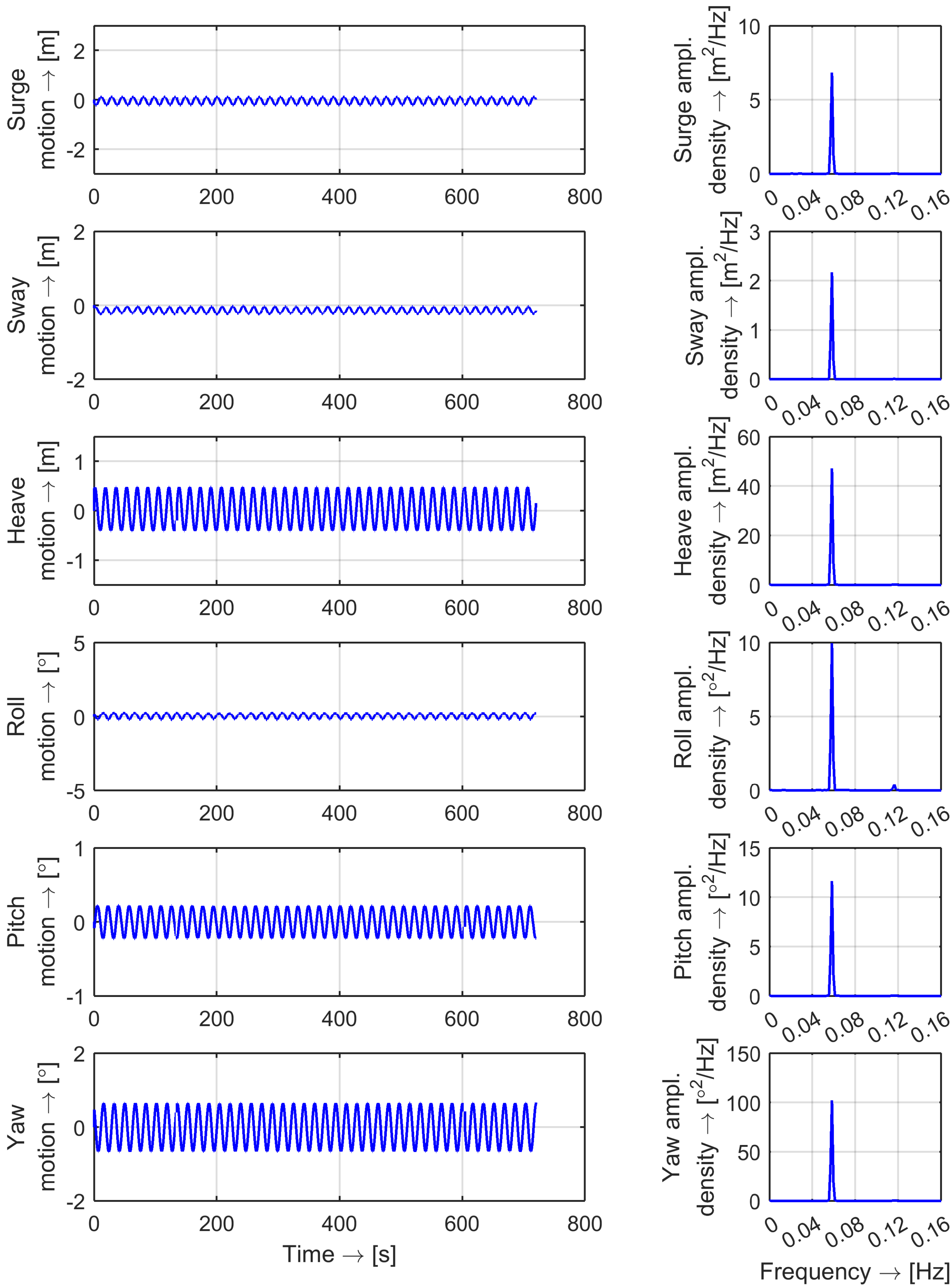

σ_{Surge} = 0.12 m, σ_{Sway} = 0.07 m, σ_{Heave} = 0.32 m, σ_{Roll} = 0.15°, σ_{Pitch} = 0.16°, σ_{Yaw} = 0.46°

Ship motions at centre of gravity (CoG) Depth = 18.0 m, H = 1.50 m, T = 17.20 s Bow-quartering waves	Monochromatic	M172c
	C4_M172c	
Deltares	11202696	App. G.148-2

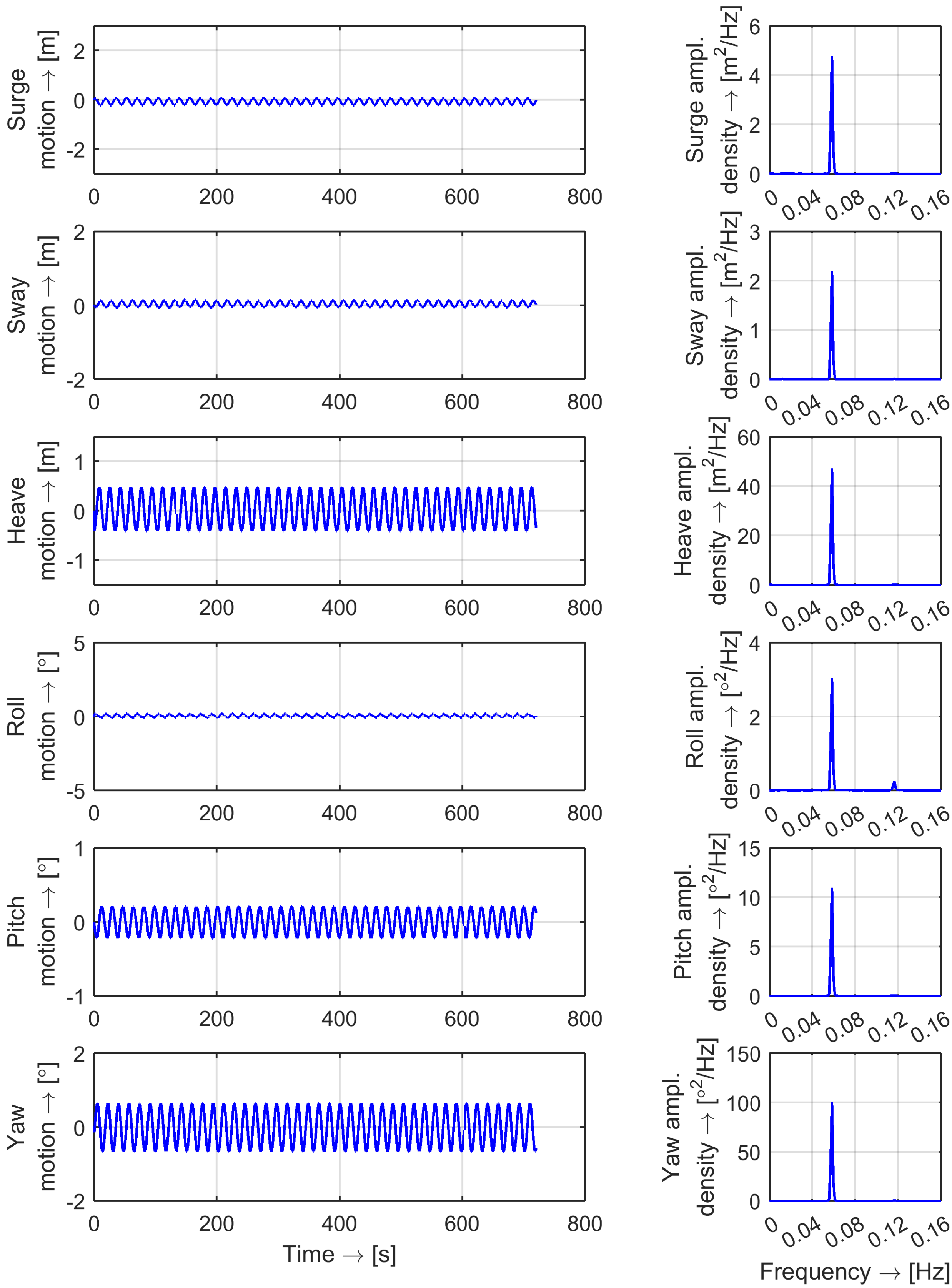

σ_{Surge} = 0.10 m, σ_{Sway} = 0.07 m, σ_{Heave} = 0.32 m, σ_{Roll} = 0.08°, σ_{Pitch} = 0.15°, σ_{Yaw} = 0.46°

Ship motions at centre of gravity (CoG) Depth = 18.0 m, H = 1.50 m, T = 17.20 s Bow-quartering waves	Monochromatic	M172c
	C4_M172c_noST	
Deltares	11202696	App. G.149-2

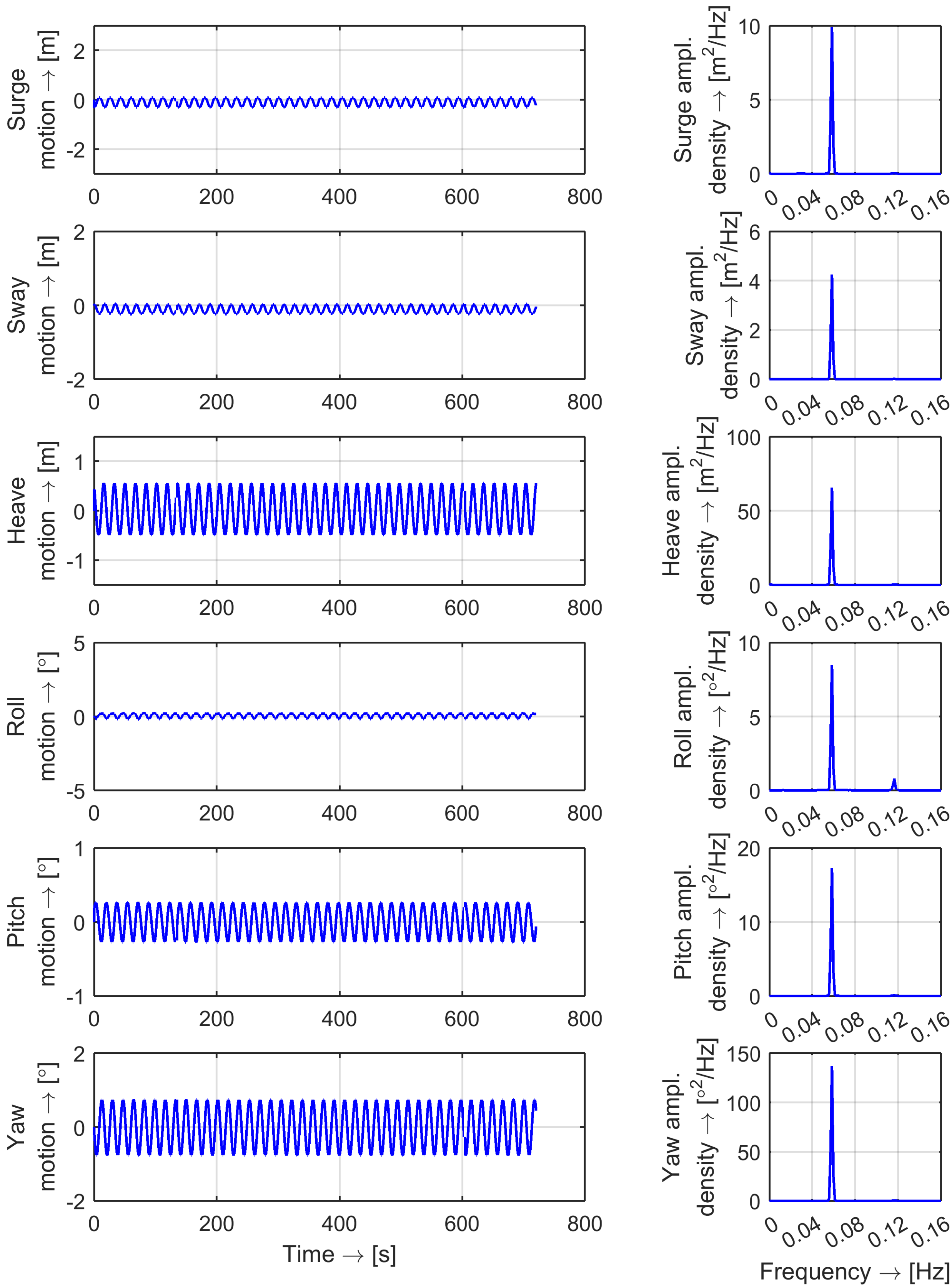

σ_{Surge} = 0.14 m, σ_{Sway} = 0.10 m, σ_{Heave} = 0.37 m, σ_{Roll} = 0.14°, σ_{Pitch} = 0.19°, σ_{Yaw} = 0.54°

Ship motions at centre of gravity (CoG) Depth = 18.0 m, H = 1.75 m, T = 17.20 s Bow-quartering waves	Monochromatic	M172d
	C4_M172d	
Deltares	11202696	App. G.150-2

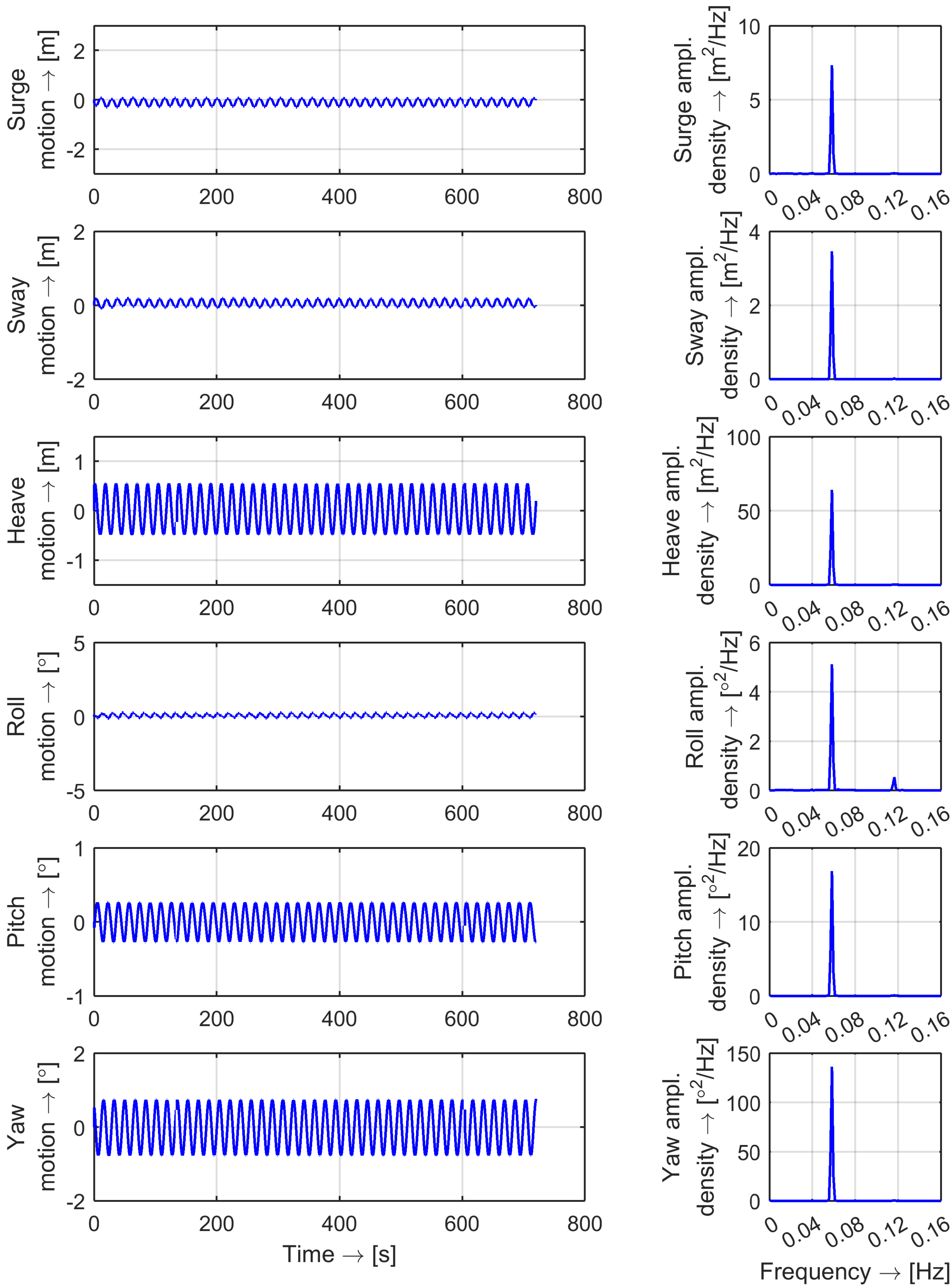

σ_{Surge} = 0.13 m, σ_{Sway} = 0.09 m, σ_{Heave} = 0.37 m, σ_{Roll} = 0.11°, σ_{Pitch} = 0.19°, σ_{Yaw} = 0.54°

Ship motions at centre of gravity (CoG) Depth = 18.0 m, H = 1.75 m, T = 17.20 s Bow-quartering waves	Monochromatic	M172d
	C4_M172d_noST	
Deltares	11202696	App. G.151-2

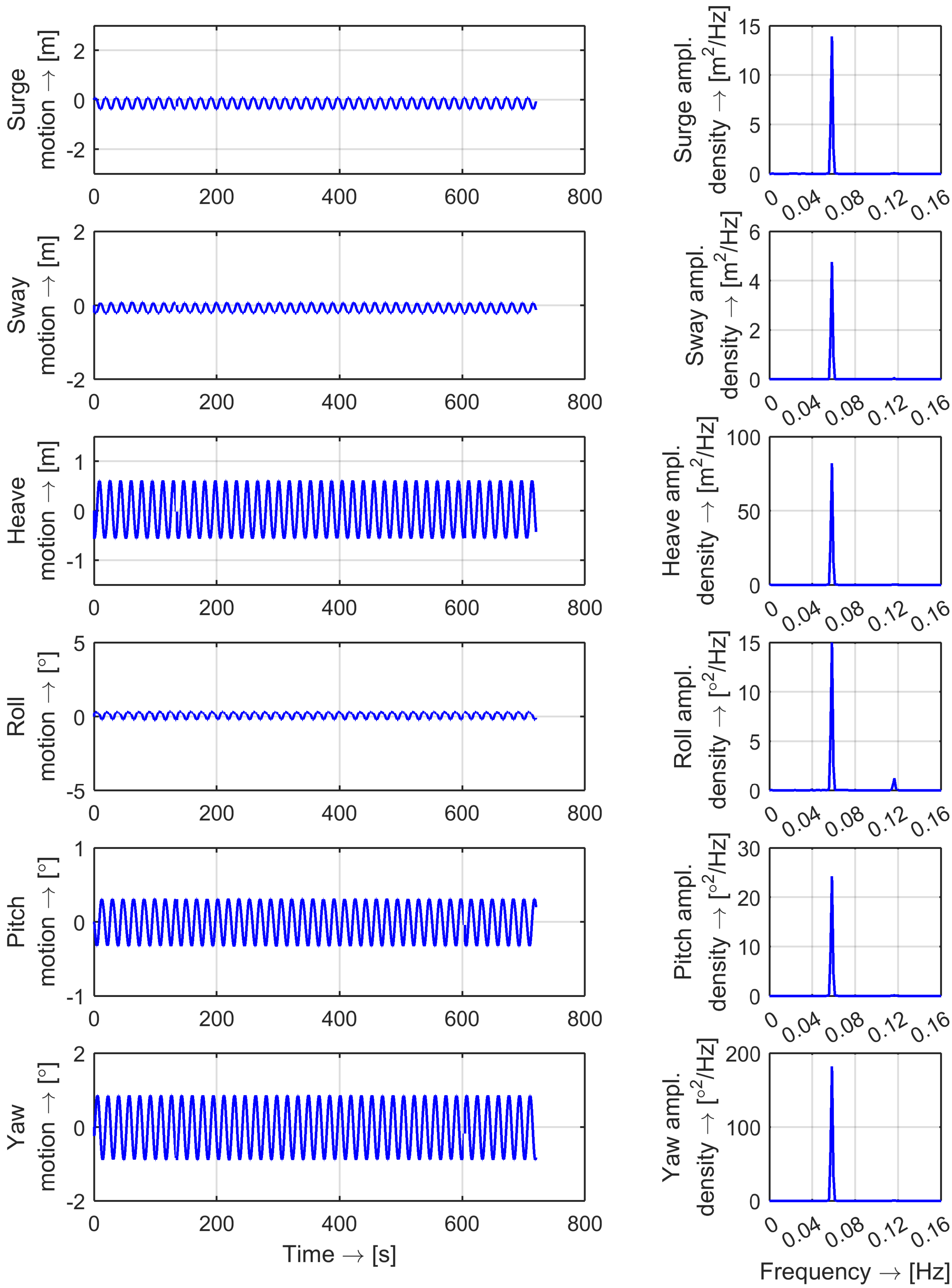

σ_{Surge} = 0.17 m, σ_{Sway} = 0.10 m, σ_{Heave} = 0.42 m, σ_{Roll} = 0.18°, σ_{Pitch} = 0.23°, σ_{Yaw} = 0.62°

Ship motions at centre of gravity (CoG) Depth = 18.0 m, H = 2.00 m, T = 17.20 s Bow-quartering waves	Monochromatic	M172e
	C4_M172e	
Deltares	11202696	App. G.152-2

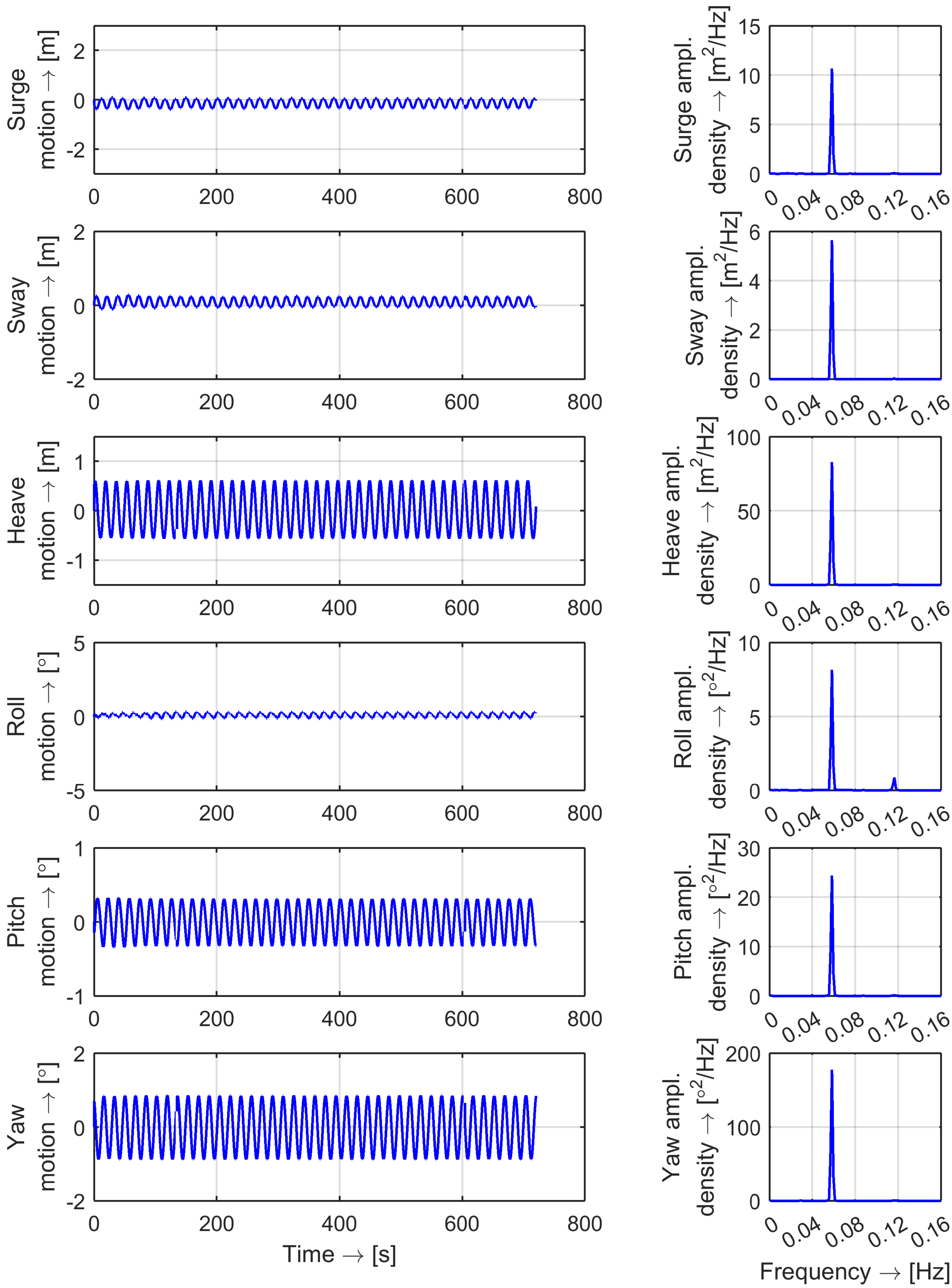

σ_{Surge} = 0.15 m, σ_{Sway} = 0.11 m, σ_{Heave} = 0.42 m, σ_{Roll} = 0.14°, σ_{Pitch} = 0.23°, σ_{Yaw} = 0.61°

Ship motions at centre of gravity (CoG) Depth = 18.0 m, H = 2.00 m, T = 17.20 s Bow-quartering waves	Monochromatic	M172e
	C4_M172e_noST	
Deltares	11202696	App. G.153-2

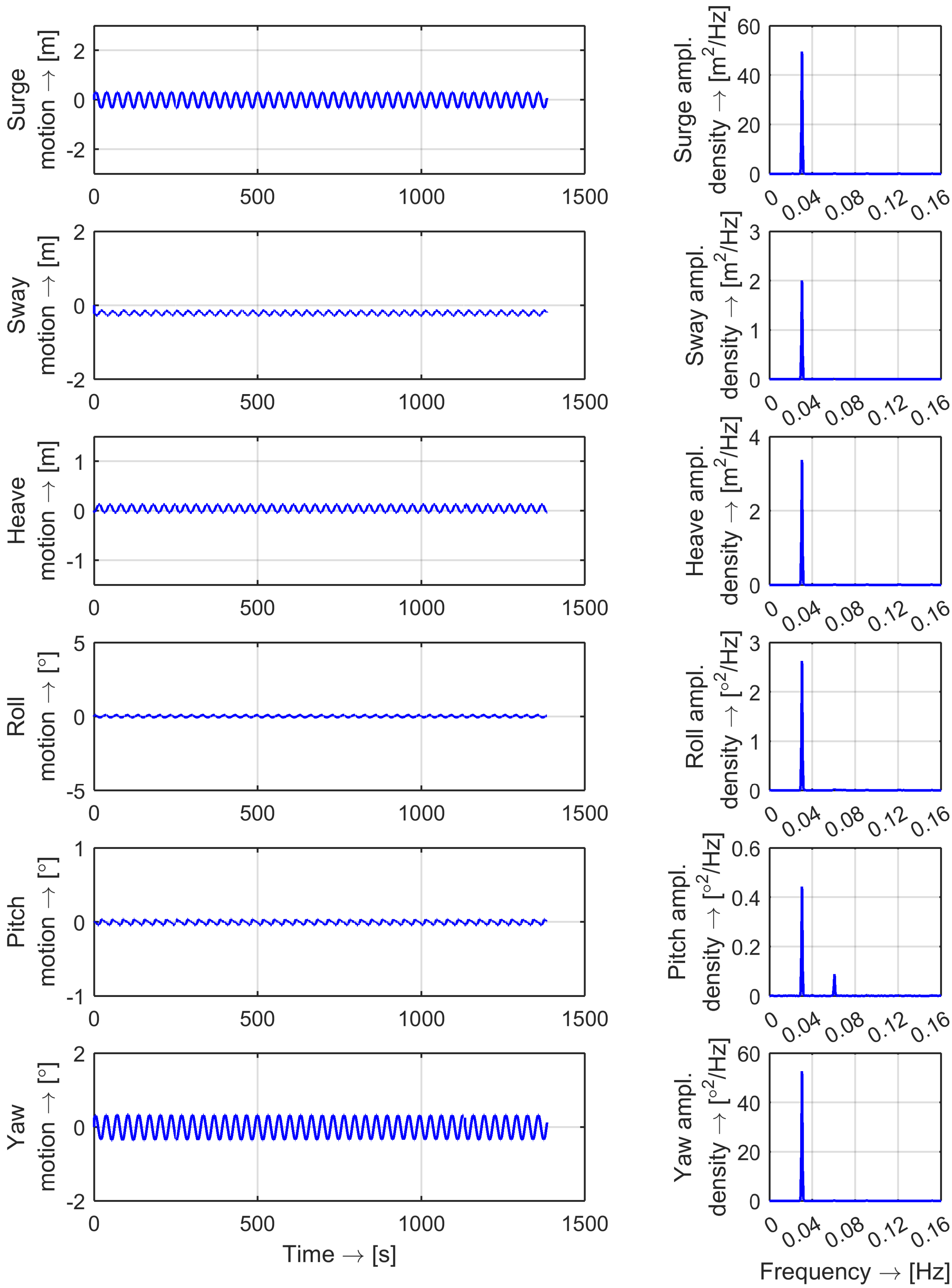

σ_{Surge} = 0.23 m, σ_{Sway} = 0.05 m, σ_{Heave} = 0.06 m, σ_{Roll} = 0.05°, σ_{Pitch} = 0.02°, σ_{Yaw} = 0.24°

Ship motions at centre of gravity (CoG) Depth = 18.0 m, H = 0.25 m, T = 33.00 s Bow-quartering waves	Monochromatic	M330a
	C4_M330a	
Deltares	11202696	App. G.154-2

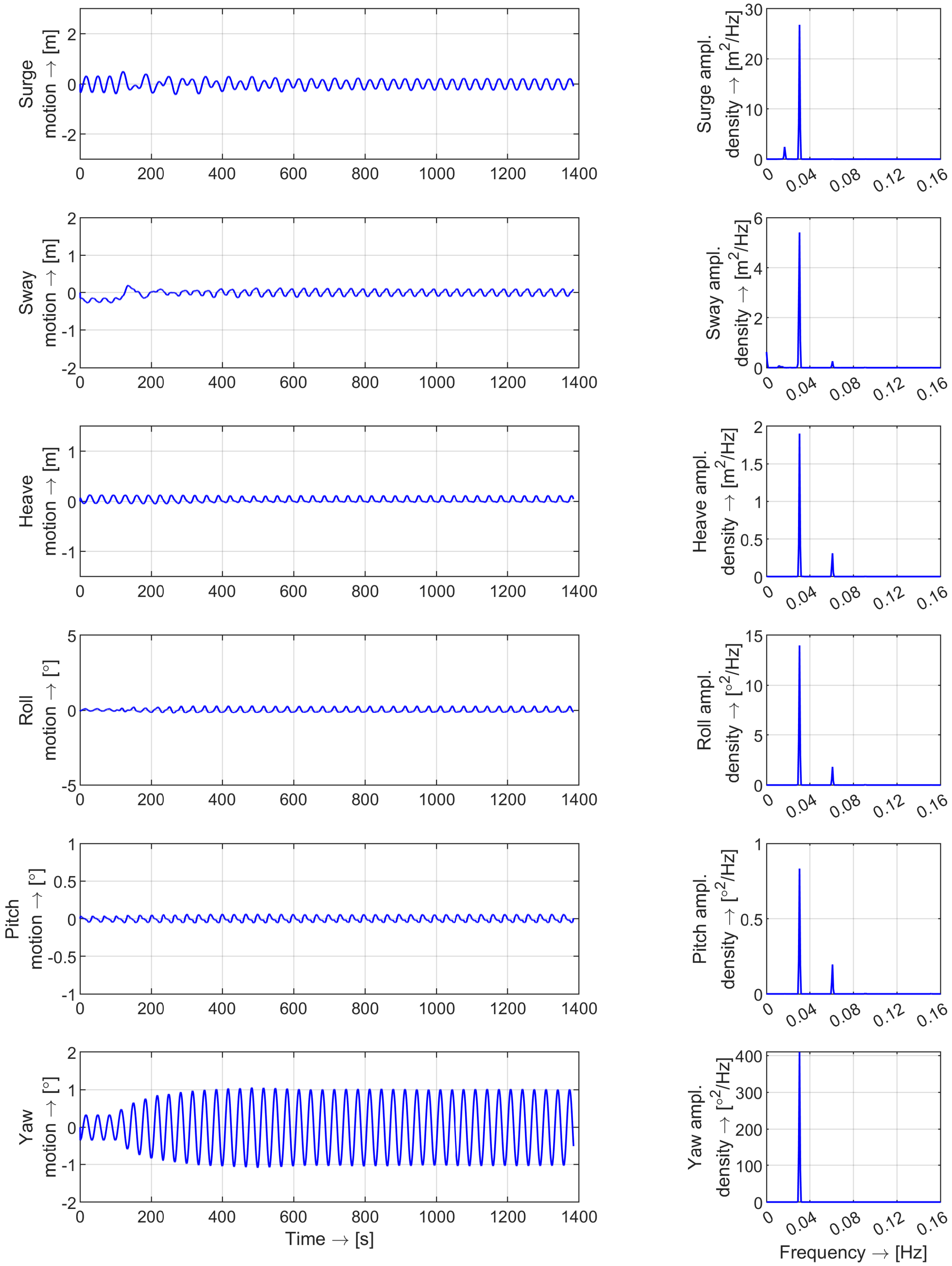

σ_{Surge} = n.a., σ_{Sway} = n.a., σ_{Heave} = n.a., σ_{Roll} = n.a., σ_{Pitch} = n.a., σ_{Yaw} = n.a.

Ship motions at centre of gravity (CoG) Depth = 18.0 m, H = 0.25 m, T = 33.00 s Bow-quartering waves	Monochromatic	M330a
	C4_M330a_Transition	
Deltares	11202696	App. G.155-2

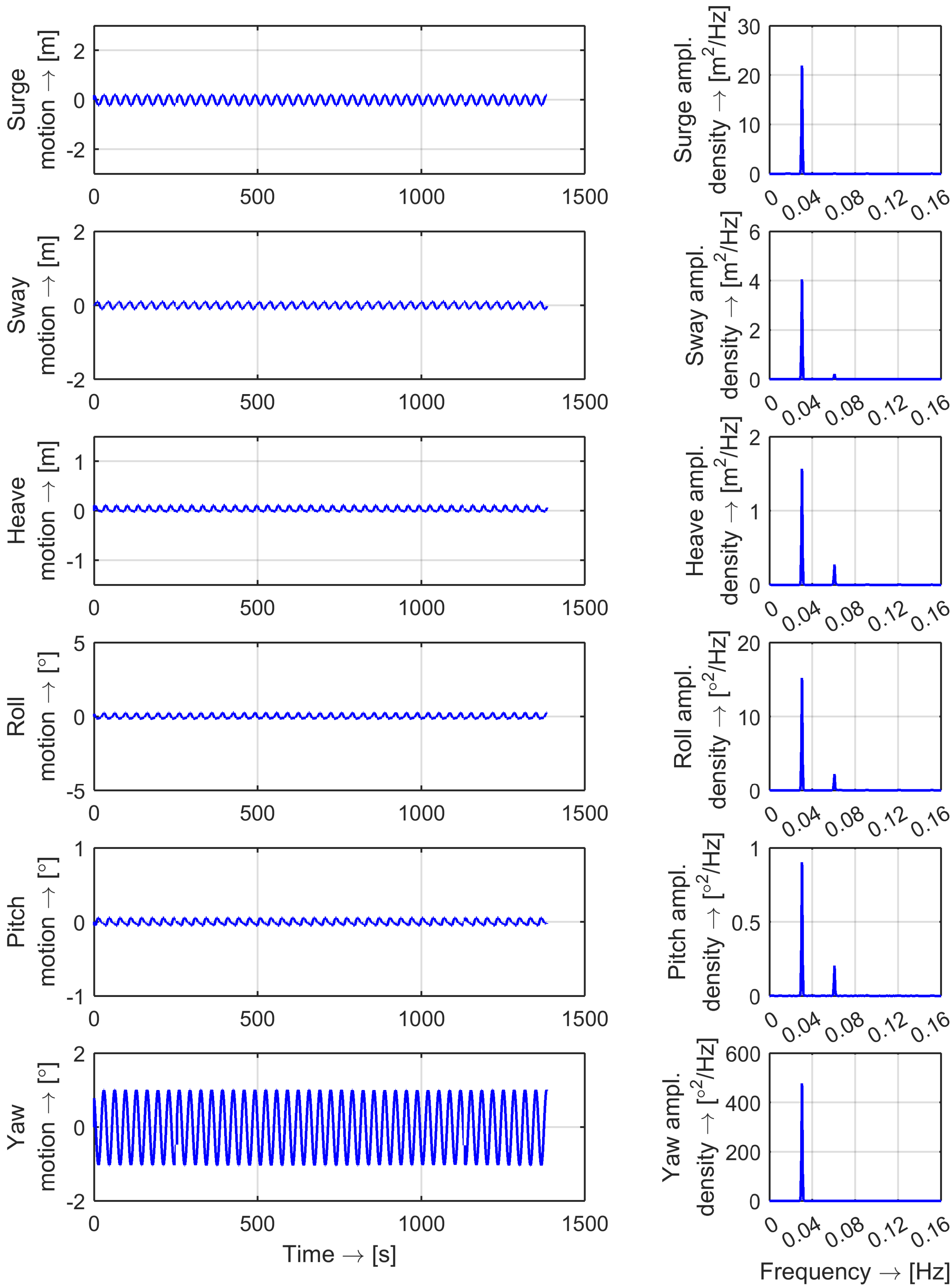

σ_{Surge} = 0.15 m, σ_{Sway} = 0.07 m, σ_{Heave} = 0.04 m, σ_{Roll} = 0.14°, σ_{Pitch} = 0.03°, σ_{Yaw} = 0.72°

Ship motions at centre of gravity (CoG) Depth = 18.0 m, H = 0.25 m, T = 33.00 s Bow-quartering waves	Monochromatic	M330a
	C4_M330a_noST	
Deltares	11202696	App. G.156-2

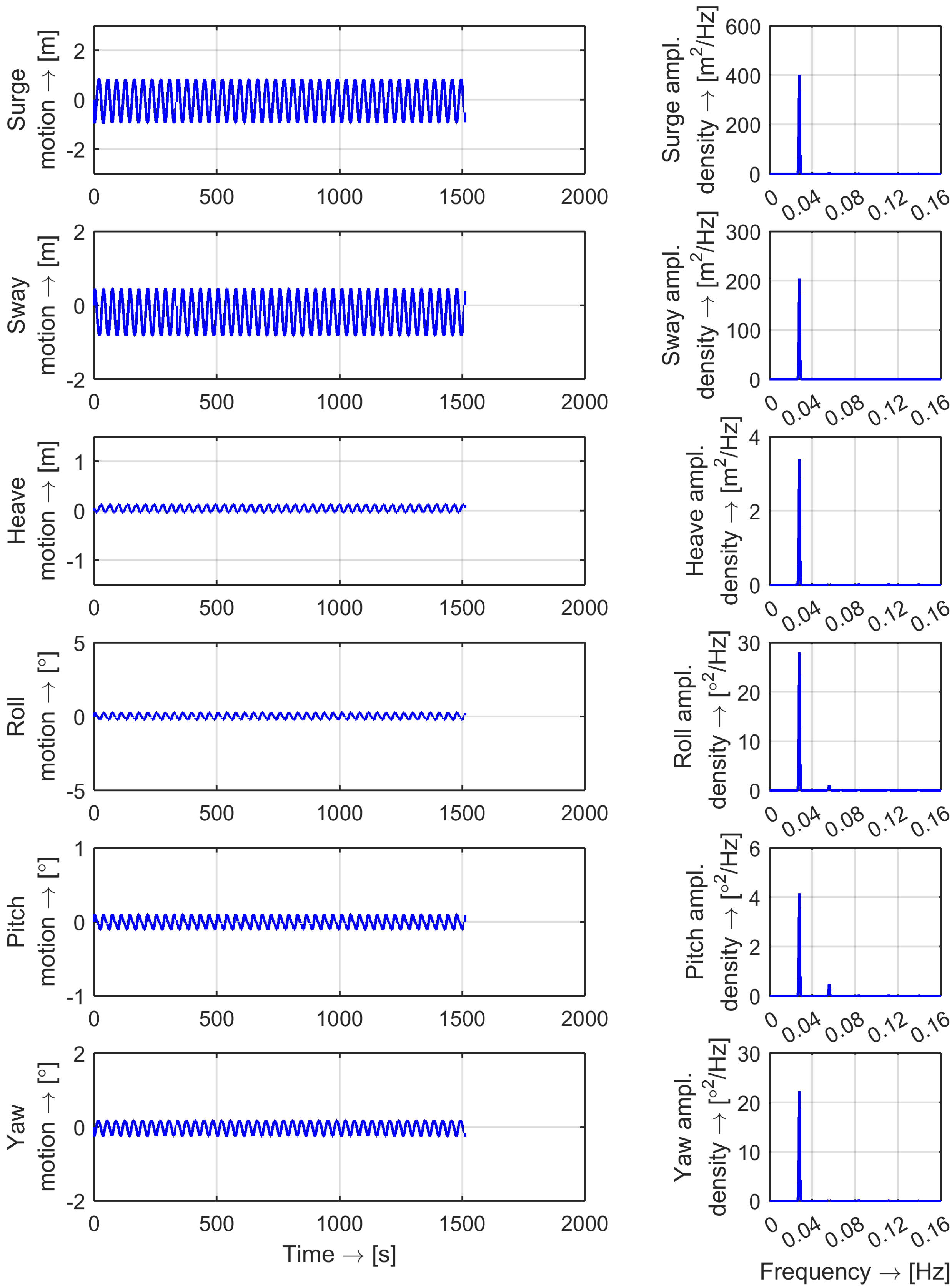

σ_{Surge} = 0.63 m, σ_{Sway} = 0.45 m, σ_{Heave} = 0.06 m, σ_{Roll} = 0.17°, σ_{Pitch} = 0.07°, σ_{Yaw} = 0.15°

Ship motions at centre of gravity (CoG) Depth = 18.0 m, H = 0.25 m, T = 36.00 s Bow-quartering waves	Monochromatic	M360a
	C4_M360a	
Deltares	11202696	App. G.157-2

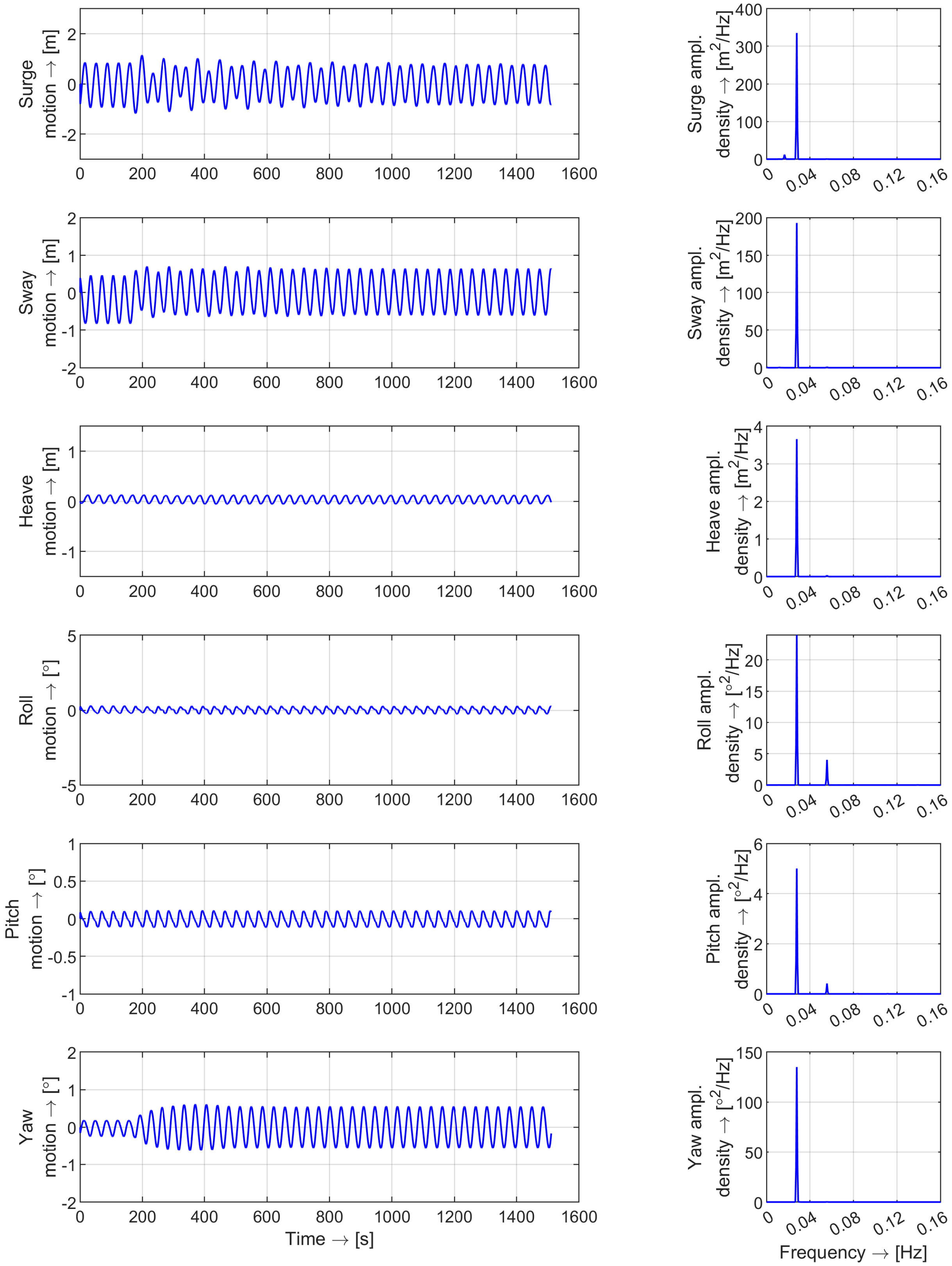

σ_{Surge} = n.a., σ_{Sway} = n.a., σ_{Heave} = n.a., σ_{Roll} = n.a., σ_{Pitch} = n.a., σ_{Yaw} = n.a.

Ship motions at centre of gravity (CoG) Depth = 18.0 m, H = 0.25 m, T = 36.00 s Bow-quartering waves	Monochromatic	M360a
	C4_M360a_Transition	
Deltares	11202696	App. G.158-2

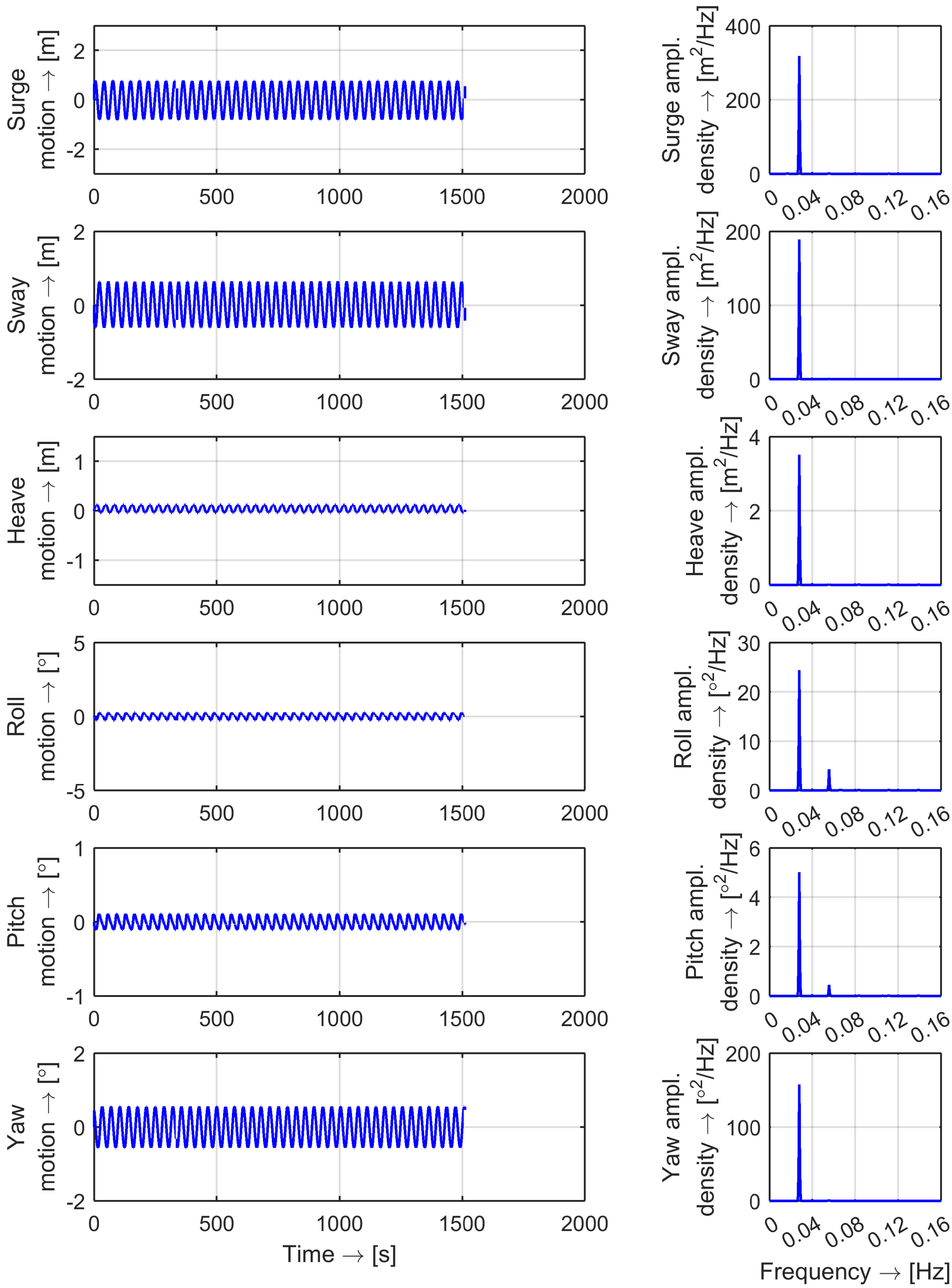

σ_{Surge} = 0.56 m, σ_{Sway} = 0.43 m, σ_{Heave} = 0.06 m, σ_{Roll} = 0.17°, σ_{Pitch} = 0.07°, σ_{Yaw} = 0.40°

Ship motions at centre of gravity (CoG) Depth = 18.0 m, H = 0.25 m, T = 36.00 s Bow-quartering waves	Monochromatic	M360a
	C4_M360a_noST	
Deltares	11202696	App. G.159-2

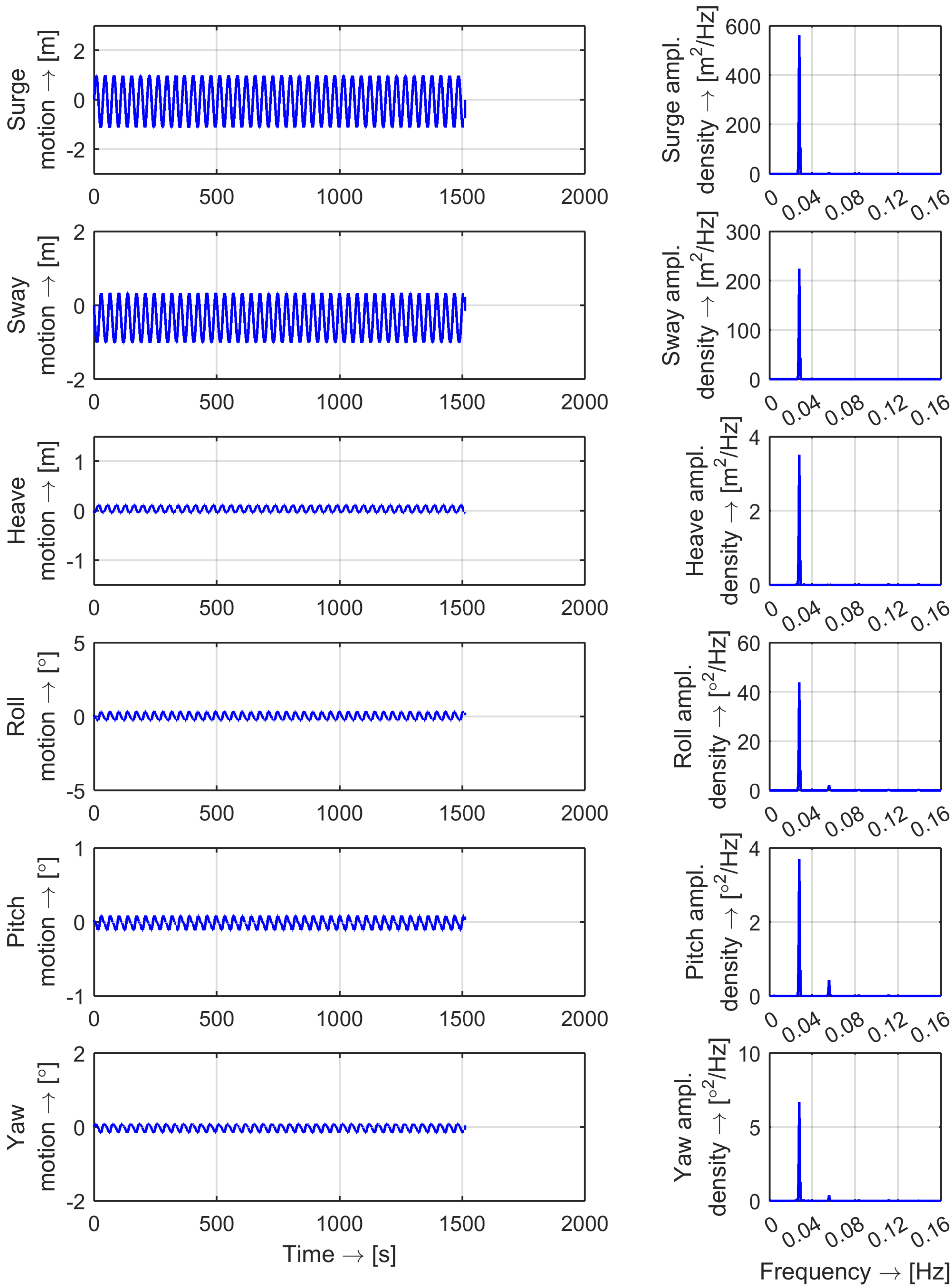

σ_{Surge} = 0.75 m, σ_{Sway} = 0.47 m, σ_{Heave} = 0.06 m, σ_{Roll} = 0.21°, σ_{Pitch} = 0.06°, σ_{Yaw} = 0.08°

Ship motions at centre of gravity (CoG) Depth = 18.0 m, H = 0.25 m, T = 36.00 s Bow-quartering waves	Monochromatic	M360a
	C4_M360a_200t	
Deltares	11202696	App. G.160-2

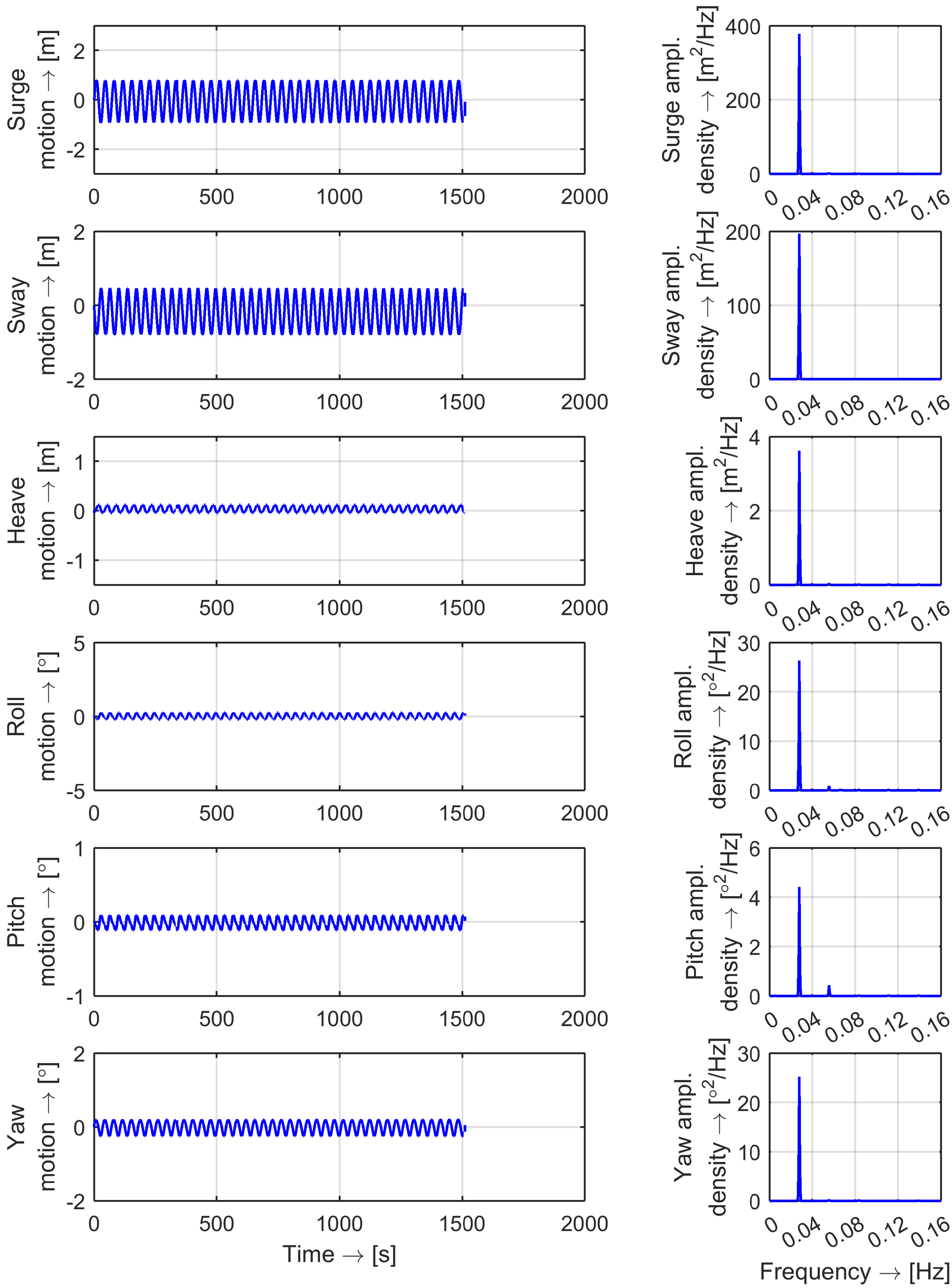

σ_{Surge} = 0.61 m, σ_{Sway} = 0.44 m, σ_{Heave} = 0.06 m, σ_{Roll} = 0.16°, σ_{Pitch} = 0.07°, σ_{Yaw} = 0.16°

Ship motions at centre of gravity (CoG) Depth = 18.0 m, H = 0.25 m, T = 36.00 s Bow-quartering waves	Monochromatic	M360a
	C4_M360a_sga	
Deltares	11202696	App. G.161-2

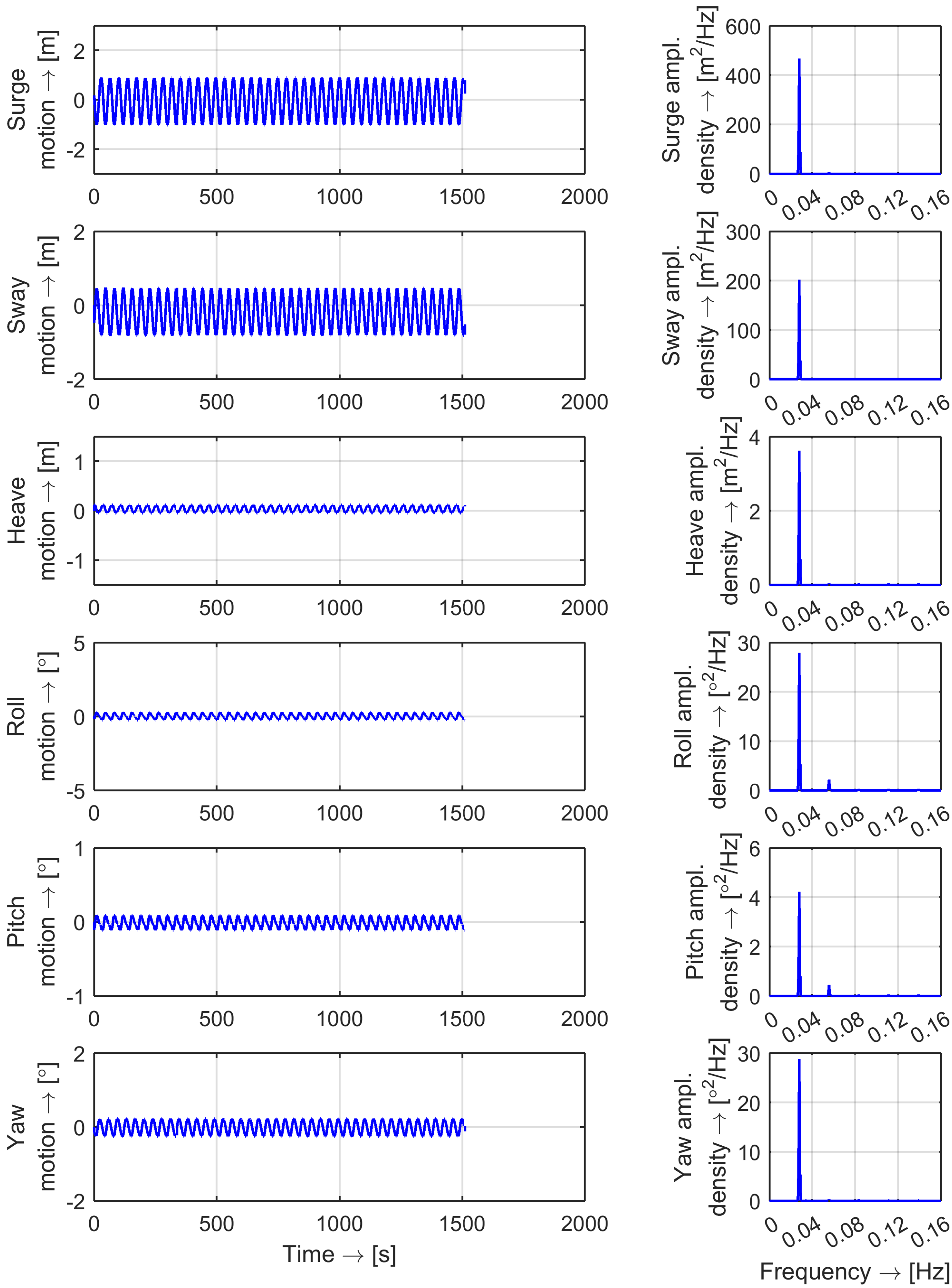

σ_{Surge} = 0.68 m, σ_{Sway} = 0.45 m, σ_{Heave} = 0.06 m, σ_{Roll} = 0.17°, σ_{Pitch} = 0.07°, σ_{Yaw} = 0.17°

Ship motions at centre of gravity (CoG) Depth = 18.0 m, H = 0.25 m, T = 36.00 s Bow-quartering waves	Monochromatic	M360a
	C4_M360a_sk	
Deltares	11202696	App. G.162-2

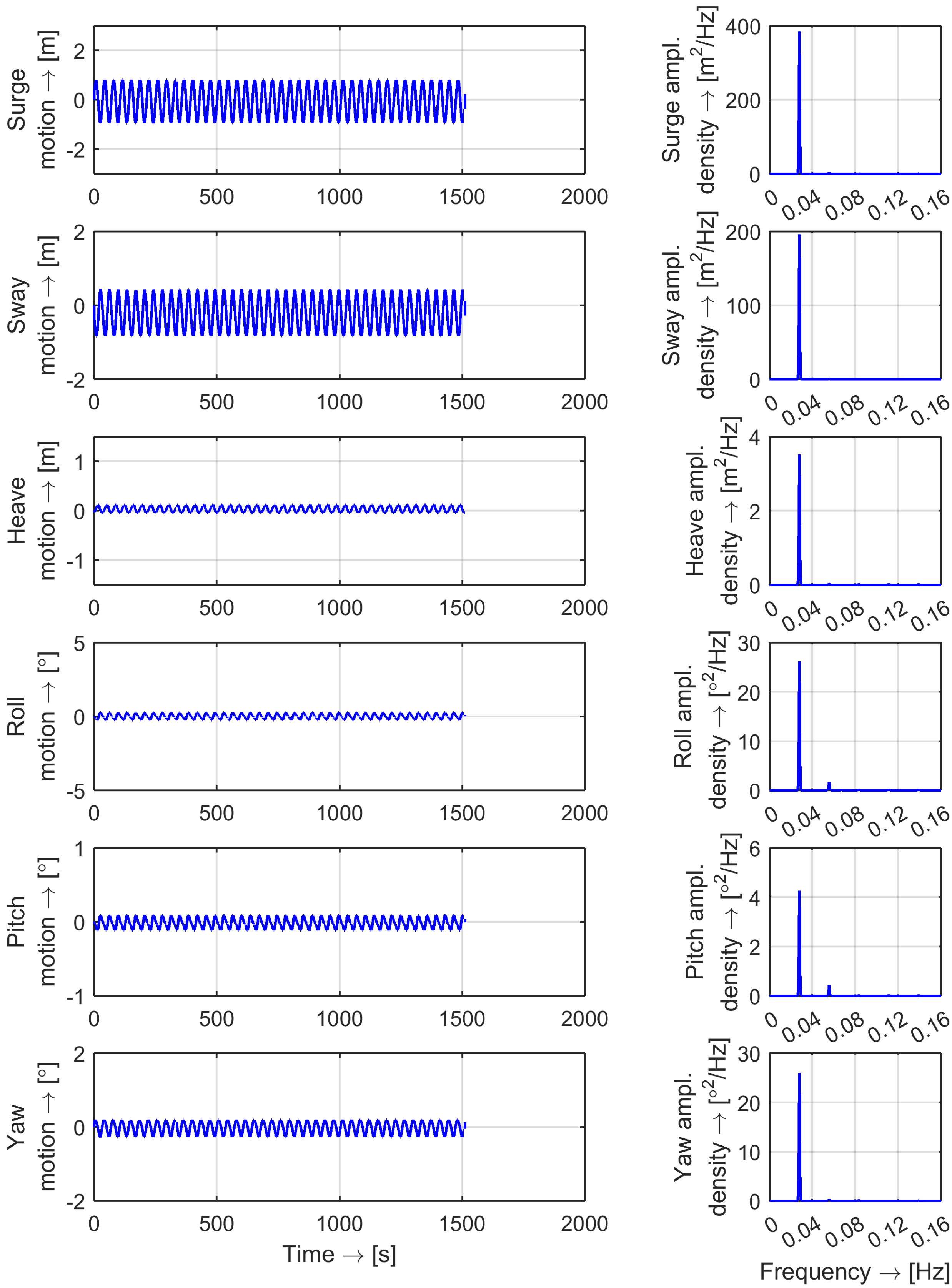

σ_{Surge} = 0.62 m, σ_{Sway} = 0.44 m, σ_{Heave} = 0.06 m, σ_{Roll} = 0.17°, σ_{Pitch} = 0.07°, σ_{Yaw} = 0.16°

Ship motions at centre of gravity (CoG) Depth = 18.0 m, H = 0.25 m, T = 36.00 s Bow-quartering waves	Monochromatic	M360a
	C4_M360a_ssk	
Deltares	11202696	App. G.163-2

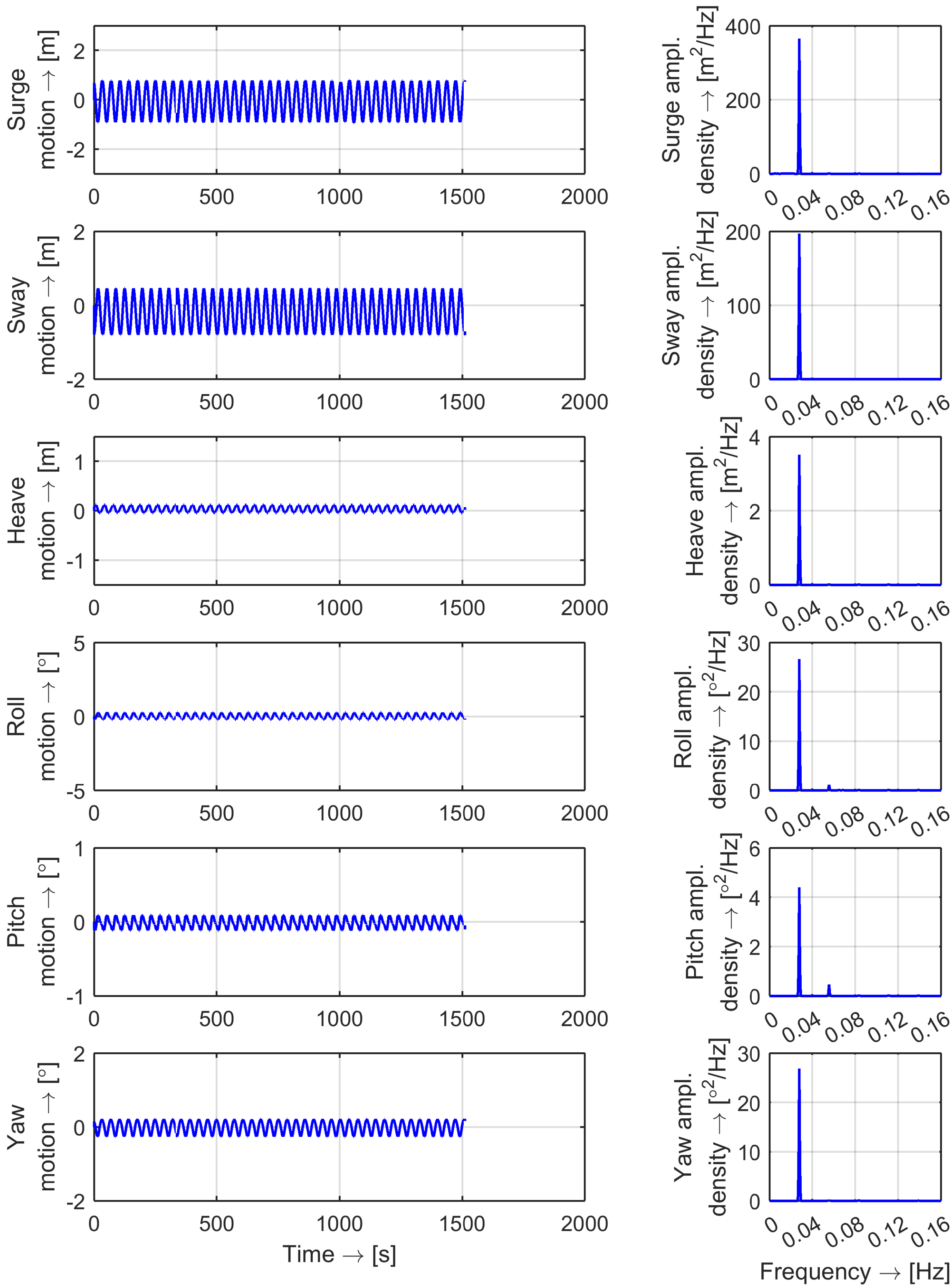

σ_{Surge} = 0.60 m, σ_{Sway} = 0.44 m, σ_{Heave} = 0.06 m, σ_{Roll} = 0.17°, σ_{Pitch} = 0.07°, σ_{Yaw} = 0.16°

Ship motions at centre of gravity (CoG) Depth = 18.0 m, H = 0.25 m, T = 36.00 s Bow-quartering waves	Monochromatic	M360a
	C4_M360a_ssk_sga	
Deltares	11202696	App. G.164-2

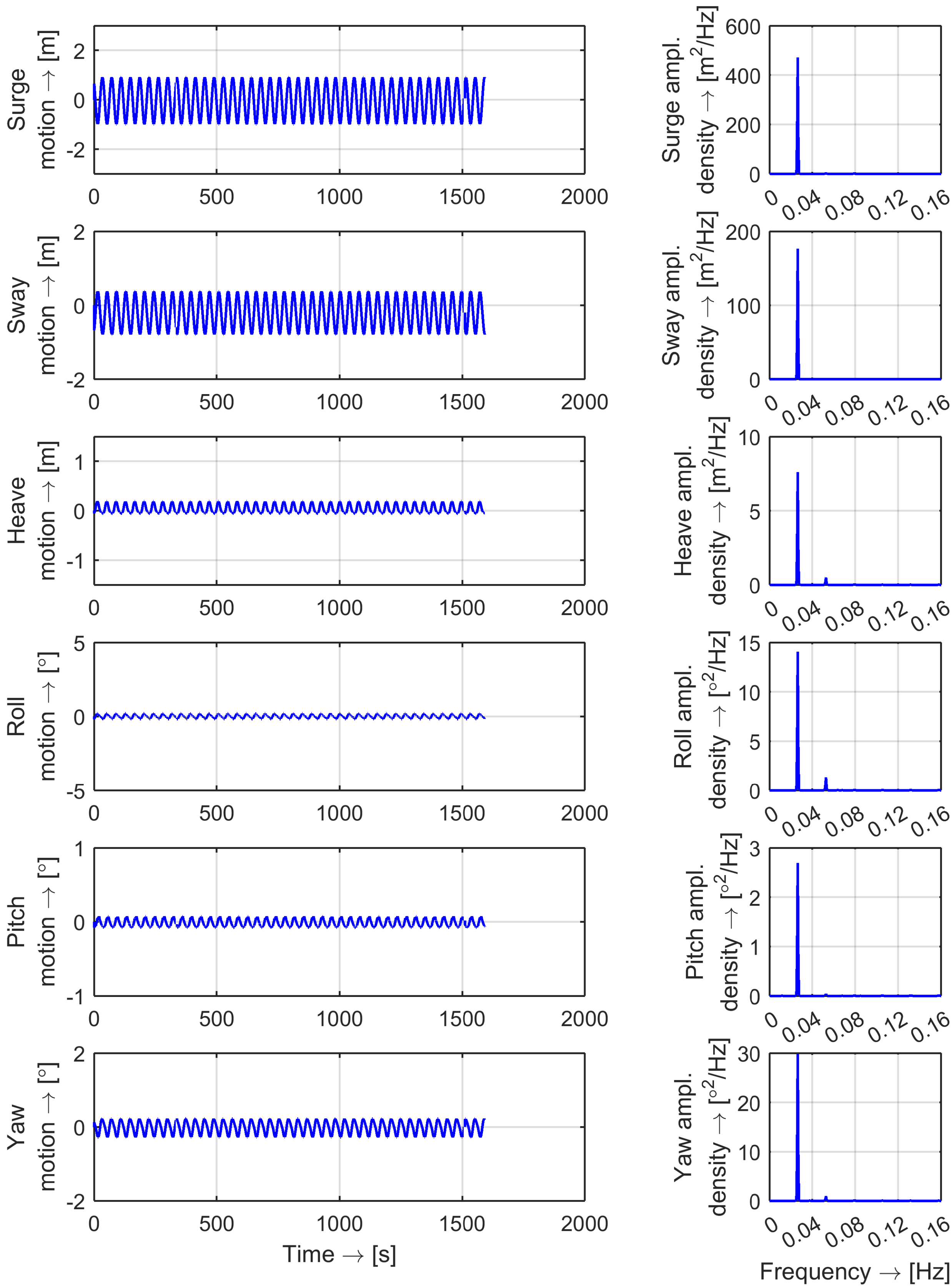

σ_{Surge} = 0.67 m, σ_{Sway} = 0.41 m, σ_{Heave} = 0.09 m, σ_{Roll} = 0.12°, σ_{Pitch} = 0.05°, σ_{Yaw} = 0.17°

Ship motions at centre of gravity (CoG) Depth = 18.0 m, H = 0.25 m, T = 38.00 s Bow-quartering waves	Monochromatic	M380a
	C4_M380a	
Deltares	11202696	App. G.165-2

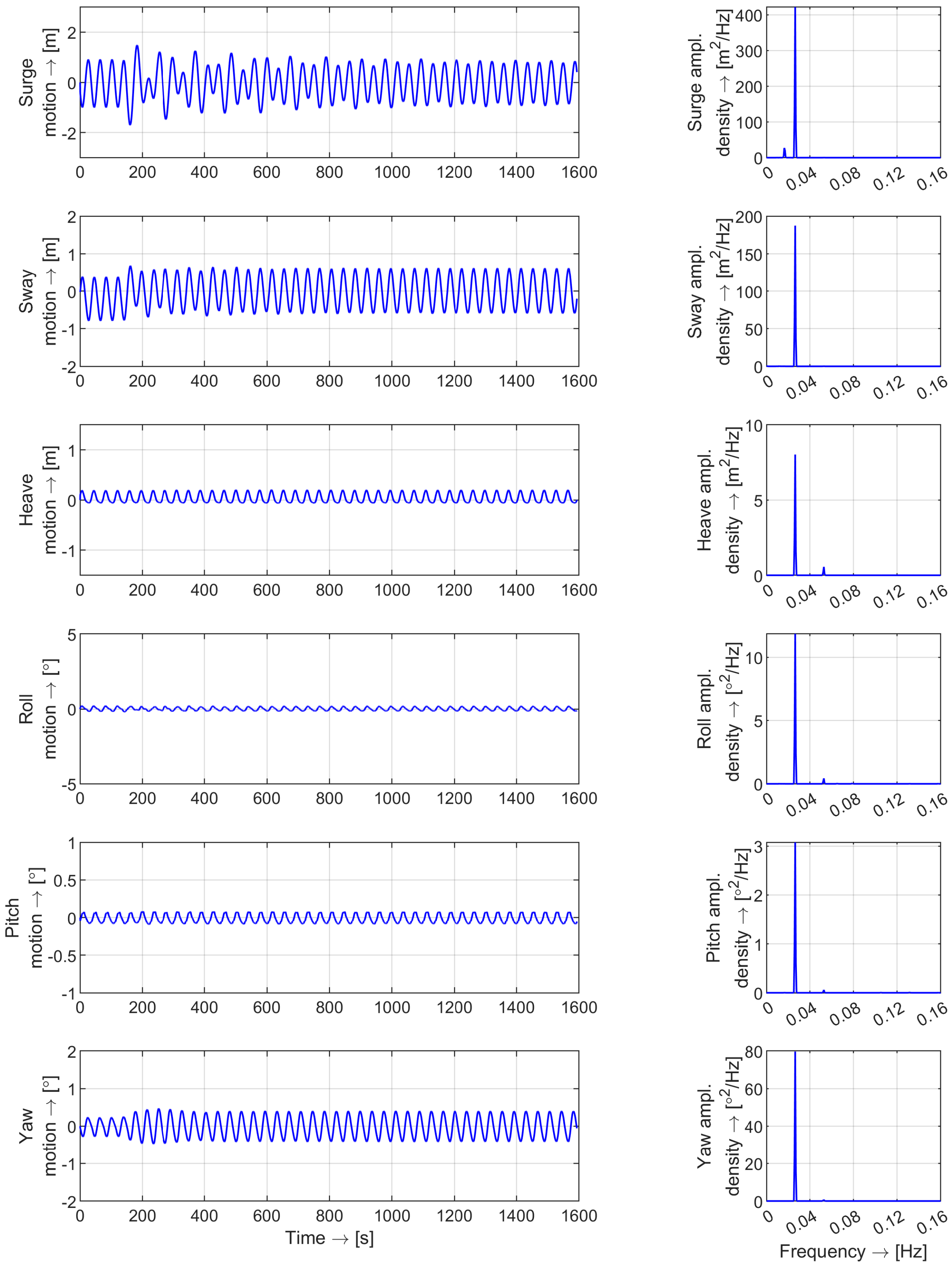

σ_{Surge} = n.a., σ_{Sway} = n.a., σ_{Heave} = n.a., σ_{Roll} = n.a., σ_{Pitch} = n.a., σ_{Yaw} = n.a.

Ship motions at centre of gravity (CoG) Depth = 18.0 m, H = 0.25 m, T = 38.00 s Bow-quartering waves	Monochromatic	M380a
	C4_M380a_Transition	
Deltares	11202696	App. G.166-2

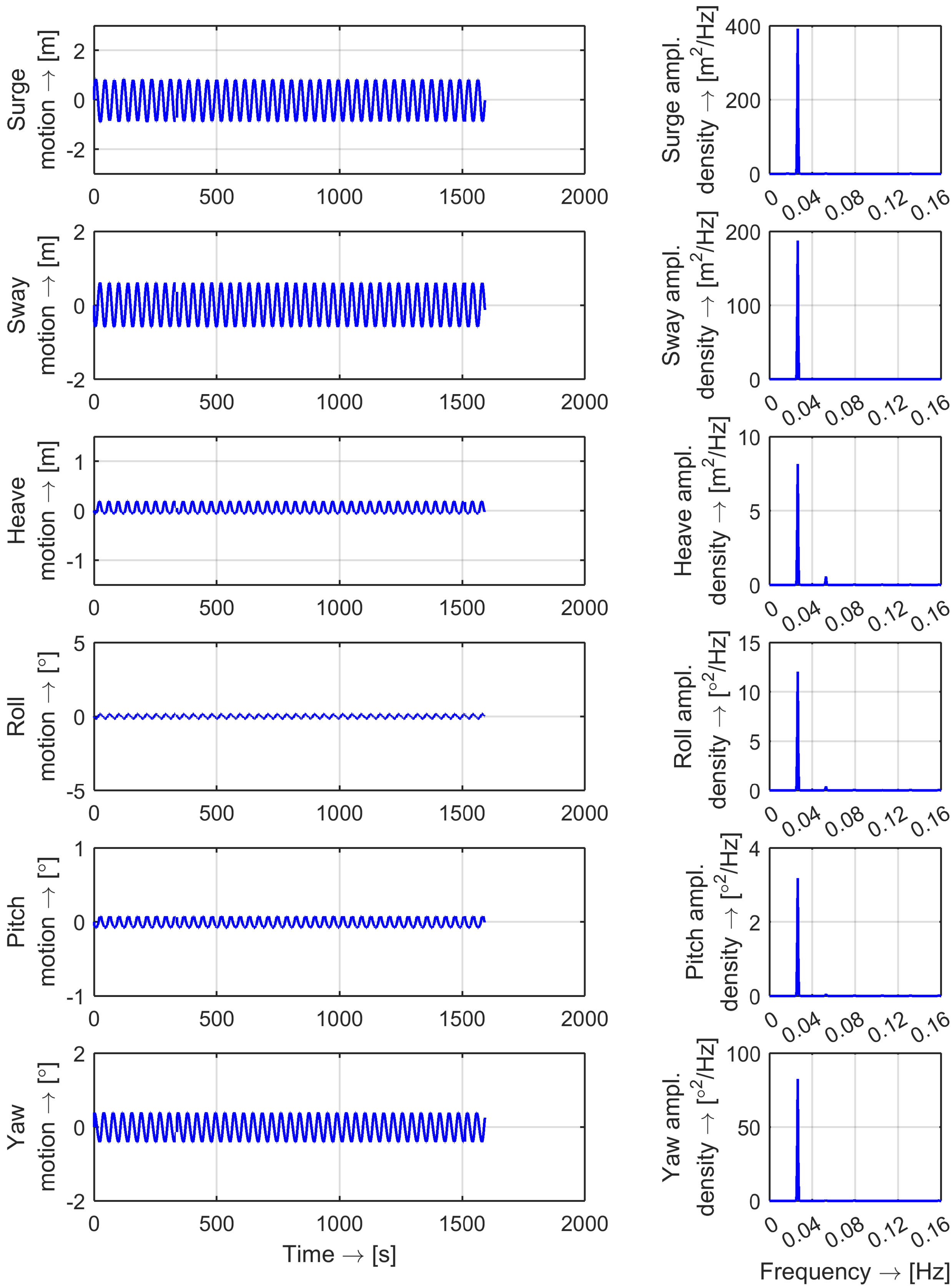

σ_{Surge} = 0.61 m, σ_{Sway} = 0.42 m, σ_{Heave} = 0.09 m, σ_{Roll} = 0.11°, σ_{Pitch} = 0.06°, σ_{Yaw} = 0.28°

Ship motions at centre of gravity (CoG) Depth = 18.0 m, H = 0.25 m, T = 38.00 s Bow-quartering waves	Monochromatic	M380a
	C4_M380a_noST	
Deltares	11202696	App. G.167-2

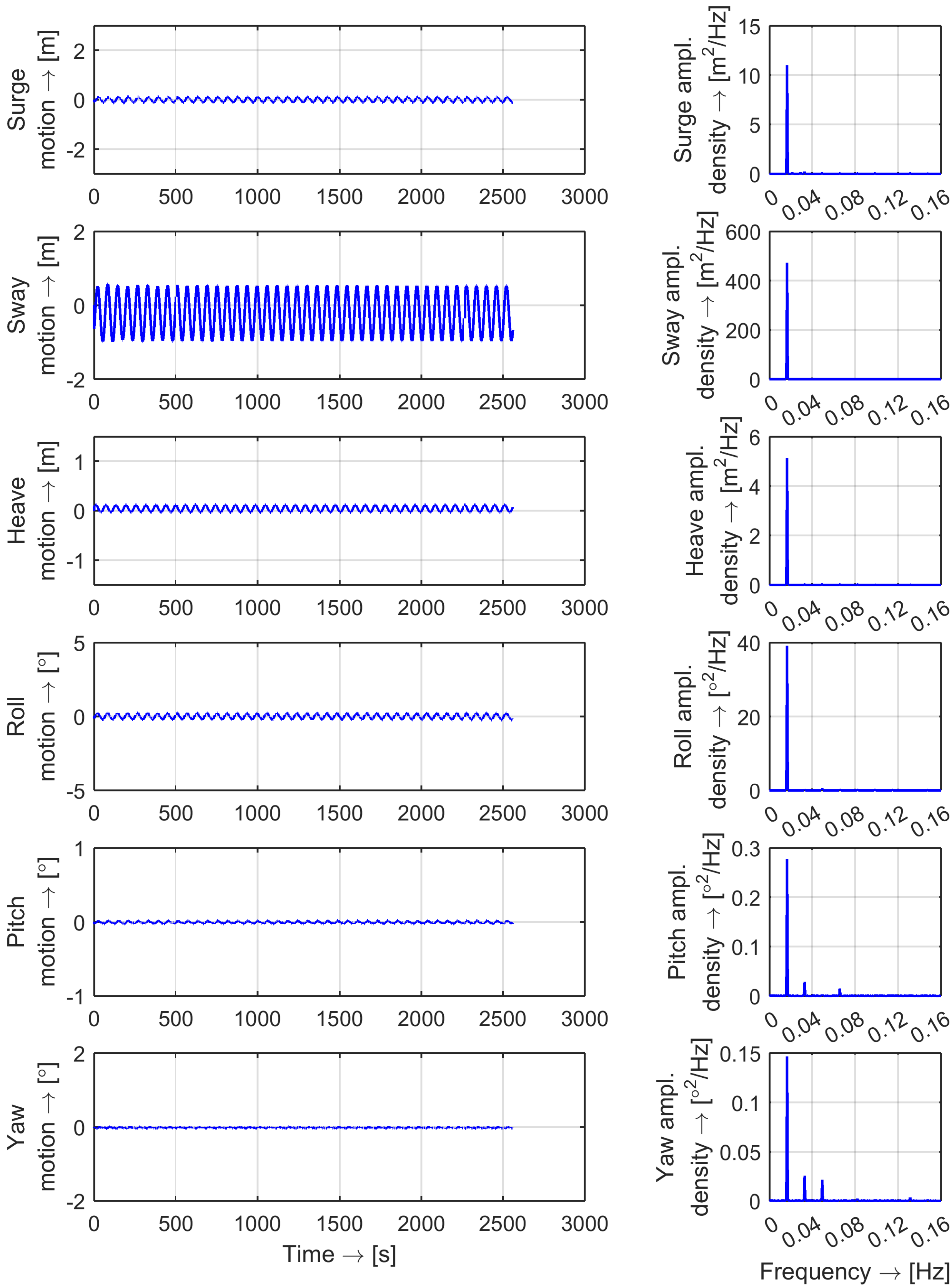

σ_{Surge} = 0.08 m, σ_{Sway} = 0.53 m, σ_{Heave} = 0.05 m, σ_{Roll} = 0.15°, σ_{Pitch} = 0.01°, σ_{Yaw} = 0.01°

Ship motions at centre of gravity (CoG) Depth = 18.0 m, H = 0.20 m, T = 61.00 s Bow-quartering waves	Monochromatic	M610a
	C4_M610a	
Deltares	11202696	App. G.168-2

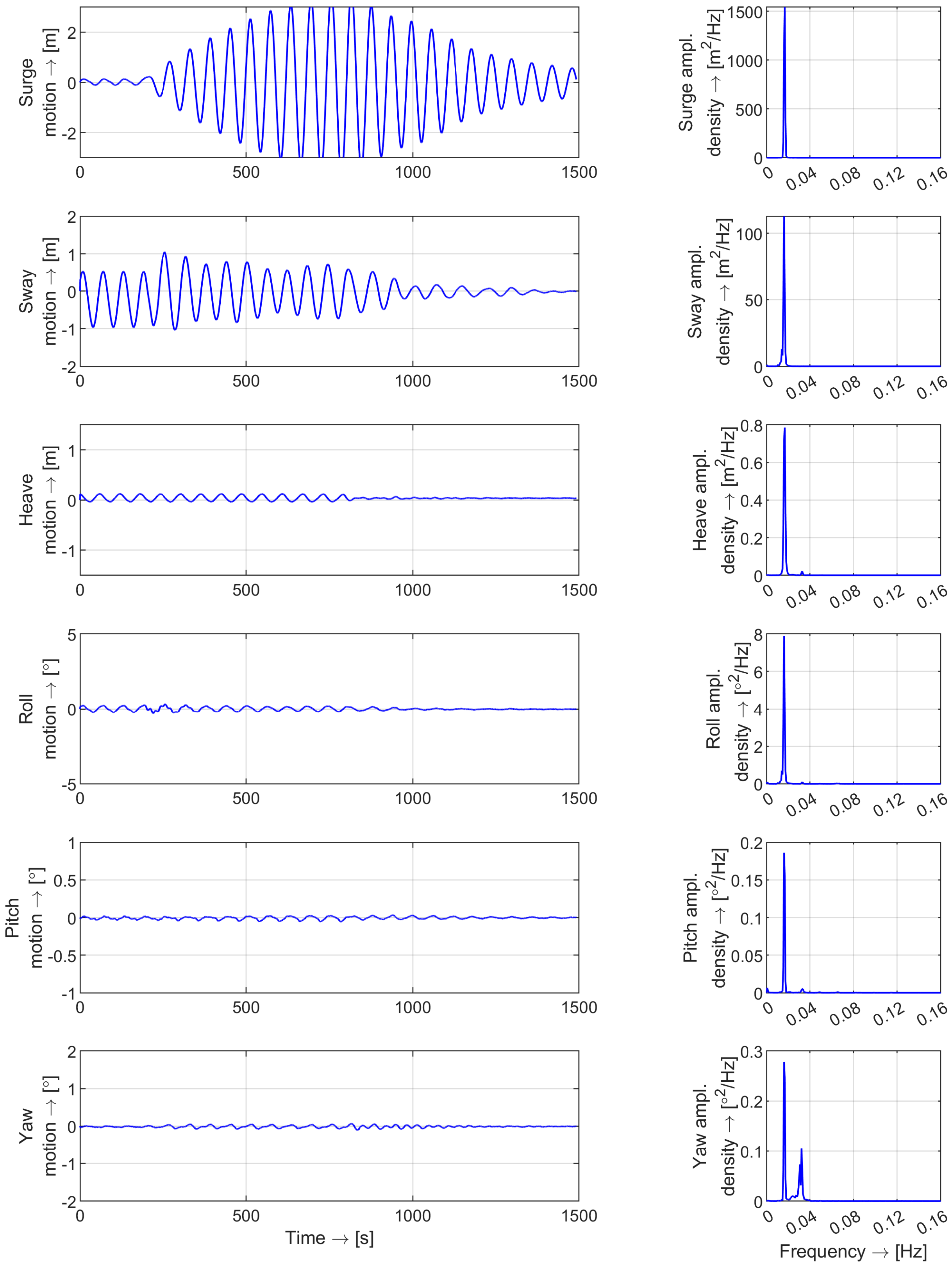

σ_{Surge} = n.a., σ_{Sway} = n.a., σ_{Heave} = n.a., σ_{Roll} = n.a., σ_{Pitch} = n.a., σ_{Yaw} = n.a.

Ship motions at centre of gravity (CoG) Depth = 18.0 m, H = 0.20 m, T = 61.00 s Bow-quartering waves	Monochromatic	M610a
	C4_M610a_Transition	
Deltares	11202696	App. G.169-2

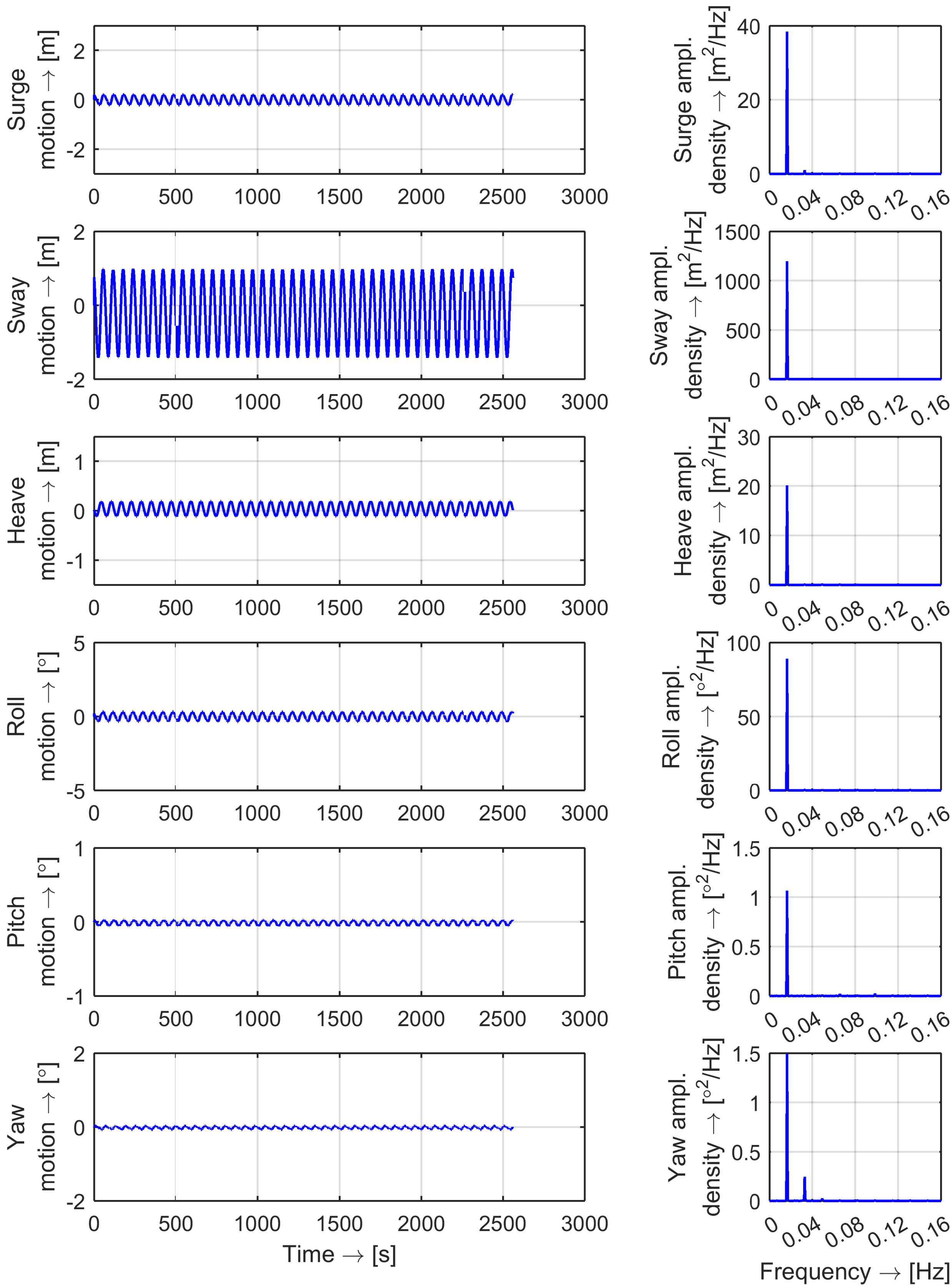

σ_{Surge} = 0.15 m, σ_{Sway} = 0.84 m, σ_{Heave} = 0.11 m, σ_{Roll} = 0.23°, σ_{Pitch} = 0.03°, σ_{Yaw} = 0.03°

Ship motions at centre of gravity (CoG) Depth = 18.0 m, H = 0.40 m, T = 61.00 s Bow-quartering waves	Monochromatic	M610b
	C4_M610b	
Deltares	11202696	App. G.170-2

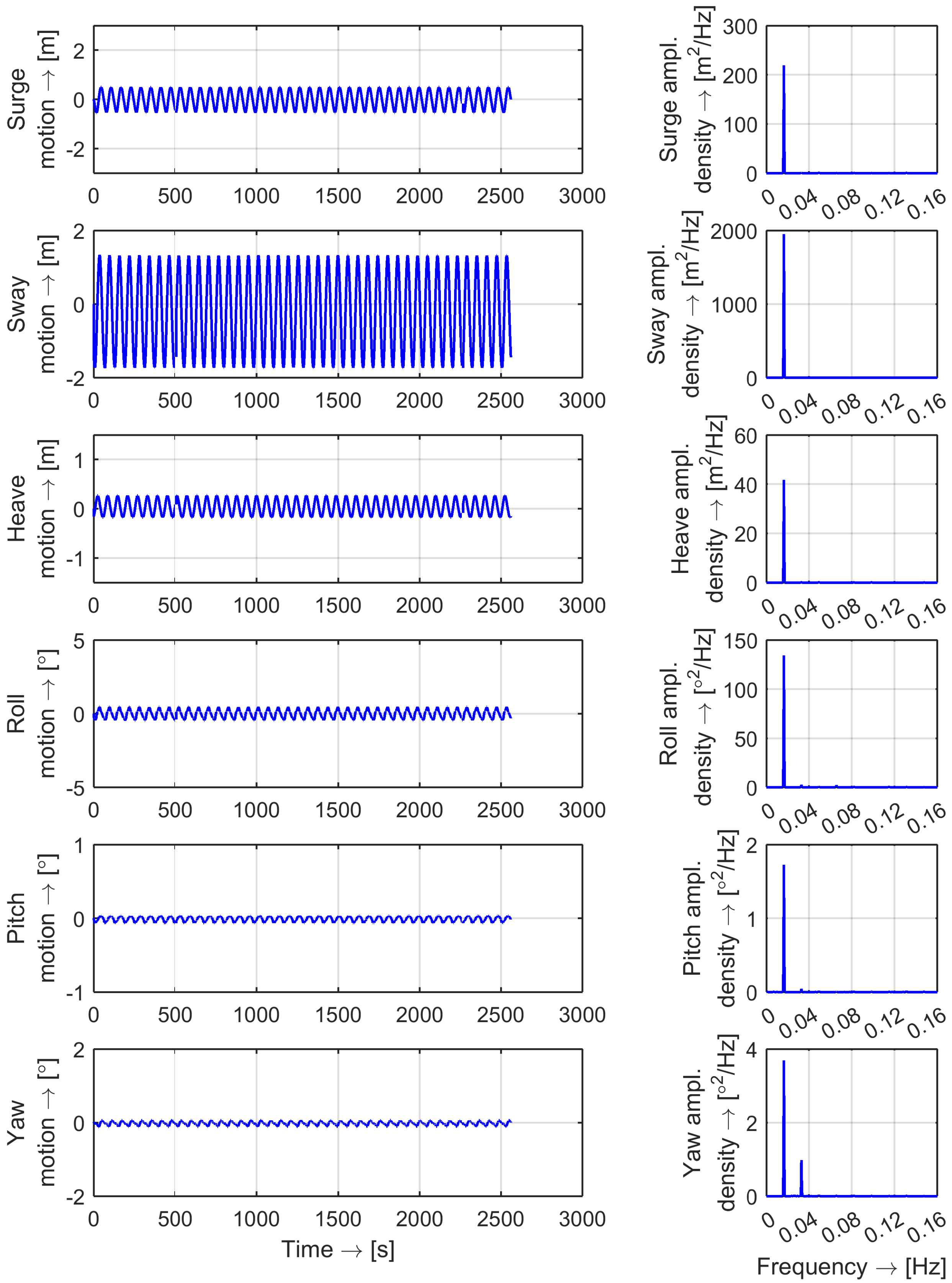

σ_{Surge} = 0.36 m, σ_{Sway} = 1.07 m, σ_{Heave} = 0.16 m, σ_{Roll} = 0.29°, σ_{Pitch} = 0.03°, σ_{Yaw} = 0.05°

Ship motions at centre of gravity (CoG) Depth = 18.0 m, H = 0.60 m, T = 61.00 s Bow-quartering waves	Monochromatic	M610c
	C4_M610c	
Deltares	11202696	App. G.171-2

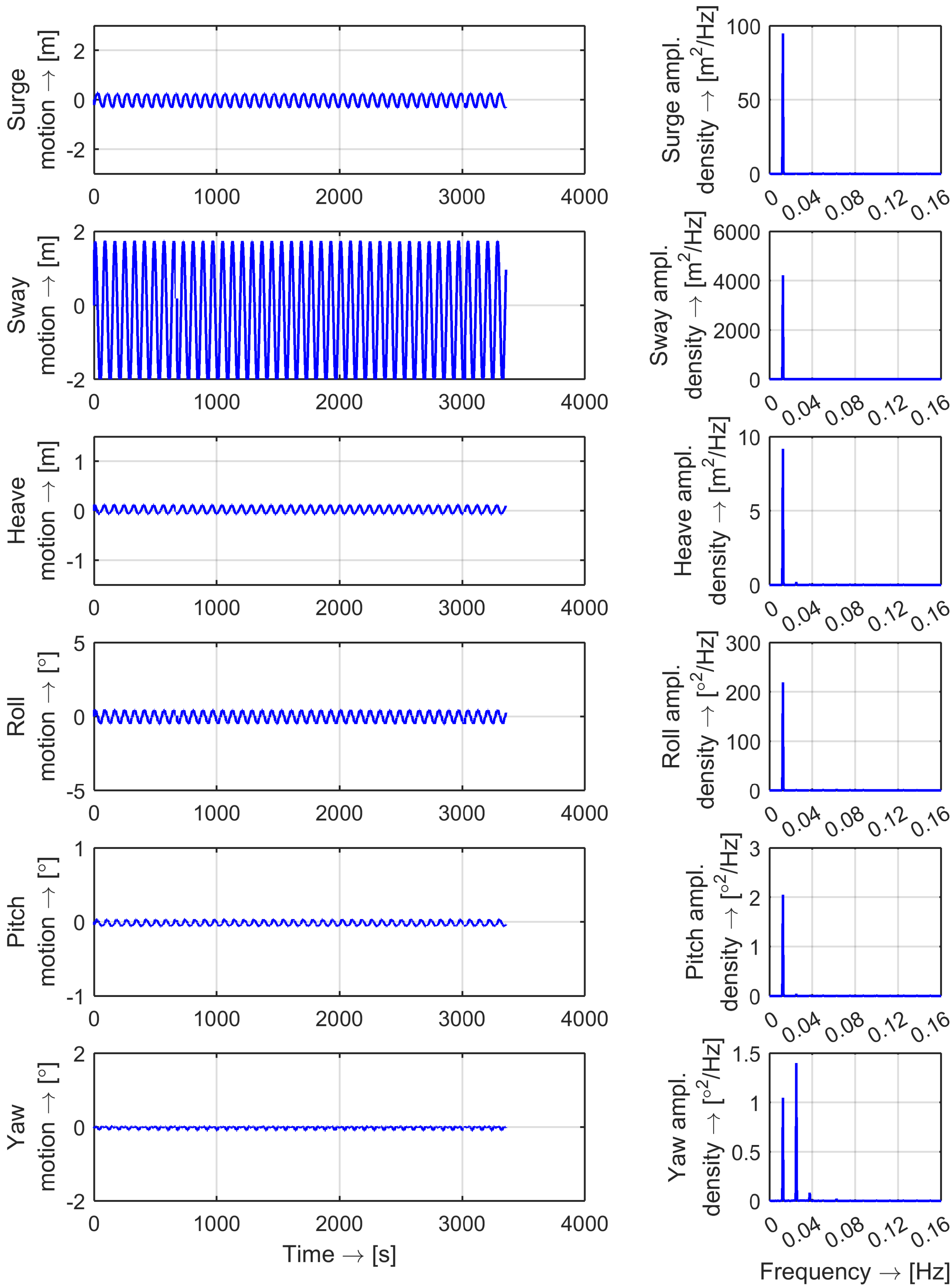

σ_{Surge} = 0.21 m, σ_{Sway} = 1.37 m, σ_{Heave} = 0.06 m, σ_{Roll} = 0.32°, σ_{Pitch} = 0.03°, σ_{Yaw} = 0.03°

Ship motions at centre of gravity (CoG) Depth = 18.0 m, H = 0.20 m, T = 80.00 s Bow-quartering waves	Monochromatic	M800a
	C4_M800a	
Deltares	11202696	App. G.172-2

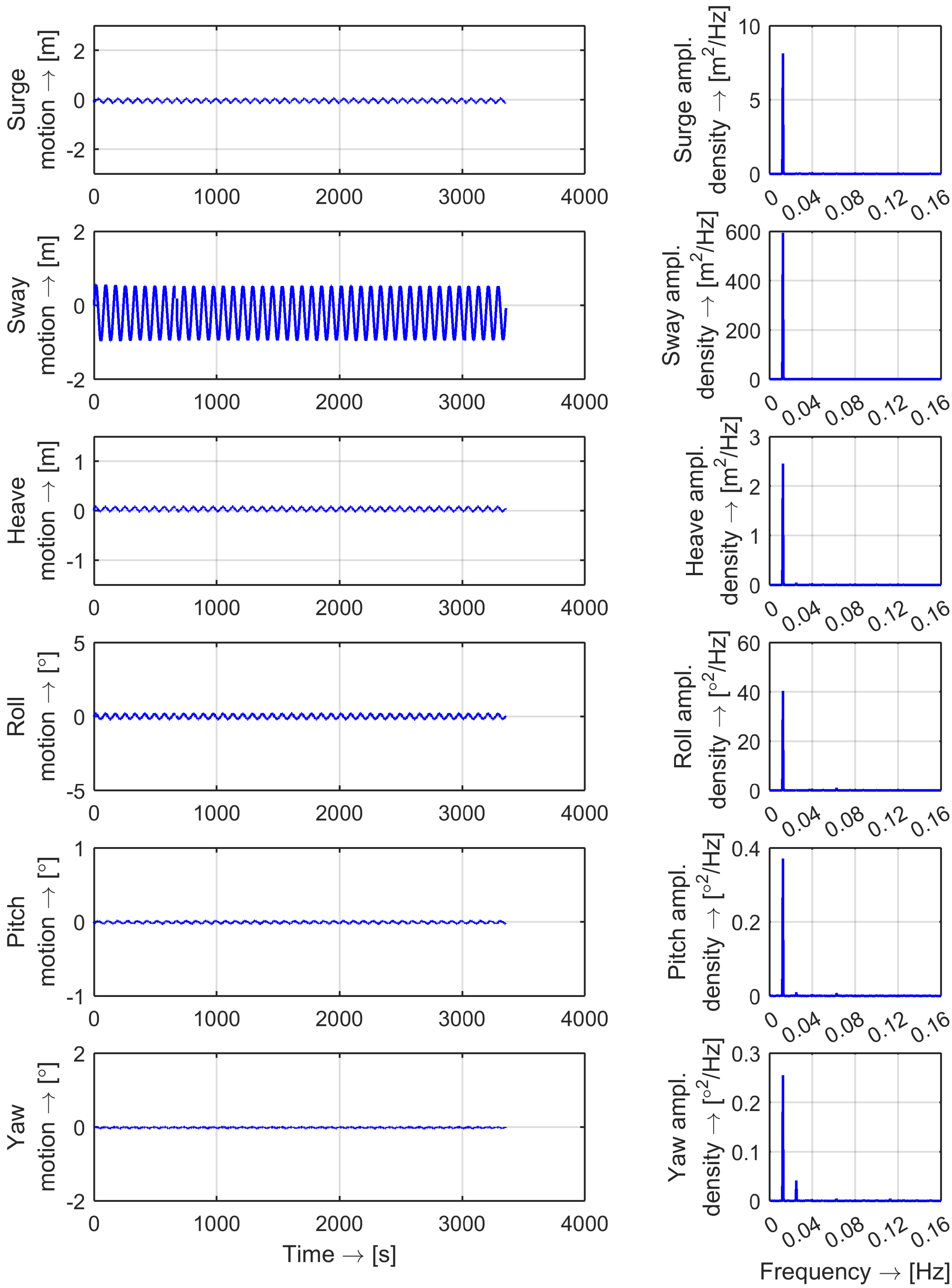

σ_{Surge} = 0.06 m, σ_{Sway} = 0.52 m, σ_{Heave} = 0.03 m, σ_{Roll} = 0.14°, σ_{Pitch} = 0.01°, σ_{Yaw} = 0.01°

Ship motions at centre of gravity (CoG) Depth = 18.0 m, H = 0.09 m, T = 80.00 s Bow-quartering waves	Monochromatic	M800d
	C4_M800d	
Deltares	11202696	App. G.173-2

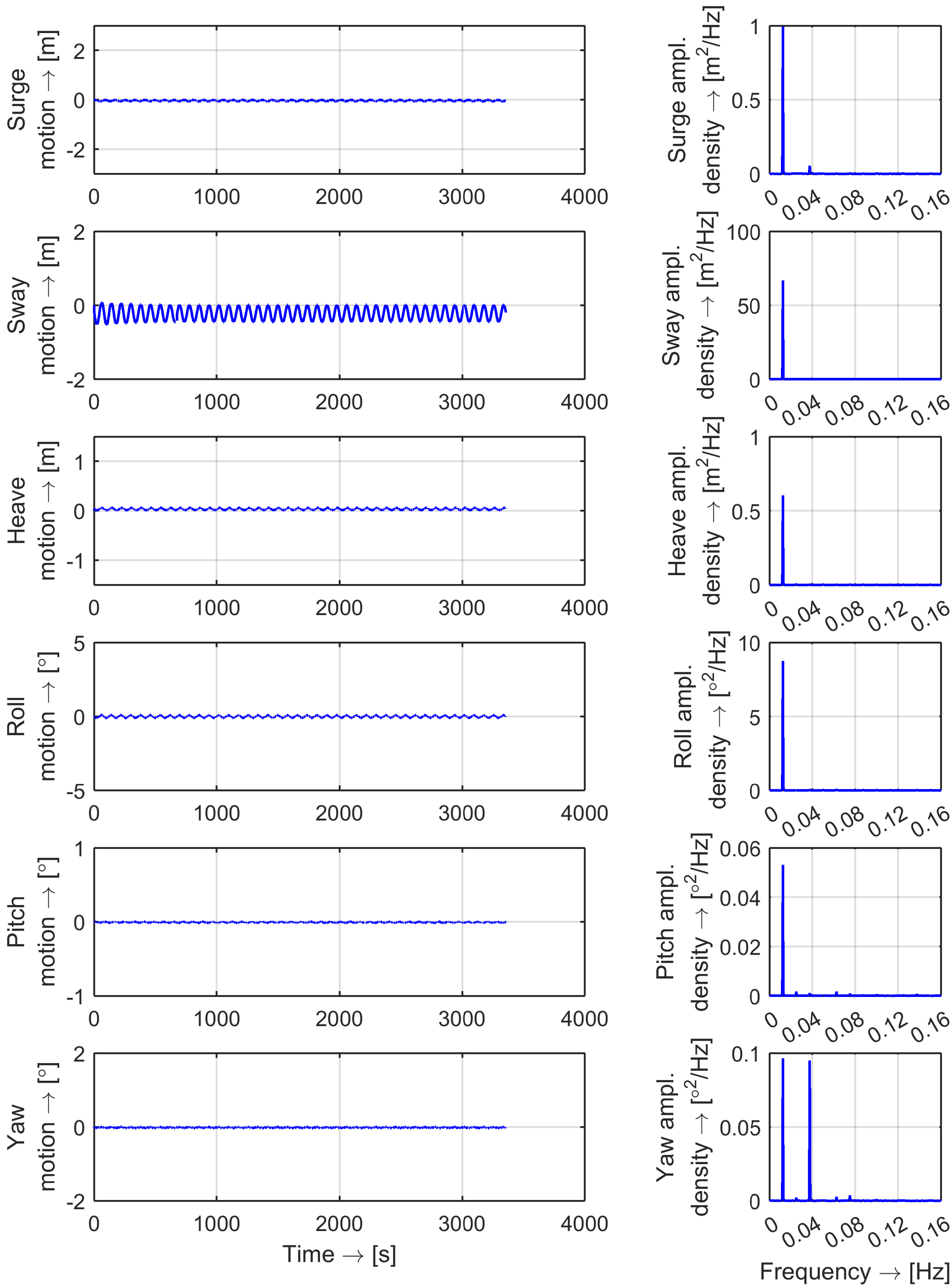

σ_{Surge} = 0.02 m, σ_{Sway} = 0.17 m, σ_{Heave} = 0.02 m, σ_{Roll} = 0.06°, σ_{Pitch} = 0.01°, σ_{Yaw} = 0.01°

Ship motions at centre of gravity (CoG) Depth = 18.0 m, H = 0.05 m, T = 80.00 s Bow-quartering waves	Monochromatic	M800e
	C4_M800e	
Deltares	11202696	App. G.174-2

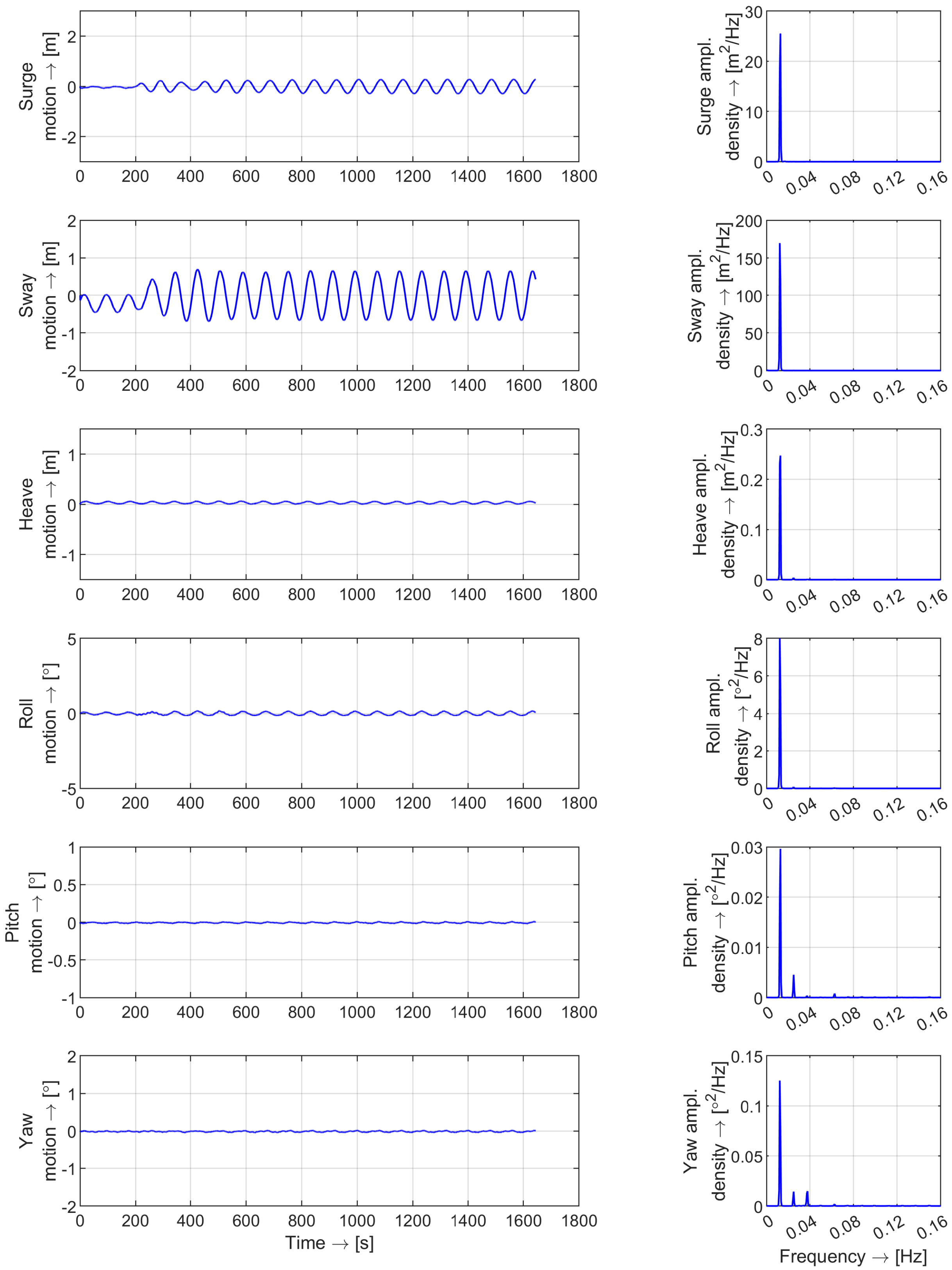

σ_{Surge} = n.a., σ_{Sway} = n.a., σ_{Heave} = n.a., σ_{Roll} = n.a., σ_{Pitch} = n.a., σ_{Yaw} = n.a.

Ship motions at centre of gravity (CoG) Depth = 18.0 m, H = 0.05 m, T = 80.00 s Bow-quartering waves	Monochromatic	M800e
	C4_M800e_Transition	
Deltares	11202696	App. G.175-2

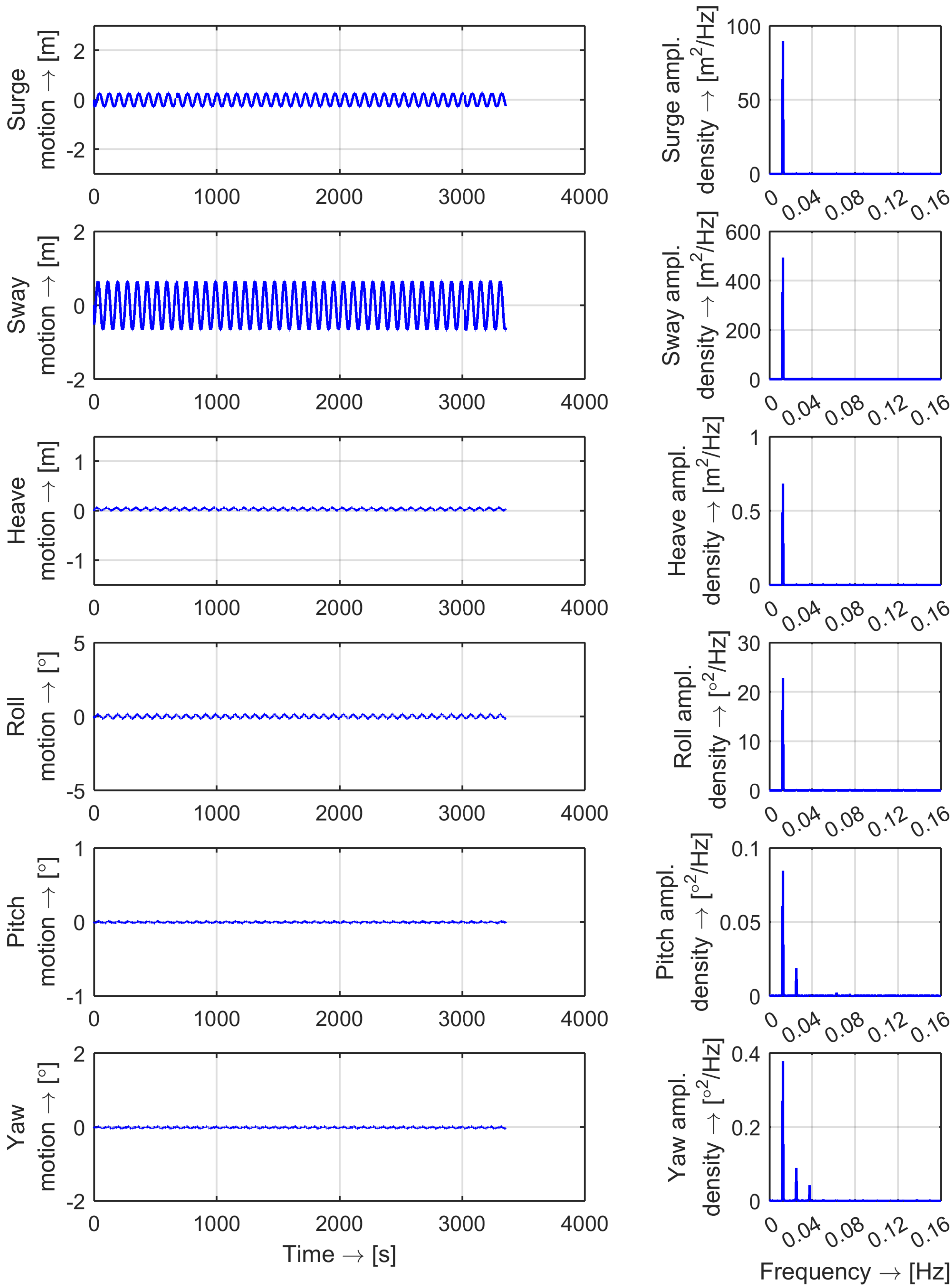

σ_{Surge} = 0.20 m, σ_{Sway} = 0.47 m, σ_{Heave} = 0.02 m, σ_{Roll} = 0.10°, σ_{Pitch} = 0.01°, σ_{Yaw} = 0.02°

Ship motions at centre of gravity (CoG) Depth = 18.0 m, H = 0.05 m, T = 80.00 s Bow-quartering waves	Monochromatic	M800e
	C4_M800e_noST	
Deltares	11202696	App. G.176-2

G.1.2 Tables with standard deviations of ship motions

Table G.1 Overview of standard deviations of ship movements per test for Case A (Part 1).

Test-ID	Surge [m]	Sway [m]	Heave [m]	Roll [°]	Pitch [°]	Yaw [°]
A1_M610a	0.11	0.12	0.06	0.02	0.02	0.01
A1_M610b	0.41	0.18	0.11	0.05	0.04	0.02
A1_M610c	1.45	0.20	0.15	0.05	0.05	0.02
A1_M800a	0.36	0.59	0.05	0.12	0.04	0.02
A1_M800b	1.61	1.26	0.10	0.26	0.09	0.07
A2_B610a	0.19	0.08	0.09	0.25	0.15	0.04
A2_B610a_Transition	n.a.	n.a.	n.a.	n.a.	n.a.	n.a.
A2_B610a_noST	0.42	0.08	0.09	0.25	0.15	0.04
A2_B610b	0.23	0.08	0.12	0.24	0.18	0.04
A2_B610b_noST	0.75	0.09	0.12	0.29	0.19	0.05
A2_B610c	0.28	0.09	0.14	0.28	0.22	0.05
A2_B610c_noST	1.37	0.10	0.14	0.32	0.22	0.05
A2_B610d	0.33	0.11	0.17	0.33	0.25	0.06
A2_B610d_Transition	n.a.	n.a.	n.a.	n.a.	n.a.	n.a.
A2_B610d_noST	1.98	0.11	0.16	0.32	0.25	0.06
A2_B610e	0.41	0.13	0.19	0.36	0.28	0.06
A2_B610e_noST	2.25	1.13	0.15	0.26	0.22	0.29
A2_B610f	0.70	0.25	0.29	0.30	0.34	0.08
A2_B800a	0.03	0.09	0.04	0.20	0.07	0.04
A2_B800a_Transition	n.a.	n.a.	n.a.	n.a.	n.a.	n.a.
A2_B800a_noST	0.05	0.09	0.04	0.20	0.07	0.04
A2_B800b	0.03	0.12	0.05	0.25	0.08	0.04
A2_B800b_noST	0.07	0.12	0.05	0.24	0.08	0.04
A2_B800c	0.04	0.17	0.06	0.30	0.11	0.05
A2_B800c_noST	0.11	0.16	0.06	0.28	0.11	0.05
A2_B800d	0.05	0.22	0.08	0.34	0.13	0.06
A2_B800d_noST	0.16	0.20	0.07	0.31	0.13	0.05
A2_B800e	0.06	0.27	0.09	0.37	0.15	0.06
A2_B800e_noST	0.22	0.26	0.09	0.33	0.15	0.06
A2_B800f	0.56	0.83	0.16	0.69	0.33	0.12
A3_B610e_200t	0.37	0.12	0.19	0.34	0.28	0.07
A3_B610e_sga	0.42	0.11	0.18	0.32	0.28	0.07
A3_B610e_ssk	0.41	0.11	0.18	0.31	0.28	0.07
A3_B610e_ssk_sga	0.44	0.11	0.18	0.33	0.28	0.07
A3_B610f_200t	0.58	0.23	0.29	0.34	0.34	0.09
A3_B800e_200t	0.07	0.26	0.09	0.34	0.15	0.06
A3_B800f_200t	0.49	0.83	0.16	0.68	0.33	0.11
A3_M610b_sga	0.42	0.18	0.11	0.05	0.04	0.02
A3_M610b_ssk	0.41	0.18	0.11	0.05	0.04	0.02
A3_M610b_ssk_sga	0.38	0.18	0.11	0.05	0.03	0.02
A4_I156a	0.03	0.03	0.02	0.10	0.04	0.01
A4_I156b	0.08	0.06	0.04	0.18	0.07	0.02
A4_I156c	0.13	0.11	0.06	0.23	0.10	0.03
A4_I156d	0.20	0.16	0.08	0.30	0.14	0.04
A4_I156e	0.31	0.19	0.11	0.28	0.17	0.05

Table G.2 Overview of standard deviations of ship movements per test for Case B (Part 1).

Test-ID	Surge [m]	Sway [m]	Heave [m]	Roll [°]	Pitch [°]	Yaw [°]
B1_M80a	0.01	0.09	0.03	0.14	0.02	0.00
B1_M80a_Transition	n.a.	n.a.	n.a.	n.a.	n.a.	n.a.
B1_M80a_noST	0.01	0.09	0.03	0.12	0.02	0.00
B1_M80b	0.01	0.17	0.07	0.27	0.04	0.01
B1_M80b_Transition	n.a.	n.a.	n.a.	n.a.	n.a.	n.a.
B1_M80b_noST	0.01	0.17	0.07	0.26	0.03	0.01
B1_M140a	0.08	0.30	0.27	1.96	0.17	0.03
B1_M140a_lwv	0.08	0.29	0.27	1.88	0.16	0.03
B1_M140a_sk	0.08	0.28	0.27	1.89	0.17	0.03
B1_M140b	0.10	0.43	0.34	2.31	0.21	0.03
B1_M140c	0.07	0.93	0.39	2.27	0.20	0.03
B1_M140d	0.13	0.96	0.43	2.42	0.25	0.03
B1_M140e	0.20	0.97	0.49	2.10	0.27	0.16
B1_M140f	0.02	0.09	0.07	0.67	0.04	0.01
B1_M140g	0.04	0.13	0.13	1.10	0.08	0.02
B1_M140h	0.06	0.19	0.20	1.51	0.12	0.03
B1_M156a	0.05	0.85	0.30	2.33	0.11	0.04
B1_M156b	0.06	0.87	0.38	2.10	0.14	0.04
B1_M156c	0.08	0.91	0.45	1.92	0.17	0.04
B1_M156f	0.02	0.42	0.09	1.48	0.04	0.02
B1_M156g	0.04	0.73	0.17	2.73	0.08	0.03
B1_M156h	0.04	0.84	0.23	2.60	0.09	0.05
B1_M172a	0.16	0.77	0.38	1.91	0.11	0.07
B1_M172f	0.01	0.15	0.10	0.33	0.03	0.02
B1_M172g	0.02	0.31	0.19	0.76	0.05	0.04
B1_M172h	0.05	0.69	0.28	2.02	0.09	0.07
B1_M800d	0.03	0.84	0.04	0.22	0.00	0.03
B1_M800e	0.01	0.23	0.02	0.08	0.00	0.01
B1_M800e_Transition	n.a.	n.a.	n.a.	n.a.	n.a.	n.a.
B1_M800e_noST	0.00	0.68	0.02	0.15	0.00	0.02
B2_B610f	0.03	0.34	0.08	0.94	0.04	0.04
B2_B610f_noST	0.03	0.39	0.08	1.23	0.04	0.04
B2_B610g	0.05	0.66	0.14	2.02	0.07	0.06
B2_B610g_noST	0.05	0.71	0.14	2.32	0.06	0.06
B2_B610h	0.22	0.76	0.19	2.01	0.08	0.07
B2_B610h_noST	0.23	0.77	0.19	2.09	0.07	0.07
B2_B800f	0.01	0.20	0.08	0.64	0.02	0.03
B2_B800f_noST	0.01	0.24	0.08	0.79	0.02	0.03
B2_B800g	0.03	0.42	0.16	1.39	0.04	0.05
B2_B800g_noST	0.03	0.49	0.16	1.55	0.04	0.05
B2_B800h	0.04	0.62	0.23	2.01	0.06	0.07
B2_B800h_noST	0.04	0.66	0.24	1.93	0.06	0.06

Table G.3 Overview of standard deviations of ship movements per test for Case B (Part 2).

Test-ID	Surge [m]	Sway [m]	Heave [m]	Roll [°]	Pitch [°]	Yaw [°]
B3_B800g_50t	0.03	0.42	0.16	1.34	0.04	0.04
B3_B800g_200t	0.03	0.42	0.16	1.42	0.04	0.06
B3_B800g_sga	0.03	0.40	0.16	1.29	0.04	0.05
B3_B800g_sk	0.03	0.44	0.16	1.48	0.04	0.05
B3_B800g_ssk	0.03	0.40	0.16	1.33	0.04	0.05
B3_B800g_ssk_sga	0.03	0.40	0.16	1.27	0.04	0.05
B3_M156f_50t	0.02	0.41	0.09	1.44	0.04	0.02
B3_M156f_200t	0.02	0.41	0.09	1.43	0.04	0.02
B3_M156f_sga	0.02	0.39	0.09	1.36	0.04	0.02
B3_M156f_sk	0.02	0.44	0.09	1.59	0.04	0.02
B3_M156f_ssk	0.02	0.40	0.09	1.39	0.04	0.02
B3_M156f_ssk_sga	0.02	0.39	0.09	1.36	0.04	0.02
B3_M800d_sk	0.03	0.91	0.04	0.23	0.00	0.03
B3_M800e_50t	0.00	0.37	0.02	0.10	0.00	0.01
B3_M800e_200t	0.01	0.22	0.02	0.08	0.00	0.01
B3_M800e_sga	0.01	0.21	0.02	0.08	0.00	0.01
B3_M800e_ssk	0.01	0.21	0.02	0.08	0.00	0.01
B3_M800e_ssk_sga	0.01	0.18	0.02	0.07	0.00	0.01
B4_I156a	0.04	0.43	0.11	1.51	0.05	0.03

Table G.4 Overview of standard deviations of ship movements per test for Case C (Part 1).

Test-ID	Surge [m]	Sway [m]	Heave [m]	Roll [°]	Pitch [°]	Yaw [°]
C1_B610a	0.27	0.34	0.14	0.52	0.15	0.16
C1_B610b	0.33	0.42	0.18	0.62	0.18	0.21
C1_B610c	0.41	0.50	0.22	0.74	0.22	0.26
C1_B610d	0.49	0.57	0.25	0.87	0.25	0.30
C1_B610e	0.55	0.70	0.29	1.27	0.27	0.35
C1_B800a	0.06	0.10	0.18	0.32	0.07	0.24
C1_B800b	0.08	0.12	0.22	0.39	0.08	0.29
C1_B800c	0.09	0.16	0.26	0.48	0.10	0.35
C1_B800d	0.12	0.20	0.30	0.56	0.12	0.40
C1_B800e	0.15	0.26	0.35	0.62	0.15	0.47
C2_B610c_200t	0.41	0.52	0.22	0.69	0.22	0.27
C2_B610c_sga	0.41	0.49	0.23	0.67	0.22	0.26
C2_B610c_sk	0.36	0.50	0.23	0.67	0.22	0.26
C2_B610c_ssk	0.41	0.50	0.23	0.69	0.22	0.26
C2_B610c_ssk_sga	0.41	0.49	0.22	0.71	0.22	0.26
C3_I120a	0.11	0.18	0.06	0.33	0.12	0.13
C3_I140a	0.06	0.10	0.07	0.25	0.10	0.11
C3_I156a	0.05	0.08	0.05	0.21	0.06	0.08
C3_I156b	0.10	0.15	0.10	0.32	0.12	0.16
C3_I156c	0.16	0.24	0.16	0.43	0.18	0.24
C4_M140a	0.02	0.11	0.08	0.34	0.11	0.20
C4_M140b	0.03	0.14	0.09	0.41	0.14	0.25
C4_M140c	0.03	0.16	0.11	0.49	0.18	0.30
C4_M140d	0.04	0.18	0.13	0.56	0.21	0.34
C4_M140e	0.04	0.21	0.15	0.63	0.23	0.39

Table G.5 Overview of standard deviations of ship movements per test for Case C (Part 2).

Test-ID	Surge [m]	Sway [m]	Heave [m]	Roll [°]	Pitch [°]	Yaw [°]
C4_M156a	0.05	0.11	0.14	0.52	0.11	0.21
C4_M156a_noST	0.04	0.07	0.14	0.43	0.12	0.21
C4_M156b	0.06	0.12	0.18	0.55	0.15	0.27
C4_M156b_noST	0.06	0.07	0.17	0.49	0.15	0.27
C4_M156c	0.07	0.11	0.21	0.53	0.18	0.33
C4_M156c_noST	0.07	0.07	0.21	0.50	0.19	0.33
C4_M156d	0.09	0.11	0.24	0.49	0.21	0.39
C4_M156d_noST	0.09	0.07	0.24	0.52	0.23	0.38
C4_M156e	0.10	0.12	0.27	0.50	0.25	0.44
C4_M156e_Transition	n.a.	n.a.	n.a.	n.a.	n.a.	n.a.
C4_M156e_noST	0.10	0.06	0.27	0.53	0.26	0.43
C4_M172a	0.08	0.02	0.20	0.15	0.09	0.31
C4_M172a_Transition	n.a.	n.a.	n.a.	n.a.	n.a.	n.a.
C4_M172a_noST	0.06	0.03	0.20	0.06	0.08	0.30
C4_M172b	0.10	0.03	0.26	0.15	0.12	0.39
C4_M172b_noST	0.08	0.05	0.26	0.08	0.12	0.38
C4_M172c	0.12	0.07	0.32	0.15	0.16	0.46
C4_M172c_noST	0.10	0.07	0.32	0.08	0.15	0.46
C4_M172d	0.14	0.10	0.37	0.14	0.19	0.54
C4_M172d_noST	0.13	0.09	0.37	0.11	0.19	0.54
C4_M172e	0.17	0.10	0.42	0.18	0.23	0.62
C4_M172e_noST	0.15	0.11	0.42	0.14	0.23	0.61
C4_M330a	0.23	0.05	0.06	0.05	0.02	0.24
C4_M330a_Transition	n.a.	n.a.	n.a.	n.a.	n.a.	n.a.
C4_M330a_noST	0.15	0.07	0.04	0.14	0.03	0.72
C4_M360a	0.63	0.45	0.06	0.17	0.07	0.15
C4_M360a_Transition	n.a.	n.a.	n.a.	n.a.	n.a.	n.a.
C4_M360a_noST	0.56	0.43	0.06	0.17	0.07	0.40
C4_M360a_200t	0.75	0.47	0.06	0.21	0.06	0.08
C4_M360a_sga	0.61	0.44	0.06	0.16	0.07	0.16
C4_M360a_sk	0.68	0.45	0.06	0.17	0.07	0.17
C4_M360a_ssk	0.62	0.44	0.06	0.17	0.07	0.16
C4_M360a_ssk_sga	0.60	0.44	0.06	0.17	0.07	0.16
C4_M380a	0.67	0.41	0.09	0.12	0.05	0.17
C4_M380a_Transition	n.a.	n.a.	n.a.	n.a.	n.a.	n.a.
C4_M380a_noST	0.61	0.42	0.09	0.11	0.06	0.28
C4_M610a	0.08	0.53	0.05	0.15	0.01	0.01
C4_M610a_Transition	n.a.	n.a.	n.a.	n.a.	n.a.	n.a.
C4_M610b	0.15	0.84	0.11	0.23	0.03	0.03
C4_M610c	0.36	1.07	0.16	0.29	0.03	0.05
C4_M800a	0.21	1.37	0.06	0.32	0.03	0.03
C4_M800d	0.06	0.52	0.03	0.14	0.01	0.01
C4_M800e	0.02	0.17	0.02	0.06	0.01	0.01
C4_M800e_Transition	n.a.	n.a.	n.a.	n.a.	n.a.	n.a.
C4_M800e_noST	0.20	0.47	0.02	0.10	0.01	0.02

G.1.3 Tables with absolute maxima of ship motions

Table G.6 Overview of absolute maxima of ship movements per test for Case A (Part 1).

Test-ID	Surge [m]	Sway [m]	Heave [m]	Roll [°]	Pitch [°]	Yaw [°]
A1_M610a	0.22	0.19	0.12	0.10	0.04	0.04
A1_M610b	0.69	0.28	0.20	0.17	0.06	0.05
A1_M610c	2.18	0.32	0.26	0.16	0.09	0.07
A1_M800a	0.60	0.88	0.13	0.24	0.06	0.06
A1_M800b	2.50	1.83	0.20	0.45	0.14	0.14
A2_B610a	0.41	0.16	0.21	0.47	0.27	0.09
A2_B610a_Transition	0.86	0.16	0.21	0.45	0.27	0.09
A2_B610a_noST	0.91	0.16	0.21	0.46	0.28	0.09
A2_B610b	0.49	0.18	0.26	0.45	0.34	0.11
A2_B610b_noST	1.46	0.19	0.26	0.51	0.35	0.10
A2_B610c	0.62	0.22	0.31	0.51	0.41	0.11
A2_B610c_noST	2.46	0.22	0.30	0.55	0.41	0.11
A2_B610d	0.73	0.27	0.35	0.60	0.47	0.13
A2_B610d_Transition	3.47	0.26	0.32	0.57	0.48	0.14
A2_B610d_noST	3.36	0.26	0.34	0.58	0.47	0.13
A2_B610e	0.90	0.30	0.41	0.62	0.54	0.14
A2_B610e_noST	4.43	4.38	0.40	0.59	0.54	2.87
A2_B610f	1.82	0.61	0.66	0.71	0.69	0.19
A2_B800a	0.16	0.23	0.11	0.41	0.14	0.09
A2_B800a_Transition	0.23	0.21	0.12	0.40	0.14	0.09
A2_B800a_noST	0.20	0.21	0.11	0.40	0.14	0.09
A2_B800b	0.10	0.28	0.14	0.49	0.18	0.10
A2_B800b_noST	0.25	0.28	0.13	0.48	0.18	0.10
A2_B800c	0.13	0.36	0.17	0.58	0.23	0.12
A2_B800c_noST	0.33	0.35	0.15	0.54	0.23	0.12
A2_B800d	0.15	0.45	0.18	0.67	0.27	0.13
A2_B800d_noST	0.42	0.42	0.17	0.59	0.27	0.13
A2_B800e	0.20	0.53	0.20	0.71	0.32	0.15
A2_B800e_noST	0.54	0.51	0.19	0.64	0.32	0.14
A2_B800f	1.56	1.39	0.37	1.49	0.63	0.28
A3_B610e_200t	0.88	0.27	0.37	0.58	0.54	0.15
A3_B610e_sga	1.00	0.26	0.37	0.54	0.54	0.15
A3_B610e_ssk	0.95	0.27	0.37	0.54	0.54	0.15
A3_B610e_ssk_sga	1.04	0.26	0.37	0.56	0.54	0.15
A3_B610f_200t	1.79	0.57	0.67	0.74	0.69	0.23
A3_B800e_200t	0.34	0.56	0.17	0.75	0.31	0.14
A3_B800f_200t	1.65	1.40	0.37	1.49	0.63	0.28
A3_M610b_sga	0.71	0.28	0.20	0.16	0.06	0.05
A3_M610b_ssk	0.69	0.28	0.20	0.16	0.06	0.04
A3_M610b_ssk_sga	0.65	0.29	0.20	0.16	0.06	0.05
A4_I156a	0.17	0.14	0.13	0.42	0.13	0.06
A4_I156b	0.40	0.27	0.20	0.69	0.28	0.10
A4_I156c	0.62	0.47	0.25	0.92	0.41	0.16
A4_I156d	1.14	0.65	0.30	1.21	0.56	0.23
A4_I156e	1.82	0.80	0.39	1.15	0.62	0.30

Table G.7 Overview of absolute maxima of ship movements per test for Case B (Part 1).

Test-ID	Surge [m]	Sway [m]	Heave [m]	Roll [°]	Pitch [°]	Yaw [°]
B1_M80a	0.02	0.28	0.06	0.22	0.03	0.01
B1_M80a_Transition	0.02	0.30	0.07	0.24	0.04	0.02
B1_M80a_noST	0.02	0.18	0.06	0.19	0.04	0.01
B1_M80b	0.04	0.27	0.13	0.43	0.08	0.02
B1_M80b_Transition	0.03	0.59	0.12	0.42	0.07	0.03
B1_M80b_noST	0.03	0.46	0.12	0.38	0.07	0.02
B1_M140a	0.16	0.45	0.40	2.87	0.28	0.07
B1_M140a_lwv	0.16	0.42	0.41	2.71	0.26	0.07
B1_M140a_sk	0.16	0.42	0.41	2.76	0.26	0.08
B1_M140b	0.21	0.72	0.53	3.44	0.33	0.07
B1_M140c	0.57	1.52	0.56	3.74	0.32	0.09
B1_M140d	0.56	1.75	0.67	4.33	0.47	0.10
B1_M140e	0.67	2.12	0.80	4.47	0.51	0.44
B1_M140f	0.04	0.26	0.12	0.96	0.06	0.07
B1_M140g	0.08	0.30	0.20	1.56	0.13	0.07
B1_M140h	0.12	0.36	0.31	2.17	0.18	0.08
B1_M156a	0.19	1.22	0.45	3.47	0.18	0.09
B1_M156b	0.27	1.36	0.55	3.27	0.22	0.08
B1_M156c	0.33	1.48	0.64	3.11	0.28	0.07
B1_M156f	0.04	0.73	0.15	2.15	0.08	0.07
B1_M156g	0.07	1.16	0.29	3.87	0.12	0.09
B1_M156h	0.11	1.25	0.35	3.78	0.14	0.10
B1_M172a	0.35	1.61	0.61	3.66	0.22	0.19
B1_M172f	0.03	0.34	0.16	0.48	0.06	0.08
B1_M172g	0.05	0.60	0.30	1.09	0.08	0.10
B1_M172h	0.10	1.24	0.43	3.24	0.15	0.14
B1_M800d	0.05	1.42	0.06	0.35	0.02	0.06
B1_M800e	0.02	0.54	0.04	0.14	0.01	0.03
B1_M800e_Transition	0.02	0.98	0.04	0.26	0.01	0.04
B1_M800e_noST	0.01	0.98	0.04	0.26	0.01	0.04
B2_B610f	0.07	0.94	0.16	1.68	0.09	0.07
B2_B610f_noST	0.07	0.80	0.16	2.03	0.08	0.08
B2_B610g	0.11	1.62	0.31	3.48	0.14	0.13
B2_B610g_noST	0.11	1.50	0.33	3.84	0.13	0.14
B2_B610h	0.42	1.88	0.42	4.09	0.17	0.15
B2_B610h_noST	0.45	1.71	0.43	4.16	0.16	0.17
B2_B800f	0.04	0.53	0.17	1.06	0.05	0.07
B2_B800f_noST	0.04	0.48	0.17	1.28	0.06	0.06
B2_B800g	0.07	1.04	0.33	2.31	0.09	0.13
B2_B800g_noST	0.07	1.05	0.34	2.56	0.09	0.11
B2_B800h	0.12	1.56	0.50	3.41	0.13	0.17
B2_B800h_noST	0.12	1.48	0.50	3.30	0.13	0.15

Table G.8 Overview of absolute maxima of ship movements per test for Case B (Part 2).

Test-ID	Surge [m]	Sway [m]	Heave [m]	Roll [°]	Pitch [°]	Yaw [°]
B3_B800g_50t	0.07	1.02	0.33	2.26	0.09	0.11
B3_B800g_200t	0.06	1.09	0.33	2.35	0.09	0.12
B3_B800g_sga	0.07	1.00	0.33	2.18	0.09	0.11
B3_B800g_sk	0.07	1.05	0.33	2.42	0.09	0.10
B3_B800g_ssk	0.07	1.04	0.33	2.22	0.09	0.11
B3_B800g_ssk_sga	0.07	1.01	0.33	2.15	0.09	0.11
B3_M156f_50t	0.04	0.71	0.15	2.06	0.08	0.03
B3_M156f_200t	0.04	0.78	0.14	2.06	0.08	0.05
B3_M156f_sga	0.04	0.69	0.14	1.93	0.07	0.05
B3_M156f_sk	0.04	0.75	0.14	2.25	0.08	0.04
B3_M156f_ssk	0.04	0.73	0.14	1.98	0.07	0.06
B3_M156f_ssk_sga	0.04	0.69	0.14	1.93	0.07	0.05
B3_M800d_sk	0.06	1.48	0.07	0.38	0.01	0.06
B3_M800e_50t	0.01	0.65	0.06	0.16	0.01	0.02
B3_M800e_200t	0.02	0.56	0.06	0.13	0.01	0.02
B3_M800e_sga	0.02	0.48	0.05	0.17	0.01	0.02
B3_M800e_ssk	0.03	0.55	0.05	0.15	0.01	0.03
B3_M800e_ssk_sga	0.02	0.44	0.05	0.15	0.01	0.03
B4_I156a	0.28	1.56	0.40	4.39	0.21	0.14

Table G.9 Overview of absolute maxima of ship movements per test for Case C (Part 1).

Test-ID	Surge [m]	Sway [m]	Heave [m]	Roll [°]	Pitch [°]	Yaw [°]
C1_B610a	0.51	0.78	0.30	1.11	0.30	0.33
C1_B610b	0.66	0.90	0.39	1.35	0.37	0.42
C1_B610c	0.86	1.02	0.47	1.64	0.44	0.52
C1_B610d	1.05	1.14	0.55	1.89	0.51	0.61
C1_B610e	1.17	1.51	0.64	2.98	0.56	0.70
C1_B800a	0.15	0.43	0.35	0.54	0.14	0.43
C1_B800b	0.19	0.42	0.42	0.66	0.16	0.53
C1_B800c	0.23	0.43	0.50	0.81	0.20	0.64
C1_B800d	0.30	0.47	0.58	1.00	0.23	0.75
C1_B800e	0.37	0.56	0.66	1.20	0.28	0.88
C2_B610c_200t	0.80	1.31	0.45	1.58	0.45	0.55
C2_B610c_sga	0.86	0.98	0.45	1.54	0.45	0.52
C2_B610c_sk	0.80	1.01	0.45	1.49	0.45	0.54
C2_B610c_ssk	0.85	1.01	0.45	1.49	0.45	0.52
C2_B610c_ssk_sga	0.90	0.96	0.45	1.57	0.45	0.51
C3_I120a	0.67	0.97	0.25	1.31	0.47	0.52
C3_I140a	0.41	0.59	0.24	0.90	0.36	0.39
C3_I156a	0.19	0.55	0.21	0.74	0.23	0.27
C3_I156b	0.45	0.83	0.45	1.12	0.46	0.61
C3_I156c	0.72	1.12	0.68	2.00	0.60	0.95
C4_M140a	0.06	0.34	0.16	0.52	0.17	0.29
C4_M140b	0.08	0.35	0.17	0.63	0.22	0.37
C4_M140c	0.10	0.34	0.20	0.78	0.27	0.43
C4_M140d	0.13	0.33	0.21	0.89	0.31	0.50
C4_M140e	0.15	0.34	0.23	1.02	0.35	0.57

Table G.10 Overview of absolute maxima of ship movements per test for Case C (Part 2).

Test-ID	Surge [m]	Sway [m]	Heave [m]	Roll [°]	Pitch [°]	Yaw [°]
C4_M156a	0.11	0.38	0.24	0.86	0.17	0.32
C4_M156a_noST	0.11	0.14	0.24	0.70	0.17	0.32
C4_M156b	0.15	0.34	0.29	0.84	0.21	0.40
C4_M156b_noST	0.16	0.16	0.28	0.77	0.22	0.39
C4_M156c	0.17	0.29	0.33	0.82	0.26	0.48
C4_M156c_noST	0.21	0.18	0.33	0.80	0.28	0.48
C4_M156d	0.21	0.27	0.37	0.78	0.31	0.56
C4_M156d_noST	0.27	0.20	0.36	0.86	0.33	0.56
C4_M156e	0.26	0.26	0.40	0.82	0.36	0.65
C4_M156e_Transition	0.35	0.32	0.40	0.99	0.38	0.76
C4_M156e_noST	0.32	0.21	0.39	0.90	0.38	0.63
C4_M172a	0.14	0.22	0.33	0.27	0.13	0.45
C4_M172a_Transition	0.16	0.22	0.33	0.34	0.13	0.53
C4_M172a_noST	0.12	0.06	0.33	0.15	0.13	0.45
C4_M172b	0.19	0.21	0.40	0.23	0.17	0.56
C4_M172b_noST	0.17	0.10	0.41	0.18	0.17	0.57
C4_M172c	0.23	0.24	0.48	0.24	0.23	0.67
C4_M172c_noST	0.24	0.16	0.48	0.22	0.22	0.67
C4_M172d	0.32	0.25	0.56	0.24	0.28	0.77
C4_M172d_noST	0.31	0.20	0.55	0.28	0.28	0.78
C4_M172e	0.40	0.23	0.62	0.35	0.33	0.89
C4_M172e_noST	0.41	0.29	0.62	0.34	0.35	0.88
C4_M330a	0.35	0.28	0.13	0.11	0.05	0.36
C4_M330a_Transition	0.50	0.27	0.13	0.30	0.06	1.09
C4_M330a_noST	0.24	0.12	0.11	0.29	0.06	1.04
C4_M360a	0.97	0.84	0.13	0.29	0.11	0.25
C4_M360a_Transition	1.18	0.83	0.13	0.30	0.12	0.63
C4_M360a_noST	0.83	0.65	0.12	0.29	0.11	0.57
C4_M360a_200t	1.14	1.03	0.12	0.37	0.12	0.16
C4_M360a_sga	0.94	0.80	0.12	0.29	0.12	0.26
C4_M360a_sk	1.03	0.83	0.12	0.31	0.12	0.26
C4_M360a_ssk	0.96	0.84	0.12	0.29	0.12	0.28
C4_M360a_ssk_sga	0.95	0.81	0.12	0.30	0.12	0.27
C4_M380a	1.00	0.79	0.19	0.22	0.08	0.28
C4_M380a_Transition	1.70	0.79	0.20	0.22	0.09	0.47
C4_M380a_noST	0.92	0.62	0.20	0.19	0.08	0.41
C4_M610a	0.14	0.99	0.12	0.27	0.03	0.05
C4_M610a_Transition	3.67	1.05	0.12	0.32	0.06	0.11
C4_M610b	0.23	1.42	0.20	0.37	0.06	0.08
C4_M610c	0.56	1.74	0.27	0.48	0.07	0.12
C4_M800a	0.34	2.17	0.13	0.51	0.06	0.10
C4_M800d	0.13	0.97	0.09	0.24	0.03	0.05
C4_M800e	0.08	0.53	0.06	0.11	0.02	0.03
C4_M800e_Transition	0.30	0.70	0.06	0.18	0.02	0.04
C4_M800e_noST	0.30	0.68	0.06	0.17	0.02	0.04

G.2 Case D

G.2.1 Result plots

Due to confidentiality, the figures including ST-results (i.e. forces, cylinder positions, characteristics) are not publicly available. Only the figures including the vessel motions have been published in this document.

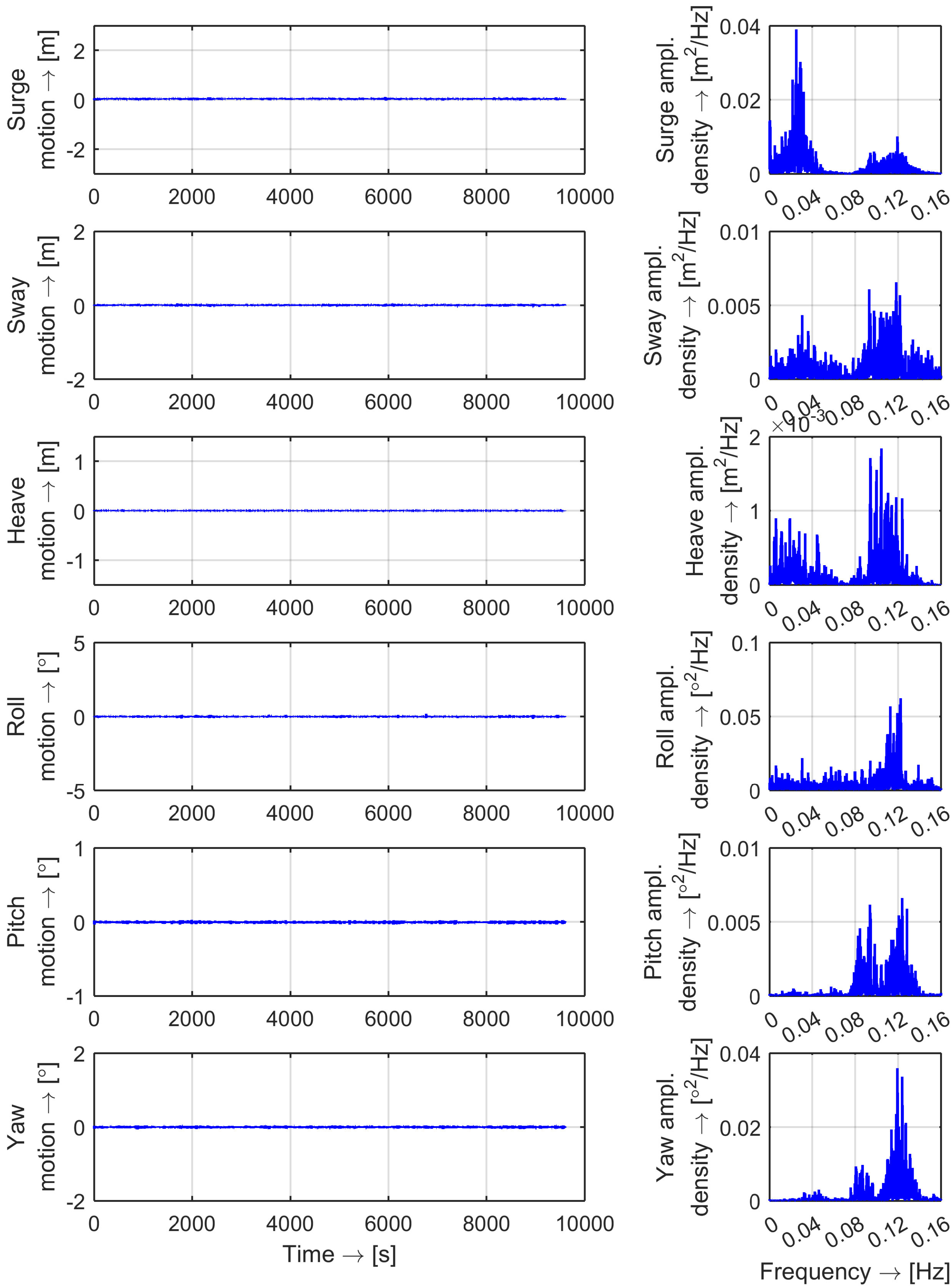

σ_{Surge} = 0.02 m, σ_{Sway} = 0.01 m, σ_{Heave} = 0.00 m, σ_{Roll} = 0.02°, σ_{Pitch} = 0.01°, σ_{Yaw} = 0.02°

Ship motions at centre of gravity (CoG) Depth = 18.0 m, H_s = 1.000 m, T_p = 8.00 s, γ = 3.3 Bow-quartering waves	Irregular	I80a
	D1_I80a	
Deltares	11202696	App. G.177-2

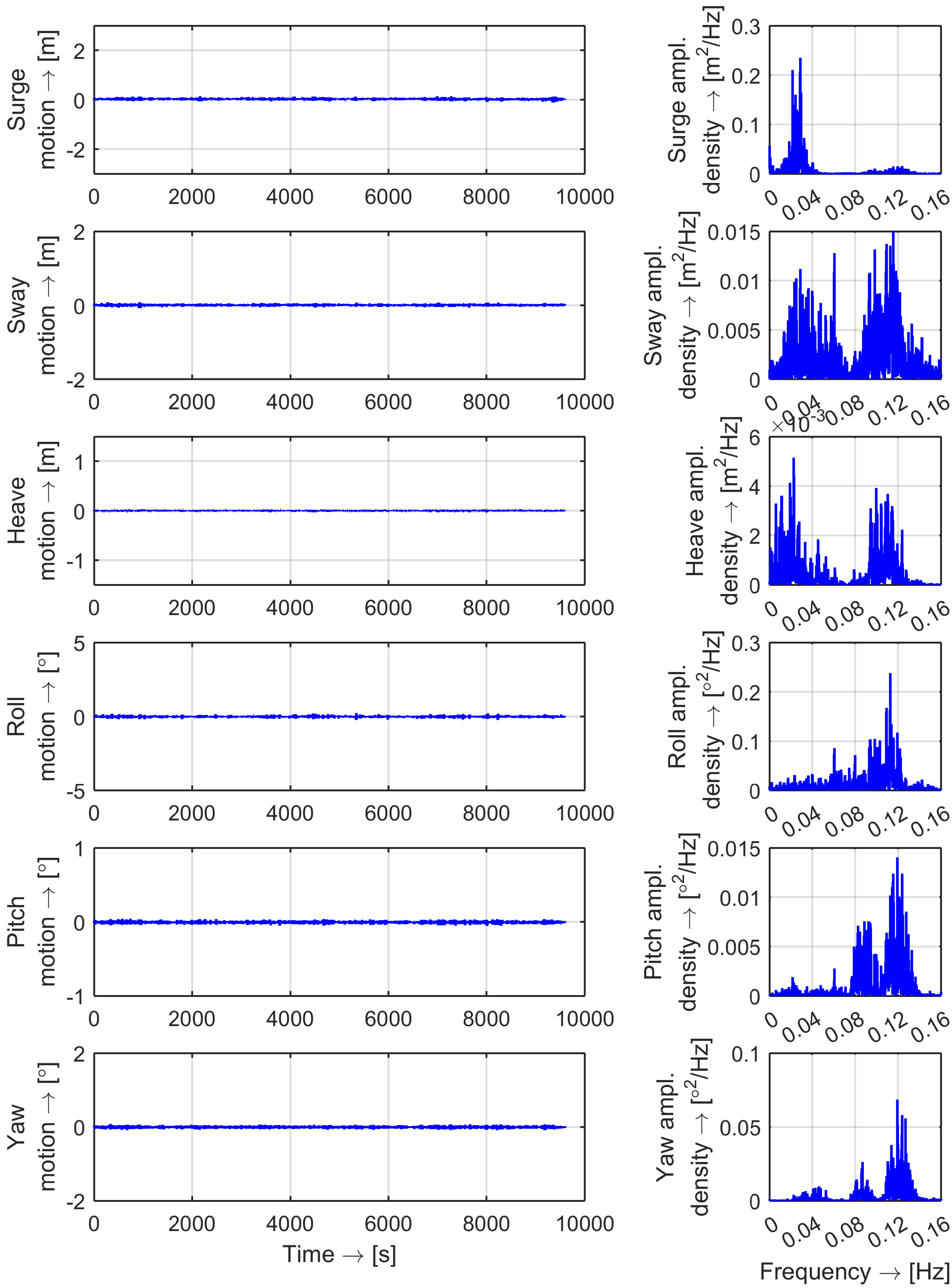

σ_{Surge} = 0.03 m, σ_{Sway} = 0.02 m, σ_{Heave} = 0.01 m, σ_{Roll} = 0.04°, σ_{Pitch} = 0.01°, σ_{Yaw} = 0.02°

Ship motions at centre of gravity (CoG) Depth = 18.0 m, H_s = 1.500 m, T_p = 8.00 s, γ = 3.3 Bow-quartering waves	Irregular	I80b
	D1_I80b	
Deltares	11202696	App. G.178-2

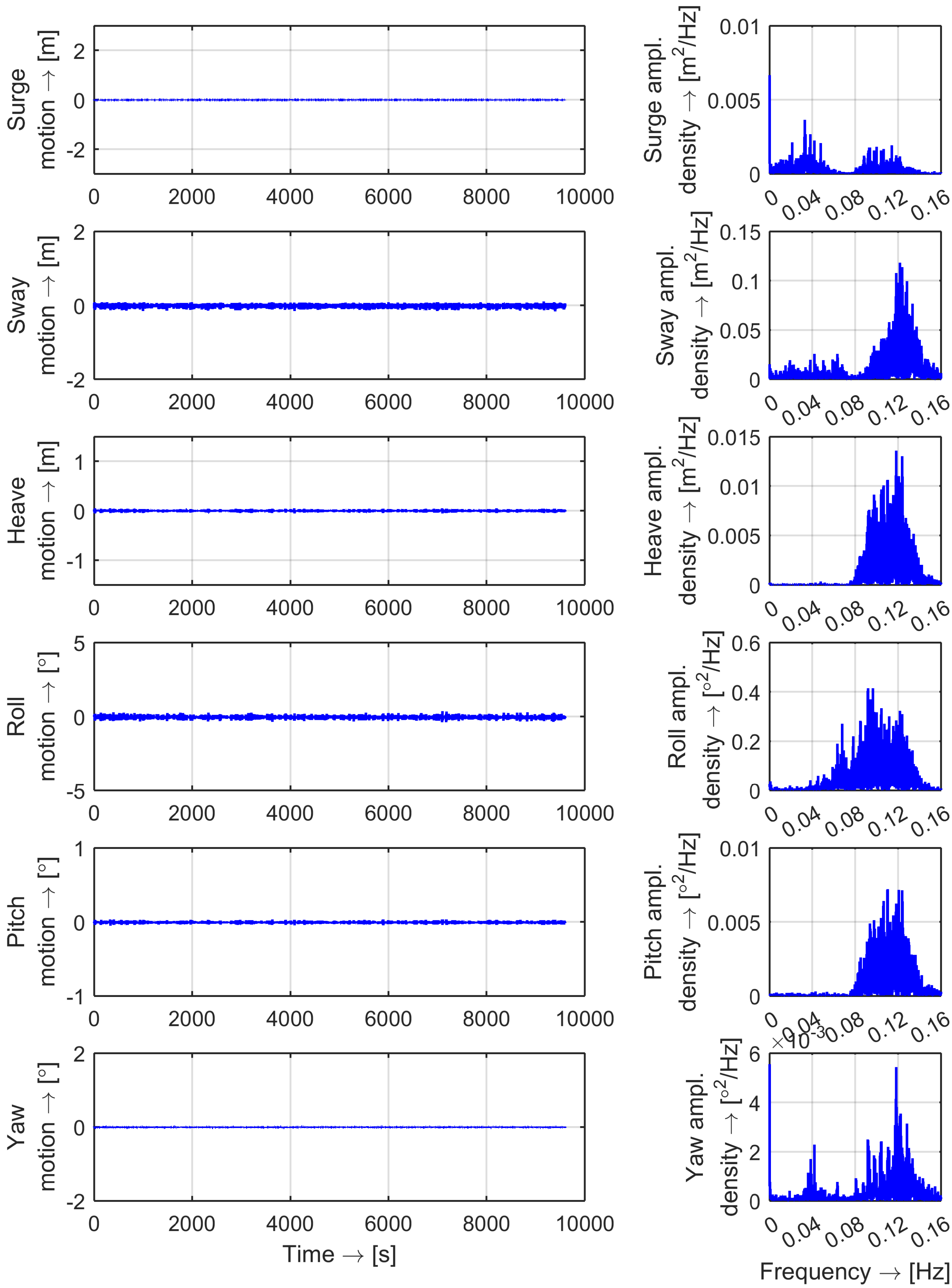

σ_{Surge} = 0.01 m, σ_{Sway} = 0.04 m, σ_{Heave} = 0.01 m, σ_{Roll} = 0.08°, σ_{Pitch} = 0.01°, σ_{Yaw} = 0.01°

Ship motions at centre of gravity (CoG) Depth = 18.0 m, H_s = 0.500 m, T_p = 8.00 s, γ = 3.3 Beam-on waves	Irregular	I80c
	D1_I80c	
Deltares	11202696	App. G.179-2

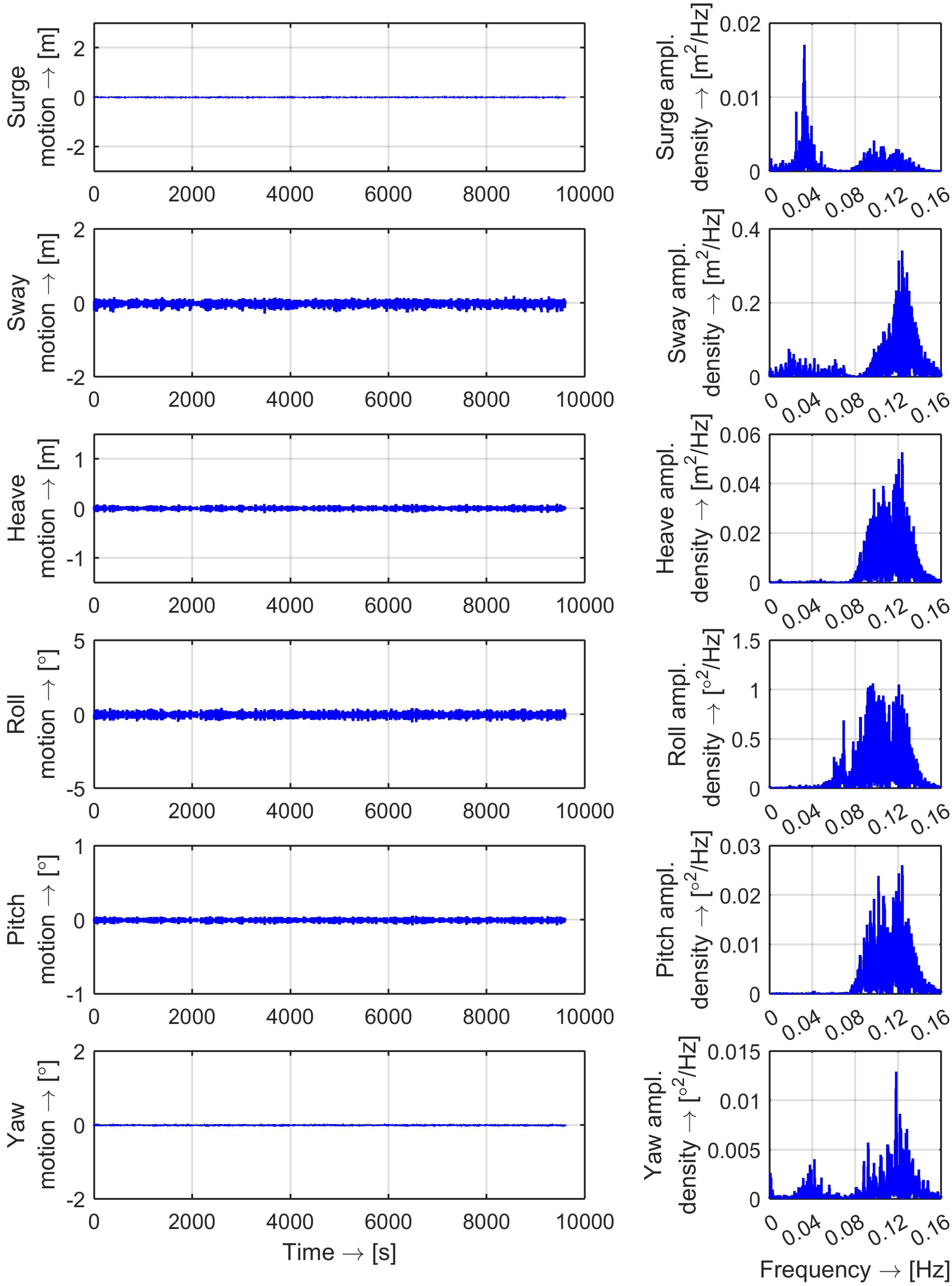

σ_{Surge} = 0.01 m, σ_{Sway} = 0.07 m, σ_{Heave} = 0.03 m, σ_{Roll} = 0.14°, σ_{Pitch} = 0.02°, σ_{Yaw} = 0.01°

Ship motions at centre of gravity (CoG) Depth = 18.0 m, H_s = 1.000 m, T_p = 8.00 s, γ = 3.3 Beam-on waves	Irregular	I80d
	D1_I80d	
Deltares	11202696	App. G.180-2

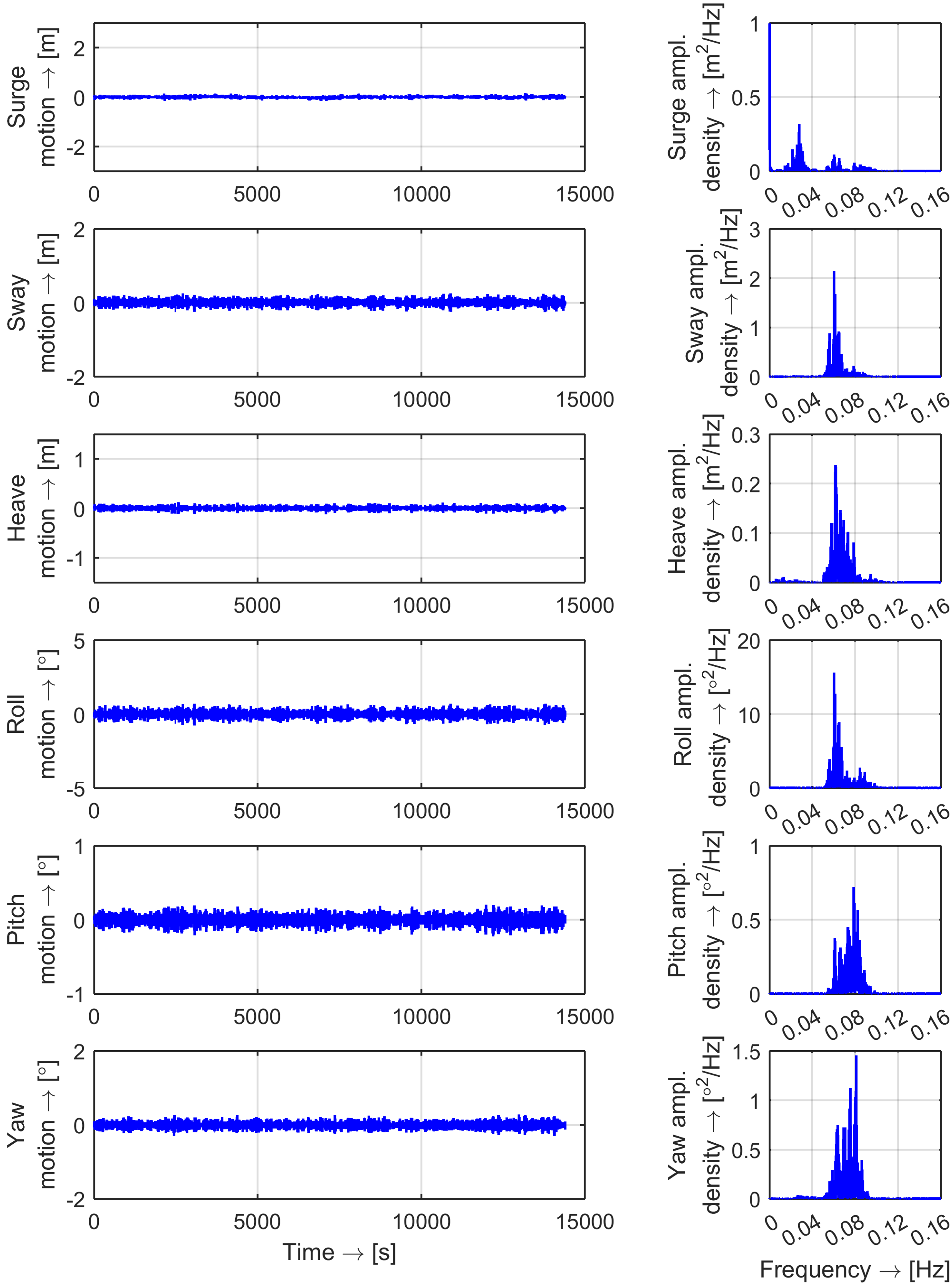

σ_{Surge} = 0.04 m, σ_{Sway} = 0.07 m, σ_{Heave} = 0.03 m, σ_{Roll} = 0.21°, σ_{Pitch} = 0.06°, σ_{Yaw} = 0.08°

Ship motions at centre of gravity (CoG) Depth = 18.0 m, H_s = 1.000 m, T_p = 12.00 s, γ = 3.3 Bow-quartering waves	Irregular	I120a
	D1_I120a	
Deltares	11202696	App. G.181-2

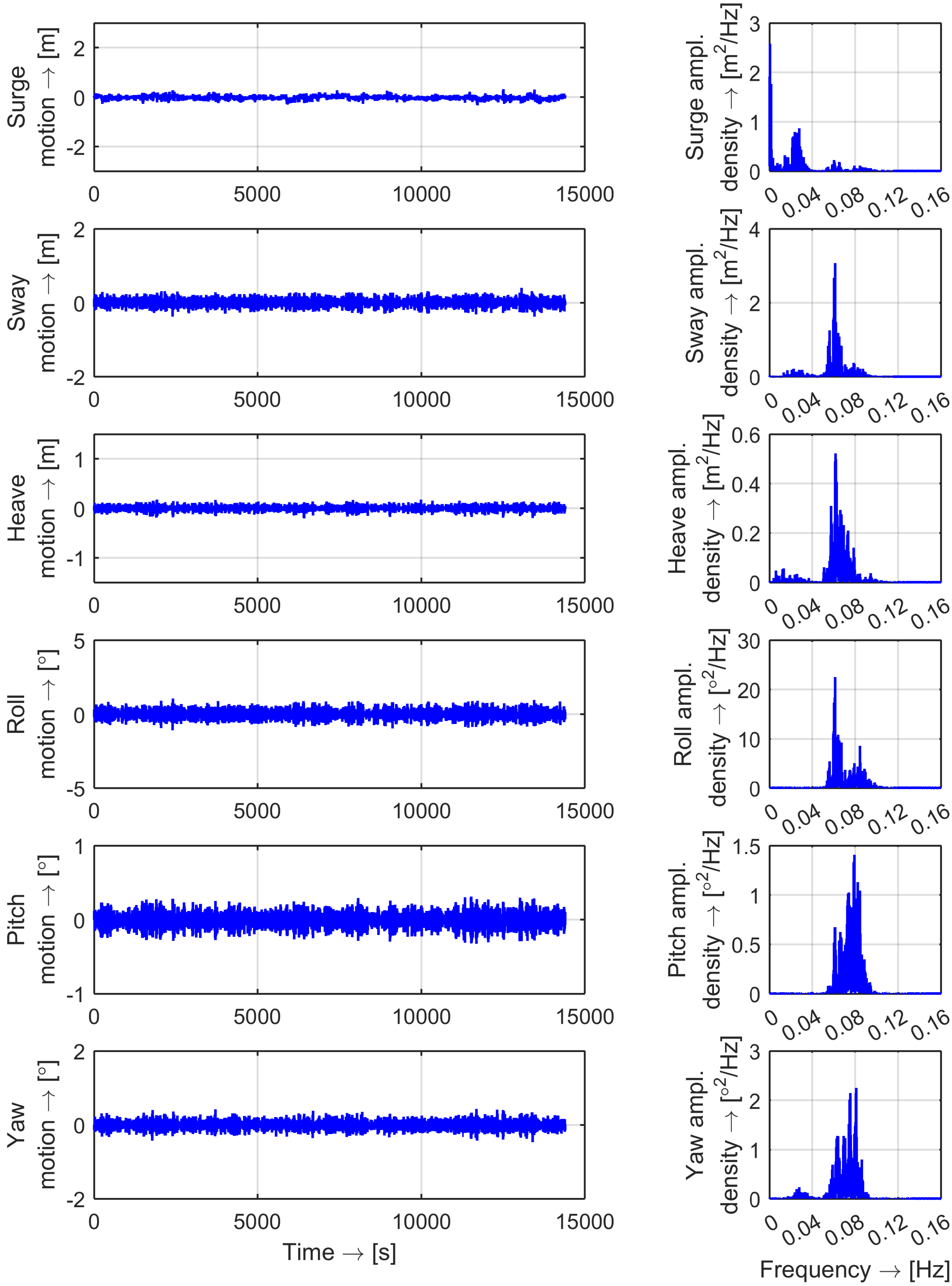

σ_{Surge} = 0.08 m, σ_{Sway} = 0.10 m, σ_{Heave} = 0.05 m, σ_{Roll} = 0.29°, σ_{Pitch} = 0.09°, σ_{Yaw} = 0.12°

Ship motions at centre of gravity (CoG) Depth = 18.0 m, H_s = 1.500 m, T_p = 12.00 s, γ = 3.3 Bow-quartering waves	Irregular	I120b
	D1_I120b	
Deltares	11202696	App. G.182-2

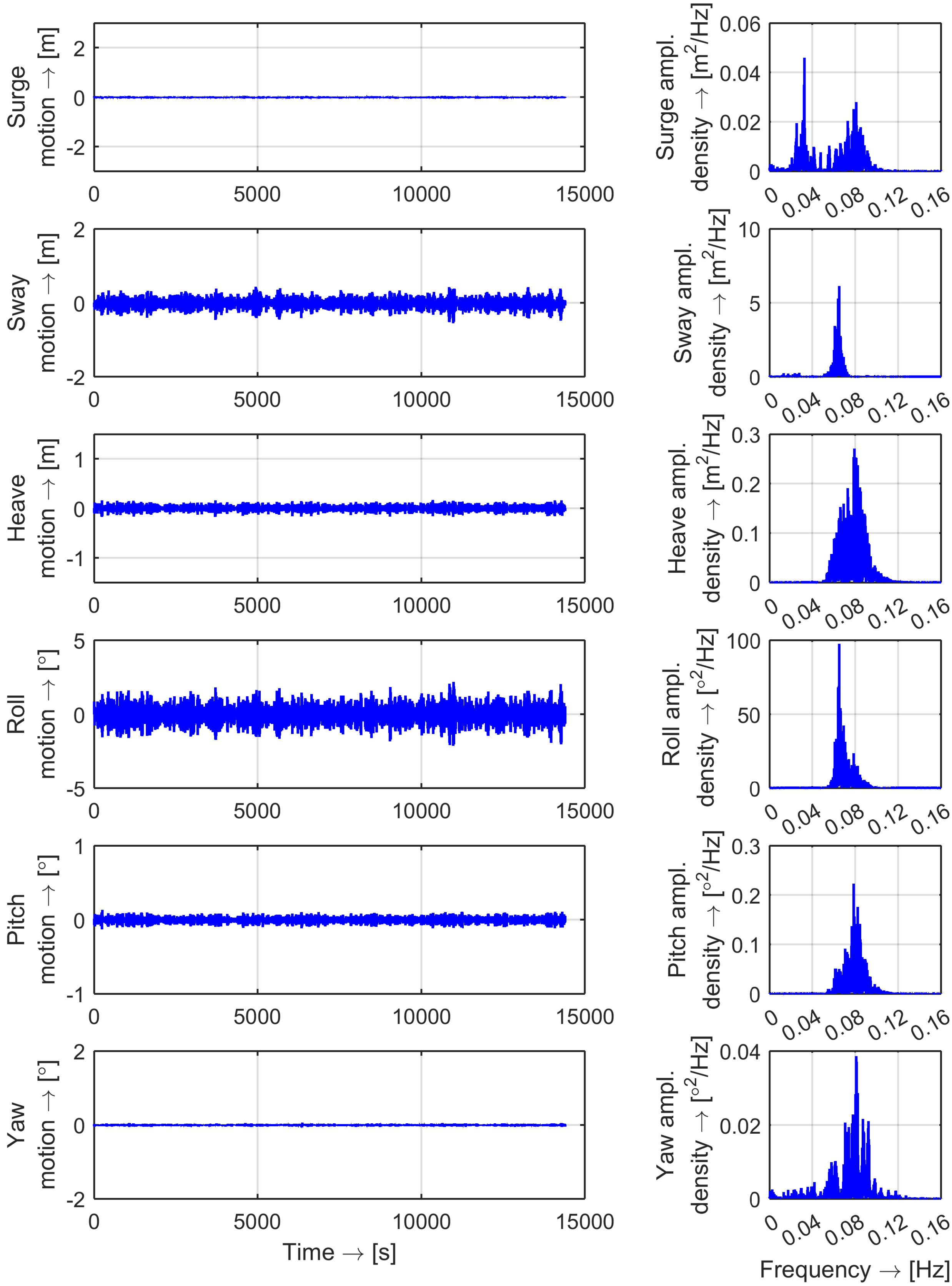

σ_{Surge} = 0.02 m, σ_{Sway} = 0.13 m, σ_{Heave} = 0.05 m, σ_{Roll} = 0.56°, σ_{Pitch} = 0.04°, σ_{Yaw} = 0.02°

Ship motions at centre of gravity (CoG) Depth = 18.0 m, H_s = 0.500 m, T_p = 12.00 s, γ = 3.3 Beam-on waves	Irregular	I120c
	D1_I120c	
Deltares	11202696	App. G.183-2

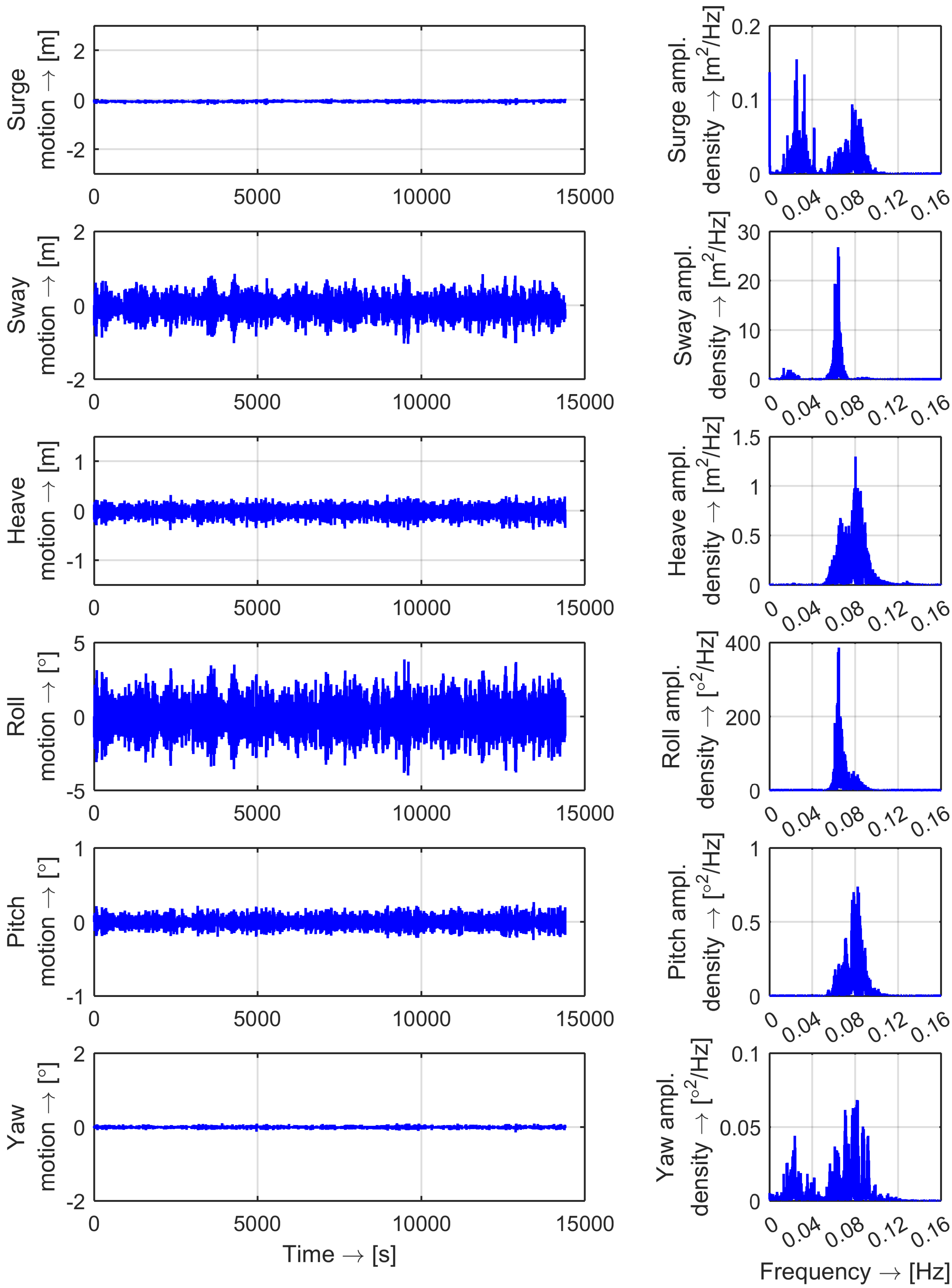

σ_{Surge} = 0.03 m, σ_{Sway} = 0.27 m, σ_{Heave} = 0.10 m, σ_{Roll} = 1.09°, σ_{Pitch} = 0.07°, σ_{Yaw} = 0.03°

Ship motions at centre of gravity (CoG) Depth = 18.0 m, H_s = 1.000 m, T_p = 12.00 s, γ = 3.3 Beam-on waves	Irregular	I120d
	D1_I120d	
Deltares	11202696	App. G.184-2

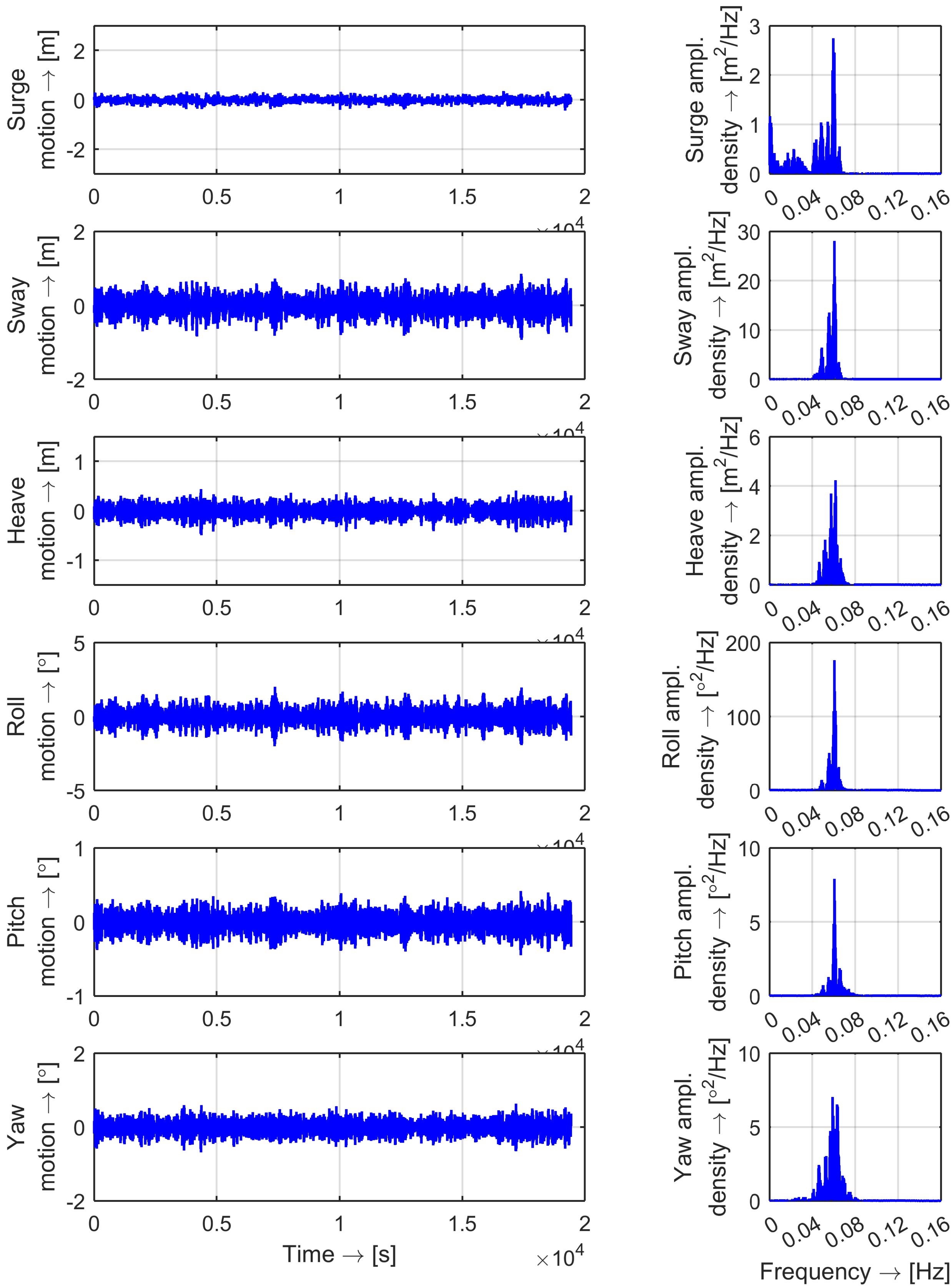

σ_{Surge} = 0.10 m, σ_{Sway} = 0.24 m, σ_{Heave} = 0.12 m, σ_{Roll} = 0.53°, σ_{Pitch} = 0.12°, σ_{Yaw} = 0.18°

Ship motions at centre of gravity (CoG) Depth = 18.0 m, H_s = 1.000 m, T_p = 16.20 s, γ = 5.0 Bow-quartering waves	Irregular	I162a
	D1_I162a	
Deltares	11202696	App. G.185-2

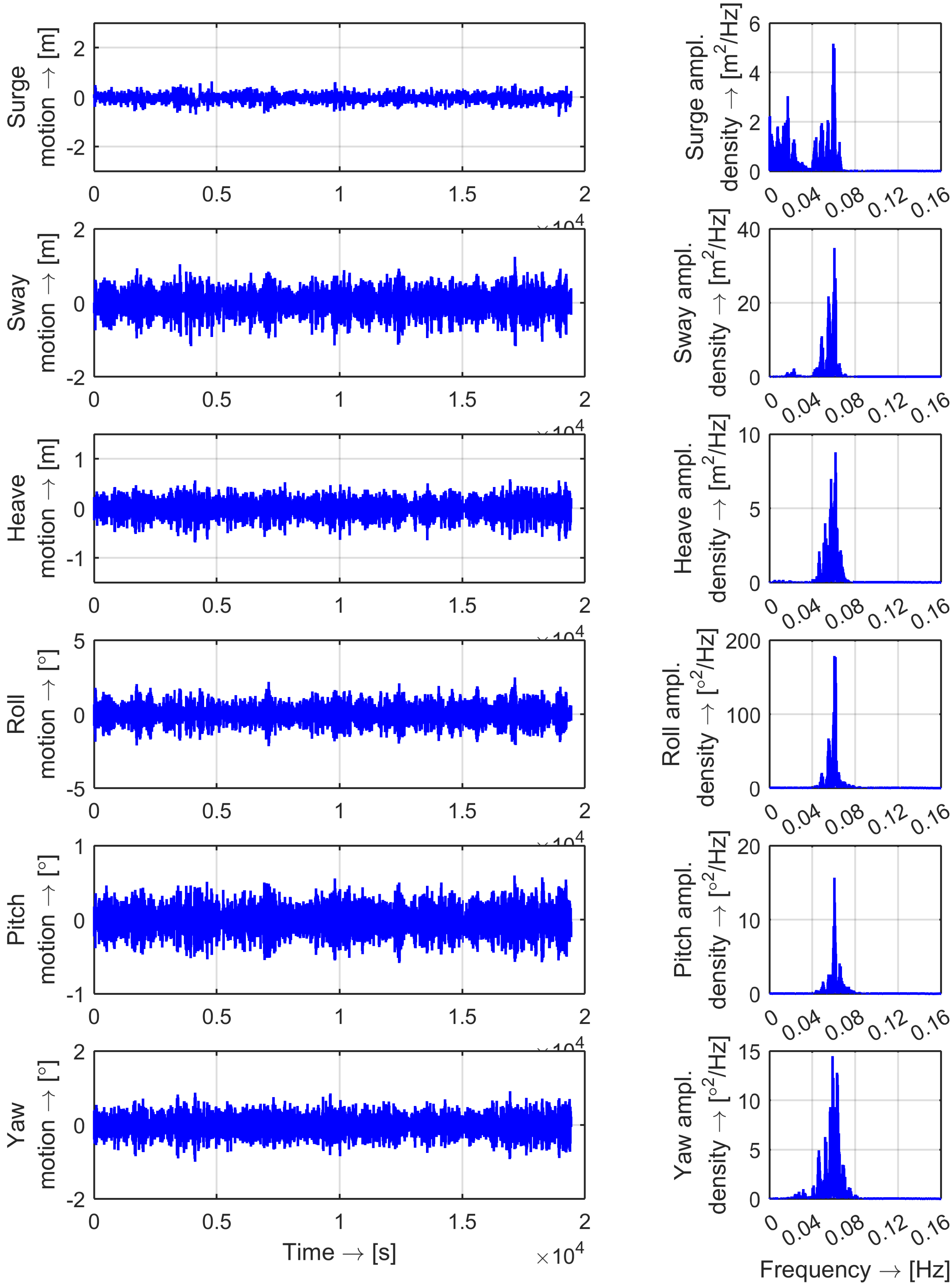

σ_{Surge} = 0.16 m, σ_{Sway} = 0.30 m, σ_{Heave} = 0.18 m, σ_{Roll} = 0.61°, σ_{Pitch} = 0.17°, σ_{Yaw} = 0.25°

Ship motions at centre of gravity (CoG) Depth = 18.0 m, H_s = 1.500 m, T_p = 16.20 s, γ = 5.0 Bow-quartering waves	Irregular	I162b
	D1_I162b	
Deltares	11202696	App. G.186-2

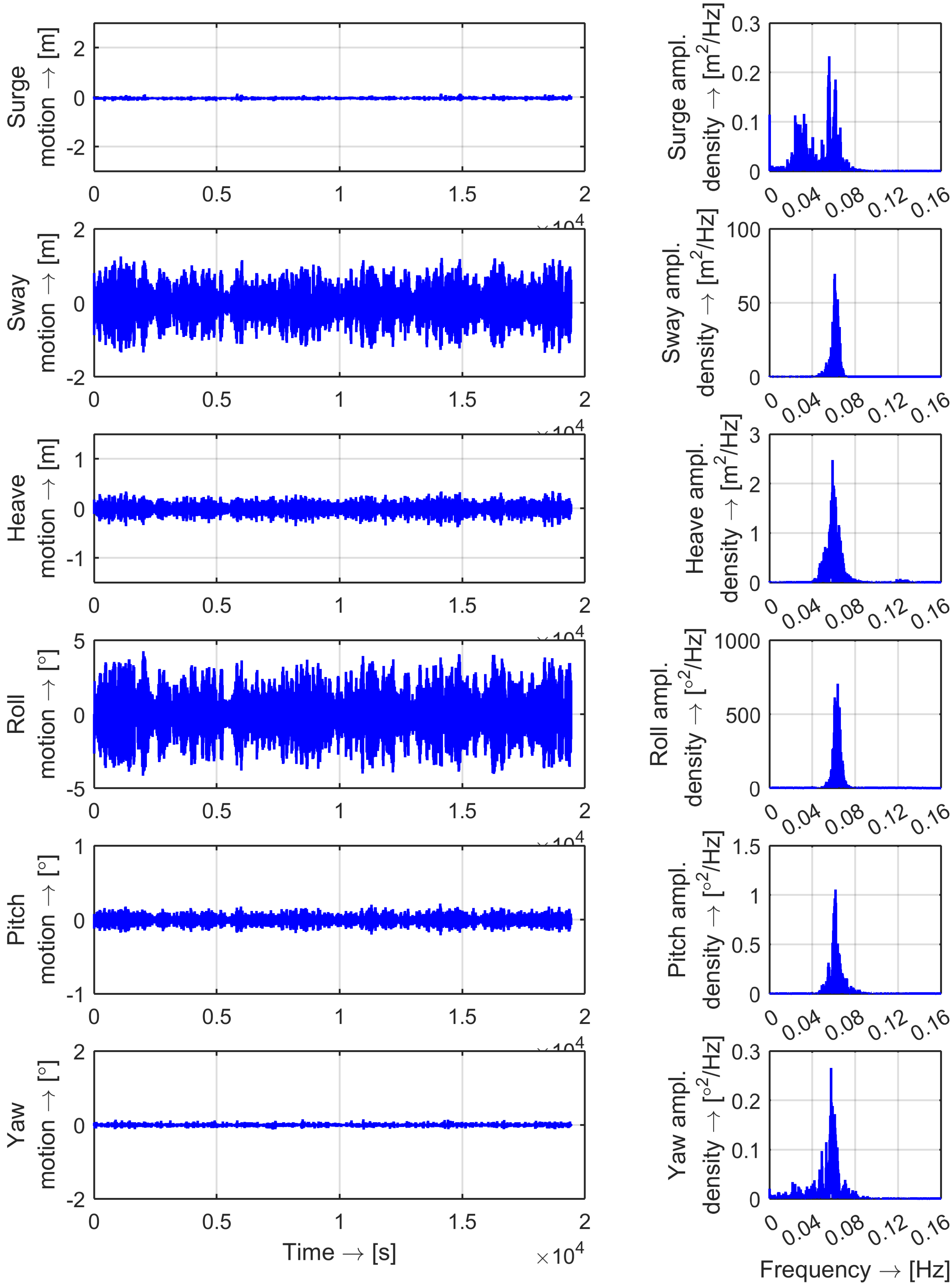

σ_{Surge} = 0.03 m, σ_{Sway} = 0.44 m, σ_{Heave} = 0.10 m, σ_{Roll} = 1.45°, σ_{Pitch} = 0.06°, σ_{Yaw} = 0.03°

Ship motions at centre of gravity (CoG) Depth = 18.0 m, H_s = 0.500 m, T_p = 16.20 s, γ = 5.0 Beam-on waves	Irregular	I162c
	D1_I162c	
Deltares	11202696	App. G.187-2

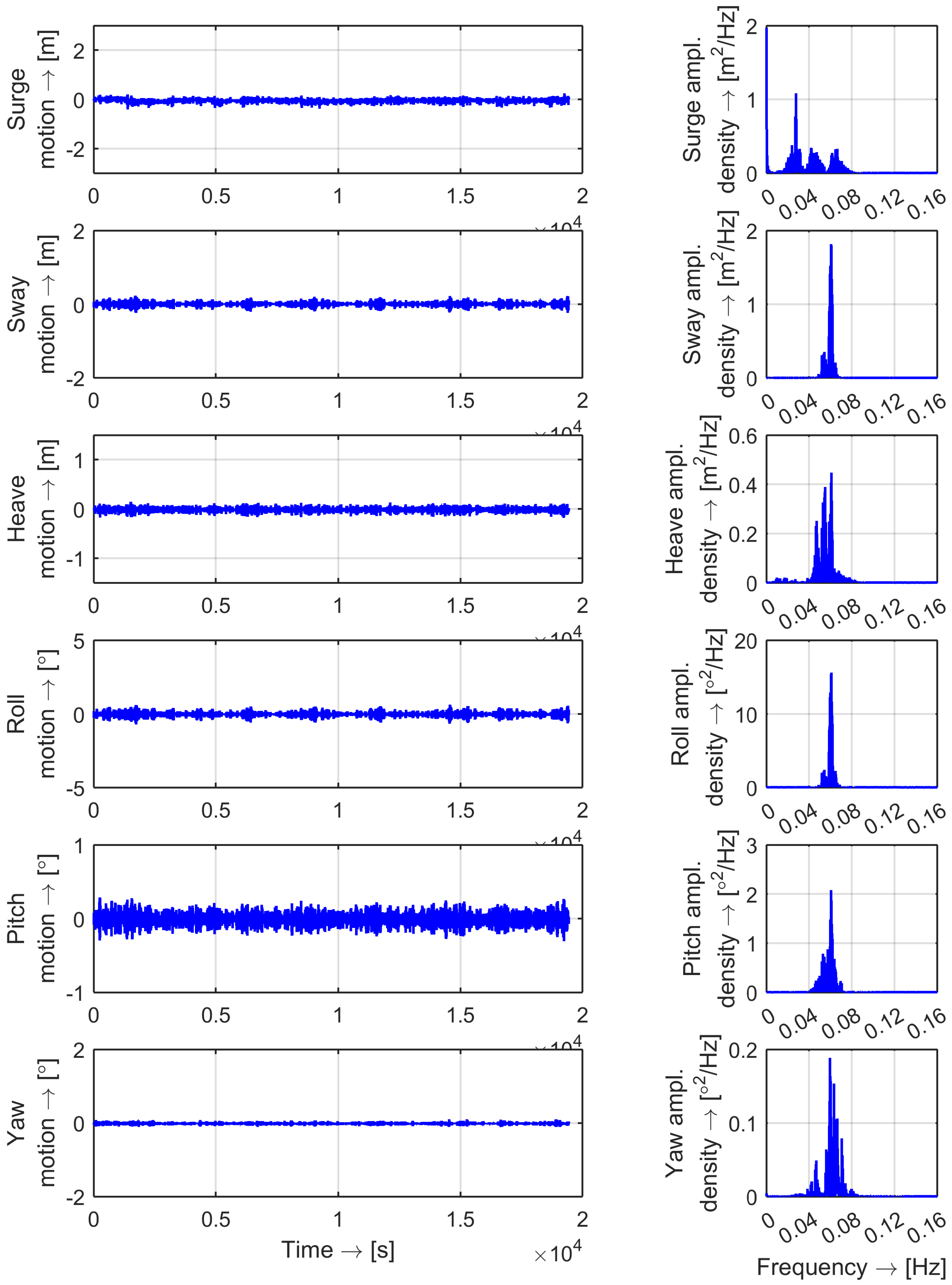

σ_{Surge} = 0.07 m, σ_{Sway} = 0.06 m, σ_{Heave} = 0.04 m, σ_{Roll} = 0.16°, σ_{Pitch} = 0.08°, σ_{Yaw} = 0.03°

Ship motions at centre of gravity (CoG) Depth = 18.0 m, H_s = 1.000 m, T_p = 16.20 s, γ = 5.0 Head-on waves	Irregular	I162e
	D1_I162e	
Deltares	11202696	App. G.188-2

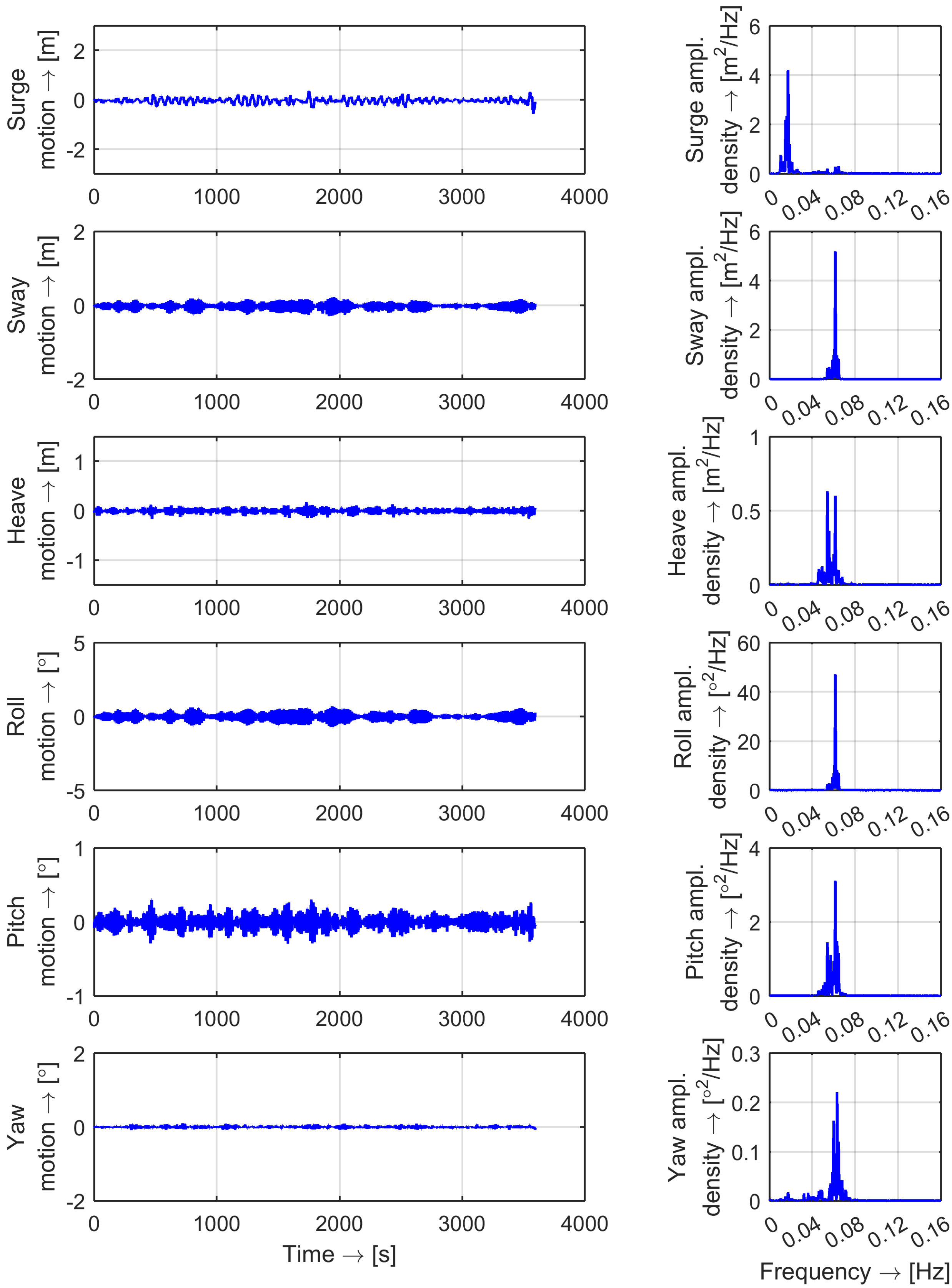

σ_{Surge} = 0.10 m, σ_{Sway} = 0.09 m, σ_{Heave} = 0.05 m, σ_{Roll} = 0.25°, σ_{Pitch} = 0.09°, σ_{Yaw} = 0.03°

Ship motions at centre of gravity (CoG) Depth = 18.0 m, H_s = 1.000 m, T_p = 16.20 s, γ = 5.0 Head-on waves	Irregular	I162e
	D1_I162e_noST	
Deltares	11202696	App. G.189-2

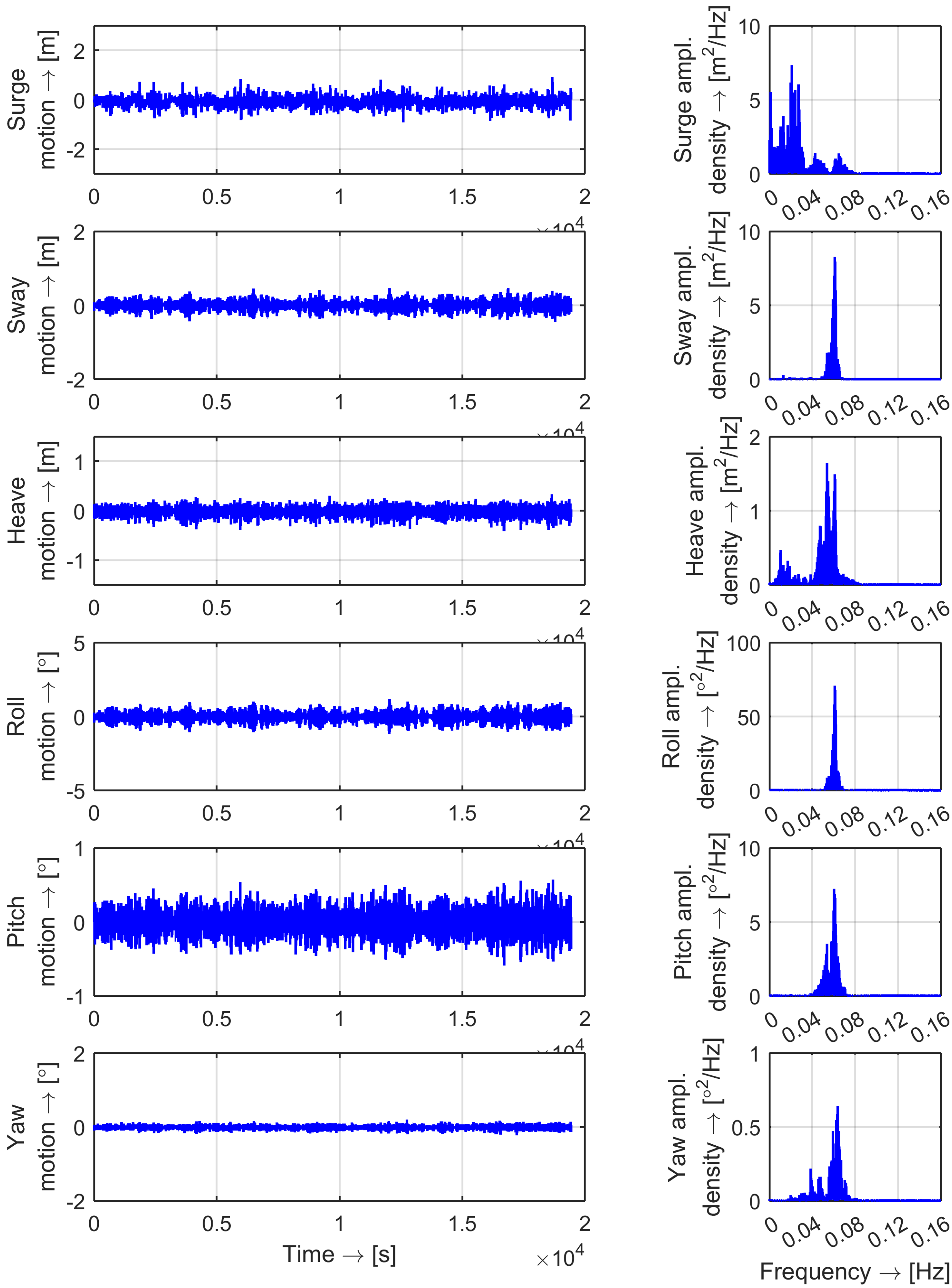

σ_{Surge} = 0.20 m, σ_{Sway} = 0.12 m, σ_{Heave} = 0.09 m, σ_{Roll} = 0.33°, σ_{Pitch} = 0.16°, σ_{Yaw} = 0.05°

Ship motions at centre of gravity (CoG) Depth = 18.0 m, H_s = 2.000 m, T_p = 16.20 s, γ = 5.0 Head-on waves	Irregular	I162f
	D1_I162f	
Deltares	11202696	App. G.190-2

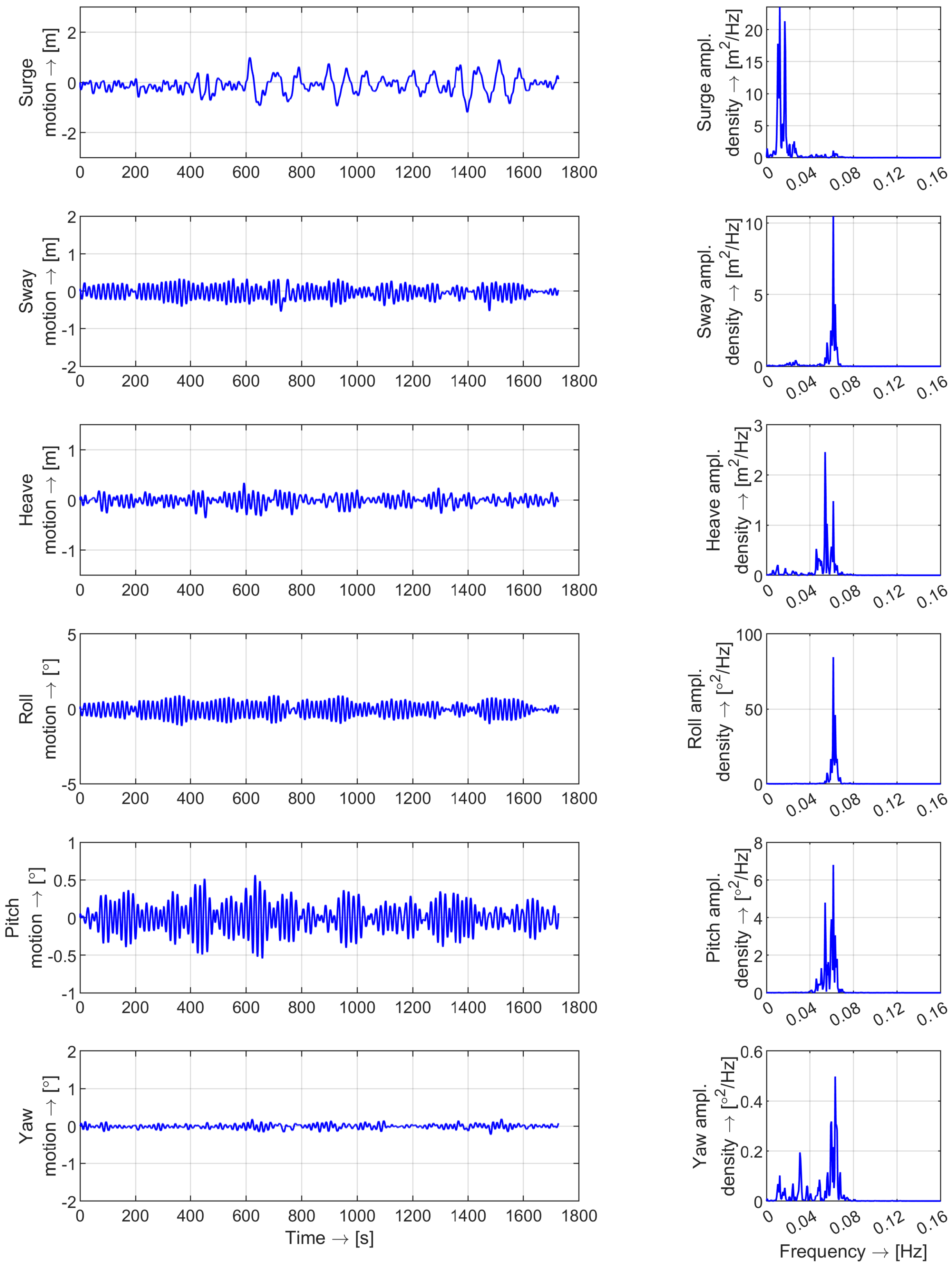

σ_{Surge} = n.a., σ_{Sway} = n.a., σ_{Heave} = n.a., σ_{Roll} = n.a., σ_{Pitch} = n.a., σ_{Yaw} = n.a.

Ship motions at centre of gravity (CoG) Depth = 18.0 m, H_s = 2.000 m, T_p = 16.20 s, γ = 5.0 Head-on waves	Irregular	I162f
	D1_I162f_transition	
Deltares	11202696	App. G.191-2

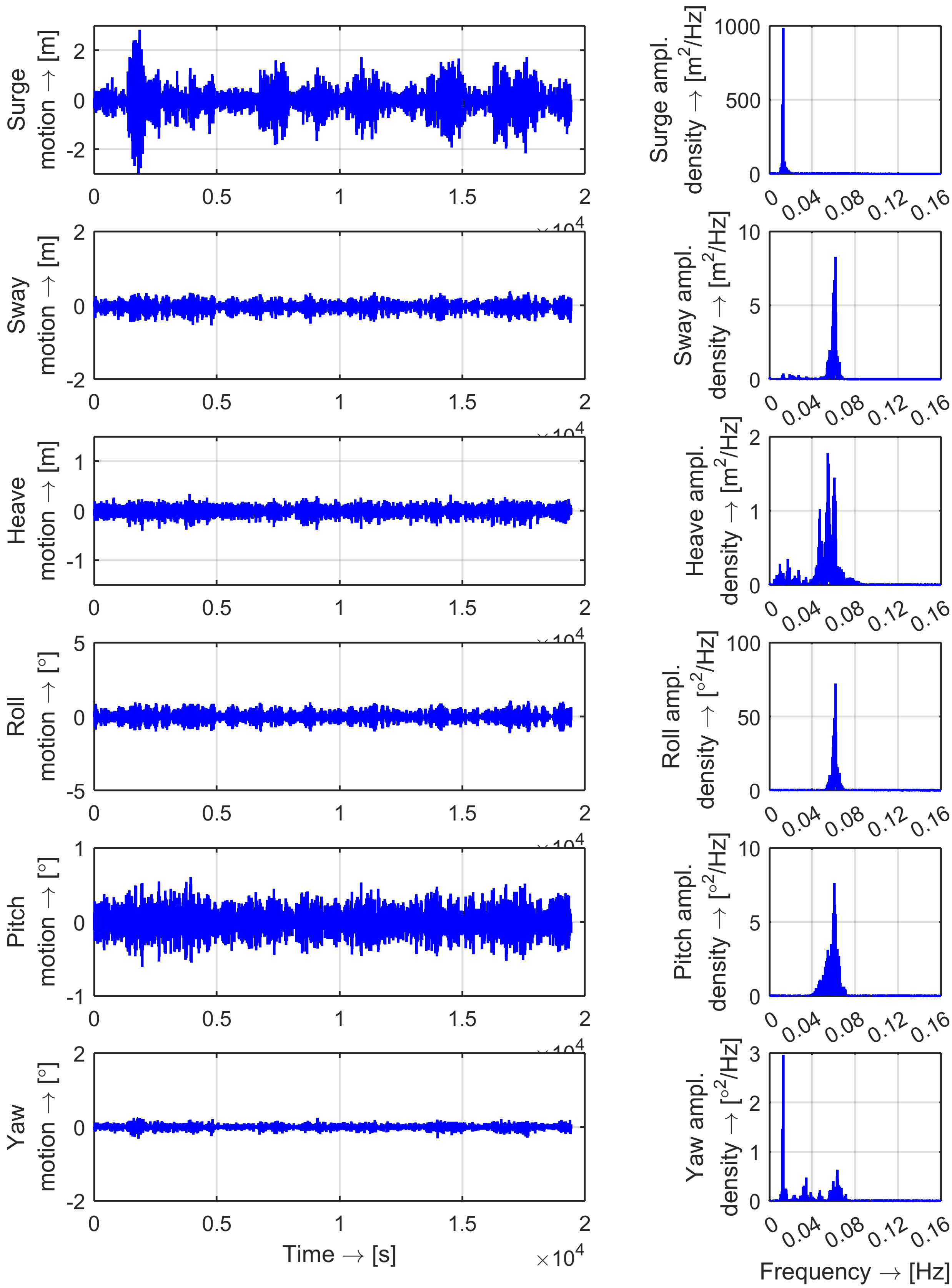

σ_{Surge} = 0.61 m, σ_{Sway} = 0.13 m, σ_{Heave} = 0.09 m, σ_{Roll} = 0.33°, σ_{Pitch} = 0.16°, σ_{Yaw} = 0.06°

Ship motions at centre of gravity (CoG) Depth = 18.0 m, H_s = 2.000 m, T_p = 16.20 s, γ = 5.0 Head-on waves	Irregular	I162f
	D1_I162f_noST	
Deltares	11202696	App. G.192-2

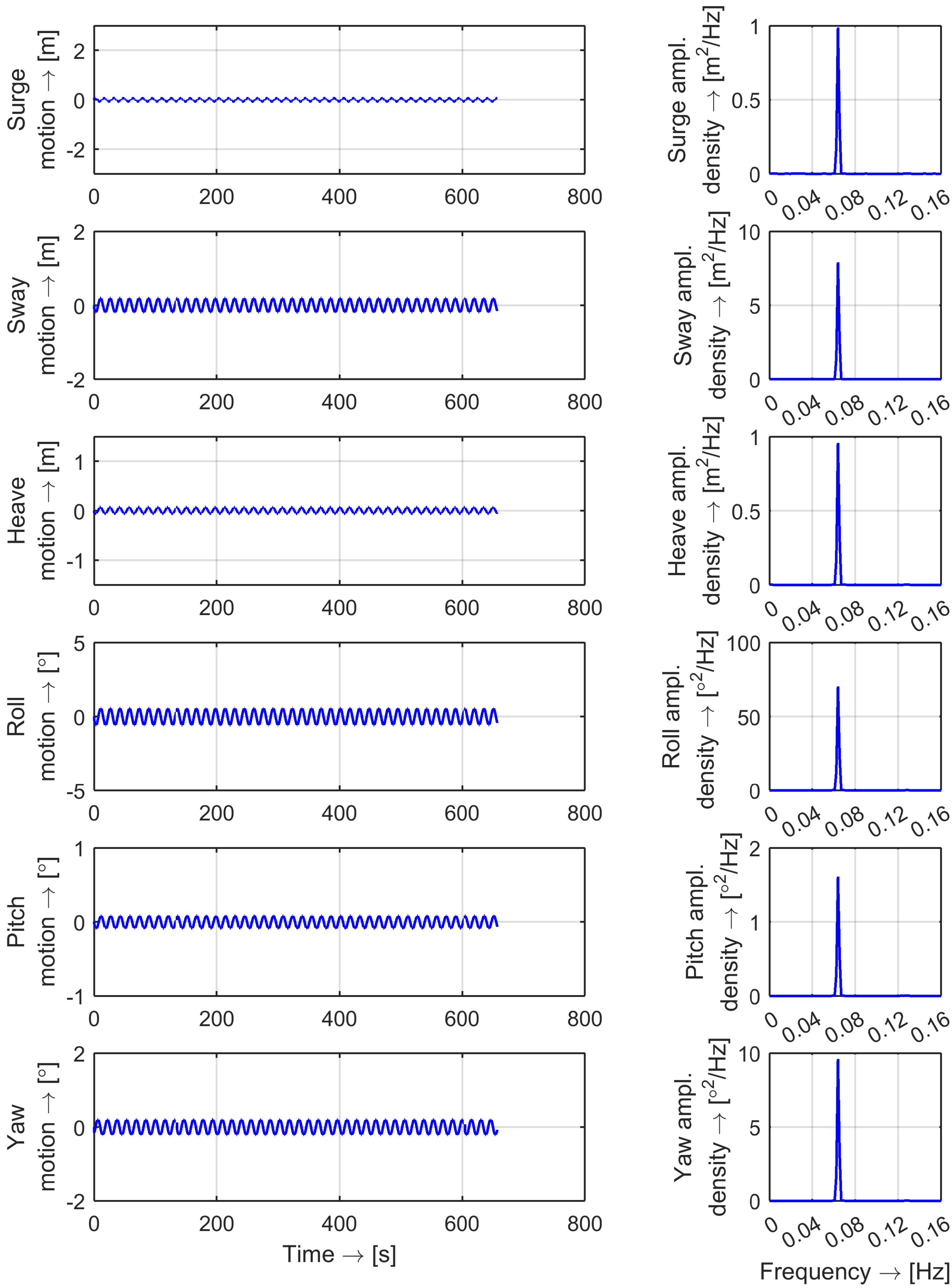

σ_{Surge} = 0.05 m, σ_{Sway} = 0.14 m, σ_{Heave} = 0.05 m, σ_{Roll} = 0.40°, σ_{Pitch} = 0.06°, σ_{Yaw} = 0.15°

Ship motions at centre of gravity (CoG) Depth = 18.0 m, H = 0.500 m, T = 15.60 s Bow-quartering waves	Monochromatic	M156a
	D2_M156a	
Deltares	11202696	App. G.193-2

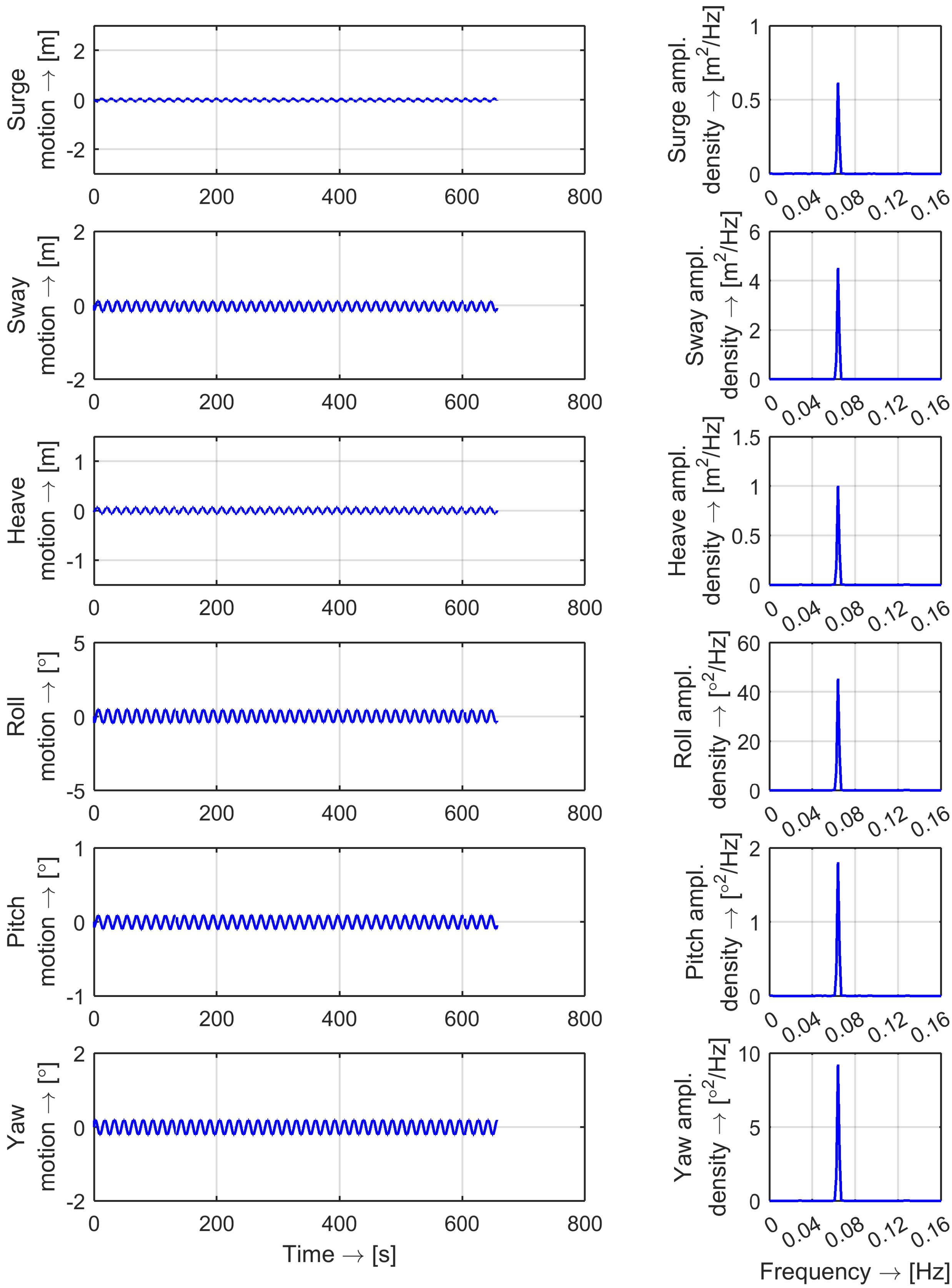

σ_{Surge} = 0.04 m, σ_{Sway} = 0.10 m, σ_{Heave} = 0.05 m, σ_{Roll} = 0.32°, σ_{Pitch} = 0.06°, σ_{Yaw} = 0.15°

Ship motions at centre of gravity (CoG) Depth = 18.0 m, H = 0.500 m, T = 15.60 s Bow-quartering waves	Monochromatic	M156a
	D2_M156a_noST	
Deltares	11202696	App. G.194-2

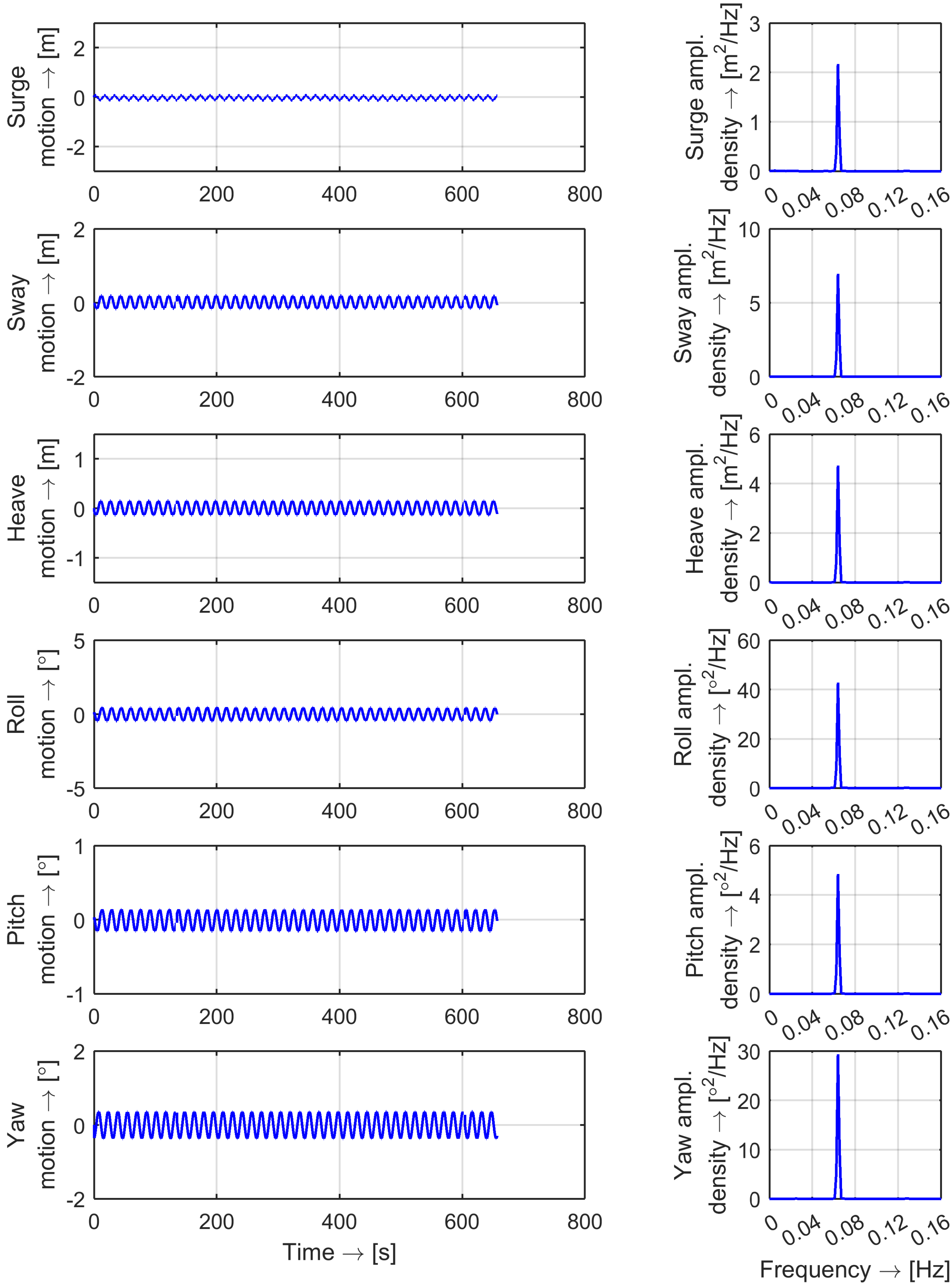

σ_{Surge} = 0.07 m, σ_{Sway} = 0.13 m, σ_{Heave} = 0.10 m, σ_{Roll} = 0.32°, σ_{Pitch} = 0.11°, σ_{Yaw} = 0.26°

Ship motions at centre of gravity (CoG) Depth = 18.0 m, H = 1.000 m, T = 15.60 s Bow-quartering waves	Monochromatic	M156b
	D2_M156b	
Deltares	11202696	App. G.195-2

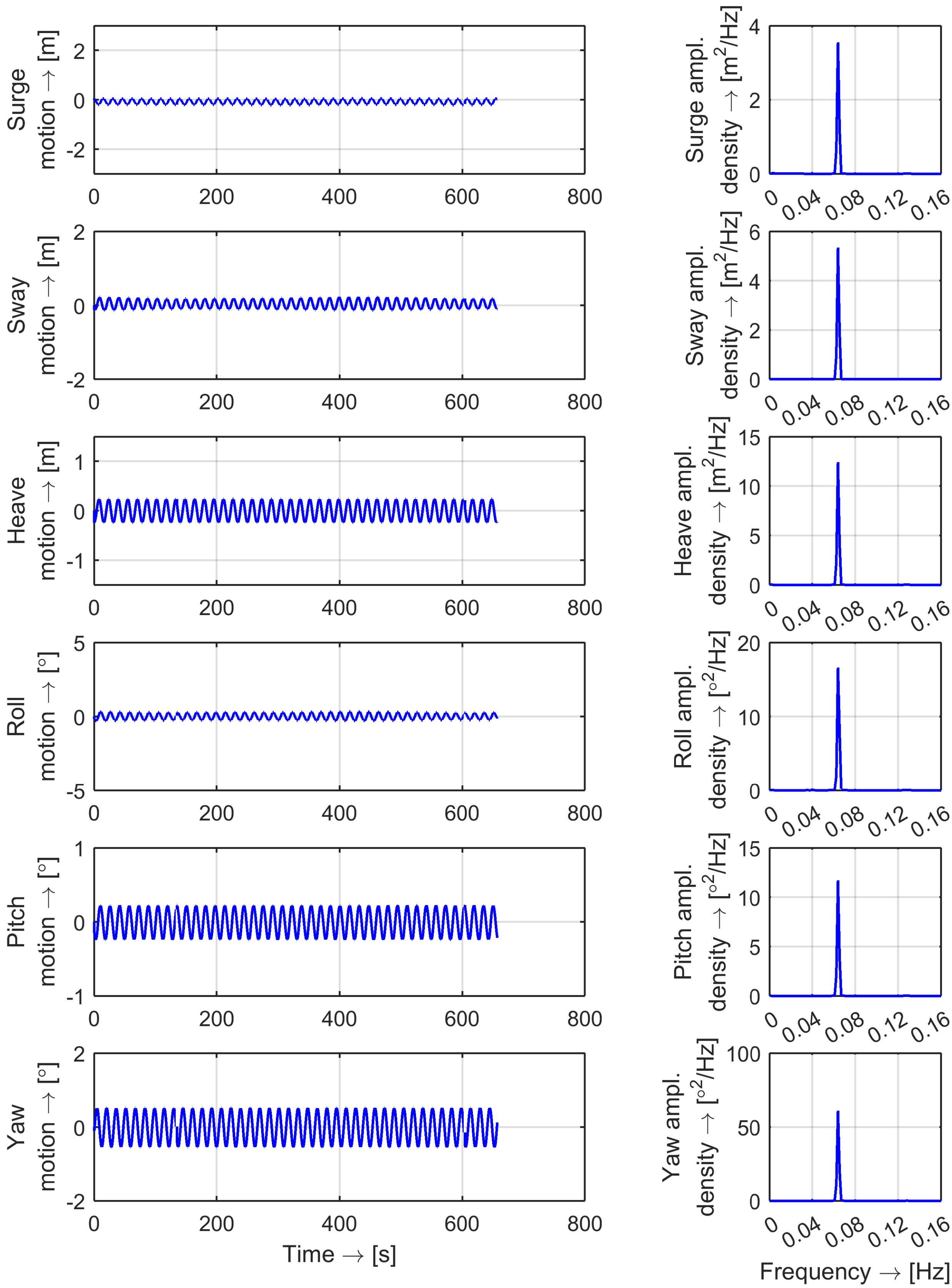

σ_{Surge} = 0.09 m, σ_{Sway} = 0.11 m, σ_{Heave} = 0.17 m, σ_{Roll} = 0.20°, σ_{Pitch} = 0.16°, σ_{Yaw} = 0.38°

Ship motions at centre of gravity (CoG) Depth = 18.0 m, H = 1.500 m, T = 15.60 s Bow-quartering waves	Monochromatic	M156c
	D2_M156c	
Deltares	11202696	App. G.196-2

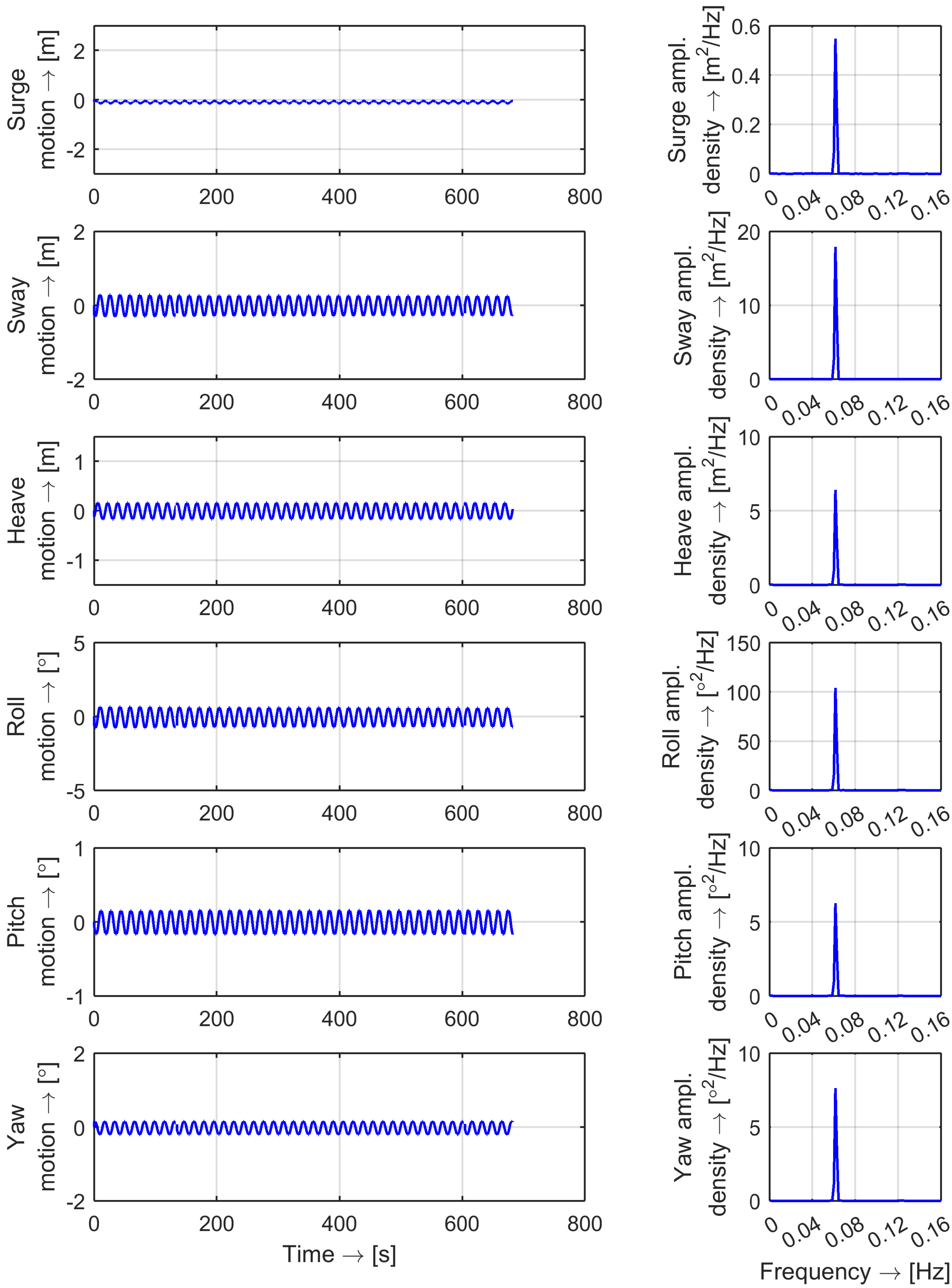

σ_{Surge} = 0.04 m, σ_{Sway} = 0.20 m, σ_{Heave} = 0.12 m, σ_{Roll} = 0.49°, σ_{Pitch} = 0.12°, σ_{Yaw} = 0.13°

Ship motions at centre of gravity (CoG) Depth = 18.0 m, H = 0.500 m, T = 16.20 s Bow-quartering waves	Monochromatic	M162a
	D2_M162a	
Deltares	11202696	App. G.197-2

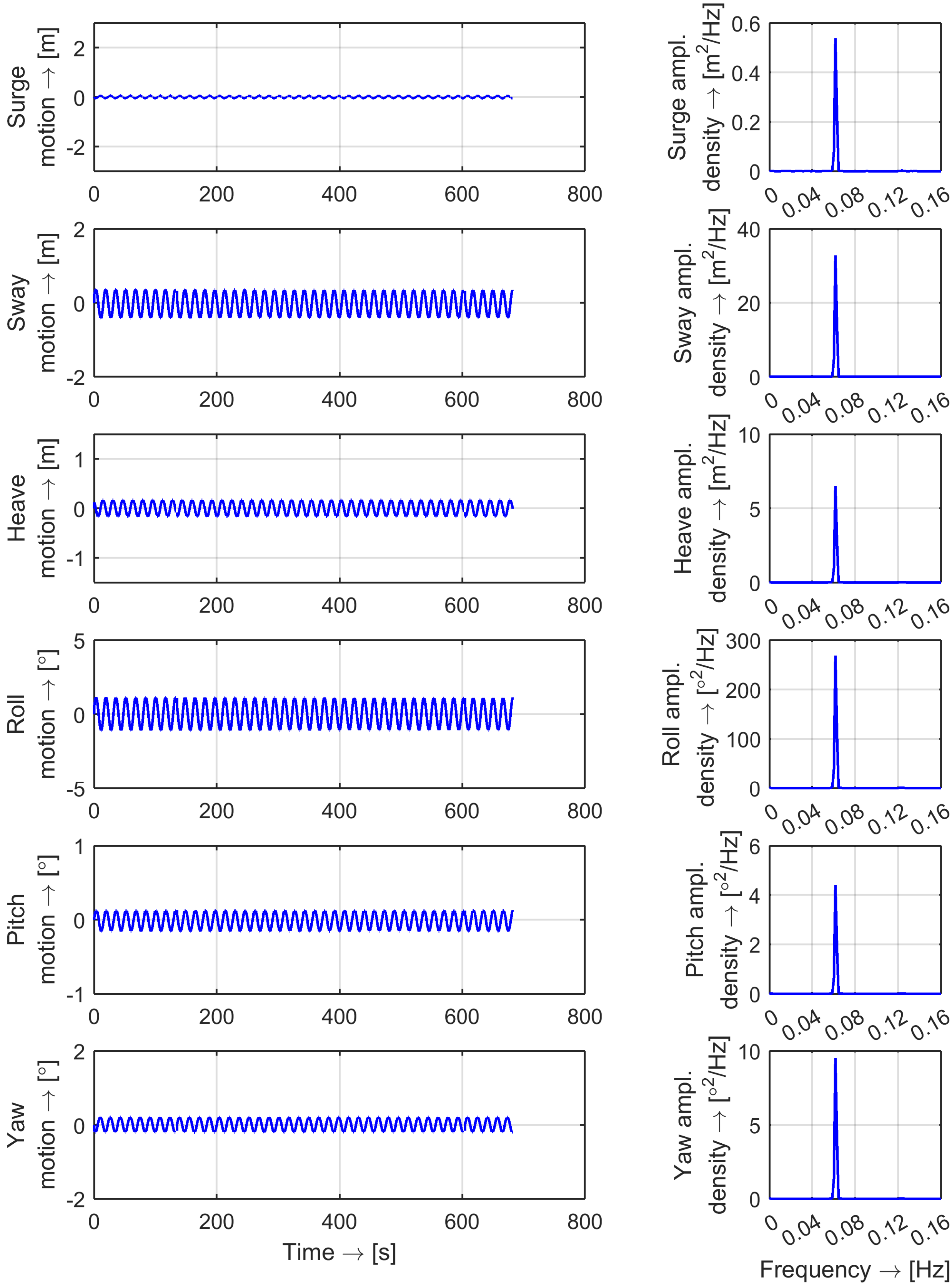

σ_{Surge} = 0.04 m, σ_{Sway} = 0.27 m, σ_{Heave} = 0.12 m, σ_{Roll} = 0.79°, σ_{Pitch} = 0.10°, σ_{Yaw} = 0.15°

Ship motions at centre of gravity (CoG) Depth = 18.0 m, H = 0.500 m, T = 16.20 s Bow-quartering waves	Monochromatic	M162a
	D2_M162a_noST	
Deltares	11202696	App. G.198-2

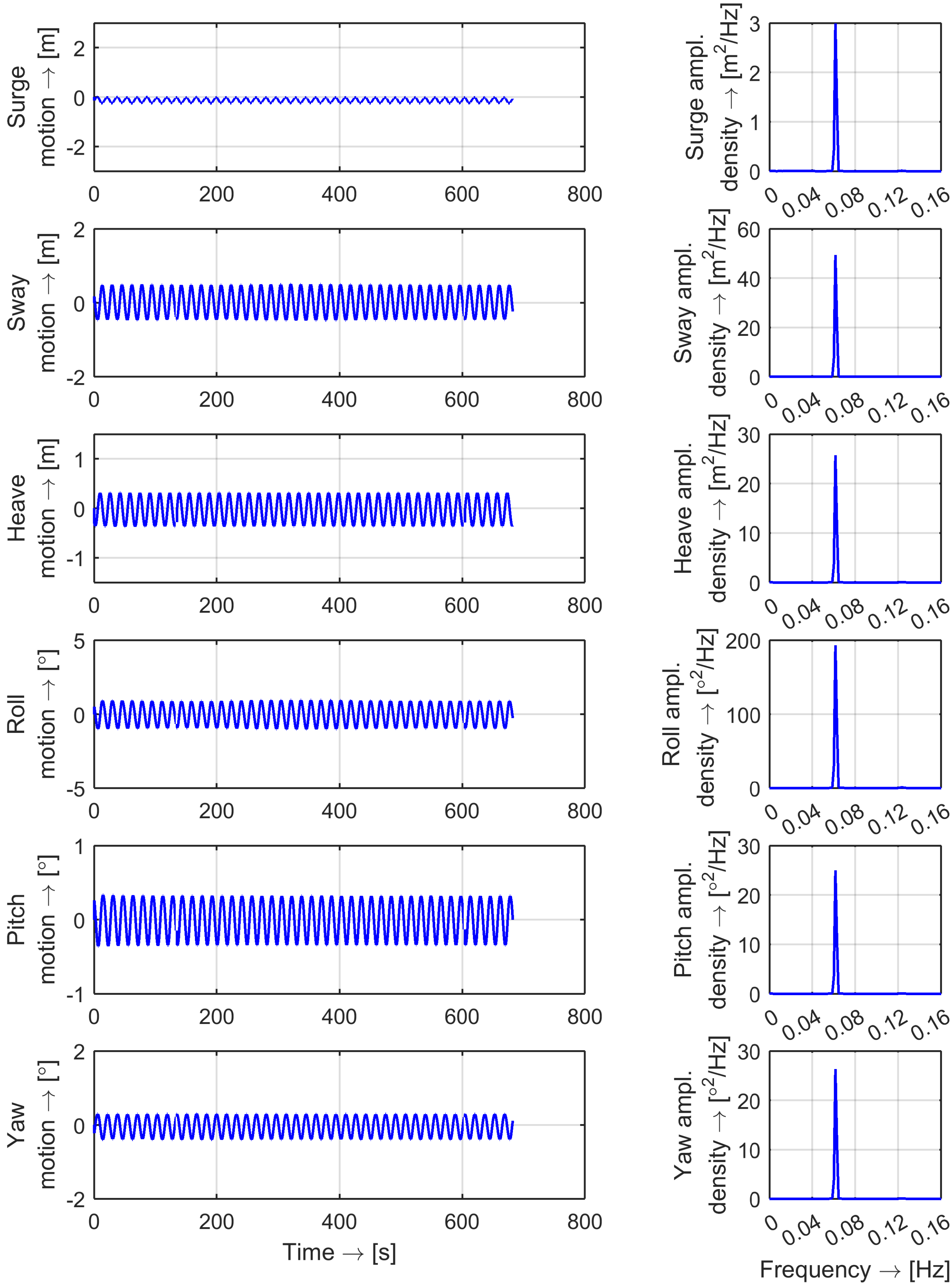

σ_{Surge} = 0.08 m, σ_{Sway} = 0.34 m, σ_{Heave} = 0.24 m, σ_{Roll} = 0.67°, σ_{Pitch} = 0.24°, σ_{Yaw} = 0.25°

Ship motions at centre of gravity (CoG) Depth = 18.0 m, H = 1.000 m, T = 16.20 s Bow-quartering waves	Monochromatic	M162b
	D2_M162b	
Deltares	11202696	App. G.199-2

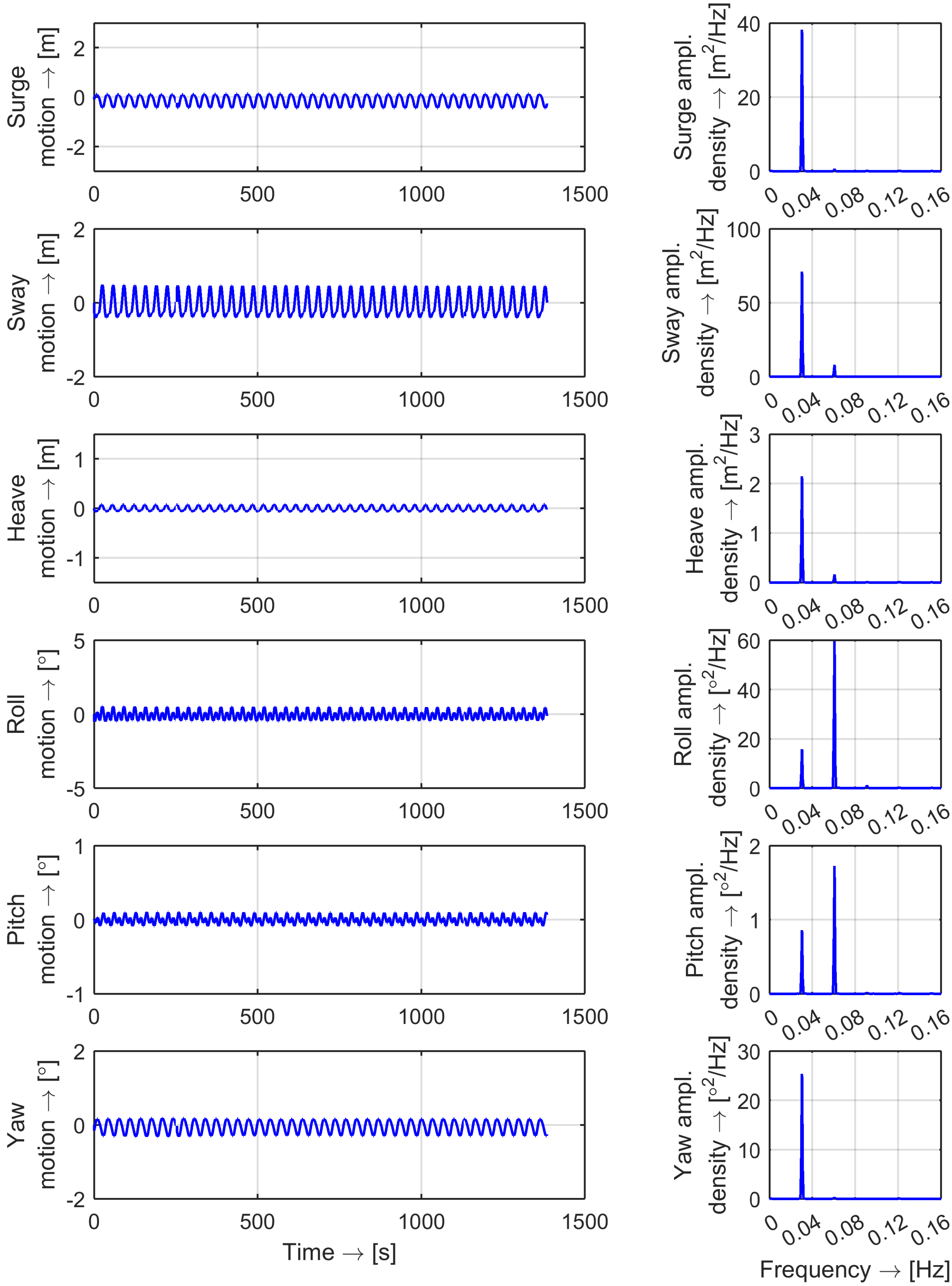

σ_{Surge} = 0.21 m, σ_{Sway} = 0.29 m, σ_{Heave} = 0.05 m, σ_{Roll} = 0.29°, σ_{Pitch} = 0.05°, σ_{Yaw} = 0.17°

Ship motions at centre of gravity (CoG) Depth = 18.0 m, H = 0.120 m, T = 33.00 s Bow-quartering waves	Monochromatic	M330e
	D2_M330e	
Deltares	11202696	App. G.200-2

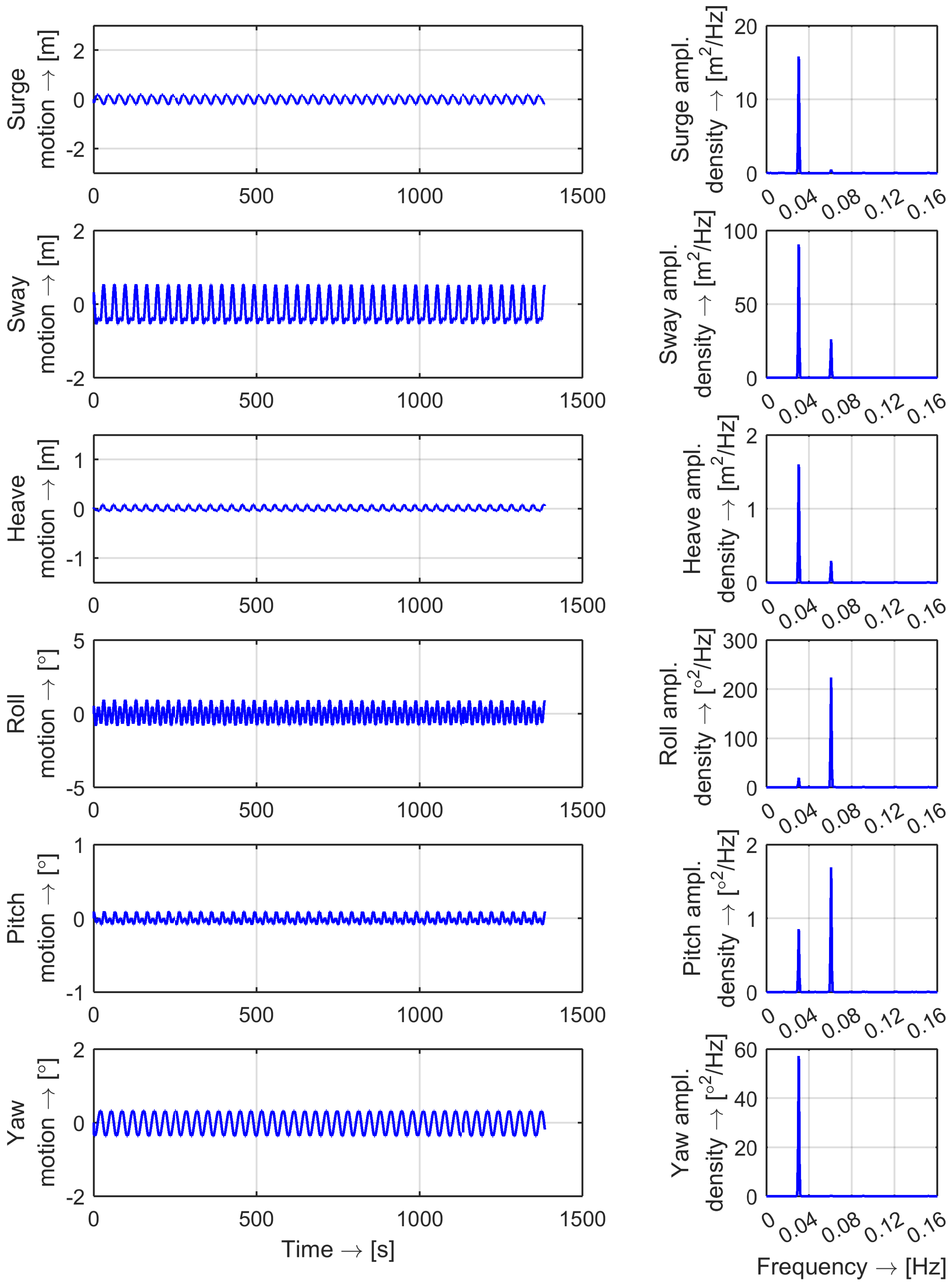

σ_{Surge} = 0.13 m, σ_{Sway} = 0.36 m, σ_{Heave} = 0.05 m, σ_{Roll} = 0.52°, σ_{Pitch} = 0.05°, σ_{Yaw} = 0.25°

Ship motions at centre of gravity (CoG) Depth = 18.0 m, H = 0.120 m, T = 33.00 s Bow-quartering waves	Monochromatic	M330e
	D2_M330e_noST	
Deltares	11202696	App. G.201-2

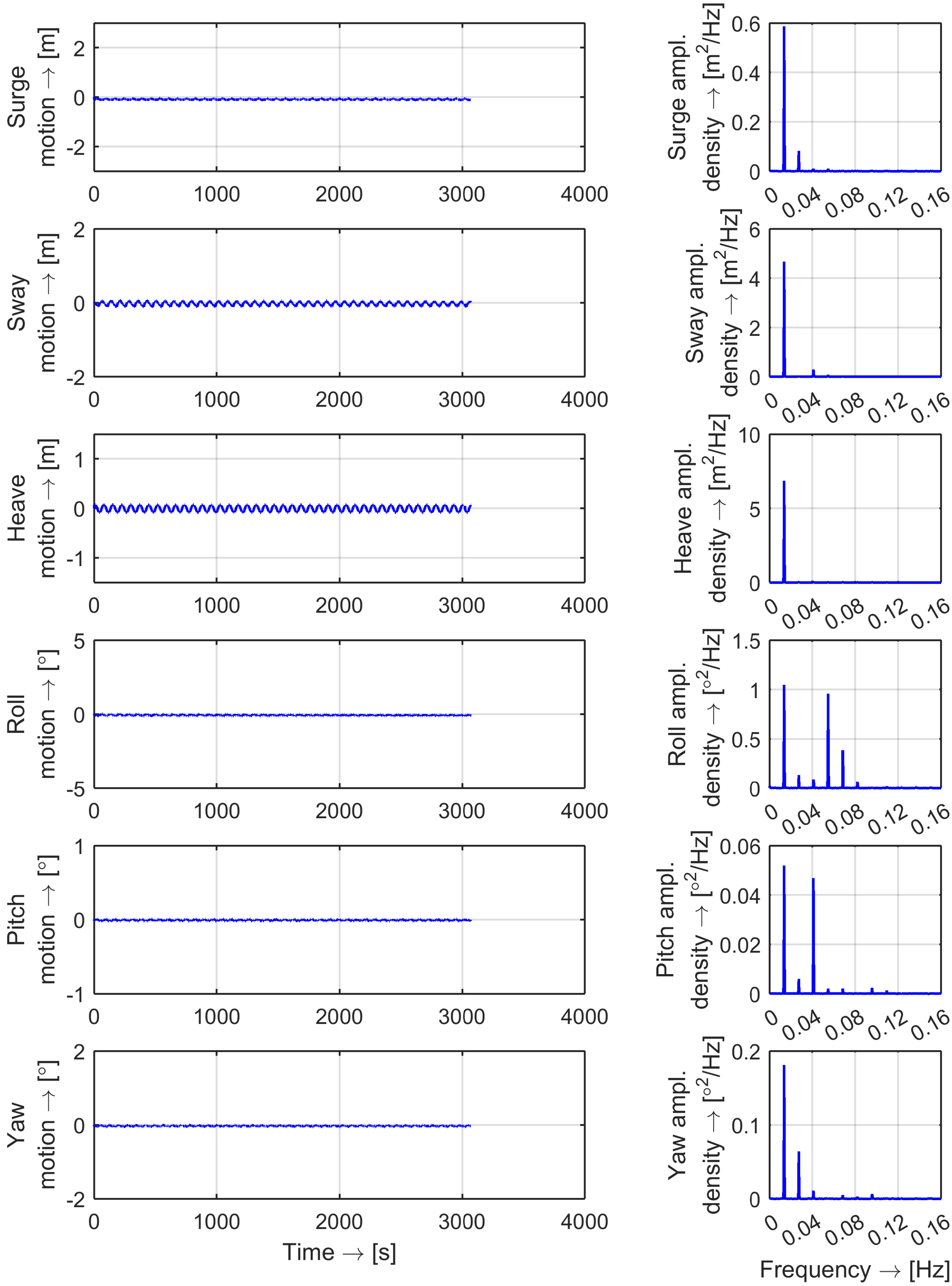

σ_{Surge} = 0.02 m, σ_{Sway} = 0.05 m, σ_{Heave} = 0.06 m, σ_{Roll} = 0.04°, σ_{Pitch} = 0.01°, σ_{Yaw} = 0.01°

Ship motions at centre of gravity (CoG) Depth = 18.0 m, H = 0.200 m, T = 73.12 s Bow-quartering waves	Monochromatic	M7312a
	D2_M7312a	
Deltares	11202696	App. G.202-2

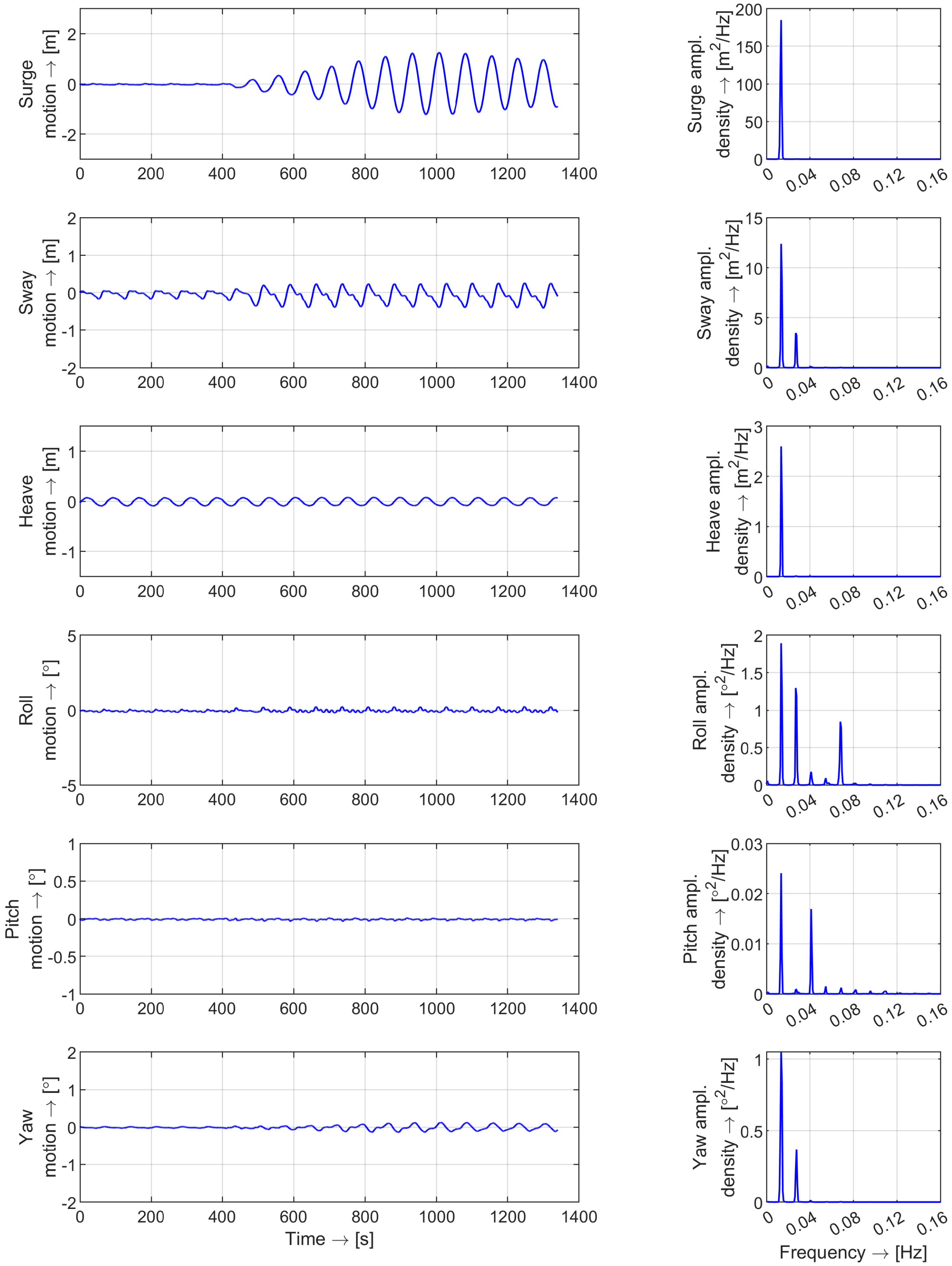

σ_{Surge} = n.a., σ_{Sway} = n.a., σ_{Heave} = n.a., σ_{Roll} = n.a., σ_{Pitch} = n.a., σ_{Yaw} = n.a.

Ship motions at centre of gravity (CoG) Depth = 18.0 m, H = 0.200 m, T = 73.12 s Bow-quartering waves	Monochromatic	M7312a
	D2_M7312a_transition	
Deltares	11202696	App. G.203-2

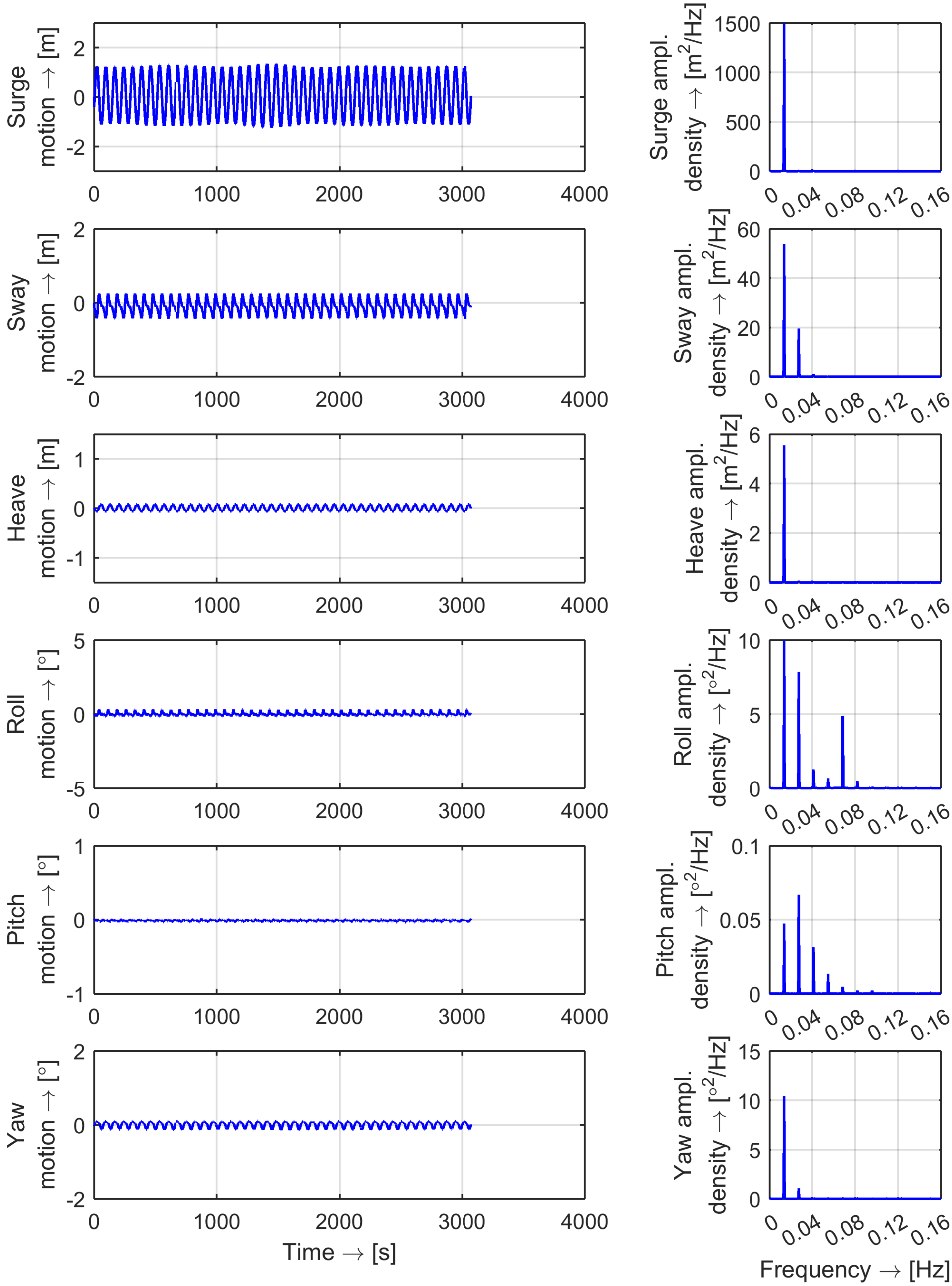

σ_{Surge} = 0.86 m, σ_{Sway} = 0.19 m, σ_{Heave} = 0.05 m, σ_{Roll} = 0.11°, σ_{Pitch} = 0.01°, σ_{Yaw} = 0.08°

Ship motions at centre of gravity (CoG) Depth = 18.0 m, H = 0.200 m, T = 73.12 s Bow-quartering waves	Monochromatic	M7312a
	D2_M7312a_noST	
Deltares	11202696	App. G.204-2

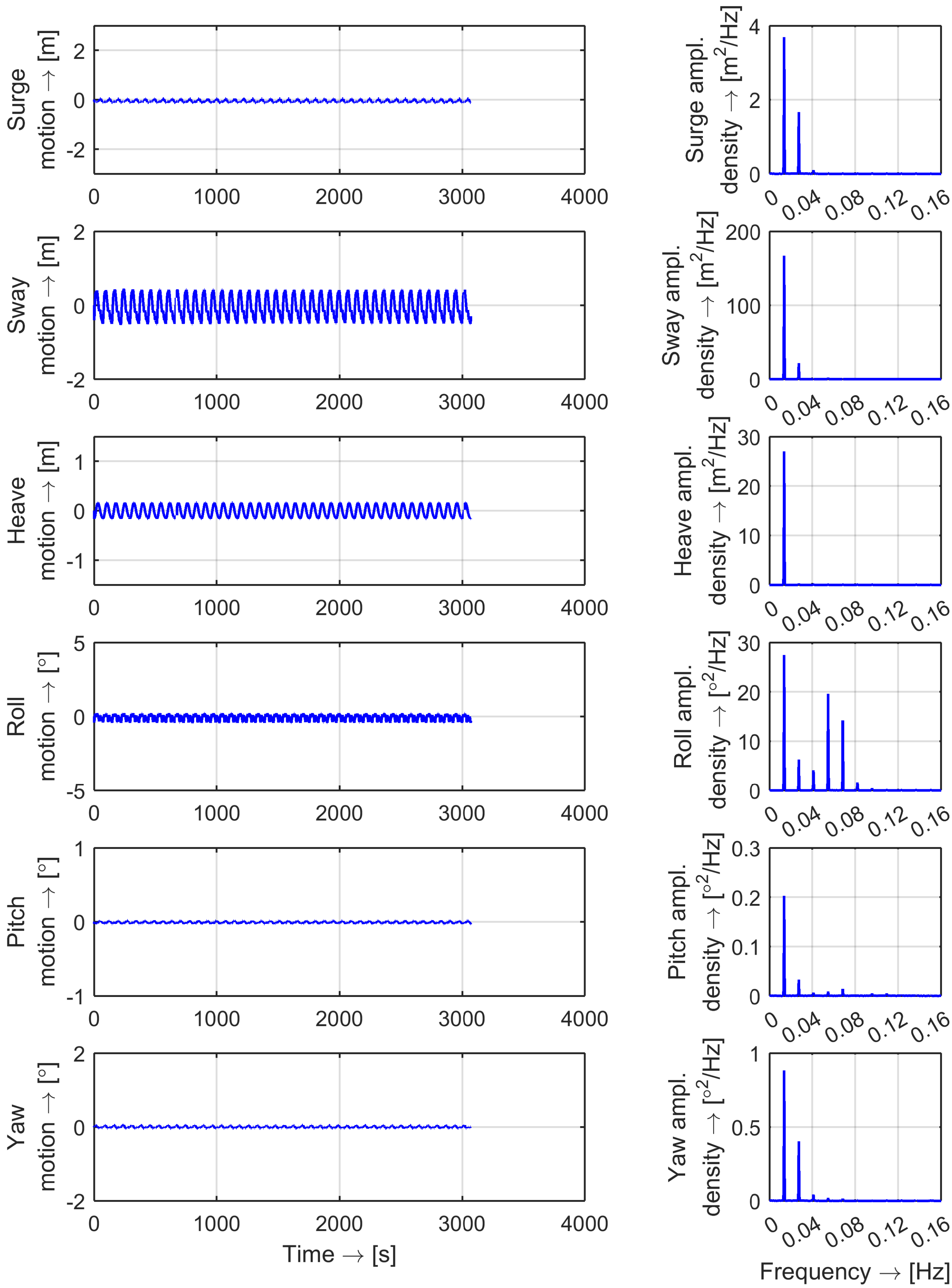

σ_{Surge} = 0.05 m, σ_{Sway} = 0.31 m, σ_{Heave} = 0.12 m, σ_{Roll} = 0.19°, σ_{Pitch} = 0.01°, σ_{Yaw} = 0.03°

Ship motions at centre of gravity (CoG) Depth = 18.0 m, H = 0.400 m, T = 73.12 s Bow-quartering waves	Monochromatic	M7312b
	D2_M7312b	
Deltares	11202696	App. G.205-2

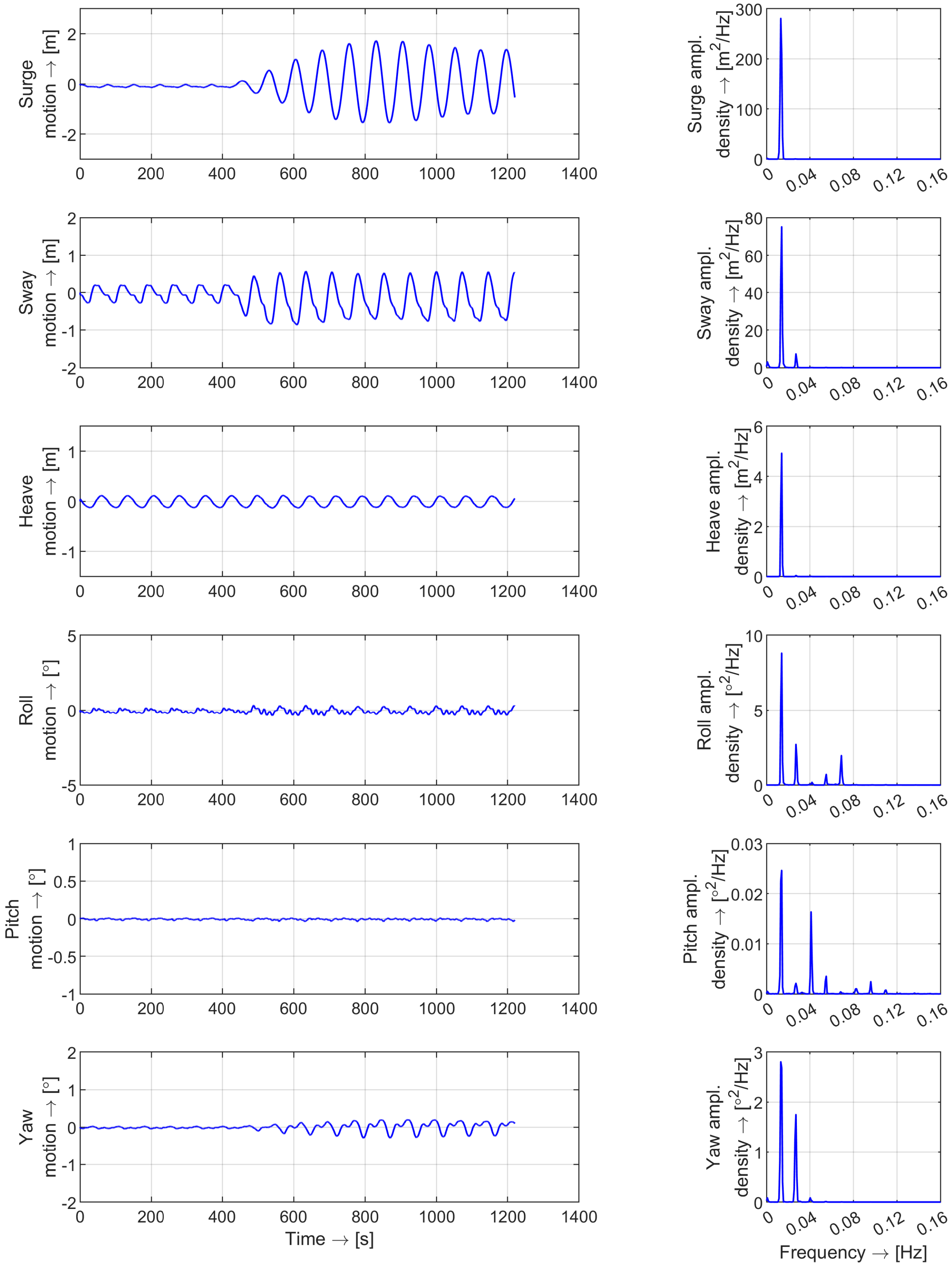

σ_{Surge} = n.a., σ_{Sway} = n.a., σ_{Heave} = n.a., σ_{Roll} = n.a., σ_{Pitch} = n.a., σ_{Yaw} = n.a.

Ship motions at centre of gravity (CoG) Depth = 18.0 m, H = 0.300 m, T = 73.12 s Bow-quartering waves	Monochromatic	M7312d
	D2_M7312d_transition	
Deltares	11202696	App. G.206-2

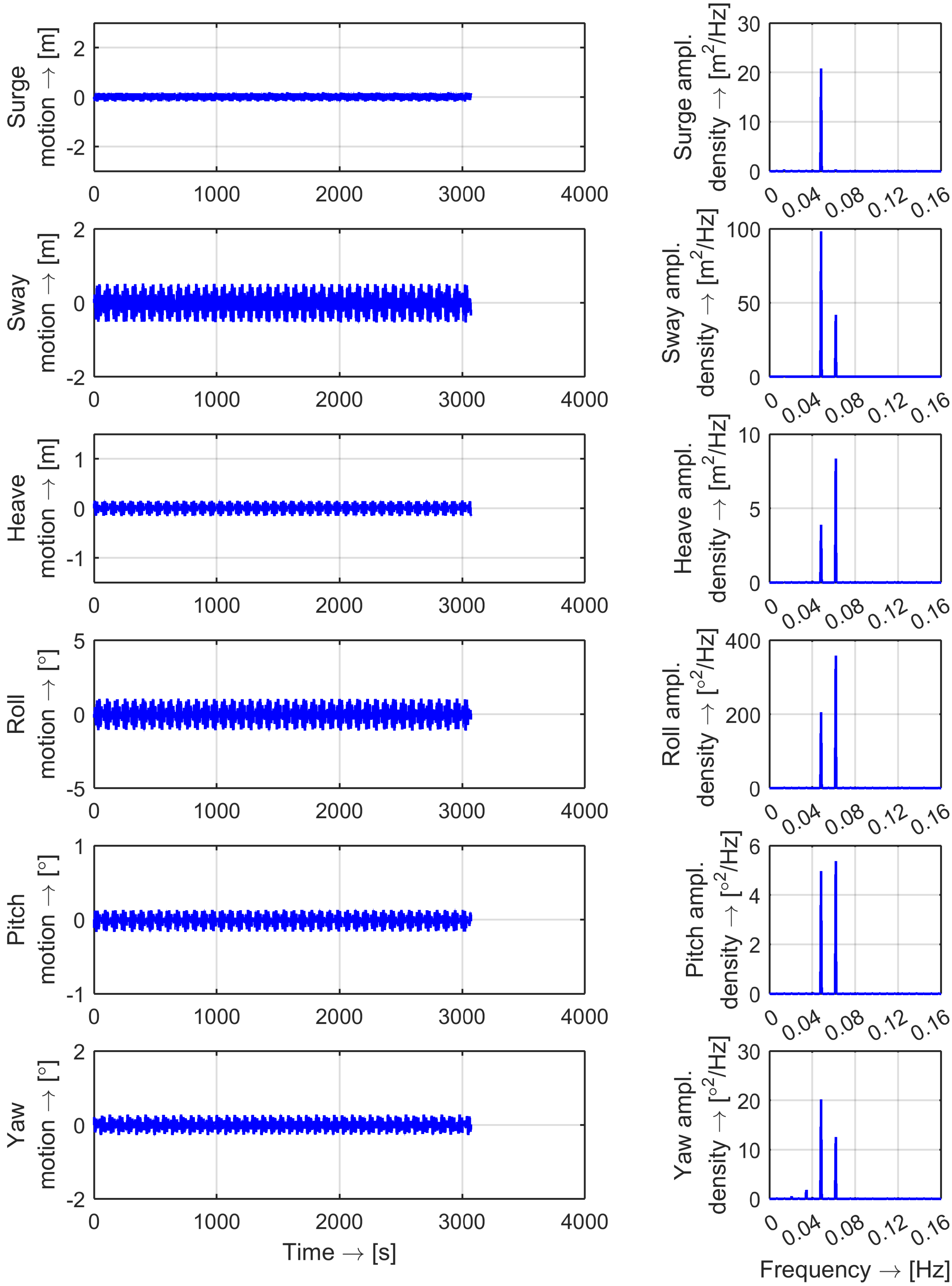

σ_{Surge} = 0.11 m, σ_{Sway} = 0.27 m, σ_{Heave} = 0.08 m, σ_{Roll} = 0.54°, σ_{Pitch} = 0.07°, σ_{Yaw} = 0.14°

Ship motions at centre of gravity (CoG) Depth = 18.0 m, H = 0.500 m, T_1 = 16.20 s, T_2 = 20.81 s Bow-quartering waves	Bichromatic	B7312a
	D3_B7312a	
Deltares	11202696	App. G.207-2

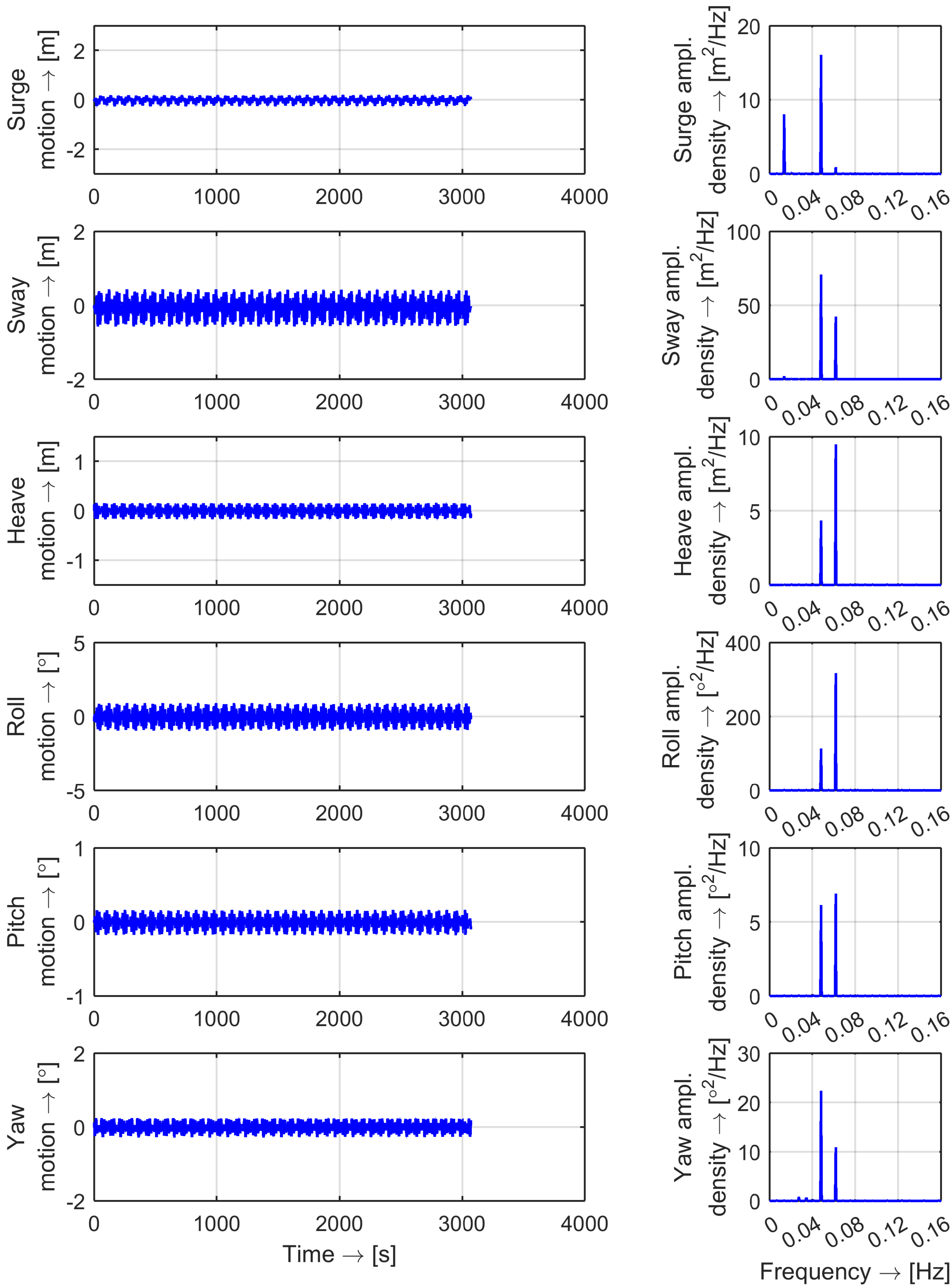

σ_{Surge} = 0.12 m, σ_{Sway} = 0.25 m, σ_{Heave} = 0.08 m, σ_{Roll} = 0.47°, σ_{Pitch} = 0.08°, σ_{Yaw} = 0.14°

Ship motions at centre of gravity (CoG) Depth = 18.0 m, H = 0.500 m, T_1 = 16.20 s, T_2 = 20.81 s Bow-quartering waves	Bichromatic	B7312a
	D3_B7312a_noST	
Deltares	11202696	App. G.208-2

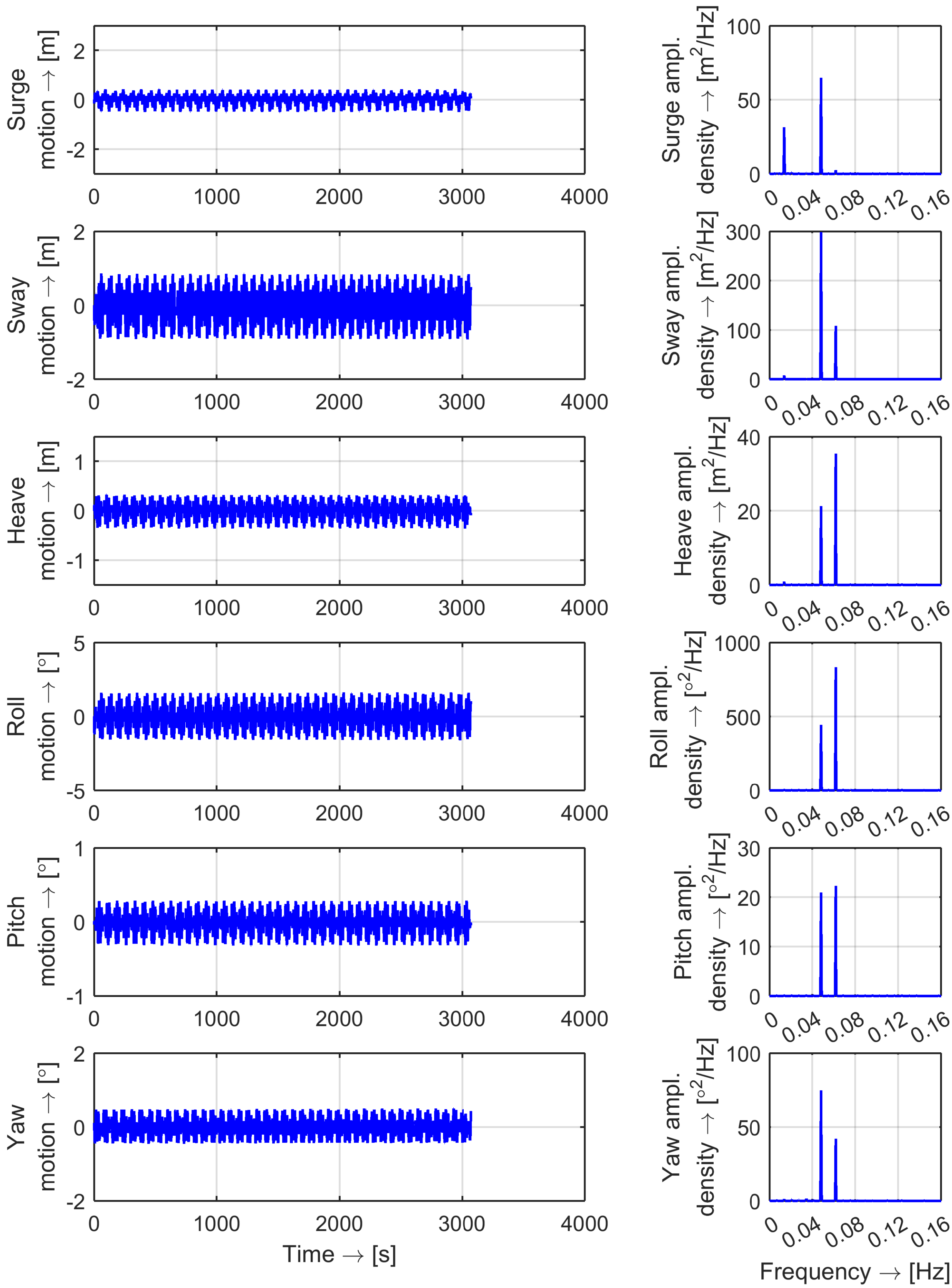

σ_{Surge} = 0.23 m, σ_{Sway} = 0.47 m, σ_{Heave} = 0.17 m, σ_{Roll} = 0.81°, σ_{Pitch} = 0.15°, σ_{Yaw} = 0.25°

Ship motions at centre of gravity (CoG) Depth = 18.0 m, H = 1.000 m, T_1 = 16.20 s, T_2 = 20.81 s Bow-quartering waves	Bichromatic	B7312b
	D3_B7312b	
Deltares	11202696	App. G.209-2

G.2.2 Tables with standard deviations of ship motions

Table G.11 Overview of standard deviations of ship movements per test for Case D.

Test-ID	Surge [m]	Sway [m]	Heave [m]	Roll [°]	Pitch [°]	Yaw [°]
D1_I80a	0.02	0.01	0.00	0.02	0.01	0.02
D1_I80b	0.03	0.02	0.01	0.04	0.01	0.02
D1_I80c	0.01	0.04	0.01	0.08	0.01	0.01
D1_I80d	0.01	0.07	0.03	0.14	0.02	0.01
D1_I120a	0.04	0.07	0.03	0.21	0.06	0.08
D1_I120b	0.08	0.10	0.05	0.29	0.09	0.12
D1_I120c	0.02	0.13	0.05	0.56	0.04	0.02
D1_I120d	0.03	0.27	0.10	1.09	0.07	0.03
D1_I162a	0.10	0.24	0.12	0.53	0.12	0.18
D1_I162b	0.16	0.30	0.18	0.61	0.17	0.25
D1_I162c	0.03	0.44	0.10	1.45	0.06	0.03
D1_I162e	0.07	0.06	0.04	0.16	0.08	0.03
D1_I162e_noST	0.10	0.09	0.05	0.25	0.09	0.03
D1_I162f	0.20	0.12	0.09	0.33	0.16	0.05
D1_I162f_transition	n.a.	n.a.	n.a.	n.a.	n.a.	n.a.
D1_I162f_noST	0.61	0.13	0.09	0.33	0.16	0.06
D2_M156a	0.05	0.14	0.05	0.40	0.06	0.15
D2_M156a_noST	0.04	0.10	0.05	0.32	0.06	0.15
D2_M156b	0.07	0.13	0.10	0.32	0.11	0.26
D2_M156c	0.09	0.11	0.17	0.20	0.16	0.38
D2_M162a	0.04	0.20	0.12	0.49	0.12	0.13
D2_M162a_noST	0.04	0.27	0.12	0.79	0.10	0.15
D2_M162b	0.08	0.34	0.24	0.67	0.24	0.25
D2_M330e	0.21	0.29	0.05	0.29	0.05	0.17
D2_M330e_noST	0.13	0.36	0.05	0.52	0.05	0.25
D2_M7312a	0.02	0.05	0.06	0.04	0.01	0.01
D2_M7312a_transition	n.a.	n.a.	n.a.	n.a.	n.a.	n.a.
D2_M7312a_noST	0.86	0.19	0.05	0.11	0.01	0.08
D2_M7312b	0.05	0.31	0.12	0.19	0.01	0.03
D2_M7312d_transition	n.a.	n.a.	n.a.	n.a.	n.a.	n.a.
D4_B7312a	0.11	0.27	0.08	0.54	0.07	0.14
D4_B7312a_noST	0.12	0.25	0.08	0.47	0.08	0.14
D4_B7312b	0.23	0.47	0.17	0.81	0.15	0.25

G.2.3 Tables with absolute maxima of ship motions

Table G.12 Overview of absolute maxima of ship movements per test for Case D.

Test-ID	Surge [m]	Sway [m]	Heave [m]	Roll [°]	Pitch [°]	Yaw [°]
D1_I80a	0.11	0.05	0.02	0.17	0.04	0.06
D1_I80b	0.14	0.08	0.04	0.23	0.05	0.09
D1_I80c	0.03	0.16	0.05	0.37	0.05	0.03
D1_I80d	0.04	0.29	0.10	0.57	0.08	0.05
D1_I120a	0.17	0.25	0.13	0.75	0.22	0.29
D1_I120b	0.33	0.40	0.21	1.07	0.33	0.46
D1_I120c	0.08	0.55	0.18	2.17	0.13	0.06
D1_I120d	0.22	1.04	0.39	3.96	0.26	0.14
D1_I162a	0.43	0.94	0.50	1.99	0.45	0.68
D1_I162b	0.80	1.24	0.69	2.47	0.59	0.98
D1_I162c	0.18	1.35	0.38	4.23	0.22	0.15
D1_I162e	0.41	0.23	0.18	0.71	0.30	0.11
D1_I162e_noST	0.57	0.29	0.17	0.71	0.30	0.10
D1_I162f	0.92	0.46	0.42	1.17	0.59	0.22
D1_I162f_transition	1.19	0.54	0.36	1.16	0.56	0.22
D1_I162f_noST	2.98	0.54	0.41	1.12	0.61	0.31
D2_M156a	0.07	0.20	0.07	0.60	0.09	0.21
D2_M156a_noST	0.07	0.18	0.07	0.51	0.11	0.22
D2_M156b	0.14	0.20	0.16	0.48	0.16	0.38
D2_M156c	0.23	0.23	0.24	0.34	0.24	0.55
D2_M162a	0.15	0.31	0.18	0.79	0.17	0.21
D2_M162a_noST	0.06	0.42	0.18	1.14	0.16	0.22
D2_M162b	0.26	0.51	0.37	1.03	0.36	0.40
D2_M330e	0.46	0.49	0.09	0.54	0.10	0.32
D2_M330e_noST	0.22	0.55	0.09	0.96	0.10	0.37
D2_M7312a	0.12	0.12	0.09	0.14	0.02	0.05
D2_M7312a_transition	1.25	0.42	0.09	0.24	0.04	0.13
D2_M7312a_noST	1.35	0.43	0.08	0.33	0.04	0.14
D2_M7312b	0.13	0.53	0.17	0.44	0.03	0.06
D2_M7312d_transition	1.72	0.86	0.13	0.38	0.04	0.29
D4_B7312a	0.19	0.53	0.16	1.11	0.17	0.29
D4_B7312a_noST	0.28	0.58	0.17	0.96	0.18	0.28
D4_B7312b	0.51	0.92	0.36	1.63	0.32	0.50

www.deltares.nl

Deltares